On the Electronic Absorption Spectra and the Dipole Moment of the Molecular Compound between Stannic Chloride and Naphthalene

By Hiroshi TSUBOMURA

(Received July 13, 1953)

Introduction

It has been well known for many years that stannic chloride as well as the halides of various metals, e.g., aluminium, boron, titanium, tin, mercury, etc., can form molecular compounds with organic compounds.[1][2][3] The organic compounds which combine with stannic chloride may be divided into two groups according to whether they contain oxygen or nitrogen atoms or not. Organic compounds of the former group, e.g., ethers, aldehydes, ketones, amines or nitrils, combine with stannic chloride with evolution of heat. On the other hand, for the latter group, composed mainly of aromatic hydrocarbons, it is known that the bond is very weak and in most cases accompanies changes of electronic absorption spectra and dielectric polarizations.

Briegleb and Kambeitz[4] have, by the optical measurements, found that, in a dilute carbon tetrachloride solution, the MC's (molecular compounds) between stannic chloride and aromatic hydrocarbons exist in a 1:1 form. Ulich and his co-workers[5] have measured the molecular polarization of the MC between stannic chloride and benzene, and gave 0.8D for the dipole moment of the MC, assuming that the concentration of the MC is equal to that of the stannic chloride. Strictly speaking, however, this assumption seems to be incorrect.

As for the experimental data concerning the physico-chemical properties of such MC's, not more than those described above have been reported. Also, it seems that no satisfactory theoretical explanation about the nature of the binding forces has yet been made. In an attempt to obtain more experimental knowledge which may be useful for the clarification of these problems, the present author made the following researches on the electronic absorption spectra and dielectric polarizations.

1) Gmelins Handbuch der anorganischen Chemie, 8 Aufl., 1937, Verlag Chemie G.m.b.H., Berlin; J.W. Mellor, "A Comprehensive Treatise on Inorganic and Theoretical Chemistry," Longmans, Green, London, 1929.
2) P. Pfeiffer, "Die organische Molekülverbindungen," Ferdinand Enke, Stuttgart, 1927.
3) G. Briegleb, "Zwischenmolekulare Kräfte und Molekülstruktur," Ferdinand Enke, Stuttgart, 1937.
4) Ref. 3, p. 124.
5) H. Ulich, E. Hertel and W. Nespital, *Z. physik. Chem.*, **B17**, 369 (1932).

Experimental

The stannic chloride used was prepared by introducing dry chlorine into a flask which contained fused tin heated to about 350°C. The stannic chloride vapor which was generated in the flask was led, through a cooler, into another vessel. The stannic chloride thus prepared was refluxed with tin for several hours in order to convert the contained chlorine to stannic chloride. The stannic chloride thus obtained is a clear colorless liquid which shows almost an constant b.p. of 113°C. Naphthalene was recrystallised twice from methanol solutions, and dried in a vacuum desiccator containing phosphorus pentoxide for several weeks. (m.p., 80.6°C). Benzene was purified by washing with concentrated sulfuric acid, followed by fractional distillation. Ethyl acetate was dried with calcium chloride and fractionated. (b.p., 76.8°C). Cyclohexane was purified according to the method described by Hinrichsen and Kempf[6].

The measurements of the absorption spectra were made by the Beckman spectrophotometer, model DU. For the measurement of the dielec-

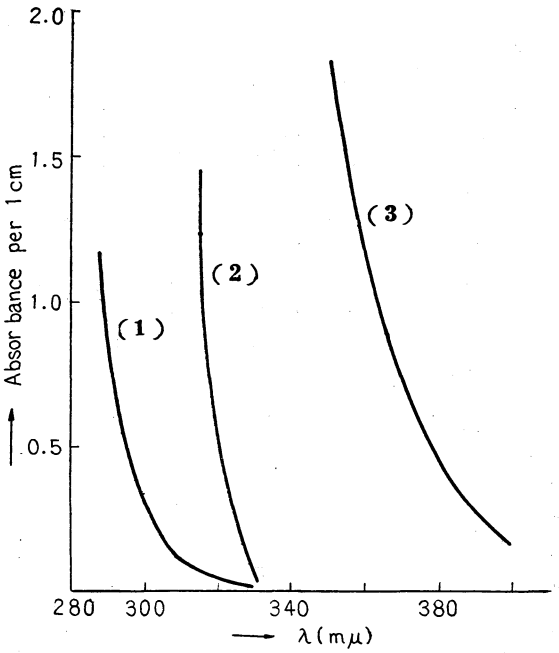


Fig. 1.—Absorption spectra of
(1) pure stannic chloride
(2) 0.0100 M naphthalene in cyclohexane
(3) 0.667 M stannic chloride and 0.0251 M naphthalene in cyclohexane.

6) Hinrichsen and Kempf, *Ber.*, **45**, 2106 (1912).

tric constant, the same instrument as reported by K. Kozima and T. Yoshino[7] has been used in this case. Since stannic chloride is very sensitive to moisture, care was taken to protect it as far as possible during the measurements. As a very small amount of white precipitation was inevitably formed during the preparation of solutions, the solutions were transferred through a glass filter, protected from moisture, into the cells used for the absorption or dielectric measurements.

Results

1. Absorption Spectra—In Fig. 1, curves (1) (2), and (3) show the absorbance per 1 cm of stannic chloride for pure liquid state, that of naphthalene in cyclohexane and that of a mixture of stannic chloride and naphthalene in cyclohexane, respectively. From these curves, it can be seen that, in the region of wavelength longer than 330 mμ, the absorbances of both stannic chloride and naphthalene are negligible, and so the absorbance of (3) in this region is entirely to be attributed to the molecular compound.

Next, the isothermal dilution change of the absorption of this MC was measured for eleven solutions at 18°C. It was confirmed that the results can be expressed by the following equation,

$$c^0_{Mi}\, c^0_{Ni}(d_{x0}/d_{xi}) = (d_{x0}/\varepsilon_x)c^0_{Mi} + d_{x0}/(\varepsilon_x \cdot K) \quad (1)$$

where c^0_{Mi} and c^0_{Ni} are the total concentration (in mole/l.) of stannic chloride and naphthalene (including those which are associated) for the ith solution, d_{x0}/d_{xi} is the ratio of the absorbance between zeroth and ith solutions which was derived by averaging these ratios at many different wavelengths, and ε_x and K are constants. (See Fig. 2). It may be easily proved that equation (1) can be derived from the following equation expressing the equilibrium of the 1:1 association

$$c_x/c^0_M(c^0_N - c_x) = K^* \quad (2)$$

and in fact K and ε_x appearing in (1) are the equilibrium constant and the molar absorptivity of the MC, respectively. Therefore, the results indicate that in dilute solution the concentration of the MC is governed by equation (2), in agreement with the Briegleb and Kambeitz's results. From the data, K and ε_x were detemined by use of the method of least square. The results are:

$K=0.06$ (M^{-1}), $\varepsilon_x = 2\times10^3$ (cm^{-1}. M^{-1}) at 350 mμ

Since in this case K is very small, it seems difficult to get these values more accurately.

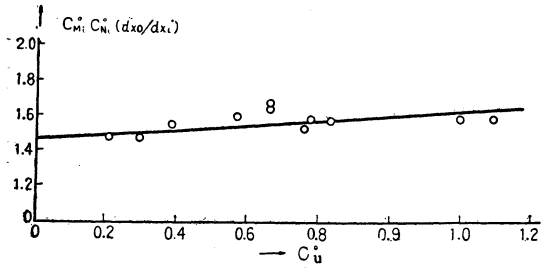


Fig. 2.

TABLE I

at 18°C

	x*	d	ε	P_1, cc.	$N_x\Delta P$	Nx, M/gr.	ΔP, cc
$SnCl_4$	0	2.2358	2.9031	45.231	/	/	
Soln. 1	0.01070	2.2198	2.9058	/	0.00093	3.16×10^{-5}	30
Soln. 2	0.03380	2.1897	2.9131	/	0.00303	10.01×10^{-5}	30

at 40°C

	x*	d	ε	P_1, cc.	$N_x\Delta P$
$SnCl_4$	0	2.1784	2.8269	45.267	/
Soln. 1	0.01070	2.1635	2.8245	/	0.00058
Soln. 2	0.03380	2.1368	2.8307	/	0.00242

* The x's are the molarities of naphthalene calculated without assuming the formation of the *MC*.

2. Polarization Measurements

The dielectric constants and densities of liquid stannic chloride and two solutions of naphthalene in stannic chloride were measured at 18°C and 40°C. The results obtained are given in Table 1. The dielectric constant and density of stannic chloride itself are in good agreement with those reported by Ulich and others[5]. First, it was found that the polarizations of the solutions were considerably greater than the weighted means of the molecular polarizations of stannic chloride and naphthalene. This indicates that the molecular polarization of the *MC* is larger than the sum of those of stannic chloride and naphthalene.

In a dilute solution, it was confirmed spectrophotometrically that the *MC* was of 1:1 form. But in this case the situation is not quite the same because now naphthalene is dissolved in the liquid of stannic chloride. Nevertheless the author tentatively assumes here that still in this case the *MC* is of 1:1 form, and that the molecular polarization of the *MC*, P_x, is given by the following formula:

$$P_x = P_M + P_N + \Delta P \quad (3)$$

Then the polarization per one gram of the solution is given by

$$P_{12} = (\varepsilon_{12}-1)/(\varepsilon_{12}+2)\cdot d_{12} = N^\circ_M P_M + N^\circ_N P_N + N_x \Delta P, \quad (4)$$

7) K. Kozima and T. Yoshino, *J. Chem. Soc. Japan*, **72**, 20 (1951).

* This is an approximate equation which is exact when c^0_M is far larger than c^0_N. All the solutions investigated were, of course, prepared so as to satisfy this condition.

where N_x is the number of moles (per one gram of the solution) of the *MC* and N°_M and N°_N are those of stannic chloride and naphthalene, including the associated ones, respectively. Concerning P_M and P_N, the former was calculated from the experimental values of ε_M and d_M, and the latter may be taken from the experimental value reported by Briegleb[8], (33.84 cc.). Thus ($N_x \Delta P$) can be determined by use of equation (4). The results obtained are given in Table 1.

The second step is to determine N_x. The concentrations of the *MC* in dilute cyclohexane solutions can be obtained by use of equation (2) with the K value determined from the results of isothermal dilution change. But it is clear that we cannot apply this equation to the solution for the dielectric measurement because the activity coefficient of the medium must differ in the two cases. Therefore the concentration of the *MC* in the solution for the dielectric measurement was estimated by comparing the absorbance of the *MC* in it with that in the dilute cyclohexane solution. The N_x and ΔP thus obtained are given in Table 1.

We may conclude that the orientation polarization constitutes most part of the ΔP. The dipole moment is then calculated from the averaged value of ΔP to be 1.2 *D*. It was found that about 80% of the naphthalene molecules were associated. It is worth while to note that the dipole moment calculated by assuming complete association is 1.0 *D*. This is a little larger than the corresponding value for the *MC* of stannic chloride with benzene reported by Ulich et al.

From Table 1, it can be seen that the $N_x \Delta P$ at 40°C is considerably smaller than that at 18°C. If we assume the dipole moment of the *MC* does not vary with rising temperature, ΔP should be proportional to $1/T$. In such a case we find that the N_x at 40°C is about 60–80% of that at 18°C. From this result, and by use of the *reaction isochore*, the heat of formation is calculated to be 2–4 kcal/mole. But this result should be regarded to be only semi-quantitative, since the agreement between these values for the two solutions was not satisfactory.

The spectra of the MC's of stannic chloride with benzene or ethyl acetate.

From the resemblance of the electronic and molecular structure of benzene and naphthalene, and also from Ulich's polarization data, it was supposed that an absorption spectrum similar to the stannic chloride-naphthalene system would occur in the stannic chloride-benzene system. In order to check this, the spectrum of a stannic chloride solution of benzene has been measured, and the result obtained was in agreement with the expectation mentioned above. (Fig. 3). A quantitative analysis was not made in this case. Simply it was observed that the absorption band of the *MC* was of considerably shorter wavelength than that of the stannic chloride-naphthalene system.

8) G. Briegleb, *Z. physik. Chem.* B **16**, 276 (1932).

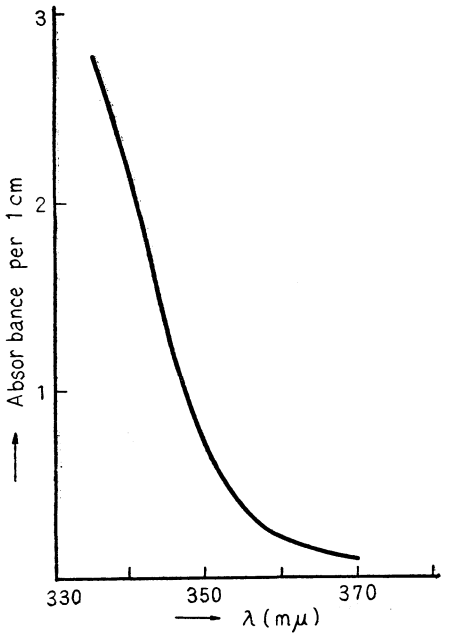


Fig. 3.—Absorption spectra of 0.187 M benzene in stannic chloride.

In an attempt to investigate the spectra of the *MC*'s of stannic chloride with oxygenated organic compounds, ethyl acetate was chosen as an appropriate example. It was observed that much heat was evolved when stannic chloride was dissolved in it. The mixtures are clear viscous liquid and the wavelengths of their spectra are a little longer than that of stannic chloride, but considerably shorter than that of the stannic chloride-naphthalene system. The absorbance of this *MC* was found to be roughly proportional to the concentration of stannic chloride in the mixture. (Fig. 4).

Discussion

It is highly probable that the linkages between stannic chloride and compounds containing oxygen or nitrogen atoms are very strong, since heat is evolved when these substances are mixed. It may be supposed that these linkages are of a type of coördination linkage between the lone pair AO of oxygen or nitrogen atom and the MO of stannic chloride including the d-shell of tin atom.[9] We might explain the linkages between stannic chloride and aromatic hydrocarbons by an analogous model, basing our explanation on the fact that for many cases aromatic hydrocarbons are regarded to be of the electron-donor type. But in this case the orbital of the electron-donor molecule which interacts with that of metal halides is

9) L. Pauling, The nature of the Chemical Bond, Cornell Univ. Press, Ithaca, N.Y., 1940, p. 93.

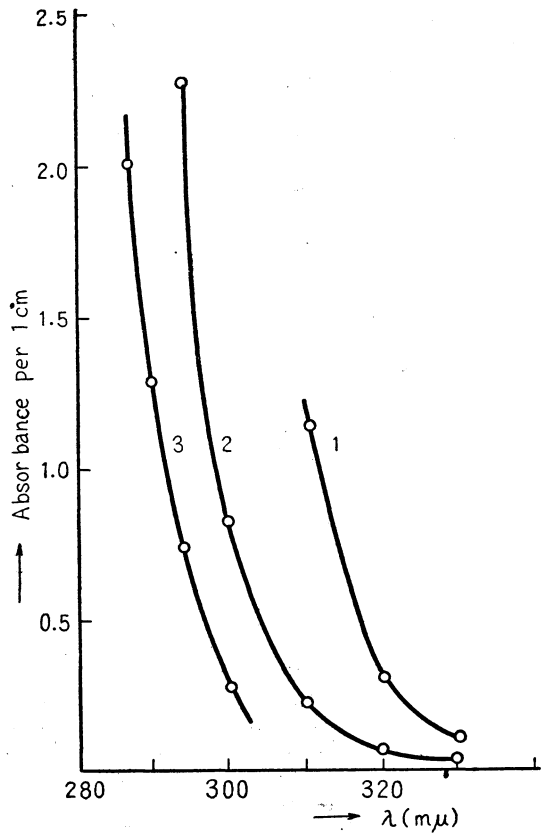


Fig. 4.—Absorption spectra of stannic chloride in ethyl acetate.
(1) 3.57 M stannic chloride
(2) 0.714 M "
(3) 0.202 M "

not confined to one special atom in it, but extends throughout the whole molecule. Then the absorption spectra of such MC's may be understood as the charge-transfer spectra similar to those of the benzene-iodine complex[10] or quinhydrone.[11] If this is true, the dipole moments observed for these MC's may possibly be caused mainly by the charge-transfer.*

Although the energy of the linkage in the MC between stannic chloride and ethyl acetate is very different from those between stannic chloride and aromatic hydrocarbons, it must be concluded that a similar charge-transfer spectrum will exist still in the former MC. The band which was experimentally found to be proportional to the concentration of stannic chloride in the ethyl acetate solution will probably be this charge-transfer spectrum.

From the experimental results, it is likely that the wavelengths of the MC's of stannic chloride become longer as the electron-donors are varied in the sequence of ethyl acetate, benzene, and naphthalene. It is worth while to note that the lowest ionization potentials of the electron-donors become smaller in the same sequence.** The charge-transfer spectra may be roughly assigned to the transition between two energy levels formed by the perturbation between the lowest unfilled MO of the electron-acceptor and the highest filled MO of the electron-donor, and hence the wavelength of this spectrum depends largely on the energy difference between the original unperturbed MO's.[11] Now it is clear that such energy differences become larger, the larger the ionization potentials of the electron-donor. Thus, the relation between the ionization potentials of the electron-donors and the wavelengths of the MC's may be explained by the previously given MO theory.

Summary

The 1:1 form of the molecular compound between stannic chloride and naphthalene in dilute solution has been confirmed by the measurements of electronic absorption spectra. The exaltation of the molecular polarization of this molecular compound has been determined from both optical and dielectric measurements and the dipole moment has been calculated from it. The absorption spectra of other similar molecular compounds have also been measured. It has been proposed that the intermolecular linkages may be explained as the charge-transfer bond.

The author wishes to express sincere thanks to Prof. K. Kozima for his valuable discussions and kind advice.

Tokyo Institute of Technology,
Meguroku, Tokyo

10) R.S. Mulliken, *J. Am. Chem. Soc.*, **74** 811 (1952).
11) H. Tsubomura, This Bulletin, **26**, 304 (1953).

* Briegleb took the dipole moment of such *MC*'s as were caused by the deformation of stannic chloride molecule from the tetrahedral structure. (ref. 3, p. 84). It seems that such a cause should also be taken into account as an additive factor of the dipole moment of these *MC*'s. But his explanation for the original nature of the bonds in these *MC*'s seems to be unsuccessful.

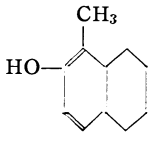
** This fact was kindly suggested to the author by Dr. S. Nagakura.

Studies on Santonin. I. Experiments on the Synthesis of Santonin. Part I. Preparation of 2-Keto-1, 10-dimethyl-decalin

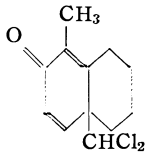
By Masanao MATSUI, Seiichi KITAMURA, Yoshio SUZUKI and Michiko HAMURO

(Received July 22, 1953)

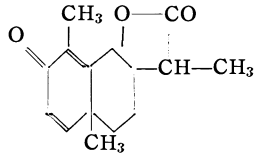
ac-Tetrahydro-1-methyl-2-naphthol (I) is easily obtained from β-naphthol through methylene-dinaphthol and 1-methyl-2-naphthol[1)2)]. T. Harukawa and H. Ishikawa[3)] prepared 2, 5, 6, 7, 8, 10 - hexahydro - 2 - oxo - 1 - methyl - 10 - dichloro - methyl - naphthalene (II) from *ac*-tetrahydro-1-methyl-2-naphthol by the method analogous to that of Woodward[4)]. We who aimed from this material to prepare the substance resembling santonin (III), checked



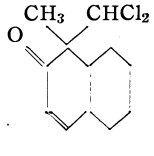
I



II



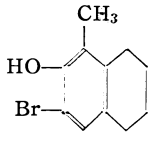
III



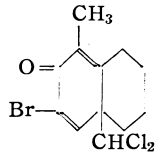
IV

We knew therefore that it is difficult to introduce any radical into the hydrobenzene ring of (II).

Then we turned our attention to the starting material, *ac*-tetrahydro-1-methyl-2-naphthol (II) and tried to introduce a double linkage into its hydrobenzene ring. We treated this naphthol with bromosuccinimide to introduce bromine to the 8-position, but this trial also failed. Considering the fact that the substance obtained by this trial was not dehydrobrominated by alkali in the warm, and showing that bromine exists in the benzene ring and from the results of the bromination of other phenols, replacement of the 3-position of (II) was the most probable. The product obtained was considered to be 1-methyl-3-bromo-tetrahydro-2-naphthol (V), which reacted with chloroform in the presence of sodium hydroxide and yielded dichloromethyl-dienone (VI), mp. 153°.

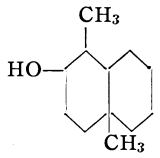


V

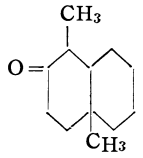


VI

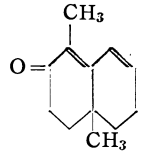
We gave up the first plan and tried to prepare 2, 3, 4, 5, 6, 10-hexahydro-2-oxo-1, 10-dimethyl - naphthalene (IX) from dichloromethyl dienone (II) above mentioned.



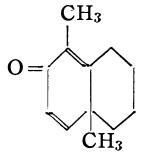
VII



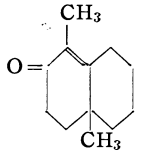
VIII



IX



X



XI

(II) was hydrogenated in an autoclave with Raney Nickel at room temperature. The temperature gradually rose with the consumption of hydrogen and at the end of hydrogenation reached 80°. One mol. of the sample (II) absorbed about 5 mol. of hydrogen and dimethyl-decahydro-naphthol (VII) was obtained. It is a light yellow oil, boiling at 85-100°/0.5 mm. n_D^{18} 1.5075. 3,5-Dinitrobenzoate was oil which was probably the mixture of stereoisomerides. (VII) was oxidized by chromium trioxide in acetic acid and a ketone, bp. 75—85°/0.5 mm. n_D^{18} 1.4955 was obtained. This ketone is 2-oxo-1, 10-dimethyl-decaline (VIII), because its 2,4-dinitrophenyl-hydrazone (mp. 186°) was the same as the

1) K. Fries and E. Hubner, *Ber.* **39**. 439, 441 (1906).
2) Cornforth, Cornforth and Robinson. *J. Chem. Soc.*, **1942**, 682.
3) *J. Pharm. Japan*, **70**, 338 (1950).
4) Woodward, *J. Am. Chem. Soc.*, **62**, 1208 (1940).

one derived from hydrogenation product of 2,3,4,5,6,7,8,10-octahydro-2-oxo-1,10-dimethylnaphthalene (XI) which was prepared from 2-methyl-cyclohexanone and dimethylaminopentanone methiodide by the method of Gunstone and Heggie[5].

Bromination and dehydrobromination by pyridine yielded liquid unsaturated ketone boiling at 65—85°/0.3 mm. n_D^{20} 1.5145—1.5300, 2,4-dinitrophenylhydrazone melting at 189°. This product was probably the mixture of IX, X and XI. (n_D^{20} of IX, X and XI are 1.5590—1.5320 and 1.5260 and 2,4-dinitrophenylhydrazones of IX, X and XI melt at 216°, 238—239° and 198—199° respectively[5].

Experimental

1. *ac*-Tetrahydro-1-methyl-2-naphthol (I)

β-Naphthol condensed with formaldehyde in the presence of sodium acetate in alcohol to give methylene-dinaphthol, mp. 192°, in a theoretical amount. The methylene-dinaphthol was reduced by zinc and sodium hydroxide aqueous solution to 1-methyl-2-naphthol[1], bp. 160–162°/25 mm., mp. 110° (60%). The naphthol was reduced at 110°/100 atm. p. with hydrogen and Raney nickel in alcohol to give *ac*-tetrahydro-1-methyl-2-naphthol, mp. 113° (82%)[6]

2. 2, 5, 6, 7, 8, 10-Hexahydro-2-oxo-10-dichloromethyl-naphthalene (II)[3]

(I) (70 g.) was dissolved in 700 g. of 10% sodium hydroxide aqueous solution in a 3 l four necked flask. Chloroform (250 g.) and 190 g. of 40% sodium hydroxide aqueous solution were dropped separately but simultaneously from two dropping funnels at 75° during 3 hrs. with stirring which was continued for 45 min. after the addition was over. The cooled mixture was extracted with chloroform (500 cc.) and the extract was washed with 5% sodium hydroxide aqueous solution and then with water. After the evaporation of the solvent, the residue was dissolved in 70 cc. of methanol and the solution was left to stand overnight in a refrigerator. Separated crystals (15 g.) were collected and recrystallized from methanol. 11 g. of (II), mp. 155°, was obtained. (Found: C, 58.70; H, 5.1%; Calcd. for $C_{12}H_{14}OCl_2$ C, 58.8; H, 5.7%.)

The mother liquor of the crystals was distilled, and the fraction boiling at 150–175°/0.25 mm. was collected (35 g.) It was dissolved in methanol (100 cc.) and cooled by dry ice, to give crystals (11 g.), mp. 57–59°. The sample was treated with ether and 3 g. of insoluble crystals (mp. 155°) were obtained. The ether solution, separated from the crystal was washed with 5% sodium hydroxide aqueous solution several times and with water 3 times. Then the ether was removed and the residue was recrystallized from methanol. The substance melting at 63°, a yellowish large prism, was obtained. This is considered to be 1,2,5,6,7,8-hexahydro-2-oxo-1-methyl-1-dichloromethyl-naphthalene (IV). (Found: C, 59.5; H, 5.0; Cl, 28.3% Calcd for $C_{12}H_{14}OCl_2$: C, 58.8; H, 5.7; Cl, 28.7%)

3. *ac*-Tetrahydro-1-methyl-3-bromo-2-naphthol (V)

A mixture of *ac*-tetrahydro-1-methyl-2-naphthol (158 g.), bromosuccinimide (178 g.) and carbon tetrachloride (1 l) was refluxed for 1 hour. After 100 g. of succinimide were recovered by filtration, carbon tetrachloride was removed. The crystals obtained were recrystallized from petroleum ether (bp. 40–60°), giving 78 g. of (V) mp. 71°, (Found: C, 55.06; H, 5.20; Br, 33.5%, Calcd. for $C_{11}H_{11}OBr$: C, 55.2; H, 5.0; Br, 29.2%)

4. 2, 5, 6, 7, 8, 10-Hexahydro-2-oxo-1-methyl-10-dichloromethyl-3-bromo-naphthalene (VI)

The substance (V) (120 g.), 10% sodium hydroxide aqueous solution (1500 g.) and chloroform (280 g.) were treated in the same manner as case 2. and 12 g. of the desired product (VI) mp. 153°, was obtained. (Found: C, 44.2; H, 4.4%; Calcd. for $C_{12}H_{13}OCl_2Br$: C, 44.4; H, 4.3%)

5. 2-Hydroxy-1, 10-dimethyl-decalin (VII)

A solution of 20 g. of (II) in 200 cc. of 5% potassium hydroxide-methanol solution was hydrogenated with 5 g. of Raney nickel catalyst under an initial pressure of 50 atm. p. in 0.5 l. autoclave at first at 20° and at 80° when hydrogenation was over. Twenty hrs. were required and ca. 10 l. of hydrogen was consumed. The hydrogenated solution, after removing the catalyst, was distilled. The fraction boiling at 85–100°/0.3 mm., n_D^{18} 1.5075, which was (VII), was collected. The yield was 16.8 g. (Found: C, 78.2; H, 10.4%; Calcd. for $C_{12}H_{22}O$: C, 79.1; H, 12.1%.) 3,5-Dinitrobenzoate was an oil. Hence the existence of stereoisomerides is probable.

6. 2-Oxo-1, 10-dimethyl-decalin (VIII)

In a solution of (VIII) (32 g.) and 500 cc. of acetic acid, 15 g. of chromium trioxide in 120 cc. of water dissolved in 300 cc. of acetic acid was dropped under stirring at 15°. After the addition, when the required 2 hrs., was over, stirring was continued for 3 hrs. and the reaction mixture was left to stand overnight. Water (1.9 l) was added and the mixture was extracted with petroleum ether (bp. 40–60°) five times, using each time 200 cc, of the solvent. The extract was combined and washed with water. 2-Oxo-1, 10-dimethyl-decalin (VIII) yellowish oil boiling at 75–85°/0.5 mm., n_D^{18} 1.4955 was obtained, (Gunstone and Heggie reported bp. 76–78°/0.5 mm., n_D^{19} 1.4945)[5]. 2,4-Dinitrophenylhydrazone melting at 186°, recrystallized from methanol, gave no melting point depression on admixture with the sample (186°) prepared by another method[5]. (Found: C, 60.4; H, 7.0%; Calcd. for $C_{18}H_{24}O_4N_4$: C, 60.0; H, 6.7%.)

7. Bromination and Dehydrobromination of (VIII)[5].

Three g. of 2-oxo-1, 10-dimethyl-decalin was dissolved in 100 cc. anhydrous ether and 2.8 g of bromine was dropped under stirring and cooled with ice-water. After decolorization, ether was removed and 10 cc. of pyridine was added. The

5) *J. Chem. Soc.*, **1952**, 1441.
6) R.H. Martin and Robert Robinson, *J. Chem. Soc.*, **1943**, 491-7.

mixture was refluxed for 2 hrs. An unsaturated ketone (1.1 g.), bp. 65–85°/0.3 mm., n_D^{20} 1.5145–1.5300, was obtained. 2, 4-Dinitrophenylhydrazone, recrystallized from ethanol, was dark red and melted at 189°.

Summary

2-oxo-1, 10-dimethyl-decalin (VIII) was synthesized from (I), according to the following course, (I)→(II)→(VII)→(VIII). The sample obtained was the same as the one derived from the condensation product of 2-methyl-cyclohexanone and diethylamino-pentanone methiodide.

The writers wish to express their hearty thanks to Dr. Ryo Yamamoto for his stimulating interest in this work, and they are also indebted to Messrs. S. Takai, N. Nishimura, T. Sano and Miss. J. Kigami for the microanalyses.

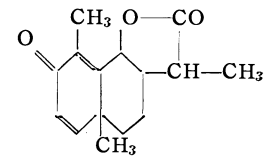
Sumitomo Chem. Co. Ltd, Osaka

Studies on Santonin. II. Experiments on the Synthesis of Santonin. Part II. Preparation of a Stereoisomeride of Santonin

By Masanao MATSUI, Katsuyuki TOKI, Seiichi KITAMURA, Yoshio SUZUKI and Michiko HAMURO

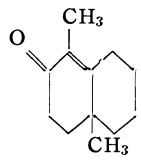
(Received July 22, 1953)

Since the structure (I) had been established for santonin by Clemo, Ruzicka and others[1-5] the synthesis of this compound was unsuccessful, despite of the efforts of several investigators[6][7][8]. Recently Abe, Harukawa, Ishikawa, Miki, Sumi and Toga in Japan[9][10] reported the success of the synthesis of one active and three racemic stereoisomerides of santonin, though the details of the investigations are not published. The present writers have also succeeded independently synthesizing by another route a stereoisomeride of santonin which differs probably from the isomerides obtained by Abe et al.

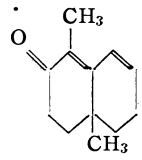


I

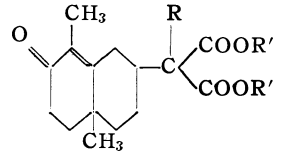
Gunstone and Heggie[11] showed the easy way to obtain 2, 3, 4, 5, 6, 10-hexahydro-2-oxo-1, 10-dimethyl-naphthalene (III) through 2, 3, 4, 5, 6, 7, 8, 10-octahydro-2-keto-1, 10-dimethyl-naphthalene (II) in a moderate yield. The writers found that alkyl malonates condensed with the dienone (III) on the 7-position in the presence of sodium methylate and produced



II



III

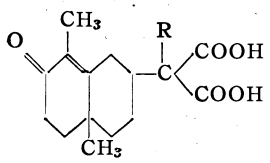


IV

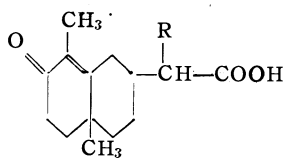
2, 3, 4, 5, 6, 7, 8, 10-octahydro-2-oxo-7-naphthyl-malonates (IV) in a moderate yield. Malonates generally condense with α,β-unsaturated carbonyl system C=C−C=O at the β-position; the condensation is widely known as Michael-condensation. But this condensation never occurs with the enone (II), because probably the β-position (9-position of naphthalene) is highly sterically hindered. On the contrary, malonates easily condense with dienone (III) at the δ-position (7-position of naphthalene). The position was confirmed by selenium-dehydrogenation of the compound obtained by hydrogenation of the condensation product of diethyl methylmalonate and (III) the compound obtained by selenium-dehydrogenation was identified with 1-methyl-7-ethyl-naphthalene by the mixed melting point determination of picrate, mp. 94°.

1) Clemo, Haworth, Walton, *J. Chem. Soc.*, **1929**, 2368; *ibid.* **1930**, 1110.
2) Clemo, Haworth, *ibid.* **1930**, 2579.
3) Ruzicka, Eichenberger, *Helv. Chim. Acta.*, **13**, 1117.
4) Tshitschibabin, Schtschukina, *Ber.* **63**, 2793.
5) Wedekind, Tettweiler, *Ber.* **64**, 387; *ibid.* **64**, 1117.
6) Paranjape, Phalnikar, Bhide, Nargrund, Rasayanam **1**, 233 (1943); *C. A.* **38**, 4266 (1944). (Note: They reported the synthesis of santonin, but none has succeeded to check it.)
7) Gunstone, Heggie, *J. Chem. Soc.*, **1952**, 1354, 1437.
8) Clemo, McQuillin, *ibid.* **1952**, 3835, 3839.
9) *Japan Acad.*, **28**, 425 (1952).
10) *ibid.* **29**, 113 (1953).
11) *J. Chem. Soc.*, **1952**, 1440.

Dicarboxylic acids (V) were obtained by alkaline hydrolysis of esters (IV), and divided into a crystalline substance and a semisolid oil. Acids (V) were changed by decarboxylation to monocarboxylic acids (VI) which were divided into crystal and semisolid oil.



V

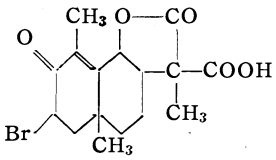


VI

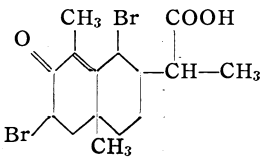
The melting point of (V), (VI) and 2, 4-dinitrophenyl-hydrazone was as follows:—

R	System	V	VI	2, 4-dinitro-phenyl-hydrazone
H	A	185°	145°	245°
	B	oil	135°	235°
CH_3	A	183°	125°	235°
	B	oil ?	oil ?	?

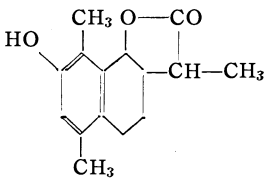
By bromination, crystalline forms of (V) and (VI) ($R=CH_3$) yielded bromolactone-carboxylic acid (VII) (mp. 176°) and dibromo-carboxylic acid (VIII), (mp. 146°) respectively. The constitution of these compounds was proved by analysis and sequent reactions.



VII



VIII



IX

They were dehydrobrominated by heating in an oil bath of about 170° with lutidine (In the case of (VII), decarboxylation also occurred) and produced the same santonin C*, a new isomeride of santonin, melting at 189—190°; λ_{max}^{EtOH}245 mμ(log ε=4.10). The melting point depressed to 138° when santonin C was admixed with an equal amount of natural santonin. The lactone is stable, never colorizes in the sun light, is easily soluble in chloroform and is able to be recrystallized from alcohol, etc. the attitude for various solvents resembling that of natural santonin.

When santonin C was treated with conc. hydrochloric acid, it yielded (±) β-desmotroposantonin (IX), melting at 231°, by dienone-phenol rearrangement, more easily than natural santonin. The desmotropo-santonin was identified by comparing with an authentic sample derived from natural santonin.

Experimental**

1. 2, 3, 4, 5, 6, 7, 8, 10-Octahydro-2-oxo-1, 10-dimethyl-naphthalene (II).[11]

2-Methylcyclohexanone (99 g.), sodamide (18.4 g.) and ether (150 cc.) were stirred for 2–4 hours at room temperature in a three necked flask protected with calcium chloride tube. (A stream of dry nitrogene is not necessary.) 1-Diethylaminopentan-3-one methiodide (135 g.) dissolved in methanol (50 cc.) was added gradually and stirring was continued for 4 hours. The mixture was left to stand overnight. Next day, the mixture was stirred for 2 hours at boiling point. The solution acidified with dil. hydrochloric acid, was extracted with ether. The ether extract was washed with 10% alkali carbonate solution, then with water, was dried, and the ether was distilled out. Octahydro-oxo-naphthalene (II), 45 g. (57%), thus obtained was light yellow oil, bp. 91–92°/0.5 mm. n_D^{29} 1.5217. 2, 4-dinitrophenylhydrazone was recrystallized from ethylacetate-methanol, scarlet plate: mp. 198-199°. (Found: C, 60.3; H, 6.5; N, 15.4%; Calcd. for $C_{18}H_{22}O_4N_4$: C, 60.3; H, 6.2; N, 15.6%.)

2. 2, 3, 4, 5, 6, 10-Hexahydro-2-oxo-1, 10-dimethyl-naphthalene (III).[11]

Dry powder of N-bromosuccinimide (79 g.) was added to a solution of (II) (79 g.) in carbon tetrachloride (200 cc.) and the mixture was refluxed for 30 minutes after the first vigorous reaction ceased. Remaining succinimide was removed from the cold solution. After the removal of the solvent, the residue was refluxed with pyridine (200 cc.) for 2 hours. Hexahydro-oxo-naphthalene (III) (58 g. 73%), bp. 92–96°/0.25 mm., n_D^{18} 1.5562, was obtained. Semicarbazone melted at 210–212° (from alcohol.)

* Since Abe et al. disignated their three isomerides, santonin A. B. and D. The writers named our sample santonin C.

** The melting point reported in this paper is uncorrected.

3. 2,3,4,5,6,7,8,10-Octahydro-2-oxo-1,10 dimethyl-7-naphthyl-malonic acid (V), (R=H).

Diethyl malonate (19 g.) and 10 g. of (III) were added with stirring to a solution of metalic sodium (1.3 g.) in methanol (15 cc.) at room temperature (20°). Stirring was continued for several hours and left to stand for 12–38 hours. The mixture was warmed at 50° with stirring for 2 hours. Acetic acid (5 cc.) was added to the cooled reaction mixture, then water was added, and the mixture was extracted with ether. The ether extract was washed with water and ether was distilled out. The fraction boiling at 160–185°/0.5 mm. (7 g.), which became a semisolid mass, was hydrolysed by refluxing with the solution of potassium hydroxide (7 g.) in aqueous methanol (45 cc.) for 2 hours. The reaction mixture was diluted with water and extracted with ether to remove neutral substances. An oil, alkali soluble, was obtained. It deposited crystals (2.0 g.), which were collected and washed with ether. This crystal is an isomeride of (V) (R=H), mp. 185° (with evolution of CO_2). (Found: C, 64.0; H, 6.8%, Calcd. for $C_{15}H_{20}O_5$; C, 64.3; H, 7.1%.) The mother liquor contains another isomeride of (V), (R=H).

4. 2,3,4,5,6,7,8,10-Octahydro-2-oxo-1,10-dimethyl-7-naphthyl-acetic acid (R=H).

I) *Acid A*:—The Above mentioned crystalline octahydro-oxo-dimethyl-naphthyl-malonic acid (2.0 g.) was distilled under reduced pressure in an oil bath held at 220°. The whole material distilled at ca. 190°/0.5 mm. and soon crystallized, mp. 144–145° (from ether). (Found: C, 71.2; H, 8.7%; Calcd. for $C_{14}H_{20}O_3$: C, 71.2; H, 8.5%.) 2,4-dinitrophenylhydrazone was scarlet crystal, mp. 244–245° (from acetic acid and methanol). (Found: C, 57.8; H, 5.6; N, 13.5; Calcd. for $C_{20}H_{24}O_6N_4$: C, 57.8; H, 5·8; N, 13.5%).

II) *Acid B*:—Mother liquor of crystalline octahydro-oxo-dimethyl-naphthyl-malonic acid (V) described in 3. was distilled in the same manner as the case of acid A and 2 g. of semisolid mass was obtained. It was dissolved in ether. When the ether solution was concentrated, crystals (1.5 g.) were obtained; mp. 135° (from methanol). (Found: C, 71.5; H, 8.1%; Calcd. for $C_{14}H_{20}O_3$: C, 71.2; H, 8.5%.) 2,4-dinitrophenyl-hydrazone was scarlet crystal, mp. 235° (from acetic acid and methanol) (Found: C, 56.8; H, 6.5; N, 13.2 %; Calcd. for $C_{20}H_{24}O_6N_4$: C, 57.8; H, 5.8; N, 13.5%).

5. α-(2,3,4,5,6,7,8,10-Octahydro-2-oxo-1,10-dimethyl-7-naphthyl)-α-methyl-malonic acid (V), (R=CH_3).

Diethyl methylmalonate (20 g.), hexahydro-oxo-naphthalene (III) (10 g.), sodium (1.3 g.) and methanol (15 cc.) were used. The processes were the same as in the case of 3. The product, distilled at 170–190°/0.3 mm., 8.5 g. was hydrolysed by using potassium hydroxide (8 g.) and aqueous methanol (80 cc.) From alkali soluble material obtained, crystals (2.8 g.) melting at 181–183° (when quickly heated, under the evolution of CO_2), recrystallized from methanol, were obtained. The weight of mother liquor was 2.8 g. The crystal is an isomeride of (V), (R=CH_3). (Found: C, 65.8; H, 7.7%; Calcd. for $C_{16}H_{22}O_5$: C, 65.4; H, 7.5%).

6. α-(2, 3, 4, 5, 6, 7, 8, 10-Octahydro-2-oxo-1, 10-dimethyl-7-naphthyl) propionic acid (VI) (R=CH_3).

(VI) (R=CH_3) was obtained as a crystal mass by decarboxylation which occurred at distillation of crystalline naphthyl-methyl-malonic acid (V) (R=CH_3) (2.8 g.), bp. 180–185°/0.3 mm. The crystal of naphthyl propionic acid (1.9 g.) melted at 125° after recrystallization from ether. (Found: C, 72.3; H, 9.0%; Calcd. for $C_{15}H_{22}O_3$: C, 72.0; H, 8.8%.) 2,4-Dinitrophenylhydrazone was scarlet crystal, mp. 234–235° (from ethyl acetate-methanol) (Found: C, 57.2; H, 6.0; N, 13.1%; Calcd. for $C_{21}H_{26}O_6N_4$: C, 58.7; H, 6.0; N, 13.0%).

Dehydrogenation. Naphthyl-propionic acid mentioned above (1 g.) was hydrogenated in 20 cc. of acetic acid with Adams' platinum oxide (2 mol. of hydrogen was absorbed). The hydrogenated product was treated with selenium (4 g.) at 320° for 18 hours. The neutral product obtained by this treatment was distilled with sodium and converted directly into the picrate, golden yellow needles, mp. 94° (recrystallized from alcohol). Its melting point was underpressed on admixture with 7-ethyl-1-methyl-naphthalene picrate prepared by analogous treatment from natural santonin.

The mother liquor of (V), (R=CH_3) in the case of 5. was also distilled, and semisolid monocarboxylic acid (mixture ?) (2 g., after purification by dissolving in potassium carbonate solution) which did not crystallize, was obtained. 2, 4-Dinitrophenylhydrazone were obtained in two forms, one scarlet crystal, melted at ca. 220° and one ca. 195°. The one having higher melting point seems to be that of crystalline acid, mp. 125°, above mentioned, but both of them seem not pure. The semisolid carboxylic acid was also dehydrogenated by selenium after hydrogenation and 7-ethyl-1-methyl-naphthalene picrate, mp. 94°, was also obtained.

7. Santonin C

i) Octahydro-oxo-naphthyl-methyl-malonic acid V (R=CH_3), mp. 183°, (5 g.) was dissolved in 50 cc. of acetic acid under slight heating, and bromine (5.5 g.) dissolved in acetic acid (5 cc.) was added gradually. Bromine was soon decolorized and evolution of HBr occurred. The mixture was poured into 100 cc. of ice water. A crystal (2 g.) separated, was collected and washed with ether. It was bromolactone carboxylic acid (VII) mp. 176°. (Found: C, 50.0; H, 5.3%; Calcd. for $C_{16}H_{21}O_5Br$: C, 51.5; H, 5.6%).

The bromolactone carfoxylic acid (2 g.) and lutidine (10 cc.) were heated at 170° in an oil bath for 2 hours. The mixture was poured into ice water and dil. hydrochloric acid was added. The mixture was extracted with ether and the extract was washed with 10% alkali carbonate solution and then with water. The ether solution was concentrated by evaporation. Crystals separated were collected and recrystallized from ethanol with small amount of active carbon. Rhombic plate (0.4 g.) mp. 189–190°, easily soluble in chloroform, was obtained;

λ_{max}^{EtOH} 245 mμ (log ε=4.10) (Found: C, 73.3; H, 7.2%, Calcd. for $C_{15}H_{18}O_3$: C, 73.2; H, 7.3%). It was stable in sun light and never colorized.

ii) Octahydro-oxo-naphthyl-propionic acid (VI), (R=CH_3), mp. 125° (1.5 g.) was dissolved in chloroform (12 cc.) and bromine (2.0 g.) was added under stirring in the sun light. After decolorization of bromine, dry air was passed through the solution and chloroform was removed together with hydrogen bromide. A small amount of ether was added and crystals (0.8 g) separated were collected and washed with ether. It was (VIII), mp. 145–146°. (Found: C, 44.9; H, 5.3%; Calcd. for $C_{15}H_{20}O_3Br_2$: C, 44.2; H, 4.9%).

The dibromo-compound (0.8 g.) and lutidine (5 cc.) were heated in an oil bath held at 170° for 1 hour and by the same treatment as i), rhombic plate crystal of santonin C, mp. 189–190° (0.1 g.) was obtained.

Santonin C was obtained by the same treatment from crude bromolactone carboxylic acid or dibromocarboxylic acid from which crystals had not been separated.

Mother liquor of naphthyl-methyl-malonic acid and monocarboxylic acid derived from it also yielded santonin C, though the yield was small.

8. Dienone-phenol Rearrangement of Santonin C.

Santonin C (100 mg.) was mixed with 1 cc. of conc. hydrochloric acid. The crystals gradually dissolved and soon different crystals, needles ((±)β-desmotroposantonin) were deposited. The sample, recrystallized from methanol, mp. 231°, which was undepressed on admixture with authentic (±)β desmotroposantonin obtained from natural santonin. (Found: C, 73.5; H, 7.2%; Calcd. for $C_{15}H_{18}O_3$: C, 73.2; H, 7.3%).

Summary

A new isomeride of santonin, santonin C, was synthesized. The route consists of condensation of 2, 3, 4, 5, 6, 10-hexahydro-2-oxo-1, 10-dimethyl-naphthalene and diethyl methylmalonate, hydrolysis, bromination and dehydrobromination by lutidine.

The writers wish to express their grateful acknowledgement to Dr. Ryo Yamamoto for his stimulating interest in this work. They are also indebted to Messrs. S. Takai, N. Nishimura and Miss J. Kigami for the microanalyses and to Messrs. N. Ohi and M. Isaoka for the determination of ultraviolet absorption.

Sumitomo Chem. Co. Ltd., Osaka

Emploi du péroxyde d'argent dans le dosage volumétrique et colorimétrique du vanadium[1]

Motoharu TANAKA

(Reçu le 4, Août, 1953)

Introduction

D'études précédentes[2] nous avons conclu que le péroxyde d'argent est un oxydant énergique du manganèse et du chrome. En conséquence nous sommes conduits à lui reconnaître la même propriété dans le dosage volumétrique et colorimétrique du vanadium. Pour cette dernière expérience, on a employé jusqu'à nos jours, le persulfate,[3] l'acide perchlorique,[4] le bromate,[5] et le permanganate.[6] Notre présent travail voudrait ajouter à ces réactifs le péroxyde d'argent.

Dosage Volumétrique du Vanadium

Deux méthodes sont en vigueur pour le dosage volumétrique du vanadium. Dans l'une[7] le gaz sulfureux réduit le vanadium en quadrivalent. Bien que cette méthode aboutisse à d'excellents résultats, elle nous oblige à chasser l'excès de ce gaz par une opération ennuyeuse. Dans l'autre méthode le vanadium est oxydé en quinquivalent par les réactifs mentionnés plus haut.

Il y a longtemps que la séparation éléctrolytique[8] du vanadium d'avec le chrome est faite par l'emploi du cathode de mercure, qui nous donne le vanadium quadrivalent. Cette liqueur éléctrolysée peut être convenablement oxydée par le péroxyde d'argent.

1) Ce rapport a déjà été présenté au "Symposium" de chimie analytique de la Société chimique et de la Société analyticochimique du Japon qui s'est tenu à Tokio, au mois de Mai, 1953.

2) M. Tanaka, This Bulletin **23**, 165 (1950); ibid., **26**, 299 (1953); *J. Chem. Soc. Japan, Section de la chimie pure*, **72**, 29 (1951).

3) R.F. Goddn et D.N. Hume, *Anal. Chem.*, **22**, 1314 (1950); H.H. Willard et P. Young, *Ind. Eng. Chem.*, **20**, 769 (1928).

4) T.D. Parks et E.J. Agazzi, *Anal. Chem.*, **22**, 1179 (1950).

5) I.M. Kolthoff et E.B. Sandell, *Ind. Eng. Chem.*, Anal. Ed., **2**, 140 (1930).

6) B. Bagshave et al., *J. Iron Steel Inst.* (London) **170**, 343 (1952).

7) W.F. Hillebrand et al., Applied Inorganic Analysis, pp. 456-9 (1952).

8) W.F. Hillebrand et al., op. cit., pp. 138-141.

Réactifs Nécessaires

1° Péroxyde d'argent (en suspension dans l'eau distillée).
2° Acide sulfurique.
3° Solution titrée de permanganate de potassium.
4° Solution titrée de sulfate ferreux.
5° Solution d'o-phénanthroline à 0,2%.

Mode Opératoire

1° Absence de chrome et de manganèse.

On dissout dans l'acide sulfurique étendu (1 : 20) un échantillon comprenant 0.5~10 mgr. de vanadium. Après la dissolution complète, on filtre la portion non dissoute. A la liqueur filtrée mélanger de l'eau oxygénée, dont l'excès est subséquemment détruit par ébullition. Refroidir à la température ordinaire et y ajouter du péroxyde d'argent. Chauffer au bain-marie pendant deux minutes. Après disparition de l'oxydant, soumettre à nouveau à la température ordinaire. On y verse alors un excès de sulfate ferreux et 0,5 cc. de solution d'o-phénanthroline. On titre avec le permanganate de potassium jusqu'à la disparition de la teinte rose du complexe fer(II)-phénanthroline. 1 cc de solution centinormale de permanganate correspond à 0,5095 mgr. de vanadium.

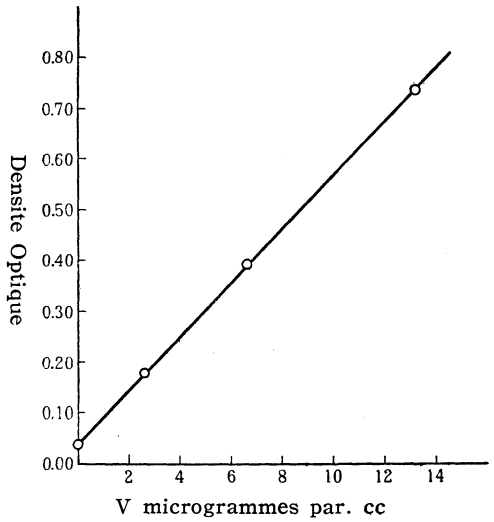
2° Présence de chrome.

Après la dissolution d'un échantillon, on sépare le vanadium d'avec le chrome par l'électrolyse en employant le cathode de mercure. A l'aide du péroxyde d'argent on oxyde ensuite la liqueur électrolysée et on opère suivant le procédé donné plus haut.

3° Présence de manganèse.

S'il existe du manganèse, il est oxydé par le péroxyde d'argent pour former le permanganate. Mais celui-ci est réduit facilement par addition d'une solution de sulfate ferreux jusqu'à disparition de la teinte rose du permanganate.

Fig. 1
Courbe d'étalonnage
Longueur d'onde : 410 mμ
Epaisseur de cuvette : 13,06 mm



Autre procédé pour séparer le manganèse d'avec le vanadium : faire précipiter ce dernier avec le fer ferreux par emploi de bicarbonate de sodium[9], ou encore, par une opération analogue à celle du chrome séparer par l'électrolyse le vanadium d'avec le manganèse, dont il reste cependant des traces dans la solution électrolysée.

Exactitude de la Méthode.

Nous avons répété les titrages sur diverses quantités de vanadium. Ces expériences nous montrent que l'on peut doser la teneur en vanadium avec un écart absolu inférieur à 0,01 mgr. Le tableau I reproduit les résultats.

TABLEAU I

EXACTITUDE DE LA MÉTHODE VOLUMÉTRIQUE

V présent (mg.)	V trouvé (mg.)	Écart absolu (mg.)
0,64	0,66	+0,02
„	0,66	+0,02
„	0,65	+0,01
1,12	1,12	±0
„	1,12	±0
„	1,13	+0,01
1,60	1,60	±0
„	1,59	−0,01
„	1,59	−0,01
3,20	3,20	±0
„	3,20	±0
„	3,21	+0,01
4,80	4,80	±0
„	4,81	+0,01
„	4,81	+0,01

Exemples d'Analyse

Nous donnons ci-dessous les résultats d'analyse des aciers. Pour établir leurs teneurs en vanadium nous avons utilisé la méthode de réduction par gaz sulfureux. Si nous comparons les résultats des deux méthodes, nous sommes frappés par leur coincidence. C'est dire en d'autres termes que le procédé par le péroxyde d'argent que nous avons proposé peut être employé avec succès dans le dosage volumétrique du vanadium.

TABLEAU II

EXEMPLES D'ANALYSE DE LA MÉTHODE VOLUMÉTRIQUE

Échantillons	V trouvé (%)	
	Méthode par le péroxyde d'argent	Méthode employant le gaz sulfureux
Acier	2,52	2,30
„	4,30	4,39
„	4,73	4,72
Ferrovanadium	45,82	45,82
„	45,88	„

9) W.W. Scott, Standard Methods of Chemical Analysis, 5th Ed., p. 1458 (1939).

Dosage Colorimétrique du Vanadium

Pour estimer colorimétriquement la teneur en vanadium on emploie généralement les trois méthodes suivantes;

1°[10] Extraction de l'oxinate de vanadium par l'alcool amylique,

2°[11] Méthode par l'eau oxygénée formant un composé pervanadique,

3°[12] Méthode de E.B. Sandell qui s'appuie sur la coloration du phosphotungstovanadate. Cette dernière est préférée pour deux raisons: peu d'éléments font obstacle au dosage; et par ailleurs la loi de Beer se verifie dans une très grande étendue de la concentration. L'emploi de cette méthode nécessite l'oxydation du vanadium en quinquivalent. Cette oxydation est faite avec succès par le péroxyde d'argent.

Réactifs Nécessaires.

1° Péroxyde d'argent (en suspension dans l'eau distillée).
2° Acide phosphorique, G.P.
3° Acide sulfurique, G.P.
4° Tungstate de sodium à 5 M.
5° Solution d'acide oxalique à environ décinormale.

Mode Opératoire.

A une solution froide (2～3 N d'acide sulfurique) ajouter du péroxyde d'argent et chauffer ensuite au bain-marie pour détruire son excés. Si on y observe une teinte rose due à la présence du manganèse, la décolorer par des gouttes de solution d'acide oxalique. Refroidir à la température ordinaire et diviser la solution en deux parts égales. L'une sera utilisée comme référence. A chaque 10 cc de l'autre, verser 1 cc d'acide phosphorique (1:2) et 0,5 cc de tungstate de sodium. En suite faire bouillir cette dernière solution pendant quelques minutes; comparer la coloration après refroidissement.

Influence des Éléments Étrangers.

Les éléments suivants formant les composés peu solubles sont à écarter[12];

K, Ammonium, Ti, Zr, Bi, Sb, Sn.

Cependant si on n'observe qu'une petite quantité de précipité, la filtration simple nous amène à un résultat satisfaisant. L'introduction de l'argent ne gêne pas ce dosage. Si le chlorure d'argent se produit, on peut facilement le rendre soluble par addition du sulfate mercurique[13].

Exactitude de la Méthode.

En employant une solution de vanadium quadrivalent de concentration précédemment fixée par la méthode volumétrique, nous avons cherché à établir la relation entre la concentration et la densité optique (longueur d'onde, 410 mμ). La figure 1 nous montre cette relation. Nous avons aussi obtenu l'équation suivante à l'aide de la méthode des moindres carrés:

$$X=\frac{E-0,036}{0,0537}$$

X: concentration du vanadium (microgrames V par cc.)

E: densité optique (épaisseur de cuvette, 13,06 mm.)

Nous avons répété les dosages sur diverses quantités connues du vanadium quadrivalent. A l'aide de l'équation précédente nous arrivons aux résultats du tableau III.

TABLEAU III

EXACTITUDE DE LA MÉTHODE COLORIMÉTRIQUE

V. présent (mg.)	V. trouvé (mg.)	Ecart absolu (mg.)
0,000	<0,0005*	<0,0005*
0,066	0,066	±0
„	0,067	+0,001
„	0,067	+0,001
0,165	0,165	±0
„	0,166	+0,001
„	0,166	+0,001
0,330	0,326	−0,004
„	0,326	−0,004
„	0,323	−0,007

* Résultat de plusieurs expériences répétées.

La conclusion est que par la méthode proposée nous pouvons doser 0,00～0,20 mg. de vanadium avec un écart absolu de ±0,001 mg.

Exemples d'Analyse

Nous donnons di-dessous deux exemples d'analyse par cette méthode:

TABLEAU IV

ÉXEMPLES D'ANALYSE DE LA MÉTHODE COLORIMÉTRIQUE

Échantillons	V. trouvé (%)	
	Méthode par le péroxyde d'argent	Méthode employant le gaz sulfureux
Échantillon composé (Fe 100 mg., Cr 10 mg.	1,52	1,50
Acier au nickel et chrome	0,065	0,064

La coïncidence entre le résultat obtenu par le dosage volumétrique et celui par la colorimétrie est frappante.

Résumé

Nous proposons le péroxyde d'argent comme oxydant dans le dosage du vanadium. Ce réactif peut s'appliquer à la méthode soit volumétrique soit colorimétrique. Quand il existe en même temps diverses substances

10) J.M. Bach et R.A. Trelles, *Sol. obras. sanit. nacion Buenos Aires*, **5**, 127 (1941); E. Sudo, *J. Chem. Soc. Japan*, Section de la chimie pure, **72**, 817 (1951).
11) E.R. Wright et Mellon, *Ind. Eng. Chem.*, Anal. Ed., **9**, 375 (1937).
12) E.B. Sandell, Colorimetric Determination of Traces of Metals, pp. 607-9 (1950).
13) M. Tanaka, *J. Chem. Soc. Japan*, Section de la chimie pure, **72**, 136 (1951).

réductrices et le vanadium dont la valence est inconnue, le péroxyde d'argent peut oxyder tout le vanadium en quinquivalent. La puissance de ce réactif sera observée dans le cas suivants:

1° Quand on se sert de la cathode de mercure pour la séparation du vanadium d'avec le fer et le chrome.

2° Quand il existe du vanadium quadrivalent et quinquivalent et que l'on désire évaluer les deux séparément. C'est surtout dans le cas où l'on emploie la résine à ion-échange pour la séparation préliminaire de cet élément.[14]

3° Quand on coprécipite le vanadium avec l'hydroxyde ferreux.

Nous ne voulons pas manquer, en terminant, de remercier cordialement Monsieur le Professeur Sugawara qui nous a encouragé pendant cette recherche et Monsieur le Professeur Hirano qui a mis à notre disposition les échantillons nécéssaires.

Notre étude a été facilitée par le "Coleman's Model 14 Universal Spectrophotometer" donné à la Faculté des Sciences de l'Université de Nagoya par "Elizabeth Thompson Sciencé Fund", à qui nous offrons notre profonde gratitude.

Institut de Chimie, Faculté des Sciences,
Université de Nagoya

14) J.E. Salmon et H.R. Tieteze, *J. Chem. Soc.*, **1952**, 2324.

Studies on the Oxy-acid Phosphors. II. Vanadate Phosphors (Part 1)

By Yoshihide KOTERA and Tadao SEKINE

(Received August 19, 1953)

Introduction

Study of the vanadate phosphors was begun by R. Robl[1] who reported the emission of alkali-earth pyrovanadates. A. Schloemer,[2] W. A. Weyl[3] and L. Burns[4] studied the magnesium and zinc vanadates, but the details of their preparations, characteristics, etc. are unknown. We prepared the vanadate phosphors and measured their brightness and emission spectra.

Experiments and Results

Purification of Ammonium Metavanadate and Metallic Salts.

In the preparation of the phosphor, a chemically pure grade of commercial ammonium metavanadate was used as one of the starting materials. The ammonium metavanadate was dissolved in a dilute solution of caustic soda (ca. 5%) until it was saturated. By the addition of recrystallized ammonium chloride to this solution, ammonium metavanadate was crystallized out, and filtered. After this purification procedure was repeated once more, the product was used as one of the batch materials for the dry process. For the wet process, the aqueous solution of this product was used.

Other batch materials were used for the purified metallic carbonate, oxide or hydroxide for the dry process, and for the wet one the aqueous solution of the purified metalic chloride or sulfate. A chemically pure grade of commercial metallic salts was purified as follows. Calcium, strontium or barium chloride was dissolved in water, the impurities due to iron and other heavy metals were removed by the usual chemical methods. This purification procedure was repeated once more, and the filtrate was used for the wet process. The sodium carbonate solution, which was treated in almost the same way as the purification procedure described above, was added to the purified metallic salt solution and the precipitated carbonate thus obtained was used for the dry process. When metallic oxide was needed, the carbonate was heated. The purification of zinc or cadmium sulfate solution was carried out in almost the same way as the procedure described above, except that hydrogen sulfide was passed until a small amount of zinc or cadmium sulfide was precipitated, and that the metallic zinc or cadmium was added to remove the traces of heavy metals which might be present.

As to magnesium salt, magnesium sulfate solution was purified in the same manner. For the dry process, purified basic magnesium carbonate or Merck's unpurified magnesium oxide was employed.

The purity of these batch materials was tested spectroscopically and colorimetrically.

Mixing and Firing

In the wet process, each metallic salt solution was added to the ammonium vanadate solution, and the metallic oxide or carbonate was mixed to the precipitated metallic vanadate in the agate mortar. As for the dry one, crystal of ammonium vanadate was mixed well with the metallic oxide or carbonate in the dry state. The mixed batch was heated at 640°C. for 2 hours.

The firing was done in air in the electric furnace. Three weight percent of ammonium perchlorate was added before firing, because the rise of brightness was expected.[5]

Read before the Third Annual Meeting of the Chemical Society of Japan 1950. Report I was published in the *J. Chem. Soc. Japan Ind. Chem. Sect.*, **54**, 625 (1951). (in Japanese)

1) R. Robl, *Z. Angew. Chem.*, **39**, 608 (1926).
2) A. Schloemer, *J. prakt. Chem.*, **133**, 51 (1932).
3) W.A. Weyl, *U.S. Pat.* 2,322,265; *Ind. Eng. Chem.*, **34**, 1035 (1942).
4) L. Burns, *U.S. Pat.* 2,452, 518.
5) Y. Kotera and T. Sekine, *J. Chem. Soc. Japan, Ind. Chem. Sect.*, **54**, 625 (1951). (in Japanese)

TABLE I

THE COLOR OF EMISSION OF PYROVANADATE PHOSPHORS

	3650 Å	2537 Å	cathode-ray or X-ray	previous results
$Ca_2V_2O_7$	no luminescence	blue	no luminescence	red brown (U. V.)[1]*
$Sr_2V_2O_7$	yellowish green	blue	white	yellow (U.V.)[1]
$Ba_2V_2O_7$	bluish green	yellowish green	bluish green	yellow (U.V.)[1]
$Mg_2V_2O_7$	yellow	yellowish brown	orange	—— §
$Zn_2V_2O_7$	yellow	orange	yellow	yellow[3,4]
$Cd_2V_2O_7$	yellow	orange	yellow	——

A. Schloemer reported that calcium metavanadate emits the very weak luminescence of wine red color.[2]

§ A. Schloemer reported that magnesium metavanadate emits the green luminescence at-180°C.[2]

TABLE II

THE OPTIMUM MIXING RATIO OF PYROVANADATE PHOSPHORS

	Wet process (Metallic vanadate) : (MO or MCO_3)	Dry process (NH_4VO_3) : (MO or MCO_3)
$Ca_2V_2O_7$	10 : 1 (wt., CaO was used)	1 : 1.5 (mol., CaO was used)
$Sr_2V_2O_7$	10 : 1 (wt., $SrCO_3$)	1 : 1.25 (mol., $SrCO_3$)
$Ba_2V_2O_7$	10 : 1 (wt., BaO)	1 : 1.25 (mol., BaO)
$Mg_2V_2O_7$	2.5 : 1 (mol., MgO)	1 : 3.5 (mol., basic Mg carbonate)
$Zn_2V_2O_7$	1 : 1 (mol., ZnO)	1 : 2 (mol., ZnO)
$Cd_2V_2O_7$	1 : 1 (mol., $CdCO_3$)	——

TABLE III

THE RESULTS OF THE CHEMICAL ANALYSIS OF PYROVANADATE PHOSPHORS

	Experimental		Theoretical for $R_2V_2O_7$	
	V_2O_5	RO	V_2O_5	RO
Strontium pyrovanadate	36.4	56.0	46.74	53.26
Barium pyrovanadate	34.1	62.3	37.24	62.76
Zinc pyrovanadate	—	55.0	52.78	47.22

The Properties of Phosphors.

The colors of emissions of the heated products were listed in TAB. I, and the optimum ratios of mixing, when excited by the 2537Å excitation, were shown in TAB. II. It is common that, when oxy-acid phosphors were prepared, the nonstoichiometric compound gives the brightest phosphor by the ultraviolet excitation, and the results obtained might be explained by this rule. Especially, magnesium pyrovanadate showed the brightest value, when prepared with a great excess of magnesium oxide. For the upper three in TAB. II, the precipitates have the form of pyrovanadate ($R_2V_2O_7$), while, for the lower three, metavanadate ($R(VO_3)_2$).[6] The phosphors would be in the pyrovanadate form, and the results of the chemical analysis of some products in TAB. III support this idea. For zinc pyrovanadate, the results in TAB. III were near to the theoretical value for $Zn_3V_2O_8$, which was reported by W. A. Weyl,[3] and contains 57.20% of ZnO, but we consider that the phosphor itself would be in the form of pyrovanadate, in which the excess of ZnO might be present as solid solution.

The emission spectra of some phosphors were shown in Fig. 1, no correction being made on the spectral sensitivity of the photographic plate, and, since their exposure times were not the same, their relative intensity can not be compared strictly. Their spectral range is fairly wide, and this property may be advantageous for practical uses. Further, the emissions of zinc and cadmium pyrovanadates are rather stronger than the others.

As zinc pyrovanadate seemed to be better from the standpoint of application, the preparation of zinc pyrovanadate was studied in detail.

The Preparation of Zinc Pyrovanadate Phosphors.

Both dry and wet processes were tried and the brightness of the samples produced was measured by the apparatus as illustrated in Fig. 2, under the excitation by a low-pressure mercury discharge lamp through the filter Corning No. 7-54, whose spectral transmission is shown in Fig. 3. The reflections from samples were calibrated by measuring the reflection from magnesium oxide, which shows no luminescence. The relative value of

6) J.W. Mellor, "A Comprehensive Treatise on Inorganic and Theoretical Chemistry" (1922) Vol. IX p. 768.

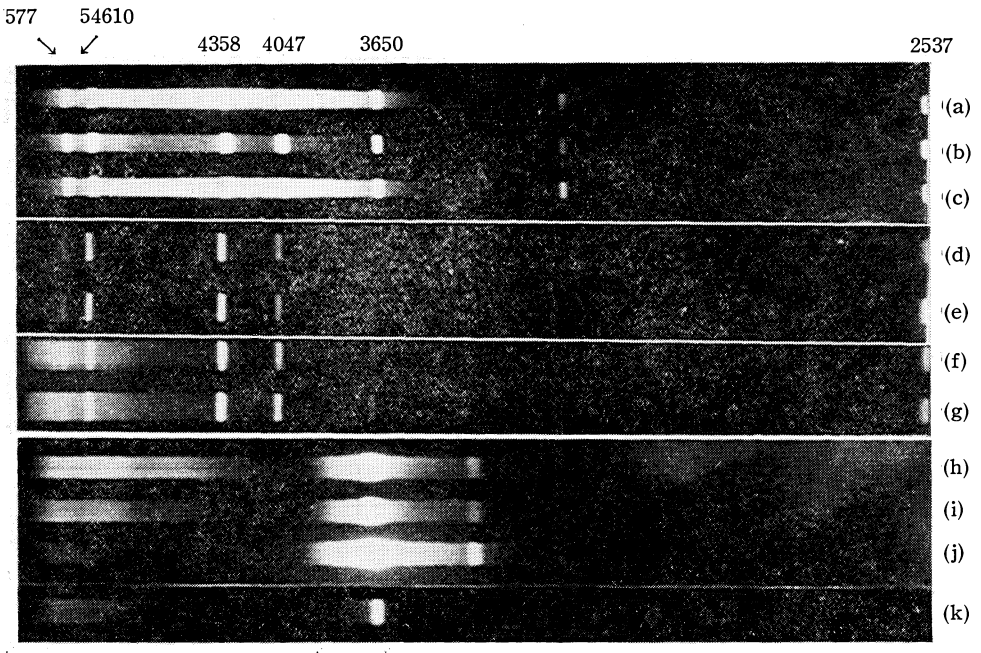


Fig. 1. The emission spectra of vanadate phosphors

(a) $Ca_2V_2O_7$, (b) $Ba_2V_2O_7$, (c) $Ca_2V_2O_7$, (d) $Sr_2V_2O_7$, (e) $Mg_2V_2O_7$, (f) $Zn_2V_2O_7$ (g) $Cd_2V_2O_7$ (h) $Ba_2V_2O_7$ (i) $Sr_2V_2O_7$ (j) $Mg_2V_2O_7$, (k) $Cd_2V_2O_7$

(a)—(g): excited by 2537Å

(h)—(k): excited by 3650Å

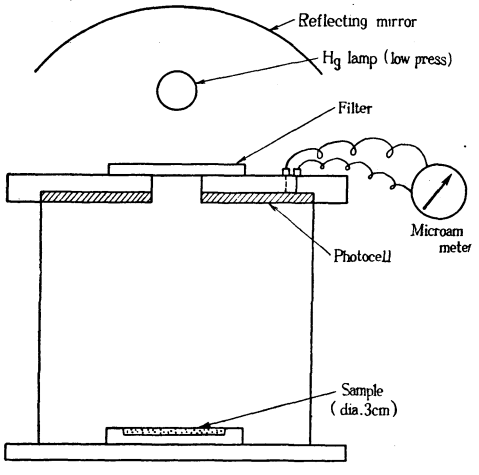


Fig. 2. The apparatus for the measurement of the relative brightness.

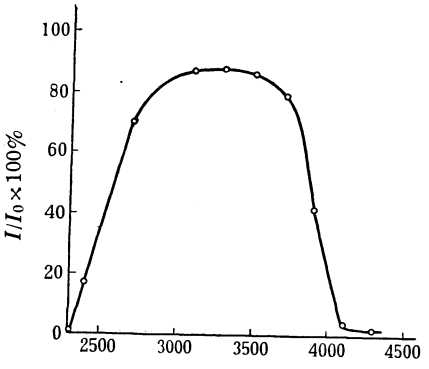


Fig. 3. The spectral transmission curve of the filter, Corning No. 7-54.

brightness was noted, the brightest sample being taken to be 10, while the value of commercial zinc beryllium silicate showed the value 17–20. In the dry process, purified ammonium vanadate and zinc carbonate were mixed well in the agate mortar, 1.2–3 folds of the latter being taken in the molar ratio, and fired 2 hours at 600°C. Results are listed in TAB. IV.

In the wet process, 2 parts of a 5% solution of purified ammonium vanadate were poured into 1 part of a 20% solution of purified zinc sulfate. In some cases alkali was added to the former, and in the other acid was added to the latter, and the effect of *p*H during the precipitation on the brightness of the fired samples was examined, 1 mol. of the precipated zinc metavanadate thus tobained was mixed with 1 mol. of purified zinc

oxide, then fired for 2 hours at 600°C. Results are shown in TAB. V.

TABLE IV

THE BRIGHTNESS OF ZINC PYROVANADATE PHOSPHORS IN DRY PROCESS

The molar ratio	brightness
$NH_4VO_3 : ZnCO_3 = 1 : 1.2$	2
$= 1 : 1.5$	3
$= 1 : 1.8$	9
$= 1 : 2.0$	9
$= 1 : 2.5$	7
$= 1 : 3.0$	6

TABLE V

THE BRIGHTNESS OF ZINC PYROVANADATE PHOSPHORS IN WET PROCESS

pH by the precipitation	brightness
ammonia alkali	9
neutral	10
acidic	9

The effects of adding some heavy metals to phosphors were investigated on the samples obtained by the wet process. Various amounts of heavy metals were added to the precipitate and the mixtures were fired in the same manner as described above. TAB. VI shows the change of

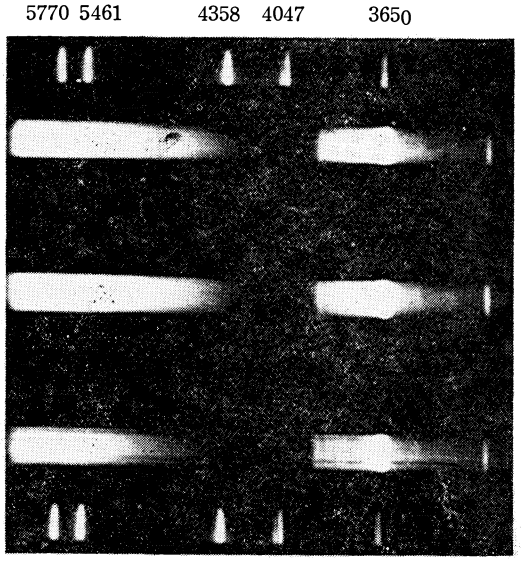


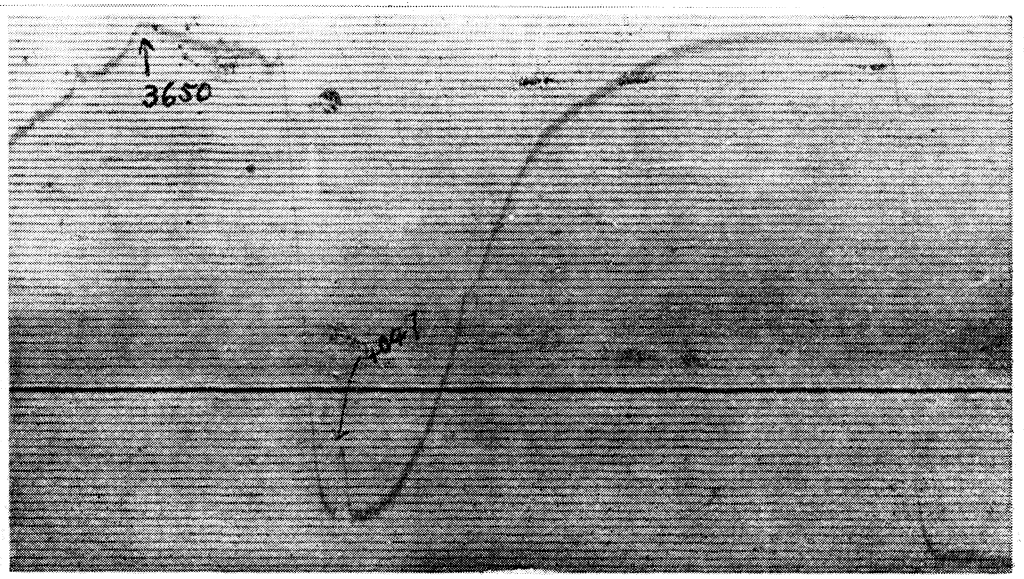
Fig. 4 The emission spectra of zinc pyrovanadate phosphors
Fig. 4—I. The emission spectra.
Fig. 4—II. The microphotometer curve
(a) $Zn_2V_2O_7$ Ag
(b) $Zn_2V_2O_7$ Pb
(c) $Zn_2V_2O_7$ Sn

TABLE VI

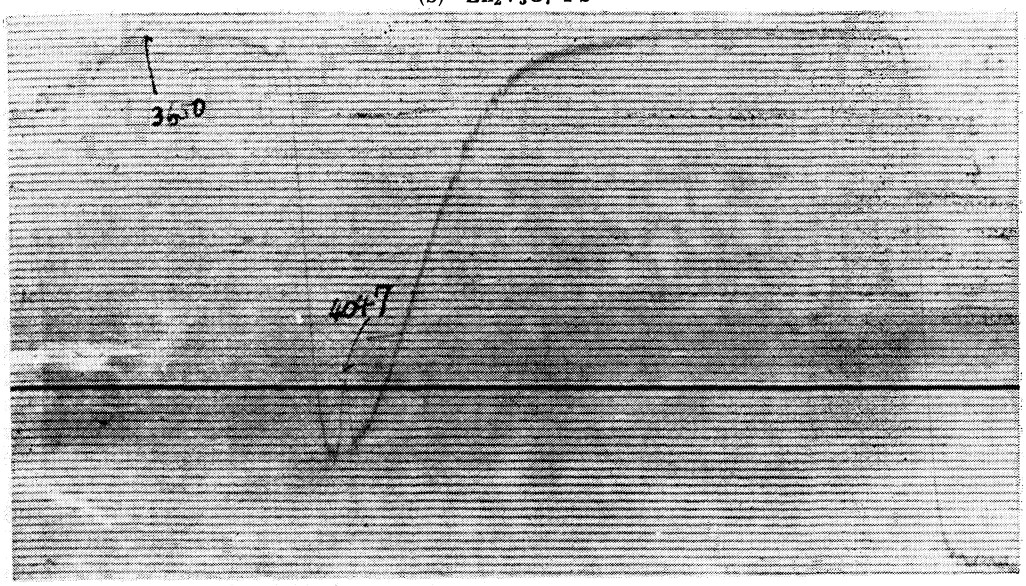
THE EFFECTS OF THE HEAVY METALS ON THE BRIGHTNESS OF ZINC PYROVANADETE

Concentration (mol %) Heavy metals	0.01	0.05	0.1	0.25	0.5	5
Ag	8	10	9	7	7	—
Cu	—	7	—	4	—	—
Pb	10	6	10	8	—	—
Bi	6	4	4	—	7	—
Mn	—	7	—	4	—	—
Sn	8	10	8	8	7	4
Ni	—	7	—	—	—	—
Ce	—	7	—	7	—	—

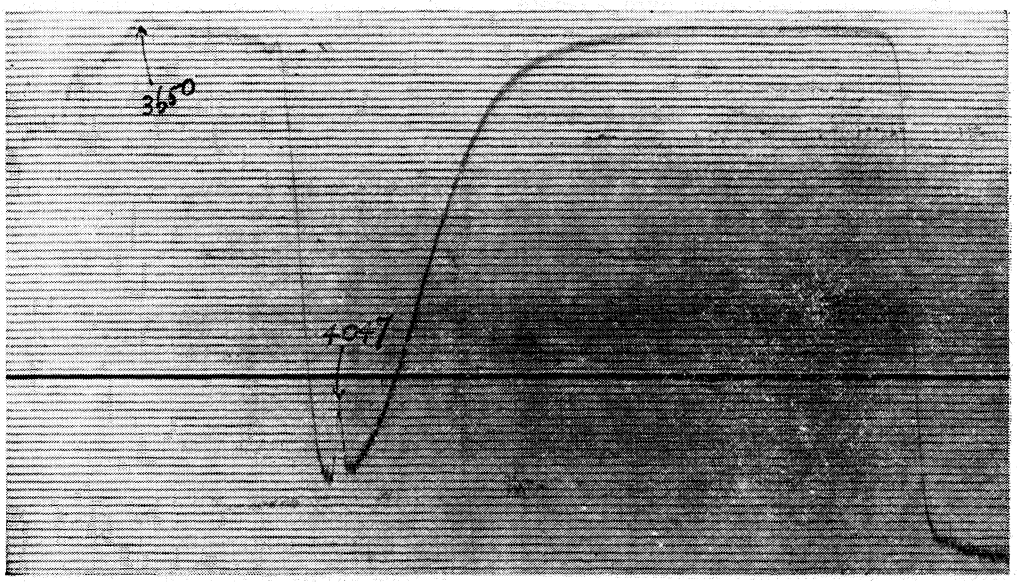
(a) $Zn_3V_2O_7$ Ag



(b) $Zn_2V_3O_7$ Pb



(c) $Zn_3V_2O_7$ Sn



← Deflection of Galvanometer

brightness, when the amounts of heavy metals were changed from 0.01 to 5 mol. % for 1 mol. zinc pyrovanadate. The emission spectra of some samples were shown in Fig. 4, no correction being made on the spectral sensitivity of the photographic plate.

These results indicate that the wet process gives somewhat better results than the wet one in the preparation of zinc pyrovanadate phosphors and the greatest brightness is about a half of that of commercial zinc beryllium silicate, and the heavy metals scarcely change the emission spectra but have the effect of intensifying the brightness.

Discussion

According to Robl, calcium, strontium and barium pyrovanadates show the emission of colors listed in Tab. I. These discrepancies of colors with our results are difficult to explain. As for calcium pyrovanadate, we could recognize its luminescence at 3500–5850Å only by the 2537Å excitation, and could not obtain such a calcium pyrovanadate as emits the red-brown luminescence under any kind of excitation method. Robl found the range of luminescence of strontium pyrovanadate to be 6000–4830Å and that of barium salt 6000–4570Å, while we recognized the luminescence at 4370–5830Å and 3900–5850Å respectively. Strontium pyrovanadate phosphor may be of use for the single white luminescent material

for the Braun tube, but its brightness is much lower than that of the current phosphors, and further studies of its preparation should be made.

We found that magnesium, zinc and cadmium pyrovanadates emit the luminescence whose characteristics are shown above. It is to be noted that magnesium pyrovanadate phosphor was prepared with a great excess of magnesium oxide, like the case of other oxy-acid phosphors, for example, tungstate phosphors. Zinc and cadmium pyrovanadate phosphors are excited both by 2537Å and 3650Å, and, if they are used in the fluorescent lamp, ultraviolet radiation from it will decrease, and this might be the reason why zinc pyrovanadate phosphor is used in the so-called nonactinic fluorescent lamp.[4] The wet process gives comparatively good results in the preparation of zinc pyrovanadate. The firing condition will be studied more precisely, for example, the atmosphere of the firing.

It is ascertained that zinc pyrovanadate shows a slight change of distribution of emission by the addition of heavy metals, and other pyrovanadate phosphors showed similar results. We conclude that the pyrovanadate salts belong to the phosphors of unactivated type similar to the tungstate phosphors. This conclusion is supported by other experiments, for example, by the measurements of the temperature dependence of the intensity of luminescence.[7] Their emission centers may be vanadium, or in precise expression, pyrovanadate radical.

Summary

The preparations and the measurements of the general characteristics of the pyrovanadate phosphors have been carried out. When excited by the ultraviolet, zinc pyrovanadate shows a relatively strong emission. Strontium pyrovanadate emits white color on irradiation by the cathode ray. Magnesium, calcium, barium, and cadmium salts show emission by the various methods of excitation. It has been suggested that pyrovanadate phosphors belong to the unactivated type similar to the tungstate phosphors.

The authors wish to thank Mr. Shigeo Shionoya for the measurements of spectral distribution of emission, Mr. Tetsutaro Hashimoto for the measurement of absorption of filter, and Mr. Hiromi Nishida and Mr. Shoji Makishima for the general discussion on the subject and the experimental work they had done.

Government Chemical Industrial Research Institute, Tokyo
Hatagaya, Tokyo

7) S. Makishima, J. Yamanouchi, T. Mukaibo, S. Shionoya: *Ann. Rep. Eng. Res. Institute*, University of Tokyo, 9, 33 (1951).

On Derivatives of α-Thujaplicin. II. On Nitroderivatives of α-Thujaplicin (o-Isopropyl-tropolone)[1]

By Kameji YAMANE and Shiro MOROSAWA

(Received August 25, 1953)

T. Nozoe and his collaborators[2] previously reported the occurence of hinokitiol and its isomer, α-thujaplicin (I) in the acidic constituents of the essential oil of Thujopsis dolabrata, Sieb. et Zucc. ("Hiba"-wood) produced in Aomori Prefecture in Japan. Again T. Nozoe et al.[3] reported on the derivatives of (I), halogen-, nitroso-, amino-derivatives of (I) and *p*-tolyl-azo-dye, etc. The present authors studied nitro-derivatives of (I) and their rearrangement products.

The authors carried out various mono- and di-nitration of (I) with nitric acid, nitrogen peroxide, cupric nitrate and benzoylnitrate. One kind of mononitro-α-thujaplicin m.p. 112–113° (II) and one kind of dinitro-α-thujaplicin 92–93° (III) are obtained. The separation of (III) from (II) is accomplished by adding aniline or *p*-toluidine to a benzene solution of the mixture of (II) and (III), to precipitate a yellow addition compound of (III). Decomposition of the addition compound with acid gives (III). The cupric nitrate method gives a better yield than any other nitration method: that is, the application of three molar equivalents of cupric nitrate to (I) in acetic acid yields (II) (42%) and (III) (21%), in the case of four molar equivalents of cupric nitrate, it yields (II) (30%) and (III) (24%). But when the mix-

1) This work was presented at the 6th Annual General Meeting of the Chemical Society of Japan in Kyoto, April 2, 1953.

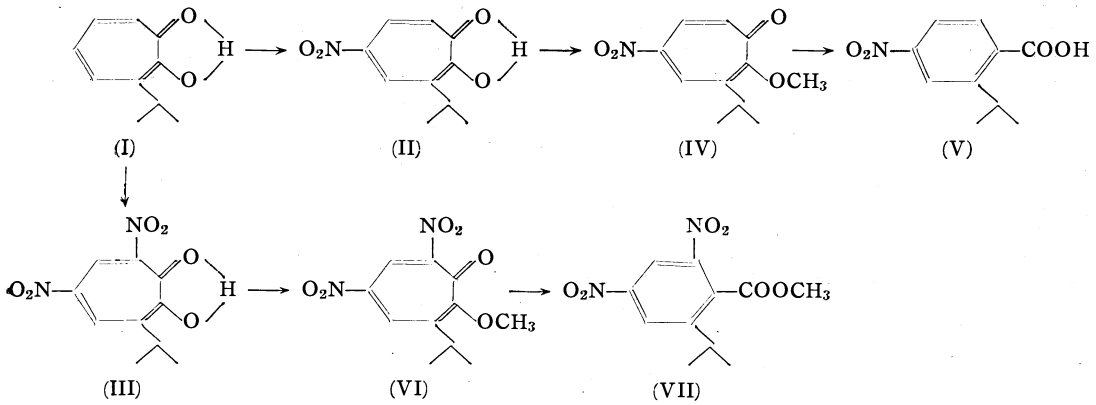
2) T. Nozoe, A. Yasue and K. Yamane, *Proc. Japan Acad.*, **27**, 15 (1951).

3) T. Nozoe, Y. Kitahara K. Yamane, and I. Ikemi, *ibid.*, **27**, 193 (1951).

ture of four molar equivalents of cupric nitrate and (I) in acetic acid is allowed to stand over for five days, (II) (55%) and (III) (14%) are obtained.

The existence of another kind of position isomer of (II) can be considered, but the attempt to find it out during the course of this study was a failure. Moreover, it is noticeable that (II) is unaffected by further nitration with cupric nitrate in an acetic acid solution.

Yellow needles, (II) do not give aniline and *p*-toluidine addition compound but produces a red coloration with ferric chloride. Potassium salt is red prisms, and sodium salt, orange-yellow needles. (II) absorbs three molar equivalents of hydrogen when hydrogenated in methanol with palladium-charcoal as a catalyst, giving amino-α-thujaplicin m.p. 172–173° in a good yield, which is the same substance as that previously obtained by T. Nozoe et al.[3], by the catalytic reduction of the nitroso-derivative and azo-dye of (I). (II) does not couple with the *p*-tolyl-diazonium compound. From these facts and investigations of the substitution reaction of tropolone, hinokitiol and other tropoloides by T. Nozoe et al.[4], the nitro group in (II) is assumed to be at the *p*-position. Methylation of (II) with diazomethane in ether yields a mononitro-α-thujaplicin methylether m.p. 106.2–106.5° (IV) as yellow prisms in a 92% yield. When heated in methanol with sodium methoxide as a catalyst, (IV) undergoes the rearrangement to yield colorless needles m.p. 143–145° (V) in 86% yield, which is assumed to be a mononitro-*o*-cumic acid from the analytical value, the aromatization of other tropoloides and no coloration by ferric chloride characteristic to tropolone nucleus. The determination of the structure of (V) will be reported on the following paper. (V) gives anilide of m.p. 156–156.5°, and *p*-toluidide of m.p. 189°.



(III) forms yellow prisms m.p. 92–93°, which give a red coloration by ferric chloride characteristic to tropolone nucleus. (III) is soluble in 2N-potassium hydroxide and sodium hydroxide to give a red coloration, but it soon changes to yellow. (III) does not undergo any rearrangement when heated with alcohol, as dinitrohinokitiol[5] does. With aniline, (III) gives an addition compound of orange-yellow needles m.p. 120–122° (decomp.), which are slightly soluble in benzene. With *p*-toluidine, (III) gives also an addition compound of yellow needles m.p. 152–153° (decomp.), but it changes to orange-red crystals of m.p. 161–162° (decomp.) when left for a long time. *o*-Phenylendiamine addition compound forms yellow needles m.p. 155–156° (decomp.), and phenylhydrazine also gives an addition compound m.p. 104–106° in cold benzene, but does not give phenylhydrazone.

Methylation of (III) with diazomethane in an ethereal solution yields a dinitro-α-thujaplicin methylether m.p. 101–102° (VI) as faintly yellow prisms or needles. (VI) undergoes the rearrangement when heated in methanol with sodium methoxide as a catalyst to yield colorless needles m.p. 97–98° (VII) in a 61% yield, which do not show any coloration with ferric chloride. A trial to obtain the free acid by hydrolysis with 2N-sodium hydroxide without isolating the rearrangement product of (VI) gives colorless prisms m.p. 158–160°, which are assumed to be a mononitro-monohydroxy-*o*-cumic acid from the analytical value, but no detailed studies are made. From the investigations of substitution products of tropolone, hinokitiol and other tropoloides by T. Nozoe et al.[4,5], the nitro groups in (III) are assumed to be at the *o'*- and *p*-position. The determination of the structure of (VII) will be reported later.

Ultraviolet absorption spectra of nitro derivatives of (I) and their rearrangement products are shown in Fig. 1 and 2. (II), (III)

and (IV) have absorption maxima of 350–450 mμ characteristic to tropolone nucleus, while (V) and (VII) have not. It is noticeable that (VI) has also no maximum of 350–450 mμ.

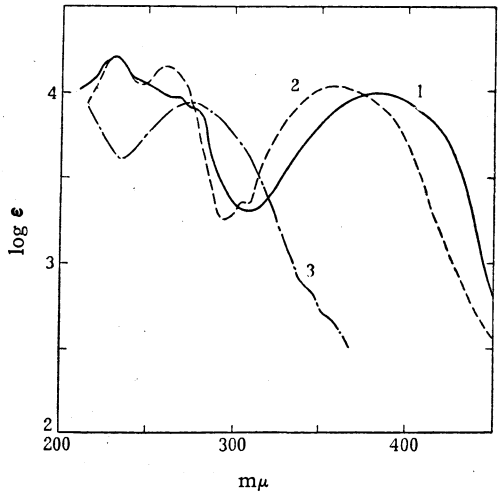


Fig. 1.—Ultraviolet spectra of mononitro-α-thujaplicin (II). (curve 1), mononitro-α-thujaplicin methyl ether (IV), (curve 2), mononitro-o-cumic acid (V), (curve 3) in methanol.

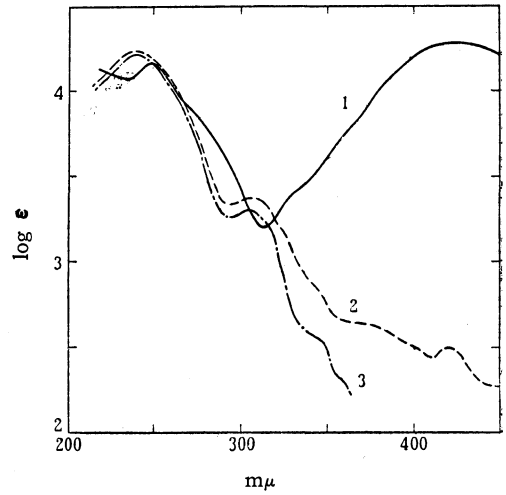


Fig. 2.—Ultraviolet spectra of dinitro-α-thujaplicin (III), (curve 1), dinitro-α-thujaplicin methyl ether (VI), curve 2), dinitro-o-cumic acid methyl ester (VII), curve 3) in methanol.

Experimental

Nitration of α-Thujaplicin (I).

(a) **With Nitric Acid.** 1). To a solution of 1.18 g. of α-thujaplicin (I) in 2 cc. of glacial acetic acid, 0.67g. of sp. gr. 1.42 (68%) nitric acid is added dropwise. The first drop is added at the room temperature, but the subsequent addition is made under ice-cooling during 20 minutes. After the completion of the addition, the mixture is stirred for an hour under ice-cooling, and 0.32g. of yellow crystal of m.p. 105–109° are gained. The recrystallization from benzene gives yellow prisms m.p. 112–113° (II), which give a red coloration with ferric chloride characteristic to tropolones but do not give a p-toluidine compound. Yield 20%. Found: C, 57.12; H, 4.82; N, 7.22, Calculated for $C_{10}H_{11}O_4N$: C, 57.41; H, 5.30; N, 6.69%. 2). To a solution of 1.06g. of (I) in 1 cc. of glacial acetic acid, 1.49 g. of sp. gr. 1.42 (68%) nitric acid is added dropwise. The first drop is added at the room temperature, but the subsequent addition is made under ice-cooling during 33 minutes. Yellow crystals begin to separate out after about 10 minutes from the beginning of dropping. After the completion of the addition, the mixture is stirred for an hour under ice-cooling, then the precipitate containing crystals is filtered, and dissolved in benzene and removed from the syrupy matter by decantation. 0.18 g. of (II) are obtained from the benzene solution. Yield 13%. To the filtrate of the precipitation 30 cc. of water is added and the mixture is extracted with benzene. The benzene solution is evaporated to a smaller volume, and aniline is added. Yield, 0.18 g. of an aniline addition compound of (III). Yield of (III), 6%. The recrystallization from benzene gives orange-yellow needles m.p. 118–120° (decomp.). Found: C, 55.38; H, 4.36; N, 11.96, Calculated for $C_{16}H_{16}O_6N_3$; C, 55.48; H, 4.67; N, 12.12%. The decomposition of the addition compound with acid yields (III). The recrystallization from benzene and petroleum ether gives yellow prisms m.p. 92.5–93° (III). Found: C, 47.49; H, 4.04; N, 11.12, Calculated for $C_{10}H_{10}O_6N_2$: C, 47.24; H, 3.96; N, 11.02%.

(b) **With Cupric Nitrate.** To a solution of 2.32 g. of cupric nitrate, $Cu(NO_3)_2 \cdot 3H_2O$, in 5 cc. of glacial acetic acid, a solution of 0.53 g. of (I) in 3 cc. of glacial acetic acid is added dropwise under ice-water-cooling with stirring, and the mixture is left over night in ice-water. To the mixture 25 cc. of water is added, and on standing for an hour, the cupric complex is precipitated. 0.63 g. of the cupric complex is obtained by the filtration, which is decomposed with hot 6N-hydrochloric acid, and extracted with benzene. The benzene solution is evaporated to a smaller volume, and p-toluidine is added, yielding an addition compound of (III.) The recrystallization from benzene gives yellow needles m.p. 152–153° (decomp.). Found: N, 12.21, Calculated for $C_{17}H_{19}O_6N_3$: N, 11.63%. The addition compound of p-toluidine changes to orange-red prisms m.p. 161–162° (decomp.) when left for a long time, and (III) is obtained from both by the decomposition with acid. 0.17 g. of (III) is gained. Yield 21%. From the filtrate of the p-toluidine addition compound of (III), 0.28 g. of (II) is gained. Yield 42%.

Amino-α-thujaplicin. A solution of 0.14 g. of (II) in 25 cc. of methanol is catalytically reduced

4) T. Nozoe, *Science of Drugs*, **3**, 174 (1949); *Sci. Rep. of Tōhoku Univ.*, (I), **34**, 199 (1950); T. Nozoe et al., *Proc. Japan Acad.*, **26**, 25, 33, 45 (1950); *ibid.*, **27**, 156, 190, 231, 565 (1951); *ibid.*, **28**, 483 (1952).

5) T. Nozoe, Y. Kitahara, K. Yamane and K. Yamaki, *Proc. Japan Acad.*, **26**, 14 (1950).

with 20 mg. of 5% palladium-charcoal at ordinary temperature and pressure, by which 44 cc. of hydrogen is absorbed. The removal of the catalyst followed by the distillation of methanol gives 0.17 g. of the residue. The recrystallization from benzene and petroleum ether gives yellow prisms, m.p. 172–173°, which do not show any depression of the melting point when fused with amino-α-thujaplicin obtained previously[3] by the catalytic reduction from nitroso-α-thujaplicin and *p*-tolyl-azo dye of (I).

Mononitro-α-thujaplicin Methyl Ether (IV). To a solution of 0.14 g. of (II) dissolved in a mixture of absolute methanol 5 cc. and absolute ether 10 cc., an etherial solution of diazomethane is added under ice-cooling until the mixture no longer gives a coloration with ferric chloride. The removal of the solvent gives 0.6 g. of crystal m.p. 87–99° by standing over in a vaccum desiccator. Yield 92%. The recrystallization from ether gives yellow prisms (IV) m.p. 105–106°. Found: C, 58.75; H, 5.66; N, 6.12, Calculated for $C_{11}H_{13}O_4N$: C, 59.18; H, 5.87; N, 6.77%.

Rearrangement of Mononitro-α-thujaplicin Methyl Ether (IV). A mixture of 70 mg. of (IV) in a methanolic solution of sodium methoxide, prepared from 20 mg. of sodium and 1.5 cc. of methanol, is refluxed for six hours. To this mixture is added 1 cc. of 2N-hydrochloric acid and the mixture is heated in a water bath for an hour, cooled and filtered. 60 mg. of colorless crystals m.p. 140.5–142.5° are obtained. The recrystallization from 50% alcohol gives colorless needles, m.p. 143–145° (V), which are assumed to be a mononitro-*o*-cumic acid, and does not show any coloration with ferric chloride. Yield 86%. Found: C, 57.86; H, 4.86; N, 6.57, Calculated for $C_{10}H_{11}O_4N$: C, 57.41; H, 5.30; N, 6.69%. Anilide of (V) forms colorless prisms m.p. 156–156.5° (from alcohol). Found: N, 9.99, Calculated for $C_{16}H_{16}O_3N_2$: N, 9.86%. *p*-Toluidide of (V) forms colorless needles m.p. 189°. Found: N, 9.40, Calculated for $C_{17}H_{18}O_3N_2$: N, 9.40%.

Addition Compounds of Dinitro-α-thujaplicin (III). Aniline and *p*-toluidine compounds are described above. *o*-Phenylendiamine addition compound forms orange-yellow fine needles, m.p. 155–156° (decomp.) (from alcohol). Found: C, 53.87; H, 4.94; N, 15.00, Calculated for $C_{16}H_{18}O_6N_4$: C, 53.03; H, 5.01; N, 15.41%. Phenylhydrazine addition compound is an orange yellow crystal m.p. 104–106° (decomp.).

Dinitro-α-thujaplicin Methyl Ether (VI). To a solution of 0.13 g. of (III) dissolved in a mixture of absolute methanol 2.4 cc. and absolute ether 7.2 cc., an etherial solution of diazomethane is added under ice-cooling until the mixture no longer gives a coloration with ferric chloride. The removal of the solvent gives 0.087 g. of crystal of (IV) by standing over in a vaccum desiccator. Yield 61%. The recrystallization from methanol gives pale yellow prisms or needles m.p. 99–100° (IV). Found: C, 48.78; H, 4.05; N, 10.17, Calculated for $C_{11}H_{12}O_6N_2$: C, 49.23; H, 4.51; N, 10.45%.

Rearrangement of Dinitro-α-thujaplicin Methyl Ether (VI). (a) A mixture of 48 mg. of (VI) in methanolic solution of sodium methoxide, prepared from 5 mg. of sodium and 1.5 cc. of methanol, is refluxed for six hours. The removal of the solvent gives 36 mg. of colorless scaly crystal m.p. 97–98° (VII). Yield 74%. This crystal is assumed to be a dinitro-*o*-cumic acid methyl ester (VII). Found: C, 49.51; H, 4.55; N, 10.29, Calculated for $C_{11}H_{12}O_6N_2$: C, 49.23; H, 4.51; N, 10.45%. (b) A mixture of 82 mg. of (VI) in a methanolic solution of sodium methoxide, prepared from 5 mg. of sodium and 1.5 cc. of methanol, is refluxed for six hours. After the removal of the solvent, 2 cc. of 2N-sodium hydroxide is added and warmed for two hours in a water bath to effect the hydrolysis. The acidification of the solution with 2N-hydrochloric acid, yields 60 mg. of colorless crystals m.p. 139–150°. The recrystallization from benzene gives colorless prisms m.p. 158–160.5°, which are assumed to be probably a mononitro-monohydroxy-*o*-cumic acid from the analytical value. Found: C, 52.44; H, 4.67; N, 6.79, Calculated for $C_{10}H_{11}O_5N$: C, 53.31; H, 4.92; N, 6.22%.

The authors take this opportunity to express their deep gratitude to Professor T. Nozoe (Tōhoku Univ.) and Professor A. Yokoo (Okayama Univ.) who have given kind guidance during the course of this study. The authors also express their deep gratitude to Takasago Chemical Industries Co. Ltd., for the donation of the essential oil of Hiba-wood, and to the Ministry of Education for their Grant in Aid for Scientific Research.

Department of Chemistry,
Faculty of Science, Okayama
University, Okayama

Photoconductivity of the Condensed Polynuclear Aromatic Compounds

Hiroo INOKUCHI

(Received August 29, 1953)

Introduction

In previous works, H. Akamatu and the present author have reported that violanthrone, isoviolanthrone and pyranthrone have photoconductivity and intrinsic semi-conductive characters.[1,2] Similar behaviour was found for the other related compounds, that is, the condensed polynuclear aromatic and aza-aromatic compounds.[3,4] For example, indanthrone black ($C_{34}H_{14}N_2O_2$) has the electrical resistivity of $2.5\times10^8\,\Omega$cm. and ovalene ($C_{32}H_{14}$) has $2.3\times10^{15}\,\Omega$cm. Such particular pure compounds as these have never been found as shown in Fig. 1 in measurings of the electrical conductivity of many sorts of compounds. And also, this group of compounds shows luminescent character by the actions of cathode-ray and ultra-violet light in the solid state.[5] These characters will be attributed to the intermolecular overlappings of the electron clouds of π-electrons in the polynuclear condensed aromatic rings.

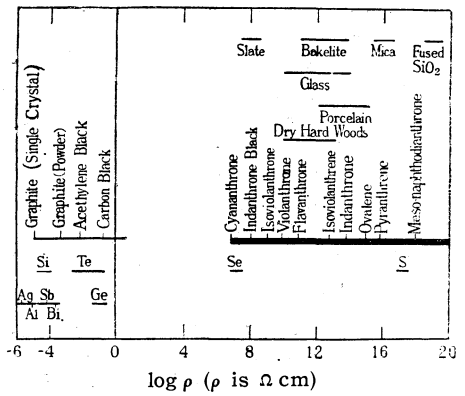


Fig. 1. The electrical resistivity diagram of substances.

Up to the present, the researches of semiconductors have been mostly restricted to the field of inorganic substances, thus these compounds occupy a new field in the branch of semi-conductive materials. We may call these organic compounds—*organic semi-conductors.*

Experimental Procedure

In these compounds, the photoconductivity of isoviolanthrone, violanthrone, isoviolanthrene, violanthrene, pyranthrone, pyranthrene, ovalene, flavanthrone, indanthrone and indanthrazine was measured. These materials have been purified chemically by the usual methods, and then sublimed *in vacuo* more than twice until the electrical conducitvity became constant[3)4)6)].

Excepts for violanthrone and isoviolanthrone, a photocell was made following the so-called "sandwich" type as illustrated in Fig. 2. The cells were formed by evaporating organic semi-conductors (1)* on a quartz plate (dimension is 1 mm × 10 mm × 50 mm) (2) which had been previously coated with a transparent aluminum conducting film (3). The second electrode (4) could be made by depositing a thin layer of aluminum by evaporation on the surface of the film of the organic substances. Further, both sides of this plate were painted with colloidal graphite (5), (6) as electrical terminals. Further details are shown in Fig. 2.

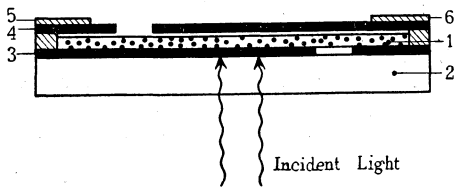


Fig. 2. "Sandwich" type photocell for photoconductivity measurements. (1) photoconductive organic semi-conductor, (2) quartz plate, (3) transparent aluminum electrical conducting film, (4) thin layer of aluminum as a second electrode, (5) & (6) colloidal graphite electrodes as electrical terminals.

For violanthrone and isoviolanthrone, the film of these compounds was deposited by vacuum evaporation between tin foils, 10 mm in width, which were stuck on a quartz plate, keeping the gap between them 1 mm.

The photoelectric current of the cells was produced by illumination of monochromatized light

1) H. Akamatu and H. Inokuchi, *J. Chem. Phys.*, **20**, 1431 (1952).
2) H. Akamatu and H. Inokuchi, *J. Chem. Phys.*, **18**, 810 (1950).
3) H. Inokuchi, This Bulletin, **24**, 222 (1951).
4) H. Inokuchi, This Bulletin, **25**, 28 (1952).
5) H. Akamatu, unpublished.
6) H. Akamatu and K. Nagamatsu, *J. Colloid Sci.*, **2**, 593 (1948).

* For example, violanthrene are sublimed, at 300°—350°, at 10^{-4} mm.Hg and pyranthrene, at 250°—300°, at 10^{-4} mm.Hg. Heats of sublimation of those are 52.3+2.1 kcal. mol. and 45.3+1.6 kcal. mol. respectively. Details of this problem were reported in this Bulletin, **25**, 299 (1952). H. Inokuchi, S. Siba, T. Handa and H. This Bulletin, **26**, 364 (1853).

from a 500 watts tungsten lamp, operating at a constant voltage of 75 volts.

These condensed aromatic compounds are typical molecular crystals and have no impurities, that is, they are intrinsic semi-conductors. Therefore, their physical properties don't change by further steps of sublimation. This character is very advantageous for the measurement of photoconductivity compared with inorganic semi-conductors, such as Sb_2S_3 and CdS.

The optical absorption of solid state was observed by the LiF monochrometer. In this experiment, the organic substances were evaporated on a quartz plate or a glass one, as a thin layer, which had from 10 to 100 micron thickness.

Results and Discussions

Gudden and Pohl have described in their famous works[7], that a photoelectric current is separated into two types, viz., primary current and secondary current. The former is a motion of charges, electrons and holes, released throughout the illuminated volume by the action of photoelectrons and the latter is introduced with the contribution of the lowering of electronic barriers by the primary current, thus permitting the flow of additional electrons.

The photoelectric current observed here is proportional to the intensity of the incident light as shown in Fig. 3. This character is one of the most distinct properties of a primary current. Then, it may be reasonable to say that the observed photocurrent in this experiment is a primary current.

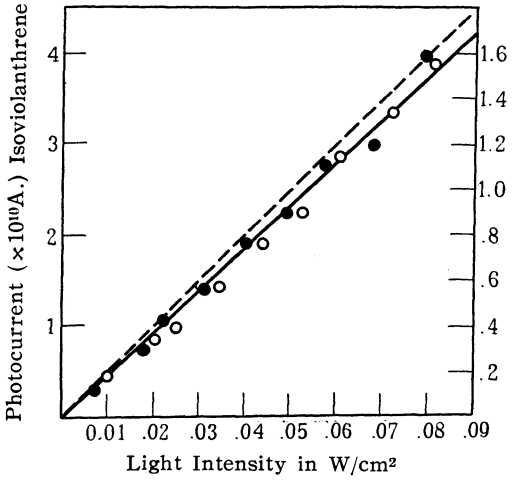


Fig. 3. Photoelectric current as a function of the intensity of illumination for ovalene photocell (—○—○—) and isoviolanthrene photocell (—●— - —●—) at 270 V. potential difference across these layers.

When "isoviolanthrene photocell" was illuminated by the white light (0.055 W./cm.²), the photoelectric current of this cell was changed with applied potential across the isoviolanthrene layer as shown in Fig. 4. When the thickness of film was from 50 up to 100 micron, then a 10^2 V. potential difference across the layer corresponded to 10^4 V./cm. This character was similar to the amorphous selenium film[8]. The photoelectric current increased nearly linearly with applied voltage and didn't indicate any saturation

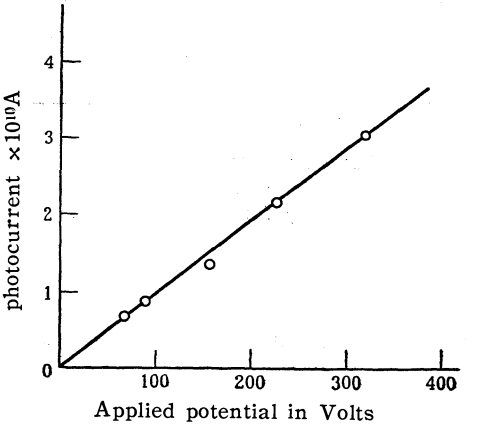


Fig. 4. Photoelectric current plotted against the Voltages applied across the isoviolanthrene photocell for the illumination of the white light (0.055 W./cm.²).

at the possible high voltage (270 V.). The ordinary semi-conductors, such as ZnS, have a saturated photocurrent at 10^3 V./cm[9].

The photocells of ten organic substances, described already, were made and the photoelectric current at 270 V. potential difference across these organic semi-conductive layers, which was illuminated at $10^{-3}-10^{-4}$ W./cm.² intensity monochromatized light, was measured. The spectral response of photoelectric current is shown in Fig. 5-7.

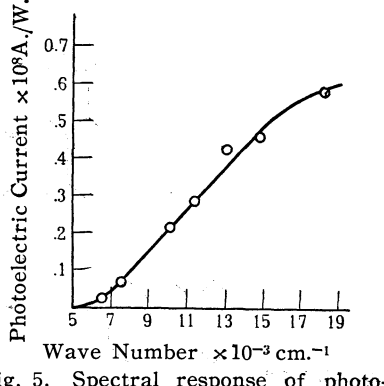


Fig. 5. Spectral response of photoconductivity for the flavanthrone photocell.

7) B. Gudden, "Lichtelektrische Erscheinungen," Julius Springer, Berlin, 1928.

8) P. K. Weimer and A. D. Cope, *R. C. A. Rev.*, **12**, 314 (1951).

9) B. Gudden and R. Pohl, *Z. f. Phys.*, **17**, 331 (1923).

The photocurrent decreased as the wavelength of the incident light increased in each case, and the threshold was found. The value of light quantum in e.V. at each threshold is illustrated in TABLE I.

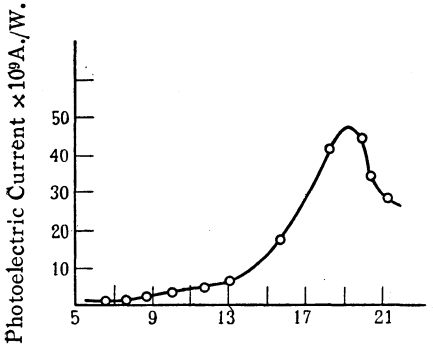


Fig. 6. Spectral response of photoconductivity for the isoviolanthrene photocell.

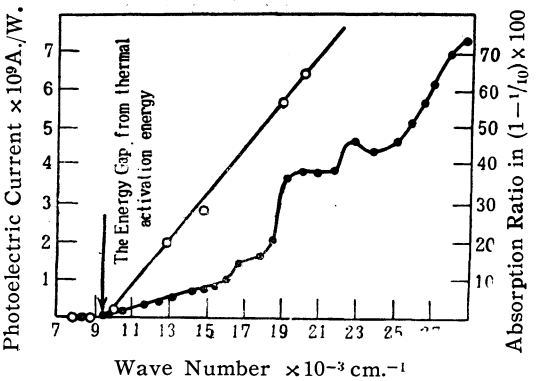
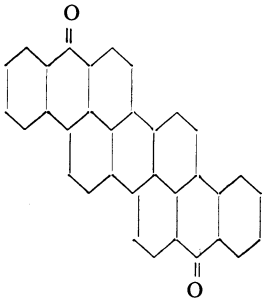
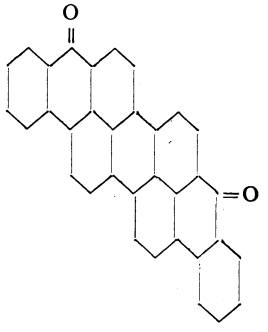
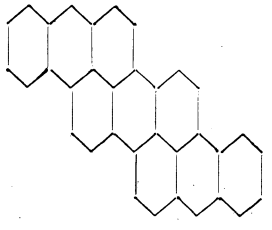
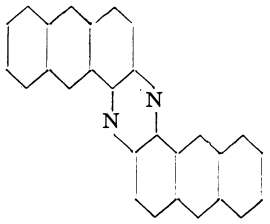


Fig. 7. Spectral response of photoconductivity and optical absorption curve for ovalene —○—○—○— photoconductive response, —●—●—●— optical absorption curve.

TABLE I. THE ENERGY GAP OF THE CONDENSED POLYNUCLEAR AROMATIC AND AZA-AROMATIC COMPOUNDS

Substance	Structure	Energy gap in e.V. unit: from photoconductivity	from optical absorption	from thermal activation energy
Isoviolanthrone		0.93	$0.7—0.7_5$	0.75
Violanthrone		0.84	0.7_5	0.78
Isoviolanthrene		0.85	—	0.82

Violanthrene	0.88	0.8	0.85
Ovalene	1.20	1.2	1.13
Pyranthrone	1.14	$0.8—0.8_5$	1.06
Pyranthrene	0.85	$0.7_5—0.8$	1.07
Flavanthrone	0.76	$0.7—0.7_5$	0.70
Indanthrone	0.74	0.6_5	0.63

Indanthrazine  0.80 0.6_5—0.7 0.66

The observed dark currents were changed with substances measured, with thickness of films and with other conditions. However, when the photocell was illuminated with the tungsten lamp, which had 0.1 W/cm^2 intensity, the ratio of photocurrent to dark current was about from 5 to 20 times. For example, the photocurrent and dark current of indanthrone were 5.14×10^{-11} A and 1.37×10^{-11} A, pyranthrone 19.6×10^{-11} A and 2.7×10^{-11} A and this ratio of "ovalene photocell" was very large, such as 140×10^{-10} A of photoelectric current and 1.54×10^{-10} A of dark current at room temperature. This is very

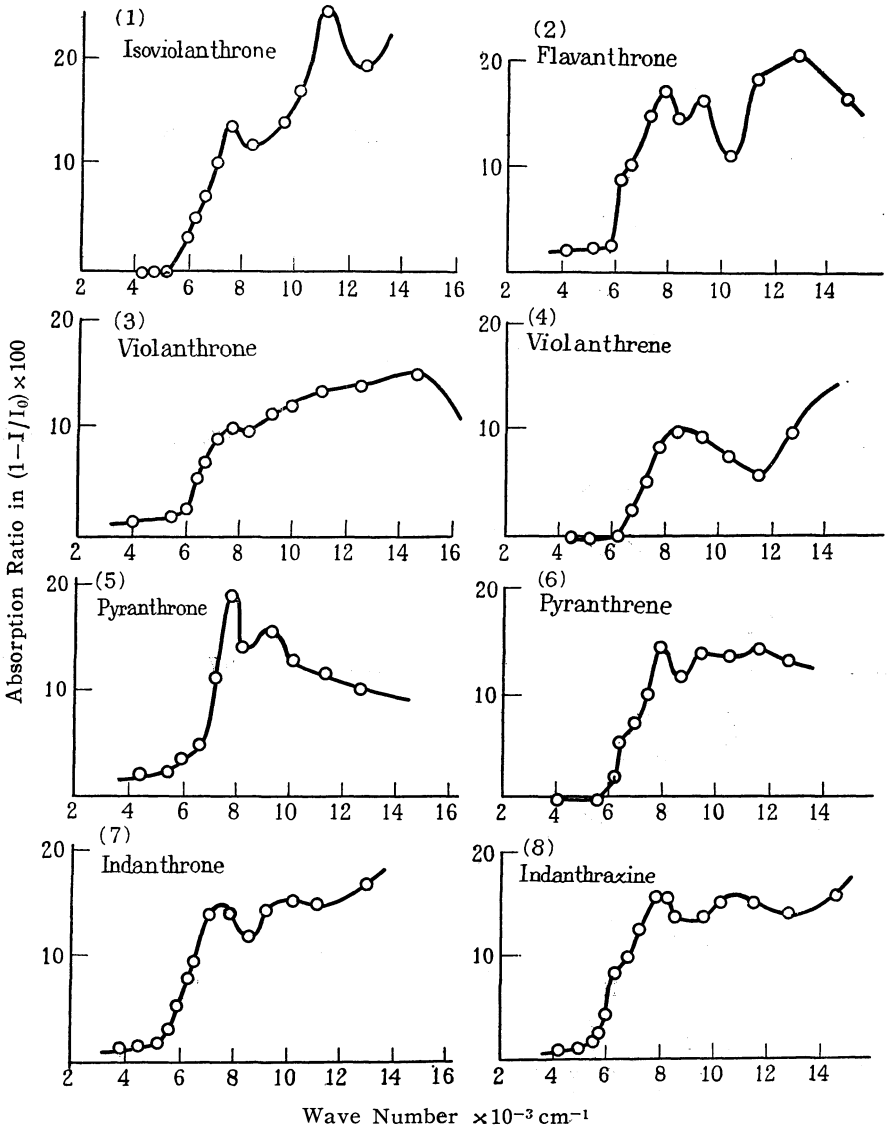


Fig. 8. Optical absorption of the organic semi-conductors. (1) isoviolanthrone, (2) flavanthrone, (3) violanthrone, (4) violanthrene, (5) pyranthrone, (6) pyranthrene, (7) indanthrone and (8) indanthrazine.

interesting when compared with the molecular structure.

These organic semi-conductors have no impurities—intrinsic semi-conductors. Then, assuming a crystal band structure, the threshold values correspond to the energy gap between the full band and the empty band.

To study the correlation between the photoconductivity and the optical absorption of crystals, the author has measured the absorption spectrum of layers of these organic substances. The spectral response of this character is shown in Fig. 8, and the threshold values are tabulated in TABLE I in e. V. unit. In TABLE I, results of photoconductivity, the optical absorption of solid and the temperature dependence of electrical conductivity satisfactorily coincide with each other. For example, these three characteristics of ovalene are shown in Fig. 7.

This will be due to the fact that the organic semi-conductors studied here are intrinsic ones having molecular lattice.

Summary

Photoconductivity and optical absorption in the solid state of the organic semi-conductors, that is, isoviolanthrone (I), violanthrone (II), isoviolanthrene (III), violanthrene (IV), pyranthrone (V), pyranthrene (VI), ovalene (VII), flavanthrone (VIII), indanthrone (IX) and indanthrazine (X) were measured. From the threshold values of the spectral response of the photoelectric current and optical absorption in the solid state, the energy gap between the full band and the empty band were estimated as (I) 0.93 eV, 0.7 eV, (II) 0.84 eV, 0.75 eV, (III) 0.85 eV, —, (IV) 0.88 eV, 0.8 eV, (V) 1.14 eV, 0.85 eV, (VI) 0.85 eV, 0.8 eV, (VII) 1.20 eV, 1.2 eV, (VIII) 0.76 eV, 0.75 eV, (IX) 0.74 eV, 0.65 eV, (X) 0.80 eV, 0.7 eV respectively. Also from the experimental facts that the photocurrent is proportional to the applied potential and to the light intensity, the author thinks that the photocurrent observed here is a primary current. These results, photoconductivity and absorption spectra, are in good agreement with that estimated from the temperature dependence of the electrical resistivity. It may be reasonable that this agreement is due to the fact that the organic semi-conductors studied here are intrinsic ones having molecular lattice.

The author expresses his hearty thanks to Prof. H. Akamatu for his kind direction of this study. The cost of this research has been defrayed from the Grant in Aid for Fundamental Scientific Research from the Ministry of Education, to which the author's thanks are due.

Department of Chemistry, Faculty of Science, The University of Tokyo

Thermal Diffusion Factor of Hydrogen-Nitrogen Mixture

Kozo HIROTA*) and Kazuo SASAKI

(Received September, 10, 1953)

Introduction

Recently it becomes easy to discuss intermolecular potential by the theoretical and experimental development. Considering the fact that the effect of thermal diffusion is affected more sensitively by the intermolecular potential than any other transport phenomena, such as viscosity, ordinary diffusion, etc., it will be interesting to treat the effect in relation to this standpoint. Actually, several authors have already attacked the problem theoretically[1], but it seems to us that they did not extend their research in such details so far as to check whether or not the experimental data agree with their theory over the entire range of composition. It was, therefore, attempted in the present paper to treat the problem from another direction, adopting hydrogen-nitrogen mixture as the system to be studied, because it has been the most studied of all the binary mixtures.

Theoretical Consideration

To begin with, thermal diffusion factors α of this system were collected from the reports hitherto published, instead of k_t, for

*) Now, Science Faculty, Osaka University, Nakanoshima, Kita-ku, Osaka.

1) S. Chapman, *Proc. Roy. Soc.*, A **177**, 38 (1940). R.C. Jones, *Phys. Rev.*, **58**, 111 (1940); **59**, 1019 (1941). M. Kotani, *Proc. Math.-Phys. Soc. Japan*, **24**, 76 (1942). T. Kihara and M. Kotani, *ibid.* **25**, 602 (1943). Hirschfelder, Bird, and Spotz, *Chem. Rev.*, **44**, 205 (1949). K. E. Grew, *Proc. Roy. Soc.*, A **189**, 402 (1947), K. E. Grew, *Proc. Phys. Soc.*, **62**, 655 (1949). E. R. S. Winter, *Trans. Faraday Soc.*, **46**, 81 (1950), etc.

the reason that the former constant varies less against composition than the latter*).

All these values, except those which were obtained at the mean temperatures much lower than 0°C, are plotted in solid circles against molar fraction of hydrogen (c), as shown in Fig. 1, where some of them had to be determined by evaluating from the data of original papers. The four points designated in the triangle are those determined under 1-12.6 atm. pressure recently by Hirota and Kobayashi[2], using the Clusius-Dickel column, and the numerals attached to them indicate the pressure under which the experiment was carried out. It will be important that these data at high pressure also coincide with those obtained at ordinary pressure, though, according to Becker, it will increase to some extent under 80 atmospheric pressures[3].

If we exclude, for the time being, the values marked by the triangle and the open circle which will be explained in the present paper, it is evident that the observed α's increase linearly with hydrogen concentration**), but there is a tendency for their mutual difference to increase more greatly at the same time, especially in the concentration above $c=0.80$. Such a dispersed state of the results cannot be caused by the temperature difference among the measurements, because the difference is too small to be explained on both theoretical and experimental grounds, while also it cannot be caused by the slight pressure difference[4], as described above.

On the other hand, the first approximate values[5] of α were calculated by using the Lennard-Jones 12 : 6 potential:

$$V(r)=4\epsilon\left\{\left(\frac{r_0}{r}\right)^{12}-\left(\frac{r_0}{r}\right)^{6}\right\}$$

(ϵ is the depth of the potential energy minimum and r_0 is the low velocity collision diameter). The difficult numerical calculation could be avoided by use of the tables given by Hirschfelder, et al.[1,6], the basic constants required in the procedure are as follows:

$\epsilon(H_2)/k=33.3°K$,
$r_0(N_2)=2.968Å$ (from viscosity),
$\epsilon(N_2)/k=91.46°K$,
$r_0(N_2)=3.681Å$ (from viscosity),
and $\epsilon(N_2\sim H_2)/k=47.8°K$,
$r_0(N_2\sim H_2)=3.325Å$.

(k is the Boltzmann constant.) The temperature was assumed to be 321.6°K in the calculation.

The calculated result is shown by the full line in Fig. 1, where the dotted is the one when a rigid sphere potential is adopted in calculation, using 2.730Å, 3.756Å and 3.243Å as the collision diameter of hydrogen, nitrogen and nitrogen-hydrogen, respectively. It is clearly shown, as ought to be, that the latter cannot reproduce the experiment, while that of the Lennard-Jones potential can reproduce the experimental values better. But even this potential cannot give the decreasing tendency of α in high hydrogen concentration.

Experiment and Discussion

Considering the situation, thermal diffusion

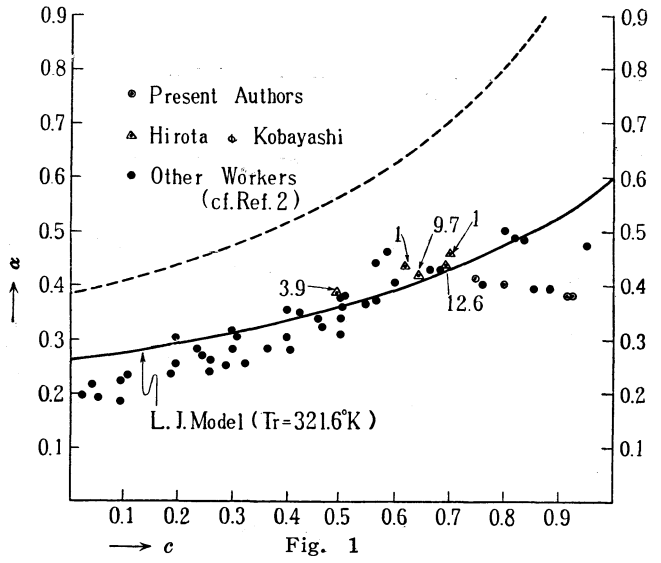


Fig. 1

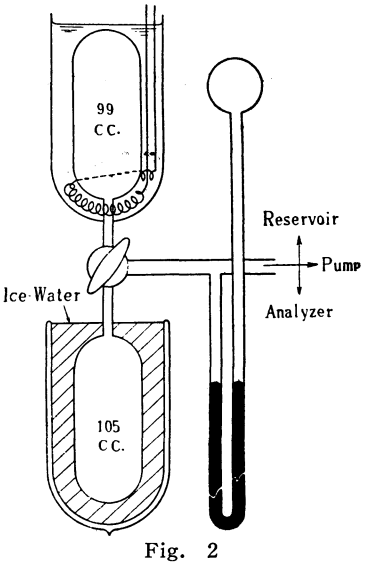


Fig. 2

*) Between a and kt, there is a relation: $kt=ac(1-c)$, where c is the concentration in molar fraction.

**) The present data of Hirota and Kobayashi differ slightly wih those of the former report, due to the accurate determination done later.

2) K. Hirota and Y. Kobayashi, *J. Chem. Phys.*, **21**, 246 (1953).

3) E.W. Becker and A. Schulzeff, *Naturw.*, **35**, 219 (1948).

4) Regarding this system, E. Whalley (private communication) obtained the result that separations at one atmosphere and 1 mm.Hg. seem to be identical within a few percent, if two bulbs were maintained for a sufficient time at 295°K and 427°K, respectively.

5) Chapman and Cowling, "Mathematical Theory of Non-Uniform Gases" (1939).

6) Hirschfelder, Bird and Spotz, *J. Chem. Phys.*, **16**, 968 (1948).

factors of relatively high hydrogen concentration were determined by the two-bulb-method. The main apparatus consisted of two bulbs (about 100 cc.) as shown in Fig. 2. Higher and lower temperatures were kept at 0°C. and 100°C. by ice-water and boiling water, respectively. The purity of the samples was tested mass-spectrometrically, and the impurity, being mostly oxygen, was found to be less than 0.1%. The concentration of hydrogen in the samples was analyzed by the volume decrease, oxidizing it with CuO heated at 300°C. During sampling care was taken that no concentration change should occur due to the difference of the diffusion rate of hydrogen and nitrogen through the tubing. Each experiment was carried out for a much longer time—five or more times —than the relaxation time (ca. 1.5 hours) defined by

$$t_r=\left(\frac{L}{\rho DS}\right)\left(\frac{mm'}{m+m}\right)\cdot\frac{1}{2}\cdot\left(\frac{T+T'}{T-T'}\right)\cdot\ln\left(\frac{T'}{T}\right),$$ [7]

where L, length of the connecting tube = 11 cm;
ρ, density;
D, diffusion coefficient;
S, cross section of the tube = (π/4.0 cm^2);
$m(m')$, mass in the reservoir of higher (lower) temperature;
$T(T')$, higher (lower) temperature.

The experimental data and α obtained from them are shown in table 1 and by the open circles in Fig. 1 (c=0.74, 0.79, 0.88 and 0.89). It is shown that the experimental points are still lower than the theoretical line. Therefore, the discrepancy already mentioned in the region of higher concentration does not disappeared, but rather seems to be confirmed. Considering the fact that the potential adopted by the present paper holds fairly well to other transport phenomena, such an unexpected disagreement between theory and experiment may be brought out by the use of Chapman's first approximate formula of α besides as well as becauce of the incompleteness of the intermolecular potential adopted.

TABLE I

Mean hydrogen conc. (molar fraction)	Separation (molar fraction)	Thermal diffusion factor α
0.741_4	0.023_8	0.39_7
0.792_8	0.020_4	0.39_8
0.879_5	0.010_7	0.32_5
0.890_0	0.010_5	0.34_4

Summary

The thermal diffusion factor of the nitrogen-hydrogen system has been discussed theoretically. It has been found that the Lennard-Jones potential can reproduce the experimental result, if the hydrogen concentration is below 0.8 in molar fraction. Each experiment done by use of the two-bulb-method in hydrogen concentration 0.74−0.89 has given similarly smaller value than expected theoretically. Such discrepancy may be caused by the theoretical formula of α as well as by the incomplete intermolecular potential.

Chemical Branch, Research Institute of Applied Electricity, Hokkaido University, Sapporo

7) H. Brown, *Phys. Rev.*, **58**, 661 (1940).

Studies on the Degradation of Yeast Ribonucleic Acid by Lanthanum Hydroxide. On the Existence of a Resistant Fraction

By Michio SHIMOMURA

(Received September, 11, 1953)

Ribonucleic acid (RNA) was shown in the previous paper[1] to be hydrolysed almost completely into nucleosides and inorganic phosphate by the action of lanthanum hydroxide. However, it was still ambiguous as to whether the nucleic acid is completely dephosphorylated or not, since it is a compound of high complexity. In the case of the enzymatic degradation of RNA by ribonuclease (RNase), a non-dialysable residue has been known to remain which comprises 15 to 50 per cent of the original[2)3)], and this fact has offered a clue for the research on the ribonucleic acid structure[4)5)6)].

1) M. Shimomura and F. Egami, This Bulletin, **26**, 263 (1953).

2) H. S. Loring, F. H. Carpenter and P. M. Roll, *J. Biol. Chem.*, **169**, 601 (1947).

3) G. Schmidt, R. Cubiles, B.H. Swartz and S.J. Thannhauser, *J. Biol. Chem.*, **170**, 759 (1947).

4) E. Chargaff, *J. Cell. Comp. Physiol.*, **38**, Supplem. 1, 41 (1951).

5) G. Schmidt, R. Cubiles and S. J. Thannhauser, *J. Cell. Comp. Physiol.*, **38**, Supplem. 1, 61 (1951).

6) B. Magasanik and E. Chargaff, *Biochim. Biophys. Acta*, **7**, 396 (1951).

In the work to be described it was found that the action of lanthanum hydroxide can not lead to the perfect dephosphorylation of RNA, but that a resistant fraction (LaRF) remains. Some properties of the resistant fraction were studied and compared with those of the ribonuclease resistant fraction (RNaseRF).

Materials and Analytical Methods

Yeast Ribonucleic Acid A commercial sample of RNA prepared from brewer's yeast by the method of Clark and Schryver[7] (Kirin Institute) was used after purification by the usual chloroform method.[8] The phosphorus content of the purified preparation was 8.0 per cent.

Lanthanum Carbonate The purification procedure of the carbonate has been described previously.

Ribonuclease The enzyme was extracted from calf. spleen and partially purified by the method of McDonald[9] up to the step of B Fraction. The preparation was freed from salt by washing with aqueous ethanol and then with absolute ethanol and dried in vacuum. Yeast RNA liberated no inorganic phosphate by the action of this preparation.

Ribonuclease Resistant Fraction 200 mg. of RNA were digested with 10 mg. of RNase in 15 cc. of M/100 magnesium sulfate. The digestion proceeded at 37° for 3 hours and occasional addition of dilute alkali maintained the mixture at *p*H 7—8. A 5 cc. aliquot was then removed and the residual 10 cc. of digested nucleic acid solution was dialysed through cellophane first against 500 cc of 2M solution of sodium chloride[10] then against 1 litre of distilled water for 24 hours, respectively. The estimation of the phosphorus content of the dialysis residue showed that 80 per cent of the original material had been removed.

Analytical Methods The same methods as those in the previous paper[1] were used.

Methods and Results

Estimation of LaRF The reaction mixture, similar to that described in the previous paper[1], was constructed as follows: 200 mg. of lanthanum carbonate were suspended in distilled water in a 50 cc. Erlenmeyer flask and dissolved by adding hydrochloric acid. On adjustment of the solution to *p*H 8.5 by the addition of aqueous ammonia, lanthanum hydroxide was precipitated. To this suspension a RNA solution containing 10.8 mg. of the purified material, 10 cc. of M/5 borate buffer solution at *p*H 8.5 and then water were added till the final volume was 40 cc. The reaction proceeded at 80°.

Preliminary experiments showed certain difficulties in the estimation of undephosphorylated RNA from the difference between the total and the inorganic phosphorus of the reaction mixture, since the difference was small. Fortunately, however, it was found that the liberated nucleosides are not adsorbed on lanthanum hydroxide, a powerful precipitating agent of nucleic acid. Therefore, the measurements were carried out in the following manner. A 4 cc. sample was withdrawn at intervals and centrifuged. The precipitates were washed twice with 8 cc. of dilute lanthanum hydroxide suspension respectively in order to remove nucleosides, and analysed for RNA by the orcinol method. It is a well known fact that in this colorimetric method the color is given by purine-bound ribose. The results of the experiment, which are presented in Table, 1, have been calculated on the assumption that the purine/pyrimidine ratio of the undephosphorylated fraction is the same as that of the original material.

TABLE I

ESTIMATION OF UNDEPHOSPHORYLATED RNA

Time (hrs.)	Undephosphorylated RNA (%)
40	7.8
56.5	7.3
99	5.9

It can be seen in TABLE I that some amounts of RNA remain undephosphorylated, although they are not completely stable to the action of lanthanum hydroxide. At any rate, they are remarkably resistant in view of the fact that 99.9 per cent dephosphorylation might be expected in 40 hours from the calculation based on the first order reaction constant of the reaction up to 85 per cent dephosphorylation.

Preparation of LaRF An RNA solution containing 15 g. of the material was mixed with a lanthanum hydroxide suspension which was prepared from 30 g. of the carbonate. The final volume was about 1 litre. This mixture was adjusted at *p*H 8.5 by the addition of aqueous ammonia and maintained at 80° for 40 hours. The occasional addition of ammonia prevented the lowering of *p*H of the mixture during the hydrolysis. The precipitate was subsequently filtered while warm, washed with hot water to remove nucleosides and suspended in about 150 cc. of 5 per cent solution of sodium bicarbonate which had previously been adjusted at *p*H 8 with dilute hydrochloric acid. After standing for about 2 hours, lanthanum carbonate was removed by centrifugation. The clear supernatant, which contained RNA, was made slightly acid (*p*H 5) with acetic acid, freed from the excess of bicarbonate by a current of air under reduced pressure and neutralized with ammonia.

The above procedure was repeated once more with lanthanum hydroxide prepared from 10 g. of the carbonate. LaRF solution thus obtained contained a small amount of inorganic phosphate, which was removed by the addition of a small amount of lanthanum hydroxide and subsequent centrifugation. The final yield of LaRF was calculated on the basis of its phosphorus yield to be about 1.5 per cent of the original material.

Analysis of LaRF The LaRF solution prepared as described contained about 15 per cent of

7) G. Clark and S. B. Schryver, *Biochem. J.*, **11**, 319 (1917).
8) M. G. Sevag, D. B. Lackman and J. Smolens, *J. Biol. Chem.*, **124**, 425 (1938).
9) M.R. McDonald, *J. Gen. Physiol.*, **32**, 39 (1948).
10) R. Markham and J. D. Smith, *Biochem. J.*, **52**, 565 (1952).

DNA (TABLE II); it may be explained by the facts that DNA is not dephosphorylated by lanthanum hydroxide, and that yeast RNA preparation is generally contaminated by a small amount of DNA. Its purine-bound ribose/RNA-P was much greater than that of the original RNA.

TABLE II

COMPARISON OF ANALYTICAL FIGURES OF VARIOUS FRACTIONS

	DNA-P	Purine-bound Ribose
	Total P	RNA-P
	%	mol./mol.
LaRF	15	1.08
RNaseRF		0.80
RNA		0.50 (Standard)

DNA-P was measured by the diphenylamine method on the assumption that the purine/pyrimidine ratio was 1. Purine-bound ribose was calculated from the color intensity of the orcinol test on the assumption that the original RNA preparation contained equimolecular purine-and pyrimidine-bound riboses. RNA-P was taken as the difference between total P and DNA-P.

Dephosphorylation of Various Fraction by Lanthanum Hydroxide The dephosphorylation of LaRF by lanthanum hydroxide was very slow (Curve 1), and this was also the case even after digestion by RNase (Curve II), while RNaseRF (Curve III) and the whole digest of RNA by RNase (Curve IV) were dephosphorylated as easily as RNA itself.

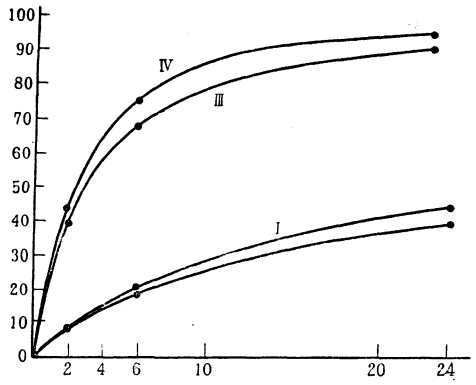


Fig. 1. Dephosphorylation of various fractions by lanthanum hydroxide. The preparation of RNaseRF and the whole digest of RNA by RNase are described in the text. The digestion of LaRF by RNase; LaRF solution containing about 400 μg. of phosphorus was incubated with 1 mg. of RNase at *p*H 7.0—7.5 and 37° for 3 hours. The incubations with lanthanum hydroxide were carried out at *p*H 8.5 and 80°. (The methods were described in the previous paper.)

Discussion

In the present experimental conditions, LaRF was not completely resistant to the action of lanthanum hydroxide. Anyhow, the observations presented here indicate that the structure of a certain specific portion of RNA is different from the rest.

The recent study in this laboratory showed that RNA becomes, by methylation of the hydroxyl group at C_2' of the sugar residue, as lanthanum hydroxide resistant as DNA, which has no hydroxyl group at C_2', and that the methylated RNA is not attacked by RNase[11]. In this connection, it is interesting that LaRF itself and LaRF treated with RNase were not easily dephosphorylated by lanthanum hydroxide, although the resistibility of LaRF to lanthanum hydroxide was not so great as that of the methylated RNA. It may be supposed that the hydroxyl group at C_2' might be masked in some way in LaRF. Anyhow this fact will offer a new clue for the elucidation of the structure of RNA.

Summary

1. Yeast ribonucleic acid is, as reported in the previous paper, hydrolysed almost completely into nucleosides and inorganic phosphate by lanthanum hydroxide, but the remaining fraction is considerably resistant to the action of the hydroxide.

2. Purine-bound ribose/RNA-p ratio of the resistant fraction is about 1.

3. Even after the treatment with ribonuclease, dephosphorylation of the resistant fraction by lanthanum hydroxide is not easy.

4. The ribonuclease resistant fraction is dephosphorylated by lanthanum hydroxide as easily as ribonucleic acid itself.

The present author wishes to express his thanks to Professor Fujio Egami for suggesting this investigation as well as constant encouragement in the course of the work. A part of the cost of this investigation was defrayed from the Scientific Research Encouragement Grant from the Ministry of Education, to whom I extend my thanks.

Chemical Institute, Faculty of Science, Nagoya University, Nagoya

11) F. Egami, H. Ishihara and M Shimomura, *Z. Physiol. Chem.*, **295**, 349 (1953).

Dielectric Behaviours of Hydrated Crystals I. Strontium Formate Dihydrate, Potassium Copper (II) Chloride Dihydrate and Ammonium Copper (II) Chloride Dihydrate[1]

By Ryôiti KIRIYAMA and Hideko IBAMOTO

(Received September 21, 1953)

Introduction

The investigations of the dielectric behaviours of the hydrated crystals will render some strong clues about the binding state of the water molecules in the crystal lattices. In these measurements, however, it is difficult to obtain reliable data owing to some sorts of lattice imperfections, especially liquid inclusions or efflorescent nuclei, and the surface leakage originated probably from the adsorbed water molecules. For the purpose of avoiding such phenomena, it will be desirable to use large, transparent, single crystals which make it possible to minimize these troublesome effects. In the present paper, the temperature and frequency dependences of the dielectric properties of one rhombic crystal, strontium formate dihydrate, $Sr(HCO_2)_2 \cdot 2H_2O$ and two isomorphous tetragonal crystals, potassium copper (II) chloride dihydrate, $K_2CuCl_4 \cdot 2H_2O$ and ammonium copper (II) chloride dihydrate, $(NH_4)_2CuCl_4 \cdot 2H_2O$ which contain directly coordinated water molecules to the divalent metal ions are reported and the anisotropies of the permittivities of the cupric salts are discussed.

Experimental

Crystals and Specimens of Strontium Formate Dihydrate. As the temperature dependence of the solubility of this anhydrate in water is rather small, a single crystal of this substance can be obtained by slow cooling, together with slow vaporization from the seed crystal placed on the bottom of a glass vessel, filled with a slightly supersaturated aqueous solution, which is kept in an air-thermostat with a regulator of $\pm 1°$ in the range of 40–30°C.[2] Cutting and grinding these transparent large single crystals perpendicular to three crystallographic axes, we obtain suitable specimens of about 1.5×1.5 cm². in area and 1.0–1.5 mm. in thickness in each case. These slices are pasted by tin foils with vacuum grease on both sides. Then this specimen is inserted into the plate condenser mentioned below.

Crystals and Specimens of Potassium Copper (II) Chloride Dihydrate and Ammonium Copper (II) Chloride Dihydrate. These crystals are grown by slow cooling of the supersaturated aqueous solutions by the same process mentioned above. But the temperature dependences of the solubilities being rather steep, it is necessary to regulate the temperature-fluctuation within less than $\pm 0.1°$. Consequently, the growing vessels are placed in a water-thermostat and the temperature is carefully controlled. Large crystals thus obtained are cut and ground to form suitable slices which are perpendicular to two crystallographic axes. Among these specimens we select nearly perfect, single crystals which are scarcely optically anomalous and not twinned according to the examination using a polarizing microscope. The slice is directly put between silver-coated brass electrodes forming a crystal condenser in the measuring circuit.

Equipment. The crystal condenser for the measurement at room temperature is a somewhat improved type of the previously used condenser in our laboratory,[3] and the permittivities of the crystal are determined from the ratios of the capacities of the specimens to those of the artificial rock salt of which permittivity is adopted at 5.62 as the standard value.[4] This rock salt was prepared by Stockberger's method in our laboratory.

The cell for the observation of the temperature dependence is also an improved type of that previously reported.[3] The temperature of the specimen in the cell is measured by a copper-constantan couple in the limit of ±1°C. The heating rate is about 0.2°/min. in every case. For the purpose of avoiding the condensation of water vapour upon the crystal surface when the cell is cooled down, a small member of calcium chloride grains have been spread on the bottom of the cell.

The measurements at audio-frequencies are carried out using a capacity-resistance bridge with RC-type oscillator. In these cases, there are no remarkable dispersions between 20 kc–1 kc, thus the measurements are performed mainly at 5 kc.

1) This paper was partly presented at the annual meeting of the Crystallographic Society of Japan on May 14, 1950 and partly at the meeting of the Chemical Society of Japan on Sept. 20, 1952 (a symmposium on structural chemistry) and also on Nov. 17, 1952 (a symmposium on complex salt).

2) R. Kiriyama, Studies on the velocities of crystal growth I. The growth condition of the single crystal of strontium formate dihydrate, *J. Chem. Soc. Japan*, **70**, 260 (1949), in Japanese.

3) T. Suita, K. Suenaga and I. Nitta, Abstract of the Electrical Engineering Section of the 4th general meeting of Nippon Kogakukai on April, 1940, page 18.

4) K. Höjendahl, *K. Danske Vidensk. Selskab.*, **16**, No. 2, (1938).

The measurements at radio-frequencies are carried out by a resonance circuit and the dielectric losses are obtained by resistance-substitution. The frequencies used are 600 kc. and 3 Mc. stabilized by quartz oscillators.

Result

Strontium Formate Dihydrate. The permittivities along three crystallographic axes at a room temperature are as follows,

$$\varepsilon_a=5.2,\quad \varepsilon_b=4.9,\quad \varepsilon_c=4.3$$

In these cases, the frequency dependences between 5 kc. and 3 Mc. are not observable, and these values may be more precise than those previously reported by one of the authors.[5]

The temperature dependences between −170°C. and the dehydration point at 3 Mc. are shown in Fig. 1. The temperature coefficients of the permittivities along three axes are very small and it shows a horizontal straight line up to about 70°C. in every case. But the permittivities show slightly decreasing tendencies of at least 1% when the temperature rises above about 70°. However the permittivities increase suddenly at 75° and the crystal collapses, followed by dehydration of the total water of crystallization.

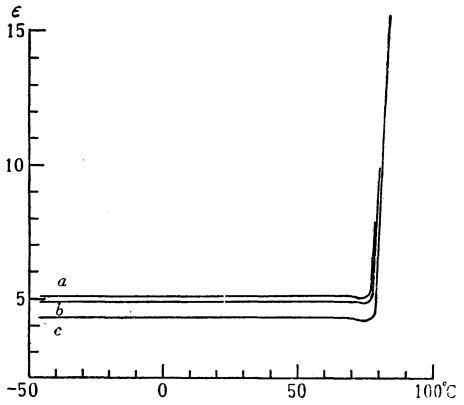


Fig. 1. Strontium formate dihydrate: Anisotropy and temperature dependences of the permittivities along its three crystallographic axes.

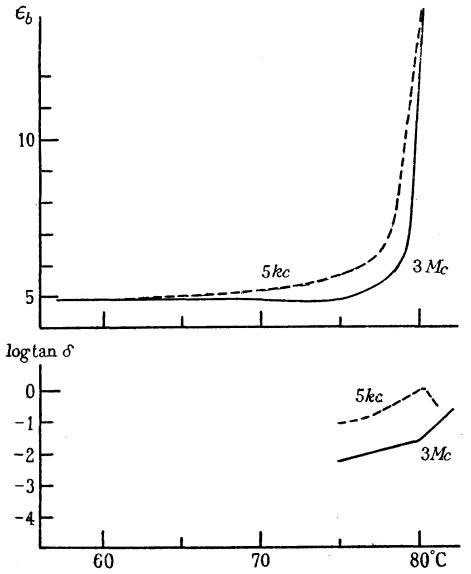


Fig. 2. Strontium formate dihydrate: Dispersion at 3Mc. and 5kc.

The change and dispersion of the dielectric behaviour before and after the dehydration are shown in Fig. 2 in which the curves along *b*-axis are picked up as an example. The permittivity at 5 kc is higher than that at 3 Mc above 65° and the dielectric loss at 5 kc is also far greater than that at 3 Mc. The cause of such a high dielectric loss will be attributed to the surface conduction of the dehydrated polycrystals. Actually, it is confirmed that the loss diminishes when a thin mica foil has been inserted between the crystal specimen and one of the electrodes.

Potassium Copper (II) Chloride Dihydrate and Ammonium Copper (II) Chloride Dihydrate. The permittivities at room temperature are as follows,

$K_2CuCl_4\cdot 2H_2O$: $\varepsilon_a=8.5,\ \varepsilon_c=5.1$
$(NH_4)_2CuCl_4\cdot 2H_2O$: $\varepsilon_a=7.2,\ \varepsilon_c=5.6$

There are no detectable dispersions between 3 Mc. and 5 kc at room temperature. But, it is remarkable that, in spite of the isomorphous structure, the potassium salt shows greater anisotropy than that of ammonium salt.

The temperature dependences of the permittivities and the losses of both salts are shown in Fig. 3 and 4. The temperature coefficients of the permittivities $\frac{1}{\varepsilon}\left(\frac{d\varepsilon}{dT}\right)$ are obtained from these experimental curves.

$K_2CuCl_4\cdot 2H_2O$: −170 — −20°C. (3 Mc. and 5 kc.)
along *a* nearly zero; along *c* 2.2×10^{-4}
$(NH_4)_2CuCl_4\cdot 2H_2O$: −170 — −130°C. (3Mc. and 5 kc.)
along *a* -7×10^{-4}; along *c* 9×10^{-4}
−130 — 0°C. (3 Mc. and 5 kc.)
along *a* nearly zero; along *c* nearly zero
0 — 100°C. (3 Mc. and 5 kc.)
along *a* 1.7×10^{-4}; along *c* 2.2×10^{-4}

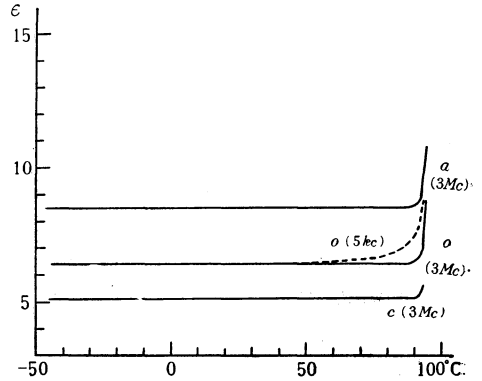


Fig. 3. Potassium copper (II) chloride dihydrate: Temperature dependences of the permittivities and the dispersion perpendicular to *o*(111) -plane.

5) R. Kiriyama, *Kagaku*, **17**, 239 (1947), in Japanese.

100 — 125°C. (3 Mc.)
along a 1.1×10^{-3}; along c 0.6×10^{-3}
100 — 125°C. (5 kc.)
along a 6.5×10^{-3}; along c 6×10^{-3}

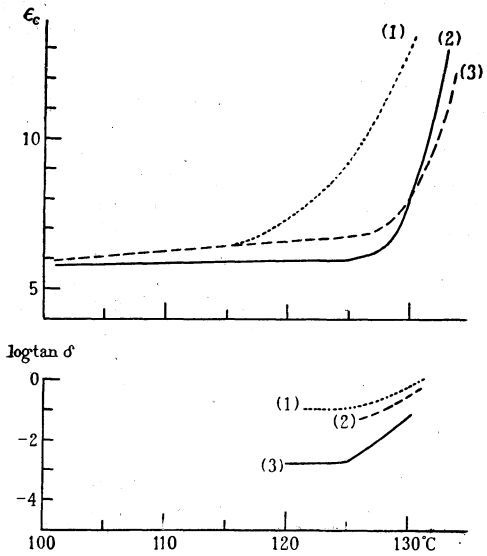


Fig. 4. Ammonium copper (II) chloride dihydrate: Temperature dependences of the permittivities and the dielectric losses; (1) 5kc., direct; (2) 5kc., both sides mica foils; (3) 3Mc., one side mica foil.

Thereupon, in the case of the ammonium salt at low temperatures, we found a rather curious anisotropy of the temperature coefficients which are negative in a-direction and positive in c-direction. The dielectric behaviour of the potassium salt is analogous to that of strontium formate dihydrate which shows no remarkable change up to the dehydration temperature. Especially, in the case of this potassium salt, it shows also a little decreasing tendency at 3 Mc. before the dehydration occurs.

The dehydration of the ammonium salt takes place at a considerably higher temperature than that of potassium salt and this temperature difference will cause some effects originated in the dehydrated water molecules. In the experiments of the ammonium salt, we have often met with the emergence of electrochemical reactions between the specimen and the brass electrodes of which the silver-coating had been perhaps imperfect.

For the purpose of investigating both effects of the surface conduction and the electrode reaction, we have tried to observe the temperature dependences of the specimens in the following ways.

(1) The specimen was directly put between two electrodes.
(2) A mica foil was inserted between the specimen and the lowerside electrode.
(3) Mica foils were inserted between the specimen and two electrodes to separate the effect of d.c. conduction.

Three examples along c-direction of these experiments in the neighbourhood of the dehydration temperature are plotted in Fig. 4.

Discussion

The crystal structure of strontium formate dihydrate was analysed by I. Nitta and K. Osaki[6]. According to their result, one water molecule is coordinated directly to the strontium ion but the other is packed in the lattice surrounded by oxygen atoms and water molecules with hydrogen bond distances. The anisotropy of the permittivities is rather small. This may be expected from the less anisotropic arrangement of the constituent atoms, radical ions and molecules. The negligible smallness of temperature and frequency dependences of permittivities may suggest that there exist fairly strong hydrogen bonds in the lattice and that no rotation-like motions of the water molecules or, unquestionably, of the formate ions will occur up to the collapse of the lattice accompanied with the dehydration of the water of crystallization.

The slight depression of the permittivities immediately below the dehydration temperature at 3 Mc. may be attributed to the loosening of the hydrogen bonds as in the case of the predehydration of copper sulphate pentahydrate[7]. But it is questionable whether the larger value at 5 kc in the same temperature region is a true dispersion caused by some rotation-like motion or originated by slight conduction on the crystal surface.

The abrupt increases of the permittivities due to the surface conduction at the dehydration temperature are analogous to many hydrated salts observed by us.

The crystal structures of both potassium and ammonium copper (II) chloride dihydrates are isomorphous and the perspective is shown in Fig. 5[8]. In this structure, $[CuCl_2(H_2O)_2Cl_2]$ rhombic octahedron is found, but we ought to adopt the planar rhombic $[CuCl_2(H_2O)_2]$ group parallel to c-axis rather than the rhombic planar $[CuCl_2Cl_2]$ group perpendicular to the c-axis as the copper (II)-complex ion in both crystals from the evidences of the atomic distances between the central Cu-atom and the ligands determined by the structure analysis.

Contrary to our expectation based on this isomorphic structure, there is found a larger anisotropy of the permittivities of the potassium salt than of the ammonium salt. The

6) I. Nitta and K. Osaki, read before the annual meeting of the Chemical Society ot Japan, April 5, 1947.
7) R. Kiriyama and H. Ibamoto, This Bulletin, **25**, 359 (1952).
8) S.B. Hendricks and R.G. Dickinson, *J. Am. Chem. Soc.*, **49**, 2149 (1627); L. Chroback, *Z. Krist.*, **88**, 35, (1934).

most reliable reason for this discrepancy may be due to the atomic polarization of the hydrogen atom of the water molecule which

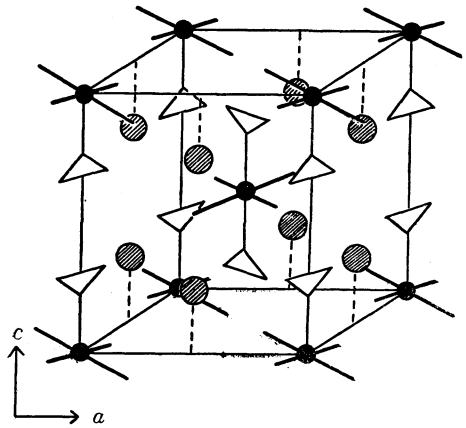


Fig. 5. The crystal structure of $K_2CuCl_4 \cdot 2H_2O$; Cu-black circle; K-hatched circle; H_2O-triangle; Cl is omitted but thick full lines indicate Cl—Cl distances in the orthorhombic octahedron.

has some different interactions in every lattice of both salts. It has been confirmed that the proton-proton distances were 1.62 ± 0.02Å in the potassium salt and 1.59 ± 0.02Å in the ammonium salt by means of the proton magnetic resonance experiments[9]. These values are considerably greater than that of the free water molecule, 1.51Å, determined by the spectroscopic method. The larger discrepancy found in the potassium salt may be caused by the fact that there is a stronger interaction between the O-H···Cl system in two neighbouring $[CuCl_2(H_2O)_2Cl_2]$ octahedrons. Moreover, the protonic polarization in the hydrogen bond is larger in the lateral direction of the bond axis than in the direction parallel to the line joining the two electronegative atoms as found in some crystals which contain O-H···O hydrogen bond systems in their crystal lattices[10]. Thus the stronger hydrogen bond of O-H···Cl in the potassium salt causes a larger anisotropy of the permittivity than that of the ammonium salt. Also this effect will clarify the difference of the dichroisms of the potassium and ammonium salts. The fact that one is strong and the other is weak respectively, is due to the difference of the bond strengths between the copper atom and the ligand water molecule. In the potassium salt, the copper-water bond is weaker than that of the ammonium salt owing to the stronger O-H···Cl bond mentioned above, therefore, the rhombic $[CuCl_2Cl_2]$ group on the *c*-plane will have more covalent nature than that of the ammonium salt. This difference of the bond nature, in other words, the polarization of the electron cloud of the chlorine atom will result in a stronger dichroism of the potassium salt than that of the ammonium salt.

The temperature dependences of the permittivities of the potassium salt are very small in a wide temperature range. And the slight dispersion above 50–60°C. may be attributed to the slight orientation of the dipoles of the water molecules occupying disordered lattice points which must often exist in this optically anomalous crystal. And, in this connection, it is noticeable here that there has been no temperature change of the biaxial interference figure of this optically anomalous crystal up to the dehydration temperature, therefore, this optical anomaly is not attributable to the somewhat regular misfit of the water molecules in the lattice. The sudden increase at the dehydration temperature is due to some conductive effects as in the case of the strontium formate dihydrate mentioned above.

In the case of the ammonium salt, the temperature dependences are analogous to that of the potassium salt and the principal explanation of these behaviours will be analogous to that above discussed. The reason for the slight negative temperature coefficient along *a*-axis at low temperatures, is not made clear at present, but it is noticeable that such a tendency is found also in ammonium mercury (II) chloride monohydrate and not in postassium mercury (II) chloride monohydrate[11].

In conclusion the authors wish to express their thanks to Prof. I. Nitta for his encouragement and suggetions during this work. The expense of this work was defrayed partly from the Scientific Research Grant from the Ministry of Education, to whom I extend my thanks.

Department of Chemistry, Faculty of Science, Osaka University, Nakanoshima, Osaka

9) J. Itoh, R. Kusaka, Y. Yamagata, R. Kiriyama and H. Ibamoto, *Physica*, **19**, 415, (1953).

10) In gypsum by the authors and in resorsinol and pentaerysritol by S. Yabumoto and R. Kiriyama; These results will be published shortly.

11) The results of these mercury (II) salts will be published in the following paper sbortly.

Oxidation of Carbon Monoxide on Silver Surface

By Noboru YAMADA

(Received October 9, 1953)

Introduction

Kinetic studies on a catalytic reaction with the same catalyst have often shown different results by different investigators. On the oxidation of carbon monoxide with silver as catalyst, Benton and Bell[1] showed that the reaction rate was proportional to the pressure of carbon monoxide and independent of the oxygen pressure. On the other hand, Titani et al.[2] showed that the reaction rate was proportional to the oxygen pressure and independent of the carbon monoxide pressure. In both cases the reaction rate was measured by the flow method. The catalyst used by Benton and Bell was the reduced silver catalyst, silver powder prepared by reduction of silver oxide with hydrogen, and those used by Titani et al. were the reduced silver powder and electrolysed silver powder obtained by the electrolysis of acidic silver nitrate solution. The temperature range of experiment was 80–140°C with Benton and Bell, and 150–450°C with Titani et al. Thus the results so obtained by these investigators were inconsistent with each other.

The main aim of the following experiments have been to determine which was the real case, and to make clear why those conflicting results were obtained by the investigators.

Experimental

The measurements of the reaction rate were made by the flow method. The apparatus and procedure employed were almost the same as those used by Titani et al.[2]

Carbon monoxide was generated by dropping formic acid on hot concentrated sulfuric acid. Oxygen was obtained electrolytically from sodium hydroxide solution. Each gas was purified in the usual manner, and stored over water in each reservoir. They were forced out of each reservoir under pressure, dried in the liquid oxygn traps, their flow rate controlled by the glass capillary tubes and inserted wires, and mixed before the entrance of the reaction tube. The total flow rate was fixed at 20 cc. (0°C, 760 mm. Hg.) per min. Controlling the flow rate of each gas, mixed gas having various proportion of carbon monoxide and oxygen were passed over the catalyst at atmospheric pressure. The reaction tube of hard glass was 16 mm. in inside diameter and 230 mm. in length. In the middle of the tube 4 g. of the catalyst was packed ca. 20 mm. in length. The reaction tube was heated by a cylindrical electric furnace.

Both catalysts, the reduced silver powder prepared by reduction of precipitated silver oxide with hydrogen at a low temperature as Benton and Bell[1], and the electrolysed silver powder obtained by electrolysis of acidic silver nitrate solution as Titani et al.[2], were used and compared with each other.

Results

(a) The Experiments with the Reduced Silver Catalyst.

The results are shown in Fig. 1, where the amount of carbon dioxide produced for a minute,

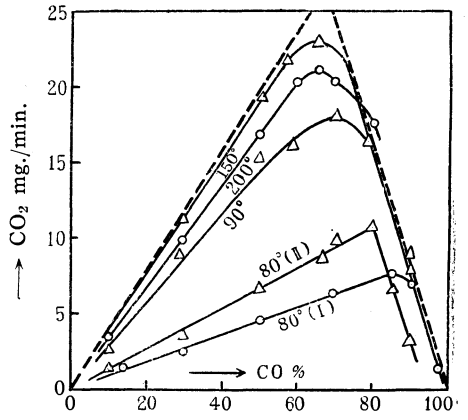


Fig. 1. Reaction rate with reduced silver catalyst.

the reaction rate, is plotted against mole percent of carbon monoxide in the mixed gas. The experiments were made at 80°, 200°, 150°, 90°, and again at 80°C. Benton and Bell[1] made their experiment in two limited composition ranges of the mixed gas, 0–20% and 90–100% of carbon monoxide. Now the reaction rate has been measured in the whole range of carbon monoxide-oxygen composition. The broken line in Fig. 1 shows the boundary, the maximum amount of carbon dioxide allowed for the composition of the mixed gas. Every curve in Fig. 1 increases with carbon monoxide content and falls at the boundary line. Comparing the curves 80° (I) and 80° (II), it is recognized that the catalyst has gradually increased its activity during the experiments. This may be due to the preliminary reduction with hydrogen before every run in order to avoid the deactivation of the catalyst by oxidation during the experiment. The data of the left hand part of every curve, which increases with carbon monoxide content in the

1) A.F. Benton and R.P. Bell, *J. Am. Chem. Soc.*, **56**. 501 (1934).

2) T. Titani and T. Ishiwatari, *J. Am. Chem. Soc.*, **65**, 13 (1944); T. Titani and N. Yamada, *ibid*, **65**, 224 (1944); T. Titani and S. Nakata, *ibid*, **65**, 305 (1944).

mixed gas, obey the following relation.

$$v=kP_{CO} \qquad (1)$$

where v is the reaction rate, number of mg. of carbon dioxide produced in one minute, k is the rate constant, and P_{CO} is the average partial pressure of carbon monoxide in the entering and exit mixed gas. Though the reaction rate in these experiment was larger than those of Benton and Bell[1], the kinetic relation (1) was qalitatively the same as theirs. That is, the reaction rate is proportional to the pressure of carbon monoxide and independent of the oxygen pressure.

(b) **The Experiments with the Electrolysed Catalyst.**

In the first experiment the electrolysed catalyst well-washed and dried was used without preliminary reduction with hydrogen. The results at

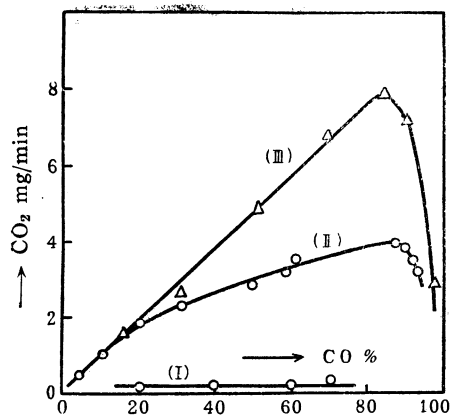


Fig. 2. Reaction rate with electrolysed silver catalyst at 80°C.

80°C are plotted as (I) in Fig. 2. The amount of carbon dioxide produced was very small. Then the catalyst was reduced in the hydrogen stream at 200°C for thirty minutes. The results of the second experiment after this treatment are plotted as (II) in Fig. 2. The catalyst was markedly activated and the reaction rate increased with the partial pressure of carbon monoxide. The data of the experiment with the reduced silver catalyst at 80°C, 80°(1) in Fig. 1, are plotted in Fig. 2 as (III) for comparison. It can be seen that by reduction with hydrogen the electrolysed catalyst was activated and approached to the reduced silver catalyst prepared from silver oxide.

(c) **The Effect of Reduction and Poisoning with Hydrogen.**

As mentioned above, it may be thought that when the surface of the silver catalyst has been fully reduced, the reaction rate increases with the partial pressure of carbon monoxide, the '*ascending*' type like the curve (II) and (III) in Fig. 2. If so, the surface of silver catalyst, which showed such low activity as (I) in Fig. 2 might have been oxidized or poisoned with oxygen. To make sure of this, the following experiment was made. The results are shown in Fig. 3. The electrolysed silver catalyst dried but not reduced preliminarily with hydrogen was used. The reaction rate was measured at 200°C in the first, the curve (I) in Fig. 3. The reaction rate decreased with carbon monoxide content in the mixed gas. The curve (I) in Fig. 3 is the '*descending*' type. This is the same type of curve as has been seen

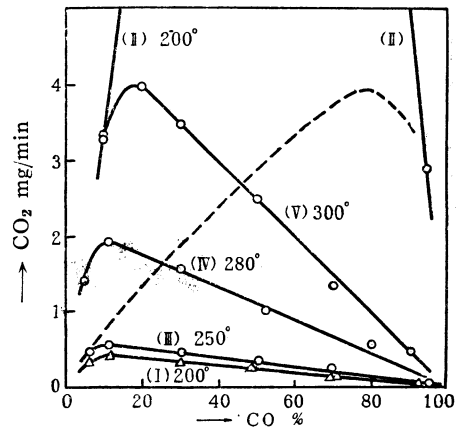


Fig. 3. Reaction rate with electrolysed silver catalyst and its changes by reduction and oxygenation.

in the experiment of Titani *et al*[2]. After the reduction of this catalyst in the hydrogen stream at 200°C, the reaction rate was measured again at 200°C. As was expected, the catalyst was remarkably activated, and the mixed gas reacted almost completely during the passage of the catalyt layer as was seen partially by (II) in Fig. 3. Then the catalyst was heated at 300°C in an oxygen stream for four hours, in order to poison the silver surface with oxygen. The results of three series of experiments at 250°, 280° and 300°C after this treatment are shown as (III), (IV), and (V) in Fig. 3. Clearly the catalyst was deactivated and the curves were of the '*descending*' type. The data on the straight line parts of these curves obey the following relation.

$$v=k'P_{O_2} \qquad (2)$$

where v is the reaction rate as the equation (1), k' is rate constant, and P_{O_2} is the average partial pressure of oxygen in the mixed gas. The reaction rate was proportional to the partial pressure of oxygen and independent of the carbon monoxide pressure. This was the case in the experiment of Titani *et al.*[2] For comparison with the curve (II) in Fig. 2, the results of the experiment at 80°C on the electrolysed silver catalyst reduced with hydrogen, is drawn into Fig. 3 as the broken line curve. It can be seen that the type of the curves is changed from '*ascending*' into '*descending*' type. The experiments by the use of the reduced silver catalyst from silver oxide was made also in a procedure similar to the above, and the same change by the treatment with oxygen could be seen.

Discussion

The results of the above experiments are

summarized and represented schematically in Fig. 4.

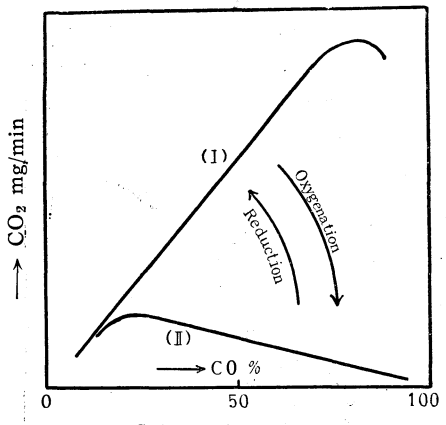


Fig. 4. Schematic representation of results.

When the surface of the silver powder has been fullly reduced with hydrogen, the rate of the catalytic oxidation of carbon monoxide on the surface describes the '*ascending*' type of reaction rate-composition curve as shown in Fig. 4 (I). The rate of reaction increases proportionally to the partial pressure of carbon monoxide and independently to the oxygen pressure. This is the case when the silver powder has been prepared by electrolysis of silver nitrate solution as well as by reduction of silver oxide. On the other hand, when the surface of silver powder has not been fully reduced or poisoned with oxygen, the catalyst is less active, and the reaction rate-composition curve is the '*descending*' type like (II) in Fig. 4. The reaction rate increases with the partial pressure of oxygen and is independent of the carbon monoxide pressure. This is the case when the catalyst is of the reduced silver from silver oxide as well as of the electrolysed silver. The 'ascending' type (I) in Fig. 4 corresponds to the result of the experiment of Benton and Bell[1], and the 'descending' type (II) corresponds to that of Titani et al[2]. One of these two different features of reaction rate dependency can be changed to the other by heating the surface of the silver catalyst in the stream of oxygen, or hydrogen.

These results indicate the following mechanism of oxidation of carbon monoxide on silver surface. This catalytic reaction consists mainly of the following two steps.

(i) $O_2 \longrightarrow 2O$ (chemisorption)

(ii) $O + CO \longrightarrow CO_2$

The step (i) is the chemisorption of oxygen on the surface of the silver catalyst. The oxygen molecules in the gas phase collide against the bare catalyst surface and are chemisorbed into atoms on it. In the next step (ii) the carbon monoxide molecules in the gas phase strike the chemisorbed oxygen on the surface of the silver catalyst and combine with them into carbon dioxide. If this is the mechanism of oxidation of carbon monoxide with silver catalyst, the following two limiting cases may occur.

(I) The case in which plenty of oxygen is chemisorbed on the catalyst surface.

In this case the amount of chemisorbed oxygen on a unit area of the surface of the silver catalyst must be large enough, and almost independent of the oxygen pressure. In consequence the reaction rate may be proportional to the rate of collision of carbon monoxide molecules on the catalyst surface, and accordingly to the partial pressure of carbon monoxide. That is,

$$v = kP_{CO}$$

This is the case when the silver powder prepared by the reduction of silver oxide with hydrogen is used, or generally when a silver catalyst has been treated with hydrogen and the catalyst surface has been fully reduced.

The activation energy for this case was calculated by the relation of the rate constant and the reaction temperature of the experiment (a) with the reduced silver catalyst.

$$A = 4.9 \text{ kcal.}$$

It may be presumed that the activation energy has the following content.

$$A = A_2 - Q/2$$

A_2 is the activation energy of the reaction step (ii), and Q is the heat of reaction step (i), or the heat of chemisorption of oxygen on the catalyst surface.

(II) The case in which only a little oxygen is chemisorbed on the catalyst surface.

In this case oxygen, as soon as it is chemisorbed on the catalyst surface, combines instantly with carbon monoxide. In consequence the total reaction rate is determined by the rate of chemisorption of oxygen on the catalyst surface. Accordingly it is proportional to the partial pressure of oxygen and independent of the carbon monoxide pressure, as following

$$v = k'P_{O_2}$$

This is the case when the electrolysed silver catalyst not reduced is used, or generally when a silver catalyst has been treated with oxygen and poisoned the surface.

The activation energy was calculated from the data of the experiments (III), (IV), and (V) in Fig. 3.

$$A' = 23.6 \text{ kcal.}$$

This activation energy A' must be the activation energy A_1 of the reaction step (i), or of chemisorption of oxygen on this poisoned catalyst surface.

$$A' = A_1$$

Thus, it can be explained by the above consideration that the different features of the reaction appear with reduction or oxydation of a catalyst surface. It my be concluded that Benton and Bell measured the reaction rate on the fully reduced silver surface, and that Titani et al. on the surface poisoned with oxygen. The difference between the two is by no means contradictory.

Summary

The catalytic oxidation of carbon monoxide on the surface of silver powder has been studied. The reaction rate has been measured by the flow method. The reaction rate on the fully reduced silver surface is proportional to the pressure of carbon monoxide and independent of the oxygen pressure. On the other hand, when the surface has not been reduced with hydrogen, or has been treated preliminarily in an oxygen stream at a high temperature, the reaction rate is proportional to the oxygen pressure and independent of the carbon monoxide pressure. One of these two features of the reaction can be changed to the other by heating the surface in the stream of oxygen, or hydrogen. These results indicate that the chemisorption of oxygen and the reaction between this chemisorbed oxygen and carbon monoxide are the main steps of the oxidation, and its reaction rate is determined by either of these steps.

The author wishes to express his cordial thanks to Dr. T. Titani, Professor of Tokyo Metropolitan University, for helpful discussion and encouragement.

Faculty of Liberal Arts and Science, Toyama University

Sterols and Other Unsaponifiable Substances in the Lipids of Shell Fishes, Crustacea and Echinoderms. XIII. Sterol Components of Star Fish, Luidia quinaria von Martens

By Yoshiyuki TOYAMA and Toru TAKAGI

(Received October 9, 1953)

Among the sterol components of star fish, stellasterol ($C_{27}H_{44}O$, m.p. 149~150°, m.p. of its acetate 176~177°)[1] in *Astropecten aurantiacus* and asteriasterol (m.p. 70°)[2] in *Asterias forbesi* were known in earlier times. Later studies,[3] however, revealed that asteriasterol, like astrol[4] in *Astropecten aurantiacus*, is identical with batyl alcohol. Bergmann and Stansbury[5] separated a sterol fraction resembling stellasterol from *Asterias forbesi*, but they found that this fraction is not a single sterol but a mixture of two sterols, $C_{28}H_{46}O$ (F_2) and $C_{28}H_{48}O$ (F_1). Although neither components were separated from each other, both components were shown to have an ethylenic linkage at C-8, the di-unsaturated component having one more ethylenic linkage at the 22 : 23-position. These authors retained the name stellasterol for the di-unsaturated $C_{28}H_{46}O$, and designated the mono-unsaturated $C_{28}H_{48}O$ as stellastenol. According to Barton,[6] who examined the relations between the optical activities of these sterols and their esters, the ethylenic linkage common to stellasterol and stellastenol is located at the 7 : 8-position. One of the present authors, Toyama, and Matsumoto[7] separated hitodesterol (m.p. 167~168°, m.p. of its acetate 181~182°) from *Asterina pectinifera* (Müller et Troschel). Although the formula $C_{28}H_{42}O$ or $C_{29}H_{44}O$ was given for hitodesterol at that time, this formula has been found to be erroneous by later investigation in our laboratory[8] and hitodesterol was assumed now to have the formula $C_{28}H_{46}O$ or $C_{29}H_{48}O$, having a close resemblance to stellasterol, chondrillasterol, and spinasterol, possibly identical with one of them. Meanwhile, the occurrence

1) A. Kossel and S. Edelbacher, *Z. Physiol. Chem.*, **94**, 264 (1915).
2) J.H. Page, *J. Biol. Chem.*, **57**, 471 (1923).
3) l. c., (*f*).
4) T. Matsumoto, M. Yajima and Y. Toyama, *J. Chem. Soc. Japan*, **64**, 1203 (1943); W. Bergmann and H. A. Stansbury, Jb., *J. Org. Chem.*, **8**, 283 (1943).
5) W. Bergmann and H.A. Stansbury, Jb., *J. Org. Chem.*, **9**, 281 (1944).
6) Cf. L. F. Fieser and M. Fieser, "Natural Products Related to Phenanthrene" 1949, p. 297.
7) T. Matsumoto and Y. Toyama, *J. Chem. Soc. Japan*, **64**, 1069 (1943).
8) Y. Toyama, not yet published.

of another sterol (m.p. 144~146°, m.p. of its acetate 160~162°) in *Asterina pectinifera* (*Patiria pectinifera*) was reported by Kuwata and Ban.[9] This sterol, named patiriasterol, was concluded to be identical with $\Delta^{22:23}$-ergostenol by these authors.

In this paper, the results of our studies on the sterol components of star fish, *Luidia quinaria* von Martens, are recorded. The sterol mixture, as a whole, consisted chiefly of mono-unsaturated sterol. The acetate of the sterol mixture was subjected to fractional crystallization, yielding several acetate fractions which had somewhat different iodine values by the perbenzoic acid method. The acetate fraction of higher melting point showed a higher iodine value than the acetate fraction higher iodine value than the acetate fraction of lower melting point, indicating the presence of a lesser amount of saturated and di-unsaturated sterols in addition to mono-unsaturated sterol in the original sterol mixture. By repeated fractional crystallizations of the acetate mixture, two sterol fractions I (m.p. 145~147°, m.p. of its acetate 157°) and II (m.p. 135°, m.p. of its acetate 149°) were obtained. Both fractions consisted of mono-unsaturated sterol. The acetates of the fractions I and II absorbed no hydrogen in the presence of palladium black in glacial acetic acid, but they underwent isomerization, as is the case with a $\Delta^{7:8}$-sterol. Bromination-debromination of the acetate of the fraction I resulted in the formation of 7:8, 9:11-conjugation which presented a further evidence for the presence of 7:8-ethylenic linkage in the fraction I.[10] Although the fraction II might consist of another $\Delta^{7:8}$-sterol which is different from the $\Delta^{7:8}$-sterol of the fraction I, it is also possible that both fractions consist of the same $\Delta^{7:8}$-sterol and differ only in their purity. Comparing the fraction I and patiriasterol, the melting points of free sterols and their corresponding esters are fairly close to each other, but they differ decisively in their behavior toward hydrogenation. While patiriasterol has its ethylenic linkage at the 22:23-position, the ethylenic linkage of the fraction I is located convincibly at the 7:8-position. On the other hand, the fraction I agrees with stellastenol in the position of ethylenic linkage, both having 7:8-ethylenic linkage, but it is not yet decided whether the sterol in the fraction I is C_{28}-sterol or C_{29}-sterol. For the sake of comparison, the properties of γ-spinastenol (C_{29}), $\Delta^{7:8}$-ergostenol, patiriasterol, and the sterol fractions I and II, together with some derivatives of the respective sterols are shown in Table I.

TABLE I

	Free sterol		Acetate		Benzoate		α-Isomer		Acetate of α-isomer	
	m.p., °C	$[\alpha]_D^\circ$	m.p., °C	$[\alpha]_D^\circ$	m.p., °C	$[\alpha]_D^\circ$	m.p., °C	$[\alpha]_D^\circ$	m.p., °C	$[\alpha]_D^\circ$
γ-Spinastenol (11)	144–145	+11	156–157	+8	180.5	+13	112–113	+23	116–117	+12
$\Delta^{7:8}$-Ergostenol (12)	148	−2	157–159	+4	180.5	+2	132	+11	109	0
Patiriasterol	144–146	+4.4	160–162	+4.2	175–176	+7.1	—	—	—	—
Sterol fract. I	145–147	+9	157	+6	177	—	115	—	111–112	+18
Sterol fract. II	135	+2	149	+2	171	—	114	—	115	+8

Experimental

A lot of star fish, *Luidia quinaria* von Martens, caught around the Osaki-Shimojima Island in the Inland Sea of Seto in August, 1952, were sun-dried. The dried material (1,030 g.) was cut into small pieces and then extracted with ether, yielding 29 g. (2.8%) of ether extract which was a viscous liquid of reddish orange color and deposited a large amount of solid in the winter season. On treating the ethereal extract with 300 cc. of acetone, 22.1 g. of acetone-soluble portion (fat) and 6.9 g. of acetone-insoluble portion (phosphatide) were separated. The acetone-soluble portion was a reddish orange oil having the following characteristics: d_4^{20} 0.9405, n_D^{20} 1.4740, acid value 111.8, saponification value 143.9, iodine value by the Wijs method 132.4, unsaponifiable matter 28.16%.

The acetone-insoluble portion gave only 0.3 g. of unsaponifiable matter by extraction of the saponified product with ether. The unsaponifiable matter (6 g.) obtained from the acetone-soluble

9) S. Kuwata and Shoichi Ban, *J. Pharm. Soc. Japan*, **69**, 212 (1949).
10) Cf. R. C. Anderson, R. Stevenson and F. S. Spring, *J. Chem. Soc.*, **1952**, 2901.
11) D. H. R. Barton and J. D. Cox, *J. Chem. Soc.*, **1948**, 783.
12) D. H. R. Barton and J. D. Cox, *J. Chem. Soc.*, **1948**, 1354.

portion was recrystallized twice from methanol, yielding 2.2 g. of crude sterol, which had m.p. 125~129°, iodine values 65.6 by the perbenzoic acid method and 177.4 by the pyridine sulfate dibromide method. The ultraviolet absorption spectra of the crude sterol indicated the absence of provitamin D. The steryl acetate (2.0 g.) prepared by acetylation of crude sterol had m.p. 135~141° and saponification value 127.1. This was subjected to repeated recrystallizations as shown in Table II.

TABLE II

No. of recrystallization	Solvent	Acetate, crystallized out		Acetate, recovered from mother liquor	
		Yield g.	m.p. °C.	m.p. °C.	Iodine v. by the perbenzoic acid method
1	Methanol	1.9	143–144	104–106	43.4
2	Ethanol	1.6	146–148	105–110	—
3	„	1.1	147–152	124–126	—
4	Acetone	0.5	156–159	147–149	—
5	„	0.25	156–159	147–149	62.6
6	„	0.10	162–165	157–159	70.7
7	„	0.08	162–165		
8	"	0.02	174–175	165–166	—

Iodine values, calculated: $C_{30}H_{50}O_2$ (F_1) 57.3, $C_{31}H_{52}O_2$ (F_1) 55.6

Sterol Fraction I. The acetate of m.p. 157–159°, recovered from the mother liquor of recrystallization in Table II, was fractionally crystallized from acetone, yielding 1st crop of m.p. 160°, 2nd crop of m.p. 157° and 3rd crop of m.p. 152°. The 2nd crop showed no change in its melting point by further recrystallizations from acetone and ethanol-ether and the final product had saponification value 124.9 (calculated, $C_{30}H_{50}O_2$ 126.7, $C_{31}H_{52}O_2$ 122.8), iodine values 63.5 by the perbenzoic acid method 190.1 by the pyridine sulfate dibromide method, and $[\alpha]_D^{16}$+5.6°. The free sterol obtained by saponification of the acetate had, after recrystallization from methanol, m.p. 145–147° and $[\alpha]_D^{16}$+9.0°. Benzoylation of the free sterol gave a benzoate of m.p. 177°.

A solution of the acetate of m.p. 152° with a palladium black catalyst in glacial acetic acid was shaken under the atmosphere of hydrogen for 3 hours at room temperature. Absorption of hydrogen did not occur at all, but the acetate underwent isomerization during this treatment, forming an isomer (α-isomer) which showed, after recrystallization from methanol, m.p. 111–112° and $[\alpha]_D^{25}$+18.1°. The free sterol obtained by saponification of this acetate melted at 115°.

The acetate (0.05 g.) of m.p. 152° was dissolved in 10 cc. of ether, and 5 cc. of a 2% solution of bromine in ether was added dropwise. After standing for one hour, a mixture of 0.25 g. of potassium iodide dissolved in a small amount of water and 10 cc. of ethanol was added to the solution of brominated product, and the mixture was allowed to stand for 48 hours in order to complete debromination. An aqueous solution of sodium bisulfite was then added, and the mixture was extracted with ether. The ethereal extract, after recrystallization from methanol, melted at 164° and exhibited the characteristic ultraviolet absorption spectra of 7:8, 9:11-conjugated sterol; log ε_{235} 3.91, log ε_{242} 3.88, log ε_{251} 3.80.

Sterol Fraction II. The acetate of m.p. 147~149°, recovered from mother liquors of recrystallization in Table II, was fractionally crystallized from acetone. After removing higher and lower melting fractions, a fraction of m.p. 148~149° was separated and further recrystallized from acetone, ethanol-ether and methanol-acetone until an acetate of a constant melting point of 149° was obtained. It had saponification value 123.4, iodine values 60.1 by the perbenzoic acid method and 170.9 by the pyridine sulfate dibromide method, and $[\alpha]_D^{12}$+2.2°. Saponification of the acetate gave a free sterol of m.p. 135° and $[\alpha]_D^{12}$+1.6°. Benzoylation of the free sterol gave a benzoate of m.p. 171°.

On shaking a solution of acetate of m.p. 149° with a palladium black catalyst in glacial acetic acid under the atmosphere of hydrogen for 3 hours, isomerization without absorption of hydrogen occurred, yielding an isomerized product (α-isomer) of m.p. 115° and $[\alpha]_D^{25}$+7.9°. Saponification of this product gave a free sterol of m.p. 114°.

Summary

Sterol mixture of star fish, *Luidia quinaria* von Martens, has been found to consist largely of mono-unsaturated sterol with a lesser amount of saturated and di-unsaturated sterols. By fractional crystallization of steryl acetate mixture, sterol fractions I (m.p. 145° and m.p. of its acetate 157°) and II (m.p. 135° and m.p. of its acetate 149°) were separated. Both fractions were found to consist of $\Delta^{7:8}$-sterol of C_{28} or C_{29} series. It requires some further research to decide whether each fraction consists of a different individual sterol or both fractions consist substantially of the same sterol, differing only in their purity.

Department of Applied Chemistry,
Faculty of Engineering,
Nagoya University, Nagoya

Enzymatic Reduction of Aromatic Nitro, Nitroso and Hydroxyl amino Compounds

Ikuo YAMASHINA, Shogo SHIKATA and Fujio EGAMI

(Received October 16, 1953)

In the previous paper[1], the nature of the enzyme system participating in the reduction of aromatic nitro-compounds was described.

This paper describes the route of the enzymatic reduction of nitro-compounds to amino-compounds. It is well known that when aromatic nitro-compounds such as trinitrotoluene or dinitrophenol are administrated to animals, the corresponding amino, hydroxylamino, and azoxy compounds are excreted in the urine[2)3)]. These products are considered as intermediate or by-products in the biological reduction of nitro-compounds to amino-compounds[4)5)6)7)8)]. Concerning the route of the reduction, we assumed at first the following successive reduction of the nitro to the amino, taking into consideration that biological oxido-reductions generally take place by the two-electron steps:

Nitro→Nitroso→Hydroxylamino→Amino

However, we paid attention also to such substances as azoxy, azo, and hydrazo compounds, which are known to be intermediates in organo-chemical reduction of aromatic nitro-compounds.

Experimental Methods

We used as substrates nitroso[9)], hydroxylamino[9)], azoxy[10], azo[11)], and hydrazo[12)] compounds in the series of *o*-benzoic acid, because they are all sufficiently water-soluble and stable for the enzymatic study. The preparation of the enzymes from a halotolerant bacterium, the experimental conditions, and the methods of estimation of the reaction velocity were the same as for those described in the preceding report.

1) I. Yamashina, This Bulletin in the press.
2) R.T. Williams, G.T. Mills and H.J. Channon, *Biochem. J.*, **38**, 72 (1944).
3) H. Mayer, A. Mayer and L. Plantefol, *Ann. physiol. physicochem. biol.*, **8**, 1 (1932).
4) G.D. Greville and K.G. Stern, *Biochem. J.*, **29**, 487 (1949).
5) H.G. Bray, W.V. Thorpe and P.B. Wood, *Biochem. J.*, **44**, 39 (1949).
6) D. Robinson, J.N. Smith and R.T. Williams, *Biochem. J.*, **48**, xxvii (1951).
7) H.G. Bray, R.C. Clowes and W.V. Thorpe, *Biochem. J.*, **49**, lxv (1951).
8) H.G. Bray, Z. Hyhs and W.V. Thorpe, *Biochem. J.*, **49**, xcv (1651).
9) E. Bamberger and F.L. Pyman. *Ber.*, **42**, 2307 (1909).
10) G. Heiler, *Ber.*, **41**, 2690 (1908).
11) J. Maier, *Ber.*, **34**, 4135 (1901).
12) R. Loewenherz, *Ber.* **25**, 2797 (1892).

Results and Discussion

Enzymatic Reduction of *o*-Nitroso- and *o*-Hydroxylamino Benzoic Acid:

The measurements of the reaction velocity were carried out by the determination of the

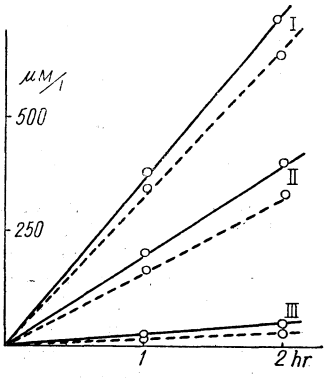


Fig. 1. The formation of anthranilic acid from *o*-nitroso, *o*-hydroxylamino benzoic acids in the presence of hydrogen carriers, -o- nitroso, --o-- hydroxylamino. System: Substrate (6×10^{-3}M) 1 cc., Reductase 1 cc., H. Carrier (10^{-3}M) 0.4 cc., Dehydrogenase (5 mg./cc.) 1 cc., Buffer (pH 6.8, 10^{-1}M, phosphate) 1 cc., HCOONa (10^{-1}M) 1 cc., H_2O 1.6 cc., I: Nile Blue, II: Methylene Blue, III: no carrier.

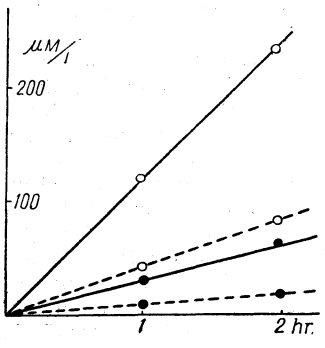


Fig. 2. The formation of anthranilic acid with leuco M.B. as hydrogen donator, -o- nitroso, -o- hydroxylamino, ----- no enzyme.
System: Substrate (6×10^{-3}M) 1 cc., Leuco M.B. (10^{-2}M) 2 cc., Buffer 1 cc., Reductase 1 cc..

anthranilic acid produced. As shown in Fig. 1 and Fig. 2, they were reduced enzymatically by the hydrogen donator system such as the

system consisting of hydrogen donator, dehydrogenase and an appropriate intermediary hydrogen carrier or by the leuco-form of appropriate redox dyes.

It is noteworthy that methylene blue is effective as a hydrogen carrier in these cases, contrary to the case of the reduction of the nitro group. From these results it may be concluded that the water-extract of the freeze-dried cells of the halotolerant bacterium contains the enzymes which accelerate the reduction of aromatic nitroso and hydroxylamino groups. We should like to call them "nitroso-reductase" and "hydroxylamino-reductase" respectively. The effects of various inhibitors on nitroso- and hydroxylamino- reductases are shown in TAB. I. The inhibiting action of cyanide and azide are so strong that the participation of some heavy metal to the enzyme reaction may be supposed. The inhibition is even greater than that on nitro-reductase.

TABLE I
THE EFFECTS OF SEVERAL INHIBITORS

	Nitroso	Hydroxylamino
KCN 10^{-3} M	80%	70%
NaN_3 10^{-2} M	40	30
NaF 10^{-2} M	10	10
Mn^{++} 10^{-4} M	—	0

As shown in Fig. 1 and Fig. 2, the velocity* of the enzymatic reduction of nitro is larger than that of hydroxylamino. It is not due to the inhibition by the excess of substrate in the latter case, because the velocity of the formation of amino from hydroxylamino is quite proportional to the concentration of the substrate (Fig. 3).

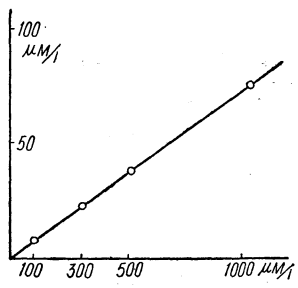


Fig. 3. The relation of the formation of anthranilic acid and the conc. of substrate (*o*-hydroxylamino benzoic acid.
System: Substrate 1 cc., Reductase 1 cc., Leuco M.B. (10^{-2}M) 2 cc. Buffer 1 cc.
Time: 2 hr.

These facts suggest that the hydroxylamino compound may not be a normal intermediate in the enzymatic reduction of nitroso compounds.

Experiments with *o, o'*-Azoxy, *o, o'*-Azo, and *o, o'*-Hydrazo Benzoic Acids:

They were not reduced in the presence of our enzyme preparation by the hydrogen donator-dehydrogenase system (nile blue or methylene blue as hydrogen carriers) nor by leuco methylene blue. So these substances can be excluded from the possible intermediates of the reduction from the nitro compound to the amino compound. However *o, o'*-azoxy benzoic acid was formed as a by-product in the reduction of *o*-nitrobenzoic acid as will be shown later (Fig. 5).

Route of the Enzymatic Reduction:

As the velocity of the enzymatic formation of amino group from nitroso group is larger than that from hydroxylamino group as mentioned above, the main route of nitroso to amino cannot be

nitroso→hydroxylamino→amino,

but it must be

nitroso→X→amino
nitroso→amino.

As azoxy, azo and hydrazo compounds, which had been supposed to be X in the reaction scheme, were not reduced enzymatically, we have been led to the conclusion that the direct four-electron reduction from nitroso to amino may be the main route of the enzymatic reduction.

In order to further ascertain the conclusion, we tried to detect the intermediates and the by-products of the enzymatic reaction by paper-chromatography. The reaction mixture (Each of the above-mentioned compounds and dehydrogenase system) was extracted with other, dried in the refrigerator and the residue was dissolved in a small quantity of ether and tested by paper chromatography. The composition of the developing solvents and *Rf* values of various compounds are shown in TAB. II.

TABLE II. THE DEVELOPING SOLVENTS AND *Rf* VALUES

Solvents; (1)

Ethanol	40%	Butanol	33%
Butanol	20	Pyridine	33
Ammonia (s.g.=0.90)	20	sat. NaCl aq.	33
Benzene	20	The organic layer of above mixture	

(2) *Rf* Values: Solvent

Benzoic acids	(1)	(2)
o-nitro	0.63	0.68
o-amino	0.51	0.91
o-nitroso	0.20	0.30
o-hydroxyl-amino	0 02	—
o, o'-azoxy	0.24	0.65
o, o'-azo	0.28	—
o, o'-hydrazo	0.33	—

*) Measured by the formation of amino group.

For the detection of each spots, Ehrlich's reaction for amino compounds was carried out directly or after the reduction by $SnCl_2$-HCl. Axoxy, azo and hydrazo compounds appeared as red spots and others as yellow spots.

The enzymatic reduction of nitroso was followed by paper chromatography as shown in Fig. 4. At the first stage of the reaction the spot of hydroxylamino appeared intensely; it then gradually became feeble and afterwards disappeared. From these results it must be considered that besides the direct route there is also a route by which the nitroso is reduced enzymatically to amino via hydroxylamino.

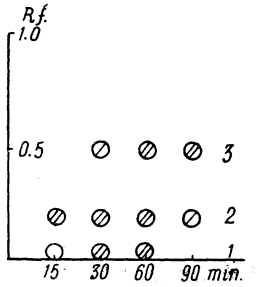


Fig. 4. Solvent (1) (Table II)
1: *o*-hydroxylamino benzoic acid
2: *o*-nitroso " "
3: *o*-amino " "

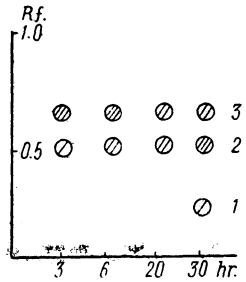


Fig. 5. Solvent (1) (Table II)
1: *o,o'*-azoxy benzoic acid
2: *o*-amino " "
3: *o*-nitro " "

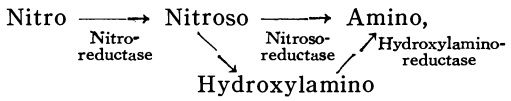
On the paper chromatogram of the reduction products of the nitro to the amino, as shown in Fig. 5, the spot of azoxy compound was detected, besides the spots of decreasing nitro and of increasing amino. Taking into consideration the fact that the azoxy compound cannot be reduced by our enzyme preparation, it must be regarded as a by-product. The reason why any substance other than nitro, amino and azoxy benzoic acids was not detected may be explained by assuming that the possible intermediates, nitroso and hydroxylamino benzoic acids, are so rapidly reduced that they do not accumulate appreciably. This consideration is also supported by the fact that the quantity of the amino compound formed was equivalent to that of the nitro compound reduced, which in turn was estimated by the polarography.

TABLE III.

	0 hr.	9 hr.	Degree of diminution or formation
nitro	100%	68%	32%
amino	0	33	33
nitro	100	76	20
(in the presence of 10^{-3} M KCN)			(degree of inhibition is 25%)

Moreover, the paper chromatography disclosed the existence of the nitroso compound as a reduction product in the enzymatic reduction of the nitro compound under the presence of 10^{-3} M KCN. In this condition, the enzymatic formation of amino from nitro was reduced to 30%, that from nitroso to 20% and that from hydroxylamino to 30%, while the rate of the enzymatic reduction of nitro measured by polarography was reduced only to 75%. These facts are easily explained by considering the that primary product of the enzymatic reduction of the nitro compound is the nitroso compound and that this stage of successive reduction is less inhibited by KCN than the latter stages.

All of the results concerning the reduction process of nitro to amino may be summarized as follows:



although it must be mentioned that we have as yet not been able to obtain experimental evidence that nitroso-reductase and hydroxylamino-reductase are different. The accumulation of azoxy compound, a by-product, is probably due to the condensation of nitroso and hydroxylamino compound.

Summary

1) A cell-free enzyme preparation of a halotolerant bacterium activates aromatic nitroso and hydroxylamino compounds as well as nitro compounds and accelerates their reduction by hydrogen donator systems.
2) The enzymatic reduction of nitroso and hydroxylamino was more strongly inhibited by cyanide and azide than that of nitro.
3) Methylene blue, which can not be used as an intermediary hydrogen carrier in the case of nitro reduction, can be used in the

cases of nitroso and hydroxylamino reduction.

4) From these facts, we have been led to the consideration that there exist special enzymes such as nitroso-reductase and hydroxylamino-reductase besides nitro-reductase.

5) Azoxy, azo, and hydrazo compound cannot be reduced by the enzyme preparation.

6) From the studies of reaction velocity and paper chromatography of the intermediates and the end products, we proposed a scheme concerning the enzymatic reduction of nitro to amino, namely:

$$\text{Nitro} \rightarrow \text{Nitroso} \rightarrow \text{Amino}$$
$$\searrow \quad \nearrow$$
$$\text{Hydroxylamino}$$

The expenses of this study were defrayed in part by a grant from Japanase Biological Research Works, Ltd. and Seikagaku-Kenkyujo Ltd., to both of which the authors' thanks are due.

Chemical Institute, Faculty of Science, Nagoya University

Isopropoxypolysiloxanes

Rokuro ŌKAWARA, Toshio TANAKA and Iwao ISHIMARU

(Received September 3, 1953)

The preparation of tetraisopropoxysilane from silicon tetrachloride and isopropanol was attempted in vain by Dearing[1]. Recently Bradley and his co-workers[2] reported briefly its formation from the same materials. We wish now to report on the preparation and properties of tetraisopropoxysilane $((CH_3)_2CHO)_4Si$ (I), hexaisopropoxydisiloxane $((CH_3)_2CHO)_3SiOSi((CH_3)_2CHO)_3$ (II), and octaisopropoxytrisiloxane $((CH_3)_2CHO)_3SiOSi((CH_3)_2CHO)_2OSi((CH_3)_2CHO)_3$ (III).

For the starting material isopropanol of Shell Chemicals (b.p. 82.2°C, n_D^{20} 1.3776) was used without further purification. For the preparation of (I) and (II) redistilled silicon tetrachloride (b.p. 57–58°C), and for the preparation of (III) octachlorotrisiloxane $Cl_3SiOSiCl_2OSiCl_3$ were used. This substance was obtained from the distillation residue of industrial silicon tetrachloride with rigorous fractionation through the helices packed column of about 20 plates under reduced pressure. (b.p. 73°C./13 mm., Anal. Calcd. for $Cl_8Si_3O_2$: Cl, 70.9. Found: Cl, 70.8.)

Preparation of Tetraisopropoxysilane (I) and Hexaisopropoxydisiloxane (II):—In the 1 *l.* three-necked flask equipped with an efficient stirrer, dropping funnel and reflux condenser, isopropanol (240 g., 4 mol.) was placed. Redistilled silicon tetrachloride (170 g., 1 mol.) was added with vigorous stirring for 2 hours. During the addition, the mixture was kept under 5°C. After addition the temperature was gradually raised to 40°C. for an hour and kept at this temperature for additional 3.5 hours. The mixture amounted to 360 g. (Cl content 62%). At this temperature, the mixture was dehydrochlorinated by bubbling dry air through the mixture until the chlorine content of the mixture became constant, the final value was 0.2% after 7 hours aeration. The volume of air passed was 400 *l.* At this stage the weight of the mixture amounted to 245g. (Yield: 91% theory). Hydrated sodium carbonate (5 g.), containing about 2 moles H_2O to Na_2CO_3, was added and the mix-

TABLE ISOPROPOXYPOLYSILOXANES

Name	Formula	Boiling Point °C./mm.	Refractive Index n_D^{20} n_D^{30}	Density d_4^{20} d_4^{30}	Molar Refraction Found (Calcd.)**	Molecular Weight Found*** (Calcd.)	% Si Found (Calcd.)
Tetraisopropoxysilane	$[(CH_3)_2CHO]_4Si$ (I)	93–4/28*	1.3835 1.3787	0.8744 0.8656	70.7 (70.4)	267 (265)	10.59 (10.62)
Hexaisopropoxydisiloxane	$[(CH_3)_2CHO]_6Si_2O$ (II)	82–3/2	1.3921 1.3875	0.9236 0.9150	110.1 (109.0)	420 (427)	13.14 (13.17)
Octaisopropoxytrisiloxane	$[(CH_3)_2CHO]_8Si_3O_2$ (III)	121–2/2	1.3960 1.3912	0.9504 0.9419	148.9 (147.7)	585 (589)	14.37 (14.31)

* 74°C/13 mm., 116°C./85 mm. Bradley, *et. al., loc. cit.*

** Calculated from bond refrativities by E. L. Warrick, *J. Am. Chem. Soc.* **68**, 2455 (1946)

*** Cryoscopic measurements in benzene

1) A.W. Dearing and E.E. Reid, *J. Am. Chem. Soc.*, **50**, 3058 (1928).

2) D.C. Bradley, R.C. Mehrotra and W. Wardlaw. *J. Chem. Soc.*, **1952**, 5020.

ture was warmed to 80°C, with shaking. The filtrate (240 g.) was distilled under reduced pressure by a Claisen flask, and the fraction boiling at 90°–95°C./30 mm. was collected. (Crude (I), 230g., Yield: 85% theory) This fraction and the residue of several runs, from which the (II) was obtained, were fractionated rigorously by a Stedman column of about 20 plates respectively. The properties of these fractions are summarized in the following Table.

If the treatment of hydrated sodium carbonate was not carried out, the distillate obtained after several fractionations usually still contained a trace of isopropoxychlorosilane which fumes in moist air. After the treatment with an excess of hydrated sodium carbonate equivalent to convert Si–Cl to Si–O–Si no trace of fuming compound was found in the filtrate. Furthermore the decomposition of the isopropoxysilane was not observed even after prolonged heating at about 80°C.

Preparation of Octaisopropoxytrisiloxane (III):—In the 300 cc. three-necked flask equipped as above, was placed octachlorotrisiloxane. (40 g., 0.1 mol.) Isopropanol (48 g., 0.8 mol.) was added with vigorous stirring for 1.5 hours. During the addition, the temperature of the mixture was kept under5 °C. after which the temperature was gradually raised to 40°C. for 0.5 hour and kept at this temperature for additional one hour. The weight of the mixture amounted to 60 g. This mixture was aerated at this temperature until the chlorine content became constant. The volume of air passed was 280 *l* during a course of 8 hours and the final chlorine content was 1.2%. (Yield: 55 g., 94.8% theory) To this was added hydrated sodium carbonate (7 g.) and treated as above. The filtrate (51 g.) was rigorously fractionated by the Stedman column. About 5 g. of low boiling fraction (80°–110°C./2 mm.) was obtained. Judging from the boiling point, this may be considered to be hexaisopropoxydisiloxane (II) produced by a fission of siloxane chain, but was not further examined. The properties of constant boiling fraction (III) are given in the Table together with (I) and (II).

The authors wish to express their sincere thanks to Dr. Watase for his gracious encouragement during this work. Our thanks are also due to the Ministry of Education for a grant in aid of this research.

Department of Applied Chemistry,
Faculty of Engineering,
Osaka University, Osaka

Chemical Studies On Ion Emission from Solids. II. A Method of Micro-Determination of An Alkali Salt in Aqueous Solution by Measuring Positive-Ion Emission

By Nobuji SASAKI and Toshiyoshi YUASA

(Received May 28, 1953)

Commercial alumina-coated tungsten filament operating as a heater in a vacuum tube, emits positive ions at about 800°C. They consist of sodium and potassium ions, as shown mass-spectrographically by H. Inoue[1] in our laboratory. The emission decays[2] with respect to time nearly exponentially. To the filament thus freed from alkalis by long heating was mounted* a known amount (about one mg.) of aqueous sodium chloride solutions in various ranges of concentration. The total number of positive ions emitted from the filament by heating was measured and plotted against the concentration of sodium. The resulting smooth curve may be used for determining the extremely low concentration of sodium, only one milligram of sample solution (e.g. a rain drop) being required.

Experimental

A piece of alumina-coated tungsten filament, 60 mm. in length and 0.051 mm. in diameter, was mounted as anode along the axis of a cylindrical cathode of 15 mm. diameter by screw-binders for convenient dismounting. The ions reaching to the cathode were measured by a galvanometer (1.1×10^{-11} amp./mm.) under the following conditions—applied voltage being 60 V., temperature of the filament about 750°C, pressure about 10^{-5} mm.Hg. Further details of the apparatus were explained in the previous report.[2] For preparing sample solutions only quartz apparatus was used to avoid any contamination of alkalis.

Determination of the Total Number of Positive Ions Emitted.—Aqueous sodium chloride solutions of various ranges of known concentration were prepared as standard using distilled water. Reading of the galvanometer was taken fifteen seconds after the heating current of filament was switched in. The current-time curves

1) The results were read at the Meeting of the Chemical Society of Japan (Kinki-Branch), Oct., 1949.

2) N. Sasaki and T. Yuasa, *J. Chem. Soc. Japan*, **73**, 273 (1952).

* The weight of a small amount of a volatile liquid such as the sample solution mounted to the filament was determined by a method to be described elsewhere.

of some representative results (No (3), (5), (7), (12), (14)) are shown in Fig. 1. The total number of

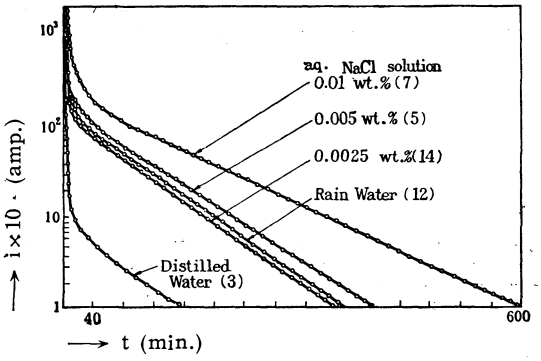


Fig. 1.—Emission Current-time curve

positive ions for each solution was obtained by integrating the emission currents with respect to ime (Table I). They give a smooth curve when plotted against the concentration (Fig. 2).

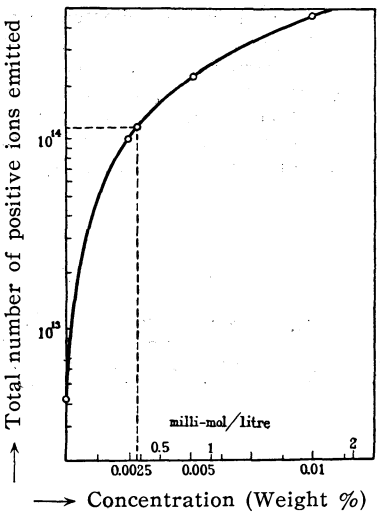


Fig. 2.—Total number of positive ions VS. Concentration curve

TABLE I

Samples	Order of measurement	Weights of the samples applied (W) in mg.	Total number of positive ions emitted (N)	N/W	Means
NaCl aq. soln.	(7)	0.864	3.70×10^{14}	4.28×10^{14}	
0.01 wt. %	(8)	1.093	4.77×10^{14}	4.36×10^{14}	4.29×10^{14}
	(9)	0.870	3.70×10^{14}	4.25×10^{14}	
	(4)	1.016	2.00×10^{14}	1.96×10^{14}	
0.005 wt. %	(5)	0.907	1.86×10^{14}	2.05×10^{14}	2.05×10^{14}
	(6)	0.851	1.82×10^{14}	2.13×10^{14}	
	(13)	0.901	8.41×10^{13}	0.93×10^{14}	
0.0025 wt. %	(14)	1.078	1.10×10^{14}	1.02×10^{14}	1.01×10^{14}
	(15)	0.924	9.98×10^{13}	1.08×10^{14}	
	(1)	0.909	3.75×10^{12}	4.12×10^{12}	
Distilled Water	(2)	1.091	4.64×10^{12}	4.25×10^{12}	4.19×10^{12}
	(3)	1.007	4.23×10^{12}	4.20×10^{12}	
	(10)	1.005	4.23×10^{12}	4.20×10^{12}	
Rain Water	(11)	1.013	1.17×10^{14}	1.15×10^{14}	1.13×10^{14}
	(12)	1.062	1.18×10^{14}	1.11×10^{14}	

The total number of positive ions emitted from one mg. of distilled water is nearly equal to the probable errors of N/W of aqueous sodium chloride solutions of various ranges of concentration, so that no correction was made for the blank value of distilled water.

The ratios of N/W to N_0, the total number of sodium ions contained in one mg. of solutions, are strikingly constant for wide ranges of concentration, namely, 0.38, 0.39 and 0.41 respectively for 0.0025, 0.005 and 0.01 weight per cent aqueous sodium chloride solutions. The rest of sodium ions seem to have evaporated as neutral molecules or atoms.

Similar measurements were made with aqueous potassium chloride solutions and a calibration curve of the same type was obtained.

Ionic emission from mixed KCl-NaCl solutions have been found greater than those calculated by the additive law. Ionic emission from more complicated mixtures was investigated by H. A. Barton and coworkers[3], and B. Toubes and coworker[4], finding that only alkali metal ions were emitted at about 800°–1000°C from the mixture of alkali and alkaline earth salts, while the alkaline earth salts required higher temperatures to produce emission.

Analysis of rain water in Nagoya and Kiryu Cities has been carried out by K. Sugahara[5], and S. Muto[6] respectively. The results show that the most important constituents are sodium and chloride ions with minor constituents such as K, Fe, Al, Ca, Mg, SO_4 and SiO_2.

3) H. A. Barton, G. P. Harnwell, and C. H. Kunsman, *Phys. Rev.*, **27**, 739 (1926).
4) B. Toubes and G. K. Rollefson, *J. Chem. Phys.*, **8**, 495 (1940).
5) K. Sugahara, *Kagaku (Science)*, **18**, 485 (1948).
6) S. Muto, *J. Chem. Soc. Japan*, **74**, 420 (1953).

A few rain drops were collected in a quartz vessel in Kyoto City, February 25,1953 and submitted to measurement. The result obtained $N/W=1.13\times10^{14}$ consists of sodium ions with a small portion of potassium ions. If we neglect the effect of the other salts and simply make use of the calibration curve in Fig. 2, N/W may be turned into a more familiar quantity 0.48 millimol./litre.

Inorganic Chemistry Laboratory, Department of Chemistry, Faculty of Science, and Department of Chemistry, Yoshida College, Kyoto University, Kyoto

Mikroanalyse Mit Hilfe von Ionenaustauschenden Harzen I. Über Den Nachweis Geringer Menge Des Kobalts Mit Ammoniumrhodanid[1]

Von Masatoshi FUJIMOTO

(Eingegangen am 6. Juni, 1953)

Einleitung. Bedeutend charakteristische Färbungen[2] liefern oft die farblosen oder hellgelben ionenaustauschenden Harze bei Gegenwart von der wässerigen Lösung verschiedenartiger Komplexsalzen. Diese Färbungen, die vielleicht von austauschender Adsorption der Komplexionen auf das Harz herrühren, sind manchmal ganz verschieden von den der wässerigen Lösungen der entsprechenden Komplexsalzen und häufig sehr deutlich. Der Verfasser, während seiner Untersuchung über die Rhodanidkomplexsalzen mit den ionenaustauschenden Harzen, hat gefunden, dass bei Gegenwart des überschüssigen Ammoniumrhodanids selbst kleinste Menge von Kobalt in der Lösung dem anionenaustauschenden Harze eine klare himmelblaue Färbung gab, die man für vorzüglichen Nachweis des Kobalts verwenden konnte.

Das in dieser Untersuchung benutzte anionenaustauschende Harz. Amberlite IRA-400[3]: Das Harz wurde durch zweimaliges Durchlaufen der 2N Salzsäure und destilliertes Wassers in die RCl-Form übergeführt. Die Korngrösse ist ungefähr 30 Maschen von Tyrerschem Normalsieb.

Versuchsanordnung. Man bringt einen Tropfen (0.02 ccm. mit Kapillarpipette) der neutralen oder sauren Versuchslösung auf eine weisse Tüpfelplatte[4], dazu fügt man einige Körnchen von anionenaustauschenden Harze mit einer kleinen Platindrahtöse, danach schüttelt um, und versetzt man mit einem Tropfen der 1M Ammoniumrhodanidlösung[5]. Nach einigen Minuten bis einem Tage, je nach der Kobaltmenge der Probelösung, entsteht am Rande oder über das Ganze der Harzkörnchen eine klare himmelblaue Farbe, welche unter Beleuchtung mit einer elektrischen Lampe von 60 Watt und durch etwa zwanzigfache Vergrösserung mit einer Lupe wohl nachweisbar ist.

Bestimmung der Erfassungsgrenze.

(1) Unter Erfassungsgrenze versteht man bei diesem Versuche solche Kobaltmenge in Gamma ($\gamma = 10^{-6}$ g) in jeder Probelösung, die sich in den zwölf Vertiefungen der Tüpfelplatte findet, wenn unter gleichen Bedingungen alle diese positive Reaktion zeigen, d, h., wenn sie nach einer Stunde klar erkennbare, hell himmelblaue Färbung am Rande der allen Harzkörnchen geben.

(2) Massflüssigkeit wurde aus der Lösung des extrareinen Kobalt (II) chlorids dargestellt, deren 1 ccm. von der Lösung 78.1 mg. von Kobalt enthielt[6].

(3) Die Resultate der Experimente stehen in Tabelle I.

Daher wurde die Erfassungsgrenze 0.16 γ und die Grenzkonzentration $1:1.3\times10^5$ für Kobalt an dieser Reaktion festgestellt.

Einflusse der Begleitionen. (1) Eisen (III): Die intensiv blutrote Färbung, die bei Anwesenheit der Eisen (III) salze mit Ammoniumrhodanid auf die Harzkörnchen entsteht, stört stark den Nachweis. Durch Zusatz von überschüssigem Kaliumfluoride entfärben sich die Harzkörnchen sehr leicht unter Bild-

1) Eingebracht in der sechsten Jahrsversammlung der Japanischen Chemischen Gesellschaft, Kyoto, April, 1953.

2) Z. B., vgl. K. Kimura und T. Asano, *Chemistry and Chemical Industry* (Kagaku to Kogyo), **2**, 258 (1949).

3) Amberlite XE-98 sowie Dowex 2 wurden gleichfalls benutzt, wobei befriedigende Ergebnisse erhalten wurden.

4) Eine Tüpfelplatte mit zwölf Vertiefungen: Vor dem Gebrauch wurde sie in warmer 1N Salzsäure etwa 10 Min. lange eingetaucht, mit Wasser gewaschen, in einem Luftbad bei 50°C getrocknet, und einige Zeit stehen gelassen.

5) Der Verfasser hat geringe Menge des Eisens mit einer Säule des anionenaustauschenden Harzes (RSCN-Form) von dem Ammoniumrhodanid erfolgreich beseitigt: *Japan Analyst*, **2**, 360 (1953).

6) Die Menge von Kobalt wurde folgenderweise bestimmt: 1) Wägung als $CoSO_4$: 2) Titration von H^+, die durch eine Säule des kationenaustauschenden Harzes, HR, ausgetauscht wurde.

TABELLE I. DIE RESULTATE DER EXPERIMENTE FÜR ERFASSUNGSGRENZE

Nr.	Menge von Co^{2+} (γ in 0.02 ccm.)	Zeit nach der Mischung (Min.)	Reaktionsresultate 1	2	3	4	5	6	7	8	9	10	11	12
1.	0.016	60	−	−	−	−	−	−	−	−	−	±	−	−
	„	1*	±	±	−	±	+	+	−	+	±	+	±	+
2.	0.16	2	±	±	±	−	±	−	±	±	±	±	−	−
	„	10	+	±	+	±	+	+	±	+	±	+	±	−
	„	60	+	+	+	±	+	+	±	+	+	+	+	+
3.	1.6	0.5–1	+	+	+	+	+	+	+	+	+	+	+	+
	„	10	⫴	⫴	⫴	⫴	⫴	⫴	⫴	⫴	⫴	⫴	⫴	⫴

− : nicht erkennbar, ± : unsicher, + : sicher, ⫴ : intensiv gefärbt.

* 1 Tag nach der Mischung.

ung vom farblosen Komplexfluoride[7].

(2) **Nickel (II):** Die grössere Menge von Nickel(II)salze färbt die Harzkörnchen gelbgrün und hindert ziemlich den Nachweis. Jedoch, a) durch Verdünnung der Lösung bis zum ungefähr 0.5 prozentigen oder noch kleineren Nickelgehalt[8], und danach b) durch einen Blindversuch, der mit der kobaltfreien Nickelsalze ausgeführt wurde, konnte man die obengenannte Störung fast beseitigen.

(3) **Kupfer (II):** Eine dunkelbraune Färbung, die auf die Harzkörnchen durch Reaktion von Kupfersalze mit Ammoniumrhodanid entsteht, wurde durch Zusatz der Kristallchen des Kaliumjodids und des Natriumthiosulfats leicht entfärbt.[9]

(4) **Mangan (II):** Grosser Überschuss der Mangan(II)salze stört nicht den Nachweis.

(5) **Chrom (III):** Weil Chrom(III)salze bei Anwesenheit des Ammoniumrhodanids das Harzkörnchen nicht färben, stört die intensiv dunkelgrüne bzw. blaue Farbe der Lösung von Chrom(III)salze den Nachweis gar nicht.

(6) **Uran (VI) als Uranylacetat:** Uranylsalze färben die Harzkörnchen lebhaft gelb, und verhindern die Reaktionsempfindlichkeit. Neben einem Blindversuche miteinander gestellt wurde dieser Nachweis mit genügender Empfindlichkeit ausgeführt.

(7) **Anionen:** Bei Gegenwart von OH^- oder CN^- findet die Färbung von Harze nicht statt, aber durch Zusatz von 1N Salzsäure konnte man diese Störung leicht beseitigen. Entschieden grosser Überschuss von F^-, I^-, und $S_2O_3^{2-}$ stört nicht den Nachweis. (Vgl. (1) und (3)).

(8) **Mineralsäuren:** 0.7 mg. Salz-, 1.0 mg. Schwefel-, 1.5 mg. Salpeter-, 7.2 mg. Phosphor-, und 1.2 mg. Perchlorsäuren stören nicht den Nachweis von 0.16 γ Kobaltmenge.

(9) **Karbonsäuren:** Bei Anwesenheit von 1.8 mg. Essig-, 2.0 mg. Oxal-, 2.0 mg. Wein-, und 1.5 mg. Zitronensäuren wurde der Nachweis von 0.16 γ Kobaltmenge nicht gestört.

Die so erhaltenen Resultate werden in Tabelle II. kurz zusammengestellt.

TABELLE II. EINFLUSSE DER BEGLEITSTOFFE

Begleitstoffe	Menge von Begleitstoffen	Nachweisbare Kobaltmenge	Grenzverhältnis	Anmerkungen
Fe^{3+}	700 γ	0.32 γ	$1:2.2\times10^3$	+KF (überschüssig).
Ni^{2+}	320 γ	0.32 „	$1:10^3$	<Ni 0.5 proz. u. Neben Blindversuche.
Cu^{2+}	1 mg	0.5 „	$1:2\times10^3$	+KI (Kristallchen) +$Na_2S_2O_3$ („ „).
Mn^{2+}	1 mg	0.2 „	$1:5\times10^3$	.....
Cr^{3+}	400 γ	0.32 „	$1:1.3\times10^3$	Neben Blindversuche.
UO_2^{2+}	700 γ	1.6 „	$1:4.5\times10^2$	Neben Blindversuche.
OH^-, CN^-	Grosser Überschuss.	0.16 „	.....	+1N·HCl (überschüss.).
F^-, I^- $S_2O_3^{2-}$	Grosser Überschuss.	0.16 „	.....	.....
A:	Grosser Überschuss.	0.16 „	.....	.....
B:	Grosser Überschuss.	0.16 „	.....	.....

A: HCl, H_2SO_4, HNO_3, H_3PO_4 und $HClO_4$.
B: Essig-, Oxal-, Wein- und Zitronensäuren.

7) I.M. Kolthoff, *Mikrochemie*, 8, 176 (1930).

8) F. Feigl, „Qualitative Analyse mit Hilfe von Tüpfelreaktionen," 3. Aufl. 1938, S. 220.

9) M. Ishibashi, „Qualitative chemische Analyse (Teisei Bunseki-Kagaku)," Band 1., 3. Aufl. 1947, (japanisch), S. 237.

Beidem oben ausgeführten Versuche, wurde es auch gefunden, dass in der einigen sogenannten „extrareinen" Probe von Nickel(II)chlorid, Nickel(II)karbonat, und Mangan(II)sulfat eine kleine Menge des Kobalts enthalten war.

Zusammenfassung

1. Der Nachweis von Kobalt mit Ammoniumrhodanid wird verbessert durch die Anwendung von der farblosen oder hellgelben ionenaustauschenden Harzkörnchen, und eine neue Tüpfelmethode wird vorgeschlagen.

2. Nach dieser Methode kann man den Nachweis geringer Menge des Kobalts bei Anwesenheit verschiedenartiger Ionen (Fe^{3+}, Ni^{2+}, Cu^{2+}, Mn^{2+}, Cr^{3+}, UO_2^{2+}, OH^-, CN^-, F^-, I^-, und $S_2O_3^{2-}$) sowie der Säuren (HCl, H_2SO_4, HNO_3, H_3PO_4, $HClO_4$, Essig-, Oxal-, Wein-, und Zitronensäuren) ausführen.

3. Wie oben erörtert, hat diese methode die folgenden Vorzüge:

(1) Grössere Empfindlichkeit und leichte Erkennbarkeit,

(2) Mit der Zeit steigende Deutlichkeit der Reaktion (vgl. Tabelle I),

(3) Erhaltbarkeit des Ergebnisses nach dem Trocknen der gefärbten Harzkörnchen,

(4) Ausführbarkeit ohne spezielle Reagenzien und lästige Verfahren,

(5) Ausführbarkeit für saure sowie neutrale Probelösung und seine höhere Spezifität (vgl. Tabelle II), u.s.w..

Zum Schluss möchte der Verfasser Herren Prof. Dr. E. Minami, Dr. M. Honda, und Dr. H. Kakihana für ihre wertvolle Ratschläge bei dieser Untersuchung seinen herzlichen Dank aussprechen.

Laboratorium der analytischen Chemie,
Chemisches Institut der
wissenschaftlichen Fakultät,
Tokyo Universität, Tokyo

Hydrogen Sulfide Cookings of p-Oxybenzyl Alcohols. I.

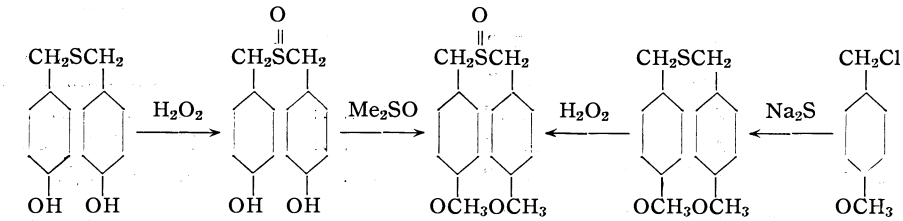
Hiroshi MIKAWA

(Received August 3, 1953)

The first experiments on model compounds in connection with the mechanism of kraft cooking processes were made by Enkvist[1]. Among others[2] he obtained a very important result that vanillyl alcohol gives vanillyl disulfide on cooking with an aqueous solution of hydrogen sulfide of *pH* 7 during 72 hours at 100°C. He proposed a theory of mechanism of kraft cooking mainly from the behaviours of vanillyl disulfide against aqueous alkali and his opinion has been generally accepted by the chemists of this field[1)3)].

In connection with the following paper, which deals with the hydrogen sulfide cookings of *p*-oxybenzyl ether, the reactivity of *p*-oxybenzyl alcohol was investigated at first. The expected product 4, 4′-dioxydibenzyl disulfide was not obtained but 4, 4′-dioxydibenzyl sulfide[1] was the only product obtainable when *p*-oxybenzyl alcohol was cooked during 6.5 hours or 70 hours. The yields of the monosulfide were 82 and 61% respectively for each cooking hours.

The structure of the monosulfide[1] was determined by the method shown in the scheme 1. As on methylation of the mono-

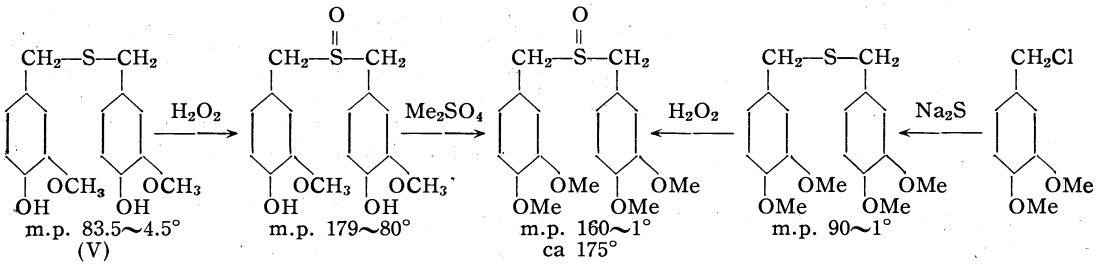


Scheme 1.
Determination of the constitution of 4, 4′-dioxydibenzyl sulfide

1) Enkvist and Moilanen, *Svensk Papperstidn.*, **52**, 183 (1949).
2) Enkvist and Hägglund, *festskrift tillägnad* J. Arvid Hedvall, **1948**, 149.
Enkvist, *Svensk Papperstion.*, **51**, 225 (1948).
3) Cf. Hägglund, "Chemistry of Wood", Academic Press Publishers, Inc., New York, N.Y. 1951. p. 484.

sulfide (I) sulfur was split off (probably as dimethyl sulfide) and dianisyl sulfide (IV) was not obtained by this process, that was oxidized at first to sulfoxide (II) and then methylated to dianisyl sulfoxide (III). According to our experience, on methylation of thiolignin with dimethyl sulfate and alkali similar splitting off of sulfur occurs probably as dimethyl sulfide.

As *p*-oxybenzyl alcohol did not give the expected disulfide, vanillyl alcohol was also examined in the similar way. It gave again monosulfide (72%) (V) and a very small amount of divanillyl disulfide as the result of 8 hours cooking. The constitution of divanillyl sulfide was determined in the same way as in 4, 4′-dioxydibenzyl sulfide according to the scheme 2. Diveratryl sulfoxide has two melting points.



Scheme 2.
Determination of the constitution of divanillyl sulfide

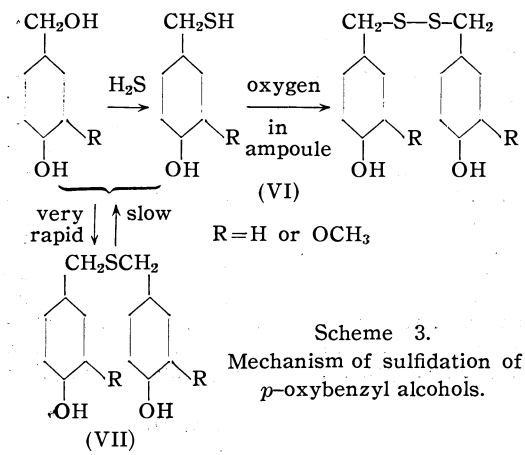
The reactivities of 4, 4′-dioxydibenzyl sulfide (I) and divanillyl sulfide (V) with aqueous alkali were also tested in the same manner as the procedure used by Enkvist in the case of divanillyl disulfide[1]. Monosulfides also split off sulfur as hydrogen sulfide, as is shown in the following table.

Table I. Desulfidation of Monosulfide (I) and (V) with Aqueous Alkali.
(5% NaOH, 100°)

	hrs.	splitted.
4, 4′-dioxydibenzyl	3	10.8%
Sulfide (I)	5	88.0%
Divanillyl sulfide (V)	3	19.7%

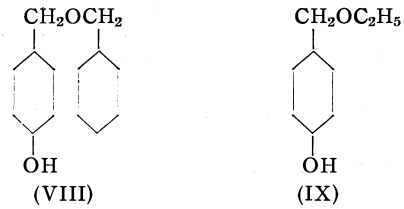
1) On the Mechanism of Sulfidation of *p*-Oxybenzyl Alcohols.

The following mechanism (scheme 3) is assumed to be most probable. At the beginning, hydrogen sulfide reacts with *p*-oxybenzyl alcohol so as to give *p*-oxybenzyl mercaptan (VI), which condenses rather rapidly with the remaining alcohol. The primary reaction product is thus monosulfide (VII). Monosulfide is, however, not completely stable; there it is in equilibrium with the alcohol and mercaptan.



Scheme 3.
Mechanism of sulfidation of *p*-oxybenzyl alcohols.

This assumption is not unreasonable, because, as will be shown in the next paper, benzyl ether linkage is very susceptible of being hydrolysed when it is activated by the phenolic hydroxyl group in its paraposition



(e.g. VIII and IX) and, therefore, the benzyl thioether linkage activated by both hydroxyl groups in 4 and 4′ positions may be surely

4) Enkvist communicated privately a preliminory opinion as follows: The first product in each case will be vanillyl mercaptan. If the solution has a high concentration of hydrosulfide ion and if its *p*H is slightly lower than 7—in his case it was about 5 after the digestions, as he reported proviously (cf. (1))—the substance will remain as vanillyl mercaptan until the opening of the tube. Then, the outer air will oxidize it during crystallization to vanillyl disulfide. If the concentration of hydrogen sulfide is slightly less and the *p*H is 7 or slightly higher as in our case, the vanillyl mercaptane will find occasion to react with vanillyl alcohol or sodium vanillyl mercaptide under the formation of vanillyl monosulfide.

hydrolyzable. Molecular oxygen in the air space of glass ampoule will oxidize the mercaptan, which exists in equilibrium with the monosulfide although its concentration is very low. Thus, monosulfide and disulfide are expected in our experiment, as the oxygen in the ampoule is rather limited. The reaction product obtained by Enkvist consisted mainly of disulfide, but this is not explainable by the above mechanism, as according to his private communication the ampoule used by him was not large enough to supply the necessary amount of oxygen. It is therefore possible that some other unknown factors are determining the course of the reaction; in one case mainly monosulfide and in the other mainly disulfide is obtained as reaction product[4].

2) On the Mechanism of the Kraft Cooking Process.

The monosulfide group of thiolignin had been assumed to be stable to aqueous alkali, but the present results indicate that this group is not stable just as disulfide group, at least when this is activated by both phenolic hydroxyl groups in 4 and 4′ positions. It seems, therefore, to be possible to explain the mechanism of sulfidation of lignin and desulfidation of thiolignin without considering the formation of the disulfide group. The mechanism may be explained more reasonably if the formation of both mono- and di-sulfide groups are taken in consideration. Because the side chain of lignin contains oxygen atoms of various oxidation stages, the formation of the disulfide group by self-oxidation will be easier in the case of lignin than in the model compounds. However, quantitatively speaking, the main part of the sulfur atoms, split off by alkali in the kraft cooking process may exist as a form of monosulfide.

As Mikawa et al. observed[5], X group of lignin was sulfidated with hydrogen sulfide quite rapidly and this reaction was completed after about 5 hours. The velocities of sulfidation of *p*-oxybenzyl alcohol and vanillyl alcohol are not yet clear. But the fact that they are sulfidated to a considerable extent during less than 10 hours cooking will support the opinion that X group of lignin is a benzyl alcoholic hydroxyl group with a phenolic hydroxyl in its para-position.

Experimental Part

1. Hydrogen Sulfide Cooking of *p*-Oxybenzyl Alcohol.

3.7 g. of *p*-oxybenzyl alcohol was added to a solution (final *p*H was adjusted to just 7) of $Na_2S \cdot 9H_2O$ (7.2 g.) in 300 cc. of Clark-Lubs buffer solution (108 g. of KH_2PO_4 and 15 g. of NaOH in 1000 cc. of water). The mixture was heated at 100° for 6.5 hours in a stainless autoclave of just 550 cc. capacity. On cooling, crystals of almost pure 4, 4′-dioxydibenzyl sulfide separated (3.29 g., 82%), which were recrystallized from toluene containing a little dioxane, m.p. 141–2°. Found: S, 12.9%, Calculated for $C_{14}H_{14}O_2S$: S, 13.0%.

The same reaction was performed during 70 hours in a rotating glass ampoule of 150 cc. capacity (*p*-oxybenzyl alcohol 2.0 g., $Na_2S \cdot 9H_2O$ 3 g., buffered hydrogen sulfide water of *p*H 7, 100 cc.). The yield of melting point pure 4, 4′-dioxydibenzyl sulfide was 1.2 g. (61%). 4, 4′-dioxydibenzyl disulfide was not obtained from the reaction mixture.

2. Hydrogen Sulfide Cooking of Vanillyl Alcohol.

The reaction was performed mainly as in the experiment 1 (vanillyl alcohol 2.5 g., $Na_2S \cdot 9H_2O$ 3 g., hydrogen sulfide water 100 cc., 8 hours at 100°, capacity of autoclave just 150 cc.). The separated crystals were filtered off, dissolved in alcohol, passed through a layer of active Al_2O_3, the alcohol was evaporated and the residue was recrystallized from toluene. Yield 1.8 g. (72%), m.p. 83.5–4.5°. This is divanillyl sulfide. Found: S, 10.5; MeO, 19.8, Calculated for $C_{16}H_{18}O_4S$: S, 10.4 MeO, 20.3%.

The mother liquor of this crystal separates after about a week, forming a mixture of large crystals of monosulfide and fine crystals of disulfide, from which the former were separated with a pincette and the latter were dissolved in acetone and purified by reprecipitation by water (50 mg.). It melted at 128–9° and does not show any m.p. depression in admixture with the authentic sample of divanillyl disulfide, which was synthesized according to the method of Manchot and Zahn[6].

3. Syntheses of 4, 4′-Dioxydibenzyl Sulfoxide and Divanillyl Sulfoxide.

4, 4′-Dioxydibenzyl sulfide (100 mg.) was dissolved in 4 cc. of glacial acetic acid, 0.3 cc. of 30% H_2O_2 was added and the solution was set aside over night at the ordinary temperature[7]. The reaction mixture was diluted with water and neutralized with $NaHCO_3$. The separated crystals were filtered, washed with water, dissolved in alcohol and reprecipitated with water, yield 70 mg., m.p. 184.5–5.0°. The analysis agrees with the compound, 4, 4′-dioxydibenzyl sulfoxide. Found: S, 11.8, Calculated for $C_{14}H_{14}O_3S$: S, 12.2%.

Divanillyl sulfoxide was also synthesized similarly from divanillyl sulfide (100 mg.). Yield 50 mg. Found: S, 9.7, Calculated for $C_{16}H_{18}O_5S$: S, 9,95%.

4. Methylation of Sulfoxides.

4, 4′-Dioxydibenzyl sulfoxide or divanillyl sulfoxide (80 mg.) was dissolved in 10 cc. of sodium hydroxide solution (NaOH 0.8 g.). 0.8 cc. of dimethyl sulfate was added and the whole shaken until it disappeared. The separated dianisyl or

4) Mikawa, Sato, Takasaki and Okada, *J. Soc. Chem. Ind. Japan*, 54, 299 (1951); TAPPI in the press. Mikawa, *J. Soc. Chem. Ind. Japan*, 54, 651, 762 (1951).

6) Manchot and Zahn, *Ann.*, **345**, 320 (1906).

7) Hinsberg, *Ber.*, **41**, 2838 (1908).

diveratryl sulfoxide (yields were very good) was filtered, washed and purified by reprecipitation from its acetone solution with water. Their melting points were not depressed in admixture with the authentic samples synthesized according to the experiments 5 and 6.

5. Syntheses of 4, 4′-Dimethoxydibenzyl Sulfide and Sulfoxide.

$Na_2S \cdot 9H_2O$ (2.40 g.) was dissolved as far as possible in alcohol (40 cc.), anisyl chloride (1.56 g.) was added and the whole refluxed for about 30 min.[8]. Water was added to the mixture, extracted with ether, washed with water, the ether was evaporated and the residue (1.5 g.) was distilled at 0.005 mmHg (bath temp. 150°). The residue (0.7 g.) was dissolved in several grams of glacials acetic acid. 0.8 cc. of 30% H_2O_2 was added (during which some heat was evolved), and after about 4 hours poured into water. The precipitated crystals were filtered, washed with water, dried and recrystallized twice from ethyl alcohol containing a little water, m.p. 172–3°. Found: MeO, 20.4; S, 11.3, Calculated for $C_{16}H_{18}O_3S$: MeO, 21.4; S, 11.0%.

6. Syntheses of Diveratryl Sulfide and Sulfoxide.

Veratryl alcohol (3 g.) was converted to chloride according to the method of Freudenberg[9]. The somewhat crude veratryl chloride obtained was subjected to reaction with 2.5 g. of $Na_2S \cdot 9H_2O$ in 80 cc. of alcohol. NaCl was filtered and the filtrate was concentrated in vacuo, water was added and the neutral reaction product extracted with benzene, the benzene extract was dried with Na_2SO_4, the solvent was evaporated and the residue was crystallized from its ether solution by petroleum ether. Recrystallisation from the mixture of benzene and petroleum ether yielded a product (1.0 g.), which melted at 90–1°. The analysis agrees with the theory that the compound is diveratryl sulfide. Found: S, 10.8, Calculated for $C_{18}H_{22}O_4S$: S, 9.6%.

Diveratryl sulfide (100 mg.) and H_2O_2 (30%, 0.4 cc.) was dissolved in 4 c.c. of glacial acetic acid and set aside overnight at the room temperature. Water was added to the solution, neutralized with $NaHCO_3$ and the separated crystals were filtered, dissolved in acetone and reprecipitated with water (70 mg.), which melted at 169.5–70.5° when heated rapidly and at ca. 175° when heated slowly. The analysis agrees with the theory that the compound is diveratryl sulphoxide. Found: S, 9.0, Calculated for $C_{18}H_{22}O_5S$: S, 9.14%.

7. Reactions of 4, 4′-Dioxydibenzyl Sulfide (1) and Divanillyl Sulfide (2) with Aqueous Solution of Alkali.

100 mg. of (1) or (2) was heated at 100° with 5% (cf. reference (1)) aqueous solution of NaOH in a micro-methoxyl apparatus due to Zeisel in the atmosphere of hydrogen. The solution was cooled and acidified with glacial acetic acid and the liberated hydrogen sulfide was swept with hydrogen into dilute NaOH in wash trap and receiver. The combined sodium hydroxidesolution was oxidized with bromine water and SO_4'' was determined as usual. Results obtained are shown in the table.

The author wishes to express his gratitude to the following members of the laboratory, Dr. H. Okada, the head, Miss. S. Suehiro and Mr. K. Sato for their encouragement and help.

Research Laboratory of the KOKUSAKU Pulp Ind. Co. Ltd.
184, 1-chome, Kamiochiai, Shinjuku-ku, Tokyo, Japan

8) Märker, *Ann.*, **136**, 88 (1965).
9) Freudenberg, Carrara and Cohn, *Ann.*, **446**, 87 (1925).

p-Hydroxy-Benzyl Ethers As Lignin Models. II.

Hiroshi MIKAWA

(Received August 3, 1953)

It is now generally accepted that the sulfonatable groups of lignin are not unique and consist of three different types of groups, namely X, Z, and B[1]. The constitutions of these groups are concluded mainly from the experiments on model compounds and the analyses of lignosulfonic acids. Recently Lindgren and Adler gave very useful reviews concerning the sulfonatable groups of lignin[2].

In the present paper the constitution of X group is discussed from the results of the hydrogen sulfide cookings of *p*-hydroxybenzyl ethers as lignin models. A series of experiments of Lindgren, Enkvist, Erdtman, Adler, Leopold and Migita et al. On the sulfonation (rapid sulfonation of *p*-hydroxybenzyl alcohols and slow sulfonation of *p*-methoxybenzyl alcohols[3]) and sulfidation (former compounds

1) Lindgren, *Acta Chem, Scand.* **5**, 603 (1951). Mikawa, Sato, Takasaki and Okuda, *J. Soc. Chem. Ind. Japan*, **54**, 299 (1951); TAPPI in the press. Mikawa, *ibid*, **54**, 651. 741, 762 (1951). **55**, 294, 342 (1952).

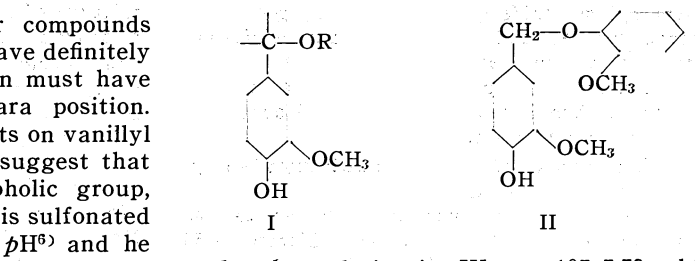
2) Lindgren, *Svensk Papperstidn.* **55**, 78 (1952). Adler and Lindgren, *ibid.* 565.

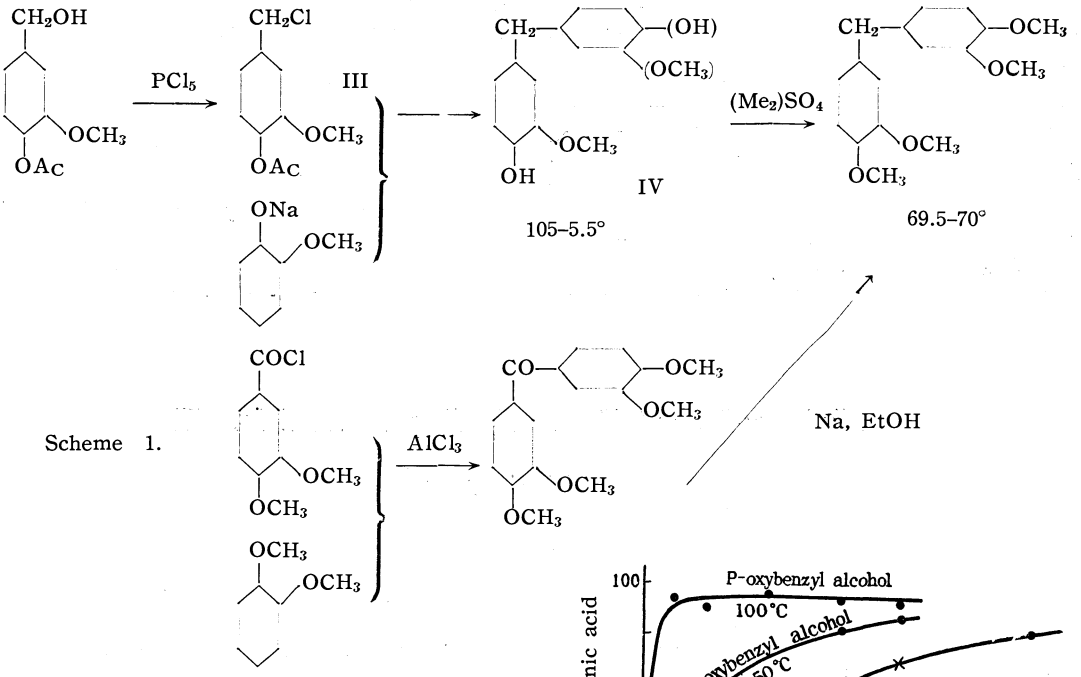
3) Lindgren, *Acta. Chem. Scand.* **1**, 779 (1947); **3**, 1011 (1949). Erdtman and Leopold, *ibid*, **3**, 1358 (1949). Adler and Yllner, *Svensk Papperstidn.* **55**, 238 (1952). Adler, Lindgren and Saeden, *ibid.* **55**, 245 (1952). Migita, Nakano, Ichino and Mikawa, *Tech. Assoo. Pulp and Paper Ind. Japan*, in the press.

react with H_2S[4] but the latter compounds do not[5]) of model compounds have definitely established that X group of lignin must have phenolic OH group in its para position. Though the results of experiments on vanillyl alcohol and *p*-oxybenzyl alcohol suggest that X group is a free benzyl alcoholic group, Lindgren found that pinoresinol is sulfonated comparatively rapidly at higher *p*H[6]) and he pointed out the possibility that X group is the benzyl alkyl ether grouping.

As we have demonstrated, one of the most striking characteristics of X group is its reactivity with H_2S at *p*H 7[1]). It will be, therefore, most desirable to test at the same *p*H the reactivity of H_2S with benzyl ethers which have a phenolic OH group in its para position[7]).

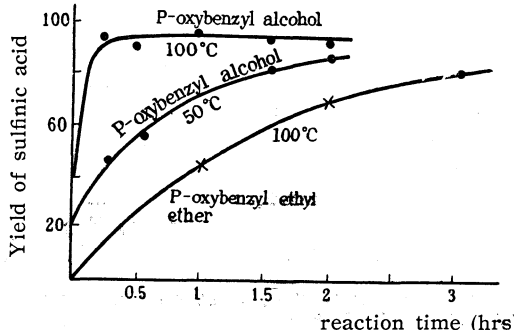
The syntheses of compounds of the type, for example, I is highly desirable for our purposes. Synthesis of II was attempted at first according to scheme 1, but the condensation of sodium guaiacolate and III in toluene (which contains a little alcohol) gave diphenylmethane derivative IV, m.p. 105–5.5°, which on methylation gave 3, 4, 3′, 4′-tetramethoxydiphenylmethane. The melting point, 69.5–70°, of the methylated product of IV was not depressed in admixture with the authentic sample of 3, 4, 3′, 4′-tetramethoxydiphenylmethane (which was synthesized from 3,4,3′,4′-tetramethoxybenzophenone according to the method of Robinson[8]) but showed marked depression with the authentic sample of veratryl guaiacyl ether, m.p. 78–9°. The structure of IV is therefore either 4, 4′-dioxy-3, 3′-dimethoxy- or 4, 3′-dioxy-3, 4′-dimethoxydiphenyl-methane, although, of course, the former structure is by far the more probable.





Scheme 1.

As, therefore, the syntheses of the compounds of type I seemed to be comparatively



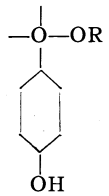
×: *p*H 7.65 Sulfination of *p*-oxybenzyl
●: *p*H 6.22 alcohol (5% SO_2, 1% NaOH)
and
p-oxybenzyl ethyl ether (*p*H 6.22 & 7.65)

4) Enkvist and Mollanen, *Svensk Papperstidn.* **52**, 183 (1949). Mikawa, cf. previous paper.
5) Enkvist, unpublished (cf. (2)).
6) Iindgren, *Acta Chem. Scand.* **6**, 91 (1952).
7) T. Enkvist made recently profound investigations on the sulphidation of model compounds. cf. *Svensk Papperstidn.* **55**, (1952). In this paper he reaches already the conclusion that the compounds with benzyl ether linkage activated by phenolic OH group in its orth and para position combine with sulfur by hydrosulfide cooking at *p*H 7.
8) Robinson, *J. Chem. Soc.*, **107**, 273 (1915).

TABLE 1. SULFONATIIN OF *p*-OXYBENZYL ETHYL ETHER 100°C

pH	hr 1	2	3
6.22	45.8	—	86.3
7.65	46.4	73.2	—

difficult[9], it was aimed at reaching the compounds of the type V, as it was made clear from the following results (a) and (b) that the methoxyl group in the meta position does not seem to exert any significant effect on the reactivity of the groups in the side chain, which fact Lindgren has already suggested in his review[2].



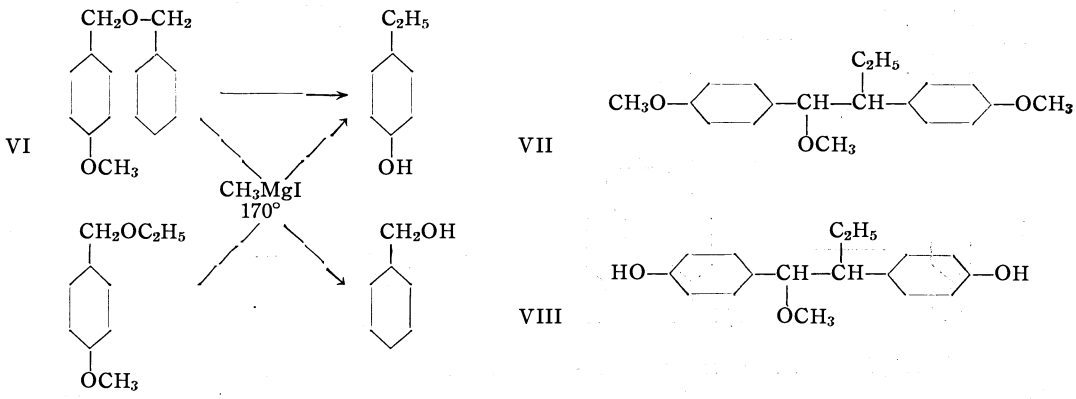
V

(a) *p*-Oxybenzyl alcohol is sulfonated as vanillyl alcohol quite rapidly and almost quantitatively with sulfite solution to give *p*-oxybenzyl sulfonic acid, as is evident from the figure[3].

(b) As was shown in the previous paper, *p*-oxybenzyl alcohol reacts with H_2S at *p*H 7 very easily and 4, 4′-dioxydibenzyl sulfide was obtained, just as vanillyl alcohol is.

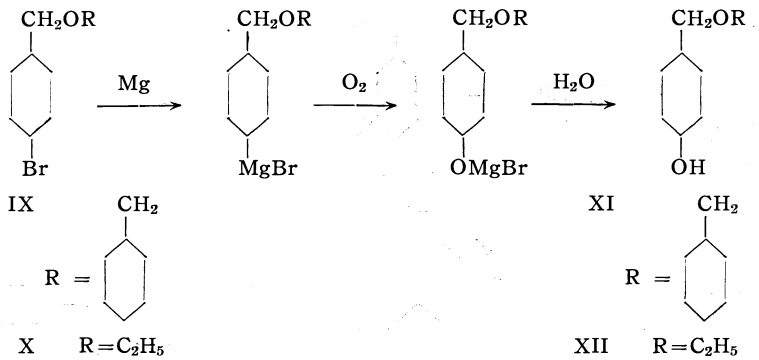
Demethylations of *p*-methoxybenzyl ethers with methyl magnesium iodide were attempted at first[10]. *p*-Methoxydibenzyl ether VI gave a considerable amount of benzyl alcohol and *p*-ethylphenol, when treated with methyl magnesium iodide at 170°. *p*-Methoxybenzyl ethyl ether gave similarly *p*-ethylphenol under the same conditions (see scheme 2). It was therefore made clear that the selective cleavage of arylether linkage of these compounds with the reservation of benzyl ether linkage is fairly difficult under these conditions. T. Takahashi was able, however, recently to demethylate VII to VIII with methyl magnesium iodide[11].

Scheme 2.



At last, *p*-oxybenzyl ethers (XI and XII) were synthesized from the corresponding *p*-bromobenzyl ethers (IX and X) via their Grignard compounds as shown in the scheme 3[12]. The actual Yeilds of XI and XII were 20 and 23% of the theoretical respectively.

Scheme 3.



9) However, B. Leopold synthesized recently vanillyl methyl ether in a very simple way. cf. *Svensk Papperstidn*, **55**, 816 (1952).

10) Späth, *Monatsh.* **35**, 319 (1914); **36**, 6 (1915). Luttinghaus and Saar: *Angew. Chem.*, **51**, 915 (1938). Kharasch and Huang, *J. Org. Chem.*, **17**, 669 (1952).

11) Takahashi: *J. Chem. Soc. Japan*, in the press.

12) Porter and Steel, *J. Am. Chem. Soc.*, **42**, 2650 (1920). Ivanoff, *Bull. Soc. Chim.*, **1**, 47 (1925). Bert and Dorier, **182**, 63 (1926). Smith, Hoehn and Ungnade, *J. Org. Chem.*, **4**, 351 (1939).

The boiling and melting points of these compounds and the melting points of some of their derivatives were shown in Table II.

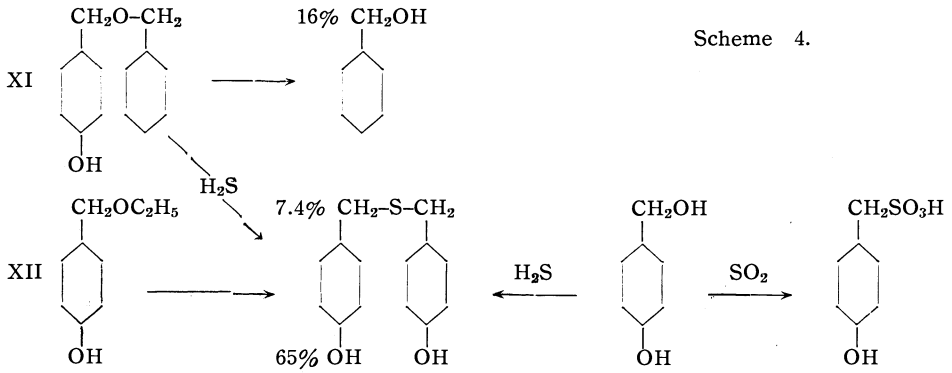
TABLE II.

		b.P., m.p.		*p*-nitro-benzoate	3, 5-dinitro-benzoate	acetate
HO—⟨⟩—CH_2OCH_2—⟨⟩	XI	b.p. 0.005	130–5°	m.p. 74–5°	—	m.p. 45.5–6°
HO—⟨⟩—$CH_2OC_2H_5$	X	b.p. 0.8	105°	m.p. 74–5°	m.p. 107–8°	—
		m.p.	50–1°			

p-Oxydibenzyl ether XI was sealed in an ampoule with H_2S water of *p*H 7, shaken well and heated for 15 hours at 100°C. Because of the low solubility of this compound the reaction was heterogeneous. 4,4'-dioxydibenzyl sulfide and benzyl alcohol were obtained in the yields of 7.4 and 16% (of the theory) respectively. The former was separated as such and the latter as its 3,5-dinitrobenzoate. The yields were calculated from those of the products of correct melting points.

p-Oxybenzyl ethyl ether XII was treated similarly for 18 hours. Pure 4,4'-dioxydibenzyl sulfide was obtained in the yield of 65% (of the theory). In this case the reaction was homogeneous. These results were shown in scheme 4.

Scheme 4.

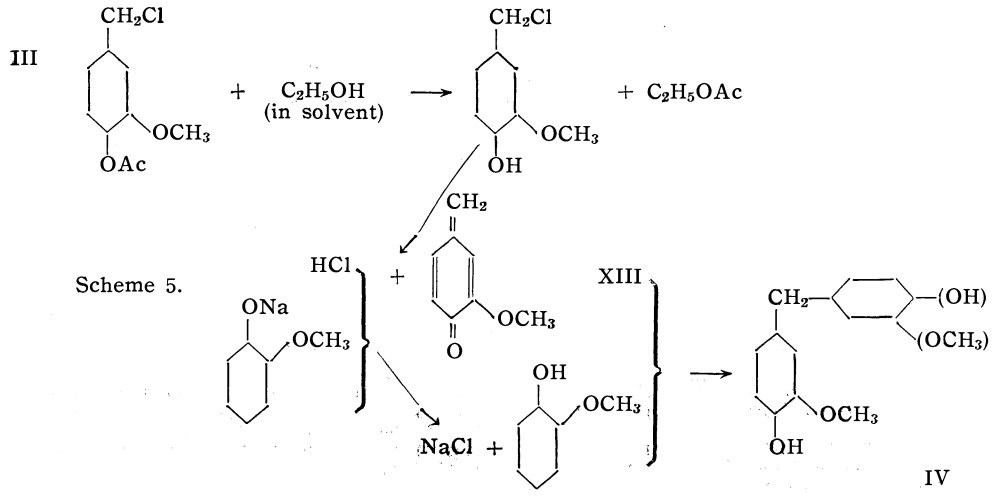


p-Oxybenzyl ethyl ether XII was sulphonated at pH 6.22 and 7.65. As is shown in the figure and Table 1, the sulfonation was very rapid.

Discussion

i) The Condensation of sodium guaiacolate and III in toluene containing a small amount of alcohol to give diphenylmethane derivative IV at comparatively low temperature suggests to us that the reaction has proceeded via the methylene quinone structure XIII as is shown in scheme 5. It is a well known fact,

Scheme 5.



that pseudophenol alcohol halides condense with phenols or dimethylanilines to give diphenylmethane derivatives[13].

ii) No attempt have been made to cleave lignin molecule with grignard reagent of its building stones[14]. As at least about 50% of the building stones of native lignin are thought to be linked through aryl ether linkage between the hydroxyl group of the side chain and the phenolic OH group in its para position[2], it will be very interesting to use grignard reagent to cleave these linkages.

iii) The fact that the *p*-oxybenzyl ethers XI and XII are easily hydrolyzed even at pH 7 at 100°C and react with H_2S to give 4,4'-dioxydibenzyl sulfide is completely in line with the properties of X group[1].

The fact suggests to us again a possibility that this group is a benzyl alkyl ether group with phenolic OH group in its para position. As the sulfidation velocity of X group is approximetely known[1], we will be able to compare the velocity with that of the models, if the latter is measured with sufficient accuracy. It is, therefore, very interesting to measure accurately the sulfidation velocity of model compounds with the so-called dilution method[15] using radioactive mono sulfide.

p-Oxybenzyl ethyl ether was sulfonated with neutral sulfite solutions and moreover the velocities of sulfonation do not seem to depend on the pH values. These findings are also completely parallel with the properties of X group.

Added in proof. According to the private communication of Dr. J. de Jonge, Philips Research Laboratories, Holland, our sample of *p*-hydroxybenzyl ethyl ether was hydrolyzed very quickly. i.e., at pH 6.8 after 3 hours and at pH 5.2 after 6 hours it was completely hydrolyzed into *p*-hydroxybenzyl alcohol at 100° and somewhat less completely at pH 8.1 after 6 hours at 100°. It may, therefore, safely be concluded that in the reaction with H_2S hydrolysis of ether to the corresponding alcohol predeeds the formation of the sulfide.

Experimental Part

1. Synthesis of 3-Methoxy-4-acetoxybenzyl Chloride. Acetylvanillin was reduced to acetylvanillyl alcohol according to the method used by Carothers and Adams[16]. 0.2 g. of $PtO_2 \cdot H_2O$ (according to Adams et al.[17]) was added to a solution of acetylvanillin (14 g.) and $FeCl_2$ (0.5 cc. of 0.2 mol. solution) in 200 cc. of absolute ethanol and was shaken with hydrogen (4 atm.) until no more hydrogen was absorbed. Acetylvanillyl alcohol (11.2 g.) was obtained as a very viscous oil.

2 g. of this acetylvanillyl alcohol was dissolved in 20 cc. of dry chloroform and pulverized PCl_5 (2 g.) was added slowly (during which some heat and HCl gas were evolved). The chloroform solution was washed well with water, dried with Na_2SO_4, the solvent removed in vacuo and the residue (1.9 g.) crystallized from petroleum ether (1.0 g.). The product obtained melted at 46–7° and the analyses agree with the compound being 3-methoxy-4-acetoxybenzyl chloride. Found: Cl, 15.9; CH_3O, 14.0, Calculated for $C_{10}H_{11}O_3Cl$: Cl, 16.6; CH_3O, 14.4%.

2. Condensation of 3-Methoxy-4-acetoxybenzyl Chloride with Sodium Guaiacolate. Sodium (1.1 g.) was dissolved in 20 cc. of anhydrous ethanol and guaiacol (7 g.) and toluene (40 cc.) were added. 3-Methoxy-4-acetoxybenzyl chloride (8 g.) was dissolved in toluene (70 cc.). The two solutions were mixed at once and the whole was warmed at 40° for 30 minutes, the rest stood over-night and was poured into a dilute solution of NaOH and well shaken. Neutral fraction (4.22 g.) was extracted with ether. The aqueous layer was acidified, extracted with ether, and the solvent removed. The residue (6.1 g.) solidified on standing, which was rubbed on a clay plate, dissolved in ether, passed through active Al_2O_3, ether removed and recrystallized from benzene to give white needles (4.06 g.), m.p. 105–5.5° (I).

(I) was methylated with dimethyl sulfate and alkali and recrystallized from aqueous ethanol to give white leaflets, melting at 69.5–70° (II), which was not depressed in admixture with the authentic sample of 3, 4, 3', 4'-tetramethoxydiphenylmethane. (I) was therefore either 4, 4'-dioxy-3, 3'-dimethoxydiphenylmethane or 4, 3'-dioxy-3, 4'-dimethoxydiphenylmethane. The methoxyl values of (I) and (II) and the mixed melting points of them with several compounds are as follows:

(I), m.p. 105–5.5°, mixed melting point with vanillyl alcohol, 90–2°. Found: CH_3O, 23.5, Calculated for $C_{15}H_{16}O_4$: CH_3O, 23.8%.

(II), m.p. 69.5–70°, mixed melting points with diveratryl ether and veratryl guaiacyl ether, 54–7° and 58–61° respectively. Found: CH_3O, 42.5, 42.6, calculated for $C_{17}H_{20}O_4$: CH_3O, 43.0%.

3. Synthesis of Veratryl Guaiacyl Ether. Veratryl chloride was synthesized according to the method of Freudenberg[18]. Metallic sodium (0.31 g.) was dissolved in 100 cc. of absolute ethanol, guaiacol (2 g.) added, a solution of veratryl chloride (2.2 g.) in 10 cc. of benzene added and the whole was refluxed for 1 hour. The neutral fraction of the product was recrystallized from alcohol (1.5 g.), m.p. 78–9°. The analysis shows that the compound is veratryl guaiacyl ether. Found:

13) Richter-Anshütz: "Chemie der Kohlenstoffverbindungen" Leipzig 1935, Bd. II$_2$ Seite 371.
14) Brauns, "Chemistry of Lignin" New York 1952, page 574.
15) Wahl and Bonner: "Radioactivity Applied to Chemistry" New York 1951, page 94.
16) Carothers and Adams, *J. Am. Chem. Soc.*, **46**, 1680 (1924).
17) Adams, Voorhees and Shriner, *Org. Synth.* **8**, 92 (1928).
18) February, Carrara and Cohn, *Ann.* **446**, 87 (1925).

CH_3O, 33.7; Calculated for $C_9H_{11}O_4$: CH_3O, 33.9%.

4. Synthesis of *p*-Oxybenzyl Sulfonic Acid. *p*-Oxybenzyl alcohol (3.02 g.) was dissolved in a sulfite solution containing 5 and 1% of SO_2 and NaOH respectively and heated in an autoclave at 100° for 1 hour. The solution was boiled in vacuo, filtered, passed through ion exchange resin IR 120, boiled again in a vacum, neutralized with excess $BaCO_3$, filtered and the solution of the barium salt was evaporated to dryness. The residue was leached with a little water, filtered and again evaporated to dryness. The residue was extracted with ethanol, which contains a little water, ether was added and the precipitated barium salt was filtered (4.0 g.). The analysis shows that the compound is a salt of *p*-oxybenzyl sulfonic acid. Found: Ba, 26.8; Calculated for $C_7H_7O_4SBa_{1/2}$: Ba, 26.8%.

1.0 g. of the barium salt was dissolved in water, passed through ion exchange resin IR 120, the same pyridine added and the whole was evaporated to dryness in vacuo. The residue was recrystallized from a mixture of dioxane acetone and alcohol to give pyridinium salt of *p*-Oxybenzyl sulfonic acid (0.8 g.) m.p. 129–30°. Found: S, 13.0, Calculated for $C_{12}H_{13}O_4NS$: S, 12.0%.

5. Synthesis of *p*-Methoxydibenzyl Ether. 4.2 g. of sodium was dissolved in a solution of anis alcohol (50 g.) in toluene (50 cc.) and when almost all of the metal disappeared, 20 g. of anis alcohol was added in order to complete the reaction. A solution of benzyl chloride (22.7 g.) in 30 cc. of toluene was then added and the mixture refluxed for 1 hour. The toluene solution was washed with water, dried with Na_2SO_4, the solvent removed, and the residue was distilled repeatedly in a vacuum in order to remove anis alcohol as far as possible. The yield of *p*-methoxydibenzyl ether of $bp_{0.8}$ 155–60° was 22 g. Found: CH_3O, 13.1, Calculated for $C_{15}H_{16}O_2$: CH_3O, 13.6%.

6. Attempted Demethylation of *p*-Methoxybenzyl Ethyl Ether to *p*-Oxybenzyl Ethyl Ether. *p*-Methoxybenzyl ethyl ether (1.7 g.) was added to a solution of methyl magnesium iodide, which was prepared from 8.5 g. of methyl iodide, 1.45 g. of magnesium and 50 cc. of ether. The ether was distilled off and the residue was heated in an oil bath for 2 hours (the temperature was raised during 1 hour to 170° and kept at that temperature for 1 hour). On cooling, the residue solidified. This was decomposed with a concentrated aqueous solution of NH_4Cl, acidified and extracted with ether. The ether extract was shaken with dilute alkali, acidified, extracted with ether, dried with Na_2SO_4, the solvent removed and the phenolic residue was converted to its *p*-nitrobenzoate. Repeated recrystallizations from ethanol yielded a product of m.p. 80–1°, not depressed in admixture with *p*-nitrobenzoate of *p*-ethylphenol (m.p. 80–1°) obtained from *p*-methoxydibenzyl ether, when it was decomposed with methyl magnesium iodide (see experiment 7).

7. Attempted Demethylation of *p*-Methoxydibenzyl Ether to *p*-Oxydibenzyl Ether. *p*-Methoxydibenzyl ether (2.19 g.) was added to a solution of methyl magnesium iodide, which was prepared from 8.5 g. of methyl iodide, 1.45 g. of magnesium and 50 cc. of ether. The ether was distilled off and the residue was heated as in the experiment 8. The residue was decomposed with a concentrated aqueous solution of NH_4Cl, acidified and extracted with ether, the solvent removed and the residue (2.01 g.) was separated into neutral (I) and phenolic (II) fractions.

(I) was distilled in a vacuum and the distilled oil (0.84 g.) converted to its *p*-nitrobenzoate, which melted after recrystallization from ethanol at 82–3° (1.4 g.), not depressed in admixture with the authentic *p*-nitrobenzoate of benzyl alcohol (82–3°).

(II) was also distilled in a vacuum and the distilled oil (0.65 g.) converted again to its *p*-nitrobenzoate, which melted after recrystallization from ethanol at 80–1° (0.9 g.), not depressed in admixture with the *p*-nitrobenzoate obtained in the experiment 8. A part of this *p*-nitrobenzoate was hydrolysed with ethanolic NaOH and converted as usual to the carboxymethyl ether, which melted after recrystallization from water at 96–6.5°. These melting points agree well with those of *p*-ethylphenol[19].

8. Synthesis of *p*-Bromodibenzyl Ether. 3g. of potassium was dissolved at the boiling point of toluene in 20 g. of benzyl alcohol, which was diluted with 20 g. of toluene. When almost all of the metal disappeared, 2 g. of K, 5 g. of benzyl alcohol and 5 g. of toluene were added and the reaction was completed. 27 g. of *p*-bromobenzyl bromide in 40 cc. of toluene, which was boiled in a vacuum in order to expel a trace of HBr, was added at once to the suspension of the alcoholate. During ca. 1/2 hours the mixture was maintained at its boiling temperature. Water was added and the reaction product was taken up in ether. The solvent was driven off and the residue was fractionary distilled in a vacuum. The yield of *p*-bromodibenzyl ether of $bp_{0.8}$ 142–45°C was 28 g. (92.5%). Found: Br, 28.9, Calculated for $C_{14}H_{13}OBr$: Br, 28.9%.

9. Synthesis of *p*-Oxydibenzyl Ether. A solution of *p*-bromodibenzyl ether (27.6 g.) and ethyl bromide (10.9 g.) in 90 cc. of ether was gradually added during 5 hours to magnesium in a three necked flask, which was equipped with a dropping funnel, stirrer and a reflux condenser. After the reaction was completed, dry oxygen was bubbled through the reaction mixture for 2.5 hours (during which process some heat was evolved and the solution was separated gradually into two layers). All of the reaction products were decomposed with concentrated aqueous solution of NH_4Cl and then with dilute HCl. The products were extracted exhaustively with ether and separated into neutral (16.0 g.) and phenolic (5.5 g.) fractions. The latter was distilled in a high vacuum. Almost all of the oil (yield 4.3 g., 20% of the theoretical) was distilled at a very constant tmperature of 130–5° 0.005 mmHg.

p-Nitrobenzoate: This was synthesized as usual with *p*-nitrobenzoyl chloride and pyridine

19) McElvain: "The Characterisation of Organic Compounds" New York 1949, page 251.

and recrystallized from methanol. It melted at 74–5°.

Acetate: This was synthesized as usual with acetic anhydride and pyridine and recrystallized from methanol containing a little water. It melted at 45.5–46°. Found: CH_3CO, 16.9, Calculated for $C_{14}H_{14}O_2$: CH_3CO, 16.8%.

10. Synthesis of *p*-Oxybenzyl Ethyl Ether. A solution of *p*-Bromobenzyl ethyl ether (21.5 g.) and ethyl bromide (10.9 g.) in 85 cc. of ether was added dropwise during 2 hours to magnesium (5 g.) in a three necked flask in an atmosphere of hydrogen (during which the content separated into two layers, but the oily heavier layer did not disturb the reaction, because this was not so viscous). After the reaction was completed, the content was evaporated in order to expel hydrogen. Dry oxygen was then passed through the mixture (during which time a very viscous grayish colored mass was deposited, which was stirred frequently during the oxidation). After about 2 hours, the entire content was decomposed with concentrated aqueous solution of NH_4Cl and then acidified with dilute HCl, and extracted with ether. The ether extract was shaken with dilute NaOH solution, which was acidified and extracted again with ether, the solvent removed, and the residual oil (4.63 g.) distilled in a high vacuum. Almost all the oil distilled at 105°/0.8 mmHg (3.9 g., 23% of the theoretical), which solidified the next day, m.p. 50–1°. The analysis shows that the compound is *p*-oxybenzyl ethyl ether. Found: C_2H_5O, 28.8, calculated for $C_9H_{12}O_2$: C_2H_5O, 28.6%. *p*-Nitrobenzoate: m.p. 74–5°. Found: C_2H_5O, 14.5, Calculated for $C_{16}H_{15}O_5N$: C_2H_5O, 15.0%. 3, 5-Dinitrobenzoate: m.p. 107–8°. Found: C_2H_5O, 13.5, Calculated for $C_{16}H_{14}O_7N$: C_2H_5O, 13.0%.

11. Hydrogen Sulfide Cooking of *p*-Oxydibenzyl Ether. *p*-Oxydibenzyl ether (1.05 g) was added to a solution of $Na_2S \cdot 9HO$ (1.2 g.) in 100 cc. of Clark-Lubs buffer solution (final pH was adjusted to just 7). The mixture was heated in a glass ampoule at 100° for 15 hours (during which the ampoule was shaken vigorously). Because of the low solubility of the phenol the reaction was heterogeneous. After the reaction the organic materials were extracted with ether. The ether extract was dried, the solvent removed, and the faintly pink coloured residual oil (1.10 g.) was let to stand for crystallization. After several days a small amount of crystals separated. Ca. 1 cc. of petroleum ether was added, which did not mix with the oil, and the mixture was kept in a refrigerator further 2–3 days (during which time the amount of the crystalls increased). They were filtered and weighed (50 mg.) (I). The filtrate was diluted with benzene and kept again in a refrigerator to give further 0.13 g. of crystalline material (II), which was filtered and the mother liquor so obtained was separated into phenolic (III) and neutral fractions (IV) which weighed 0.53 and 0.38 g. respectively.

(I) was recrystallized from aqueous ethanol to give leafy plates (40 mg.), m.p. 170.5–71°, which was soluble in dil. NaOH. This was not investigated further.

(II) was also recrystallized from aqueous ethanol, to give 5 mg. or (I) and 50 mg. of 4, 4′-dioxydibenzyl sulfide, having m.p. and mixed m.p. 139–40°.

(III) was acetylated with pyridine and acetic anhydride. 70 mg. of *p*-acetoxydibenzyl ether of correct m.p. was recovered.

(IV) was converted to its 3, 5-dinitrobenzoate, which was recrystallized from ethanol to give 300 mg. of 3, 5-dinitrobenzoate, of benzyl alcohol, having m.p. and mixed m.p. 113–13.5°.

12. Hydrogen Sulfide Cooking of *p*-Oxybenzyl Ethyl Ether. *p*-Oxybenzyl ethyl ether (0.76 g.) was added to a solution of $Na_2S \cdot 9H_2O$ (1.2 g.) in 100 cc. of Clark-Lubs buffer solution (pH was adjusted to just 7). The mixture was heated in a glass ampoule at 100° for 18 hours (during which time the phenol went into solution and the reaction proceeded in a homogeneous phase). On cooling, beautiful crystalls of 4, 4′-dioxydibenzyl sulfide separated (final pH of the solution was 7.2), which was filtered (0.61 g.) and recrystallized three times from aqueous ethanol (450 mg.), m.p. and mixed m.p. 139–40°. The yield was 65% of the theory.

13. Sulfonation of *p*-Oxybenzyl Ethyl Ether at Various pH (cf. figure). *p*-Oxybenzyl ethyl ether was dissolved (concentration 0.056 mol/l) in a sulfite solution (total SO_2 5%, pH 6.22 or 7.65, 35 cc.), heated at 100° for 1–3 hours in a glass ampoule. The whole content was passed through ion exchange resin IR 120, to remove cations. 7 cc. of 1N H_2SO_4 was added, boiled in vacuo to expel SO_4, 40 cc. of saturated solution of $Ba(OH)_2$ was added, filtered and passed again through IR 120. The solution so obtained was titrated with 1/10 N NaOH with methyl red as an indicator. Results were shown in the figure and Table 1.

The author wishes to express his gratitude to Messrs. M. Takahashi and T. Takahashi at the Tokyo University for their kind advice and to the follwoing members of the laboratory, Dr. H. Okada, Miss S. Suehiro and Mr. K. Sato for their encouragement and help.

Research Laboratory of the KOKUSAKU Pulp Ind. Co. Ltd.
184, 1-chome, Kamiochiai, Shinjuku-ku, Tokyo, Japan

Terminally Phenylated Conjugated Unsaturated Ketones II.[1] *Silver Acetate on Dibenzylidenecycloalkanone Tetrabromides*

Ping-Yuan YEH

(Received August 4, 1953)

In the course of a study of the aromatization of 2,6-dibenzylidenecyclohexanone[2] the action of silver acetate on dibenzylidenecycloalkanone tetrabromides was studied.

Diacetoxy-dibromo-2, 5-dibenzylidenecyclopentanone was obtained by the action of silver acetate on 2,5-dibenzylidenecyclopentanone tetrabromide in acetic acid even when 4 mole equivalents of silver acetate were used. The corresponding tetraacetoxy-derivative was obtained, however, when 4 mole equivalents of silver acetate were reacted with 2,6-dibenzylidenecyclohexanone tetrabromide. On using 2 mole equivalents of silver acetate and heating them at 85~90° for an hour, both diacetoxydibromo- and triacetoxymonobromo-derivatives were obtained with a 10% recovery of 2, 6-dibenzylidenecyclohexanone tetrabromide. If the temperature was maintained at 85~90° for more than 2 hours or the reaction mixture was refluxed for half an hour the only crystalline product identified was 2,6-dibenzylidenecyclohexanone. By refluxing half an hour in acetic acid, however, tetraacetoxy- and tetrabromo-2,6-dibenzylidenecyclohexanone did not give 2,6-dibenzylidenecyclohexanone.

Two isomers of diacetoxy-dibromo-2,5-dibenzylidenecyclopentanone, m.p. 213~214° (decomp.), colorless plates, and m.p. 185~186°, colorless prisms, and two isomers of tetraacetoxy-2,6-dibenzylidenecyclohexanone, m.p. 227~228° (decomp.), colorless needles, and m.p. 220~221° (decomp.) colorless polygonal crystals, were obtained in the present work.

Experimental[3]

Materials. 2, 5-Dibenzylidenecyclopentanone tetrabromide and 2, 6-dibenzylidenecyclohexanone tetrabromide were prepared according to the published methods[4][5] and had m.p. 175° (with decomposition) and 193°, respectively.

Action of silver acetate on 2, 5-dibenzylidenecyclopentanone tetrabromide. A mixture of 20 g. (0.034 mole) of 2, 5-dibenzylidenecyclopentanone tetrabromide, 24.2 g. (0.136 mole) of silver acetate, and 180 ml. of glacial acetic acid was refluxed for 3 hours under mechanical stirring. After removing the silver bromide and adding water the crude diacetoxydibromo-derivative separated out as a white precipitate (14.0 g., 76%) which was recrystallized from ethanol; colorless plates, m.p. 213–214° (decomp.). It gave positive Beilstein test. *Anal.* Calcd. for $C_{23}H_{22}O_5Br_2$: C, 51.32; H, 4.12. Found: C, 51.78 and 51.63; H, 4.27 and 3.96.

From the mother liquor of the above recrystallization, a small number of colorless prismatic crystals, m.p. 185–186°, were obtained. These also gave positive Beilstein test. *Anal.* Calcd. for $C_{23}H_{22}O_5Br_2$: C, 51.32; H, 4.12. Found: C, 50.84; H, 3.70.

Action of silver acetate on, 2, 6-dibenzylidenecyclohexanone tetrabromide. a) 2, 6-Dibenzylidenecyclohexanone tetrabromide (15 g., 0.025 mole), silver acetate (8.4 g., 0.05 mole), and 70 cc. of glacial acetic acid were heated at 85–90° for an hour and treated in the same manner as in the above experiment. By extracting the silver bromide precipitate with benzene, 10% (1.5 g.) of the unreacted tetrabromide was recovered. The crude product (12.7 g., 90%) was recrystallized from ethanol. Colorless needles, m.p. 210–211° (decomp.). Yield 5.7 g. (40%). It gave positive Beilstein test. *Anal.* Calcd. for $C_{24}H_{24}O_5Br_2$: C, 52.19; H, 4.38. Found: C, 52.52 and 51.94; H, 4.50 and 4.38.

From the mother liquor of the above recrystallization colorless polygonal crystals melting at 200–201° (0.2 g.) were obtained which gave positive Beilstein test. *Anal.* Calcd. for $C_{25}H_{27}O_7Br$: C, 58.76; H, 5.12. Found: C, 58.28; H, 4.78.

When the reaction mixture was refluxed for half an hour or heated at 85–90° for more than 2 hours, instead of heating for an hour, the crystalline product was 2, 6-dibenzylidenecyclohexanone, (m.p. and mixed m.p. with authentic specimen, 117–118°, no depression) and no diacetoxydibromo-derivative could be obtained. *Anal.* Calcd. for $C_{20}H_{18}O$: C, 87.56; H, 6.61. Found: C, 87.23; H, 6.51.

b) A mixture of 15 g. (0.025 mole) of 2, 6-dibenzylidenecyclohexanone tetrabromide, 16.8 g. (0.1 mole) of silver acetate, and 200 ml. of glacial acetic acid was refluxed for an hour under mechanical stirring and treated in the same manner as in the above experiment. The precipitate (3.8 g.) thus obtained was recrystallized from benzene. Colorless needles, m.p. 227–228° (decompn.), yield 3.3 g. (26%). This gave negative Beilstein test. *Anal.* Calcd. for $C_{28}H_{30}O_4$: C, 65.87; H, 5.92. Found: C, 66.32; H, 5.95.

1) Ping-Yuan Yeh, "Isomerization and dimerization of 2,6-dibenzylidenecyclohexanone" J. Taiwan Pharmaceutical Association, 5, 2 (1953).

2) Ping-Yuan Yeh, "Aromatization of 2, 6-dibenzylidenecyclohexanone". In this series of manuscript.

3) All melting points are corrected.

4) D. Vorländer and K. Hobohm, *Ber.*, **29**, 1837 (1896).

5) C. E. Garland and E. E. Reid, *J. Am. Chem. Soc.*, 2336 (1925).

Besides this product, some colorless polygonal crystals (less soluble in benzene than the needles, m.p. 220–221° (decomp.), yield 0.3 g. (2.3%), were obtained. These also gave negative Beilstein test. *Anal.* Calcd. for $C_{28}H_{30}O_4$: C, 65.87; H, 5.92. Found: C, 66.19; H, 5.83.

Summary

The action of silver acetate on 2,6-dibenzylidenecyclohexanone tetrabromide and 2,5-dibenzylidenecyclopentanone tetrabromide was studied.

The author wishes to express his gratitudes to Prof. Tetsuo Nozoe, Tohoku University, and Prof. Eigai Sebe, Kumamoto University for their adyice.

Department of Chemistry,
National Taiwan University,
Formosa, China

Deformation of the Regenerated Cellulose Fibers III. Deformation and Refractive Indices of Air-Dried Filament

Saburo OKAJIMA and Shigeru HAYAMA

(Received September 4, 1953)

This problem has already been studied by one of these authors and it was found[1] that the refractive indices of the air-dried filament change by stretching according to the first theory of Kratky or sometimes according to the second theory or along some courses between the two limits. Of course it was only in the early stage of deformation ($v_d<1.4$) that the second theory can be applied with a good conformity. The cause of this variation has not been found and here the study was continued and it was found that the deformation can be rather satisfactorily explained by the first theory of Kratky and the irregularity in the early stage is related to the drying condition of the fresh filament.

Experiment

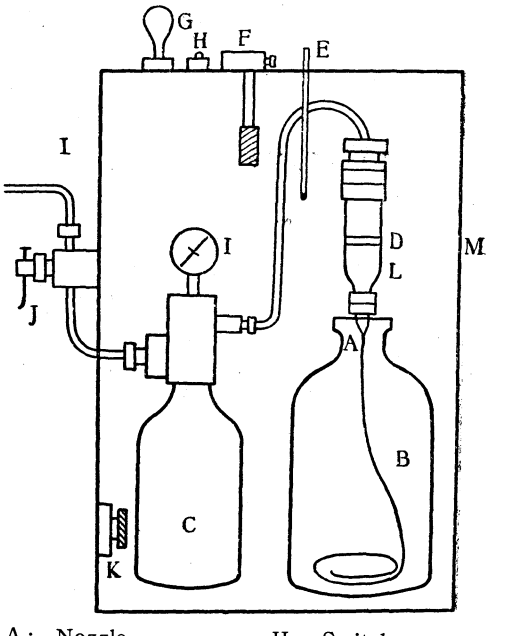
(1) **Model Filament.** A sample of commercial raw ramie was purified by extracting with ether, alcohol and then boiled in 1% NaOH solution repeatedly and bleached. The average degree of polymerization, DP, of it was about 1000.

The purified ramie was then hydrolysed with N-H_2SO_4 at 60°C for some time, followed by boiling with a 1% NaOH solution. Three samples of DP 1000, 540 and 350 were prepared by controlling the duration of hydrolysis.

These samples were dissolved in the cuprammonium solution and spun into isotropic filament of regenerated cellulose. For this purpose the cellulose was placed in a small flask having a thick wall with appropriate amounts of $Cu(OH)_2$ and NH_3-solution and its dissolution was accelerated by kneading in an atmosphere of H_2 which was supplied to the flask through a layer of conc. NH_3-solution. A glass rod (stirrer) was inserted into the flask and was connected to the flask at the mouth elastically and air-tightly by means of a rubber tube.

1) S. Okajima, *J. Soc. Chem. Ind. Japan*, 48, 86 (1945).

The spinning apparatus was placed in a closed air thermostat as shown in Fig. 1. In the figure,



A: Nozzle
B: Coagulating bath
C: Air tank
D: Oil
E: Thermometer
F: Thermoregulater
G: Signal lamp
H: Switch
I: Manometer
J: Valve
K: Heater
L: Spinning Solution
M: Air thermostat

Fig. 1. Spinning Apparatus

A is a glass nozzle of 0.2~0.3 mm diameter and B, the coagulating bath, is an aq. solution of NaOH (5%). The spinning solution, L, is kept from contact with the atmospheric oxygen by covering with a thin layer of oil D. The pressure added on L was 0.2~0.4 atm. according to the viscosity of the spinning solution. This apparatus was also used in the experiments reported in the preceding.

communications on the same problem.[2]

The coagulated filament, which was deposited on the bottom of B, was taken out of B and decoppered at 25~30°C for 70 min. with a solution containing 200 g. of Na_2SO_4 and 50 g. of CH_3COOH per litre. As the regeneration is followed by a remarkable longitudinal shrinkage of the filament, it was carefully carried out under a condition that allows free shrinkage in order to keep it from the slightest tension at the regeneration.

TABLE 1

Filament No.	Composition of the spinning solution			Temp., °C	DP of the filament
	Cellulose, %	Cu, %	NH_3, %		
S-1	13.6	5.9	18.7	25	270
S-6	11.8	5.5	21.5	30	380
S-10	8.0	3.6	12.0	20	380
S-11	8.0	3.6	12.0	30	370
S-14	12.4	4.9	10.1	30	380
S-15	9.2	3.1	6.1	25	370
S-20	3.0	1.5	8.0	20	580
S-21	8.0	3.0	10.0	25	470

The spinning conditions and some of the properties of the model filaments thus obtained are summarized in Tab. 1.

(2) **Stretching of the Model Filament.** A model filament of about 1 meter length was air-dried under a very slight tension, but being sufficient to prevent the curling up. This is designated as "isotropic filament" in this paper, although it has a small intrinsic double refraction. This slight anisotropy is of course corrected in the calculation of the final stretching degree v_d as is described later.

The air-dried isotropic fiber of known length, l_{0d}, was elongated by hanging overnight a weight W at the lower end and the residual length, l_{2d} was read after removing the weight and waiting until the equilibrium state was obtained (after 1 day). The stretching degree, v_d, was then l_{2d}/l_{0d}. Various amounts of v_d were obtained by changing the value of W. The maximum amount of v_d is a function of the air humidity around the filament as shown in Fig. 2. It was very difficult to carry out the stretching in the relative humidity lower than 60% in our case.

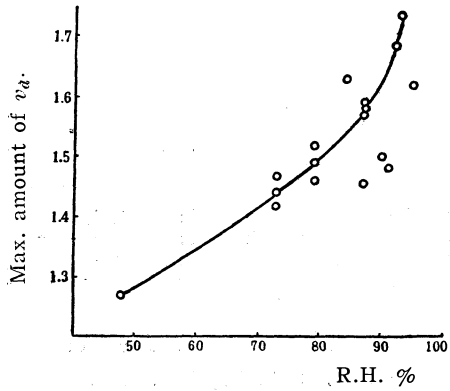


Fig. 2. Effect of the humidity upon the stretching degree.

(3) **Double Refraction.** The stretched filaments were dried in vacuum at 60°C and their refractive indices $n_{\parallel}$ and $n_{\perp}$ were measured by Becke's method and corrected as already reported by the authors.[3] The intrinsic double refraction is then given by $n_{\parallel}-n_{\perp}$.

Experimental Results

(1) Effect of the Temperature of Spinning.—The samples S-10 and -11 were spun from the same spinning solution under the same conditions except the temperatures only, which were 20 and 30°C respectively. But the effect of this temperature difference can not be observed and the curves follow well the first theory as shown in Fig. 3.

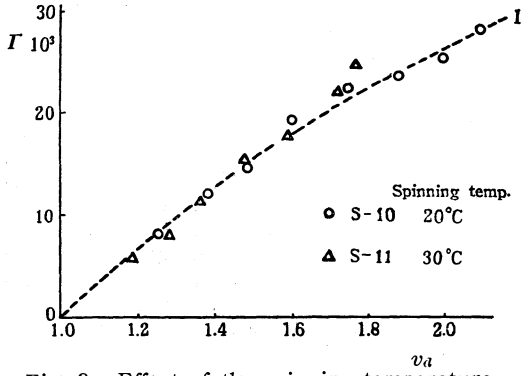


Fig. 3. Effect of the spinning temperature.

In the figure the values of v_d are corrected so as the first point of each curve is placed on the theoretical curve 1 which was calculated on the assumption of the first theory of Kratky.

(2) Effect of the NH_3-concentration in the Spinning Solution.—The spinning solutions of S-6, -14 and -15 are of different

2) S. Okajima, *Bull. Yamagata University*, 1950, No. 1, 21; S. Okajima and Y. Kobayashi, This Bulletin, **24**, 85 (1951); S. Okajima and S. Hayama, ibid, **24**, 90 (1951).

3) S. Okajima and Y. Kobayashi, *J. Soc. Chem. Ind. Japan*, 1943, **46**, 941; S. Okajima, *Bull. Yamagata University*, 1950, No. 1, 21.

NH_3-concentration, while their DP are equal to each other. The solutions of the latter two were evacuated for some time after preparing by the ordinary recipes and the NH_3-concentration was lowered to 10.1 and 6.1% form the original concentrations of 18 and 10% respectively.

The deformations of these filaments are also similar to that of the highest concentration, S-6, and all three coincide with curve 1. (rf. Fig. 4).

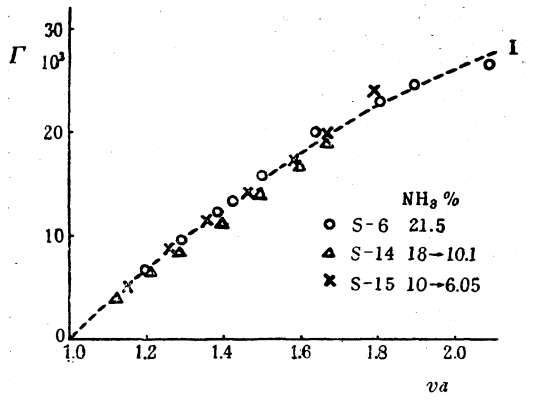


Fig. 4. Effect of NH_3-concentration.

(3) Effect of the Cellulose Concentration of the Spinning Solution.—A series of filaments were prepared from the spinning solution of varying cellulose concentration from 3.0 to 13.6%. Of course DP of the cellulose in the solution was higher in the case of the lower concentration and vice versa for the sake of keeping the viscosity of the solution within comparatively narrow limits, which was necessary for the smooth spinning.

It is seen from Fig. 5 that all the curves are in the vicinity of the theoretical curve

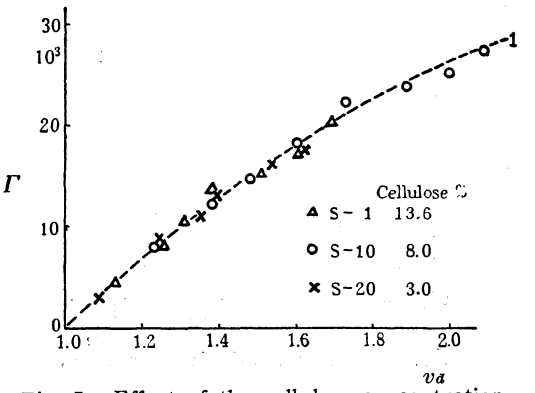


Fig. 5. Effect of the cellulose concentration

1. The effect of the concentration appears remarkably in the swelling degree of the regenerated filaments[4], but in the dry state it nearly disappears and the double refraction changes along the same course.

(4) Effect of the Drying Condition.—As is well known the drying of the freshly prepared fibre affects some properties of the fibre irreversibly and so now the effect of the air humidity in drying is observed.

For this purpose each of the two samples (S-20 and S-21) were divided into three parts and dried in the air of 30, 60 and 80% R.H. (S-20-1～-3 and S-21-1～-3). Each of S-21 series was further divided into two parts (S-21-1～-3 and S-21-1′～-3′) and the former were stored in a room controlled 70% R.H., while the latters in a desiccator of 90% R.H. They were stretched in the as me surroundings to observe the effect of the drying conditions. These air conditions are summarized in Tab. 2.

TABLE 2

Filament No.	S-20			S-21			S-21		
	1	2	3	1	2	3	1′	2′	3′
Drying: T, °C	34	34	9.5	33	18	16	33	18	16
R.H., %	30	60	80	30	60	78	30	60	78
l_{0d}/l_{0w}: before aging	0.656	0.678	0.692	0.666	0.675	0.687	0.666	0.675	0.687
after aging	—	—	—	0.666	0.675	0.687	0.693	0.688	0.697
Aging: T, °C					19			20	
R.H., %					70			80	
Stretching: T, °C		11–13			18–22			18–22	
R.H., %		74–79			73			87–88	

Figs. 6～8 indicate that in the first two series the influence of different drying conditions is apparent: the filament dried at lowes R.H. has a steeper initial change while that dried at 80% R.H. shows an ordinary change. But this difference does not exist between S-21-1′～-3′ and three curves coincide with each other and also with the curve 1.

The above phenomena may be explained by a concept that difference in drying

4) P. H. Hermans, "Physics and Chemistry of Cellulose Fibre", 1949.

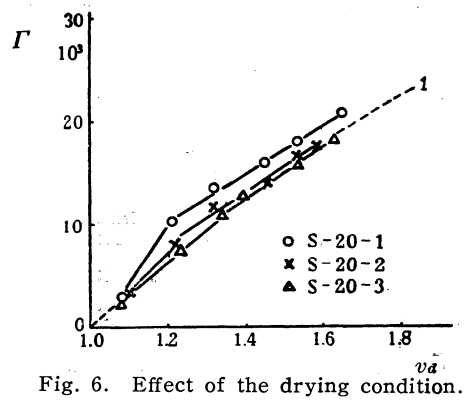


Fig. 6. Effect of the drying condition.

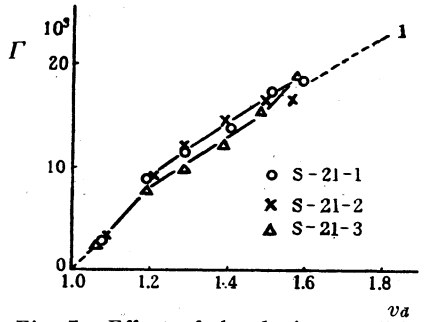


Fig. 7. Effect of the drying condition.

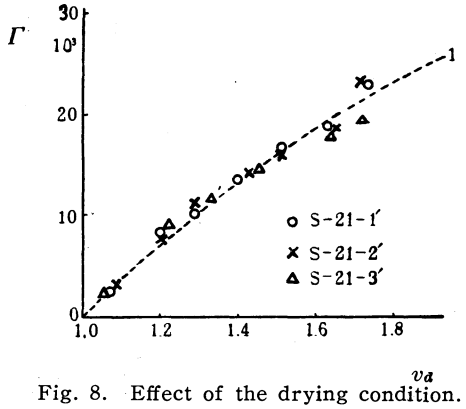


Fig. 8. Effect of the drying condition.

condition brings about some structural difference which disappears while being aged in such humid air as 90% R.H. but does not disappear in the low humidity. This concept is supported by the data in Tab. 2, according to which the dry length of the isotropic filament relative to the wet increases appreciably as the air becomes humid, and this difference disappears while the filaments are aged in 90% R.H. although it remains in the low humidity. These behaviors will have some connection with the change in weak junctions of cellulose molecules which will become less cohesive in the higher moisture content of the filament.

Summary and Discussion

Deformation of the dried filament can be expressed in the term of the first theory of Kratky on the whole as in the case of swollen filament[2]. And this behavior is not affected by the slight change of the spinning conditions of the filament such as the temperature and the composition of the cellulose solution. But in the case of the fila ment dried in the less humid air the orientation occurs more prominently in the early stage of the stretching but soon follows the above deformation mechanism.

This drying effect will illustrate the variation seen in the previous paper.[1] Of course it is noteworthy that the value of l_{0d} changes a few percent with the variation of the air humidity during measuring and, therefore, this factor must be taken into consideration when l_{0d} and l_{2d} are read under the different air conditions. Some of our older data are thought to contain small fuctuations due to this fact.

One of the authors has also reported[5] that a filament stretched in water to some degree seems to have the same molecular orientation pattern as that given by stretching in the dry state to the corresponding anisotropy and this anisotropic filament deforms further by restretching in the dry state according to the same mechanism which is shown by the isotropic filament in the dry deformation. This seemedto be a very curious and interesting fact but now becomes clear as the deformation mechanisms of the fresh (swollen) and driedfilaments are similar to each other.

Faculty of Engineering,
Tokyo Metropolitan University, Tokyo
and
Faculty of Engineering,
Yamagata University, Yonezawa

5) S. Okajima, *J. Soc. Chem. Ind. Japan*, **48**, 87, (1949); **49**, 52, (1944.).

Removal of Dissolved Oxygen by Sodium Sulfite. Application to the Polarographic Study

By Shinichi KIKUCHI, Kenichi HONDA and Seckchill KIM

(Received October 20, 1953)

As is well known, in most cases of the polarographic study, the dissolved oxygen in the test solution must be removed before measuring because of its own waves which interfere with that of the substance being determined. Usually inactive gases as hydrogen or nitrogen are bubbled through the test solution for that purpose. But this is a rather time-consuming and elaborate procedure and as a result it influences the speed and efficiency of the determination. Against this physical method, the chemical method that is to adsorb the dissolved oxygen by the reducing agent, sodium sulfite, was reported by E. Varasova[1] and also was recommended by Heyrovsky[2] and Hohn[3]. Though this method seems rather simple if adequately effective, the quantitative investigation for the efficiency of sodium sulfite is not yet reported.

So there is little knowledge in the literature of the subject for the use of sodium sulfite. Of course, considering the change of the constitution of the solution which may affect the wave form of the substance being determined, its volume of addition should be as little as possible, providing it adsorbs the dissolved oxygen effectively.

From this standpoint, the effect of sodium sulfite upon the oxygen wave and its relation to the time after adding it to the test solutions were investigated. Effect to the *p*H, effect to the wave-height of the substance to be determined and effective *p*H range are also reported here.

Experimental

The concentration of dissolved oxygen was determined polarographically in the solutions of various kinds of supporting electrolyte, such as Sörensen's phosphate, glycocol–NaOH and borate-NaOH buffer solutions, 0.1M LiCl, KCl and NaOH solutions, their mixture with methanol and so on. All those solutions were made up from the reagents of "guaranteed" grade. To obtain the desired concentration of sodium sulfite, one of the freshly prepared 10, 5 and 1% solutions of it was added to the test solution. Gelatine was not used. Electrolysis was carried out in an open cell with the saturated calomel reference electrode on a liquid paraffine bath thermostatted at 25±0.1 °C. Polarographic apparatus used here was the d.c. amplification system recording polarograph which was constructed in this laboratory[4]. The capillary characteristics were 0.96 $mg^{2/3}$ $sec.^{-1/2}$ as $m^{2/3}$ $t^{1/6}$ in 0.1M KCl with no applied potential.

Results and Discussions

In order to show the concentration of dissolved oxygen, its wave-height is adopted. This is done because the object of the present study is not the direct determination of the dissolved oxygen; moreover the relative variation of dissolved oxygen corresponding to the volume of added sodium sulfite is more important. The wave-height is measured at the point of −0.5 V. vs. S.C.E. where it is accepted that there is the linear relation between the concentration and the wave-height[5].

(A) Effect in Neutral and Alkaline Solutions.

Concentration∼time relations are shown in Figs. 1∼7; solutions of each figure are 0.1M LiCl, KCl, phosphate buffer of *p*H 8.6, borate-NaOH buffer of *p*H 9.4.10,9,12.2 and 0.1N NaOH respectively. Each curve in the

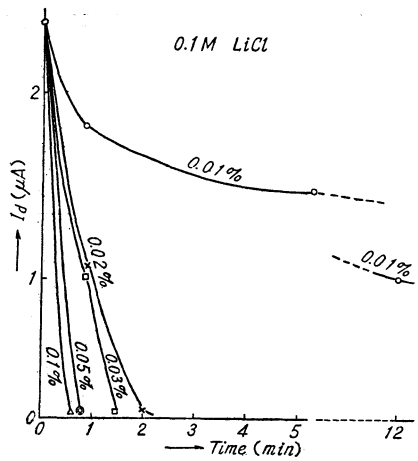


Fig. 1.

1) E. Varasova, *Collection Czech. Chem. Comms.*, **2**, 8 (1930).
2) J. Heyrovsky "Polarographisches Praktikum", Springer-Verlag, Berlin, 1948, S. 55.
3) H. Hohn, "Chemische Analysen mit dem Polarographen", Springer-Verlag, Berlin, 1937, S. 44.
4) S. Kikuchi, Y. Sakaguchi and K. Honda, This Bulletin, **25**, 98 (1952).
5) G. A. Marsh, *Anal. Chem.*, **23**, 1427 (1950).

figures represents the wave-height decrease with the time lapse after the addition of sodium sulfite; the value in percentage beside the curve shows its concentration. The wave-height at the point of time 0 indicates that of dissolved oxygen in blank solution.

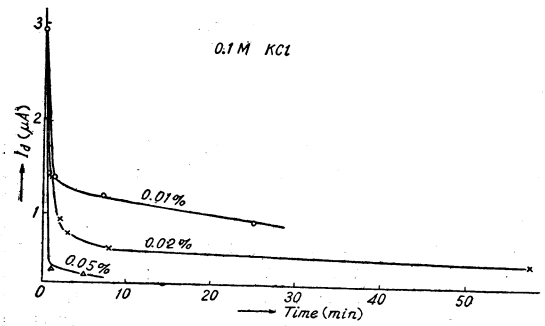


Fig. 2.

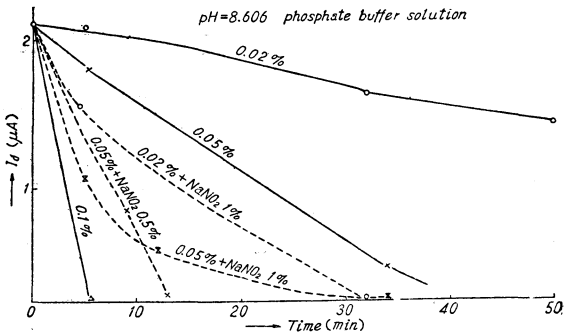


Fig. 3.

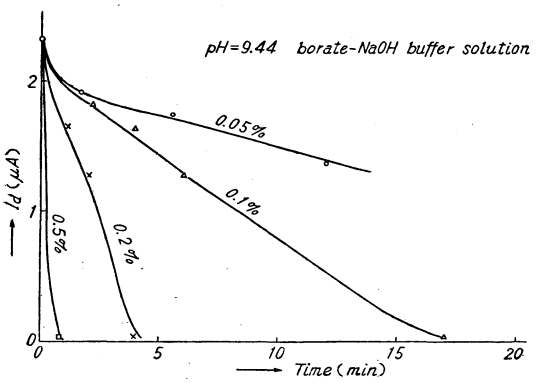


Fig. 4.

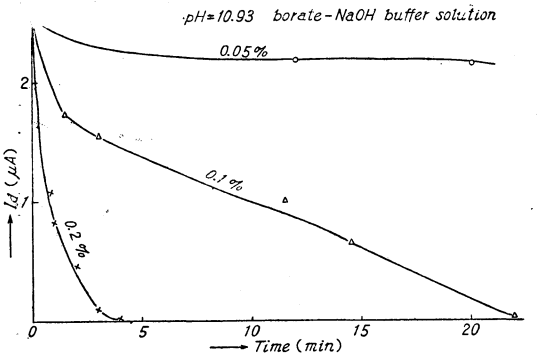


Fig. 5.

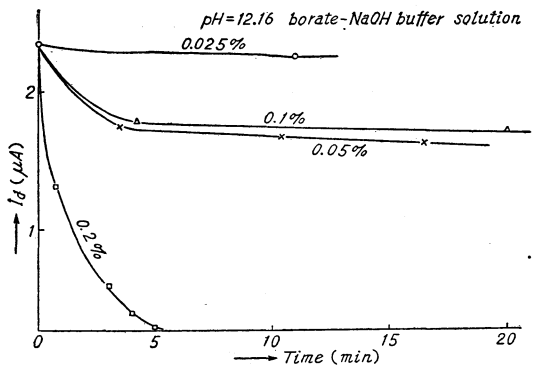


Fig. 6.

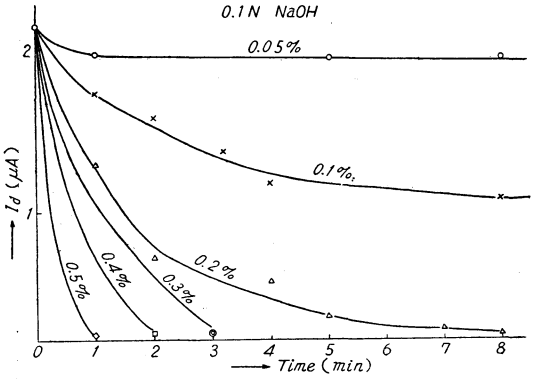


Fig. 7.

Of course, the necessary degree of removal of dissolved oxygen depends upon the magnitude of the wave to be interfered with, so minimum but adequate concentration of sodium sulfite can be determined from the figures according to the individual case. But from the practical standpoint, supposing that it is necessary that the height of the oxygen wave should decrease about one-fiftieth of ts original height within 5 minutes, the minimum concentration of sodium sulfite are as follows;

0.02% in 0.1M LiCl
0.05 " 0.1M KCl
0.1 " *p*H 8.6 buffer
0.2 " *p*H 9.4 buffer
0.2 " *p*H 10.9 buffer
0.2 " *p*H 12.2 buffer
0.3 " 0.1N NaOH

From the figures and values above, it is

found that the reducing power of sodium sulfite is most efficient in a neutral solution and becomes less effective towards the alkaline side. The reducing reaction proceeds quickly in the first five minutes and after that proceeds more slowly.

(B) **Influence of Positive and Negative Catalyzer upon the Reducing Power of Sodium Sulfite.**

As to the reaction between oxygen and sodium sulfite, several positive and negative catalysts are described in the literature of the subject[6]. Alcohol, glycocol, aldehyde, etc. which are often encountered in organic polarography are known as negative catalyzers. In the solutions which contain the substances mentioned above, the efficiency of of sodium sulfite is markedly diminished. Those appearances are shown in Figs. 8, 9 and 10, in which the constitutions of the solutions are glycocol-NaOH buffer of *p*H 19.0, 0.1M KCl-methanol (volume ratio 1:1) and phosphate buffer of *p*H 8, 6-methanol (9:1) respectively.

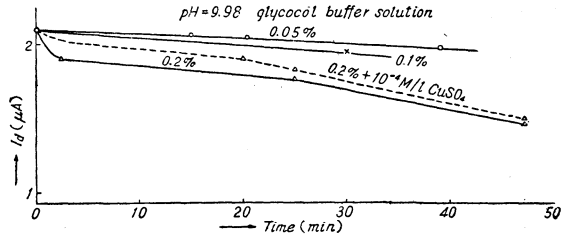


Fig. 8.

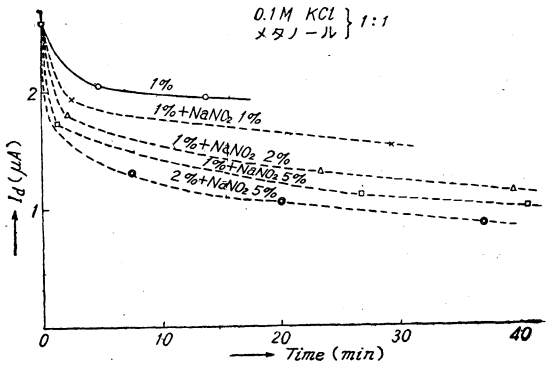


Fig. 9.

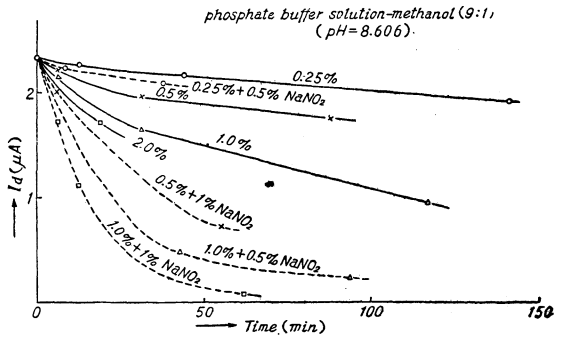


Fig. 10.

As shown in accompanying figures, the addition of sodium sulfite even up 0.2~2% is not yet sufficient and it seems unsuitable for the practical use for it may cause some important change of the constitution of the solution. To supplement this deficiency, some positive catalysts are tested. As a matter of course, it is demanded that the catalysts itself produces no reducing waves polarographically. Nevertheless, cupric sulphate is first selected, because in spite of having a well-defined wave of cupric copper, it appears at comparatively noble potential and so it seems less likely to interfere with other waves, if used in a very dilute state. Its behavior is shown as a dotted line in Fig. 8. As shown, the addition in such a concentration of 10^{-4} M/l. does not bring any effective result. But it is assumed that in the case of determination of copper the effect of sodium sulfite would be accelerated. Secondly sodium nitrite which generally is not reduced at dropping mercury electrode before the discharge of sodium ion provided that there are no polyvalent cations such as La^{+++} and Ca^{++}, is tested. Its behavior is shown as the dotted lines in Figs. 3, 9 and 10. In Fig. 3, in the phosphate buffer solution, the addition of 0.5~1% nitrite increased the removing effect somewhat more than threefold, but when the methanol content is half the volume as in Fig. 9, its effect is not so pronounced and the addition of 5% increases the power of sodium sulfite about twofold. In Fig. 10 when methanol is 10%, its catalytic effect is promoted more than before. 1% addition of nitrite promotes the reaction more than twofold.

In conclusion, when a hindering substance is contained, it is possible to remove oxygen by the addition of a promoting reagent, but from the fact of its being time-consuming, its utility still remains doubtful.

(C) **Influence to the *p*H of the Solution.**

By the addition of different substances, a change of the constitution of the solution is more or less inevitable. From the standpoint of organic polarography, the variation of *p*H value corresponding to the addition of sodium sulfite is measured roughly in the buffered solutions. The results are shown in Table 1.

6) Mellor "Inorganic and Theoretical Chemistry".

TABLE I.

Na_3SO_3 %	Sörensen's borate-NaOH Buffer *p*H	*p*H
0	9.29	12.12
0.05	9.3	12
0.1	9.3	〃
0.5	9.5	〃
1.0	9.5	〃

As seen in this table, the addition causes little variation in strong alkaline solutions, but some increase of *p*H value in neutral and weak alkaline solutions and so will bring on a shift of half-wave potential of organic compounds. As a result, when the addition is more than 0.5% the calibration of *p*H is necessary even if the solution is buffered.

(D) Influence to the Wave-height of the Substance being Determined.

If the sodium sulfite which is known as the reducing reagent reduces the substance to be determined, its use would be nonsense. For the example of *p*-nitroanthranilic acid, this propriety is examined in the mixture of buffer solution and methanol. The wave-heights are compared in both the cases, wheh nitrogen is bubbled and when sodium sulfite in cooperation with sodium nitrite is added. The results are shown in Table II.

TABLE II. WAVE-HEIGHT OF *p*-NITROANTHRANILIC ACID

(A) 8×10^{-4} M/1. in *p*H 8.6 Buffer and Methanal (11 : 1)

	Nitrogen passed (10 min.)	0.8% Na_3SO_3+1.2% $NaNO_2$		
Time (min.)	—	41	84	200
Wave-height (μA.)	4.2_8	4.2_8	4.2_8	4.3_9

(B) $1+10^{-3}$ M/1. in *p*H 12.2 Buffer and Methanol (9 : 1)

	Nitrogen passed (10 min.)	0.5% Na_2SO_3+3% $NaNO_2$	
Time (min.)	—	35	77
Wave-height (μA.)	5.0_5	4.9_6	5.0_5

As shown in Table II, both wave-heights coincide within experimental error after the elapse of more than an hour. The results indicate that sodium sulfite will not affect the wave of organic compound.

(E) Effect in the Acidic Solution.

Hitherto it is acknowledged that the efficacy of sodium sulfite is restricted in neutral and alkaline range because on the acidic side the reduction wave of HSO^-_3 appears.[7] From the experimental result, in the buffer solution of *p*H 5.6 the oxygen wave reduces more than 90% of its original height within 10 min. Qualitatively it is found that its reducing action still proceeds in acidic solution.

As a result when the wave of the substance being determined appears at the nobler potential than that of HSO^-_3, it is possible to use this method.

7) I. M. Kolthoff and C. S. Miller, *J. Am. Chem. Soc.*, **63**, 2818 (1944).

Summary

(1) From the polarographic standpoint, the behavior of reducing the dissolved oxygen by sodium sulfite is investigated in various kinds of supporting electrolytes.

(2) The efficiency is most prominent in neutral solution and becomes less effective towards basic.

(3) Influence upon the *p*H of the solution by the addition should not be neglected.

(4) There would be no effect to the reducible substance.

(5) Its reducing action still proceeds in acidic solution.

(6) The stock solution of sodium sulfite should be as fresh as possible. But a too fresh solution in 5~10 min. after preparation does not show the effect. The reason is not yet clarified. Ten or more days after preparation, it becomes less effective.

Laboratory of Electro-and Photochemistry
Institute of Industrial Science,
University of Tokyo, Chiba

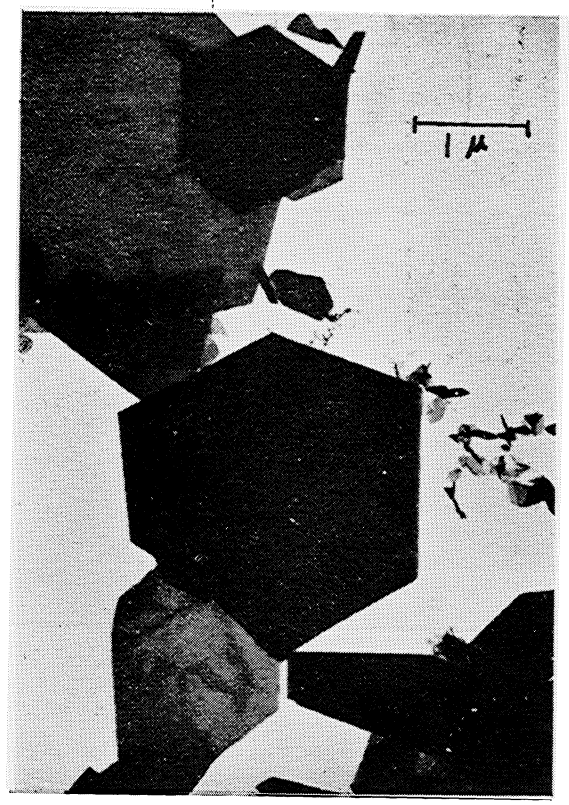


Fig. 1. Electron micrograph of the smoke of $CdCl_2$. ×15.000

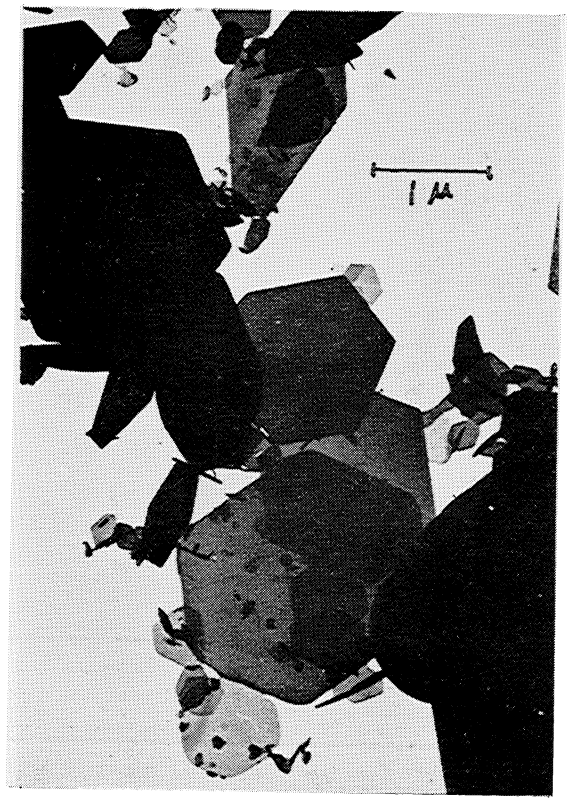


Fig. 2. Electron micrograph of the smoke of $CdBr_2$. ×15.000

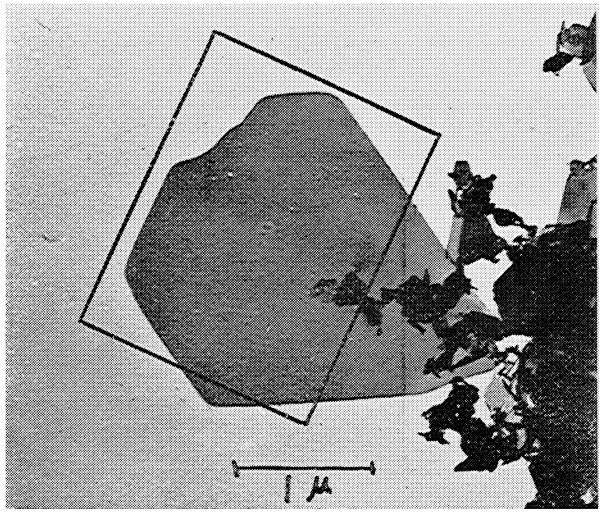
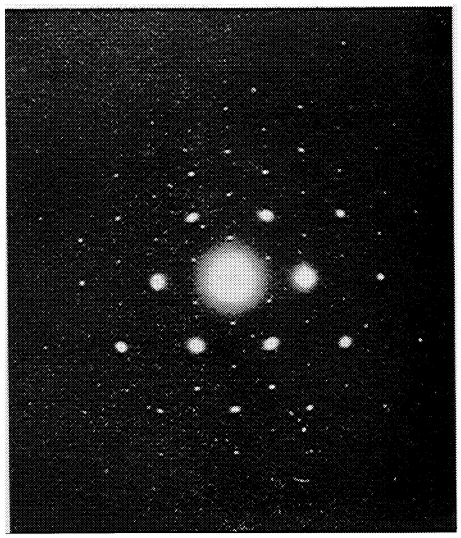


Fig. 3. (a) Electron micrograph of flakes of $CdCl_2$. ×18.000



(b) Diffraction pattern produced by transmission perpendicular to the portion indicated in the rectangle in (a).

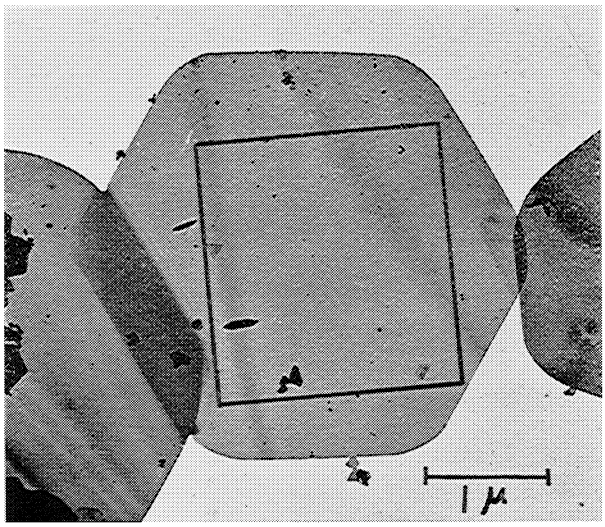
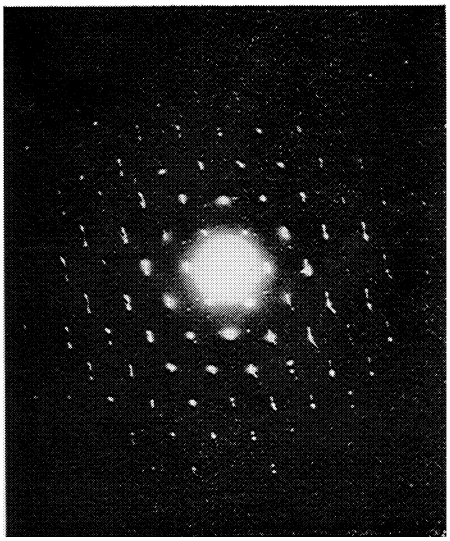


Fig. 4. (a) Electron micrograph of flakes of $CdBr_2$. ×18.000



(b) Diffraction pattern produced by transmission perpendicular to the portion indicated the rectangle in (a).

LETTER

The Study of the Smoke of $CdCl_2$ and $CdBr_2$ by Means of Electron Microscope

By Sho SUZUKI

(Received September 9, 1953)

In the course of the study of the smoke of a metal halide by means of the electron microscope[1], it was found that the smoke of $CdCl_2$ and $CdBr_2$ was made up of very thin, and hexagonal flakes. In this experiment the smoke of each cadmium halide was prepared by heating the substance in a porcelain crucible at about 800°-900°C. On heating, the substance melted at first, and then evaporated gradually in a white smoke. The smoke thus produced was deposited directly on a bronze wire screen (diameter; 0.5 mm), and was observed in the electron microscope.

Fig. 1 is the micrograph of the smoke of $CdCl_2$, and Fig. 2 that of $CdBr_2$. Both photographs reveal thin, flaky, and hexagonal crystals. The diffraction patterns of these flaky crystals were also obtained by employing the U-6 type three stage electron microscope. These flaky crystals give electron diffraction patterns as of Fig. 3(b) and 4(b). Fig. 3(b) shows the electron diffraction pattern caused by transmission nearly perpendicular to a portion of the flaky crystal of $CdCl_2$, the portion of which is indicated in the rectangle in Fig. 3(a). The electron diffraction pattern for $CdBr_2$ is shown in Fig. 4(b), and the portion of the crystal subjected to the electron diffraction is shown in the rectangle in Fig. 4(a).

The spacings for the substances are calculated from the N-pattern diagrams obtained here and are shown in Table 1, and it is confirmed that these flakes are $CdCl_2$ and $CdBr_2$. In addition, because of the hexad symmetry appearing in the N-pattern, it is evident that the electron beam is nearly perpendicular to the (III)-plane.

$CdCl_2$ and $CdBr_2$ have the typical layer structure and each layer is parallel to the (III)-plane, hence it is concluded that the flake in the present micrographs is formed as a result of the layer formation of crystals with the layer structure.

The author wishes to express his sincere appreciation to Mr. Matsuo of Shimazu Seisakusho Co. Ltd., who carried out the operation of the U-6 type three stage electron microscope, for his technical assistance, and also wishes to acknowledge the assistance of Dr. Shimazu, who gave him a chance to use the instrument.

Table I[2]

$d_{obs.}$	$d_{x\text{-}ray.}$	hkl	substance
1.93	1.93	$1\bar{1}0$	$CdCl_2$
1.98	1.98	$1\bar{1}0$	$CdBr_2$

Government Chemical Industrial Research Institute, Tokyo
Hatagaya-Honmachi, Shibuya-ku, Tokyo, Japan

1) S. Suzuki, This Bulletin **25**, 279 (1952).

2) S. Yamaguchi, This Bulletin **18**, 81 (1943).

The Low-temperature Luminescence Newly Found with a Number of Silver Salts

By Shoji MAKISHIMA and Takeshi TOMOTSU

(Received October 10, 1953)

The low temperature luminescence of silver halides has been reported by several investigators[1] and been criticised recently by F. Seitz[2]. We have studied the luminescence of a number of common silver salts other than halides with a view to finding a more general relation between the luminescence and the photolytic discoloration of silver salts.

Insoluble silver salts were precipitated in the excess state of either anion or silver ion by mixing the solutions of silver nitrate and various precipitants, each of A.R. grade. At first a small quantity of precipitates was formed in the solution of both reagents by adding a small portion of the one to the other. Then the precipitates were filtered off, and finally the filtrates were mixed. The action of actinic light was carefully avoided throughout the procedures of preparation and measurements.

The luminescence was examined at room and liquid air temperature in a Dewar vessel furnished with two quartz windows under the excitation of 365 mμ of a mercury vapor lamp. The emission spectra consist of a single broad band at liquid air temperature in most cases. The luminescent characteristics are given below:

sulfite Ag_2SO_3 (orange, strong), sulfate Ag_2SO_4 (orange, medium), pyrophosphate $Ag_4P_2O_7$ (orange, medium), oxalate $Ag_2C_2O_4$ (orange, medim; white purple*, weak*), carbonate Ag_2CO_3 (red, medium), molybdate Ag_2MoO_4* (red, weak; red*, weak*), tungstate Ag_2WO_4 (red, very weak), nitrite

1) W. Meidinger, *Phys. Z.*, **40**, 517 (1939); **41**, 277 (1940) G. C. Farnell, P. C. Burton and R. Hamalla, *Phil. Mag.* **41**, 157, 545 (1950).

2) F. Seitz, *Rev. Mod. Phys.*, **23**. 349 (1951).

$AgNO_2$* (greenish yellow, very strong; yellow*, medium*), sulfocyanide AgCNS (green, strong), cyanide AgCN (blue, medium), perchlorate $AgClO_4$ (yellow, weak), mercuri-iodide Ag_2HgI_4* (green, strong; red*, weak*).

Fluoride, nitrate, ferrocyanide, ferricyanide and phosphate are not luminescent at both room and liquid air temperatures, the last one, however, fluorescing probably infrared. The salts with asterisk are luminescent at room temperature, whose luminescence characteristics are also marked with asterisks.

Evidences were obtained that these fluorescences are not ascribed to the print-out silver. On the contrary, the fluorescences depend sometimes on whether the salt is of silver or of anion body. So, for instance, the emission color changes from silver body to anion body as follows: AgCNS (green→orange), AgCN (blue→yellowish orange), Ag_2SO_4 (orange→white purple). This indicates an intimate connection of luminescence with lattice defects. The same light as excites the luminescence leads to the blackening of the salts at higher temperature, but not at liquid air temperature. The blackening is generally less remarkable in the salts of an anion body. The authors concluded that silver salts can be luminescen in their pure state by the reverse process of photolytic absorption, in which, however, some lattice defects are undoubtedly involved. The mechanism suggested by F. Seitz, namely the transition $d^9s \rightarrow d^{10}$ within the silver ion, seems to be invalid, for similar emission spectra (orange~red) appear in some cases (as in Ag_2SO_3, Ag_2SO_4, Ag_2CO_3, $Ag_4P_2O_7$), whereas spectra are quite different with one another in other cases (as in $AgNO_2$, Ag_2HgI_4, AgCN etc.). Spectroscopic and other details are to be published in later reports.

The Institute of Science and Technology, University of Tokyo, Tokyo

Critical Concentration for Micelle Formation and its Aggregation Number in Aqueous Solutions of Paraffin Chain Salts

By Kozo SHINODA and Kyoji KINOSHITA

(Received February 14, 1953)

1. Introduction

The abrupt change in many physico-chemical properties (refractive index, freezing point, conductivity, osmotic pressure, viscosity, surface tension, absorption spectrum of dye etc.) and the appearance of colloidal properties have been attributed to the aggregation of paraffin chain salts into micelles and the concentration at which such change occurs has been termed the critical concentration for the formation of micelles.

With respect to the aggregation number of paraffin chain salts in aqueous solutions, it has become clear that the aggregation number is represented by a counter balance between the electrical work due to the aggregation of charges in the "heads" of paraffin chain ions and the decrease of the short-range non-electrical energy due to the aggregation of hydrocarbon portion[1,2], i.e., the decrease of oil-water interface. The electrical work which will be compeled at the micelle formation of paraffin chain salts (ions) increases much more rapidly than the aggregation number, while the decrease of the cohesive energy at the micelle formation is approximately proportional to the aggregation number. Hence, the energy decrease of the short-range force accompanied by the increase of one paraffin chain ion in the micelle becomes definite, while the energy increase of electrical force becomes greater with the increasing number of aggregations.

The increase of aggregation number, therefore, must be stopped, when the micelle is enlarged to the right size. If the aggregation number increases more than this, the energy depression per paraffin chain ion passing from the bulk of the solution into the micelle begins to decrease and the micelle of such an aggregation number can not exist. This is the reason why a paraffin chain salt shows a definite number of aggregation and a distinct critical micelle concentration at a given temperature. Thus the critical micelle concentration of a paraffin chain salt in equilibrium with its micelle is analogous to the solubility of ordinary substances in equilibrium with a separate phase. As the micelle formation is a reversible process, a paraffin chain salt in the bulk of the solution must be in equilibrium with the salt in the micelle. The critical micelle concentration can be calculated by equating the partial potential of a paraffin chain ion in the bulk of the solution and that in the micelle.[3]

2. Energy Change at the Micelle Formation

In the present paper, a cylindrical double layer model has been adopted as the micelle shape, its thickness is just twice the length of the long-chain salts molecule. We may express the total energy change at the micelle formation, E, in terms of electrical energy, E_e, and the short range cohesive energy, E_m.

A paraffin chain salt consists of the non-polar portion of hydrocarbon chain and the polar ionic group. If it is assumed that the former is a cylinder of radius r_0 and length l, the following values are given using surface-chemical data.

$$\begin{aligned} l &= 1.3\times m\text{Å} \\ s_0 &= \pi r_0^2 = 20.5\text{Å}^2 \\ r_0 &= 2.56\text{Å} \end{aligned} \qquad (3.1)$$

where m is the number of carbon atoms which construct a hydrocarbon chain, s_0 is the cross-sectional area of a hydrocarbon chain, and r_0 is its radius. Above the critical micelle concentration scores of these detergent molecules are aggregated to the micelle. If the micelle consists of n molecules of paraffin chain salts, the area of the cross section of this cylindrical micelle is $ns_0/2$, and the radius becomes

$$R=(ns_0/2\pi)^{1/2} \qquad (3.2)$$

Although the edge of an actual micelle may probably be more circular than this model, calculation will be made according to this cylindrical double layer model. The side area of this cylindrical micelle is

$$S=4\pi(ns_0/2\pi)^{1/2}\times 1.3m\text{Å}. \qquad (3.3)$$

The total inter-facial energy at the side of a cylindrical micelle is

$$\frac{4\pi(ns_0/2\pi)^{1/2}\times 1.3m\omega}{1.3\times 2\pi r_0}=(2n)^{1/2}m\omega \qquad (3.4)$$

1) P. Debye: *J. Phys. & Colloid Chem*, **53**, 1 (1949).
2) M. Nakagaki: *J. Chem. Soc. Japan.*, **72**, 113 (1950); **73**, 802 (1951).
3) K. Shinoda: This Bulletin, **26**, 101 (1953).

where ω is the non-electrical work required to take one methylene radical from the micelle to the bulk of the solution, the denominator of the left-hand side of (3.4) being equal to the area per methylene radical.

As to the estimation of ω we have given attention to the fact that the solubility ratio of homologous aliphatic compounds into water diminishes to about 1/3 with the increase of each methylene radical.[3]

That is $\omega \fallingdotseq 1.08kT$.

The total energy decrease due to the short-range force is given as follows, considering that the short-range energy depression per paraffin chain molecule is $m\omega$ and using (3.4),

$$E_{nm} = nm\omega - (2n)^{1/2}m\omega \tag{3.5}$$

Here E_{nm} is the short-range energy decrease at the micelle formation when the aggregation number is n.

In estimating the electrical work due to the micelle formation we have neglected the interaction between the two end discs, because there is an experimental fact that a non-polar oil such as benzene or hexane which is solubilized between the monolayer of the micelle shows an increase of x-ray spacing, but shows only a slight effect on the critical micelle concentration.[4,5]

Let us now calculate the electrical energy due to one disc, assuming that the disc has a uniform charge density, σ. Consider a surface element P on the end of a small disc, at a distance x from the center of the disc, as shown in Fig. 1.

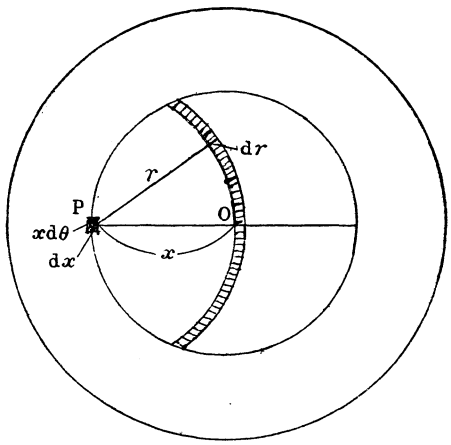


Fig. 1. disc

The area, at the distance of $r \sim r+dr$ from P on this small disc is

$$2\cos^{-1}(r/2x)r\,dr$$

and if we assume the surface charge density of this disc to be σ, the potential at the surface element P due to this portion is

$$\frac{2\cos^{-1}(r/2x)r\sigma^2 dr x d\theta dx}{Dr} \tag{3.6}$$

Integrating all over the small disc, and then integrating all over the disc, we obtain

$$\int_0^{(ns_0/2\pi)^{1/2}}\int_0^{2\pi}\int_0^{2x}\frac{2\cos^{-1}(r/2x)r\sigma^2 dr x d\theta dx}{Dr}$$

$$=\int_0^{(ns_0/2\pi)^{1/2}}\int_0^{2\pi}\frac{4\sigma^2x^2}{D}d\theta dx$$

$$=\int_0^{(ns_0/2\pi)^{1/2}}\frac{8\sigma^2x^2\pi}{D}dx=\frac{(2ns_0)^{3/2}\sigma^2}{3D\pi^{1/2}} \tag{3.7}$$

This is the electrical energy for the formation of one disc, which is composed of $n/2$ molecules. The total electrical energy for the formation of micelle, E_{ne}, is twice this.

Then we must consider the effect of an ion atmosphere. The correct treatment of the ion atmosphere is, however, not yet achieved and we have adopted an experimental parameter to express the effect of the ion atmosphere. That is to say, a reasonable constant must be multiplied to the electrical energy term at the micelle formation. Experimental constants given by Corrin and Harkins[6] for the effect of added salts on the critical micelle concentration are adopted as the parameter, considering that each long-chain ion instead of contributing a charge e to the micelle, would contribute less charge than this because of the adsorbed gegenions :[3]

Thus the total energy change at the micelle formation is

$$E_n = E_{nm} + E_{ne} = nm\omega - (2n)^{1/2}m\omega - \sqrt[4]{2}\,\sigma^2K^2n^{3/2}s_0^{3/2}/3D\pi^{1/2} + ne^2\kappa/3D \tag{3.8}$$

With respect to the value of K reference may be made later, (4.7). The electrical energy of the long-chain ion in the bulk of the solution is expressed by $e^2\kappa/3D$.

3. Aggregation Number and the Critical Micelle Concentration

The aggregation number might be explained by the counter balance between the short-range energy and the electrical long-range energy. From this point of view it may be said that the micelle which requires maximum energy to take out one paraffin chain salt molecule must be the most stable, and the aggregation number is calculated by differentiating the energy for the micelle formation with respect to the aggregation number as follows.[7]

4) E. C. Lingafelter, O. L. Wheeler, and H. V. Tartar: *J. Am. Chem. Soc.*, **68**, 1940 (1946).

5) R. W. Mattoon, R. S. Stearns, and W. D. Harkins: *J. Chem. Phys.*, **16**, 644 (1948).

6) M. L. Corrin and W. D. Harkins: *J. Am. Chem. Soc.*, **69**, 683 (1947). cf. S. H. Herzfeld; *J. Phys. Chem.*, **56**, 959 (1952).

7) Y. Ooshika: *Butseiron-Kenkyu* **44**, 30 (1951).

$$\frac{\partial E_n}{\partial n}=m\omega-m\omega/(2n_0)^{1/2}$$
$$-2\sqrt{2}\sigma^2K^2n_0^{1/2}s_0^{3/2}/D\pi^{1/2}+e^2\kappa/3D$$
$$=max \qquad (4.1)$$

and

$$\frac{\partial^2 E_n}{\partial n^2}=m\omega/\sqrt{2}n_0^{3/2}-2\sqrt{2}\sigma^2K^2s_0^{3/2}/D\pi^{1/2}n_0^{1/2}$$
$$=0 \qquad (4.2)$$

Calculating (4.2) we obtain the aggregation number of the micelle,

$$n_0=m\omega D\pi^{1/2}/4\sigma^2K^2s_0^{3/2} \qquad (4.3)$$

Substituting n_0 (4.3) into the equation (4.1), we obtain

$$\frac{\partial E_{n0}}{\partial n}=m\omega-\sqrt{2}\,m\omega/n_0^{1/2}+e^2\kappa/3D \qquad (4.4)$$

This is the maximum energy difference between the paraffin chain salt in micellar state and in non-aggregated state. Those micelles which would require maximum energy are certainly most stable, and other micelles which are smaller or larger will tend to increase or decrease their aggregation number until they assume the right size. This condition is given in (4.3), and the critical micelle concentration will be given by using (4.4).

As the micelle formation is a reversible process, paraffin chain salts in the bulk of the solution are in statistical equilibrium with those in the micelle. The critical micelle concentration can be obtained by equating the partial potential of each state. The relation has been derived already in the previous paper.[3] That is

$$\log C=\log 1000/v-(\chi-\chi')/kT-1 \qquad (4.5)$$

Where $\chi-\chi'$ is the energy difference between the paraffin chain ion in the micellar state and that in the solute state; v is free volume per molecule; C is the critical micelle concentration in moles per liter.

Substituting the relation (4.4) into the equation (4.5), we obtain

$$\log C=\log 1000/Nv-m\omega/kT+\sqrt{2}\,m\omega/n_0^{1/2}kT$$
$$-e^2\kappa/3DkT-1 \qquad (4.6)$$

Introducing $\omega=1.08\,kT$, $D=80.8$ $\sigma=e/20.5\text{Å}^{-2}$, $e=4.8\times10^{-10}$ *esu*, and $s_0=20.5\text{Å}^2$ into (4.3) we obtain n_0, and then introducing n_0 into (4.6) and assuming $Nv=10$ *c.c.*, we obtain

$$\log C=3.60-1.08m+2.77m^{1/2}K-0.77C^{1/2}-1 \qquad (4.7)$$

where K is 0.57 for fatty acid soaps and 0.46 for sodium alkyl sulfate. Critical micelle concentrations of common soaps are calculatd using these values.

4. Qualitative Discussion of the Effect of Added Salts, Polar Oil and Non-polar Oil

1) The paraffin chain ions aggregated into the micelle attract the gegenions to positions near the micelle surface. But the gegenions, which tend to move away by thermal agitation, also attract the paraffin chain ions and tend to take them away from the micelle. This is one of the reasons why the ionic detergents are much more soluble into water than non-electrolyte of the same hydrocarbon chain length. As the adsorption of gegenions to the micelle increases with the increasing concentration of added gegenions, the aggregation number of long-chain ions in the micelle increases according to (4.3), and the critical micelle concentration decreases with the increase of the aggregation number according to (4.6). In other words the decrease of the critical micelle concentration in the presence of added salts is due to the decrease in the repulsive forces between the polar head groups of the molecules (ions) in the micelle. As the same ions are apart from the micelle due to the Coulombic repulsive force, the effect of salts is independent of the kind or valency of the ions of the same sign and only depends on the concentration and valency of gegenions.

2) Solubilization of polar compounds such as alcohols, fatty acids, etc. can be considered to involve penetration into the palisade layer of the micelle rather than incorporation into the micelle center.[8,9] Thus the effective charge density on the micelle surface decreases with the increase of the penetration of the polar-nonpolar molecules into the micelle. If the mole fraction of alcohols penetrated into the micelle is x, the charge density will become from σ to $(1-x)\sigma$, and the aggregation number of paraffin chain salts increases according to (4.3), and the critical micelle concentration decreases according to (4.3), (4.6) and the free energy of mixing.[3]

3) The extensive x-ray work of many investigators[10-14] shows that the nonpolar oil enters the hydrocarbon center of the micelle. Thus the solubilization of nonpolar molecules does not affect the charge density, but only affects the interaction between discs. Since the thickness of the micelle is just twice the length, of the paraffin chain salts, the repul-

8) W. D. Harkins, R. W. Mattoon, and R. Mittelmann: *J. Chem. Phys.*, **15**, 763 (1947).
9) J. H. Schulmann, and A. H. Hughes: *Biochem. J.*, **29**, 1243 (1935).
10) K. Hess, and J. Gundermann: *Ber.*, **70B**, 1800 (1937).
11) H. Kiessig, and W. Philippoff: *Naturwissenschaften*, **27**, 593 (1939).
12) J. Stauff: *Kolloid-Z.*, **89**, 224 (1939): **96**, 244 (1942).
13) E. W. Hughes, W. M. Sawyer, and J. R. Vinograd: *J. Chem. Phys.*, **13**, 131 (1945).
14) W. D. Harkins, R. W. Mattoon, and M. L. Corrin: *J. Colloid Sci.*, **1**, 105 (1946).

sion due to the same ions between discs and the attraction due to the gegenions around the micelle may be ignored, and the interaction between discs is supposed to be small. This anticipation coincides with the experimental results that the critical micelle concentration decreases slightly with the added hydrocarbons.[4,5,15]

Summary

The cylindrical double layer model for the micelle was adopted and the aggregation number was calculated by the condition that $\partial^2 E_n/\partial n^2=0$, and by using the aggregation number given by the above condition, an equation for the critical micelle concentration was derived. This equation shows that the critical micelle concentrations depend on the number of carbon atoms in the hydrocarbon chains and not on the kind of gegenions of the same valency. Moreover, the effect of added salts, polar oil and nonpolar oil on the aggregation number and on the critical micelle concentration in aqueous solution of paraffin chain salts was discussed qualitatively.

The expense of this research has been partly defrayed by the Ministry of Education, to which our thanks are due.

Department of Physical Chemistry,
Faculty of Engineering,
Yokohama National University,
Yokohama, Japan

15) H. B. Klevens: *J. Phys. & Colloid Chem.*, **54**, 1012 (1950).

Quantitative Separation of Copper by Thiourea from Homogeneous Solution[1]

By Shigenari WASHIZUKA

(Received April 9, 1953)

It was reported by Y. Uzumasa and T. Okura[2], that on boiling alkaline solution containing the copper sub-group ions in the presence of thiourea, sulfides precipitate in crystalline and easily filterable form. These authors suggested that a new method of qualitative analysis without using hydrogen sulfide might be possible by the homogeneous precipitation with this reagent.

The author made, following this suggestion, a thorough study on the conditions for the complete precipitation of copper sulfide and for the quantitative separation of copper in the presence of other cations such as nickel, cobalt, zinc, manganese, calcium and magnesium. Finally the author found that the use of urea and ammonium chloride together with thiourea made this trial succeed. Urea[3] added to the acidified solution, when boiled, gradually diminishes the hydrogen ion concentration in the solution, owing to its hydrolytic decomposition, and the proper conditions for the complete precipitation of copper sulfide by thiourea are attained. Thus the satisfactory results were obtained in the case of copper alone, but the separation of copper is less satisfactory in the presence of other cations.

The selective reactions of thiourea against cations[4], or formation of metal sulfides are promoted with the increase of *p*H value in the solution. At a desirable high *p*H range, coprecipitation of some cations with copper sulfide occurs and unsatisfactory results as mentioned above are obtained. To avoid this, the increasing tendency of *p*H caused by the decomposition of these reagents should be controlled so as to be in the lower limit of *p*H value required for the formation of copper sulfide. The addition of ammonium chloride to the homogeneous solution containing these reagents successfully solves this problem. The realization of this optimum *p*H value is ascribed to the buffer action of urea and ammonium chloride.

Experimental

(A).—Complete precipitation of copper sulfide.

Materials.—Pure cupric oxide, ignited at 900°C., was dissolved in hydrochloric acid and the solution was diluted with water to a liter. The copper solution thus prepared was found to be

1) On September 26, 1952, part of this paper was read before the Meeting of the Hokkaido Section of the Chemical Society of Japan.

2) Y. Uzumasa and T. Ôkura, This Bulletin, **23**, 163 (1950).

3) The characteristic separation method from homogeneous solution by urea has been developed by H. H. Willard and others. H. H. Willard and N. K. Tang, *J. Am. Chem. Soc.*, **59**, 1190 (1937); H. H. Willard and N. K. Tang, *Ind. Eng. Chem., Anal. Ed.*, **9**, 357 (1937); H. H. Willard and J. L. Sheldon, *Anal. Chem.*, **22**, 1162 (1950); H. H. Willard, *Anal. Chem.*, **22**, 1372 (1950); L. Gordon, *Anal. Chem.*, **24**. 459 (1952).

4) J. H. Yoe and L. G. Overholser, *Ind. Eng. Chem., Anal. Ed.*, **14**, 435 (1942).

free from other metallic ions. The concentration was determined as cupric oxide. Thiourea was recrystallized from water, while urea from ethanol.

Experimental Procedure.—Approximately 300 ml. of solution containing about 50 mg. of copper together with 2 grams of urea and one or more ml. of 10% thiourea solution, was placed in a 500 ml. Erlenmeyer flask. The solution was properly adjusted to give the desired initial *p*H value with diluted hydrochloric acid or alkali hydroxide solution. The homogeneous solution thus prepared was then heated to boiling point. A white turbidity first appeared, which gradually blackened upon the formation of copper sulfide. The solution was kept boiling, about thirty minutes later the black precipitate appeared, then it was cooled and kept at room temperature for one hour. The precipitate aggregated at the bottom of the flask was dense and not bulky.

The precipitate was filtered off, and washed with water. Unlike the precipitates formed by hydrogen sulfide, this precipitate was not oxidized by air, and no peptization was noticed during filtration and washing. The precipitate was ignited, and weighed as cupric oxide. *p*H values of the filtrates or solutions were measured with a glass electrode *p*H meter throughout this study.

(1). *Quantity of Thiourea Required.*—To find out the most suitable quantities of thiourea for precipitating copper, a series of experiments were conducted. The results obtained are given in Table 1. These results indicate that more than 1.7 of the mole ratio of thiourea added to copper are required to obtain accurate results. Although an excessive reagent seems to be harmless for the quantitative precipitation of copper, it is desirable to avoid an exceedingly excessive use, as it makes successive analytical procedures complicated. The proper amount required for 50 mg. of copper is 1 ml. of 10% solution of thiourea.

TABLE I

RELATION BETWEEN QUANTITY OF Cu AND THIOUREA ADDED (CuO Taken 62.6 mg.)

10% thiourea solution added, ml.	mole ratio to Cu	CuO found, mg.	Diff. mg.
0.6	1.0	61.9	−0.7
0.8	1.3	62.7	+0.1
1.0	1.7	62.8	+0.2
2.0	3.4	62.9	+0.3
3.0	5.1	62.5	−0.1
4.0	6.8	62.8	+0.2

Initial *p*H of the solution is 4.0. Boiling duration is 30 min., and urea added is 2 g./300 ml. of the total volume.

(2). *Relation between Final pH Value, and Urea Added.*—As urea forms ammonia and carbon dioxide or ammonium carbonate gradually with hydrolysis, the resulting *p*H values of the solution depend on the molar concentrations of urea added. Table II shows the effect of varied quantities of urea on the final *p*H value. Final *p*H values of the solutions containing less than 1.5 g. of urea were low, and experimental errors were negative. It should be noted that copper is completely precipitated when *p*H is above 8.0 and the concentration of urea added is over 0.08 in molar concentration. As the length of time necessary for the appearance of copper sulfide precipitate was found to differ from each other, boiling should be continued for thirty minutes or more in each case.

TABLE II

RELATION BETWEEN FINAL *p*H, AND UREA ADDED (CuO taken 62.6 mg./300 ml.)

Urea added, g.	mol. × 10²/1.	Final *p*H,	CuO found, mg.	Diff. mg.	Time elapsed from boiling to the appearance of black turbidity min.
0.5	2.8	7.72	61.5	−1.1	15
1.0	5.6	7.85	61.9	−0.7	10
1.5	8.4	8.00	62.4	−0.2	7
2.0	11.2	8.48	62.6	±0.0	5
2.5	14.0	8.84	62.5	−0.1	5
3.0	16.8	9.00	62.6	±0.0	3

Initial *p*H of the solution is 4.0, thiourea added is 1 ml. of 10% solution. Boiling was continued for 30 min. or more after first black turbidity appeared.

(3). *Effect of Duration of Boiling.*—Table III gives the results for the various durations of boiling. The precipitation, at the urea content of 2.0 g., was found to be complete after thirty minutes from the appearance of black turbidity. Continuing the boiling, the precipitates coagulated and settled to the bottom of the flask. When the copper content is about 50 mg., boiling for forty minutes is ideal for practical purposes. Further experiments confirmed that sixty minutes of boiling is needed for 100 mg. of copper.

TABLE III

EFFECT OF BOILING DURATION (CuO taken 60.9 mg.)

Boiling duration min.	CuO found, mg.	Diff. mg.
15	60.0	−0.9

30	60.8	−0.1
45	61.2	+0.3
60	60.7	−0.2
60	60.9	±0.0
60	61.1	+0.2

Initial pH of the solution is 4.0, urea added is 2.0 g./300 ml. of the total volume, and thiourea added is 1 ml. of 10% solution.

(4). *Effect of initial pH Value.*—Table IV shows that the amount of copper precipitated is affected by the initial pH of the homogeneous solution. As the hydroxyl ion evolved with the hydrolysis of urea neutralizes the hydrogen ion, resulting pH value of solutions with lower initial pH do not reach to the extent of complete precipitation. In the case of the initial pH 1.6, a white turbidity appeared after the solution began to boil, and took nearly thirty minutes till the black colored copper sulfide appeared. When the initial pH value was lower than 2.6, the coagulation of copper sulfide was incomplete. It is revealed that the precipitation is completely carried out when the initial pH value is regulated at 4.0 or more.

TABLE IV
EFFECT OF INITIAL pH VALUE (CuO taken 62.6 mg.).

Initial pH,	Final pH,	CuO found,	Diff.	Time elapsed from boiling to the appearance of black turbidity.
		mg.	mg.	min.
1.6	7.00	60.6	−2.0	30
2.0	7.24	60.9	−1.7	15
2.6	7.60	61.7	−0.9	7
3.4	8.00	62.3	−0.3	5
4.4	8.55	62.5	−0.1	5
5.2	8.80	62.4	−0.2	2

Urea added is 2 g./300 ml. of the total volume, and thiourea added is 1 ml. of 10% solution. Boiling was continued for 30 min. or more after first black turbidity appeared.

(B).—Separation of Copper From Other Metals.

(1) *Preliminary Investigation*:—Relation between final pH, and ammonium chloride.—

In order to ascertain the influence of the other cations, 50 mg. of copper was precipitated following the above mentioned procedure from the solution containing 0.5 g. of one of other cations respectively. The precipitates thus formed were ignited to constant weight, which compared with that obtained in the case where copper alone exists. It was found that calcium and magnesium had no affect, whereas the coprecipitated amounts of cobalt as well as nickel were 25%, while zinc and manganese were 70% and 1% respectively. Because of the interferences of these other cations, the procedure resulted in unsatisfactory separation of copper. To avoid these interferences, various amounts of ammonium chloride (from 0.5 to 4.0 g.) were added to the solution and boiling was continued to complete precipitation. Converse to the amount of ammonium chloride, the quantity of the coprecipitation gradually diminished, and satisfactory results were obtained by adding 2.0 g. of the salt.

To determine the influence of the amounts of ammonium chloride upon the final H value and the precipitation of copper, two series of attempts were made in which various amounts of ammonium chloride were added to the solution containing 62.0 mg. of cupric oxide, and 2 g. of ammonium chloride was added to the solution containing various concentrations of copper. The former results are shown in Fig. 1, and the latter in Table V. Fig. 1 indicates that the final H value of the solution decrease with the increase of ammonium chloride added, and the addition of more than 2 g. of it tends to make the precipitation less satisfactory. Table V indicates the relations between various concentrations of copper and the final pH. In order to guard against any reduction of the quantity of the precipitate, 2 g. of the salt is ideal, and in this state final pH is 8.0.

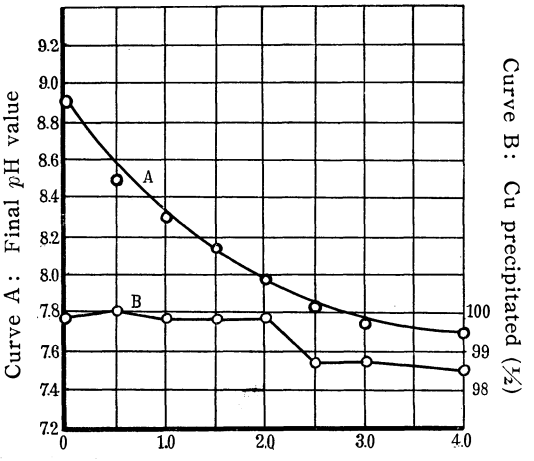


Fig. 1. Relation between final pH, quantity of copper precipitated, and amm. chloride added

Curve A. The final pH versus the amount of amm. chloride added.

Curve B. Percentages of precipitates versus the amounts of amm. chloride added.

Quantity of amm. chloride added (g./300ml.)

Surface Chemistry of High Polymers. III. Some Relationships between the Monolayer of Non-electrolytic Linear Polymers

By Hiroshi HOTTA

(Received July 18, 1953)

In the previous papers[1,2] we have studied the monolayer of copolymers of vinyl acetate and stearate at the air/water and oil/water interfaces to obtain information for the general behaviour of the non-electrolytic linear polymer. As a result of studying afterwards some other similar linear polymers, we found some interesting relationships between them. Therefore, we shall describe these results as the addendum to the previous studies.

Experimental

We measured the surface pressure by the hanging plate method, and the surface potential by the vibrating electrode method at the air/water interface at room temperature (10~15°C.), and the interfacial pressure by the ring method at the petroleum ether (b.p. 100~140°C.)/water interface at about 20°C. The apparatus and procedure were almost the same as in the previous papers[1,2], but the specific caution for each individual polymer and some modifications for the rise in accuracy were taken.

Polymethyl methacrylate was spread on distilled water from benzene solution, polyacrylonitrile from dimethylformamide solution, and amilan (ε-aminocaproic acid polymer) from the solution in a mixture of concentrated sulphuric acid (10%), isopropyl alcohol (50%), and water (40%), respectively. Polymethacrylic acid was spread on ca. 0.01 N HCl from aqueous 20% pyridine solution.

Materials—Polymethyl methacrylate was reprecipitated with methyl alcohol from the benzene solution of a commercial product. Polyacrylonitrile was kindly supplied by Prof. M. Imoto in Osaka City University. Amilan was the same as in the preceding paper.[2] Polymethacrylic acid was prepared by the usual method by Mr. S. Otsuka in our institute. Although the degrees of polymerization of these samples were not properly measured, it is sure that they are far greater than the corresponding value in Table II to be discussed below.

Results and Discussion

Polymethyl Methacrylate and Undissociated Polymethacrylic Acid at the Air/water Interface:

The observed surface pressure-area curves and surface potential-area curves of polymethyl methacrylate and undissociated polymethacrylic acid are shown in Figs. 1 and 2, respectively, in which the result of polymethyl

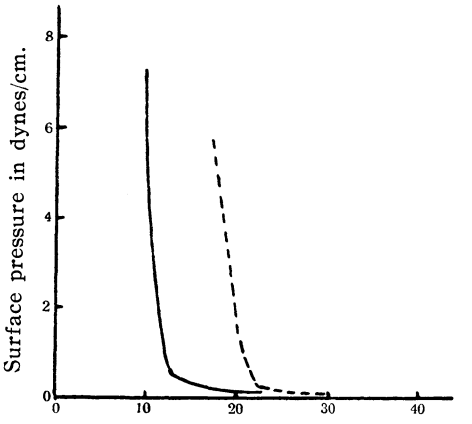


Fig. 1. The surface pressure-area curves of polymethyl methacrylate (- - - -) and polymethacrylic acid on *p*H 1.6 (——) at the air/water interface

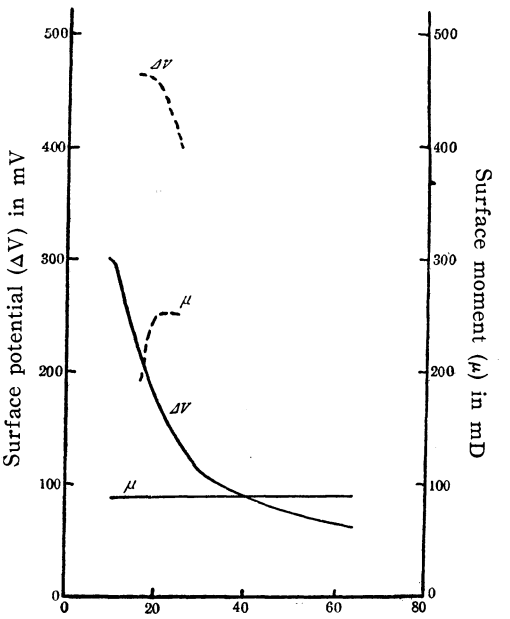


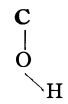
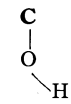
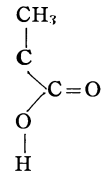
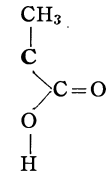
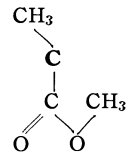
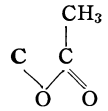
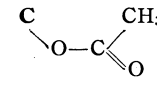
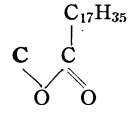
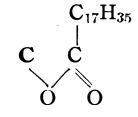
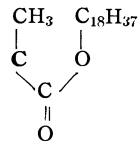
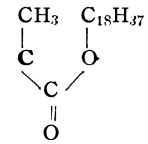
Fig. 2. The surface potential (ΔV) or surface moment (μ)-area curves of polymethyl methacrylate (- - - -) and polymethacrylic acid on *p*H 1.6 (——) at the air/water interface

1) T. Isemura, H. Hotta and T. Miwa, This Bulletin, **26**, 380 (1953).
2) H. Hotta, ibid, **26**, 386 (1953).

methacrylate is shown by a dotted line and is almost identical with that reported by other investigators.[3,4] Especially, the reliable surface potential could not be obtained up to 25 Å²/residue, similar to Crisp.[4] On the contrary, the curve for polymethacrylic acid could be obtained reliably at the wider range. The latter film might be sufficiently undissociated under the present condition as mentioned in the following paper.[5]

When we summarize the present results as well as the previous one,[1] the surface moment of some linear polymer films, calculated by the usual method as mentioned in the previous paper, was various in spite of their similar formulas as shown in Table I, in which the surface moment at the both areas of 25 Å² and 50 Å² per residue is listed in mD unit in parenthesis in the corresponding column and the carbon atom in the main chain is shown by **C**. The surface moment of polyvinyl alcohol in this table, which is quoted from the result of Crisp,[4] is corrected for residual acetate groups. On the other hand, the bond moment of C=O and C−O in vacuo is 2.5 and 0.86 D. unit, respectively.[6] Therefore, on considering these magnitudes and the orientation of these polar bonds at the air/water interface, their most plausible models consistent with the observed value of their surface moment as shown in Table I are proposed to make clear the differences between them. The area, from which the reliable surface moment could be obtained, is given in Table I. The physical meaning of these areas will be given in the next section.

TABLE I THE SURFACE MOMENT OF POLYMERS AT THE AIR/WATER INTERFACE

Polymer	Surface moment (in mD unit) and the corresponding model at 25 Å² per residue		at 50 Å² per residue		Area, from which the reliable surface moment can be obtained (in Å² unit)	Literature
Polyvinyl alcohol		(40)		(40)	50	(4)
Undissociated polymethacrylic acid		(90)		(90)	65	The present
Polymethyl methacrylate		(250)	—	—	25	The present
Polyvinyl acetate		(260)		(340)	70	(1)
Polyvinyl stearate		(260)		(260)	55	(1)
Polyoctadecyl methacrylate		(460)		(460)	45	(4)

3) H. G. Saraswat and A. Kalyanasundaren, *J. Polymer Sci.*, **7**, 325 (1951).
4) D. J. Crisp, *J. Colloid Sci.*, **1**, 161 (1946).
5) T. Isemura, H. Hotta and S. Otsuka, to be published in This Bulletin.
6) C. P. Smyth, *J. Am. Chem. Soc.*, **60**, 183 (1938).

It is understood, first of all, by the low bond moment of C−O in comparison with that of C=O, that polyvinyl alcohol has the lowest surface moment in these polymers. Next, the various surface moments among polymethyl methacrylate, polyvinyl acetate and stearate and polyoctadecyl methacrylate in spite of their similar formula, can be understood by the present models in this table, that is, these models are designed so as to have a higher surface moment with the increase of the inclination of C=O bond, and a similar surface moment for a similar inclination. The remarkably low surface moment of undissociated polymethacrylic acid may be attributed to the horizontal orientation of C=O bond. The difference of the limiting area between polymethyl methacrylate and polymethacrylic acid shown in Fig. 1 is also understood in the light of these models. The difference of the surface moments of polyvinyl acetate at 25 Å^2 and at 50 Å^2 per residue is understood by using these models in consideration of their high flexibility as discussed thoroughly in the preceding papers.[1,2] The difference of the surface moment of polyvinyl stearate from that of polyoctadecyl methacrylate was already discussed in the previous paper.[1]

Polymethyl Methacrylate and Polyacrylonitrile at the Petroleum Ether/water Interface:

The observed interfacial pressure-area curves of polymethyl methacrylate and polyacrylonitrile at the petroleum ether/water interface are shown in Fig. 3. We had to wait 25 minutes for the perfect spreading of them prior to every successive measurement.

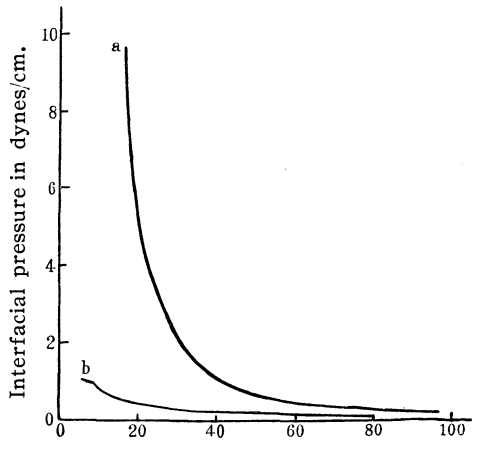


Fig. 3. The interfacial pressure-area curves at the petroleum ether/water interface: curve a, polymethyl methacrylate and curve b, polyacrylonitrile

Polyacrylonitrile could not be spread at the air/water interface. We calculated their statistical kinetic unit at the oil/water interface by inserting the results into the equation of

$$\pi A = \frac{kT}{n}\left(1+\frac{b}{A}\right) \qquad (1)$$

and extrapolating to infinite area as shown in Fig. 4, where π is the interfacial pressure, A the area per residue, n the degree of of polymerization of this unit, and b an interaction constant. The explanation of this equation is described in detail in the preceding paper.[2] The results shown in Table II, give the various values for the number of atoms in the main chain of this statistical kinetic unit, n_{atom}. In this table, the datum for polyvinyl acetate reported in the previous paper is also shown for comparison. The value for amilan was measured over again as mentioned in the next section.

TABLE II

THE STATISTICAL KINETIC UNIT OF LINEAR POLYMER AT THE OIL/WATER INTERFACE

Polymer	$(n)_{A=\infty}$ in equation (1)	n_{atom} (The number of atoms in the main chain of this unit)
Polyvinyl acetate	19	37
Polymethyl methacrylate	23.5	47
Polyacrylonitrile	36.5	73
Amilan (ε-aminocaproic acid polymer)	6.9	48

In these polymers as shown in Table II, polyvinyl acetate gives the film of perfectly expanded type and the same surface pressure-area curve at the air/water and oil/water interfaces as mentioned in the preceding paper. Amilan and polymethyl methacrylate give the film of condensed type at the air/water interface, and the expanded film at the oil/water interface as shown in figures. Polyacrylonitrile can not be spread at the air/water interface, but gives the film of considerably condensed type even at the oil/water interface as shown in Fig. 3, and this film gives the negative slope in Fig. 4. Both the latter polymers take 25 minutes for perfect spreading at the oil/water interface, but the former both polymers can spread within 10 minutes. On the other hand, the areas, from which the reliable surface moment begins to be obtained, are shown in Table I.

When we compare the relationship between the type of film, the time needed for perfect spreading, the largest area per residue for

giving the reliable surface moment and the value of n_{atom}, we notice that they are not independent of each other. That is, each quantity serves as a measure showing how the molecules are flexible (or rigid), or, how much they are interacted mutually, accompanying the effect of linkage as discussed in detail in the preceding paper.[2] With increasing flexibility, the surface pressure and the largest area for reliable surface moment increase, and the time for perfect spreading and the value of n_{atom} decrease. The more quantitative interpretation of n_{atom} will be given in the following paper.

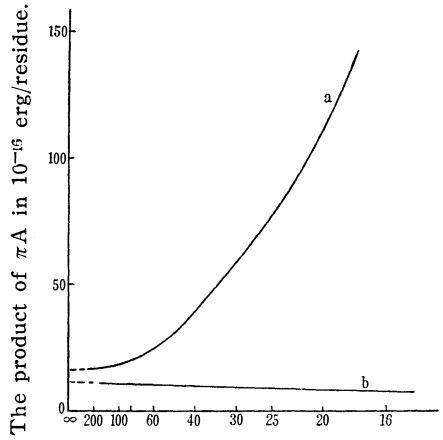


Fig. 4. The $\pi A - \frac{1}{A}$ curves of polymer at the petroleum ether/water interface: curve a, polymethyl methacrylate and curve b, polyacrylonitrile

The slightly negative slope of polyacrylonitrile in Fig. 4 seems to be due not to imperfect spreading, but to the increasing degree of condensation of film, on comparing the kink point in Fig. 3 with that of polymethacrylic acid in Fig. 1, which has no side chain in the surface as polyacrylonitrile. It is also consistent with the fact that polyacrylonitrile is insoluble except in dimethylformamide.

Surface Chemical Effect of Hydrolysis of Amilan-in Dilute Surphuric Acid:

When we studied the monolayer of amilan in the preceding paper,[2] it was spread from the solution in 10% surphuric acid. Since it is well-known that the molecular weight of amilan decreases in surphuric acid by hydrolysis,[7] we examined this effect on its film by the above-mentioned methods. These results are shown in Figs. 5, 6 and 7 as the function of surface area per monomer.

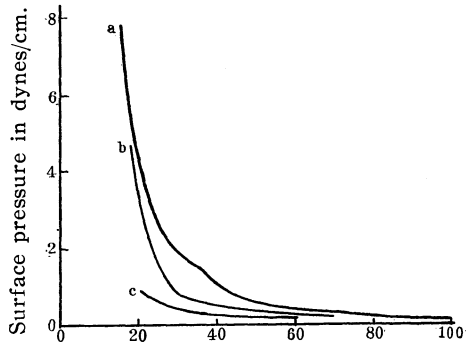


Fig. 5. The surface pressure-area curves of amilan at the air/water interface: curve a, within a first month, curve b, after 4 months and curve c after 8 months

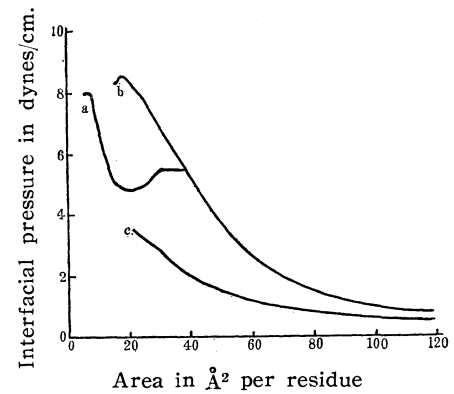


Fig. 6. The interfacial pressure-area curves of amilan at the petroleum ether/water interface: curve a, within a first month, curve b, after 4 months and curve c, after 8 months

The surface pressure-area curves at the air/water interface suffered no change within a month after preparing the solution and the curves were quite identical with the curve shown in Fig. 5. It has a kink point at 35 Å², below the area of which the pressure changed considerably with time. However, the curves obtained by using the solutions stood over four or eight months after preparation (curves b and c in Fig. 5), were lower in surface pressure than curve a, and there was no kink point in the former curves. On the other hand, the curves at the petroleum ether/water interface were also essentially unchanged within the first month. However, the kink point disappeared gradually with the age of the solution as shown in Fig. 6. Nevertheless the values of n_{atom} in

7) K. Hoshino and M. Watanabe, *J. Chem. Soc. Japan*, **70**, 170 (1949); *J. Am. Chem. Soc.*, **73**, 4816 (1951).

Table II were not affected even after 8 months.

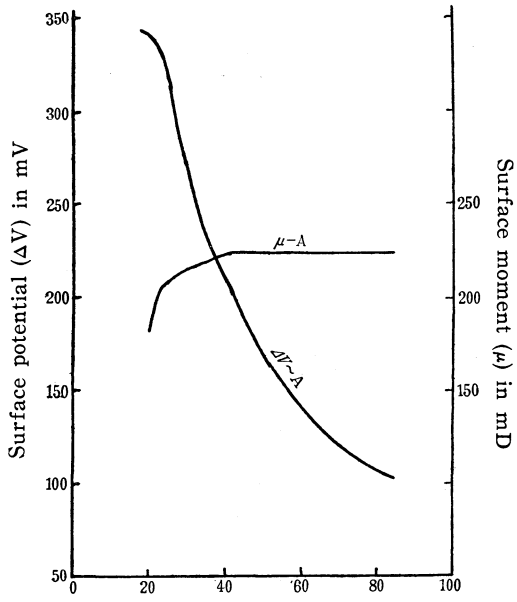


Fig. 7. The surface potential or surface moment of amilan at the air/water interface

The corresponding surface potential-area curves were almost unchanged even after 4 months as noticed from Fig. 7, and the reliable surface potential could be obtained from about 80 Å². However, the saturated tendency of surface potential at the area smaller than 23Å², became gradually indistinct with the age of the solution. On the other hand, the surface viscosity measured by the oscillating disk method is rapidly raised from about 80 Å².[8]

From these facts, it is concluded that there are two characteristic points, namely, 35 Å² and 80 Å² in amilan film at the air/water interface. The former corresponds perhaps to the intrachain transition as mentioned in the preceding paper. On the other hand, as the film is compressed, the polymer molecules at the surface begin to contact each other, and to construct a loose but homogeneous network structure. Such an area, where the homogeneous interchain structure is completed, corresponds to the latter characteristic point, from which the surface potential can be obtained reproducibly and the surface viscosity is rapidly raised.

Although it has been mentioned above that the effect of hydrolysis was not so remarkable during the first month, the observed values in the repeated experiments were fluctuated from the standard curve with the lapse of time, and the transition points became gradually indistinct with age. The surface pressure was fairly lower even in curve a in Fig. 5 than that reported by Isemura and Hamaguchi.[9] It might be due to either the strong hydrolysis in the initial period or to the difference of solvent and concentration at spreading.

Summary

1. The various surface moments of like polymers can be understood in the light of the models in Table I, which are designed by considering the orientation of C=O bond at the interface.

2. The flexibility of polymer film can be measured not only by surface pressure but also by the time for perfect spreading, the largest area from which the reliable surface moment can be obtained, or the number of atoms in the main chain of the statistical kinetic unit.

3. The effect of hydrolysis of a milan solution by sulphuric acid on its film was examined.

In conclusion, the author expresses his hearty thanks to Prof. T. Isemura for his kind guidance throughout the present work, and to Prof. M. Imoto of Osaka City University and Mr. S. Otsuka in our institute who kindly supplied the present samples. The cost of this research has been partly defrayed from the grant for Scientific Research Encouragement from the Ministry of Education given to Prof. T. Isemura, to whom the author's thanks are due.

The Institute of Scientific and Industrial Research Osaka, University, Sakai, Osaka

8) T. Isemura and K. Hamaguchi, to be published in This Bulletin.

9) T. Isemura and K. Hamaguchi, This Bulletin, **25**, 40 (1952).

Enzymatic Reduction of Aromatic Nitro Compounds

By Ikuo Yamashina

(Received July 23, 1953)

There have been found only two nitro compounds in nature, e. g. β-nitro-propionic acid and chloramphenicol, but it is well known that many species of micro-organisms have the ability to reduce aromatic nitro compounds. The bacterial reduction of chloramphenicol is considered to be one of the reasons for the tolerance.[1,2] And it is also known that in animals, amino-, hydroxylamino and azoxy compounds are excreted in urine when aromatic nitro compounds are administered[3].

In our laboratory, Egami, Ebata and Sato prepared a cell-free bacterial enzyme preparation which accelerates the reduction of chloramphenicol and other aromatic nitro compounds[2]. However, the present author has found that the cell-free extract[4] of a halotolerant bacterium, *Bacillus pumilus* var., has a stronger activity. Utilizing the enzyme preparation of the bacterium, the author studied the nature of the enzyme system and at the same time reinvestigated the identity of nitrite reductase and the enzyme "nitroreductase" because the identity was suggested by Egami and others in our laboratory. It may be worthy to note here that the bacterium has a series of enzymes participating in the successive reduction of nitrate to ammonia[4] and has a strong activity of denitrification[5].

Experimental

Extraction of Nitro-Reductase.—The bacterium was cultured on peptone-bouillon agar containing 10% NaCl, and 1% KNO_3 at 37°C. After 40 ~50 hours the cultured cells were gathered, washed with 10% NaCl by centrifugation and then lyophilized. A clear enzyme solution was obtained by extracting the lyophilized cells with 10^{-1} M phosphate buffer solution (*p*H 6.8, 50~100 mg. cells/cc.) overnight.

Methods of Measurements.—The enzyme activities were measured under anaerobic condition by using Thunberg tubes at 37°C. Before the estimation, the reaction mixture (6~7 cc.) was deproteinized by $Cd(OH)_2$ gel, which was formed by adding 2 cc. $CdSO_4$ solution ($CdSO_4$ 13 g. in 300 cc. H_2O containing 20 cc. N H_2SO_4) and 0.5 cc. N NaOH to the reaction medium. When the dyes such as methylene blue or nile blue were employed, Japanese acid clay or Kaolin was used as the adsorbing agent. The measurements of the reaction were carried out by the determination of the amino compounds formed, or bypolarography of the remaining nitro compounds[3,7]. The methods of the determination of various amino compounds are as follows:

***p*-, *m*-Aminobenzoic Acids (PABA, MABA) and *p*-Aminosalicylic Acid.**—The solution containing amino compounds (8 cc.) was diazotized by adding 1 cc. 6 N HCl and 0.5 cc. 0.2% $NaNO_2$ at room temperature. After 15 min. excess nitrite was removed by some solid aminosulfonic acid. Then, 0.5 cc. 0.2% β-diethylaminoethyl-α-naphthylamine oxalate was added and the optical density of the red dyes formed was measured by Coleman's spectrophotometer at 650 mμ.

***o*-Aminobenzoic Acid.**—In place of 6N HCl, 2N HCl was employed and diazotization was carried out under cooling in ice water. And the measurement of the optical density was carried out after keeping the solution for 15~20 hours at 37°C. after the addition of the coupling agent.

***m*-Aminophenol[8].**—Diazotization was carried out under cooling in ice water and the optical density was measured at 570 mμ after keeping the coupled solution for 15~20 hours at 37°C.

***p*-Aminophenol.[8]**—To the solution of *p*-aminophenol were added 2 cc. 1N Na_2CO_3, 0.4 cc. 5% phenol, 2 cc. 0.1% $K_3Fe(CN)_6$ and 1.6 cc. dist. water. After 30 min. the measurement of the optical density was carried out at 650 mμ.

Measurement of the Reduction of Chloramphenicol[9].—The solution of the reduction product of chloramphenicol was treated similarly as the solution of PABA. By the measurement of the optical density of the red dye formed, the relative velocity of the reduction of chloramphenicol could be estimated. But, for the determination of the absolute velocity polarography was employed. So, after the removal of most of the dyes by some Japanese acid clay, the test solution was deoxygenated by the stream of H_2 gas for 15 min. and measured by SHIMAZU's polarograph.

1) G. N. Smith and C. S. Worrel, *Arch. Biochem.*, **21**, 216 (1949).
2) F. Egami, M. Ebata and R. Sato. *Nature*, **167**, 118 (1951); *J. Agr. Chem. Soc. Japan*, **25**, 347 (1952).
3) R. T. Williams, G. T. Mille and H. J. Channon, *Biochem. J.*, **38**, 73 (1944).
4) S. Taniguchi, H. Mitsui, J. Toyada, Y. Yamada, and F. Egami, *J. Biochem.*, **40**, 175 (1953).
5) I. Yamashina, unpublished.
6) J. E. Page, J. W. Smith and J. G. Waller, *J. Phys. & Colloid. Chem.*, **53**, 545 (1949).
7) J. W. Smith and J. G. Waller, *Trans. Farad. Soc.*, **46**, 290 (1950).
8) D. Robinson, J. N. Smith and R. T. Williams, *Biochem. J.*, **50**, 221 (1951).
9) G. B. Hess, *Analyt. Chem.*, **22**, 649 (1950).

Results and Discussion

Reaction System[10,11,12,13].—It is known that the enzymatic reductions of nitrate, nitrite and hydroxylamine proceed according to the following reaction system:

Substrate—Reductase—Intermediary—Hydrogen Carrier—Dehydrogenase—Hydrogen Donator.

So, in the case of aromatic nitro compounds the existence of a similar reaction system was expected and it was really ascertained (Table I, Fig. 1).

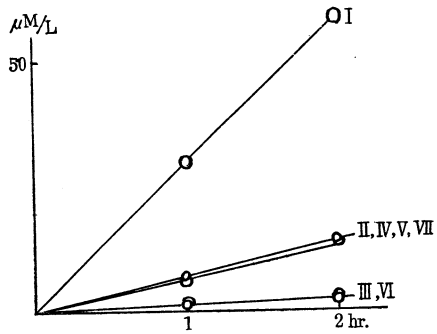


Fig. 1. The formation of PABA at various conditions (Table 1)

TABLE I

	I	II	III	IV	V	VI	VII
Substrate (PNBA 6×10^{-3} M)	1	1	1	1	1	—	1
Reductase*1	1	—	1	1	1*3	1	1
H. Carrier (Nile Blue 2×10^{-3} M)	1	1	1	—	1	1	1
Dehydrogenase*2	1	1	—	1	1	1	1
Buffer (10^{-1} M, *p*H 6.8, phosphate)	1	1	1	1	1	1	1
H. Donator (10^{-1} M, HCOONa)	1	1	1	1	1	1	—
H_2O	—	1	1	1	—	1	1 cc.

*1 The enzyme extracted from halotolerant bacterium
*2 Lyophilized cells of Pseud. fluor. (5 mg/cc.).
*3 heated at 100°C, for 5 min.

Intermediary Hydrogen Carrier.—As intermediary hydrogen carriers, brilliant cresyl blue, thymol blue, *o*-chlorophenolindophenol, methylene blue, K-indigotetrasulfonate, nile blue, neutral red, pyocyanine and several pteridine derivatives were tested. Among these substances only nile blue and brilliant cresyl blue were effective (Fig. 2). The structures and the redox potentials of these two dyes are as follows:

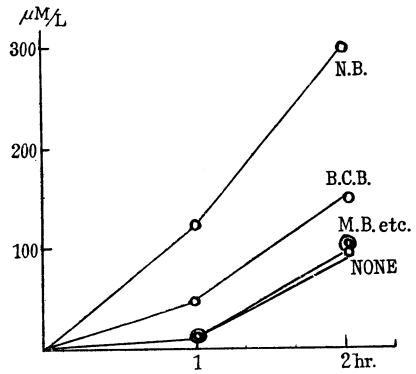
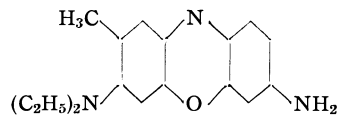
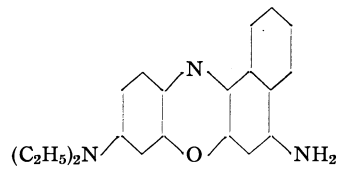


Fig. 2. The formation of PABA in the presence of various hydrogen carriers (3×10^{-5}M)



brilliant cresyl blue

E_0(*p*H 7.0 30°C.) +0.047 volts



nile blue

−0.125 volts

It is interesting to note that the nitroreductase requires the specially shaped molecule, oxazine ring, as the intermediary hydrogen carrier. But, as to the relation between the velocity of the reaction and the concentration of dyes, a marked difference has been observed between two dyes; in the case of nile blue the activity was proportional to the concentration, on the other hand, in the case of brilliant cresyl blue there was an optimum (Fig. 3). The natural hydrogen carrier we have not yet investigated, however, coenzymes such as DPN and FAD may be supposed to function in the reduction of nitro compounds in vivo.

Reaction by the use of leuco dyes.—In order to ascertain the reaction system above mentioned, it was tested whether the reaction proceeds in accordance with the following simple system;

10) B. B. Westfall, *J. Pharmacol.*, **79**, 23 (1944).
11) B. B. Westfall, *J. Pharmacol.*, **78**, 386 (1943).
12) E. Bueding and N. Jolliffe, *J. Pharmacol.*, **88**, 300 (1946).
13) V. H. Parker, *Biochem. J.*, **51**, 363 (1952).

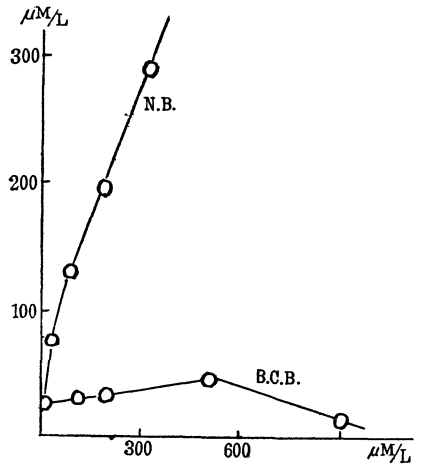


Fig. 3. The relation of the formation of PABA and the conc. of hydrogen carriers

Substrate—Nitro-Reductase—Leuco Dyes. The leuco base of nile blue or brilliant blue was prepared by the catalytic reduction, Pa-$BaSO_4$ being used as the catalyser. In the case of the nile blue, the enzymatic reduction of PNBA was confirmed. An example was

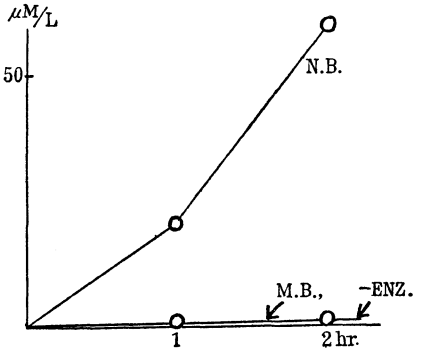


Fig. 4. The formation of PABA with leuco dyes as hydrogen donators System: Substrate (6×10^{-3} M) 1 cc., Reductase 1 cc., Leuco Dye (10^{-2} M) 2 cc., Buffer 1 cc.

shown in Fig. 4, but the curve of the formation of amino compounds plotted against time was not always monotonous. It may be attributed to the low solubility of leuco nile blue in neutral solution, especially in the presence of phosphate. Accordingly, it is unsuitable to use leuco nile blue for the investigation of the reaction velocity. On the other hand, in the case of brilliant cresyl blue, the enzymatic reduction of PNBA was not confirmed. This may be explained by the inhibitory action by the excess of brilliant cresyl blue mentioned above. From these results it was concluded that the enzymatic reduction of aromatic nitro compounds proceeds by the mechanism analogous to that of nitrate, etc.

Michaelis constants were obtained graphically from PS-activity curve in the enzymatic reduction of *o*-, *m*-, and *p*-amino-benzoic acid (Fig. 5).

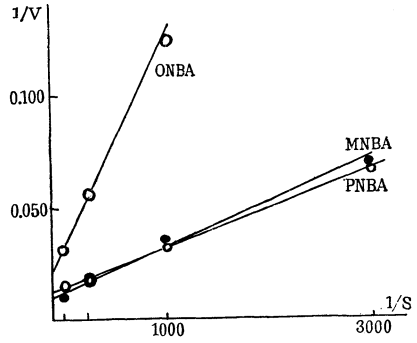


Fig. 5. v=the formation of amino benzoic acids (*o*-, *m*-, *p*-) in 1 hr. in μM/L. s=the conc. of substrates (M/L.)

Specificity, Especially the Relation to Nitrite Reductase.—Various aromatic nitro compounds such as *o*-, *p*-, *m*-nitro benzoic acids (ONBA, PNBA, MNBA), *m*-, *p*-nitrophenols, *p*-nitro salicylic acid. and chloramphenicol were reduced to the respective amino compounds by the enzyme system mentioned above. In the series of nitro benzoic acids the ratio of the reduction velocities at the same concentration of the substrates was *o*-: *m*-: *p*-=0.25 : 0.78 : 1.00.

According to Michaelis equation

$$v=-\frac{kES}{S+K_m}$$

using each K_m values, the ratio of the velocity constants (k) was estimated.

$$o\text{-}:m\text{-}:p\text{-}=0.5:1.2:1.0$$

If K_m values or the ratio of k values were estimated on many nitro compounds, the material for discussing the problems as to the combination of enzyme and its substrate or the influences of the substituents in the reducibility of nitro group could be obtained.

The enzyme solution which was used as nitro-reductase contained also active nitrite reductase. Moreover, as the intermediary hydrogen carrier in nitrite reduction, various substances besides nile blue, brilliant cresyl blue and methylene blue are effective[4]. On the other hand, it was previously shown that methylene blue was not effective in nitro reduction. Now, the competitive inhibition of enzyme action by nitrite reported[2] was reinvestigated and confirmed (Fig. 6). The

effects of aromatic nitro compounds on nitrite reduction were studied as follows. In these experiments, the hydrogen carrier being effective in both cases, nile blue was used and as the carrier effective only in nitrite reduction, methylene blue was used (Table II). As

TABLE II

THE DEGREE OF INHIBITION OF NITRITE REDUCTION BY NITRO COMPOUND (PNBA)

Conc. of PNBA (M/L.)	Conc. of nitrite (M/L.) 10^{-3} N.B.	10^{-3} M.B.	10^{-2} N.B.	10^{-2} M.B.
10^{-3}	5%	0%	5%	0%
10^{-2}	40	0	60	0

shown in Table II, only in the presence of the common carrier, nile blue, the competitive inhibition of nitrite reduction by aromatic nitro compounds was observed. These facts show the possibility of the presence of the

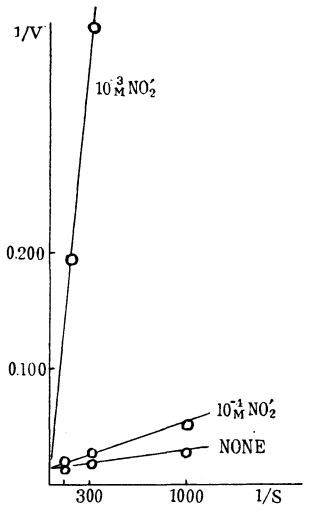
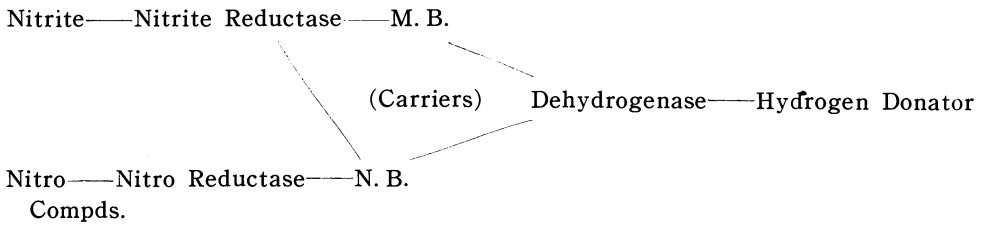


Fig. 6. v=the formation of PABA (μM/L.) in 1 hr.
s=the conc. of PNBA (M/L.)

competition of the two different enzyme systems to the common intermediary hydrogen carrier, as illustrated below:



Then, the effects of several inhibitors on the reduction of nitro compounds compared with that on nitrite reduction are as follows (Table III)[3]. In this case, the inhibition to

TABLE III

THE DEGREES OF INHIBITION BY SEVERAL INHIBITORS

	Nitro	Nitrite
KCN 10^{-3} M	70%	40%
NaN_3 10^{-2} M	5	20
NaF 10^{-2} M	0	0
Mn 10^{-4} M	0	80
Thiourea 10^{-2} M	0	0

formic dehydrogenase was negligibly small. In these data it is shown that the effects of *Mn* are remarkably different in the two cases.

These results seem to be contradictory to the idea that nitrite reductase and nitroreductase may be one and the same enzyme. Anyhow the final solution of the problem will be given by the separation of the enzymes.

Discussion.—The results and the theories described above seem to be consistent with all of the previous reports on the reduction of aromatic nitro compound. E. g. furacin, by bacteria is also considered to take place by a simillar mechanism, taking into consideration the observations that the reduction of furacin by bacteria proceeds only in the presence of oxazine dyes such as nile blue.[14-16]

The author expects that aromatic nitro compounds are not directly but stepwise re-

14) J. S. Gots, V. E. Jordan and A. F. Brodie, *Arch. Biochem.*, **36**, 285 (1952).
15) J.S. Gots, R.E. Asnis and A.F. Brodie, *Arch. Biochem.*, **30**, 25 (1951).
16) J. S. Gots, R. E. Asnis and A. F. Brodic, *Arch. Biochem.*, **30**, 35 (1951).

duced to amino compounds, then there must be many reductases in the enzyme solution which may be named nitro-reductase, nitroso-reductase etc.

Summary

1) The enzyme "nitro-reductase", which activates aromatic nitro-compounds and accelerates their reduction, was extracted from a halotolerant bacterium.

2) The reduction proceeds by the mechanism analogous to that of nitrate reduction, namely, by the system consisting of nitro-reductase, intermediary hydrogen carrier, dehydrogenase and hydrogen donator.

3) Oxazine dyes such as nile blue and brilliant cresyl blue are the only effective hydrogen carriers so far examined for the reaction.

4) Various aromatic nitro compounds can be reduced to amino compounds by the enzyme system. Some kinetic studies were performed.

5) The relation between nitro-reductase and nitrite reductase, the identity of which was suggested formerly, was reinvestigated. The competitive inhibition of nitro reduction by nitrite was confirmed, but taking into consideration various experimental evidences, it may be concluded that the two enzymes are not identical.

The author would like to thank Prof. F. Egami for his kind guidance and encouragement throughout this study. The expence of this study was defrayed in part by a grant from Japanese Biological Research Works, Ltd. and Seikagaku-Kenkyujo Ltd. to which the author's thanks are due.

Chemical Institute, Faculty of Science, Nagoya University

État du fer dans les eaux des lacs[1]

Par Motoharu TANAKA

(Reçu le 5, Août, 1953)

Des études récentes sur l'état de certains éléments dans l'hydrosphère attirent de plus en plus l'attention des géochimistes.[2,3] On pourra y employer l'une des méthodes suivantes:

1°) Pour déterminer la charge des colloides .....Cataphorèse

2°) Pour la recherche quantitative des colloïdes et des particules plus grosses.....
- Centrifugation
- Résine à ion-échange

3°) Pour étudier la valence et la liaison des éléments.....
- Analyse chimique
- Mesure du potentiel d'oxydo-réduction
- Résine à ion-échange
- Polarographie[3]

Toutes les eaux des lacs contiennent plus ou moins de fer dont l'agissement dans l'hydrosphère nous intéresse particulièrement. Dans les eaux des lacs dont le *p*H est au voisinage de 7, le fer ferrique ne peut être à l'état soluble sauf s'il forme un complexe quelconque (minéral ou organique). Le fer ferreux n'existe que dans la couche inférieure où l'on ne peut déceler l'oxygène qu'en très petite quantité. Mais les expériences nous révèlent qu'il existe du fer à toutes les couches d'eau. Ce fer est-il contenu dans les particules relativement grosses ou dans les particules plus petites? Est-il à l'état soluble formant des complexes minéraux ou organiques? Cet exposé a pour but d'éclaircir ces questions.

Expériences à l'aide de la centrifugation

Au lac Aburagafuchi,[4] nous avons pris trois échantillons aux profondeurs respectives de 0 m, 2 m, et 3 m de la superficie. Ces échantillons, centrifugés à 3500 révolutions par minute pendant vingt minutes, nous donnent la teneur en fer inséparable par la centrifugation. Nous avons aussi évalué la teneur en fer des eaux non-centrifugées.

Cette expérience s'effectuant dans la période de stagnation, on constate une diminution d'oxygène avec la profondeur d'un côté, et de l'autre un acroissement de la proportion de fer qui ne peut être séparé de l'eau

1) Ce rapport a été présenté à l'assemblée annuelle de la société chimique du Japon qui s'est tenue à Tokyo, au mois d'avril 1952.

2) T. Kawamoto: Umi to sora (La mer et le ciel) **29**, 24 (1952). T. Okura a fait une conférence sur l'état du fer dans les eaux naturelles au "Symposium" de la géochimie de la société chimique du Japon, à Nagoya au mois de novembre 1952.

3) M. Le Peintre et H. R. Olivier, Compt. rend., **234**, 353 (1952). Ces auteurs se sont servis de la polarographie pour déterminer la valence de l'arsenic dans l'eau thermale à La Bourboule.

4) Ce lac se trouve prés de l'embouchure de la rivière Yahagi, Préfecture d'Aichi. Sa profondeur maxima est 5, 5 m et sa transparence souvent approche à plusieurs centimètres.

par centrifugation. Les figures du tableau I nous démontrent ce phénomène. Ce fait

TABLEAU I
EXPÉRIENCE A L'AIDE DE LA CENTRIFUGATION.
Le lac Aburagafuchi. Le 10, Sept. 1951.
Centrifugation: 3500 Rev./min. 20 min.

Profondeur (m)	Fe(t)(mg/l)	Proportion du fer inséparable (%)	O_2 (cc/l)
0 m	0,67	47,8	5,27
2 m	0,53	79,4	3,98
3 m	0,33	87,7	1,33

nous invite à croire que les grosses particules qui se trouvent près de la superficie sont détruites au fur et à mesure de leur descente en donnant des particules plus fines.

Étude par la méthode analytico-chimique

Poursuivant davantage notre étude, nous avons défini les trois états du fer:

1°) Fer qui réagit directement avec α,α'-bipyridyle dans une solution tamponnée par l'acétate de sodium.....Fe(II)

2°) Fer qui réagit avec α,α'-bipyridyle après la réduction de la solution.....Fe(s)

Méthode: On ajoute, à 5 cc d'échantillon d'eau, 0,2 cc d'acide chlorhydrique (6 N) et 0,3 cc de réductif (une solution saturée d'acide sulfureux). 10 minutes après l'addition de ces réactifs, on traite la solution par α,α'-bipyridyle et une solution tampon d'acétate de sodium et on compare la coloration.

3°) Fer dosé après la fusion du résidu d'évaporation d'eau avec du pyrosulfate de sodium.....Fe(t)

Ici, Fe(II) est la quantité de fer ferreux soluble (constante de dissociation $4{,}0-8{,}7\times10^{-18}$ [5]). Fe(s) signifie la quantité de fer ferreux et de fer qu'on peut rendre soluble facilement. Enfin Fe(t) désigne tout le fer qui existe dans un échantillon d'eau.

Dans les couches supérieures le rapport Fe(s)/Fe(t) varie de quelques centièmes à quelques dixièmes (Fig. 1), mais progressivement avec la profondeur il approche du pourcentage 100% dans la période de stagnation. Autrement dit, le fer soluble augmente avec la profondeur durant cette période. Dans la section précédente, nous avons observé que le fer inséparable par la centrifugation augmente en proportion du décroissement d'oxygène. Quant au Fe(s), il aussi s'enrichit dans les couches pauvres en oxygène. D'un autre côté, dans ces dernières couches s'accumulent des matières organiques qui peuvent stabiliser le fer en donnant des complexes ferriques, même s'il est à l'état ferrique. On peut donc logiquement conclure que des matières organiques provoquent le déficit d'oxygène et que dans le milieu pauvre en oxygène plus grande quantité du fer peut exister sans précipitation.

Considérons la variation saisonnière de la teneur en fer au lac Aburagafuchi (Fig. 1): Au mois d'avril, au commencement de la période de stagnation, on ne peut déceler le fer ferreux dans la couche tout près du fond, même si l'on y voit le manque plus ou moins complet d'oxygène. Mais on y peut constater une augmentation du rapport Fe(s)/Fe(t), et au mois de juillet et d'octobre ce rapport est très proche de 1 dans les couches inférieures au niveau d'oxydo-réduction. Au mois de novembre, après la circulation automnale, on n'y trouve naturellment pas, au fond, la couche anaérobie, et on ne découvre pas une telle couche dans laquelle le rapport Fe(s)/Fe(t) est au voisinage de 1.

Nous avons constaté le même phénomène dans les autres lacs japonais, dont les résultats ne sont pas encore publiés.

La teneur plus forte en fer observée à la superficie

Des expériences essayées jusqu'à présent on conclut que plus on descend vers le fond, plus la teneur en fer augmente. Nous avons aussi constaté qu'ordinairement Fe(s) augmente avec la profondeur. Ayant fait des recherches dans les eaux de différents lacs, nous nous sommes trouvés en présence d'un phénomène non constaté jusqu'ici: celui de la présence d'une quantité notable de fer à la superficie (lac Aburagafuchi, sept. 1950: oct., nov. 1951: lac Kizaki,[6] oct. 1950; mai, sept. 1951: lac Nakatsuna,[6] oct. 1950; mai, oct. 1951). Cela s'explique: une grande quantité du fer contenu dans les particules apportées par les affluents et par les mouvements d'eau est à l'état insoluble en milieu légèrement acide (0,2 cc de 6 N HCl dans 5 cc de l'eau, v. plus haut). Même si ce fer n'est pas à l'état soluble, la rapidité apparente de sa descente est ralentie par les vagues de la superficie. C'est pourquoi on y observe souvent une plus forte teneur en Fe(t). Cette explication s'appuie sur le fait que les eaux de la superficie contient une assez grande quantité de silice et d'aluminium, éléments constitutifs des

5) G. Baxendale, *Trans. Faraday Soc.*, **46**, 55, 736 (1950), Krumholz, *Anais. Acad. Brasil Ciencias*, **22**, 263 (1950).

6) Les lacs, Kizaki, Nakatsuna et Aoki, sont situés dans la préfecture de Nagano, le long de la vallée, au pied Est des Alpes Japonaises du Nord. Nous en donnons ci-dessous quelques précisions morphométriques:

	Aoki	Kizaki	Nakatsuna
Superficie (km^2)	1,863	1,413	0,141
Profondeur (m)	62,0	29,5	12,0
Altitude (m)	822	764	815

Ces trois lacs sont mis en communication par une rivière.

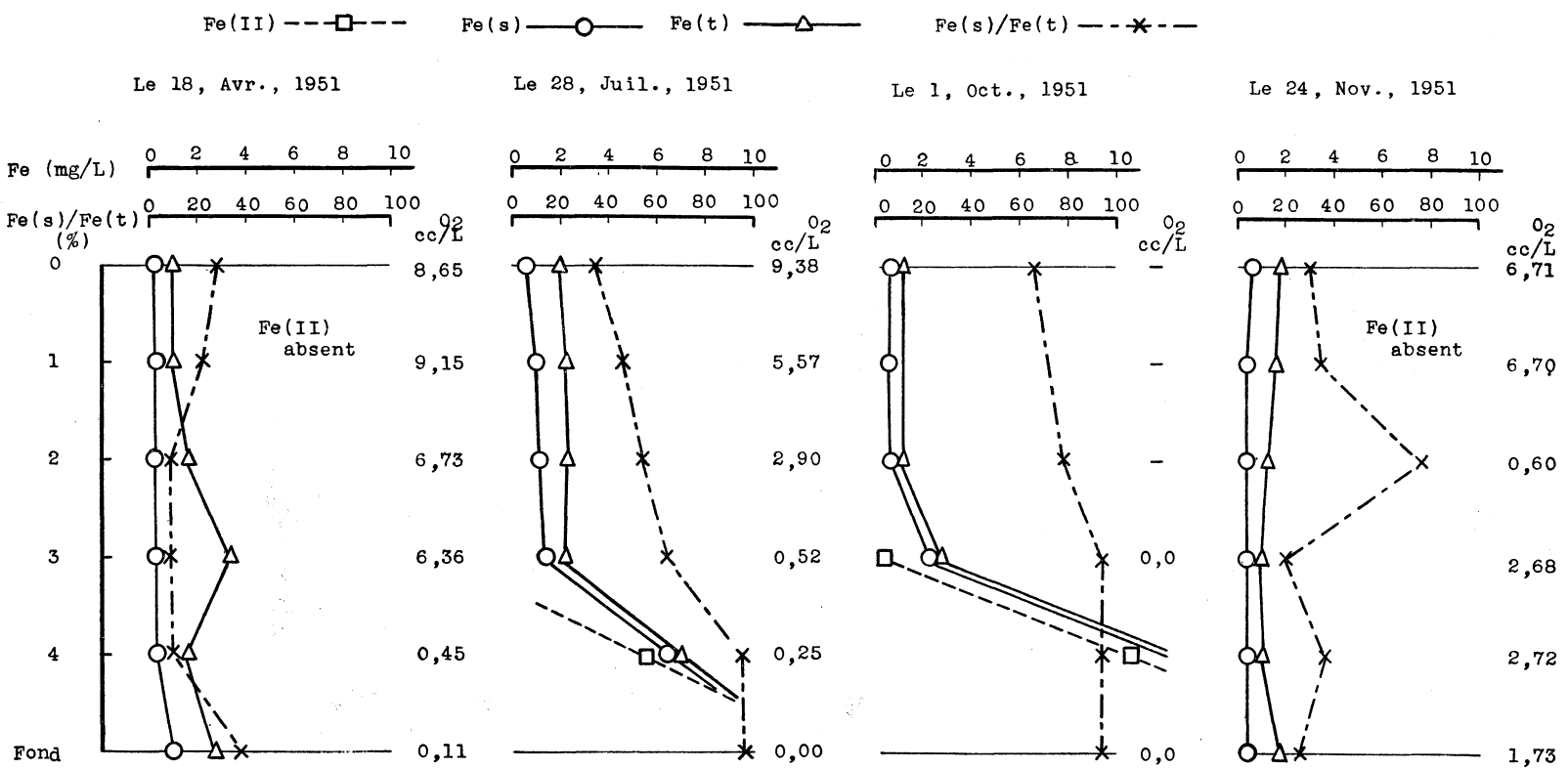


Fig. 1. Variation saisonnière de la distribution verticale de divers états du fer et de Fe(s)/Fe(t). Le lac Aburagafuchi. 1951.

roches silicieuses (ou des argiles) (v. Tableau II). Les conditions météorologiques, le vent

TABLEAU II
LES TENEURS PLUS FORTES EN FER TOTAL, ALUMINIUM ET SILICE OBSERVÉES À LA SUPERFICIE.

a) Lac Aburagafuchi (le 1, Oct. 1951).

Profondeur (m)	Fe (t)(mg/l)	Al (mg/l)	Si (mg/l)
0	0,90	0,80	7,1
2	0,43	0,33	4,4
3	2,72	0,28	4,6
4	—	0,21	—
4,5	17,8	0,53	—

b) Lac Kizaki (le 19, Mai, 1951).

Profondeur (m)	Fe (t)(mg/l)	Al (mg/l)	Si (mg/l)
0	0,17	0,17	5,6
2,5	0,18	0,13	5,2
5	0,19	0,14	5,2
7,5	0,08	—	5,2
10	0,06	0,10	4,8
12,5	0,05	0,04	4,3
15	0,07	0,09	4,3
20	0,07	0,12	4,8
28	0,45	0,25	4,8

c) Lac Nakatsuna (le 21, Mai, 1951).

Profondeur (m)	Fe (t)(mg/l)	Al (mg/l)	Si (mg/l)
0	0,15	0,30	5,8
2,5	0,12	0,10	6,8
5	0,11	0,19	5,8
7,5	0,10	0,19	4,8
10	0,19	0,17	6,4

et les précipitations atmosphériques, naturellement entrent ici en cause. Au lac Yogo[7] qui n'a aucun affluent et qui est entouré de montagnes rocheuses (non argileuses), il est cependant intéressant de n'avoir pu découvrir un tel phénomène à la superficie (v. Tableau III).

TABLEAU III
DISTRIBUTION VERTICALE DU FER TOTAL, DE L'ALUMINIUM ET DE LA SILICE.
(Lac Yogo). Le 21. Août, 1951.

Profondeur (m)	Fe(t)(mg/L)	Al(mg/L)	Si(mg/L)
0	0,22	0,22	1,8
2,5	0,24	0,35	2,3
5	0,27	0,25	2,5
7,5	0,32	0,30	2,7
10	3,28	0,29	3,4

Génèse du fer ferreux dans les couches inférieures

Dans la couche près du fond des lacs, s'accumulent le fer et le manganèse[8] dans la période de stagnation estivale. On pensait depuis longtemps que la plupart de ces éléments étaient fournis par la vase. C'est à bon droit, mais dans le lac d'eau saumâtre comme Aburagafuchi, où les bactéries réductrices des sulfates sont très actives, on ne peut doser le fer dans l'eau-pore (eau contenue dans la vase) de la vase qu'en hiver et toutes les particules y sont enveloppées de pellicules de fer sulfuré (v. Tableau V). Une telle vase ne peut donc fournir le fer ferreux dans les couches inférieures. D'un autre côté, on décèle une grande quantité de fer ferreux dans la couche près du fond (v. Tableau IV). Cette quantité n'est pas inférieure à celle des autres lacs d'eau douce. Dans ceux-ci, contrairement aux lacs d'eau saumâtre, l'eau-pore de la vase contient plusieurs centigrammes du fer ferreux (v. Tableau V).

TABLEAU IV
QUANTITÉ DU FER PEREUX DANS L'EAU DE LA COUCHE PRÈS DU FOND.

Lacs	Date	Fe(II)mg/l	Epaisseur de la couche anaérobie
Aburagafuchi	10. Sept. 1950	max. 34,6	50 cm
Kizaki	10. Oct. 1950	max. 31,3	25 cm
Nakatsuna	14. Oct. 1950	max. 24,0	100 cm

TABLEAU V
QUANTITÉ DU FER FERREUX DANS L'EAU-PORE DE LA VASE.

Lacs	Fe(II) dans l'eau-pore (mg/l)
Aburagafuchi (lac d'eau saumâtre)	
Période de stagnation	$<0,02$
Après la circulation automnale	2,0～10,5
Kizaki (lac d'eau douce)	47,4～69,0
Nakatsuna (lac d'eau douce)	60,7～70,9

Nous sommes alors conduits à la conclusion que la plus grande partie du fer ferreux dans la couche près du fond provient des particules de la couche supérieure.

En résumé, nous pouvons déduire qu'il existe dans le lac d'eau saumâtre un état stationnaire donné schématiquement dans la Fig. 2. Mais dans les lacs d'eau douce comme Kizaki et Nakatsuna, par contre, il faut tenir compte de la quantité du fer fourni par la vase (Fig. 3).

7) Ce lac se trouve dans la préfecture de Shiga, au nord du lac Biwa. Sa profondeur maxima est 13 m. Les montagnes paléozoïques séparent le lac Yogo du lac Biwa.

8) Par exemple, M. Tanaka, *J. Earth Sciences*, Nagoya University, **1**, 119 (1953); F. Ruttner, *Archiv. f. Lagerstättenforschung*, **75**, 16 (1942); S. Yoshimura, *Japanese J. Geol. Geogr.*, **6**, 61 (1931).

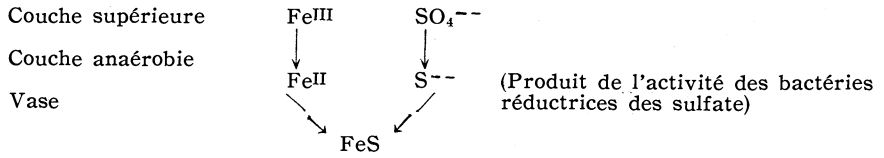


Fig. 2
Génèse du fer ferreux dans le lac d'eau saumâtre

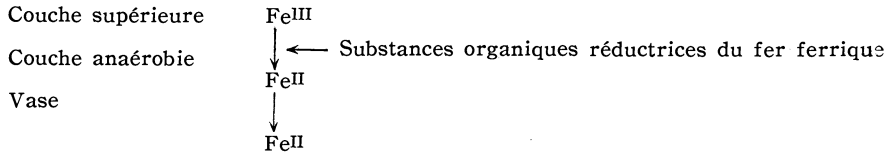


Fig. 3.
Génèse du fer ferreux dans le lac d'eau douce.

Résumé

1°) Nous proposons des méthodes de recherche de l'état d'un élément chimique dans l'hydrosphère.

2°) En employant les résultats obtenus par la centrifugation et les méthodes analytiques, nous sommes conduits à la conclusion que plusieurs dizaines de pourcentages du fer centenu dans les eaux superficielles sont à l'état insoluble. Plus exactement, la constante de sa dissociation est inférieure à $4{,}0 \sim 8{,}7 \times 10^{-18}$.

3°) Le rapport fer soluble-fer total, s'approche de 1 avec la profondeur. Cela signifie que le fer est rendu soluble au cour de sa descente progressive dans le lac.

4°) Le fer ferreux dans les couches d'eau tout près du fond : dans les lacs d'eau saumâtre, provient de la superficie ; dans les lacs d'eau douce, il faut de plus tenir compte du fer fourni de la vase.

Au terme de cet exposé, nous tenons à exprimer à Monsieur le Professeur K. Sugawara qui nous a aidé de ses conseils très précieux et très utiles, notre profonde gratitude.

Institut de Chimie,
Faculté des Sciences,
Université de Nagoya

Surface Chemistry of High Polymers. IV. The Monolayer of Polymeth-acrylic Acid and its Copolymers with Diethylaminoethyl Vinyl Ether at the Air/Water Interface

By Toshizo ISEMURA, Hiroshi HOTTA and Seinosuke OTSUKA

(Received August 20, 1953)

As mentioned in the previous paper, there are some investigations on the film of non-electrolytic synthetic polymers.[1-5] There is, however, only a little investigation on that of synthetic polyelectrolytes.[6,7] The investigation of the latter film has many interesting points not only as the pure physical chemistry but also as an important model of biocolloidal substances, as pointed out by Katchalsky.[8] For these reasons, we studied first the monolayer of polymethacrylic acid (PMA) and its copolymers with diethylaminoethyl vinyl ether (DAV) at the air/water interface, and investigated how the ionization of these polymers affects their behaviour at the interface. The results obtained will be described in the present paper. The result at the oil/water interface will be published later.

Experimental

The polymers used in the present investigation

1) T. Isemura, H. Hotta and T. Miwa, This Bulletin, **26**, 380 (1953).
2) H. Hotta, This Bulletin, **26**, 386 (1953).
3) H. Hotta, This Bulletin, **27**, 80 (1954).
4) T. Isemura and K. Hamaguchi, This Bulletin, **25**, 40 (1952); **26**, 425 (1953).
5) D. J. Crisp, *J. Colloid Sci.*, **1**, 49 and 161 (1946).
6) T. Isemura and K. Hamaguchi, to be published in This Bulletin.
7) A. J. G. Allen and A. E. Alexander, *Trans. Faraday Soc.*, **46**, 316 (1950).
8) A. Katchalsky, *J. Polymer Sci.*, **7**, 393 (1951).

were prepared as follows. Polymethacrylic acid (sample M) was prepared by the usual method. Copolymers of methacrylic acid (MA) and diethylaminoethyl vineyl ther ($(C_2H_5)_2$–N–C_2H_4–O–CH$=CH_2$) (DAV) were prepared by two different methods. Sample L was copolymerized from an equimolar mixture of MA and DAV dissolved in 60% aqueous methanol solution, using potassium persulphate as catalyst (0.2 mole percentage). On the other hand, sample K was copolymerized from an equimolar mixture of MA and DAV dissolved in N/2 hydrochloric acid, using potassium persulphate as catalyst (0.1 mole percentage), and obtained as hydrochloric acid salt. The composition of these copolymers, which was estimated by nitrogen analysis, is shown in Table I with the mean molecular weight per vinyl unit. The details of the copolymerization and the properties in the bulk phase of these copolymers will be reported elsewhere.

TABLE I
THE COMPOSITION OF COPOLYMERS OF METHACRYLIC ACID (MA) AND DIETHYLAMINOETHYL VINYL ETHER (DAV).

Sample	Mole percentage of DAV in copolymer	Mean molecular weight per vinyl unit
K	31	112
L	20	97
M	0	86

We measured their surface pressure by the hanging plate method, and their surface potential by the vibrating electrode method at room temperature (10–15°C.). The apparatus and procedure for these measurements were almost the same in the previous paper[1] except some modification for the development of accuracy. The film was spread from aqueous 20% pyridine solution on the aqueous phase at various *p*H, which was controlled with hydrochloric acid or sodium hydroxide, and determined by "TOYO" test paper.

Results

The surface pressure-area curves and surface potential (or surface moment)-area curves on the aqueous phase at various *p*H are shown in Figs. 1, 2 and 3, and in Figs. 4, 5 and 6, respectively. Although the surface potential-area curves for sample K at *p*H 5.8, 8.0 and 12.1 were not entirely identical with curve in Fig. 4, they were not essentially different from it. The surface moment-area curves, shown by dotted lines in the figures, were calculated by the usual method as mentioned in the previous paper.[1] The surface moment of all samples at the constant range obtained was plotted against the *p*H of aqueous phase in Fig. 7 to clarify the relation between them. The points under the ground line of surface moment in this figure correspond to the negative as curve e in Figs. 4 and 6. In these figures, the area was calculated as the mean area per vinyl unit with the mean molecular weight in Table I.

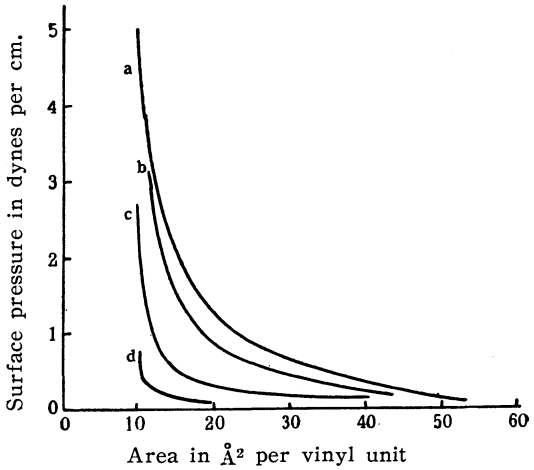


Fig. 1. The surface pressure-area curves of samle K on various *p*H. Curve a (*p*H 1.4); curve b (*p*H 2.4); curve c (*p*H 3.9); and curve d (*p*H 4.4)

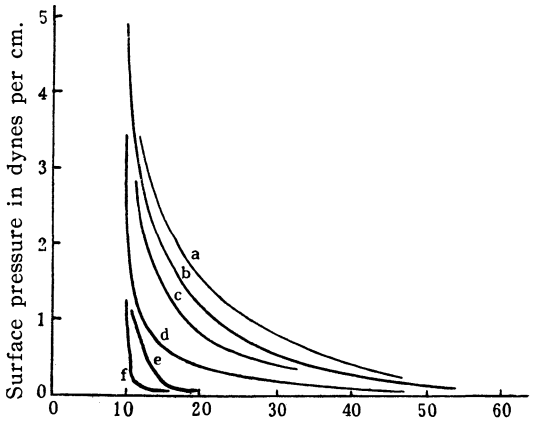


Fig. 2. The surface pressure-area curves of sample L on various *p*H. Curve a (*p*H 1.0); curve b (*p*H 1.4); curve c (*p*H 2.6); curve d (*p*H 3.8); curve e (*p*H 4.9); and curve f (*p*H 5.3)

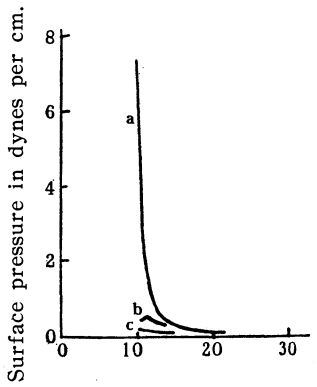


Fig. 3. The surface pressure-area curves of polymethaerylic acid (sample M) on various *p*H. Curve a (*p*H 1.6, 3.4, 4.0, and 4.4); curve b (*p*H 4.7); and curve c (*p*H 7.5)

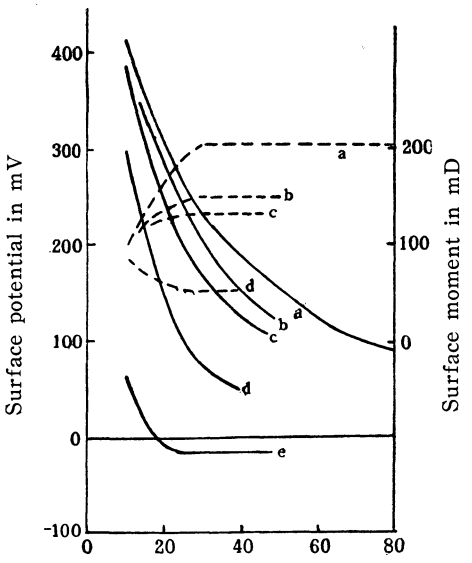


Fig. 4. The surface potential (or surface moment)- area curves of sample K on various *p*H. The surface moment is shown by dotted line. Curve a (*p*H 1.0, 1.4, 2.6, and 3.8); curve b (*p*H 4.5); curve c (*p*H 4.8); curve d (*p*H 5.3); and curve e (*p*H 5.8, 8.0 and 12.1)

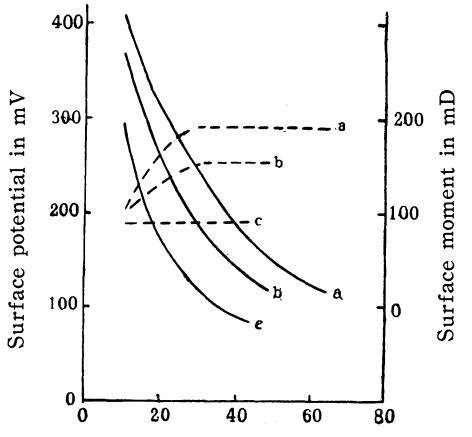


Fig. 5. The surface potential- (or surface moment)- area curves of sample L on various *p*H. The surface moment is shown by a dotted line. Curve a (*p*H 1.4, 2.4, and 3.8); curve b (*p*H 4.4); and curve c (*p*H 4.9)

Discussion

Since even the interpretation of the properties of the solution of linear polyelectrolyte is a subject recently developed, its theory at the interface is scarcely established at present. However, since there are some exact investigations on the solution of polymethacrylic acid as the representative of

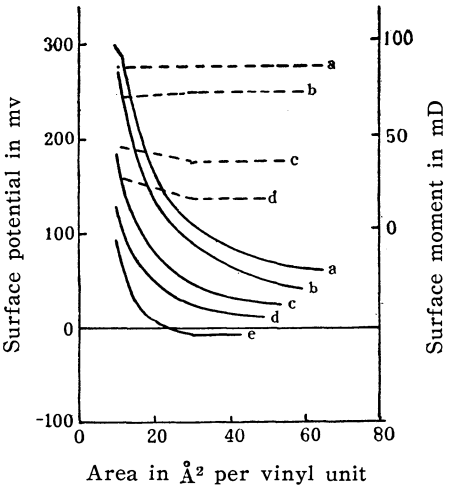


Fig. 6. The surface potential- (or surface moment)- area curves of polymethacrylic acid (sample M) on various *p*H. The surface moment is shown by a dotted line. Curve a (*p*H 1.6, 3.4 and 4.0); Curve b (*p*H 4.4); Curve c (*p*H 4.7); Curve d (*p*H 5.3); and Curve e (*p*H 7.5)

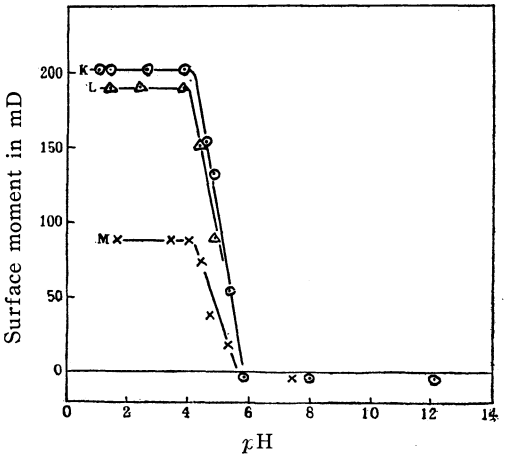


Fig. 7. The relation between surface moment and the *p*H of substrate. Sample K (⊙), L (△), and M (×), respectively

linear polyelectrolytes, we shall consider the present result of monolayer in comparison with the knowledge of the behaviour of this polyelectrolyte in the bulk phase.

The Monolayer of Polymethacrylic Acid (PMA) (sample M)—It is evident from Figs. 3, 6 and 7 that the surface pressure and surface moment of PMA were completely identical up to nearly *p*H 4.0, and fell rapidly down to zero between *p*H 4.0 and 5.5, and the surface potential became even negative at *p*H greater than 5.5. This trend of change of the surface behaviours with *p*H corres-

9) A. Katchalsky, O. Künzle and W. Kuhn, *J. Polymer Sci.*, 5, 283 (1590).

ponds entirely to the properties of the bulk solution of PMA, which were interpreted in detail by Katchalsky.[8,9] It is found as mentioned below that the former is also perfectly understood by his interpretation of the relationships between the state of molecules and the degree of ionization of polyelectrolyte in solution[8].

Since the molecules are rigid and not affected by ionization at a low degree of ionization up to *p*H 4.0 in consideration of his interpretation, the surface pressure and surface moment are entirely unchanged by *p*H, and then, since they open up with increasing ionization and take the form of freely kinked threads up to about 10% ionization (*p*H 5), the surface moment is lowered due to the negative charge of carboxyl groups, and, since the spreading molecules begin to dissolve into the aqueous phase due to their stretching with more increasing ionization, the apparent surface pressure and surface moment are more and more decreased. Finally, since the molecules can no more stand at the interface in the same form as that in the aqueous phase, namely, in the form of rodlike filaments at the higher degree of ionization, the greater part of spreading molecules tends to take the further stable form and therefore dissolves into the aqueous phase as shown as curve e in Fig. 6. That is, the difference of energy between the forms of molecules at the interface and in the aqueous phase rapidly increases with the increase of degree of ionization.

The Monolayer of Copolymers with DAV (sample K and L)—From Figs. 1, 2, 4, 5 and 7, it can be recognized that the surface pressure and surface moment of both copolymers at the same *p*H were almost the same, in spite of their different compoistion, while the surface pressure increased with decreasing *p*H. The change with *p*H was exactly parallel to that of PMA over all *p*H range investigated.

Before discussing these phenomena, it may be considered how the side chains of the present copolymers orientate at the interface. It was concluded from the surface pressure and surface moment in the preceding paper[3] that the carboxyl groups of PMA are immersed in the aqueous phase. Furthermore, diethylaminoethyl groups may also be immersed in the aqueous phase for the following reasons. (I) Triethylamine, which resembles this group, is appreciably soluble in water. (II) The shape of surface pressure-area curves of the present copolymers are independent of their composition and similar to that of PMA, in the condensed state at low ionization, in contrast with the copolymers of vinyl acetate and stearate,[1] and do not show any kink point which should appear if the side chains lie flat in the interface. (III) Their surface potential is very regular and reproducible in contrast with the copolymers of vinyl acetate and stearate.[1] Therefore, the discussion of the behaviour of the monolayer of these polymers in the light of the effect of ionization and without any consideration of the steric effect of side chains causes no serious error in this case.

Subsequently, we notice the phenomenon up to *p*H 4.0 from *p*H 1.0. In this *p*H range, the amine groups may be completely dissociated in accordance with their fraction in the polyelectrolytes and the dissociation constant of monomer. However, as shown in Fig. 7, the surface moment of both copolymers is nearly equal in spite of their different composition. When we evaluate the surface moment of dissociated amine groups, on the assumption of their perfect dissociation and of the perfect undissociation of carboxyl groups of methacrylic acid, of which the surface moment was found to be 88 mD from curve M in Fig. 7, we found the surface moment of ionized amine groups is 450 mD for sample K and 600 mD for sample L, respectively. On the other hand, the surface moment of $C_{18}H_{37}N(CH_3)_3^+$ was reported to be 600 mD or more.[10] From these facts, it is concluded that the amine groups of both copolymers are almost equally dissociated by about 20%,[11] and the remainder of amine groups are not dissociated and have the surface moment nearly equal to that of undissociated PMA (90 mD). It is also understood on the same basis that the surface pressure of these copolymers at the same *p*H was almost identical as shown in Figs. 1 and 2 in spite of their different composition.

The dissociation of amine groups is imperfect because the condensation of film, due to the action of hydrogen bonds operative between the undissociated carboxyl groups of MA, makes them too close for their perfect ionization. The film is, of course, expanded in nature, but seems to be still fairly condensed even at *p*H 1.4 in comparison with the result at the oil/water interface which will be published in the following paper. It is also explained by considering the relation between the shape of the molecule and the degree of ionization interpreted by Katchalsky.[8]

10) J. T. Davies, *Proc. Roy. Soc.*, (London), **208** A, 224 (1951).

11) The total ionizable groups, namely, the sum of MA and DAV is taken hereafter as the standard of the degree of ionization.

From all the figures we notice that the surface moment-area curves are bent at about 30 Å^2, and approach to about 90 mD at about 10 Å^2, in Fig. 5 shows the surface moment of 90 mD, and has no bending point. This tendency is shown not only in the case of the present copolymers, but also in that of PMA in Fig. 6. However, it does not show such a bending point in the undissociated or slightly dissociated state of PMA as shown in curve a and b in Fig. 6. From these facts, it is also concluded that the too close approaching of ionizable groups hinders the ionization due to the same mechanism as mentioned above and the above assumption, that the value of surface moment of undissociated amine groups may be 90 mD, is confirmed here. McBain and Peaker had already suggested the idea that the film of stearic acid can not be so much ionized in the solid state.[12] This is also related to the phenomenon that the conductivity of soap solution falls rapidly down with increasing concentration from the critical micelle concentration.[13]

Although the constancy of surface moment in this *p*H range in Fig. 7 appears at first sight to be contradictory to the fact that the surface pressure increases with decreasing *p*H as in Figs. 1 and 2, it is understood on considering that the surface pressure is more sensitive to the degree of ionization than the surface moment. The similar fact was already been pointed out in the previous paper.[14,15]

As mentioned above, the carboxyl groups of MA begin to dissociate appreciably from *p*H 4.0 with increasing *p*H. Consequently, since the positivity of the whole molecule decreases, the mean apparent surface moment gradually decreases. Since the effective charge density for the mutual repulsion of molecules is gradually decreased, the film is condensed. Therefore, the surface pressure-area curve at *p*H 4.9 (see Fig. 2) becomes similar to that of undissociated PMA (see Fig. 3), and the corresponding surface moment-area curve (curve c in Fig. 5) does not show a bending point as mentioned above. This fact is understood on assuming that the degrees of ionization of respective constituents, namely, MA and DAV balance each other at this *p*H, and therefore the molecule has essentially no charge as a whole. This *p*H is the surface isoelectric point of this copolymer. This is considerably less than that expected from the dissociation constant of both monomers and the composition of copolymer. It may be caused by the following facts. Since the molecules are condensed more strongly at the interface due to the larger content of MA than in the solution, the amine groups can not dissociate, due to too closely approaching at the interface, as much as in the solution.

With the further increase of *p*H, MA of the greater part of the copolymer is more and more ionized and then the molecules tend to stretch to rodlike form. Therefore, since the molecules can not stand in the stable form at the interface, they dissolve into the aqueous phase as mentioned in the section of PMA. It is because of the great content of MA in comparison with DAV that we could not obtain the stable film due to undissociated DAV at the higher *p*H as we could at the low *p*H.

Summary

As the result of the measurements of the surface pressure and surface potential of polymethacrylic acid and its copolymers with diethylaminoethyl vinyl ether on the aqueous phase at various *p*H, their surface moment was constant up to *p*H 4.0, then rapidly fell down to zero between *p*H 4.0 and 5.5, and finally their stable film could not be found at the higher *p*H range than 5.5, but the surface pressure decreased with increasing *p*H even up to *p*H 4.0. These tendencies are discussed in the light of Katchalsky's interpretation in regard to the relation between the shape of molecules and the degree of ionization.

The important conclusions from the present experiments are:

(1) all the side chains of the present polymer are immersed in the aqueous phase;
(2) the degree of ionization of amine groups may be of about 20% even at its maximum; and
(3) the isoelectric point of the present copolymer at the interface exists at about *p*H 5.0 of the aqueous phase.

The Institute of Scientific and Industrial Research, Osaka University, Sakai, Osaka

12) J. W. McBain and C. R. Peaken, *Proc. Roy. Soc.*, (London), **125** A, 394 (1929).
13) J. W. McBain, "Colloid Science", Chap. 17 (1950).
14) H. Hotta and T. Isemura, This Bulletin, **25**, 101 (1952),
15) A. E. Alexander, *Trans. Faraday Soc.*, **37**, 15 (1941).

Aluminium dans les eaux des lacs[1]

Par Motoharu TANAKA

(Reçu le 21, Septembre, 1953)

Nous avons déjà publié l'étude sur le fer dans les eaux des lacs[2]. Bien que nous ayons de nombreuses recherches sur les éléments comme le fer, le manganèse, le phosphate et la silice qui se trouvent dans les eaux des lacs, nous ne pouvons trouver que très peu d'études sur l'aluminium dans l'hydrosphère; surtout, dans les eaux des lacs, nous n'avons aucun travail systématique au sujet de cet élément.

L'aluminium est un élément indifférent à la réaction d'oxydoréduction. Il occupe une grande partie de la lithosphère, et cependant nous n'en pouvons déceler qu'une très petite quantité dans l'hydrosphère et la biosphère. Ce sont ces points qui ont excercé tant d'influence sur nous que nous avons entrepris l'étude qui suit.

De plus, le dosage de l'aluminium, fait sur les eaux naturelles, nous pouvons souvent rendre plus claire l'élucidation de l'état des autres éléments. Nous en avons déjà obtenu quelques résultats.[3]

Méthode d'Analyse

Après l'évaporation à sec de l'échantillon d'eau au bain-marie, fondre le résidu avec du bisulfate de sodium; dissoudre la masse fondue dans quelque 20 cc de l'eau contenant 0.5 cc d'acide nitrique et filtrer la silice qui y est restée insoluble. A la liqueur filtrée, ajouter 2 cc de solution de sulfocyanure d'ammonium à 25%. Extraire le sulfocyanure de fer en utilisant le mélange de solvant organique (Ether: alcool amylique = 2:5)[4]. Séparer la couche aqueuse, et la neutraliser au moyen de l'indicateur de *p*-nitrophénol; en contrôler le *p*H à 4,2[5] avec la solution tampon (acide acétique et acétate de sodium). Y ajouter 1 cc de la solution à 0.2% d'aluminon (aurintricarboxylate d'ammonium). 15 minutes après, la densité optique obtenue à l'aide du spectrophotomètre, à la longueur d'onde de 535 mμ, nous permet de calculer la teneur en aluminium. La présence d'une quantité comparable de phosphate ne gêne pas ce dosage.

Agissement de l'Aluminium dans les Eaux des Lacs

L'aluminium ne devient pas plus soluble dans un milieu réductif comme le fer et le manganèse. Donc on imagine que sa distribution verticale soit homogène; et pourtant, l'inspection précise nous amène aux phénomènes suivants. Tableau 1 nous montre la distribution verticale de l'aluminium et des autres éléments au lac Aburagafuchi[6].

TABLEAU I

DISTRIBUTION VERTICALE DES ÉLÉMENTS CHIMIQUES AU LAC ABURAGAFUCHI.

(Le 8, Sept. 1950 (La période de stagnation) Profondeur; 5,0 m)

Profondeur	O_2	Fer ferreux	Fer total	Mn	Al	Si
m	cc/l	mg/l	mg/l	mg/l	mg/l	mg/l
0	5,27	<0,02	0,67	0,40	1,20	10,0
1	5,40	„	0,66	0,16	1,25	8,0
2	3,98	„	0,53	0,16	0,98	6,7
3	1,33	„	0,33	0,32	0,94	4,8
4	2,91	„	0,43	0,44	0,60	3,6
4,54*		3,7	24,8	2,20	0,80	11,0
4,69*	0,0	23,8	24,8	2,30	0,80	11,3
4,89*		28,6	37,3	2,50	2,90	12,1
4,94*		29,0	38,0	2,65	4,45	18,7
4,99*	0,0	27,4	35,5	2,60	7,30	36,4
5,00*		34,6	39,5	2,75	8,10	42,4

* Profondeurs mesurées du fond.

i) Teneur plus forte en aluminium à la superficie.

Dans une étude précédente sur le fer[2], nous avons indiqué la teneur plus forte en aluminium et en fer à la superficie. Là, nous avons déjà expliqué que les particules argileuses étant apportées par les affluents et par les mouvements d'eau, la rapidité de leur descente se relentit par

1) Nous avons déjà présenté une partie de cette recherche á l'assemblée annuelle de la société chimique du Japon, qui s'est tenue á Tokyo en avril 1951.

2) M. Tanaka, Ce Bulletin, **27**, 89 (1954).

3) Nous allons publier bientôt un exposé qui concerne l'état de la silice dans les eaux naturelles.

4) J. T. Woods avec M. G. Mellon: *Ind. Eng. Chem.* Anal. Ed., **13**, 551 (1941).

5) W. H. Smith et al., *Anal. Chem.*, **21**, 1334 (1949).

6) La description sur ce lac a été donnée par MM. T. Koyama et K. Sugawara dans "*J. Earth Sciences, Nagoya University*", **1**, 24 (1952).

les vagues aux couches superficielles. Cette explication est soutenue par la teneur plus forte de la silice, principal élément constitutif des argiles, à la superficie.

Le même phénomène était observé aux autres lacs[2].

ii) Accumulation de l'aluminium dans les couches tout près du fond. Bien qu'il ne soit pas plus soluble dans un milieu réducteur que dans un milieu oxydant, l'aluminium, qui par ailleurs ne constitue pas un élément nutritif, s'accumule dans la couche tout près du fond durant la période de stagnation. Nous nous mettons à expliquer ce phénomène par l'exemple du lac Aburagafuchi. (Tab. I).

Les eaux étant examinées vers le fond, on décèle le fer ferreux pour la première fois à la profondeur de 4.54 m. C'est là que le fer total et le manganèse commencent à augmenter, mais l'aluminium ne s'accoît pas encore. Subitement, la concentration d'aluminium augmente à la profondeur de 4.89 m. Ce phénomène de l'accumulation de l'aluminium dans la couche inférieure à celle où s'accumulent le fer et le manganèse n'est pas spécial dans le lac Aburagafuchi, et on peut le constater encore aux autres lacs (v. Tab. II et III et Fig 2).

TABLEAU II

DISTRIBUTION VERTICALE DES ÉLÉMENTS CHIMIQUES AU LAC YOGO.

(Le 21 août, 1951. Profondeur: 12,5 m.)

Profondeur	0_2	Fer férreux	Mn	Al	Si
m	cc/l	mg/l	mg/l	mg/l	mg/l
0	5,47	<0,02	<0,02	0,22	I,8
2,5	4,61	„	„	0,35	2,2
5	4,14	„	0,12	0,25	2,5
7,5	1,19	„	0,17	0,30	2,7
10	0,39	2,66	2,0	0,29	3,3
12,00*	0,25	6,02	2,12	0,28	4,3
12,25*	0,14	6,02	2,02	0,26	4,7
12,40*	0,20	6,12	2,17	0,28	4,8
12,45*	0,31	6,55	2,18	0,30	4,8
12,50*	1,44	6,85	2,25	0,44	6,1

* Profondeurs mesurées du fond.

TABLEAU III

DISTRIBUTION VERTICALE DES ÉLÉMENTS CHIMIQUES AU LAC NAKATSUNA.

(Le 14 Oct. 1950. Profondeur: 12,5 m.)

Profondeur	0_2	Fer ferreux	Mn	Al
m	cc/l	mg/l	mg/l	mg/l
0	5,75	0,02	0,11	0,28
6	5,75	0,02		0,29
11,5	1,76	7,27	1,03	0,25
12,30*	0,18	22,8	1,33	0,40
12,40*	0,15	24,6	1,40	0,46
12,45*	0,00	24,0	1,25	1,05
12,50*	0,00	24,0	1,28	1,03

* Profondeurs mesurees du fond.

Explications de l'accumulation de l'aluminium: Les particules ou les débris minéraux apportés par les affluents ou par les mouvements d'eau parvenus à la couche anaérobie, le fer et le manganèse deviennent solubles et plus ou moins se dégagent de ces particules. Enfin ces dernières, composées principalement de silice et aluminium, plus ou moins se gonflent et de plus en plus ralentissent leur vitesse de précipitation.

De plus, les substances organiques accumulées dans les couches plus basses pourront former des complexes avec l'aluminium[7] (v. la section suivante).

Ainsi l'aluminium s'accumule dans la partie

TABLEAU IV

TENEUR EN ALUMINIUM DANS L'EAU CONTENUE DANS LA VASE. (mg/l)

Nom du lac	Kizaki	Nakatsuna
Date	Le 10 Oct. 1950	Le 14, Oct. 1950
Eau tout près du fond	0,78	1,03
Eau contenue dans la vase	6,05～17,5	1,94～2,92

7) Nous avons essayé l'extraction du phyllite avec l'eau pure et l'eau contenant des substances organiques (extrait des aiguilles du pin). Cette dernière dissout beaucoup plus aisément l'aluminium que l'autre, comme le tableau suivant nous montre:

Résultats de l'extraction de l'aluminium

30 g du phyllite pulvérisé (200 mailles) par un litre. Durée de l'extraction: 60 jours.

Solvant	Aluminium mg/l	Remarque
Eau pure	0,14	pH=6.9
Eau contenant de substances organiques (exempte d'oxygène)	1.33	pH=6.6

inférieure de la couche anaérobie. Il faut encore y tenir compte de ce qu'il peut être fourni de la vase qui en contient une quantité considérable (v. Tab. IV).

Après la circulation automnale, l'aluminium ainsi accumulé dans la couche tout près du fond se précipite avec le fer et le manganèse, de la même manière que la silice et le phosphate. Sa concentration n'y est plus considérable, comme l'indiquent Tab. V et Fig. 2.

TABLEAU V

DISTRIBUTION VERTICALE DES ÉLÉMENTS CHIMIQUES AU LAC ABURAGAFUCHI

(Le 20 jan. 1951 Après la circulation automnale) Profondeur : 5,0 m)

Profondeur	O_2	Fer ferreux	Fer total	Mn	Al	Si
0	cc/l	mg/l	mg/l	mg/l	mg/l	mg/l
0	8,15	0,02	0,29	0,039	0,44	11,8
1	8,68	„	0,39	0,061	0,42	8,2
2	9,25	„	0,25	0,086	0,50	4,3
3	9,75	„	0.48	0,065	0,51	2,2
4	7,72	„	0,25	0.084	0,49	3,0
4,70*	6,78	„	0,42	0,078	0,68	1,6
4,90*	7,14	„	0,58	0,081	0,62	1,7
5,00*	7,07	„	0,43	0,080	0,70	1,7

* Profondeurs mesurées du fond.

État de l'Aluminium dans les Eaux des Lacs

Notre étude approfondie sur l'aluminium a pour but d'éclaircir l'état de cet élément dans les eaux des lacs. Les états suivants de l'aluminium seront possibles dans les eaux naturelles :

1° Al^{+++}

2° Complexes minéraux d'aluminium ($Al(OH)^{++}$, $Al(OH)^{+}_2$, AlF_6^{---}, $AlCl_6^{---}$ etc.).

3° Complexes organinues d'aluminium.

4° Aluminium dans les débris minéraux.

An voisinage de pH 7 que l'on rencontre souvent dans les eaux naturelles, Al^{+++} ne peut exister qu'en très petite quantité. Quant à la deuxiéme forme d'aluminium, complexes minéraux, seule une solution très concentrée permet son existence. Donc la troisième et la quatrième seront les formes principales de l'aluminium dans les eaux des lacs ordinaires.

i) *Expériences à l'aide de la centrifugation.*

Nous avons essayé la centrifugation des eaux prises aux profondeurs differentes du lac Aburagafuchi (le 8, sept., 1950). L'analyse de l'aluminium de l'eau centrifugée et de celle noncentrifugée étant faite, elle nous donne le rapport Al inséparable—All total. Ce rapport augmente avec la profondeur comme suit :

Profondeur m	Rapport Al inséparable —Al total	O_2 cc/l
0	0.85	5.27
3	0.98	1.33

L'accroissement de ce rapport correspond à la diminution de l'oxygène.

ii) *Études à l'aide de la résine à ion-échange.*

Il est bien entendu que l'aluminium non-ionisable(+) n'est pas absorbé à la résine à cation-échange. Nous le désignons $Al_{non\text{-}ion.}$, qui comprend l'aluminium contenu dans les débris minéraux et à l'état colloïdal. Alors, nous pensons comme suivant :

$$Al_{total} - Al_{non\text{-}ion} = Al_{ion}.$$

où Al_{ion} est l'aluminium qui est positivement ionisable.[8]

Ainsi faisant, les expériences étaient conduites au lac Kizaki à partir du mois de mars 1952 jusqu'en mars 1953.

a) Mode opératoire.

Nous avons employé le type $R^{NH_4}_{H}$ de l'Amberlite IR 120. Comme nous traitons les eaux pauvres en oxygène, les échantillons d'eau sont pris par un injecteur. Ce dernier est subséquemment lié à la colonne de résine qui est précédem-

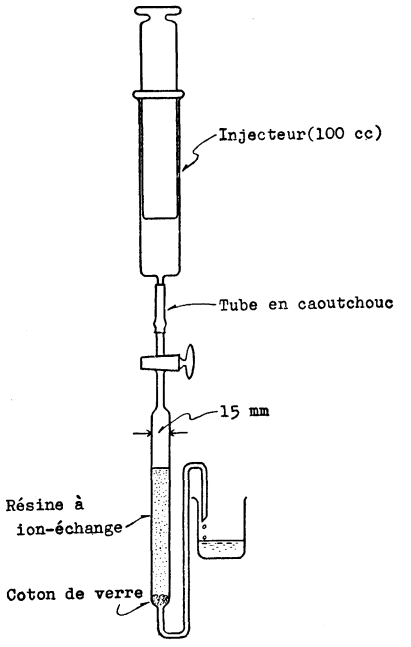


Fig. 1. Appareil pour ion-échange

8) D'aprés M. Honda, l'aluminium dans le complexe AlF_6^{---} est absorbé par la résine à cation-échange (*J. Chem. Soc. Japan*, **71**, 59 (1950)).

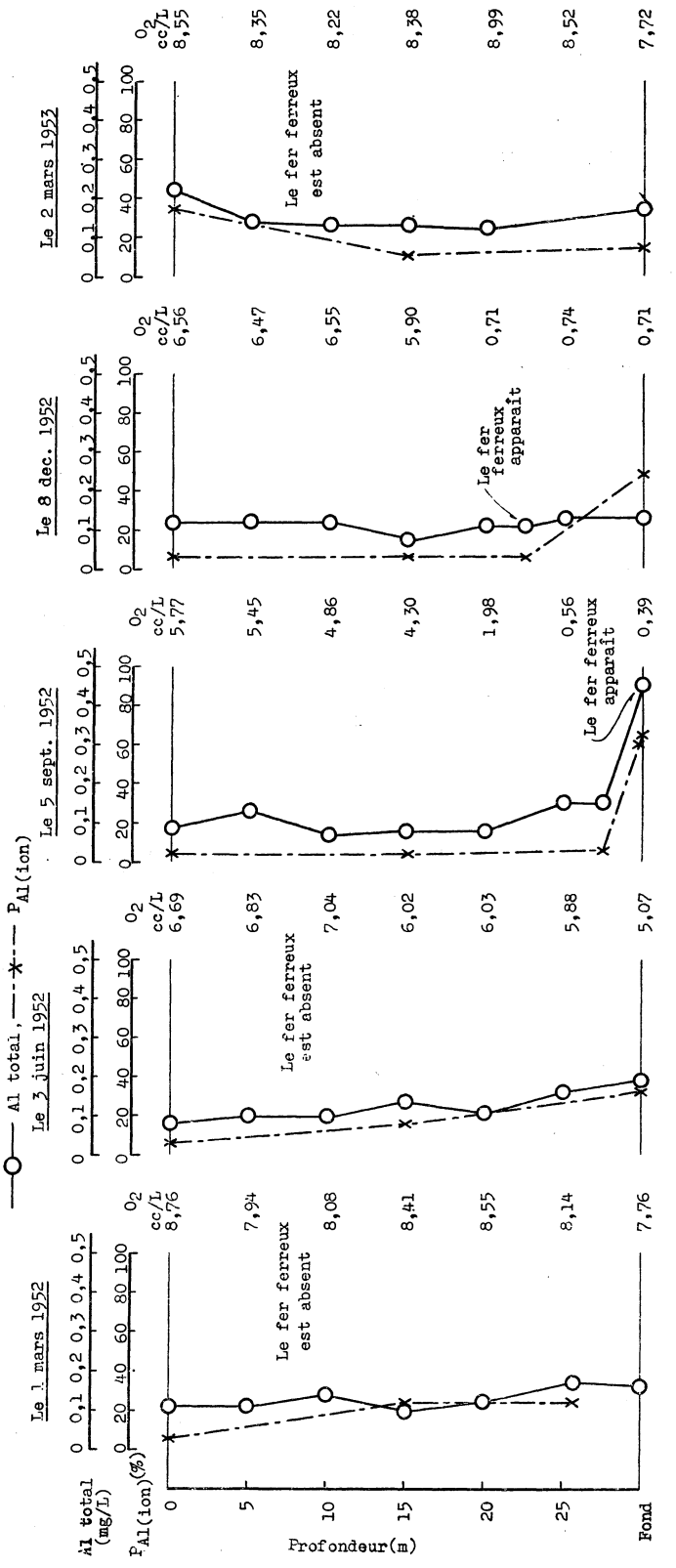


Fig. 2. Variation saisonnière du rapport Al ionisable—Al total. Le lac Kizaki (1952~1953).

lavé par de l'eau bien exempte d'oxygène (Fig. 1). La rapidité de coulement est près 5 cc par minute. Après avoir fait couler 100 cc d'échantillon, on lave la colonne avec l'eau bien exempte d'oxygène. On utilise toute cette liqueur effluente pour le dosage de l'aluminium non-ionisable.

b) *Résultat et discussion.*

Nous désignons $(Al_{ion}/Al_{total}) \times 100$, $P_{Al(ion)}$. $P_{Al(ion)}$ veut dire alors le pourcentage de l'aluminium positivement ionisable pour Al_{total}. Fig. 2 nous montre la variation saisonnière de $P_{Al(ion)}$ et de la teneur en aluminium au lac Kizaki.

En général, $P_{Al(ion)}$ est au voisinage de 10%. Néanmoins, pendant la période de stagnation, il augmente avec la profondeur et il atteint 50—60% près du fond. Comme nous ne trouvons pas d'accumulations de OH^-, Cl^-, F^- près du fond, nous devons chercher ailleurs la cause de l'augmentation de $P_{Al(ion)}$. Nous savons, d'autre côté, un accroissement de substances organiques près du fond pendant la période de stagnation. De plus, l'aluminium constitue souvent le complexe organique. Nous pourrons alors penser que l'aluminium devient plus ionisable par de substances organiques qui s'accumulent près du fond pendant la période de stagnation. L'expérience d'extraire le phyllite mentionnée plus haut soutient ce point de vue.

Résumé

1° L'aluminium s'accumule dans les couches tout près du fond du lac. L'accumulation de substances organiques et la destruction des débris minéraux y entrent en cause. Après la circulation automnale, l'aluminium ainsi accumulé coprécipite avec le fer et le manganèse.

2° La teneur en aluminium est souvent plus forte à la superficie.

3° Dans le lac Kizaki, le pourcentage de l'aluminium positivement ionisable pour l'aluminium total est 50–60% près du fond pendant la période de stagnation. Durant les autres saisons ce pourcentage est au voisinage de 10% dans toutes les couches d'eau. Des substances organiques joueraient un rôle important dans le phénomène d'accroissement de l'aluminium positivement ionisable.

Qu'il soit permis à l'auteur, en terminant cet exposé, d'exprimer ses profonds remerciements à Monsieur le professeur Sugawara, et à Monsieur le docteur Koyama, qui l'ont soutenu sans cesse par leurs conseils très précieux et très utiles.

Institut de Chimie
Faculté des Sciences,
Université de Nagoya

Über die Reinigung des Rubidiums.—Umkrystallisation der Doppelsulfate des Rubidiums mit den zweiwertigen Metallen.

Von Airi SUETUNA

(Eingegangen am 28, September, 1953)

Einleitung

Weil sich das Rubidium in der Mitte der Elementenreihe der Kaliumgruppe befindet und infolgedessen die meisten Rubidiumsalze solche Löslichkeiten zeigen, welche zwischen denjenigen der entsprechenden Kaliumsalze und Cäsiumsalze stehen, so reichert die fraktionierte Umkrystallisation der meisten Rubidiumsalze das Rubidium in den mittleren Teilen der Fraktionierreihe an. Aber wenn es nun ausnahmsweise ein Rubidiumsalz gibt, welches als sowohl das entsprechende Kaliumsalz wie das Cäsiumsalz schwerer löslich ist, so darf man mit Recht erwarten, daß die einfache Wiederholung der Umkrystallisation dieses Rubidiumsalzes schließlich das reine Rubidiumpräparat geben werde. Es ist in der Tat gefunden, daß man die Reinigung des Rubidiums durch die wiederholte Umkrystallisation des Tetraoxalates durchführen kann[1].

Merkwürding ist die Tatsache, daß alle Doppelsulfate des Rubidiums mit den zweiwertigen Metallen, welchen die allgemeine Formel $M_2^{I}SO_4 \cdot M^{II}SO_4 \cdot 6H_2O$ zuzuschreiben ist, mehr oder weniger schwerer löslich als die entsprechenden Kaliumdoppelsulfate sowie die Cäsiumdoppelsulfate sind. Und hiermit wäre es wohl möglich, durch die wiederholte Umkrystallisation solcher Doppelsulfate die Rubidiumsalze rein zu erhalten. Je größer der Löslichkeitsunterschied unter den Doppelsulfaten, welcher der Verschiedenheit von den darin vorhandenen Alkalimetallen entspricht, ist, desto zweckmäßiger wären die Doppelsulfate für die Reinigung. Also wurden nun vor allem 3 Doppelsulfate, die Doppel-

1) A. Suetuna; Dieses Bulletin. **25**, 248 (1952).
2) J. Locke: *Am. Chem*, J., **27**, 459 (1902).

sulfate des Rubidiums mit Nickel, Kobalt und Kupfer, als die zweckmäßigsten herausgelesen und jede für sich oftmaligen Umkrystallisationen unterworfen.

TABELLE I. DIE LÖSLICHKEIT DER DOPPELSULFATE

Die Löslichkeit der Doppelsulfate, $M_2^{I}SO_4 \cdot M^{II}SO_4 \cdot 6H_2O$, wurde von J. Locke gegeben[2]. Die hier gegebenen Werte sind von den originalen Werten auf g. Salz/100 g. H_2O umgerechnet.

$K_2SO_4 \cdot NiSO_4 \cdot 6H_2O$	$Rb_2SO_4 \cdot NiSO_4 \cdot 6H_2O$	$Cs_2SO_4 \cdot NiSO_4 \cdot 6H_2O$
9.4	7.6	32.7
$K_2SO_4 \cdot CoSO_4 \cdot 6H_2O$	$Rb_2SO_4 \cdot CoSO_4 \cdot 6H_2O$	$Cs_2SO_4 \cdot CoSO_4 \cdot 6H_2O$
17·9	11.9	55.5
$K_2SO_4 \cdot CuSO_4 \cdot 6H_2O$	$Rb_2SO_4 \cdot CuSO_4 \cdot 6H_2O$	$Cs_2SO_4 \cdot CuSO_4 \cdot 6H_2O$
16.1	13.3	61.3

Außerdem wurde bei dieser Gelegenheit die oben genannte Methode mittels Tetraoxalates wieder von neuem untersucht, worüber der Verfasser auch hier hinzufügend mitteilen möchte.

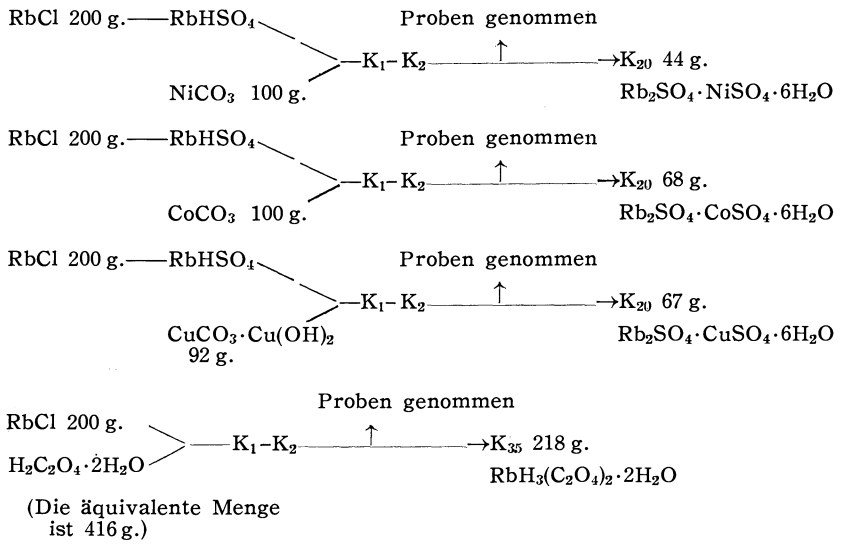
Experimentales

Ausgangsmaterial.—Dies war bei jedem Falle rohes Rubidiumchlorid, anscheinend K 15~20%, C_5 15~20% und Rb 60~70%. Zur Herstellung der Doppelsulfate wurde dieses ins Rubidiumhydrosulfat umgewandelt, und in die wässrige Lösung des Hydrosulfates das Carbonat (im Falle des Kupfers das basische Carbonat) des gewünschten Metalls eingetragen. Die so erhaltenen 3 Doppelsulfate wurden jede für sich 20 mal, anderseits das Tetraoxalat 35mal aus reinem Wasser umkrystallisiert, bei jeder Umkrystallisierungsreihe unterwegs von Zeit zu Zeit Proben genommen, welche samt den Endprodukten einer Spektralanalyse unterworfen und auf ihre Reinheit geprüft wurden.

Nickelrubidiumsulfat.—Die Umkrystallisation dieses Salzes ist mit keiner Schwierigkeit verbunden. Nur muß man natürlich dabei besorgen, zum Vermeiden der Hydrolyse des Nickels dann und wann einige Tropfen reiner Schwefelsäure in die Lösung hineinzutropfen.

Kobaltrubidiumsulfat.—Beim Umkrystallisieren dieses Salzes wurde manchmal sehr weitgehende Übersättigungserscheinung beobachtet, welche vermutlich auf Überschüsse freier Schwefelsäure beruhen möchte.

Kupferrubidiumsulfat.—Die Umkrystallisation dieses Salzes leidet darunter, daß beim Sieden der wässrigen Lösung sich ein grünes Salz, wahrscheinlich das basische Kupferrubidiumsulfat, abscheidet, welches gefährliches Stoßen verursacht.



K_n: Krystall nach n-maliger Umkrystallisation.

Die nach den Formeln nötigen Mengen Carbonate auf 200 g. RbCl.

$NiCO_3$ 98 g. $CoCO_3$ 98 g. $CuCO_3 \cdot Cu(OH)_2$ 91 g.

Die angewandten Carbonate wurden jedoch durch Analyse beziehungsweise

$NiCO_3$ 52% $CoCO_3$ 78% $CuCO_3 \cdot Cu(OH)_2$ 90%

enthaltend gefunden Fig. Experimentales.

Nachdem alle 4 Umkrystallisierungsreihen vollgebracht worden waren, wurden alle Proben ins Carbonat umgewandelt und somit zur Analyse vorbereitet. Die Doppelsulfate wurden dazu in den wässrigen Lösungen mit den kleinen Überschüssen von Oxalsäure heiß versetzt, die Niederschläge, die Oxalate der respektiven Metalle, abfiltriert, in die Filtrate Überschüsse von Oxalsäure eingetragen, nach Erkalten das abgeschiedene Rubidiumtetraoxalat plus Oxalsäure abgesaugt. Die so erhaltenen Salzmassen wurden dann auf einer Platinschale mäßig erhitzt, bis das Aufblasen der Schmelze aufhörte, und somit ins Carbonat umgewandelt.

Die semi-quantitative Spektralanalyse wurde mit Littrowschem Spektrograph nach der Glimmschicht-spaltabbildungsmethode ausgearbeitet. Die letzte Probe von der Umkrystallisierungsreihe des Nickelrubidiumsulfates und 3 letzte von derjenigen des Tetraoxalates erwiesen sich als besonders reine Rubidiumpräparate. Wie man anfangs aus den Löslichkeitsverhältnissen vorausgesehen hat, läßt sich das Cäsium durch diese Methoden rasch genug beseitigen, dagegen das Kalium vielmehr schwer vollständig entfernen.

TABELLE II

DIE RESULTATE DER SEMI-QUANTITATIVEN SPEKTRALANALYSE DER PRODUKTE

Probe		Li (%)	Na (%)	K (%)	Cs (%)
Rb-Ni-sulfat	K_5	Keine Linien	Keine Linien	~0.5	~5
	K_{10}	〃	〃	~0.1	0.5~0.1
	K_{15}	〃	〃	0.1~0.05	~0.01
	K_{20}	〃	〃	0.1~0.05	~0.001
Rb-Co-sulfat	K_5	〃	<0.01	1~0.5	~5
	K_{10}	〃	Keine Linien	0.5~0.1	1~0.5
	K_{15}	〃	〃	~0.1	0.5~0.1
	K_{20}	〃	〃	~0.1	0.05~0.01
Rb-Cu-sulfat	K_5	〃	〃	~1	~5
	K_{10}	〃	〃	0.5~0.1	1~0.5
	K_{15}	〃	〃	~0.1	0.5~0.1
	K_{20}	〃	〃	~0.1	0.05~0.01
Tetraoxalat	K_{20}	〃	〃	~0.5	~0.005
	K_{25}	〃	〃	~0.05	Keine Linien
	K_{30}	〃	〃	~0.05	〃
	K_{35}	〃	〃	00.5~0.01	〃

K_n: Krystall nach n-maliger Umkrystallisation.
Na-Keine Linien <0.001 (%)
Cs-Keine Linien <0.001 (%)

Im allgemeinen leidet man beim Reinigen des Rubidiumsalzes auch durch andere Methoden ebenfalls daran, daß nicht das Cäsium, sondern das Kalium hartnäckig dem Rubidiumpräparat anhaftet und schwer vollständig beseitigt werden kann. Dies ist eine Tatsache, welche wohl nicht bloß auf Verbrauch der Glasgeräte zurückzuführen sein möchte.

Zur Berechnung der Ausbeute der Umkrystallisierungsreihe, z.B., des Nickelrubidiumsulfates, wobei das Rubidiumchlorid im Überschuß verwandt wurde, nimmt man an, daß aus der anfänglichen Salzmenge (232 g.), welche der verwandten Menge (100 g.) des Nickelcarbonates (Gehalt an $NiCO_3$ 52%) entspräche, nach 20-maliger Umkrystallisation 44 g. des Endproduktes gewonnen würden. Der aus diesen Zahlwerten berechnete Wert der Ausbeute wurde weiter in Rücksicht auf die Menge bisweilen genommener Proben berichtigt. Die Ausbeuten der Umkrystallisierungsreihen anderer Doppelsulfate und des Tetraoxalates wurden in gleicher Weise berechnet.

TABELLE III

DIE AUSBEUTEN DER UMKRYSTALLISATIONEN

Rb-Ni-sulfat	A_1	92.9%
	A_{20}	22.7%
Rb-Co-sulfat	A_1	92.5%
	A_{20}	21.3%
Rb-Cu-sulfat	A_1	91.7%
	A_{20}	17.8%
Tetraoxalat	A_1	97.9%
	A_{20}	64.7%
	A_{35}	46.7%

A_n: Ausbeute n-maliger Umkrystallisation.

Zusammenfassung

1) Man kann reine Rubidiumpräparate erhalten, indem man das Nickelrubidiumsulfat, Kobaltrubidiumsulfat, oder Kupferrubidiumsulfat oftmals aus Wasser umkrystallisiert.

(2) Weiter darf man sicher erwarten, daß alle Doppelsulfate des Rubidiums mit den zweiwertigen Metallen, $M_2^{I}SO_4 \cdot M^{II}SO_4 \cdot 6H_2O$, durch oftmaliges Umkrystallisieren gereinigt werden können.

(3) Das Nickelrubidiumsulfat läßt sich unter den 3 Doppelsulfaten am raschesten durch Umkrystallisieren reinigen.

Herren Prof. K. Kimura und M. Fujimoto möchte ich für ihre vielen wertvollen Ratschläge bei der vorliegenden Untersuchung meinen besonderen Dank aussprechen.

Chemisches Institut der Wissenschaftlichen Fakultät, Universität zu Tokyo

Studies on the Chemical Constitution of Agar-agar. XVI[1]. *Isolation of Crystalline Agarobiose Diethylmercaptal by Mercaptolysis of Agar-agar*[2]

By Susumu HIRASE and Choji ARAKI

(Received October 14, 1953)

In Part XV the present authors reported the isolation of crystalline diethylmercaptals of D-galactose, 3,6-anhydro-L-galactose and of DL-galactose, and the non-crystalline residue (designated as R_I) from the products of the first forty eight hours mercaptolysis of agar. They suggested, moreover, that R_I, which upon further mercaptolysis produced monosaccharide derivatives above mentioned, would comprise some oligosaccharide diethylmercaptals. On the other hand, one of the authors could isolate agarobiose (4-D-galactopyranosyl 3,6-anhydro-L-galactose) from the partial hydrolysis products of agar[3]. Hence, in a search for agarobiose diethylmercaptal, R_I has been investigated.

R_I was shown to be divided into the *n*-butanol-soluble fraction and the insoluble one. Acetylation of the former produced a crystalline compound, which proved to be hexaacetyl agarobiose diethylmercaptal (I) for the reasons described later. Upon saponification, the acetate regenerated crystalline agarobiose diethylmercaptal (II).

It appears probable that the prolonged mercaptolysis described above has led to the further cleavage of agarobiose units once produced into monosaccharide units. In order to obtain the agarobiose derivative in a better yield, the partial mercaptolysis has been carried out under the milder condition, namely, for five hours at 3~5°. The reaction mixture gave crude agarobiose diethylmercaptal by the solvent fractionation in a yield of 46.2% of agar employed. This result and the isolation of D-galactose diethylmercaptal and of 3,6-anhydro-L-galactose diethylmercaptal in almost equimolar proportion[1] demonstrate that agarobiose units extend over approximately half, at least, of the molecule of agar.

The assignment of the structures of agarobiose diethylmercaptal (II) and its hexaacetate (I) to the compounds isolated as above mentioned arises for the following reasons. Mercaptolysis of II yielded D-galactose diethylmercaptal (III) and 3,6-anhydro-L-galactose diethylmercaptal (IV), indicating that II was a disaccharide diethylmercaptal, the component sugars of which were D-galactose and 3,6-anhydro-L-galactose. Demercaptalation of II regenerated the parent free sugar, the phenylosazone of which was found to have the same characteristics as agarobiose phenyosazone described by one of the authors before.[3] On the other hand, methylation of II with dimethyl sulfate and sodium hydroxide solution followed by subsequent demercaptalation with mercuric chloride afforded crystalline hexamethyl *aldehydo*-agarobiose (VI), which was then oxidized to hexamethyl agarobionic acid (VII). Methyl ester of VII showed no increase of the methoxyl content on further methylation with methyl iodide and silver oxide. When VII was submitted to the hydrolysis with N-sulfuric acid, there were produced 2,3,4,6-tetramethyl D-galactose (VIII) and crystalline 2,5-dimethyl 3,6-anhydro-L-galactonic acid (IX). The former was identified as its crystalline anilide. The latter was identified by its properties and also by its conversion to the crystalline amide[3]. The identification of these two cleavage fragments enables the statement to be made that the structure of hexamethyl agarobionic acid (VII) is represented by that, in which C_1 of 2,3,4,6-tetramethyl D-galactose (VIII) is united glycosidically to C_4 of 2,5-dimethyl 3,6-anhydro-L-galactonic acid (IX). This agrees well with the assignment of the structures of agarobiose diethylmercaptal and its hexaacetate to the compounds under question.

Experimental

Evaporation and concentration were carried out under reduced pressure below 40°. The specific rotation was measured in the aqueous solution unless otherwise stated. The thioethoxyl content was determined by the method of these authors[4]. The yield, the specific rotation and the thioethoxyl content of the ash-containing sample are calculated into the case of the ash-free one. All melting points are uncorrected.

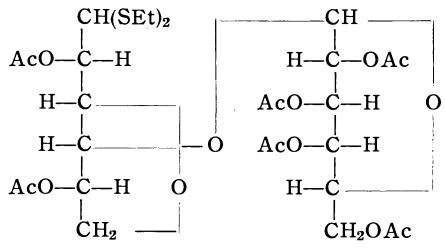
Mercaptolysis of agar. a) for 48 hrs.:— Agar (60.0 g., dry weight 49.1 g.) was mercaptolysed

1) Part XV: C. Araki and S. Hirase, This Bulletin, **26**, 463 (1953).

2) Read at 5th (1952) and 6th (1953) Annual Meetings of the Chemical Society of Japan.

3) C. Araki, *J. Chem. Soc. Japan*, **65**, 533, 627 (1944).

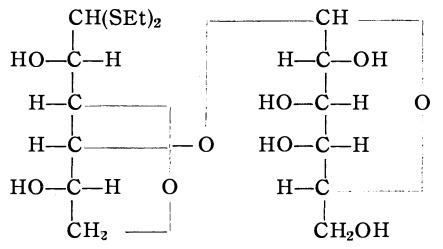
4) The method will be published elsewhere.



(I)

Hexaacetyl agarobiose diethylmercaptal

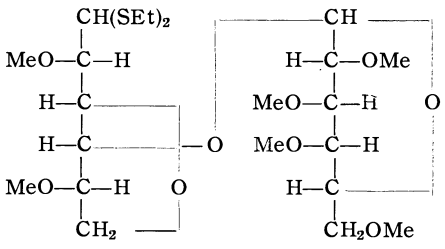
NH_3 (MeOH)



(II)

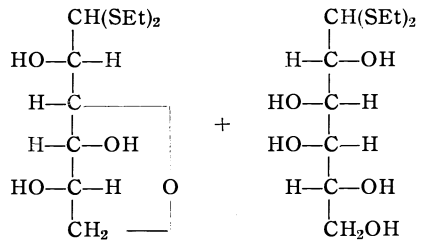
Agarobiose diethylmercaptal

Me_2SO_4 (NaOH)



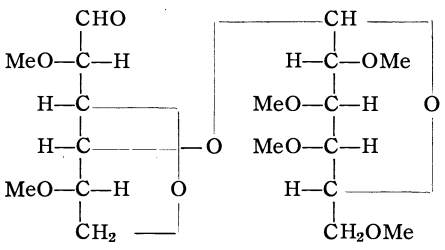
(V)

EtSH (HCl)



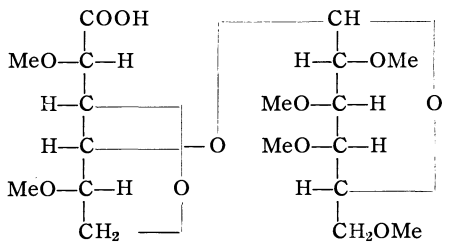
(IV) (III)

H_2O ($HgCl_2$)



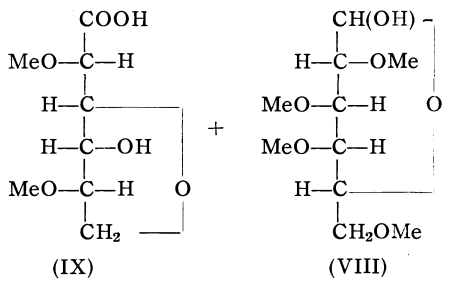
(VI)

O ($KMnO_4$)



(VII)

H_2O (H_2SO_4)



(IX) (VIII)

Me: $-CH_3$

Et: $-C_2H_5$

Ac: $-COCH_3$

exactly in the same manner as described in Part XV[1]. The non-crystalline residue, designated as R_1, was obtained as a hygroscopic amorphous powder (ash 2.86%); yield 29.1 g., $[\alpha]_D^7$ −8.0° (*c* 2.62), SC_2H_5 23.08%.

This was dissolved in absolute methanol (50 cc.) and *n*-butanol (500 cc.) was added with vigorous shaking. The insoluble precipitate was filtered, washed first with *n*-butanol and then with ethyl acetate, and dried, when a hygroscopic white powder (ash 6.40%) was obtained; yield 5.9 g., $[\alpha]_D^{25}$ −18.6° (*c* 2.09), SC_2H_5 15.82%.

The combined filtrate and the butanol washings, in which agarobiose diethylmercaptal was contained, were concentrated with occasional additions of water to a sirup, which was dried by repeatedly adding absolute methanol and subsequent distilling off, forming an amorphous powder (ash 2.00%); yield 23.2 g., $[\alpha]_D^{25}$ −7.1° (*c* 2.12), SC_2H_5 25.17%.

b) for 5 hrs.:—Agar (60.0 g., dry weight 49.1 g.) was mercaptolysed for 5 hrs. at 3~5° (ice-cooling) by the reaction with concentrated hydrochloric acid (*d* 1.20, 200 g.) and ethylmercaptan (80 g.). The solution of the reaction products, from which inorganic substances had been removed in the same manner as described before[1], was concentrated to about 200 cc. and allowed to stand overnight in an ice-box. Since no crystals were deposited, the solution was concentrated to 150 cc., and extracted with ether for continuous 140 hrs. in a Soxhlet's apparatus. From ether extracts, D-galactose diethylmercaptal (1.04 g.) and 3,6-anhydro-L-galactose diethylmercaptal (0.78 g.) were obtained in a crystalline state.

The remaining water solution was then concentrated to a sirup, which was dissolved in absolute methanol (500 cc.). The precipitate formed was filtered, washed and dried, a hygroscopic white powder (ash 9.08%) being obtained; yield 5.4 g., $[\alpha]_D^{25}$ −26.8° (*c* 0.96), SC_2H_5 6.18%. The combined filtrate and the washings were evaporated to dryness, and the residue was redissolved in absolute methanol (50 cc.). To this solution was added *n*-butanol (500 cc.) with shaking. After overnight standing it was treated in the same way as in the case of *a*. The butanol-insoluble precipitate was obtained in the form of a hygroscopic white powder (ash 2.46%); yield 10.1 g., $[\alpha]_D^{25}$ −24.0° (*c* 1.18), SC_2H_5 13.17%. The butanol-soluble fraction, being considered as crude agarobiose diethylmercaptal from its specific rotation and its thioethoxyl content, was obtained in the form of a hygroscopic amorphous powder (ash 0.68%) with a pale yellow color; yield 29.8 g. (46.2% of the agar employed, when calculated as its parent free sugar), $[\alpha]_D^{25}$ −8.8° (*c* 1.21) and −46.9° in pyridine (*c* 0.86), SC_2H_5 25.71% (agarobiose diethylmercaptal requires SC_2H_5 28.39%).

Hexaacetyl agarobiose diethylmercaptal (I). *a*) The butanol-soluble fraction (12.0 g.) of 48 hrs. mercaptolysis products was acetylated with pyridine (100 cc.) and acetic anhydride (100 cc.) for 2 days at room temperature. The reaction product (16.0 g.), isolated by the solvent removal of the chloroform extract in the usual way, was dissolved in methanol (25 cc.), and water (5 cc.) was added to give a turbidity. Deposited crystals were filtered, washed with 50% aqueous methanol and dried; yield 7.6 g., m.p. 96~99°. An additional specimen (1.4 g.) was obtained from the mother liquor, m.p. 96~99°. Pure hexaacetyl agarobiose diethylmercaptal was obtained after recrystallization twice from methanol-water (7 : 3) as long needles; m.p. 101~103.5°, $[\alpha]_D^{26}$ −11.8° in chloroform (*c* 1.02), −22.1° in benzene (*c* 1.27) and −16.7° in ethanol (*c* 1.38). *Anal.* Found: C, 49.05; H, 6.13; CH_3CO, 37.71; SC_2H_5, 18.45, M.W. (Rast' method), 688. Calcd. for $C_{28}H_{42}O_{18}S_2$: C, 49.25; H, 6.20; CH_3CO, 37.82; SC_2H_5, 17.94%; M.W., 682.8.

b) The butanol-soluble fraction (14.9 g.) of the 5 hrs. mercaptolysate was acetylated in the same manner as above mentioned. The yield of crude crystals (m.p. 96~99°) of the hexaacetate was 17.0 g. (71.7% of the theoretical amount).

Agarobiose diethylmercaptal (II). A solution of hexaacetyl agarobiose diethylmercaptal (10.0 g.) in absolute methanol (100 cc.) was saturated with dry ammonia under ice-cooling, and allowed to stand overnight. The solution was evaporated to a sirup, which was then dissolved in ethyl acetate (50 cc.). White crystals separated immediately; yield 5.3 g. (83.2% of the theoretical amount), m.p. 168~170°. The recrystallization was repeated twice from absolute ethanol, giving pure agarobiose diethylmercaptal, m.p. 171~172°, $[\alpha]_D^{23}$ −8.47° (*c* 3.07), −20.9° in methanol (*c* 1.39) and −51.7° in pyridine (*c* 1.47). It is readily soluble in water, methanol, pyridine and hot ethanol. *Anal.* Found: C, 44.38; H, 6.95; SC_2H_5, 28.49. Calcd. for $C_{16}H_{30}O_9S_2$: C, 44.65; H, 7.02; SC_2H_5, 28.39%.

Agarobiose. Agarobiose diethylmercaptal (5.0 g.), mercuric chloride (7.5 g.) and excess lead carbonate were treated in the same way as in the demercaptalation of 3,6-anhydro-L-galactose diethylmercaptal[1]. A solution of the resulting sirup (3.4 g.) in absolute methanol (10 cc.) was poured into absolute ethanol (50 cc.) with stirring, forming the precipitate of agarobiose, which was obtained as a hygroscopic white powder after filtration and drying; yield 2.0 g., $[\alpha]_D^{27}$ −21.5° (initial, *c* 1.16)→−16.4° (equilibrium). It reduced a cold Fehling's solution, showed a strong Seliwanoff's reaction, and restored the color to a Schiff's reagent.

Phenylosazone[3]: Yellow fine needles, m.p. 221~222° (decomp.), $[\alpha]_D^{15}$ −135.5° (initial)→−110.8° (equilibrium) in pyridine-ethanol (2 : 3) (*c* 0.406).

Mercaptolysis of agarobiose diethylmercaptal. The mercaptolysis of agarobiose diethylmercaptal (2.0 g.) was accomplished by dissolving it in concentrated hydrochloric acid (*d* 1.20, 5 cc.) and shaking with an addition of ethylmercaptan (3 cc.) at 10~12° for 24 hrs. Successive treatments of the reaction mixture with lead carbonate, hydrogen sulfide, silver carbonate and again hydrogen sulfide removed inorganic ions. The water solution (about 50 cc.) thus obtained upon concentration gave crystals of D-galactose diethyl-

mercaptal (III) (0.53 g.), m.p. alone or on admixture with an authentic specimen, 140~142°, $[\alpha]_D^{10}$ −4.5° (*c* 0.85).

The mother liquor was further evaporated to dryness, from which 3,6-anhydro-L-galactose diethylmercaptal (IV) (0.50 g.) was obtained by the repeated extraction with cold ethyl acetate followed by evaporation, m.p. and mixed m.p. 109~110°, $[\alpha]_D^{10}$ +14.1° (*c* 0.78).

The residue of the extraction was proved to be unaffected agarobiose diethylmercaptal by its m.p. and its specific rotation.

Hexamethyl agarobiose diethylmercaptal (V). Hexaacetyl agarobiose diethylmercaptal (20.0 g.) was methylated in a 80% acetone solution three times by the reaction with dimethyl sulfate and a 30% sodium hydroxide solution in the usual way. The methylated product distilled at 188~191°/0.040 mmHg. (bath temperature 240~260°), giving a viscous liquid; yield 10.6 g. (71% of the theory), n_D^{25} 1.4952, $[\alpha]_D^{10}$ −17.5° in chloroform (*c* 1.15), −12.5° in ethanol (*c* 1.12). It is hardly soluble in cold water, but readily soluble in organic solvents. *Anal.* Found: C, 51.11; H, 7.96; SC_2H_5, 23.05. Calcd. for $C_{22}H_{42}O_9S_2$: C, 51.33; H, 8.23; SC_2H_5, 23.20%.

Hexamethyl *aldehydo*-agarobiose (VI). According to the procedure of Wolfrom and others[5], hexamethyl agarobiose diethylmercaptal (4.8 g.) was demercaptalated by the action of mercuric chloride (10 g.) in an acetone solution containing water for 6 hrs. at room temperature in the presence of cadmium carbonate. The product was a brown sirup, which was then dissolved in water, a brown oily precipitate being removed by decantation. The aqueous solution, after being decolorized with charcoal, was concentrated to dryness. The resulting colorless sirup (3.4 g.) crystallized almost completely. Recrystallization of the crude crystals from dry ether gave fine needles of the *aldehydo*-sugar; yield 2.6 g. (67% of the theoretical amount), m.p. 92~93°, $[\alpha]_D^{10}$ −4.0° (initial) → −9.33° (equilibrium) in water (*c* 0.75), −9.77° (initial) → −53.71° (equilibrium after 2 hrs.) in chloroform (*c* 1.024). It reduced a hot Fehling's solution, decolorized a neutral permanganate solution, and restored the color to a Schiff's solution. *Anal.* Found: C, 52.68; H, 7.78; OCH_3, 45.31. Calcd. for $C_{18}H_{32}O_{10}$: C, 52.93; H, 7.90; OCH_3, 45.58%.

Hexamethyl agarobionic acid (VII). To a solution of the *aldehydo*-sugar (8.0 g.) in water (50 cc.) was dropped a solution of potassium permanganate (2.2 g.) in 0.1N potassium hydroxide solution under stirring at room temperature. The oxidation proceeded immediately. The precipitate of manganese oxide was removed by filtration and the potassium ion was exchanged by a cation resin Amberlite IR-120. The solution was then neutralized exactly with 0.1N barium hydroxide solution, and concentrated to dryness. The residue, from which the unaffected *aldehydo*-sugar was extracted with ether, was dissolved in water. The treatment of the solution with a cation resin Amberlite IR-120 followed by subsequent evaporation gave hexamethyl agarobionic acid as a glassy solid; yield 4.5 g. (54% of the theoretical amount), $[\alpha]_D^{10}$ −25.5° (*c* 0.55). *Anal.* Found: OCH_3, 43.55; Neut. Equiv., 423. Calcd. for $C_{18}H_{32}O_{11}$: OCH_3, 43.86%; Neut. Equiv. 424.

Hexamethyl methyl agarobionate. The free acid (3.8 g.) above mentioned was esterified by the reaction with diazomethane in an ethereal solution, yielding a viscous liquid with a pale yellow color; yield 3.6 g., b.p. 161~163°/0.030 mmHg., n_D^{25} 1.4681, $[\alpha]_D^{14}$ −23.4° (*c* 1.03), −31.1° in chloroform (*c* 1.16). *Anal.* Found: C, 49.99; H, 7.78; OCH_3, 47.21; Sapn. Equiv., 436. Calcd. for $C_{19}H_{34}O_{11}$: C, 49.76; H, 7.47; OCH_3, 47.37%; Sapn. Equiv., 438.

This was methylated twice with methyl iodide and silver oxide in the usual way; b.p. 160~161°/0.027 mmHg., $[\alpha]_D^{17}$ −23.0° (*c* 2.73), OCH_3 found 47.25%.

The reaction with ammonia or phenylhydrazine failed to give any crystalline derivative.

Hydrolysis of hexamethyl agarobionic acid. Hexamethyl agarobionic acid (1.1 g.) was hydrolysed in N-sulfuric acid (50 cc.) in a boiling water bath. The reaction was followed polarimetrically: $[\alpha]_D$ −22.8° (initial); −15.9° (0.5 hr.); −13.6° (1 hr.); +0.05° (3 hrs.); +15.9° (8 hrs.); +27.6° (14 hrs.) +30.5° (24, 32 and 40 hrs., constant). The solution was neutralized with barium carbonate, filtered and evaporated. From the resulting sirup, 2,3,4,6-tetramethyl D-galactose was extracted with boiling ether, leaving barium 2,5-dimethyl 3,6-anhydro-L-galactonate.

a) 2,3,4,6-Tetramethyl D-galactose (VIII)—The ether extract upon concentration gave a colorless sirup of 2,3,4,6-tetramethyl D-galactose; yield 0.51 g., $[\alpha]_D^{10}$ +113.0° (*c* 0.46), OCH_3 found 52.35% ($C_6H_8O_2(OCH_3)_4$ requires OCH_3 52.55%).

Anilide: m.p. alone or when mixed with an authentic specimen, 192°, $[\alpha]_D^{10}$ −79.2° (initial) → +41.7° (equilibrium) in acetone (*c* 0.48).

b) 2,5-Dimethyl 3,6-anhydro-L-galactonic acid (IX)—Barium 2,5-dimethyl 3,6-anhydro-L-galactonate, described above, was converted to the free acid by means of a cation exchange resin Amberlite IR-120. The resulting product crystallized completely; yield 0.41 g., m.p. 159~160°. Recrystallization from ethyl acetate gave a pure substance[3]; m.p. 161°, $[\alpha]_D^{7}$ −58.6° (*c* 0.44). *Anal.* Found: C, 46.38; H, 6.63; OCH_3, 29.97; Neut. Equiv., 205. Calcd. for $C_8H_{14}O_6$: C, 46.58; H, 6.85; OCH_3, 30.12%; Neut. Equiv., 206.

Amide: The free acid (0.12 g.) above mentioned was esterified with diazomethane in an ethereal solution. The methyl ester (0.12 g.), obtained as a colorless sirup with $[\alpha]_D^{15}$ −39.3° (*c* 2.52), was then converted to the corresponding amide in the usual way[3]; flakes, m.p. 172°, $[\alpha]_D^{15}$ −67.0° (*c* 0.63). *Anal.* Found: C, 46.74; H, 7.39. Calcd. for $C_8H_{15}O_5N$: C, 46.80; H, 7.37%.

The authors wish to express their thanks

5) M. L. Wolfrom et al., *J. Am. Chem. Soc.*, **51**, 2188 (1929); **52**, 2464, 3619 (1930); 53, 4379 (1931); **56**, 880, 985 (1934).

to Mr. K. Arai for carrying out the micro-analysis, and to Mr. K. Yamanouchi for his assistance in this study. This research has been aided by the Grant for the Fundamental Scientific Research from the Ministry of Education to whom thanks are also expressed.

Institute of Chemistry, Faculty of Industrial Arts, Kyoto Technical University, Kyoto

Studies on the Chemical Constitution of Agar-agar. XVII[1] *Isolation of Crystalline Agarobiose Dimethylacetal by Partial Methanolysis of Agar-agar*[2]

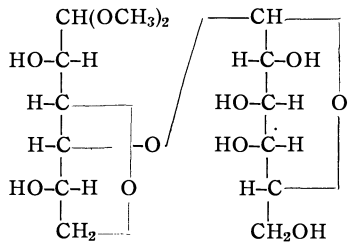
By Choji ARAKI and Susumu HIRASE

(Received October 14, 1953)

Constitutional studies on agar carried out in this laboratory have revealed that the chief component monosaccharides, so far as known hitherto, are D-galactose and 3,6-anhydro-L-galactose, and that these two are joined by 1-4-linkage to build the agarobiose[3] (4-D-galactopyranosyl 3,6-anhydro-L-galactose) unit in the molecule of agar. Moreover, it has been suggested that agarobiose units would extend over approximately half of the molecule of agar[1,4]. But difficulty was encountered in the quantitative treatment of the material in the preceding works, and consequently it has not been possible to estimate the precise content of agarobiose units. However, the partial methanolysis method, dealt with in the present paper, has proved to make possible not only the isolation of crystalline agarobiose dimethylacetal (I) but also its quantitative separation to some extent to be effected.

The partial methanolysis of agar was accomplished by treatment with boiling methanolic hydrogen chloride for a short period, a portion of agar still remaining undissolved.

The reaction products on solvent fractionation gave rise to a crystalline compound,



(I)

which was identified as agarobiose dimethylacetal (I) for the following reasons. Acetylation gave a crystalline hexaacetate, indicating the presence of six available hydroxyl groups in the molecule. Complete methanolysis produced methyl D-galactoside and 3,6-anhydro-L-galactose dimethylacetal[5] in equimolar proportion. Mild acid hydrolysis regenerated the reducing sugar, the phenylosazone of which was found to be identical with the well-established agarobiose phenylosazone.[3]

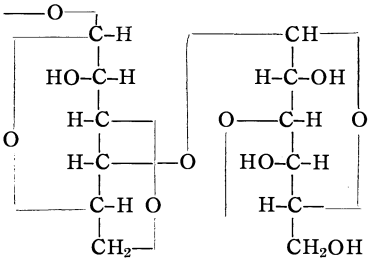
Further constitutional evidence was provided by the fact that, when authentic agarobiose diethylmercaptal[1] was submitted to demercaptalation by the action of mercuric chloride in absolute methanol, there was obtained a crystalline compound having the same characteristics as those of the compound under question. The direct formation[6] of a sugar acetal from the corresponding mercaptal can scarcely occur unless hydroxyl groups in the same molecule are protected by some substituents from the lactol formation. In the case above mentioned, however, the dimethylacetal resulted because the 3,6-anhydro-galactose residue in the agarobiose unit prefers[7] an open-chain structure to a lactol-ring structure on account of the steric hindrance caused by the preexistence of the 3,6-anhydro-ring.

The non-crystalline portion of the methanolysate was separated by means of partition chromatography on a column of starch, which led to the isolation of an additional specimen

1) Part XVI: S. Hirase and C. Araki, This Bulletin. **27**, 105 (1954).
2) Read at 6th Annual Meeting of the Chemical Society of Japan held at Tokyo in 1953.
3) C, Araki, *J. Chem. Soc. Japan*, **65**, 533, 627 (1944).
4) C. Araki, *Memoirs of the Faculty of Industrial Arts, Kyoto Technical Univ., Science and Technology Edition*, **2** (B), 46 (1953).
5) C. Araki, *J. Chem. Soc. Japan*, **65**, 725 (1944).
6) J. W. Green and E. Pacsu, *J. Am. Chem. Soc.*, **60**, 2288 (1938).
7) S. Pea , Advances in Carbohydrate Chemistry, **2**, 37 (1946).

of agarobiose dimethylacetal, together with 3,6-anhydro-L-galactose dimethylacetal and methyl D-galactoside. Thus the total yield of agarobiose units, including not only the yield of agarobiose dimethylacetal itself but also those of advanced methanolytic products, namely, of 3,6-anhydro-L-galactose dimethylacetal and methyl D-galactoside, amounted to 69.5% of the reacted agar, when calculated as the parent free sugar.

Although the chromatographic separation has been unsatisfactory, this result, along with the fact that D-galactose residues are united to other residues at 1,3-positions,[8] and that 3,6-anhydro-L-galactose residues are present as the pyranose form[9] in the molecule of agar, brings us to the conclusion that such constitutional units as illustrated in formula II would extend over approximately two-thirds of the agar molecule. Consequently the constitutional formula for agar, proposed by Jones and Peat[10] in 1942, represents by no means the real feature of the molecule.



(II)

Experimental

Evaporation and concentration were carried out under reduced pressure below 40°. The specific rotation was measured in an aqueous solution unless otherwise stated. All melting points are uncorrected.

Partial Methanolysis of Area. Commercial powdered agar (50 g., dry weight 41.9 g.) was refluxed with 1% (w/v) methanolic hydrogen chloride (500 cc.) for 1.5 hrs. After cooling, the undissolved agar (3.3 g.) was removed by filtration, and the filtrate was submitted to neutralization with silver carbonate followed by filtration and subsequent evaporation. The resulting sirup was treated with 0.2N aqueous barium hydroxide solution (500 cc.) at 60° for 2 hrs. The solution was then neutralized with carbon dioxide, filtered and concentrated to a sirup, which was dried by repeated additions of absolute methanol followed by subsequent evaporation to give rise to an amorphous powder (44.0 g.).

Solvent Fractionation of the Methanolysate. The methanolysate thus obtained was dissolved in absolute methanol (120 cc.), and then *n*-butanol (600 cc.) was added with vigorous shaking. The voluminous precipitate (17.4 g.) formed was filtered, washed first with *n*-butanol and then with ethyl acetate. The combined filtrate and washings were concentrated to dryness, when an amorphous powder (fraction A) was obtained; yield 26.5 g., $[\alpha]_D^{14}$ −13.0°. The precipitate was redissolved in absolute methanol (30 cc.), and then absolute ethanol (150 cc.) was added with shaking. The precipitate formed was again filtered, washed with methanol-ethanol (1:5) and dried, when a hygroscopic white powder (fraction C)was obtained; yield 11.9 g. (30.8% of the reacted agar), $[\alpha]_D^{13}$ −22.8°, OCH_3 found 7.58%. The filtrate and washings were combined and concentrated to dryness, when an amorphous powder (fraction B) was obtained; yield 5.5 g. (14.3% of the reacted agar), $[\alpha]_D^{13}$ −18.1°, OCH_3 found 15.14%.

Isolation of Agarobiose Dimethylacetal. The fraction A was dissolved in absolute ethanol (30 cc.), and acetone (60 cc.) was added, and the transparent solution was left in an ice box for a week. The deposited crystals of agarobiose dimethylacetal were filtered and washed first with ethanol-acetone (1:2) and then with absolute ethanol; yield 13.3 g. (30.2% of the reacted agar, calculated as its parent free sugar), m. p. 160~163°. The combined filtrate and washings upon concentration to dryness gave an amorphous powder (fraction A'); Yield 13.1 g. (33.9% of the reacted agar), $[\alpha]_D^{14}$ +0.65°, OCH_3 found 20.53%. Pure agarobiose dimethylacetal was obtained as prisms on recrystallization of the crude one from absolute ethanol; m. p. 162~164°, $[\alpha]_D^{10}$ − 29.1° (c 1.58) and −37.4° in methanol (c 1.10). It is readily soluble in water and methanol, and scarcely soluble in cold ethanol. *Anal.* Found: C, 45.69; H, 7.23; OCH_3, 16.69. Calcd. for $C_{14}H_{26}O_{11}$: C, 45.46; H, 7.09; OCH_3, 16.76%.

Hexaacetyl Agarobiose Dimethylacetal. Agarobiose dimethylacetal (1.0 g.) was acetylated with pyridine and acetic anhydride in the usual way. Crude crystals were deposited when the reaction mixture was poured into ice-water; yield 1.6 g., m. p. 84~86°. Recrystallization twice from methanol-water (1:2) gave flakes of the pure substance; m.p. 87~88°, $[\alpha]_D^{13}$ −5.76° in chloroform (c 1.22) and −12.5° in benzene (c 1.20). *Anal.* Found: C, 50.09; H, 6.00; CH_3CO, 41.30. Calcd. for $C_{12}H_{14}O_9(CH_3CO)_6(OCH_3)_2$: C, 50.16; H, 6.15; CH_3CO, 41.49%.

Methanolysis of Agarobiose Dimethylacetal. Agarobiose dimethylacetal (2.0 g.) was refluxed with 2% methanolic hydrogen chloride (100 cc.), the reaction being followed polarimetrically: $[\alpha]_D$ −38.5° (initial); −6.0° (1 hr.); +10.0° (3 hrs.); +18.0° (10 hrs.); +21.5° (15 hrs.); +22.5° (20 hrs.); +23.0° (25, 30 and 35 hrs.). After 35 hrs. the reaction solution was neutralized with silver

8) C. Araki, *J. Chem. Soc. Japan*, **58**, 1362 (1937); E. G. V. Percival and J. C. Somerville, *J. Chem. Soc.*, **1937**, 1615.
9) C. Araki, *J. Chem. Soc. Japan*, **61**, 775 (1940).
10) W. G. M. Jones and S. Peat, *J. Chem. Soc.*, **1942**, 225.

carbonate, filtered and concentrated to a sirup (2.0 g.), which was shown by paper chromatography to be a mixture of 3, 6-anhydrogalactose dimethylacetal and methyl galactoside. This indicative evidence was confirmed by the isolation of each component by means of the chromatographic separation on a starch column, at first *n*-butanol saturated with water and then 80% methanol being used as a mobile phase. 3,6-Anhydro-L-galactose dimethylacetal was obtained on solvent removal of the butanol effluent as a colorless sirup: yield 46.7% of the sample used, $[\alpha]_D^{19}$ −28.7° (*c* 0.76), OCH_3 found 25.8%. Its structure was confirmed by hydrolysing it to free sugar and then converting the latter to the crystalline diphenylhydrazone in the usual way[5]; m.p. and mixed m.p. 154°.

Methyl D-galactoside, obtained on evaporation of the 80% methanol effluent in a yield of 53.6% of the sample used, was hydrolysed with N-sulfuric acid in the usual way to give free D-galactose, m.p. and mixed m.p. 165°, $[\alpha]_D^{16}$ +81.9° (equilibrium, *c* 0.56).

Hydrolysis of Agarobiose Dimethylacetal. Agarobiose dimethylacetal (5.0 g.) was hydrolysed with 0.01 N-aqueous oxalic acid solution (50 cc.) in a boiling water bath, the reaction being followed polarimetrically; $[\alpha]_D$ −29.0° (initial); −21.0° (0.5 hr.); −18.5° (1.0 hr.); −17.5° (1.5 and 2.0 hrs.). After 2 hrs. the solution was neutralized by means of an anion exchange resin Amberlite IR-4B, and then evaporated to a sirup, which was dried over phosphorus pentoxide in vacuum to form a hygroscopic powder of agarobiose; yield 4.4 g., $[\alpha]_D^{23}$ −17.4° (initial, c2.18)→−14.2° (equilibrium). Crystallization from methanol, ethanol, acetic acid, or from combined solvent systems of them was unsuccessful.

Phenylosazone: m.p. 220~221° (decomposition), not depressed on admixture with an authentic specimen[1,3], $[\alpha]_D^2$ −136.8 (initial)→−108.8° (after 24 hrs.) in pyridine-ethanol (2:3) (*c* 0.432).

Agarobiose Dimethylacetal from the Corresponding Diethylmercaptal. Agarobiose diethylmercaptal[1] (3.0 g.) in absolute methanol (60 cc.) was treated with mercuric chloride (5.6 g.) and yellow mercuric oxide (6 g.), according to the procedure of Green and Pacsu[11] for the preparation of thioglycosides. The resulting product was a colorless sirup, which gave crystals of agarobiose dimethylacetal on crystallization from ethanol-acetone (1:2); yield 1.1 g., m.p. 161~163°. Recrystallization from ethanol afforded a pure substance, m.p. 162~164°, not depressed on admixture with the specimen isolated from the agar-methanolysate described above; $[\alpha]_D^{17}$ −28.9° (*c* 1.21), OCH_3 found 16.62 (calcd. for $C_{14}H_{26}O_{11}$ 16.76%),

The mothor liquor separated from the crude crystals was concentrated to a sirup (1.2 g.); $[\alpha]_D^{17}$ −23.2° (*c* 1.11), OCH_3 found 16.25%. Paper chromatographic examination revealed the spot of agarobiose dimethylacetal only.

Examination of the Fraction A', B and C on Paper Chromatograms. A small portion of each of the fraction A', B and C was examined by paper chromatography, using *n*-butanol-ethanol-water (4:1:2) as a mobile phase and *o*-aminophenol as a color-developer[12]. All of the revealed spots showed a yellow coloration caused by 3,6-anhydrogalactose. Thus, the fraction A' gave the spots of 3,6-anhydrogalactose dimethylacetal (*Rf* 0.66), an unidentified compound (a trace, *Rf* 0.43) and of agarobiose dimethylacetal (*Rf* 0.34). The fraction B showed the spots of agarobiose dimethylacetal and unidentificable compounds (*Rf* 0.43 and 0.19). The fraction C showed the spots of agarobiose dimethylacetal (a trace) and unidentified, probably higher oligosaccharide derivatives (*Rf* 0.19 and those less than 0.19). Methyl galactoside was detected nowhere, although expected to be present, as it moves to the position (*Rf* 0.31) near the agarobiose derivative in the above condition. The same results were obtained when paper strips were sprayed with a lead tetraacetate reagent[13].

Separation of the Fraction A', B and C on Starch Columns. General Procedure:—The sample to be separated was dissolved in *n*-butanol nearly saturated with water (if necessary, a small amount of methanol was added), and placed on the top of the chromatographic column, which had been prepared by pouring a thick slurry of potato starch in *n*-butanol saturated with water into a glass tube and allowing the excess solvent to percolate down. The column was then washed with *n*-butanol saturated with water. Small portions of the effluent were examined on the paper chromatograms in the same way as described in the preceding section, and the effluent was divided into several sub-fractions in such a manner as to lead to the highest possible recovery of each component. After agarobiose dimethylacetal had been completely washed out, the column was then washed with 80% aqueous methanol until nothing came into the effluent. The sub-fractions thus obtained were separately evaporated to dryness.

The Fraction A':—The sample (799 mg.) was separated on a column (4×18 cm.) into four sub-fractions listed in Table I. The sub-fraction A'

Table I. The chromatographic separation of the fraction A'

Sub-fraction	Yield %a	Yield %b	$[\alpha]_D^{15}$	*Rf* value
A'—I	18.5	4.9	−25.0°	0.67
A'—II	7.2	—	−12.0°	0.67, 0.43, 0.34
A'—III	50.1	14.9	−15.2°	0.34
A'—IV	20.0	6.3	+45.3°	(0.31)

a. of the sample used, by weight.
b. of the reacted agar when calculated as the parent free sugar.

11) J. W. Green and E. Pacsu, *J. Am. Chem. Soc.*, **59**, 1205 (1937).

12) S. Hirase, C. Araki and S. Nakanishi, This Bulletin, **26**, 183 (1953).

13) J. G. Buchanan, C. A. Dekker and A. G. Long, *J. Chem. Soc.*, **1950**, 3162.

—I was confirmed to be 3,6-anhydro-L-galactose dimethylacetal by its *Rf* value and its hydrolysis to the free sugar followed by subsequent conversion to the crystalline diphenylhydrazone,[5] m.p. and mixed m.p. 154°. A′—II was a mixed fraction. A′—III was chromatographically pure agarobiose dimethylacetal, and when crystallized from ethanol-acetone, it gave a crystalline specimen, m.p. and mixed m.p. 161~163°, $[\alpha]_D^{17}$ −28.8° (*c* 0.67). A′—IV, a methanol effluent, gave only a faint spot on a paper chromatogram when sprayed with an *o*-aminophenol reagent, but it revealed an apparent zone moving to the same position (*Rf* 0.31) as α-methyl D-galactoside when sprayed with a lead tetraacetate reagent. When crystallized from ethanol, it gave crystalline α-methyl D-galactoside hydrate, m.p. and mixed m.p. 108 ~ 110°, $[\alpha]_D^{16}$ +175.8° (*c* 0.41). Thus A′—IV was considered to be mainly a mixture of α- and β-methyl D-galactoside.

The Fraction B:—The sample (799 mg.) was separated on a column (4×14 cm.) into three sub-fractions shown in Table II. The sub-fraction B—I was a mixed fraction. B—II was pure agarobiose dimethylacetal which crystallized completely; m.p. and mixed m.p. 161~163°, $[\alpha]_D^{16}$ −28.8°(c 0.66). B—III, a methanol effluent, was shown to contain an unidentified substance and a trace of methyl galactoside on paper chromatograms.

TABLE II THE CHROMATOGRAPHIC SEPARATION OF THE FRACTION B

Sub-fraction	Yield %a	Yield %b	$[\alpha]_D^{15}$	*Rf* value
B—I	3.9	—	−13.8°	0.43, 0.34
B—II	69.3	8.7	−24.2°	0.34
B—III	20.7	—	−3.4°	0.19, (0.31)

a. of the used sample, by weight.
b. of the reacted agar when calculated as the parent free sugar.

The Fraction C:— This was considered from its methoxyl content and its paper chromatographic examination to be chiefly composed of higher oligosaccharide derivatives. Hence, it was submitted again to mild methanolysis, and agarobiose dimethylacetal produced thereby was analysed: a portion of the fraction C (2.38 g.) was boiled with 1% methanolic hydrogen chloride (20 cc.) for 1.5 hrs., and the reaction solution was treated in the similar manner to that described for the methanolysis of agar. The product (2.40 g.) was divided into two parts, the ethanol-methanol (5: 1)-soluble part (1.55 g.); $[\alpha]_D^{16}$ −10.3°, and the insoluble part (0.78 g.); $[\alpha]_D^{16}$ −22.9°. Paper chromatographic examination indicated that the former contained agarobiose derivative, but the latter did not. Separation of the former on a starch column exactly in the same way as described for the fraction A′ afforded the chromatographically pure sub-fraction of agarobiose dimethylacetal in a yield of 25.5% of the used sample (5.1% of the reacted agar, when calculated as its parent free sugar), from which a crystalline specimen could be isolated; m.p. and mixed m.p. 161—163° $[\alpha]_D^{17}$—28.5° (c 0.42). Other sub-fractions were shown paper-chromatographically to contain unidentified compounds, which will be studied later.

Thus, the total yield of agarobiose units was calculated by summing up the yield of agarobiose dimethylacetal (the crystalline specimen isolated from A, the sub-fraction A′—III and B—II, and a sub-fraction from C), 3,6—anhydro-L-galactose dimethylacetal (the sub-fraction A′—I) and of methyl D-galactoside (the sub-fraction A′—IV), namely, 69.5% of the reacted agar (38.6 g.) when each is calculated as its parent free sugar.

The authors wish to express their thanks to Mr. K. Arai for carrying out the microanalysis and to Mr. K. Yamanouchi for his assistance in this study. This research has been aided by the Grant for Fundamental Scientific Research from the Ministry of Education to whom thanks are also expressed.

Chemical Institute, Faculty of Industrial Arts, Kyoto Technical University, Kyoto

The Crystal Structure of Zinc Oxyacetate, $Zn_4O(CH_3COO)_6$

By Hirozo KOYAMA and Yoshihiko SAITO

(Received October 23, 1953)

Introduction

Zinc oxyacetate $Zn_4O(CH_3COO)_6$ has an analogous composition to beryllium oxyacetate $Be_4O(CH_3COO)_6$. Its stability, volatility[1] and, furthermore, its crystal structure reported in a study by Wyart[2] showed that it must be of the same type as $Be_4O(CH_3COO)_6$. However, the accurate shape and size of the molecule have not yet been reported. As an

1) N. V. Sidgwick: "Chemical Elements and their Compounds" p. 283, Oxford, (1950).

2) J. Wyart: *Bull. Soc. Franç. Min.*, **49**, 148 (1926).

extension of our work on beryllium oxyacetate[3,4], we have undertaken its complete structure determination.

Determination of the Structure

According to the method described by Auger and Robin[5] the compound was prepared by slowly distilling powdered anhydrous zinc acetate in a high vacuum. Zinc oxyacetate sublimed gradually and was collected as a crystalline crust on the cool place of the container. After being allowed to cool, the crystalline crust was examined and well-formed single crystals were picked out. They form small (up to 0.8 mm) transparent octahedra, which on prolonged exposure to moist air are hydrolysed and become opaque, while the corresponding beryllium compound is extremely stable. Crystals selected for the present study were octahedra of about 0.6 mm in each dimension and showed no remarkable cleavage.

Laue and complete sets of oscillation photographs were prepared. The latter were taken using Fe K_α radiation ($\lambda=1.937$ Å). The dimension of the unit cell, space group and other crystallographic data were found to be in good agreement with those obtained by the previous investigator[6]:

System: Cubic

Unit-cell dimension: $a=16.45$ Å ± 0.03 Å

Space group: O_h^7-Fd3m

Number of molecules per cell:
$Z=8$ units of $Zn_4O(CH_3COO)_6$

Density: $\rho_{obs.}=1.903$ g cm^{-3}.
$\rho_{calc.}=1.901$ g cm^{-3}.

The intensities of reflection were visually estimated with the aid of calibrated scales. The above-mentioned crystallographic data and general features of intensity of reflection indicated that the structure would be close to the cubic modification of beryllium oxyacetate. Referring to the structure of beryllium compound and making use of Patterson projection, atomic parameters were deduced and refined by the method of double Fourier series. Final atomic parameters are listed in Table I.

TABLE I

ATOMIC PARAMETERS

8	$O_{(1)}$	in 8(a)	000		
32	Zn	32(e)	xxx	with	$x=-0.069$
48	$C_{(1)}$	48(f)	$x00$		$x=0.220$
48	$C_{(2)}$	48(f)	$x00$		$x=0.314$
96	$O_{(2)}$	96(g)	xxz		$x=-0.047$
					$z=-0.185$

Structure amplitudes calculated and observed are given in Table II. The agreement was good and the value of $R=\Sigma||F_0|-|F_c||/\Sigma|F_0|$ is 0.18 for all (hkl) reflections. The temperature factor used is of the form $\exp -B(\sin\theta/\lambda)^2$, where $B=0.4$ Å^2.

3) T. Watanabe, Y. Saito and H. Koyama: *Nature*, **164**, 1046 (1949).
4) Y. Saito: X-rays, **7**, 9 (1952) (in Japanese).
5) V. Auger et I. Robin: *Compt. rend.* **178**, 1546 (1924).
6) J. Wyart: loc. cit.

TABLE II OBSERVED AND CALCULATED F-VALUE

hkl	$F_{obs.}$	$\|F_{calc.}\|$	hkl	$F_{obs.}$	$\|F_{calc.}\|$	hkl	$F_{obs.}$	$\|F_{calc.}\|$
111	19.8	24.4	1020	—	1.1	1244	—	2.3
220	7.4	9.3	862	9.5	8.7	1331	—	2.6
311	10.7	9.9	951	10.7	10.6	1175	4.5	4.0
222	18.7	21.9	773	8.7	8.0	1084	2.0	4.3
400	14.7	15.7	1022	11.4	12.9	1262	8.7	9.6
331	11.8	13.0	666	13.0	12.0	1333	10.1	10.8
422	11.3	10.0	953	10.3	10.9	995	1.5	2.2
511	10.9	11.0	864	3.0	5.7	1351	—	1.7
333	15.3	14.5	1042	4.2	4.2	1175	—	1.2
440	11.5	11.1	1111	1.4	3.5	1264	4.5	6.6
531	11.2	11.1	775	15.6	12.6	10100	7.9	6.1
442	19.0	20.5	880	31.1	27.4	1420	9.3	4.4
620	7.9	8.8	971	17.5	13.9	1086	4.0	3.3
533	10.9	9.6	1131	9.0	9.4	1191	2.2	3.5
622	15.4	13.9	955	9.4	8.1	1353	3.8	3.4
444	7.7	5.4	882	—	3.5	10102	11.1	11.7
551	2.1	1.7	1044	23.0	20.6	1422	3.8	5.4
711	15.0	16.6	1060	12.0	8.5	1280	2.3	2.0
642	5.8	4.8	866	16.7	15.0	1193	9.4	10.7
731	8.6	7.9	973	7.8	7.0	1282	1.6	0.8
553	14.0	11.7	1133	11.2	9.1	1442	—	2.2
800	27.7	32.7	1062	9.3	8.9	10104	—	1.6
733	6.3	4.6	1200	8.9	7.9	1371	6.9	7.5
644	10.2	10.0	884	—	1.4	1284	—	1.8
660	25.8	23.3	1151	7.4	9.3	1511	7.8	9.1

822	16.1	15.2	1222	2.8	4.8	1373	—	0.5
751	13.9	11.9	1064	—	1.0	1444	1.0	2.4
555	9.3	7.7	1153	11.6	14.5	1460	9.9	12.7
662	13.3	12.5	975	6.1	5.8	1531	3.5	4.3
840	3.5	4.6	1240	1.1	1.0	1462	2.6	4.9
911	12.4	11.8	991	11.8	11.0	1533	—	4.4
753	—	0.1	1242	13.6	12.3	11111	6.2	7.6
842	4.8	6.8	886	—	2.7	12102	4.9	6.1
664	—	0.2	1082	5.1	5.0	1464	2.2	3.6
931	2.7	3.7	1311	12.2	9.6	1551	6.2	8.2
844	—	0.8	1171	—	0.8	1391	3.0	3.3
771	14.2	14.4	993	9.5	9.0	11113	3.6	4.8
933	17.6	18.4	1155	9.1	9.8	1600	21.1	22.0
755	2.1	3.2	1066	4.7	6.0	1622	3.1	3.5

TABLE III

INTERATOMIC DISTANCES AND INTERBOND ANGLES

$Zn_4O(CH_3COO)_6$			$Be_4O(CH_3COO)_6$ (16°C)		
$O_{(1)}$	Zn	1.96 Å	$O_{(1)}$	Be	1.65 Å
$O_{(2)}$	Zn	1.98	$O_{(2)}$	Be	1.61
Zn	Zn	3.20	Be	Be	2.76
$C_{(2)}$	$C_{(1)}$	1.55	$C_{(2)}$	$C_{(1)}$	1.55
$C_{(2)}$	$O_{(2)}$	1.24	$C_{(2)}$	$O_{(2)}$	1.26
$O_{(2)}$	$O_{(2)}$	2.20	$O_{(2)}$	$O_{(2)}$	2.24
$O_{(2)}$	$O_{(2)}$	2.71	$O_{(2)}$	$O_{(2)}$	2.51
$\angle O_{(2)}C_{(2)}O_{(2)}$		125°	$\angle O_{(2)}C_{(2)}O_{(2)}$		126°

Description of the Structure

The interatomic distances and interbond angles calculated on the basis of the atomic parameters listed in Table 1 are given in Table III, together with those found in crystals of $Be_4O(CH_3COO)_6$.

The structure consists of $Zn_4O(CH_3COO)_6$ molecules having the shape shown in the Figure. The molecular symmetry is Td–$\bar{4}3m$, whereas that of $Be_4O(CH_3COO)_6$ is T–23. This difference in molecular symmetry arises from slightly different orientations of the acetate groups in the molecule. In $Zn_4O(CH_3COO)_6$ molecule, each acetate group lies on the plane containing central oxygen atom and one edge of Zn-tetrahedron, while in the case of the beryllium compound below the transition temperature (40°C) the planes containing OCO radicals are inclined at an angle of 12.7° with the planes of $O_{(1)}$ and one Be-Be edge. The Zn-O distances are in good agreement with those found in crystals of ZnO. In spite of the molecular nature of this compound, the size and shape of the acetate groups are, though not significant, in agreement with those found in other ionic structures.

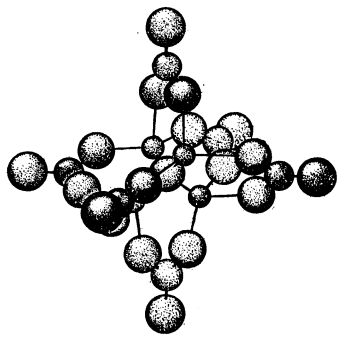


Fig. A molecule of zinc-oxyacetate

Summary

The crystal structure of $Zn_4O(CH_3COO)_6$ has been examined by the method of X-ray Fourier analysis (Fe K_α, $\lambda = 1.937$ Å). The general features of the structure reported by Wyart in 1926 are confirmed and the atomic co-oridinates which hitherto remained unfixed have been completely determined. Lengths of Zn-O bonds are 1.96 and 1.98 Å respectively, which are in good accord with those found in crystals of ZnO. The significance of the structure is discussed briefly and compared with that of $Be_4O(CH_3COO)_6$.

We are grateful to Prof. T. Watanabé for suggesting this problem and to Profs. I. Nitta and H. Kuroya for their continued interest and encouragement. Part of the cost of this study has been defrayed by a Grant of the Ministry of Education.

Institute of Polytechnics, Osaka City University, Osaka

Dielectric Behaviour of Crystalline Pentaerythritol

By Ryoiti KIRIYAMA, Shigeru YABUMOTO and Isamu NITTA

(Received December 21, 1953)

Introduction

The crystal structure of tetragonal pentaerythritol shows a particular arrangement of hydrogen bonds, these lying in the plane perpendicular to the tetragonal axis and forming a closed square configuration.[1] Owing to this arrangement, exceptionally perfect cleavage parallel to this plane appears.

Therefore, this crystal seems to be an adequate case where the dielectric behavior of a hydrogen bond might be elucidated in respect to its anisotropic nature. Moreover, this tetragonal modification transforms at 188°C. to a cubic one, which is looked upon as an example of the so-called plastic crystals and it has been assumed that the hydrogen bonds in a closed square configuration of the low modification are likely to be broken suddenly, at least partly, at transformation temperature.

From the X-ray and thermal studies,[2] it has been concluded that in the high modification, pentaerythritol molecules will rotate about their centers of gravity with some internal rotations of constituting radicals. If such radical and molecular rotations will occur in the crystal lattice, they must be observable in some dielectric behaviours, in addition to the existence of the non-zero dipole moment of the molecule revealed by the molecular beam method carried out by Estermann.[3] Thus we have studied the dielectric behaviours of pentaerythritol in both low and high modifications.

This paper contains the results of the experiment together with some discussion about the nature of the so-called atomic polarization of the hydrogen atom in hydrogen bond and the role of rotating hydroxyl radicals in the dielectrical phenomena.

Material

About 1 kg. of fairly pure pentaerythritol powder was purified by recrystallization several times from its aqueous solution and we obtained about 500 g. of a sufficiently pure sample with melting point 257°C.

The growth of a large single crystal suitable for the anisotropy measurement of its dielectric properties was difficult to achieve to a certain extent on account of spontaneous nucleation or germination of conidiospore frequently occurring in its solution during the growth-process. After various attempts, we have succeeded in obtaining single crystals suitable for these measurements by slow cooling of a supersaturated aqueous solution filled in a sealed glass-vessel, on the bottom of which a seed crystal had been laid beforehand. The optimum temperature region was 60~65°C. and the cooling-rate was several degrees in 3—4 weeks. We have successfully obtained single crystals more easily than the above mentioned by improving a thermostat as seen in Fig. 1. The

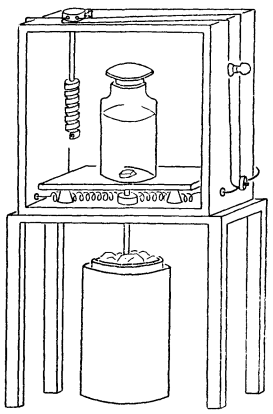


Fig. 1. The thermostat for preparing a large single crystal of pentaerythritol using convection current arised in the solution by strong temperature gradient at the bottom of the glass vessel

temperature of this thermostat was maintained constantly at a point between 60~65°C. and the upper end of the copper rod dipped in an ice-filled Dewar vessel was brought into contact with the bottom of the solution vessel in such a way that the seed placed inside came just above the upper end. This then gave rise to some slow convection currents downwards meeting onto the seed, thus the crystal grows up satisfactorily several times faster than in the case of the above procedure.

The specimens have been prepared from such crystals by cutting and grinding to plates of 1.1~1.8 mm. thick and 1.2~2.0 cm^2. in area and affixing aluminum or tin foils of 1×1 cm^2. on both their

1) I. Nitta and T. Watanabé, *Sci. Papers Inst. Phys. Chem, Research (Tokyo)*, **34**, 1669 (1938); E. G. Cox, F. J. Llewellyn and T. H, Goodwin, *J. Chem. Soc.*, **1937**, 882.

2) I. Nitta, S. Seki and M. Momotani, *Proc. Japan Acad.*, **26** (9), 25 (1950); I. Nitta, S. Seki, M. Momotani, K. Suzuki and S. Nakagawa, ibid (10) 11; I. Nitta, T. Watanabe, S. Seki and M. Momotani, ibid (10) 19).

3) J. Estermann, *Z. physik. Chem.*, B**2** 287 (1929), B**20** 195 (1933).

sides using vacuum grease or vaseline or sometimes coating with aquadag.

Apparata and Measurements

In the high frequency region two sorts of resonance circuits were used in the present experiment. The one is constructed of a push-pull oscillator of 30 Mc and a variable precision-condenser of 50pF in the resonance circuit in which the current is measured by means of a crystal detector and a microammeter. The other is composed of either quartz oscillator of 600 kc or 3 Mc and a coupling resonance circuit with a variable precision-condenser of 500 pF, the resonance being detected as above. In order to follow quickly the change of temperature, we read equivalent resistance from the lowering of the microammeter reading calibrated previously by substitution method.

In audio-frequencies, a capacity-resistance bridge was constructed suitable for the measurements, especially for high dielectric losses in the high temperature modification. In this bridge, the oscillator is an RC type one and the balancing is attained by a variable precision-condenser of 1500 pF, a set of variable non-inductance dial type resistance and a number of fixed condensers and resistances which are used to change arm-ratios. To detect the balancing, a set of crystal detector and galvanometer or a Brown-tube oscilloscope with preamplifier was used, the dielectric losses being calculated from the observed data.

The crystal condenser used for the accurate capacity measurement at room temperature was carefully constructed to have almost no stray capacity. The dielectric constant was determined from the ratio of the capacity of the sample to that of rock salt plate with the same thickness. This rock salt single crystal was made by Stockbarger's method in this laboratory. The standard dielectric constant adopted for rock salt was 5.62 throughout this study.

The cell for the measurement of the temperature dependence was made of a copper cylinder and a small-stray-capacity crystal condenser as shown in Fig. 2. The temperature was measured by a copper-constantan thermocouple with a millivoltmeter.

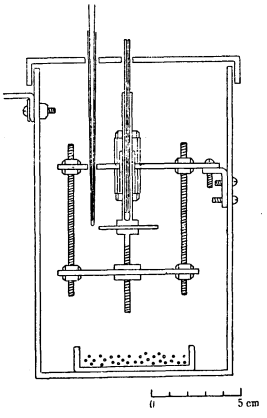


Fig. 2. The measuring cell for the dielectric constant and loss of the high-temperature modification of pentaerythritol

In order to avoid sublimation and decomposition of the sample at high temperatures, we have covered the bottom of the cylinder with pentaerythritol powder and raised the temperature somewhat rapidly, the rate being about 0.7°C. per minute.

For the measurement of direct current (D. C.) conductivity, the specimen was coated with aquadag, then dried at about 110°C., and the measurement carried out using a Wheatstone bridge with a battery of 4V. For the purpose of avoiding the effect of electrolytic polarization in the specimen, the successive readings were at longer intervals and the field direction was altered every time.

Results

The dielectric constants at room temperature for the respective field directions parallel to the *c*- and *a*-axes of the crystal are as follows:

$$\epsilon_c = 2.89, \text{ and } \epsilon_a = 3.7,$$

at frequencies from 5 kc to 30 Mc and at 17°C., where ϵ_a is calculated from the value 3.37 of the plate measured perpendicular to the natural *o*(111) plane. Thus these values show no appreciable dispersion. It may be added that the dielectric losses are too small to be observed in our experiments for the mentioned region of frequencies at room temperature.

Up to the transition point, there is no appreciable temperature dependence of these dielectric phenomena at every frequency. Even at about 130°C. where a small anomaly of its specific heat curve has been reported in a previous paper,[2] there is observed nothing anomalous in the present dielectric study.

On heating a single crystal specimen through and above the transition point, its dielectric constant and loss both increase suddenly as shown in Fig. 3.

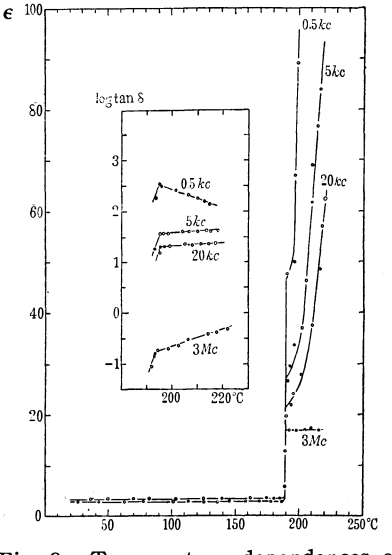


Fig. 3. Temperature dependences of the dielectric constants and losses of pentaerythritol in both low- and high- temperature modifications

The dielectric behaviour of the high temperature modification was carefully measured up to 220°C. at the above-mentioned frequencies except for 0.5kc, at the latter frequency the measurement became somewhat uncertain because of the scaling out of the instrument. As seen in Fig. 3 a remarkable dielectric dispersion in the audio-frequency region appears. And, it is worth noticing that the measured capacities of the specimens with the metal foils are always considerably larger than those coated with aquadag at every temperature as well as frequency.

At the transition point, dielectric losses appear suddenly at every frequency used, and above it they increase rapidly with temperature. In audio frequencies, the loss of a metal-foiled plate is higher than that of an aquadag-coated plate but in high frequencies such a phenomenon was not observed. The frequency dependence of the dielectric constants and losses is shown in Fig. 4.

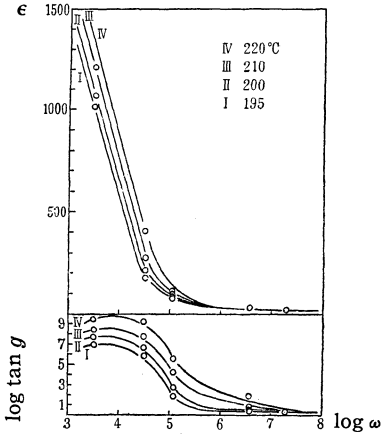


Fig. 4. Frequency dependences of the dielectric constant and loss of the high-temperature modification of pentaerythritol

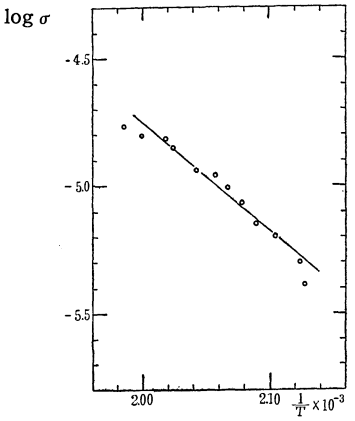


Fig. 5. Specific conductivities of pentaerythritol crystal at various temperatures

The specific conductivities at various temperatures are plotted against reciprocals of absolute temperatures in Fig. 5. In spite of inaccuracy of the D.C. conductivity measurements, many points are distributed in the form of a straight line. The value of the conductivities are unexpectedly large compared with those of ordinary molecular crystals.

Discussion

I. The Low Temperature Modification (tetragonal form)

Refractive indices and their temperature dependences were measured formerly by one of the authors (Kiriyama).[4] The values at room temperature, listed in Table I,[4] agree fairly well with those quoted in Groth's Chemische Krystallographie. This crystal is optically negative, refractive indices n_ω and n_ε corresponding to n_a and n_c repectively, of which their suffixes respresent the directions of the electric field of the light wave. In Table II the squares of the refractive indices, extrapolated to infinitely long wave length by Cauchy's dispersion formula, are given in comparison with corresponding dielectric constants. The latter are appreciably larger than the former in both directions. These differences may be attributed chiefly to the socalled atomic polarization of a hydrogen bond, the O-H···O system, or roughly speaking, ionic polarization of a proton of the system.

TABLE I
REFRACTIVE INDICES OF PENTAERYTHRITOL

λ(mμ)	n_ω	n_ε
486	1.5628	1.5218
589	1.5559	1.5146
659	1.5537	1.5109

TABLE II
DIELECTRIC CONSTANTS AND SQARES OF REFRACTIVE INDICES OF PENTAERYTHRITOL

ε_a	3.7	n_a^2	2.38
ε_c	2.89	n_c^2	2.24

From our previous studies on the double refraction of the tetragonal molecular crystal (Nitta)[5] and the above-mentioned temperature dependence of the double refraction of the present crystal (Kiriyama)[4], it was found that the Lorentz-Lorenz relation held approximately for the present crystal and the observed temperature dependence was primarily due to the anisotropic thermal expansion of the lattice, there being no evidence that the electronic polarization of the molecule itself had changed with the temperature.

4) Read before the annual meeting of the Chemical Society of Japan (1939).

5) I. Nitta, *Sci. Papers Inst. Phys. Chem. Research (Tokyo)*, **37**, 114 (1940).

Thus assuming that the Lorentz-Lorenz and Clausius-Mosotti formulae hold goods, we obtain somewhat formally the two components of the atomic polarization per mole to be approximately,

$$P_{Ac}=9.1\,\text{cc.} \quad \text{and} \quad P_{Aa}=15\,\text{cc.}$$

which correspond to 24 % and 34 % of the total polarization P_T($P_{Tc}=38$, $P_{Ta}=46$ cc.) in each direction. The fact that we have still a considerable amount of P_{Ac} and P_{Aa} will imply that the hydrogen bond is largely of the ionic nature and relative displacement of the hydrogen atoms or protons induced by the external field will be considerable, being more in the case of P_{Aa}. In this connection it will be interesting to reexamine the experimental result of the infra-red study carried out by Ellis and Bath for this crystal.[6]

The temperature dependence of the dielectric constants up to the transition point is negligibly small in spite of the large expansion coefficient along the *c*-axis.[2] This may be explained by the cancellation of the decrease of the dielectric constants due to decreasing density by the increase of ionic polarization due to the increasing thermal loosening of the lattice. It may be added that, according to Bayley's low temperature observation,[7] this substance shows no significant dielectric change in the region from −100° to 0°C. which is outside of the region of our experiment.

II. The High Temperature Modification (cubic form)

The high temperature form is isotropic and it is one example of the so-called plastic crystals, resembling the liquid state in many points. The molecule possesses statistically a mean shape of cubic or spherical symmetry owing to the internal rotation around the C–C and C–O bonds as well as finite or infinite possible molecular orientations.

At higher temperatures than the transition point, the dielectric phenomena are somewhat unusual. The large dielectric constant and losses as well as their remarkable temperature dependences at audio frequencies are evidently due to the D.C. conduction, as confirmed by the directly observed large D.C. conductivity. Similar phenomena have been observed with long chain alcohols and monoglycerides.[8] Their abnormally high dielectric constants with dispersion in the solid phase decrease by a considerable amount at the melting points and show no dispersion effects in the molten state. However, in the present case of pentaerythritol we could not extend such measurement because of the considerably rapid decomposition as well as sublimation near the melting point.

The observed conductivity must be due to a kind of protonic transfer. From the temperature dependence of the D.C. conductivity σ, the activation energy E is estimated to be roughly 20kcal./mole assuming the usual relation $\sigma=A\exp(-E/RT)$. This energy value is appreciably larger than that of ice which is estimated to be about 10 kcal./mole. It is interesting to notice that, while the latter is approximately equal to the heat of sublimation, the former value, 20 kcal./mole, is again nearly equal to the heat of sublimation of pentaerythritol in the high temperature modification as has been measured in this laboratory.[9] Thus, formally speaking, in regard to the electrical conduction it seems as if the molecule which has approximately the same energy as in the vapour state plays some role in transporting the protonic charge. It should be added that in the measurement of the dielectric constant we obtained greater values in the case of the specimen plate metal-foild with vaseline or vacuum grease than in the case when it was coated with aquadag. The higher value is thus due to the interfacial polarization of accumulated protons caused by the high resistance of vaseline or vacuum grease.

The appreciable dispersion effect in these audio frequency regions is not observed any more in the high frequency region (600kc to 30Mc). This will mean that the time of relaxation concerning the transport of the protonic charge is by far larger than the period of these alternating fields. Nevertheless the dielectric constant of the high temperature modification at these high frequencies is still considerably greater than that of the low temperature modification. This fact is due to the acquisition of a dipole moment of pentaerythritol molecule arising from the internal molecular rotation above the transition point, the molecule in the tetragonal from having the symmetry of S_4–$\bar{4}$, and thus no dipole moment. This supports qualitatively the conclusion of the X-ray study already mentioned. Moreover the time of relaxation for the dipole orientation may have something to do with that of the internal rotation and be considerably shorter than the applied high frequencies. It is also interesting to notice

6) J. W. Ellis and J. Bath, *J. Chem. Phys.*, **7**, 862 (1939); *cf.* E. F. Westrum, Jr. and K. S. Pitzer, *J. Amer. Chem. Soc.*, **71** 1940 (1949).
7) S. T. Bayley, *Trans. Faraday Soc.*, **47**, 518 (1951).
8) Y. Kakiuchi, *Proc. Japan Acad.*, **23**, (6) 65 (1947); J. D. Hoffman and C. P. Smyth, *J. Amer. Chem. Soc.*, **71**, 431 (1949); R. W. Crowe and C. P. Smyth, ibid., **72** 4427 (1950).
9) I. Nitta, S. Seki and K. Suzuki, This Bulletin, **24**, 63 (1951); P. G. Owsten, *Quart. Rev.*, 5, 344 (1951).

that as far as our measurement covers the dielectric constant it remains almost unchanged at various temperatures.

From the formal application of the well-known Debye formula[10] for the orientation polarization using the dielectric constant 16.7 and the refractive index 1.439 calculated from the average refractive index of the low temperature form and the volume change at the transition point, the dipole moment of the molecule in the crystal at 200°C. was calculated to be 1.8D, which agrees fairly well with Estermann's value 2D obtained by the molecular beam method, though these should not be compared with the other directly. Another formal application of the Debye formula for hindered dipole rotation,[11] assuming the Estermann value 2D we obtain for the hindering potential $U=1.3$kcal./mole so as to be able to account for the peculiar behaviour when the dielectric constant remains approximately the same in the high temperature region.

Evidently the two Debye formulae used above are not satisfactory in respect to the consideration of the reaction field. If we next use the formula of Onsager[12] we obtain the moment in vacuum $\mu_v=3.9$D which is by far greater than Estermann's and will mean that all the local dipole moments in the molecule orientate themselves to a considerable extent in the same direction. This difficulty comes out of course from the neglect of the short range interaction. Thus we come now to the Kirkwood formula for polar liquid.[13]

$$\epsilon_s-n^2=\frac{3\epsilon_s}{2\epsilon_s+n^2}\left(\frac{n^2+2}{3}\right)^2\frac{4\pi}{3}\frac{\mu_v^2N_0}{kT}(1+z\cos\gamma)$$

where $\cos\gamma$ is the averaged cosine of angles between nieghbouring dipoles and z is the number of the nearest nieghbours which is in the present case equal to 12. Substituting the following numerical values for the static dielectric constant $\epsilon_s=16.7$ and $\mu_v=2\times10^{-18}$, we obtain $\cos\gamma=0.244$. In the case of water the value of $\cos\gamma$ is equal to 1/3, assuming the free rotation of one of the OH bonds of water molecule about the other OH bond which is fixed in a direction towards the neighbouring oxygen atom.[14] Hence the value 1/4 would mean that the short range interaction can not be neglected. It would be better not to go further in detail because of the difficulties as follows; the molecules in the cubic form carrying out complicated internal rotations which cause the dipole moment of the molecule as a whole change from time to time, thus the theories of Onsager and Kirkwood are not directly applicable to the present case, in which the statistical average of short range interactions due to changing dipole moment is very difficult to compute with accuracy.

Department of Chemistry, Faculty of Science, Osaka University, Nakanoshima, Osaka

10) P. Debye, "Polare Molekeln" Leipzig, 1929, p. 27.
11) P. Debye, *Physik. Z.*, **36**, 160 (1935); *Chem. Rev.* **19**, 171 (1936).
12) L. Onsager, *J. Amer. Chem. Soc.*, **58**, 1486 (1936).
13) J. G. Kirkwood, *J. Chem. Phys.*, **7**, 911 (1939).
14) J. G. Kirkwood, *Trans. Faraday Soc.*, **42**, 7 (1946); *cf.* H. Fröhlich, "Theory of Dielectrics", Oxford, 1949, P. 140.

LETTER

Hexamethoxy Disilane

By Rokuro OKAWARA and Toshio TANAKA

(Received November 13, 1953)

Among the alkoxyds of disilane, hexaethoxy-[1,2] and hexapropoxy[2]- disilane only have been studied. Now we wish to report on the preparation and properties of hexamethoxy disilane $(CH_3O)_3SiSi(OCH_3)_3$, the lowest member of the alkoxyds of disilane.

Hexachlorodisilane (b.p. 69.8° C./49 mm. Hg. m.p. $-1.2°\sim-0.8°$C., *Anal.* Calcd. for Si_2Cl_6: Cl, 79.18, Found: Cl, 79.05) (36 g., 0.134 mol.) was placed in a 300 cc. three-necked flask, equipped with an efficient stirrer, a dropping funnel and a reflux condenser, and was cooled with an ice-salt bath. The outlet tube from the upper end of the condenser was led above the surface of the alkali solution which was placed to absorb the hydrogen chloride gas. After the hexachlorodisilane was completely solidified, the purified and dehydrated methanol (0.05% H_2O, determined

1) G. Martin, *J. Chem. Soc.*, **105**, 2860 (1914).
2) E. W. Abrahamson, I. Joffe and H. W. Post, *J. Org. Chem.*, **13**, 275 (1948).

by the Kahr-Fischer reagent) (26.5 g., 0.83 mol.) was added drop by drop to the solid. When the solid was made to disappear by the reaction, the temperature of the mixture was gradually raised to 30°C. with vigorous stirring. If the temperature was raised to 40°C., the floating white mass was suddenly increased on the surface of alkali solution under the outlet tube. Since this mass may be regarded as a decomposition product appearing from the fission of Si-Si bond, the dehydrochlorination of the mixture was carried out by bubbling nitrogen slowly through the mixture at the temperature not over 30°C. After bubbling for five hours, 28 g. of the mixture was obtained, of which the chlorine content was 3%. Repeated addition of methanol, followed by aeration with nitrogen could not markedly reduce the chlorine content.

When the product was fractionated adding a small amount of methanol, there was obtained impure hexamethoxy disilane contaminated by a trace of methoxy chlorodisilane, which fumes in air and causes the hexamethoxy disilane to decompose when the product is exposed to air. To prepare the pure hexamethoxy disilane, a trace of methoxy chlorodisilane should be completely expelled before the fractionation.

For this purpose the following ammonia treatment was found to be effective. A small amount of methanol (3 g.) was added to the mixture (28 g.) and dry ammonia gas was slowly bubbled through the mixture, until the odor of hydrogen chloride disappeared. After filtration, the precipitate was washed with a small quantity of dehydrated ethyl ether. The filtrate was repeatedly evacuated until the odor of ammonia practically disappeared.

The product was rigorously fractionated through a semi-micro Stedman column of about 15 plates under reduced pressure. The constant boiling fraction (I): 63°~4°C./86 mm.Hg (6 g.), (II): 100°~101°C./20 mm.Hg (8 g., yield: 25%) and the residue (6 g.) were obtained.

Judging from the boiling point, fraction (I) may be methyl orthosilicate. The fraction (II), which was analysed, was a transparent liquid having a faint odor and did not decompose in air. n_D^{20} 1.4070, d_4^{20} 1.095. *Anal.* Calcd. for $C_6H_{18}O_6Si_2$ (mol. wt. 242), C: 29.73. H: 7.49, Si: 23.18, Found for (II), C: 29.48, H: 7.60, Si: 23.0, mol. wt. 235 (in benzene).

The authors wish to express their sincere thanks to Dr. Watase for his gracious encouragement during this work. Our thanks are also due to the Ministry of Education for aid in this research.

Deyartment of Applied Chemistry, Faculty of Engineering, Osaka University, Osaka

*Formation and Aging of Precipitates. I. Electron Microscopic Studies of the Formation of Barium Sulfate Precipitate**

By Eiji SUITO and Kazuyoshi TAKIYAMA

(Received September 17, 1953)

Introduction

The relations between the formation of the precipitates and their physical and chemical properties have been studied by a number of investigators. Especially the precipitation of barium sulfate has been investigated as a fundamental case. Fischer[1] and Okada[2] employed the electron microscope to study the precipitates of barium sulfate. The authors also used an electron microscope to study the formation, the aging and the growth mechanism of the crystals of barium sulfate. In this paper the relation between the concentration of the reagents and the shape and size of the precipitated particles is described.

Experimental Procedure

Barium sulfate precipitates were formed on mixing barium hydroxide with sulfuric acid to keep out the disturbance of other ions. But at concentrations higher than 0.2 M barium acetate and manganous sulfate were used because of their solubilities. These reagents were all guaranteed. The reagents of equal volumes and of the same concentrations were mixed rapidly by pouring into a large test tube at 18°C. Directly after mixing, a drop of the reaction products was placed on a specimen holder for the electron microscope and was dried. The specimens were observed directly or after chromium shadowing by the electron microscope SM—T4.

Experimental Results

Fifteen kinds of precipitates were prepared, varying the total concentration of barium sulfate from 1.0000 to 0.0001 M (i.e. the concentration of the reagents from 2.0000 to 0.0002 M). Several specimens for electron microscopy were prepared from each precipitate, and several electron micrographs were taken for each of the specimens. The shape and the size of the particles of each precipitate were observed, then the length of the longest part of the particles was measured. From about 200 particles the size distribution curves of each precipitate were obtained as shown in Fig. 1, in which the relative frequency is plotted against the length of the particle. These distribution curves are for

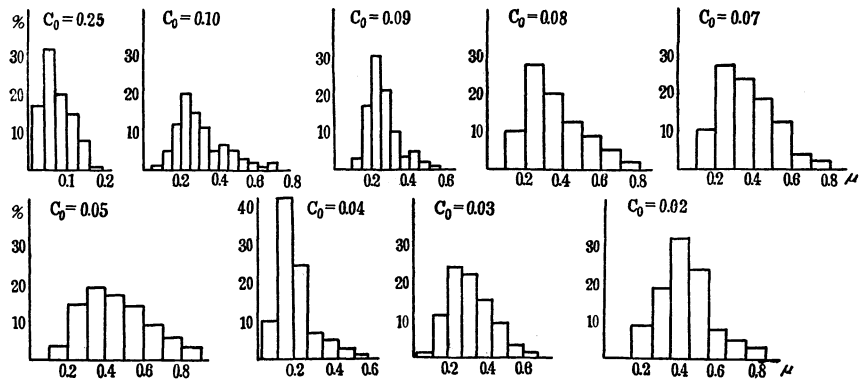


Fig. 1. Frequency histogram of particle size.
abscissa: size of particles (μ).
ordinate: relative frequency (% of particles).

the samples ranging from 0.25 to 0.02 M in the total concentration. From these distribution curves the arithmetic mean sizes of the particles were calculated. The shape and the size of barium sulfate precipitates formed in different total concentrations are shown collectively in Table 1.

* Some parts of this experiment were published in *Proc. Japan Acad.*, **28**, 133 (1952) as a preliminary report.

1) R. B. Fischer, *Anal. Chem.*, **23**, 1667 (1951).

2) S. Okada, M. Kawane and S. Magari, *Mem. Faculty Eng. Kyoto Univ.*, **13**, 198 (1951).

TABLE I

THE RELATION OF THE SHAPE AND SIZE TO THE TOTAL CONCENTRATION OF BARIUM SULFATE PRECIPITATES

Group	No.	Total concentration C_0(M)	Particle size (mean) L(mμ)	$C_0 \times L$	Particle shape
A	1	1.00	13	13.0	Amorphous
„	2	0.50	25	12.5	„
„	3	0.25	51	12.7	Sphere
B	4	0.10	251	25.1	Spindle
„	5	0.09	266	23.9	„
„	6	0.08	307	24.5	„
„	7	0.07	317	22.2	„
„	8	0.05	470	23.5	„
C	9	0.04	182	7.3	Cross spindle
„	10	0.03	270	8.1	„
„	11	0.02	466	9.3	„
D	12	0.01	1650	16.5	Diamond (rugged)
E	13	0.001	2030	20.3	Diamond (round)
F	14	0.0003	850	0.255	Rectangle
„	15	0.0001	110	0.011	

I. The Shape of Barium Sulfate Precipitates.

The natural habit of barium sulfate is orthorhombic. But several kinds of different shapes were formed by changing the total concentrations as shown in Table I. The degree of perfection of the crystals was excellent at lower concentration.

At the total concentration of 1.0 M the colorless and transparent jelly was formed immediately after mixing the reagents. This jelly turned white in a few minutes. The precipitates prepared over the range 1.0 to 0.5 M in the total concentrations were jelly or gel. One of the electron micrographs is shown in Photo 1. It seems to be in an amorphous state according to the resolving power of the electron microscope used today. At the total concentration of 0.25 M the precipitate was crystalline, each particle being an irregular sphere as shown in Photo 3.

It seemed that the precipitates prepared in this range (A group in Table I) were affected by acetate and manganous ions. When barium hydroxide saturated in boiling water reacted with 6 N sulfuric acid, beautiful spherical particles, 80 mμ in diameter, were formed.

In the range of the total concentrations, 0.10~0.05 M (B group), the powdery precipitates appeared directly after mixing the reagents and the shape of the precipitated particles was like a spindle with rugged edges as shown in Photo 4. The ratio of major axis to minor axis was almost constant, namely, 10 : 5.5. The number of projections was eight or ten, and the crystal seemed to have grown in the direction of the projections.

In the range of the total concentrations, 0.04~0.02 M (C group), many cross spindle shaped particles were found besides simple spindle shaped ones as shown in Photo 5. The both lengths of the cross spindles were the same and the projections decreased in number.

At the total concentration of 0.01 M (D group) the precipitate appeared a few seconds after mixing the reagents, and it was diamond shaped having rugged edges as shown in Photo 7. The particles were flat and the ratio of thickness to length was 1 : 10.

At the total concentration of 0.001 M (E group) the precipitate formed about ten seconds after mixing the reagents and consisted of large diamond shaped particles having smooth edges and small spindle shaped ones, which were about 1/10 in size of the large ones, as shown in Photo 8.

In the range of the total concentrations below 0.0003 M (F group) the precipitates appeared about one or two minutes after mixing the reagents. The particles sampled before the completion of the crystals were flat and rectangular, consisting of irregular sizes as shown in Photo 10.

II. The Particle Size of Barium Sulfate Precipitates.

The size of particles of freshly precipitated barium sulfate generally increased with the decrease of the total concentration as shown in Table I. In the A, B and C groups, each of which has the same shape, the relation of the total concentration C_0 (M) to the size

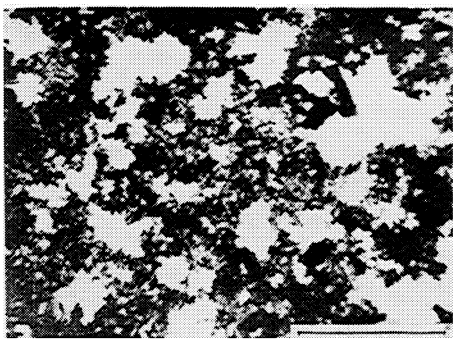


Photo. 1. $C_0=1.0$ M
(×20,000)

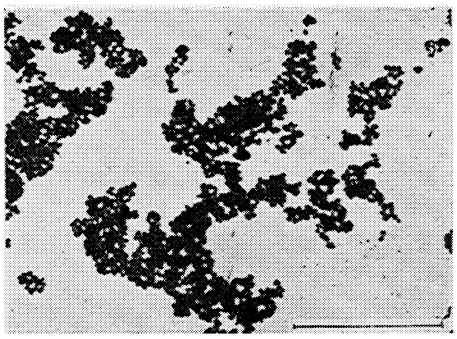


Photo. 2. $C_0=1.0$ M
After 3 months (×20,000)

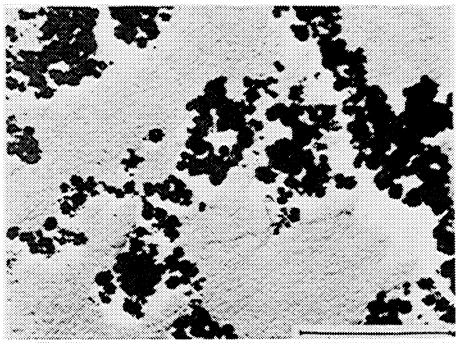


Photo. 3. $C_0=0.25$ M
(Cr-shadowing, ×20,000)

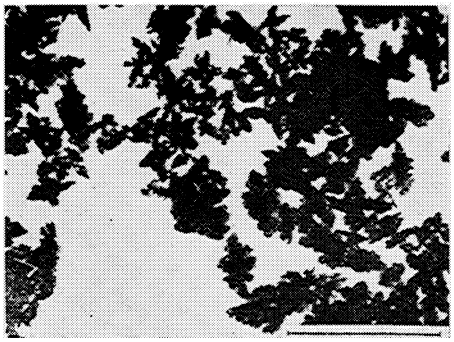


Photo. 4. $C_0=0.10$ M
(×20,000)

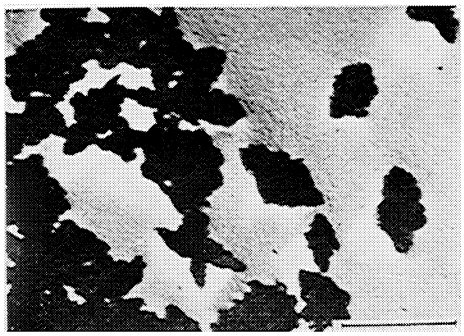


Photo. 5. $C_0=0.02$ M
(Cr-shadowing, ×15,000)



Photo. 6. $C_0=0.02$ M
After 2 years (Cr-shadowing, ×15,000)

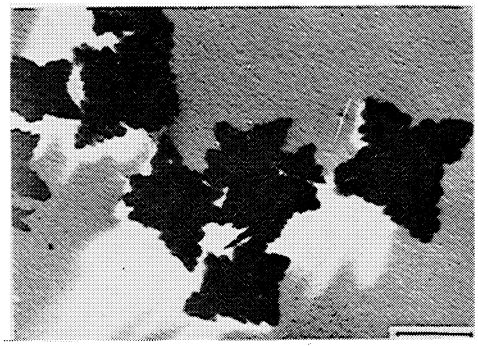


Photo. 7. $C_0=0.01$ M
(Cr-shadowing, ×10,000)



Photo. 8. $C_0=0.001$ M
(×10,000)

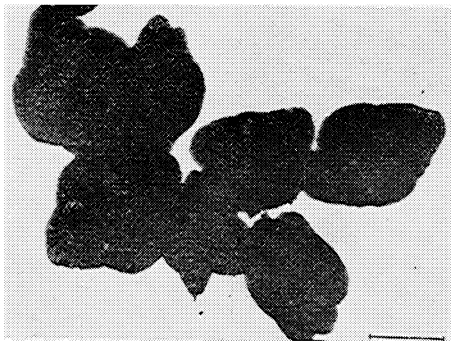


Photo. 9. $C_0=0.001$ M
After 5 hours (×10,000)

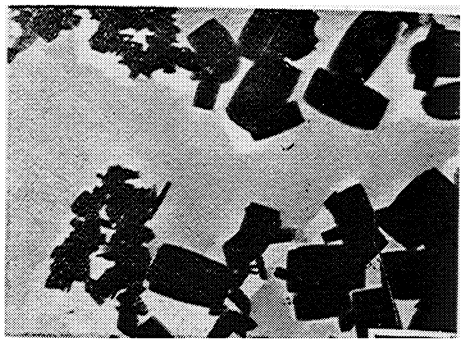


Photo. 10. $C_0=0.0003$ M
(Cr-shadowing, ×10,000)

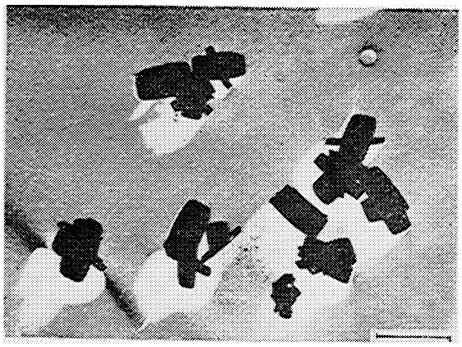


Photo. 11. $C_0=0.0003$ M
After 5 hours (Cr-shadowing, ×10,000)

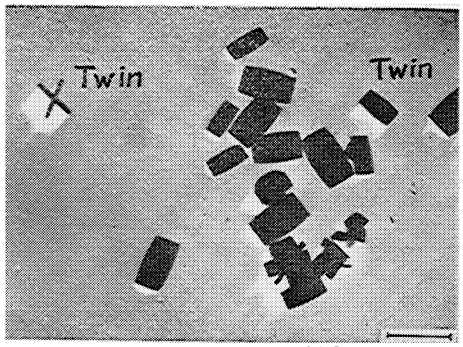


Photo. 12. $C_0=0.0003$ M
(Cr-shadowing, ×8,000)

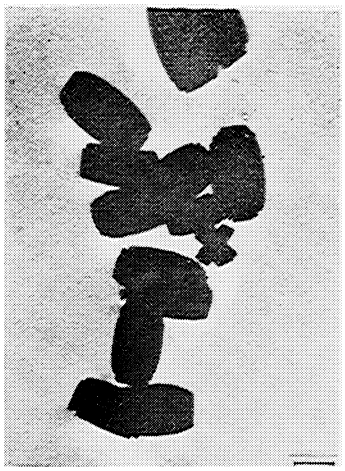


Photo. 13.
Precipitation condition
(Cr-shadowing, ×5,000)



Photo. 14.
Crystalline nuclei
(Cr-shadowing, ×5,000)

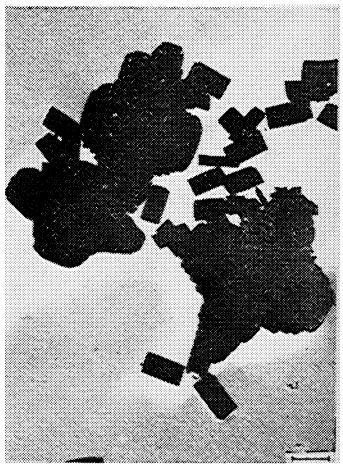


Photo. 15.
Produced crystals
(Cr-shadowing, ×5,000)

of the precipitated particles L (mμ) is hyperbolic, i.e. $C_0 \times L$ = constant, as indicated in Fig. 2. Accordingly, so long as the particles

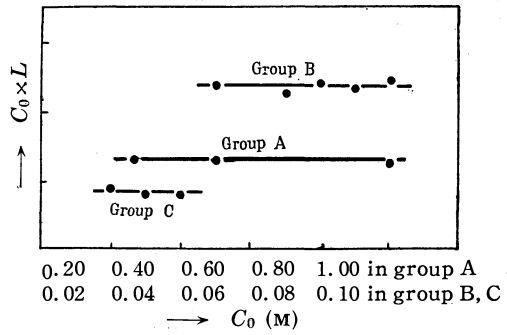


Fig. 2. The relation between the total concentration and the particle size.

of the same shape were concerned, the precipitation law advocated by von Weimarn accorded well with this experiment.

Summary

The shape and the size of barium sulfate precipitate prepared within the range of the total concentrations from 1.0000 to 0.0001 M were observed by an electron microscope. The particles were observed to precipitate in various forms (spherical, spindle, diamond and rectangular) in response to the total concentration of barium sulfate. It was confirmed that the precipitation law advocated by von Weimarn was still substantiated so far as the particles of the same shape were concerned.

The cost of this research has been partly defrayed from the Scientific Research Encouragement Grant of the Ministry of Education, to which the author's thanks are due.

Institute for Chemical Research, Kyoto University, Takatsuki, Osaka

Formation and Aging of Precipitates. II. Electron Microscopic Studies of the Aging of Barium Sulfate Precipitate

By Eiji SUITO and Kazuyoshi TAKIYAMA

(Received September 17, 1953)

Introduction

The aging of the precipitate is not only significant for the study of its properties, but also interesting from the view-point of the production of powdered materials in the chemical industry. The aging of barium sulfate precipitate has been studied by many investigators by means of various methods. Nowadays, as the electron microscope has made it possible to observe the colloidal dimension, the aging process can be studied in detail.

The authors previously described the shape and size of freshly precipitated barium sulfate[1]. In this paper the aging of the precipitates and the process of the growth of the crystals are described.

I. Aging Process in various Concentrations.

Barium sulfate precipitates produced as described in the previous paper[1] were kept in mother liquor and they were sampled out for electron microscopy at various intervals of time.

(*a*) *Crystallization of Gel* In the range of the total concentrations, 1.0~0.5 M, the fresh precipitates were colorless and transparent jellies and seemed to be amorphous. These jellies changed to a white gelatinous mass in a few minutes and settled down after a few days. These sedimented precipitates were composed of spherical particles, which were crystalline, as shown in Photo 2.

(*b*) *Precipitates uniform in Shape and Size* In the range of the total concentrations from 0.10 to 0.01 M the freshly precipitated particles were spindle shaped, cross spindle shaped and diamond shaped and each precipitate had homodisperse or uniform size distribution[1]. In these cases no change of the shape and size was observed for a few months. But the particles precipitated over the range 0.10 to 0.02 M, which had been dendritic and spindle shaped, changed to smooth spindle or hexahedron (rectangle in cross section) shaped ones after about 2 years as shown in Photo 6. Nevertheless, the size of the particles was almost unchanged as shown in Photos 5 and 6. The dendritic particles, which were probably unstable, re-

1) E. Suito and K. Takiyama, This Bulletin, **27**, 121 (1954).

oriented to ideal crystals, which were rectangular and stable, during the digestion in the mother liquor.

(*c*) *Precipitates not uniform in Shape and Size* At the total concentration of 0.001 M the freshly precipitated particles consisted of two different sizes and shapes, i. e. large diamond shaped particles of about 2 μ and small spindle shaped ones of about 0.2 μ as shown in Photo 8. These smaller ones disappeared after several hours as shown in Photo 9. Two kinds of particles must have appeared by heterogeneous mixing of the reagents. The disappearance of the smaller particles is explained by recrystallization, that is to say, the smaller particles, which were more soluble than the larger ones, dissolved and were deposited on the larger ones.

In the range of the total concentrations below 0.0003 M, the precipitates, which were sampled out immediately after mixing the reagents, consisted of various sizes. In this case the size of the particles changed to uniform as shown in Photo 11 and Ostwald's ripening theory was proved to be valid.

II. Growing Process of Crystal.

In order to study the process of growth of the crystal, the changes of the electric conductivity and the turbidity were measured during the formation of the ideal crystal, whose shape was rectangular.

(*a*) *Change of Conductivity* 10 cc. of barium hydroxide solution and sulfuric acid, whose concentrations were both 0.0021 M, were added simultaneously in to 40 cc. of water. The conductivity of the suspension was measured at ten seconds intervals. The change of the conductivity is indicated by curve 1 in Fig. 1. A rapid change occured about forty seconds after mixing.

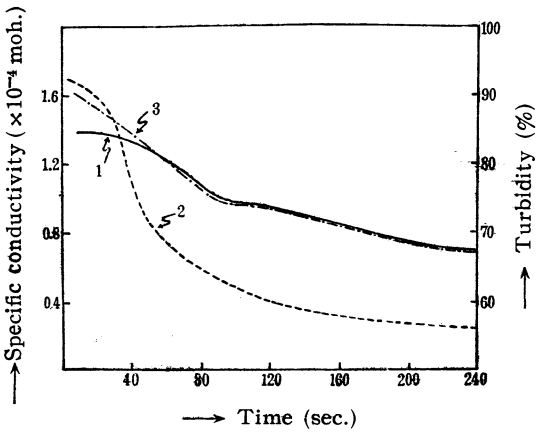


Fig. 1. The change of conductivity and turbidity during the formation of the precipitate.

(*b*) *Change of Turbidity* 2 cc. of barium hydroxide solution and sulfuric acid, whose concentrations were both 0.0021 M, were added into 8 cc. of water. The intensity of the light that passed through the specimen was compared with the intensity of the light that passed through water by means of photocolorimeter. In Fig. 1, curve 2 indicates the intensity of the passed light in percentage. The turbidity changed rapidly about thirty seconds after mixing the reagents.

As indicated in Fig. 1, the curve of the conductivity and the turbidity have a similar form. From these curves, a certain induced period, ten to sixty seconds, is considered to be needed for the formation of the nucleus which grew slowly to the perfect crystal.

(*c*) *Change of Conductivity during the Crystallization in the Presence of Nucleus* 20 cc. of barium hydroxide solution and sulfuric acid, whose concentrations were both 0.0021 M, were added into 40 cc. of the suspension described in (a). The change of the conductivity is indicated by curve 3 in Fig. 1. When the nucleus is present, the crystallization does not require the induced period.

III. Morphology of the Crystals slowly formed and in the Presence of Nucleus.

(*a*) *Crystals slowly formed* The precipitated particles of barium sulfate described above in (II. a) are rectangular as shown in Photo 12, and this shape is ideal for barium sulfate. The ratio of the length of the two edges was almost constant, namely, 2 : 1. Occasionally twin crystals appeared besides these rectangular single crystals. As marked in Photo 12, two twins are observed from different directions by shadowing. As the facet of the twin of orthorhombic crystal is (110), the angle between the two crystals of the twin ought to be about 63°11′, but the angle of the twin shown in Photo 12 is 70° because of the inclination of the crystal to the specimen holder.

(*b*) *Precipitates formed in the Presence of Nucleus* As mentioned above the deposition of the precipitate was promoted by the addition of nucleus. The precipitated particles, which were prepared in the presence of the nucleus as described in (II. c), contained two kinds of rectangular particles, large and small.

The rectangular particles shown in Photo 13 appeared a few minutes after mixing dilute reagents. Before mixing reagents the nuclei, which were diamond shaped as shown in Photo 14, were added to barium hydroxide solution. Immediately after mixing the

reagents, the precipitate shown in Photo 15 appeared. The nuclei grew to angular edged particles and many new rectangular particles appeared. It seems that the nuclei accelerate the separation of the crystals and do not affect the shape of the precipitated particles.

Summary

1. The amorphous precipitate of barium sulfate changed to a crystalline state by aging.

2. The precipitated particles produced in uniform size remained almost unchanged for a few months, but they became perfect for a long period (i. e. a few years).

3. When the particles of two different sizes formed directly after mixing the reagents, the smaller particles went into solution and the larger particles grew at the expense of the small ones.

4. In the case of dilute reagents the rapid change of conductivity was observed in an early stage of the reaction. The nucleus probably formed during this stage.

5. The precipitation was promoted by the nucleus added before the reaction, but the presence of the nucleus did not affect the shape of the precipitated particles.

The authors are grateful to Professor Ishibashi for the use of the facilities of his laboratory in the conductivity and turbidity measurements. The cost of this research has been partly defrayed from the Scientific Research Encouragement Grant of the Ministry of Education, to which the author's thanks are due.

Institute for Chemical Research, Kyoto University, Takatsuki, Osaka

Surface Chemistry of Synthetic Protein Analogues. III. On the Surface Viscosity of Monolayers of Non-electrolytic Synthetic Polypeptides

By Toshizo ISEMURA and Kozo HAMAGUCHI

(Received October 9, 1953)

Introduction

In the preceding papers of this series,[1),2)] the properties of spread monolayers of some synthetic polypeptides on water investigated by surface pressure measurements were reported in relation to the models of proteins. It was found that poly-DL-α-aminocaproic acid showed very close resemblance of force-area relation to natural proteins such as pepsin and egg albumin among other polypeptides such as poly-DL-α-aminocaprylic acid, poly-DL-α-aminocapric acid and poly-DL-α-aminolauric acid. The latter polypeptides having longer side chains than six carbon atoms in length, gave quite different force-area relation. In F–A curves of these polypeptides, plateau of high compressibility appeared. Poly-γ-methyl-L-glutamate gave condensed film on distilled water. In this case, the polypeptide chain assumed presumably the structure of α-type. This film was expanded on the acidified substrate, and the polypeptide chain may be transformed into β-keratine type. The appearance of the plateau in the F–A curve was attributed to the reorientation of the side chain of the polypeptide. The surface pressure at the plateau depends on temperature and also on the number of carbon atoms in the side chains. From the temperature dependence of the transition pressure and the difference of the areas before and after transformation, the energy needed for reorientation was estimated experimentally.

It is generally accepted that the force-area curves of various natural proteins are not profoundly changed by the species of the proteins. Consequently, it is very difficult to know some characteristics of various proteins from their force-area relations of spread monolayers. On the other hand, it is well-known that the proteins are widely different from each other in their surface viscosity.[3)] Accordingly, the measurements of surface viscosity of the spread monolayers of synthetic polypeptides seemed to be very significant for the comprehension of the natural proteins. In the present paper, the results of the

1) T. Isemura and K. Hamaguchi, This Bulletin, **25**, 40 (1952).
2) T. Isemura and K. Hamaguchi, ibid., **26**, 424 (1953).
3) M. Joly, *J. chim. phys.*, **36**, 285 (1939).

measurements of surface viscosity of polypeptide monolayers and also some consideration of the results will be described.

Experimental

Surface viscosity was measured by the damping of the oscillatory motion of rotating disc on the surface of liquid. The method was essentially the same with that adopted by Langmuir and Schaefer[4] and by Joly[5]. The surface pressure was measured simultaneously by the hanging plate method. The moment of inertia of the oscillatory disc (I) was 66.51, and the radius of the disc (R_1) 1.27 cm. The torsion constant of the torsion wire was 42.0. The radius of the film surrounding the oscillatory disc (R_2) was 5.04 cm. The surface viscosity was calculated by the following formula,

$$\eta = \Delta\lambda_{10} \frac{2.3I}{2\pi P}\left(\frac{1}{R_1^2}-\frac{1}{R_2^2}\right)$$

where P is the period of the oscillatory pendulum and $\Delta\lambda_{10}$ is the difference between logarithmic decrements of oscillation both in the presence of film and in the absence of film. The polypeptides examined in the present experiments and their solvents used for the spreading are tabulated in Table I. Side chains and residue weight for amino acid are also shown in the Table.

TABLE I

Polypeptides	Side chains	Residue weight	Solvents
Poly-DL-α-aminocaproic acid	$-(CH_2)_3\cdot CH_3$	113.1	benzene
Poly-DL-α-aminocaprylic acid	$-(CH_2)_5\cdot CH_3$	141.1	benzene
Poly-DL-α-aminocapric acid	$-(CH_2)_7\cdot CH_3$	169.1	benzene
Poly-DL-α-aminolauric acid	$-(CH_2)_9\cdot CH_3$	197.1	benzene
Poly-γ-methyl L-glutamate	$-(CH_2)_2COOCH_3$	143.1	pyridine
Copolypeptide of glycine and alanine			dichloroacetic acid+benzene (1:4)
Poly-γ-benzyl-DL-and L-glutamate	$-(CH_2)COOCH_2C_6H_5$	219.1	chloroform
Amilan		99.1	cresol+benzen (1:3)

Results and Discussion

(I) Viscosity-area Curves of Poly-DL-α-aminocaproic Acid, Poly-DL-α-aminocaprylic acid, Poly-DL-α-aminocapric Acid and Poly-DL-α-aminolauric Acid.

The η–A curves of these polypeptides are shown in Fig. 1. From this figure, it can be

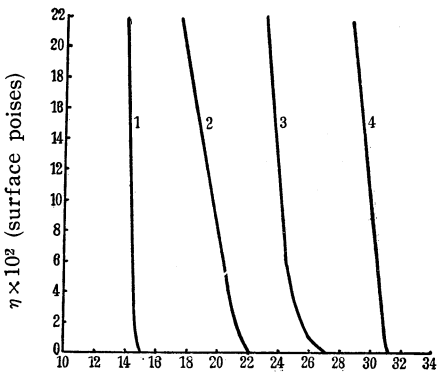


Fig. 1. The surface viscosity-area curves of poly-DL-α-aminocaproic acid (1), poly-DL-α-aminocaprylic acid (2), poly-DL-α-aminocapric acid (3) and poly-DL-α-aminolauric acid (4) (25°C.).

readily seen that the area where surface viscosity was first detected, was related to the side chains. However, the limiting area of the amino-acid residue obtained from the η–A curve for poly-DL-α-aminocaproic acid was 14.7Å². This is an area occupied by an amino-acid residue if the polypeptide of β-keratine configuration was packed closely and it also corresponds to the area per residue estimated from X-ray data as already reported in the previous paper.[1] Cumper and Alexander[6] also found 14.7 Å² as the limiting area per residue for the monolayer of poly-alanine at liquid/liquid and air/water interfaces and for the monolayer of poly-phenylalanine at air/water interface. However, if the length of the side chain becomes longer than six carbon atoms, as in the case of poly-DL-α-aminocaprylic acid, the limiting area becomes larger with the length of the side chain. Consequently, it seems that the increase of the length of the side chains laid on the surface profoundly affects the increase of surface viscosity. The surface viscosity of these polypeptides with longer side chains reaches considerably high values even under the extremely low surface pressure. So, we can not interpret the η–A curve in relation to the F–A curve of the respective polypetide. When the surface fluidity, namely, the reciprocal of surface viscosity was plotted as a function of the area per residue, the change of the nature of film could be readily detected from the relation of the fluidity and the area per residue, even at low surface pressure and

4) I. Langmuir and V. J. Schaefer, *J. Am. Chem. Soc.*, 59. 2400 (1937).
5) M. Joly, *Kolloid-Z.*, 89, 26 (1939).
6) C. W. N. Cumper and A. E. Alexander, *Trans, Faraday Soc.*, 46, 235 (1950).

rather high surface viscosity region where any change can hardly be detected from F–A and η–A relations.

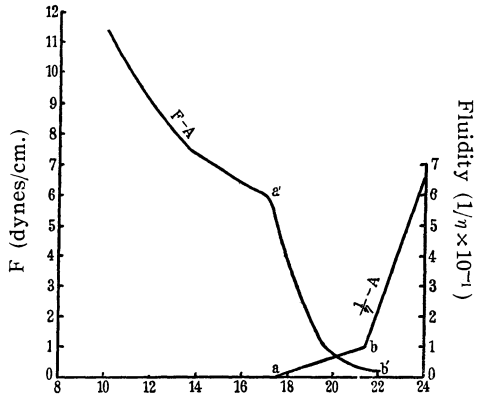


Fig. 2. The force-area and fluidity-area curves of poly-DL-α-aminocaprylic acid (24°C.).

F–A and $1/\eta$–A curve for poly-DL-α-aminocaprylic acid are shown in Fig. 2 and those for poly-DL-α-aminocapric acid in Fig. 3. In these $1/\eta$–A curves, there exist definite kink points b and c. a is the intercept of $1/\eta$–A

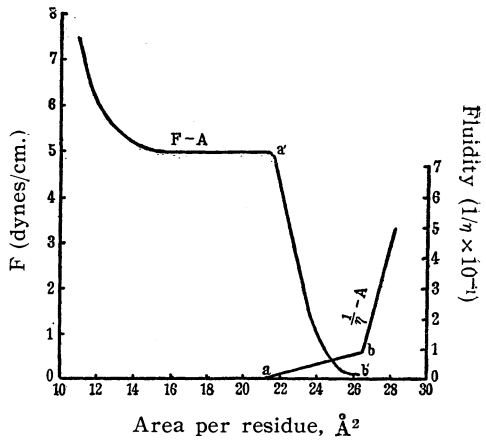


Fig. 3. The force-area and fluidity-area curves of poly-DL-α-aminocapric acid (23°C.).

curve, with area axis extrapolated to zero fluidity. On the other hand, b′ is the area where the surface pressure becomes detectable in the F–A curve and a′ is the area where the plateau begins. These areas are listed in Table II. From the table it will be seen that a is in good agreement with a′ and b with b′.

TABLE II

Polypeptides	Area (Å²/residue) a	a′	b	b′	c	
Poly-DL-α-aminocaprylic acid	17.3	17.2	31.5	21.5	25.3	(24°C.)
Poly-DL-α-aminocapric acid	21.0	22	26.5	24.5	28	(22°C.)
Poly-γ-benzyl-DL-glutamate	19.0	19.5	23.7	24		(9°C.)

(II) Change of Configuration of Poly-γ-methyl-L-glutamate in the Monolayer.

As already reported in the previous paper[1], the monolayer of poly-γ-methyl-L-glutamate behaves differently from other polypeptides, and has a limiting area of 9.8 Å²/residue which was determined by the F–A relation. However, when it was spread on the substrate acidified by formic acid or acetic acid, the monolayer gave the F–A curve analogous to those for other polypeptides with shorter side chain as poly-DL-α-aminocaproic acid and its limiting area per residue was found to be 14.7 Å². The change was interpreted in the light of the results of the infra-red observation of this polypeptide by Ambrose and Hanby[7] and by Bamford, Hanby and Happey[8]. It was concluded that on aqueous substrate the polypeptide assumes the α_{II} configuration proposed by Shimanouchi and Mizushima,[9] and by Ambrase and Hanby[7] independently, and on formic acid or acetic acid solution it turns

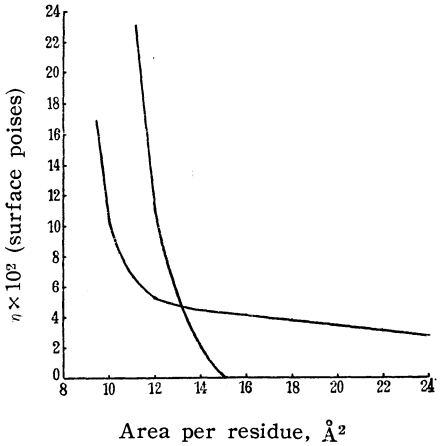


Fig. 4. The surface viscosity-area curves of poly-γ-methyl-L-glutamate. (10°C.): curve I, on distilled water; curve II, on 0.02 N formic acid.

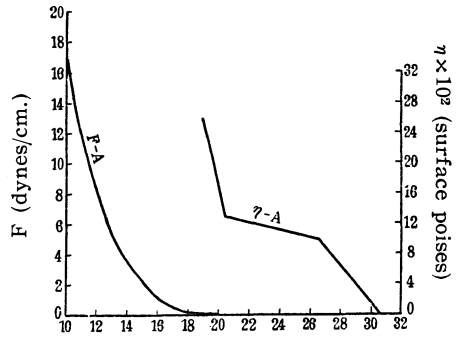
7) E. J. Ambrose and W. E. Hanby, *Nature*, **163**, 483 (1949).
8) C. H. Bamford, W. E. Hanby and F. Happey, *Nature*, **166**, 829 (1950).
9) T. Shimanouchi and S. Mizushima, *Science (Japan)*, **17**, 24, 52 (1947). This Bulletin, **21**, 1 (1948).

to β-keratine type. The difference between both films spread on aqueous and on formic or acetic acid substrate was definitely demonstrated from the results of the surface viscosity measurement. The results are shown in Fig. 4. Curve I in the figure is the η-A curve on the distilled water and Curve II is that obtained on aqueous formic acid substrate (0.02 N). The film, assumed to be as of α-modification on the water surface, was viscous even in low surface concentration which exerts no detectable surface pressure with our surface balance. This is the distinct difference with films of other polypeptides examined. Below the area of 9.8 Å²/residue, the surface viscosity was rapidly increased with small reduction of area. On the other hand, the viscosity of the film spread on formic acid substrate increases below the area of 14.7 Å²/residue as other polypeptides of shorter side chains such as poly-DL-norleucine. It is very interesting that this may be the surface chemical indication of the $\alpha \rightarrow \beta$ transformation of poly-γ-methyl-L-glutamate by formic acid.

Recently, our conclusion that the α_{II}-structure proposed by Shimanouchi and Mizushima and by Ambrose and Hanby is plausible for the structure of α-keratine from our result of film area measurement, was criticised by Low[10]. He insisted that our conclusion is invalid because the area was reduced in proportion to the reduction of the length of the main chain, and no consideration for inter-chain packing and orientation was paid. However, in our opinion, when the polypeptide chain was compressed, the polypeptide chain is closely packed so as to orientate the side chain of one side in air and the other in water, irrespective of the structure of the polypeptide in either α- or β-configuration. The thickness of polypeptide chain lying flat should be the same, in the case of both α- and β-structure. This could lead to our conclusion that the area occupied by the closely packed polypeptide chain depends only on the length of the main chain.

(III) Surface Viscosity-area Relation of Copolymer of Glycine and Alanine.

The polypeptides so far investigated were of more than four carbon atoms in length. It is very interesting to investigate how the polypeptides behave at the surface if the polypeptides have no side chains or very short ones. When the polypeptides have long side chains, the coiling of the main chains might be difficult on account of the mutual hindrance of the side chains. In this connection the glycine-alanine copolymer was studied. This copolymer may be easily coiled. It is interesting to compare the behaviour of such a polypeptide with a linear polymer having no side chains such as amilan, on which we will discuss in the later part.



Area per glycine-alanine residue, Å²

Fig. 5. The surface pressure-area and surface viscosity-area curves of glycine-alanine copolymer (22°C.).

The F-A curve and η-A curve of the glycine-alanine copolymer are shown in Fig. 5. The present investigation of F-A curve, the limiting area per glycine-alanine residue was about 20 Å², namely, about 10 Å² per amino-acid residue. This fact suggests that this polymer may assume also the structure of folded type as in the case of poly-γ-methyl-L-glutamate. The F-A curve for this copolymer film is, however, different from that for poly-γ-methyl-L-glutamate in its behaviour against the nature of substrate. Although the latter film expands on the acidic substrate considerably, the former film gave the same F-A curve on the acidic substrate as on the distilled water. On the other hand, the surface viscosity of this copolymer film was detected at the area of 30 Å² per glycine-alanine residue, namely at the area of 15Å² per amino-acid residue, and at the area of 20 Å² per glycine-alanine residue, the surface viscosity was again suddenly increased. This area corresponds to the area from which the surface pressure was suddenly exerted. When the main chain of polypeptide in β-keratine type was packed closely, the residue of amino-acid in polypeptide occupies 15 Å² on the surface. On the other hand, the residue of amino-acid occupied 10 Å² on the surface, when the main chain of the polypeptide takes the folded structure of α_{II}-type and was packed closely. Accordingly, we might conclude that the copolymer was spread as a film assuming β-keratine type. However, the polypeptide chain will be readily trans-

10) B. W. Low, "The Proteins" ed. by H. Neurath and K. Bailey, Vol. I, Part A, p. 376 (1953).

formed into α-type by slight compression that this transformation cannot be detected by the surface pressure measurement. In the region of this transformation the film may be heterogeneous and the surface viscosity was somewhat fluctuated. From this result mentioned above the polypeptides having very short side chains or none tend to assume readily folded structure. This inference seems plausible from the recent observation of A. Elliott[11] on the infra-red spectrum of poly-DL-alanine. He described in his recent paper, that it is evident that in poly-DL-alanine the equilibrium between α- and β-forms is very nicely balanced, and the transformation from one to the other is readily induced. This conclusion might be applied generally to the polypeptide of very short side chain such as glycine-alanine copolymer. From this viewpoint, our results on the surface viscosity-area relation of this copolymer could be explained successfully.

(IV) The Difference between L-and DL-Polypeptides of γ-Benzyl Glutamate.

For the investigation of the difference between the behaviour of optical active and of racemic polypeptide, the film of poly-γ-benzyl-L-glutamate and of poly-γ-benzyl-DL-glutamate were studied. The F-A and η-A curves of these polypeptides are shown in Fig. 6. On

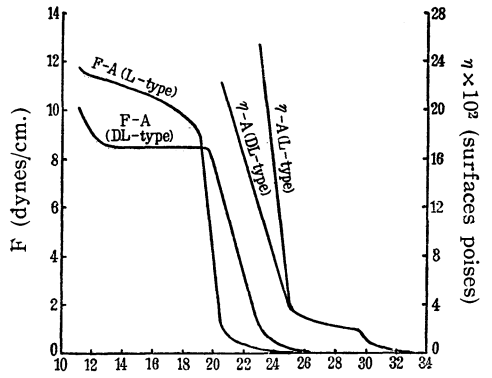


Fig. 6. The surface pressure-area and surface viscosity-area curves of poly-γ-benzyl L- and DL-glutamates (10°C.).

the one hand, F-A curves and η-A curves of these polypeptides showed generally similar trends respectively, and plateaus appeared in the F-A curves for both polypeptides. However, we can notice the following differences by careful inspection of these curves. (1) The limiting area determined from F-A curves were 24 Å/residue for DL-type polypeptide and 21 Å²/residue for L-type polypeptide. (2) The compressibility of the film up to the pressure at which the plateau appears was smaller for L-type polypeptide than for DL-type polypeptide. (3) The F-A curve of poly-γ-benzyl-DL-glutamate was strikingly influenced by temperature as reported in the previous paper.[2] The pressure where the plateau appearing in the F-A curve was decreased with the rise of temperature as in the cases of the films such as poly DL-α-aminolauric acid. On the contrary, in the case of poly-γ-benzyl-L-glutamate, temperature scarcely affected on the F-A relation and the pressure at which the plateau appears, was almost independent of temperature and nearly 8.5 dynes/cm. (4) The area at which the surface viscosity is suddenly increased, was about 25 Å²/residue irrespective of the type of polypeptide. However, the inclination of η-A curve, namely $\partial\eta/\partial A$ was smaller for L-polypeptide than for DL-polypeptide. To clarify the inter-relation between F-A curve and η-A curve, $1/\eta$-A curve was considered. (Fig. 7). a, b, a′ b′,

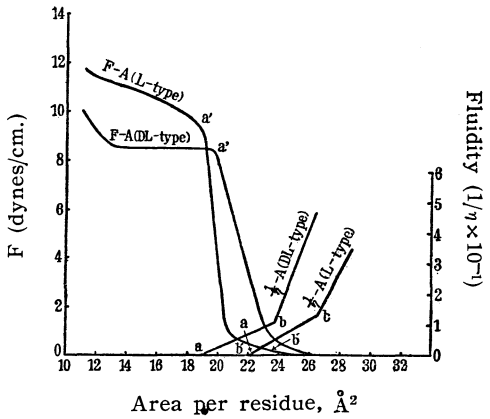


Fig. 7. The force-area and fluidity-area curves of poly-γ-benzyl-DL- and L-glutamates (10°C.).

for L-polypeptide and DL-polypeptide were summarized in Table III. The results shown

TABLE III

Poly-γ-benzyl glutamate	Area (Å²/residue) a	a′	b	b′
L-type	22.3	18.5	26.5	22
DL-type	19.0	19.5	23.7	24

in Table III were obtained as already described, with poly-γ-benyl-DL-glutamate. The area from which the plateau begins to appear, a′, coincides with the area found from extrapolation of $1/\eta$-A curve to $1/\eta=0$. Whereas, with the film of poly-γ-benzyl-L-glutamate, the area from which the surface pressure becomes appreciable, b′ (22 Å²) corresponded to the area found by extrapolation

11) A. Elliott, *Nature*, **170**, 1066 (1952).

of $1/\eta$-A curve to $1/\eta=0$ (21.5Å^2).

From these experimental facts, it can be concluded that the films compressed up to the pressure where the plateau begins to appear, are entirely different for L- and DL-polypeptide, respectively. The arrangement of the L-polypeptide chains is far more closely packed. The film of L-polypeptide in such condition is in a nearly solid state.

(V) The Surface film of Amilan.

F–A curve of the monolayer of amilan was already reported in the previous paper[1]. In F–A curve, a kink point was found at about 32 Å^2/residue. This area is in good agreement with the area occupied by the residue calculated in the basis of the molecular scale model.[6),12)] On the other hand, it was found that some change occurs at the area of 80 Å^2/residue from the sudden change of surface viscosity as shown in Fig. 8. This is

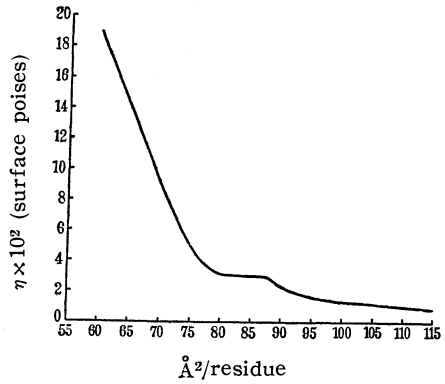


Fig. 8. The surface viscosity-area curve of amilan (22°C.).

entirely different from the films of poly-DL-α-aminocaproic acid and glycine-alanine copolymer. From the surface potential measurement it was found that the potential fluctuated down to the area 80~90 Å^2/residue, below which it changes regularly as reported by Hotta[13)] in our Laboratory. Amilan was quite different from the polypeptides films. From this result, our conclusion that amilan is not adequate as the model of protein, was again confirmed.

12) D. J. Crisp, *J. Colloid Sci.*, **1**, 49 (1946).
13) H. Hotta, This Bulletin, **27**, 80 (1954).

Summary

The surface viscosity of the spread monolayers of synthetic polypeptides with non-electrolytic side chains was investigated in relation to the surface area and to the surface pressure. If the length of a side chain becomes longer than six carbon atoms, the limiting area becomes larger with the length of the side chain. Polypeptide with no side chains or very short ones such as glycine-alanine copolymer might be changed to α-configuration from "extended" β-configuration merely by compression. The ease of transition from one configuration to another corresponds to the discovery by Elliott in bulk solution with poly-alanine. $\alpha_{II} \rightarrow \beta$ transformation of poly-γ-methyl-L-glutamate which had been reported in the previous paper, was observed also by the surface viscosity measurements. The difference of the nature of films of optical active and of racemic polypeptide was investigated. The polypeptide consisting of single optical isomeride was able to be more closely packed in the film than that of racemic. Our discovery by surface pressure measurement that the polymer of ϵ-aminocaproic acid, namely, amilan is not adequate as the model of protein, was again confirmed from the study of surface viscosity.

The authors wish to express their sincere thanks to Dr. H. Tani and Mr. H. Yuki in the Faculty of Science, Osaka University and to Dr. J. Noguchi at Kanazawa University who gave them the valuable samples of synthetic polypeptides. A part of the expense for the experiment has been defrayed from a grant given by the Ministry of Education, to whom the authors' thanks are due.

The Institute of Scientific and Industrial Research.
Osaka University, Sakai, Osaka

The Condensation of Benzaldehyde with Methyl Ethyl Ketone by Aqueous Sodium Hydroxide

By Hiroshi MIDORIKAWA

(Received November 4, 1953)

Harries and Müller[1] demonstrated that, when aqueous sodium hydroxide was employed as the condensing agent, benzaldehyde condensed with methyl ethyl ketone at the α-methyl group of the ketone at ordinary temperature, forming 1-phenyl-1-penten-3-one, and, when hydrogen chloride was employed as the condensing agent, benzaldehyde reacted with methyl ethyl ketone at its α-methylene group, giving 3-methyl-4-phenyl-3-buten-2-one.

In the preceding report[2], it was indicated that furfural condensed with methyl ethyl ketone chiefly by aqueuos sodium hydroxide at its methylene group at the lowered reaction temperature 0~5°, giving the chief product 4-(2-furyl)-3-methyl-4-butanol-2-one, whereas furfural condensed with the ketone chiefly at its α-methyl group at the elevated reaction temperature 60~65°, giving 1-(2-furyl)-1-penten-3-one.

In the present experiment, the condensation of benzaldehyde with methyl ethyl ketone by aqueous sodium hydroxide at lowered and elevated reaction temperatures was studied in order to compare it with the result of furfural in the preceding report[2].

At the elevated reaction temperature 60~65°, the condensation of benzaldehyde with methyl ethyl ketone gave only 1-phenyl-1-penten-3-one (I) as illustrated below, since this condensation product afforded an oxime melting at 86~87° which was identical with that of 1-phenyl-1-penten-3-one obtained by Harries and Müller.[1] The semicarbazone of this ketone melted at 181~182°.

At the lowered reaction temperature 3~5°, benzaldehyde and methyl ethyl ketone underwent aldol condensation by sodium hydroxide, giving a mixture of 3-methyl-4-phenyl-4-butanol-2-one (II) and 1-phenyl-1-pentanol-3-one (III), as illustrated below. The mixture of these condensation products gave no semicarbazone, but, after the dehydration with acetic anhydride, gave a mixture of a semicarbazone melting at 218~219° in a larger proportion and the semicarbazone (m.p. 181~182°) of 1-phenyl-1-penten-3-one in a smaller proportion. The semicarbazone melting at 218~219° was identified with that of 3-methyl-4-phenyl-3-buten-2-one obtained by condensing benzaldehyde with methyl ethyl ketone by hydrogen chloride. Consequently, it was confirmed that the condensation products at the reaction temperature 3~5° were a larger amount of 3-methyl-4-phenyl-4-butanol-2-one (II) and a smaller amount of 1-phenyl-1-pentanol-3-one (III), and, on the dehydration with acetic anhydride, gave the corresponding unsaturated ketones, 3-methyl-4-phenyl-3-buten-2-one (IV) and 1-phenyl-1-penten-3-one (I).

Furthermore, 3-methyl-4-phenyl-3-buten-2-one was oxidized by sodium hypochlorite to α-methylcinnamic acid (V), while 1-phenyl-1-penten-3-one (I) was not acted upon by this oxidizing agent.

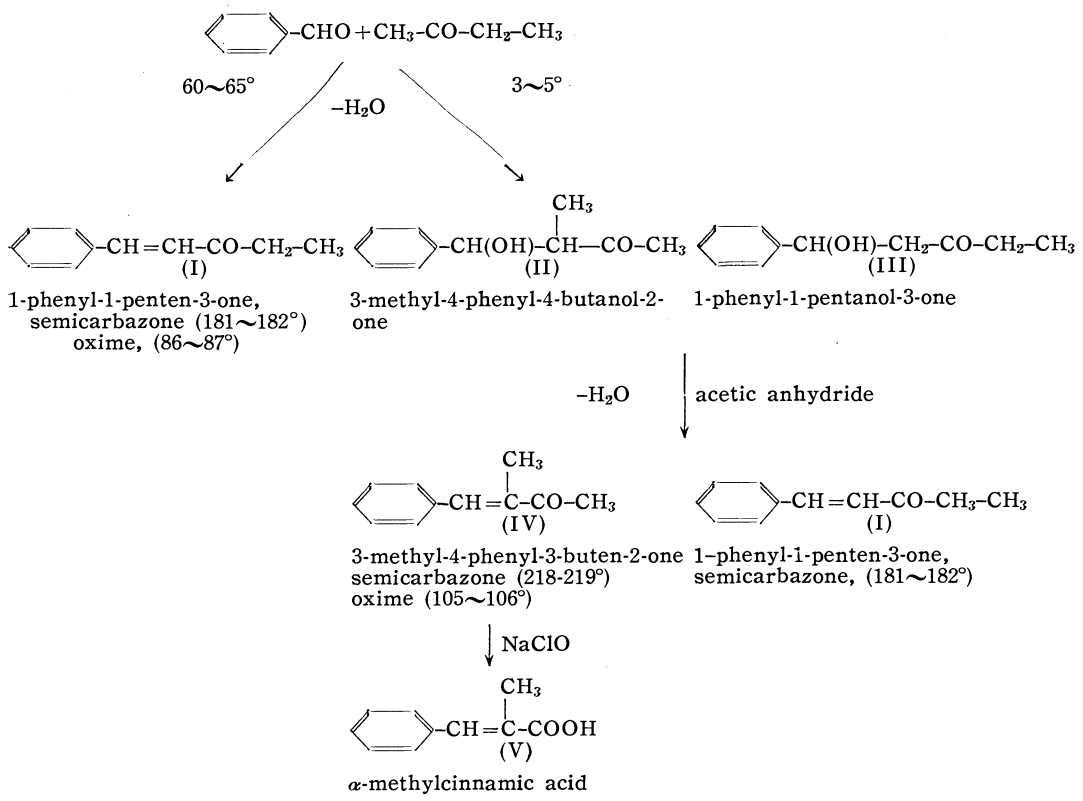
The overall reactions are illustrated by the following formulation.

3-Methyl-4-phenyl-3-buten-2-one (IV) and 1-phenyl-1-penten-3-one (I) obtained here gave respective 2,4-dinitrophenylhydrazones. It was of interest that the mixture of the aldol condensation products at the reaction temperature 3~5°, on the reaction with 2,4-dinitrophenylhydrazine in methanolic sulfuric acid, gave the 2,4-dinitrophenylhydrazones of 1-phenyl-1-penten-3-one (I) and benzaldehyde, but no 2,4-dinitrophenylhydrazone of 3-methyl-4-phenyl-3-buten-2-one (IV). This result appeared to indicate that, under such a reaction condition, 1-phenyl-1-pentanol-3-one (III) gave 2,4-dinitrophenylhydrazone of 1-phenyl-1-penten-3-one (I) with simultaneous dehydration, and 3-methyl-4-phenyl-4-butanol-2-one (II) initially dissociated to methyl ethyl ketone and benzaldehyde, which subsequently gave its 2,4-dinitrophenylhydrazone.

Experimental

Condensation at Reaction Temperature 3~5° Into a stirred suspension of benzaldehyde (20 g.) and methyl ethyl ketone (40 g.) in water (300 cc.) was at once introduced 10% aqueous sodium hydroxide (15 cc.) at 3°. The reaction was complete after prolonged stirring for 6 hrs. at 3~5°. The reaction mixture was neutralized with dilute sulfuric acid, the oily layer separated and the aqueous solution extracted twice with ether. The oily layer and the ether extract were combined and dried over anhydrous sodium sul-

1) C. Harries and G. H. Müller, *Ber.*, **35**, 966 (1902).
2) H. Midorikawa, This Bulletin, **26**, 460 (1953).



fate. Fractionation of the ethereal solution gave a pale yellow liquid (25 g.), b.p. 122~129°/6 mm. This fraction was considered to consist of 3-methyl-4-phenyl-4-butanol-2-one (II) in a larger proportion and 1-phenyl-1-pentanol-3-one (III) in a smaller proportion. Calcd. for $C_{11}H_{14}O_2$: C, 74.11 H, 7.92; Found: C, 72.22, H, 7.67%.

This analysis appeared to show that this fraction contains a small quantity of the dehydrated ketones $C_{11}H_{12}O$, but the fraction gave no semicarbazone. From this fraction were obtained two 2,4-dinitrophenylhydrazones in equal proportions, which were readily separable from each other by the difference of the solubility in nitrobenzene. The more soluble one crystallised in red needles, m.p. 212~213°, undepressed on admixture with 2,4-dinitrophenylhydrazone of 1-phenyl-1-penten-3-one (I) as indicated below. The less soluble one formed orange prisms melting at 235~236°, undepressed on admixture with benzaldehyde 2,4-dinitrophenylhydrazone.

Dehydration of the Condensation Product at the Reaction Temperature 3~5C° The foregoing aldol condensation product (5 g.) at the reaction temperature 3~5° was refluxed with acetic anhydride (15 g.) for 16 hrs. Fractionation of the reaction mixture gave a pale yellow oil (4 g.), b.p. 112~114°/6 mm.

This oil (0.5 g.) was suspended in an aqueous semicarbazide-sodium acetate solution, and methanol added until a clear solution was obtained. The solution, after heating on the water-bath for a short time and standing for 3 hrs., gave colourless crystals (0.4 g.), which was recrystallised from methanol as plates, m.p. 218~219°, undepressed on admixture with the semicarbazone of 3-methyl-4-phenyl-3-buten-2-one (IV) indicated below. The filtrate on standing overnight gave colourless crystals (0.1 g.), which were recrystallised twice from methanol in needles, m.p. 181~182°. This specimen was identical with the semicarbazone of 1-phenyl-1-penten-3-one (I).

The oil (1 g.), above mentioned was suspended in an aqueous sodium hypochlorite solution[2] (8 cc.) at ordinary temperature with occasional shaking for 2 days. The reaction mixture was freed of oily matter by extraction with ether, and acidified with dilute hydrochloric acid to yield crystals (0.3 g.) on cooling, which were recrystallised from water as colourless prisms, m.p. 77~78°. This specimen was identified with α-methylcinnamic acid (V); lit[3]., m.p. 78°. Calcd. for $C_{10}H_{10}O_2$: C, 74.04, H, 6.22%; Found: C, 73.96, H, 6.11%.

Cndensation at the Reaction Temperature 60~65° Into a stirred suspension of benzaldehyde (15 g.) and methyl ethyl ketone (30 g.) in water (200 cc.) was at once introduced 10% aqueous sodium hydroxide (7 cc.) at about 60°. After prolonged stirring for 3 hrs. at 60~65°, the reaction was over. The reaction mixture was worked up as described above. Fractionation of the ether solution, after drying over calcium chloride, gave a pale yellow oil (19 g.), b.p. 117~118°/6 mm., which solidified at ordinary temperature. This fraction was composed of 1-phenyl-1-penten-3-one (I). Calcd. for $C_{11}H_{12}O$: C, 82.45 H, 7.55%; Found:

C, 82.29 H, 7.70%.

This fraction gave the oxime melting at 86~87°, which was identical with the oxime (m.p. 85~86°) of 1-phenyl-1-penten-3-one (I) obtained by Harries and Müller[1]. Its semicarbazone formed colourless needle crystals melting at 181~182° (lit[4]., m.p. 173°), and its 2,4-dinitrophenylhydrazone, carmine rhombic crystals, melting at 212~213° on crystallisation from pyridine. Calcd. for $C_{17}H_{16}O_4N_4$: C, 59.97, H, 4.74, N, 16.46 %; Found: C, 59.78, H, 4.59, N, 16.50 %.

3-Methyl-4-phenyl-3-buten-2-one (IV) was synthesised from benzaldehyde and methyl ethyl ketone by the use of hydrogen chloride as the condensing agent, as reported by Harries and Müller[1]. This ketone gave the oxime melting at 105~106° (lit[1]., m.p. 103~104°), the semicarbazone melting at 218~219° (lit[4]., m.p. 204°) and a 2,4-dinitrophenylhydrazone, red needles, melting at 199~200°. Calcd. for $C_{17}H_{16}O_4N_4$: C, 59.97, H, 4.74, N, 16.46%; Found: C, 59.52, H, 4.56, N, 16.51%.

3) R. Stoermer and R. Wehlu: *Ber.*, **35**, 3552 (1902).
4) C. V. Gheroghiu and B. Arwentiew: *Bull. Soc. Chim.*, **47**, 195 (1930).

Summary

In the condensation of benzaldehyde with methyl ethyl ketone by aqueous sodium hydroxide, the lowered reaction temperature (3~5°) favored the aldol condensation at the α-methylene group of the ketone as in the condensation of furfural with the ketone[2]. On the other hand, the elevated reaction temperature (60~65°) conducted exclusively the condensation at the α-methyl group of the ketone, giving 1-phenyl-1-penten-3-one (I).

3-Methyl-4-phenyl-4-butanol-2-one (II), obtained by the aldol condensation at the lowered reaction temperature (3~5°), was dehydrated with acetic anhydride to 3-methyl-4-phenyl-3-buten-2-one (IV), which was oxidized by sodium hypochlorite to afford α-methylcinnamic acid (V).

The author expresses his sincere thanks for Dr. T. Hayashi for his kind advice.

Scientific Research Institute, Komagome, Bunkyo-ku, Tokgo

Visco-Elasticity Measurement by the Torsional Rheometer. Simple Treatment by the Application of the Four-Terminal Network

By Tsurutaro NAKAGAWA

(Received November 10, 1953)

Introduction

Some polymer and colloidal solutions, in contrast to ordinary liquids of low molecular weight, have been known to show elastic nature besides viscosity, and rheological peculiarities of these "elastic liquids"—e. g. "Fliesselastizität" (H. Freundlich, 1932), "structural viscosity" (W. Philippoff, 1935), "thread-forming ability" (H. Erbring, 1936), "Weissenberg effect" (K. Weissenberg, 1947) etc. have been studied by various workers. As it has recently become desirable to analyse such rheological behaviors of those solutions, various rheometers or elastoviscometers suitable for the measurement of their visco-elastic properties have been proposed, and among them it is thought that the rheometers in which the most rigorous treatment has been given are those of coaxial-cylinder type which provide a means of maintaining a liquid in a state of torsional oscillation in a narrow annular gap between two vertical coaxial cylinders.

In this paper, the author gives a simple general view of the rheometers of this type by the application of the four-terminal electrical network theory. The treatment by the four-terminal network is better than that by the ordinary two-terminal network from the view-point that the former can include all modifications of the rheometer by a single four-terminal circuit diagram.

It goes without saying that the treatment presented here is only approximate; the inertia of the sample liquid is neglected here. This approximation, however, is satisfactory in the measurement at very low frequencies.*

Survey of the Four-Terminal Network Theory

An electrical network which has two input and two output terminals is called a four-terminal network.

When the generalized Kirchhoff's law is applied to the four-terminal network N (Fig. 1.), the fundamental equation of the network is derived in terms of the "four-terminal

* T. Nakagawa, Third Rheological Meeting, Japan, 1953.

constants" A, B, C and D as

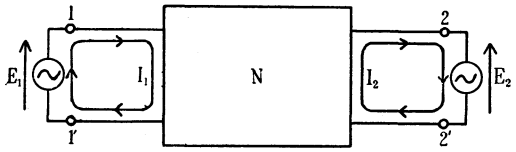


Fig. 1. Four-terminal network.

$$\begin{cases} E_1 = AE_2 + BI_2 & \text{(1a)} \\ I_1 = CE_2 + DI_2 & \text{(1b)} \end{cases}$$

or, according to the matrix expression,

$$\begin{pmatrix} E_1 \\ I_1 \end{pmatrix} = \begin{pmatrix} A & B \\ C & D \end{pmatrix} \begin{pmatrix} E_2 \\ I_2 \end{pmatrix} \qquad (2)$$

where E_1 and I_1 are the input voltage and the input current respectively; E_2 and I_2 are the quantities relating to the output. The four-terminal constants A B C D are shown to satisfy the next relation.

$$\begin{vmatrix} A & B \\ C & D \end{vmatrix} = AD - BC = 1 \qquad (3)$$

According to the theory, the four-terminal constants of a circuit which has a single impedance Z as shown in Fig. 2 are

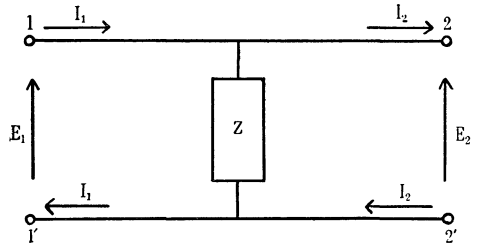


Fig. 2. Single-impedance network (I).

$$\begin{pmatrix} A & B \\ C & D \end{pmatrix} = \begin{pmatrix} 1 & 0 \\ 1/Z & 1 \end{pmatrix} \qquad (4)$$

and for a circuit of Fig. 3, they are

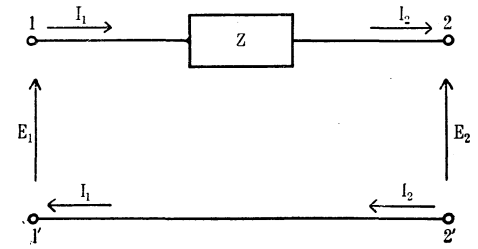


Fig. 3. Single-impedance network (II).

$$\begin{pmatrix} A & B \\ C & D \end{pmatrix} = \begin{pmatrix} 1 & Z \\ 0 & 1 \end{pmatrix} \qquad (5)$$

When a four-terminal circuit N_2 is connected tandem to the right hand side of a four-terminal circuit N_1, a new four-terminal circuit N is constructed and its four-terminal constants A B C D are obtained from the product of two matrices

$$\begin{pmatrix} A & B \\ C & D \end{pmatrix} = \begin{pmatrix} A' & B' \\ C' & D' \end{pmatrix} \begin{pmatrix} A'' & B'' \\ C'' & D'' \end{pmatrix} = \begin{pmatrix} A'A''+B'C'' & A'B''+B'D'' \\ C'A''+D'C'' & C'B''+D'D'' \end{pmatrix} \qquad (6)$$

where A' B' C' D' and A'' B'' C'' D'' are four-terminal constants of the network N_1 and N_2 respectively (Fig. 4.).

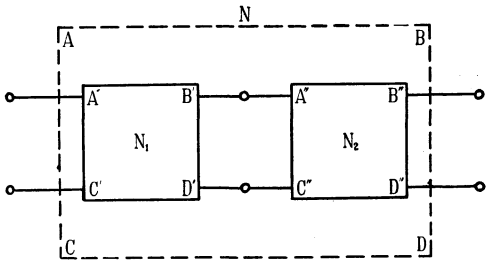


Fig. 4. Tandem connection of two four-terminal networks.

From the above-stated, the four-terminal constants of a π-type network which is composed of three impedances as shown in Fig. 5 are easily obtained as follows by the cascade connection of three circuits illustrated in Fig. 2 and 3.

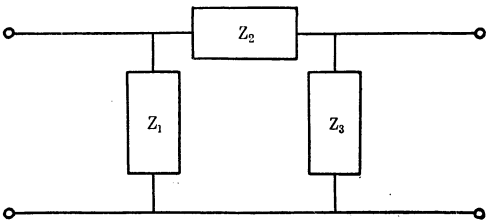


Fig. 5. π-type network.

$$\begin{pmatrix} A & B \\ C & D \end{pmatrix} = \begin{pmatrix} 1 & 0 \\ 1/Z_1 & 1 \end{pmatrix} \begin{pmatrix} 1 & Z_2 \\ 0 & 1 \end{pmatrix} \begin{pmatrix} 1 & 0 \\ 1/Z_3 & 1 \end{pmatrix} = \begin{pmatrix} 1+Z_2/Z_3 & Z_2 \\ (Z_1+Z_2+Z_3)/(Z_1Z_3) & 1+Z_2/Z_1 \end{pmatrix} \qquad (7)$$

The Torsionally Oscillating Rheometer and the Four-Terminal Circuit

In this rheometer, a cylinder of radius r_1 is suspended coaxially to a depth l in a liquid contained in a cup of radius r_2. The rheometer of this type is used in two modi-

fications. In one,[1,1',2,3,3'] the external cup is caused to oscillate through a small fixed angular amplitude Θ_0, while the top end of the suspension wire is fixed; in the other[1',4,5,6], the top end of the suspension wire is put into the torsional oscillation $\Theta=\Theta_0 e^{j\omega t}$, the cup being fixed. In both cases the rheological properties of the sample liquid are known from the analysis of the motion of the internal cylinder relative to that of the external cup or to that of the top of the suspension wire.

When the experiment is carried out at very low frequencies (period $T=2\pi/\omega$, greater than several seconds) a simple approximate treatment seems to be permissible*. Here the inertia of the sample is assumed to be negligible and to have no effect on the motion of the inner cylinder. And moreover, the next two relations, in which viscosity η and rigidity G are related to the resistance R and the stiffness E by a simple shape factor K_0, are assumed to hold. Of the reason for employing this shape factor reference will be made in the later section on the rotational viscometer and Schwedoff's apparatus.

$$\eta=\frac{R}{4\pi l}\left(\frac{1}{r_1^2}-\frac{1}{r_2^2}\right)\equiv K_0 R \quad \text{poises} \qquad (8)$$

$$G=\frac{E}{4\pi l}\left(\frac{1}{r_1^2}-\frac{1}{r_2^2}\right)\equiv K_0 E \quad \text{dyn./cm}^2. \qquad (9)$$

Analogous Four-Terminal Network.—A simple consideration enables us to construct an analogous four-terminal network a in Fig. 6 corresponding to our rheometer where the electro-mechanical correspondence is as is listed in Table 1. Fig. 6 is a π-type

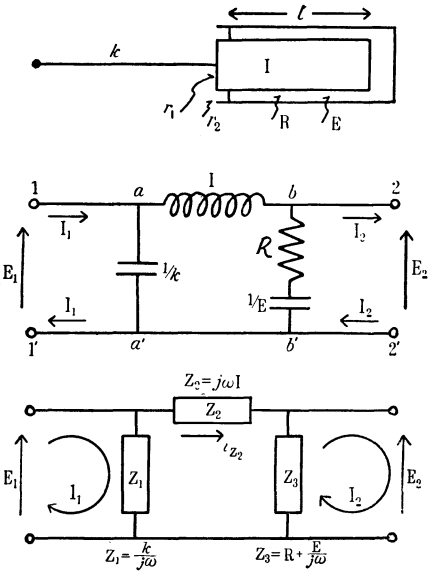


Fig. 6. Torsionally oscillating rheometer and the analogous four-terminal network.

TABLE I

ELECTRO-MECHANICAL CORRESPONDENCE

Mechanical System	Electrical System
k : Torsion constant of suspension wire	Reciprocal capacitance
I : Moment of inertia of inner cylinder	Inductance
R : Viscous resistance of sample	Resistance
E : Stiffness of sample	Reciprocal capacitance
$\dot{\theta}$: Velocity	i : Current
θ : Displacement	Q : Charge

circuit which was stated above, and since

$$\begin{cases} Z_1=\dfrac{k}{j\omega} \\ Z_2=j\omega I \\ Z_3=R+\dfrac{E}{j\omega} \end{cases} \qquad (10)$$

the four-terminal constants $A\ B\ C\ D$ are calculated by Eq. 7; and, for example,

$$C=(Z_1+Z_2+Z_3)/(Z_1Z_3)=\frac{(j\omega R-\omega^2 I+k+E)}{k\left(R+\dfrac{E}{j\omega}\right)} \qquad (11)$$

1) J. R. Van Wazer and H. Goldberg, *J. Appl. Phys.*, **18**, 207 (1947).
1') H. Goldberg and O. Sandvik, *Anal. Chem.*, **19**, 123 (1947).
2) J. R. Van Wazer, *J. Colloid Sci.*, **2**, 223 (1947).
3) H. Markovitz et al., *Rev. Sci. Instr.*, **23**, 430 (1952): H. Markovitz, *J. Appl. Phys.*, **23**, 1070 (1952).
3') J. G. Oldroyd et al., *Proc. Phys. Soc.*, B, **64**, 44 (1951): J. G. Oldroyd, *Quart. Journ. Mech. and Applied Math.* **4**, Pt. 3, 271 (1951).
4) T. Nakagawa, *J. Chem. Soc. Japan*, **72**, 759 (1951) (in Japanese).
5) T. Nakagawa, This Bulletin **24**, 191 (1951).
6) T. Nakagawa, ibid., **25**, 93 (1952).
* The exact treatment of the torsionally oscillating rheometer taking account of the inertia of the sample has recently been done by various authors; so for the cup-drive system, see for example, J. G. Oldroyd,[3'] A. A. K. Ibrahim and A. M. Kabiel, *J. Appl. Phys.*, **23**, 754 (1952), and H. Markovitz[3]; for the top-drive system, see S. Oka, *Bull, Kobayashi Inst. of Phys. Res.*, 3, 9 and 17 (1953) (in Japanese).

where $j=\sqrt{-1}$, and ω is 2π times the frequency ν ($\omega=2\pi\nu$).

The angular velocity $\dot{\theta}$ of the inner cylinder corresponds to the current i_{Z_2} which flows through the inductance I, and to know the angular displacement of the inner bob it is enough to compute the charge Q_{Z_2}

$$Q_{Z_2}=\frac{i_{Z_2}}{j\omega} \tag{12}$$

(1) **Top-Drive System.**—First is discussed the case in which the cup is fixed and the top end of the suspension wire is subjected to oscillational displacement

$$\Theta=\Theta_0 e^{j\omega t}$$

This situation is electrically as follows (Fig. 7). The input current at the terminal 1—1′ is

$$I_1=j\omega\Theta_0 e^{j\omega t},$$

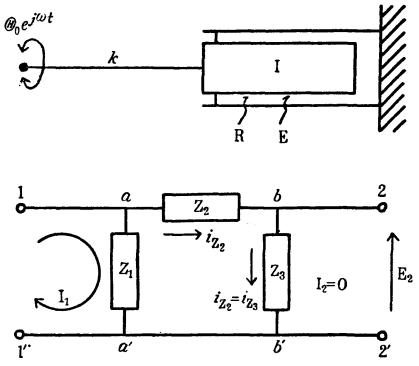


Fig. 7. Top-drive rheometer.

and the velocity of the cup is zero, that is, the terminal 2—2′ is opened

$$I_2=0$$

From Eq. (1b) of the four-terminal equation

$$E_2=\frac{I_1}{C}$$

The angular velocity of the inner cylinder $\dot{\theta}$ corresponds to i_{Z_2}, and

$$i_{Z_2}=i_{Z_3}=\frac{E_2}{Z_3}=\frac{I_1}{CZ_3}$$

$$=\frac{k\Theta_0 e^{j\omega t}}{R+j\left(\omega I-\dfrac{k+E}{\omega}\right)}$$

So that

$$\theta=\frac{\dot{\theta}}{j\omega}=\frac{k\Theta_0 e^{j\omega t}}{[(k+E)-\omega^2 I]+j\omega R}$$

$$\therefore\ \theta=\frac{k\Theta_0}{\sqrt{(k+E-\omega^2 I)^2+\omega^2 R^2}}e^{j(\omega t-\phi)}\equiv Ae^{j(\omega t-\phi)}$$

where $$\tan\phi=\frac{\omega R}{(k+E-\omega^2 I)} \tag{13}$$

This result of course agrees with that obtained by the direct solution of the equation of motion of the inner cylinder

$$I\ddot{\theta}=k(\Theta-\theta)-R\dot{\theta}-E\theta$$

If m, the amplitude ratio A/Θ_0 and ϕ, the phase angle are observed, R and E are known from Eq. 13 or from

$$\begin{cases} R=\dfrac{kT\sin\phi}{2\pi m} \\ E=k\left(\dfrac{\cos\phi}{m}-1\right)+\dfrac{4\pi^2 I}{T^2} \end{cases} \tag{14}$$

where $T=2\pi/\omega$, and consequently η and G can be calculated from Eqs. 8 and 9. Or the observation of the amplitude resonance enables us to calculate η and G[4,5],** from

$$\begin{cases} \omega_{res}=2\pi\nu_{res}=\sqrt{n_e^2-2\epsilon^2} \\ A_{res}=L/\sqrt{4\epsilon^4+4\epsilon^2\omega^2_{res}} \end{cases}$$

where ν_{res} and A_{res} are the resonance frequency and the resonance amplitude respectively, and

$$2\epsilon=R/I,\quad n_e^2=(k+E)/I,\quad L=k\Theta_0/I.$$

(2) **Cup-Drive System.**—In this case the external cup is put into sinusoidal oscillation, and the top end of the suspension wire is fixed (Fig. 8.). This condition corresponds electrically to the case in which, contrary to that of the top-drive system,

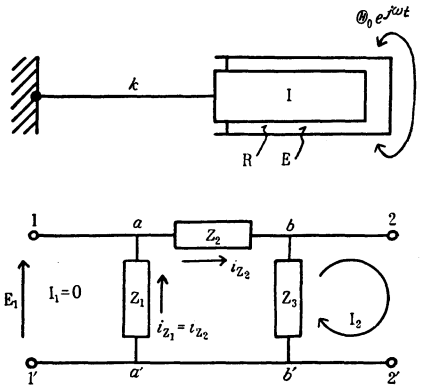


Fig. 8. Cup-drive rheometer.

$$I_1=0$$
$$I_2=j\omega\Theta_0 e^{j\omega t}$$

** The resonance method starting from Eq, (13) which implies the neglect of the inertia of the sample, however, seems to be doubtful, for in this case the observation is ordinarily made at the frequencies several cycles per second or more, and then the inertia of the liquid can not be neglected. With the phase angle method, on the other hand, very low frequencies can be adopted and then Eq. 13 is satisfactory.

and the four-terminal equation is

$$\begin{cases} E_1 = AE_2 + BI_2 & \text{(1a)} \\ I_1 = 0 = CE_2 + DI_2 & \text{(1b)} \end{cases}$$

From (1a), (1b) and (3)

$$E_1 = \left(B - \frac{AD}{C}\right) I_2 = \frac{(BC-AD)}{C} I_2 = \frac{-1}{C} I_2$$

$$= -\frac{Z_1 Z_3}{(Z_1+Z_2+Z_3)} \cdot j\omega\Theta_0 e^{j\omega t}$$

$\dot{\theta}$ corresponds to i_{Z_2}, and

$$i_{Z_2} = i_{Z_1} = -\frac{E_1}{Z_1}$$

So that

$$\theta = \int \dot{\theta} dt = \frac{\dot{\theta}}{j\omega} = \frac{(E+j\omega R)\Theta_0}{[(k+E-\omega^2 I)+j\omega R]} e^{j\omega t}$$

or
$$\theta = \frac{\sqrt{E^2+\omega^2R^2} \cdot \Theta_0}{\sqrt{(k+E-\omega^2 I)^2+\omega^2 R^2}} e^{j(\omega t-\phi)} \qquad (15)$$

$$\tan\phi = \frac{\omega R(\omega^2 I - k)}{E(k+E-\omega^2 I)+\omega^2 R^2}$$

This is somewhat complicated in comparison with Eq. 13. It is not possible to obtain a relation as simple as Eq. 14 for the calculation of R and E from the observed m and ϕ***.

(3) Impedance-Less Suspension In the rheometer which was used by J. R. Van Wazer and H. Goldberg[1] the internal cylinder is suspended from a thin thread whose mechanical loss and elastance are both assumed to be negligible in comparison with those of the liquid under study. The external cup is set into oscillation. This situation corresponds to Fig. 9 in which the terminals a and a' are short-circuited and

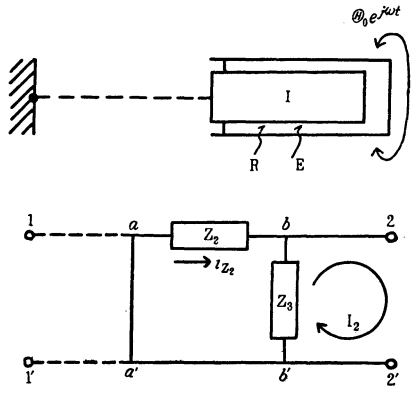


Fig. 9. Impedance-less suspension rheometer.

*** In this case the rigorous analysis[3,3'] is rather convenient to use.

$$Z_1 = \frac{k}{j\omega} = 0$$

When we put $k=0$ in Eq. 15, motion of the internal cylinder in the case of the impedance-less suspension is obtained as

$$\theta = \frac{\sqrt{E^2+\omega^2R^2} \cdot \Theta_0}{\sqrt{(E-\omega^2 I)^2+\omega^2 R^2}} e^{j(\omega t-\phi)} \equiv A_0 e^{j(\omega t-\phi)}$$

$$\tan\phi = \frac{\omega^3 RI}{E(E-\omega^2 I)+\omega^2 R^2}$$

If we differentiate A_0 and set $\partial A_0/\partial\omega$ equal to zero, the condition for a maximum, or for the amplitude resonance, is fulfilled and we find that

$$\omega^2_{res} = \frac{-n_e^4 + n_e^4 \cdot \sqrt{1+8\varepsilon^2/n_e^2}}{4\varepsilon^2}$$

at resonance, where $2\varepsilon = R/I$ and $n_e^2 = E/I$. When $\varepsilon^2 \ll n_e^2$, or when the elastic nature is very strong in the liquid under study,

$$\omega^2_{res} = \frac{-n_e^4 + n_e^4(1+4\varepsilon^2/n_e^2)}{4\varepsilon^2} = n_e^2 = \frac{E}{I}$$

So that it is possible to know the elastic constant of an elastic liquid approximately from

$$G = \frac{I}{4\pi l}\left(\frac{1}{r_1^2} - \frac{1}{r_2^2}\right)\omega^2_{res}$$

(It is of course possible to calculate the true shear modulus and the damping viscosity by the appropriate correctional procedure[1].)

The resonance method, however, as was mentioned previously, seems to be incorrect from the point that the inertia of the sample can not be neglected in the frequency range usually adopted.

(4) Rotational Viscometer and Schwedoff Apparatus Apart from the oscillating devices, two simple rheometers will be mentioned; one of them is the rotational viscometer and the other is the apparatus which was used by Th. Schwedoff[7] and others[8] to measure the shear modulus of gel-like matter.

Rotational Viscometer. — In the ordinary type rotational viscometer (Couette-Hatschek apparatus) the external cylinder rotates with a constant angular velocity Ω, while the top end of the suspension wire is kept in position. The stationary state is reached after the inner cylinder is deflected to a certain extent θ.

The electrical analog is illustrated in Fig. 10; the input terminals $1-1'$ are opened and the output direct current $I_2 = \Omega$ (D.C.). In

7) Th. Schwedoff, *J. de Phys.*, [2] 8, 341 (1889).
8) E. Hatschek and R. S. Jane, *Koll. Z.*, 39, 300 (1926); H. J. Poole, *Trans. Farad. Soc.*, 22, 82 (1926).

the stationary state the inductance I is inactive because no current flows in it, and counter-electromotive force at the resistor part balances with that of the capacitor

$$R\Omega=\frac{\theta}{1/k}$$

or

$$R\Omega=k\theta$$

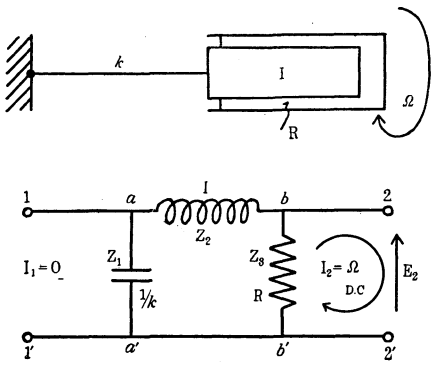


Fig. 10. Rotational viscometer.

The well-known Couette-Hatschek formula of the rotational viscometer is

$$\frac{4\pi l}{\left(\frac{1}{r_1^2}-\frac{1}{r_2^2}\right)}\eta\Omega=k\theta$$

and then

$$\eta=\frac{R}{4\pi l}\left(\frac{1}{r_1^2}-\frac{1}{r_2^2}\right)\equiv K_0R \qquad (8)$$

It has simply been assumed in the present discussion that the relation 8 holds in the oscillatory case too.

Schwedoff Apparatus.—In the Schwedoff method for measuring the elasticity of typical elastic gels—e.g. gelatin gel, agar-agar gel and so on, the top end of the suspension wire is twisted to an angle θ_1 and the equilibrium deflection θ_2 of the internal cylinder is observed.

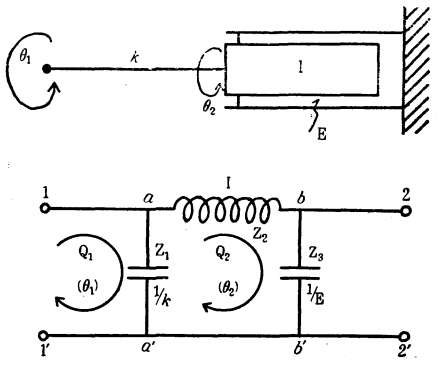


Fig. 11. Schwedoff apparatus.

The situation is that at the equilibrium the inductance is inactive and the voltage Q (charge)/C (capacitance) of the one capacitor is equal to that of the other (cf. Fig. 11 and Table I).

$$\frac{(\theta_1-\theta_2)}{1/k}=\frac{\theta_2}{1/E}$$

or

$$E=k\frac{(\theta_1-\theta_2)}{\theta_2}$$

The exact formula derived by Schwedoff is

$$G=\frac{k}{4\pi l}\left(\frac{1}{r_1^2}-\frac{1}{r_2^2}\right)\cdot\frac{(\theta_1-\theta_2)}{\theta_2}$$

Then

$$G=\frac{E}{4\pi l}\left(\frac{1}{r_1^2}-\frac{1}{r_2^2}\right)\equiv K_0E \qquad (9)$$

The author has extended this shape factor K_0 to the case of the dynamic elasticity throughout the discussion.

As to the time effect of the elastic deformation of gels, (a) the elastic after-effect (retarded elasticity or parallel visco-elasticity) is described by a resistor element inserted in series to the capacitor of Z_3, and (b) flow (relaxed elasticity or series visco-elasticity) is analogized by a leakage resistance inserted in parallel in Z_3.

(5). More Complicated Cases.—When the cup and the upper end of the wire are both driven, the general case must be solved in

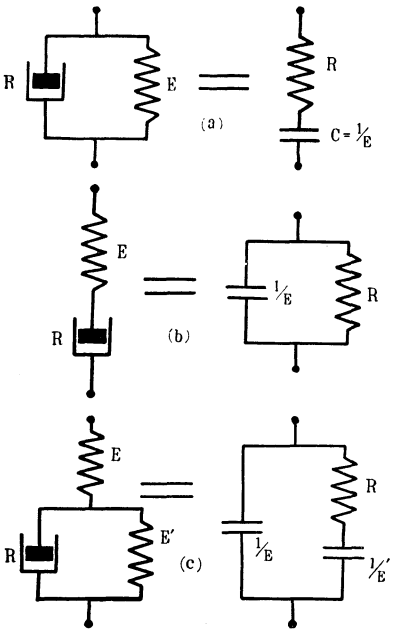


Fig. 12. Mechanical models and corresponding networks.

which $I_1 \neq 0$, $I_2 \neq 0$ and they are in some phase difference.

Throughout the discussion the $R-C$ series circuit was assumed as to the components of Z_3, corresponding to the parallel mechanical model (Voigt model) as is shown in Fig. 12 a, in which $Z_3=R+E/(j\omega)$. If necessary, however, other impedance functions may be adopted—e.g. $R—C$ parallel circuit corresponding to Maxwell model (Fig. 12 b), or three-element model (Fig. 12 c) in which

$$Z_3=\frac{1}{\frac{1}{E/(j\omega)}+\frac{1}{R+E'/(j\omega)}}$$

Summary

(1) The four-terminal electrical network is shown to be useful in the schematic representation of various mechanical systems.

(2) A simple review on various types of torsionally oscillating rheometers is given according to the theory of four-terminal networks.

(3) It is shown that complicated viscoelastic systems are easily solved so far as their formalistic treatment is concerned.

The author hereby expresses his thanks to Prof. H. Akamatsu for his interest and the support given to him in this study.

Department of Chemistry,
Faculty of Science,
Tokyo University, Tokyo

Radiochemical Studies on Ultra-Micro Quantities of Organometallic Compounds. I. On the Determination of the Composition of an Organometallic Compound in an Ultra-Micro Amount

By Tomitaro ISHIMORI

(Received November 11, 1953)

The composition of an organometallic complex compound is usually determined by the chemical analysis of the pure crystals of the complex compound. For the determination of the composition of a complex compound in a minute amount, some optical or electrochemical methods are available, but these methods are not applicable for a complex salt in an ultra-micro amount. However, there are many complex compounds which can be prepared only in extremely minute quantities, e.g. organometallic compounds of much rarer elements such as polonium, promethium and so on.

Recently the present author[1] reported the formation of polonium dithizonate by the dithizone extraction method. The dithizonate has been used in the determination of radium A and radium F in waters of some strongly radioactive hot springs. Also in Europe, G. Bouissieres et al.[2] purified polonium by means of the extraction of polonium dithizonate. Further, radium B content of waters of hot springs was determined by the extraction in the form of lead (radium B) dithizonate.[3]

Such being the circumstances, the author attempted to determine the composition of organometallic compounds which are difficult to prepare in a large amount and devised a method suitable for this purpose. In the present paper, the theoretical basis of the method and the results of the experiments with lead (thorium B) dithizonate and lead (thorium B) hydroxyquinolate, both of the well known compositions, are described.

(A) Theoretical Basis of the Method.

In 1941, I. M. Kolthoff and E. B. Sandell[4] studied the extraction of zinc dithizonate quantitatively and gave an equation relating the extraction coefficient of the metallic dithizonate, the *p*H of the aqueous solution being extracted and the concentration of the chloroform solution of dithizone used for the extraction.

Recently the principles of solvent extraction were outlined by M. Calvin.[5] Basing his results on his theory, Furman determined

1) T. Ishimori and H. Sakaguchi, *J. Chem. Soc. Japan*, **71**, 327 (1950).

2) G. Bouissieres and C. Ferrandini, *Anal. Chem. Acta*, **4**, 610 (1950).

3) H. Umemoto, *Japan Analyst*, **2**, 201 (1953).

4) I. M. Kolthoff and E. B. Sandell, *J. Am. Chem. Soc.*, **63**, 1906 (1941).

5) M. Calvin, *Experientia*, **6**, 135 (1950); *Manhattan Project Report* CN-2486, December 19, 1944; cf. A. E. Martell and M. Calvin, "Chemistry of the Metal Chelate Compunds", N. Y., Prentice Hall Inc., 1952, p. 451.

the chemical formulea of various dithizonates.[6] Moreover, also in Sweden, comprehensive studies on thorium acetylacetonate seem to be carried out from the theoretical points of view.[7]

In a similar way the present author studied the equilibrium between the aqueous solution of a definite *p*H containing a tracer amount of radioisotope of a metallic element and the chloroform solution of an organic reagent, both being in mutual contact.

In such a system the following equilibria are established after thorough shaking and standing:

(organic solvent phase) (aqueous phase)

$$HR \overset{p_r}{\rightleftarrows} HR \overset{k_r}{\rightleftarrows} H^+ + R^-$$

Here, an organic reagent, HR, is considered as a weak acid and k_r and p_r respectively indicate the dissociation constant and the partition coefficient as given by Eq. 1 and 2:

$$k_r = [H^+]_w \cdot [R^-]_w / [HR]_w \quad (1)$$

$$p_r = [HR]_w / [HR]_o \quad (2)$$

Here the suffixes, r, w, and o respectively represent the organic reagent, aqueous phase, and organic solvent phase, and the square bracket represents concentration.

Further, the reaction of the metal ion, M^{n+}, with the organic anion and the partition of the organometallic compound, MR_n, between two liquid phases are written as

organic solvent phase) (aqueous phase)

$$MR_n \overset{p_c}{\rightleftarrows} MR_n \overset{k_c}{\rightleftarrows} M^{n+} + nR^-$$

Therefore, the equilibrium constant for this reaction is

$$k_c = [M^{n+}]_w \cdot [R^-]^n_w / [MR_n]_w, \quad (3)$$

and the partition coefficient of the complex compound between the aqueous and organic phases is

$$p_c = [MR_n]_w / [MR_n]_o. \quad (4)$$

In these equations, the suffix c represents the complex compound.

The extractability, E, namely the ratio of the radioactivity due to the total amount of the radioactive metallic cation taken into the system and that extracted into the organic phase, is written as

$$E = [MR_n]_o \cdot v_o / ([MR_n]_o \cdot v_o + [MR_n]_w \cdot v_w + [M^{n+}]_w \cdot v_w), \quad (5)$$

where v_o and v_w represent respectively the volumes of the organic and aqueous phases. Introducing values from Eqs. 2, 3 and 4, Eq. 5 beomes

$$E = p_c^{-1} \cdot [MR_n]_w \cdot v_o / [MR_n]_w \cdot \{(p_c^{-1} v_o + v_w) + k_c v_w [R^-]_w^{-n}\}. \quad (6)$$

Because p_c and k_c are constant at a definite temperature and v_o and v_w can be kept constant in a series of experiments, Eq. 6 is simplified as

$$E = 1/(A + B'[R^-]_w^{-n}) \quad (7)$$

or

$$E^{-1} = A + B'[R^-]_w^{-n}, \quad (8)$$

where A and B' are constants.

In Eq. 7 or 8, $[R^-]_w$ is difficult to determine experimentally, but in these cases we consider, $[R^-]_w$ is proved to be proportional to the amount of the organic reagent, (HR), taken into the system. Namely in the equation

$$(HR) = [HR]_o v_o + n[MR_n]_o v_o + [HR]_w v_w + n[MR_n]_w v_w + [R^-]_w v_w, \quad (9)$$

the total amount of metal is so small that second and fourth terms on the right hand side can be neglected. Therefore, Eq. 9 becomes

$$(HR) = [HR]_o v_o + [HR]_w v_w + [R^-]_w v_w. \quad (10)$$

Introducing values from Eq. 1 and 2, Eq. 10 is rewritten as

$$(HR) = [R^-]_w \{k_r^{-1}(p_r^{-1} v_o + v_w)[R^+]_w + v_w\}, \quad (11)$$

where all quantities in the right hand side except $[R^-]_w$ are kept constant. Thus $[R^-]_w$ is proved to be proportional to (HR), and Eq. 8 is rewritten as

$$E^{-1} = A + B(HR)^{-n}, \quad (12)$$

in which A and B are constants.

According to Eq. 12, we can determine the value of n, the ratio between the number of organic anions and that of metallic cation, in the following manner.

An aqueous solution of a definite hydrogen ion concentration containing a known amount of the radioactive tracer of a metal is prepared. In a small separating funnel known volumes of this aqueous solution and an organic solvent containing a known quantity of an organic reagent are shaken together until the equilibrium is established. The organic solvent is then separated and dried in a glass dish. The radioactivity of the residue is measured and the extractability, E is calculated.

Similar procedures are repeated for a series of varying amounts of the organic reagent. The values of E^{-1} are plotted against $(HR)^{-n}$, taking for n the values 1, 2, 3 and so on, so that we can find out the integer, n, which gives the best linearity between E^{-1} and $(HR)^{-n}$.

Thus we can determine the actual value of n, but this method does not give any

6) cf. Martel and Calvin, ibid p. 463. The present author can not find where this paper appeared originally.

7) J. Rydberg, *Arkiv für Kimi*, 5, 517 (1953). This is the eleventh report of Rydberg's study. The rest of this series have not been accesible to the present author.

knowledge concerning the water bound to the complex molecule. Moreover it can not be adopted in the case where two or more kinds of organometallic compounds are formed, and also in the case where the formation of radiocolloids prevents the establishment of the equilibria underlying the derivation of Eq. 12.

In addition to these defects, we can not estimate the effects of impurities introduced into the system by chemicals used in the experiment. Any way the amount of these impurities is supposed to be much greater than the radiochemical amount of the metallic cation taken into the system.

(B) Experimental Examination of the Validity of the method.

As mentioned above, there are many uncertain facts which may disturb the results of the method. Therefore, the author intended to check the validity of the above reasoning for some organometallic compounds such as lead dithizonate and lead hydroxyquinolate, the composition of which are known already. In these experiments carrier-free radioisotope of lead, thorium B, is used.

(1) Preparation of thorium B solution.

According to the usual method recommended by O. Hahn[8], the radioactive deposits of thoron are collected on a platinum plate. About 50 g. thorium nitrate is placed in a closed metal container into which an insulated, negatively charged (250 volts) platinum plate is also introduced. The active deposit proceeding from the emanation, i. e. thorium B with its disintegration products, is collected on the platinum plate for about 24 hours, and then dissolved into hot dilute nitric acid (1 : 15). The solution is made up to 25cc. and divided into aliquot portions for both the preparation of the standard specimen of thorium B and the following experiments.

The radiochemical purity is examined by the measurement of the decay curve shown in Fig. 1, in which the logarithm of the activity is plotted against the time elapsed. From this figure the apparent half-life of the activity is calculated as about 10.5 hours. So we can conclude that the "thorium B" will not have any detectable radiochemical impurity except its daughter, thorium C group, in an equilibrium amount.

The measurements of the activities are carried out by a Lauritsen electroscope made by the Scientific Research Institute, Tokyo.

Owing to its relatively short half-life (10.6 hours), the solution of thorium B must be prepared just before each series of experiments so that its radioactivity is measured accurately.

(2) On the composition of lead dithizonate.

5cc. of 50% sodium citrate solution and and 5cc. of 10% potassium cyanide are added to 20cc, of thorium B solution obtained as above. Ammonium hydroxide is added to the mixture dropwise to make it weakly alkaline, and the resultant solution is made up to 100cc. The *p*H of the solution is checked by a *p*H test paper and estimated to be about 9.5.

The stock chloroform solution of dithizone (about 1.25×10^{-4} mol./l.)[9] is diluted successively with chloroform and a series of chloroform solutions of dithizone, 1, 1/5, 1/10, 1/25 and 1/50 times the concentration of the original stock solution, is prepared. Dilution of the solutions is made just before use to prevent the decomposition of dithizone.

To 10 cc. of the aqueous solution prepared as above, 5 cc. of the chloroform solution of dithizone (known concentration) are added in a separating funnel. The system of the two liquid phases is shaken vigorously for one minute and is left to stand aside for a while so that it separates into two liquid phases. The chloroform phase is taken into a glass dish, dried up and left to stand overnight before the measurement of radioactivity. During the overnight standing, thorium B disintegrates to a considerable extent, so it looks unfavorable for the measurement of radioactivity, but it is necessary to make sure the condition of radiochemical equilibrium between thorium B and its daughters, members of thorium C group.

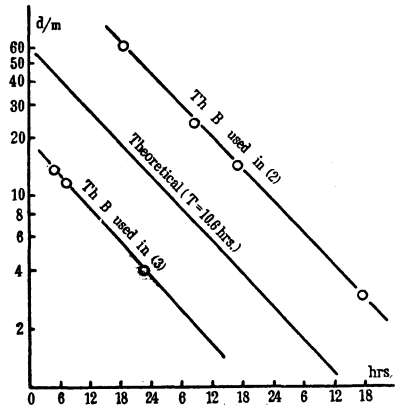


Fig. 1

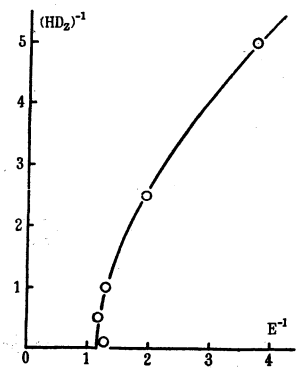


Fig. 2 a

8) Otto Hahn, "Applied Radiochemistry" Cornell Univ. Press, New York, N. Y., p. 44 (1936).

9) The concentration of dithizone in chloroform is determined by titrating a dilute solution of silver nitrate.

Taking the ratio of the activity due to the extracted thorium B to that of the standard specimen of the same age, the extractability, E, is calculated.

Similar procedures are repeated for varying concentrations of dithizone in chloroform.

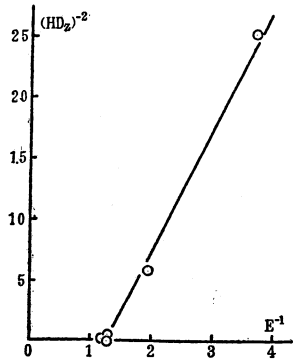


Fig. 2 b

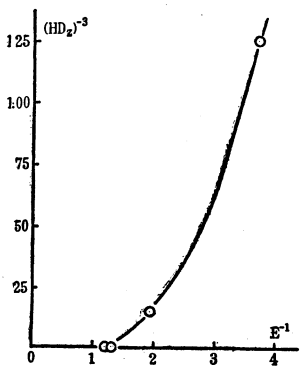


Fig. 2 c

TABLE I

RESULTS FOR LEAD DITHIZONATE

No.	(HDz)	$(HDz)^{-1}$	$(HDz)^{-2}$	$(HDz)^{-3}$	E^{-1}
1	10	0.1	0.01	0.001	1.27
2	2	0.5	0.25	0.125	1.19
3	1	1.0	1.0	1.0	1.30
4	0.4	2.5	6.3	15.6	1.97
5	0.2	5.0	25.	125.	3.72

(HDz): Amount of dithizone in an arbitrary unit in which about 6.3 10^{-7} mol. dithizone corresponds to (HDz)-10

E : Extractability

Results obtained are shown in Table I and Fig. 2 (a, b, c). As can be seen in these figures, E^{-1} is linear to $(HDz)^{-2}$. (cf. Fig. 2 b) So we can conclude that the composition of lead dithizonate is of such a ratio as when one atom of lead is bound to two anions of dithizone, Dz.

On the other hand Liebhasky and Winslow[10] reported that lead dithizonate corresponds to the formula $PbDz$, but Clifford[11] showed that the complex compound is actually $PbDz_2$, which is generally accepted by most chemists.[12] The conclusion obtained by the present method also coincides with that of Clifford. Therefore, the present method is considered to be applicable for the determination of the composition of organometallic compounds. And the disturbing factors mentioned above proved to result in no serious error.

(3) On the composition of lead hydroxyquinolate.

To the solution which contains 5g. sodium citrate and 20 cc. thorium B solution described in (1), ammonium hydroxide is added dropwise until *p*H of the solution becomes about 9. The resultant solution is made up to 50 cc.

About 100 mg. 8-hydroxyquinoline is dissolved in 50 cc. chloroform. Diluting this solution with chloroform, a series of solutions of 8-hydroxyquinoline is prepared. Their concentrations are 1, 2/5, 1.5/5, and 1.2/5 times that of the original solution.

Using the aqueous solution of thorium B and the chloroform solution of 8-hydroxyquinoline, a series of experiments is carried out in a similar way as described in the case of lead dithizonate.

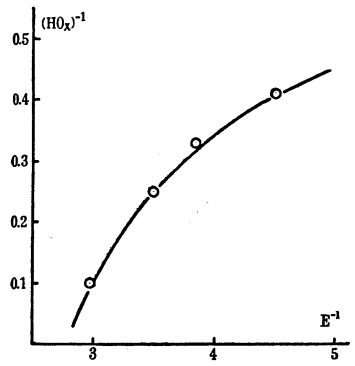


Fig. 3 a

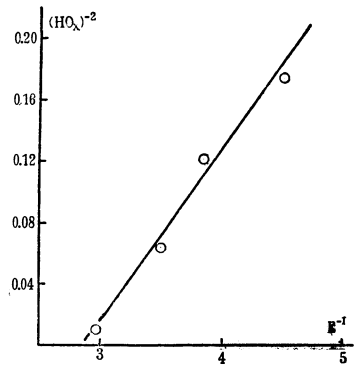


Fig. 3 b

10) H. A. Liebhasky and E. H. Winslow, *J. Am. Chem. Soc.* **59**. 1966 (1937).

11) P. A. Clifford, *J. Official Agr. Chem.* **26**, (1943); *C. A.*, **37**, 3009.

12) The formula given by Clifford which coincides with that of H. Fischer (*Z. anorg. Chem.*, **47**, 685 (1934).) is quoted by F. J. Welcher ("Organic Analytical Reagents", vol. 3, D. van Nostrand Co., Inc., New York, 1947. p. 470.).

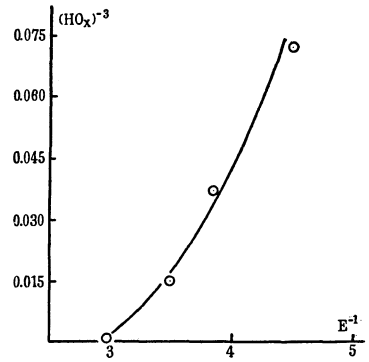


Fig. 3 c

TABLE II.

RESULTS FOR LEAD HYDROXYQUINOLATE

No.	(HOx)	$(HOx)^{-1}$	$(HOx)^{-2}$	$(HOx)^{-3}$	E^{-1}
1	10	0.1	0.01	0.001	2.97
2	4	0.25	0.063	0.015	3.50
3	3	0.33	0.111	0.037	3.84
4	2.4	0.41	0.174	0.072	4.51

(HOx): Amount of 8-hydroxyquinoline in an arbitrary unit in which (HOx) = 10 corresponds to about 10 mg. 8-hydroxyquinoline.

E : Extractability

The results are shown in Table II and in Fig. 3 (a, b, c). In Fig. 3 b, we can see a linear relationship between E^{-1} and $(HOx)^{-2}$. Therefore we can conclude that lead hydroxyquinolate corresponds to the formula $Pb(Ox)_2$. This conclusion agrees with the generally accepted formula[13] for lead hydroxyquinolate, again showing the applicability of the present method method for such a problem.

In the following papers results for some organometallic compounds which have unknown compositions will be reported.

The author has to thank to Professor Tsunetaka Sasaki, Kyushu University, for his encouragement and criticism in several discussions on the theoretical considerations of the present study.

Department of Chemistry, Faculty of Science, Kyushu University, Fukuoka

13) V. Maarson and L. W. Haase, *Chem. Ztg.* **52**, 993 (1928); *C. A.* **23**, 1077 (1928).

On the Ring-opening Reactions of the Furan Compounds. IV. The Condensation Products of Furfural with Methyl Propyl Ketone, Methyl Isopropyl Ketone and Pinacolin by Alkali

By Hiroshi MIDORIKAWA

(Received November 17, 1953)

In the previous paper[1] it was reported that, in the condensation of furfural and benzaldehyde with methyl ethyl ketone by alkali, the lowered reaction temperature (0~5°) favored the aldol condensation at the α-methylene group of the ketone and the elevated reaction temperature (60~65°) the condensation at the α-methyl group of the ketone. In the present work were studied the condensation of furfural with methyl propyl ketone by alkali and the ring-opening of the condensation products of furfural with methyl isopropyl ketone and pinacolin.

The condensation of furfural with methyl propyl ketone was carried out in two cases of lowered and elevated reaction temperatures, 0~5° and 60~63°.

In both cases, the condensation products afforded two species of semicarbazone—a greater amount of colorless needle crystals melting at 143~144° and a much smaller amount of colorless needles melting at 223~225°. The ratios of the semicarbazone melting at 143~144° to that melting at 223~225° in the two cases were nearly equal. Considered from the analysis, the condensation product at the lowered reaction temperature appeared to contain a small quantity of the aldol condensation product which corresponds to that of furfural with methyl ethyl ketone.

The condensation product at the reaction temperature 0~5°, after heating with dilute hydrochloric acid in order to dehydrate the aldol[2] which was considered to be contained, was oxidized by sodium hypochlorite to give α-ethyl-2-furanacrylic acid (IV), in the fol-

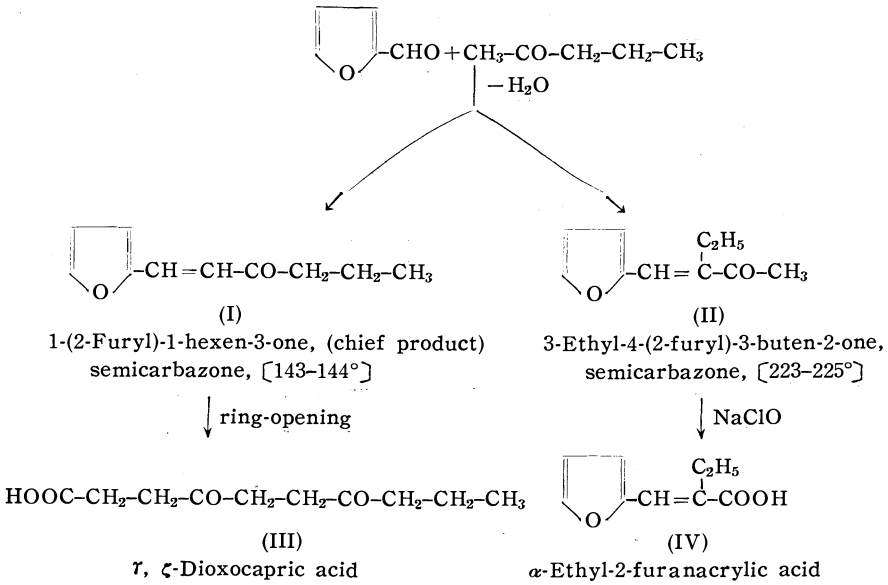
1) H. Midorikawa: This Bulletin, **26**, 460 (1953).

2) H. Midorikawa: This Bulletin, **26**, 462 (1953).

lowing formulation, although in a very poor yield. Consequently it is evident that 3-ethyl-4-(2-furyl)-3-buten-2-one (II) is contained in it and methyl propyl ketone reacts with furfural at the α-methylene group of the ketone. The condensation product at the reaction temperature 0~5°, after being heated with dilute hydrochloric acid, gave a mixture of a larger proportion of the semicarbazone melting at 143~144° and a much smaller proportion of that melting at 223~225°.

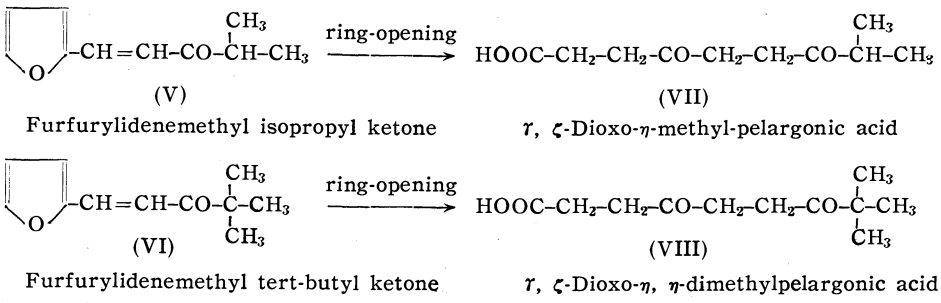
The condensation product at the reaction temperature 60~63°, on the ring-opening in alcoholic hydrochloric acid[3], gave a dioxocarboxylic acid in a good yield. This acid was considered to be identical with the dioxocarboxylic acid which was reported as γ, ζ-dioxocapric acid (III) by Breusch and Ulusoy[4].

From the stand-point of the poor yield of α-ethyl-2-furanacrylic acid (IV) and the good yield of γ, ζ-dioxocapric acid (III), it was infered that 3-ethyl-4-(2-furyl)-3-buten-2-one(II), which furnished the former acid on the treatment with sodium hypochlorite, gave the semicarbazone of colourless needles (m. p. 223~225°), and the furfurylidene ketone which gave the semicarbazone of colorless minute needles (m. p. 143~144°) was 1-(2-furyl)-1-hexen-3-one (I) yielding γ, ζ-dioxocapric acid (III) by the ring-opening, as shown below.



The poor yield of α-ethyl-2-furanacrylic acid (IV) appeared to reveal a weaker reactivity of the α-methylene group of methyl propyl ketone in comparison with that of methyl ethyl ketone.

The condensation products of furfural with methyl isopropyl ketone and pinacolin by alkali, furfurylidenemethyl isopropyl ketone (V) and furfurylidene-methyl tert-butyl ketone (VI), gave γ, ζ-dioxo-η-methylpelargonic acid (VII) and γ, ζ-dioxo-η, η-dimethylpelargonic acid (VIII) respectively, on the ring-opening in alcoholic hydrochloric acid. These reactions are illustrated as follows:



3) E. A. Kehrer and P. Igler: *Ber.*, **32**, 1177 (1899).
4) F. L. Breusch and E. Ulusoy: *C. A.*, **42**, 5850 (1948).
5) I. Kashiwagi: This Bulletin, **1**, 94 (1926).

Experimental

Condensation of Furfural with Methyl Propyl Ketone Into a stirred suspension of methyl propyl ketone (13 g.) and furfural (7 g.) in water (150 cc.) was at once introduced 5 % aqueous sodium hydroxide (10 cc.) at 60~63°. The reaction was complete after stirring for 2.5 hrs. at 60~63°. The reaction mixture was neutralised with dilute sulfuric acid. The oily layer was separated and the aqueous solution extracted twice with ether. The combined ethereal solution of the oily layer and the ether extract, after drying over anhydrous sodium sulfate, was fractionated to give a yellow liquid (7 g.), b. p. 119~121°/8 mm.

This fraction was considered to consist of 1-(2-furyl)-1-hexen-3-one (I) in a larger proportion and 3-ethyl-4-(2-furyl)-3-buten-2-one (II) in a much smaller proportion.

Calcd. for $C_{10}H_{12}O_2$: C, 73.12, H, 7.37 %; Found: C, 72.92, H, 7.60 %.

This oil gave a mixture of two species of semicarbazone. The greater part consisted of colorless microscopic needles, which were fairly soluble in methanol and melted at 143~144° on recrystallisation from methanol-water. In addition, fewer colorless needles, which were sparingly soluble in cold methanol and recrystallised from methanol, m.p. 223~225°, were obtained.

The semicarbazone melting at 143~144° was considered to be that of 1-(2-furyl)-1-hexen-3-one (I).

Calcd. for $C_{11}H_{15}O_2N_3$: C, 59.69, H, 6.83, N, 18.99 %; Found: C, 59.55, H, 6.86, N, 19.12 %.

In a solution of 2, 4-dinitrophenylhydrazine in methanolic sulfuric acid, this semicarbazone was converted to a 2, 4-dinitrophenylhydrazone, which was recrystallised from pyridine in red foliated crystals, m. p. 171~172°.

Calcd. for $C_{16}H_{16}O_5N_4$: C, 55.79, H, 4.68, N, 16.27 %; Found; C, 55.74, H, 4.43, N, 16.57 %.

The semicarbazone melting at 223~225° was considered to be the one of 3-ethyl-4-(2-furyl)-3-buten-2-one (II).

Calcd. for $C_{11}H_{15}O_2N_3$: C, 59.69, H, 6.83, N, 18.99 %; Found: C, 59.69, H, 6.89, N, 18.79 %.

This semicarbazone was also converted to 2, 4-dinitrophenylhydrazone which was recrystallised from pyridine in carmine prisms, m. p. 183~184°.

Calcd. for $C_{16}H_{16}O_5N_4$: C, 55.79, H, 4.68, N, 16.27 %; Found: C, 55.81, H, 4.45, N, 16,21 %.

The condensation at 0~5° also was carried out by stirring a mixture of methyl propyl ketone (15 g.), furfural (8 g.), water (150 cc.) and 10 % aqueous sodium hydroxide (10 cc.) for 7 hrs. The reaction mixture was kept overnight below 10°, and then worked up in the same manner as in the condensation at 60~63°. A fraction (7.5 g.) distilling at 119~123°/8 mm was collected.

Calcd. for $C_{10}H_{12}O_2$: C, 73.12, H, 7.37 %; Found: C, 70.34, H, 7.62 %. (This analysis seems to show that this fraction contains a small amount of the aldol condensation product, $C_4H_3O\cdot CH(OH)CH(CH_3)\cdot CO\text{-}CH_3$, which requires C, 65.89 %; H, 7.74 %.)

This fraction gave the same semicarbazones as the condensation product at the reaction temperature 60~63°.

Ring-opening of the Condensation Product of Furfural with Methyl Propyl Ketone The condensation product (2 g.) at the reaction temperature 60—63° was refluxed with conc. hydrochloric acid (1.5 cc.) and alcohol (5 cc.) for 3 hrs. The reaction mixture was evaporated till dry in the water-bath, and a small quantity of dil. hydrochloric acid was added to evaporate till dry once more. The residue was extracted with a sufficient quantity of water, and the extract was concentrated on the water-bath to give the dioxocarboxylic acid which was considered to be γ, ζ-dioxocapric acid (III) (0.7 g.). The acid was recrystallised from ligroin as colorless hexagonal plates, m.p. 83~84°; lit.,[4] m.p. 83~84°.

Calcd. for $C_{10}H_{16}O_4$: C, 59.96, H, 8.00 %; Found: C, 60.40, H, 8.14 %.

Sodium Hypochlorite Oxidation of the Condensation Product of Furfural with Methyl Propyl Ketone The condensation product(2.3g.) at the reaction temperature 0~5° was suspended in 6 % hydrochloric acid (5 cc.) and heated by shaking in the water-bath for a short time. The separated oil was suspended in the aqueous sodium hypochlorite solution[2] (15 cc.) and kept at ordinary temperature for two days, with occasional shaking. The reaction mixture was freed of the oily matter by extraction with ether and acidified with dilute hydrochloric acid to yield a small number of crystals, which were dissolved in a requisite quantity of hot water, decolorised with active charcoal and crystallised as colorless needles on cooling, m.p. 95~96°. This specimen showed no depression on admixture with α-ethyl-2-furanacrylic acid which was synthesised by the reaction of furfural with butyric anhydride and anhydrous sodium butyrate.[6]

Ring-openings of Furfurylidenemethyl Isopropyl Ketone (V) and Furfurylidenemethyl *tert*-Butyl Ketone (VI) Furfurylidenemethyl isopropyl ketone (V) and furfurylidenemethyl *tert*-butyl ketone (VI) were respectively synthesised by the condensations of furfural with methyl isopropyl ketone and pinacolin, using sodium hydroxide as the condensing agent.[5]

Furfurylidenemethyl isopropyl ketone (b.p. 101~102°/5 mm.) gave a semicarbazone crystallising from methanol-water as colorless needles, m.p. 148~149°, and a 2, 4-dinitrophenylhydrazone crystallising from pyridine as orange needles, m.p. 175~176°.

Semicarbazone. Calcd. for $C_{11}H_{15}O_2N_3$: C, 59.69, H, 6.83, N, 18.99 %; Found: C,59.98, H, 6.89, N, 18.97 %. *2, 4-Dinitrophenylhydrazone* Calcd. for $C_{16}H_{16}O_5N_4$: C, 55.79, H, 4.68, N, 16.27 %; Found: C, 55.57, H, 4.33, N, 16.30 %.

Furfurylidenemethyl *tert*-butyl ketone (b.p. 101~102°/5 mm.) gave no semicarbazone, as reported by Kashiwagi,[5] but gave a 2, 4-dinitrophenylhydrazone crystallising from pyridine-methanol as scarlet lustrous needles, m.p. 121~123°.

6) A. S. Carter: *J. Am. Chem. Soc.*, 50, 2299 (1928).

Calcd. for $C_{17}H_{18}O_5N_4$: C, 56.98, H, 5.07, N, 15.63 %; Found: C, 57.03, H, 5.03, N, 15.62 %.

The ring-opening of furfurylidenemethyl isopropyl ketone (2 g.) was carried out by refluxing with conc. hydrochloric acid (1.5 cc.) and alcohol (5 cc.) for 3 hrs. By the same procedure as in the case of the foregoing ring-opening reaction was obtained γ, ζ-dioxo-η-methylpelargonic acid, which was recrystallised from ligroin as colorless needles, m.p. 72~73°.

Calcd. for $C_{10}H_{16}O_4$: C, 59.96, H, 8.00 %; Found: C, 59.93, H, 7.89 %.

The ring-opening reaction of furfurylidenemethyl *tert*-butyl ketone to γ, ζ-dioxo-η, η-dimethylpelargonic acid (VIII) was performed by the same procedure as in the case of furfurylidenemethyl isopropyl ketone. The ketone (2 g.) gave the crude acid (0.5 g.) as a viscous oil. It was recrystallised from ligroin as colorless leaflets, m.p. 46~47°.

Calcd. for $C_{11}H_{18}O_4$: C, 61.64, H, 8.47 %; Found: C, 61.57, H, 8.39 %.

Summary

Methyl propyl ketone condensed with furfural by alkali both at the α-methyl and α-methylene groups of the ketone, giving 1-(2-furyl)-1-hexen-3-one (I) in a larger proportion and 3-ethyl-4-(2-furyl)-3-buten-2-one (II) in a much smaller proportion.

The former furfurylidene ketone (I) gave γ, ζ-dioxocapric acid (III) on the ring-opening in alcoholic hydrochloric acid, and the latter (II) was oxidized by sodium hypochlorite to α-ethyl-2-furanacrylic acid (IV).

The ring-opening of furfurylidenemethyl isopropyl ketone (V) and furfurylidenemethyl *tert*-butyl ketone (VI) in alcoholic hydrochloric acid gave γ, ζ-dioxo-η-methylpelargonic acid (VII) and γ, ζ-dioxo-η, η-dimethylpelargonic acid (VIII) respectively.

The author expresses his sincere thanks to Dr. T. Hayashi for his kind advice.

Scientific Research Institute,
Komagome, Bunkyo-ku,
Tokyo

The Structure of Surface-Denatured Protein. VI. The Effect of pH of Substrate upon the Limiting Area of Protein Monolayer

By Kazutomo IMAHORI

(Received November 26, 1953)

Introduction

Gorter[1] has investigated the influence of *p*H of the substrate upon the spreading of various proteins, by measuring the spreading areas after the protein has been in contact with solutions of different *p*H for a period of one or two minutes. He observed that such protein as egg albumin or serum albumin, spread well at the *p*H of its isoelectric point, as well as in the case of strong alkaline and strong acid solutions, but on both sides of the isoelectric point, little spreading could be obtained. But the low spreading disappeared, when enough salt was added to the substrate. These results can be explained[2] by assuming that at *p*H values, where the effective protein charge is high, the spreading tendency is at a minimum. Yet, the truth of the above assumption has not been ascertained. The author has studied the size and the shape of protein molecules expanded on substrates of various *p*H values, and has considered the cause of spreading from these results.

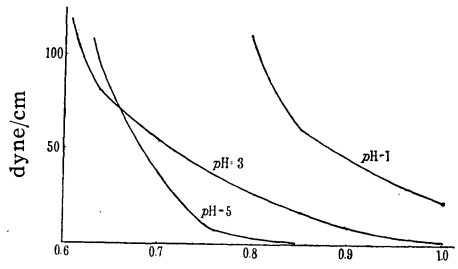
1) E. Gorter, H. Ormondt, and F. Dom, *Proc. Kon. Akad. v. Wet.*, **35**, 838 (1933).
2) E. Gorter 'Surface tension and films' Schmit's Chem. of the amino acids and proteins. p. 428.

The Limiting Area

The limiting areas of the surface films of egg albumin as well as horse serum albumin have been measured. Both samples are in the pure crystalline state, being prepared by Drs. S. Nakamura and H. Sugano at the Chem. Inst. of Tokyo University. The apparatuses used for this measurement are a surface balance and than ellipsometer, the former of which has been described in the first report of this series[3], while the details of the latter will be published shortly. Three buffer solutions having the *p*H values of 1, 3, (HCl buffer) and 5 (acetate buffer), are used as the substrates.

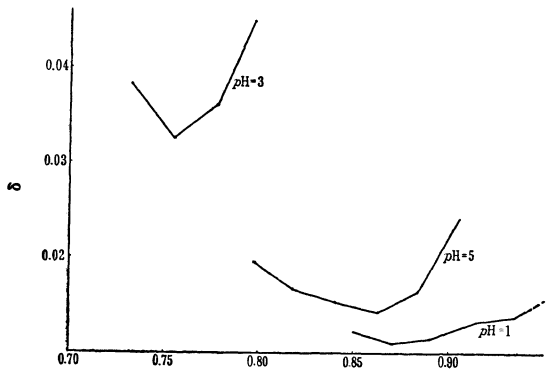
The F—A relations of serum albumin films on these three buffers are shown in Fig. 1. These would suggest many things. First of all, the curve on *p*H=5 is of a condensed type, while the other two are of an expanded type. The curve of *p*H=1 breaks at the area of 0.845 m^2/mg, and the curve of *p*H=5, at 0.76 m^2/mg, but the curve of *p*H=3, at the area of 0.637 m^2/mg.

Similar features can be seen in the case of egg albumin. In Fig. 2, δ—A relations of egg albumin



m^2/mgs

Fig. 1.



m^2/mg

Fig. 2

are shown instead of those of F—A, where δ means the compressibility, being defined by the following relation:

$$\delta = -\frac{1}{A} \cdot \frac{dA}{dF}$$

The δ—A relations on pH=1 and pH=5 are similar, and the minima of both curves are at 0.87 and 0.86 m^2/mg respectively. But the curve of pH=3 has a far smaller limiting area (0.755 m^2/mg). Fig. 2 shows also that the δ min (the value of δ at the minimum point) on pH=3 is greater than those on pH=1 and pH=5. This means of course, that the film of egg albumin which expanded on the substrate of pH=3 is more compressible than those on pH=1 and pH=5. This fact seems to have some relation to the results of the following experiment.

The films which expanded on the substrates of various pH values were transferred on the metallic slide, by Blodgett's method, under the surface pressure of 13 dynes/cm, and 30 dynes/cm.

The thicknesses of these films were measured by using the ellipsometer. The results were as follows. The films expanded on pH=1 and pH=5 showed the same and constant thickness,—about 10 Å—if they were built up under the pressure of 13 dynes/cm or 30 dynes/cm. But the film on pH=3 had as well the thickness of 10 Å when it was built up under the pressure of 13 dynes/cm., but its thickness increased to 25 Å, when it was built up under the pressure of 30 dynes/cm. This result would suggest that the egg albumin molecules, which were denatured and expanded on the solution of pH=3, might be easily again folded into thicker ones, being in accordance with the fact of the large δ value of this film.

The Size and the Shape

The molecular weight of egg albumin which expanded on the solutions of pH=1 and pH=3, has been determined by the method of Bull and Guastalla[4]. The molecular weight thus obtained was about 42,000 in both cases. This value is just between those obtained by Bull and Guastalla. On the other hand, the molecular weight of serum albumin has been obtained as 70,000 in the previous paper[3].

From these values and the limiting areas obtained above, we can calculate the surface area of each protein molecule as shown on the third line of Table I.

The shape of a protein on each substrate might be determined by the experiment of surface diffusion. The details of the experiment and also of the way of calculation, were given in the second and third reports of this series[5,6].

TABLE I

	Egg albumin			Serum albumin		
pH	1	3	5	1	3	5
surface area per molecule	6065 Å²	5260 Å²	60000 Å²	9830 Å²	7380 Å²	8840 Å²
axial ratio	30 : 1	15 : 1		20 : 1	10 : 1	8 : 1
short axis	28.5 Å	37.5 Å		44.4 Å	54.5 Å	66.7 Å
long axis	855 Å	562 Å		888 Å	545 Å	533 Å

The results are also shown on the fourth line of Table I. The shape, being assumed to be an elliptic disk, is expressed in terms of the axial ratio. On the fifth line of the table, the lengths of two axes are given.

The data in Table I suggest that the shape of the snrface-denatured protein molecule of both albumin species depends on the pH value of the substrate. The molecules expanded on the acid substrate have extremely elongated shapes. This conclusion ascertained by experiment of surface viscosity. Fig. 3 shows the results of the mea-

3) K. Imahori, This Bulletin, **27**, 7 (1952).
4) H. B. Bull, "Advances in Protein Chemistry." Vol. 3.
5) K. Imahori, This Bulletin **27**, 9, (1952).
6) K. Imahori, This Bulletin **27**, 11 (1952).

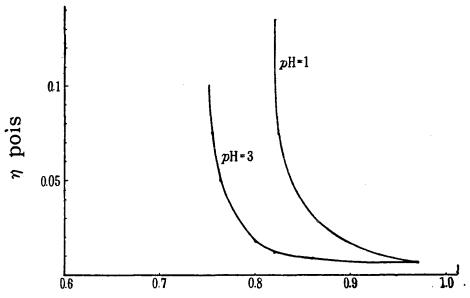


Fig. 3

surements of surface viscosity against the surface area, indicating that the film of egg albumin expanded on pH=1 solution has far greater viscosity than that on pH=3. Similar results are obtained, if we measure the surface viscosity of the serum albumin on pH=1 and pH=5. The high viscosity of both albumins on pH=1, shows that these protein molecules have elongated shapes on the acid substrate.

Discussions

The results of the preceding experiments show that each molecule of two albumin species takes a different form in the three different solutions. The molecule expanded on the solution of pH=1, has the most elongated shape. It forms well expanded, quite thin, and the least compressible rigid films.

The molecule expanded on pH=3, shows a less elongated shape. As it is more compressible than that on pH=1, it is presumably folded into the thicker film under high surface pressure.

The molecule on pH=5, shows also a less elongated shape as in the case of pH=3. But it makes a well-expanded, incompressible rigid film.

The F—A curve of this latter film is of the condensed type, indicating that interaction between molecules is fairly small.

These differences may be explained to some extent as follows. On the solution of pH=1, the basic residues of the albumin molecule, such as arginine, or lysine are ionized and carry the positive charge, while the acid residues such as glutamic acid or asparatic acid are not ionized in this pH range and consequently carry no charge.

The positive charges of those basic residues act repulsively on each other. On the other hand, they are very hydrophilic and are apt to put themselves into the water. The former causes the albumin molecules to be perfectly unfolded, and to take an extremely elongated shape. The latter causes them to lie flat on the water surface, and to make a stable rigid film. Each molecule carries a number of net positive charges, which cause the molecules to repulse each other, and makes the F—A curve into an expanded one.

On the substrate of pH=5, on the other hand, most of the acid and basic residues are ionized, and the albumin molecule contains about an equal number of negative and positive charges upon it. These charges of different signs, acting attraction force on each other and leading to inter- and intramolecular salt-like bonds, as well as hydrogen bonds, and S-S bonds, will prevent the albumin molecule from being perfectly unfolded. Thus, the albumin molecule on pH=5, containing bended structure, takes rather a round shape. The intra-molecular bonds also make the polypeptide chain assume a definite structure, which leads to the comparatively large limiting area and low compressibility as is seen in the above experiment. As the molecule contains many ionized and hydrophilic residues, it can make the stable, incompressible and rigid film. On the substrates of pH=3, the number of positively charged residues of the albumin molecule is less than that of pH=1, while, some of the acid residues can be ionized in this case. Thus, the intra-molecular repulsive force is not so strong as that of pH=1, while the intramolecular bonds are not enough to hold the rigid and bended structure, on the water surface. Thus, the molecule on pH=3 is very flexible, yields easily to external force and causes the low limiting area. A small number of charges make the film somewhat hydrophobic and compressible into a thicker film, under high surface pressures.

This contraction and expansion of the film caused by the variation of pH of the substrate was observed with a mixed film of octadecyl amine and stearic acid as well.

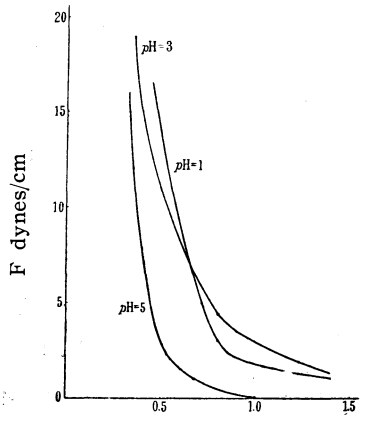


Fig. 4

The details of the experiment will be published elsewhere in the near future.

The following experiment supports our explanation. In Fig. 4, the F—A curve of the heat denatured serum albumin is shown. The procedure was nearly the same as that of S. Staelberg[7]. The same crystalline serum albumin was dissolved in 60% n-propyl alcohol containing 0.5 M sodium acetate, and denatured by heating at 100°C for 30 minutes. The protein spread from this solution gave the limiting areas of 0.82 and 0.55 m^2./mg. on the substrates of pH=1 pH=5 respectively. The F—A curve of the film on pH=3 broke slightly at the area of about 0.82 m^2./mg., but the film might be compressed to the limiting area of 0.55 m^2./mg. The small limiting area on pH=5 means that the intra-molecular bonds were broken by heat, and so the molecules were readily compressible by the attraction between residues of different signs. On the substrate of pH=1, however, few differences were found between the heat-denatured and not heat-denatured proteins. The breaking of intra-molecular bonds by heat resulted in a good expansion of protein on the substrate of pH=3. As the repulsive force was not so remarkable as on pH=1, the molecule could be easily compressed into the compact state as on pH=5.

7) Stina Staelberg, *Trans. Faraday Soc.*, **35**, 1416 (1939).

Conclusion

(1) The size and shape of the egg and serum albumins have been measured on three buffer solutions having the pH values of 1, 3, and 5 respectively.

(2) The film on pH=1 is a well-expanded, incompressible and rigid one. That on pH=5 is as well expanded, but the film on pH=3 is of a not well expanded but easily compressible type.

(3) These differences have been discussed from the points of charges and intra-molecular bonds.

The author wishes to express his hearty thanks to Prof. Bun-ichi Tamamushi, for his kind inspection of this paper. Some part of the present work has been aided by Miss Mitsuko Hachiwaka and Miss Harumi Matsui, to whom the author's thanks are due. This experiment is aided by the Scientific Research Encouragement Grant from the Ministry of Education.

Chemical Iustitute, College of General Education, Tokyo University, Tokyo

The Condensation of Furfural with Methyl Ethyl Ketone by Aqueous Sodium Hydroxide

By Hiroshi MIDORIKAWA

(Received December 7, 1953)

In the previous paper[1], it was reported that, in the condensation of furfural with methyl ethyl ketone by aqueous sodium hydroxide, a mixture of two furfurylidene ketones was obtained and one of those was 4-(2-furyl)-3-methyl-3-buten-2-one (I), and the other was considered to be 1-(2-furyl)-1-penten-3-one (II). In the present experiment, these furfurylidene ketones were completely separated from each other, and the results[1] previously obtained were confirmed.

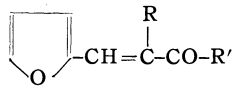
The condensation was carried out at the reaction temperature 60~63°. The resulting condensation product gave a mixture of three species of semicarbazone, foliated crystals (m.p. 212~213°), needle crystals (m.p. 183~184°) and tabular crystls (m.p. 166~167°).

The semicarbazone of foliated crystals (m.p. 212~213°), separating from the other two species by the less solubility in methanol, regenerated a ketone, a pale yellow oil, on heating with dilute hydrochloric acid. This oil afforded α-methyl-2-furanacrylic acid (III) in a good yield on sodium hypochlorite oxidation. Consequently it is evident that this oil is 4-(2-furyl)-3-methyl-3-buten-2-one (I). The reactions are illustrated in the formulation shown below.

By refluxing with alcoholic hydrochloric acid, this ketone did not give γ, ζ-dioxo-ε-methylcaprylic acid, $CH_3-CO-\underset{\displaystyle CH_3}{\underset{|}{CH}}-CH_2-CO-CH_2-CH_2-COOH$, which was considered to be obtained by the furan ring opening. This result corresponds to the noteworthy fact

1) H. Midorikawa, This Bulletin, **26**, 460 (1953).

that the furfurylidene ketone

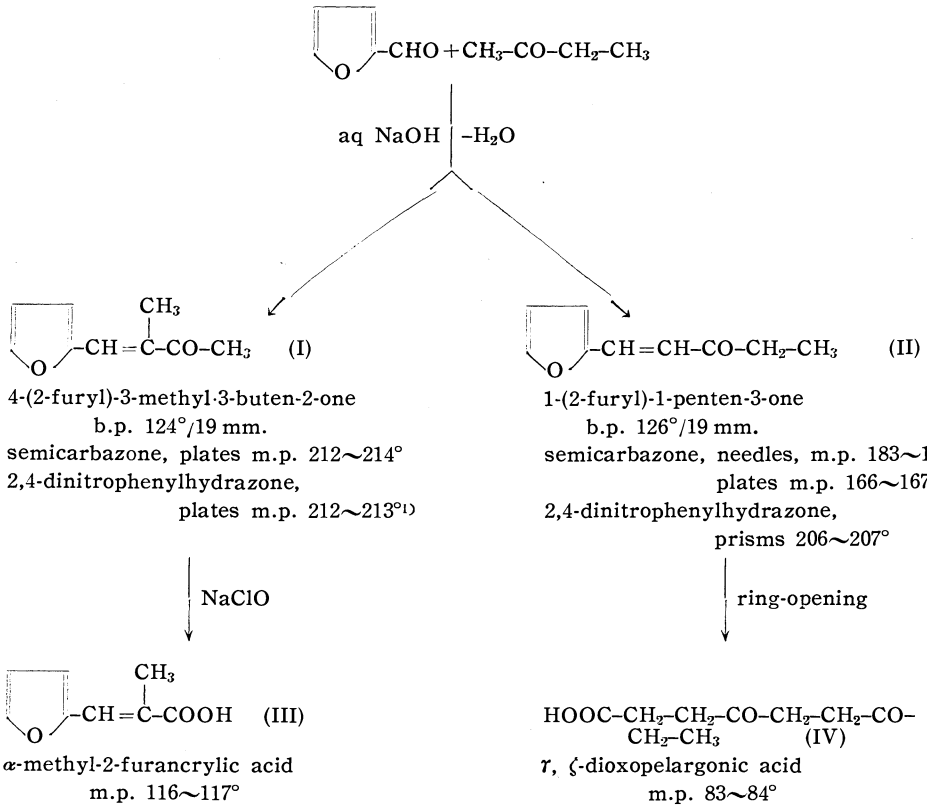


which possesses the alkyl group (R) at the carbon atom joining its carbonyl and furfurylidene groups, as in this keton, does not give the dioxocarboxylic acid R′-CO-CH(R)-CH_2-CO-CH_2-CH_2-COOH by the cleavage of the furan ring when refluxed with alcoholic hydrochloric acid[2], although there are a few exceptions[3].

The semicarbazones of needle crystals (m.p. 183~184°) and tabular crystals (166~167°) which were more soluble in methanol were selected from each other, after several recrystallisations. The latter crystals were not detected in the previous experiment[1]. The needle crystals appeared to shift to the tabular crystals comparatively less soluble in methanol on repeated recrystallisation by methanol-water. These two species of crystals were converted into the identical 2,4-dinitrophenylhydrazone of carmine needles (m.p. 206~207°), when reacted with 2,4-dinitrophenylhydrazine in alcoholic sulfuric acid. Obviously, one species of ketone gave the two species of semicarbazone, although it was not clear whether these two species are two forms in dimorphism or in syn-anti isomerism.

The mixture of these needle and tabular crystals of semicarbazone, on heating with dilute hydrochloric acid, generated a faintly yellow oil. This oil was considered to be 1-(2-furyl)-1-penten-3-one (II), since it generated no heat and gave no chloroform on treatment with aqueous sodium hypochlorite. This ketone gave the dioxocarboxylic acid (m.p. 83~84°) in a good yield, on refluxing with alcoholic hydrochloric acid. It seemed certain that this dioxocarboxylic acid is γ, ζ-dioxopelargonic acid (IV).

The reactions described above are illustrated in the following formulation.



Experimental

Condensation of furfural with methyl ethyl ketone Furfural (60 g.) and methyl ethyl ketone 120 g.) were dissolved in water (1000 cc.), and 10% aqueous sodium hydroxide (50 cc.) was at once run in at 60° with stirring. After prolonged

2) H. Midorikawa: This Bulletin, **26**, 317 (1953).
3) D. L. Turner: *J. Am. Chem. Soc.*, **71**, 612 (1949).

stirring for 1 hr. at 60°, the reaction mixture was worked up in the same manner as in the case of the previous report[1] to give a pale yellow oil (70 g.) distilling at 126~127°/20 mm.

This fraction (30 g.) was suspended in a solution of semicarbazide hydrochloride (30 g.) and sodium acetate (50 g.) in water (40 cc.) and methanol added, until a homogeneous solution was obtained. On standing overnight, crystals (40 g.) of semicarbazone separated out.

The crystals (40 g.) of semicarbazone were heated with methanol (200 cc.) on a water-bath, and, on cooling, a fraction(16 g.) of crystals melting at 205~210° was obtained. This fraction was once more washed with hot methanol (50 cc.) to give colourless crystals (15 g.) melting at 211~213°. From the filtrate pale yellow crystals (25 g.) melting at 130~140° were obtained by addition of a sufficient quantity of water. Several recrystallisations of these crystals from methanol gave a mixture (15 g.) of needles (m.p. 183~184°) previously reported[1] and plates (m.p. 166~167°), which were picked out from each other. On repetition of the recrystallisation, the needle crystals appeared to shift to the tabular crystals less soluble in methanol. Analysis of the tabular crystals (m.p. 166~167°): Found: C, 57.75, H, 6.12, N, 20.16. Calcd. for $C_{10}H_{13}O_2N_3$: C, 57.94, H, 6.32, N, 20.28%.

Both needle and tabular crystals were converted into the 2,4-dinitrophenylhydrazone (m.p. 206~207°), which showed no depression of the mixed melting point with 2,4-dinitrophenylhydrazone (m.p. 205~206°) obtained in the previous experiment[1].

4-(2-Furyl)-3-methyl-3-buten-2-one (I) The crystals (12 g.) melting at 211~213° were suspended in a mixture of conc. hydrochloric acid (20 cc.) and water (40 cc.), and heated for a brief time in the water-bath. The liberated oil, on extraction with ether, dehydration over calcium chloride and fractionation, gave a pale yellow oil (7 g.) distilling at 124°/19 mm. This sweet smelling ketone did not solidify at room temperature, and colourised on standing. Found: C, 71.53, H, 6.55. Calcd. for $C_9H_{10}O_2$: C, 71.96, H, 6.71%.

This ketone (1 g.) was suspended in sodium hypochlorite solution[1] (10 cc.) and the vessel kept in water at ordinary temperature for 2 days, with occasional shaking. The resulting chloroform was removed and the aqueous solution acidified with dilute hydrochloric acid to yield α-methyl-2-furanacrylic acid (III) (0.6 g.).

This ketone (2 g.) was refluxed with conc. hydrochloric acid (1.5 cc.) and alcohol (5 cc.) on the water-bath for 3 hrs. The reaction mixture, worked up in the same manner as previously reported,[1] did not give any dioxocarboxylic acid.

1-(2-Furyl)-1-penten-3-one (II) A semicarbazone mixture (12 g.) of the needle crystals (m.p. 183~184°) and tabular crystals (m.p. 166~167°) was treated with dilute hydrochloric acid in the same manner as in the case of 4-(2furyl)-3-methyl-3-buten-2-one (I) to give a pale yellow oil (7 g.) distilling at 126°/19 mm. This sweet smelling ketone also did not solidify at room temperature and colourised on standing. Found: C, 71.34, H, 6.57. Calcd. for $C_9H_{10}O_2$: C, 71.96, H, 6.71%.

This ketone, on suspencion in sodium hypochlorite solution at room temperature for 2 days, did not undergo any reaction.

This ketone (2 g.) was refluxed with conc. hydrochloric acid (1.5 cc.) and alcohol (5 cc.) for 3 hrs. in the water-bath. The reaction mixture, worked up in the same manner as previously reported, gave the dioxocarboxylic acid (0.8 g.) melting at 83~84° which was considered to be γ, ζ-dioxopelargonic acid (IV).

Summary

From the condensation product of furfural with methyl ethyl ketone by aqueous sodium hydroxide were isolated 4-(2-furyl)-3-methyl-3-buten-2-one (I) and 1-(2-furyl)-1-penten-3-one (II).

The former ketone (I) was oxidised by sodium hypochlorite to yield α-methyl-2-furanacrylic acid, (III) but gave no γ, ζ-dioxo-ε-methylcaprylic acid by refluxion with alcoholic hydrochloric acid.

The latter ketone (II) gave γ, ζ-dioxopelargonic acid (IV) by refluxion with alcoholic hydrochloric acid, but was no acted upon by sodium hypochlorite.

The semicarbazone of 1-(2-furyl)-1-penten-3-one (II) existed in two forms of the needle crystals melting at 183~184° and the tabular crystals melting at 166~167°.

The author expresses his sincere thanks to Dr. T. Hayashi for his kind advice.

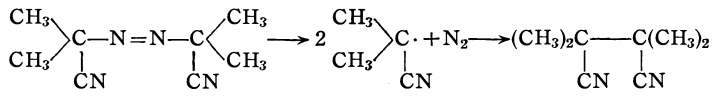
Scientific Research Institute, Komagome, Bunkyo-ku, Tokyo

The Dimerization of Trichloroethylene Induced by the Decomposition of α, α'-Azodiisobutyronitrile and the Structure of the Dimer

By Osamu SIMAMURA and Naoki INAMOTO

(Received December 14, 1953.)

α, α'-Azodiisobutyronitrile first prepared by Thiele and Heuser[1] decomposes thermally to give tetramethylsuccinonitrile and nitrogen, involving homolysis to intermediate radicals $(CH_3)_2\dot{C}CN$:



It acts therefore as a powerful initiator of the vinyl polymerization. The synthetical aspects of the chemistry of this and related compounds pertaining to this property have been reviewed by Ziegler[2]. The thermal decomposition of these compounds and the chemical nature of the radicals thereby produced have recently been the subject of numerous investigations[3]. It appeared to be of interest, as part of a study of chemical behavior of radicals in solution, to investigate the decomposition of α, α'-azodiisobutyronitrile in trichloroethylene which is known to give no high polymeric substances except in copolymerization with other reactive monomers[4]. In the present paper an account is given of the determination of the structure of the dimer of trichloroethylene produced by the agency of α, α'-azodiisobutyronitrile, and a mechanism of the dimerization is proposed.

By boiling trichloroethylene with 1 to 1.5 mole % of α, α'-azodiisobutyronitrile added in portions over a period of 35 to 64 hours and fractionating the reaction mixture a dimer, $C_4H_2Cl_6$, of trichloroethylene was obtained as a main product in 25 to 28% conversion (see Table I). The fractionation of higher polymeric products was not carried out, and the ratio of the weight of the dimer obtained to the weight of the residue from the distillation was shown in the column headed "Dimer/Polymers" in Table I. As Frank and Blackham[5] had reported the dimerization of trichloroethylene by means of dibenzoyl peroxide, we also repeated their experiment and the dimerized product was shown to be identical with that obtained by the action of α, α'-azodiisobutyronitrile by comparing their infrared spectra (see Fig. 1 and Table II).

TABLE I

DIMERIZATION OF TRICHLOROETHYLENE

Expt. No.	C_2HCl_3 g.	Azodinitrile mole %	Benzoyl peroxide mole %	Reaction time hrs.	Yield of dimer g.	B.p. °C/mm. Hg	Conversion %	Dimer/Polymers
1	131	1.5		35.5	27	103–5/10	25.3	4.4
2	168	1.0		38	31	117–8/18	24.5	3.0
3	320	1.0		64	79.5	111–3/12	28.3	7.3
4	240		1.0	41	120	98–100/7–8	58.3	6.0
Data from ref. 5			1.2	95		104.4/10	68.3	9.0

TABLE II

PROPERTIES OF DIMER $C_4H_2Cl_6$

Source	B.p. °C/mm. Hg*	d_4^{20}	n_D^{20}	MR_D
Expt. 3	104/10	1.6786	1.5452	49.51
Expt. 4	98–100/7–8	1.6727	1.5471	49.72
Ref. 5	104.4/10	1.6760	1.5461	49.66
				Calcd. 49.41

* Redistilled.

1) J. Thiele and K. Heuser, *Ann.*, **290**, 1 (1896).
2) K. Ziegler, *Brennstoff-Chem.*, **30**, 181 (1949).
3) See *Ann. Rep. on Progr. Chem.*, **49**, 115 (1952).
4) K. W. Doak, *J. Am. Chem. Soc.*, **70**, 1525 (1948).
5) C. E. Frank and A. U. Blackham, ibid., **72**, 3283 (1950).

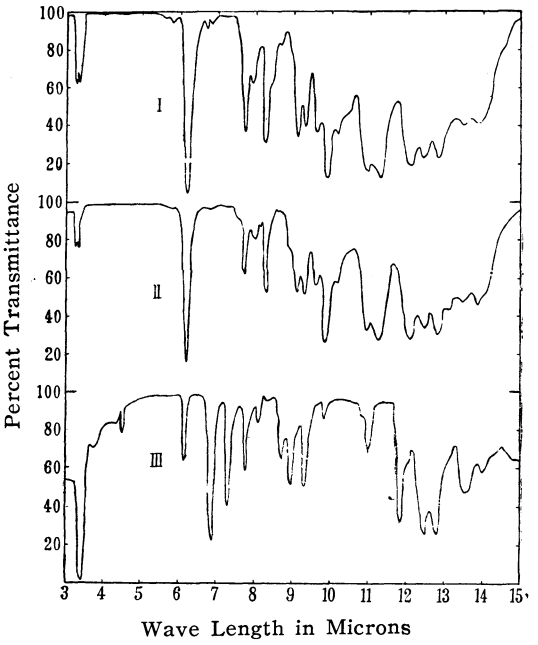
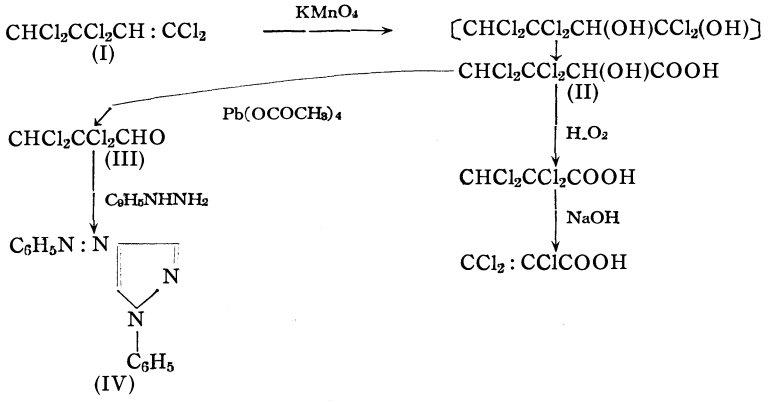


Fig. 1. Infrared absorption spectra of trichloroethylene dimers (I and II) obtained in the presence of azodiisobutyronitrile and dibenzoyl peroxide, respectively, and of 1, 1, 3, 3, 4-pentachloro-5-cyano-5-methyl-1-hexene(III).

The chemical constitution of the dimer of trichloroethylene (I) was established to be 1, 1, 3, 3, 4, 4-hexachloro-1-butene on the basis of the following degradations (see the annexed scheme). The oxidation of the dimer with potassium permanganate in cold aqueous acetone gave a crude acid (II), but it could be neither crystallized nor distilled without decomposition, and no attempt at characterization was therefore made. It was shown, however, that it is an α-hydroxy acid, because, in the first place, the action of the Fenton reagent[6] converted it to an acidic substance which gave a reddish brown precipitate with 2, 4-dinitrophenylhydrazine showing that an α-keto acid was formed, and secondly, on oxidation with lead tetraacetate according to Oeda[7], it gave an aldehyde (III). This aldehyde also was not isolated in a pure state, but it developed a purple color with Schiff's reagent and gave with excess phenylhydrazine 1-phenyl-4-phenylazopyrazole (IV), m. p. 126–7°, demonstrating that the aldehyde (III) contains three carbon atoms. The formation of the pyrazole from aldehyde III, which must be 2, 2, 3, 3-tetrachloropropanal, as will be seen below, is readily understandable from its structure; for α and β carbon atoms of the aldehyde carry respectively two chlorine atoms and their function may therefore be equivalent to a carbonyl group. The same pyrazole is obtained by the action of phenylhydrazine on compounds with analogous structural features, namely, 1, 1, 3, 3-tetrachloropropanone[8] and 1, 3-bisphenylhydrazone of propanonedial[9]. By heating the crude hydroxy acid (II) with 30% hydrogen peroxide 2, 2, 3, 3-tetrachloropropanoic acid, m. p. 79–80°, was obtained, which was dehydrochlorinated to 2, 3, 3-trichloropropenoic acid, m. p. 75–6°, by heating with aqueous sodium hydroxide. Thus, the grouping $CHCl_2CCl_2$- must be present in the dimer molecule and the double bond is accordingly located at the terminal position, the structure of the dimer having to be either $CHCl_2CCl_2CH:CCl_2$ or $CHCl_2CCl_2CCl:CHCl$. That the former structure is the correct one is shown by the formation of the three-carbon aldehyde (III) by the two-step cleavage of the double bond, which requires that carbon atom 2 of the dimer must bear a hydrogen atom. The structure of the hydroxy acid (II) must be 2-hydroxy-3, 3, 4, 4-tetrachlorobutanoic acid which is derived from the dimer (I) by hydroxylation at the double bond followed by hydrolysis and dehydration at carbon atom 1.



6) H. J. H. Fenton and H. O. Jones, *J. Chem. Soc.*, **77**, 71 (1900).
7) H. Oeda, This Bulletin, **9**, 8 (1934).
8) S. Levy and F. C. Witte, *Ann.*, **252**, 345 (1889); Th. Zincke and O. Kegel, *Ber.*, **22**, 1478 (1889).
9) H. v. Pechmann and L. Vanino, *Ber.*, **27**, 222 (1894).

Henne and Ruh[10] had attempted the determination of the structure of the trichloroethylene dimer obtained by means of dibenzoyl peroxide, but they could not decide between several possibilities. Frank and Blackham,[5] without presenting any experimental proof, had inferred the same structure as above by assuming that the dimerization of trichloroethylene follows a similar course to those of chlorinated olefins the structures of whose dimers are well established.[11,12] Since the identical dimer is obtained from trichloroethylene, as has been mentioned earlier, by means of either benzoyl peroxide or α, α'-azodiisobutyronitrile, the present structural proof is valid also for the dimers obtained by the American workers.

The residue from the fractionation of the dimer (Expt. No. 3) yielded a small amount of a new crystalline compound, m. p. 167–168°, which analyzed for $C_8H_8Cl_5N$ (see Fig. 1 for the infrared spectrum). In view of the established structure of the dimeric product and of the initiation of this reaction by α, α'-azodiisobutyronitrile, it is highly probable that this compound is 1, 1, 3, 3, 4-pentachloro-5-cyano-5-methyl-1-hexene (VI), which should result from the successive addition of 1-cyano-1-methylethyl radical produced from an initiator molecule to two molecules of trichloroethylene followed by loss of a chlorine atom (reactions 1, 3 and 4 shown in the following scheme). The isolation of the compound $C_8H_8Cl_5N$ is significant in that, in the first place, it contains a radical moiety from the initiator molecule, thus demonstrating the mechanism of the initiation, and further, it affords an experimental proof of the chlorine atom being transferred from a growing radical chain to a molecule of trichloroethylene, a new chain being thereby initiated. Thus, we are led to formulate the initiation, propagation and termination of the dimerization as follows:

$$(CH_3)_2\dot{C}(CN) + CHCl:CCl_2 \longrightarrow (CH_3)_2CCHCl\dot{C}Cl_2(CN) \quad \cdots(1)$$

$$(CH_3)_2CCHCl\dot{C}Cl_2(CN) + CHCl:CCl_2 \longrightarrow \begin{cases} (CH_3)_2CCH(CN):CCl_2 + CHCl_2\dot{C}Cl_2 & \cdots(2) \\ \quad (V) & \\ (CH_3)_2CCHClCCl_2CHCl\dot{C}Cl_2(CN) & \cdots(3) \end{cases}$$

$$(CH_3)_2CCHClCCl_2CHCl\dot{C}Cl_2(CN) + CHCl:CCl_2 \longrightarrow \begin{cases} (CH_3)_2CCHClCCl_2CH:CCl_2(CN) \\ \quad (VI) \\ \quad + CHCl_2\dot{C}Cl_2 & \cdots(4) \\ (CH_3)_2C(CHClCCl_2)_2CHCl\dot{C}Cl_2(CN) & \cdots(5) \end{cases}$$

$$CHCl_2\dot{C}Cl_2 + CHCl:CCl_2 \longrightarrow CHCl_2CCl_2CHCl\dot{C}Cl_2 \quad \cdots(6)$$

$$CHCl_2CCl_2CHCl\dot{C}Cl_2 + CHCl:CCl_2 \longrightarrow \begin{cases} CHCl_2CCl_2CH:CCl_2 + CHCl_2\dot{C}Cl_2 & \cdots(7) \\ CHCl_2(CCl_2CHCl)_2\dot{C}Cl_2 & \cdots(8) \end{cases}$$

In the above formulation the transference of the chlorine atom is shown as occurring by a collision between a radical and a molecule of trichloroethylene. However, the possibility could not be excluded experimentally that the transference is effected by initial decomposition of the radical into a stable molecule and a chlorine atom, the latter adding subsequently to a molecule of trichloroethylene to give radical $CHCl_2\dot{C}Cl_2$.

A search for 1, 1-dichloro-3-cyano-3-methyl-1-butene (V) failed, the formation of which should be expected from the mode of initiation and the comparative ease of transference of the chlorine atom to trichloroethylene. Reactions 5 and 8 giving rise to higher polymeric products are of subordinate importance, as is seen from the last column in Table I, in line with the observation that trichloroethylene is unable to give high polymeric

10) A. L. Henne and R. P. Ruh, *J. Am. Chem. Soc.*, **69**, 279 (1947).
11) K. E. Wilzbach, F. R. Mayo and R. Van Meter, ibid., **70**, 4069 (1948).
12) M. S. Kharasch and G. Büchi, *J. Org. Chem.*, **14**, 84 (1949).

substances on account of the steric hindrance exerted by the chlorine atoms at the double bond.

The dimerization by a chain transer reaction in which a halogen atom is transferred from the dimer radical to the monomer has originally been suggested by Wilzbach and Mayo[11] for methallyl chloride, and Kharasch and Büchi[12] explained the formation of 5-bromo-4-(bromomethyl)-1-pentene in the decomposition of acetyl peroxide in allyl bromide on the basis of a similar mechanism. The present study has brought foward another case in which such a mechanism is operative.

Experimental

Materials α, α'-Azodiisobutyronitrile was prepared according to Thiele and Heuser[1], and recrystallized from ether, m. p. 104° with decomposition. Commercial trichloroethylene was washed with aqueous potassium carbonate and then with water, dried with calcium chloride and fractionated. A fraction boiling at 87.0° was used.

Dimerization To boiling tricholoroethylene under reflux 1 to 1.5 mole % of α, α'-azodiisobutyronitrile was added in portions over a period of 35 to 64 hours, towards the end of which the temperature of the heating bath had to be elevated to 135° to keep the liquid refluxing. The results of three runs are shown in Table I. A reaction mixture, on cooling, deposited tetramethylsuccinonitrile (e.g., 0.14 g. in Expt. No. 3), m.p. 169°; the filtered solution was repeatedly fractionated through a Vigreux column 50 cm. in length; unreacted trichloroethylene was recovered and the dimer distilled over at 104° at 100 mm. Hg (Found: C, 18.7; H, 1.0; Cl, 80.86. Calcd. for $C_4H_2Cl_6$: C, 18.3, H, 0.8; Cl, 80.99%.). The residue from the fractionation, treated with ether, deposited 0.4 g. of 1, 1, 3, 3,4-pentachloro-5-cyano-5-methyl-1-hexene (VI), m. p. 167–8° (from alcohol) (Found: C, 32.7; H, 2.6; N, 4.73; Mol. wt. (Rast), 296. Calcd. for $C_8H_8Cl_5N$: C, 32.5; H. 2.7; N, 4.74%; Mol. wt., 295.5). When the mother liquor was subjected to distillation at 0.04 mm. Hg., 5.6 g. of unidentified viscous oil (probably a trimer etc.) passed over at 122–124°, from which a further 0.3 g. of the pentachlorocyanomethylhexene crystallized out.

Degradation of the Dimer Potassium permanganate (6.5 g.) was added in portions with shaking to 5.0 g. of the dimer dissolved in 30 cc. of acetone and 5 cc. of water cooled with water at 10°. The mixture was filtered from the manganese dioxide, which was then washed with acetone. The filtrate and the washing were combined and evaporated on a water bath. The residue was neutralized with hydrogen sodium carbonate, the solution evaporated under diminished pressure of a water pump, and the residue extracted with ether to remove neutral substances. It was acidified with dilute hydrochloric acid and saturated with sodium chloride, and the solution was extracted repeatedly with ether. The ethereal extracts were combined and dried with anhydrous sodium sulfate and the ether was removed on a water bath giving 2.5 g. of a liquid residue comprising 2-hydroxy-3, 3, 4, 4-tetrachlorobutanoic acid (II), which could not be brought to crystallization by keeping over concentrated sulfuric acid in an evacuated desiccator for seven days.

To the crude α-hydroxy acid (II) (2.0 g.) in 5 cc. of water heated in a boiling water bath 30% hydrogen peroxide was added drop by drop over a period of one hour until the presence of its excess was shown by potassium iodide-starch paper. The reaction mixture was cooled and extracted with ether and the ether removed. The liquid residue (1.2 g.), on being kept over concentrated sulfuric acid in an evacuated desiccator for three days, deposited 0.3 g. of hygroscopic crystals of 2, 2, 3, 3-tetrachloropropanoic acid, m. p. 79–80° (from petroleum ether, reported m. p. 76°[13]) (Found: Cl, 66.63; neutralization equivalent, 222. Calcd. for $C_3H_2Cl_4O_2$: Cl, 66.98%; neutralization equivalent, 212). Further crops of the acid (a total of 0.8 g.) were obtained after several days. This acid (1 g.) was heated with 0.4 g. of sodium hydroxide in 5 cc. of water, the mixture acidified with hydrochloric acid and extracted with ether, the ether removed and the residue recrystallized from petroleum ether to give 0.8 g. of 2, 3, 3-trichlropropenoic acid, m. p. 75–6° (reported m. p. 76°[14]) (Found: neutralization equivalent, 182.5. Calcd. for $C_3HCl_3O_2$: 175.5).

To a stirred solution of 0.5 g. of the α-hydroxy acid (II) in 25 cc. of benzene at 60–80° lead tetraacetate was added in portions until the oxidizing power began to persist in the solution (potassium iodide-starch paper). It took about one hour. The excess lead tetraacetate was destroyed by heating for 30 minutes with anhydrous oxalic acid. The benzene solution developed a purple color with Schiff's reagent. It was distilled on a water bath to remove benzene, the residue added with 30 cc. of alcohol and filtered. The filtrate was heated with 2 g. of phenylhydrazine, some precipitate filtered off, and the filtrate concentrated on a water bath to give golden yellow crystals of 1-phenyl-4-phenylazopyrazole, m. p. 126–7° (from alcohol, yield 50 mg.) (Found: N, 22.9. Calcd. for $C_{15}H_{12}N_4$: 22.57%).

Infrared Data The infrared spectra were recorded on a Baird Double Beam Spectrophotometer equipped with rock salt optics. They were shown in Fig. 1. The spectrum of 1, 1, 3, 3, 4-pentachloro-5-cyano-5-methyl-1-hexene suspended in liquid paraffin shows an absorption band of the nitrile group at 4.5 μ and that of the ethylenic bond at 6.13 μ.

Summary

1. Trichloroethylene has been dimerized by

13) C. F. Mabery and A. W. Smith, *Ber.*, **22**, 2659 (1889).
14) J. Böeseken and P. Dujardin, *Rec. trav. chim.*, **32**, 97 (1913).

boiling with α, α'-azodiisobutyronitrile to $C_4H_2Cl_6$, which has been identified as 1, 1, 3, 3, 4, 4-hexachloro-1-butene by degradation.
2. A compound of molecular formula $C_8H_8Cl_5N$, whose structure is presumably 1, 1, 3, 3, 4-pentachloro-5-cyano-5-methyl-1-hexene, has been isolated. This fact indicates that the reaction is initiated by the addition of 1-cyano-1-methylethyl radical to trichloroethylene and propagated by the transference of a chlorine atom from the dimeric radical to a molecule of the monomer.
3. The decomposition of dibenzoyl peroxide in trichloroethylene gives the same dimer as above, the structural identity being confirmed infrared spectrometrically.

The authors' thanks are due to Dr. H. Kamada and Mr. S. Tanaka, Engineering Research Institute, for measuring the infrared spectra and to the Ministry of Education for a Grant-in-Aid for Scientific Research.

Department of Chemistry, Faculty of Science, Tokyo University, Tokyo

Spectrochemical Study of Microscopic Crystals. V. Relation between Dichroism and Direct Interaction between Metal Atoms in the Crystals of Bis (Dimethylglyoximo)-Copper (II), Nickel (II) and Platinum (II)[1]

By Shoichiro YAMADA and Ryutaro TSUCHIDA

(Received December 24, 1953)

In the earlier papers the present authors reported on the dichroism of those complex compounds which exhibit unusually deep colours in the crystalline state as compared with those in solution, and concluded that in the crystals of Magnus's green salt[2] and salts of tetracyanoplatinate (II)[3] there exists direct interaction between the central platinum atoms of planar complexes, which are arranged in such a way that they are piled one just above and below another. Recently Godycki and Rundle[4] reported on the crystal structure of bis (dimethylglyoximo)-nickel (II) and suggested the possibility of a direct, though weak, interaction between nickel atoms. They also asserted that the pleochroism of the crystal supported the above assumption, but gave no experimental value for the absorption coefficients. Moreover, their descriptions of the dichroism contradict our measurements, though the conclusion arrived at through their argument on the basis of their qualitative observation happens to be similar to ours. In this paper we report on the quantitative dichroism measurement of the crystals of bis (dimethylglyoximo)-copper (II), nickel (II) and platinum (II), and discuss the relation between the dichroism and the state of the complex molecules in these crystals.

1) Read before the meeting of the Symposium on Coordination Compounds, Nagoya, Japan, November 8, 1953.

2) R. Tsuchida and S. Yamada, *J. Chem. Soc. Japan*, **70**, 44 (1949); S. Yamada, *J. Am. Chem. Soc.*, **73**, 1579 (1951).

3) S. Yamada, This Bulletin, **24**, 125 (1951).

4) L. E. Godycki and R. E. Rundle, *Acta Cryst.*, **6**, 478 (1953).

Experimental

Materials. Bis (dimethylglyoximo) Copper (II) Black monoclinic prisms were obtained from solutions of copper acetate and of dimethylglyoxime in 50% alcohol. The crystal is remarkably dichroic; it appears to be dark reddish brown with linearly polarized light having its electric vector along the c-plane, the c-axis being the needle axis, and brownish yellow with that having its electric vector perpendicular to the c-plane. The Dichroism measurement was made with reference to the above two directions.

Bis (dimethylglyoximo) Nickel (II) The compound was prepared from an aqueous solution of nickel sulphate and an alcoholic solution of dimethylglyoxime, and recrystallized from chloroform. Red acicular crystals of orthorhombic system were obtained. A distinct dichroism was observed with a thin crystal under the microscope; the crystal appears red with linearly polarized light having its electric vector parallel to the needle axis, and orange with that having its electric vector perpendicular to the axis. The measurement was made in reference to these two directions.

Bis (dimethylglyoximo) platinum (II) Chocolate-coloured acicular crystals were prepared from an aqueous solution of potassium tetrachloroplatinate (II) and an alcoholic solution of dimethylglyoxime.[5] The crystal is strongly dichroic; it appears greenish black with the electric vector

5) Gmelins Handbuch der anorg. Chem., 7. Aufl., Band 5, 1915, p. 604.

parallel to the needle axis, and orange with the electric vector perpendicular to the above. The dichroism measurement was per formed on the prism face in the above mentioned directions.

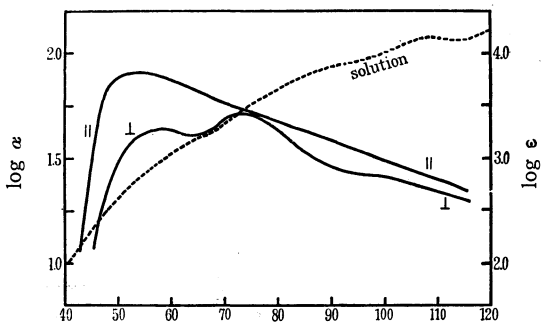
Measurements.—Quantitative dichroism measurement of the crystals was performed by the Tsuchida-Kobayashi's microscopic method.[6] α denotes absorption coefficient per mm. of a crystal. Molecular absorption coefficients of a crystal, k, were calculated from the relation, $k=10\alpha M/\rho$, where M and ρ represent molecular weight of the compound and density of the crystal, respectively.

Absorption spectra were obtained with a Beckman DU spectrophotometer in a chloroform solution of the nickel compound, and in an alcoholic solution of the copper compound. Extinction coefficients, ε, are given by the following expression, $\varepsilon=1/\text{cd.}\ \log(I_0/I)$.

$\parallel$-or $\perp$-absorption means absorption of light with the electric vector parallel or perpendicular to the plane of the molecule, respectively.

Results and Discussion

Bis (dimethylglyoxime) copper (II) Results of the measurement are shown in Fig. 1, and tabulated in Table I. The crystal



Frequency (ν), 10^{13}/sec.

Fig. 1. Absorption spectra of bis (dimethylglyoximo) copper (II).

structure analysis was reported by Bezzi et al.[7] According to their results, the planes of the planar molecules are parallel to each other and als to othe c-plane of the crystal. That is, the absorption spectrum with the electric vector along the c-plane corresponds to the $\parallel$-absorption and the absorption with the electric vector perpendicular to the c-plane corresponds to the $\perp$-absorption.

TABLE I

ABSORPTION MAXIMA OF BIS (DIMETHYLGLYOXIMO) COPPER (II)

	10^{13}/sec. ν	log α	k
$\parallel$-abs.	54	1.91	182×10^3
$\perp$-abs.	58	1.64	98×10^3

$\Delta\nu=4\times10^{13}$/sec., $\Delta\log\alpha_{max}=0.27$, $\alpha_{\parallel}:\alpha_{\perp}=1.86:1$.

It has been known that complexes of copper (II), in general, show in the visible or infrared region an absorption band which can be ascribed to the linkages between the metal and the ligands. Comparing the absorption curves of copper-dimethylglyoxime with those of other cupric complexes, the band at $\nu=58\times10^{13}$/sec. (Band A) for the $\perp$-absorption is considered as due to the linkages between copper and the ligands. Most metallic compounds with dimethylglyoxime or similar compounds,[8,9] which have π-electron system, exhibit absorption curves of complicated structure and also a band which can be supposed to be originated from dπ interaction between d-electrons of a transition metal atom and electrons of a ligand.[10] Thus the band at $\nu=73.2\times10^{13}$/sec. (Band B) is tentatively assumed to be of a similar nature to the above band associated with dπ interaction.

The $\parallel$-absorption shows only a flat curve without a definite peak; it may be a superposition of the band A and band B.

With the absorption band A, the following regularity on the dichroism is obtained: *the $\parallel$-absorption is bathochromic and hyperchromic to the $\perp$-absorption.* The relation is similar to that which had been induced previously with planar quadri-coordinated complexes of transition metals,[11,12] and therefore can be understood in the same way as previously reported. Thus, since the electric moment associated with the linkage between copper and nitrogen atoms should be larger in the direction along the complex plane than in the direction perpendicular to the plane, $\parallel$-absorption is expected to be hyperchromic to the $\perp$-absorption. This was found to be the case with the cupric complex. Hence,

6) R. Tsuchida and M. Kobayashi, "The Colours and the Structures of Metallic Compounds," Zoshindo, Osaka, Japan, 1944, p. 180. See also the previous papers of this series.

7) S. Bezzi, E. Bua and G. Schiavinato, *Gazz. Chim. Ital.*, **81**, 856 (1951).

8) Some of curves are found in Ref. 6, p. 194.

9) Data with cobaltic compounds are given in H. Kuroya, *J. Inst. Polytech. Osaka City Univ.*, **1**, 11 (1951).

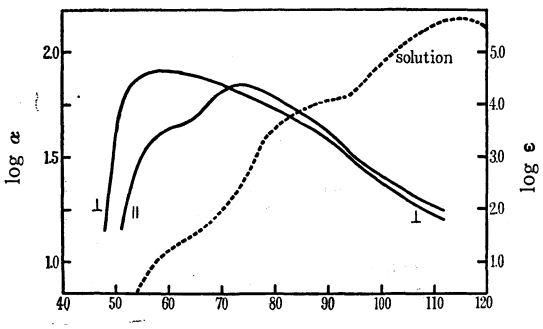
10) P. Krumholz, *J. Am. Chem. Soc.*, **75**, 2163 (1953), etc.

11) About palladium (II) and platinum (II) complexes, see S. Yamada, *J. Am. Chem. Soc.*, **73**, 1182 (1951); S. Yamada and R. Tsuchida, This Bulletin, **23**, 439 (1953).

12) About cupric complexes, to be published later.

the dichroism indicates that the molecules in this crystal exist as independent units, in agreement with the result of the crystal structure analysis.[7]

Bis (dimethylglyoximo) nickel (II) Results of the measurement are shown in Fig. 2, and tabulated in Table II. According to



Frequency (ν), 10^{13}/sec.

Fig. 2. Absorption spectra of bis (dimethylglyoximo) nickel (II).

the crystal analysis by Godycki et al.,[4] the planes of the complexes are parallel to each other and perpendicular to the c-axis, with the nickel atoms situated on lines along the c-axis. As in the case of the corresponding copper complex, it is supposed that the band of the ∥-absorption with its maximum at $\nu=60\times10^{13}$/sec. (Band A) is originated from transitions directly related to the linkages between the metal and the co-ordinating atoms, and that the band (Band B) with its maximum at $\nu=74\times10^{13}$/sec., which is reasonably considered as corresponding to the band at $\nu=86\times10^{13}$/sec. with the solution, may be due to the specific dπ interaction between the metal with d-electrons and atoms of the ligands with π-electrons. Instead of the two distinct bands in the ∥-absorption, only a broad absorption band is observed in the ⊥-absorption; in the latter both the bands would come so close together that only superposition of them may be observed. As to the band A, which has been assumed to

TABLE II

ABSORPTION MAXIMA OF BIS (DIMETHYLGLYOXIMO) NICKEL (II)

	10^{13}/sec. ν	log α	k
∥-abs.	61	1.63	76×10^3
⊥-abs.	59	1.91	144×10^3

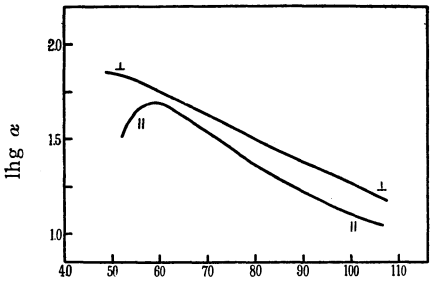
$\Delta\nu=2\times10^{13}$/sec., $\Delta\log\alpha_{max}=0.28$, $\alpha_{\parallel}:\alpha_{\perp}=0.53:1$.

be ascribed to the co-ordination linkages, there can be found the following relation: *the ⊥-absorption is by far hyperchromic to the ∥-absorption.* The relation is reverse to those observed with the corresponding copper compound, and also with metallic planar complexes of the normal type, that is, the type without the interaction between adjacent molecules.[11,12] The above relation that the electric vector perpendicular to the complex plane is more strongly absorbed than the vector along the plane indicates that the planar complexes are under some effect in the direction perpendicular to the planes of the complex molecules, and that the effect must be of such a nature as to cause a direct influence on the co-ordination linkages.

Such an effect would be considered to be a direct interaction between the nickel atoms which are arranged one just above and below another. Godycki et al.[4] also suggested, on the basis of their erroneous observation, similar interaction in this compound; their observation that the electric vector is more strongly absorbed along the plane of the complex than in the direction perpendicular to the plane is quite incomprehensible and seems incorrect.

Interactions between π-electrons might be considered besides the metal-metal interaction. However, since the complex molecules piled above and below one another are rotated about ninety degrees with respect to each other, the interaction between the π-electron systems of adjacent molecules may be ruled out. It is also probable that π-π interaction between the nitrogen atoms may contribute to this result to some extent, judging from the distance between nitrogen atoms of adjacent molecules. It seems reasonable, however, to consider that the motal-metal interaction should be dominant, compared with the contribution of the π-π interaction.

Bis (dimethylglyoximo) platinum (II) Results of the measurement are shown in Fig. 3. The crystal structure analysis of the compound has not been reported. However, judging from the crystal structure of the corresponding nickel and palladium compounds,[4] it is probably certain that the complex planes in the platinum (II) compound are parallel to each other and perpendicular to the needle axis, just as in the case of the other two. On the basis of the above assumption was assigned the ∥-and ⊥-absorp-



Frequency (ν), 10^{13}/sec.
Fig. 3. Absorption spectra of bis (dimethylglyoximo) platinum (II).

tion. Since the ⊥-absorption stretches out beyond the region of measurement, the maximum could not be determined. It is seen that the crystal of the platinum-dimethylglyoxime compound shows its absorption in the extraordinarily long wave-length region, in comparison with other platinum compounds such as potassium tetrachloro-, tetrabromo-,[11,13] and dioxalato-[14] platinate (II), and others. This suggests that some effect might be exerted upon the planar molecules in the former compound. Further, by inspecting the dichroism, the following relation is found: *the ⊥-absorption is much more hyperchromic and bathochromic than the ∥-absorption.* The above relation is reverse to that in case of complexes of the normal type. The reversal of the effect as to the dichroism indicates that the effect, which has direct influence on the absorption closely connected with the linkages between the metal and the ligands, should be taken into consideration. Hence, as in the case of the corresponding nickel compound, a direct interaction is supposed to exist between platinum atoms.

The Nature of the Metal-Metal Interaction The metal-metal interaction as proposed in the nickel-and platinum-dimethylglyoxime compounds is considered to be of a similar nature to the interaction which was previously reported by the present authors in the case of Magnus's green salt[2] and salts of tetracyano-platinate (II).[3] In order to explain the metal-metal interaction in the latter crystals, the following assumption was presented in the former report.[2,3] In the quadri-coordinated planar complexes of platinum (II), four atoms of the ligands with two pairs of electrons around the central metal form octahedral hybridization.[15] The pairs of electrons above and below platinum cores of the complexes exert mutual effects upon one another, overlapping of electronic density being naturally expected (Fig. 4).

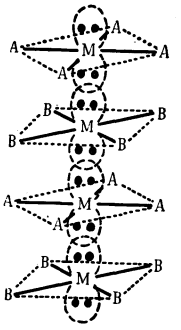


Fig. 4. Metal-metal interaction in the Magnus's type compounds.

The same assumption may apply to the crystal of the nickel (II)-and platinum (II)-dimethylglyoxime compounds. When the above metal-metal interaction is getting stronger, the overlapping of the electrons may also become larger. In other words, the greater the overlapping of the electrons, the more the sharing of electrons. In the extreme structure, in which the overlapping might reach the extremity, complete sharing of electrons might happen (Extreme structure II in Fig. 5).[16] It may be reasonably supposed that the more stable the extreme structure, the larger would be the overlapping and the greater the contribution of the structure would result, in which sharing of the electrons is complete. It is to be noted that the metal-metal interaction of the said type has been found mostly with the compounds

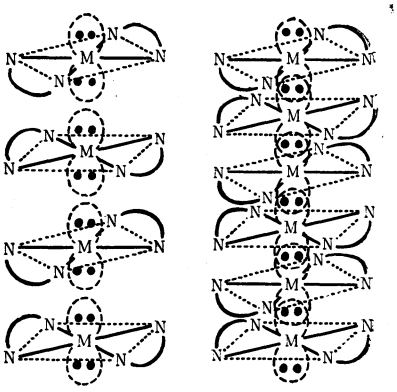


Fig. 5. Extreme structures of some metallic dimethylglyoximo compounds involving metal-metal interaction.

13) S. Yamada, H. Yoneda and R. Tsuchida, *J. Chem. Soc., Japan.* **69**, 145 (1948).
14) R. Tsuchida and S. Yamada, unpublished.
15) About the possibility of octahedral hybridization in quadri-coordinated planar complexes, see, for example, R. Tsuchida, M. Kobayashi and H. Kuroya, *Rev. Phys. Chem. Japan*, **13**, 158 (1939).
16) The contribution of the extreme structure, in which complete sharing of an electron pair occurs, was recently pointed out by Godycki et al. (Ref. 4).

of Ni (II), Pd (II) and Pt (II). In order to explain such tendency, we wish to propose the following hypothesis: *When complete sharing of electrons would occur between complex molecules arranged above and below one another (structure II), Ni (II), Pd (II) and Pt (II) would attain the effective atomic number of the rare gases and thereby the extreme structure II (Fig. 5) might be stabilized.* Thus the larger contribution of the extreme structure II, and hence the greater stability of the metal-metal interaction, could be explained in terms of the above hypothesis with Ni (II), Pd (II) and Pt (II) compounds.

The same assumption applies satisfactorily also to the stability of the molecule of copper acetate, $Cu_2(CH_3CO_2)_4 \cdot 2H_2O$,[17] in which, according to the above hypothesis, the copper atoms in the extreme structure would attain the effective atomic number of krypton by sharing one pair of electrons between two copper atoms.

Summary

Dichroism of the crystals of bis (dimethylglyoximo)-copper (II), nickel (II) and platinum (II) has been quantitatively determined by the microscopic method in the region from 2400 to 7000 Å.

The crystal of the copper compound has been found to show dichroism of the normal type, indicating that no specific metal-metal interaction can be expected in this crystal.

The crystals of the nickel (II) and platinum (II) compounds exhibit anomalous dichroism. It has been concluded that in these crystals there should exist metal-metal interaction.

A hypothesis has been presented, in order to explain the tendency that the specific metal-metal interaction similar to that proposed above has been found mostly with Ni (II), Pd (II) and Pt (II) compounds.

The authors wish to thank Mr. E. Hongo of Nisshin Chemicals Co. for his help in the experimental work and the Analytical Laboratory of our department for measurement of absorption spectra in solution. Thanks are also due to the Ministry of Education for a grant.

Department of Chemistry, Faculty of Science, Osaka University, Nakanoshima, Osaka

17) About the configuration of the molecule, see J. N. van Niekerk and F. R. L. Schoening, *Acta Cryst.*, **6**, 227 (1953).

*Dipole Moments of Cyclic Siloxanes and Thiosiloxanes**

By Yukio KURITA and Michio KONDO

(Received December 25, 1953)

Introduction

The molecular structures of cyclic siloxanes have been studied in various ways, especially by electron diffraction[1,2] and by X-ray study[3]. Although Sauer and Mead[4] calculated the dipole moments of several cyclosiloxanes from the dielectric measurements on pure liquids, they did not discuss the configuration in detail. The physicochemical studies of cyclothiosiloxanes have not yet been carried out extensively, but Yokoi and Nomura[5] have made electron diffraction studies on these compounds.

The measurement of the dipole moments of these compounds in nonpolar solvents seemed to be desirable to elucidate the geometrical configurations and atomic polarizations of these compounds as well as the polarity of Si-O and Si-S bonds. Hence we measured the dipole moments of hexamethyldisiloxane, two cyclosiloxanes, and two cyclothiosiloxanes in benzene solution.

Experimental

The materials used were kindly given to us by Mr. M. Yokoi of Nagoya University. They are:

I. Hexamethyldisiloxane. b.p. 98°.
II. Hexamethylcyclotrisiloxane. m.p. 64.5°, b.p. 135°.
III. Octamethyltetracyclosiloxane. m.p. 17.4°, b.p. 171°.

* Read before the Annual Meeting of the Chemical Society of Japan held on April 4, 1953.

1) E. H. Aggerwal and S. H. Bauer, *J. Chem. Phys.*, **18**, 42 (1950).
2) M. Yokoi, (to be published shortly).
3) L. K. Frevel and M. J. Hunter, *J. Am. Chem. Soc.*, **67**, 2275 (1945).
4) R. O. Sauer and D. J. Mead, *J. Am. Chem. Soc.*, **68**, 1794 (1946).
5) M. Yokoi and T. Nomura, (to be published shortly).

IV. Tetramethylcyclodithiosiloxane*. m. p. 105.5°, b.p. 172–3°.
V. Hexamethylcyclotrithiosiloxane*. m. p. 17–8°, b.p. 151.5–3.5°
(38 mm. Hg.)

The apparatus and the method of measurements were the same as given already in our previous paper[6]. For the calculation of $P_{2\infty}$, we used a modified Hedestrand's method[7]. The results are shown in Table I. The values of P_0+P_A of these compounds are not very large, and the calculated moments therefore depend sensitively upon the assumed values of P_A. The values in Table I are considered to be most reasonable, as will be discussed in the following.

TABLE I

DIPOLE MOMENTS OF CYCLOSILOXANES AND CYCLOTHIOSILOXANES IN BENZENE SOLUTION

	temp.	ε_1	d_1 (g./cc.)	α	(g./cc.)	$P_{2\infty}$ (cc.)	R_D	P_A	μ(D)
I	20°	2.2845	0.87610	0.13	−0.12	67.1	48.9	4.9=0.1R	0.80
II	30°	2.2632	0.86642	−0.070	0.047	66.7	55.8	10.9=0.2R	0.0
III	25°	2.2750	0.87114	0.11	0.082	98.1	74.5	14.5=0.2R	0.67
IV	30°	2.2652	0.86554	0.348	0.133	64.3	55.3	9.0	0.0
V	20°	2.2839	0.87635	0.804	0.162	116.0	82.9	10.9	1.03

The data found in the literature of the subject to be compared with the present results are that of the compound I 0.79D measured by Freiser, Eagle and Speier[8], which is in good agreement with ours. Sauer and Mead found the values 0.74D and 1.09D for the moment of I and III respectively. Their results, however, should not be compared directly with our results, since their measurements were carried out on pure liquids.

Discussion of the Results

Polarity of Si-O bond If we use ∠SiOSi =130°, evaluated from electron diffraction data of the experiment on I,[9] and the moment of 0.80D observed for I, the moment of Me_3SiO-group can be calculated as 0.80/(2 cos 65°)=0.95D**, which is identical with the value estimated by Freiser and others. It is only half as great as the value, 2.2D estimated by Sauer and Mead[4]. On the assumption that the bond moment of O-H is equal to 1.5D and the valency angle SiOH to 110°, the moment of trimethylsilanol is calculated to be 1.5D or 2.2D, according to the value of Me_3SiO-group moment of 0.95D or 2.2D. If we compare these values with the observed moment of Et_3SiOH[10], 1.50D, it may be concluded that the Me_3SiO-group moment estimated by us is more proper than that of Sauer and Mead***. Subtracting the bond moment of Si-C (1.0D) and H-C (0.4D) algebraically from the Me_3SiO-moment (0.95D), we obtain the Si-O bond moment as 1.55D.

If we take into consideration the contribution of the ionic structure $Si^+—O^-$ only, the Si-O moment is calculated to be 3.2D, twice as large as the observed value. This discrepancy is explained as follows. It has generally been acknowledged by many authors that silicon has an ability to expand the valency shell beyond octet and to from multiple bonds. Therefore the $Si^-=O^+$ double bond structure contributes to the normal state in such a manner as to cancel the moment of $Si^+—O^-$ structure partly. Pauling[11] presented an elaborate method of calculating the percentage character of the polar and the double bond structure in oxygen acid, such as silicate ion. If we apply his method to the bond of siloxane, the ionic character of $Si^+—O^-$ is estimated to be 41%, the double bond character of $Si^-=O^+$ to be 27% and the Si-O bond length to be 1.63A. From these values, SiO moment is calculated to be 1.1D, which agrees fairly well with the observed value of 1.55D, considering the approximations made in the calculation.

Atomic Polarization of Cyclotrisiloxane and Cyclodithiosiloxane From an electron diffraction study of hexamethylcyclotrisiloxane II, Aggerwal and Bauer[1] concluded that it has a planar structure. Frevel and Hunter[3] reached the same conclusion from an X-ray investigation on it. Accordingly it is reasonable to assume that it has a planar structure with no permanent moment even in

* T. Nomura, M. Yokoi and K. Yamasaki, *Proc. Japan Acad.*, **29**, 342 (1953).

6) Y. Kurita, T. Nozoe and M. Kubo, This Bulletin, **21**, 10 (1951).

7) Y. Kurita, T. Nozoe and M. Kubo, This Bulletin, **26**, 242 (1951).

8) H. Freiser, M. V. Eagle and J. Speier, *J. Am. Chem. Soc.*, **75**, 2824 (1953).

** If we use the value of ∠SiOSi=137° cited in *Ann. Rev. Phys. Chem.*, **2**, 224 (1951) instead of 130°, the moment of Me_3SiO-group is calculated as 1.09D.

*** From the constancy of the moments per monomeric units of dimethylsiloxane polymers greater than tetramers, they concluded that −O=160° and that the group moment of Me_3SiO is equal to 2.2D. However, the observed moments can be explained adequately with our value for the bond moment, if a slight hindrance of rotation about Si-O bond is assumed to be present.

9) K. Yamasaki, A. Kotera and M. Yokoi, *J. Chem. Phys.*, **18**, 1414 (1950).

10) M. Pizotti, *Gazz. Chim. Ital.*, **73**, 143 (1943).

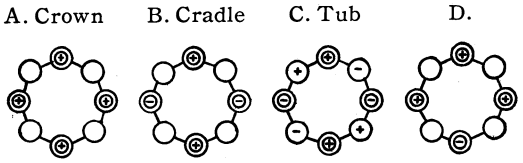
11) L. Pauling, *J. Phys. Chem.*, **56**, 361 (1952).

solution. Then we are led to the conclusion that II has the atomic polarization of 10.9 cc., amounting to 20% of the electronic polarization. It is not an unreasonable value as compared with the large atomic polarization of compounds with a similar ring structure, such as paraldehyde (11.4 cc.) and trioxane[12] (13 cc.). Baker et al.[13] obtained large atomic polarizations for linear polysiloxanes.

In the molecule IV, the distortion of the valency angle of SiSSi and SSiS and the repulsion between methyl groups across the ring are minimum for the planar configuration. This supposition was confirmed by Yokoi and Nomura[5] with an electron diffraction study. Hence it can be assumed that IV has a planar structure with no permanent dipole moment. Then the atomic polarization is estimated as $P-R_D=9$ cc.

These results will be used later for the estimation of the atomic polarizations of III and V.

Configuration of Octamethylcyclotetrasiloxane If the atomic polarization of III is assumed, from analogy to II, to be 14.5 cc. or 20% or R_D, the moment of III is calculated to be 0.67D. From the electron diffraction study Yokoi[2] determined the valency angles of O and Si and bond lengths, but he failed to draw a definite conclusion concerning the configuration of the molecule. Among the possible symmetrical configurations, only the crown form has a finite moment (1.7D)*, while the cradle and tub forms have no moment. The possible explanation of the observed moment (0.67D) is that III exists either as mixture of these symmetrical forms or as a certain less symmetrical form intermediate between these symmetrical forms. For example, D-form has a moment of 0.6–0.7D.



○ Oxygen. + Above the plane.
◎ Silicon. − Below the plane.

Fig. 1

Configuration of Hexamethylcyclotrithiosiloxane V has a moment of 1.03D, even if it has an atomic polarization 10.9 cc., the same value in magnitude as that of the corresponding oxygen compound II. The large of 1.03D for V rules out the planar symmetrical model similar to that in II.

The theoretical values for the chair and the boat configurations were calculated as follows. The moment of the chair form is given by $\mu=3\sin\theta\mu_{SSiS}$. In this expression, θ, the angle between the SSS plane and the SSiS plane, is calculated from the relation,

$$\cos\theta=(2\sin\alpha/2-\sin\beta/2)(\sqrt{3}\cos\beta/2),$$

where α is the valency angle of SiSSi and β the valency angle of SSiS. Assuming the bond moment of Si-S**, Si-C and H-C to be equal to 1.0D, 1.0D and 0.4D, respectively, and the valency angle of Si to be tetrahedral, the SSi(Me_2)S group moment, μ_{SSiS}, is calculated as 0.62D. On these assumptions, the resultant moment of the chair form is calculated to be 1.06±0.14D for the value of α equal to 110±5°, obtained from the electron diffraction by Yokoi and Nomura[5]. The moment of the boat form is calculated to be equal to about one third of that of the chair form. From the comparison of these values with the observed one, V appears to have predominantly the chair configuration. As the moment of the boat form is relatively smaller than that of the chair form, the existence of a small amount of the former does not affect appreciably the theoretical value of the moment of the mixture. When $\alpha=110°$, a mixture composed of 94% of the chair form and 6% of the boat form gives exactly the observed value, 1.03D. When $\alpha=105°$, the composition is 73%–27%. Hence the apparent agreement between the observed and the calculated moments does not preclude the existence of the boat form definitely. On the other hand, it is expected also from the consideration of the moleular model that the boat form of V is not significantly unstable compared with the chair form since the large Si-S distance will decrease steric repulsions. It is desirable to study the possibility of the existence of the boat form.

Summary

The dipole moments of several cyclosiloxanes and cyclothiosiloxanes were measured in benzene solution. The values obtained are: Hexamethyldisiloxane (I), 0.80D; octamethylcyclotetrasiloxane (III), 0.67D; hexamethylcyclotrithiosiloxane (V),

12) R. J. W. Le Fèvre, J. W. Mully and B. M. Smyth, *J. Chem. Soc.*, **1950**, 290.

13) E. B. Baker, A. J. Barry and M. J. Hunter, *Ind. Eng. Chem.*, **38**, 1117 (1946).

* In obtaining this value, we used the following values ∠SiOSi=140°, ∠OSiO=115° evaluated from electron diffraction study by Yokoi and H-C=0.4D, Si-C=1.0D and Si-O =1.55D estimated above.

** The ionic character of the Si—S bond is estimated to be equal to 11% from the electronegativity difference of Si and S. Then the Si—S moment may be taken as 1.0D, using 2.14 Å as the Si—S distance.

1.03D. The atomic polarizations obtained are: hexamethylcyclotrisiloxane (II), 10.9 cc.; tetramethylcyclodithiosiloxane (IV), 9.0 cc. The unexpectedly small bond moment of Si-O (1.55D) can be explained by the double bond character of the bond. For the configuration of (III) and (V), it is impossible to draw any definite conclusion from the study of the dipole moment alone.

We wish to express our sincere thanks to Prof. M. Kubo for his kind advice and encouragement, and to Mr. M. Yokoi for placing the samples at our disposal and for many stimulating discussions. Our tnanks are also due to the Ministry of Education for a contribution in aid of this research.

Chemical Department, Faculty of Science, Nagoya University, Nagoya

Molecular Structural Studies on Compounds Containing C—O Bond[1] *by Electron Diffraction. I. Molecular Structure of Gaseous p-Benzoquinone*

By Masao KIMURA and Shuzo SHIBATA

(Received December 25, 1953)

It is well-known that the quantum mechanical treatment can be applied to the problem of the π-electron distribution in a molecule to obtain the relationship between the bond order and bond length[2]. For C-C bond, such treatments have been carried out by many workers and there is much reliable information useful in the discussion of a molecular structure[1], whereas for C-O bond, the relation between the bond order and bond length has not yet been clarified in spite of its interest from the viewpoint of molecular structural theory. This is mainly due to the fact that we lack any abundant informations regarding geometrical configurations. The C-O bond length is affected sensitively by groups or atoms coexistent in the molecule. The difference between the values of the double and the single carbon-oxygen bond distances is larger than that for other heteropolar bonds, e.g. C-N and C-S. The facts mentioned above attract our interests strongly. But we must take into account the state in which the molecular configuration is determined, since the configurations of molecules containing carbonyl, carboxyl and hydroxyl groups are often affected by intermolecular interactions, such as hydrogen bond in crystals[3], in some cases even in the gaseous state. Therefore, it seems to be preferable to determine molecular structures not only by X-ray diffraction but also by gas electron diffraction. Our investigations have been undertaken in order to determine molecular structures in the gaseous state and to discuss the relationship between the bond order and bond length. The structure of methyl and ethyl alcohol[4], 1.4-dioxane[5], trioxane[5] and acetone[6] have already been investigated in our laboratory. It is desirable to choose, as material, molecules, whose physicochemical properties are well-known. The ultraviolet absorption[7] and diamagnetic anisotropy[8] of *p*-benzoquinone suggest that C=O bond is conjugated with another double bond in the molecule. It is also known that *p*-benzoquinone and hydroquinone form a molecular compound, quinhydrone. Therefore these were taken as the materials for our first investigation. The molecular structure of *p*-benzoquinone has already been studied by Robertson[9] with X-ray diffraction by crystal. Though it may be considered that the molecular structure of *p*-benzoquinone in the crystalline state is identical to that in the gaseous state, for the reason mentioned above we believe that it is necessary to determine the molecular structure of gaseous *p*-benzoquinone by the electron diffraction method and to compare the result with the value obtained by X-ray diffraction method. We could not determine the molecular structure of hydroquinone by use of the visual method with sufficient accuracy to discuss the properties of C-O bond. Therefore the result for hydroquinone will

1) Cf. e.g. C.A. Coulson and H.C. Longuet-Higgins, *Proc. Roy. Soc.*, A193, 450 (1948).
2) Cf. e. g. C. A. Coulson, *Proc. Roy. Soc.*, A169, 413 (1939).
3) M. Kimura and M. Aoki, This Bulletin, **26**, 429 (1953).
4) M. Kimura, *J. Chem. Soc. Japan*, **71**, 18 (1950).
5) M. Kimura and K. Aoki, *J. Chem. Soc. Japan*, **72**, 169 (1951).
6) M. Kimura and Y. Kurita, *J. Chem. Soc. Japan*, **72**, 396 (1951).
7) H. L. McMurry, *J. Chem. Phys.*, **9**, 231 (1941).
8) K. Lonsdale, *Proc. Roy. Soc.*, A171, 559 (1939).
9) J. M. Robertson, *Proc. Roy. Soc.*, A150, 106 (1935).

be reported after reinvestigation is carried out by the electron diffraction method with a rotating sector.

TABLE I
OBSERVED VALUES OF q FOR p-BENZOQUINONE

Max.	Min.	q	Max.	Min.	q
2		18.41	8		58.17
3		24.70		8	61.48
4		29.73	9		64.25
	4	32.79		9	65.96
5		35.15	10		68.57
	5	38.31		10	71.63
6		41.77	11		74.03
	6	48.27		11	76.64
7		51.96	12		79.80
	7	55.08			

Experimental

p-Benzoquinone was prepared by the oxydation of aniline, and was purified before use: m.p. 116°C. A temperature nozzle[3] was used in order to obtain the vapor of p-benzoquinone. Seven photographs were taken using a camera length of about 11 cm.[10] and an electron wavelength of about 0.06 Å. Measurements were, as usual, carried out by the visual method[11].

The characteristic features of the photograph are shown in curve V of Fig. 2, and q values of maxima and minima are listed in Table I. The observed values of the second and third minima are inaccurate owing to the background. Hence these are not listed in Table I. The radial distribution curve was calculated by the use of the formula

$$rD(r)=\sum_{q=1}^{\max} I(q)\cdot\exp(-aq^2)\,\sin(\pi qr/10)$$

where a was taken as $\exp(-aq^2_{\max})=0.1$. The dotted line in the visual curve was obtained by the use of the theoretical intensity curve for a model obtained from preliminary calculation of the radial distribution curve. The final radial distribution curve is shown in curve R.D. in Fig. 2. The curve has sharp maxima at 1.50 Å, 2.46 Å and 3.55 Å, corresponding to C_1—C_2, C_1—C_3, C_2—C_6 and C_3—O_1 respectively. The shelf at the left side of the peak at 1.50 Å is attributable to C_1—O_1 and C_2—C_3 (cf. Fig. 2). The peaks corresponding to the other interatomic distances could not be distinguished from ghosts since they contribute negligibly to the radial distribution curve. Though the peak at 1.50 Å might be affected slightly by the contribution of shorter interatomic distances represented as a shelf, it may be concluded that C_1—C_2 and C_2—C_3 interatomic distances are definitely different from each other and that C_1—C_2 distance is approximately equal to 1.50 Å.

The simplified theoretical intensity curves

$$I(q)=\sum_{i<j}\sum\frac{z_iz_j}{r_{ij}}\sin(\pi qr_{ij}/10)$$

were calculated for the values ranging from 106° to 103° for $\angle\alpha$, 1.48 Å to 1.54 Å for r(C—C), 1.28 Å to 1.36 Å for r(C=C), as-

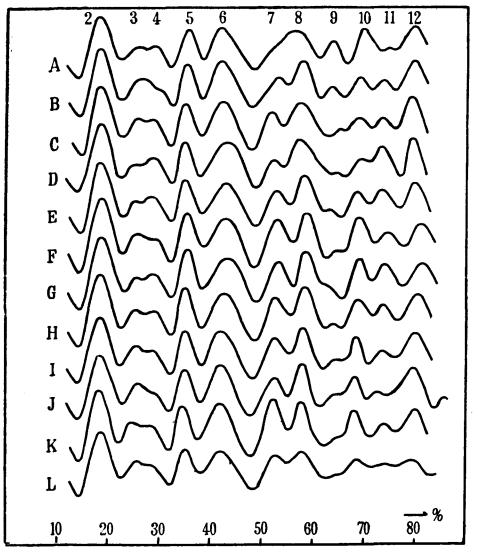


Fig. 1. p-benzoquinone.

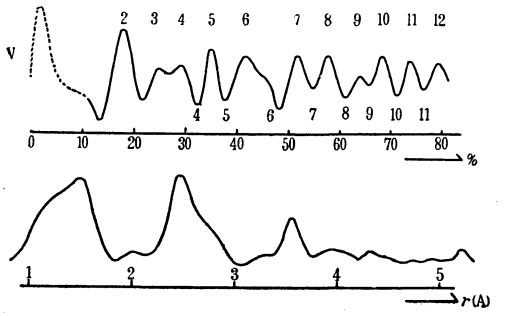


Fig. 2. Visual and radial distribution curves.

Fig. 3. Theoretical intensity curves for p-benzoquinone.

10) M. Kimura, Chemical Research, Vol. 9, p. 53.
11) Cf. e. g. L. O. Brockway, *Rev. Mod. Phys.*, 8, 231 (1937).

TABLE II
MODELS FOR *p*-BENZOQUINONE

	C=O (A)	C—C (A)	C=C (A)	$\angle\alpha$
A	1.14	1.52	1.32	116
B	1.14	1.52	1.32	112
C	1.14	1.52	1.32	110
D	1.14	1.50	1.34	110
E	1.14	1.50	1.32	110
F	1.14	1.50	1.28	116
G	1.14	1.48	1.30	110
H	1.14	1.50	1.30	110
I	1.14	1.52	1.30	110
J	1.14	1.54	1.30	110
K	1.14	1.52	1.30	108
L	modified I taking the effect of molecular vibrations into account.			

suming that r(C=O) 1.14 Å. A coplanar model was assumed with C—H distance equal to 1.09 Å. With the assumption that r(C=O)=1.14 Å, molecular forms are settled by three parameters, $\angle\alpha$, r(C—C)/r(C=O) and r(C=C)/r(C=O).

Thirty-four theoretical intensity curves were drawn and the relative positions and features of maxima and minima were compared with the visual curve. Some of them are depicted in Fig. 3. The models corresponding to these curves are listed in Table II. With the increasing angle $\angle\alpha$, the positions of the 8th and the following maxima shift to larger q values, and the relative intensity of the 7th and 8th maxima and that of the 9th and 10th maxima change as shown in the curves A, B and C in Fig. 3. r(C=O)/r(C=O) is related mainly to the relative intensities of the 3rd and 4th maxima, of the 7th and 8th maxima and of the 9th and 10th maxima (Curve D, E and F). r(C—C)/r(C=O) is related mainly to the relative intensity of the 9th and 10th maxima (curve G, H, I and J). From the criterion mentioned above, the models F, J and K are chosen as the models in good agreement with the visual curve in qualitative sense. The quantitative comparison with the observed values of maxima and minima was made for the calculated values of the models F, I and K.

The effect of molecular vibrations was taken into account in calculations with the following formula,

$$I(q)=\sum_{i}\sum_{i<j}\frac{z_i z_j}{r_{ij}}\exp(-b_{ij}q^2)\sin(\pi q r_{ij}/10)$$

in which the values of parameters b_{ij} for carbon-carbon and carbon-oxygen atomic pairs were estimated from the spectroscopic data for benzene and other compounds. In Fig. 3, the curve I is that of the fixed model. When the effect of vibration is taken into account we obtain the curve L. As a result it was shown that the features of intensity curves did not change, except the positions of the maxima farther apart than the 9th one, whose changes were surely within experimental errors.

The following values were obtained for the molecular structure of *p*-benzoquinone: $\angle\alpha$=110°±2°, r(C—C)=1.52 Å±0.02 Å, r(C=C)=1.31 Å±0.02 Å, r(C=O)=1.15 Å±0.02Å.

Discussion

Robertson[8] determined the molecular structure of *p*-benzoquinone using X-ray diffraction method. His values are as follows: $\angle\alpha$=109°, r(C−C)=1.50 Å, r(C=C)=1.32 Å, r(C=O)=1.14 Å. These values agree excellently with ours. It follows that intermolecular forces are weak in p-benzoquinone crystal and that a molecule in crystal is in an electronic state similar to a free molecule.

The value of C=O 1.15 Å is very short compared with the normal value of C=O distance in ketotype compounds, such as acetone[5]. The value of C=C distance is nearly equal to a pure double bond distance within experimental errors. In spite of the information of conjugation between C=O and C=C, the result obtained from the diffraction experiments suggests that C=O and C=C double bonds are localized to greater extent. The theoretical discussion in regard to these results will be made in our later paper.

We should like to express our thanks to Prof. M. Kubo for his helpful advice. Our thanks are also due to the Ministry of Education for grants in aid of this research.

Chemical Department, Faculty of Science, Nagoya University, Nagoya

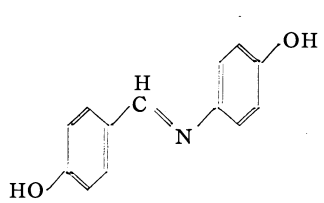
Estrogenic Action of Methylenimine Derivatives

By Yujiro NOMURA

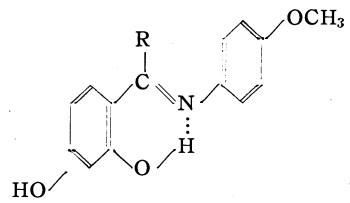
(Received January 11, 1954)

F. W. Schueler suggested that a compound, constituted of a rather large, rigid, relatively inert, and lipoid soluble molecular structure with two active hydrogen-bond forming groups located at an optimum distance of 14.5 Å units from each other may show estrogenic action.[1] He prepared sixteen azomethines and found an example to meet his hypothesis in 4, 4′-dihydroxydiphenylmethylenimine (I), which, administered subcutaneously, produced a true estrogenic response in rats in a total dose of 12.5 mg.[2] However, it must be noted that the activity is rather small for the fulfilment of the requirements.

M. Ōki and Y. Urushibara deduced the non-planar structure of stilbestrol and its homologs from their ultraviolet absorption data and presented a hypothesis that in addition to other requirements an optimum thickness of the molecule is an important factor for a strong estrogenic action.[3] The 4, 4′-dihydroxydiphenylmethylenimine prepared by Schueler has a thin structure, and its low activity might be attributed to the lack of the moderate thickness favorable for the development of a high activity.



I



II

R
a) CH_3
b) C_2H_5
c) $(CH_3)_2CH$

The author prepared alkyl 2,4-dihydroxyphenyl-4′-methoxyphenylmethylenimines (II), which probably have rigid structures by virtue of the chelate ring formation between the nitrogen atom and the ortho-standing phenolic hydrogen atom[4], and at the same time a thickness given by the steric interference of the alkyl substituent with the 4′-methoxyphenylimino group.[5]

The substituted methylenimines were prepared by condensing alkyl 2, 4-dihydroxyphenyl ketone with *p*-anisidine in the presence of anhydrous zinc chloride:

1-$RCOC_6H_3(OH)_2$-2,4+*p*-$NH_2C_6H_4OCH_3$→II

Estrogenic activities were evaluated by the vaginal smear test with ovariectomized mice by subcutaneous injection of oil solutions in two portions. Substance IIa (R: CH_3) was inactive in 1 mg. dosage. The substance IIb (R: C_2H_5) was fully active in 1 mg. dosage, and the substance IIc (R: $(CH_3)_2CH$) produced estrus in 40 % of the animals in the same dosage. The ethyl compound was the most active of the present series as in the stilbestrol homologs. As Schueler pointed out[2], a stronger estrogenic response may be expected when applied by intravaginal injection, because the methylenimine linkage is probably in part cleavaged in vivo before the compound reaches its site of action.

Experimental Part*

Alkyl 2, 4-dihydroxyphenyl Ketone. 1-$RCOC_6H_3(OH)_2$-2, 4.—Prepared according to Org. Syn. Vol. XXI, p. 103 (1941). 55 g. of resorcinol yielded 49 g. of methyl 2, 4-dihydroxyphenyl ketone melting at 142.3–144.3°C, and 48.5 g. of ethyl 2, 4-dihydroxyphenyl ketone melting at 98.2–99.2°C., respectively. 16 g. of resorcinol yielded 8.5 g. of isopropyl 2, 4-dihydroxyphenyl ketone bioling at 164°C./5 mm.

Methyl-2,4-dihydroxyphenyl-4′-methoxyphenyl-methylenimine (II a) 5 g. of methyl 2, 4-dihydroxyphenyl ketone and 6 g. of *p*-anisidine were mixed in a 20 cc. flask and 0.1 g. of anhydrous zinc chloride was added. The flask was immersed in an oil bath and heated at 140°C. for five minutes in a stream of carbon dioxide. The reaction mixture was cooled to the room tempera-

1) F. W. Schueler, *Science*, **107**, 94 (1948).
2) F. W. Schueler, *J. Amer. Pharm. Assoc.*, **39**, 87 (1950).
3) M. Oki and Y. Urushibara, This Bulletin, **25**, 109 (1952).
4) Cf. Y. Urushibara and T. Takahashi, This Bulletin, **26**, 162 (1953).
5) Cf. Reference 3.

* Melting points of methylenimines were determined in sealed capillaries, and corrected.

ture and digested with methanol. Recrystallization from acetone gave yellow plates melting at 262°C. with decomposition (Yield 8.2 g.). Found: C, 70.26; H, 5.80; N, 5.43. Calculated for $C_{15}H_{15}O_3N$ (II a): C, 70.02; H, 5.88; N, 5.44 %.

Ethyl- and isopropyl-2, 4-dihydroxyphenyl-4'-methoxyphenyl-methylenimine (IIb and IIc) Synthesized in the same way as the methyl compound. 5 g. of ethyl 2,4-dihydroxyphenyl ketone and 6 g. of *p*-anisidine yielded 6 g. of ethyl-2, 4-dihydroxyphenyl-4'-methoxyphenyl-methylenimine. Recrystallization from acetone gave yellow leaflets melting at 213°C. with decomposition. Found: C, 71.07; H, 6.07; N, 5.21. Calculated for $C_{16}H_{17}O_3N$ (II b): C, 70.83; H, 6.32; N, 5.16 %.

7.26 g. of isopropyl 2, 4-dihydroxyphenyl ketone and 7.06 g. of *p*-anisidine yielded 4 g. of isopropyl-2, 4-dihydroxyphenyl- 4'-methoxyphenyl-methylenimine. Recrystallization from methanol gave pale yellow crystals melting at 197°C. with decomposition. Found: C, 71.42; H, 6.88; N, 4.82. Calculated for $C_{17}H_{19}O_3N$ (II c): C, 71.56; H, 6.71; N, 4.91 %.

These methylenimine derivatives were readily hydrolyzed by diluted hydrochloric acid to *p*-anisidine and corresponding alkyl 2, 4-dihydroxyphenyl ketone.

The author wishes to express his hearty thanks to Professor Y. Urushibara for his kind guidance and encouragement. Thanks are also due to Mr. F. Ueno, Teikoku Hormone Manufacturing Co., Ltd., Kawasaki, for the bio-assays and to the Ministry of Education for the Grant in Aid for Fundamental Scientific Research.

Chemical Institute, College of General Education, Tokyo University, Tokyo

*A Nitrogen Analog of Hexestrol, Ethyl-p-hydroxyphenyl-(1-p hydroxyphenyl-propyl)-amine, and Its Derivatives**

By Yujiro NOMURA

(Received January 11, 1954)

Various oxygen and sulfur analogs of hexestrol have been prepared and found to have estrogenic activities [1] These facts show that the member constituting the molecular skeleton of hexestrol may be replaced by a different atom without destroying totally the estrogenic activity, unless a significant change in the molecular shape and the appearance of any new physiological properties are associated with the introduction of the different atom.

The author prepared a nitrogen analog of hexestrol, ethyl-*p*-hydroxyphenyl-(1-*p*-hydroxyphenyl-propyl)-amine, *p*-$HOC_6H_4N(C_2H_5)CH(C_2H_5)C_6H_4OH$-*p*, as follows Dry hydrogen bromide was passed into an ethereal solution of anethole (3 11 g), and the resulting solution of the addition product was mixed with a pyridine solution containing an equivalent amount of ethyl-*p*-methoxyphenyl-amine, prepared according to King and Tonkin [2] After standing overnight the reaction mixture was shaken with water. From the upper layer ethyl-*p*-methoxyphenyl - (1-*p* - methoxyphenyl-propyl)-amine (3.39 g) was isolated and recrystallization from methanol gave colorless prisms, melting at 64 5–65 0°C Found C, 76 20 , H, 8.50; N, 4 70 Calculated for $C_{19}H_{25}O_2N$. C, 76 22 , H, 8 42 , N, 4 68%.

This amine developed incomplete but distinct durable estrus in the dosage of 60 γ by subcutaneous injection into ovariectomized mice in two portions in oil solution as referred to elsewhere.[3]

Ethyl-*p*-hydroxyphenyl-(1-*p*-hydroxyphenyl-propyl)-amine was obtained by the demethylation of the above substance with red phosphorus and hydroiodic acid (d=1.7) in colorless crystals melting at 100 5°C. after recrystallization from benzene Found: C, 75 32 , H, 7 61; N, 5 30. Calculated for $C_{17}H_{21}O_2N$ · C, 75 24 , H, 7 80; N, 5 16%.

Acetylation of ethyl-*p*-hydroxyphenyl-(1-*p*-hydroxyphenyl-propyl)-amine with acetic anhydride gave a diacetate melting at 54–55°C. Found N, 3 61. Calculated for $C_{21}H_{25}O_4N$: N, 3 94%.

The author wishes to express his hearty thanks to Professor Y. Urushibara for his kind guidance and encouragement. Thanks are also due to Mr. F. Ueno, Teikoku Hormone Manufacturing Co., Ltd., Kawasaki, for the bio-assays and to the Ministry of Education for the Grant in Aid for Fundamental Scientific Research

Chemical Institute, College of General Education Tokyo University, Tokyo

* All melting points are corrected

1) Y Urushibara and M Oki, This Bulletin, **23**, 35 (1950) Y Urushibara and T Takahashi, ibid, **23**, 53 (1950), Y Urushibara and M. Oki and R Ikeda, ibid, 25, 66 (1952)

2) Harold King and Isabel M Tonkin, *J. Chem Soc*, **1946**, 1063

3) Y. Urushibara and T. Takahashi, This Bulletin, **23**, 54 (1950).

On Derivatives of α-Thujaplicin. III.[1] *Azo Dyes of α-Thujaplicin (o Isopropyl tropolone)*[2]

By Kameji YAMANE

(Received December 16, 1954)

T. Nozoe and his coworkers[3,4,5] carried out the detailed study about the azo dyes of hinokitiol (*m*-isopropyltropolone) but only *p*-tolyl-azo-dye of α-thujaplicin was reported.[6,7]

Fourteen kinds of azo dyes of α-thujaplicin are described in this paper. The alkali salt of α-thujaplicin was coupled with diazonium salts of aromatic amines in cold aqueous solution to yield orange yellow to reddish brown azo dyes easily and in good yield. The application of an excess diazonium salt gave only a mono-azo compound. The azo dyes obtained are given in Table I.

TABLE I
AZO DYES OF α-THUJAPLICIN OBTAINED

Aromatic amines used.	Color and form	m.p.	Solvents (for recrystallization)
Aniline	red prisms	132.8–134°	alcohol
o-Toluidine	red prisms	120–121°	cyclohexane
p-Toluidine	orange red prisms	130–131°	benzene
p-Anisidine	orange fine needles	107–108°	alcohol
p-Chloroaniline	yellowish brown fine crystal	123–124°	cyclohexane
p-Bromoaniline	reddish brown needles	123–124°	alcohol
m-Nitroaniline	reddish brown fine crystal	144–145.3°	benzene
p-Nitroaniline	reddish brown fine crystal	166–167°	benzene
Sulfanilic acid	orange brown fine crystal	275°<(dec.)	water
p-Sulfanilamide	yellow fine needles	227–228°	acetic acid
p-Aminobenzoic acid	yellow fine crystal	267–268° (dec.)	water (K-salt)
α-Naphthylamine	brownish red plates	135–136°	acetic acid
β-Naphthylamine	red prisms	136–137°	pet.-ether
Benzidine	dark brown fine crystal	249–250° (dec.)	benzene

Most of the azo dyes are soluble in benzene, alcohol, petroleum ether, cyclohexane and glacial acetic acid, but some derived from sulfanilic acid, *p*-sulfanilamide and *p*-aminobenzoic acid are slightly soluble in these solvents. The azo dyes dissolve in a caustic alkali solution to give an orange red or deep red solution, and precipitate with acid. The azo dyes show a red coloration by ferric chloride, characteristic to tropolone nucleus.

p-Tolyl-azo-α-thujaplicin absorbed two molar equivalents of hydrogen when hydrogenated in ethyl acetate with Adams' PtO_2 catalyst, giving amino-α-thujaplicin m. p. 172–173° and *p*-toluidine. Methylation of *p*-anisyl-azo-α-thujaplicin with diazomethane in ether gave *p*-anisyl-azo-α-thujaplicin methyl-ether m. p.

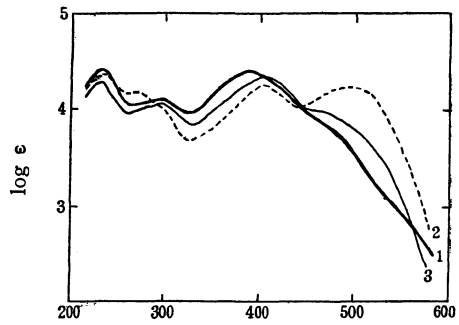
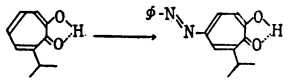


Fig. 1. Ultraviolet absorption spectra of phenyl-azo-α-thujaplicin (Curve 1), *m*-nitro-phenyl-azo-α-thujaplicin (Curve 2), *p*-sulfo-phenyl-azo-α-thujaplicin (Curve 3).

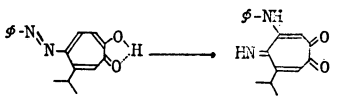
1) H. K. Yamane and S. Morosawa, This Bulletin, **27**, 18, (1954).
2) This work was presented at the Hiroshima District Meeting of the Chemical Society of Japan, Nov. 15 (1953).
3) T. Nozoe, E. Sebe and S. Ebine, *Proc. Japan. Acad.*, **26**, (8) 24 (1950).
4) T. Nozoe, S. Ebine, S. Ito and I. Takasu, Ibid., **27**, 197 (1951).
5) T. Nozoe, E. Sebe, Y. Kitahara and H. Fujii, *Sci. Rep. of Tohoku Univ.*, Ser. I., **33**, 166 (1952).
6) T. Nozoe, A. Yasue and K. Yamane, *Proc. Japan Acad.*, **27**, 15 (1951).
7) T. Nozoe, Y. Kitahara, K. Yamane and T. Ikemi, Ibid., **27**, 193 (1951).

99–100°. Ultraviolet absorption spectra of some azo dyes are given in Fig. 1. Absorption maximum of about 400 mμ is characteristic to tropolone nucleus.

T. Nozoe et al.[4,5] have reported that the azo dyes of hinokitiol (B) rearranged when heated with alcohol or acetic acid containing one drop of hydrochloric acid, giving dark reddish purple crystals, that is "hinopurpurins", which have a tropoquinonoid structure (C). It is interesting, however, that all the azo dyes of α-thujaplicin do not undergo rearrangement by the same procedure.



α-Thujaplicin (A)



(B) (C)

T. Nozoe and E. Sebe[5] have reported that the position of the azo group in azohinokitiols was at the para (5) position in spite of steric interference of the isopropyl group. In the case of azo-α-thujaplicin, the position of the azo group must be either at the para (5) or the ortho (7) position of the cycloheptatrienolone ring.

Amino-α-thujaplicin m. p. 172–173° obtained by the catalytic reduction of *p*-tolyl-azo-α-thujaplicin as described above, is the same substance prepared from the catalytic reduction of nitroso-α-thujaplicin[7] and mononitro-α-thujaplicin m. p. 112–113°.[1]

T. Nozoe et al.[8] have reported that the electrophilic substitution takes place predominantly at the *p*-position in the nitration and the nitrosation of tropolones. From these facts, therefore, the azo coupling of α-thujaplicin may take place at the *p*-position as in (A).

A trial to obtain azoxy-compound by the oxidation of phenyl-azo-α-thujaplicin with 30 per cent hydrogen peroxide solution in glacial acetic acid failed, yielding a syrupy matter which gave no red coloration with ferric chloride.

Beside the crystals of m. p. 131° of *p*-tolyl-azo-α-thujaplicin, the author obtained yellow prisms of m. p. 124° in small amount, but no detailed study has yet been made.

8) (a) T. Nozoe, *Science of Drugs*, **3**, 174 (1949); *Sci. Rep. of Tohoku Univ.*, I, **34**, 199 (1950). (b) T. Nozoe et al., *Proc. Japan. Acad.*, **26**, 33 (1950). (c) T. Nozoe et al, Ibid., **27**, 190 (1950). (d) T. Nozoe and E. Sebe, Ibid., **26**, 45 (1950). (e) T. Nozoe et al., Ibid., **27**, 565 (1951). (f) T. Nozoe et al., Ibid., **28**, 488 (1952).

Experimental

Phenyl-azo-α-thujaplicin [(A)*: φ=C_6H_5-]:—To a solution of 0.11 g. aniline dissolved in 3.3 cc. of 0.93 N-hydrochloric acid, a solution of 0.1 g. of sodium nitrite in 1.5 cc. of water was dropped in, and the resultant cold diazonium solution was added dropwise to the cold solution of 0.2 g. of α-thujaplicin in a mixture of 1.5 cc. of 1.7 N-potassium hydroxide solution and 15 cc. of water. After the completion of the addition, the mixture was stirred for ten minutes and 1 cc. of 2 N-hydrochloric acid was added. The mixture was stirred for a further 30 minutes in the cold, and the crystals were collected by filtration. 0.34 g. of azo dye was obtained. The recrystallization from alcohol yielded red prisms, m. p. 133–134°. Found: C, 71.32; H, 5.87; N, 10.39, Calculated for $C_{16}H_{16}O_2N_2$: C, 71.62; H, 6.01; N, 10.44%.

Azo-α-thujaplicins derived from *o*- and *p*-toluidine, *p*-anisidine, *p*-chloroaniline, *p*-bromoaniline, *m*- and *p*-nitroaniline, sulfanilic acid, *p*-sulfanilamide, *p*-aminobenzoic acid, α- and β-naphthylamine and benzidine were prepared in a manner like the above (ordinary method). The color, crystalline form and melting point of these azo dyes are shown in Table I. [(A): φ=*o*-CH_3·C_6H_4-]. Found: N, 10.04, Calculated for $C_{17}H_{18}O_2N_2$: N, 9.92%. [(A): φ=*p*-CH_3·C_6H_4-]. Found: N, 9.39, Calculated for $C_{17}H_{18}O_2N_2$: N, 9.92%. [(A): φ=*p*-CH_3O·C_6H_4-]. Found: N, 9.16, Calculated for $C_{17}H_{18}O_3N_2$: N, 9.39%. [(A): φ=*p*-Cl·C_6H_4-]. Found: N, 9.20, Calculated for $C_{16}H_{15}O_2N_2Cl$: N, 9.25%. [(A): φ=*p*-Br·C_6H_4-]. Found: N, 7.99, Calculated for $C_{16}H_{15}O_2N_2Br$: N, 8.07%. [(A): φ=*m*-NO_2·C_6H_4-]. Found: N, 13.63, Calculated for $C_{16}H_{15}O_4N_3$: N, 13.41%. [(A): φ=*p*-NO_2·C_6H_4-]. Found: N, 13.63, Calculated for $C_{16}H_{15}O_4N_3$: N, 13.41%. [(A): φ=*p*-HO_3S·C_6H_4-]. Found: N, 7.87, Calculated for $C_{16}H_{16}O_5N_2S$: N, 8.04%. [(A): φ=*p*-H_2NO_2S·C_6H_4-]. Found: N, 12.20, Calculated for $C_{16}H_{17}O_4N_2S$: N, 12.09%. [(A): φ=*p*-HOOC·C_6H_4-]. Found: N, 9.04, Calculated $C_{17}H_{16}O_4N_2$: N, 8.97%. [(A): φ=α-$C_{10}H_9$-]. Found: N, 8.82, Calculated for $C_{20}H_{18}O_2N_2$: N, 8.80%. [(A): φ=β-$C_{10}H_9$-]. Found: N, 8.32, Calculated for $C_{20}H_{18}O_2N_2$: N, 8.80%. *p*, *p*′-Diphenyl-bisazo-α-thujaplicin: Found: N, 10.60, Calculated for $C_{32}H_{30}O_4N_4$: N, 10.48%.

Catalytic reduction of *p*-tolyl-azo-α-thujaplicin:—A solution of 5.22 g. of *p*-tolyl-azo-α-thujaplicin in 150 cc. of ethyl acetate was catalytically reduced with 0.21 g. Adams' PtO_2 at ordinary temperature and pressure, by which 1050 cc. of hydrogen was absorbed. The removal of the solvent and the catalyst gave a solid residue, crude amino-α-thujaplicin. The recrystallization from benzene yielded yellow prisms m. p. 172–173°. Found: C, 67.20; H, 7.26; N, 7.59, Calculated for $C_{10}H_{13}O_2N$: C, 67.04: H, 7.26; N, 7.80%.

The author wishes to express his sincere thanks to Prof. A. Yokoo for his kind guidance, also to Prof. T. Nozoe (Tohoku Univ.) for helping him with this work. The author

* Formula of azo-dyes of α-thujaplicin

thanks also Miss K. Kato and Miss Iwanaga (Nozoe Laboratory) for carrying out the measurements of ultraviolet absorption spectra, and also Mr. Furukawa (Sankyo Co.) and Miss H. Iwata (Kyoto Univ.) for carrying out the microchemical analysis.

Department of Chemistry, Faculty of Science, Okayama University, Okayama, Japan

Molecular Structure Investigations by Electron Diffraction Method. I. The Molecular Structures of Isopropyl Alcohol and -Chloride

By Mashio YAMAHA

(Received January 19, 1954)

Previous electron diffraction investigations of substituted paraffines, having the number of carbon atoms up to C_3 or C_4, gave various kinds of information about the structures of respective molecules, that is, reliable molecular parameters including the informations about the internal rotations in some kinds of molecules were obtained. In Table I, there are shown several data obtained recently by many authors. Nowadays, the investigations have been carried out using the visual method and also more quantitatively by the use of the apparatus having a sector.

TABLE I
THE LIST OF MOLECULAR CONSTANTS OF SEVERAL PARAFFINE DERIVATIVES FROM RECENT INVESTIGATIONS

Molecules	C-C (Å)	C-X (Å)	Other parameters	References
CH_3–CH_3	(C–H/C–C=1.115/1.54)		∠CCH=110.5°	(6)
CH_3–CH_2OH	1.54	C–O=1.48±0.04		(7)
CH_2Cl–CH_2OH	1.54	C–O=1.45 (1.43)	(Gauche form is predominant at room temperature.)	(8), (9)
CH_2Cl–CH_2Cl	1.49±0.03	C–Cl=1.78±0.01 C′···Cl=2.69±0.02,	(Gauche=27±5% at 22°C.)	(10)
CH_3–CCl_3	1.54±0.04	C–Cl=1.77_5±0.02		(11), (12), (13)
CH_3–CCl_2–CH_3	1.54±0.04	C–Cl=1.77_6±0.02,	∠ClCCl=109.5±2° ∠CCCl=109°±3°	(11)
CH_2Cl–$CHCl$–CH_3	1.56	C–Cl=1.79±0.035 C′···Cl=2.715±0.025,	∠CCCl=108±4°	(14)
CH_3–CF_3*	1.52±0.02	C–F=1.37±0.02		(15)
CF_3–CF_3*	1.45(±0.06)			(16)

*Origin of the deviations of molecular parameters seem to be somewhat different for fluorinated derivatives from that for other substituted paraffines.

There seem to be disagreements on several points of molecular parameters among a few examples shown in Table I. But whether these discrepancies are within a range of errors or whether they indicate real differences among the molecules could not be decided at present. As regards the C—C bond distances, for example, the value 1.54 Å has so far been usually considered to be reliable for saturated paraffines and their derivatives, but the value 1.49 Å has been obtained for 1,2-dichloroethane molecule[10], and 1.56 Å for 1,2-dichloropropane molecule[14]. The present author is trying to investigate some substituted paraffines as regards the C—C distances and other molecular parameters.

Isopropyl alcohol and -chloride molecules have been investigated, because the contribution of C—C atom-pairs to the intensity curves seems to predominate in these molecules over the cases of ethane derivatives. In this study, we may not ignore the question how the equilibrium positions of two methyl groups will contribute to the intensity

curves. But in the reinvestigation of isopropyl chloride molecule[1], unfortunately, the problem of internal rotations of methyl groups has not been made clear by using the visual method.

Experimental Procedures

Commercial isopropyl alcohol was carefully dried on quick lime and distilled several times (boiling point: 82 °C). The chloride was synthesized[2] from purified alcohol and distilled carefully (b.p. 37°C).

The apparatus of electron diffraction is the one which was described in the previous report[3]. Eight maxima and five minima have been observed visually in the range $9<q<80$ for isopropyl alcohol, and twelve maxima and eight minima in the range $9<q<95$ for isopropyl chloride from ten or more photographic plates in both cases.

The experimental visual curve obtained for each case is shown in the top-most place of Fig. 3A and 3B respectively, and $q_{obs.}$'s, the corresponding observed q-values of maxima and minima, are shown in the third column in Table IV A and IV B.

The theoretical intensity curves for the assumed molecular models have been calculated by the use of the well-known formula[4]:

$$I=k\sum_i\sum_j Z_iZ_j/l_{ij}\cdot\left(\sin\frac{\pi}{10}ql_{ij}\right)\cdot\exp(-b'_{ij}q^2)$$

where $q=10\,s/\pi$, $s=(4\pi\sin\theta/2)/\lambda$, θ the scattering angle, and λ the wave length of the beam.

In constructing the assumed molecular models, the rotations of methyl groups about each C-C bond are considered. (The figures of molecular models are shown in Fig. 1, in which various parameters are given out.) That is, all the hydrogen atoms of methyl groups, which contribute to intensity curves as the variations of C″···H and X″···H* distances, are taken into account**.

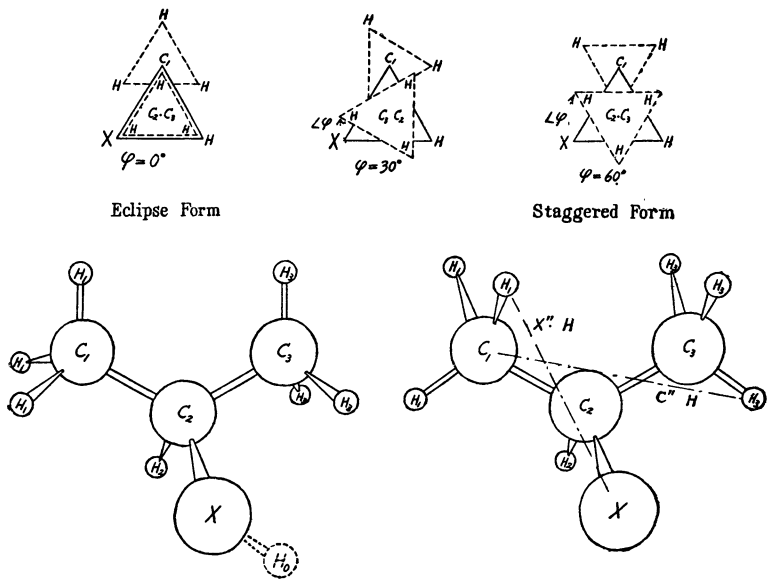


Fig. 1. Schematic models which show the interatomic configurations in relation to the rotations of methyl groups for isopropyl derivatives.

In case of isopropyl alcohol, the atom X is the hydroxyl oxygen and the hydroxyl hydrogen atom H_0 attached to the X atom, which are shown with dotted figure. In case of isopropyl chloride, X is the chlorine atom. One of the six $C''\cdots H$ and one of the six $X''\cdots H$ interatomic distances are hereby exemplified, and the meaning of the signs ($''$) and ($\cdots$) will be clear from this figure.

1) J.Y. Beach and D.P. Stevenson, *J. Am. Chem. Soc.*, **61**, 2643 (1939).
2) "Organic Synthesis" Collective Vol. 1. p. 142 (1948), (Analogous method for *n*-Butyl Chloride.)
3) T. Yuzawa and M. Yamaha, This Bulletin, **26**, (No. 8) 414 (1953).
4) V. Schomaker and R. Spurr, *J. Am. Chem. Soc.*, **64**, 2693 (1942).
* The sign (...) shows the distance between two atoms which are non-bonded. The sign ($''$) shows that there are two other atoms in between along three successive bonds (assigned the mark of *two* dashes), e.g. C″...H shows one of the three $C_1''\ldots H_3$ distances in the case of C_1-C_2-C_3-H_3 as well as $C_3''\ldots H_1$ in C_3-C_2-C_1-H_1.
** The hydrogen atom H_0 attached to the oxygen atom of hydroxyl group is neglected, because the contributions of O-H_0, $C_2'\ldots H_0$ and those of farther distances between H_0 and other atoms to the intensity curves are negligibly small.

The variations of these distances in relation to the rotational angle φ of methyl group (the angle φ is conveniently taken from the C_1C_2X plane for $(methyl)_1$ group) are shown

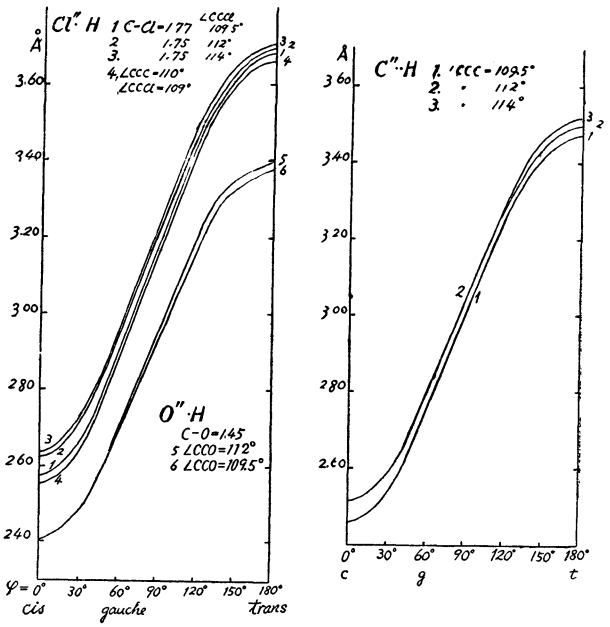


Fig. 2. The diagrams of interatomic distances C''...H, O''...H and Cl''...H versus the rotational angle φ. (In case of C—H=1.10)
Angle φ=0°, 60° and 180° correspond to cis, gauche and trans position respectively about the C—C bond.

in Fig. 2 for each molecule. The contributions of these distances to the intensity curves are remarkable for the alcohol in the range $25<q<55$, where the influences of the thermal vibrations are comparatively small. For the chloride, on the contrary, these contributions appear in the range $q<35$ of the curve, where the exact estimation of the intensity relations is difficult.

The vibration factors b'_{ij} used in the formula are shown in Table II. For isopropyl

TABLE II
THE LIST OF THE APPROXIMATE VIBRATION FACTORS USED FOR THE CALCULATION OF INTENSITY CURVES

Atom pairs	nz_iz_j/l_ij**	Distances (Å)	$<l_i^2j>_{Av}^{1/2}$	$b_{ij}=\pi/200<1^2_{ij}>_{Av}$.	b'_{ij}
C —C	46	1.52—1.56	0.057	0.00015	0
C'...C	14	2.48—2.55	0.084	0.00035	0.00020
C —H	46	1.09—1.13	0.078 (0.064)*	0.00030	0.00015
C'...H	27	2.14—2.23	0.091 (0.086)*	0.00041	0.00025
C —Cl	58	1.75—1.80	0.061 (0.064)*	0.00018	0.00003
C'...Cl	75	2.68—2.75	0.068 (0.070)*	0.00023	0.00008
C —O	33	1.43—1.48	0.055+	0.00015	0
C'...O	39	2.42—2.46	0.066+	0.00022	0.00008
C''—H (cis, gauche) 6, 11					(0.00060)***
C''—H (120°, trans) 9, 4					(0.00040)***
Cl''...H (cis, gauche) 15, 28					(0.00076)***
Cl''...H (120°, trans) 24, 11					(0.00046)***
C''...H (cis, gauche) 8, 14					(0.00060)***
C''...H (120°, trans) 11, 6					(0.00040)***

Table II. *Reference (10)
**The values are to be some what changed from these values.
***Roughly assumed values.
+Calculated with consideration of reference (5).

alcohol, the values have been assumed by the force constants calculated from vibration frequencies of ethyl alcohol[9]. For isopropyl chloride, the values have been assumed from the values suggested by J. Karle et al.[10].

(The valency agles ∠CCH and ∠HCH are assumed to be 109.5° throughout the investigation.)

Isopropyl Alcohol With the visual curve, the theoretical intensity curves are shown in Fig. 3A in accordance with the variations of assumed molecular models. As shown in Table III A, corresponding theoretical intensity curves to molecular constants of models

TABLE IIIA

THE LIST OF MOLECULAR MODELS AND CORRESPONDING ASSUMED MOLECULAR CONSTANTS FOR ISOPROPYL ALCOHOL

Models	C—C (Å)	C—O (Å)	∠CCC°	Configulation of two $-CH_3$ groups	$q/q_{obs.}$
A	1.54	1 48	109.5	Eclipse	0.991_5
B_E	〃	1.45	〃	〃	1.000_2
C	〃	1.43	〃	〃	1.002_0
D	〃	1.48	112	〃	—
E	〃	1.45	〃	〃	0.995_1
F	〃	1.43	〃	〃	—
B_{30}	〃	1.45	109.5	$\varphi=30$	0.991_9
B_S	〃	〃	〃	Staggered	0.998_3*
P_E	1.52	1.45	109.5	Eclipse	1.012_5
P_S	〃	〃	〃	Staggered	1.006_4*
Q_E	1.56	〃	〃	Eclipse	0.990_6
Q_S	〃	〃	〃	Staggered	0.987_2*
X_E	1.54	1.45	109.5	Eclipse	0.997_6 (C-H=1.13 Å)
Y_S	〃	〃	112	Staggered	— (∠CCO=112°)
Y_{30}	〃	〃	〃	$\varphi=30$	— (〃)

* The 3rd and 5th maxima are not taken into account in these mean values.

TABLE IVA

OBSERVED q-VALUES AND CALCULATED $q/q_{obs.}$ VALUES FOR BETTER MOLECULAR MODELS OF ISOPROPYL ALCOHOL

Max.	Min.	$q_{obs.}$	wt.	A	B_E	B_{30}	C	E	X_E	B_S
	2	(14.39)								
2		18.43	1	1.010	1.023	1.004	1.028	1.010	1.031	0.982
	3	23.13	2	0.997	1.003	0.999	1.002	0.990	1.007	0.994
3		27.20	2	0.995	1.004	1.011	1.007	1.002	1.007	—*
	shelf									
	4	(38.61)								
4		42.59	2	0.991	1.003	0.996	1.003	0.993	0.998	0.996
	5	48.21	2	0.991	1.000	0.975	0.998	0.994	0.994	(1.008)
5		52.36	1	0.974	0.980	0.951	0.985	0.976	0.974	—*
6		58.33	2	0.991	0.998	0.996	1.001	1.000	0.989	1.006
	7	63.79	1	0.979	0.992	0.991	0.992	—	0.986	0.995
7		68.33	1	—	0.995	0.988	—	—	0.985	0.995
8		(76.23)	(See Fig. 3A.)							
Weighted mean:				0.991_5	1.000_2	0.991_9	1.002_0	0.995_1	0.997_6	0.998_3
Wtd. mean sq. deviation:				0.008_3	0.008_2	0.015_0	1.008_7	0.008_8	—	—

*These values can not be taken into account since the features are different from that of visual one. (See Fig. 3A).

are specified as follows:

1) For the groups of curves from A to C and D to F, the C–O distance increase successively in each group. The angles ∠CCC are 109.5°, 112° in the two groups respectively and other parameters, ∠CCO and rotational configurations, remain constant.

2) Curves assigned P, B, Q in order correspond to the increase of C–C distance with constant other parameters.

The $q_{obs.}$'s of the maxima and the minima

(abbreviated as "*q-values*" in this and next sections) of each curve in the cases 1) and 2), are slightly different from one another with the parameters mentioned, and the curves assigned B, including the subscripts, seem to be the most acceptable ones.

3) Curves assigned the same letters with different subscripts (e. g. B_E, B_{30}, B_S; P_E, P_S; Q_E, Q_S; and Y_E, Y_S) show the different rotational configurations of methyl groups with the same other parameters in each case, i. e. "E", "30" and "S" show the cases in which the angles φ are 0°, 30° and 60° respectively.

Through each group, for example B_E, B_{30} and B_S, the remarkable variations of the curves are shown by the features of the third maximum with the shelf-like maximum and the fifth maximum. The curves with subscripts "S" are at least to be rejected through these groups, and curves B_E and B_{30} are the acceptable ones. This selection seems to be confirmed, although the visual method used.+

4) The curves X_E and X_S, correspond to the case of C–H = 1.13 Å, and have shown slight disagreements in *q-values*. The curves Y correspond to the model having the both angles $\angle CCC = \angle CCO = 112°$, and are to be rejected because the *q-values* and the shapes of the fifth minimum and the fifth maximum are different obviously from the visual one.

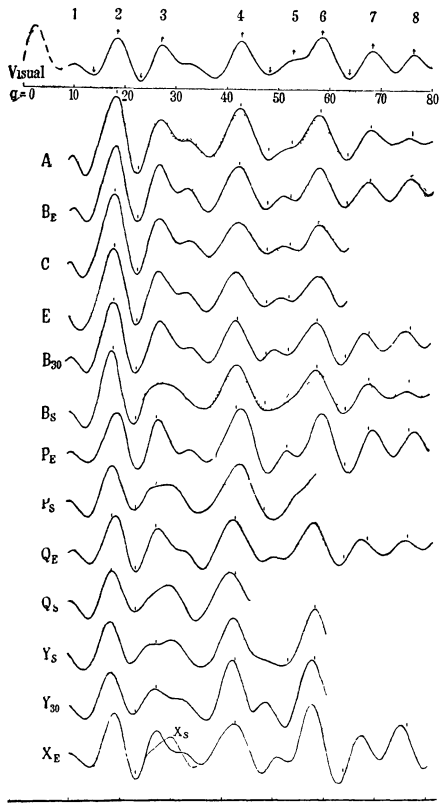


Fig. 3 A. Visual and theoretical intensity curves for isopropyl alcohol molecule.

Dotted curves on *A* and *B*s correspond to the curves of each rigid model, and real curves *A* and *B*s to the curves in which the vibration factors for each atomic distance as shown in Table II are taken into account. (In the other real curves, the factors are not taken into account for convenience, because the effects of the factors are not large enough to change the features of each maximum and minimum.)

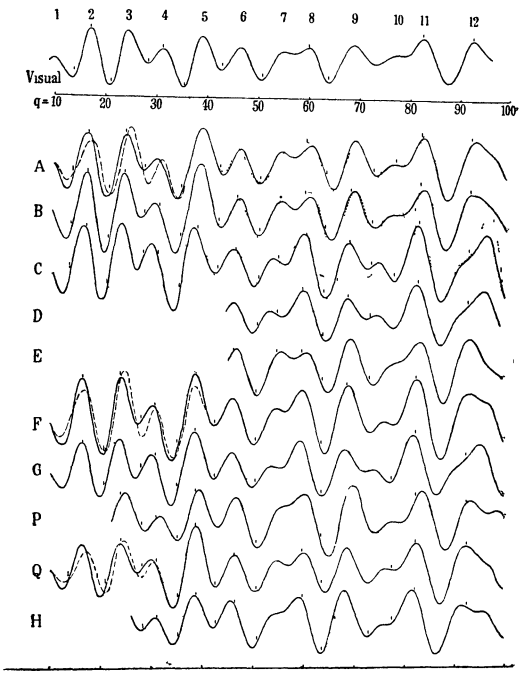


Fig. 3B. Visual and theoretical intensity curves for isopropyl chloride molecule.

Broken curves on A, F and Q in the range of $q < 45$ correspond to each eclipse model, and all real curves in this *q*-range to each staggered model. Dotted curves on A, B and C in the range of $q > 40$ correspond to the curves of each rigid model, and in all real curves from A to R in this *q*-range, the vibration factors are taken into account. The damping effects to the features of the curves seem to be remarkable in the range of $q > 50$, especially the tenth maximum and the eleventh minimum.

+ In order to obtain the better visual curve, especially to confirm the intensity relation of the third maximum with the following shelf and the fifth small maximum, we have photographed by the use of a new apparatus, which has $1/s^2$ sector and the camera length about 11.82 cm., which has recently been constructed and is now in regulating. But since the microphotometry could not yet be applied, we have measured carefully by the visual method.

The influence of the vibration factors using the values above mentioned are shown with the dotted curves on the curves A and Bs.

The radial distribution curve was computed using the best visual intensity curve (see Fig. 4), The background line is almost smoothed out and the each peak of the

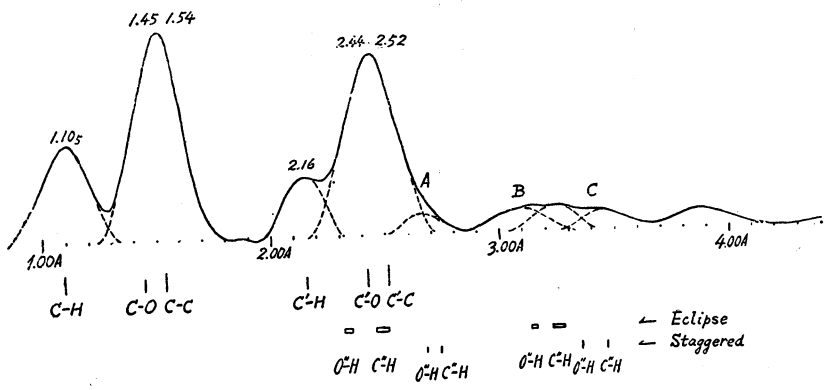


Fig. 4. Radial distribution curve for isopropyl alcohol molecule computed using the visual curve.

Under the curve, the interatomic distance corresponding to each peak is shown, and O''...H and C''...H distances are pointed out at lower levels. Interatomic distances, O''...H and C''...H, are to correspond to either level, (eclipse or staggered), in accordance with the variation of the rotational configurations. But the figures indicated by A, B and C are somewhat obscure.

curve seems to correspond almost correctly to each distance of all atom-pairs of the best model. The combinations of atomic distances O'' . . . H and C'' . . . H, corresponding to both the eclipse and staggered form of methyl groups seem to appear. From the feature of this curve, however, the fact can not be decided whether these might be the ghost maxima or not (marked with A, B and C in Fig. 4).

Isopropyl Chloride.—The visual curve and theoretical intensity curves are shown in Fig. 3B. Molecular parameters used in obtaining each theoretical curve are listed in Table IIIB. The characteristic features of the curves, which change with the variations of corresponding parameters, and the interpretation and selection based on these features of intensity curves are specified as follows:

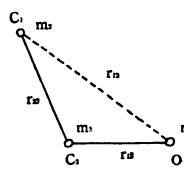
TABLE III B

THE MOLECULAR MODELS AND CORRESPONDING ASSUMED MOLECULAR CONSTANTS FOR ISOPROPYL CHLORIDE

Models	C—C (Å)	C—Cl (Å)	∠CCC°	∠CCCl°	$q/q_{obs.}$
A	1.54	1.75	109.5	109.5	1.006_0
B	〃	〃	112	109.5	1.006_8
C	〃	〃	112	112	0.989_0
D	〃	〃	114	112	(0.994_7)
E	1.54	1.77	112	108	(1.011_7)
F	〃	〃	109.5	109.5	1.002_5
G	〃	〃	114	112	0.984_5
P	1.52	1.77	109.5	109.5	(1.016_3)
Q	1.56	1.77	〃	〃	0.993_9
H	1.54	1.80	109.5	109.5	0.990_9

1) For the groups of curves from A to D and E to G, the angles ∠CCC and ∠CCCl increase in an orderly way in each group from A to D and E to G. The C-Cl distances are 1.75 Å and 1.77 Å respectively, and other parameters, C-C and rotational configurationes, remain constant.

When compared with those of the visual curve, nearly equal heights of the seventh



5) P. C. Cross and J. H. Van Vleck [*J. Chem. Phys.* **1**, 350 (1933)] have calculated that the parameters of the equation, $V=1/2\{c_{13}(\Delta r_{13})^2+c_{23}(\Delta r_{23})^2+c_{12}(\Delta r_{12})^2\}$, are $c_{13}=4.0\times10^5$dyne/cm., $c_{23}=3.5\times10^5$, and $c_{12}=1.7\times10^5$dyne cm. respectively, where V is the potential function for the ethyl alcohol molecule (XXY type molecule), Δr_{ij}'s denote the displacements of interatomic distances as shown in the figure.

6) V. Schomaker et al., *J. Am. Chem. Soc.*, **73**, 1482 (1951).

7) M. Kimura, *J. Chem. Soc. Japan.* **71**, 18 (1950) (Japan).

8) O. Bastiansen, *Acta Chem. Scand.*, **3**, 415 (1949).

9) M. Kimura and M. Yamaha, the work was reported in the First Annual Meeting of the Chemical Society of Japan, April 3rd, 1948 (at Tokyo University, Tokyo).

10) J. Ainsworth and J. Karle, *J. Chem. Phys.*, **20**, 425 (1952).

TABLE IV B

OBSERVED q-VALUES AND CALCULATED $q/q_{obs.}$ VALUES FOR BETTER MOLECULAR MODELS OF ISOPROPYL CHLORIDE

Max.	Min.	q_{obs}	wt.	A	B	C	F	Q
	2	(13.66)		(0.908)	(0.922)			(0.930)
2		16.55	1	1.003	1.009	0.982	1.015	0.997
	3	20.72	1	0.982	0.980	0.965	1.014	0.965
3		23.97	2	1.008	1.010	0.989	1.030	0.997
	4	28.10	1	0.982	0.980	0.959	1.012	0.966
4		30.82	2	0.980	0.980	0.964	1.003	0.972
	5	35.12	1	0.978	0.974	0.968	0.978	0.974
5		38.63	3	1.015	1.015	1.003	1.004	1.002
	6	42.59	2	1.021	1.017	0.997	0.997	1.006
6		46.25	3	1.012	1.012	0.995	0.995	1.002
	7	50.54	2	1.005	1.003	0.989	0.995	0.999
7		54.55	2	1.001	1.007	0.982	0.999	0.999
8		59.56	2	1.017	1.021	1.002	1.004	1.006
	9	63.60	2	1.022	1.022	1.008	1.009	1.011
9		68.60	3	1.010	1.013	0.997	1.001	0.997
	10	72.83	1	1.011	1.013	0.989	1.002	0.998
10		(77.31)	1	0.995	0.999	0.962	0.979	0.986
11		82.24	1	(1.010)	(1.010)	0.998	1.001	1.013
12		(92.33)		(1.007)	(1.007)	(1.045)	(1.001)	(0.996)
	Weighted mean:			1.006_0	1.006_8	0.989_0	1.002_5	0.990_9
	Wtd. mean sq. deviation:			0.012_9	0.013_5	0.014_4	0.010_9	0.013_9

and the eighth maxima, the small shelf-like tenth maximum on the eleventh maximum and the position of the twelveth maximum, the features in the curves A, B, E and F seem to be satisfactory. For angles ∠CCC and ∠CCCl≥112°, the features above pointed out become less satisfactory while further deviations occur, as shown in the curves D and G.

2) Curves P and Q, having constant C-Cl =1.77Å and ∠CCC=∠CCCl=109.5°, show the changes of *q-values* according to the variation of C-C distances, from 1.52Å to 1.56Å. The $q/q_{obs.}$ values of curve Q are almost acceptable, but the values of P are so large that it seems to be out of the range of errors.

3) On the curves A, F and Q, the contributions of the rotational configurations of methyl groups appear in the range $10<q<35$. The broken curve on each curve corresponds to the eclipse form of each model, and real curves in the same q-range correspond to the staggered form. By the visual method, it is hardly possible to determine exactly the intensity ratio of the second to the third maxima, because of the coexistence of background in the q-range. So the difference of this ratio which appears in the theoretical intensity curves is not remarkable enough for us to distinguish it.

4) The effects of vibration factors are approximately taken into account in all the cases A to H. Dotted curves on A, B and C in the range $40<q$ show the curves in which these factors are neglected, i.e. they correspond to the rigid models. The damping effect agrees roughly with the visual curve in the intensity relations of maxima and minima in the range $q>60$, that is, the pictures from the curves including the factors seem to require the tenth maximum to be lower and the tenth and the eleventh minima to be shallower than the respective lines joining the mentioned adjacent features of the curves in which the factors are ignored.

Various molecular parameters obtained from this investigation seem nearly to agree with and confirm those from the previous data[1], in which the results were obtained from the observation of maxima and minima up to the range $q<50$, because the observation of this report has been obtained from wider range up to $q<95$, in which the variations of features of intensity relations are conspicuously clear in this range ($50<q<95$).

Results and Discussions

From these considerations above pointed out, the models corresponding to the curves B_S, P_S, Q_S, Y_S and Y_E for isopropyl alcohol and C, D, G, P and R for isopropyl chloride are at least to be rejected in our experiment.

We have obtained the final results as follows:

Isopropyl alcohol, C−O : 1.45±0.03Å, C−C : 1.54±0.02Å, ∠CCC≈∠CCO : 110±2.5° and

the angle ∠CCO and ∠CCC are not equal to or larger than 112° simultaneously. And also the relative equilibrium position of the methyl groups against the central −CHOH group is not at least the rigorously staggered position.

Isopropyl chloride, C−Cl : 1.76±0.02Å, C−C : 1.55±0.02Å and ∠CCC≈∠CCCl : 109.5 ±1.5°.

These conclusions are reasonable, except in the case of the equilibrium position of methyl groups in the isopropyl alcohol molecule, compared with the structures of several related compounds of these molecules, but some discrepancies are found, for example, in comparison with the results of 1, 2-dichloropropane molecule by V. Schomaker et al.[14] which have shown the values 1.56Å and 1.79Å for C-C and C-Cl distances respectively.

From the results of this investigation, it seems to be hoped that we could obtain some aspects about the problems of methyl groups from the electron diffraction investigations, if we would choose adequate samples and could determine the intensity relations more quantitatively.

Summary

The molecular structures of isopropyl alcohol and -chloride have been investigated by the electron diffraction method. The atomic distances, C-O : 1.45±0.03Å, C-C : 1.54±0.02Å and valence angles, ∠CCC≈∠CCO : 110°±2.5° are determined for the former molecule, and distances C-Cl : 1.76±0.02Å, C-C : 1.55±0.02Å and angles ∠CCC≈∠CCCl : 109.5±1.5° for the latter.

The approximate thermal vibration factors have been taken into account for the determination of the best molecular models. The rotational configurations of methyl groups have been considered, but the equilibrium position of two methyl groups cannot be determined conclusively, in spite of the fact that this effect upon the intensity curves are not to be ignored in the case of isopropyl alcohol molecule.

The author wishes to express his hearty thanks to Professor Y. Morino, in the Faculty of Science, Tokyo University, Professor A. Kotera and Assistant Professor K. Suzuki in our University for their kind advice and discussions throughout this work, and to Mr. K. Kuchitsu for his kind help for the calculations of the thermal vibration factors.

Chemical Institute, Faculty of Science,
Tokyo University of Education,
Ootsuka, Tokyo, Japan

11) J. W. Coutts and L. Livingston, *J. Am. Chem. Soc.*, **75**, 1542 (1953).
12) M. Yamaha, this work was reported in the sixth Annual Meeting of the Chem. Society of Japan, April 4th, 1953 (at Kyoto Univ.).
13) W. Gordy et al., *J. Chem. Phys.*, **20**, 605 (1952), (Microwave spectroscopy).
14) V. Schomaker et al., *J. Chem. Soc.*, **20**, 555 (1952).
15) W. F. Edgell et al., *J. Chem. Soc.*, **16**, 1002 (1948), (Microwave spectroscopy). cf. W. Shard and R. A. Spur, *J. Am. Chem. Soc.*, **66**, 16 (1944).
16) See. J. R. Nielsen and C. M. Richards, *J. Chem. Phys.* **16**, 67 (1948).

The Dipole Moments of Some Polyhalocyclohexanes and their Related Compounds. I.

By Ichiro MIYAGAWA, Yonezo MORINO, and Randolph RIEMSCHNEIDER

(Received January 21, 1954)

As is well known, it is possible for the atoms attached to a carbon atom of the cyclohexane ring to exist at two positions: the polar and the equatorial ones, with regard to the relative direction of the bonds to the plane of the ring.[1,2,3a] It follows that a poly-substituted compound of cyclohexane has a lot of geometrical isomers. A good example is the case of BHC: it has actually six isomers, α to η forms,[4] due to the various combinations of the polar and equatorial bonds, and its γ-isomer is characterized by its mar-

1) O. Hassel and E. Naeshagen, *Tids. Kjemi Bergvesen Met.* **10**, 126 (1930).

2) K. Kojima and T. Yoshino, *J. Am. Chem. Soc.*, **75**, 166 (1953).

3) R. Riemschneider, a) Communication XXI. . . . The method of representation of the chair form of cyclohexane ring described in Comm. XXI is not used in the present paper; b) Comm. X, *Monat Chem.*, **83**, 394 (1952) and Comm. XXII, *Zeit. Naturforschung*, **8b**, 000 (1953); c) Comm. XXIII, ibid. **8b**, 000 (1953): d) Comm. XXV, ibid., **8b**, 161 (1953); e) Comm. XXVII, *Monat. Chem.*, **84**, 512 (1953); f) Comm., III and IV, *Zeit. Naturforschung*, **5b**, 307 (1950) and **6b**, 48 (1951).

4) As for η-BHC of the configuration of e.e.p.e.p.p. compare: R. Riemschneider, Komm., XXIV, *Monat. Chem.* **84**, 000 (1953).

vellous power as an insecticide.

Thus the determination of the geometrical configuration of the isomers of these compounds is most desirable, but it usually requires much time. As the halogen-carbon bond has a large dipole moment, its measurement would afford an effective means for this purpose, as in the case of the isomers of BHC.[5]

The critical discussions of the structure of the compounds stated here have already been presented elsewhere by one of the present authors (R.R.)[3b-f], also taking into account the dipole moment. The aim of this paper is to report the details of the measurement as well as the full information of the calculation.

Experimental

Materials All the samples measured had been prepared by one of the present authors (R.R.)[3b-f] and their dipole moments were measured by another (I. M.) without further purification.

The solvent benzene was made free from thiophene by aluminium chloride, dried over metallic sodium and then distilled, the fraction boiled within 0.1°C being collected for use.

Measurement The density d and dielectric constant ε of the solution in benzene were measured with a pycnometer and a heterodyne beat apparatus in a manner previously described.[5] The wavelength used was about 150 meters. The polarization $p_{2\infty}$ of the solute was calculated by the following formula derived by Halverstadt-Kumler's method[6]:

$$p_{2\infty}=\frac{\varepsilon_1-1}{\varepsilon_1+2}\frac{1}{d_1}\left[1+\frac{3a}{(\varepsilon_1-1)(\varepsilon_1+2)}-\frac{b}{d_1}\right] \quad (1)$$

where ε_1, and d_1 are respectively the dielectric constant and density of the solvent, and a and b are the coefficients of the linear expansion of dielectric constant and density of the solution with respect to the weight fraction w:

$$\varepsilon=\varepsilon_1+aw, \quad (2)$$

and

$$d=d_1+bw. \quad (3)$$

Then the dipole moment μ is given by the equation:

$$\mu=0.0128\left[(P_{2\infty}-P_E-P_A)\,T\right]^{1/2}, \quad (4)$$

where $P_{2\infty}=M_2p_{2\infty}$ is the molecular polarization, (M_2 being the molecular weight), P_E and P_A are the electronic and atomic polarization of the solute respectively. P_E was taken to be equal to the molar refraction MR_D for sodium D line, which was calculated by the use of the atomic refraction given in "Landolt-Börnstein Tabellen" and P_A was assumed to be 5 percent of MR_D.

The temperature of the thermostat was kept all through at 30°C, because at the time when this measurement was undertaken the room temperature sometimes exceeded 25°C.

5) Y. Morino, I. Miyagawa, and T. Oiwa, *Botyu-kagaku*, **15**, 181 (1950).
6) I. F. Halverstadt and W. D. Kumler, *J. Am. Chem. Soc.*, **64**, 2988 (1942).

Results

The weight fraction of the solute, w, the dielectric constant, ε and the density, d, of the solution are given in Table I, together with the coefficients a and b calculated from them. The molecular polarization, $P_{2\infty}$, and the dipole moment μ thus obtained are listed in Table II.

TABLE I
DIELECTRIC CONSTANTS AND DENSITIES OF BENZENE SOLUTIONS AT 30°C

w	ε	d
1. Tetrabromodichlorocyclohexane, $C_6H_6Cl_2Br_4$, m. p. 203°.		
0.00000	2.2615	0.8685
0.01814	2.2823	0.8789
0.02971	2.2947	0.8865
	$a=1.11_9$	$b=0.603$
2. Dibromotetrachlorocyclohexane, $C_6H_6Cl_4Br_2$, m. p. 178°.		
0.00105	2.2738	0.8742
0.01937	2.2846	0.8792
0.03143	2.3007	0.8862
0.04298	2.3142	0.8923
	$a=1.22_6$	$b=0.555$
3. Dibromotetrachlorocyclohexane, $C_6H_6Cl_4Br_2$, m. p. 285°.		
0.01092	2.2632	0.8738
0.01894	2.2644	0.8777
	$a=0.153$	$b=0.487$
4. Decachlorocyclohexene, C_6Cl_{10}, m. p. 95°.		
0.01464	2.2646	0.8755
0.02455	2.2668	0.8809
0.03551	2.2692	0.8865
0.05274	2.2728	0.8955
	$a=0.214$	$b=0.511$
5. Octachlorocyclohexane, $C_6H_4Cl_8$, m. p. 93°.		
0.01328	2.2755	0.8742
0.02259	2.2858	0.8791
0.04094	2.3053	0.8879
0.06166	2.3274	0.8983
	$a=1.069$	$b=0.475$
6. $C_6H_5O_2Cl$, m. p. 123-124°		
0.01371	2.3661	0.8724
0.02393	2.4425	0.8762
0.03737	2.5404	0.8809
0.05014	2.6324	0.8856
	$a=7.39_7$	$b=0.359$
7. 2, 2, 6, 6,-Tetrachlorocyclohexanone, $C_6H_6OCl_4$, m. p. 84°.		
0.01371	2.3757	0.8737
0.02772	2.4980	0.8789
0.04252	2.6300	0.8846
0.05905	2.7803	0.8910
	$a=8.98_1$	$b=0.381$

8. 1,4-Dichlorocyclohexadiene-(1,4), $C_6H_6Cl_2$, m. p. 63°.

0.03516	2.2661	0.8778
0.05975	2.2694	0.8844
	$a=0.132$	$b=0.265$

TABLE II
MOLECULAR, ELECTRONIC, AND ATOMIC POLARISATIONS, AND DIPOLE MOMENTS AT 30°C

Compounds	m.p.	$P_{2\infty}$(cc)	P_E+P_A (cc)	μ(D)
Tetrabromodichloro-cyclohexane	203	148.0	71.9	1.93
Dibromotetrachloro-cyclohexane	178	135.4	65.8	1.84
Dibromotetrachloro-cyclohexane	285	67.8	65.8	0.3
Decachlorocyclo-hexene	95	77.2	75.9-79.9	0.
Octachlorocyclo-hexane	93	128.8	70.0	1.69
$C_6H_5O_2Cl$	123-124	236	34.2	3.14
2,2,6,6-Tetrachloro-cyclohexanone	84	451	50.0	4.40
1,4-Dichlorocyclo-hexadiene-(1,4)	63	39.1	37.2	0.3

1. Tetrabromodichlorocyclohexane $C_6H_6Cl_2Br_4$ m. p. 203° and Dibromotetrachlorocyclohexanes, $C_6H_6Cl_4Br_2$ m. p. 178° and 285°. Judging from the method of preparation of these compounds, there is no doubt that they are 1, 2, 3, 4, 5, 6-substituted ones,[3b-c] exactly similar to BHC, though the accurate positions of the bromine atoms are not definitely assigned. The spacial configurations of the six isomers of BHC are schematically shown in Fig. 1, where the cyclohexane ring is represented by a hexagonal ring, the chlorine atom in an equatorial bond (e-bond) by a short line, the chlorine atom in a polar bond (p-bond) by a small circle on the hexagonal ring, the white and black circles denoting chlorine atoms above and below the central plane.

Now the moments of these compounds are considered to be nearly the same as, or slightly smaller than, those of the corresponding isomers of BHC, since the bond moment of the C–Br bond is nearly the same as that of the C–Cl bond. The moments of the isomers of BHC were found to be α: 2.2D, β: 0D, γ: 2.8D, δ: 2.2D, and ε: 0D. The moment of η-isomer has not been measured, but according to the rule suggested by Y. Morino, I. Miya-

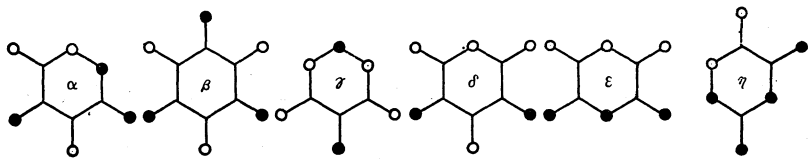
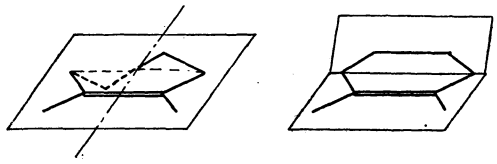


Fig. 1. Configuration of the Isomers of BHC.

gawa, and T. Oiwa,[5] it is estimated to be 1.88 D. Therefore, the observed values of the dipole moments of $C_6H_6Cl_2Br_4$, m.p. 203° (1.93 D) and of $C_6H_6Cl_4Br_2$, m.p. 178° (1.84 D) apparently indicate that they are neither β nor ε, but α, δ or η type compounds. The η-form may be safely eliminated from our consideration, because the abundance of the corresponding chlorine compound is extremely small. It can not be discriminated, however, whether they are of α-type or of δ-one.

Similarly it is concluded that $C_6H_6Cl_4Br_2$, m.p. 285° is of β type or of ε one, since its moment is negligibly small. Considering the fact that its melting point is as high as that of the β-isomer of BHC (310°), it seems probable that $C_6H_6Cl_4Br_2$, m.p. 285° has the configuration of β-form.

2. Decachlorocyclohexene, C_6Cl_{10}. For the cyclohexene ring two forms should be considered: first, the C_2 form corresponding to the chair form of the cyclohexane ring, and second, the C_s form corresponding to the boat form (See Fig. 2). The dipole moments for both forms are calculated to see which form is actually realized in this case. The assump-



C_2-form C_s-form

Fig. 2. The two forms Cychohexene Ring

tions used are as follows: the moment of the group $\begin{matrix} Cl \\ \diagdown \\ \quad C=C \\ \diagup \\ \quad Cl \end{matrix}$ is 1.74 D, located in the plane ClC=CCl and perpendicular to the double bond. The moments of the C–Cl bonds attached to other carbon atoms are 1.86 D. At the same time the induction effect suggested by us[5] are taken into account it is assumed that the C–Cl bond which is marked

by a circle in Fig. 3, induces at each bond in the direction along the bond the moment shown in the figure, the moments induced perpendicularly to the bonds being all disregarded. Of course this rule is an empirical one, but it has served to enable us to compute with reasonable accuracy not only the moments of fourteen chlorinated aliphatic hydrocarbons but also those of eleven compounds which have a cyclohexane ring.

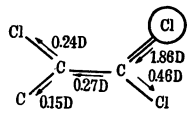


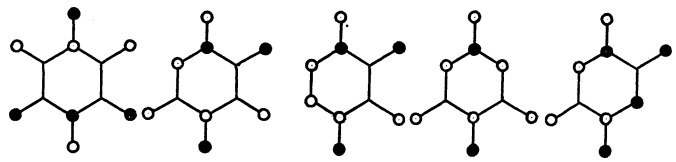
Fig. 3. The Induction Moments due to C–Cl Dipole

The calculated values of the dipole moments by use of these assumptions are found to be 0.40 D for C_s form and 0.14 D for C_2 form. Both of them lie in the allowed region from the observed value 0D, so that the configuration of the cyclohexene ring can not be decided by this discussion.

Though the present calculation gave no discrimination between the two forms, it has the merit of providing a strong evidence that in the vector addition for computing the dipole moment of a molecule, the induction effect can by no means be put out of the consideration, because, otherwise, it will result in values larger even than 2D for decachlorocyclohexene, in sharp contrast to the observed zero moment.

3. **Octachlorocyclohexane, $C_6H_4Cl_8$, m.p. 93°.** The sample was prepared by the chlorination of *p*-dichlorobenzene.[3e] It is evident that it is 1,1,2,3,4,4,5,6-substituted compound, so that the geometrical configuration of this compound must be one of the following five forms:

(1)	(1pe, 2e, 3e, 4pe, 5e, 6e)	0 D
(2)	(1pe, 2p, 3e, 4pe, 5e, 6e)	1.47 D
(3)	(1pe, 2p, 3p, 4pe, 5e, 6e)	1.86 D
(4)	(1pe, 2p, 3e. 4pe, 5e, 6p)	1.93 D
(5)	(1pe, 2p, 3e, 4pe, 5p, 6e)	0 D



(1) (2) (3) (4) (5)

Fig. 4. The Configurations of the Isomers of Octachlorocyclohexane

Their spacial configurations are illustrated in Fig. 4. The computed moments of these isomers are also given in the above, the assumptions for the calculation being the same as those used in the preceding case. The observed value, 1.69 D, suggests that it is neither (1) nor (5), but one of (2), (3), and (4). It cannot be confirmed which one of them should be assigned to $C_6H_4Cl_8$, m.p. 93°, but the most stable form (2) may be the most favourable. The reason is that the form (2) has one pair of polar C–Cl bonds, while the form (3) has two pairs and the form (4) three pairs of them. The most important part of the intramolecular potential energy of this molecule may be due to the steric repulsion between this pair of polar C–Cl bonds, which project toward the same direction at a very close proximity. The difference 0.22 D between the calculated and the observed may be ascribed to the rough approximation of the calculation.

4. **Tetrachlorocyclohexanone, $C_6H_6OCl_4$.** It was prepared by the chlorination of cyclohexanol, and the substitution by chlorine atoms was confirmed to take place at 2,2,6,6-positions.[3d] In order to estimate the dipole moment of this molecule, some additional assumptions are necessary for the value of C=O moment itself and the induction effect due to C=O bond, besides the induced moments by C–Cl bond shown in Fig. 3. The C=O bond moment may be taken to be 2.80 D from the moment of cyclohexanone.[8] If we tentatively assume for the induction effect upon and by the C=O bond the same amounts as those of the C–Cl bond, then 3.78 D is obtained for the total moment of this molecule.* The discrepancy between this and the observed value, 4.40 D, should, of course, be attributed to the provisional assumptions for the induced moment. In fact, larger induced moments should be assigned to them, since the bond moment of C=O is larger than that of the C–Cl bond. If the moments induced by the C=O dipole are increased by the ratio 2.80 / 1.86,** (Fig. 5 shows the individual values of the induced moments in this case), the computed values of the moment of this molecule becomes 4.21 D.

8) J. W. Williams *J. Am. Chem. Soc.* **52** 1831 (1930).

* The valency angles are all assumed to be tetrahedral.

** The moment induced at the C=O bond C-Cl bond remains 0.24 D, the same as that at the C-Cl bond.

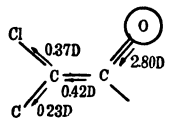
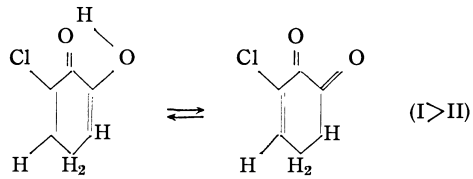


Fig. 5. The Induction Moments due to C=O Dipole

5. **$C_6H_5O_2Cl$, m.p. 123-124° from 2,2,6,6-Tetrachlorocyclohexanone.**[3d] It has been found that this compound has the following two tautomers in equilibrium in the ratio of I>II.[3d]



In order to make sure of this conclusion, the moments of the two forms (I) and (II) are calculated by the ordinary assumptions that C–Cl : 1.60 D, C–O : 1.10 D, C=O : 2.80 D, O–H: 1.53D, ∠HOC : 100°, and the bonds C–Cl, C=O, and O–H are all located in one plane,* and that the induced moments are the same as those of 2,2,6,6-tetrachlorocyclohexanone, which gave 3.78 D for its moment. The calculated moment of the form I is 1.98 D, and that of the form II is 4.33 D.** Thus, in order to explain the observed moment 3.14 D, it must be assumed that the forms I and II coexist in equilibrium at the ratio of 60 % to 40 %. Needless to say, no great credit should be laid to the value of this ratio,*** since the moments of the two forms used for the calculation are based upon many hypothetical assumptions. Yet it is enough to support the conclusion stated above that this compound is a tautomeric mixiure of the two forms, form I predominating.

6. **1,4-Dichlorocyclohexadiene-(1,4).**[3f] Since the four bonds attached to the ethylenic carbon atoms are located in one plane, this molecule has to be folded by the axis through the central two carbon atoms. If the angle ∠C=C–Cl be denoted by θ, and the angle between the two planes by φ (See Fig. 6), then the resultant moment is simply given by

$$\mu = 2\mu_{ccl} \sin\theta \sin\frac{1}{2}(\pi - \varphi)$$

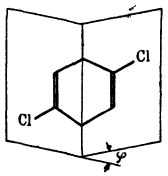


Fig. 6. The Configuration of 1,4-Dichlorocyclohexadiene-(1,4)

Therefore, inserting the value of $\mu = 0.30$ D, together with $\mu_{ccl} = 1.60$ D, and $\theta = 120°$, we get $\varphi = 14°$.

On the other hand, if we assume the angle of ∠C=C–C to be 120°, and the angle of ∠C–C–C of the central carbon atoms to be tetrahedral, then the angle between the two planes is geometrically obtained to be 40°. At a glance, it seems that there exists a serious difference between the calculated and the observed, but, if some allowance be made for the valency angles, the observed value of φ stated above can be brought into the allowed region of the molecular model. For instance, the application of the the angles ∠C=C–C : 123°, and ∠C–C–C : 112°, gives $\varphi = 17°$ instead of 40°. In fact, the widening of the valency angle are readily acceptable if we consider the fact that the repulsion between the nonbonded carbon atoms has the possibility of making the valency angles wider by a few degrees.

Here it should be noted that the values of φ computed from the dipole moment may have some errors, because the observed moment is so small that the values obtained for the angle are greatly affected by the assumption employed for the atomic polarisation. If we take $P_E + P_A = MR_D$ in place of 1.05 MR_D, the moment will increase to 0.42 D, resulting in the increase of the angle to 20°. Thus it can be concluded that the cyclohexadiene-(1,4) ring is folded, but flatter than expected by an ordinary tetrahedral angle.

Department of Chemistry,
Faculty of Science,
Tokyo University,
and Chemisches Institut der
Freien Universität, Berlin-Dahlem

* It can be easily shown that the actual deviation from the plane is virtually small.

** The interaction of two double bonds in the conjugated position is not considered for the time being.

*** The complete neglect of the induction effect provides 2.65 D and 5.11 D for the moment of the two forms, resulting in 85% to their concentrations.

The Studies of Molecular Structures by Electron Diffraction. III. The Structures of m- and p Difluorobenzene

By Hajime OOSAKA†, Hiroshi SEKINE and Takahide SAITO

(Received January 26, 1954)

Introduction

The results of the recent electron diffraction studies on the carbon-fluorine distances in aromatic compounds are collected in Table I.

TABLE I

THE PREVIOUS RESULTS OF THE C-F DISTANCES OF FLUORINE-CONTAINING AROMATIC COMPOUNDS

Substance	C-F distance (Å)	Reference
C_6H_5F	1.34±0.04	1
C_6H_5F	1.31±0.03	2, 4
o-$C_6H_4F_2$	1.35±0.03	1
p-$C_6H_4F_2$	1.31±0.03	3
o-C_6H_4FCl	1.31±0.03	3
p-C_6H_4FBr	1.30±0.03	3

As shown in it, one of us[1] reported that the distance is shorter in monofluorobenzene and o-difluorobenzene than in aliphatic compounds, but soon later Hassel[2] reported an even shorter distance in monofluorobenzene, which seemed compatible with the recent data of chlorine-or bromine-containing compounds[3]. In these, it is difficult to determine the precise C—F distance, because the chlorine or bromine atom has much greater scattering power than fluorine. That is the reason why we feel an interest in the difluorosubstitutes, although we may find different C—F distances from the monofluorobenzene.

Experimental

The samples, m-difluorobenzene[5] and p-difluorobenzene,[6] were prepared by the Schiemann reaction. They showed the boiling points 82°C. and 88°C., respectively.

The camera length is about 9.1 cm. The electron wave length, about 0.055 Å, was calibrated with gold foil diffraction.

1) H. Oosaka, This Bulletin, **15**, 31 (1940).
2) O. Hassel and H. Viervoll, *Acta chemica Scand.*, **1**, 149 (1947).
3) H. Oosaka and Y. Akimoto, This Bulletin, **26**, 433 (1953).
4) T. Yuzawa and M. Yamaha, This Bulletin, **26**, 414 (1953).
5) G. Schiemann and T. Pillarsky; *Ber*, **62**, 3039 (1929), 3035 (1929).
6) P. Ruggli and E. Capser, *Helv. Chim. Acta.* **18**, 1414 (1435).

Interpretation

The diffraction photographs were interpreted by the usual visual method. For the calculation of the theoretical intensity curves, the formulae

$$I(q)=k\sum_i\sum_j \frac{Z_iZ_j}{r_{ij}} \exp(-a_{ij}q^2)\sin\frac{\pi}{10}qr_{ij}$$

$$q=(40/\lambda)\sin(\theta/2) \qquad a_{ij}=(\pi^2/200)l_{ij}^2$$

are used, where r_{ij} is the distance between the i-th and j-th atom, λ is the electron wave length, θ is the scattering angle, Z_i is the atomic number of i-th atom, and l_{ij} is the mean amplitude of r_{ij}. The thermal vibration terms are neglected as a first approximation, i.e., we put $l_{ij}=0$. It is assumed that the hydrogen and fluorine atoms are coplanar with the regular hexagon benzene ring, and that the distances of C—C and C—H are 1.39 Å. and 1.08 Å. respectively. All the interference terms except those of hydrogen atoms are taken into account. The five theoretical curves calculated for these molecules with C—F distances of 1.27, 1.29, 1.31, and 1.35 Å and a visual intensity curve obtained by photographs are compared in Fig. 1 and 2. The values of q of the observed and calculated maxima, and their ratios $q_{calc.}/q_{obs.}$ are given in Table II and III.

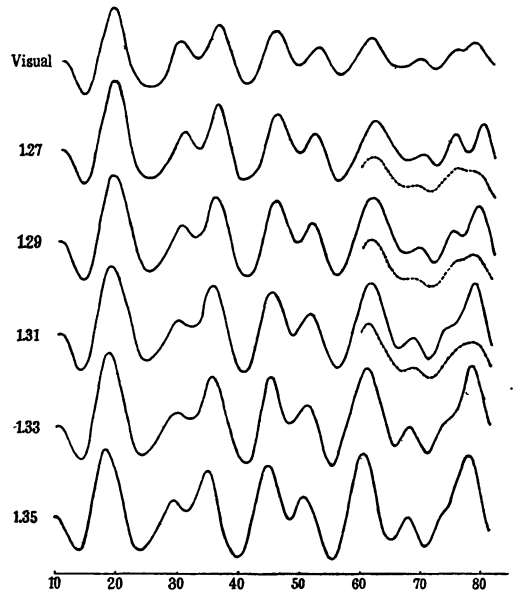


Fig. 1. The visual and theoretical curves of m-Difluorobenzene.

7) I. Karle, *J. Chem. Phys.*, **20**, 65 (1952).
8) Y. Morino and Kuchizu, private communication.

TABLE II

$q_{calc.}/q_{obs.}$ OF *m*-DIFLUOROBENZENE

	C-F	1.27	1.29		1.31		1.33
Max.	$q_{obs.}$	$q_{calc.}/q_{obs.}$	$q_{calc.}/q_{obs.}$		$q_{calc.}/q_{obs.}$		$q_{calc.}/q_{obs.}$
1	18.5	1.011	1.005		1.000		0.995
2	29.6	1.024	1.020		1.017		1.014
3	35.9	0.994	0.989		0.983		0.981
4	45.2	1.011	1.007		1.002		0.998
5	52.1	0.996	0.992		0.989		0.984
6	61.0	1.012	1.008	1.005+	1.003	1.000+	1.000
7	68.8	1.016	1.006	0.999	0.999	0.991	0.994
8	74.8	1.004	1.000	1.006	0.996	1.006	0.992
9	78.5	1.013	1.006	0.996	1.000	0.993	0.996
Arithmetical mean		1.009	1.003	1.002	0.999	0.998	0.995
Mean square root deviation		±0.009	±0.009	±0.009	±0.007	±0.007	±0.009

+: These values were estimated from the dotted curves in Fig. 1, which contained the thermal vibrational terms.

Finally, as a second approximation, the thermal vibration terms l_{ij}, roughly estimated (in Table IV) in reference to the calculated aliphatic data,[7,8] are introduced into the most probable three models, for $q \geqq 60$. (The values $q_{calc.}/q_{obs.}$ are given in Table II and III.)

The radial distribution function is not calculated, since the C—F distance is the only one variable.

Details and Results

(a) ***m*-Difluorobenzene** (Fig. 1 and Table II). In glancing over the intensity curves, the models for C—F=1.29, 1.31 and 1.35 Å seem right. According to the careful examination of these models on the relative intensities of the corresponding maxima, especially max. VII, the $q_{calc.}/q_{obs.}$ values, and their mean deviations, it is reasonable for the C—F distances of *m*-difluorobenzene to be 1.30±0.03 Å.

(b) ***p*-Difluorobenzene** (Fig. 2 and Table III). A procedure similar to the above, leads us to the conclusion that the C—F distance of this molecule is 1.30±0.03 Å.

They agree well with the results of the previous investigations.

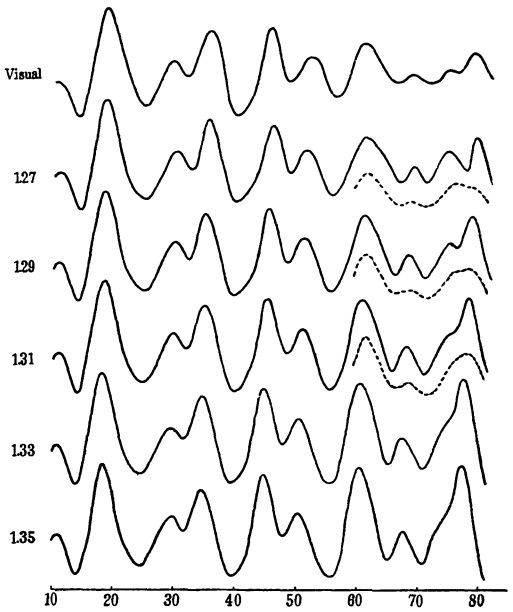


Fig. 2. The visual and theoretical curves of *p*-Difluorobenzene.

TABLE III

$q_{calc.}/q_{obs.}$ OF *p*-DIFLUOROBENZENE

	C-F	1.27	1.29		1.31		1.33
Max.	$q_{obs.}$	$q_{calc.}/q_{obs.}$	$q_{calc.}/q_{obs.}$		$q_{calc.}/q_{obs.}$		$q_{calc.}/q_{obs.}$
1	18.5	1.016	1.011		1.005		1.005
2	29.5	1.027	1.024		1.017		1.014
3	35.8	0.992	0.986		0.980		0.975
4	45.6	1.007	1.002		0.996		0.991
5	52.3	0.987	0.985		0.979		0.973
6	61.1	1.002	1.000	1.000+	0.998	1.000+	0.997
7	68.9	1.004	0.993	0.991	0.988	0.984	0.985
8	74.8	1.005	1.007	1.009	1.005	1.004	0.999
9	79.0	1.008	1.000	1.000	0.995	0.995	0.989
Arithmetical mean		1.005	1.001	1.001	0.996	0.996	0.991
Mean square root deviation		±0.011	±0.012	±0.012	±0.012	±0.011	±0.012

+: These values were estimated from the dotted curves in Fig. 2, which contained the thermal vibrational terms.

TABLE IV
THE COEFFICIENTS OF THE THERMAL VIBRATIONAL TERMS; a_{ij}

$a_{ij}=0.04935\times 1_{ij}^{2}$

Atomic pair	a_{ij}	Atomic pair	a_{ij}
C—C	0.000049	C—F	0.000089
C···C′	0.000064	C···F′	0.000160
C···C″	0.000089	C···F″	0.000253
C—H	0.000128	C···F‴	0.000287
C···H′	0.000226	H—F	0.000130
C···H″	0.000400	$(H\cdots F)_m$	0.000240
C···H‴	0.000460	$(H\cdots F)_p$	0.000350
		$(F\cdots F)_m$	0.000260
		$(F\cdots F)_p$	0.000350

Summary

The C—F distances of *m*-difluorobenzene and *p*-difluorobenzene are investigated to be almost equal, 1.30±0.03 Å.

We have great pleasure in acknowledging our debt of gratitude to Professor A. Kotera for his continued encouragement during this research. We wish to express our thanks to Mr. M. Yamaha, Mr. M. Igarashi and Mr. Y. Akimoto for their helpful discussions and suggestions.

Chemical Laboratory, Tokyo Bunrika University, Tokyo

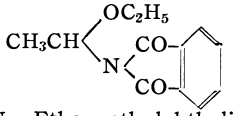
LETTER

Addition Reactions of Amino Compounds to Ethyl Vinyl Ether

By Junji FURUKAWA, Akira ONISHI, Teiji TSURUTA, and Shiro OSHIMA

(Received November 27, 1953)

A new product (A) was obtained in the reaction between phthalimide and ethyl vinyl ether without any added catalyst. The analysis and the molecular weight determination suggest that (A) is likely to be an addition product, the structure of which being assumed to be either (I) or its β-isomer. In view of the fact that similar addition reactions of alcohols[1] and phenols[2] form acetals, the α-adducts, the adduct (A) may be expected to be (I).



(I) N-α-Ethoxyethylphthalimide

On decomposition by hydrochloric acid, the adduct (A) gave rise to acetaldehyde along with phthalimide. The formation of acetaldehyde is in favor of the structure of N-α-isomer (I).

A similar addition product (B) has likewise been obtained from a reaction with carbazole as the amino component. On the other hand, Voronkov[3] reported that vinyl ethers condense with monocarboxylic acid amides to yield ethylidene-di-O-acylamide, $CH_3CH[OC(=NH)R]_2$, in the presence of hydrochloric acid. The structure of the O-acylamide type is obviously excluded from the possible structures for the adduct (B), but is not for the adduct (A).

It was found that vinyl acetate also may condense with phthalimide to give rise to a similar adduct.

Detailed examinations as to the structure of the adducts as well as experiments on the reactions between vinyl compounds and various amino compounds (imides, amides and amines) are now in progress in our laboratory.

Experimental

A mixture of 22.0 g. (0.15 mol.) of phthalimide and 32.4 g. (0.45 mol.) of ethyl vinyl ether was heated at 155° for 5 hours in a 100 cc.-autoclave. Evaporating the unreacted vinyl ether, a viscous oily residue was obtained, which gradually turned into a crystalline matter. The yield of the adduct was quantitative. Being recrystallized from petroleum benzine and alcohol, colorless crystals (A) were obtained which showed m.p. 64~65°. *Anal.* Calcd. for (I), $C_{12}H_{13}O_3N$: C, 65.74, H, 5.98, N, 6.39. Found: C, 65.92, H, 5.52, N, 6.82. *Molecular weight*: Calcd. 219.23; Found: 216 (cryoscopic method). Boiling 5 g. of (A) with 14 cc. of hydrochloric acid (1:1), phthalimide and acetaldehyde were formed in almost equimolecular amount, which were identified by mixed melting with authentic specimens of the imide and of the 2.4-dinitrophenylhydrazone, respectively.

The experiment for carbazole was essentially the same as stated above.

This work was supported by a grant in aid for the Miscellaneous Scientific Research from the Ministry of Education.

Institute for Chemical Research, Kyoto University, Takatsuki, Osaka

1) N. A. Gershtein and M. F. Shostakovskii, *J. Gen. Chem.* (U. S. S. R.), **18**, 451 (1948); *Chem. Abst.*, **42**, 7243 (1948).
2) M. F. Shostakovskii, ibid., **20**. 608 (1950); *Chem. Abst.*, **44**, 7754 (1950).
3) M. G. Voronkov, *J. Gen. Chem.* (U. S. S. R.), **21**, 1631 (1951); *Chem. Abst.*, **46**., 8002 (1952)

Photopolymerization of Vinyl Chloride by Mercury Sensitization

By Masao KOIZUMI, Kazuo NAKATSUKA and Shunji KATO

(Received August 19, 1953)

A. Introduction

In the course of the study of photopolymerization of vinyl compounds, we have found that the polymerization of vinyl chloride (in the vapor phase) initiated by the light of a low pressure mercury lamp, is mainly a photosensitized reaction by mercury vapor and that the effective light is 1850 Å and not 2537 Å. The present paper will report the main features of the reaction and some kinetic studies about it.

B. Apparatus and Procedure

The main part of the apparatus ordinarily used is shown in Fig. 1. It is somewhat similar to the one used by H. W. Melville[1]. B is the reaction vessel of about 20cc. (quartz) and A is a mercury-cut through which the sample is led into the reaction vessel, which is also utilized as a manometer to trace the reaction. The temperature was usually controlled by streaming water. The mercury lamp is a simple D. C. type of about 20 cm. long (300 W).

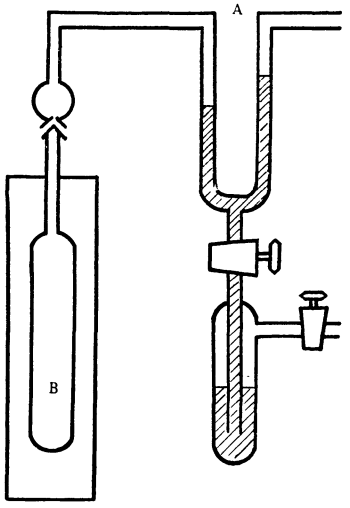


Fig. 1 The main part of the apparatus

C. Some Features of the Reaction

1. When the illumination is commenced, the pressure begins to decrease and a white polymer is deposited on the surface of the vessel. The deposition is observed only on the front part, and when the vessel is covered by Al foil partly, the back side of the covered part is completely free from the deposit, the boundary being as sharp as the foil itself. There is no sign of any side reactions.

2. When the illumination is cut off, the reaction stops at once, showing that there is no active material surviving such as observed by Melville in the case of methyl metacrylate[1]

3. When the wall of the vessel is lined with the material transparent down to 2000Å such as NaCl or paraffin, the reaction is affected remarkably. When pieces of metal such as steel or bronz are previously thrown into the vessel, the rate is slightly increased while pieces of quartz rods of the same origin as that of the vessel slightly retards the rate.

4. When only the light 2537 Å is employed, the reaction scarcely goes on. This fact was particularly confirmed by the following experiment. Using the reaction vessel with two parallel plates, it was ascertained that the intensity of light 2537 Å which had passed through the reaction vessel was quite strong and yet there was observed no pressure decrease nor the white deposit on the wall of the vessel. On the other hand, when the light of mercury lamp was filtered by a thick layer of water, the reaction was often suppressed remarkably. These facts strongly suggest that the effective light is the one of such short wave length that is liable to be absorbed by a trace of impurity in water.

5. When mercury vapor is cautiously eliminated, the reaction is reduced to a very small quantity. This fact was confirmed by the apparatus particularly designed, the pressure decrease being measured with a membrane manometer.

All the above facts strongly support the view that the present photopolymerization is initiated by 1850 Å line of Hg lamp, the intensity of which is so weak that it is almost completely absorbed in the region near the front part of the vessel and that the reaction is heterogeneous taking place on the wall of the vessel at least in some steps of the overall reaction. In addition, the mercury vapor supposedly acts as photosensitizer.

1) H. W. Melville, *Proc. Roy. Soc.*, **A163**, 511 (1938); *Proc. Roy. Soc.*, **A167**, 99 (1937).

D. Some Kinetic Studies

1. The Effect of the Pressure of Vinyl Chloride—In the present experimental condition, the pressure decrease is very small compared with the initial pressure of vinyl chloride, and it goes on linearly against time. The pressure decrease during initial 60 minutes is completely proportional to the initial pressure of vinyl chloride showing that the reaction is of the first order with regards vinyl chloride. (See Fig. 2)

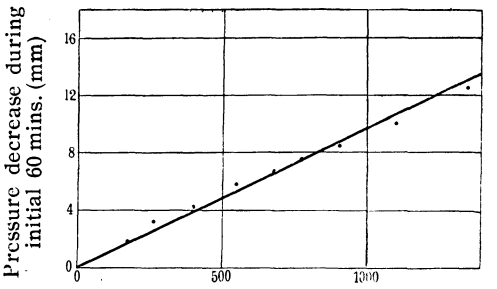


Fig. 2. Dependence of the rate upon the pressure of vinyl chloride

2. The Effect of Light Intensity—The reaction rate is proportional to the intensity of light as shown in the following table.

THE EFFECT OF INTENSITY OF LIGHT UPON THE RATE

	P (Press. of $CH_2=CHCl$)	I (Relative intensity)	ΔP (Press. decrease per hr.)	k' ($\Delta P/P$)	k'/I
1	760.5 mm	1	9.5 mm	0.0125	0.0125
2	763.0	$\frac{1}{2}$	5.2	0.0068	0.0136
3	768.0	1/3	3.4	0.0044	0.0132
4	761.2	$\frac{1}{4}$	2.4	0.0032	0.0128

In this experiment the intensity of light was varied with the use of blackened copper nets or black perforated celluloid plates.

3. The Effect of Temperature—The reaction rate was measured at three temperatures 10°C, 41°C and 95°C. At all temperatures, the pressure decrease is linear against time, and the reaction rate calculated from the slope of each line is proportional to the pressure of vinyl chloride.

Under the present experimental condition, the rates at various temperatures are expressed by the following formulas.

10°C $v=0.00017\ P_{C_2H_3Cl}$ (mm./min.)

41°C $v=0.000025\ P_{C_2H_3Cl}$

95°C $v=0.00001\ P_{C_2H_3Cl}$

The measurement at 95°C is somewhat unreliable but it is evident that the rate decreases with the rise of temperature. The activation energy is calculated to be about −6 Kcal.

4. The Effect of the Pressure of Mercury Vapor—The effect of the pressure of mercury vapor was examined by comparing the results of the two series of experiment at elevated temperatures of which the one was performed in the presence of a mercury drop at the bottom of the vessel while the other was done in the ordinary condition. The result is that the rate increases monotonously with the rise of the pressure of mercury vapor as shown in the following table (mean value of several experiments).

Temp.	Mercury pressure	Rate of pressure decrease
	mm.	mm./min.
41 °C	0.0005	0.000025
	0.0065	0.00025
95 °C	0.0005	0.000007
	0.21	0.0014

The rate may be regarded as approximately proportional to the mercury pressure in its low pressure region.

To sum up the above results, the reaction rate can be expressed as follows.

$$v=k\ [CH_2=CHCl]\ [Hg]\ I \qquad (1)$$

where I is the intensity of the incident light, which is absorbed completely.

E. Discrimination of the Function of Mercury Vapour on the Basis of the Photopolymerization by Al Spark

In section C, it was shown that the existence of mercury vapor is essential for the reaction.

To decide whether the function of mercury is sensitization or catalysis, the investigation of photopolymerization induced by the light of different wave length other than 1850 Å is expected to be much helpful. Thus if the polymerization takes place by another light and the accelerating action of mercury vapor is still perceived, then the function of mercury vapour in the case of mercury lamp would perhaps be catalytic in nature, while on other hand, if no effect of mercury vapour is existent in the case of another light, the action of

mercury in the case of mercury lamp ought to be a sensitizing one.

From such a viewpoint, we examined the photopolymerization by Al spark and particularly the effect of mercury vapour on the reaction rate. The conditions of Al spark employed are as follows: spark gap 0.5 cm., voltage 10000V; condenser inserted; capacity, 0.02μF. By taking the emission spectrum, three strong lines near 1850 Å were confirmed to exist in this condition. We were much indebted to Dr. T. Kuzirai of Kyoto University for taking the spectrum.

1. The polymerization occurs in the ordinary condition (mercury vapour is existent) just in the same order of magnitude as in the case of mercury lamp.
2. The polymer deposited is quite different in appearance from that obtained in the case of mercury lamp. It is transparent and looks like liquid. Even when mercury vapour is excluded as cautiously as possible, the reaction rate is not influenced beyond the experimental error. It seems rather to be accelerated to some extent.

The above results lead us to the conclusion that the polymerization by Al spark is quite a different reaction from that by mercury lamp, and that in the former case it is a simple photochemical one, while in the latter it is a photosensitized reaction by mercury vapor.

F. Discussion of the Mechanism on the Basis of Kinetic Formula

In Section D. the kinetic formula (1) was derived from the experimental results.

The reaction mechanism must be such as conforms to the above relation, and this condition gives us the criterion to decide the probable mechanism.

The problem is therefore to tabulate all the mechanisms conceivable and to give for each of them an appropriate reaction formula.

Let us therefore classify, at first, the types of reaction in the following way.

α) Complete homogeneous gaseous reaction

β) Heterogeneous reaction

β) is further classified into seven types according to the circumstances that each step of the overall reaction, that is initiation, propagation, and termination, be a gaseous or a wall reaction. They are

	β							α
	(i)	(ii)	(iii)	(iv)	(v)	(vi)	(vii)	(viii)
Init.	W	W	W	W	G	G	G	G
Prop.	W	W	G	G	W	W	G	G
Term.	W	G	W	G	W	G	W	G

In the above list, G and W means a gaseous or wall reaction, respectively. All these types must be further classified according to the detailed scheme of initiation, propagation and termination.

Case (α) Let us first consider case (α). To derive an overall kinetic formula, one must give the rate expression for each step.

I) *Initiation*

$$Hg+h\nu \rightarrow Hg^* \quad Hg^*+M \rightarrow M^*+Hg$$

The velocity of initiation is given by the following equation.

$$v_i = k_i I \frac{\alpha_{Hg}[Hg]}{\alpha_M[M]+\alpha_{Hg}[Hg]}[M]$$

where I is the intensity of light to be absorbed, α_{Hg} and α_M are the molecular extinction coefficients of mercury and vinyl chloride vapour respectively. The above equation is derived on the assumption that the spontaneous deactivation of excited mercury atoms is not important.

The magnitude of α_{Hg} and α_M are unknown but there is no doubt that the vapor of vinyl chloride absorbs the light in the region of 1850 Å not so little. Besides $[M] \gg [Hg]$. Therefore, it may safely be assumed that $\alpha_M[M] \gg \alpha_{Hg}[Hg]$. This relation may also be supported to some extent by the experimental result. Thus if $\alpha_M[M] \approx \alpha_{Hg}[Hg]$ the reaction formula can not be so simple as (1). Again, if $\alpha_{Hg}[Hg] \gg \alpha_M[M]$, v_i ought to be independent of [Hg] and the overall reaction rate cannot be proportional to [Hg] irrespective of any scheme of the two succeeding steps, if the gaseous initiation really holds at all.

For these reasons, the above formula can be put as follows

$$v_i = k_i I \frac{\alpha_{Hg}[Hg]}{\alpha_M} \qquad (2)$$

II) *Propagation*

$$M^*+M \rightarrow M_2^* \quad M_2^*+M \rightarrow M_3^*$$

There may be no question as to the propagation process,

$$v = k_p[M][R]$$

where R is an active radical.

III) Termination

Types of termination conceivable are as follows.

a) R+R→P
b) R+Hg→P
c) R+M→P

Now the velocity of the overall reaction is given by v, that of the propagation process, and the application of the stationary state method easily leads to the following kinetic formulas for each case.

a) $v=k_p\sqrt{\frac{k_i}{k_t}\frac{I}{\alpha_M}}\alpha_{Hg}[Hg]\,[M]$

b) $v=k_p\frac{k_i}{k_t}\frac{I}{\alpha_M}\alpha_{Hg}[M]$

c) $v=k_p\frac{k_i}{k_t}I\frac{\alpha_{Hg}}{\alpha_M}[Hg]$

All the above formulas contradict the experimental result. Thus the conclusion that the reaction is not homogeneous, can be derived merely from the kinetic formula.

Case (β) The analogous deduction can be made for case (β). The details of the discussion will be given eleswhere and only essential points will be described here briefly.

I) Initiation when the initiation takes place in the gaseous phase, the result is just the same as in the case α.

When the initiation takes place on the wall, v_i will be given by the following equation

$$v_i=k_i\,I\,\frac{\alpha_{Hg}[Hg][[M]]}{[M]} \qquad (3)$$

where [[M]] represents the surface concentration of vinyl chloride monomer.

This relation can be derived as follows.

Excited mercury atoms which can arrive at the wall during its life are those which exist in the extremely close neighbourhood of the surface. If the mean distance through which activated atoms can reach the wall be put as Δd, v_i may be put as follows:

$$v_i=k_i\,I\,\alpha_{Hg}[Hg]\,\Delta d\,[[M]]$$

Δd depends on various factors, but in the present case it is essential how it is influenced by the pressure of vinyl chloride. Taking account of the fact that the experimental relation (1) is very simple, it may be most probable to put Δd as inversely proportional to the latter, since it is theoretically expected to decrease as the pressure of vinyl chloride increases. Thus the equation 3) is obtained*.

Using 2) or 3) for initiation, the following possibilities were criticized for i), ii), iii), iv), v), vi), vii) of case (β).

I) Initiation Gas or wall

II) Propagation Radicals combine with monomer molecules (in the vapour phase) irrespective whether the reaction takes place in the gaseous phase or on the wall.

III) Termination Gas: Three possibilities similar to a), b), c) of (α)

Wall: d) [R]+[R]→[P]
e) [R]+R→[P]
f) [R]+Hg→[P]
g) [R]+M→[P]
h) [R]+[S]→[P]
i) [R]+[M]→[P]
j) R+[M]→[P]
k) R+[S]→[P]

where S means the wall of the vessel, and [ ] represents the molecular species in the adsorbed state.

The result of the critique is that five types of mechanisms conform the relation (1) and if one takes account of the fact that the addition of quartz rod decrease the rate to some extent, then the selected mechanisms are as follows.

	Init.	Prop.	Term.	Type of termination kinetic formula
v)	G	W	W	h) [R]+[S]→P $v=\frac{k_pk_i}{k_t}I\frac{\alpha_{Hg}}{\alpha_M}[Hg][M]$
				i) [R]+[M]→P $v=\frac{k_pk_i}{k_t}I\frac{\alpha_{Hg}}{\alpha_M}\frac{[Hg][M]}{[[M]]}$
Vii)	G	G	W	k) R+[S]→P $v=\frac{k_pk_i}{k_t}I\frac{\alpha_{Hg}}{\alpha_M}[Hg][M]$
				j) R+[M]→P $v=\frac{k_pk_i}{k_t}I\frac{\alpha_{Hg}}{\alpha_M}\frac{[Hg][M]}{[[M]]}$

It is to be noted that the adsorption of vinyl chloride must be saturated in order that the scheme v) i) and vii) j) may be adopted.

The conclusion is that the mechanism of the principal polymerization reaction by mercury lamp is given as follows.

Initiation takes place in the gaseous phase

* Any relations other than (3) can not lead to (1), how the succeeding steps may be assumed.

Propagation proceed in the gaseous phase or on the wall. Termination takes place on the wall and the radical in the gaseous phase is stabilized either by its collision against the surface or by the interaction with adsorbed monomer molecules, while in the case that propagation proceeds on the wall, the radical is stabilized spontaneously or by the interaction with adsorbed monomer.

Thus the scheme of the reaction is given as follows.

$$\text{Init.} \quad \begin{cases} Hg + h\nu \rightarrow Hg^* \\ Hg^* + M \rightarrow M^* \end{cases}$$

$$\text{Prop} \quad \begin{cases} M^* + M \rightarrow M_2 \\ \text{or} \begin{cases} M^* \rightarrow [M^*] \\ [M^*] + M \rightarrow [M_2^*] \end{cases} \end{cases}$$

$$\text{Term.} \quad \begin{cases} [R] + [S] \rightarrow P \\ \text{or } [R] + [M] \rightarrow P \\ \text{or } R + [S] \rightarrow P \\ \text{or } R + [M] \rightarrow P \end{cases}$$

Summary

It was found that the photopolymerization of vinyl chloride in the presence of mercury vapor is mainly a sensitized reaction due to the latter. The effective light is 1850 Å and not 2537 Å.

As a result of some kinetic studies, it was confirmed that the initiation of the chain takes place in the gaseous phase, the propagation proceeds in the gaseous phase or on the wall, and lastly, the termination occurs only on the wall of the vessel.

Details of the experiment and full discussions will be published in Journ. Polytech. Osaka City University.

The cost of the present research has been partly defrayed from the Scientic Research Grant from the Ministry of Education.

Institute of Polytechnics,
Osaka City University, Osaka

Studies on the Organic Phosphorescence. I.

Shunji KATO and Masao KOIZUMI

(Received August 19, 1953)

Introduction

According to the current interpretation of the organic phosphorescence[1] which is emitted by many unsaturated compounds under suitable conditions, such as in solid solution or in adsorbed state, the whole process of phosphorescence concerns mainly the isolated molecule, and the phosphorescent state is a triplet state (T-state).

Now, the triplet state, which is considered to be of a biradical nature, deserves special attention from the photochemical standpoint[2] owing to its reactivity and especially to its extraordinary long life compared with the ordinary excited state (S′-state). But the role of the triplet state in connection with the photochemical reaction is not quite certain as yet, and the systematic studies are very much desirable.

The present authors have constructed an apparatus for the accurate measurement of decay of organic phosphorescence and are attacking the above problems by studying the quenching effects of many substances upon the phosphorescence, and especially are trying to determine whether quenchers affect on S′-state or T-state. The purpose of the present paper is to give some mathematical relations which may help to elucidate the mechanism of the quenching action, and to report some results as to the self-quenching (concentration quenching) of filter paper-Trypaflavine phosphor.

A. Kinetic Expressions for the Initial Intensity and the Life of Phosphorescence

From the standpoint of photochemistry, it may be essential to decide whether the quenching action operates selectively on the singlet S′-state or triplet T-state or alternatively on both states equally well. We considered about this problem on the basis of Lewis' scheme and arrived at the conclusion that the measurement of both the initial intensity and the life of phosphorescence in the absence and in the presence of quenching materials, may be much helpful for this decision. The mathematical procedure will be stated briefly below.

Lewis' scheme of phosphorescence is schematically represented as follows. (cf. Fig. 1)

* Physicochemical Studies of Organic Dyestuffs in Relation to Photochemistry V.

1) G. N. Lewis and M. Kasha, *J. Am. Chem. Soc.*, **66**, 2100 (1944); G. N. Lewis, M. Calvin and M. Kasha, *J. Chem. Phys.*, **17**, 804 (1949).

2) M. Calvin and G. D. Dorough, *J. Am. Chem. Soc.*, **70**, 699; **71**, 4024 (1949).

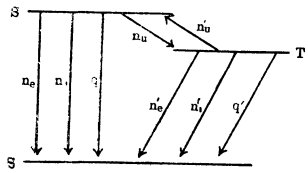


Fig. 1

1) S→S′: excitation by light absorption.
2) Fluorescence is the emission accompanied when the molecule excited by the process (1) directly falls down to S-state.
3) S′→T: transition to the triplet state.
4) β-phosphorerescence is the emission which is accompanied with the transition T→S.
5) α-phosphorescence is the emission accompanied with S′→S which succeeds the process T→S′.

Put the various transition probabilities as follows.

From S′

n_e: transition to the ground state accompanied with the emission

n_i: transition due to inner quenching effect (including the effect due to the interaction between adsorbent and dye molecule. The effect of inevitable impurity may also be included)

q: quenching effect of a substance

n_u: transition to the triplet state

From T

n_e': transition to the ground state accompanied with the emission

n_i': transition due to inner quenching effect (analogous to n_i)

q': quenching effect of a substance

n_u': transition to S′-state

Using these constants, the differential equations for the number of molecules in S′-state (N_S) and in T-state (N_T), after the interruption of illumination are given as follows:

$$\frac{dN_S}{dt}=-(n_e+n_i+n_u+q)\,N_S+n_u'\,N_T \qquad (1)$$

$$\frac{dN_T}{dt}=-(n_e'+n_i'+n_u'+q')\,N_T+n_u\,N_S \qquad (2)$$

If we take account of the fact that the life time of S′-state is $10^{-7}\sim10^{-8}$ sec, while that of triplet T-state is of the order of 0.1 sec, the exact solutions which consist of the exponential terms can be approximately expressed by a single exponential term. Thus N_T and N_S after the interruption of illumination are given as follows.

$$N_T=\frac{n_u Q}{\pi_s\pi_t-n_u n_u'}\cdot e^{-\left\{\pi_t-\frac{n_u n_u'}{\pi_s}\right\}t} \qquad (3)$$

$$N_S=\frac{n_u Q}{\pi_s\pi_t-n_u n_u'}\cdot\frac{n_u'}{\pi_s}e^{-\left\{\pi_t-\frac{n_u n_u'}{\pi_s}\right\}t} \qquad (4)$$

where Q is the number of molecules excited per second during illumination, and

$$\pi_s=n_e+n_i+n_u+q$$
$$\pi_t=n_e'+n_i'+n_u'+q'$$

From (3) and (4) the intensity of phosphorescence at an arbitrary time (t) is given as follows.

$$I_p=n_e'N_T+n_e N_S=\frac{Q n_u}{\pi_s\pi_t-n_u n_u'}\left[n_e'+\frac{n_u' n_e}{\pi_s}\right]e^{-\left\{\pi_t-\frac{n_u n_u'}{\pi_s}\right\}t} \qquad (5)$$

The formula (5) gives the decay constant α (reciprocal of the average life τ, $\alpha=\frac{1}{\tau}$) and the initial intensity of phosphorescence as follows.

$$\alpha=\pi_t-\frac{n_u n_u'}{\pi_s}=(n_e'+n_i'+q')+\frac{n_u'(n_e+n_i+q)}{\pi_s} \qquad (6)$$

$$I_{po}=\frac{n_u Q}{\pi_s\pi_t-n_u n_u'}\left(n_e'+\frac{n_u' n_e}{\pi_s}\right)=\frac{n_u Q}{\alpha}\cdot\frac{n_e'\pi_s+n_u' n_e}{(\pi_s)^2} \qquad (7)$$

(6) and (7) are the general expressions when the quencher acts both on S′-and T-states.

(6) and (7) are completely correct in the practical sense so long as the natural life of T-state is extraordinary long compared with that of S′-state which is $10^{-7}\sim10^{-8}$ sec.

When the quenching substance is absent, α and I_{po} in (6) and (7) are put as $\alpha^{(0)}$ and $I_{po}^{(0)}$ respectively, then the formulas for $\alpha^{(0)}$ and $I_p^{(0)}$ are given as follows.

$$\alpha^{(0)}=\pi_t^{(0)}-\frac{n_u n_e'}{\pi_s^{(0)}}=n_e'+n_i'+\frac{n_u'(n_e+n_i)}{\pi_s^{(0)}} \qquad (8)$$

$$I_{po}^{(0)}=\frac{Q}{\alpha^{(0)}}\cdot\frac{n_u(n_e'\pi_s^{(0)}+n_e n_u')}{(\pi_s^{(0)})^2}=\frac{Q}{\alpha^{(0)}}\cdot\frac{n_u\{n_e'(n_e+n_i+n_u)+n_e n_u'\}}{(n_e+n_i+n_u)^2} \qquad (9)$$

where

$$\pi_s^{(0)}=n_e+n_i+n_u$$
$$\pi_t^{(0)}=n_e'+n_i'+n_u'$$

Now when the quenching substance affects only T-state, a remarkably simple relation holds as described below. Putting α and I_{po} in this case as $\alpha^{(q')}$ and $I_{po}^{(q')}$, these are easily derived from (6) and (7). $\alpha^{(q')}$ and $I_p^{(q')}$ thus obtained, when compared with $\alpha^{(0)}$ and $I_p^{(0)}$ (eq. (8) and (9)), lead to the following relation.

$$\alpha^{(q')}=\alpha^{(0)}+q'$$

$$I_{po}^{(q')}=\frac{Q}{\alpha^{(q')}}\cdot\frac{n_u\{n_e'\pi_s^{(0)}+n_e n_u'\}}{(\pi_s^{(0)})^2}=\frac{Q}{\alpha^{(q')}}\cdot\frac{n_u\{n_e'(n_e+n_i+n_u)+n_e n_u'\}}{(n_e+n_i+n_u)^2}=I_{po}^{(0)}\frac{\alpha^{(0)}}{\alpha^{(q')}}$$

therefore

$$\frac{I_{po}^{(q')}}{I_{po}^{(0)}}=\frac{\alpha^{(0)}}{\alpha^{(q')}} \qquad (10)$$

Thus in this case, the inital intensity of phosphorescence and the average life is proportional to each other.

Next, when the quenching substance affects only S′-state, the result is not so simple as in the former case. The formulas for I_{po} and α in this case are as follows.

$$\alpha^{(q)} = n_e' + n_t' + \frac{n_u'(n_e + n_t + q)}{\pi_s} \qquad (11)$$

$$I_{po}{}^{(q)} \frac{Q}{\alpha^{(q)}} \quad \frac{n_u(n_e'\pi_s + n_e n_u')}{(\pi_s)^2} \qquad (12)$$

Comparing with (8) and (9)

$$\frac{I_{po}{}^{(q)}}{I_{po}{}^{(0)}} = \frac{\alpha^{(0)}}{\alpha^{(q)}} \times \frac{(n_e + n_t + n_u)^2}{(n_e + n_t + n_u + q)^2}$$

$$\times \frac{n_e'(n_e + n_t + n_u + q) + n_e n_u'}{n_e'(n_e + n_t + n_u) + n_e n_u'} \qquad (13)$$

From (13) it may be anticipated that the intensity of phosphorescence decreases remarkably in contrast to a rather small change of life; because on the right side of equation (13), the quenching factor (q) exists in the denominator as a quadratic term in addition to the ratio $\alpha^{(0)}/\alpha^{(q)}$. It may be mentioned that there exists (q) term in the numerator of the third factor, but at ordinary temperature, when the condition $n'_e < n'_u$ holds in many cases, the effect is presumably rather small.

To sum up the above results, one can hope to judge whether quenchers affect on S′-state or T-state predominantly, if one measures the initial intensity and average life of the quenched phosphorescence and compares them with those of unquenched one.

B. Apparatus and Procedure

The life of filter paper-Trypaflavine phosphor being of the order of 0.1 sec, it can be measured accurately by the use of electromagnetic oscillograph. But, the intensity being so weak that it is necessary to use a photomultiplier and amplify the photocurrent further to some extent. We have designed our apparatus to control the amplificaction in a wide range and at the same time, made use of a relay circuit to record, on the same oscillograph paper, the initial and the final stage of the one decay curve with the same order of accuracy. Two kinds of vessels were used for the sample; A) one is an ampule of a simple type, which contains a piece of filter paper (immersed previously in the aqueous solution of Trypaflavine and evacuated) close to the inner surface of the vessel. B) The other is of a Dewar-flask type with a ground joint, of which the vacuum part contains several kinds of samples fitted close arround the inner brass wall. The latter vessel is convenient for measuring at various temperatures. The details of the apparatus for the measurement and of the vessels of samples will be reported elesewhere.

C. Some of the Experimental Results

a) Results obtained with the vessel A. When the logarithm of the phosphorescence intensity is plotted against time, an almost straight line is obtained in most cases; some of the examples are shown in Fig. 2. It is

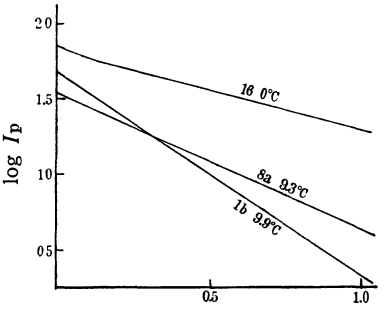


Fig. 2

certain that the decay curve is expressed by a single exponential form.

$$I_p = I_{po} e^{-\alpha t} \qquad (1)$$

where I_{po} is the initial intensity and α is the reciprocal of the average life or the decay constant.

From the inclination of the line one can easily calculate α, and by exterpolating the line to $t=0$ one can get the value I_{po} (relative). Some reults are tabulated in Table I.

TABLE I

α AND I_{po} AT VARIOUS DYE CONCENTRATION

Sample	Conc. of adsorbed dye 10^{-6} mol/g.	(at 10°C) α*	(Vessel A) I_{po} (relative)
1a		3.23	44
1b		3.07	31
„	15.3	3.13	47
„		3.05	49
2a		2.75	80
„	9.02	2.74	98
2b		2.62	75
3b		2.43	146
„	2.84	2.41	133
4		2.00	110
	1.11	2.00	123
		2.13	136
5	0.602	2.01	99
		1.98	68
6	0.361	1.94	75
7	0.241	2.08	50
8a		2.08	34
„	0.120	2.02	36
8c		2.04	34
8d		2.02	43
W1**	5.81	2.11	109
W2	1.11	1.92	141
W3	0.182	1.76	53

The small temperature effect is corrected for the experimental value.

The filter paper was washed with distilled water for a long time.

1. Reproducibility. As is seen from Table I, each measurement is quite reliable and the process of phosphorescence is quite reproducible so long as the treatment of the sample is the same, although a special pretreatment of the filter paper such as washing with distilled water for a long time gives a different α-value (cf. W in Table I).

2. Effect of Temperature. The result is that I_{po} scarecely depends upon the temperature, while α shows a conspicuous increase with the rise of temperature. The activation energy is calculated to be about several Kcal. by the use of Arrhenius equation. (Of course the calculation is approximate in nature and it was made merely for the purpose of correcting the experimental results in order to compare at the same temperature.

3. Effect of the Incident Light Intensity. Under the present experimental conditions, I_{po} is completely proportional to the intensity of incident light, while α does not depend upon it.

4. Effect of Concentration of Dye. When one plots the α-values and I_{po}-values against the dye concentration, curves as shown in Fig. 3 are obtained. In this figure a dotted curve is an adsorption isotherm plotted against the equilibrium concentration of the solution given along the right side ordinate.

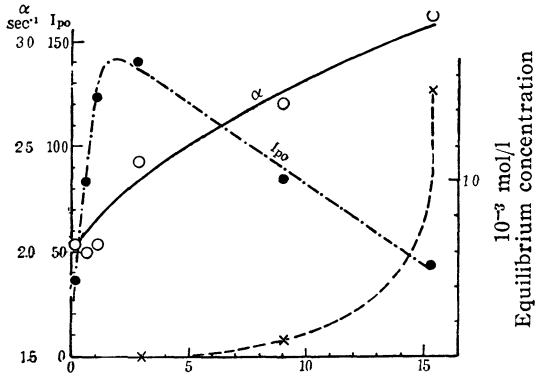


Fig. 3. I_{po} and α against the dye concentration (10°C) (Vessel A)

As is apparent from the figure, I_{po} increases quite rapidly in the range of small concentration, and after reaching a maximum, decreases almost linearly down to 1/3~1/4 of the maximum value in the region of saturated adsorption. On the contrary, α-value is almost constant in the region where I_{po} curve rises but thereafter it increases monotonously until it reaches the value about 30% larger than the original one.

b) The Results Obtained with the Vessel B. In this case log I_p~t curve shows a slight curvature at the initial stage and this curvature seems to increase with the concentration of dye (see Fig. 2). But the magnitude of this curvature being very small, α value was calculated from the linear part. The results at 0°C and 10°C are given in Table II and Fig. 4. I_{po} varies with the dye concentration in the same way as in the case of vessel A. α seems to show a different tendency from the former curve, the reason of which is not certain. But the magnitude of increase is quite the same as before.

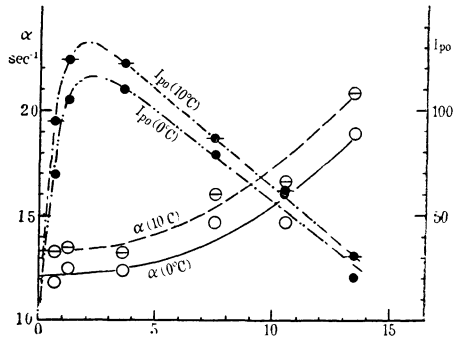


Fig. 4. I_{po} and α against the dye concentration (0°, 10°C) (Vessel B)

TABLE II

α AND I_{po} AT VARIOUS DYE CONCENTRATION

Sample	Conc. of adsorbed dye 10^{-6} mole/g (at 10°C and 0°C) (vessel B)	α 0°C	α 10°C	I_{po} 0°C	I_{po} 10°C
11	13.5	1.89	2.08	21	31
12	10.5	1.47	1.66	62	60
13	7.5	1.47	1.60	79	87
14	3.6	1.24	1.33	110	122
15	1.22	1.25	1.35	105	124
16	0.64	1.18	1.33	69	95

D. Discussion

It still remains open to question that the mechanism of organic phosphorescence, especially in the case of adsorbed phosphor, is completely explained by Lewis' model. But our results show quite definitely that the process is expressed as a unimolecular reaction and there is no reason to reject Lewis' scheme.

Let us consider, therefore, the concentra-

1) Filter paper used for this series was washed thoroughly with distilled water.

tion effect according to the results derived in (A) on the ground of Lewis' model. As seen from Fig. 3 and Fig. 4, I_{po}~c and α~c curves show the same features for both cases at least qualitatively, and so the main characters of the phosphorescent process may be discussed upon the data of the present report, though the detailed discussion such as about the various transition probabilities may require more exact measurements.

In the present case, there is no special quencher added, but if the self-quenching due to the interaction of the adsorbed dye molecules exists, it may conventionally be represented by q and q'. Other transition constants n_e, n_i, n_u, n_e', n_i', n_u' might be affected by the dye concentration, but are approximated to be constant tentatively in the following discussion.

Let us consider at first how the rise of I_{po} in the low concentration region can be explained. In this region α is almost constant and therefore, the self-quenching can be neglected completely, and it may also be certain that all other transition probabilities keep the same value. Then, from (7) I_{po} must be proportional to Q, the number of molecules excited to S'-state per second during illumination (or the number of photons absorbed per sec.), which can be put as $(1-e^{-\varepsilon cd})$, where ε is the molecular extinction coefficient and cd is the number of moles of dye (in the ground state) in 1000 cm^2 of the cross section of the light path.

Now, as was stated in the previous section the intensity of phosphorescence is completely proportional to that of the incident light. Therefore, the state of affairs is far below the photosaturation and the number of molecules in the ground state can be put equal as an analytical quantity.

Now, it turned out that up to the region of max. I_{po}-value (about 1.11×10^{-6} mol/g), the experimental relation between I_{po} and c(analytical) could be expressed successfully by the equation

$$I_{po}=\text{const}\ (1-k^{-\varepsilon cd})$$

where ε is put as 7×10^4. With regard to the above value of ε, we could demonstrate that its order was very plausible by measuring the absorption coefficient for a cellophane Trypaflavine phosphor.

Thus it can safely be concluded that the increase of I_{po} in the region of small dye concentration is due to the increase of absorption of light.

Next, let us consider the high concentration region. Using the above ε value, it can be confirmed that beyond 2.2×10^{-6} mol/g, the absorption of light is more than 95% and so Q can be put as constant. Therefore, the decrease of I_{po} must be attributed to the selfquenching in the broad sense of the word.

The following three possible phenomena may be considered as the cause for the self quenching.

1) Accompanied with the increase of concentration, the dye molecules aggregate into such polymers (including dimers) that can not emit fluorescence nor phosphorescence at all.

2) The interaction between excited dye molecule and the neighbouring normal molecule causes the excess energy of the former to be dissipated into thermal energy.

In such a case, two possibilities must be discriminated.

a) The state affected is S'-state.

b) The state affected is T-state.

Of course it may be possible that the above three phenomena superpose. Among these three phenomena, the first is quite plausible in view of the fact that the absorption spectrum of Trypaflavine adsorbed on cellophane, changes conspiquously with the increase of dye concentration. Evidently, the electronic states in question (ground and excited states), in this case, are not concerned with a monomeric dye molecule but concerned, so to speak, a different molecular species. But there is no doubt that they are singlet states.

If 2b) is the case, then I_{po} must be reciprocally proportional to α, which contradicts the experimental results; thus I_{po} at 15×10^{-6} mol/g. of the dye concentration is only about one third of that at 1.5×10^{-5} mol/g., while the increase of α-value is about 30%.

Therefore the possibility that 2b) is the main and principal process of quenching is definitely denied. On the other hand 2a) does not contradict with the experimental results, since in this case I_{po} ought to decrease conspicuously in contrast to a rather small increase of α.

The conclusion is that the states related with the quenching process are chiefly singlet states, irrespective whether the mechanism be 1) or 2a).

Summary

Assuming Lewis' scheme, mathematical formulation was given for the decay of organic phosphorescence, which would help us to judge whether the quenching action of the added substance affects on singlet or triplet state. The decay curves of Trypa-

flavine-filter paper phosphor in various concentrations, were accurately measured by and oscillograph, and from the results obtained, it was tentatively concluded that the triplet state is not affected much in the concentration quenching.

Full accounts of the experiment and more detailed discussions will be published in Journ. Polytech. Osake City University.

The cost of this research has been partly defrayed from the Scientific Research Grant from the Ministry of Education, to which the present authors wish to express their gratitude.

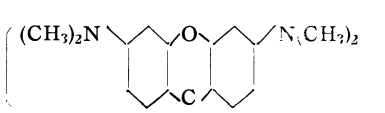
Institute of Polytechnics, Osaka City University, Osaka

Influence of the Addition of High Molecular Electrolytes upon the Absorption Spectra and Fluorescence of Organic Dyestuffs. II.

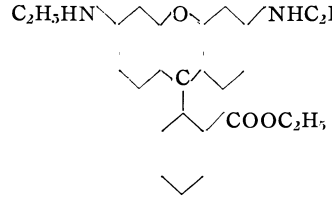
By Masao KOIZUMI and Noboru MATAGA

(Received August 19, 1953)

In the second paper[1] of our series of physicochemical studies of organic dyestuffs*, the influence or addition of K-polyvinylsulfate (PVSK) upon the absorption spectra and fluorescence of Rhodmaine 6G was reported, and the results were explained almost quantitatively as due to the change of aggregation of dye ions, which is caused by the accumulation of the latter in the neighbourhood of PVSK. Now in the course of our extensive study of the influence of PVSK upon various basic dyes, which was continued since then, we have found another interesting example which can be comprehended almost quantitatively as due to the change of aggregation of dye ions. It is Pyronine G, which



Pyronine G



Rhodamine 6G

belongs to Xanthen dyestuffs and its structure is somewhat more simple than Rhodamine 6G. In this case a new metachromatic band appears by the addition of PVSK, in contrast to the case of Rhodamine 6G, and yet the main features of the change of absorption spectrum are so simple and orderly that the quantitative treatment is possible. Pyronine G—PVSK system may be regarded as another ideal case of metachromasy which can be interpreted on the basis of the change of aggregation of dye ions.

Experimental

a) Some examples of the absorption spectra of Pyronine G in the aqueous solution at various concentrations are shown in Fig. 1.

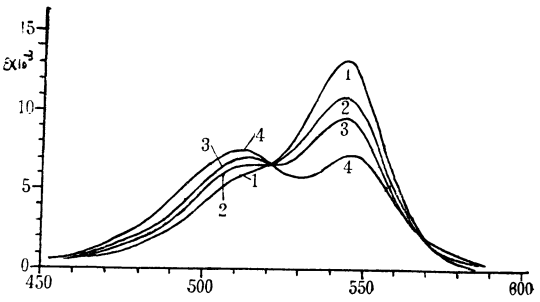


Fig. 1. Absorption spectra of the aqueous solution of Pyronine G.

	concentration	temperature
1.	5×10^{-5} mol/l	27°C
2.	2×10^{-4} „	
3.	6×10^{-4} „	
4.	2×10^{-3} „	

* Physicochemical Studies of Organic Dyestuffs in relation to Photochemistry. III.

**) The paper will, hereafter, be refered to as Part I of "Influence of the addition of high molecular electrolytes upon the absorption spectra and fluorescence of organic dyestuffs".

1) M. Koizumi and N. Mataga, This Bulletin **26**, 165 (1953); See also: N. Mataga and M. Koizumi, *J. Inst. Polytech. Osaka City Univ.*, **3**, 21 (1952).

The absorption curve has two maxima at 545 mμ and 512.5 mμ. The former is prominent in the region of low concentration, while the latter gradually grows with the increase of concentration. Thus two maxima 545 and 512.5 mμ are expected to belong respectively to monomer (α-band) and dimer (β-band), an equilibrium existing between the two, as in the case of Rhodamine 6G[1,2,3,4]. (The equilibrium constant of dimerization was calculated to be 6.38×10^{-4} at 27°C.).

b) The effect of addition of PVSK is characteristic in its simplicity. Up to 2×10^{-4} mol./l. of dye the concentration, no change is produced in the spectrum. If the concentration of dye is a little above 4×10^{-4} mol./l. the absorption curve changes its shape with the addition of PVSK. Thus both α- and β-bands gradually decline apparently in a parallel way and a new metachromatic band appears at the position 800 Å shorter than the α-band, and it gradually grows with the addition of more PVSK. When the concentration of added PVSK reaches a certain critical concentration, however, the metachromatic band begins to decline accompanied with the rise of α- and β-band, until the shape of the curve coincides almost completely with that of the aqueous solution without PVSK. But as the concentration of dye increases, the phenomenon of recovery commences at a larger concentration of PVSK, and at last, when the dye concentration is about 2×10^{-3} mol./l. the recovery occurs only very slightly. (See Fig. 2)

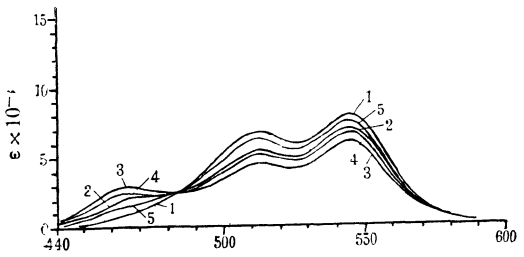


Fig. 2. Change of absorption spectra of Pyronine G by the addition of PVSK. (Dye conc. 8×10^{-4} mol./l.)

	PVSK	temperature
1.	0 and 1000 (7.56×10^{-3}gr/cc)	27°C
2.	5	,,
3.	10	,,
4.	50	,,
5.	500	,,

If one compares the above result with that of Rhodamine 6G[1], the chief points of difference are the rise and fall of α- and β-band occuring apparently in a parallel way. and the appearance of a new metachromatic band. As regards to the phenomenon of recovery, it is qualitatively similar to that in the case of Rhodamine 6G, but it is more elegant and complete in the region of low concentration of dye. It may be worthy to add that the positions of α-, β- and metachromatic band are invariable during the whole change.

Discussion

Let us consider the mechanism of metachromasy in the present case on the ground of the following experimental results.

1) Below 2×10^{-4} mol./l. of the dye concentration, no change is produced in the absorption spectrum, even if large excess of PVSK is added.

2) In the case of dye concentration a little above 4×10^{-4} mol./l. the addition of PVSK produces a metachromatic band with the fall of α- and β-band, but with the excess of added PVSK the spectra become similar to that of pure aqueous solution.

3) When the concentration of dye is increased furthermore, the change of absorption spectra, including the appearance of a metachromatic band, becomes more prominent and at the same time, the recovery is retarded and quite reduced.

To explain the result (1), we must recognize one of the following two situations.

A) The change of the electronic state of dye ions may be produced by their interaction with the electrolyte ions, but in the region of low concentration of dye, the number of interacted molecules, is so small that it cannot be observed as any change in spectra (It may alternatively be said that there is approximately no adsorption, provided that the model of adsorption[1] is adopted.)

B) Dye ions are adsorbed on the high molecular substance, but neither the equilibrium between monomer and dimer, nor the optical properties of both monomer and dimer in relation to the absorption, spectrum, are affected by the adsorption.

Of the two possibilities mentioned above, A) cannot be reconciled with the facts (2) and (3) consistently. Thus the fact (3) might be attributed to the increase of adsorption (though small), but as long as one recognizes A), the quantity of adsorbed dye is so small as compared with the added high molecular substance, that the conditions around the adsorbed dye ion cannot be expected to be affected much by the addition of excess PVSK. Therefore, the fact (2) cannot be explained along this line, and some additional assumption is necessary. For example, if the structure of high molecular substance changes, in the region of its high concentra-

2) V. L. Levshin, *Acta Physicochim. U. R. S. S.* **1**, 684 (1935).

3) E. Rabinowitch and L. F. Epstein, *J. Am. Chem. Soc.*, **63**, 69 (1941).

4) S. E. Sheppard, *Rev. Mod. Phys.*, **14**, 303 (1942); S. E. Sheppard and A. L. Geddes. *J. Am. Chem, Soc.*, **66**, 1995, 2003 (1944).

tion, so remarkably in such a manner that it cannot adsorb the dye ions any longer, then the fact (2) could be explained. But this is also improbable in view of the fact (3) and also of the equilibrium dialysis experiment of Levine and Schubert[5].

The conclusion is, therefore, that one must assume the situation B). According to B), the fact 3) can be interpreted, for example, as due to the formation of a multiple associate of dye ions in the region of high concentration of dyes, and the result 2) can naturally be expected since the concentration of adsorbed dye ions decreases with the addition of an excess quantity of PVSK.

On the ground of the above qualitative deduction, it is much probable to attribute the change of absorption spectra of Pyronine-G, induced by the addition of PVSK, to a change of aggregation of dye ions.

Let us criticize this idea more quantitatively in the region of small concentration of dye, where the quantitative treatment is possible. Assume that in a certain range of the concentration of adsorbed dye ions, there is formed a new molecular species other than normal monomer and dimer, which produces a metachromatic band and it does not participate in monomer-dimer association equilibrium. (It may be added that this molecular species is probably a multiple associate but the calculation below does not necessarily require to be so).

Molar extinction coefficients at the position of α- and β-maximum in the pure aqueous solution are correlated with the experimentally obtained extinction coefficient λ by the following equations.

$$\left.\begin{aligned}\lambda_m &= C_0\varepsilon_m \\ \lambda_d &= C_0\varepsilon_d\end{aligned}\right\} \qquad (1)$$

where C_0 is the analytical concentration of dye (mol./l.) and ε_m, ε_d are the molar extinction coefficients at α- and β-maxima, respectively.

Now, when PVSK is added enough for a new molecular species to appear, the concentration of dye ions participating in association equilibrium may be reduced to some extent. If the reduced concentration be put as $(C_0-\Delta C_0)$, then the molecular extinction coefficient ε_m', ε_d' at the present condition ought to be given as follows:

$$\left.\begin{aligned}\lambda_m' &= C_0\varepsilon_m' = (C_0-\Delta C_0)\varepsilon_m \\ \lambda_d' &= C_0\varepsilon_d' = (C_0-\Delta C_0)\varepsilon_d\end{aligned}\right\} \qquad (2)$$

It is to be added that the above relations (2) assume that a pure metachromatic band is negligible at the position of α- and β-maximum, which is very much plausible in view of the experimental results.

From (2), the following relations must hold.

$$\varepsilon_m' = \frac{(C_0-\Delta C_0)}{C_0}\varepsilon_m, \quad \varepsilon_d' = \frac{(C_0-\Delta C_0)}{C_0}\varepsilon_d \qquad (3)$$

$$\frac{\varepsilon_m'}{\varepsilon_d'} = \frac{\varepsilon_m}{\varepsilon_d}$$

Thus if one calculates and tabulates previously, $\frac{\varepsilon_m}{\varepsilon_d}$-values against various concentrations of dye from the spectrum of the pure aqueous solution, then by comparing the experimentally obtained $\frac{\varepsilon_m'}{\varepsilon_d'}$-value with the table, one can decide the value of $(C_0-\Delta C_0)$ or ΔC_0.

The value of $\frac{(C_0-\Delta C_0)}{C_0}\varepsilon_m$, obtained by the above procedure ought to coincide with ε_m' as long as the starting assumption is correct. The results of the calculation satisfy this requirement almost completely as shown in Table 1.

TABLE I

COMPARISON BETWEEN ε_m' AND $\frac{(C_0-\Delta C_0)}{C_0}\varepsilon_m$

a) Concentration of dye $C_0 = 8\times10^{-4}$ mol./l.

P*	0	1	5	10	50	100	500	1000
$\Delta C_0(\times10^4)$	0	0.1	1.6	2.0	1.4	1.4	0.1	0
ε_m'	8.0	7.95	7.0	6.1	6.7	7.1	7.6	7.8
ε_m	8.0	8.2	8.8	9.0	8.7	8.7	8.2	8.0
$\frac{(C_0-\Delta C_0)}{C_0}\frac{\varepsilon_m}{\varepsilon_m'}$	1.0	1.0	1.0	1.1	1.0	1.0	1.0	1.0

5) A. Levine and M. Schubert, *J. Am. Chem. Soc.*, **74**, 5702 (1952).

b) Concentration of dye $C=10^{-3}$ mol./l.

P	0	1	5	10	50	100	500	1000
$\Delta C_0(\times 10^4)$	0	1.4	2.4	3.4	3.8	3.9		1.8
ε_m'	7.7	8.2	6.75	5.7	4.5	4.9		6.3
ε_m	7.7	8.0	8.7	8.8	8.9	8.94		8.0
$\frac{(C_0-\Delta C_0)}{C_0}\frac{\varepsilon_m}{\varepsilon_m'}$	1.0	0.8	0.97	1.0	1.2	1.1		1.0

* P: Quantity of PVSK added (Unit.: 7.56×10^{-6} g./cc.)

Thus it has been quantitatively proved that what produces a metachromatic band behaves as a new molecular species and lies outside monomer-dimer equilibrium. There scarcely remains any doubt that this new molecular species is polyassociate and is neither monomer nor dimer attached to PSVK in views of the qualitative discussion already stated. It is possible to discuss quantitatively other possibilities than the above one which is most probable, but the detailed discussion including them will be reported in Journ. Polytech. Osaka City University, with the full account of experimental results.

Institute of Polytechnics, Osaka City University, Osaka

Influence of the Addition of High Molecular Electrolyte upon the Absorption Spectra and Fluorescence of Organic Dyestuffs. III.

By Noboru MATAGA and Masao KOIZUMI

(Received August 19, 1953)

Introduction

In the first paper[1] of the series of investigation about "the influence of the addition of high molecular electrolyte upon the adsorption spectrum and intensity of fluorescence of dyestuffs", it was stated at first that two kinds of mechanisms for metachromasy are to be taken into account in order to treat the problem from a general standpoint.

One is a) the change of electronic state of dye ions, directly produced by their interaction with high molecular electrolyte, and the other is b) the change in the state of aggregation of dye ions, which is caused by the accumulation of dye ions in the neighbourhood of high molecular electrolyte. In that paper, we succeeded in interpreting quantitatively the behaviour of Rhodmaine 6G–PVSK system, in which no metachromatic band appears, upon the basis of monomer-dimer equilibrium. In Part II we gave strong evidence that the spectral behaviour of Pyronine G–PVSK system, in which a metachromatic band appears, can also be explained only by the change of aggregation of dye.

Hitherto we have intentionally chosen such systems in which the change of aggregation is expected to be important, and the above two examples are the ideal case of b) which are interpreted quantitatively. Among various dyes so far investigated, there are many which can be comprehended along the same line, though not so quantitatively and accordingly not so definitely as the above two examples.

Now, turning our attention to the other case, we have chosen various Na and K–alkyl sulfate esters of different chain length as the electrolyte with only one functional group, and studied their influences upon the absorption spectra and fluorescence intensities of many dyes, in order to find out such a system as can be interpreted as an ideal case a).

As a result of a systematic study of many dyes, it has been confirmed quite definitely that in such cases the change of aggregation of dye ions still plays an important role. In addition, we have obtained some evidences which suggest that prior to micell-formation (at which a remarkable change of absorption spectrum and fluorescence intensity occurs,

* Physicochemical Studies of Organic Dyestuffs in relation to Photochemistry IV.

1) M. Koizumi and N. Mataga, This Bulletin **26**, 115 (1953), See also: N. Mataga and M. Koizumi, *J. Inst. Polytech. Osaka City Univ.*, **3**, 21 (1952).

as is observed usually in other cases[2]) the high molecular electolyte lies in some aggregated state or in an orderly array of some kind. By virtue of it, the dye ions also take such a special state of aggregation as produce a peculiar type of change in absorption spectra and intensity of fluorescence.

In this paper some experimental results which support the above viewpoint, especially those about Rhodamine 6G, will be reported in a rather condensed form, the details of which will be published in Journ. Inst. Polytech. Osaka City University.

The chief points which we have investigated are 1) the effect of chain length of alkyl sulfate, 2) the effect of the dye concentration and 3) the effect of temperature.

The discussion will be given not separately but along with the experimental results in each part.

Experimental Results and Interpretation of Them

(1) The Effect of Chain Length of Alcohol Sulfate Ester—Methyl and butyl sulfate do not affect the spectrum nor the fluorescence at all, irrespective of the magnitude of addition. Amyl sulfate gives a slight effect only at its high concentrations. In the case of octyl sulfate, the quenching of fluorescence is observed accompanied by the complicated change of absorption in the region above 5×10^{-4} mol./l. When the concentration reaches C. M. C., the fluorescence recovers and the spectrum becomes simple again similar to that of pure aqueous solution.

Na-lauryl sulfate (LASNa) shows an analogous effect as octyl sulfate except that the effect becomes observable at a little lower concentration, ca. 10^{-5} mol./l. Analogous phenomena are also observed in some dyestuffs other than Rhodamine 6G such as Trypaflavine and Acrydine yellow, which have a tendency to polymerize in the pure aqueous solutions [1,3]) while Rhodamine B, which does not dimerize in the aqueous solution[1]) suffers no effect, however much LASNa is added. All these results strongly support the view that only in the case when such electrolytes as can form the micelle are added to dimerizable dyestuffs, the fluorescence is quenched and the absorption changes prior to C. M. C.

(2) The Effect of the Concentration of the Dye.—When the dye concentration is small (2×10^{-6} mol./l.), the effect comes to be observed at higher concentration of LASNa while the recovery of fluorescence begins at a far lower concentration than C. M. C. reported in the literatures[4]), which was determined, for example, from the measurement of electric conductivity. As regards the absorption spectrum, α-band declines and β-band slightly rises in the region where the quenching of fluorescence is remarkable. The above results can be comprehended if the dye ions in the proper concentration of added LASNa are assumed to exist as something like dimer sandwiched in between the ions of added electrolytes, and have no power of fluorescence. The interpretation is quite analogous to the case of PVSK. Thus when the concentration of dye is low, the gradual increase of LASNa soon comes to provide, prior to C. M. C., such a situation in which the dye ions in the neighbourhood of the aggregate of LASNa begins to decrease, and this causes the above phenomenon of recovery.

On the other hand, when the concentration of dye is large, the quenching is observed in a wider range of concentration of LASNa, and the magnitude of quenching is more remarkable than in the case of lower concentration of dye. Quenching is removed sharply in the close neighbourhood of C. M. C. of LASNa. As for the absorption spectra, both α-and β-band decline at first, with the addition of LASNa ; then a broad band appears extending to the longer wave length than α-maximum, which in the suitable concentration of LASNa has two peaks in the opposite side of the position of α-band. Thus the spectrum is quite different from that of simple or PVSK added[1]) aqueous solution, and this result may reasonably be comprehended if one assumes that dye ions are sandwiched in between the orderly array of electrolyte, and interaction between these dye ions are such that the situation is somewhat analogous to but different from that of dimerization or polymerization in the aqueous solution. It goes without saying that the quenching is also interpreted on the basis of the same model. It may be added that in the case of high concentration of dye, the number of sandwiched dye ions between the orderly array of electrolyte ions would be so large that it could not be decreased so much, prior to C. M. C., and this may be the reason why the recovery takes place at C. M. C. without any sign of it beforehand. The similar changes in absorption spectrum and intensity of fluorescence are also observed in the case of other dyes which

2) See for example; M. L. Corrins and W. D. Harkins, *J. Am. Chem. Soc.*, **69**, 683 (1947); *J. Chem. Phys.*, **14** 641 (1946), R. C. Merrill and R. Getty, *J. Phys. Colloid Chem.*, **52**, 774 (1948).

3) V. Zanker, *Z. Phys. Chem.*, **199**, 225 (1952).

4) See for example; F. D. Haffner, G. A. Piccione and C. Rosenblum, *J. Phys. Chem.*, **46**, 662 (1942).

have some tendency of polymerization such as Trypaflavine and Acridine yellow[1,3] and they are also considered to be due to the same circumstances. On the other hand, Pyronine G which sustains no effect by PVSK in the small concentration of dye (Part II), also shows no change in either absorption spectrum or fluorescence in the present case, as long as the concentration of dye is low. As for Rhodamine B which has no tendency of polymerization, the result was already mentioned in section 1.

The difference of spectrum in the case of LASNa from that with PVSK seems to exist generally. Thus Pyronine G, in a very limited region of dye concentration, shows a similar metachromatic band as in the case of PVSK, but elswhere, it commonly gives a broad band different from that of the aqueous solution. Other dyestuffs such as Thionine and Toluidine blue etc., show similar behaviour. The problem would be worthy of further study with regards to the change of electronic state of dye ion influenced by the ions of electrolyte.

Judging from the above results, it may be safe to conclude that the change of spectrum and fluorescence in the case of LASNa is essentially related to the change in aggregation of dye ions just as in the case of PVSK.

(3) **The Effect of Temperature.**—The intensities of fluorescence were measured at 13° C. and at 55°C. in various corresponding conditions and were compared with each other. It was found that as long as the concentration of dye is small (2×10^{-6} mol./l.), the intensity is reduced by the elevation of temperature when the quantity of added LASNa is small (up to 2×10^{-4} mol./l.); while at higher concentration of LASNa the intensity is stronger at a higher temperature. Now, as for the effect of temperature, two phenomena must in general be taken into account. One is the collisional quenching[5], which increases at higher temperature, and the other is the shift of association equilibrium between dye ions or between electrolyte and dye ion, which generally tends toward dissociation at higher temperature. If it is assumed that the above two effects are operative in the present system, then the results can at least qualitatively be well interpreted. Thus the collisional quenching naturally predominates at low concentration of LASNa where the aggregates of LASNa are not existent in measurable quantity, and the result is that the intensity is reduced at higher temperature. While at higher concentration of LASNa, a relatively large portion of dye ions are sandwhiched in between the orderly array of LASNa ions, and the shift of association equilibrium determines the resultant temperature effect. According to the above interpretation, the temperature effect ought to be, in general, positive at higher concentration of dye, and the experimental result is just as expected.

It may further be added that the features of absorption spectrum becomes relatively simpler at higher temperature, which is also reconciled with the above interpretation. Thus the temperature effect can also be comprehended if one assumes that the dye ions sandwiched in between the orderly array of electrolyte ions, interact with each other in a somewhat similar manner as in the bulk solution.

General Conclusion

From the above-mentioned experimental results and discussions, it has become quite clear that the change of absorption spectra brought about by the addition of an electrolyte with only one functional group, is essentially correlated with the change of aggregation of dye ions. But, in contrast to such substances with many functional groups as PVSK, it seems indispensable that some kind of specific aggregation or orderly array of ions exists on the part of added electrolyte. The structure of it is naturally considered to be quite labile, and accordingly the aggregation of dye ions, an orderly array of electrolyte ions and the interaction between dye and electrolyte ions, all these phenomena, are entangled with each other in so delicate a manner that the spectrum is expected to be influenced by various factors very sensitively as is the case.

This problem would be very interesting from the standpoint of the change of electronic state of dye affected by the neighbouring electrolyte ion, that is from the standpoint of case (a) mentioned at the beginning of the present paper.

To sum up our results reported in three papers, it can be concluded that in the case of basic dyes such as Xanthene or Thiazine dyestuffs, metachromasy produced by the addition of anionic electrolyte is chiefly caused by the change of aggregation of dye ions (mechanism b) though the change of electronic state of dye directly produced by the interaction between dye and electrolyte ions (mechanism a) may be superposed in some cases. Our general conclusion is quite similar to that of Michaelis[6], but our reasoning is more

5) See for example: P. Pringsheim, "Fluorescence and Phosphorescence", 322. 349 (1949).

6) L. Michaelis and S. Granick, *J. Am. Chem. Soc.*, **67**. 1212 (1945), L. Michaelis, *J. Phys. Colloid Chem.*, **54**, 1 (1950).

definite being supported by some quantitative discussions.

More detailed discussions involving other dyestuffs will be reported in Journ. Inst. Polytech. Osaka City University. The cost of this reseach has been partly defrayed from the Scientific Grant from the Ministry of Education.

Institute of Polytechnics,
Osaka City University, Osaka

Hydroxylamine dans les eaux lacustres[1] —*Variation saisonnière et importance biogéochimique*—

Par Motoharu TANAKA

(Reçu le 23 Décembre 1953)

Les recherches nombreuses[2] sur les azotes combinés dans l'hydrosphère ne datent pas d'aujourd'hui. D'un autre côté, les biochimistes et les bactériologistes étudient sans cesse les mutuelles transformations bactériologiques des azotes combinés.

Récemment, les biochimistes ont démontré la production intermédiaire d'hydroxylamine dans le cas de transformation $NO_2^- \rightleftarrows NH_3$. Ainsi Novak et Wilson[3] ont constaté la formation d'hydroxylamine au cours de la fixation d'azote, et Taniguchi et d'autres[4] l'ont verifiée dans la réduction successive de l'azote nitrique. Procédant par méthode indirecte, Lees[5] a conclu la possibilité d'une formation intermédiaire d'hydroxylamine dans la nitrification bactériologique.

Nous avons déjà présenté une étude[6] sur l'existence d'hydroxylamine dans les eaux lacustres. Dans le présent exposé nous allons compléter les résultats d'observation durant une année entière. L'argumantation en sera faite dans le détail.

Lac étudié Pour cette recherche nous avons choisi le lac Kizaki. La stratification très prononcée des azotes combinés y est observée dans la période de stagnation estivale[7].

Le lac Kizaki se trouve dans la Préfecture de Nagano, le long de la vallée, au pied Est des Alpes Japonaises Nord. Par une rivière il se trouve mis en communication avec le lac Nakatsuna. Sa transparence de quelques métres nous montre sa nature mésotrophique.

Méthode d'analyse Nous avons employé la modification par Endre et Kaufmann[3),8)] de la méthode de Blom[9], dans laquelle l'hydroxylamine est oxydée en nitrite avec une solution d'iode; avec l'acide sulfanilique le nitrite forme un composé diazoïque qui est subséquemment couplé avec l'α-naphtylamine en produisant une coloration rose. On compare cette coloration et en déduit la teneur en hydroxylamine.

Les réactifs nécessaires sont:

Acide sulfanilique Mélanger 10.5 g. d'acide sulfanilique, 6.8g. d'acétate de sodium, 300cc. d'acide acétique cristallisable et 600 cc. d'eau distillée. Faire bouillir la solution et diluer à 1 litre.

α-Naphtylamine A un litre d'eau distillée, bouillante, ajouter 5.0 g. d'α-naphtylamine et continuer l'ébullition pendant 5 minutes. Filtrer immédiatement et introduire l'acide chlorhydrique suffisant pour clarifier la solution.

Iode 1.3 g. d'iode est dissous dans 100 cc. d'acide acétique cristallisable.

Hyposulfite 2.5 g. d'hyposulfite de sodium sont dissous dans 100 cc. d'eau distillée. Conserver en glacière. Tous les réactifs doivent être contenus dans des bouteilles brunes.

Mode opértoire de l'analyse A 5 cc. d'échantillon d'eau, ajouter 1 cc. d'acide sulfanilique et 0.5 cc. d'iode: maintenir la température de la solution à 30–40°C pendant 15 minutes; décolorer ensuite l'excèsd'iode avec l'hyposulfite. Y introduire 1 cc. d'α-naphtylamine et comparer la coloration avec celle qu'on obtient par le nitrite de sodium, parce que l'oxydation de l'hydroxylamine en nitrite est vraiment quantitative.

S'il existe du nitrite dans l'échantillon, soustraire son équivalence de la teneur obtenue en hydroxylamine.

Résultats d'observations Nos observations ont débuté au mois de juin 1952 et ont été poursuivies jusqu'en mars 1953 par intervalle-

1) Cet exposé a été déjà présenté à l'assemblée annuelle de la société chimique de Japon qui s'est tenue à Kyoto au mois d'avril 1953.

2) Par example, B. P. Domogalla, E. B. Fred et W. H. Peterson, *J. Amer. Water Works Assoc.*, **15**, 369 (1929); S. Yoshimura, *Archiv f. Hydrobiol.*, **24**, 155 (1932).

3) R. Novak et P. W. Wilson, *J. Bact.*, **55**, 517 (1948).

4) S. Taniguchi, H. Mitsui, J. Toyoda, T. Yamada et F. Egami, *J. Biochem.*, **40**, 1775 (1953).

5) H. Lees, *Nature*, **169**, 156 (1952).

6) M. Tanaka, *Nature*, **171**, 1160 (1953).

7) M. Tanaka, *J. Earth Sciences, Nagoya University*, **1**, 119 (1953).

8) G. Endres et L. Kaufmann, *Ann. Chem.*, **53**, 184 (1937).

9) J. Blom, *Biochem. Z.*, **194**, 385 (1928).

de trois mois. Les tableaux 1-4 nous montrent les rèsultats.

En juin, l'eau de lac se stratifie, et on constate vers le fond que l'oxygène tend légèrement à diminuer. Le nitrite et l'hydroxylamine ne sont décelés qu'a la couche de 15 m., c'est-à-dire au-dessous de la "couche du saut". Quant au nitrate, il se trouve dans les couches au-dessous de 17.5 m. et il augmente avec la profondeur. La teneur en azote ammoniacal oscille entre 0.012 et 0.030 mg. par litre.

Au mois de septembre, la stagnation se complète et les eaux au-dessous de 25 m. contiennent moins d'un cc. d'oxygène par litre d'eau. On décèle du fer ferreux dans la couche tout près du fond. L'azote nitrique augmente jusqu'à la couche de 26 m. et il diminue au

TABLEAU I

DISTRIBUTION VERTICALE DE L'OXYGÈNE ET DES AZOTES COMBINÉS DANS LE LAC KIZAKI (a)

Le 3 juin 1952* Profondeur atteinte: 29 m.

Profondeur m	Température °C	O_2 cc/l	$N\text{-}NO_3$ mg/l	$N\text{-}NO_2$ mg/l	$N\text{-}NH_2OH$ mg/l	$N\text{-}NH_3$ mg/l
0	16.25	6.69	<0.02	<0.001	<0.001	0.018
2.5	15.78	7.07	"	"	"	0.012
5	15.68	6.83	"	"	"	0.016
7.5	13.71	6.83	"	"	"	0.030
10	9.93	7.04	"	"	"	0.016
12.5	8.83	6.84	"	"	"	<0.01
15	8.08	6.02	"	0.0075	tr.	"
17.5	7.36	6.02	0.04	<0.001	<0.001	0.012
20	6.81	6.03	0.04	"	"	<0.01
22.5	6.60	5.99	0.06	"	"	0.018
25	6.42	5.88	0.05	"	"	0.018
27.5	6.40	5.22	5.22	"	"	0.018
28.8	——	4.63	0.06	"	"	0.018
28.9	——	4.63	0.06	"	"	0.022
28.95	——	4.79	0.07	"	"	0.030
29.0	——	5.07	0.04	"	"	0.030

Dans toutes les couches d'eau, on ne décèle aucune trace de fer ferreux.

TABLEAU II

DISTRIBUTION VERTICALE DE L'OXYGÈNE ET DES AZOTES COMBINÉS DANS LE LAC KIZAKI (b)

Le 5 sept. 1952 Profondeur atteinte: 28.5 m.

Profondeur m	Température °C	O_2 cc/l	$N\text{-}NO_3$ mg/l	$N\text{-}NO_2$ mg/l	$N\text{-}NH_2OH$ mg/l	$N\text{-}NH_3$ mg/l
0	24.8	5.77	<0.02	<0.001	<0.001	<0.01
2.5	24.71	5.67	"	"	"	0.018
5	24.60	5.45	"	"	"	0.018
7.5	18.90	5.71	"	"	"	0.018
10	13.82	4.86	"	"	"	0.016
12.5	10.76	4.33	0.08	"	"	0.016
15	9.74	4.30	0.07	"	"	0.018
17.5	——	4.08	0.15	"	"	0.018
20	——	1.98	0.20	"	"	0.016
22.5	——	1.73	0.16	"	"	0.018
25	——	0.56	0.28	"	"	0.018
26	——	——	0.28	0.004	0.004	0.018
27.5	——	——	0.19	0.012	0.007	0.016
28	——	——	0.11	0.014	0.011	0.016
28.1	——	0.42	0.09	0.016	0.011	0.020
28.3	——	0.31	0.08	0.019	0.011	0.020
28.45	——	0.49	0.06	0.019	0.011	0.020
28.50*	6.60	0.39	0.05	0.015	0.021	0.023

* Apparition de fer ferreux.

TABLEAU III

DISTRIBUTION VERTICALE DE L'OXYGÈNE ET DES AZOTES COMBINÉS DANS LE LAC KIZAKI (c)

Le 8 déc. 1952 Profondeur atteinte: 28.7 m.

Profondeur m	Température °C	O_2 cc/l	$N\text{-}NO_3$ mg/l	$N\text{-}NO_2$ mg/l	$N\text{-}NH_2OH$ mg/l	$N\text{-}NH_3$ mg/l
0	8.5	6.52	<0.02	<0.001	<0.001	<0.01
5	8.63	6.47	0.09	〃	〃	〃
10	8.25	6.55	0.03	〃	〃	〃
15	8.65	5.90	0.04	〃	〃	〃
20	8.60	0.71	0.02	〃	〃	0.016
21.5	——	——	0.025	0.006	0.004	<0.01
22.5*	8.42	0.82	<0.02	0.005	0.005	0.025
24	——	——	〃	<0.001	tr.	0.030
25	8.52	0.74	〃	〃	<0.001	0.032
25.5	——	——	〃	〃	〃	0.032
26.5	——	——	〃	〃	〃	0.035
27.5	8.65	1.51	〃	〃	〃	0.035
28.3	——	——	〃	〃	〃	0.040
28.5	——	0.71	〃	〃	〃	0.040
28.6	——	——	〃	〃	〃	0.040
28.65	——	0.61	〃	〃	〃	0.045
28.7	7.02	0.71	〃	〃	〃	0.045

* Au-dessous de cette couche existence de fer ferreux.

TABLEAU IV

DISTRIBUTION VERTICALE DE L'OXYGÈNE ET DES AZOTES COMBINÉS DANS LE LAC KIZAKI (d)

Le 2 mar. 1953* Profondeur atteinte: 26.5 m.

Profondeur m	Température °C	O_2 cc/l	$N\text{-}NO_3$ mg/l	$N\text{-}NO_2$ mg/l	$N\text{-}NH_2OH$ mg/l	$N\text{-}NH_3$ mg/l
0	3.3	8.55	<0.02	<0.001	<0.001	0.014
5	3.04	8.35	0.02	〃	〃	0.022
10	3.10	8.22	<0.02	〃	〃	0.022
15	3.10	8.38	〃	〃	〃	0.022
20	3.10	8.99	〃	〃	〃	0.022
25	——	8.52	〃	〃	〃	0.022
26.3	——	8.18	〃	〃	〃	0.025
26.45	——	8.35	〃	〃	〃	0.022
26.5	3.05	7.72	0.06	〃	〃	0.022

* Aucune trace de fer ferreux dans les couches d'eau.

delà de cette couche.

C'est dans cette couche que l'hydroxylamine et le nitrite apparaissent en proportion du décroissement de l'azote nitrique. Le nitrite atteint son maximum entre 20 et 5 cm. au-dessus de la superficie de la vase. La teneur en hydroxylamine est la plus forte dans la couche la plus basse (la couche tout près du fond). L'ammoniaque varie de 0.016 à 0.023 mg. par litre.

A la fin de la période de stagnation, en décembre, on décèle du fer ferreux au-dessous de 22.5 m., bien que la stabilité verticale ne soit pas assez grande. On peut doser l'azote nitrique entre les profondeurs 5 et 21.5 m m.; sa teneur varie de 0.02 mg. jusqu'à 0.09 mg. par litre. L'hydroxylamine et le nitrite sont décelables aux couches de 21.5 m. et de 22.5 m. La teneur en hydroxylamine est supérieure dans cette dernière couche où le nitrite est moins abondant. L'ammoniaque apparaît dans les couches au-dessous de 20 m. et ses concentrations y sont de 0.016 à 0.045 mg. par litre.

Après la circulation hivernale, en mars 1953, on ne décèle le nitrate qu'à la profondeur de 5 m. et tout près du fond. On ne constate plus l'existence d'hydroxylamine et de nitrite dans aucune couche d'eau. Les teneurs en azote ammonical oscillent entre 0.014 et 0.026 mg. par litre.

Résumons nos résultats—A mesure que la période de stagnation avance, l'hydroxyl-

amine apparaît dans les couches dont la teneur en oxygéne est inférieure à 1 cc par litre d'eau.

Le maximum est atteint à la partie la plus haute des couches où l'on décèle le fer ferreux (niveau d'oxydo-réduction). Au-dessous, l'hydroxylamine diminue et disparaît. A ce dernier point de vue il ressemble au nitrite, mais leurs tenenrs les plus fortes apparaissent aux couches différentes; vers le fond, dans la période de stagnation, on observe comme suit les maxima des teneurs en azotes combinés: nitrate, nitrite, hydroxylamine et ammoniaque.

Après la circulation hivernale, on ne décèle ni nitrite ni hydroxylamine dans aucune couche d'eau.

Argumentation Considérons d'abord comment se forme l'hydroxylamine dans les eaux du lac Kizaki:

Avant l'apparition d'hydroxylamine, le nitrate est le plus abondant parmi les azotes combinés (Tableau I). L'augmentation de l'hydroxylamine et du nitrite correspond à la diminution du nitrate et de l'oxygène (Tableaux II et III).

En nous appuyant sur ces deux faits, nous pouvons conclure que l'hydroxylamine dans ce lac se forme comme produit intermédiaire de la réduction bactériologique du nitrate favorisée par l'environment pauvre en oxygène.

L'apparition du nitrite (et probablement de l'hydroxylamine) à la profondeur de 15 m. en juin 1952 (Tableau I) est plus dfficile à expliquer, car on n'y constate pas la diminution d'oxygène. Cette profondeur correspond à "compensation depth" où l'assimilation et la décomposition des matières organiques sont presque égales. Bien que l'on y puisse supposer un milieu microscopiquement anaérobie où des bactéries peuvent réduire le nitrate en nitrite, ce phénomène serait plus probablement dû à la réduction du nitrate par les êtres autotrophes, par exemple algues, au fur et à mesure de l'assimilation de l'azote nitrique dans l'épilimion. On sait que l'algue peut réduire le nitrate dans un milieu aérobie, comme récemment Kessler[10] l'a étudié en détail à l'aide de la méthode biochimique. On peut ainsi expliquer de plus la présence de nitrate au-dessous de 15 m. et son absence au-dessus de cette couche.

Résumé

1° Nous avons étudié la variation saisonnière des composés d'azote, surtout celle de l'hydroxylamine.

2° Dans le lac Kizaki, à la période de stagnation, nous avons trouvé de l'hydroxylamine au niveau d'oxydo-réduction.

3° Nous avons conclu que cet hydroxylamine est un produit intermédiaire de la réduction bactériologique du nitrate.

4° L'apparition de l'azote nitreux (et probablement de l'hydroxylamine) au-dessous de la "couche du saut", au début de la période de stagnation, serait due sans doute à la réduction de l'azote nitrique par les algues.

En terminant ce compte-rendu, nous tenons à mentionner les noms des MM. les Professeurs K. Sugawara et F. Egami à qui va notre gratitude pour l'aide précieuse qu'ils n'ont pas cessé de nous donner.

Institut de chimie, Faculté des Sciences, Université de Nagoya

10) E. Kessler, *Flora*, **140**, 1 (1953).

Rheology of Surface Films. II. A Surface Rheometer for Measuring the Film Creep under Constant Shear Stress[1]

By Kiyoshi INOKUCHI

(Received February 18, 1954)

Introduction

In a previous paper[2], it has been proved that the rheological study of monomolecular films is a valuable tool for gaining more insight into the structure of materials. Before further development of this study is attempted, it is first necessary to establish the standard procedure of the measurement. The most simple and convenient method of this study would be to determine the creep as a function of time after applying the constant stress to the film materials. The apparatus[2]

1) Presented at the Symposium of Colloid Chemistry of the Chemical Society of Japan, Nov. 1952, Fukuoka.

2) K. Inokuchi, This Bulletin, **25**, 500 (1953).

used in the previous paper, although it involves the determination of creep against time, was not satisfactory in achieving the quantitative analysis of the creep curve, since the stress was not kept constant during the test, but decayed with the creep. In fact, quantitative analysis of the data obtained with the previous apparatus becomes rather involved and often impractical, when the experiment is carried out with films, the rheological properties of which are more or less complicated. The desirable condition is that the stress remains constant throughout the creep test. In this paper, an apparatus useful under such condition is described.

Construction of Apparatus

The essential elements of the apparatus consist of a ring and a suspending wire similar to those used in the previous case. The torque applied to the ring is supplied from the distorsion of the wire. In order to realize the condition of constant stress, it is only necessary to maintain the twisted angle of the torsion wire, which is given at the beginning of the measurement, to be constant during the experiment. In the present apparatus, such mechanism is automatically conducted by a phototube relay system. The essential part is divided into the following two systems: (1) optical system, and (2) driving system.

(1) Optical System Fig. 1 illustrates the

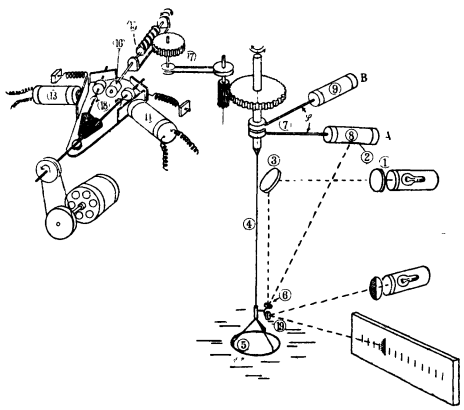


Fig. 1. Schematic view of the apparatus

schematic view of the apparatus. A beam of parallel light, passed through a condensing lens (1), is projected to the first mirror (3) which is fixed closely near the torsion wire with oblique inclination so that the light beam is made parallel to the torsion wire (4). The ring (5) provides a small concave mirror (6) of about 4 mm. in diameter which moves with the rotation of the ring. This second mirror (6) reflects a part of the parallel light from the first mirror (3) to form an intense light spot at a certain point within the plane determined by the wire (4) and the center of the mirror (6). Such a design of the optical system would enable the angular displacement of the light spot to be equal to that of the ring, because the projecting light is made parallel to the rotating axis of the mirror (6). Thus, if the driving of the torsion head is so conducted that it always moves together with the light spot, the condition of constant stress would be satisfied. The conduction mechanism of the torsion head is as follows.

The torsion head provides two rods (7) of about 15 cm. long, extending outwards at right angles to it, at each end of which phototube housings (8, 9) are attached respectively. These rods can be turned around the torsion head and be fixed at any position desired. Each of the housings encases two RCA-921 phototubes (A, B) respectively with each photosurface downwards. Each housing provides a narrow and long slit (2) of 2×40 mm. along the median line of its ventral side respectively, so that the photosurface can receive the light beam through the slit, when the position of the rod is properly adjusted.

(2) Driving System The driving of the torsion head is wholly conducted by a phototube relay system. The principal manner is as follows: as soon as a photosurface receives light, the driving system of the torsion head is so actuated that the head rotates toward one direction, whereas once the photosurface becomes dark, it is inversely actuated so that the head rotates toward the opposite direction. Such mechanism would render the torsion head a reciprocating motion about the light spot if the motion of the light spot is sufficiently slow compared with that of the torsion head. Such a function is quite similarly given to both phototubes (A) and (B), and the alternative use of these tubes, either (A) or (B), is achieved by the switch (10) (see Fig. 3).

The essential elements of the arrangement employed in the driving system are indicated in the functional block diagram of Fig. 2. The

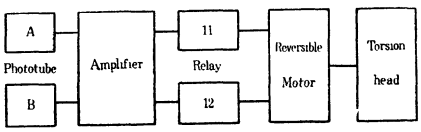


Fig. 2. Block diagram of driving mechanism using phototube relay.

two-step amplifier is ordinarily designed as illustrated in Fig. 3. The amplified photocurrent actuates the relays (11, 12) which transfer the photosignal to the reversible motor, which in turn drives the torsion head toward the alternative directions. Each of the relays (11, 12) is separately actuated by the phototubes (A) and (B), respectively, and the alternative use of them is also accomplished by the reversible switch (10). Each relay provides two contacts respectively, which intermit the rectified current for the reversible motor according to the following mechanism. Even when the relay is

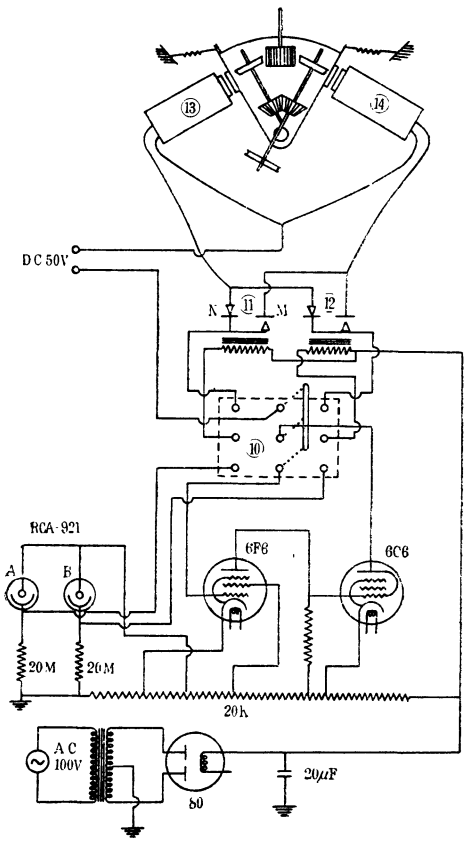


Fig. 3. Schematic circuit of phototube amdlifier

at rest, one of these contacts (for example, M) is closed by means of a spring, while another contact (N) is opened. Once the relay is actuated, however, the situation is inverted, that is, the contact (M) is opened, and (N) is closed. Since each contact is connected to the magnets (13, 14) of the reversible motor respectively, the reciprocating motion of the motor takes place according to whether or not the relay is actuated.

The construction of the reversible motor will be apparent when referred to Fig. 1 and 3. The gear shaft (15) with a friction rotor (16) is connected to the torsion head through the gear system (17). The reciprocating motion of the rotor is transmitted through the friction gear clutch assembly (18) which alternatively works by actuation of the magnet, either (13) or (14).

Principle of Operation

Suppose that the ring is allowed to touch the surface of the water covered with the film materials, being suspended by untwisted torsion wire, and the position of the phototube (A) is so adjusted that the photosurface just receives the light beam from the mirror (6) of the ring. If the switch (10) is so turned that the phototube (A) becomes active, and the phototube (B) is at rest, the torsion head would, according to the mechanism mentioned above, be driven toward one direction until the light spot is left outside of the slit of the phototube housing and accordingly the photosurface becomes dark, whereas once the surface becomes dark, the torsion head begins to return to the position where the light spot again enters into the slit. Here the situation becomes the same as at the beginning, and such to and fro motion further continues. In other words, the torsion head exercises a reciprocating motion about the light spot.

It must be mentioned here that the ring on the film, although suspended by a reciprocally twisted torsion wire, caused hardly perceptible reciprocating motion, but took a static position, so long as the amplitude as well as the period of the reciprocating motion of the torsion head was sufficiently small. Accordingly the film does not suffer any alternative shear in spite of the reciprocating motion of the torsion head. In the present apparatus, the frequency of the reciprocating motion was about 2–3 times per second and the amplitude of the motion was not more than 0.5 degree when the system was well adjusted.

Now let the second tube (B) be set by φ angles with respect of the first tube (A) and the switch (10) be so turned that the second tube (B) becomes active, leaving the first (A) at rest. Since, in this instance, the photosurface of the tube (B), which becomes newly active, remains still dark, the torsion head will be so driven until the second tube (B) catches the light spot. Here, the wire is twisted by φ. If the ring thereafter causes rotation owing to the stress imposed on it, the torsion head would also moves together with the moving light spot making a fine reciprocating motion about it, and the constant distortion of the wire will be maintained during the experiment.

At a later time, if the switch is returned to the original position so that the first tube (A) becomes active while the second (B) is at rest, the torsion head would inversely be driven so that the torsion of the wire is always set to the original state (zero). Such a condition would provide the curve of the after-effect of the testing film upon removal of the stress.

In the present study, where the motion of the ring in question was sufficiently slow compared with the rate of motion of the torsion head, there was no appreciable time lag of the head for pursuing the light spot, and the relative situation between the ring and the torsion head is considered to be constant throughout the experiment.

Performance

Briefly, the operation of the present apparatus is as follows. The ring is allowed to touch the clean surface of water. The phototubes are so set that the light spot from the mirror (6) just fits at the photosurface of the first tube (A) through the slit, and the second (B) is laid by φ angles with respect of the first (A). The testing film is now spread on the water surface. The position of the ring at respective time

is measured by means of a lamp and scale system using the mirror (19) attached to the ring. The switch (10) is so turned that only the tube (A) is active, being the tube (B) at rest, and the original position of the ring is marked on the scale. Then, in order to impose the stress on the ring, the switch (10) is changed so that only the tube (B) is active, leaving the tube (A) at rest, and the deflection of the ring is recorded with time. If a study of the after-effect upon removal of the stress is intended, it is enough to return the switch (10) to the original position.

The equations to calculate the surface shear modulus of rigidity (G) and surface viscosity coefficient (η) may be expressed as follows

$$G = \frac{k}{4\pi}\left(\frac{1}{r_1^2} - \frac{1}{r_2^2}\right)\frac{\varphi}{\theta} \qquad (1)$$

$$\eta = \frac{k}{4\pi}\left(\frac{1}{r_1^2} - \frac{1}{r_2^2}\right)\frac{\varphi}{\dot{\theta}} \qquad (2)$$

where r_1, r_2 are the radii of the ring and of the circular film coaxial to the ring, respectively, θ, the angular displacement of the ring, and k, the torsion constant.

Test and Results

The measured extent of coincidence between the rotating angles of the ring and the corresponding angles of the light spot was shown in Fig. 4. Fairly good coincidence

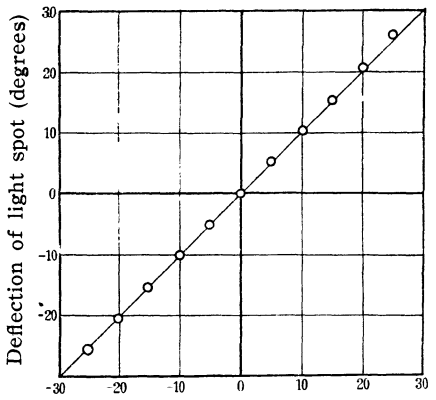


Fig. 4. Relation between rotating angles of the ring and the corresponding deflection angles of light spot.

was seen over the range of about 50 degrees within the error of a few per cent.

Fig. 5 shows the deformation-time curve (θ—t curve) of serum albumin monolayer determined with the present apparatus. Here, it was intended that the present apparatus was tested by being referred to the data obtained with the apparatus presented in a previous paper. Fig. 6 gives the $\theta-t$

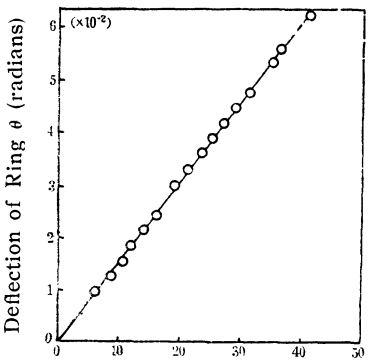


Fig. 5. $\theta-t$ plot of serum albumin monolayer determined by the present apparatus on 5% ammonium sulfate aqueous solution, surface area, 1.03 sq. m. per mg., temperature, 16°C.

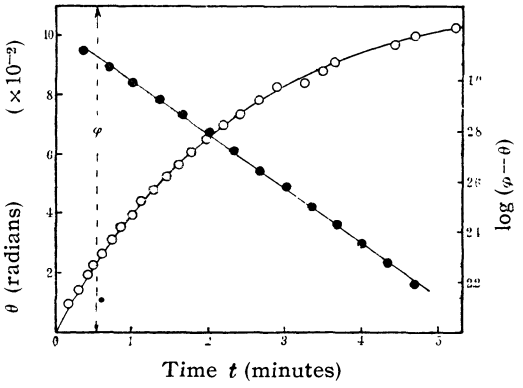


Fig. 6. $\theta-t$ curve (open circles) and $\log(\varphi-\theta)-t$ curve (full circles) of serum albumin monolayer, determined by the previous apparatus.

curve together with the $\log(\varphi-\theta)-t$ plot when the previous apparatus was applied to the same film. From the linearity of $\log(\varphi-\theta)-t$ plot[3], it was found that this film behaves as a simple viscous matter of Newtonian nature. This fact predicts that the present apparatus would give a straight line to the $\theta-t$ plot if only the stress is kept constant during the test, in contrast with the droop curve in case of the previous apparatus. This prediction was verified in Fig. 5 in which good linearity was yielded in the $\theta-t$ plot. The basic requirement of this apparatus—constant stress—was found to be fulfilled within experimental error.

As an example of a less simple creep curve, a monolayer of ovalbumin film was subjected to our test. The deformation-time

3) V. E. Hatschek and R. S. Jane, *Koloid-z.* **39**, 300 (1926).

curve determined by the present apparatus was given in Fig. 7, where the experimental

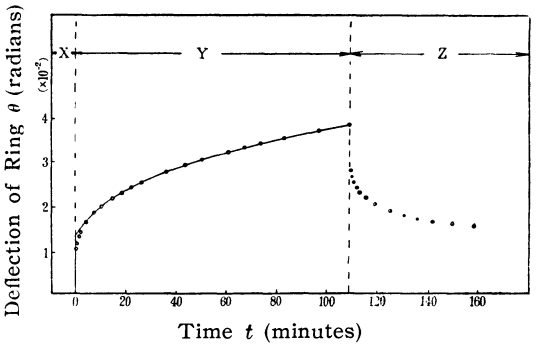


Fig. 7. $\theta-t$ curve for ovalbumin monolayer on 5% ammonium sulfate solution, surface area, 0.904 sq. m. per mg., temperature, 19°C. Full circles indicate the observed values, and solid line, the calculated curve. (X) represents the dead time, (Y), the time in which the stress was imposed, and (Z), the time. after the stress was removed.

conditions are indicated in the legend. From inspection of the shape of the curve, it will be apparent that the curve is characterized by instantaneous elastic response, retarded elastic response and irreversible flow. The solid curve represents the trace which was drawn according to the following well-known equation, putting the proper numerical values into the respective variables

$$\theta=\theta_0+A(1-e^{-t/\tau})+\lambda t \qquad (3)$$

where θ represents the angular displacement of the ring at time t, θ_0, an initial displacement of the ring due to an instantaneous elasticity, λ, the constant motion rate of the ring in viscous flow region, A, the final and maximum response due to a retarded elasticity, and τ, the retardation time. It was noted here that, except for the initial transcient creep region, the observed values were well expressible by such a simple equation. Putting θ_0, A, and λ into the equation (1) and (2), an instantaneous surface shear modulus of rigidity (G_1), a retarded surface shear modulus of rigidity (G_2), and surface viscosity coefficient (η) of the constant rate flow were calculated as follows: $G_1=2.7$ dynes/cm. $G_2=3.2$ dynes/cm., $\eta=2.1\times10^4$ dynes/cm./sec., and $\tau=21.7$ minutes.

Summary

A surface rheometer was presented which enables the creep of surface films to be measured under constant shear stress. The main construction consists of a ring and a suspending torsion wire. Automatic adjustment of the torsion head driving, which made distorsion of the wire to be constant throughout the creep test, was accomplished by means of a phototube relay mechanism. The creep curve and its analysis data of ovalbumin monolayer were also presented.

The author wishes to express his hearty thanks to Prof. T. Tachibana for his helpful advice and encouragement, and to Dr. J. Sakagami of the Department of Physics of this University for his valuable discussion concerning the construction of the apparatus.

Department of Chemistry,
Faculty of Science,
Ochanomizu University, Tokyo

The Syntheses from Levulinic Acid. A Possible Use of Some 2-Methyl-5-oxopyrrolidine-2-carboxylic Esters as Plasticizers[1]

By Tadao TAKENISHI and Osamu SIMAMURA

(Received February 18, 1954)

The object of the present investigation is to search for possible uses as chemical intermediates of levulinic acid, which is often obtained in quantities as a by-product from carbohydrate materials in food industries. The application of the Strecker synthesis[2] to levulinic acid gave 2-amino-2-methylglutaric acid, from which several derivatives were prepared including 2-methyl-5-oxopyrrolidine-2-carboxylic acid. Since esters as a class are of general interest as plasticizers, some 2-methyl-5-oxopyrrolidine-2-carboxylic esters were prepared and those of higher alcohols were tested for plasticizer performance. They are compatible and efficient for

1) Part of the material of this report was presented at a meeting of the Chemical Society of Japan held on Oct. 2, 1952. at Niigata.

2) A. Strecker, ***Ann.***, **75**, 27 (1850).

plasticizing vinyl chloride resin; with regard to heat stability, they are unsatisfactory only in one respect in that the plasticized sheets of polyvinyl chloride, heated at 110° for six hours, became colored light brownish violet. The results are recorded in the accompanying table.[3]

PROPERTIES OF POLYVINYL CHLORIDE SHEETS PLASTICIZED WITH 2-METHYL-5-OXOPYRROLIDINE-2-CARBOXYLIC ESTERS

	n-Octyl Ester		2-Ethylhexyl Ester		Dodecyl Ester	
Plasticizer (parts for 100 parts polyvinyl chloride with 2 parts lead stearate)	30	50	30	50	30	50
Modulus at 100% Elongation, kg./cm².	157	64	183	65	200	82
Elongation, %	268	305	263	335	275	315
Tensile Strength, kg./cm².	282	192	300	208	322	205
Tear Resistance, kg./cm.	118	74	140	82	136	78
Oil Extraction (*a*)	—	10.78	—	5.32	—	15.05
Water Extraction(*b*)	—	5.83	—	3.91	—	0.20
Low Temperature Flexibility(*c*)	—	9.30	—	13.27	—	7.65

(*a*) % gasoline-soluble substances, at 18~23°, for 24 hrs.
(*b*) % water-soluble substances, at 50°, for 24 hrs.
(*c*) Elongation at 25~26° / Elongation at −4 to −5°.

Experimental

2-Amino-2-methylglutaric Acid A solution of 102 g. (1.9 moles) of ammonium chloride in 240 cc. of lukewarm water was added, followed by 120 cc. (1.7 moles) of 28% ammonium hydroxide, to a solution of 86 g. (1.7 moles) of sodium cyanide in 170 cc. of water placed in a round-bottomed flask fitted with a ground-glass stopper. The mixture was stirred while 200 g. (1.7 moles) of ammonium levulinate in aqueous solution was added. The flask was then stoppered, the stopper secured firmly by means of adhesive tape, and the flask kept half immersed for six hours in a water bath at 65~70°. The reaction mixture was then cooled, poured into 2 l. of concentrated hydrochloric acid contained in a round-bottomed flask cooled by a stream of water, and the mixture saturated with hydrogen chloride. After standing overnight, it was refluxed for three hours to hydrolyze the acid amide produced. After cooling, the precipitated inorganic salts were filtered off on a Büchner funnel. The filtrate was concentrated under reduced pressure on a water bath, and the deposited inorganic salts were filtered. When the filtrate was neutralized to a pH 3.2 with aqueous sodium hydroxide and the inner wall of the vessel scratched vigorously, 2-amino-2-methylglutaric acid separated in fine crystals, which were collected on a Büchner funnel. The yield of the product was 210 g. (70% of the theoretical amount). This crude amino acid was dissolved in hot water, charcoaled and filtered, giving fine crystalline product, m.p. 170° (Found: C, 44.73; H, 6.88; N, 8.69. Calcd. for $C_5H_{11}O_4N$: C, 44.10; H, 7.20; N, 8.23%).

2-Benzamido-2-methylglutaric Acid Benzoyl chloride (6.2 g.) was added to 2-amino-2-methylglutaric acid (8 g.) dissolved in a solution of 6.5 g. of sodium hydroxide in water, the mixture shaken for 30 minutes, acidified with hydrochloric acid, the precipitated benzoic acid filtered off, the filtrate concentrated to half the original volume, extracted with ether and ethyl acetate, the combined extracts dried over anhydrous sodium sulfate, and the solvent removed on a water bath. Recrystallization of the residue from aqueous alcohol gave the benzoyl derivative, m.p. 196~7° (Found: N, 5.45; neutralization equiv., 132.5. Calcd. for $C_{13}H_{15}O_5N$; N, 5.28%; neutralization equiv., 132.5.).

2-Acetamido-2-methylglutaric Anhydride 2-Amino-2-methylglutaric acid (8 g.) was refluxed with 20 cc. of acetic anhydride and 15 cc. of acetic acid for 4 hours. After the excess of acetic anhydride was decomposed with water, the mixture was concentrated in vacuo and the remaining oil was induced to crystallize by rubbing with ethyl acetate, giving 2-acetamido-2-methylglutaric anhydride, m.p. 141~2° (from ethyl acetate) (Found: N, 7.71. Calcd. for $C_8H_{11}O_4N$; N, 7.58%,).

2-Acetamido-2-methylglutaric Acid To 8 g. of 2-amino-2-methylglutaric acid and 25 cc. of acetic anhydride, aqueous sodium hydroxide was added drop by drop with vigorous shaking until the mixture was alkaline. After shaking for thirty minutes, the mixture was neutralized with hydrochloric acid, concentrated in vacuo, the precipitated inorganic salts filtered off, the

3) The authors are indebted to Mr. S. Takazawa of Yamato Rubber Works, Tokyo, for the performance data.

filtrate concentrated to dryness in vacuo, and the residue triturated with ethyl acetate and filtered off, giving crude crystals melting at 126~135°. An analytically pure sample was prepared by repeated crystallization from water, m.p. 182~3° (Found: N, 6.76; neutralization equiv., 110.5. Calcd. for $C_8H_{13}O_5N$: N, 6.89%; neutralization equiv., 101.5).

Diethyl 2-Amino-2-methylglutarate The diethyl ester was prepared by Fischer's method[4]. 2-Amino-2-methylglutaric acid (20 g.) was heated on a water bath with 120 cc. of absolute ethanol which had previously been saturated with dry hydrogen chloride until all the amino acid dissolved, and the heating was continued for a further five hours. The mixture was then concentrated under diminished pressure, added with 100 cc. of ethanol saturated with dry hydrogen chloride, heated and concentrated as above, the whole cycle of procedures being repeated three times. The oily product thus obtained was dissolved in a small amount of water, the solution neutralized and the ester extracted several times with ether. The combined ether extracts were dried over sodium sulfate, evaporated, and the residue distilled in vacuo, giving 7 g. of diethyl ester, b.p. 102~4° at 0.5 mm. Hg, d_4^{20} 1.0550, n_D^{20} 1.4428 (Found: N, 6.45; MR_D, 54.56. Calcd. for $C_{10}H_{19}O_4N$: N, 6.45%; MR_D, 55.11.).

2-Methyl-5-oxopyrrolidine-2-carboxylic Acid 2-Amino-2-methylglutaric acid was dehydrated to 2-methyl-5-oxopyrrolidine-2-carboxylic acid by heating at 180~200° in a practically quantitative yield, m.p. 144~5° (from hot water) (Found: N, 9.78; neutralization equiv., 143. Calcd. for $C_6H_9O_3N$: N, 9.86%; neutralization equiv., 143.).

Ethyl 2-Methyl-5-oxopyrrolidine-2-carboxylate 2-Methyl-5-oxopyrrolidine-2-carboxylic acid (15 g.), 150 cc. of ethanol, 200 cc. of benzene and 1 cc. of concentrated sulfuric acid were heated in a round-bottomed 1 l. flask fitted with a refluxing condenser and separator so arranged that the upper layer of the condensing liquid containing benzene and ethanol was returned to the reaction flask and the lower water layer withdrawn from time to time. The flask was heated until no further separation of water occurred. The solvent was removed from the reaction mixture in vacuo, the residue dissolved in ether, the ether solution washed with aqueous solution of sodium bicarbonate, the ether removed, the residue subjected to fractional distillation under reduced pressure, giving 10 g. of ethyl ester, colorless liquid, b.p. 126~130° at 0.5 mm. Hg, d_4^{20} 1.1283, n_D^{20} 1.4690 (Found: N, 8.39; MR_D, 43.24. Calcd. for $C_8H_{13}O_3N$: N, 8.18%; MR_D, 42.21.).

Butyl 2-Methyl-5-oxopyrrolidine-2-carboxylate This ester was prepared from 2-methyl-5-oxopyrrolidine-2-carboxylic acid similarly to the ethyl ester in 95% yield, b.p. 141~2° at 0.5 mm. Hg (Found: N, 7.05. Calcd. for $C_{10}H_{17}O_3N$: N, 7.03%.). It was also synthesized from 2-amino-2-methylglutaric acid by the same procedure in 80% yield, b.p. 141~2° at 0.5 mm. Hg, d_4^{20} 1.0698, n_D^{20} 1.4676 (Found: N, 7.13; MR_D, 51.68. Calcd. for $C_{10}H_{17}O_3N$; N, 7.03%; MR_D, 51.45.).

Octyl, 2-ethylhexyl, dodecyl and benzyl esters were prepared from 2-methyl-5-oxopyrrolidine-2-carboxylic acid by the same procedure as above.

Occtyl 2-Methyl-5-oxopyrrolidine-2-carboxylate (yield 75%), b.p. 173~4° at 1.0 mm. Hg, d_4^{20} 1.0062, n_D^{20} 1.4652 (Found: N, 5.63; MR_D, 70.29. Calcd. for $C_{14}H_{25}O_3N$: N, 5.48%; MR_D, 69.80.).

2-Ethylhexyl 2-Methyl-5-oxopyrrolidine-2-carboxylate (yield 85%), b.p. 179~181° at 3.0 mm. Hg, d_4^{20} 1.0106, n_D^{20} 1.4668 (Found: N, 5.48; MR_D, 70.29. Calcd. for $C_{14}H_{25}O_3N$: N, 5.48%; MR_D, 69.80.).

Dodecyl 2-Methyl-5-oxopyrrolidine-2-carboxylate (yield 50%), b.p. 198~199° at 0.5 mm. Hg, m.p. 37~9° (from ethanol) (Found: N, 4.47. Calcd. for $C_{18}H_{33}O_3N$: N, 4.49%.).

Benzyl 2-Methyl-5-oxopyrrolidine-2-carboxylate (yield 70%), b.p. 237~240° at 1 mm. Hg, m.p. 94~95° (from carbon tetrachloride) (Found: N, 6.01. Calcd. for $C_{13}H_{15}O_3N$; N, 6.00%.).

Summary

The synthesis of 2-amino-2-methylglutaric acid from levulinic acid by Strecker's method is reported. This acid gives 2-methyl-5-oxopyrrolidine-2-carboxylic acid on dehydration, and some of its esters were prepared and tested for plasticizer performance.

The authors are indebted for generous supplies of materials to the Management of Sanko Co., Tokyo, to which the thanks of T.T. are also due for leave of absence to participate in this work.

Department of Chemistry, Faculty of Science, Tokyo University

4) E. Fischer, *Ber.*, **34**, 433 (1901).

The Condensations of Furfural with Methyl Isobutyl Ketone and Phenylacetone by Aqueous Sodium Hydroxide

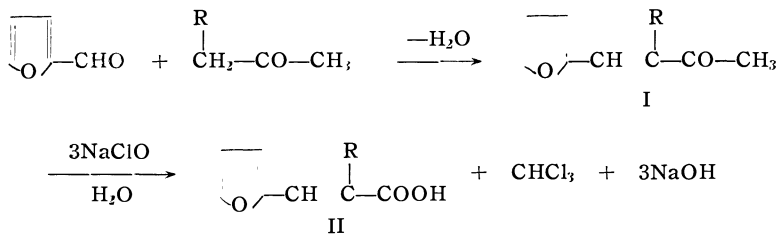
By Hiroshi MIDORIKAWA

(Received February 23, 1954)

In the previous reports[1] were represented the following facts: At the lowered reaction temperature 0–5°, methyl ethyl ketone tends to condense with furfural or benzaldehyde by alkali at its α-methylene group, and methyl propyl ketone, though slightly, has such a tendency in the condensation with furfural by alkali. At the elevated reaction temperature 60–65°, methyl ethyl ketone, as well as methyl propyl ketone, condenses with furfural chiefly at their α-methyl groups. In the condensation with benzaldehyde at the elevated reaction temperature 60–65°, methyl ethyl ketone reacts exclusively at its α-methyl group.

The present work consists in studying whether methyl isobutyl ketone and phenylacetone, on the condensation with furfural by aqueous sodium hydroxide, react at their α-methylene groups or not. In the reaction of furfural with methyl isobutyl ketone by alkali, there are few reports[2,3,4]. But those appear to have no such consideration.

When the condensation of furfural with the ketone $CH_3—CO—CH_2—R$ takes place at its α-methylene group, the resulting furfurylidene ketone (I) must be oxidised by sodium hypochlorite to α-R-2-furanacrylic acid (II), as in all cases so far examined[1]. The reaction is represented in the following formulae.



On the condensation of furfural with methyl isobutyl ketone by aqueous sodium hydroxide, both condensation products at the lowered and at the elevated reaction temperatures gave only one species (m.p. 177–178°) of semicarbazone, which was considered to be identical with the semicarbazone (m.p. 175–176°) of the condensation product obtained by Wienhaus and Leonhardi[3]. On suspension of these condensation products in sodium hypochlorite solution for 2 days with occasional shaking, no α-isopropyl-2-furanacrylic acid and no smell of chloroform were detected. Consequently, it seemed certain that the condensation products were composed of 1-(2-furyl)-5-methyl-1-hexen-3-one (III) resulting from the condensation of furfural at the α-methyl group of methyl isobutyl ketone irrespective of the reaction temperatures, as illustrated below.

This semicarbazone (m.p. 177–178°) was converted into two species of 2,4-dinitrophenylhydrazone. One was reddish-orange, flattened needles (m.p. 196–197°) and the other red, long needles (m.p. 144–145°). These two forms also were directly obtained from both the condensation products at the lowered and elevated reaction temperatures. Furthermore, it was of interest that the red, long needles shifted readily to the reddish-orange needles in dilute alcoholic sulfuric acid. Probably, these two forms of 2,4-dinitrophenylhydrazone may be the syn- and antiisomers as two *o*-tolyhydrazones of N-phenacyl-*p*-anisidine.[5]

Refluxion of the condensation product at the reaction temperature 60–65° with alcoholic hydrochloric acid and subsequent hydrolysis gave a dioxocarboxylic acid (m.p. 79–80°) in a good yield, which was considered to be γ,ζ-dioxo-ϑ-methylcapric acid (IV), as reported by Breusch and Ulusoy[4]. The reaction sequence is illustrated in the accompanying formulae.

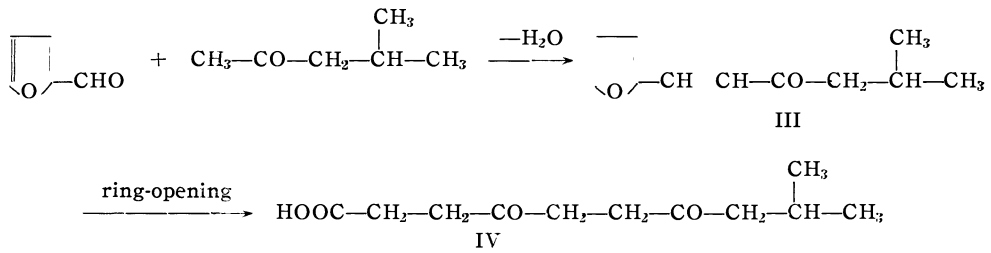
1) H. Midorikawa, This Bulletin, **26**, 460 (1953); **27**, 131 (1954), **27**, 143 (1954); **27**, 149 (1954).

2) J. T. Thurston, *C. A.*, **39**, 5023 (1945); H. Wachs and O. F. Hedenburg, *J. Am. Chem. Soc.*, **70**, 2695 (1948).

3) H. Wienhaus and H. Leonhardi, *C. A.*, **24**, 2127 (1930).

4) F. L. Breusch and E. Ulusoy, *C. A.*, **42**, 5850 (1948).

5) M. Busch, G. Friedenberger and W. Tischbein, *Ber.*, **56**, 999 (1926).



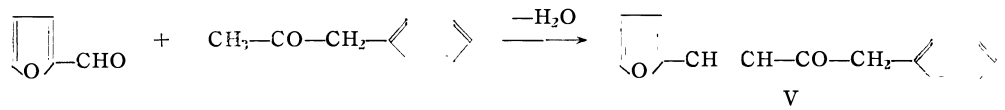
III

IV

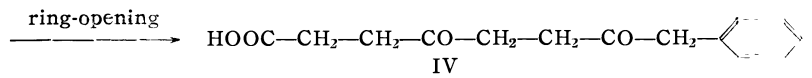
Phenylacetone was also condensed with furfural at the lowered and elevated reaction temperatures, 5° and 60–70°. Neither of the condensation products at the lowered and elevated reaction temperatures, on sodium hypochlorite oxidation, gave any α-phenyl-2-furanacrylic acid nor any smell of chloroform. It seemed certain that the condensation of phenylacetone with furfural gave 4-(2-furyl)-1-phenyl-3-buten-2-one (V), reacting at the α-methyl group of the ketone irrespective of the reaction temperatures, as illustrated below.

On the other hand, both condensation products at the lowered and elevated reaction temperatures gave two species of semicarbazone, colourless prisms (m.p. 210–212°) and colourless prisms (m.p. 163–164°), which were converted respectively into 2,4-dinitrophenylhydrazones of red, flattened needles (m.p. 183–184°) and reddish-orange leaflets (m.p. 178–179°). The condensation product at the elevated reaction temperature gave these two semicarbazones in equal proportions, and the condensation product at the lowered reaction temperature gave the semicarbazone of prisms (m.p. 210–212°) chiefly.

Moreover, both condensation products at the lowered and elevated temperatures afforded a dioxocarboxylic acid in nearly equal yields on the ring-opening in alcoholic hydrochloric acid, which was considered to be γ,ζ-dioxo-η-phenylcaprylic acid (VI). From these results, it may be supposed that the compound (V) obtained here consists of the cis- and trans-isomers. The reaction sequence is illustrated by the following formulation.



V



IV

Ultimately, methyl isobutyl ketone and phenylacetone appeared difficult to condense with furfural at their α-methylene groups, in contrast with methyl ethyl ketone and methyl propyl ketone. This fact may perhaps be attributed to the presence of the bulky group adjacent to the α-methylene group of these ketones, such as isopropyl and phenyl groups.

Experimental

Condensation of Methyl Isobutyl Ketone with Furfural Into a stirred suspension of furfural (15 g.) and methyl isobutyl ketone (30 g.) in water (200 cc.) was at once introduced 5% aqueous sodium hydroxide (10 cc.) at 60°, with stirring. After prolonged stirring for 2 hrs. at 60–65°, the reaction mixture was neutralised with dilute hydrochloric acid and the oily layer separated. The aqueous solution was extracted twice with ether and the ether extract combined with the oil. Fractionation of the ether solution gave a yellow oil (12.7 g.) distilling at 124–126°/6 mm., which was considered to consist of 1-(2-furyl)-5-methyl-1-hexen-3-one (III), $C_{11}H_{14}O_2$. (Found: C, 73.84; H, 7.61%; Calcd. for $C_{11}H_{14}O_2$: C, 74.11; H, 7.96%).

This fraction gave a semicarbazone crystallising from methanol-water as colourless needles, (m.p. 177–178°; lit[3]., m. p. 175~176°.) (Found: C, 61.09; H, 6.94; N, 17.65%; Calcd. for $C_{12}H_{17}O_2N_3$; C, 61.24; H, 7.29; N, 17.86%).

This fraction gave nearly equal amounts of two 2,4-dinitrophenylhydrazones, reddish-orange, flattened needles (m.p. 196–197°) and red, long needles (m.p. 145–146°). The former 2,4-dinitrophenylhydrazone was comparatively sparingly soluble in pyridine and the latter fairly soluble in pyridine. Those isomers were separated by the solubility difference. Needles (m.p. 196–197°) (Found: C, 57.09; H, 4.79; N, 15.22%; Calcd. for $C_{17}H_{18}O_5N_4$: C, 56.96; H, 5.07; N, 15.63%). Needles (m.p. 145–146°) (Found: C, 57.12; H, 4.74; N, 15.50%; Calcd. for $C_{17}H_{18}O_5N_4$: C, 56.96; H, 5.07; N, 15.63%).

The latter needles (m.p. 145–146°) were readily transformed into the former (m.p. 196–197°), being suspended in hot dilute methanolic sulfuric acid for a short time.

The semicarbazone (m.p. 177–178°) was also converted into a mixture of these two 2,4-dinitrophenylhydrazones, reacting with 2,4-dinitrophenylhydrazine in alcoholic sulfuric acid.

The condensation of furfural with methyl isobutyl ketone at the reaction temperature 0–5° was carried out by stirring a mixture of furfural (15 g.), methyl isobutyl ketone (30 g.), water (250 cc.) and 10% aqueous sodium hydroxide (30 cc.) for 6 hrs. The reaction mixture was worked up in the same manner as in the case of the foregoing condensation, and a fraction (20 g.) distilling at 121–124°/5 mm. was collected. This fraction also gave the same semicarbazone and 2,4-dinitrophenylhydrazones as in the case of the condensation at the reaction temperature 60–65°.

Both condensation products at the reaction temperatures, 60–65° and 0–5° were suspended in the sodium hypochlorite solution[6], but no heat was generated and no α-isopropyl-2-furanacrylic acid detected.

Condensation of Furfural with Phenylacetone Furfural (15 g.) and phenylacetone (30 g.) were suspended in water (200 cc.), and 5% aqueous sodium hydroxide was at once run in at about 60° with stirring. After prolonged stirring for 5.5 hrs. at 60–70°, the reaction mixture was worked up in the same manner as in the foregoing condensation, and a fraction (22 g.) distilling at 172–177°/5 mm. was obtained, which was considered to be 4-(2-furyl)-1-phenyl-3-buten-2-one (V), $C_{14}H_{12}O_2$. (Found: C, 78.71; H, 5.69%; Calcd. for $C_{14}H_{12}O_5$: C, 79.28; H, 5.71%).

This fraction afforded nearly equal amounts of two semicarbazones, colourless prisms (m.p. 163–164°) fairly soluble in methanol and colourless needles(m.p. 210–212°)sparingly soluble in methanol. These isomers were separated by the solubility difference. Prisms (m.p. 163–164°)(Found: C, 66.48; H, 5.50; N, 15.45%; Calcd. for $C_{15}H_{15}O_2N_3$: C, 66.88; H, 5.62; N, 15.61%). Needles (m.p. 210–212°) (Found: C, 66.68; H, 5.61; N, 15.43%; Calcd. for $C_{15}H_{15}O_2N_3$: C, 66.88; H, 5.62; N, 15.61%).

The former semicarbazone was converted to a 2,4-dinitrophenylhydrazone crystallising from pyridine as reddish-orange, lustrous leaflets (m.p. 178–179°), and the latter semicarbazone to a 2,4-dinitrophenylhydrazone crystallising from pyridine as red, flattened needles (m.p. 183–184°). Orange leaflets (m.p. 178–179°) (Found: C, 60.90; H, 4.04; N, 13.94%; Calcd. for $C_{20}H_{16}O_5N_4$: C, 61.20; H, 4.12; N, 14.28%). Red, flattened needles (m.p. 183–184°) (Found: C, 60.88; H, 4.03; N. 14.17%; Calcd. for $C_{20}H_{16}O_5N_4$: C, 61.20; H, 4.12; N, 14.28%).

Furfural (15 g.) and phenylacetone (30 g.) were suspended in a mixture of alcohol (50 cc.) and water (250 cc.), whereupon 10% aqueous sodium hydroxide was run in at about 5° with stirring. After prolonged stirring for 6.5 hrs. at 5°, the reaction mixture was worked up as described above, and a fraction (8 g.) distilling 170–178°/5 mm. obtained. This fraction gave the red flattened needles (m.p. 183–184°) mainly.

Both condensation products at the reaction temperatures 60–70° and 5° were suspended in the sodium hypochlorite[6], but no heat was generated and no α-phenyl-2-furanacrylic acid detected.

Ring-opening The condensation product (III) (2 g.) of furfural with methyl isobutyl ketone at the reaction temperature 60–65° was refluxed with conc. hydrochloric acid (1.5 cc.) and alcohol (5 cc.) on the water-bath for 3 hrs. The reaction mixture, after addition of an equal volume of dilute hydrochloric acid, was evaporated to dryness on the water-bath. The residue was extracted with a sufficient quantity of water, and the extract evaporated on the water-bath to give an oily matter which on cooling formed a crystalline mass (1 g.). It was recrystallised from ligroin as colourless leaflets, m.p. 79–80°. This specimen was considered to be γ,ζ-dioxo-ϑ-methylcapric acid (IV)[4], $C_{11}H_{18}O_4$. (Found: C, 61.57; H, 8.23%; Calcd. for $C_{11}H_{18}O_4$: C, 61.64; H, 8.47%).

The condensation product (V) (2 g.) of furfural with phenylacetone at the reaction temperature 60–70° was refluxed with conc. hydrochloric acid (1.5 cc.) and alcohol (5 cc.) for 3 hrs. The reaction mixture, after being worked up as described above, gave a crystalline mass (0.3 g.), which was recrystallised from ligroin-ethyl acetate as colourless rhombic plates, m.p. 88–89°.

By the same procedure, the condensation product (V) (2 g.) of furfural with phenylacetone at the reaction temperature 0–5° yielded the same crystals (0.3 g.). This specimen was considered to be γ,ζ-dioxo-η-phenylcaprylic acid (VI), $C_{14}H_{16}O_4$. (Found: C, 67.37; H, 6.62%; Calcd. for $C_{14}H_{16}O_6$: C, 67.71; H, 6.49%).

Summary

Methyl isobutyl ketone and phenylacetone, unlike methyl ethyl ketone[1], condensed with furfural by sodium hydroxide at their α-methyl groups irrespective of the reaction temperature, giving 1-(2-furyl)-5-mthyl-1-hexen-3-one (III) and 4-(2-furyl)-1-phenyl-3-buten-2-one (V) respectively.

1-(2-Furyl)-5-methyl-1-hexen-3-one (III) gave the two forms of 2,4-dinitrophenylhydrazone. One (m.p. 145–146°) shifted readily to the other (m.p. 196–197°) in dilute alcoholic sulfuric acid, and those may be the syn- and anti-isomers.

4-(2-Furyl)-1-phenyl-3-buten-2-one (V) obtained here gave the two species of semicarbazone which were converted into the respective two species of 2,4-dinitrophenylhydrazone. It may perhaps be composed of the cis- and trans-isomers. This furfurylidene ketone gave γ,ζ-dioxo-η-phenylcaprylic acid (VI) by the ring-opening in alcoholic hydrochloric acid.

The author expresses his sincere thanks to Dr. T. Hayashi for his kind advice.

Scientific Research Institute, Komagome, Bunkyo-ku, Tokyo

6) H. Midorikawa, This Bulletin, **26**, 462 (1953).

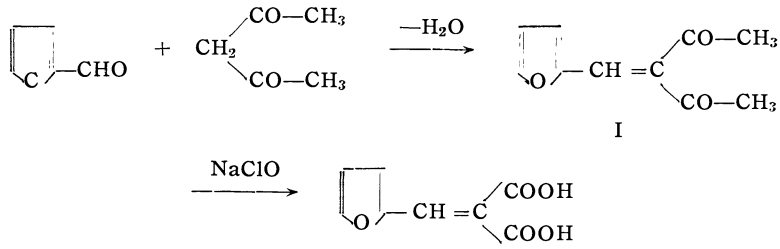
The Condensations of Furfural with Acetylacetone and Ethyl Propionylacetate

By Hiroshi MIDORIKAWA

(Received February 23, 1954)

In the present paper were tried the condensations of furfural with acetylacetone and ethyl propionylacetate which have a reactive methylene group. In these cases, piperidine was a more suitable condensing agent than alkali, as in the condensation of ethyl acetoacetate with benzaldehyde[1] or furfural[2].

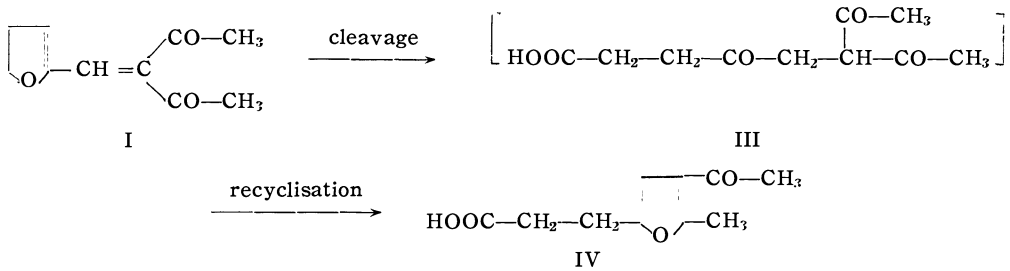
The condensation of furfural with acetylacetone by piperidine or aqueous sodium hydroxide gave 3-acetyl-4-(2-furyl)-3-buten-2-one (I), which was oxidised by sodium hypochlorite to furfurylidenemalonic acid (II). The reaction sequence is shown in the following formulae.



I

II

Furthermore, by refluxing with alcoholic hydrochloric acid and subsequent hydrolysis, 3-acetyl-4-(2-furyl)-3-buten-2-one (I) gave an acid, $C_{10}H_{12}O_4$, which gave a semicarbazone, $C_{11}H_{15}O_4N_3$. It was infered that this acid did not possess the group $-CH(COCH_3)_2$ and the ordinary unsaturated nature, because it did not colorise aqueous ferric chloride and did not decolorise bromine water. Consequently, this compound $C_{10}H_{12}O_4$ was considered to be β-(4-acetyl-5-methyl-2-furyl)-propionic acid (IV) which was given by the ring-cleavage of the furfurylidene ketone (I) and the subsequent recyclisation[3] of the resulting cleavage product (III) with loss of water, as illustrated below. The analogous examples had already been reported with respect to furfurylidene-ethyl phenyl ketone[4] and furfurylidene-(3-methyl-4-methoxy-6-chloroacetophenone)[5].



I

III

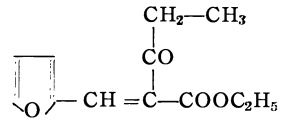
IV

In this case the saturated cleavage product (III) was not isolated. The related furan (IV) obtained here showed no remarkable pine-splint reaction.

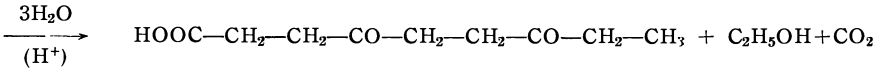
On the condensation of furfural with ethyl propionylacetate by piperidine was obtained ethyl α-propionyl-2-furanacrylate (V). This compound (V) yielded a dioxocarboxylic acid $C_9H_{14}O_4$ (m. p. 83–84°) on refluxing with alcoholic hydrochloric acid and subse-

1) E. Knoevenagel and W. Ruschhaupt, *Ber.*, **30**, 1026 (1898).
2) E. Knoevenagel, *Ber.*, **29**, 172 (1896).
3) A. P. Dunlop and F. N. Peters, "The Furans," p. 653, New York, Reinhold Publishing Corp., (1953).
4) D. L. Turner, *J. Am. Chem. Soc.*, **71**, 612 (1949).
5) R. H. Martin and R. Robinson, *J. Chem. Soc.*, 497 (1953).

quent hydrolysys. The present author* had already investigated that ethyl α-acetyl-2-furanacrylate yielded γ,ζ-dioxocaprylic acid by the same procedure. It was certain, therefore, that this dioxocarboxylic acid was γ, ζ-dioxopelargonic acid (VI), as illustrated by the following formulation.

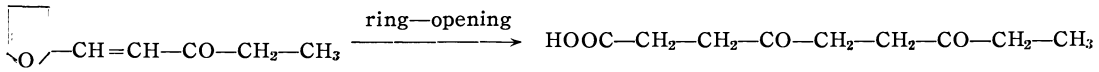


V



VI

In the preceding report[6], two furfurylidene ketones were obtained on the condensation of furfural with methyl ethyl ketone by alkali. One (b. p. 126°/19 mm.) of those, which gave the two forms of semicarbazone, needles (m. p. 183~184°) and plates (m. p. 166~167°), and the carmine needles (m. p. 206~207°) of 2, 4-dinitrophenylhydrazone, had been considered to be 1-(2-furyl)-penten-3-one (VII), owing to there being no reaction with sodium hypochlorite. The dioxocarboxylic acid (m. p. 83~84°) arising from this furfurylidene ketone on the ring-opening in alcoholic hydrochloric acid, which had been expected to be γ, ζ-dioxopelargonic acid, showed no depression on admixture with the authentic specimen (VI) obtained from ethyl α-propioyl-2-furanacrylate (V). Therefore, the considerations in the preceding paper were confirmed. The reaction sequence is illustrated by the accompanying formulation.



V VI

Experimental

3-Acetyl-4-(2-furyl)-3-buten-2-one (I). To a mixture of furfural (7 g.) and acetylacetone (7 g.) was added piperidine (0.1 g.) and the vessel was immersed in water at ordinay temperature for 2 days. The reaction mixture was extracted with ether. The ether extract, washed with dilute hydrochloric acid, was dried over calcium chloride. Fractionation of the ethereal solution gave a pale yellow, viscous oil (9 g.) distilling at 128~129°/4 mm., which solidified on standing for a short time. It formed colourless prisms on two recrystallisations from ether, m. p. 58~59°, which was the required ketone (I), $C_{10}H_{12}O_3$. (Found; C, 67.95; H, 5.65 %; Calcd. for $C_{10}H_{10}O_3$: C, 67.37; 5.66 %).

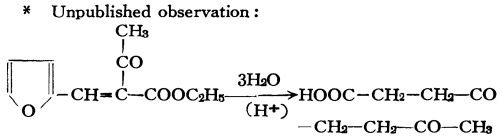
Its mono-2,4-dinitrophenylhydrazone formed lustrous, carmine prisms melting at 224~225° on crystallisation from pyridine. (Found: C, 53.72; H, 4.06; N, 15.27 %; Calcd. for $C_{16}H_{14}O_6N_4$; C, 53.61; H, 3.94; N, 15.61 %).

3-Acetyl-4-(2-furyl)-3-buten-2-one (I) (1 g.) was suspended in the sodium hypochlorite solution[6] (15 cc.) and the vessel immersed in water at ordinary temperature for 2 days, with occasional shaking. The reaction mixture was acidified with dilute hydrochloric acid and extracted twice with ether. The ether extract on evaporation gave colourless prismatic crystals (2 g.), which were recrystallised from acetic acid as colourless prisms melting at 206° with decomposition. This specimen was identical with furfurylidenemalonic acid (II), $C_8H_6O_5$; lit.,[7] m. p. 205°. (Found: C, 52.64; H, 3.32%; Calcd. for $C_8H_6O_5$: C, 52.73; H, 3.32 %).

3-Acetyl-4-(2-furyl)-3-buten-2-one (I) (2 g.) was refluxed with conc. hydrochloric acid (1.5 cc.) and alcohol (5 cc.) on the water-bath for 3 hrs. The reaction mixture, after the addition of an equal volume of dilute hydrochloric acid, was evaporated to dryness on the water-bath. The residue was extracted with a sufficient quantity of water, and the extract decolourised by active charcoal. Concentration of the solution on the water-bath gave faintly yellow needle crystals (0.1 g.), which recrystallised from ligroin-ethyl acetate, m. p. 125~126°; soluble in alcohol, benzene and acetone; sparingly soluble in ether. This specimen was considered to be β-(4-acetyl-5-methyl-2-furyl)-propionic acid (IV). (Found: C, 61.21; H, 6.03 %; Calcd. for $C_{10}H_{12}O_4$: C, 61.19; H, 6.16 %). Molecular weight: Found (Micro-Rast): 198; Calcd. for $C_{10}H_{12}O_4$:196.

This acid gave a semicarbazone which formed colourless minute crystals (m. p. 206~207°); spar-

* Unpublished observation:



6) H. Midorikawa, This Bulletin, **26**, 460 (1953); **27**, 149 (1954).

7) C. Liebermann, *Ber.*, **27**, 287 (1894).

ingly soluble in methanol. (Found: C, 52.09; H, 5.95; N, 16.53 %; Calcd. for $C_{11}H_{15}O_4N_3$: C, 52.15; H, 5.97; N, 16.59 %).

The condensation of furfural with acetylacetone by alkali was also carried out at O°. From the reaction mixture was obtained a pale yellow, viscous oil distilling at 127~135°/3 mm., in a poor yield. This oil did not solidify on standing, but gave the same reaction products as in the case of the condensation product by piperidine—the 2,4-dinitrophenylhydrazone melting at 224~225°, furfurylidenemalonic acid (II) by sodium hypochlorite oxidation and β-(4-acetyl-5-methyl-2-furyl)-propionic acid (IV) on refluxing with alcoholic hydrochloric acid.

Ethyl α-propionyl-2-furanacrylate (V). Into a mixture of furfural (7 g.) and ethyl propionylacetate(10 g.) synthesised by Blaise's method[8] were introduced five drops of piperidine at −15°. After standing for 24 hrs. at −15~5°, five drops of pideridine were added to the mixture, and whole kept at −15~5° for 2 days. The reaction mixture was extracted with ether. The ether extract was washed with dilute hydrochloric acid and dried over calcium chloride. Fractionation of the ether solution gave a pale yellow oil (5 g.) distilling at 147°/5 mm., which solified on standing. This fraction recrystallised from ether-ligroin as colourless prisms, m. p. 57~58°. (Found: C, 64.70; H, 6.10 %; Calcd. for $C_{12}H_{14}O_4$: C, 64.83; H, 6.35 %).

Its 2,4-dinitrophenylhydrazone crystallised from pyridine as scarlet, fibrous needles, m. p. 223~224°. (Found: C, 53.40; H, 4.34; N, 13.81 %; Calcd. for $C_{18}H_{18}O_7N_4$: C, 53.71; H, 4.51; N, 13.92 %).

γ,ζ-Dioxopelargonic Acid (V). Ethyl α-propionyl-2-furanacrylate (V) (2 g.) was refluxed with conc. hydrochloric acid (2 cc.) and alcohol (5 cc.) on the water-bath for 5 hrs. The reaction mixture, after addition of an equal volume of dilute hydrochloric acid, was evaporated to dryness on the water-bath. The residue was extracted with hot water, and the extract was concentrated on the water-bath to yield a crystalline mass (0.2 g.) of the required acid. It was recrystallised from ligroin-ethyl acetate as colourless leaflets, m. p. 83~84°. (Found: C, 57.30; H, 7.28 %; Calcd. for $C_9H_{14}O_4$: C, 58.03; H, 7.59 %.).

This acid showed no depression of the mixed melting point with the dioxocarboxylic acid, obtained by the ring-opening of the furfurylidene ketone (b. p. 126°/19 mm.) in alcoholic hydrochloric acid which was considered to be 1-(2-furyl)-1-penten-3-one in the previous papers[6].

8) R. Willstatter and C. H. Clarke: *Ber.*, **47**, 298 (1914).

Summary

3-Acetyl-4-(2-furyl)-3-buten-2-one (I) and ethyl α-propionyl-2-furanacrylate (V) were obtained by the condensations of furfural with acetylacetone and ethyl propionylacetate by piperidine, respectively.

3-Acetyl-4-(2-furyl)-3-buten-2-one (I) was oxidised by sodium hypochlorite to furfurylidenemalonic acid (II), and, on refluxing with alcohoric hydrochloric acid and subsequent hydrolysis, gave β-(4-acetyl-5-methyl-2-furyl)-propionic acid (IV).

Ethyl α-propionyl-2-furanacrylate (V) gave γ,ζ-dioxopelargonic acid (VI) by refluxing with alcoholic hydrochloric acid and subsequent hydrolysis.

The dioxocaboxylic acid (m. p. 83~84°), obtained by the ring-opening of the furfurylidene ketone (b. p. 126°/19 mm.) in alcoholic hydrochloric acid which was considered to be 1-(2-furyl)-1-penten-3-one (VII) in the previous reports, was identical with this γ,ζ-dioxopelargonic acid (VI). It was confirmed, therefore, that the ideas in the previous reports[6] was correct.

The author expresses his sincere thanks to Dr. T. Hayashi for his kind advice.

Scientific Research Institute,
Komagome, Bunkyo-ku, Tokyo

The Effect of Conversion on the Mechanism of Vinyl Polymerization. I. Styrene

By Saburo FUJII

(Received February 20, 1954)

Introduction

Although the detailed mechanism of the initial stage of vinyl polymerization has been studied by many workers with various methods, little has been published which clarifies the effect of conversion on the chain mechanism of polymerization. As already reported, the polymerizations of several vinyl monomers in the liquid phase are strongly accelerated after certain conversions[1),2),3)], and this rate of acceleration has been attributed by Trommsdorff[4)] to a decrease in the termination rate constant of polymer radicals with the increasing viscosity of the system. His suggestion has recently been confirmed by Matheson and his coworkers[5)] with the measurement of the lifetime of kinetic chains, but the further investigations at high conversions may yet be necessary to make clear the chain mechanism in the later stage of polymerization.

In an attempt to obtain further information on this point the present author has studied photochemically the polymerizations of several vinyl monomers in the range 0 to about 70% conversion. This paper reports the work on styrene.

Theoretical

The following facts are implicitly assumed in this work (1) The radical polymerization consists of four kinds of elementary reactions; thermal or light initiation, propagation, transfer with monomer and termination. (2) These elementary rate constants are independent of the length[6)] or valence character (mono- or di-radical) of the polymer radicals, and further the rate constants of propagation and transfer are assumed to be approximately independent of conversion[7)]. (3) The irradiated light is absorbed uniformly in the reaction cell and causes no decomposition of the monomer or of the polymer. (4) The rate of light initiation is proportional to the absorbed light intensity, this intensity being proportional to that of illumination. (5) The light absorption by the polymer is negligible compared to that by the monomer. (6) An instantaneous steady state is reached in the light initiation. (7) The rate of thermal initiation is unaffected by light. (8) The assumptions in the sector experiment are almost the same as those described in Matheson's papers[5)]; precautions to insure the correctness of the assumptions (3) to (8) except (6) were made in the present experiment.

On the basis of the absorption spectra of styrene and its polymer[8)], the assumptions (4) and (5) may be adequate and the absorbed light intensity, I_{abs}, will be represented by

$$I_{abs} = \varepsilon l[M] I_0 , \qquad (1)$$

where I_0 is the intensity of illumination, $[M]$ the monomer concentration, l the depth of the reaction cell and ε the mean molecular extinction coefficient of the monomer in the neighborhood of 3660 Å. In the present work, the production and disappearance of kinetic chains are mainly discussed, but neither the question whether the active polymer is monoradical or biradical or whether the termination is a recombination or a disproportionation are considered. From this stand-point by the concentration of kinetic chains, $[R]$, will be given by

$$\frac{d[R]}{dt} = qI_{abs} + k_i[M]^2 - k_t[R]^n \qquad (2)$$

and also the rate of monomer consumption at any stage by

$$-\frac{d[M]}{dt} = V_p = k_p[R][M] \qquad (3)$$

Here q is the quantum efficiency of production of kinetic chains, and k_t, k_p and k_i are the rate constants of termination, propagation and thermal initiation respectively.

1) G. V. Schulz and F. Blaschke, *Z. physik. Chemie*, **B50**, 305 (1941).
2) G. M. Burnett and H. W. Melville, *Nature*, **153**, 661 (1945); *Proc. Roy. Soc. London*, **A189**, 456 (1947).
3) M. H. Mackay and H. W. Melville. *Trans. Faraday Soc.* **45**, 323 (1949).
4) Trommsdorff, "*Colloquium on High Polymers*" Freiburg, 1944.
5) (a) M. S. Matheson, E. E. Auer, E. B. Bevilacqua and E. J. Hart, *J. Am. Chem. Soc.*, **71**, 497 (1949); (b) ibid., **73**, 1700 (1951) (c) ibid., **73**, 5395 (1951).
6) F. R. Mayo, *J. Am. Chom. Soc.*, **70**, 3689 (1948); R. A. Cregg and F. R. Mayo, ibid., **70**, 2373 (1948).
7) M. F. Vaughan, *Trans. Faraday Soc.*, **48**, 576 (1952).
8) (a) T. G. Majury and H. W. Melville, *Proc. Roy. Soc. London*, **A205**, 496 (1951); (b) J. H. de Boer, R. Houwink and J. F. H. Custers, *Rec. trav. Chim.*, **52**, 709 (1933).

Further if the condition, $q\boldsymbol{I}_{abs} \gg k_i[M]^2$, is held in the stationary state of this chain reaction, the following two equations are easily derived from eqns. (1), (2) and (3).

$$\ln V_{pL} = \ln\left\{(q\varepsilon l)^{1/n}\frac{k_p}{k_t^{1/n}}[M]^{1+\frac{1}{n}}\right\} + \frac{1}{n}\ln \boldsymbol{I}_0 \qquad (4)$$

and

$$E_a = -R\frac{\partial(\ln V_{pL})}{\partial(1/T)} = E_p - \frac{1}{n}\left\{E_t + R\frac{\partial(\ln q)}{\partial(1/T)}\right\} \qquad (5)$$

where V_{pL} is the stationary rate of photo-polymerization, E_a the over-all activation energy of photo-polymerization, T the absolute temperature, and E_p and E_t are the activation energies of propagation and termination respectively. These eqns. (4) and (5) will be used in the discussion of the experimental results.

Next, if the chain termination is of the second order ($n=2$), the average life-time of kinetic chains, τ_s, in the stationary state of polymerization may be defined by

$$\tau_s = \frac{1}{k_t[R]_s} \qquad (6)$$

and then

$$\frac{\tau_s V_{pL}}{[M]} = k_p/k_t \qquad (7)$$

is obtained from eqn. (3). Thus, by measuring τ_s the value of k_p/k_t can be estimated.

Under the present experimental conditions the value of τ_s at low conversion (0~1%) was of the order of second and could be measured with rotating sector technique, but the one at high conversions became so long (over 10^3 seconds) that the photochemical after-effect could easily be observed dilatometrically. For the after-effect the equation governing $[R]$ after the interruption of illumination will be

$$-\frac{d[R]}{dt} = k_t[R]^n - k_i[M]^2 \qquad (8)$$

This equation can be integrated in the case of $n=2$ under the conditions ($[R]=[R]_s$ at $t=0$, $[R]=(k_i/k_t)^{1/2}[M]=[R]_d$ at $t=\infty$) and combined with eqns. (3) and (6) to give

$$\ln\left(\frac{V_p+V_d}{V_p-V_d}\right) = \ln\left(\frac{V_{pL}+V_d}{V_{pL}-V_d}\right) + 2\frac{V_d}{V_{pL}}\frac{t}{\tau_s} \qquad (9)$$

where V_d is the steady rate of thermal polymerization (dark rate) V_p the rate of polymerization at the time, t, after the interruption of illumination. Hence if

$$\left[\frac{V_{pL}}{2V_d}\ln\left(\frac{V_p+V_d}{V_p-V_d}\right)\right]$$

is plotted as a function of t, a straight line will be obtained with a slope of $1/\tau_s$, that is, τ_s can be estimated.

The theory and experimental method of the rotating sector are fully presented in Matheson's papers[5]. In the present experiment the ratio of the dark period to the light period was 3 and the thermal initiation during light periods was negligible compared to the light initiation. Therefore the theoretical ratio of the intermittent light rate to the steady light rate as a function of flash time and dark rate is the same as the one calculated by Matheson and his co-workers.[5a]

Experimental

Styrene was prepared by the dehydration of pure β-phenyl-ethyl alcohol with solid potassium hydroxide over 240°C. and purified by successive washing with dilute sulphuric acid, dilute sodium hydroxide and distilled water. After drying with calcium chloride it was distilled twice through a fractionating column of 1 meter long at 15 mm. pressure, and the fraction boiling at 40.0°C. was collected and stored in an evacuated flask in the dark. Immediately before use this monomer was allowed to polymerize to about 5% thermally and with the illumination of ultra-violet light longer than 3300 Å, and then it was redistilled with dry ice into the reaction cell. These procedures were carried out in a glass system evacuated to 10^{-3}mm. pressure.

The rate of monomer consumption was measured with a dilatometer shown in Fig. 1, and a reading-microscope was used to read the mercury level in the capillary C to 0.01 mm. This dilatometer was immersed in a thermostat, which was regulated to ±0.001°C. In the experiments at high conversions the reaction cell A in Fig. 1. was heated in a small electric furnace at 130± 5°C. for desirable duration[9], left alone at room

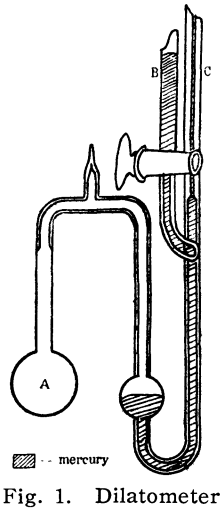


Fig. 1. Dilatometer

9) The number average degree of polymerization for the polymer formed by this procedure may be estimated as about 1700 (R. A. Gregg and F. R. Mayo, *Discussions of the Faraday Soc.*, No. 2 (1947). *The Labile Molecule.* p. 528.)

temperature over half a day, and then the experiments were carried out, where the polymer concentration in A was estimated from the lowering of the mercury level in B. Matheson's data[5b] about the densities of the monomer and of the polymer in monomer were used to estimate the rate of polymerization and the polymer concentration in the cell.

The source of light was a 200 watt ultra high pressure mercury lamp fed from a constant voltage transformer. The light was passed through a 5% aqueous solution of copper sulphate and through two lenses made of soda glass. Considering the intensity distribution of absorbed light the photo-polymerization may be mainly caused by the light of 3660 Å.[10] During an experiment the constancy of light was checked by a vacuum photocell with a Mazda UVD_1 filter (for 3660 Å). Also, using the above optical filter, the light intensity at the front of the reaction cell was measured with an uranyl-oxalate actinometer and its full intensity was 4×10^{-8} Einsteins per second.

The sector was made of a 46 cm. diameter aluminum disk and one-fourth part of it was cut off to a radical depth of 7 cm. The disk speed could be varied in steps from 1/20 to 150 r.p.m. The set of sector apparatus and the method of sector experiment were almost the same as the ones reported by Matheson and his co-workers.[5a]

Unless otherwise noticed, the reaction system did not contain any photo-sensitizer or thermal catalyser. The rate of photo-polymerization under the present experimental conditions did not exceed over 10^{-4} mol./l./sec., so that the apparent change of monomer concentration may be negligible during illumination. When the lifetime of kinetic chains was very long, a long period of preliminary illumination was necessary to the determination of the stationary rate of photo-polymerization.

Results

The stationary rates of photo-polymerization under a constant light intensity (4×10^{-8} Einsteins/sec.) and of thermal polymerization were measured at three different temperatures between 0 to 60 % conversion, and these were found to be strongly accelerated with increasing conversion (Table I). Plotting log (relative rate) against the reciprocal of the absolute temperature gives an over-all activation energy at each conversion and the result is indicated in the last column of Table I.

TABLE I

RATES* OF PHOTO- AND THERMAL-POLYMERIZATIONS AND OVER-ALL ACTIVATION ENERGIES FOR STYRENE

Conversion %	25°C.	30°C.	40°C.	$E_{act.}$ (k cal./mol.)
(a) Light rate (unit; 10^{-6}mol./l./sec.)				
0~1	1.15	1.52	2.65	10.4
38±1	6.25	7.91	12.0	8.1
60±2	21.3	25.8	37.2	6.9
(b) Thermal rate (unit; 10^{-6}mol./l./sec.)				
0~1	0.097	0.170	0.417	18.1
38±1	0.396	0.630	1.40	15.7
60±2	0.645	1.01	2.17	14.5

* All the rate measurements were corrected for the thermal reaction taking place in the unilluminated appendages to the reaction cell, by subtracting the proper fraction of thermal rate from the apparently observed rates. The polymer concentration in the unilluminated appendages to the cell did not exceed a few per-cent even after the experiments at high conversions, so that the magnitude of the thermal rate in that part, which was necessary to the above correction, was considered to hold the initial value in a complete run.

In this experiment the rate acceleration was found to be accompanied with the photochemical inital- and after-effects (Fig. 2) and also with by a decrease in the reaction order of chain termination (Table II). Here Fig. 2 was obtained in the direct observation of the volume change with time of the reaction system after the interruption of light, where these results had been confirmed to be mainly caused by the chemical after-effect but not by the temperature depression of the system. In the low rate of polymerization

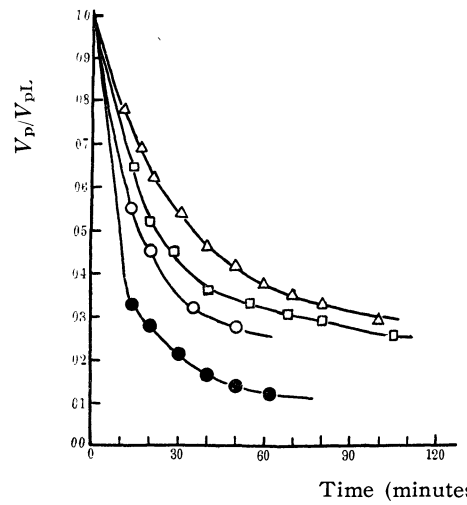


Fig. 2. Photochemical after-effects at 30°C.

	Conversion %	V_{pL} mol./l./sec.	V_d/V_{pL}
●	38	7.91×10^{-6}	0.081
○	38	3.58×10^{-6}	0.180
□	43	9.32×10^{-6}	0.054
△	60	25.8×10^{-6}	0.038

used in these experiments (of the order of 10^{-5} mol./l./sec.) the temperature within the reaction cell exceeded that of the thermostat

10) G. M. Burnett, *Trans. Faraday Soc.*, **46**, 772 (1950).

bath only by the order of 0.01°C. under the stationary conditions, and the volume change due to the disappearance of this temperature difference might be negligible, at high conversions, compared to the total change caused by the after-effect. The data in Table II were obtained, with the use of eqn. (4), from the measurement of V_{pL} in one run in the same reaction cell, (i) under the full intensity from the lamp and (ii) with the intensity reduced by covering the window with calibrated screens.

TABLE II
REACTION ORDER OF CHAIN TERMINATION AT 25°C.

(a) An example at 68 % conversion

Transmission of screen, S	V_{pL} (10^{-5} mol./l./sec.)	$\log S$	log (Relative rate	n
1.00	2.25	0.00	0.00	
0.41	1.24	−0.38	−0.25	1.5
0.19	0.79	−0.73	−0.45	1.6

(b) Summarized result

conversion, %	n
0	1.9～2.1
38±1	1.9～2.1
60±2	1.7～1.8
68±2	1.4～1.6

Also the lifetime of kinetic chains was measured or estimated at several conversions in order to obtain the relationship between the above results and the relative change of k_t with increasing conversion. Since the overall rate of photo-polymerization in the initial stage was proportional to the square-root of the absorbed light intensity ($n=2$, as shown in Table II) and was constant during a considerable period of illumination, τ_s at extremely low conversions could be measured with rotating sector. A typical run in the sector experiments is indicated in Fig. 3.

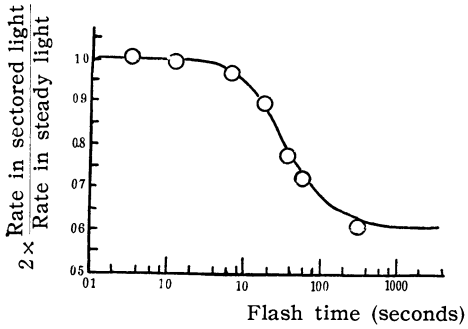


Fig. 3. Rates of polymerization in intermittent light for different times of flash: Curve, theory for dark rate 7 % of steady light rate; ○, experimental point under the conditions (temp. 30°C., coversion 0 % and steady light rate $=2.27\times10^{-6}$ mol./l./sec.)

On the other hand the values of τ_s at high conversions were too great to be measured by with the usual sector techniqe and so these were estimated by the use of eqn. (9) from the observed after-effect. The allowance for the deviation of n from 2 was not considered in this estimation. Therefore both the τ_s values estimated on the basis of the eqn. (9) and the corresponding k_p/k_t values on the eqn. (7) may have a considerable error at the conversions over about 60 %, since n becomes less than 2 at those high conversions. Few examples of the analytical representation for the after-effect observed are illustrated in Fig. 4 and the results of all lifetime runs are summerized in Table III.

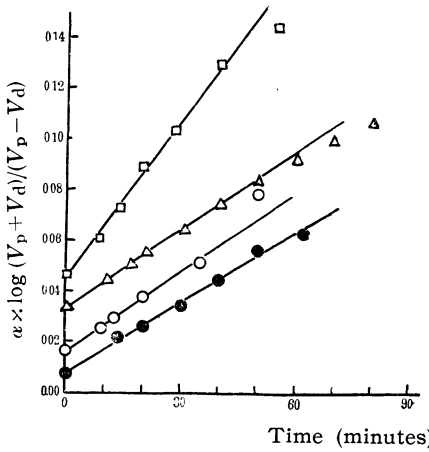


Fig. 4. Analytical representations for the observed after effects; the kinds of experimental points are the same as the ones shown in Fig. 2.
●, ○ ····· $\alpha=0.1$
□, △ ····· $\alpha=1.0$

Discussions

Rate acceleration Trommsdorff[4] examined several vinyl monomers and found that the rates of polymerization were accelerated after certain conversions, styrene alone showing no such acceleration under his experimental conditions. Also it has been well known after Schulz's work[11] that the rates of thermal polymerization of styrene at comparatively high temperatures are apparently proportional to the monomer concentration in the range up to about 90 % conversion. Therefore, compared with these previous results, the abnormal rate acceleration observed in this work seems to throw the possibility (a) on the production of an unstable substance which may induce the rate acceleration and the after-effect or (b)

11) G. V. Schulz, *Ergeb. d. exakt. naturwis.*, **17**, 364 (1938).

TABLE III KINETIC CHAIN LIFETIMES AND RATE CONSTANT RATIO IN RTYRENE

Conversion x %	Temp., °C.	V_{pL} mol./l./sec.	τ_s sec.	Av. τ_s at $V_{pL}=10^{-5}$	k_p/k_t	k_{tx}/k_{to} (b)
0	20	2.18×10^{-5}	0.26	0.48	0.55×10^{-3} (a)	
		1.12×10^{-5}	0.35			
	30	2.27×10^{-5}	9.8	2.0	2.36×10^{-3}	1
		1.52×10^{-5}	12.			
38±1	30	7.91×10^{-5}	453.	358.	6.36×10^{-4}	3.75×10^{-1}
		3.58×10^{-5}	1000.			
43±2	30	9.32×10^{-5}	1356.	1261.	2.56×10^{-3}	9.22×10^{-4}
60±2	30	2.58×10^{-5}	1932.	4980.	1.30×10^{-2}	1.81×10^{-4}
70±2	30	1.76×10^{-5}	2274.	4002.	1.37×10^{-2}	1.71×10^{-4}

(a) α-Azo-bisisobutyronitrile was used as a photo-sensitizer in this experiment, no sensitizer in the others.

(b) The ratio of k_{tx} at x % conversion to k_{t0} at nearly 0 %; the assumption (2) was used in this estimation.

on the abnormal increase of q. However the theoretical examination for the case (a) will give a constant τ_s value, which is independent of V_{pL} and conversion, in contradiction to the present result, and also the simple calculation for the case (b) will lead to the unreal conclusion that the few hundred-fold increase of q must be necessary to explain the observed rate acceleration. On the other hand, if the rate acceleration is attributed to a decrease in k_t as suggested by Trommsdorff in the other vinyl polymerizations, the expected ratios of V_{pL} at 38 % and 60 % conversions to the initial value may eb estimated as about 7.9 and 18.8 respectively at 30°C. by the use of eqn. (4) with the data in the last column of Table III, while the corresponding experimental ratios are about 5.2 and 16.9 respectively. The difference between the above two values at each conversion is accepted to be within an experimental error under the present conditions. Thus the allowance for the above discussions will lead to the conclusion that the rate acceleration is due to an extreme decrease in k_t as the system becomes more viscous.

Decreases in the overall activation energy and n It is an expected result in this work that an extreme decrease in k_t is accompanied with a considerable decrease in the over-all activation energy, and this kinetic behaviour has also been found by the present author in the thermal- and photo-polymerizations of methyl methacrylate near room temperatures[12] and by Cowley & Melville[13] in the photo-degradation (by 2537 Å line) of polymethyl methacrylate over 130°C. This result can be explained by the fact that E_t in eqn. (5) increases steadily as the mutual termination of polymer radicals become diffusion-controlled with the increasing viscosity of the system. Using the following equation, which has been suggested by Spencer and Williams[14],

$$\eta = 3.63\times10^{-10}\, exp\,\{0.0572\sqrt{M} + \sqrt{w_2}(22.54-0.045\sqrt{M}+5000/T)\},$$

where η=bulk viscosity of the styrene-polystrene system in centipoises, M=Staudinger molecular weight and w_2=weight fraction of polymer, it may be estimated that the activation energies of diffusion of polymer radicals at 38 % and 60 % conversions are about 6.1 and 7.7 kcal./mole respectively. If 2.4 kcal./mole is used as an apparent E_t value in the initial stage[5b], the estimated increase in E_t will cause it to decrease E_a (in eqn. (5)) by about 1.8 kcal./mole at 38 % and by about 3.0 kcal./mole at 60 %, while Table I shows the decreases in the over-all activation energies as 2.3~2.4 kcal./mole at 38 % and as 3.5~3.6 kcal./mole at 60 %. The difference between the above estimated and experimental decreases in E_a may be within an experimental error.

The value (1.9~2.1) of n, the reaction order of chain termination, measured in the range 0 to nearly 40 % conversion shows that mutual termination only takes place. However its decrease over about 60 % conversion suggests strongly that self-termination occurs considerably in the highly viscous medium. It is not difficult to visualize a mechanism by which polymer radicals become apparently terminated without mutual collision. There will be a finite probability that the active end of a growing radical will become shielded by the coiling of the molecule. The fine net of polymer chains at high conversion would be expected greatly to enhance the

12) Unpublished work from this Laboratory.

13) P. R. E. J. Cowley and H. W. Melville, *Proc. Roy. Soc. London*, **A211**, 320 (1952).

14) Spencer and Williams, *J. Colloid Sci.*, **2**, 117 (1947).

degree of shielding. Thus a considerable portion of radicals become unable to react freely with monomer for steric reasons and appear to be deactivated by itself alone. In this sense the extreme decrease in k_t is an inevitable result and also the rate constants of propagation and transfer may be more or less reduced at very high conversions. On the other hand such a shielding effect may be expected to be diminished by the following factors; (i) thermal disturbance, (ii) a decrease in the molecular weight of polymer present and (iii) the addition of a chain transfer substance which is able to pass freely through the polymer network. The factor (iii) has been confirmed experimentally by the addition of a small amount of carbon tetrachloride as a chain transfer substance in the photo-polymerization of styrene[15]. Also it is expected from the factor (i) that neither the extreme decrease in k_t nor the change of $\bar{n}$ are observed at comparatively high temperatures. The discrepancy between the present experimental results and those of the previous authors may perhaps be due to a great difference in the degree of this shielding effect, though it can not be explained precisely at present.

Summary

The polymerization of pure styrene has been studied photochemically near room temperatures and in the range 0 to about 70 % conversion, and the following results have been obtained.

With increasing conversion; (1) both the direct photo-polymerization and the thermal polymerization are accelerated strongly, (2) the over-all activation energies in both polymerizations decreases, (3) the lifetime of kinetic chains increased steadily and the photochemical initial and after effects are easily observed dilatometrically over 30 % conversion. Also (4) the reaction order of chain termination is 2 in the range 0 to about 40 % conversion, but it becomes less than 2 at the conversions over 60 %.

Thus these results have been discussed on several assumptions and it has been concluded that they are attributed to a considerable change in the mechanism of radical termination with increasing conversion of the reaction system, i. e., the change from an activation-controlled termination to a diffusion-controlled one.

The author wishes to express his hearty thanks to Dr. Shoji Shida of this Institute for his helpful advice and encouragement, and to Dr. Hideya Funahasi to Takasago Perfumery Co. for his kind gift of β-phenylethyl alcohol.

Laboratory of physical chemistry,
Tokyo Institute of Technology,
Ookayama, Meguro-ku, Tokyo

15) Unpublished work by the present author.

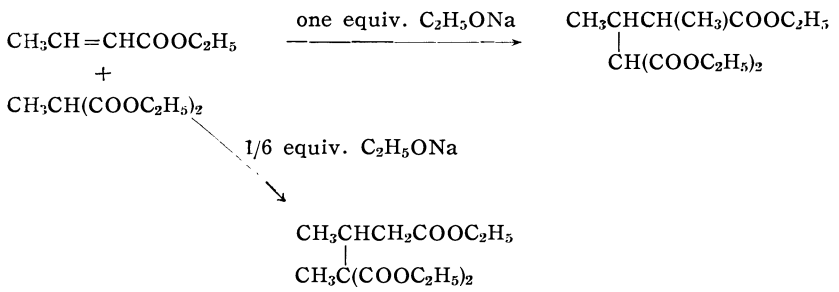
The Michael Addition of Diethyl Methylmalonate to Ethyl Crotonate-(carbonyl C^{14}). A Contribution to the Elucidation of the Mechanism of the Abnormal Addition

By Osamu SIMAMURA, Naoki INAMOTO and Tadashi SUEHIRO

(Received March 15, 1954)

In the course of a paper on the constitution of ethyl sodiocyanacetate and of ethyl sodiomethylcyanacetate, Thorpe[1] has put forth a view that these sodio compounds, RC(CN):C(ONa)OC_2H_5 (R=H or alkyl), add to the double bond of α,β-unsaturated carboxylic esters with R- and -C(CN):C(ONa)OC_2H_5 acting as addendum components. More recently, Michael and Ross[2] have shown that diethyl methylmalonate in the presence of one sixth equivalent of sodium ethoxide adds to ethyl crotonate to yield diethyl α-ethoxycarbonyl-α,β-dimethylglutarate, whereas, with one equivalent of sodium ethoxide, the product is diethyl α-ethoxycarbonyl-β,γ-dimethylglutarate in accordance with Thorpe's view. A product of the former type in the Michael addition is often referred to as normal by later workers and one of the latter type as abnormal.

1) J. F. Thorpe, *J. Chem. Soc.*, **77**, 923 (1900).
2) A. Michael and J. Ross, *J. Am. Chem. Soc.*, **52**, 4598 (1930).



It has then been suggested by Holden and Lapworth[3] that the abnormal addition product with a structure expected from Thorpe's theory could result equally well by migration, during the addition process, of an ethoxycarbonyl group from the malonic ester part of the adduct; however, they were unable to produce any convincing experimental evidence in favour of the theory. Gardner and Rydon[4] have subsequently shown that all the then available observations can be accounted for on the basis of the Holden-Lapworth mechanism; but it has been viewed with some suspicion because of the strained four-membered cyclic structure postulated as an intermediate. It has now been definitely established by a tracer method with carbon-14 that, in the Michael addition of diethyl methylmalonate to ethyl crotonate with one equivalent of sodium ethoxide, it is an ethoxycarbonyl group which migrates to yield the abnormal addition product.

Labelled ethyl crotonate was condensed with diethyl sodiomethylmalonate, and the resulting diethyl α-ethoxycarbonyl-β,γ-dimethylglutarate hydrolyzed with sodium hydroxide to the corresponding tricarboxylic acid, which was subsequently decarboxylated by heating at 170–180°. The carbon dioxide evolved was found to contain about 42 % of the radioactive carbon of the original ethyl crotonate. This observation demonstrated beyond doubt that in the course of the condensation migration of an ethoxycarbonyl group took place from the methylmalonate moiety to the carbon atom α to the labelled ethoxycarbonyl group giving a product (II) with a malonic ester grouping labelled with C^{14}. If a methyl group had become attached to the carbon atom α to the labelled ethoxycarbonyl group as postulated by Thorpe[1] and Michael and Ross[2], the resulting condensation product could have contained no labelled malonic ester grouping, and the subsequent hydrolysis followed by pyrolysis could have consequently given no radioactive carbon dioxide. The sequence of the reactions followed is shown as follows and the measured activities of the products at each stage of the reactions given in Table I.

3) N. E. Holden and A. Lapworth, *J. Chem. Soc.*, **1931**, 2368.
4) J. A. Gardner and H. N. Rydon, ibid., **1938**, 48.

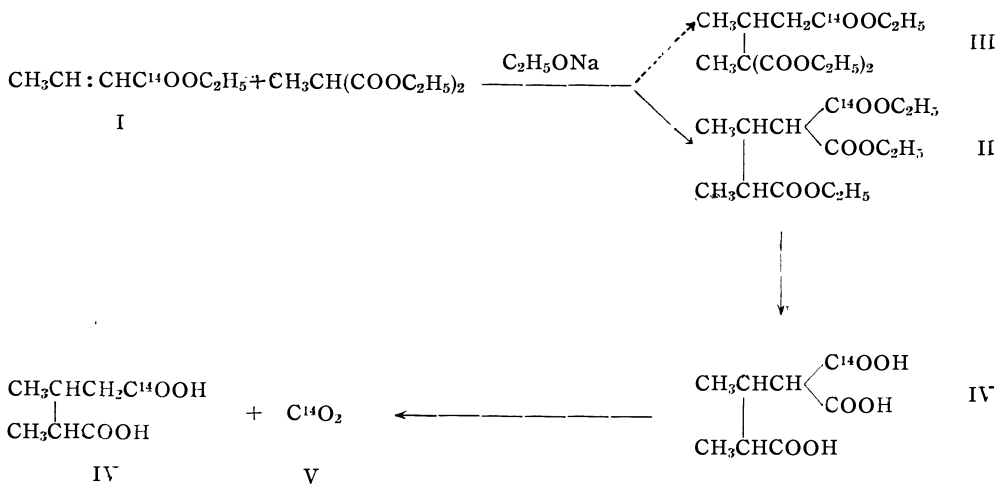


TABLE I

MOLAR ACTIVITIES* OF THE REACTION PRODUCTS

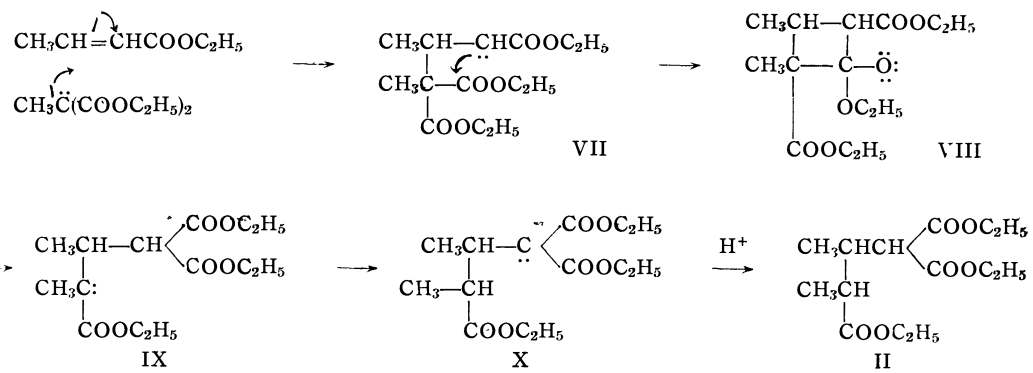
	Expt. 1 mc./mol.	Expt. 2 mc./mol.
Ethyl crotonate (I)	0.0805±0.0013	0.0285±0.0006
Diethyl α-ethoxycarbonyl-β,γ-dimethylglutarate (II)	0.123 ±0.003	0.0415±0.0018
α-Carboxy-β,γ-dimethylglutaric acid (IV)	0.120 ±0.003	0.0399±0.0013
Carbon dioxide from decarboxylation (V)	0.0335±0.0007	0.0120±0.0004
Carbon dioxide from combustion of the residue (VI)	——	0.0043±0.0002

* Indicated deviations are standard errors.

In the course of the investigation some difficulty arose with regard to some molar activity values. Molar activities of diethyl α-ethoxycarbonyl-β,γ-dimethylglutarate (II) and the corresponding free tricarboxylic acid were unusually high compared with the theoretical values of 0.0805 and 0.0285 expected from the activities of the starting materials. This anomaly is probably attributable to the contamination with labelled diethyl α-ethylidene-β-methylglutarate, which may have been formed by the dimerization of the labelled ethyl crotonate in the presence of basic reagents[5]. It seems that the fractionation was not carried out effectively owing to the smallness of the quantity of the material to be handled. On the basis of the measured molar activities, the contents of the dimer of ethyl crotonate in the condensation products are calculated to be 49 and 39 mole% for Expts. 1 and 2, respectively. The alkaline hydrolysis of the condensation product did not give crystalline acid; this is due to the presence of diastereomeric forms of the tricarboxylic acid (IV) in addition to the acid from the above dimer. The observed neutralization equivalents of the products (72.7 and 73.9 for Expts. 1 and 2, respectively) were higher than the theoretical value of 68.1 for α-carboxy-β,γ-dimethylglutaric acid; the differences are accounted for quantitatively by correcting for the presence of the crotonic acid dimer. Further, the activity of the carbon dioxide obtained by oxidation of the residue from the decarboxylation was found to be 0.0043 mc./mol., which agrees well with 0.0044 mc./mol. calculated from the composition of the condensation product.

It is generally recognized that the C^{12}-carboxyl group is eliminated as carbon dioxide from malonic and substituted malonic acids several per cent more frequently than the C^{14}-carboxyl group.[6] On the tentative assumption that the difference in the reaction rate is ten par cent, the molar activity of the carbon dioxide evolved from α-carboxy-β,γ-dimethylglutaric acid in, for example, Expt. 2 should be 0.0285/(1.10+1.0)=0.0136 mc./mol. The observed value of 0.0120 mc./mol. appears therefore to be too low. This is probably attributed to the possible presence of a small quantity of the unrearranged normal product (III).

An essential part of the mechanism of the Michael addition with migration of an ethoxycarbonyl group may be formulated as follows:



5) H. v. Pechmann, *Ber.*, **33**, 3323 (1900); A. Michael and J. Ross, *J. Am. Chem. Soc.*, **53**, 1150 (1931).

6) G. A. Ropp, *Nucleonics*, **10**, No. 10, 22 (1952)

The carbonyl oxygen of the migrating ethoxycarbonyl group plays a role in helping the carbonyl carbon to accept a lone pair of electrons from the carbon atom α to the ethoxycarbonyl group on the original ethyl crotonate resulting in a four-membered cyclic structure provisionally shown as VIII. Objection might be raised to such a structure which may suffer from a considerable strain, but the four-membered cyclic compounds are not so strained that their existence should be rendered impossible. It may be considered that structure VIII represents a transitional state of the rearrangement rather than a more or less stable intermediate, the acceptance of the lone pair being synchronized with the release of the electron pair which has originally linked the migrating group with the α carbon atom of the original diethyl methylmalonate, giving rise to IX. The migration of the ethoxycarbonyl group is followed by a transfer of a proton in the reverse direction to it, X thus being formed, in which a carbanion group is more stabilized than in IX. It is possible that the transfer of the proton may be simultaneous with the migration of the ethoxycarbonyl group. This is a natural consequence of the difference in acidity between a CH group activated by one ethoxycarbonyl group and one activated by two such groups, the acidity of the former being less strong than the latter. Finally, X gives the rearranged product (II) on working up with aqueous acid.

If there is, in the reacting mixture, a stronger acid which can donate a proton to a lone pair of electrons shown in structure VII, the migration of an ethoxycarbonyl group will not take place. This is indeed the case with the Michael condensation with one sixth equivalent of sodium ethoxide[2]; diethyl methylmalonate which had not completely been converted to the sodio compound served as a proton donor. Tsuruta, Yasuhara and Furukawa[7] investigated the effect of variation of experimental conditions, specially of the amount of sodium ethoxide in the Michael addition of diethyl ethylmalonate to diethyl fumarate on the relative yield of the normal and abnormal products and pointed out a competition between the reaction of the initially formed adduct anion (similar to VII) with a proton donor giving the normal product and the isomerization of the adduct anion leading to the abnormal product; but the mechanism of the latter reaction was obscure to them.

As regards what types of reactants will show abnormality and what types will be normal, the theory of the abnormal addition discussed above predicts that condensation of unsaturated compounds of the type CR_2: $CHCOOC_2H_5$ with alkylmalonic ester and similar compounds can be abnormal, and that those of unsaturated substances of the type CR_2: $CRCOOC_2H_5$ with malonic esters will be normal.

Experimental

Crotonic Acid-(carboxyl-C^{14}) This acid was synthesized by the carbonation with radioactive carbon dioxide of allymagnesium bromide prepared according to Shoemaker and Boord[8] followed by the isomerization with hot 50% sulfuric acid[9] according to the following scheme.

$$CH_2:CHCH_2MgBr + C^{14}O_2 \longrightarrow CH_2:CHCH_2C^{14}OOH$$

$$CH_2:CHCH_2C^{14}OOH \longrightarrow CH_3CH:CHC^{14}OOH$$

Starting from 393 mg. of active barium carbonate containing 0.12 mc. of C^{14} and diluting the resulting crude labelled crotonic acid with a total of 2.0 g. of pure unlabelled crotonic acid as a carrier for ease of manipulation, 0.48 g. of labelled crotonic acid with constant activity of 0.245 ± 0.0043 mc./mol., m.p. 70.5–72.0°, was obtained after crystallization four times from petroleum ether. On the basis of the molar activity of the crotonic acid the overall yield of the above synthesis is estimated at 4.9% based on the carbon dioxide used. The poor yield is attributed to the carbonation step, as the isomerization appears to be effected with an almost quantitative yield of 98% according to the literature.[9]

Another approach to labelled crotonic acid followed consisted in the action of labelled potassium cyanide on allyl bromide at 100° in a sealed tube, and the subsequent hydrolysis and simultaneous isomerization to crotonic acid by heating the resulting ally cyanide with 50% sulfuric acid on a water bath.

$$CH_2:CHCH_2Br + KC^{14}N \longrightarrow CH_2:CHCH_2C^{14}N$$

$$CH_2:CHCH_2C^{14}N \longrightarrow CH_3CH:CHC^{14}OOH$$

7) T. Tsuruta, Y. Yasuhara and J. Furukawa, *J. Org. Chem.*, **18**, 1246 (1953).
8) B. H. Shoemaker and C. E. Boord, *J. Am. Chem. Soc.*, **53**, 1505 (1931).
9) E. J. Boorman and R. P. Linstead, *J. Chem. Soc.*, **1933**, 577.

This method gave an overall yield of 25 % based on the cyanide used.

Ethyl Crotonate-(carbonyl-C^{14}) The synthetic procedure was similar to that for ethyl acetate by Ropp.[10] Crotonic acid-(carboxyl-C^{14}) (1.1 g.) was neutralized with aqueous sodium hydroxide, the resulting solution evaporated to dryness on a water bath, and the remaining labelled sodium crotonate desiccated at 120° under 5×10^{-4} mm.Hg. This was heated for one hour at 180–210° with 3.8 cc. of ethyl phosphate, b. p. 104–5° at 20 mm. Hg, prepared according to the method of Dutton and Noller.[11] Distillation of the reaction mixture at 2×10^{-4} mm. Hg gave 1.3 g. of ethyl crotonate-(carbonyl-C^{14}). This procedure yielded pure specimen of ethyl crotonate, n_D^{20}1.4247, in a preliminary experiment with unlabelled crotonic acid.

The Michael Addition Two similar runs were carried out, one of which (Expt. 2) is described as an example. Sodium (0.5 g.) was melted by heating in xylene and powdered by shaking, the xylene decanted, the sodium washed with ether, and 100 cc. of ether and 1.3 g. of absolute ethyl alcohol added to prepare sodium ethoxide. To this mixture 3.8 g. of diethyl methylmalonate prepared from methyl iodide and diethylsodiomalonate in alcohol according to the usual practice, b. p. 114.0–114.5° at 46 mm Hg, was added. Ethyl crotonate-(carbonyl-C^{14}) (2.21 g., 0.0285 mc./mol.) in 50 cc. of ether was then added dropwise to the stirred mixture and the mixture was refluxed for 5 hours. Acetic acid (1.6 g.) in 12.5 cc. of water was added with stirring, the ethereal layer separated, dried with anhydrous sodium sulfate, the ether removed on a water bath and the residue subjected to distillation under diminished pressure, giving 1.7 g. of a fraction (II) boiling at 130–131° at 3 mm. Hg. The condensation product was heated with 1.0 g. of sodium hydroxide in a mixture of 5 cc. each of water and alcohol for two hours and a half on a water bath, the alcohol removed, the residue diluted with water to 80 cc. and filtered through a column of Amberlite IR 120. A fraction with *p*H 2.2 was collected and evaporated to dryness over sulfuric acid in a vacuum desiccator, giving 1.1 g. of acid (IV) (neutralization equivalent, 73.9; activity, 0.0399±0.0013 mc./mol.).

Decarboxylation of α-Carboxy-β,γ-dimethylglutaric Acid The above acid (170 mg.) was heated gradually to 180° in an evacuated vessel, and the vessel was kept at that temperature for one hour. The carbon dioxide evolved was condensed in a trap cooled with liquid air attached to the reaction vessel. When the decarboxylation was over, the condensed carbon dioxide was transferred, also in vacuum, to aqueous sodium hydroxide contained in another flask. Ammonium chloride was added to the sodium hydroxide solution, barium carbonate precipitated by adding barium chloride solution, collected on a filter paper and assayed for radioactivity (Found: 0.0120 ±0.0004 mc./mol.). The same result was obtained, if the decarboxylation and absorption of carbon dioxide by aqueous sodium hydroxide was carried out in an apparatus for Van Slyke-Folch oxidation[12], thus eliminating the operation of condensing carbon dioxide by liquid air.

Radioactivity Determinations Radiocarbon assays were carried out by oxidizing samples according to Van Slyke and Folch[13], and converting the resulting carbon dioxide to barium carbonate, which was counted with a Geiger-Müller counter on an "infinitely thick" layer with a surface area of 4.9 cm^2, the counts being all corrected for background and compared with the count of a standard barium carbonate with known molar activity.

Summary

The Michael addition of diethyl methylmalonate to ethyl crotonate-(carbonyl-C^{14}) was carried out with one equivalent of sodium ethoxide; the addition product, diethyl α-ethoxycarbonyl-β,γ-dimethylglutarate, was hydrolyzed and the resulting acid decarboxylated by heating. The evolved carbon dioxide contained 42 % of the radiocarbon of the original ethyl crotonate. Thus it was demonstrated that the migration of an ethoxycarbonyl group took place in the course of the reaction from the methylmalonate moiety to the carbon atom α to the labelled ethoxycarbonyl group. The mechaism of the reaction is discussed.

The authors are indebted to the Ministry of Education for a Grant-in-Aid for Scientific Research.

Department of Chemistry, Faculty of Science, Tokyo University, Tokyo

10) G. A. Ropp, *J. Am. Chem. Soc.*, **72**, 2299 (1950).
11) R. G. Dutton and C. R. Noller, "Organic Syntheses," **16**, 9 (1936).
12) M. Calvin et al., "Isotopic Carbon", John Wiley & Sons, Inc., New York, 1949, p. 93.
13) D. D. Van Slyke and J. Folch, *J. Biol. Chem.*, **136**, 509 (1940).

An Equation of State in Analytical Form (Continued)

By Tetsuya ISHIKAWA

(Received December 21, 1953)

From the successive studies on this subject[1], the author is convinced that his equation of state is, among the hitherto pubished equations of state, the only one which has applicability to liquids as well as to vapours. As a supplementary example, it is necessary to add a comparison between his equation and Beattie-Bridgeman's equation, the latter having generally been accepted to hold with high accuracy for vapours. Fig. 1 shows a

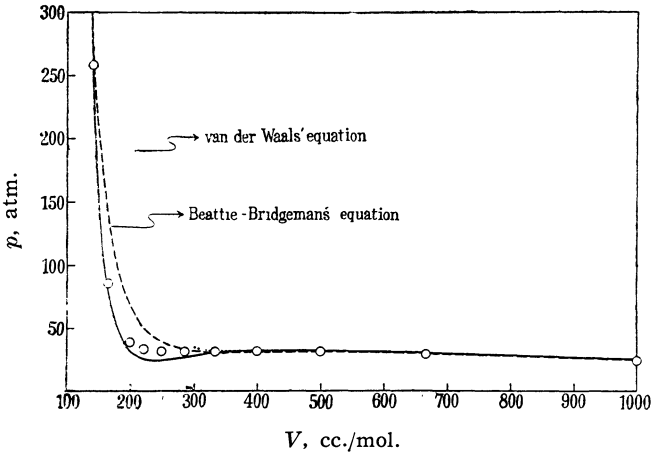


Fig. 1. Critical Isotherm of $C(CH_3)_4$

graphical comparison between these two equations by quoting gaseous neopentane, $C(CH_3)_4$, at the critical isotherm from Beattie, Douslin, and Levine's recent measurements[2] (the author's equation, full line; Beattie-Bridgeman's equation, broken line; observed values, ○). Their calculated values above 3.5 mole/l were not given, and they were computed by use of their determined constants: $A_0=23.3300$, $B_0=0.33560$, $a=0.15174$, $b=0.13358$, $c=400\times10^4$. For the author's curve $(2-\varepsilon)$ the value at the critical isotherm was taken to be 1.922, the mean of the values: 1.913, 1.914, 1.917, 1.920, 1.924, 1.927, 1.928, 1.928, 1.927, and 1.926 at 1.0, 1.5, 2.0, 2.5, 3.0, 3.5, 4.0, 4.5, 5.0 and 6.0 mole/l respectively.

As seen from the figure in which van der Waals' equation is also shown by a dotted line, Beattie-Bridgeman's equation behaves like, but far better than, van der Waals' equation as reported in the latest paper. Similar facts are found for a certain range above the critical temperature and also in the case of normal pentane, whose data are quoted from the measurements of the same investigators[3], hence it appears that Beattie-Bridgeman's equation fails at pressures so high as to correspond to the liquid portion in the neighbourhood of the critical temperature. On the other hand, the author's equation, which is valid even at such high pressures as stated above, displays a signoidal curve (showing a maximum and minimum) still above the critical temperature, the reason being easily understood from its derivation from van der Waals' equation. In fact, such a signoidal curve occurs even at a temperature from a few (e.g. H_2) to a few tens degrees (e.g. CO_2, $C(CH_3)_4$, C_2H_4[4]) above the critical temperature, though its supersaturated vapour portion, including the maximum, nearly coincides with the observed values. The necessity of this discrepancy in analytical meaning will be elucidated hereafter.

Phillips[5] carried out interesting experiments on the viscosity of carbon dioxide under a wide range of pressures both above and below the critical temperature. His observed

1) T. Ishikawa, This Bulletin, **26**, 78, 530 (1953); T. Ishikawa, M. Ikeda, ibid., **26**, 516 (1953).
2) J. A. Beattie, D. R. Douslin, S. W. Levine, *J. Chem. Phys.*, **20**, 1619 (1952).
3) J. A. Beattie, S. W. Levine, D. R. Douslin; *J. Am. Chem. Soc.*, **74**, 4778 (1952).
4) Adopted from "International Critical Tables", III, p. 15.
5) P. Phillips, *Proc. Roy. Soc., London*, A**87**, 48 (1912).

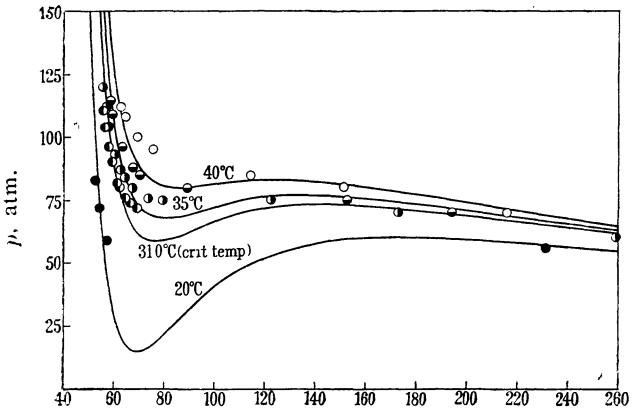


Fig. 2. Isotherms of CO_2

$p-V$ values at and above the critical temperature (denoted by ●, ◐, ◑, ◒, and ○ at 20, 30, 32, 35, and 40°C respectively in Fig. 2) lie fairly close to each isotherm except that which, if vapour and liquid still coexist, corresponds to the superheated liquid portion and the never realizable portion, $(\partial V/\partial p)>0$, of plots of the author's equation (full line), in which $(2-\varepsilon)$ values are computed from the previously obtained linearity, $2-\varepsilon=1.912+0.00028\,(T-T_c)$, except the value, 1.903 at 20°C, which is determined directly from Phillips' data for the reason that the availability of the linearity for vapour state down to a temperature below the critical temperature is at present questionable.

TABLE I

Tests for constancy of H (V-b) and of $H\,V^{2-\varepsilon}$ (H, poise; V, cc./mol.)

20°C			30°C			32°C		
p atm.	H (V-b)	$H\,V^{2-\varepsilon}$ $2-\varepsilon=1.903$	p atm.	H (V-b)	$H\,V^{2-\varepsilon}$ $2-\varepsilon=1.912$	p atm.	H (V-b)	$H\,V^{2-\varepsilon}$ $2-\varepsilon=1.912$
83	0.0171	1.56	110.5	0.0181	1.66	120	0.0188	1.72
72	0.0172	1.54	104	0.0179	1.64	112	0.0183	1.67
59	0.0177	1.55	96	0.0180	1.63	104	0.0181	1.64
			90	0.0172	1.58	93	0.0179	1.60
mean	0.0173	1.55	82	0.0175	1.56	87	0.0182	1.62
			80	0.0172	1.53	84	0.0183	1.62
			76	0.0174	1.52	80	0.0186	1.65
			74	0.0170	1.51	76	0.0187	1.67
			73	0.0170	1.50	75	0.0192	1.74
			72	0.0171	1.52			
						mean	0.0185	1.66
			mean	0.0174	1.57			

35°C			40°C		
p atm.	H (V-b)	$H\,V^{2-\varepsilon}$ $2-\varepsilon=1.913$	p atm.	H (V-b)	$H\,V^{2-\varepsilon}$ $2-\varepsilon=1.915$
114.5	0.0183	1.64	112	0.0177	1.57
109	0.0181	1.63	108	0.0176	1.56
96	0.0184	1.63	100	0.0180	1.59
88	0.0181	1.61	94	0.0181	1.62
85	0.0175	1.56			
			mean	0.0179	1.59
mean	0.0181	1.61			

Total average value of H (V-b), 0.0178 with 2.8% deviation; total average value of $H\,V^{2-\varepsilon}$, 1.60 with 2.7% deviation.

6) A. J. Batschinski, *Z. phys. Chem.*, **84**, 643 (1913).

According to Batschinski's formula[6] for normal liquids, the product of viscosity coefficient η by specific free volume $(v-\omega)$ is independent of temperature, where $M\omega$ (M= molecular weight) is nearly equal to van der Waals' b ($=V_c/3$). His formula can be rewritten as follows: $\eta(V-b)$=a constant independent of temperature where V is the molecular volume. Applying the latter formula to Phillips' viscosity data, we find that the formula holds good at high pressures for the measured temperature even above the critical temperature, and further, a like constancy is also obtained if we assume η to be simply proportional to cohesive pressure, $a/V^{2-\epsilon}$, in the author's equation (see Table 1).

Moreover, between the constant range of $\eta(V-b)$ or $\eta V^{2-\epsilon}$ at each temperature (see Table 1) and its corresponding superheated liquid portion of the author's curve (see Fig. 2) there may exist a parallelism, or in other words, the lowest pressure limit of the former appears to come near the end point (close to the minimum) of the latter.

The above results lead to the conclusion that the occurrence of a superheated liquid portion above the critical temperature is necessary for elucidating the persistence of a liquid molecular state above the critical temperature, which no equation except the author's presents, this phenomenon being also in accord with the recent Swietoslawski and Markowska's observation on the critical region, that density difference between the lower and upper parts of the tube was still noticeable after the disappearance of the meniscus[7].

The author is indebted to Nagasaki American Cultural Center for furnishing him with American journals in which Beattie and his coworkers published their compressibility measurements.

Sasebo Commercial Junior College,
Sasebo, Nagasaki

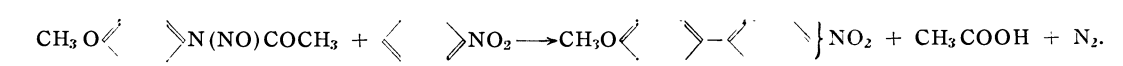
7) W. Swietoslawski, H. Markowska, *Roczniki Chem.*, **26**, 207 (1952); *C.A.* **47**, 10302 (1953).

Influence of Substituent Groups on Nuclear Reactivity in Formation of Substituted Biphenyls through Reactions of Aromatic Diazo and Cognate Compounds with Aromatic Liquids. III. The Substitution of Nitrobenzene by the p-Anisyl Radical

By Osamu SIMAMURA and Toshihiko MIGITA

(Received March 22, 1954)

In a previous paper[1] in this series, it has been shown that the ortho, para and even meta positions of nitrobenzene are activated by the nitro group over the benzene nucleus itself towards the substitutive attack by the phenyl radical produced by the decomposition of N-nitrosoacetanilide or of benzenediazo hydroxide, the order of the reactivities of the three isomeric positions being para> ortho>meta. Augood, Hey and Williams[2] have later reported on the phenylation of nitrobenzene by the decomposition of benzoyl peroxide, the trend of the influence of the nitro group being similar to that found in the above investigation. It seemed of interest to examine how a substituent placed in the phenyl radical alters the nature of the influence of the substituent in an aromatic compound to be attacked by the radical. The present paper deals with the results of experiments on the substitution of nitrobenzene by the *p*-anisyl radical formed by the decomposition of N-nitroso-*p*-acetanisidide, which yields isomeric nitro-4-methoxybiphenyls as follows:



1) O. Simamura, T. Inukai and M. Kanazashi, This Bulletin, **23**, 205 (1950).

2) D. R. Augood, D. H. Hey and G. H. Williams, *J. Chem. Soc.*, **1952**, 2094.

N-Nitroso-*p*-acetanisidide (7.6 g., 0.04 mol.) was decomposed at room temperature in 246 g. (2 mol.) of nitrobenzene giving 0.82 g. of 4-methoxy-4′-nitrobiphenyl, m. p. 110°, and 1.29 g. of 4-methoxy-2′-nitrobiphenyl, m. p. 60° (for the identification of these compounds see the experimental part). When 15 g. (0.077 mol.) of N-nitroso-*p*-acetanisidide was decomposed in a mixture of 288 g. (2.34 mol.) of nitrobenzene and 360 g. (4.62 mol.) of benzene and the reaction mixture worked up as described in the experimental part, 4-methoxybiphenyl, 4-methoxy-4′-nitrobiphenyl and 4-methoxy-2′-nitrobiphenyl were obtained in yields of 2.56 g., 2.38 g. and 3.85 g., respectively, that is, in a millimolar ratio of 13.9 : 10.4 : 16.8. The ratio of the two isomeric methoxynitrobiphenyls formed in the competitive reaction in a mixture of nitrobenzene and benzene was thus found to be in good agreement with that in the reaction in nitrobenzene alone. Any trace of 4-methoxy-3′-nitrobiphenyl could not be detected in the product from this reaction.

On the basis of the molar ratio in which the products were formed and of the amount of the reactants competing for the radical the relative reactivities[1] of the ortho, meta and para nuclear positions of nitrobenzene towards the *p*-anisyl radical are calculated to be 7.24, 0, and 8.95, respectively the reactivity of one nuclear position of benzene itself towards the same radical being taken as unity. These values are compared with the corresponding ones for the reactivity towards the phenyl radical (see Table I); it is noted

TABLE I

RELATIVE REACTIVITIES OF THE ISOMERIC NUCLEAR POSITIONS OF NITROBENZENE.

Source of radical	Relative reactivity			Reference
	o	*m*	*p*	
N-Nitroso-*p*-anisidide	7.24	0	8.95	Present work
Diazotized aniline	6.6	2.8	11	(1)
N-Nitrosoacetanilide	15–5.4	5.8	9.8–30	(1)
Dibenzoyl peroxide	7.0	1.2	7.9	(2)

that the trend is alike in both cases, as far as the ortho and para positions are concerned. The meta position of nitrobenzene is, however, completely unreactive towards the attack by the *p*-anisyl radical whereas it is a little more reactive towards the attack by the phenyl radical than benzene itself. It is generally known that the methoxyl group exerts a polar effect on the para carbon atom, which tends to increase electron density at that atom. On the other hand the polar effect of the nitro group is to decrease electron density at the positions ortho and para to the nitro group below that in the benzene nucleus. Accordingly, it might be expected from a simple electrostatic consideration that the substitution by the *p*-anisyl radical will take place preferentially at the ortho and para positions of nitrobenzene. Further, with an electron-releasing methoxyl group in 4 and an electron-attracting nitro group in 2′ or 4′ position, the biphenyls produced will be more stabilized than otherwise, since such a relative orientation of both groups makes possible their mesomeric conjugation with each other; a resulting gain in extra resonance energy will contribute in lowering the energy of activation for the formation of these isomers. All these considerations point to the preponderant formation of 2- and 4-nitro-4′-methoxybiphenyls. However, as is evident from the comparison of the reactivity values towards the *p*-anisyl with those towards the phenyl radical, the effect due to the co-operation between the *p*-methoxyl group in the attacking radical and the nitro group in the molecule being attacked appears to be very small, if any. In view of both this apparent ineffectiveness of the *p*-methoxyl group in influencing the course of the reaction and the considerable reactivity of the meta position of nitrobenzene towards the phenyl radical, the *p*-anisyl radical is excepted to attack also the meta position of nitrobenzene to an appreciable extent. The reason why 4-methoxy-3′-nitrobiphenyl should actually have not been formed is not clear.

Experimental

Materials N-Nitroso-*p*-acetanisidide was prepared according to Haworth and Hey[3] by the action of nitrous fumes on *p*-acetanisidide in a mixture of acetic acid and acetic anhydride cooled with ice. The resulting dark green solution was poured into a mixture of ice and water with vigorous stirring, and the pale yellow precipitate of N-nitroso-*p*-acetanisidide was collected, washed

3) J. W. Haworth and D. H. Hey, *J. Chem. Soc.*, **1940**, 361.

well with water and dried on a porous plate. Nitrobenzene was purified by distilling commercial nitrobenzene in steam, fractionating through a Vigreux column under reduced pressure, and finally crystallizing the distillate and discarding the liquid portion. Benzene was purified by shaking with concentrated sulfuric acid and then by fractionating through a Vigreux column.

Decomposition of N-Nitroso-*p*-acetanisidide in Nitrobenzene N-Nitrosoacetanisidide (7.6 g., 0.04 mol.) was added to 246 g. (2 mol.) of nitrobenzene at room temperature. The solution turned red in ten minutes and the evolution of nitrogen began, which continued for about one hour. After standing two days, the reaction mixture which had become dark brown was distilled under diminished pressure to remove nitrobenzene. Steam-distillation of the residue (10 g.) at 145° gave 3.2 g. of a distillate, which solidified on standing. This was separated into 0.82 g. of 4-methoxy-4′-nitrobiphneyl, yellow needles, m.p. 110° (from alcohol) (Found: N, 6.18; mol. wt., 231 (Rast). Calculated for $C_{13}H_{11}NO_3$: N, 6.11%; mol. wt., 229.2), and 1.29 g. of 4-methoxy-2′-nitrobiphenyl, yellow prisms, m.p. 60° (from alcohol) (Found: N, 6.31; mol. wt., 235 (Rast). Calc. for $C_{13}H_{11}NO_3$: N, 6.11%; mol. wt., 229.2). The separation was carried out by growing large crystals of the isomers, which could easily be distinguished from each other, from an alcoholic solution and sorting them out. Repeated operations of this procedure gave finally an inseparable mixture, a further separation of which was effected by a chromatography on alumina with a method of fractional elution according to Reichstein and Shoppee.[4]

Identification of Methoxynitrobiphenyls One of the above methoxynitrobiphneyls, m.p. 110°, was identified as 4-methoxy-4′-nitrobiphenyl by oxidizing 0.08 g. of it with 0.4 g. of chromic anhydride in acetic acid on a hot water bath to *p*-nitrobenzoic acid.

The oxidation of another isomer, m.p. 60°, gave no isolable product. A synthetic method was therefore followed. Aqueous sodium hydroxide was added dropwise to a stirred mixture of 100 cc. of anisole and diazotized *o*-nitroaniline (5 g.) in dilute sulfuric acid and the mixture stirred for a further one hour. The anisole layer was separated, the anisole removed under diminished pressure, the residue distilled with superheated steam, giving 0.8 g. of reddish brown distillate, which on distillation in vacuo gave a fraction, b.p. 110° at 5 mm. Hg. When this was dissolved in hot alcohol and the solution let stand, 0.1 g. of yellow crystals was deposited, which on recrystallization from alcohol gave the same compound m.p. 60-61°, as the above methoxynitrobiphenyl, the mixed melting point showing no depression. Of the theoretically possible isomers of methoxy-2-nitrobiphenyls to be produced by this synthesis only 4′-methoxy compound can also be a product from the decomposion of N-nitroso-*p*-acetanisidide in nitrobenzene. Thus, they were identified as 4′-methoxy-2-nitrobiphenyl.

Decomposition of N-Nitroso-*p*-acetanisidide in a Mixture of Benzene and Nitrobenzene N-Nitrosoacetanisidide (1.5 g., 0.077 mol.) was added to a mixture of 360 g. (4.62 mol.) of benzene and 288 g (2.34 mol.) of nitrobenzene. The reaction took place as described for the run in nitrobenzene alone. Benzene and nitrobenzene were removed from the reaction mixture under diminished pressure yielding 32 g. of residue, which gave 4.2 g. of solid (A) and further 10.2 g. of partly solidified distillate (B) on steam-distillation at 120 to 200°. Fraction A gave 4-methoxybiphenyl, m.p. 88°, on recrystallization from alcohol. The solid substance in B was identified with 4-methoxy-4′-nitrobiphenyl. The separation of the two isomers was carried out as before first by sorting out crystals and then by chromatography of the residues from mother liquors of all recrystallizations. Thus the crystalline product isolated were in all 2.56 g. of 4-methoxybiphenyl, 2.38 g. of 4-methoxy-4′-nitrobiphenyl and 3.85 g. of 4-methoxy-2′-nitrobiphenyl. Further, the chromatography yielded 0.70 g. of a brown oil, which could not be crystallized. As it was suspected that the missing isomer, 4-methxy-3′-nitrobiphenyl, might be present in this oil, it was treated with potassium permanganate in pyridine, but no acidic substance was isolated. The action of 0.18 g. of anhydrous aluminium chloride on 0.3 g. of this oil in 100 cc. of nitrobenzene below 120° followed by decomposition with water produced no crystalline compounds. The oily product was dissolved in alkali, heated with 0.3 g. of potassium permanganate, the mixture acidified and extracted with ether. The ethereal solution was shaken with aqueous sodium carbonate, and the aqueous layer gave traces of benzoic and *o*-nitrobenzoic acids on acidification. *m*-Nitrobenzoic acid could not be detected.

Summary

The decomposition of N-nitroso-*p*-acetanisidide in nitrobenzene at room temperature yielded 4-methoxy-4′-nitrobiphenyl and 4-methoxy-2′-nitrobiphenyl in a ratio of 1 : 1.6. From the result of a similar experiment in a mixture of nitrobenzene and benzene, which compete for the *p*-anisyl radical produced

4) T. Reichstein and C. W. Shoppee, *Discussions Faraday Soc.*, No. 7, 305 (1949).

from N-nitroso-*p*-acetanisidide, the relative reactivities of the ortho, meta and para positions of nitrobenzene towards the *p*-anisyl radical are found to be 7.24, 0, and 8.95, respectively, the reactivity of one nuclear position of benzene towards the same radical being taken as unity.

The authors are indebted to the Ministry of Education for a Grant-in-Aid for Scientific Research.

Department of Chemistry,
Faculty of Science,
Tokyo University, Tokyo

Some Observations on the Reactions of α,α'-Dimethylstilbene and Related Compounds

By Osamu SIMAMURA and Hiroshi SUZUKI[1]

(Received February 23, 1954)

F. v. Wessely and H. Welleba[2] reported that α,α'-dimethylstilbene of m. p. 67° was not isomerized to the geometrical isomer by the action of iodine in benzene solution. Therefore in view of the well established fact that thermally or photochemically activated halogen can cause the cis-trans interconversion of various ethylenic compounds, it seemed of interest to study the actions of various agents which are known to be effective in causing the stereoisomerization of the ethylenic compound on the geometrical isomers of α,α'-dimethylstilbene.[3] The present paper gives an account of some observations made during this investigation.

Ramart-Lucas and Salmon-Legagneur[5] heated α,α'-dimethylstilbene with a little concentrated sulfuric acid and found that the isomerization of the trans to the cis isomer took place only to a very limited extent, but that the reverse reaction could not be effected. The re-examination of the action of sulfuric acid (for 20 hours at 210°) revealed that the isomerization, in fact, occurred from either isomer yielding an equilibrium mixture consisting of about 55 % of the trans and 45 % of the cis isomer. The implication of this result has already been discussed[4] in terms of the steric effect of substituents on the stabilization of the molecule due to the conjugation of unsaturated systems.

We repeated Wessely and Welleba's experiment[2] by boiling 0.1 g. of *cis*-dimethylstilbene and 14 mg. of iodine in 5 cc. of benzene for 4.5 hours and recovered the unchanged material, thus confirming their results. H. J. Barber et al.,[6] however, effected the isomerization of *cis*-4,4'-dibromo-α,α'-dimethylstilbene to the trans isomer by boiling in the presence of traces of iodine in nitrobenzene. When trans-α,α'-dimethylstilbene was heated at 210° for 19 hours with a little iodine an oily product was formed, from which 22 % of *meso*-2,3-diphenylbutane[7], m. p. 129-129.5°, was isolated. The cis isomer gave the same result. In none of the experiments carried out was any isomerized product detected. Part of α,α'-dimethylstilbene was apparently hydrogenated at the ethylenic double bond by the action of iodine at the expense of the remainder. No products expected from the dehydrogenation could be isolated. A similar treatment of stilbene with iodine yielded 38 % of bibenzyl.

As evidence has been obtained to show that bromine atoms can isomerize dimethyl-

1) Present address: The College of General Education, Tokyo University.

2) F. v. Wessely and H. Welleba, *Ber.*, **74**, 777 (1941).

3) α,α'-Dimethylstilbene exists in two geometrically isomeric forms, one with m.p. 107° and the other with m.p. 67°: the former was assigned the trans and the latter the cis configuration on the basis of the dielectric constant measurements by Wessely and Welleba[2], but relevant numerical data have never been available. Recently, a confirmation of this assignment has been obtained by one of us[4] from theoretical considerations concerning the ultraviolet absorption spectra of the two isomers; accordingly, in this paper the higher melting isomer will be designated as the trans and the lower melting one as the cis isomer.

4) H. Suzuki, This Bulletin **25**, 145 (1952).

5) Ramart-Lucas and Salmon-Legagneur, *Bull. Soc. Chim. France*, [4] **45**, 718 (1929).

6) H. J. Barber, R. Slack and A. M. Woolman, *J. Chem. Soc.*, **1943**, 99.

7) A small amount of this substance was also obtained as a by-product in the reduction of 3,3-diphenyl-2-butanone with sodium and alcohol to 3,2-diphenyl-2-butanol in the course of an attempted synthesis of dimethylstilbene from acetophenone. W. Thorner and Th. Zincke (*Ber.*, **11**, 1988 (1878)) claimed to have prepared 2,2-diphenylbutane, m.p. 127.5~128.5°, by the action of phosphorus and hydrogen iodide on acetophenone and pointed out the identity of the substance with 2,3-diphenylbutane formed from (1-bromoethyl)benzene by the action of zinc or sodium (Br. Radziszewsky, *Ber.*, **7**, 140 (1874); C. Engler and H. Bethgef, ibid,. **7**, 1125 (1874)). It is highly probable that 2,2-diphenylbutane of Thorner and Zincke is *meso*-2,3-diphenylbutane.

stilbene, as will be described later. it is only because of the steric repulsion exerted by large groups at the ethylenic linkage on an attacking iodine atom which is larger than a bromine atom that iodine is ineffective in causing the isomerization at lower temperatures. On the other hand at higher temperatures, at which the isomerization catalyzed by iodine atoms might take place, the disproportionation of dimethylstilbene by iodine becomes prevailing, so that any isomerization would be completely masked.

According to Barber et al.,[6] *trans*- and *cis*-4,4'-dibromo- α,α'-dimethylstilbenes are different from each other in their behavior towards bromine in chloroform at room temperature; the latter adds bromine to give 2,3-dibromo-2,3-bis-(*p*-bromophenyl)-butane, while the former does not. Further, J. Lévy[8] reported the formation of dibromide, m. p. 150-155°, from dimethylstilbene. The results of the present experiments on the action of bromine are noteworthy. When bromine was added to a carbon tetrachloride solution of *trans*- or *cis*-dimethylstilbene in diffuse room light at night the decolorization occurred and the evolution of hydrogen bromide took place immediately. Thus, one mole of dimethylstilbene consumed ultimately about two moles of bromine, approximately two moles of hydrogen bromide being evolved. Evidently, the substitution by bromine took place rather than the addition to the double bond. The product was, besides traces of α-bromoacetophenone, the same 1,4-dibromo-2,3-dimethyl-2-butene, m. p. 153.5-155°, whether the starting material was the trans or the cis isomer. The structure of this compound, which seems to be identical with that obtained from bromine and 2,3-diphenylbutadiene[9], was established on the basis of analytical data and the result of ozonolysis which gave α-bromoacetophenone. It is probable that Lévy obtained this compound and described it as dimethylstilbene dibromide. The crude product from this reaction, melting at 134-150°, contained some crystals which decomposed with effervescence at about 130°. It is suspected that dimethylstilbene dibromide may have been formed, although it could not be actually isolated. When one mole of bromine was allowed to react with one mole of *trans*-dimethylstilbene in carbon tetrachloride in the dark, about 42% of the dimethylstilbene was converted to a crystalline mixture, melting at about 130° to 150°, the bromine content of which corresponded approximately to the calculated value for 1,4-dibromo-2,3-diphenyl-2-butene, and about 27% was recovered as a crystalline mixture, melting at 50° to 77°, consisting of *cis*- and *trans*-dimethylstilbenes. When a similar experiment was carried out in a quartz flask in direct sunlight, there was a vigorous evolution of hydrogen bromide, giving a complex mixture of products from which 1,4-dibromo-2,3-diphenyl-2-butene (6%) and a small amount of α-bromoacetophenone (as 2,4-dinitrophenylhydrazone) were isolated.

The observation that the cis-trans isomerization of dimethylstilbene took place and that the intervention of oxygen occurred as revealed by the formation of α-bromoacetophenone suggests that the action of bromine on dimethylstilbene involves bromine atoms and, consequently, radicals at some stage of the reaction, because it is well established that bromine atoms induce the cis-trans isomerization of ethylenic compounds, and that the addition of bromine to a double bond can take place through a radical mechanism involving bromine atoms.[10] A bromine atom adds to one carbon atom of the central double bond of dimethylstilbene forming a radical intermediate which contains a single bond between the α,α' carbon atoms. The radical can then react in three ways: (1) cis-trans isomerization by the rotation of the groups round the single bond between the α,α' carbons followed by the expulsion of the bromine atom to regenerate a double bond between the α,α' carbons; (2) reaction with a bromine molecule to give dimethylstilbene dibromide and another bromine atom; and (3) reaction with oxygen to give an oxygenated radical which decomposes in a manner generally postulated for peroxides[11] with the fission of the bond between α,α' carbons producing eventually a molecule of acetophenone which is then brominated to α-bromoacetophenone. The mechanism of the formation of 1,4-dibromo-2,3-diphenyl-2-butene is not clear. There are two possibilities. One involves dimethylstilbene dibromide and 2,3-diphenylbutadiene as intermediates. Inspection of a model of the former constructed with Taylor-Hirschfelder atom models shows that there is considerable steric strain due to the crowding of the bulky substituent groups. Accordingly dimethylstilbene dibromide may be so unstable a substance as to decompose readily. If any decomposition takes place at a low temperature during the present reaction to yield

8) J. Lévy, *Bull. Soc. Chim. France*, [4] **29**, 878 (1921).
9) C. F. H. Allen, C. G. Eliot and A. Bell, *Can. J. Research*, **17B**, 75 (1939); *C. A.*, **33**, 6284 (1939).
10) O. Simamura, This Bulletin, **17**, 274 (1942).
11) J. E. Leffler, *Chem. Rev.*, **45**, 385(1949); C. E. Frank, ibid., **46**, 155 (1950).

hydrogen bromide and 2,3-diphenylbutadiene, then the latter would give dibromodiphenylbutene through the 1,4-addition with bromine. It is possible that oxygen may intervene at the stage where 2,3-diphenylbutadiene adds bromine, the latter attaching itself to the terminal carbon and oxygen to the α carbon atom, and the subsequent decomposition yielding α-bromoacetophenone. The other mechanism involves the substitution by bromine at the methyl group through a radical chain mechanism; a bromine atom abstracts a hydrogen atom from a methyl group of dimethylstilbene, producing a radical stabilized by a mesomeric structure, which in turn gives, by reacting with a molecule of bromine, 1-bromodiphenylbutene and a bromine atom. That 1-bromodiphenylbutene could not be isolated from the reaction mixture might suggest either that it is substituted by bromine at the remaining methyl group to give dibromodimethylstilbene much more rapidly than dimethylstilbene is substituted to give the monobromo derivative or that the bromine atom is unable to attack the methyl group as postulated above.

The action of bromine on dimethylstilbene leading to the facile substitution at the methyl group rather than the addition at the double bond seemed to be attributable to the steric effect in the molecule caused by the crowding of bulky groups; consequently, in order further to ascertain the effect of substituents in the α,α' positions on the bromination of stilbenes the following experiments were conducted. To a solution of 0.33 millimole of an α,α'-disubstituted stilbene in 5 cc. of carbon tetrachloride was added 0.16 millimole of bromine in carbon tetrachloride (about 0.17 cc.) in diffuse light, and the time required for decolorization was compared. In Table I where the results are summarized, the figures in the column headed I denote the time which had elapsed before the red color of the reaction mixture just matched that of a standard bromine solution in carbon tetrachloride, which was approximately 6 millimolar in bromine; the figures in columns II and III denote the time when the reacting solution was faintly pale yellow and completely colorless, respectively. The number of plus signs in the fifth column indicate the approximate intensity of the evolution of hydrogen bromide visually observed. The values in the last column were determined by separate experiments.

TABLE I

ACTION OF BROMINE ON VARIOUS STILBENES

	Consumption of bromine (time in min.)			Evolution of HBr	Approximate number of moles of bromine reacted
	I	II	III		
Stilbene	2-3 (hrs.)	—	—	0	1
trans-α-Methylstilbene	1-2	—	—	++	1
trans-α,α'-Dimethylstilbene	6	10	13	++++	2
cis-α,α'-Dimethylstilbene	7-9	35–45	—	+++	2
α-Methyl-α'-ethylstilbene	30	50	65	++	2
trans-α,α'-Diethylstilbene	40	60	—	+	2
cis-α,α'-Diethylstilbene	60	115	—	+	2
Methyltriphenylethylene	2-2.5 (hrs.)	—	—	+	1

Of the compounds shown in Table I stilbene and methylstilbene add bromine to the double bond, the former more slowly than the latter; this is probably due to the retarding action of atmospheric oxygen. Methylstilbene appears to react faster because a little hydrogen bromide formed by the substitution accelerates the addition of bromine by producing, in co-operation with oxygen, bromine atoms which start the chain addition reaction of bromine[10].

Methyltriphenylethylene did not add bromine, but was substituted at the methyl group only slowly in spite of the evolution of hydrogen bromide; the absence of the addition is probably due to the steric hindrance caused by the large substituents as in the case of tetraphenylethylene which also adds no bromine. The slowness of the substitution is also attributable to the steric hindrance which prevents the double bond from producing bromine atoms from hydrogen bromide and oxygen.

Experimental

Materials Dimethylstilbene was prepared according to Ott[12] by dehydration and rearrangement of 100 g. of 3, 3-diphenyl-2-butanol, b. p. 172-3° at 14 mm., n_D^{21} 1.5822 (synthesized by the method of Lévy[8]), by boiling with 13 g. of concentrated sulfuric acid in 400 g. of glacial acetic acid for 20 hours. Recrystallization of the crude product from petroleum ether yielded 34 g. of the trans

12) E. Ott, *Ber.*, **61**, 2135 (1928).

isomer, m. p. 107°. The purification of the cis isomer proved to be difficult. The best method was to grow large crystals and to pick out hexagonal plates in which the cis isomer had crystallized. Repeated recrystallization from petroleum ether gave 10 g. of the cis isomer, m. p. 67–67.3°.

α-Methylstilbene was prepared according to Hell[13] and Ley.[14] Dehydration of 43 g. of 1, 2-diphenyl-2-propanol by doiling with 80 g. of acetic anhydride and 40 g. of acetyl chloride gave an oil containing crystals. The crystals were filtered, and recrystallization from petroleum ether gave 20 g. of *trans*-α-methylstilbene, m. p. 83–83.5° The oily product was fractionally distilled in vacuo to yield 4 g. of an oil, b. p. 151–155° at 14 mm., which consisted mainly of *cis*-α-methylstilbene as revealed by the ultraviolet absorption spectrum.[4]

α-Methyl-α′-ethylstilbene was prepared by the method of Lévy.[8] The isomer which crystallized, m. p. 47–8°, was found to be the trans form by means of the ultraviolet absorption spectrum. The cis isomer could not be freed from contamination with a considerable amount of the trans isomer, as revealed by ultraviolet spectrum,[4] and formed an oily specimen.

α, α′-Diethylstilbene was prepared similarly to the synthesis of the dimethyl analogue. α, α-Diphenylbutyraldehyde, b. p. 185–190° at 18 mm. and ethylmagnesium iodide in ether gave 4, 4-diphenyl-3-hexanol, b. p. 185° at 14 mm., which, boiled with a little concentrated sulfuric acid in glacial acetic acid, yielded an oily mixture of the cis and trans forms, b. p. 166° at 12 mm. On cooling, the oil deposited crystalline trans isomer, which melted at 77–78° after repeated crystallizations from petroleum ether. The mother liquor was further fractionated and gave an oil, b. p. 177–8° at 22 mm., which was shown to consist mainly of *cis*-α, α′-diethylstilbene by measurement of the ultraviolet absorption spectrum.[4]

Methyltriphenylethylene was prepared according to Meisenheimer[15] by the action of phenylmagnesium bromide on 2, 2-diphenylpropanal, b. p. 170° at 15 mm., followed by dehydration and rearrangement of the resulting carbinol with concentrated sulfuric acid. The product melted at 88–9°, b. p. 210° at 14 mm.

Isomerization by Sulfuric Acid *cis*- or *trans*-Dimethylstilbene (about 0.8 g.) was heated for 20 hours at 210° with a few pieces of biscuit chips impregnated with concentrated sulfuric acid in a sealed tube. It was cooled, the crystals were pressed on a porous plate to remove some adhering oily matter, and the isomeric composition of the product was determined by comparing its fusing behavior with that of a standard sample of known composition. The isomerization occurred from either isomer giving an equilibrium mixture consisting of about 55% of the trans and 45% of the cis isomer. No isomerization took place at 100° for 20 hours, and only a slight isomerization in the absence of sulfuric acid at 210° for 20 hours.

13) C. Hell, ibid.. **37**, 453 (1904).
14) H. Ley, ibid., **50**, 243 (1917).
15) J. Meisenheimer, *Ann.*, **456**, 126 (1927).

Action of Iodine A sealed tube containing 1.45 g. of *trans*-dimethylstilbene and 0.03 g. of iodine was heated for 19 hours in boiling nitrobenzene. The reaction mixture, taken up in ether (with active charcoal), filtered, and the ether removed from the filtrate, gave an oil, from which 0.315 g. of *meso*-2, 3-diphenylbutane, m. p. 129.0–129.5°, crystallized, the melting point being not depressed on admixture with an authentic specimen prepared by hydrogenating *cis*-dimethylstilbene with one mole of hydrogen in the presence of palladium-barium sulfate in ether. An experiment with the cis isomer gave the same result. Similarly stilbene gave 38% of bibenzyl, m. p. 48–51°, identified by the mixed melting point with an authentic specimen.

Action of Bromine Bromine (14.5 millimoles) was added to 1.503 g. of *trans*-dimethylstilbene in 15 cc. of carbon tetrachloride. After decolorization the carbon tetrachloride was removed in vacuo at room temperature and 2.496 g. of a crystalline compound, m. p. 134–150°, was obtained. Repeated crystallizations from carbon tetrachloride gave 0.974 g. of 1, 4-dibromo-2, 3-diphenyl-2-butene, needles, m. p. 153.5–155° (Found: Br, 43.6. Calcd. for $C_{16}H_{14}Br_2$: Br, 43.72%). This substance (0.42 g.),on ozonization in 50 cc. of chloroform followed by decomposition with water, gave 0.41 g. of α-bromoacetophenone. It was observed under a microscope that the crude product melting at 134–150° contained some crystals which decomposed with effervescence at about 130°. It may be suspected that dimethylstilbene dibromide was also formed. In some experiments carried out similarly to those above, the crude product was washed with a little alcohol and the alcoholic solution deposited, on addition of 2, 4-dinitrophenylhydrazine solution, a very small amount of α-bromoacetophenone 2,4-dinitrophenylhydrazone,m. p.220°.

The action of bromine on *cis*-dimethylstilbene gave similar results. *trans*-Dimethylstilbene (0.375 g., 1.8 millimoles) in carbon tetrachloride, added in the dark with 1.8 millimoles of bromine in the same solvent (1:20), and the solvent removed in vacuo, gave a crystalline mass, which was extracted with petroleum ether. The insoluble residue, melting at 130 to 150°, weighed 0.23 g. (Found: Br, 42.4, Calcd. for $C_{16}H_{14}Br_2$: Br, 43.72%), which on repeated crystallizations from carbon tetrachloride gave 0.138 g. of 1, 4-dibromo-2, 3-diphenyl-2-butene. Evaporations of the petroleum extract gave about 0.1 g. of a crystalline mixture, m. p. 50–77°, consisting of *cis*- and *trans*-dimethylstilbenes.

trans-α-Methylstilbene consumed about 1 mole of bromine with evolution of hydrogen bromide and gave 1, 2-dibromo-1, 2-diphenylpropane, m. p. 126–7°, as isolable compound.

Methyltriphenylethylene reacted with bromine in carbon tetrachloride only slowly in the dark, but, very rapidly in sunlight, about 1 mole of bromine being taken up with the evolution of hydrogen bromide in accordance with the observation of Meisenheimer[15]. The only product isolated was 3-bromo-1, 1, 2-triphenylpropene, m. p. 121° (from petroleum ether).

cis-Diethylstilbene (2.668 g.) in 30 cc. of carbon tetrachloride reacted with nearly 2 moles of bromine in the course of a few days in the dark, hydrogen bromide being evolved. The removal of the solvent gave viscous matter and 0.78 g. of 2,5-dibromo-3,4-diphenyl-3-hexene, m. p. 156–8° (from carbon tetrachloride).

Summary

cis- and *trans*-α,α'-Dimethylstilbene, heated with a little sulfuric acid at 210°, were isomerized to an equilibrium mixture consisting of 55% of the trans and 45% of the cis isomers. Heated with iodine at 210°, they yielded *meso*-2,3-diphenylbutane. The action of bromine produced 1,4-dibromo-2,3-diphenyl-2-butene; under certain experimental conditions the concurrent cis-trans isomerization was observed. This fact, together with the isolation of a small smount of α-bromoacetophenone as a by-product, supports the view that the reaction proceeds by a mechanism involving bromine atoms. The action of bromine on some α,α'-disubstituted stilbenes was examined. The reactions observed were discussed in terms of the steric effect exerted by the bulky groups at the ethylenic linkage.

The authors' thanks are due to the Ministry of Education for a Grant-in-Aid for Scientific Research.

Department of Chemistry,
Faculty of Science,
Tokyo University, Tokyo

The Action of Hydrogen Bromide and Oxygen on α,α'-Dimethylstilbene and Related Compounds

By Hiroshi SUZUKI[1], Osamu SIMAMURA, and (in part) Toshiko ICHIHASHI

(Received March 22, 1954)

A combined action of hydrogen bromide and oxygen on ethylenic compounds induces remarkable reactions involving free radicals:[2-5] to mention a few examples which have some bearing on the subject treated in this paper, the action of hydrogen bromide on isostilbene in the presence of oxygen causes the isomerization[3,4] to stilbene, and, if a larger amount of oxygen is present, the formation of stilbene dibromide takes place[2a,4]; and the joint action of hydrogen bromide and oxygen on various ethylenic compounds causes copious liberation of bromine with those compounds which add bromine to the double bond only to a limited extent, as tetraethyl α,γ-dicarboxy-α-bromoglutaconate, and with some of those which will not do so at all, such as dimethyl dimethylfumarate.[5] These reactions are completely inhibited by a small amount of catechol. The action of hydrogen bromide and oxygen on some α, α'-disubstituted stilbene has now been investigated with special reference to the dimethyl derivative, on reactions of which some observations have been reported in a previous paper.[6]

The passage of hydrogen bromide alone (without special measures to exclude air from the apparatus) or of a mixture with oxygen through a solution of *trans*-dimethylstilbene in carbon tetrachloride in the dark at room temperature caused no reaction whatever; but, on the contrary, *cis*-dimethylstilbene, similarly treated with hydrogen bromide, isomerized partly to the trans isomer, crystals melting at 54 to 71° being recovered, and in the presence of a large amount of oxygen, it underwent a profound change giving acetophenone (9 to 20%), α-bromoacetophenone (20 to 28%) and 1,4-dibromo-2,3-diphenyl-2-butene (3 to 4%) (for a typical run see the experimental part, Expt. No. 14). These reactions were completely inhibited by catechol (37 mol.% of dimethylstilbene) added to a reaction mixture beforehand. Thus, the combined action of hydrogen bromide and oxygen caused the same type of reaction with *cis*-dimethylstilbene as observed with stilbene and other ethylenic compounds. A further point of interest is that the ethylenic bond of *cis*-dimethylstilbene was cleaved so easily

1) Present address: The College of General Education, Tokyo University.

2) (a) Y. Urushibara and O. Simamura, This Bulletin, **14**, 323 (1939).
(b) O. Simamura, ibid., **17**, 274, 326 (1942).
(c) O. Simamura and M. Takahashi, ibid., **22**, 60 (1948).

3) Y. Urushibara and O. Simamura, ibid., **12**, 507 (1937).

4) Idem, ibid., **13**, 566 (1938).

5) O. Simamura, ibid., **15**, 292 (1940).

6) O. Simamura and H. Suzuki, ibid., **27**, 231(1954).

at room temperature to give ketones. It was temporarily considered that the remarkable difference in behavior towards hydrogen bromide and oxygen between the cis and trans isomers of dimethylstilbene might be due to some difference in the electronic state of the central double bond arising from a difference in the extent of its conjugation with the two phenyl groups which are twisted out of a coplanar configuration owing to inevitable steric requirements.[7] It soon became evident, however, that the findings had been spurious. It was found that a specimen of *cis*-dimethylstilbene purified by filtering a petroleum ether solution through a chromatographic column of alumina was no more subject to the action of hydrogen bromide and oxygen than the trans isomer. The specimen which reacted with this gas mixture showed no apparent difference from that purified by the chromatographic method, as far as the melting point and the ultraviolet absorption spectrum were concerned, but the former, on standing in a bright diffuse light of summer days, decomposed slightly and the product, when treated with ferrous ammonium sulfate and aqueous ammonium thiocyanate, developed a red color revealing the presence of a peroxidic substance. It was therefore concluded that the *cis*-dimethylstilbene had retained tenaciously, through a series of purification by repeated crystallizations, traces of peroxidic impurities or those impurities which readily yielded peroxides on autoxidation. With the trans isomer, which is less soluble and crystallizes very well, the impurities must have been easily removed by mere recrystallization. Such traces of impurities undoutedly induced the autoxidative decomposition of dimethylstilbene in air producing peroxidic molecules or very reactive intermediates of a free radical nature and thus catalyzed the reaction with hydrogen bromide and oxygen. It was indeed demonstrated by separate experiments that traces of a peroxide can in fact catalyze the combined attack by hydrogen bromide and oxygen on dimethylstilbene. Thus, in the presence of traces of bonzoyl peroxide the passage of hydrogen bromide through a solution of *trans*-dimethylstilbene in carbon tetrachloride in the dark produced a mixture of the cis and trans forms (Expt. No. 55): if oxygen was passed simultaneously, the cleavage of the double bond occurred yielding the same products (Expt. No. 27) as in the case of the impure *cis*-dimethylstilbene. Similarly, traces of the impure specimen could catalyze the reaction of *trans*-dimethylstilbene. Catechol inhibited these peroxide catalyzed reactions, a fact which is in accord with the view that reactions resulting from the action of hydrogen bromide and oxygen on the ethylenic compounds involves a radical mechanism.

An agent which initiates these reactions is obviously a bromine atom produced from benzoyl peroxide and hydrogen bromide. It adds to one carbon atom of the central double bond of dimethylstilbene forming a radical intermediate which contains a single bond between the α, α' carbon atoms. The radical can then react in the following ways. The first is the cis-trans isomerization by rotation of the groups round the single bond between the α, α' carbons followed by expulsion of the bromine atom to regenerate a double bond between the α,α' carbons. The second is a reaction with oxygen to give an oxygenated radical, which, immediately or after the formation of a hydroperoxide by abstracting a hydrogen atom from hydrogen bromide and leaving a bromine atom, decomposes in a manner generally postulated for peroxides[8] to give eventually acetophenone and fragments of radical nature. The latter are assumed to react with hydrogen bromide producing bromine atoms. Bromine atoms produced in the several ways just mentioned can again attack the double bond of dimethylstilbene continuing the chain process or combine with one another to give bromine molecules. Thus, the formation of brominated compounds such as 1,4-dibromo-2, 3-diphenyl-2-butene and bromoacetophenone is readily understood as discussed in the previous report. The inhibitive action of catechol consists in the annihilation of chain carrying bromine atoms.

Ordinary ethylenic compounds are liable to the combined action of hydrogen bromide and oxygen leading to a complicated reaction, because in their presence bromine atoms can be formed from hydrogen bromide and oxygen, thus initiating chains carried by bromine atoms. Both *cis*- and *trans*-dimethylstilbenes undergo no such reaction in the absence of a catalyst, because they are unable by themselves to produce bromine atoms from hydrogen bromide and oxygen. This is probably attributable to the steric effect of the two phenyl and the two methyl groups, which hinder the approach of hydrogen bromide and oxygen to the double bond. On the other hand, once bromine atoms have been produced from hydrogen bromide and a peroxidic initiator, they are active enough, in spite of the steric repulsion, to attack the double bond of

7) H. Suzuki, This Bulletin, **25**, 145 (1952).

8) For a leading reference see J. E. Leffler, *Chem. Rev.*, **45**, 385 (1949) and C. E. Frank, ibid., **46**, 155 (1950).

dimethylstilbene, as has previously been demonstrated,[6] producing radicals which then give the isomerized product or further react with oxygen and hydrogen bromide resulting in the oxidative cleavage of the double bond.

What is of interest in connection with these observations is that, when traces of bromine was added to a solution of *trans*-dimethylstilbene through which hydrogen bromide was being passed, the cis-trans isomerization occurred, and similarly, when a mixture of hydrogen bromide and oxygen was passed in the presence of bromine, the cleavage of the double bond took place (Expt. No. 33). The action of bromine on dimethylstilbene gives 1, 4-dibromo-2, 3-diphenyl-2-butene.[5] When oxygen was passed through a reaction mixture while bromine was being added, the yield of the dibromo-compound decreased and the formation of ketones resulting from the oxidative cleavage of the double bond was observed (Expt. No. 20). That these ketones were not formed from the 1,4-dibromo-2,3-diphenyl-2-butene by the action of oxygen and the hydrogen bromide primarily produced from bromine and dimethylstilbene was demonstrated by a separate experiment, in which the dibromo-compound was recovered unchanged when subjected to the action of oxygen and hydrogen bromide, even in the presence of benzoyl peroxide or of bromine. These observations are readily explained on the basis of the radical nature of the action of bromine on dimethylstilbene as has been pointed out in the previous report.[6] Thus, some radicals formed in the course of the reaction between bromine and dimethylstilbene release the combined attack by hydrogen bromide and oxygen.

The action of hydrogen bromide and oxygen on some other α,α'-disubstituted stilbenes was also examined. *trans*-Diethylstilbene reacted with a mixture of hydrogen bromide and oxygen only in the presence of bromine or of benzoyl peroxide, producing the same type of cleavage of the central double bond as in the case of the dimethyl analogue (Expt. No. 97). The cis isomer was cleaved without added catalyst; the material used boiled at 177–8° at 22 mm. Hg, and probably contained some peroxidic impurities as no special measures of purification had been taken in the preparation. 1,1,2-Triphenylpropene did not react with hydrogen bromide and oxygen even in the presence of bromine or of benzoyl peroxide. The action of hydrogen bromide and oxygen on *trans*-α-methylstilbene gave 1,2-dibromo-1,2-diphenylpropane, corresponding to stilbene dibromide from stilbene, along with benzoic acid and α-bromoacetophenone (Expt. No. 69). The results of these experiments substantiate the view put forth above, that some molecule with a double bond sterically hindered to such an extent that it can not by itself initiate the chains involving bromine atoms is able to react with bromine atoms and propagate the chains. Further, the absence of reaction with 1,4-dibromo-2,3-diphenyl-2-butene and 1,1,2-triphenylpropene demonstrates that the steric hindrance is so great in these molecules that they are not only incapable of such initiation, but unsusceptible even to the action of bromine atoms or, if a bromine atom adds to the double bond, unable to propagate the chains efficiently.

Experimental

The stilbenes used in this study were prepared as reported previously.[6] Hydrogen bromide was generated by dropping dried bromine on hot tetralin, passed through a bottle of cooled tetralin and a tube filled with glass wool and anthracene and then dried by passage over phosphorus pentoxide.

Typical experiments which have been referred to in the discussion are described in the following. All reactions were carried out in the dark below room temperature (0 to 10°).

Expt. No. 14 *cis*-Dimethylstilbene (0.140 g.) was dissolved in 10 cc. of carbon tetrachloride and hydrogen bromide was passed for 45 minutes into the solution. The solvent was removed under diminished pressure, the oily residue containing a small amount of crystals was treated with alcohol to dissolve the oil; the crystals were collected on a filter and identified with 1,4-dibromo-2,3-diphenyl-2-butene, m.p. 147-152° (yield 10 mg.), which was not depressed on admixture with the specimen prepared from bromine and dimethylstilbene. The alcoholic extract, on treatment with 2,4-dinitrophenylhydrazine deposited 0.18 g. of yellowish brown precipitate (Found: Br, 16.25. Calcd. for $C_{14}H_{11}BrN_4O_4$: Br, 21.11%). This was separated into two components, 2,4-dinitrophenylhydrazones of acetephenone and α-bromoacetophenone, m.p. 250° and 220°, respectively, by fractional crystallization from alcohol. On the basis of the bromine content of the original mixture, the amounts of the ketones produced were estimated at 0.0735 g. of bromoacetophenone and 0.016 g. of acetophenone.

Expt. No. 20 A solution of bromine in carbon tetrachloride (1 : 20) was added gradually to 0.199 g. of *trans*-dimethylstilbene in 10 cc. of carbon tetrachloride simultaneously with the introduction of oxygen. The reaction mixture, worked up as Expt. No. 14, gave 97 mg. of 1,4-dibromo-2,4-diphenyl-2-butene and 0.22 g. of 2,4-dinitrophenylhydrazone of ketones.

Expt. No. 27 The action of hydrogen bromide and oxygen on 0.226 g. of *trans*-dimethylstilbene and 11 mg. of benzoyl peroxide in 10 cc. of carbon tetrachloride for one hour, worked up as above, yielded 12 mg. of 1,4-dibromo-2,3-diphenyl-2-butene

and ketones (0.282 g. of 2,4-dinitrophenylhydrazones).

Expt. No. 33 A mixture of hydrogen bromide and oxygen was passed into 0.13 g. *trans*-dimethylstilbene in 10 cc. of carbon tetrachloride and a few drops of carbon tetrachloride solution of bromine (1 : 20) was added through a fine capillary tube; the passage of the gas mixture was continued for a further forty-five minutes and the solution was worked up as above to give 5 mg. of 1,4-dibromo-2,3-diphenyl-2-butene and ketones (0.202 g, of 2,4-dinitrophenylhydrazone).

Expt. No. 55 Hydrogen bromide was passed through a solution of 0.102 g. of *trans*-dimethylstilbene, m.p. 107°, and 4 mg. of benzoyl peroxide in 10 cc. of carbon tetrachloride for one hour; the removal of the solvent gave a mixture of the cis and trans isomers melting over a range of 72° to 102°.

Expt. No. 69 A mixture of hydrogen bromide and oxygen was passed for one hour into a solution of 0.267 g. of α-methylstilbene, m.p. 83-83.5°, in 10 cc. of carbon tetrachloride. The mixture was shaken with dilute aqueous sodium carbonate and the aqueons layer deposited benzoic acid on acidification with sulfuric acid (the total yield of the benzoic acid, 18 mg.). The dried carbon tetrachloride solution, concentrated under diminished pressure, gave 0.134 g. of α-methylstilbene dibromide, m.p. 127°, and an oily matter which gave 0.132 g. of 2,4-dinitrophenylhydrazone, m.p. 205-216°, probably of impure α-bromoacetophenone.

Expt. No. 97 A mixture of hydrogen bromide and oxygen was passed into a solution of 0.107 g. of *trans*-α,α′-diethylstilbene, m.p. 77-8°, and 4 mg. of benzoyl peroxide in 10 cc. of carbon tetrachloride for one hour; the mixture was worked up as above to give 0.012 g. of 2,5-dibromo-3.4-diphenyl-3-hexene, m.p. 155-7°, and ketones (0.046 g. of 2,4-dinitrophenylhydrazone). A catalytic action of bromine was demonstrated by an experiment similar to Expt. No. 33.

Summary

The action of hydrogen bromide on *cis*- or *trans*-α,α′-dimethylstilbene in the presence of a peroxidic substance or of bromine in carbon tetrachloride in the dark below room temperature caused a partial isomerization to the respective geometrical isomers. The reaction was inhibited by catechol. When oxygen was allowed to react simultaneously under otherwise the same experimental conditions, the cleavage of the central double bond took place yielding acetophenone and α-bromoacetophenone along with 1,4-dibromo-2,3-diphenyl-2-butene. Similar experiments with α-methylstilbene and α,α′-diethylstilbene were conducted. The action of oxygen and bromine on α,α′-dimethylstilbene caused the same oxidative cleavage of the double bond as with hydrogen bromide and oxygen. It was pointed out that an ethylenic compound which is sterically hindered to such an extent that it is unreactive towards molecular reagents can be reactive enough towards radical reagents.

The authors' thanks are due to the Ministry of Education for a Grant-in-Aid for Scientific Research.

Department of Chemistry,
Faculty of Science,
Tokyo University, Tokyo

The Effect of Conversion on the Mechanism of Vinyl Polymerization. II. Methyl Methacrylate

By Saburo FUJII

(Received March 18, 1954)

In the first paper of this series[1] the author described the application of the photochemical method to the study of vinyl polymerization at various conversions and reported the results on styrene not containing any initiator or chain-transfer substance at room temperatures. It was noted there that the course of polymerization was accompanied by the strong rate acceleration, an extreme increase in kinetic chain lifetime and considerable decrease in apparent activation energy and in the reaction order of chain termination. Those kinds of kinetic behaviour could be explained by the supposition that, with increasing conversion of the system, the mutual termination of polystyrene radicals becomes diffusion-controlled or prevented by the shielding effect of the polymer network.

The author has now applied the same method to methyl methacrylate in an attempt to compare it with the above results on styrene[1]

1) S. Fujii, This Bulletin **27**, 216 (1954).

and with those found by several authors[2,3,4,5,6a] for the polymerization of methyl methacrylate in the later stages. This paper reports and discusses the results obtained under the analogous conditions as described in the first paper.[1]

Experimental

Commercial methyl methacrylate was purified by successive washing with dilute sulphuric acid, dilute sodium hydroxide and distilled water, and was dried with calcium chloride over a day. Then it was distilled three times through a fractionating column of 1 meter long at 105 mm. pressure, and the fraction boiling at 45.1°C. was collected and stored in an evacuated flask in the dark. This product was allowed to polymerize to about 10% at 100°C. under the irradiation of ultra-violet light longer than 3300 Å., and then the residual monomer was redistilled with dry ice into a dilatometer used for rate measurements. This operation was carried out in an all glass system evacuated to 10^{-3} mm. pressure. All of the above treatments were necessary to obtain the pure monomer completely free from impurity which may sensitize or retard the polymerization. Unless otherwise noticed, neither photosensitizer nor thermal initiator was added to the reaction system.

The experimental apparatus and procedure were essentially those described in the first paper.[1] The filteration of light from the mercury lamp and the maximum intensity of 3660 Å. light at the front of the reaction cell (4×10^{-8} Einsteins/sec.) were the same as those in the previous experiment.[1] The photo-polymerization was mainly caused by the light of 3660Å., at which wave-length the absorption by the monomer is very little (the molecular extinction coefficient is of the order of 10^{-3})[7] so that the concentration of the radicals within the cell must be uniform. The free radical initiation by the light-excited polymer must be negligible, for the polymer shows no absorption band in the neighborhood of 3660 Å.[8] The rates of photo-and thermal-polymerizations were followed dilatometrically and computed by the use of Matheson's data[6a] on the densities of the monomer and the polymer in monomer. In the same manner as described in ref. (1), all the rate measurements were corrected for the thermal reaction taking place in the unilluminated appendages to the cell. The kinetic chain lifetimes at low conversions (of the order of seconds) were measured with a rotating sector, while those at high conversions were estimated from the photochemical after-effects, which were easily observed dilatometrically. After the experiments at low conversions, the reaction system was polymerized to a desirable conversion under the intense irradiation of 3660 Å. light, left alone at room temperature over half a day, and then the experiments at high conversions were carried out.

The main different feature from styrene was the fact that the polymerization of methyl methacrylate by the same light intensity is much faster (about seven times) than that of styrene in spite of the smaller extinction coefficient. To avoid the undesirable temperature elevation and change of conversion in the reaction system, therefore, the rates of photo-polymerization at high conversions were reduced with calibrated screens. The stationary light rates at high conversions were measured after the long period of preliminary illumination.

Results

The polymerization rates and the reaction order of chain termination—The stationary rates of photo-polymerization at three different temperatures were measured at low conversions under the full intensity (4×10^{-8} Einsteins/sec.) of light from the lamp and at high conversions under the intensities reduced with calibrated screens. Table I shows the data obtained on light rate V_{pL}, thermal rate V_d, and the apparent activation energy, E_{app}, of polymerization.

TABLE I

RATES OF PHOTO- AND THERMAL-POLYMERIZATIONS AND OVER-ALL ACTIVATION ENERGIES FOR METHYL METHACRYLATE

Transmission of screen, %	Conversion %	30°C.	40°C.	50°C.	E_{app} kcal./mol.
	(a) Light rate (unit; 10^{-6} mol./l./sec.)				
100	0~1	7.94	11.0	14.1	5.6
27.4	27±1	32.9	41.9	53.4	4.7
12.0	52±2	43.1	54.6	65.8	4.1
	(b) Thermal rate (unit; 10^{-6} mol./l./sec.)				
	0~1	0.29	0.48	0.81	10.1
	27±1	1.58	2.57	3.94	8.9
	52±2	3.49	5.63	8.32	8.5

2) G. V. Schulz and F. Blaschke, *Z. physik. Chemie*, B50, 305 (1941).
3) Trommsdorff, "Coloquium on High Polymers," Freiburg, 1944.
4) G. V. Schulz and G. Harborth, *Die Makromolekulare Chemie*, **1**, 106 (1947).
5) M. H. Mackay and H. W. Melville, *Trans. Faraday Soc.*, **45**, 323 (1949).
6) (a) M. S. Matheson, E. E. Auer, E. B. Bevilacqua and E. J. Hart, *J. Am. Chem. Soc.*, **71**, 497 (1949); (b) ibid., **73**, 1700 (1951); (c) ibid., **73**, 5395 (1951).
7) T. G. Majury and H. W. Melville, *Proc. Roy. Soc. London*, **A205**, 496 (1951).
8) The absorption band of the system shifts to the shorter wave length in the disappearance of vinyl double bond.

This table as a whole shows that the indicated values were reproducible within the error of 10% or less. Also a measurement of light rate in a complete run to 60% conversion was carried out in the same reaction cell at 30°C. under the constant intensity of illumination and the result is shown diagrammatically in Fig. 1. At the same time the reaction order of chain termination, n, i. e., the reciprocal of the intensity exponent of the stationary light rate, was determined in one run in the same reaction cell at several conversions and the results are given in Table II.

TABLE II
THE REACTION ORDER OF CHAIN TERMINATION, n

Conversion %	n
0~1	1.9~2.1
45±2	1.8~1.9
60±2	1.6~1.8

It is concluded from the above tables and figure that the strong rate acceleration after about 10% conversion is accompanied with some decreases in E_{app} ane n. This kinetic behavior is analogous to that of styrene.[1]

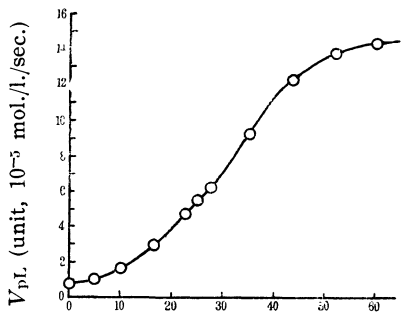


Fig. 1. The rate of photo-polymerization at 30°C. as a function of conversion.

Photochemical after-effect and kinetic chain lifetime—In the measurement of light rates, the reaction showed no detectable induction period in the initial stages, while the prolonged initial- and after-effects were clearly observed in the later stages. Since the rates were followed with a dilatometer, the temperature change of the system in the beginning of illumination and after the interruption of light caused some volume change on the system and more or less disturbed the detection of pure chemical initial- and after-effects. However the ratio of the volume change caused by this undesirable temperature change to the total one by the after-effect became very small at high conversions, so that the allowance for this temperature change was neglected, as the first approximation, in the present discussion of these effects. In a similar manner described in the previous paper,[1] it was confirmed that these effects resulted from an extreme increase in kinetic chain lifetime but not from the decomposition of any unstable substance produced during the previous illumination. A few examples of the observed after-effects are illustrated in Fig. 2, where the relative rate after the interruption of illumination is represented as a function of time.

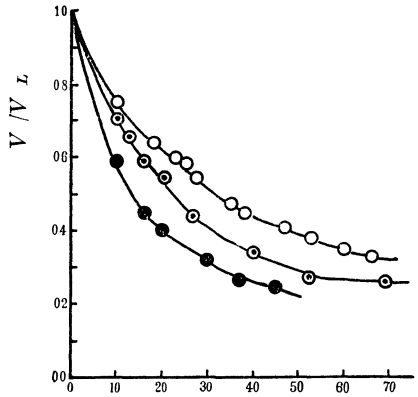


Fig. 2. Photochemical after-effects.

Experimental point	⊙	●	○
Conversion	47 %	52 %	72 %
Temperature	30°C.	50°C.	30°C.
V_{pL}(10^{-5}mol./l./sec.)	4.03	6.58	5.17
V_d/V_{pL}	0.08	0.13	0.18

With several assumptions previously justified[1] and under the case of $n=2$, the mathematical analysis of the photochemical after-effect results in the equation,

$$log\left(\frac{V_p+V_d}{V_p-V_d}\right)=log\left(\frac{V_{pL}+V_d}{V_{pL}-V_d}\right)+\frac{2\,V_d}{2.303\,V_{pL}}\times\frac{t}{\tau_s}, \quad (1)$$

and slso the accepted polymerization mechanism leads to the equation,

$$\frac{{}_sV_{pL}}{[M]}=k_p/k_t \quad \cdots\cdots\cdots\cdots (2)$$

Here V_p is the rate at the time, t, after the interruption of illumination, k_p and k_t the propagation and termination rate constants of growing radicals respectively $[M]$ the monomer concentration and τ_s the average lifetime of kinetic chains at the light rate of V_{pL}, but not the one of each growing radical. Plotting the value of the left hand side of Eq. (1) against the time will lead to a straight

line and then the τ_s value can be estimated from the slope of this line. The k_p/k_t value can be estimated from Eq. (2).

Although the deviation of n from 2 was observed at high conversions as shown in Table II, it may be admitted in the present qualitative discussion that the τ_s and k_p/k_t values at high conversions are estimated, as the first approximation was, by the use of these equations. On the basis of the above, the analytical representations of the observed after-effects are illustrated in Fig. 3, and the τ_s and k_p/k_t values obtained are summarized in Table III.

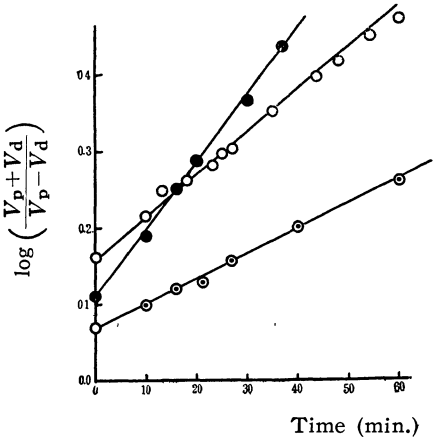


Fig. 3. Analytical representations for the observed after-effects; the experimental conditions for the indicated points are the same as those in Fig. 2.

On the other hand the kinetic chain lifetimes at low conversions were of the order of 10 seconds at the V_{pL} values indicated in Table I, and consequently these were measured with a rotating sector. A typical run in the sector experiments is indicated in Fig. 4, and the initial values of τ_s and k_p/k_t are also summarized in Table III.

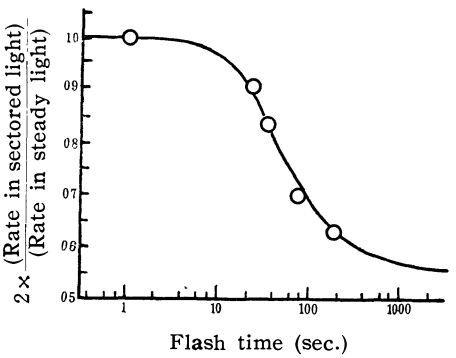


Fig. 4. Rates of polymerization of methyl methacrylate in intermittent light for different times of flash: curve, theory for dark rate 3% of steady light rate; ○, experimental point at 40°C. and steady light rate $=1.06\times10^{-5}$ mol./l./sec.

As noted previously[1,3a] the propagation step in free radical polymerizations has been admitted to be only slightly dependent upon conversion as compared with the termination step, so that the relative decrease in k_t with increasing conversion may be estimated from the k_p/k_t values shown in Table III under the assumption of constant k_p. The evaluated result is indicated in the last column of Table III, and such decrease in k_t is analogous to that previously reported on styrene.

TABLE III

KINETIC CHAIN LIFETIMES AND RATE CONSTANT RATIO IN METHYL METHACRYLATE

Conversion x %	Temp. °C.	V_{pL} mol./l./sec.	τ_s sec.	Av. τ_s at $V_{pL}=10^{-5}$	k_p/k_t	k_{tx}/k_{t0}[b]
0∼1	30	3.52×10^{-5}	1.85	[a] 7.43		
		6.83×10^{-5}	1.22			
	30	7.95×10^{-6}	21.7	17.9	1.93×10^{-5}	1
		1.08×10^{-5}	17.2			
	40	1.10×10^{-5}	20.3	22.7	2.47×10^{-5}	
		1.60×10^{-5}	14.5			
47±2	30	4.03×10^{-5}	1260	5080	9.20×10^{-3}	2.10×10^{-3}
52±2	30	4.31×10^{-5}	1098	4730	9.33×10^{-3}	2.07×10^{-3}
	40	5.46×10^{-5}	882	4810	9.48×10^{-3}	
	50	6.58×10^{-5}	762	5010	9.86×10^{-3}	
72±3	30	5.17×10^{-5}	1800	9310	2.96×10^{-2}	6.52×10^{-4}

(a) α-Azo-bisisobutyronitrile sensitizer was used in this experiment; no sensitizer in the others.

(b) The ratio of k_t at x % conversion to its initial value was estimated at 30°C.

Discussion

With the several assumptions previously described,[1] the accepted mechanism of photopolymerization leads to the equation,

$$V_{pL} = (q\varepsilon l I_0)^{1/n}\left(k_p/k_t^{1/n}\right)[M]^{1+1/n} \quad (3)$$

and also, if the thermal initiation of kinetic chains is assumed to be proportional to $[M]^2$,[9] the rate of thermal polymerization may be represented as

$$V_d = k_p\left(\frac{k_t}{k_i}\right)^{1/n}[M]^{1+1/n} \quad (4)$$

Here q is the quantum efficiency of the production of kinetic chains, ε the molecular extinction coefficient of the monomer, l the depth of the reaction cell, I_0 the intensity of illumination and k_i the rate constant of thermal initiation by the monomer. Using these equations and the data in Table III, the rate ratio at 52% conversion to the initial value at 30°C. can be estimated[10] as about 11.8 for V_{pL} and about 8.7 for V_d, while the corresponding experimental ratios are about 17.3 for V_{pL} from Fig. 1 and about 12.0 for V_d from Table I. If the k_{tx}/k_{to} value at 52% conversion is estimated to be half of that indicated in Table III,[11] the differences between the above theoretical and experimental ratios in the rate accelerations may be almost eliminated. Therefore it may be concluded that the observed rate accelerations are attributed to the extreme decrease in k_t. This conclusion has already been suggested by Trommsdorff[4] and several other authors,[2,4,5] who found the catalytic- and photo-polymerizations of several vinyl monomers to be strongly accelerated after certain conversions, and has also been confirmed by Matheson and his co-workers[6a] with the measurement of kinetic chain lifetimes in the biacetyl photosensitized-polymerization of methyl methacrylate at about 33% conversion. Following the data of the latter authors the value of k_{tx}/k_{to} at 33% conversion is in the range $4.6\sim6.6\times10^{-3}$ at 30°C., while the present work shows about 2×10^{-3} in the neighborhood of 50% at the same temperature. Allowing for the different conversions, one may accept the fact that both the results coincide with each other.

As noted previously on styrene,[1] the observed decreases in k_t and E_{app} with increasing conversion can be explained by the fact that the mutual termination of polymer radicals becomes predominantly diffusion-controlled in the later stages. Using Matheson's datum (2.8 kcal./mole)[6a] for the activation energy of chain termination, E_t, in the initial stages, the observed decrease in E_{app} (=the increase in $1/2\,E_t$) gives about 5.8 kcal./mole[12] for the E_t value at 52% conversion, i.e., the activation energy of the diffusion of polymethyl methacrylate radicals in the reaction system. The E_t values of polystyrene radicals at 38 and 60% conversions have been reported by the present author as about 7 and 9 kcal./mole respectively,[1] and these values are almost in agreement with those estimated from the viscosity equation of Spencer and Williams.[13] Flory[14] reported about 8 kcal./mole as the activation energy of the viscosity for several fused polyesters. Cowley and Melville[15] studied the photo-degradation of polymethyl methacrylate with the rotating sector technique and reported about 20 kcal./mole as the E_t value of the polymer radicals in the fused polymer. Comparing this with the author's data on styrene and Flory's data on polyesters the present value (5.8 kcal.) may be adequate, while the value (20 kcal.) of Cowley and Melville is beyond the accepted order of magnitude for the self-diffusion of polymer in the fused phase.

Some decrease in n observed over about 50% conversion seems to show that, together with the mutual termination of polymer radicals, the self-termination also takes place at very high conversions. Such self-termination may be supposed to be caused by the strong shielding action of a polymer network on the active ends of growing radicals. This suggested mechanism has been discussed in the first paper of this series[1] and supported by Bamford and Jenkins,[16] who studied the photopolymerization of acrylonitrile and found

9) P. J. Flory, *J. Am. Chem. Soc.*, **59**, 241 (1937).

10) In this calculation $n=1.8$ was used and q assumed to be constant.

11) It can be accepted under the present experimental accuracy to reduce the ratio in kt by a factor of 2.

12) Such increase in Et with increasing conversion is also detected from the temperature dependence of kp/kt. The data of k_p/kt at 52% conversion in Table 3 lead to give about 0.5 kcal./mole as the value of $(E_p\text{-}Et)$, where E_p is the activation energy of propagation. Using Matheson's datum (E_p=6.3 kcal./mole)[6a] the Et value at 52% conversion is estimated as about 5.8 kcal./mole, the value of which in good agreement with that estimated from the temperature dependence of V_pL or Vd at the same conversion.

13) Spencer and Williams, *J. Colloid Sci.*, **2**, 117 (1947).

14) P. J. Flory, *J. Am. Chem. Soc.*, **62**, 1057 (1940).

15) P. R. E. J. Cowley and H. W. Melville, *Proc. Roy. Soc. London*, **A210**, 461 (1952); ibid., **A211**, 320 (1952); In the latter reference the kt value in the fused polymer at 167°C. was reported as 4×10^4 l./mol./sec. While Matheson reported 1.22×10^7 at 30°C. and 1.87×10^7 at 60°C. as the kt value at low conversion. Using Cowley's value (20 kcal.) of Et in the fused polymer and Matheson's value (2.8 kcal.(of Et in the initial stages, the kt_x/kt_0 value at 100% conversion is estimated as about 1.2×10^{-8} at 167°C. and about 4×10^{-8} at 30°C.

16) C. H. Bamford and A. D. Jenkins, *Proc. Ror. Soc. London*, **A216**, 515 (1953).

that the photo-polymer precipitated near room temperatures occluded the active ends of polymer radicals. Recently the present author has found that the effects of conversion on V_{pL}, V_d, k_t and n are extremely reduced by the addition of chain-transfer substance, such as *n*-butylmercaptan, to the polymerization system.[17] This result seems to throw a powerful datum on the verification of the above mechanism.

Summary

The usual photochemical method and the rotating sector technique have been used to study the effect of conversion on the termination mechanism in the polymerization of methyl methacrylate. The strong rate acceleration, the extreme increase in kinetic chain lifetime and some decreases in the overall activation energy and the reaction order of chain termination have been detected with increasing conversion of the reaction system. These results are in good agreement with those reported on styrene in the first paper of this series and with the available data on this polymerization. These results have been discussed under several assumptions and confirmed to be due to a large change in the termination mechanism, i. e., from the activation-controlled termination of polymer radicals in the initial stages to the predominant diffusion-controlled termination in the later stages.

The author wishes to express his hearty thanks to Dr. Shoji Shida of this Institute for his helpful advice and encouragement during the course of this work.

Laboratory of Physical Chemistry,
Tokyo Institute of Technology,
Ookayama Meguro-ku, Tokyo

17) Unpublished

LETTER

The Structures and Lower Electronic States of Cyclobutadiene

By Shoji SHIDA

(Received March 22, 1954)

Since the earliest times of the development of quantum chemistry, cyclobutadiene has been frequently studied from the theoretical standpoint together with benzene. The molecule is of special interest because of its peculiarities in many respects when compared with benzene. On its molecular structure Coulson[1] and Craig[2,3]* have supposed that the molecule, if it exists, should not be square as usually assumed but may be rectangular in form. Until now no quantitative work has been done about this problem or as to how the lower electronic states, especially the ground state, change their location in the energy level schema on varying the structure.

The present author has calculated the energy levels of all configurations arising from four π-molecular orbitals, assuming five different structures varying from the square (I) to the rectangle (V) having the normal

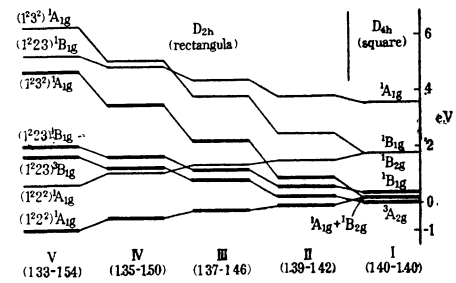


Fig. 1. The shifts of lower electronic states of cyclobutadiene with the changes of molecular dimensions.

Fine and thick stripes indicate the configuration energies computed by the ordinary ASMO method and by the method of atoms in molecules respectively. The $^3A_{2g}$ level in the square form (I) is taken as the reference state in both computations. (1.33–1.54), for instance, represents the short and long bond lengths in Å.

single and double bond lengths. The standard ASMO method without configuration

1) C. A. Coulson, private communication to the present author; C. A. Coulson and W. Moffitt, *Phil. Mag.*, **40**, 1 (1947).
2) D. P. Craig, *Proc. Roy. Soc.*, **A 202**, 498 (1950).
3) D. P. Craig, *J. Chem. Soc.*, **1951**, 3175.
* And also the earlier work of J. E. Lennard-Jones and J. Turkevich, *Proc. Roy. Soc.*, **A 158**, 297 (1937).

interaction has been used at first. Next, to the results thus obtained has been added Moffitt's correction by the method of atoms in molecules.[4] Then the two sets of results have been compared. In the figure are shown the term values for only the lower energy states which are of primary importance for the present purpose. When comparing the ground state of (I) with that of (V) as obtained by the ASMO method, one might infer that the former would be more stable than the latter. On the other hand, according to the second treatment which seems to be more reliable, the lowest singlet level referred to the lowest triplet level is lowered throughout the five structures by 1.61 e. V. and the ground state of (V) is located about 0.9 e. V. below that of (I). The effect of configuration interaction has been known to be small, in general, in the method of atoms in molecules. To cite an example, in (I) the splitting (not shown in the figure) of degenerate $^1A_{1g}$ into $^1B_{1g}$ and $^1B_{2g}$ is only 0.3 e. V.[4,5] according to the method of atoms in molecules, whereas in the ordinary ASMO method it amounts to 3.5 e. V.[2] In the above, σ-bonds have been excluded from consideration; if these are taken into account the square form will still be unstable, because the energy gained in the modification process (V to I) of the σ-framework is relatively small (at most 3 kcal.). Now, it may safely be concluded that cyclobutadiene will not be stable in a square form and that, if it exists, it will take a rectangular form.

Tokyo Institute of Technology,
Ookayama, Meguro-ku, Tokyo

The Crystal Structure of $Cs_3Fe_2Cl_9$ *and of* $Cs_3Sb_2Cl_9$

By Hideo YAMATERA and Kazumi NAKATSU

(Received February 19, 1954)

A successful attempt has been made to obtain a new double chloride of cesium and ferric iron, which was expected to be isomorphous with $Cs_3Sb_2Cl_9$, and this compound as well as $Cs_3Sb_2Cl_9$ has been found to have the $Cs_3As_2Cl_9$ type of structure.

The double chloride $Cs_3Fe_2Cl_9$ was prepared by mixing solutions of cesium chloride and ferric chloride both in concentrated hydrochloric acid. The crystal of this compound was found under the microscope to be shaped like hexagonal plates and brownish orange in color, the larger crystals looking dark red to the naked eye. Under the polarizing microscope the crystal was found to be uniaxial. The crystal is stable if kept dry, but on exposure to moist air it is readily converted into the known double chloride $Cs_2FeCl_5 \cdot H_20$ Accordingly, the accurate determination of density of this compound was not successful, but it was confirmed that this compound has a density higher than that of bromoform, 2. 9.

It is known that the three arrangements $A_3B_2X_9$ are those typified by $Cs_3As_2Cl_9$,[1] $Cs_3Tl_2Cl_9$[2] and $Cs_3W_2Cl_9$[3]. Powder photographs of these three compounds as well as those of $Cs_3Fe_2Cl_9$ and $Cs_3Sb_2Cl_9$ were prepared, Cu K_α radiation ($\lambda = 1.542$Å) being used except in the case of $Cs_3Fe_2Cl_9$ in which Fe K_α radiation ($\lambda = 1.937$Å) was used. In order to avoid decomposition by atmospheric moisture during the preparation of the photograph, $Cs_3Fe_2Cl_9$ crystals were ground under the mother liquor, sealed together with the liquor in a thinwalled capillary of borosilicate glass of diameter 0. 5mm., and then immersed in an X-ray beam. The similarity of $Cs_3Fe_2Cl_9$ and $Cs_3Sb_2Cl_9$ in the diffraction pattern suggested that the structure of these compounds belongs to the same type.

The cell dimensions derived are:

	a	c
$Cs_3Fe_2Cl_9$	7. 28±0. 05Å	8. 90±0. 05Å
$Cs_3Sb_2Cl_9$	7. 61±0. 05Å	9. 32±0. 05Å

The calculated densities are 3. 37 and 3. 41 respectively, with one formula unit per unit cell in each case. The observed intensities of reflection of $Cs_3Fe_2Cl_9$ and $Cs_3Sb_2Cl_9$ are well accounted for by means of the space group $D_{3d}^3 - P\bar{3}m1$, if the atomic positions are assumed as follows:

1Cs(1)	in	1(a) : 000	
2Cs(2)	in	2(d) : 1/3 2/3 z, with $z = 0.333$	etc.
2Fe(or Sb)	in	2(d) : 1/3 2/3 z, with $z = -0.167$	etc.
3Cl(1)	in	3(e) : 1/2 0 0,	etc.
6Cl(2)	in	6(i) : xxz, with $x = 0.167$, $z = -0.333$	etc.

As was shown by Hoard and Goldstein[1] in their study on the structure of $Cs_3As_2Cl_9$, a slight distortion from the ideal structure adopted here would cause no essential change in the calculated intensities, but improve the agreement between the observed and calculated values a little.

Institute of Polytechnics, Osaka City University

1) J. L. Hoard and L. Goldstein, *J. Chem. Phys.*, **3**, 117 (1935).

2) J. L. Hoard and L. Goldstein, *J. Chem. Ph* , **3**, 199 (1935). H. M. Powell and A. F. Wells, *J. Chem. Soc.*, **1935**, 1008.

3) C. Brosset, *Nature*, **135**, 874 (1935).

4) W. Moffitt and J. Scanlan, *Proc. Roy. Soc.*, **A220**, 530 (1953).

5) M. Wolfsberg, *J. Chem. Phys.*, **21**, 943 (1953).

Molar Volume of Polystyrene in Solution

By Gisuke MESHITSUKA and Yoshiki MATSUI

(Received May 14, 1954)

Introduction

Osmotic pressure measurements have been made on fractions of polystyrene in toluene, benzene and methylethylketone at 20°C, and the maximum molar volume b_{max} of solute have been calculated by the relation (1), which has already been reported by us[1],

$$A_2=\frac{b_{max}}{M^2} \qquad (1)$$

where A_2 represents the second virial coefficient of osmotic pressure, M the molecular weight, and b_{max} is the volume occupied by the solute molecule at its highest degree of expansion.

Many attempts have been made to deduce the relation between the degree of expansion and the molecular weight of chain molecules in dilute solutions. For example Flory[2] has shown that special interferences between distantly connected segments of a chain lead to the relation

$$R \propto M^{\alpha}, \qquad (2)$$

where R is the average radius of the expansion of chain molecules in dilute solution, and the parameter α changes between 0.5 and 0.6 with varying solvent-polymer systems.

We have examined the relation between b_{max} and M, and obtained values of α for polystyrene in toluene, benzene and methylethylketone at 20°C.

Experimental

Preparation of Polymer Samples.—Styrene monomer was sealed in tubes in atmosphere. The tubes were placed in a thermostat at 120°C for nine and a half hrs. The contents were taken up in benzene and then monomer and benzene were removed from the mixtures by the method of vacuum sublimation.

The polystyrene was separated into 19 fractions by fractional precipitation, vaporizing benzene and butanol mixture solution[3]. These fractions were reprecipitated with CH_3OH from benzene solutions and finally dried by vacuum sublimation of benzene from benzene solutions frozen by dry ice.

Measurement of Osmotic Pressure.—Osmotic pressure measurements were made in Zimm and Meyerson type osmometers, kept in a thermostat regulated to 20.000±0.003°C. Denitrated collodion was used as membranes. A static method of measurement was employed. Equilibrium was attained in about 10 hrs. The values of the osmotic pressure were accepted only when it remained constant for 12 hrs.

Results and Discussion

The osmotic pressure measurements were made on six fractions in toluene, and three fractions in both benzene and methylethylketone. Some of the plots of π/c against c are shown in Fig. 1. The unit of concentration is g.×cm^{-3} and that of pressure is g.×cm^{-2}, and hence π/c is in cm.

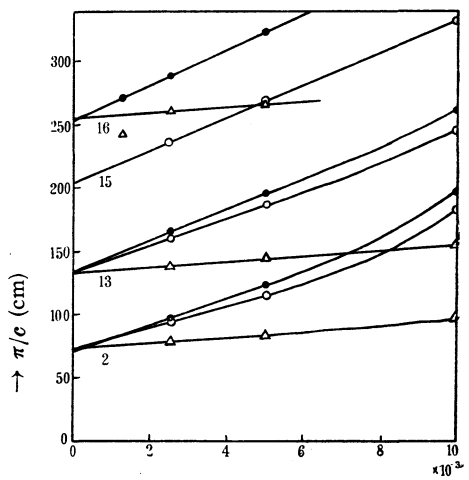


Fig. 1. Variation of π/c with c for polystyrene at 20°C; ○ toluene, ● benzene, △ methylethylketone.

Extrapolation to $c=0$ was made by free-hand drawing, and the molecular weight M was calculated from the intercept, and the second virial coefficient A_2 from the initial slope of the curve. The b_{max} was calculated by the relation (1) using the values of M and A_2. These results are summarized in Table I.

1) G. Meshitsuka, This Bulletin, **25**, 309 (1952).
2) P. J. Flory, *J. Chem. Phys.*, **17**, 303 (1949).
3) T. Titani, G. Meshitsuka, and Y. Matsui, *Chem. High Polym., Japan*, **10**, 175 (1953).

TABLE I
THE MOLECULAR WEIGHTS M, THE SECOND VIRIAL COEFFICIENTS A_2 AND THE MAXIMUM MOLAR VOLUMES b_{max}

Fraction No.	$M \times 10^{-4}$	$A_2 \times 10^4$ (cc/g²)			$b_{max} \times 10^{-4}$ (l/mole)		
		Toluene	Benzene	Methyl-ethyl-ketone	Toluene	Benzene	Methyl-ethyl-ketone
2	33.6	3.25	4.25	0.80	3.7	5.4	0.93
5	27.2	3.95	—	—	2.9	—	—
11	21.8	4.28	—	—	2.0	—	—
13	18.7	4.28	5.02	0.94	1.5	1.8	0.33
15	12.2	4.98	—	—	0.74	—	—
16	9.8	—	5.62	1.07	—	0.54	0.10
17	6.0	6.02	—	—	0.22	—	—

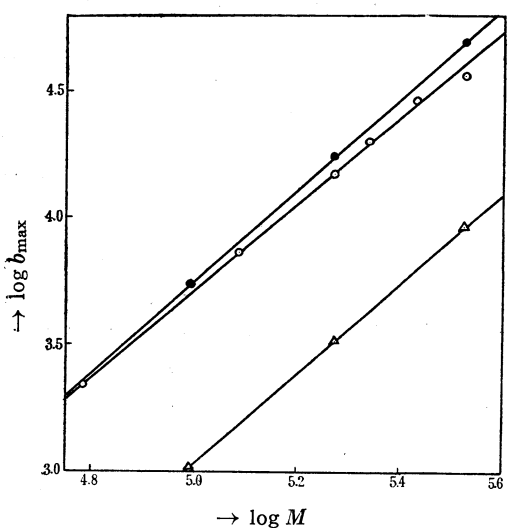


Fig. 2. Variation of log b_{max} with log M for polystyrene at 20°C; ○ toluene, ● benzene, △ methylethylketone.

Assuming the molecules to be sphere, b_{max} must be expressed as

$$b_{max}=4/3\pi\ R^3 \qquad (3)$$

Inserting the equation (2), it follows that

$$b_{max}=KM^{3\alpha}, \qquad (4)$$

or

$$\log b_{max}=\log K+3\alpha\log M, \qquad (5)$$

where K is a constant.

Fig. 2 is the plots of log b_{max} against log M for our results on the polystyrene in toluene, benzene and methylethylketone, which shows straight lines. The values of K and α determined are shown in Table II.

TABLE II
K AND α FOR POLYSTYRENE

Solvent	$K \times 10^5$	α
Toluene	1.46	0.57
Benzene	0.69	0.60
Methylethyl-ketone	0.17	0.59

The author wishes to express his sincere thanks to prof. T. Titani for his kind guidance and encouragement in the course of this study, and also to prof. K. Hirota for his earnest interest in this work.

Chemical Institute, Faculty of Science, University of Osaka

*On the Molecular Rotations of Polypeptides of Alanine**

By Hideo MURAKAMI

(Received May 18, 1953)

Introduction

Abderhalden and Gohdes observed the specific rotations $[\alpha]_D$ for a series of polypeptides of *l*-alanine.[1] Levene and Yang also observed them for a series of *d*-alanine, and obtained almost equal data concerning their absolute values.[2]

* This work was reported at the meeting for general discussion of protein structure held on May 20, 1951, in Osaka, under the auspices of the Chemical Society of Japan.

1) E. Abderhalden and W. Gohdes, *Ber.*, **64**, 2070 (1931).
2) P. A. Levene and P. S. Yang, *J. Biol. Chem.*, **99**, 405 (1932).

As was pointed out by Kauzmann and Eyring, the molecular rotation per one alanine residue $[M]_D/n$ (n is the number of residues) increases remarkably as the polypeptide chain becomes longer. This fact indicates that the neighbouring alanine residues are not optically independent and there will be some interactions. Kauzmann and Eyring gave an interesting suggestion for this point based on their consideration for the optical rotations of sugar.[3] Firstly, they noticed that the molecular rotations of ring compounds such as arabinose, xylose, mannose, galactose, glucose, etc. are relatively great (30°~260°) compared with those of corresponding alcohols (less than 10°). They interpreted these differences between ring and chain compounds by considering the statistical free rotation (restricted rotation) around a single bond. That is, in case of open chain compounds, the above-mentioned statistical free rotation is allowed, and the first order effect of optical rotation is almost entirely diminished. On the other hand, in the case of ring compounds, the rotation around the single bond is prevented on account of their rigid structures and the first-order effect of optical rotation can contribute considerably. Taking these facts into account, they suggested that the molecules of polypeptides of alanine may also form a ring involving hydrogen bond or some other type of bond. Based on this suggestion, we try to explain theoretically the observed rotations in Table I by assuming the probable model for the configuration of polypeptide.

TABLE I
OBSERVED VALUES OF SPECIFIC AND MOLECULAR ROTATION

Polypeptides	$[\alpha]_D$ in 2 N HCl		$[M]_D$	$[M]_D/n$ n is the number of residues
	Abderhalden	Levene	Levene	
alanine	+ 14.5°	− 14.5°	− 13°	−13°
alanyl-alanine	− 37.6°	+ 36.5°	+ 58°	+29°
di-alanyl-alanine	− 77.3°	+ 77.5°	+179°	+60°
tri-alanyl-alanine	−115°	+115°	+347°	+87°
tetra-alanyl-alanine	−133°	+132.5°	+494°	+99°

I. Molecular Model

Ring Strncture of Polypeptide Chain In order to calculate the molecular rotation theoretically, it is necessary that the detailed structure of the molecule is known. Conversely, if the calculated results for a probable model agree well with experimental results, the assumed model becomes more reliable.

The configurations of the polypeptide chain in protein have been studied extensively, and the numerous probable models for them have been presented by many authors.[4-9] These models are mostly based on the experimental data for crystal, fiber or film of highly polymerized large polypeptide molecules whether they be natural or synthetic.

At present, however, we are researching the configurations of small polypeptide molecules in dilute water solution, so the situations are considerably different from the above-described ones. Moreover, our model must be rigid enough and correspond to the ring structure which was demanded by Kauzmann and Eyring. Therefore, it is required that not only the known bond lengths and bond angles are satisfied approximately, but also many hydrogen bonds are formed to construct the rings. Further, it can be expected that the rigidity of the ring becomes greater as the ring becomes smaller, so long as the geometrical conditions for the stability of hydrogen bonds and internal rotations are satisfied.

Considering these conditions, we picked out (2_7 a) the model of Huggins and (2_7 b) the model of Shimanouchi and Mizushima as the most probable ones. In these models, sevenmembered rings are formed by hydrogen bonds, and concerning internal rotation, the stable configurations of the polypeptide chain are kept. At the present stage, however, the application of these models should be limited to the configurations of the relatively short polypeptide chain in solution. For the configurations of highly polymerized polypeptide chain in protein, some other factors should be taken into account, and their complete determination is a task for future study.

Equilibrium between Isomers Since the above-mentioned models have been presented for the folded α-type keratin, we denote the models (2_7 a) and (2_7 b) as $\alpha_{(1)}$ and $\alpha_{(2)}$ respectively. The only difference between $\alpha_{(1)}$ and $\alpha_{(2)}$ is the relative internal orientation between the side chain and the main chain, that is, in the case of $\alpha_{(1)}$, its orientation exists in G (Gaush) form, and in the case of

3) W. Kauzmann and H. Eyring, *J. Chem, Phys.*, 9. 41 (1941).
4) M. L. Huggins, *Chem. Rev.*, **32**, 195 (1943).
5) T. Shimanouchi and S. Mizushima, *Kagaku*, **17**, 24, 52 (1947), *Kagaku-no-Ryoiki (Journal of Japanese Chemistry)* **6**, 311 (1952), S. Mizushima, T. Shimanouchi, M. Tsuboi, T. Sugita and E. Kato. *Nature*, **164**, 918 (1949).
6) E. J. Ambrose and A. Elliott, *Proc. Roy. Soc.*, **A 205**, 47 (1951).
7) W. T. Astbury, *Nature*, **164**, 439 (1949).
8) L. Bragg, J. C. Kendrew and M. F. Perutz, *Proc. Roy Soc.*, **A 203**, 321 (1950).
9) L. Pauling and R. B. Corey, *Proc. Nat. Acad. Sci.*, **37**, 205, 241 (1951).

$\alpha_{(2)}$, exists in T (Trans) form. Other situations are equal exactly, so $\alpha_{(1)}$ and $\alpha_{(2)}$ can be said to be rotational isomers. If the energy difference between these isomers is small enough, it becomes necessary to consider the equilibrium between them in solution. According to previous experiences, T form is slightly stabler than G form except in special cases. This relation predicts that the equilibrium is shifted towards $\alpha_{(2)}$.

In the case of the polypeptide chain, however, we must take into account not only the above-mentioned interaction between the side chain and the main chain, but also the interaction between the side chain and the C=O group. In $\alpha_{(1)}$, the relative orientation between the side chain and the C=O group comes half way between G and T forms, and in $\alpha_{(2)}$, it exists in C (Cis) form. That is, C=O group takes C form with hydrogen atom on α-carbon atom in the case of $\alpha_{(1)}$, and with side chain (methyl group) in the case of $\alpha_{(2)}$. Consequently, the repulsive energy due to steric hindrance becomes greater in $\alpha_{(2)}$ than in $\alpha_{(1)}$, and $\alpha_{(2)}$ is unstabilized by this amount. Thus this repulsive energy tends to cancel the stabilization energy due to T-type configuration between the side chain and the main chain in $\alpha_{(2)}$. Though one cannot give any conclusion as to whether this cancellation is complete or not, one can expect that the energy difference between $\alpha_{(1)}$ and $\alpha_{(2)}$ is small enough.

In the following calculations, we assume as the idealized limiting case that $\alpha_{(1)}$ and $\alpha_{(2)}$ have the same stability and exist in solution with equal statistical weight. By this assumption, any unknown quantity concerning the equilibrium constant is excluded. Moreover, the main chain of polypeptide comes to have an effective plane of symmetry in the statistical meaning. Consequently, the calculations are exceedingly simplified. Later, some conclusion will be given for a case where the equilibrium is shifted towards $\alpha_{(2)}$ by the analysis of the results of calculation.

Next, we should consider the equilibrium between folded α-type configuration and that of the extended β-type or intermediate ones. In the case of water solution, the stability of the intramolecular hydrogen bond is diminished by some amount, and one can expect and larger contribution of extended or intermediate forms compared with the case in which a non-polar solvent is used. As can be easily seen, the latter ones (β- and intermediate types) have a larger degree of freedom compared with the former one (α-type), and corresponed to the state of larger entropy. Therefore the contribution of latter ones may increase rapidly with the elevation of temperature. Concerning this point, Kauzmann and Eyring suggested that the investigation of the effect of temperature on the molecular rotations of these polypeptidies would be of interest here.

In the actual calculations, the contribution of the latter ones are neglected. So it must be noticed that the calculated results correspond to the experimental results which are observed at sufficientry low temperature. Even if the contribution of latter ones could not be neglected, we might expect that the observed change of molecular rotations in a series of polypeptides would correspond well to the calculated results so long as the equilibrium constant was approximately constant regardless of the length of chains and the molecular rotations of the latter ones were sufficiently small as were inferred by Kauzmann and Eyring.

To simplify the calculations, it is assumed that the interatomic distances in C—C and C—N bonds are all 1.54 Å, and that in C=O and C—H bond is 1.26 Å and 1.1 Å respectively. Further, it is assumed that the valence angles of C and N atoms are tetrahedral angle (109°28′), and C—N bonds (C are not α-carbons) are perpendicular to a dyad axis of symmetry. In the present model, repeat distance is about 5.03 Å. In the actual molecule, true valence angles will make the molecule flatter than the assumed model and the repeat distance slightly larger.

II. Moleculur Rotation

Division of Rotatory Parameter According to the electromagnetic theory, molecular rotation $[M]$ is given as follows,

$$[M]=\frac{288\pi^2 N}{\lambda^2}\frac{n^2+2}{3}\beta \qquad (1)$$

where N is Avogadro's number, λ the wavelength of incident polarized light, and n the refractive index of the solution. Taking into account the variation of vector potential over the molecule, Rosenfeld developed a quantum-mechanical theory of dispersion, and gave the following expression for a rotatory parameter β:

$$\beta=\frac{c}{3\pi h}\sum_b{}'\frac{\mathrm{Im}\{(a\mid\vec{\mu}\mid b)\,(b\mid\vec{m}\mid a)\}}{\nu_{ba}^2-\nu^2} \qquad (2)$$

Here, $(a\mid\vec{\mu}\mid b)$ and $(b\mid\vec{m}\mid a)$ are the matrix components of electric and magnetic moments connecting state a and b; ν_{ba} the frequency of the transition between state a and b, ν the frequency of the incident plane polarized light, c the velocity of light, and h Planck's constant. Then, the theoretical problem of optical activity is merely to calculate Eq. (2) for the actual molecule. In order to proceed with the calculation, Kirkwood introduced a simplifying assumption, that is, electrons were localized in the respective constituent group not only in normal state but also in excited states. By this assumption, one can break up the total electric and magnetic moments into sums over the groups as follows,

$$\vec{\mu}=\sum_i \vec{\mu_i} \tag{3}$$

$$\vec{m}=\sum_k \frac{e}{2mc}\vec{R_k}\times\vec{P^{(k)}}+\vec{m_k} \tag{4}$$

where $\vec{\mu_i}$ is the electric moment of group i, $\vec{p^{(k)}}$ is the electric momentum of group k, and $\vec{m_k}$ is the magnetic moment referred to the center of gravity of group k situated at a point $\vec{R_k}$ from the center of gravity of the molecule as a whole. Substituting these relations in Eq. (2), Kirkwood obtained the following results.

$$\beta=\beta^{(0)}+\beta^{(1)}+\sum_k \beta^{(k)} \tag{5}$$

$$\beta^{(0)}=-\frac{1}{3h}\sum_i\sum_{k>}\sum_b \frac{\nu_{ba}}{\nu_{ba}^2-\nu_2} \times Re\{\vec{R_k}[(a\mid\vec{\mu^{(i)}}\mid b)\times b\mid\vec{\mu^{(k)}}\mid a)]\} \tag{6}$$

$$\beta^{(1)}=\frac{c}{3\pi h}\sum_j\sum_{k>}\sum_b \frac{\mathrm{Im}\{(a\ \vec{\mu^{(i)}}\ b)(b\ \vec{m^{(k)}}\ a)\}}{\nu_{ba}^2-\nu^2} \tag{7}$$

$$\beta^{(k)}=\frac{c}{3\pi h}\sum_b \frac{\mathrm{Im}\{(a\ \vec{\mu^{(k)}}\ b)\ (b\ \vec{m^{(k)}}\ a)\}}{\nu_{ba}^2-\nu^2} \tag{8}$$

$\beta^{(0)}$ is the term which was taken up and studied by Kirkwood and he considered that it was originated from the dynamical coupling between two electrons in the different groups i and k.[10,11] Not being studied in detail, the term of $\beta^{(1)}$ has usually been neglected expecting it probably to be small, $\beta^{(k)}$ is the term which was studied by Condon, Eyring, Kauzmann, Walter, et al., and they considered that it resulted from the motion of one electron in a dissymmetrical field of each group.[12,13,14]

As is obvious from the above discussion, we should consider both terms of $\beta^{(0)}$ and $\beta^{(k)}$ at least, in the calculations of molecular rotations. Accordingly, we will calculate both terms of $\beta^{(0)}$ and $\beta^{(k)}$, and give our conclusion considering both contributions from one-electron theory and dynamical coupling theory.

One-Electron Effect

a) Partial Rotation of N→E Type Transition When molecular rotation $[M]$ is observed in the visible region, the contribution from partial rotation becomes greater as the frequency of the absorption band (electronic transition), which is responsible for this partial rotation, exists nearer to the frequency of the observed light. If one remembers the factor $1/(\nu_{ba}^2-\nu^2)$ in equation of dispersion, this situation is evident. Consequently, when the special absorption band exists in the longer wavelength region far apart from the other absorptions in the ultraviolet region, most of the observed molecular rotation is determined by the partial rotation which is associated with this special transition.

In polypeptides, we are now investigating, $N\rightarrow E$ type transition in carbonyl group exists in the longest wavelength region. The calculations of the partial rotation associated with this transition have been carried out by Eyring et al. for 3-methylcyclopentanone[15] and benzoin.[16] Following Mulliken's usage, we define the coordinate of C=O group as follows. That is, we attribute the direction of π-orbitals of C and O to x-axis, that of non-bonding orbital of O to y-axis, and that of C—O bond to z-axis. In the first approximation, Eyring et al. assumed that the electron was localized in the oxygen atom throughout the process of $N\rightarrow E$ type transition, and they attributed it to the transition $2p_y\rightarrow 2p_z$. According to the study by McMurry, however, it should be attributed to the transition $2p_y\rightarrow 2p_x$ in the same approximation.[17] In this transition, the electric moment is zero and the magnetic moment is relatively large. (Even if the contribution of π-orbital of C atom is taken into account, this transition is still impossible). Then in order to obtain the non-zero value of $\beta^{(k)}$, the electric moment must have z-component, that is, one must consider the contribution of $3d_{yz}$-orbital at least in the excited state. This requirement is satisfied by using the following wave function.

$$\Psi_a=\Psi 2p_y \qquad \Psi_b=\Psi_{2px'}+C\ \Psi_{3dyz} \tag{9}$$

Substituting these wave functions in Eq. (8), one obtains

$$\beta(k)=\frac{c}{3\pi h}\frac{C}{\nu_{ba}^2-\nu^2} \mathrm{Im}\{(\Psi_{2py}\mid\mu_z\mid\Psi_{3dyz})(\Psi_{2px'}\mid m_z\mid\Psi_{2py})\} \tag{10}$$

where, C is given by first-order perturbation theory as follows,

$$C=\frac{(\Psi_{2px'}\mid\sum_i V_i\mid\Psi_{3dyz})}{E_{2px'}-E_{3dyz}} =\frac{1}{E_{2px'}-E_{3dyz}}\sum_i \gamma_x^{(i)}\gamma_y^{(i)}\gamma_z^{(i)}U_i \tag{11}$$

$$U_i=\int \Psi_{2p'}V_i\Psi_{3d}(Z^{1,i}{}_{(i)}-3X^{12}{}_{(i)}Z_{(i)}')d\tau$$

Here, V_i is the electrostatic perturbing potential from the atom i except the carbonyl group. (In practice, it is sufficient to consider the contribution from the atoms by which the center or plane of symmetry is lost). In the case of neutral atoms, these potentials originate from the incomplete screening of the nuclear charge on account of the extension of electron clouds, and fall off exponentially with the increase of distances from nuclei. Non-diagonal elements U_i of perturbing potentials

10) J. G. Kirkwood, *J. Chem. Phys.*, **5**, 479 (1937).
11) W. W. Wood, W. Fickett and J. G. Kirkwood, *J. Chem. Phys.*, **20**, 561 (1952).
12) E. U. Condon, *Rev. Mod. Phys.*, **9**, 432 (1937).
13) E. U. Condon, W. Altar and H. Eying, *J. Chem. Phys.*, **5**, 753 (1937).
14) E. Gorin, J. Walter and H. Eyring, *J. Chem. Phys.*, **6**, 824 (1938).
15) W. J. Kauzmann, J. E. Walter and H. Eyring, *Chem. Rev.*, **26**, 339 (1940).
16) T. C. Kwoh and H. Eyring, *J. Chem. Phys.*, **18**, 1186 (1950).
17) H. L. McMurry, *J. Chem. Phys.*, **9**, 231 (1941).

V_i are correlated to D_i by the following relation

$$D_i = -\frac{32}{5}\frac{a_0}{e^2}U_i$$

where the values of D_i are given by Eyring et al. as the function of distance for the cases of hydrogen and carbon atoms, and we use them in the present calculation. (In Eyring's calculation, U_i is approximated by $\int \psi_{2p}' V_i \psi_{3d} Z'^3{}_{(i)}\, d\tau$. Quantitatively, this approximation gives probably too great values). The evaluation of two center integral $(\psi_{2px}' \mid V_i \mid \psi_{3dyz})$ requires a rotation of the coordinate system in which the new Z-axis coincides with the line joining the center of the perturbing atom and the carbonyl oxygen atom. The terms γ_x, γ_y and γ_z in Eq. (11) are the direction cosines of the above-mentioned line in the old-coordinate system. The values of γ_x, γ_y and γ_z are calculated using the molecular model which is discribed in Part I.

As the value of electric moment, we assume $(\psi_{2py} \mid \mu_z \mid \psi_{3dyz}) = 0.22\ e$. This value is obtained by using the experimental absolute intensity ($f \sim 0.03$) of Rydberg series in ethylene.[18] (For carbonyl group, there is no quantitative data concerning intensity). Strictly speaking, as the value of electric moment one should take the smaller value because the above-mentioned intensity corresponds to the total intensity of a few lines in Rydberg series. For magnetic moment, we assume tentatively

$$(\psi_{2px}' \mid m_z \mid \psi_{2py}) = \frac{eh}{4\pi mci}(\psi_{2px}' \mid l \mid \psi_{2px}) = \frac{eh}{4\pi mci}0.91$$

If one considers the contribution of π-orbital of carbon atom in the excited state, this value may probably become smaller. Using these values and $n_D = 1.33$, $\nu = 0.509 \times 10^{15}$ sec^{-1} (D line of Na), one can describe the molecular rotation as follows,

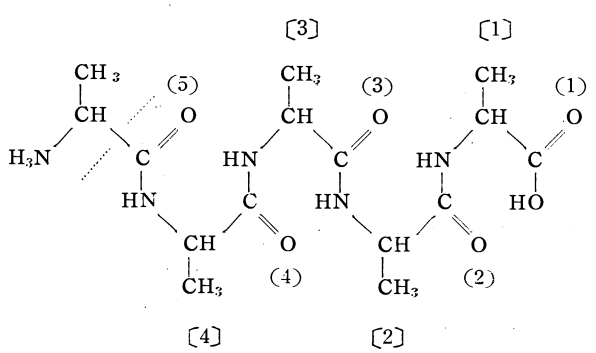
$$[M]_D = 45.87 \times 10^3 \frac{0.259}{\nu_{ba}^2 \times 10^{-30} - 0.259} \frac{1}{E_{2px}' - E_{3dyz}} \sum_i \gamma_x{}^{(i)}\, \gamma_y{}^{(i)}\, \gamma_z{}^{(i)}\, D_i \qquad (12)$$

where ν_{ba} and E_{2px}' are dependent on the nature of the atom which combines with carbonyl carbon, and use the following values:

	$\nu_{ba} \times 10^{-15}$ sec^{-1}	$E_{2px}' - E_{3dyz}$ (ev)
$H_2N\diagdown C=O$	1.68	−0.58
$HO\diagdown C=O$	1.44	−1.58

Of course, these values are not conclusive and may probably become to require some revision in the future study.

b) Method of Calculation We assume the molecular model which is described in Part I. In this model, the rotational isomers $\alpha_{(1)}$ and $\alpha_{(2)}$ have the same stability, and exist in solution with equal statistical weight. Then, the main chain of polypeptide comes to have effective plane of symmetry in the statistical meaning. This situation makes the calculations exceedingly simple, and in order to obtain the partial rotation associated with $N \rightarrow E$ type transition, it is sufficient for it by considering the perturbations from the side chain (methyl group) and the hydrogen atom which is attached to α-carbon together with the side chain. (In the following, we say that the term of methyl group is including this hydrogen atom). As a subsidiary assumption, we consider that end group COOH contributes to the formation of seven-membered ring, and another end group $-CH\langle^{CH_3}_{NH_3}$ exists in the effective plane of symmetry on account of their statistical free rotation around the single bond. Consequently, in case of tetra-alanyl-alanine, the molecular model becomes as follows:



18) J. R. Platt, H. B. Klevens and W. C. Price, *J. Chem. Phys.* **17**, 466 (1949).

As is shown in the foregoing figure, we number carbonyl oxygens as (1), (2), (3), (4), (5), and methyl groups as [1], [2], [3], [4]. Then, we can divide the perturbations (or partial rotations due to these perturbations) into three classes according to the relative positions between carbonyl oxygen and methyl group, that is:

A: {(1) [1]} {(2) [2]} {(3) [3]} {(4) [4]}
B: {(2) [1]} {(3) [2]} {(4) [3]} {(5) [4]}
C: {(3) [1]} {(4) [2]} {(5) [3]}

As described previously, interaction function D_i decreases very rapidly with the increase of r, and we neglect the interactions at intervals of more than 5 Å (for example {(2) [3]} {(5) [2]} etc.).

In each class of A, B and C, the relative orientations of the carbonyl group and the methyl group are different with the situations whether the configuration of the polypeptide chain exists in $\alpha_{(1)}$ or in $\alpha_{(2)}$. To indicate this distinction, we use the superscripts (1) and (2). In the following, we consider that the above-defined notation, for example $A^{(1)}$, corresponds to the partial rotation due to the perturbation from the methyl group to the carbonyl oxygen which exists in the relative position of class A and configuration of $\alpha_{(1)}$. So long as we assume that $\alpha_{(1)}$ and $\alpha_{(2)}$ are equally probable statistically, the mean value, for example,

$$A=(A^{(1)}+A^{(2)}/2) \qquad (13)$$

corresponds to the observed value. In the present case, the frequency of $N\rightarrow E$ type transition, consequently, the magnitude of the partial rotation depends on the atom, whether it is oxygen or nitrogen, which combines with carbonyl carbon. To distinguish these two cases, we use the subscripts O and N. Then the molecular rotations of a series of polypeptides are given as follows:

$$\left.\begin{array}{ll} \text{alanyl-alanine} & A_O+B_N \\ \text{di-alanyl-alanine} & A_O+A_N+2B_N+C_N \\ \text{tri-alanyl-alanine} & A_O+2A_N+3B_N+2C_N \\ \text{tetra-alanyl-alanine} & A_O+3A_N+4B_N+3C_N \end{array}\right\} \qquad (14)$$

The calculated values of A_O, A_N, B_N and C_N are given in Table II. Perturbations from one

TABLE II

$A_O^{(1)}=110.0°$	$A_O^{(2)}=-22.4°$	$A_O=43.8°$
$A_N^{(1)}=211.5°$	$A_N^{(2)}=-43.1°$	$A_N=84.2°$
$B_N^{(1)}=89.4°$	$B_N^{(2)}=-45.5°$	$B_N=21.9°$
$C_N^{(1)}=44.7°$	$C_N^{(2)}=36.7°$	$C_N=40.7°$

carbon atom and three hydrogen atoms in methyl group and one hydrogen atom attached to α-carbon together with methyl group are all taken into account. Using Eq. (14) and the values in Table II, we can easily calculate the molecular rotations of a series of polypeptides. These calculated values are shown in Table III together with the observed

TABLE III
CALCULATED MOLECULAR ROTATIONS $[A]_D$ DUE TO ONE-ELECTRON EFFECT

Polypeptides	Calculated values*	Observed values*
alanine	0°	0°
alanyl-alanine	66°	71°
di-alanyl-alanine	213°	192°
tri-alanyl-alanine	359°	360°
tetra-alanyl-alanine	506°	507°

* In the calculated values, $[M]_D$ of alanine is taken as the origin, and corresponding to this situation, observed values are corrected by amount of $[M]_D$ of alanine (13°).

values. As is seen in Table III, the calculated values agree well with experimental ones. It is interesting to see that each of A_0, A_N, B_N and C_N has the same sign, and this is the main reason which enables us to obtain the above-described agreement. If they had different signs, they might cancel with each other in Eq. (14) and give us much smaller molecular rotations.

We must emphasize, however, that the above-obtained quantitative agreement is only an apparent one. Firstly, as is described in the last section, the values of matrix elements U_i, $(\psi_{2py}|\mu_z|\psi_{3dyz})$ and $(\psi_{2px'}|m_z|\psi_{2py})$ belong to rather upper limits. Secondary, we can expect the appearance of the firist member of Rydberg series ($2p\rightarrow 3d$) in the slightly shorter wavelength region than the position of $N\rightarrow E$ type transition. And the theoretical consideration predicts that the partial rotation associated with this Rydberg transition has the opposite sign to that of $N\rightarrow E$ type transition, and tends to cancel it. Considering this fact, the calculated values become smaller than 20% of the observed values. (Even if we consider the contribution of $4d$, $5d$,.....functions, analogous situations are probable). The above situation is rather inferable, if one remembers that the wavelength of $N\rightarrow E$ type transition is shifted considerably towards the shorter side in case of polypeptide. In the present treatment, the partial rotation associated with the transition of the non-bonding electron in the hydroxyl group or nitrogen atoms in the main chain is not considered. The positions of these transitions, however, exist in the shorter side than that of $N\rightarrow E$ type transition, and the degree of cancellation due to the opposite partial rotation associated with Rydberg series may become greater.

At any rate, it is interesting that the theoretical and observed results agree well at least in qualitative tendency, and the

quantitative comparison will be discussed in the next section considering the dynamical coupling effect.

Dynamical Coupling Effect

a) Theoretical Foamula.—Assuming a dynamical coupling between two electrons in groups i and k (that is, a van der Waals type interaction between groups i and k), Kirkwood applied the first order perturbation calculation to Eq. (6). After some algebraic simplification, he obtained the simple expression for $\beta^{(0)}$ as follows[10,11]*:

$$\beta^{(0)}=\frac{1}{6}\sum_{i>k}^{N}\alpha_i\alpha_k\delta_i\delta_k\, G_{ik}\,\vec{R}_{ik}\,(\vec{b}_i\times\vec{b}_k) \qquad (15)$$

$$G_{ik}=\frac{1}{R_{ik}^3}\left[\vec{b}_i\vec{b}_k-3\frac{(\vec{b}_i\cdot\vec{R}_{ik})(\vec{b}_k\cdot\vec{R}_{ik})}{R_{ik}^2}\right]$$

$$\vec{R}_{ik}=\vec{R}_k-\vec{R}_i$$

where α_i is the mean polarizability of group i, δ_i is anisotropic factor of α_i and b_i is a unit vector defining the optical axis of symmetry of group i. Application of Eq. (15) is limited in the case that each group has a optical axis of symmetry, and δ_i is defined as follows:

$$\delta_i=(\alpha_{11}{}^{(i)}-\alpha_{22}{}^{(i)})/\alpha_i \qquad (16)$$

where $\alpha_{11}{}^{(i)}$ and $\alpha_{22}{}^{(i)}$ are the components of α_i parallel and perpendicular to $\vec{b}_i$. The above result obtained by Kirkwood can be considered as a quantum mechanical expression for the classical coupled-oscillator theory of Born and Kuhn. The disappearance of Planck's constant h in Eq. (15) indicates the classical character of it.

b) Method of Calculation.—The molecular model is the same as before. Since the main chain has an effective plane of symmetry in a statistical meaning, the most important factor is the term due to the interaction between methyl group and carbonyl group. In the case of dynamical coupling effect, the transition in methyl group can also contribute to the molecular rotation, and the interaction between the main chain and the side chain should also be taken into account. In the present calculation, however, we neglect this term, and the appropriateness for this omission is discussed in the last part of this paper.

Van der Waals type of interaction decreases more gradually than the interaction which is assumed in one-electron theory, so we take into account the classes of D and E together with those of A, B and C.

D: {(1)[2]} {(2)[3]} {(3)[4]}
E: {(4)[1]} {(5)[2]}

In the present case, there may be no necessity to distinguish between A_O and A_N, and the molecular rotations of a series of polypeptides are given as follows:

alanyl-alanine	$A+B$
di-alanyl-alanine	$2A+2B+C+D+$
tri-alanyl-alanine	$3A+3B+2C+2D+E$
tetra-alanyl-alanine	$4A+4B+3C+3D+2E$

(17)

In order to calculate the values of A, B, C, D and E using Eq. (15), it is necessary to know the values of $\alpha\delta$ of carbonyl group and methyl group. As the value of $\alpha\delta$, Kirkwood used that of respective group as a whole, however, we used that of respective bond, which was obtained by Wang as a result of careful analysis of Stuart's experimental value.[19] The values obtained by Wang are shown in Table IV (Carbonyl group is assumed to have an optical axis of symmetry in the first approximation). As is seen in Table IV, $\alpha\delta$ of C—H bond is much smaller than those of C—C and C=O bonds, so the contribution of it to molecular rotation can be neglected. Consequently, we consider only interactions between C=O bond and C—C bonds which combine methyl groups with the main chain, and $\vec{R}_{ik}$ is considered as a vector which combines the center of gravity of respective bond. The results of calculation are shown in Table V. It is rather surprising that each of A, B, C, D and E has the same sign in Table V. The calculated molecular rotations obtained by

TABLE IV

LONGITUDINAL AND TRANSVERSAL POLARIZABILITIES OF BONDS (10^{25} cc)

Bonds	α_{11}	α_{22}	$\alpha\delta=\alpha_{11}-\alpha_{22}$
C—H	7.2	6.2	1.0
C—C	18.2	0.2	18.0
C=O	19.4	8.0	11.4

TABLE V

$A^{(1)}=177.2°$	$A^{(2)}=-0.1°$	$A=88.6°$
$B^{(1)}=160.2°$	$B^{(2)}=-0.02°$	$B=80.1°$
$C^{(1)}=49.95°$	$C^{(2)}=4.53°$	$C=27.2°$
$D^{(1)}=0.024°$	$D^{(2)}=30.69°$	$D=15.4°$
$E^{(1)}=17.16°$	$E^{(2)}=17.23°$	$E=17.2°$

TABLE VI

CALCULATED MOLECULAR ROTATIONS $[M]_D$ DUE TO DYNAMICAL COUPLING EFFECT

Polypeptides	Calculated values	Calculated values × 0.591	Observed values*
alanine	0°	0°	0°
alanyl-alanine	169°	100°	71°
di-alanyl-alanine	380°	225°	192°
tri-alanyl-alanine	609°	360°	360°
tetra-alanyl-alanine	837°	495°	507°

* The observed values are corrected by the same way as in Table III.

* The error of signs in reference (10) is corrected in reference (11).

19) Sheng-Nien Wang, *J. Chem. Phys.*, **7**, 1012 (1939).

using Eq. (17) and the values in Table V are given in Table VI together with the observed values. The calculated values are too great compared with the observed values. But the calculated values multiplied by 0.591 agree relatively well with experimental ones. That is, the calculated results agree with experimental results, at least in qualitative tendency.

c) Discussion on the Results.—In the case of dynamical coupling effect, the calculated values are twice as large as the observed ones. As the main causes of this situation, we can consider the following three factors:

(1) The values of parameters, such as $\alpha\delta$, are too large.

(2) The assumption concerning the equilibrium between two rotational isomers $\alpha_{(1)}$ and $\alpha_{(2)}$ is not appropriate. In the actual calculation, it is assumed that $\alpha_{(1)}$ and $\alpha_{(2)}$ are equally probable, however, one can consider the case in which the equilibrium is shifted towards one side.

(3) In the present calculation, only α-type configurations are taken into account, however, one can also expect the cases in which the contribution of β-and intermediate-type configurations are not negligible.

Whether the factor (1) is real or not can be determined by the systematic study for many simple molecules, and at the present stage, it is difficult to give the decided conclusion.

Factor (2) may probably be the most important one, and we will give rather detailed consideration. Observing Tables 2 and 5, one finds that the values of A, B and C are exceedingly larger in $\alpha_{(1)}$ than in $\alpha_{(2)}$. Moreover, the sign of these quantities are definite in $\alpha_{(1)}$, on the contrary, plus and minus signs are mixed in $\alpha_{(2)}$, and tend to cancel each other. The main cause of this situation may probably exist in the fact that the side chains (methyl groups) are approximately perpendicular to the plane of main chain in the case of $\alpha_{(1)}$, on the other hand, side chains are approximately lying in that plane in the case of $\alpha_{(2)}$. If this statement is correct, molecular rotation as a whole considering not only the interaction between side chain and carbonyl group but also all the other interactions in the molecule may be sufficiently smaller in the case of $\alpha_{(2)}$ compared with the case of $\alpha_{(1)}$. Then, the shift of equilibrium towards $\alpha_{(2)}$, makes the molecular rotation of polypeptides smaller. That is, too large theoretical values suggest that the equilibrium is shifted towards $\alpha_{(2)}$ under the observed conditions. This suggestion accords with the expectation from the internal rotation. It is difficult, however, to explain the observed rotations if one neglects the contribution of $\alpha_{(1)}$ completely.

Factor (3) should also be considered, and to know the degree of contribution of this factor, it is very desirable to observe the temperature effect on the molecular rotation.

Factors (2) and (3) diminish not only the molecular rotation due to dynamical coupling effect but also due to one-electron effect as well. Since both effects predict the same sign of molecular rotations (See Table III and VI), that situation has special importance.

Lastly, we consider the degree of approximation of the present calculation. As is described in the last section, only the interaction between the side chain and the carbonyl group is taken into account, and the other interactions, for example, between the main chain and the side chain, are neglected. In order to allow this approximation, it is required that C—C bond and C—N bond (N atom has non-bonding electrons!) have the same $\alpha\delta$. As far as we know, there are no experimental results which are sufficient to verify the above-requirement. We can infer, however, that there will be no large difference between $\alpha\delta$ of C—C and C—N bonds considering the almost equal nature of both bonds. Even if the above-requirement is satisfied, it remains the contribution from the interaction between the side chain and the main chain in the case of di-alanyl-alanine and tetra-alanyl-alanine. We can expect, however, that this contribution may be small if we remember the relatively small values of D and E.

In every case, the influence of the end group $-CH\begin{matrix}CH_3\\NH_3\end{matrix}$ is neglected. Strictly speaking, these omissions may not be reasonable. If we take out the differences of molecular rotations between successive polypeptide molecules, however, the influence due to the end group may mostly be subtracted. We can expect an analogous tendency for the part due to interaction between the side chain and the main chain.

Summary

Molecular rotations of a series of polypeptides of alanine have been calculated theoretically. We have assumed the molecular model which is constructed by seven-membered rings due to intra-molecular hy-

drogen bonds (α-type configuration). Calculations are carried out for the both effects of one-electron theory and dynamical coupling theory, and the results correspond relatively well to experimental results. This fact probably indicates the appropriateness of the assumed model. In order to obtain a decisive conclusion, however, it is necessary to proceed with the calculations for other models and compare the results quantitatively. This is a task for future study.

The author wishes to express his sincere thanks to Prof. S. Akabori for his kind guidance and encouragement throughout this work.

Department of Chemistry, Faculty of Science, Osaka University, Osaka

Equilibrium of the CO_2—NH_3—Urea—H_2O *System under High Temperature and Pressure. V. Liquid-Vapor Equilibrium in the Presence of Excess Ammonia or Carbon Dioxide*[1]

By Schōhachi KAWASUMI

(Received November 4, 1953)

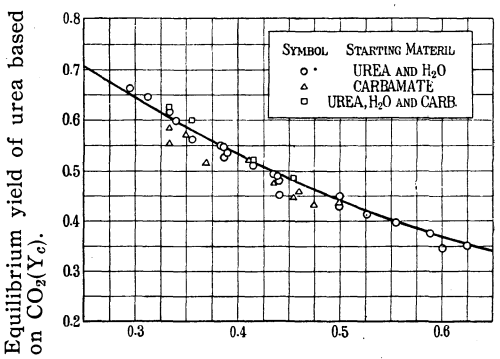
The liquid-vapor equilibrium compositions in a reaction vessel for urea synthesis from ammonia and carbon dioxide under high temperature and pressure have previously been shown in the stoichiometrical loading mole ratio of $2NH_3$ to 1 CO_2[2], assuming that the system consists of three components, ammonia, carbon dioxide and water, in the vapor phase and of four components, urea, water, unconverted ammonia and carbon dioxide in the liquid phase.

For the purpose of presenting similarly the compositions of the liquid and vapor phases of the equilibrium system starting with a mixture of ammonium carbamate and excess amount of ammonia or carbon dioxide in this paper, the yield of urea and the mole ratios of unconverted ammonia to carbon dioxide in the liquid phase of the system have been measured at a temperature of 160°C. The compositions of the system have been calculated from the present and the previous measurements[3] over the range of the loading NH_3-CO_2 mole ratio (L) from 1.6 to 3.0.

On the basis of these results, the effects of the variation of the loading mole ratio on the equilibrium compositions and the equilibrium constant of the following reaction have been discussed.

$$CO_2+2NH_3 \rightleftarrows CO(NH_2)_2+H_2O \quad \cdots\cdots(1)$$

Relation between Loading Composition and Equilibrium Yield of Urea. It is an established fact that the excess ammonia over the stoichiometrical 2 moles per mole of carbon dioxide causes an increase of the equilibrium yield of Urea (Y_c) based on the quantity of the initially charged carbon dioxide. The present measurements of the urea yield under conditions where the excess ammonia or carbon dioxide was added to the carbamate, which was loaded with a constant density of 0.60 g./cc., are plotted against the reciprocal of L in Fig. 1.



Loading CO_2 to NH_3 mole ratio (1/L)

Fig. 1.—Y_c—1/L relation at 160°C. and D=0.60 g./cc.

Y_c was measured by the following procedure: after the system reached the equilibrium, the reaction vessel was rapidly cooled and then the content was withdrawn. Water and unconverted NH_3 and CO_2 were completely evaporated out of the content at 70°C. and the amount of residual urea was weighed.

The urea yield (Y_a) based on the quantity

1) This paper was presented at the annual meeting of the Chemical Society of Japan held at Kyoto University, on April 2, 1953.

2) S. Kawasumi, This Bulletin, **25**, 227 (1952).

3) S. Kawasumi, ibid., **26**, 222 (1953).

of the initially charged ammonia, which is connected with Y_c by the equation: $Y_a \times L = 2Y_c$ is approximately constant independent of L over the range of $L<2$, while it decreases with the rise of L over the range of $L>2$.

It is a remarkable fact that the Y_c-L relation at a constant temperature and loading density depends upon the definition of the loading density. In the present experiments as mentioned above, the starting materials were prepared by loading ammonium carbamate or equi-molar urea and water into the reaction vessel with a constant loading density (D), followed by the addition of the required amount of ammonia or carbon dioxide to it. Consequently, the total loading density (D_t) including excess ammonia or carbon dioxide was varied over the range of L. Regarding the molecular weights of NH_2COONH_4, NH_3 and CO_2 as 78, 17 and 44 respectively, $D_t = \frac{D}{78}(44+17L)$ over the range of $L>2$ and $D_t = \frac{2D}{78L}(44+17L)$ over the range of $L<2$. In this case, therefore, D_t is the minimum at $L=2$ as shown in Fig. 2.

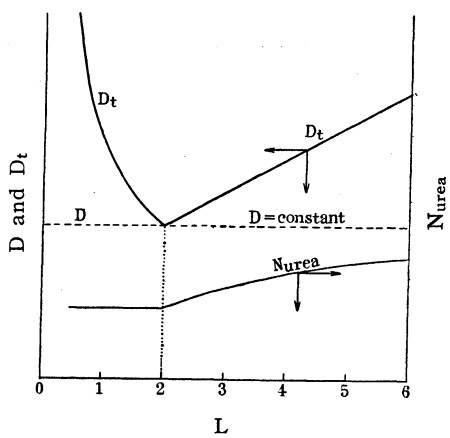


Fig. 2.—D_t—L relation in the experiment performed with a constant D.

If an experiment would be performed with a constant D_t, it would be conjectured that the amount of urea (n_{urea}) in the unit volume of the reaction vessel attains to the maximum at a certain loading mole ratio, since the loading density (D) of the carbamate is the maximum at $L=2$ as shown schematically in Fig. 3. Therefore it may be concluded that the Y_c-L relation at a constant D_t is undoubtedly different from that at a constant D.

The existence of an optimum temperature where Y_c attains to the maximum has already been discussed in the previous paper[2] under conditions where ammonia and carbon dioxide were used in the stoichiometrical proportion to form ammonium carbamate and the loading density of the carbamate was kept constant. Similarly in the presence of excess ammonia or carbon dioxide, the optimum temperature where Y_c attains to the maximum rises with an increase of D at a given L and also it rises with an increase of L at a given D. Such the Y_c-L-T-D relations may be explained to be based upon the same reason as described in the previous paper[2].

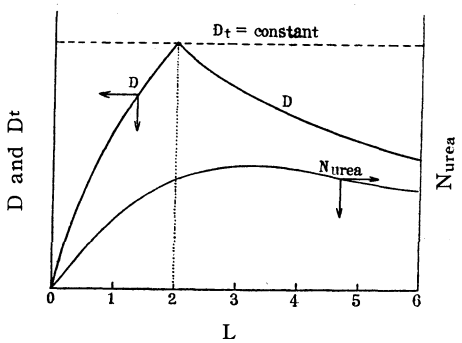


Fig. 3—D—L relation in the experiment performed with a constant D_t.

Relation between Loading-and Liquid-Composition—Under conditions where carbamate was charged at a loading density of 0.60 g. per cc. of a reaction vessel and then 0.2 to 1.0 moles of excess ammonia or 0.05 to 0.25 moles of carbon dioxide was added to one mole of the carbamate, the mole ratio (R) of unconverted ammonia to carbon dioxide in the liquid phase has been measured at 160°C. by the method reported in the previous paper.[2]

The experimental results are shown in Fig. 4. It has previously been shown that R' increases with L under the same conditions[2]. R also increases with L.

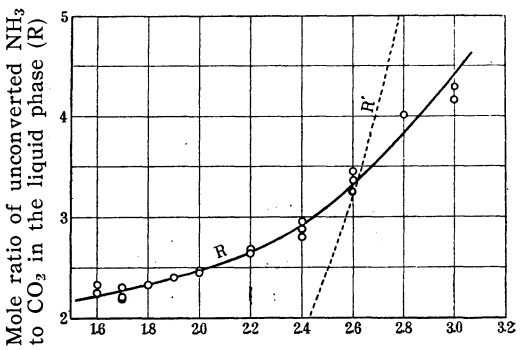


Fig. 4.—R—L relation at 160°C. and D=0.60 g./cc.

Relation between Equilibrium Composition and Loading NH_3-CO_2 Mole Ratio—A method for calculating the equilibrium concentration of each component in the two phases on the same assumption as previously employed[2] is shown in such a case as that where "c" moles of ammonium carbamate (equivalent of "$2c$" moles of ammonia and "c" moles of carbon dioxide) were initially loaded into a reaction vessel of one litre volume and then "m" moles of excess ammonia or carbon dioxide were added to one mole of the carbamate.

Equations giving Concentrations in the Presence of Excess Ammonia—In this case ($L=2+m$), we obtain from the material balance respectively,

$$n_{\text{urea}}+n_{CO_2}+n'_{CO_2}=c \quad \cdots\cdots(2)$$

$$2n_{\text{urea}}+n_{NH_3}+n'_{NH_3}=(2+m)c \quad \cdots\cdots(3)$$

Let us put,

$$n'_{NH_3}/n'_{CO_2}=R' \quad \cdots\cdots(4)$$

$$n'_{H_2O}/n'_{CO_2}=S' \quad \cdots\cdots(5)$$

$$n_{NH_3}/n_{CO_2}=R \quad \cdots\cdots(6)$$

$$n_{\text{urea}}=cY_c \quad \cdots\cdots(7)$$

and

$$n_{H_2O}=n_{\text{urea}}-n'_{H_2O} \quad \cdots\cdots(8)$$

From these seven equations, we can derive the following relations (9) to (14) which allow the equilibrium concentration of each component to be calculated.

$$n'_{CO_2}=\frac{c}{R-R'}\{(1-Y_c)(R-2)-m\} \quad \cdots(9)$$

$$n'_{NH_3}=\frac{cR'}{R-R'}\{(1-Y_c)(R-2)-m\} \quad \cdots(10)$$

$$n'_{H_2O}=\frac{cS'}{R-R'}\{(1-Y_c)(R-2)-m\} \quad \cdots(11)$$

$$n_{CO_2}=\frac{c}{R-R'}\{(1-Y_c)(2-R')-m\} \quad \cdots(12)$$

$$n_{NH_3}=\frac{cR}{R-R'}\{(1-Y_c)(2-R')-m\} \quad \cdots(13)$$

$$n_{\text{urea}}=cY_c \quad \cdots\cdots(7')$$

$$n_{H_2O}=c\left[Y_c-\frac{S'}{R-R'}\{(1-Y_c)(R-2)-m\}\right] \quad (14)$$

Equations giving Concentrations in the Presence of Excess Carbon Dioxide—Similarly in this case ($L=\frac{2}{1+m}$), we obtain the equations (15) and (16) from the material balance.

$$n_{\text{urea}}+n_{CO_2}+n'_{CO_2}=(1+m)c \quad \cdots\cdots(15)$$

$$2n_{\text{urea}}+n_{NH_3}+n'_{NH_3}=2c \quad \cdots\cdots(16)$$

In the same way from these two equations and the above five equations (4) to (8), we can derive the following relations, for example n'_{CO_2} and n_{CO_2}, which allow the equilibrium concentration to be calculated.

$$n'_{CO_2}=\frac{c}{R-R'}\{(1-Y_c)(R-2)+m\cdots\} \quad (17)$$

$$n_{CO_2}=\frac{c}{R-R'}\{(1-Y_c)(2-R')-mR'\} \quad (18)$$

Equilibrium Compositions in the Presence of Excess Ammonia and Carbon Dioxide—The liquid and vapor phase compositions have been calculated from these equations, as shown in Table 1, under the conditions

TABLE I

LIQUID-VAPOR EQUILIBRIUM COMPOSITIONS IN THE PRESENCE OF EXCESS AMMONIA OR CARBON DIOXIDE AT 160°C. AND D=0.60 g/cc

L		1.60	1.80	2.00	2.20	2.40	2.62	2.80	3.00
c, mole/l.		7.685	7.685	7.685	7.685	7.685	7.685	7.685	7.685
excess CO_2, mole/l.		1.921	0.854	—	—	—	—	—	—
excess NH_3, mole/l.		—	—	—	1.537	3.074	4.764	6.149	7.685
P, atm.		151	114	89	76	66	69.5	75	80
R′		0.156	0.287	0.547	1.035	1.850	3.380	5.350	9.250
S′		0.025	0.040	0.066	0.110	0.175	0.260	0.375	0.575
R		2.220	2.330	2.460	2.618	0.925	3.380	3.827	4.390
Yc		0.355	0.398	0.442	0.483	0.517	0.551	0.577	.0604
Concentration, mole/l.	n'_{CO_2}	2.520	1.664	1.031	0.579	0.346	0.203	0.136	0.084
	n'_{NH_3}	0.393	0.478	0.564	0.600	0.639	0.684	0.730	0.781
	n'_{H_2O}	0.063	0.067	0.068	0.064	0.061	0.053	0.051	0.049
	n_{CO_2}	3.676	3.474	3.257	3.395	3.364	3.247	3.114	2.959
	n_{NH_3}	8.150	8.100	8.012	8.887	9.854	10.980	11.915	12.990
	n_{urea}	3.410	3.400	3.397	3.710	3.975	4.235	4.435	4.640
	n_{H_2O}	3.347	3.334	3.329	3.646	3.915	4.182	4.384	4.591
Equilibrium mole fraction	N'_{CO_2}	0.874	0.754	0.620	0.466	0.330	0.216	0.149	0.092
	N'_{NH_3}	0.132	0.216	0.339	0.483	0.612	0.728	0.795	0.855
	N'_{H_2O}	0.021	0.030	0.041	0.051	0.058	0.056	0.056	0.053
	N_{CO_2}	0.198	0.190	0.181	0.173	0.160	0.143	0.130	0.118
	N_{NH_3}	0.439	0.442	0.445	0.453	0.467	0.485	0.500	0.516
	N_{urea}	0.184	0.186	0.189	0.189	0.188	0.187	0.186	0.184
	N_{H_2O}	0.180	0.182	0.185	0.185	0.185	0.185	0.184	0.182
$K_{N\text{-}(1)}$		0.870	0.911	0.974	0.985	1.000	1.025	1.049	1.073

where the equilibrium was established at 160°C. starting with a mixture prepared by loading ammonium carbamate of $c=7.685$ moles at a constant density of $D=0.60$ g./cc. into a reaction vessel of one litre volume, followed by adding a required excess amount of ammonia or carbon dioxide to the carbamate. Accordingly the total loading densities including excess ammonia or carbon dioxide are more than 0.60 g./cc. at any loading NH_3-CO_2 mole ratio.

With the increase of the excess amount of carbon dioxide added to the carbamate, the equilibrium pressure[3] rises remarkably and also Y_a is approximately constant independent of the excess amount of carbon dioxide as explained above. According to the calculation, these experimental results are undoubtedly based upon the fact that carbon dioxide is increased not in the liquid, but in the vapor phase. The table also indicates that the larger amounts of the excess ammonia initially added to the carbamate mostly exist in the liquid phase, so that the liquid volume may possibly increase with the excess amount of ammonia.

The liquid-vapor equilibrium diagram of the system at 160°C. is represented as a plot of x_i against L in Fig. 5. As shown in this diagram, x_{urea} and x_{H_2O} attain respectively to the maximum, since an increase of the

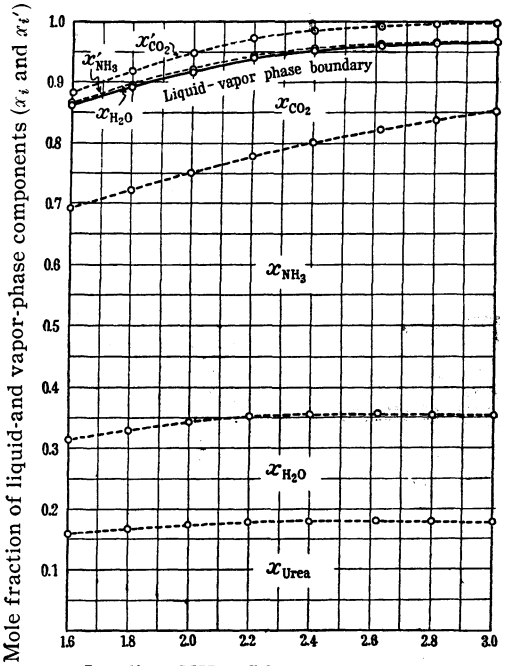


Fig. 5.—Liquid-vapor equilibria diagram of the CO_2—NH_3—Urea—H_2O system in the presence of excess ammonia or carbon dioxide at 160°C.

excess amount of ammonia in the original charge is accompanied by an increase of n_{urea} and n_{H_2O} as well as the total sum of moles (X) of every component in both liquid and vapor phases.

According to the results of Table 1, the amount of urea is approximately equal to that of water in the liquid phase due to the small amount of water vapor, so that a molecular compound of urea-water, $(NH_2)_2CO\cdot H_2O$, may be assumed for the purpose of expressing the liquid-vapor equilibrium compositions as the three component system, as such an expedient has already been employed by Davis and Black.[4]

In such a manner, a ternary diagram with the apices representing the three constituents—ammonia, carbon dioxide, and water in the vapor or urea-water in the liquid—has also been illustrated from the above data as shown in Fig. 6.

Three pressure-composition diagrams for the systems consisting of every two constituents of them are also given in Fig. 6-A, -B and -C. At a temperature of 160°C. the system exerts the minimum pressures at a point "a" on a vapor curve where the vapor is composed of ammonia and carbon dioxide in the stoichiometrical proportion to form ammonium carbamate, or $R'=2$, and this point is in equilibrium with a point "b" on a liquidus curve which has the composition of $R=2.925$. The coexisting two points of "c" on the vapor curve and "d" on the liquidus curve have the same mole ratio of ammonia to carbon dioxide, that is, $R=R'=3.38$. Usually in the binary system an azeotropic mixture in which the coexisting liquid and vapor have the same composition exerts the maximum or minimum pressure at a constant temperature. It will be seen in this diagram that "a" and "b" are not necessarily consistent with "c" or "d" in the system of three or more components such as the present system.

Further consideration will be given to the point where the coexisting liquid and vapor have the same composition. At this point,

$$R=R' \quad \cdots\cdots(19)$$

By the definitions of L and Y_c and from the material balance,

$$L=\frac{n_{NH_3}+n'_{NH_3}+2n_{urea}}{n_{CO_2}+n'_{CO_2}+n_{urea}} \quad (20)$$

$$Y_c=\frac{n_{urea}}{n_{CO_2}+n'_{CO_2}+n_{urea}} \quad (21)$$

By eliminating all of n_{CO_2}, n'_{CO_2}, n_{NH_3}, n'_{NH_3} and n_{urea} from these five equations of

4) Davis and Black, *Ind. Eng. Chem.*, **23**, 1280 (1931).

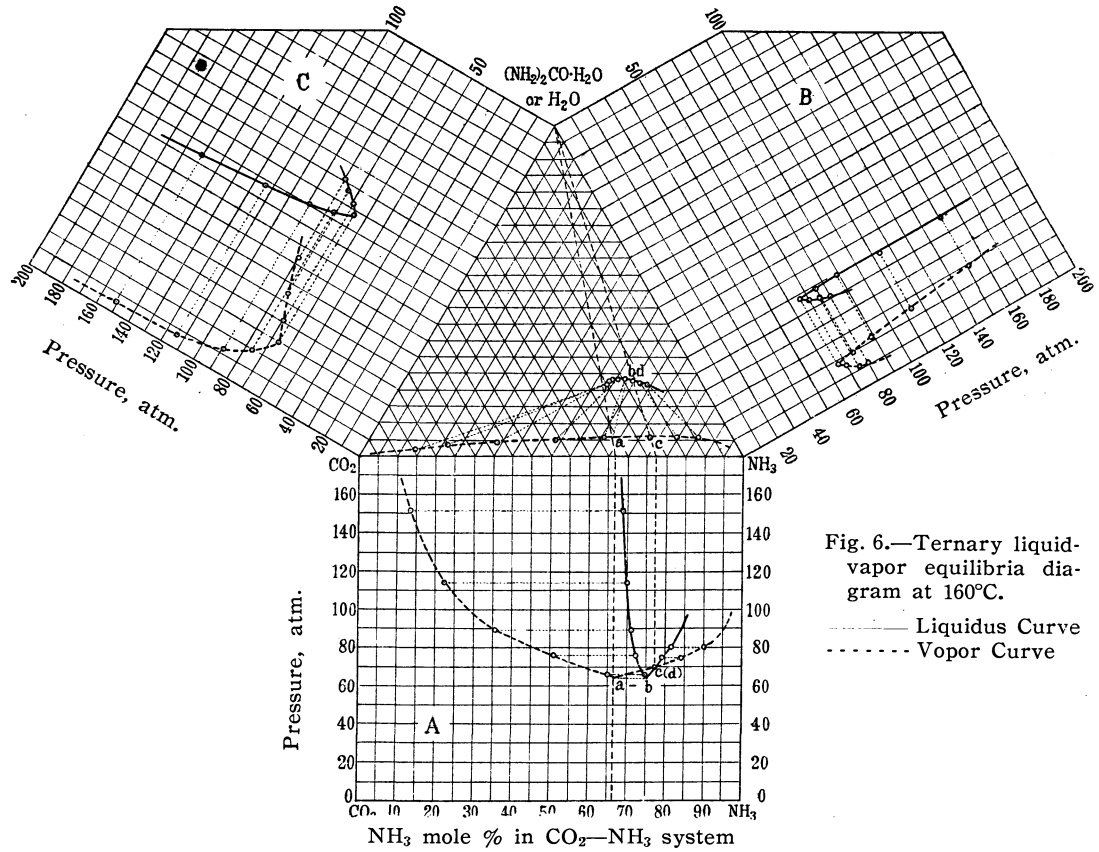


Fig. 6.—Ternary liquid-vapor equilibria diagram at 160°C.
——— Liquidus Curve
- - - - - - - Vopor Curve

(4), (6), (19), (20) and (21), the following relation is derived:

$$L-2=(1-Y_c)\ (R-2)=(1-Y_c)\ (R'-2) \quad (22)$$

The present experiments under the condition of $T=160$°C. and $D=0.60$ g./cc. showed the observed values of $R=R'=3.38$ and $Y_c=0.551$ at $L=2.62$ to be in accord with the relation represented by the equation (22).

The equilibrium constants ($K_{N-(1)}$) of the reaction (1) at 160°C. represented by mole fraction (N_i) of each component in the liquid phase ($K_{N-(1)}=\frac{N_{urea}\ N_{H_2O}}{N_{CO_2}\ N_{NH_3}^2}$) are also given in the last line of Table 1. As these values show a tendency to increase gradually with L at a constant temperature, $K_{N-(1)}$ is not an equilibrium constant in the true sense of the term as described in that case in which water has been added to mmonium carbamate.[5] The equilibrium constant should be calculated on the other assumption and explained from the other stand-point in further discussion.

Liquid Volume and Densities—Under the conditions of $T=160$°C. and $D=0.60$ and 0.40 g./cc., the liquid-vapor volume ratios in the presence of the excess amount of ammonia have been measured over the range of $L=2.0\sim3.0$ by a method which was described in the previous paper.[2] The percentage of the liquid volume to the vessel volume increases linearly with L as shown in Fig. 7. The liquid and vapor densities of

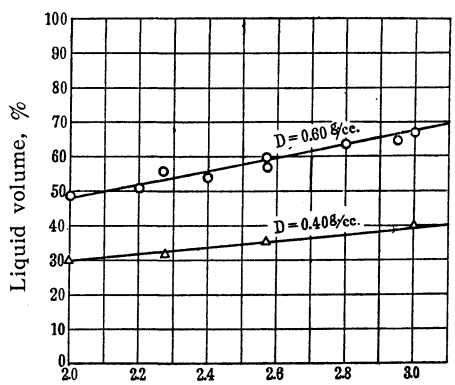
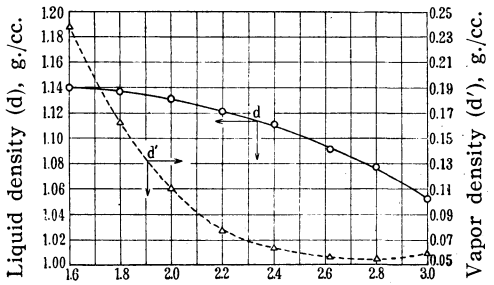


Fig. 7.—Liquid volume in the presence of excess ammonia at 160°C.

the system under high temperature and pressure are given by dividing the weight of each phase obtained from Table 1 by the liquid-and vapor-volume respectively. The

5) S. Kawasumi, This Bulletin, **26**, 218 (1953).

densities (d and d') of the two phases decrease with L, and d′ attains to the minimum at L=2.7～2.8 as shown in Fig. 8.



Loading NH_3—CO_2 mole ratio (L)

Fig. 8.—Liquid-and vapor-densities over the range of L=1.6～3.0 at T=160°C. and D=0.60 g./cc.

Summary

The liquid-vapor equilibrium compositions of the CO_2-NH_3-Urea-H_2O system starting with a mixture of ammonium carbamate and the excess amount of ammonia or carbon dioxide have been calculated at 160°C. and over the range of the loading NH_3-CO_2 mole ratio of 1.6 to 3.0 from the experimental data presented in the previous paper of this series.

The effects of the loading NH_3-CO_2 mole ratio on the equilibrium compositions have been discussed and the liquid-vapor equilibrium diagram of the system in the presence of excess ammonia or carbon dioxide has been drawn.

Symbols **Nomenclature**

c —Number of moles of ammonium carbamate loaded initially into the reaction vessel, gram mole per litre

d —Density of liquid, gram per cc.

D —Loading density, or ratio of the weights of materials to the total volume of the reaction vessel, gram per cc.

D_t —Total loading density including excess ammonia or carbon dioxide, gram per cc.

$K_{N-(1)}$ —Equilibrium constant of the reaction (1) represented by mole fraction N_i, no units

L —Loading ammonia-carbon dioxide mole ratio, no units

m —Number of moles of excess ammonia or carbon dioxide to one mole of ammonium carbamate, no units

n_i —Number of moles of a component "i" in the liquid phase per litre of the reaction vessel, gram mole per litre

N_i —Mole fraction of a component "i" in the liquid phase, or ratio of gram moles to the total gram moles in the liquid phase, no units

P —Equilibrium pressure, atm.

R —Mole ratio of unconverted ammonia to carbon dioxide in the liquid phase, no units

S —Mole ratio of water to carbon dioxide in the liquid phase, no units

T —Temperature, °C.

X_i —Mole fraction of a component "i" in the liquid phase, or ratio of gram moles to the total gram moles in the two phases, no units

X —Total sum of moles of every component of the two phases, per litre of the reaction vessel, gram mole per litre

Y_c —Equilibrium yield of urea based on carbon dioxide in the original charge, or ratio of gram moles of urea to initial loading moles of carbon dioxide, no units

Y_a —Equilibrium yield of urea based on ammonia in the original charge, no units

Superscript

′(dash) —sign to denote the vapor phase

The writer wishes to express appreciation for the kind guidance and the advice received throughout this work from Dr. Shinjiro Kodama, Prof. of Kyoto University, and for the encouragement received from Dr. Kenji Fujimura, the chief of the Research Department.

Research Department, Niihama Works, Sumitomo Chemical Co., Ltd., Niihama

On the Relation Between Viscosity and Critical Micelle Concentration of Detergent Solutions. II.[1] *Viscosity and Diffusion Coefficient of Non-ionic Detergent Solutions*[2]

By Haruhiko OKUYAMA and Kiyoshi TYUZYO[3]

(Received November 4, 1953)

Introduction

In the first paper, we proposed the method of determining the first and second critical micelle concentration (CMC) and two kinds of intrinsic viscosity from the analysis of viscosity of various ionic detergent solu-

1) The first paper of this investigation is: N. Sata and K. Tyuzyo, This Bulletin, **26**, 177 (1953).

2) Presented before the sixth Annual Meeting of the Chem. Soc. of Japan in Kyoto, April, 1953.

3) Present Address: Research Laboratory, Dai-Nippon Celluloid Co., Ltd., Sakai City, Osaka, Japan.

tions[1]. In this paper, the results concerning the aqueous solutions of non-ionic detergents are presented. Namely, not only viscosity of the solutions is measured, but also diffusion coefficient is investigated. This latter method is especially effective in determining CMC and molecular weight of micelle in the present case because this method is remarkably simplified on account of negligible action of diffusion potential in the case of non-ionic detergents, in contrast with ionic detergents[4].

Samples and Experimental Methods

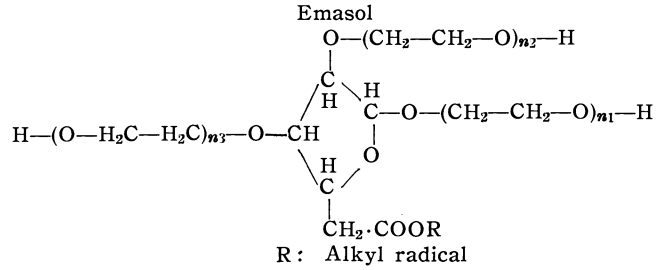
(1) **Samples:** Several kinds of non-ionic detergents (made by Kao-Soap Co. Ltd.) were used. We used series of polyoxyethylene sorbitan (Emasol) and polyoxyethylene-ether (Emulgen). These have such structures as shown below, and the coexistence of hydrophilic group and hydrophobic group in the same molecule causes the surface activity.

Emulgen

$$R{-}O{-}(CH_2{-}CH_2{-}O)_n{-}H$$

R: Alkyl radical

Emasol



R: Alkyl radical

Pure samples of Kao-Soap Co. Ltd. were used. These contain a small quantity of water, metal salt and polyoxyethylene as the impurities. The content of water is less than 1 %[5] and quantity of metal ion is too minute to hinder the measurement of viscosity and diffusion[6]. It was very difficult to remove polyoxyethylene and so we left it as it was.

(2) **Viscosity:** Viscosity was measured by an ordinary Ostwald's viscometer at 30±0.05°C. The falling time of distilled water was 127.14 sec. Each Sample was measured three times and the averaged value was adopted. But, moreover, at lower concentration (below 1 %), measurement was performed with freshly prepared solutions for three times, then the averaged value was obtained.

(3) **Partial Specific Volume:** Partial specific volume was determined by Ostwald's picnometer of 5 cc content at 30±0.05°C.

(4) **Diffusion Coefficient:** Diffusion coefficient was measured by the schlieren method using the cylindrical lens as was already shown[7,8]. This time, its accuracy was increased by using the improved diffusion cell. The temperature was 25±0.05°C. The diffusion coefficient at each concentration was obtained by the differential diffusion method[9]. The limiting concentration-gradient of our new cell was about 0.3 weight per cent, but we measured it at the concentration-gradient of 0.5~1 % considering the requirement of accuracy.

Results

(1) **Partial Specific Volume:** The temperature was 30±0.05°C. Partial specific volume of 1 % solution is shown in the Table I.

TABLE I. PARTIAL SPECIFIC VOLUME OF 1 % SOLUTION OF NON-IONIC DETERGENT AT 30°C

Substance	ρ (g/cc)	V (cc/g)
Emasol 1112	0.9972	0.849
Emasol 1115	0.9964	0.934
Emasol 1120	0.9966	0.916
Emasol 1130	0.9971	0.864
Emasol 3130	0.9978	0.796
Emulgen 120	0.9964	0.934

(2) **Viscosity:** Fig. 1 shows the relative viscosity-concentration curve of detergents at 30±0.05°C. For Emasol 1120, 1130, and Emulgen 120, the η_{sp}/C vs. C-curve becomes minimum at C_1 as is shown in the Fig. 2, but for others, η_{sp}/C simply increases with concentration.

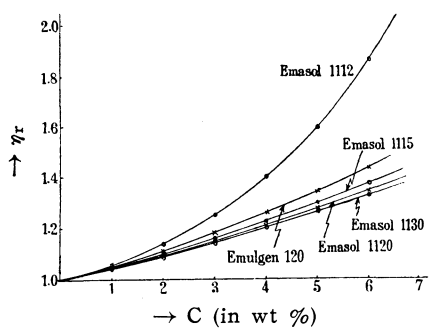


Fig. 1. Dependence of relative viscosity on concentration of several non-ionic detergent solutions.

Now, according to the first paper, the second CMC (C_2) and intrinsic viscosity ($[\eta_1]$,

4) G. S. Hartley and C. Robinson, *Proc. Roy. Soc.*, **A134**, 20 (1931).

5) Results of the analysis of water content by Mr. R. Muneyuki of Shionogi-Seiyaku Co., Ltd., were as follows:
Emasol 1112,1.9; Emasol 1115,3.26; Emasol 1120,0.6:
Emasol 1130,0.7; Emulgen 120,19.4 mg./g.

6) Results of the measured electric conductivity of several aqueous solutions were as follows:
Emasol 1112, specific electric conductivity of
1% aqueous solution=6×10^{-5}
3% aqueous solution=2×10^{-4}
Emulgen 120, 3% aqueous solution=2×10^{-4}
Potassium chloride 2/10000 N aqueous solution=2×10^{-5}
1/1000 N aqueous solution=1.5×10^{-4}

7) O. Lamm, *Nova Acta Regiae Soc. Scien. Upsal.* IV, **10**, No. 6 (1937); J. S. L. Phillipot, *Nature*, **141** 283 (1938).

8) N. Sata, H. Okuyama, K. Tyuzyo, *Kolloid-Z.* **121**, 46 (1951).

9) L. G. Longsworth, *J. Amer. Chem. Soc.*, **69**, 2510 (1947).

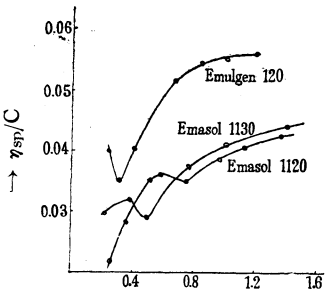


Fig. 2. Relation between η_{sp}/C and C of Emasol 1120, 1130 and Emulgen 120.

$[\eta_2]$) are obtained from the Fig. 3 and the following equation. Namely,

$$\eta_{sp}{}^0/C^0 = \frac{(\eta_r/\eta_{r\,min})-1}{C-C_1} \quad \text{.....(1)}$$

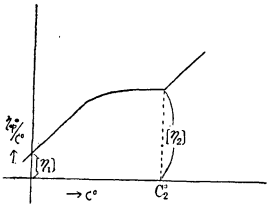


Fig. 3. Determination of C_2, $[\eta_1]$ and $[\eta_2]$.

According to the Equation 1, if we replot the curve for $\eta_{sp}{}^0/C_0$ and C^0, Fig. 3 is obtained. From the curve, the values of C_2 $[\eta_1]$, $[\eta_2]$ are gained.

$$[\eta_1] = \lim_{C^0 \to 0} (\eta_{sp}{}^0/C^0) \quad \text{.....(2)}$$

$$[\eta_2] = \lim_{C^0 \to C_2{}^0} (\eta_{sp}{}^0/C^0) \quad \text{.....(3)}$$

$$C_2 = C_1 + C_2{}^0 \quad \text{.....(4)}$$

For the species giving no minimum values of η_{sp}/C, the analogous curve as the Fig. 3 is obtained as is shown in the Fig. 4. Therefore C_2 $[\eta_1]$, $[\eta_2]$ values can easily be gained, although C_2 is not so clear as in the case of ionic detergents except Emasol 1112. But, for the species giving minimum values of η_{sp}/C at C_1, $\eta_{sp}{}^0/C^0$ vs C^0-curve becomes

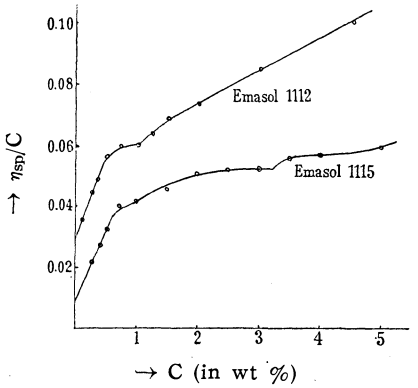


Fig. 4. Relation between η_{sp}/C and C of Emasol 1112 and Emasol 1115.

minimum at $C^0=1$ (Fig. 5). Therefore, $[\eta_1]$, $[\eta_2]$ cannot be obtained. $C^0{}_2$ is adopted as the concentration where $\eta_{sp}{}^0/C^0$ vs C^0-curve bends. The above results are summarized in the Tab. II. In the Table, C_1 (Dif.) is the

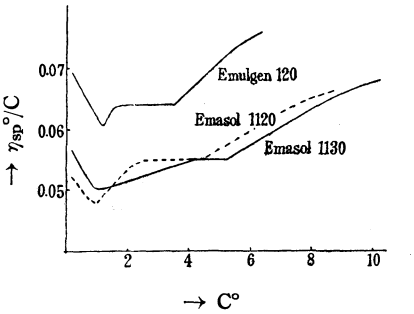


Fig. 5. Relation between $\eta_{sp}{}^0/C^0$ and C° of Emasol 1120, 1130 and Emulgen 120.

TABLE II CMC OF NON-IONIC DETERGENTS

Substance	C_1 (wt %)	C_2	C_1 (Dif.)
Emasol 1112	0∼0.3	1.10	0∼0.3
Emasol 1115	0∼0.3	3.25	0∼0.5
Emasol 1120	0.75	5.25	0∼2
Emasol 1130	0.50	5.50	0∼1
Emasol 3130	0∼0.3	1.50	.....
Emulgen 120	0.31	3.81	0∼1

concentration where the diffusion coefficient suddenly decreases as will be shown later.

(3) **Diffusion Coefficient:** In order to examine the accuracy of the diffusion cell, the diffusion of 0.1n potassium chloride solution in water was measured at 20±0.05°C. The diffusion coefficient calculated from the second moment method[10] was 168.4×10^{-7}. This value is satisfactorily consistent with the results of 0. Lamm[11] (166.6×10^{-7}) and Cohen, Bruin[12] (167.5×10^{-7}). As the accuracy of our instrument was found quite satisfactory from the above check-experiment, the following experiments were performed.

As the method of determining the diffusion coefficient from the first and second moment is too laborious and moreover very accurate data are not required in our case, the simplest inflection point method was adopted. Namely,

$$D\mu = \mu^2/2t.G^2 \quad \text{.....(5)}$$

where μ is the x-coordinate at the inflection point of a diffusion curve.

The results are shown in Fig. 6. Diffusion coefficient extrapolated to the zero concentration (D_0 (30)) at 30°C, calculated from the following equation:

$$D_{T_1}/D_{T_2} = \eta_2 T_1/\eta_1 T_2 \quad \text{.....(6)}$$

where η is the viscosity of solvent, T the absolute temperature provided that the volume of the micelle is independent of temperature, is shown in the Tab. III. It is clear from the Fig. 6 that the diffusion

10) H. Neurath, *Chem. Rev.*, **30**, 357 (1942).
11) O. Lamm, loc. cit.
12) Cohen, Bruin, *Z. Phys. Chem.*, **103**, 347 (1923).

TABLE III DIFFUSION COEFFICIENT EXTRAPOLATED TO THE ZERO CONCENTRATION AT 30°C

Substance	Emasol 1112	Emasol 1115	Emasol 1120	Emasol 1130	Emulgen 120
$D_0(30)\times10^7$	5.92	8.08	8.93	10.1	12.3

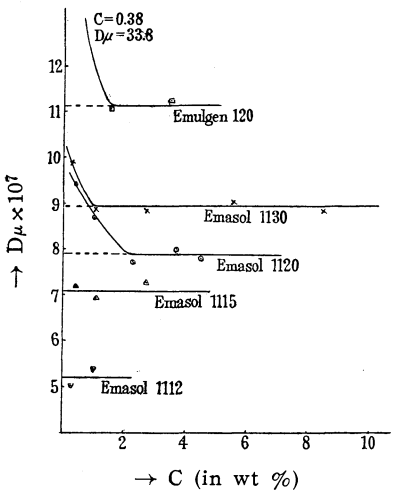


Fig. 6. Dependence of diffusion coefficient on concentration.

coefficient suddenly increases at low concentration for Emasol 1120, 1130, and Emulgen 120, but not for Emasol 1112, and 1115. Moreover, above a certain concentration, the diffusion coefficient is constant and independent of concentration. The concentration region where the diffusion coefficient suddenly increases is shown in the fourth column of Tab. II.

In the next place, the influence of electrolyte on the diffusion was examined. The addition of electrolyte to the aqueous solution of ionic detergent results in the decrease of the diffusion potential and at the same time, in the increase of the micelle size. Therefore, as a result, the diffusion coefficient decreases remarkably. But, for the aqueous solution of non-ionic detergents, the diffusion potential is small and the interaction between electrolyte and hydrophilic group is not so strong as in the case of ionic detergents. Therefore it may be supposed that the influence of electrolyte on diffusion is not so striking as in the case of ionic detergents.

TABLE IV
INFLUENCE OF ELECTROLYTE ON THE DIFFUSION OF NON-IONIC DETERGENT: EMASOL 1112, 1.5 % TO 0.75 %

KCl concentration (mol/l)	$D\mu\times10^7$
0	5.20
0.005	4.90
0.05	4.66
0.2	2.90
0.4	2.75

The used sample was Emasol 1112 and this sample was dissolved in the potassium chloride solutions of various concentrations. Diffusion of 1.5 % to 0.75 % solution was measured at 25°C. Results are shown in the Tab. IV. It is clear from the Table that diffusion coefficients moderately decrease with the increase of electrolyte concentration.

Discussion

(1) It is clear from Tab. II that the concentration at which η_{sp}/C becomes minimum is satisfactorily consistent with the concentration at which the diffusion coefficient suddenly varies. As it is rational that the rapid change of diffusion coefficient is due to the formation of micelle, it can be concluded that the concentration at which η_{sp}/C becomes minimum is CMC even for non-ionic detergents. Therefore the phenomenon that η_{sp}/C becomes minimum at CMC is the common property for both ionic and nonionic detergents and is based not only on the coulombic electrostatic interaction but also on the dipole interaction.

In the next place, it is not clear whether the diffusion coefficient becomes abnormal at C_2 (concentration at which η_{sp}^0/C^0 bends) or not, but at least for Emasol 1130, the diffusion coefficient is constant through C_2 and this fact is different from that of sodium oleate[13].

For Emasol 1112, 1115 (CMC is very low.), η_{sp}^0/C^0 vs C^0-curve is quite analogous to ionic detergents (Fig. 3). On the contrary, Emasol 1120, 1130, and Emulgen 120 show abnormality in the lower concentration region (Fig. 5).

(2) After completion of micelle formation, the diffusion coefficient is constant and independent of concentration. This phenomenon is also found in ionic detergents[14,15]. It is possible that the concentration dependence of diffusion due to the hydrodynamic and thermodynamic interaction[16] compensates with the volume effect. In this case, the diffusion coefficient is apparently

13) H. Okuyama, S. Saito and K. Tyuzyo, Presented before the 4th Annual Meeting of the Chemical Society of Japan in Tokyo, April, 1951. To be published elsewhere.
14) R. J. Vetter, *J. Phys. and Colloid Chem.*, **51**, 262 (1947).
15) O. Lamm, *Kolloid-Z.*, **98**, 45 (1942).
16) S. J. Singer, *J. Chem. Phys.*, **15**, 341 (1947). A. F. Schick and S. J. Singer, *J. Phys. and Colloid Chem.*, **54**, 1028 (1950).

constant in spite of the change of micellar volume. But this possibility is very small and micellar volume may perhaps be constant and independent of concentration.

The region where the diffusion coefficient varies suddenly covers a considerable concentration range. It cannot be concluded from this fact that the process of micelle formation is fairly gradual, because the region where the diffusion coefficient varies suddenly has a moderate width of concentration range even for ionic detergents.

(3) The influence of electrolyte on diffusion is moderately remarkable although not so much as in the case of ionic detergent.[17] The diffusion coefficient of Emasol 1112 in 0.4n potassium chloride solution is one-half what it is in pure water. This means that micellar molecular weight (M_m) becomes about eight times as great. Moreover, Emasol 1112 was dissolved in 1n, 2n, 3n, 4n aqueous solutions of potassium chloride in the concentration of 10% and was allowed to stand still for 24 hours. Then the 1n solution was almost transparent; the turbidity increased with increasing potassium chloride concentration, the 4n solution being very turbid. This behavior corresponds to the so-called "salting out" phenomenon. From this and above results, it is reasonable to consider that increase of micellar volume and salting out are equivalent phenomena in this case. It seems to be probable that with addition of electrolyte, the hydrophilic property of colloidal particles decreases and they combine with each other, increasing in size and finally they precipitate. We think this concept more probable than that the size is constant and its solubility decreases. It seems to be reasonble to classify "salting out" as follows: (a) Particle size is constant and its solubility decreases. (b) Particle size increases with the increase of electrolyte concentration. This difference may be based upon the degree of separation of hydrophilic and hydrophobic radicals in the same molecule.

(4) Assuming the micelle as a sphere, micellar molecular weight is calculated from the following equation[18]

$$M_m = \frac{(RT)^3}{162\,\pi^2\eta^3 N_A^2 D_0^3 V} \quad \cdots\cdots\cdots(7)$$

where D_0 is the diffusion coefficient extrapolated to the zero concentration, V the specific volume of the micelle which may be substituted by the partial specific volume. Results are shown in Tab. V. These values may have no important meaning, but the values of several ten thousand to hundred thousand suggest that moderately large micelles exist. This corresponds to the fact that CMC is comparatively low and may be based on the weak hydrophilic property of non-ionic detergents compared with ionic detergents.

TABLE V MICELLAR MOLECULAR WEIGHT OF NON-IONIC DETERGENT

Substance	Emasol 1112	Emasol 1115	Emasol 1120	Emasol 1130	Emulgen 120
$D_0 \times 10^7$	5.9	8.1	8.9	10.1	12.3
$M_m \times 10^{-4}$	28.9	10.1	7.8	5.8	3.1

Summary

(1) Partial specific volume, viscosity, diffusion coefficient of the aqueous solutions of non-ionic detergents are measured.

(2) η_{sp}/C becomes minimum at CMC and this concentration is quite consistent with the concentration where diffusion coefficient varies suddenly. It is interesting that this is the common phenomenon for ionic and non-ionic detergents.

(3) The form of η_{sp}^0/C^0 vs C^0-curve is analogous to that described in the first report and the second CMC (C_2) is also obtained but some abnormality occurs in the part of low concentrations for the substance of which CMC is high.

(4) After the completion of micelle formation, diffusion coefficient stays constant and is independent of concentration which suggests that micellar volume is constant and independent of concentration.

(5) The influence of an electrolyte on the diffusion is examined and a new idea of the mechanism of "salting out" is proposed.

(6) Micellar molecular weight is calculated from the diffusion coefficient assuming that a micelle is spherical.

Lastly, we heartily thank Prof. Dr. N. Sata for his kind instruction and Mr. S. Saito for his helpful suggestions. We also express our sincere thanks to Mr. R. Muneyuki of Shionogi-Seiyaku Co. Ltd. who afforded us several valuable samples and data, and Kao-Soap Co. Ltd. for offering some samples.

Department of Chemistry,
Faculty of Science,
Osaka University, Osaka

17) H. Okuyama and K. Tyuzyo, Presented before the Colloid Symposium held by the Chem. Soc. of Japan in Tokyo, November, 1951.

18) H. Neurath, loc. cit.

Sterols and Other Unsaponifiable Substances in the Lipids of Shell Fishes, Crustacea and Echinoderms. XIV. Unsaponifiable Components Other Than Corbisterol in the Lipid of Corbicula

By Yoshiyuki TOYAMA and Tatsuo TANAKA

(Received December 23, 1953)

It was indicated in the 6th report[1] of this series that a di-unsaturated sterol, apparently brassicasterol, and cholesterol in addition to corbisterol occur in the sterols from *Corbicula leana*. The present paper is concerned with a further study on the unsaponifiable components of the lipid of corbicula.

The sterol mixture separated from the unsaponifiable substances of the lipid of corbicula was converted into the steryl acetate mixture, and the latter was subjected to repeated recrystallizations until a small amount of corbisteryl acetate was finally obtained. From the mother liquors of recrystallizations the following three fractions of steryl acetate were recovered: the fraction I of m.p. 125-127°, the fraction II of m.p. 116-119° and the fraction III of m.p. 100-103°.

The fraction I was fractionally crystallized from ethanol, and the least soluble fraction thus obtained was treated with maleic anhydride to remove the component with conjugated double bonds (corbisteryl acetate) completely in form of its maleic anhydride adduct. The portion with no cunjugated double bonds (A) was subjected to a further fractional crystallization by which nine fractions (see Table II) were separated. The lst fraction consisted of an acetate of C_{29} F_2-sterol which was regarded as identical with poriferasteryl acetate. The free sterol from this acetate showed, however, a considerably lower melting point than that reported for poriferasterol. The 8th fraction consisted of an acetate of C_{29} F_1-sterol which was found to be identical with clionasteryl acetate. Hydrogenation of the 2nd fraction gave poriferastanyl (clionastanyl) acetate. These results indicate that the non-conjugated portion (A) consists chiefly of the acetates of poriferasterol and clionasterol. A portion of the fraction I was also fractionated by way of bromide. Debromination of the ether-insoluble bromide yielded a steryl acetate which was recognized as poriferasteryl acetate, but the free sterol obtained by saponification of this acetate had a melting point which was also considerably lower than that reported in the literature. Although it requires a further study on this point, it does not necessarily follow from the lower melting points of the specimens obtained in these experiments that they are inferior in purity.

The fraction II was fractionated by way of bromide, and there was obtained a bromide fraction which, after debromination, gave cholesteryl acetate. The fraction III showed m.p. 111-113° after one recrystallization and was considered to consist substantially of cholesteryl acetate.

Table I records the properties of the sterols obtained in these experiments.

It is seen from the foregoing results that the sterol mixture from corbicula contains poriferasterol, clionasterol and cholesterol in addition to corbisterol, but the presence of the F_2-sterol, apparently brassicasterol, which was found in the sterol mixture from corbicula described in the 6th report, could not be indicated. Hence another steryl acetate fraction obtained from corbicula described in the 8th report[4] was examined. This fraction was recovered from the mother liquors of recrystallizations which were performed to separate corbisteryl acetate from the steryl acetate mixture. It was then treated with maleic anhydride, by which corbisteryl acetate was completely removed in form of its maleic anhydride adduct. The non-conjugated fraction was separated and purified by recrystallization, yielding brassicasteryl acetate of m.p. 150.5-151.5° and $[\alpha]_D^{24} = -63.6°$. Accordingly brassicasterol constitutes a component of the sterol mixture from corbicula described in the 8th report. These facts appear to be ascribed to a very wide variance in the relative contents of poriferasterol, clionasterol and brassicasterol in the sterol mixtures from the different samples of corbicula; the sterol mixture from corbicula described in these experiments contains a relatively large amount of poriferasterol and

1) T. Matsumoto and Y. Toyama, *J. Chem. Soc. Japan*, **65**, 256 (1944).

2) M. Kita and Y. Toyama, *J. Chem. Soc. Japan*, **70**, 451 (1949).

TABLE I

	Free sterol		Acetate		Benzoate	
	m.p.,°C	$[\alpha]_D^{\theta}$	m.p.,°C	$[\alpha]_D^{\eta}$	m.p.,°C	$[\alpha]_D^{\theta}$
C_{29} F_2-sterol from I	141—142	—	147—148	−53.1	140.5—141	−22.2
C_{29} F_2-sterol from I, by way of bromide	145—146	−50.9	146—147	−54.6	—	—
Poriferasterol[2,3]	155—156	−49.7	146.5—147	−53	139.5—140.5	−21.9
C_{29} F_1-sterol from I	137—138	−37.1	135—136	−42.2	133—135	−17.6
C_{29} F_1-sterol from I, by way of bromide	136—137	−38.0	132—133	−40.8	—	—
Clionasterol[2]	137.5—138.5	−37	137	−41.9	134.5—135	−16.8
Stanol from I, obtained by hydrogenation	143—144	+24.5	140.5—141.5	+15.4	—	—
Poriferastanol[2]	143—144	+24.7	140—141	+16.3	—	—
Sterol from II, by way of bromide	145—146	—	114—115	−44.2	—	—
Cholesterol	148	−38	114	−43		

clionasterol but it contains brassicasterol in such a small amount that its presence could not be demonstrated, whereas the sterol mixture from corbicula described in the 8th report, like that described in the 6th report, contains a larger amount of brassicasterol. A similar fact that the content of certain sterol components in the sterol mixture from shell fish of the same species varies widely for each sample of shell fish was noted in a previous study on the sterol components of chiton in which the content of γ-cholestenol differs widely for each sample of chiton.

After separating the sterol mixture from the crude unsaponifiable substances, there was obtained a viscous oily portion (B), which was contaminated with acidic and saponifiable substances. The acetylated product of the portion (B) was subjected to a fractional distillation. There was an indication of decomposition during the distillation, yielding a total distillate in a yield of about 56% of the acetylated product. A higher fraction was saponified, the product was dissolved in acetone, the solution was cooled, and there was obtained a crystalline solid which was found to consist chiefly of a mixture of batyl and chimyl alcohols. Hydrogenation of the remainder of the saponified product gave a small amount of solid material which was considered to contain substantially batyl alcohol. Accordingly the saponified product appears to contain also an unsaturated member (selachyl alcohol) corresponding to batyl alcohol. Lower fractions were saponified, giving a product which contained a methanol-insoluble portion consisting possibly of hydrocarbons. On treating the methanol-insoluble portion with sulfuric acid, the bulk of it was converted into a tarry matter. A closer examination of the components other than alcohols of batyl alcohol series in the viscous oily portion (B) could not be performed in these experiments. However, the unidentified components including hydrocarbons were suspected to contain more or less decomposition products which might have been formed in the course of distillation.

Experimental

Preparation and Fractionation of Steryl Acetate Mixture.—Boiled meat (37.75 kg.) of corbicula was vacuum-dried at 65-75°, giving 11.44 kg. of dried material, from which 1.13 kg. of lipid was extracted with trichloroethylene.* The lipid was saponified with alcoholic potash, the diluted soap solution was treated with ether in the usual way, and there were obtained 188 g. (16.6% of lipid) of unsaponifiable substances. These were crystallized from 3.5 litres of methanol, affording 113 g. of crystalline solid (crude sterol mixture) of m.p. 132-135°. The steryl acetate mixture prepared from crude sterol was subjected to repeated recrystallizations from ethanol by which 0.3 g. of corbisteryl acetate, m.p. 151.5-152°, was separated. Concentration of the mother liquors from the 3rd and subsequent recrystallizations, the 2nd recrystallization and the lst recrystallization gave the following three fractions of steryl acetate, respectively: (1) 42 g., m.p. 125-127°; (II) 17.2 g., m.p. 116-119°; (III) 7.2 g., m.p. 100-103°.

Fractionation of Fraction I.—A portion (32 g.) of the fraction I was subjected to a further fractional crystallization from ethanol, by which

3) F. R. Valentine, Jr. and W. Bergmann, *J. Org. Chem.*, **6**, 452 (1941).

4) W. Bergmann and R. J. Feeney, *J. Org. Chem.*, **14**, 1078 (1949): W. Bergmann, F. H. McTigue, E.M. Low, W.M. Stockes and R.J. Feeney, ibid., **15**, 96 (1950).

* The fatty acid components of this lipid were studied in a previous paper by the present authors. Cf. Y. Toyama and T. Tanaka, *J. Chem. Soc. Japan*, **74**, 1016 (1953).

the least soluble fraction (5.0 g.) of m.p. 138-139° and $k_{282}=1.14$ was obtained. This was heated with maleic anhydride (1.5 g.) and xylene (30 cc.) for 10 hours at 140° in a sealed tube. After distilling off xylene under vacuum, the reaction product was saponified with alcoholic potash, and the unreacted sterol was extracted from the diluted maleate solution with ether. The ether extract (4.6 g.) showed m.p. 135-136° and $k_{282}=0$. The acetate prepared from the ether extract was fractionally crystallized from ethanol and acetone with the results given in Table II.

TABLE II

Fraction	Yield, g.	m.p., °C
1	0.82	147–148
2	0.27	145.5–146.5
3	0.27	145–146
4	0.27	142–143
5	0.39	142–143
6	0.33	139.5–140.5
7	0.48	138–139
8	0.81	135–136
9	0.84	132–133

The first fraction had $[\alpha]_D^{28}=-53.1°$,* saponification value 124.5 and iodine value by the perbenzoic acid method 110.0 (calculated for $C_{31}H_{50}O_2F_2$: saponification value 123.4, iodine value 111.6). Saponification of this fraction gave a free sterol which had m.p. 141–142° after recrystallization from ethanol. The benzoate prepared form the free sterol had m.p. 137–138° (turbid), 140.5–141° (clear) and $[\alpha]_D^{25}=-22.2°$ after recrystallization from ethanol.

The 8th fraction had $[\alpha]_D^{25}=-42.2°$, saponification value 123.9 and iodine value by the perbenzoic acid method 58.2 (calculated for $C_{31}H_{52}O_2F_1$: saponification value 122.8, iodine value 55.6).

The free sterol had m.p. 137–138° and $[\alpha]_D^{20}=-37.1°$ after recrystallization from ethanol. The benzoate had m.p. 133–135° and $[\alpha]_D^{20}=-17.6°$. The melted benzoate developed a blue-violet color in the course of its solidification.

The second fraction was hydrogenated at 60–70° in glacial acetic acid using palladium black catalyst. The product, recrystallized from ethanol, was negative for the Liebermann-Burchard reaction, and had m.p. 140.5–141.5° and $[\alpha]_D^{20}=+15.4°$. The free stanol had m.p. 143–144° and $[\alpha]_D^{20}=+24.5°$ after recrystallization from ethanol.

Fractionation of Fraction I by Way of Bromide.—A portion (10 g.) of the fraction I was dissolved in 150 cc. of ether and brominated at −10–−15°, and the insoluble bromide (1.26 g.) formed was filtered. This bromide, after being recrystallized from chloroform-methanol, had m.p. 190–191° (with decomposition), $[\alpha]_D^{12}=-42.8°$, and Br-content 42.05% (calculated for $C_{31}H_{50}O_2Br_4$ 41.28%). Debromination of this bromide gave a steryl acetate of m.p. 146–147° and $[\alpha]_D^{20}=-54.6°$.

The free sterol had m.p. 145–146° and $[\alpha]_D^{20}=-50.9°$ after recrystallization from ethanol. The ether solution separated from the ether-insoluble bromide was freed from the excess of bromine and concentrated under vacuum, and the product was fractionally precipitated by adding methanol to the ether solution. Debromination of the first precipitate (2.6 g.) and recrystallization of the debrominated product gave a steryl acetate having m.p. 132–133°, $[\alpha]_D^{20}=-40.8°$, saponification value 123.9 and iodine value* 59.6. The free sterol had m.p. 136–137° and $[\alpha]_D^{20}=-38.0°$ after recrystallization from ethanol.

Fractionation of Fractions II and III.—A portion (12.5 g) of the fraction II was dissolved in 150 cc. of ether and brominated at about −10°, and the insoluble bromide (0.5 g.) formed was filtered. The filtrate was freed from the excess of bromine and concentrated under vacuum, and the bromide was fractionally precipitated by adding methanol to the ether solution. Six precipitates were separated. Debromination of the second precipitate and recrystallization of the debrominated product gave a steryl acetate of m.p. 114–115°, $[\alpha]_D^{12}=-44.2°$, saponification value 131.1 and iodine value 64.6 (calculated for $C_{29}H_{48}O_2F_1$: saponification value 130.9, iodine value 59.2). The free sterol melted at 145–146°. Hydrogenation of the steryl acetate in glacial acetic acid in the presence of platinum black gave a stanyl acetate which had m.p. 107–108° and $[\alpha]_D^{20}=+11.9°$.

The fraction III showed m.p. 111–113° after one recrystallization from ethanol.

Separation of Brassicasterol from Sterol Mixture Described in the 8th Report.—The sterol mixture from corbicula was converted into the steryl acetate mixture, and the latter was repeatedly recrystallized to separate corbisteryl acetate (see the 8th report). From the mother liquors of recrystallization, a steryl acetate fraction (2.5 g.) of m.p. 142–143.5° and $k_{282}=2.63$ was recovered. In order to remove corbisteryl acetate completely from this fraction, it was treated with maleic anhydride. The yield of the non-conjugated fraction was about 0.6 g. due to a loss during the treatment. Recrystallization of the non-conjugated fraction from ethanol and acetone gave a steryl acetate (0.2 g.) of m.p. 150.5–151.5°, $[\alpha]_D^{24}=-63.6°$, saponification value 127.8 and iodine value 109.7 (calculated for $C_{30}H_{48}O_2F_2$: saponification value 127.3, iodine value 115.2). The free sterol from this acetate had m.p. 143.5–144.5° and $[\alpha]_D^{20}=-60.1°$ after recrystallization from ethanol.

* All rotations were taken in chloroform.

* Unless otherwise stated, the iodine values were determined by the pyridine sulfate dibromide method.

Components Other Than Sterols.—The methanol filtrate separated from the crude sterol mixture of the unsaponifiable substances contained a dark greenish-brown viscous liquid having acid value 13.3 and saponification value 41.6. This was acetylated, and a portion (35 g.) of fhe acetylated product was fractionally distilled with the results shown in Table III. There was an indication of decomposition during the distillation, and a conspicuous evolution of gas was noticed.

TABLE III

Fraction	b. p., °C/2 mm Hg	Yield, (g.)	n_D^{20}	Saponification value	Iodine value
1	—145	0.7	1.4695	133.8	54.1
2	145—170	0.9	1.4694	132.9	53.2
3	170—200	2.4	1.4671	138.9	48.2
4	200—210	3.8	1.4657	175.7	44.8
5	210—225	9.2	1.4657	187.8	42.8
6	225—227	1.8	1.4757	182.6	51.5
7	227—230	0.9	1.4827	171.8	61.4
Residue and loss		15.3			

The fractions 4, 5 and 6 were refractionated, and a fraction (3.5 g.) of b. p. 220–225°/2 mm Hg was separated. This fraction was saponified, the product was dissolved in acetone, and the solution was cooled with ice. The crystalline solid separated from the solution had iodine value 3.8, and recrystallization of this solid from acetone yielded a product (0.3 g.) of m. p. 56–57° and acetyl saponification value 266.8 (calculated for $C_{19}H_{40}O_3$: 280.1; calculated for $C_{21}H_{44}O_3$ 261.8). The oily liquid recovered from the acetone filtrate was hydrogenated at 60–70° in ethanol in the presence of Raney nickel. The hydrogenation product, after being recrystallized from 90% ethanol had m. p. 53.5–54.5°, iodine value 3.2 and acetyl saponification value 253.6.

The fractions 2 and 3 were saponified. On treating the product (2.0 g.) with 20 cc. of methanol, there was obtained 0.14 g. of methanol-insoluble portion. This was dissolved in 7 cc. of hexane, and the hexane solution was washed with an equal volume of concentrated sulfuric acid. The sulfuric acid layer became colored dark brown, and there was formed a tarry matter between the hexane and sulfuric acid layers. The hexane solution was washed several times with concentrated sulfuric acid followed by successive washing with a dilute caustic soda solution and water. After distilling off hexane from the hexane solution, there remained a small amount (30 mg.) of pale yellow liquid.

Summary

Among the sterol components of the unsaponifiable substances of corbicula, poriferasterol, clionasterol and cholesterol in addition to corbisterol are present. Among the unsaponifiable components other than sterols, the presence of a mixture of chimyl and batyl alcohols is indicated. The unsaponifiable components appear to contain also unsaturated members (selachyl alcohol series) corresponding to batyl alcohol series. Besides these components, there occur some other liquid components which contain possibly hydrocarbons. But these unidentified components appear to contain more or less the decomposition products which might have been formed during the distillation.

The sterol mixture obtained from corbicula described in the 8th report, like the sterol mixture from corbicula described in the 6th report, has been found to contain brassicasterol as a di-unsaturated sterol.

Department of Applied Chemistry,
Faculty of Engineering,
Nagoya University, Nagoya

Intermolecular Charge—Transfer Spectra. III. Organic Molecular Complexes

By Hideo MURAKAMI

(Received January 1, 1954)

In recent years, quantitative experimental studies have been undertaken concerning the absorption spectra and equilibrium constants of organic molecular complexes. We can expect that the theoretical analysis of these results will provide us with more precise information than before for their electronic structure especially for the mutual interactions between two components. In the first and second sections, we will discuss the magnitude of resonance interaction in relation with the intensities of intermolecular charge-transfer spectra. Next, the contribution of non-resonance interactions, such as van der Waals type interaction and various electrostatic interactions will be considered in comparison with the former.

The Relation between Absorption Intensity and Resonance Interaction

As is easily seen, the straightforward and quantitative calculation of resonance energy between two components is very difficult on account of the extreme complexity of the electronic system and uncertainty of the radial part of the constituent atomic wave function. It is not difficult, however, to obtain a formula which gives us a resonance interaction energy in terms of absorption intensity. Since the latter quantity is known experimentally, this formula enables us to estimate the magnitude of the former.

In the first paper of this series[1] (in the following, we refer to I) we summarized the essence of Mulliken's theory of intermolecular charge-transfer spectra in the approximation which neglects the overlap integral S between two components. In the following ,we use the simplified formulae in I, since the neglect of S does not affect the final results. According to Mulliken's theory[2], the wave function of the ground state of any molecular complex $(A\ B)$ is given by

$$\psi_N = a\,\psi_0 + b\,\psi_1 \qquad (1)$$

where ψ_0, ψ_1 is defined respectively

$$\psi_0 = \phi(A\cdot B),\quad \psi_1 = \phi(A^- - B^+)$$

In case of loose complex $(a^2 \gg b^2)$, the energy of the ground state becomes as follows,

$$W_N \simeq W_0 - H_{01}^2/(W_1 - W_0) \qquad (2)$$

where $-H_{01}^2/(W_1-W_0)$ corresponds to the resonance interaction energy and W_0 includes the exchange repulsive interaction energy together with various non-resonance interaction energies. (The derivation of Eq. (2) and the definition of W_0, W_1 and H_{01} are given in I. See Eqs. (5), (6), (7), (8) and (9) in I). From I(11), it follows

$$H_{01}^2/(W_1-W_0) \simeq b^2(W_1-W_0)/a^2 \qquad (3)$$

Further, from I (12), we obtained the relation

$$\mu_{EN}/e = Q_{EN} \simeq ab(\vec{r}_B - \vec{r}_A)$$

or

$$b^2 \simeq Q_{EN}^2/a^2(\vec{r}_B - \vec{r}_A)^2 \qquad (4)$$

Eqs. (3) and (4) provide us with the relation

$$H_{01}^2/(W_1-W_0) \simeq Q_{EN}^2(W_1-W_0)/a^4(\vec{r}_B - \vec{r}_A)^2 \qquad (5)$$

On the other hand, oscillator strength f_{EN} of transition $(E \rightarrow N)$ is given by

$$f_{EN} = (8\pi^2 mc/3h)\nu Q_{EN}^2$$

From this

$$Q_{EN}^2 = (3h/8\pi^2 mc) f_{EN}/\nu \qquad (6)$$

where

$$1/\nu = \lambda = ch/(W_E - W_N)$$

In case of loose complex, we can expect the relation

$$W_E - W_N \simeq W_1 - W_0 \qquad (7)$$

The combination of Eqs. (5), (6) and (7) provides us with the formula

$$H_{01}^2/(W_1-W_0) \simeq (3h^2/8\pi^2 m) f_{EN}/a^4(\vec{r}_B - \vec{r}_A)^2 \qquad (8)$$

If we assume

$$a \simeq 1$$

Eq. (8) is simplified as follows:

$$H_{01}^2/(W_1-W_0) \simeq (3h^2/8\pi^2 m) f_{EN}/(\vec{r}_B - \vec{r}_A)^2$$
$$= 11.5 \times 10^{-16} f_{EN}/(\vec{r}_B - \vec{r}_A)^2 ev \qquad (9)$$

In this approximation, the resonance energy is proportional to oscillator strength f_{EN} of intermolecular charge-transfer spectra and does not include the energy quentity explicitly.

In order to obtain the absolute value of the intermolecular charge-transfer interaction energy, we should take into account not only the attractive term of Eq. (8) or (9) but also the exchange repulsive term which is included in W_0 in Eq. (2). As can easily be inferred, the factors which enlarge the attractive term through the increase of H_{01} also produce the increase of exchange repulsive term by almost the same amount. Then we can expect that these two terms which have opposite signs and the nearly equal absolute value will cancel each other almost completly. This situation may probably enable us to explain the relatively large absorption intensity and the relatively small heat of formation of iodine-benzene complex.

1) H. Murakami, This Bulletin, **26**, 441 (1953).
2) R. S. Mulliken, *J. Am. Chem. Soc.*, **74**, 811 (1952).

Analysis of the Experimental Results

The absorption spectra and equilibrium constants between two components have been observed for various types of organic molecular complexes by many workers.[3-7] Their results are shown in Table I together with the representative data on halogen-aromatic complexes.[8-11] They emphasized the proportional relation between equilibrium constant K and the donor character of B-component (or the acceptor character of A-component). Since equilibrium constant K is the measure of stability of complex (strictly speaking in case of the same solvent and equal temperature), the increase of K implies the increase of attractive interaction energy. On the other hand, the increase of donor character of B-component or acceptor character of A-component seems to produce the increase of resonance interaction energy through the decrease of $(W_1 - W_0)$. (See Eq. (2)). Considering these facts, they concluded that the intermolecular charge-transfer interaction was contributing to molecular complex formation as the most essential factor.

If this is the case, Eq. (8) or (9) predicts the increase of f_{EN} with increase of K. As is well known, f_{EN} can be related with molar extinction coefficient by the formula.

$$f_{EN} = (mc^2/N\pi e^2) \cdot 10^3 \int \varepsilon_{p\tilde{a}\mu} / \log_{10} e \simeq 4.32 \times 10^{-9}\, \varepsilon_c \Delta\nu \qquad (10)$$

where $\Delta\nu$ is the half-breadth of absorption curve. Then, one has to expect the increase of ϵ_c with increase of K so long as the magnitude of $\Delta\nu$ is approximately the same for respective class of complexes. According to the data in Table I, the experimental results predict the reverse. That is, the increase of K is accompanied with the decrease of ϵ_c without exception.* In order to avoid this contradiction, one has to postulate that the contribution of intermolecular charge-transfer interaction to the total binding energy is rather smalll compared with that of the other types of

TABLE I

EXPERIMENTAL DATA FOR VARIOUS TYPES OF MOLECULAR COMPLEXES

A-Component	B-Component	Solvent	λ_{max} (Å)	ϵ_c	K	(Temperature)	Reference
s-Trinitrobenzene	Benzene	n-Heptane	2800	~4000	4.09	(21.5°)	(5)
	Aniline	Chloroform	~4000	~1550	5.1	(22°)	(4)
Oxalyl Chloride	Benzene	Heptane	2800	3333	0.27		(3)
p-Quinone	Benzene	Chloroform	2800~2900	(2800)[a]	0.42	(25°)	(7)
	Phenol	Cyclohexane	3150	1200	(0.93)[b]	(25°)	(6)
	Hydroquinone	0.05 M HCl aq. solution	4400	890	(0.97)[b]	(25°)	„
	Dimethylhydroquinone	Cychohexane	4130	370	0.60	(25°)	„
Maleic anhydride	Benzene	Chloroform	2760	3140	0.68	(25°)	(7)
	Anisol	„	3000	2020	0.84	(„)	„
	Dimethylaniline	„	4140	1590	1.5	(„)	„
Iodine	Benzene	Carbon Tetrachloride	2970	15400	1.72	(22°)	(8)
				14000	1.95	(25°)	(9)
Bromine	Benzene	Carbon Tetrachloride	2920	13400	1.04	(25°)	(10)
Chlorine	Benzene			9090	0.33	(25°)	(11)

a Extrapolated value *b* Interpolated value

3) B. D. Saksena and R. E. Kagarise, *J. Chem. Phys.*, **19**, 994 (1951).
4) J. Landauer and H. McConnell, *J. Am. Chem. Soc.*, **74**, 1221 (1952).
5) D. M. G. Lawrey and H. McConnell, *J. Am. Chem. Soc.*, **74**, 6175 (1952).
6) H. Tsubomura, This Bulletin, **26**, 304 (1953).
7) L. J. Andrews and R. M. Keefer, *J. Am. Chem. Soc.*, **75**, 3776 (1953).
8) H. A. Benesi and J. H. Hildebrand, *J. Am. Chem. Soc.*, **71**, 2703 (1949).
9) T. M. Cromwell and R. L. Scott, *J. Am. Chem. Soc.*, **72**, 3825 (1950).
10) R. M. Keefer and L. J. Andrews, *J. Am. Chem. Soc.*, **72**, 4677 (1950).
11) L. J. Andrews and R. M. Keefer, *J. Am. Chem. Soc.*, **73**, 462 (1951).

* In order to calculate the absorption intensity f_{EN} or ϵ_c, one should take into account not only the relative orientation of two components but also the following factors: 1) electron density distribution in the molecular orbitals which are essential for the intermolecular charge-transfer spectra 2) the degree of extension of each atomic orbital (for example, $2p$-function of oxygen atom is much reduced in the degree of extension than that of carbon atom). It is easy to show that these two factors make the value of $|H_{01}|$ and consequently that of ϵ_c smaller for the substituted benzene complex than that for benzene complex even if the most compact relative orientation (such as Model (α) or (β)—see later discussion) is assumed.

interactions.

Moreover, the molar extinction coefficients ϵ_c of organic molecular complexes are much smaller than those of halogen-aromatic complexes, that is about 1/10 for many cases. This fact seems to indicate to us the smallness of the intermolecular charge-transfer interaction in organic molecular complexes. Even in case of halogen-aromatic complexes, we postulated in I that the contribution of intermolecular charge-transfer interaction is negligibly small compared with that of van der Waals type interaction. Thus, in case of solution at least, we can conclude that the contribution of resonance type interaction in organic molecular complexes may be very small and the increase of K with increase of donor character of B-component may be due to the contribution of some other sorts of interactions.

In case of crystal, however, we cannot give any conclusion as to whether the contribution of intermolecular charge-transfer interaction is very small or predominant. Contrasting to the isolated 1:1 complex in solution, one molecule comes in contact with several partner molecules in case of crystal. Moreover, as was emphasized by Mulliken, intermolecular charge-transfer force has rather sharp orientational effect.[2] Consequently, there may be a case in which the relative orientation of components is governed by this force in crystal.

Non-Resonance Interactions

a) Dipole-Induced Dipole Interaction. It is evident that the van der Waals type interaction is contribution to the binding energy between two components in any molecular complex. According to our opinion, this interaction is most predominant in general. We must notice, however, that van der Waals type interaction is not characteristic for molecular complex but common for every case.

As one of the characteristic interactions, Briegleb emphasized the importance of dipole-induced dipole interaction for the molecular complexes in which A-component is polynitrobenzene and B-component is polynuclear aromatic hydrocarbon.[12] The relatively large dipole moment of NO_2 group and the large polarizability of polynuclear aromatic hydrocarbon seems to be suitable for this type of interaction. Briegleb calculated the magnitude of this interaction energy for some examples assuming the intermolecular distance as 3 Å. A part of his results is shown in Table II together with the observed heat of formation.

It is interesting to observe that the calculated and observed values of p-dinitrobenzene complex are smaller than any other case for the same B-component. This situation can be understood if we consider the relatively great distance between two NO_2 groups and the cancellation of two dipole fields due to the antiparallel orientation of two groups. Assuming the validity of the relation

$$\frac{W\ (s\text{-trinitrobenzene} \cdot \text{benzene complex})}{W\ (s\text{-trinitrobenzene} \cdot \text{anthracene complex})} \fallingdotseq \frac{W\ (p\text{-dinitrobenzene} \cdot \text{benzene complex})}{W\ (p\text{-dinitrobenzene} \cdot \text{anthracene complex})}$$

the magnitude of dipole-induced dipole interaction energy W for the case of p-dinitrobenzene · benzene complex is estimated as 0.57 Kcal/mol. If we replace p-dinitrobenzene with p-benzoquinone, this value may reduce to about 2/3, that is about 0.3~0.4 Kcal/mol on account of the smaller value of dipole moment of CO group than that of NO_2 group.

On the other hand, the magnitude of van der Waals type interaction between two benzene molecules in the most compact orientation is estimated as about 3 Kcal/mol.[13-15] Then, in case of quinone · benzene or quinone · substituted benzene complex, the magnitude of van der Waals type interac-

TABLE II

CALCULATED DIPOLE-INDUCED DIPOLE INTERACTION ENERGY W AND OBSERVED HEAT OF FORMATION ΔH IN $C_2H_2Cl_4$. (IN KCAL/MOL). BOTH DUE TO BRIEGLEB ET AL.[12]

A-Component	B-Component Anthracene	
	W	ΔH in $C_2H_2Cl_4$
o-Dinitrobenzene	3.0	2.9
m-Dinitrobenzene	1.6	1.5
p-Dinitrobenzene	1.45	1.2
s-Trinitrobenzene	4.6	3.6

W of s-Trinitrobenzene·Benzene Complex is 1.8 kcal/mol

12) G. Briegleb, *Z. physik. Chem.*, **31**B, 58 (1936). G. Briegleb, "Zwischenmolekulare Kräfte und Molekülstruktur," Stuttgart, (1937).

13) J. H. de Boer, *Trans. Faraday Soc.*, **32**, 10 (1936).

14) V. Myers, *Phys. Rev.*, **78**, 348 (1950).

15) H. A. Stuart, "Die Strucktur des Freien Moleküls", Berlin, (1952). (See p. 78)

tion may probably be ten times as great as that of dipole-induced dipole interaction. Consequently, we can expect that the relative orientation of both components in these complexes is determined by van der Waals type interaction almost completely, at least in case of solution. As is well known, two molecules which attract each other by means of van der Waals' forces will always have a tendency to orient themselves into a position where the largest possible number of atoms are in contact with each other. Thus for the case of quinone *p*-disubstituted benzene complex, we can expect the relative orientation as in Model (β). (See Fig. 2.)

b) Electrostatic Interaction In 1949, Akabori and Murakami pointed out the importance of electrostatic interaction between two components which have the complementary charge distribution.[16] For example, *p*-benzoquinone and *p*-distituted benzene (in which substituents $X^{(B)}$ are CH_3, OH, NH_2, etc.) has charge distribution as shown in Fig. 1 (1) and (2) respectively on account of

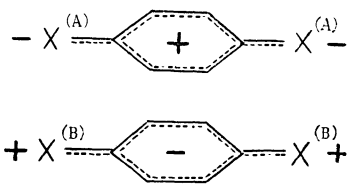


Fig. 1

the resonance effect of π-electron system. If we bring them in the relative position as in Model (β) charges of opposite sign comes nearer than in the case of any other relative orientation. Such a situation as the above suggests the contribution of Coulombic electrostatic interaction together with the van der Waals type interaction. Of course, this type of interaction is characteristic for the molecular complexes and does not exist between the same molecules.

Now we estimate the magnitude of this electrostatic interaction energy by using a point charge model. As simple and practical cases, we consider Model (α) and Model (β) which are shown in Fig. 2. We assume that each substituent $X^{(A)}$ of *A*-component has charge $-q_a$ (in electrostatic unit) and each substituent $X^{(B)}$ of *B*-component has charge q_b (also in electrostatic unit). Further, in order to simplify the calculation, we assume the uniform charge distribution in the benzene ring.

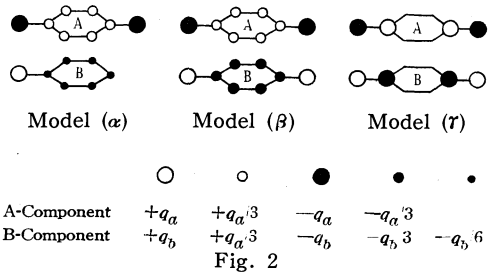


Fig. 2

Then, each carbon atom in the benzene ring of *A*-component has the charge $q_a/3$, and that of *B*-component has the charge $-q_b/6$ in Model (α) and $-q_b/3$ in Model (β). We assume that the intermolecular distance is 3 Å as was taken by Briegleb and the interatomic distances are all 1.39 Å for simplicity. Including all the attractive and repulsive interaction, we obtain the total electrostatic energy $V^{(\alpha)}$ and $V^{(\beta)}$ for Model (α) and (β) respectively as follows:

$$V^{(\alpha)} = V^{(\beta)}/2 = -0.100 \times 10^8 \qquad (11)$$

If we replace q_a and q_b with x_a and x_b which is defined by

$$q_a = ex_a,\ q_b = ex_b$$

Eq. (11) becomes as follows:

$$V^{(\alpha)} = V^{(\beta)}/2 = -1.45\, x_a x_b \text{ ev}$$
$$= -33.4\, x_a x_b \text{ Kcal/mol} \qquad (11a)$$

As another idealized model, we consider the case in which the charges in benzene ring are concentrated on 1-and 4-carbon atoms with equal proportion (Model (γ)). In this case, the straightforward calculation give the relation

$$V^{(\gamma)} \fallingdotseq 3V^{(\beta)}/4 \qquad \cdots\cdots(12)$$

Then, we can infer that the actual value is situated between $V^{(\beta)}$ and $V^{(\gamma)}$ in the cases of quinone *p*-disubstituted benzene type complexes.

The remaining task is to evaluate the magnitude of x_a and x_b for the respective molecule. Although the various methods can be adopted for this object, Sklar's method seems most attractive. According to Sklar[17] and Herzfeld[18], x_b of monosubstituted benzne is given by

$$x_b = \sum_j \Lambda_j^2 \qquad j = 2, 3 \qquad (13)$$

$$\Lambda_j = \frac{\rho_j - \omega S_j}{\omega - \omega_j} \qquad (14)$$

where

$$\omega = W + (\zeta \mid \boldsymbol{H}_R \mid \zeta) \qquad (15)$$
$$\omega_j = W_j + (\varphi_j \mid \boldsymbol{H}_{X^{(B)}} \mid \varphi_j) \qquad (16)$$

16) S. Akabori and H. Murakami, *Kagaku-no-Ryoiki* (*The Journal of Japanese Chemistry*), **3**, 10 (1949).

17) A. L. Sklar *J. Chem. Phys.* **7**, 934 (1939).

18) K. F. Herzfeld, *Chem. Rev.*, **41**, 233 (1947).

$$\rho_j = \frac{1}{2}[S_j(W+W_j)+(\varphi_j \mid \boldsymbol{H}_R+\boldsymbol{H}_{X^{(B)}} \mid \zeta)] \quad (17)$$

$$S_j=(\varphi_j \mid \zeta)$$

Here ω_j, ω are the energies of the orbitals in benzene ring R and in substituent $X^{(B)}$ as modified by the coulombic contribution of the other part, that is $X^{(B)}$ and R respectively, S_j the overlap between unoccupied orbital φ_j in R and occupied orbital ζ in $X^{(B)}$, and ρ_j the exchange integral. Numerical results for the cases of $X^{(B)}=OH$ and NH_2 have been carried out by Herzfeld,[18] Nagakura and Baba[19], and $x_b=0.075$ and 0.154 respectively. In case of $X^{(B)}=CH_3$,Ri and Eyring obtained the value $x_b=0.027$ from the rate of nitration of substituted benzene.[20] According to Herzfeld, the effect of more than one substitution ought to be additive as long as the values of A_j are sufficiently small. Then, we use twice these values for disubstituted benzene. (In case of $X^{(B)}=NH_2$, this assumption may be slightly overestimated). The charge distribution of quinone has been calculated by Nagakura and Kuboyama by the molecular orbital method.[21] Their result indicates $x_a=0.503$.

Introducing these values into Eq. (11a), the electrostatic interaction energies for Models (α), (β) and (γ) are easily obtained, and shown in Table III. The increase of interaction energy with increase of donor character of

TABLE III

CALCULATED ELECTROSTATIC INTERACTION ENERGY V IN KCAL/MOL

$X_{(B)}$	Model (α)	Model (β)	Model (γ)
CH_3	0.45	0.9	0.7
OH	1.25	2.5	1.9
NH_2	2.6	5.2	3.9

B-component may enable us to explanin the behavior of equilibrium constant K in Table I. It is evident that these interaction energies are the same order of magnitude as the dipole-induced dipole interaction energies in the case of polynitrobenzene · polynuclear aromatic hydrocarbon complexes.

Appendix

In order to complete the above discussion, we shall consider the correction factors which promote or prevent the electrostatic interaction.

Firstly, we consider the polarization effect as promoting factor. Qualitatively, it is easy to see the increase of charge separation in each component as a result of interaction between complementarily distributed charges. Here, we give a semi-quantitative discussion from the viewpoint of Eqs. (14), (15), (16) and (17). If we express the electrostatic perturbation term from the neighbouring partner molecule by $|\boldsymbol{H}|'$, ω and ω_j in the perturbed state is given by

$$\omega' = W+(\zeta \mid \boldsymbol{H}_R+|\boldsymbol{H}|' \mid \zeta) \quad (18)$$

$$\omega_j' = W_j+(\varphi_j \mid \boldsymbol{H}_X+|\boldsymbol{H}|' \mid \varphi_j) \quad (19)$$

$$\omega'-\omega_j' = (\omega-\omega_j)+[(\zeta \mid |\boldsymbol{H}|' \mid \zeta)-(\varphi_j \mid |\boldsymbol{H}| \mid \varphi_j)] \quad (20)$$

Then, For example, we assume that $|\boldsymbol{H}|'$ is the electrostatic perturbation from A-component to an electron in B-component. In this case, $(\zeta \mid \boldsymbol{H}' \mid \zeta)$ represents the decrease of effective ionization potential of substituent $X^{(B)}$ and $(\varphi_j \mid \boldsymbol{H}' \mid \varphi_j)$ represents the increase of effective electron affinity of benzene ring. (More strictly speaking, that of orbital φ_j in the ring). Elementary calculation shows that the numerical value of

$$(\zeta \mid |\boldsymbol{H}|' \mid \zeta)-(\varphi_j \mid |\boldsymbol{H}|' \mid \varphi_j)$$

is approximated by Eq. (11a) in which $x_b=-1$ and $x_a=0.503$ (the value for quinone). Then, for Model (α), we obtain the relation

$$\omega'-\omega_j' = (\omega-\omega_j)-0.73 \text{ ev}$$

According to Sklar and Herzfeld,

$$\omega-\omega_j = 12.5-7.6 = 4.9 \text{ ev}, \quad (j=2)$$

$$A_j = 0.184$$

for phenol ($X^{(B)}=OH$). By using Eq. (14), these values give us

$$\rho_j-\omega S_j = 0.902 \text{ ev}$$

In the first approximation, we assume that this value is not changed by the electrostatic perturbation. Then, perturbed value of A_2 is given by

$$A_2' = \frac{\rho_j-\omega S_j}{\omega'-\omega_j'} = 0.216$$

The relative change of electron density in the ring is given by

$$(A_2'/A_2)^2 = 1.38$$

We should emphasize that this value is rather the lower limit since the increase of the term $(\rho_j-\omega S_j)$ through the decrease of ω is neglected. It is not unreasonable to expect that the actual value of $(A_2'/A_2)^2$ exceeds 1.5. Analogous effect (though its magnitude may be small) can also be expected for A-camponent. It is evident that these situations contribute to the electrostatic interaction as promoting factor.

Next, we consider the induction effect. For the case of $X^{(B)}=OH$, some workers pointed out that the induction effect in σ-electron system might act as preventing factor.[22,23] This is the case. In OH group, however, the electron affinity of oxygen atom is reduced on account of the relatively large charge transfer from hydrogen into oxygen. Then, one can expect that the amount of σ-electron which is absorbed from neighbouring carbon by oxygen is not so great as is expected

19) S. Nagakura and H. Baba, *J. Chem. Soc. Japan*, **71**, 527 (1950).
20) T. Ri and H. Eyring, *J. Chem. Phys.*, **8**, 433 (1940).
21) S. Nagakura and A. Kuboyama, *J. Chem. Soc. Japan* **74**, 499 (1953).
22) K. Higasi, *Yakugaku Kenkyuu*, **21**, 143 (1949).
23) K. Suzuki and S. Seki, This Bulletin, **26**, 372 (1953).

from the bond moment 0.81 D of C—O bond. As is well known, this bond moment is obtained from the dipole moment of dimethyl-ether and cannot be used as that of C—O bond in C—OH group. In case of $X^{(B)}=NH_2$, electron affinity of the nitrogen atom is much smaller than that of the oxygen atom. Moreover, there are two hydrogen atoms which reduce the effective electron affinity of the nitrogen atom. Accordingly, the induction effect may probably be negligible for C—N bond in $C—NH_2$ group.

The author wishes to express his sincere gratitude to Prof. S. Akabori for his ceaseless interest and encouragement throughout the course of this series.

Department of Chemistry Faculty of Science, Osaka University, Osaka

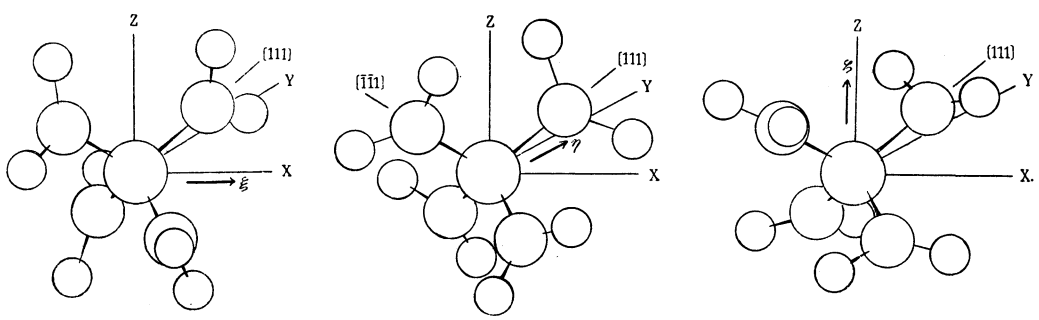
On the Diffuse Scattering of X-Rays by Single Crystals of Tetranitromethane[1)]

By Tsutomu ODA and Takeo MATSUBARA[2)]

(Received January 7, 1954)

Introduction

Oda, Iida, Watanabé and Nitta[3,4,5)] reported the crystal structure of cubic tetranitromethane using Laue and oscillation photographic data ($a=7.08$ Å $Z=2$, $T^3_d-I\bar{4}3m$). The observed high symmetry of the crystal, $T^3_d-I\bar{4}3m$, was explained by a statistical arrangement of the atomic groups or molecules within the crystal. In other words, the central carbon atoms of the two molecules in the unit cell lie at the positions 000 and $\frac{1}{2}\frac{1}{2}\frac{1}{2}$, and the eight nitrogen atoms on the four body-diagonals with the C—N bond axes are parallel to each of the other molecules, the orientation of the pairs of oxygen atoms in the nitro groups being, however, in certain disorder around the respective C—N bond axis. The simplest model will be the one in which all the pairs of oxygen atoms rotate freely around the C—N bond axes. A calculation[5)*] was carried out based on this model and the result explains well the observed intensities of Bragg reflections and the circular diffuse halo, the maximum occurring at 32° for Cu K_α. In addition to



(a) (b) (c)

Fig. 1. The three different orientations of molecules in the crystal

1) The main part of this paper was read before the Kansai meeting of the Phyiscal Society of Japan held at Osaka on January 13, 1950.

2) Present address: Department of Physics, Faculty of Science, Hokkaido University, Sapporo.

3) T. Oda, T. Iida and I. Nitta, *J. Chem. Soc. Japan*, **64**, 616 (1943).

4) T. Oda and T. Watanabé, *J. Chem. Soc. Japan*, **65**, 154 (1944). see also; P. H. Lindenmeyer and P. M. Harris, *J. Chem. Phys.*, **21**, 408 (1953).

5) T. Oda and I Nitta, *J. Chem. Soc. Japan*, **65**, 621 (1944).

*) The calculation has given the x-ray diffuse scattering expressed by

$$N(K^{\circ}-K')=Nf^2_0\{8+\sum_n^{1,2,3,4}2J_0(2c_n)-\sum_n^{1,2,3,4}4J_0^2(c_n)\}, \quad (1)$$

in which N is the number of molecules, f_0 the atomic structure factor for oxygen, $J_0(c_n)$ the Bessel function of the zeroth order with the argument c_n, c_n being

$$c_n=4\pi(\rho/\lambda)\sin(\chi/2)\sin(\alpha_n),$$

where χ is the scattering angle, α_n the angle between the reflecting plane and the plane of the two rotating oxygen atoms in the n-th nitro group in the molecule, ρ the radius of the oxygen orbit. It may be added here that this equation is essentially the same as the one (4.237) in Zachariasen's "*Theory of X-Ray Diffraction in Crystals*", 1945 p. 224.

these spot-like diffuse scattering was observed. In this paper we will show a more detailed analysis of the structure taking into consideration the mutual correlation between molecules, which enables us to explain such spot like diffuse scattering.

Theoretical

We shall assume, to simplify matters, a flat-shaped molecule having the symmetry $D_{2d}-\bar{4}2\,m$ (Fig. 1 (a), (b), (c)) which is not very different from the model given by Stosick[6] from his electron diffraction study on gaseous tetranitromethane. We shall take the X-axis in Fig. 1 (a), which is the four-fold alternating axis of the symmetry $D_{2d}-\bar{4}2\,m$, as the molecular axis. It can be shown that by the simultaneous rotation of the four nitro groups, the molecular axis will be brought into Y-(Fig. 1 (b)) or Z-axis (Fig. 1 (c)), the positions of the nitrogen atoms remaining unchanged.

Let us denote by $P_l(x_0x_l)$ the probability that the orientational character of the molecule at the l-th lattice point will be of the kind x_l, when the one at the origin is of the kind x_0. We shall normalize $P_l(x_0x_l)$ as

$$\sum_{x_0}P_l(x_0x_l)=\sum_{x_l}P_l(x_0x_l)=1 \quad .$$

Since, in the present case, x is assumed to possess three possibilities corresponding to molecular orientation in the directions of X, Y and Z axes, we shall designate them further as ξ, η and ζ. As the averaged crystal structure is a body-centered one, there are eight nearest lattice points about the l-th lattice point, which we shall designate as 1, 2, 3,⋯, μ,⋯,8. The probability $W(x_1x_2\cdots x_\mu\cdots x_8;x_l)$ that the l-th is of the kind x_l if the ones surrounding it are of the kinds x_1, x_2,⋯,x_μ,⋯,x_8 is now introduced. Then

$$P_l(x_0x_l)=\sum_{x_1}^{\xi,\eta,\zeta}\cdots\sum_{x_8}^{\xi,\eta,\zeta}\prod_{\mu=1}^{8}P_\mu(x_0x_\mu)W(x_1x_2\cdots x_\mu\cdots x_8;x_l) \qquad \cdots\cdots(2)$$

When correlation is not large, $P_l(x_0x_l)$ will take a finite value, 1/3, for large value of l.

Introducing,

$$P_l(x_0x_l)=(1/3)+R_l(x_0x_l),$$

and using the normalization condition for $W(x_1\cdots x_\mu\cdots x_8;x_l)$,

$$\sum_{x_1}\cdots\sum_{x_8}\left(\frac{1}{3}\right)^8W(x_1\cdots x_\mu\cdots x_8;x_l)=\frac{1}{3},$$

it follows that, dropping the suffix zero of x_0,

$$R_l(x\,x')=\sum_{\mu=1}^{8}\sum_{x''}^{\xi,\eta,\zeta}R_\mu(x\,x'')A_\mu(x''\,x')+N_l(x\,x'), \quad \cdots(3)$$

in which

$$A_\mu(x''\,x')=\sum_{x''_1}\cdots\sum_{x''_{\mu-1}}\sum_{x''_{\mu+1}}\cdots\sum_{x''_8}\left(\frac{1}{3}\right)^{8-1}W(x''_1x''_2\cdots x''_{\mu-1}x''x''_{\mu+1}\cdots x''_8;x'),$$

where $\sum_{x''_1}\cdots\sum_{x''_8}$ means that the summation is to be carried out over three orientations for each of the seven molecules surrounding the l-th lattice point, the μ-th neighbouring molecule being fixed to the orientation x''. In other words, $A_\mu(x''x')$ means the probability that the molecule at the l-th lattice point is of the kind x' when the one at the μ-th neighbouring point is of the kind x''. $N_l(x\,x')$ is the non-linear term of $R_l(x\,x')$.

Expressing the potential energy between two neighbouring molecules by $V_\mu(x''x')$, it is easily shown by symmetry consideration that

$$V(\xi,\xi)=V(\eta,\eta)=V(\zeta,\zeta)$$
$$V(\xi,\eta)=V(\xi,\zeta)=V(\eta,\xi)=V(\eta,\zeta)=V(\zeta,\xi)=V(\zeta,\eta).$$

Since $A_\mu(x''x')$ is expected to be proportional to the Boltzman factor $\exp\{-V_\mu(x''x')/kT\}$, we may assume that

$$A(\xi,\xi)=A(\eta,\eta)=A(\zeta,\zeta)=(1+2\alpha)/3,$$
$$A(\xi,\eta)=A(\xi,\zeta)=A(\eta,\xi)=A(\eta,\zeta)=A(\zeta,\xi)=A(\zeta,\eta)=(1-\alpha)/3,$$

where α is a function depending upon potential and temperature.

Let $\mathbf{b}=(\sigma-\sigma_0)/\lambda$ where λ is the wave length of the x-rays, σ_0 and σ the unit vectors expressing the directions of the incident and scattered rays. The averaged intensity of scattered x-rays will be given by

$$<I(\mathbf{b})>_{\text{Av.}}=\sum_l\sum_{l'}\sum_{x_l}\sum_{x_{l'}}(1/3)P_{l'-l}(x_lx_{l'})f(x_l)f^*(x_{l'})\exp\{2\pi i(\mathbf{b},\mathbf{r}_{ll'})\}, \qquad \cdots\cdots(4)$$

where $f(x_l)$ represents the "molecular" structure factor for the molecule at the l-th lattice point and $\mathbf{r}_l$ its position vector, $\mathbf{r}_{l\,l'}$ being $\mathbf{r}_l-\mathbf{r}_{l'}$. This equation can be put into the following form[7],

$$<I(\mathbf{b})>_{\text{Av.}}=I_1(\mathbf{b})+I_2(\mathbf{b}), \qquad \cdots\cdots(5)$$

in which

$$I_1(\mathbf{b})=\text{Spur}(\boldsymbol{F}\boldsymbol{S}_0),\quad I_2(\mathbf{b})=\text{Spur}(\boldsymbol{F}\boldsymbol{S}_1), \qquad \cdots\cdots(6)$$

$$\boldsymbol{S}_0=\left(\frac{1}{3}\right)^2\boldsymbol{I}\sum_l\sum_{l'}\exp\{2\pi i(\mathbf{b},\mathbf{r}_{ll'})\} \qquad \cdots\cdots(7)$$

$$\boldsymbol{S}_1=\frac{1}{3}N\sum_l\boldsymbol{R}_l\exp\{-2\pi i(\mathbf{b},\mathbf{r}_l)\}, \qquad \cdots\cdots(8)$$

$\boldsymbol{I}$ being a matrix whose elements are all one, $\boldsymbol{R}_l$ a matrix whose elements are $R_l(x\,x')$ and N the number of molecules in the crystal. $\boldsymbol{F}$ is a matrix whose elements are products of two "molecular" structure factors for the various orientations. In the present case

$$\boldsymbol{F}=\begin{pmatrix} f_\xi^*f_\xi & f_\xi^*f_\eta & f_\xi^*f_\zeta \\ f_\eta^*f_\xi & f_\eta^*f_\eta & f_\eta^*f_\zeta \\ f_\zeta^*f_\xi & f_\zeta^*f_\eta & f_\zeta^*f_\zeta \end{pmatrix}$$

In (5) I_1 stands for the Laue-Bragg scattering and I_2 for the diffuse scattering. Since $\boldsymbol{R}_l$ tends to zero for large value of l, it is possible[8] to calculate (8) and (6) by an approximate estimation of $\boldsymbol{R}_l$ for small values of l.

From (3) one finds, by introducing matrices $\boldsymbol{A}_\mu$ and $\boldsymbol{N}_l$ whose elements are $A_\mu(x''\,x')$ and $N_l(x\,x')$ respectively, the following expression,

$$\boldsymbol{R}_l=\sum_{\mu=1}^{8}\boldsymbol{R}_\mu\boldsymbol{A}_\mu+\boldsymbol{N}_l,$$

or, noting that $\boldsymbol{R}_\mu\boldsymbol{I}=0$,

6) A. J. Stosick, *J. Am. Chem. Soc.*, **61**, 1127 (1939).

7) T. Matsubara, *X-Rays*, **6**, 15 (1950).

8) T. Oda, *X-Rays*, **5**, 95 (1949).

$$\boldsymbol{R}_l=\sum_{\mu}\boldsymbol{R}_\mu\boldsymbol{A}'_\mu+\boldsymbol{N}_l, \qquad \cdots\cdots(9)$$

where

$$\boldsymbol{A}'_\mu=\boldsymbol{A}_\mu-\frac{1}{3}\boldsymbol{I}.$$

In the present case, $\boldsymbol{A}'_\mu$ is independent of μ and equal to

$$\boldsymbol{A}'=\frac{\alpha}{3}\begin{pmatrix}2&-1&-1\\-1&2&-1\\-1&-1&2\end{pmatrix}$$

The summation over l of (9) multiplied by exp $\{-2\pi i(\mathbf{b},\ \mathbf{r}_l)\}$ gives

$$\boldsymbol{S}_1=\boldsymbol{NM}(\boldsymbol{E}-\boldsymbol{B})^{-1}, \qquad \cdots\cdots(8')$$

where $\boldsymbol{E}$ is the unit matrix, and

$$\boldsymbol{B}=\sum_{\mu=1}^{8}\varepsilon_\mu\boldsymbol{A}'_\mu, \quad \varepsilon_\mu=\exp\{-2\pi i(\mathbf{b},\ \mathbf{r}_\mu)\},$$

$\mathbf{r}_\mu$ being a position vector expressing one of the eight lattice points measured from their central point, and

$$\boldsymbol{M}=\frac{1}{3}\sum_{l}\boldsymbol{N}_l\exp\{-2\pi i(\mathbf{b},\ \mathbf{r}_l)\}. \qquad \cdots\cdots(10)$$

In this case $\boldsymbol{B}$ is given by

$$\boldsymbol{B}=8(\cos\pi H\cos\pi K\cos\pi L)\boldsymbol{A}',$$

where $H=(\mathbf{b},\ \mathbf{a}_1)$, $K=(\mathbf{b},\ \mathbf{a}_2)$, $L=(\mathbf{b},\ \mathbf{a}_3)$ corresponds to a point in the reciprocal space, $\mathbf{a}_1$, $\mathbf{a}_2$, $\mathbf{a}_3$ being the cubic vector set.

By transforming $\boldsymbol{B}$ into the diagonal matrix, $I_2(\mathbf{b})$ is expressed as follows:

$$I_2(\mathbf{b})=N\sum_{i=1}^{3}\frac{m_{ii}}{1-\lambda_i}$$

where $\lambda_1=0$, $\lambda_2=\lambda_3=8\alpha\cos\pi H\cos\pi K\cos\pi L$, and m_{ii} corresponds to diagonal elements of the matrix $\boldsymbol{UFMU}^{-1}$ or $\boldsymbol{UFU}^{-1}\ \boldsymbol{UMU}^{-1}$, $\boldsymbol{U}$ being unitary and

$$U=\begin{pmatrix}1/\sqrt{3}&1/\sqrt{3}&1/\sqrt{3}\\1/\sqrt{2}&0&-1/\sqrt{2}\\1/\sqrt{6}&-2/\sqrt{6}&1/\sqrt{6}\end{pmatrix}$$

which has been used in the diagonalization of $\boldsymbol{B}$. $\boldsymbol{UFU}^{-1}$ is calculated as

$$\begin{pmatrix}(1/3)\ f_\xi+f_\eta+f_\zeta\ ^2 & (1/\sqrt{6})\ (f_\xi^*+f_\eta^*+f_\zeta^*)\ (f_\xi-f_\zeta) & (1/\sqrt{23})\ (f_\xi^*+f_\eta^*+f_\zeta^*)\ (f_\xi+f_\zeta-2f_\eta)\\ (1/\sqrt{6})\ (f_\xi^*-f_\zeta^*)\ (f_\xi+f_\eta+f_\zeta) & (1/2)\ |f_\xi-f_\zeta|^2 & (1/2\sqrt{3})\ (f_\xi^*-f_\zeta^*)\ (f_\xi+f_\zeta-2f_\eta)\\ (1/3\sqrt{2})\ (f_\xi^*+f_\zeta^*-2f_\eta^*)\ (f_\xi+f_\eta+f_\zeta) & (1/2\sqrt{3})\ (f_\xi^*+f_\zeta^*-2f_\eta^*)\ (f_\xi-f_\zeta) & (1/6)\ |f_\xi+f_\zeta-2f_\eta|^2\end{pmatrix}$$

If we neglect all higher terms except the one for $l=0$ in (10), $\boldsymbol{M}$ and $\boldsymbol{UMU}^{-1}$ are given as follows:

$$\boldsymbol{M}\fallingdotseq(1/3)\boldsymbol{N}_0 \text{ and } \boldsymbol{N}_0=\boldsymbol{R}_0-\sum_{\mu=1}^{8}\boldsymbol{R}_\mu\boldsymbol{A}'.$$

$\boldsymbol{R}_0$ can be written as

$$\boldsymbol{R}_0=\boldsymbol{E}-(1/3)\boldsymbol{I}=\frac{1}{3}\begin{pmatrix}2&-1&-1\\-1&2&-1\\-1&-1&2\end{pmatrix}.$$

Hence, if we take $\boldsymbol{R}_\mu=\boldsymbol{R}_0\boldsymbol{A}'$, $\boldsymbol{UMU}^{-1}$ becomes

$$\boldsymbol{UMU}^{-1}=\begin{pmatrix}0&0&0\\0&m'_{22}&0\\0&0&m'_{33}\end{pmatrix},$$

where $m'_{22}=m'_{33}=(1-8\alpha^2)/3$. From these calculations it follows that

$$I_2(\mathbf{b})=N\left(\frac{1}{3}\right)^2(1-8\alpha^2)\frac{|f_\xi-f_\eta\ ^2+|f_\xi-f_\zeta|^2+|f_\eta-f_\zeta|^2}{1-8\alpha\cos\pi H\cos\pi K\cos\pi L}, \qquad \cdots\cdots(11)$$

where

$$f_\xi-f_\eta=f_0\{(C_\xi-C_\eta)+i(S_\xi-S_\eta)\},$$
$$f_\xi-f_\zeta=f_0\{(C_\xi-C_\zeta)+i(S_\xi-S_\zeta)\},$$
$$f_\eta-f_\zeta=f_0\{(C_\eta-C_\zeta)+i(S_\eta-S_\zeta)\},$$

and

$$C_\zeta=4\cos2\pi Lz(\cos2\pi Hx\cos2\pi Ky+\cos2\pi Kx\cos2\pi Hy)$$
$$S_\zeta=-4\sin2\pi Lz(\sin2\pi Hx\sin2\pi Ky+\sin2\pi Kx\sin2\pi Hy),$$

f_0 being the atomic structure factor for oxygen atoms and x, y, z its parameters.

Discussion of the Results

When $\alpha=0$, $I_2(\mathbf{b})$ becomes

$$N(1/3)^2\{|f_\xi-f_\eta|^2+|f_\xi-f_\zeta|^2+|f_\eta-f_\zeta|^2\}, \qquad \cdots(12)$$

or

$$N\{(1/3)(|f_\xi|^2+|f_\eta|^2+|f_\zeta|^2)-|(f_\xi+f_\eta+f_\zeta)/3|^2\}.$$

This last equation is equivalent to

$$N\{<|f(x)|^2>_{\text{Av.}}-|<f(x)>_{\text{Av.}}|^2\},$$

which was derived in the previous paper[5] dealing with free axial rotation of nitro-groups. These equations account well for the observed halo-type diffuse scattering.

Now we will discuss the case where $\alpha\neq0$. Since there is no long-range order with respect to molecular orientation, the correlation between neighbouring molecules would be small, in other words, the value of $|\alpha|$ will not be large. So we may assume $1>8|\alpha|$. The sign of α depends upon the interaction energy $V(xx')$ between two neighbouring molecules. For example if $V(\xi,\ \xi)>V(\xi,\ \eta)$, then $\alpha<0$, and on the other hand if $V(\xi,\ \xi)<(\xi,\ \eta)$, then $\alpha>0$.

Since the function

$$|f_\xi-f_\eta|^2+|f_\xi-f_\zeta|^2+|f_\eta-f_\zeta|^2 \qquad \cdots\cdots(12')$$

changes slowly with $\mathbf{b}$, one finds that the sharp maxima of I_2 $(\mathbf{b})$ occur in the directions for which $1-8\alpha\cos\pi H\cos\pi K\cos\pi L$ possesses minimum value. When $\alpha<0$, such

directions are given by H, K, L with integers and $H+K+L=2n+1$. When H, K, L are integers, we have $H=h$, $K=k$ and $L=l$. However diffuse spots associated with {110}, and {112} (Table I) appeared. Hence, the assumption that α is negative leads to disagreement with the observation, provided that the observed diffuse spots are to be explained only by the correlation of the orientations of molecules, disregarding the influence of thermal motions. On the other hand if we take $\alpha>0$, then the maxima of I_2 (**b**) occur for the directions **b**(corresponding to $h+k+l=2n$), in agreement with the observation.

TABLE I

OBSERVED INTENSITIES OF MAXIMA OF THE DIFFUSE SPOTS WITH THE DIRECTIONS $H=h$, $K=k$ AND $L=l$ AND THEIR CALCULATED VALUES

HKL	Obs.	Calc*
110	st.	29.6
200	w.	0.9
112	st.	19.2
220	w.	12.0

* In the calculation the polarization and the usual temperature fators have been also taken into account, B in $\exp\{-B\sin^2(\chi/2)\}$ being given as 3.

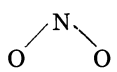
We may assume that the potantial energies $V(x\,x')$ depend primarily upon the interaction between oxygen atoms of neighbouring molecules. The calculation of the distances between these oxygen atoms was carried out, taking the bond distances of C—N, N—O as 1.47, 1.21 Å and the bond angle  as 127°. The results are shown in Table II. In this case, we could expect that the potential energies for the two kinds of mutual orientations would not differ very much, so that $|\alpha|$ would be of a small value. It is, however, difficult to decide conclusively from such a qualitative consideration which one of these two is more stable and has a higher probability.

TABLE II

CALCULATED VALUES OF THE INTERMOLECULAR ATOMIC DISTANCES BETWEEN OXYGEN ATOMS

I	II
2.73 Å	2.92 Å
2.73	3.12
3.69	3.44
3.69	3.67
3.96	3.69
3.96	3.96

I stands for the parallel orientation ξ, ξ and II for the perpendicular ξ, η.

In the theory stated above, it is seen that when $\alpha>0$, the maxima depend upon the values of (12′). In Table I are tabulated the calculated values of this equation, with the parameter values $x=0.28$, $y=0.11$, $z=0.16$ which are close to those $x=0.2675$, $y=0.054$, $z=0.1607$ derived from the bond-lengths and bond-angles as mentioned above. As is seen the calculation explained qualitatively the observed results. Further approximation will be attained by examination of the more appropriate model[4,6] of the molecule having the symmetry S_4—$\bar{4}$ and by taking into consideration of the lattice vibrations[9].

In conclusion the authors wish to express their sincere thanks to Professor I. Nitta, Professor T. Watanabé and Professor T. Nagamiya, Faculty of Science of Osaka University, for their available discussion and kind encouragement throughout this research.

Chemical Laboratory, Osaka Liberal Arts University, Osaka; Faculty of Science, Osaka University, Osaka

9) H. Faxén, *Z. Physik*, **17**, 266 (1923). I. Waller, *Z. Physik*, **17**, 398 (1923). W. H. Zachariasen, *Phys. Rev.* **57**, 597 (1940); **59**, 860 (1941). G. H. Beglie and C. M. Born, *Proc. Roy. Soc.* A **188**, 179, 189 (1947).

Perjodat-Oxydation von Ovalbumin

Von Kazuyuki MAEKAWA und Masahisa KUSHIBE

(Eingegangen Am 7, Januar, 1954)

Früher wurden häufig die Oxydationsagenzien wie Permanganate, Wasserstoffsuperoxyd, Chromsäure angewandt, um die Strukture der Eiweissstoffe mit Hilfe von Oxydation zu erklären. Bei diesen Versuchen sind sie jedoch so kräftig, dass verschiedene Stelle an dem Molekül angegriffen und damit die Reaktion kompliziert wird. Ausser bei den verhältnismässig einfachen Eiweissstoffen brachten die solchen Versuche kein ergiebiges Ergebnis[1,2]. Hinsichtlich der Beziehungen zwischen der Strukture der Eiweissstoffe und ihrer physiologischen Wirkung brachte die direkte Oxydation von Eiweissstoffen fast nichts zu Tage.

Dagegen wurden neulich einige Versuche veröffentlicht, native Eiweissstoffe unter verhältnismässig milden Bedingungen zu oxydieren. Goevel et al. fanden z.B., dass Virus, *„Western equine encephalomylitis"*, infolge der Perjodat-Oxydation seine Pathogenität verliert, dabei aber seine antigenische Spezifität zurückbleibt[3]. Ferner folgerten Goebel und Perlmann[4] aus den Veränderungen an Absorptionsspektrum und elektrophoretischer Mobilität, dass sich einige Amino-Säuren zerstören liessen, indem sie mittels $LiIO_4$ Rinde Serumalbumin oxydierten.

Desnuelle et al. berichteten[5], dass Ovalbumin durch Perjodat allmählich niedergeschlagen wurde, und dass sämtlich Cystein, Cystin, ein Teil von Tyrosin und ein Drittel von Tryptophan in dem koagulierten Ovalbumin zersetzt wurden. Vor kurzer Zeit behandelten Jansen et al.[6] mit Perjodat α-Chymotrypsin und gewannen Oxy.-α-Chymotrypsin, welche opt. *p*H mehr oder weniger verschob.

Betreffs Chemismus von Eiweiss-Oxydation befindet sich aber die eingehende Forschung noch nicht.

Schon berichtete einer von uns gemeinsam mit M. Hamada[7], dass verschiedenartige Eiweissstoffe gewissermassen das Oxydant verbrauchten und dabei gewisses Ammoniak und Aldehyd entstanden. Jedoch muss noch erklärt werden, dass dieser scheinbare Perjodat-Verbrauch von Protein verrichtet wurde, um welche Stelle von dem Proteinmoleküle wirklich zu oxydieren, und was Protein folgendessen für eine Veränderung physikalisch erlitt, und auch welche Aminosäuren welcherweise sich zersetzten. Um weiteres darüber zu erklären und zur Kenntnisse der physiologischen Wirkung und Strukture zu kommen, nahmen die Verfasser die folgenden Untersuchungen vor.

Beschreibung der Versuche

I. Direkte Oxydation von kristallizierten Ovalbumin durch Perjodat. Ovalbumin, welches nach gewöhnlichen Verfahren dargestellt, mehrfach umkristallisiert und dialyziert wurde, wurde in Michaelis'schen Phosphat-Puffer von *p*H 7.7 aufgelöst, um 5～20 mg/ccm von Eiweisslösung darzustellen. $NaIO_4$ wurde aus Wasser umkristallisiert und in demselben Puffer von *p*H 7.0, als 0.1～0.01 N Lösung gelöst. Unter Benutzung von beiden Lösungen wurden die Bestimmung von Oxydant-Verbrauch und die Darstellung von oxydierten Proben folgendermassen jede für sich verrichtet.

(A). 10 ccm dieser Ovalbuminlösung wurde in 50 ccm Glasstöpselflaschen pipettiert, hierzu wurde 20 ccm 0.02 N Natriummeta-Perjodat Lösung zugesetzt, diese wurde bei Zimmertemperatur unter gelegentlicher Pipettierung gelassen. 1 ccm von der ausgezogenen Lösung wurde mit 10 ccm gesättigter $NaHCO_3$-Lösung und 1 ccm 10%-iger KJ Lösung versetzt, danach mit 1 ccm 0.5% Stärkelösung, zuletzt mit Wasser bis zu 50 ccm

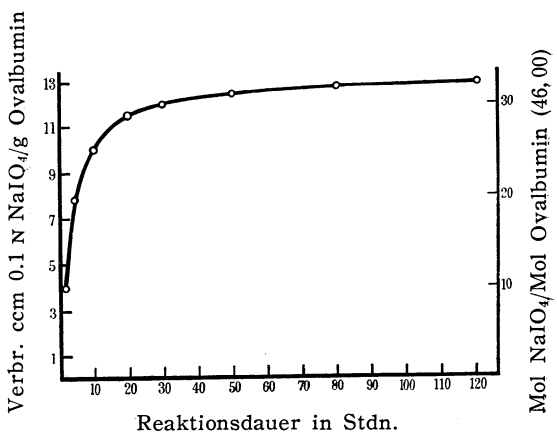


Fig. 1 Perjodat-Verbrauch von Ovalbumin.

1) S. Goldschmidt, und K. Straus, *Ann.*, **480**, 263 (1930).
2) R. M. Herriott, "Adv. in Protein Chem.", **3**, 175 (1947).
3) W. F. Goebel, P. K. Olitsky und A. C. Saenz, *J. Exp. Med.*, **87**, 445 (1948). zitiert aus *C.A.*, **42**. 5552 (1948).
4) W. F. Goebel und G. E. Perlmann, *J. Exp. Med.*, **88**. 479 (1949).
5) P. Desnuelle, S. Antonin und A. Casal, *Bull. soc. chim. biol.*, **29**. 694 (1947).
6) E. F. Jansen, A. L. Curi und A. K. Balls *J. Biol. Chem.*, **189**, 671 (1951).
7) M. Hamada und K. Maekawa, *Sci. Bull. Fac. Agric., Kyusyu Univ.*, **13**, 180 (1951).

gefüllt. Der dabei entstandene Farbenton wurde unter Anwendung von Filter 570 mμ bestimmt. Differenz der Daten für Blindprobe bezeigt Perjodat-Verbrauch. Die dabei gefundenen Ergebnisse sind wie folgende:

Wie man aus der Figur erkennt, ging die Oxydation anfangs bis zur 20 M/M Ovalbumin verhältnismässig schnell vor sich, es bedurfte aber eines Tages, um 30M von Perjodat zu verbrauchen. Diese Ziffer zeigt also, dass die von Perjodat oxydierte Stelle durchschnittlich bei Ovalbumin im Verhältnis von 1 Stelle pro 12~13 Aminosäurereste steht, wenn die Summe der Aminosäurereste in Ovalbumin als 402 angenommen wird[8].

(B). Zur Darstellung von Oxy.-Ovalbumin wurde folgendes Verfahren angewandt. Zu 200 ccm von Ovalbuminlösung (5.5 mg/ccm) wurden je 4.5 ccm (a), 9 ccm (b) und 13.5 ccm (c) von 0.1 N $NaIO_4$ Lösung zugesetzt, und diese Gemische wurden 15 Stunden lang in der Zimmertemperatur (12°) gelassen. Nachdem so gestanden, zeigten die Reaktionsgemische *p*H 6.6~6.8 und enthielten kein Perjodat ausser (c). Hierzu wurden gesättigte Ammoniumsulfatlösungen in folgenden Raten versetzt, um oxydiertes Ovalbumin niederzuschlagen.

(a) 1 ccm Lösung: 2.3 ccm $(NH_4)_2SO_4$—Lösung
(b) „ : 2.0 „
(c) „ : 1.6 „

Jeder Niederschlag wurde in Wasser gelöst und mit Ammoniumsulfat wieder behandelt. Die Umlösung wurde so oft wiederholt, bis Jodverbindung nicht mehr erkennbar war. Die wässerigen Probelösungen wurden zuletzt zu *p*H 5.3~5.5 zubereitet, mit Ammoniumsulfat versetzt, bis sich eine kaum bemerkbare Trübung zeigte, und so gelassen, um die oxydierten Proben zu fällen.

Jede Probe der erhaltenen Oxy.-Ovalbumine ist anscheinend mit Ovalbumin ganz ähnlich.

II. Veränderung in Zusammensetzung infolge der Oxydation. An den oben erwähnten oxyproben wurden Aminosäuren bestimmt, welche erwarten liessen, vermutlich oxydative Zersetzung zu erleiden. So wie es ist, unmittelbar oder nach Hydrolyse mittels Säuren oder Baryta wurde Aminosäure-bestimmung nach verchiedenem Verfahren und mutatis mutandis verrichtet. Die Resultate sind in der Tafel I zusammengestellt.

TABELLE I
VERÄNDERUNG IN ZUSAMMENSETZUNG INFOLGE DER OXYDATION

Probe / Oxydationsgrad	a 10 Mol. $NaIO_4$	b 20 Mol. $NaIO_4$	c 30 Mol. $NaIO_4$	Oxy-gelatin	Oxy-Haare
Ausbeute	90 %	83 %	64 %		
$[\alpha]_D^{20}$, (*p*H 7.7)	—55.5°	—55.5°	—83.3°	—118.3°	
Tryptophan	0.2 %	0	0		
Histidin	2.35%	2.33%	2.33%		
HS—	0	0	0		
Arginin	5.5$_0$%	5.3$_4$%	4.8$_1$%	(88%)*	
Tyrosin	3.6$_0$%	3.3$_2$%	3.0$_0$%		
Oxyprolin				(93%)*	
Cystin	1.1$_5$%	1.1$_1$%	1.1$_1$%		Spur (0.05%)

Das Zeichen* zeigt v.H. von zurückbleibenden.

Zur Eiweissbestimmung wandten wir nicht Ninhydrin, sondern Biuret-Reaktion an, weil Oxyprobe mit jenem sich nicht färbte.

Tryptophan wurde nach photokolorimetrischem Verfahren (Filter 530 mμ) bestimmt, unter Anwendung von Farbreaktion, welche aus Tryptophan und Vanillin im Gegenwart von Schwefelsäure entsteht.[9]

Wie sich aus der obigen Tafel erhellt, lässt sich Tryptophan schon in früher Stufe der Reaktion beinahe zersetzen.

Sulfhydryl-Gruppe wurde nach Ferricyanid-Methode bestimmt[10]. Es wurde erkannt, dass die Gruppe-SH auch anfangs angegriffen wurde. Dagegen ist Cystin fast unverändert zurückgeblieben. Ausserdem lässt sich vermuten, dass ein Teil von Cystein durch Perjodat zum Cystin oxydiert wurde. Haare, die zum Nachschlage mit sehr überschüssigem $NaIO_4$ monatelang durchdringend oxydiert wurden, hatten aber nach Hydrolyse nur Spur von Cystin.

Arginin erlitt wenig Veränderung. Dies wurde unmittelbar bestimmt, mit Hilfe der

8) G. R. Tristram, "Advances in Protein Chemistry," Vol, V, s. 137, Academic Press Inc., Publishers, New York, N. Y., (1949).

9) I. Iwamura, H. Hamakawa und Y. Nakahiro, *J. Agric. Chem. Soc. Japan*, **23**, 543 (1947).

10) E. S. G. Barron, "Advances in Enzymol.", Vol. 11, S. 223, Interscience Publishers, Inc., New York, N. Y. (1951).

Sakaguchi'schen Reaktion[11].

Tyrosin litt durch solch eine Oxydation keine erkennbare Veränderung.

Oxyprolin, welches bei Gelatine in Frage steht[12], zeigte keine merkbare Zersetzung.

Zusammenfassung

Ovalbumin wurde durch Perjodat in verschiedenem Grade oxydiert, ohne zu koagulieren.

Oxydiertes Ovalbumin enthielt nicht mehr Cystein und Tryptophan, aber Tyrosin, Histidin und Cystin blieben noch meistenteil zurück.

Aus dem Institut für biologische Chemie der landwirtschaftlichen Hochschule Matsuyama

11) H. T. MacPherson, *Biochem. J.*, **40**, 470 (1946).
12) R. E. Neuman und M. A. Logan, J. *Biol. Chem.*, **184**, 299 (1950).

Immunochemical Studies on Oxidized Ovalbumin

By Kazuyuki MAEKAWA and Kaoru KITAZAWA

(Received January 7, 1954)

In the preceding paper it was described that crystalline ovalbumin can, without giving any coagulation, be oxidized in the molar ratio of 10–30 moles of periodate per mole of protein[1]. The oxidized ovalbumin thus obtained was soluble in water at the isoelectric point; accordingly it appears to have been undenatured[3a]. But it is obvious that some groups on protein surface were decomposed by oxidation. Therefore, the present experiment was made with a view to elucidating what rôle those decomposed groups would, as determinant molecular ones, take in connection with the antigenicity of ovalbumin.

Experimental

1. Immune Sera Antisera were prepared by applying ovalbumin and oxi.-ovalbumin (oxidized with 30 moles of periodate) in the following way, after recrystallizing them several times (1). The aqueous protein solution (10 mg./cc.) containing phenol (0.5%) were injected into the auricular vein of rabbits four times at the interval of four days each. The initial dose was 0.5 cc. and each successive one was increased by 0.5 cc., thus the fourth and last one reaching 2 cc. After a week from the last injection, the blood of each rabbit was exsanguinated by cardiocentesia, and each serum was prepared from the blood by the usual method[2].

2. Analytical Methods (*a*) *Quantitative precipitin reaction.* Quantitative analyses in anti-ovalbumin sera and anti-oxi.-ovalbumin system were carried out as follows. Accurately measured solutions of antigens and sera were mixed and allowed to stand at 37° for 3 hours[3b]. The precipitates were centrifuged at room temperature and washed twice with 2 cc. of 1% aq. NaCl solution at 0° and centrifuged again.

(*b*) *Determination of nitrogen in the specific precipitates.* Nitrogen in the precipitates was determined as following. After 1 cc. conc. H_2SO_4 and 20 mg. K_2SO_4 (without addition of $CuSO_4$) were poured directly in the conical centrifuge tube containing precipitates, decomposition was conducted by heating for one hour. On the digested solution, ammonia was determined by the nesslerization according to modified Thompson and Morrison method[4]. Namely, the solution was poured into a 50 cc. measuring flask, neutralized completely with NaOH, and then filled up with water to the mark. To 20 cc. of this solution, were added 0.2 cc. of 50% Rochelle salt solution and 0.2 cc. of Nessler solution. After the solution was allowed to stand at 20° for 20 min., the transmittancy of light was measured by a photoelectric colorimeter using filter S 44. Previous adjustment is necessary to keep the ammonia content within a range of 1 γ—3.5 γ/cc. When the solution becomes turbid, after adding Nessler solution and warming, this sample is too conc. as to ammonia and therefore must be further diluted to repeat the same process as mentioned above.

(*c*) *Assay of supernatant solutions.* After precipitates of antigen-antibody complex were centrifuged, the supernatant solutions were tested qualitatively for both excess antigen and antibody. Approximately one-third of the solution was assayed for excess antigen and the rest for excess antibody by the addition of small amounts of antiserum and antigen respectively[5,6].

1) The foregoing report; reported in the meeting of the *Agr. Chem. Soc. Japan.* (at Kyoto, May 1951).
2) J. A. Kolmer and F. Boerner, "Approved Laboratory Technic." (New York) 1945, p. 616.
3a) P. H. Maurer and M. Heidelberger, *J. Am. Chem. Soc.*, **73**, 2070 (1951).
3b) P. H. Maurer and M. Heidelberger, *J. Am. Chem. Soc.*, **73**, 2076 (1951).
4) J. F. Thompson and G. R. Morrison, *Anal. Chem.*, **23**, 1153 (1951).
5) L. R. Wetter and H. F. Deutsch, *J. Biol. Chem.*, **192**, 237 (1951).
6) H. F. Deutsch, *J, Biol. Chem.*, **185**, 377 (1950).

TABLE I

ADDITION OF INCREASING AMOUNTS OF OVALB. AND OXI.-OVALB. TO 1.0 cc. OF ANTI-OVALBUMIN SERUM

Kind of antigen	Antigen N added, mg.	Total N pptd., mg.	Antibody N by diff., mg.	Antibody N / Antigen N	Supernatant tests
Ovalbumin	1.5760	0.0752			Excess antigen
	0.1576	0.5024	0.3448	2.2	,,
	0.0628	0.6531	0.5903	9.4	Excess antibody
	0.0314	0.4710	0.4396	14.0	,,
	0.0157	0.3014	0.2857	18.2	,,
	0.0063	0.1342	0.1279	20.3	,,
	0.0031	0.0688	0.0657	21.2	,,
Oxi. ovalbumin	1.5760	0.0837			Excess antigen
	0.1576	0.5495	0.3919	2.5	,,
	0.0628	0.6154	0.5526	8.8	Excess antibody
	0.0314	0.4145	0.3831	12.2	,,
	0.0157	0.2434	0.2277	14.5	,,
	0.0063	0.1071	0.1008	16.0	,,
	0.0031	0.0539	0.0508	16.4	,,

TABLE II

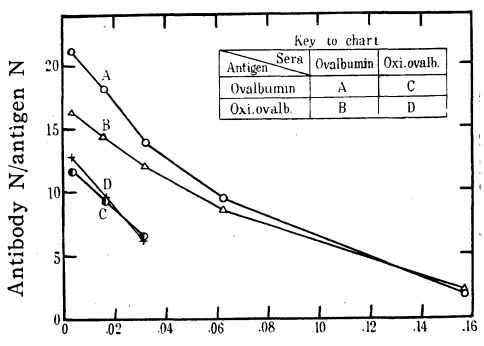
ADDITION OF INCREASING AMOUNTS OF OVALBUMIN AND OXI.-OVALBUMIN TO 1.0 cc. OF ANTI-OXI.-OVALBUMIN SERUM

Kind of antigen	Antigen N added, mg.	Total N pptd., mg.	Antibody N by diff., mg.	Antibody N / Antigen N	Supernatant tests
Ovalbumin	0.1576	0.0523			Excess antigen
	0.0314	0.2449	0.2135	6.8	,,
	0.0157	0.1649	0.1492	9.5	Excess antibody
	0.0063	0.0775	0.0712	11.3	,,
	0.0031	0.0400	0.0369	11.9	,,
Oxi. ovalbumin	0.1576	0.0542			Excess antigen
	0.0314	0.2355	0.2041	6.5	,,
	0.0157	0.1696	0.1539	9.8	Excess antibody
	0.0063	0.0832	0.0769	12.2	,,
	0.0031	0.0434	0.0403	13.0	,,

Results and Discussion

The results are shown in Tables I and II. It is apparent that there is no difference between the homogeneous reaction and the cross one in precipitin reaction upon ovalbumin-serum, except in the case of the less antigen region.

The slight difference which was found in the less antigen region, suggests that there is some loss on antigen surface which should be combined complementarily. On the other hand, there is also no difference between homogeneous and cross reaction in the reaction upon oxi.-ovalbumin-serum, except in the case of the less antigen region. In the less antigen region, the precipitate is formed somewhat more in the case of homogeneous reaction. The relation between the ratio of the antibody N to antigen N in the precipitates and the amount of antigen N increasingly added are shown in the Figure 1. As



Mg. antigen N added per cc. of serum dilution

Fig 1. Relation between the ratio of antibody N to antigen N in the precipitates and antigen N added to the serum dilution.

shown in the figure, it would seem that the oxi.-ovalbumin is not serologically heterogeneous, since the curve concerning serum of oxi.-ovalbumin is in straight line[6].

From the comparison between Tables I and II, it is clear that serological specificity was diminished considerably by the oxidation. Heidelberger and his collaborator[3b] reported that the deaminated proteins, even though one third of free NH_2-group was eliminated off, retain their serological specificity, so long as protein was not denatured.

The oxi.-ovalbumin reported here can be regarded as not denatured[3a]. Therefore, this difference between those facts is to be ascribed to the difference in the contribution to serological specificity between end-NH_2-group[7] and those groups on protein surface which were oxidized by periodate. In other words it seems that the specificity is more attributable to tryptophan, hydroxylamino acids and tyrosine, situated on protein surface, than to end NH_2-group.

7) R. R. Porter and F. Sanger, *Biochem. J.*, **42**, 287 (1948).

The decrease in serological specificity of oxi.-protein probably is not due to the fact that the surface, as in case of denatured protein, is random and has no definite folding, but to the fact that some determinant groups on the surface is decomposed by oxidation.

Summary

Using the oxidized ovalbumin, quantitative precipitin reactions were brought forward. There was some difference between the homogeneous reaction and the cross one in the precipitin reaction upon ovalbumin- and oxidized ovalbumin-serum only in the case of the less antigen region. The serological specificity of ovalbumin diminished considerably by the periodate-oxidation.

The authors wish to express their gratitude to Mr. M. Kushibe for his valuable assistance in this investigation.

Laboratory of Biological Chemistry,
Matsuyama Agricultural College

Studies on Some Physico-Chemical Properties of Ion-Exchange Resin. I. Heat of Wetting

By Tatsuo MATSUURA

(Received February 20, 1954)

Introduction

Recently, as an ion-exchange resin has been of great importance in its application in the field of chemistry and chemical engineering, it has now come to be noticed also by many physical chemists as a typical sample of an insoluble high-polymeric electrolyte. Because of its having both a high-polymeric and electrolytic nature, ion-exchange resin seems to have many characteristic properties, one of which is, unlike other high-polymers, the rapid and reproducible swelling in water, which is seen remarkably at the low cross-linked resin, while it is little seen at the high cross-linked resin. In both cases, if the sample has been dried enough, considerable heat is evolved at the moment when it is immersed in water. The author, in this paper, attempted to investigate this phenomenon as a first approach to the fundamental nature of ion-exchange resin. The measurements were made on various forms and states of some cation and anion-exchange resins, and it was found that the amounts of heat evolved depended largely on their forms in such a way that the sequence with the latter was almost parallel with the series of the heats of hydration of the ions. Theoretical considerations were also attempted with the adoption of the appropriate values for the heats of hydration of ions and some assumptions on the dry state of resion.

Experimental Procedure

Samples Used. Samples used are classified into three types; that is, the strongly acidic cation-exchange resins, the weakly acidic cation-exchange resin, and the strongly basic anion-exchange resins.

The first are polystyrene-divinylbenzene sulfonic acid exchangers and are also classified into the following three types according to their cross-linkage. The lowest cross-linked one is easily made from polystyrene by sulfonation with

chlorsulfonic acid. The other two are commercial, more or less highly cross-linked, "Amberlite IR-120" and "Amberlite IR-112," whose cross-linkage is said to be 8% to 10% and about 5% divinylbenzene (DVB), respectively.

As a sample of the weakly acidic resin, carboxylic "Amberlite IRC-50" was used. It is a copolymer of methacrylic acid and about 10% DVB.

Anion-exchange resins used, commercial "Amberlite IRA-400" and "Amberlite IRA-410," are quarternary ammonium salts with the network structures of polystyrene-divinylbenzene.

About 1 g. to 3 g. of resin was used for each run. Well-conditioned, uniform-sized (about 100 Meshes) resin was taken in a column, through which the solutions containing the concerning ion of about ten times as much as the exchange capacity of the resin bed were passed; then it was washed by distilled water, except in the cases described below, till the effluent was freed from the regenerant. In the case of the salt form of carboxylic resin, the washing was made by dilute alkali of about 0.001 N, lest the adsorbed ions might be hydrolyzed[1]. This care was also given in the case of anion-exchange resin, where the exchange was more easily obtained at a lower *p*H range. The drying of samples was done first in an air-oven, then in a desiccator, finally in a test tube with a glass joint stopper in an Abderhalden's dryer at the boiling temperatures of alcohols or water under the reduced pressure of about 0.02 mm Hg. It took from a few days to sometimes about twenty days for the samples to have the constant weights within 1 mg.

The partially desulfonated resins were prepared as follows: the synthesized resin was boiled for about one week with the mixture of conc. sulfuric acid and an almost equal volume of water, at about 150°C. The sample was blackened by this treatment, but the decrease in the exchange capacity was not so great as expected, showing the stability of this sort of resin.

The measurements on the partially wetted samples were made only on acid and sodium forms of the strongly acidic resins, which were prepared either by partial desiccating of resin or by moistening the completely dried resin with damp air. The contents of water in the samples were easily determined by titrating the exchange capacities of resins by column or batch method, and the values obtained agreed with those by the change of weight with drying or wetting.

Calorimetric Measurement. Fig. 1 shows the experimental apparatus. When the temperature of the calorimeter reached about 18°C, the readings of the Beckmann thermometer were begun at intervals of 30 seconds with the constant stirring by the stirrer S. Then the samples was carefuly and rapidly thrown from the test tube reserved at the thermostat into the water through the hole C of the vessel. The temperature rise caused by the wetting of the resin occurred immediately

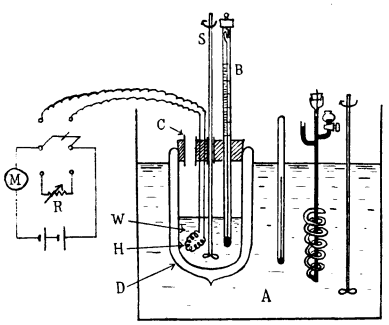


Fig. 1

A: thermostat. B: Beckman thermometer. D: Dewar vessel. S: a plastic stirrer. C: a hole. W: about 180 cc. water. H: a heater. R: resistance box almost equalled with the resistance of the heater. M: a calibrated ammeter (1 amp. range).

after that, sometimes with a noise of its decrepitation. Soon after the temperature-time diagram became flat, another temperature rise which was caused by introducing an electric current through the heater H for some seconds was added to determine the whole heat capacity. This state of matters was shown in a diagram such as Fig. 2,

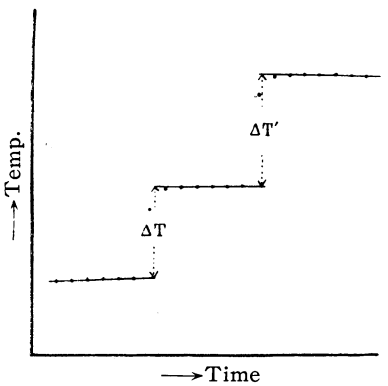


Fig. 2

in which these temperature changes were both in the order of 0.1°C to 1.5°C. By determining the weight of samples, the value of the heats of wetting was expressed in cal. per gram, as well as in kcal. per equivalent after the measurement of exchange capacity.

Exchange Capacity. Ordinarily after the calorimetric measurements were done by the above mentioned procedure, the exchange capacity of the resin, i.e., the number of exchange sites per unit, was measured by the column method. In the strongly acidic resins, each salt form was reduced to hydrogen form by the use of 4 N hydrochloric acid as regenerant and was completely washed by distilled water, then by passing the sufficient amount of neutral sodium chloride solution the hydrogen ion that was driven into the effluent was titrated by a standard alkali. In the case of weakly acidic resins, the measure-

1) M. Honda, *J. Chem. Soc. Japan* (Pure Chem. Sect.), **71**, 183, 440 (1950). *Japan Analyst*, **1**, 120 (1952).

ments were made by column or batch method, where alkaline, instead of neutral, solution was used to obtain a complete exchange and the washing was also made by dilute alkali.

At the anion exchange resins, the reduced state was selected at the chloride form, and the titration was performed by Mohr's method.

Results and Discussion

The results obtained are shown in Table I and Fig. 3. From these data it is seen at once as follows: that the values of the heat of wetting of ion exchange resin in general are considerably great as compared with the other high polymers such as starch (about 30 cal./g.)[2], and that there is a remarkable difference between them according to their forms. The sequence at the strongly acidic resin, that is, the fact that the more the valency of the ion or the higher the positon of the ion in the group, the greater is the value of the heat, coincide with the lyotropic series of ion, which undoubtedly has an important relation to the hydration of ions. The degree of difficulty in the dehydration of resin, namely, the period required for the resin to be completely dried in Abderhalden's dryer, was also consistent with this series. Thus the aluminium or magnesium form of this sort of resin was found to have the greatest heat evolution, which was contrary to the result mentioned in a review[3].

As the cation exchange resins were comparatively stable, even the treatment at 100°C did not seem to bring any serious effects, except only that some change of color (getting brown) took place at the hydrogen form, but without any change of exchange capacity. The anion exchange resins were so unstable that they decomposed more or less with a peculiar smell at comparatively low temperatures, especially at the hydroxyl ion form, which lost almost all its capacity by the drying at 65°C.

The results of the weakly acidic type resin were very interesting from the following respects. That is, the largest heat evolution per unit weight was seen with this sort of resin, and the position of the hydrogen form was much lower than that of the other forms, compared with the results of strongly acidic resins. The latter fact may be due to the undissociative nature of the hydrogen atom of the weakly acidic carboxylic group, and the value suggests the magnitude of the hydrogen bond between this hydrophylic radical and the water molecules.

In comparison with the great dependence on the variety of adsorbed ions, the heats of wetting seem scarcely to depend on the cross-linkage as far as this experiment is concerned. Only in the case of the hydrogen form of sulfonic acid type resin an effect just like this was noticed above the experimental error, that is, there was some difference depending on the cross-linkage. However, this probably is accounted for by the considerably high value of heat of dilution of hydrogen ion, and not by the difference of degree of swelling. Thus, such a rather rough measurement as this could not pursue "the swelling heat", which, even if it really exists, must be very small, because the swelling is naturally a phenomenon greatly related rather to the entropy change than to the enthalpy change.

The attempt to find any dependence on the exchange capacity led to the measurement on the desulfonated resin, where although the decrease in the exchange capacity by this method was attained to some extent, the accompanying carbonization of the resin seemed to make the matter complicated.

The calculated values of exchange capacity in a salt form of cation exchangers were derived from the standard hydrogen form by the following formula:

$$E_{MR}=\frac{E_{HR}}{1+E_{HR}\,(m/z-1)}\ (m\text{ eq. per g.}) \quad (1)$$

where E_{MR} is exchange capacity of the concerned salt form (MR), E_{HR} of acid form (HR), and m and z are molecular weight and valency of the adsorbed ion, respectively.

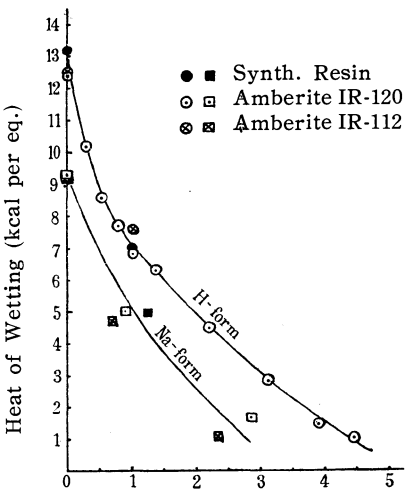


Fig. 3

2) T. Nakagawa, This Bulletin, **26**, 169 (1953).
3) G. E. Boyd, *Ann. Rev. of Phys. Chem.* **2**, 306 (1951).

TABLE I

THE HEAT OF WETTING OF ION EXCHANGE RESIN

Species of resin	Adsorbed ion form	Drying data Temperature	Drying data period	Heat of wetting		Exchange capacity obs.	Exchange capacity calc.	Apparent wet swollen volume in water
		(°C)	(days)	(cal./g.)	(kcal./eq.)		(meq/g.)	cc./g.
Synthetic		(Strongly Acidic Cation Exchange Resin)						
Resin	Al	100	20	83.8	19.3	4.15	4.34	
„	Mg	100	20	82.5	19.7	4.20	4.28	
„	H	100	5	58.7	13.1	4.49	(4.50)	10
„	H	78	7	59.4	13.2	4.50	(4.50)	
„	Ca	100	20	51.0	12.3	4.02	4.15	
„	Li	78	5	45.3	10.3	4.24	4.38	
„	Ba	78	10	35.8	10.4	3.29	3.44	
„	Na	78	5	37.2	9.1	4.08	4.09	
„	K	78	4	18.1	4.8	3.77	3.84	
„	NH_4	78	3	17.6	4.2		4.18	
„	Rb	78	5	13.5	4.3	3.12	3.26	
Amberlite								
IR-120	H	78	5	55.9	12.4	4.50	(4.50)	2.3
„	Na	78	5	37.8	9.3	4.08	4.09	
„	K	78	5	22.7	5.9	3.84	3.84	
Amberlite								
IR-112	H	78	4	56.3	12.5	4.48	(4.50)	5.4
„	Na	78	3	37.7	9.2	4.16	4.09	
„	K	78	3	18.3	4.8	3.75	3.84	
Desulfonated	H	78	5	55.6	14.6	3.81	(3.81)	8.5
Resin I	Na	78	5	37.8	10.6	3.56	3.51	
Desulfonated	H	100	5	60.5	14.1	4.30	(4.30)	9.0
Resin II	Na	100	5	34.9	8.7	3.94	3.94	
Amberlite		(Weakly Acidic Cation Exchange Resin)						
IRC-50	Ca	78	20	122		4.8	7.9	
„	Na	78	8	113.5	15.3	7.4	7.7	
„	Na : H = 2 : 3	78	6	61.6	7.6	8.1	8.6	
„	H	100	8	30.7	3.2	9.6	(9.35)	5
„	H	78	3	30.4	3.3	9.1	(9.35)	
Amberlite		(Strongly Basic Anion Exchange Resin)						
IRA-410	Cl	78	4	17.0	4.6	2.8		
„	NO_3	65	5	7.3	2.5	2.9		
Amberlite								
IRA-400	SO_4	56	20	41.8	14	3.0		
„	CH_3COO	56	4	37.4	11.4	3.3		
„	I	56	3	12.9	4.6	2.8		

*Parentheses show the standard values selected for calculating the exchange capacity of other forms by Eq. 1.

The observed and calculated values of the exchange capacity were as a whole in good agreement, except the tendency that the former were a little less than the latter. This may be accounted for as follows. (1). Incomplete drying or impurity in reagents. (2). Incomplete regeneration may be probable at the measurement of exchange capacity for the ions which have higher selectivity than hydrogen. (3). For polyvalent ion forms, the occurrence of basic ion such as $Mg(OH)^+$ may increase the apparent equivalent of the ion.

The measurement of the partially wetted samples also gave a very interesting result. As is shown in Fig. 3, at the hydrogen form of strongly acidic resins, about five water molecules per one exchange radical were found to be involved in the heat of wetting, the greatest part of which could be attributed

to the hydration of the hydrogen ion. The inflection observed on the curve at the point of one water molecule per one exchange radical may be a proof of the strong attraction between the bare hydrogen ion and one water molecule, forming the hydronium ion (H_3O^+). Considering the fact of little dependence on the cross-linkage, this number, about five water molecules per one hydrogen ion, might be said to be the hydration number of the hydrogen ion. The corresponding number for the sodium ion was found to be about three. The author believes that this can be one of the methods to estimate the hydration number of ions. On the other hand, from the wet swollen volume per gram of strongly acidic resin, the resin phase may be regarded as a concentrated solution of about 5 N for IR-120 and 0.5N for synthetic resin. These correspond to the fact that there exist from about ten to one hundred water molecules per one exchange radical, and we may say that the above mentioned five molecules are the bound water and the other are the interstitial water of hydrogen form of this resin.

The following are theoretical considerations on the heat of wetting of sulfonic acid type cation exchanger. The heat of wetting is regarded to be the negative value of the enthalpy change in wetting, ΔH_{WET}, which is the difference of heat content when the completely dried state of resin is brought to the wetted state. Now, as the model which is shown in Fig. 4, this process may be

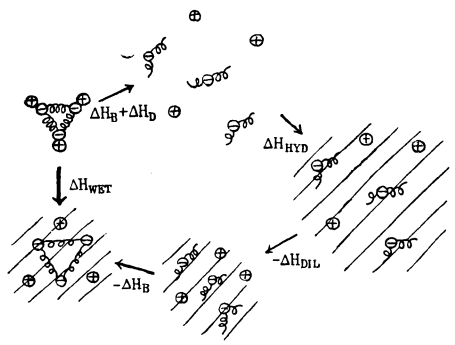


Fig. 4

divided hypothetically into the four steps. (1). The original dried sample is dissociated into fragments in a vacuum, so as for each ion pair as well as the links between structurally bound negative radicals to be separated infinitely. The enthalpy change at this stage is the sum of ΔH_D, due to the dissociation of ion pairs, and ΔH_B, which concerned with the energy required to break the bonds of the polymer network. (2). Then the completely dissociated ions (both cation and radical anion) are brought from the vacuum into the water, when the hydration of ions takes place. The enthalpy change here is caused by the hydration of both ions, ΔH_{HYD}. (3). Thirdly, the wetted yet infinitely separated ions are concentrated as far as the concentration which corresponds to the swelling state of resin. The accompanying enthalpy change is the negative value of that of dilution from the concentration to the infinite dilution, ΔH_{DIL}. (4.) Finally, while the concentration of ions are reserved constant on the other hand, the recombination into the swollen resin state takes place. Then the enthalpy change involved is only one term, which is required to combine the separated polymer bonds, thus giving $-\Delta H_B$, just the negative value of the term mentioned at the first step. After all, the change in heat content by wetting is expressed as follows:

$$\Delta H_{WET} = \Delta H_D + \Delta H_{HYD} - \Delta H_{DIL}, \quad ...(2)$$

in which ΔH_{DIL}, something similar to the heats of dilution of a few normal solution of usual salts or acids, being only 1 or 2 kcal. per mol at the most, can be neglected at the first approximation, as is compared with the order of about 100 kcal. or much more of ΔH_{HYD}. Then,

$$\Delta H_{WET} = \Delta H_D + \Delta H_{HYD}. \quad .....(3)$$

As for the energy of hydration of ions, although we have several studies in connection with the ionic radii or hydration numbers, it seems that a complete interpretation with relation to the actual hydrated radii of ions has not yet been obtained, but that only semi-empirical formula originated by Born[4] are still now prevailing[5,6]. The author, too, chose the following formula presented by Latimer[5] as the values of ΔH_{HYD}.

$$\Delta H_{HYD} = \frac{-Nz^2e^2}{2(r_i + b)}\left(1 - \frac{1}{D} - \frac{T}{D^2}\frac{dD}{dT}\right)$$

c.g.s.e.s.u. per mole, ...(4)

where N is Avogadro's number,
e, charge of electron,
z, valency of ion,
r_i, crystal ionic radius of ion,
b, correction value,
D, dielectric constant of medium, and
T, absolute temperature.

Inserting known figures at room temperature into Eq. 4, one obtains,

4) M. Born, *Z. f. Physik.* **1**, 45 (1920).
5) W. M. Latimer, K. S. Pitzer, and C. M. Slansky, *J. Chem. Phys.*, **7**, 108 (1939).
6) K. B. Yatsimirskii, *J. Gen. Chem.* (U. S. S. R.), **17**, 2019 (1947), *C. A.* **42**, 4809, (1948).

$$\Delta H_{HYD} = -\frac{165\,z^2}{r_i+b} \text{kcal. per mol.} \quad ...(5)$$

where r_i is expressed in Å. The numerical constants b, which have a serious effect on ΔH_{HYD}, were chosen 0.85 for monovalent cations except hydrogen ion, as was done by Latimer[5]. As he did not give the value for hydrogen, ΔH_{HYD} for this ion was taken from the Fajans' value, 255 kcal. per mol.[7]. b's were chosen 0.8 for divalent and trivalent cations and 0.3 for anions, respectively, followed by Yatsimirskii[6]. Thus the ΔH_{HYD} for cation is shown in the third column in Table II. The value of ΔH_{HYD} for sulfonic acid anion with polymer fragments was arbitrarily assumed to be 40 kcal. per eq., which corresponds to an ionic radius of 3.82 Å according to Eq. 5. As the following discussion refers to, the "true ionic radius of sulfonic acid group" may be assumed to have the value, 1.40 Å, for which, according to Eq. 5, ΔH_{HYD} is calculated to be 97 kcal. per Eq. The discrepancy in these values might be interpreted as follows: the attachment of the extra polymer chain may enclose the sulfonic radical, resulting the increase in effective radius; or the hydration of the sulfonic acid group is hindered sterically by the polymer network. The fourth column in Table II is the sum of ΔH_{HYD} for cation and 40 kcal.

TABLE II

THEORETICAL CONSIDERATION ON THE HEAT OF WETTING OF SULFONIC ACID TYPE CATION EXCHANGE RESIN

Ion Species	Crystallographic Ionic Radii* Å	ΔH_{HYD} for cation kcal./eq.	ΔH_{HYD} total "	ΔU "	ΔH_D calc. "	ΔH_{WET} calc. "	ΔH_{WET} obs. "
H	(0)	−255	−295		335	+40	−13.1
Li	0.60	−121.2	−161	166	149	−12	−10.3
Na	0.95	− 94.6	−135	141	127	− 8	− 9.2
K	1.33	− 75.8	−116	122	110	− 6	− 4.8
Rb	1.48	− 69.2	−109	115	104	− 5	− 4.3
Mg	0.65	−228	−268	283	255	−13	−19.7
Ca	0.99	−189	−229	243	218	−11	−12.3
Ba	1.35	−154	−194	211	190	− 4	−10.4
Al	0.50	−382	−422	425	383	−39	−19.3

* By Pauling

In order to deduce the calculated values for ΔH wet by Eq. 3, it is necessary to calculate the appropirate values for ΔH_D. For this purpose, the following assumptions were made. (1). The negative charge on a sulfonic acid group exists on the position of the oxygen atom which is the immediate neighbor of the adsorbed cation, thus as the "ionic radius of sulfonic acid group," the van der Waals radius or the ionic radius of oxygen, which both happened to have the same value, 1.40 Å[8], was taken. (2.). The dry state of resin except hydrogen form is assumed to be similar to an ionic crystal, that is, the adsorbed ion and radical anion are coupled as ions also at the dry state, but because the pairs are distributed amorphously, the electrostatic interaction is almost limited to the coupled ions, thus the Madelung constant can be assumed to be unity. (3). Thus the electrostatic attraction by the Coulomb force of ion pairs can be expressed by

$$\Delta U = \frac{Ne^2\,z'}{(r_i+1.40)} \times 10^8$$

c.g.s. e.s.u. per Eq.,.....(6)

where N, e, and r_i are as described above; z', a corrected valency of ion considering the repulsion of the ions of same charge, is 1 for monovalent adsorbed ions, 1.75 for divalent ions, and it depends on ionic radius for trivalent ion (2.44 for aluminium). (4). ΔH_D, the energy required to separate the ion pairs infinitely, so to speak the "crystal energy of ion-exchange resin," is estimated roughly as much as about ninety percent of the electrostatic attraction ΔU, considering the existence of the repulsion term. This figure was taken from the average value of several species of mono-monovalent ionic crystal[9]. (5). For

7) K. Fajans, *Naturwissenschaften*, **9**, 729 (1921).
8) L. Pauling, "The Nature of the Chemical Bond," p. 189, 346 (1939).
9) E. A. Moelwyn-Hughs, "Physical Chemistry," p. 599, (1940).

hydrogen form, we adopt a different model; that is, the atoms in the dry state of that form are no longer ionized but exist as covalent bond, and

$$\Delta H_D = D + I - E, \qquad \text{.....(7)}$$

where D is energy required to separate the covalent bond between the hydrogen atom and residual sulfonic radical, and $I-E$ is the difference between the ionization energy of hydrogen atom and the electron affinity of the sulfonic radical. As the value for D, 110 kcal. per mole, the covalent bond energy of O−H bond in water molecule, was conventionally used. The value for I is 313 cal.; and for E, 88 kcal., the value of electron affinity of oxygen atom, was conventionally used.

Thus the calculated ΔH_{WET} is shown in column 7, Table II. The fair agreement between ΔH_{WET} observed and calculated, considering the fact that it is derived as the difference of the two large values, suggests that these assumptions just made are not going too far except in some cases. At the hydrogen form, where the deviation is very large, it is necessary to use more refined values for D and E. For divalent and trivalent cation forms, both the uncertainty in ΔH_{HYD} and the probable deviation from the above mentioned factor (90%) are enough to explain the poor coincidence between theory and experiment.

Summary and acknowledgment

(1) The measurement of heats of wetting of strongly acidic and weakly acidic cation exchange resins and strongly basic anion exchange resins was made by a simple method and their great dependence on the adsorbed ion species was found.

(2) The series of heat of wetting with ion forms is almost parallel with the lyotropic series of ions, thus it has been shown that this penomenon has an important relation to the hydration of the ions. The acid form of the weakly acidic resin occupies a special position, and this is attributed to the undissociative nature of carboxylic radical.

(3) The result on the partially wetted samples supports the view that only a few water molecules which may be called "bound water" take part in the heat of wetting or hydration of ions.

(4) A theoretical interpretation based on a few assumptions was attempted and a fair agreement with the experimental results was obtained.

The author wishes to express his hearty thanks to Dr. Masatake Honda of the Department of Chemistry of the Faculty of Science in the University of Tokyo, for his kind guidance and encouragement extended to the author while he was with him at Rikkyo University.

The College of Science,
Rikkyo University

The Molecular Structure of cis-1,2-*Dichlorocyclohexane*

By Kunio KOZIMA, Kiyoshi SAKASHITA and Yoshiyuki TAKEISHI

(Received March 12, 1954)

1,2-Disubstituted cyclohexanes have two geometrical isomers. One is called the *cis*-isomer and the other the *trans*-isomer. By use of the usual symbols the molecular structure of the former is represented by (1e, 2p) or (1p, 2e). As for 1,2-dihalocyclohexanes the *cis*-isomers were not obtained for a long time. However, a new 1,2-dichlorocyclohexane, presumably the *cis*-isomer, has recently been described by Carrol et al.[1]

If the compound is really *cis*-1,2-dichloro derivative, it should have the following two properties, since its cyclohexane ring should take the chair-form as in the case of the similar derivatives[2-4] already reported: (1) The compound has not the "inverted isomer".[2-4] (2) The value of dipole moment is nearly the same as that determined by us for the (1e, 2e) form of *trans*-1,2-dichloro derivative[3], namely 3.1 D.

The main purposes of this research are to ascertain whether or not the compound is the *cis*-isomer by measuring the vibration

1) B. Carrol, D. G. Kubler, H. W. Davis and A. M. Whaley, *J. Am. Chem. Soc.*, **73**, 5382 (1951).

2) K. Kozima and T. Yoshino, ibid., **75**, 166 (1953).

3) K. Kozima, K. Sakashita and S. Maeda, ibid., **76**, 1965 (1954).

4) K. Kozima, *Bull. Tokyo Inst. Tech.*, **1952**, 1. (in Japanese).

spectra and the dipole moment and, if so, to know the properties of the compound.

Experimental

Preparation and Purification of the Compound.—According to the method of Carrol et al.[1] we prepared the 1,2-dichlorocyclohexane by reacting *trans*-1,2-cyclohexene chlorohydrin with thionyl chloride in the presence of pyridine. The product was purified by the fractional distillation in vacuo. The boiling point is 71.0~71.2° at 8.5 mm.

Electric Dipole Moment.—For the measurement of dielectric constants the same instrument was used as before. The data are listed in Table I, where f denotes the mole fraction and P_2 the molar polarization of the solute. The measured values of P_2 are in various cases almost independent of the low concentrations which were used. Therefore, the mean value of P_2 was taken as $P_{2\infty}$ in all cases. The dipole moment was calculated as $\mu=0.0128\sqrt{(P_{2\infty}-R_D)\cdot T}$ using the molar refraction R_D (37.5 cc) calculated from the atomic refractions for the D-line.

TABLE I

DIPOLE MOMENTS

in benzene

$t=30°$, $P_{2\infty}=231$, $\mu=3.10$ D.

f	ε	d	P_2
0.0000	2.2625	0.8675	
0.007093	2.3562	0.8709	230
0.008311	2.3738	0.8715	232

in heptane

$t=30°$, $P_{2\infty}=237.5$, $\mu=3.15$ D.

f	ε	d	P_2
0.0000	1.9056	0.6753	
0.01328	2.0026	0.6814	237
0.01492	2.0157	0.6823	238

in heptane

$t=45°$, $P_{2\infty}=225.5$, $\mu=3.13$ D.

f	ε	d	P_2
0.0000	1.8829	0.6625	
0.01328	1.9776	0.6687	225
0.01492	1.9837	0.6696	226

in carbon tetrachloride

$t=40°$, $P_{2\infty}=227$, $\mu=3.12$ D.

f	ε	d	P_2
0.0000	2.1928	1.5563	
0.006699	2.2690	1.5526	227
0.007255	2.2746	1.5519	227

Vibration Spectra.—For Raman spectra the same spectrograph was used as in our earlier work. The spectra of the compound were observed for the solid and liquid states. Regarding infrared spectra measurements were made with Perkin-Elmer spectrometer Model 112 equipped with NaCl and KBr Prisms. The results of the wave number readings for both spectra are shown in Table II.

TABLE II

VIBRATION SPECTRA

Raman* (solid) cm^{-1}	Raman* (liquid) cm^{-1}	infrared** (liquid) cm^{-1}
193 (1)	193 (3)	
278 (2)	278 (4)	
348 (10)	346 (10)	
365 (1)	367 (2)	
?	474 (1)	473 (vw)
510 (5)	510 (8)	511 (m)
535 (10)	541 (10)	543 (s)
681 (10)	695 (10)	695 (vs)
735 (9)	741 (9)	741 (vs)
816 (3)	818 (4)	816 (s)
833 (3)	833 (5)	834 (s)
		~845 (vw)sh
876 (2)	876 (4)	877 (vs)
902 (1)	902 (3)	906 (m)
985 (7)	987 (8)	986 (vs)
		~1008 (vw)sh
1026 (2)	1026 (4)	1025 (vw)
1057 (2)	1057 (3)	1057 (w)
1079 (2)	1079 (2br)	1078 (w)
		1085 (w)
?	1133 (1)	1131 (w)
1191 (1/2)	1191 (1)	1191 (m)
1220 (1/2)	1218 (0)	1217 (w)
	1226 (2)	1226 (m)
		~1262 (vw)sh
1267 (3br)	1267 (5br)	1270 (s)
1296 (1/2)	1296 (1)	1298 (m)
?	1314 (1)	1313 (w)
	1335 (1)	1336 (w)
1346 (1br)		~1346 (w)sh
	1355 (1)	1356 (m)
1442 (4br)	1435 (3)	1446 (vs)
	1443 (6)	
		2169 (w)
		2695 (vw)
	2847 (2)	2880 (m)
2903 (3)	2904 (4)	
2920 (3)	2920 (4)	
2941 (4)	2938	2937 (vs)br
2950 (4)	2955 (6br)	
2982 (2)	2977	

* As for the Raman spectra the numbers shown in the brackets are the visually estimated relative intensities.

** The infrared spectra were not investigated below 430 cm.$^{-1}$ The letters shown in the brackets mean the relative intensities. v=very, s=strong, m=medium and w=weak. sh=shoulder.

Discussion

It is seen from Table I that the dipole moment of the compound does not appreciably vary with temperature or solvent. From Table II the following facts may be clear:

(1) The number of the Raman bands and their relative intensities do not vary except for the disappearance of the several very weak lines of the liquid spectrum when the measuring state is changed from liquid to solid. (2) The infrared and Raman spectra agree with each other perfectly regarding the number of the bands and approximately regarding the relative intensities except the very faint bands and the region above 2000 cm^{-1}.

Two possibilities for interpreting the facts mentioned above come out: (1) The molecule does not possess the inverted isomer; or (2) The molecule has the inverted isomer, but the energy difference between the isomers is so great that only one of the two forms can exist. A case in which the energy difference between the isomers is nearly zero or small can be left out of consideration, because of the number of the bands (for instance, the number of the bands assigned to the C—Cl stretching vibrations is two, as might be naturally expected from the formula of $C_6H_{10}Cl_2$).

It is not immediately clear that the dichlorocyclohexane prepared from 1,2-cyclohexene chlorohydrin, as described above, is 1,2-dichlorocyclohexane. Taking this point into consideration these two possibilities will be discussed.

Each of the three position isomers of dichlorocyclohexanes has two geometrical isomers—the *cis*- and *trans*-isomers. Of these six isomers only three have inverted isomers; viz. *trans*-1,2-, *trans*-1,4- and *cis*-1,3-dichlorocyclohexanes. Regarding the first two of them we have already reported[2,3]. Then, only *cis*-1,3-isomer remains to be considered. The structures of *cis*-1,3-dichloro derivative are represented as follows:

$$(1p, 3p) \rightleftarrows (1e, 3e).$$

The distance between the two chlorine atoms of the (1p, 3p) structure is calculated to be about 2.5 Å, assuming the usual values for the C—C and C—Cl nuclear separations and the tetrahedral valency angle for the carbon atoms of the cyclohexane ring which has the "chair" form. Comparing this distance with twice the van der Waals' radius of the chlorine atom, we can expect that the (1p, 3p) structure will be unstable as compared with the (1e, 3e) structure so that only the latter can exist. Therefore, it is not immediately clear that the compound in question is not *cis*-1,3-dichloro derivative. However, upon the basis of simple vector addition of bond moments, it is calculated that the moment of the (1e, 3e) structure of *cis*-1,3-dichloro derivative, $\mu_{1,3}$, and that of *cis*-1,2-dichloro derivative, $\mu_{1,2}$, are represented, respectively, as follows;

$$\mu_{1,3} = 2\mu_0 \cos \theta/2$$
$$\mu_{1,2} = 2\mu_0 \sin \theta/2$$

where μ_0 is the sum of the moment of C—Cl bond and that of C—H bond, and θ is the tetrahedral valency angle of carbon atom. Estimating the value of μ_0 at 1.80 or 1.90 D, we can calculate the values of $\mu_{1,3}$ and $\mu_{1,2}$ obtaining the following results;

$$\mu_{1,3} = 2.08 \text{ or } 2.19 \text{ D}$$
$$\mu_{1,2} = 2.94 \text{ or } 3.10 \text{ D}$$

The observed value is about 3.1 D which is in good agreement with that obtained by Tulinskie, Di Giacomo and Smyth[5] in the vapor and dilute benzene solution states. The marked difference between the observed value and $\mu_{1,3}$ indicates that the compound is not *cis*-1,3-dichloro derivative. Then we can conclude that the compound is not the isomer which has the inverted isomer.

Next, we must consider the possibility (1). As for the remaining three isomers of dichlorocyclohexanes which do not possess the inverted isomer, it is easily seen that the compound is not *trans*-1,3- or *cis*-1,4-dichloro derivative. The reasons for this* are as follows:

(1) The value of the moment of *trans*-1,3-derivative which has the structure represented by (1e, 3p) or (1p, 3e) should be equal to that of the (1e, 3e) structure of *cis*-1,3-derivative. Consequently, regarding this isomer we cannot expect such a large moment as observed.

(2) The moment of *cis*-1,4-dichloro derivative should be equal to $\mu_{1,2}$ except for a small difference due to the so-called "induction effect". Therefore, we can say that the compound in question may be this isomer so far as the moment is concerned. However, we have already prepared a dichloro derivative as a by-product of the preparation of *trans*-1,4-dichloro derivative, and studied its vibration spectra and other properties. The spectra are quite different from those shown in Table II. We have concluded from such investigations that the compound mentioned above is not *cis*-1,2-dichloro derivative, but is *cis*-1,4-dichloro derivative. Details of this research will be soon described.

Next, we are in a position to discuss whether or not the compound in question is *cis*-1,2-dichloro derivative, which is the only

5) A. Tulinskie, A. Di Giacomo and C. P. Smyth, *J. Am. Chem. Soc.*, **75**, 3552, (1953).

* It may not be probable that the compound is the 1,4-dichloro derivative. But we cannot immediately see that it is out of the range of possibility.

isomer* that remains to be considered. Upon the basis of vector addition of bond moment it is expected that the moment of *cis*-1,2-dichloro derivative would be equal to $\mu_{1,2}$ calculated above and to that of the (1e, 2e) structure of *trans*-1,2-dichloro derivative, which we have already estimated at 3.1 D.[3] by the investigations of dipole moments. This value and that of $\mu_{1,2}$ agree with the data shown in Table I. The fact that the Raman and infrared spectra agree with each other indicates that the compound is of low symmetry. For comparison the following fact obtained by us should be noted, namely, regarding the infrared and Raman spectra caused mainly by the C—Cl stretching vibration of the (1p, 2p) isomer of *trans*-1,2-dichloro derivative the mutual exclusion rule for a centrosymmetric molecule holds approximately true, because the molecule has locally the center of symmetry as for the two C—Cl bonds—(the total change of polarizability or dipole moment of the molecule with such normal vibrations as mentioned above may be mainly determined by the change of C—Cl bond polarizabilities or bond moments through the vibrations)—although the molecule as a whole is only of C_2 symmetry. Thus we can, beyond any doubt, conclude that the compound in question is *cis*-1,2-isomer, in conformity with the evidence drawn from the " trans-elimination ".[1]

The authors wish to express their sincere thanks to the Ministry of Education for its financial grant.

Tokyo Institute of Technology,
Meguro-ku, Tokyo

* The possibility that the compound is 1,1-dichloro derivative can be left out of consideration, because the moment of the isomer is expected to be equal to $\mu_{1,3}$ calculated above.

Polarographic Studies on Heterocyclic Compounds. I. Kinetic Current of Isonicotinic Acid

By Yoshinosuke NAGATA and Isamu TACHI

(Received March 17, 1954)

Introduction

Polarographic studies of pyridine derivatives have been made by several scholars. The reduction mechanism of picolinic, nicotinic and isonicotinic acids, which are monocarboxylic acid of pyridine, have been studied by Tompkins and others[1-6].

The present authors investigated the limiting current of isonicotinic acid.

Experimental Part

A specimen of isonicotinic acid is offered by Prof. Dr. T. Takahashi (the Department of Pharmacy, Faculty of Medicine, Kyoto University).

The concentration of isonicotinic acid in the electrolytic solution, in which 0.1-N potassium chloride is involved as an indifferent electrolyte, is in the range of 10^{-4} to 10^{-3} mol per liter. The *p*H of electrolytic solution is changed by using the various kinds of buffer solutions, which are Mc Ilvain's phosphate buffer, Kolthoff's buffer, and Sörensen's borate buffer. The volume of buffer solution contained in the electrolytic solution corresponds to 80 vol. % of the whole solution.

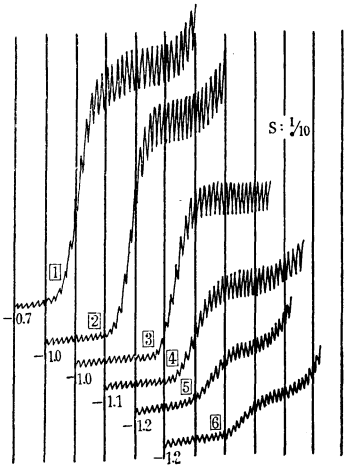


Fig. 1. Polarograms of 5×10^{-4} m./l. isonicotinic acid at various *p*H. (1) 2.2, (2) 7.0, (3) 8.2, (4) 9.0, (5) 10.0, (6) 10.8.

1) M. Shikata and I. Tachi *Chem. News.* **137**, 126 (1928).
2) P. C. Tompkins and C. L. Shmidt *J. Biol. Chem.*, **143**, 643 (1942).
3) P. C. Tompkins and C. L. Schmidt, *Univ. California Pub., Physiol.*, **8**, 229 (1943).
4) P. C. Tompkins and C. L. Schmidt, *Uuiv. California Pub., Physiol.*, **8**, 237 (1943).
5) P. C. Tompkins and C. L. Schmidt, *Univ. California Pub. Physiol.*, **8**, 247 (1943).
6) E. Knobloch, *Collection*, **12**, 407 (1947).

The Yanagimoto Type Polarograph is used and the normal calomel electrode is connected with the electrolytic solution as a reference electrode. The sensitivity of the galvanometer is 3×10^{-9} Amp./mm./m. The rate of the flow of mercury from the capillary, m, and drop time t, at -1.6 volt vs. N.C.E. are 1.202 mg./sec. and 4.26 sec. at 20°C., respectively.

Experimental Results

(1) Effects of the *p*H on the Half-wave Potential and the Limiting Current.

The polarograms obtained with 5×10^{-4} m./l. isonicotinic acid solution of various *p*H values show a so-called well-defined single reduction wave in the whole *p*H range (Fig. 1). The relationship between *p*H, the half-wave potential, and the limiting current is shown in Table I. As shown by curve (1) in Fig. 2,

TABLE I

RELATIONSHIP BETWEEN THE *p*H, $E_{1/2}$, AND THE LIMITING CURRENT OF THE REDUCTION WAVE OF 5×10^{-4} m./l. ISONICOTINIC ACID

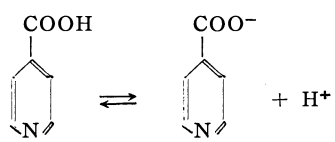
Temperature: 20°C.

*p*H	Buffer	$E_{1/2}$ (vs. N.C.E.)	i(μA)
2.2	Mc Ilvain's buffer	−0.910 v.	2.30
3.0	,,	−0.970	2.30
4.0	,,	−1.030	2.31
5.0	,,	−1.120	2.40
6.0	,,	−1.180	2.40
7.0	,,	−1.280	2.10
6.2	Kolthoff's buffer	−1.190	2.30
7.1	,,	−1.260	2.04
7.5	,,	−1.290	1.83
8.2	,,	−1.330	1.56
8.5	,,	−1.360	1.35
9.0	,,	−1.410	0.93
9.2	Sörensen's buffer	−1.420	0.72
9.5	,,	−1.440	0.48
10.0	,,	−1.460	0.26
10.8	,,	−1.470	0.18
12	,,	−1.470	—
13	in 0.1-N NaOH	—	—

the half-wave potential shifts to more negative value with increasing *p*H value and in the range of *p*H greater than 10 it remains nearly constant.

While the limiting current shows a constant value in the *p*H range from 2 to 6, it decreases gradually with increasing *p*H value in the range of *p*H greater than 7 until it diminishes at *p*H 12.

Isonicotinic acid is a weak mono-basic acid and dissociates as follows:



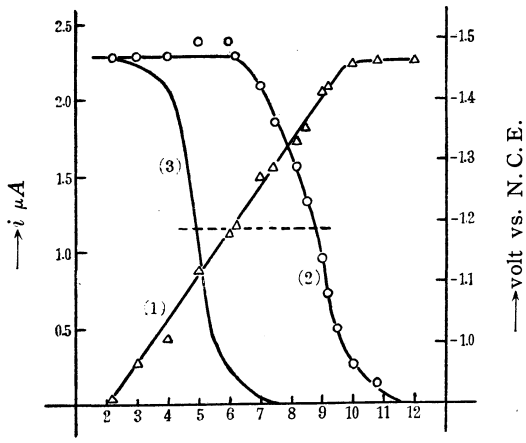


Fig. 2
(1).....$E_{1/2}$-*p*H curve
(2).....i-*p*H curve
(3).....Dissociation curve

Its dissociation constant, K, is equal to 1.09×10^{-5} [7]. Curve (3) in Fig. 2 represents the dissociation curve of isonicotinic acid and the course of i-*p*H curve (curve (2) in Fig. 2) runs similarly to it. Therefore, provided the reduction wave is due to the reduction of undissociated molecules of isonicotinic acid, curve (2) is to be regarded to show the apparent polarographic dissociation curve.

(2) Effect of the Concentration of Isonicotinic Acid on the Limiting Current.

The relationship between the concentration of isonicotinic acid, the half-wave potential, and the limiting current at *p*H 5.0 at 22°C. is shown in Table II. As shown in column 4 (Table II) and Fig. 3 the limiting current is

TABLE II

RELATIONSHIP BETWEEN THE CONCENTRATION OF ISONICOTINIC ACID AND ITS LIMITING CURRENT AT *p*H 5.0

Temperature: 22°C.

Conc. ($\times10^{-4}$ m./l.)	$E_{1/2}$ (vs. N.C.E.)	i(μA)	i/Conc.
9	−1.050 v.	4.56	0.506
8	−1.040	4.11	0.512
7	−1.030	3.54	0.505
6	−1.040	3.06	0.510
5	−1.030	2.52	0.504
4	−1.030	2.04	0.510
3	−1.020	1.56	0.520
2	−1.020	1.02	0.510
1	−1.030	0.54	0.540

[7] H. Scudder, "Conductivities and Ionization Constants of Organic Compounds", 267 (1914).

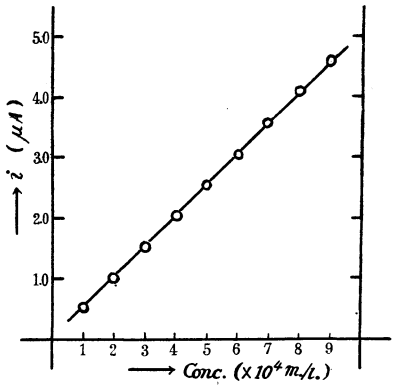


Fig. 3

proportional to the concentration of isonicotinic acid. Hence the quantitative analysis of isonicotinic acid is possible at *p*H 5.0 in the range from 10^{-4} to 10^{-3} mol per liter. The half-wave potential is hardly influenced by the change of concentration (Column 2 in Table II).

(3) Effect of the Height of Mercury Reservoir on the Limiting Current.

Table III represents the relationship between the mercury reservoir height, *h*, and the limiting current at *p*H 3.0 and 9.5. The fact that the limiting current at *p*H 3.0 is proportional to $\sqrt{h}$ (column 5 in Table III) means that this current is controlled by a diffusion process as shown by the Ilkovič theory[8]; whilst, the limiting current at *p*H 9.5 is independent of *h*, i.e., it can be concluded that the limiting current at *p*H 9.5 shows the characteristics of kinetic current[9,10].

TABLE III

DEPENDENCE OF THE HEIGHT OF MERCURY RESERVOIR ON THE LIMITING CURRENT OF 5×10^{-4} m./l. ISONICOTINIC ACID

Temperature: 20°C.

		*p*H 9.5	*p*H 3.0	
h	$\sqrt{h}$	*i*	*i*	$i/\sqrt{h}$
60 cm.	7.75	0.495 μA	2.400 μA	0.31
55	7.42	0.495	2.280	0.31
50	7.07	0.510	2.265	0.32
45	6.71	0.510	2.175	0.33
40	6.33	0.510	2.070	0.33
35	5.92	0.499	1.950	0.33
30	5.48	0.495	1.830	0.33
25	5.00	0.510	1.665	0.33

TABLE IV

INFLUENCE OF THE TEMPERATURE ON THE LIMITING CURRENT OF 5×10^{-4} m./l. ISONICOTINIC ACID

*p*H 3.0			*p*H 9.5		
t°C.	*i*	Temp.-Coeff.	*t*°C.	*i*	Temp.-Coeff.
22.4	2.40 μA		21.2	0.548 μA	
26.4	2.58		25.2	0.630	3.19%
30.0	2.70		30.5	0.705	2.67%
35.7	2.97	Av.	36.2	0.774	2.27%
41.0	3.24	1.62%	39.4	0.819	1.92%
45.5	3.48		45.0	0.870	1.89%
50.5	3.78		50.5	0.910	1.80%
55.2	4.08		55.5	0.975	1.63%

(4) Effect of the Temperature on the Limiting Current.

The relationship between the temperature and the limiting current at *p*H 3.0 and 9.5 is shown in Table IV. The temperature coefficient of the limiting current which is expressed by $\left(\frac{1}{i}\frac{di}{dT}\right)\times100\%$ is about 1.6% per degree at *p*H 3.0 and it is equal to that of the diffusion current[11]. The coefficient at *p*H 9.5 is greater than at *p*H 3.0 (Column 6), but it decreases gradually with rising temperature. This tendency seems to be opposite to the general one concerning the temperature coefficient. The reason why such a phenomenon presents itself cannot be interpreted and must to be investigated furthermore.

Discussion

As the limiting current at *p*H 3.0 is controlled by diffusion process, the theoretical diffusion current can be calculated from Ilkovič's equation[8]

8) D. Ilkovič *Collection*, **6**, 498 (1934).
9) R. Brdička and K. Wiesner, *Collection*, **12**, 138 (1947).
10) J. Koutecký and R. Brdička, *Collection*, **12**, 337 (1947).
11) D. Ilkovic, *Collection*, **10**, 249 (1938).

$$i_d = 0.605nFCD^{1/2}m^{2/3}t^{1/6} \quad (1)$$

where i_d denotes the diffusion current, n electron number involved in the reduction, F Faraday's constant, C the concentration of the depolarizer, D its diffusion coefficient, m the rate of flow of mercury from the capillary, and t drop time. Employing the following numerical values: $C=5\times10^{-4}$ m./l., $D=8.86\times10^{-6}$ (assuming that the diffusion coefficient of isonicotinic acid is equal to that of benzoate[12]), $m=1.201$ mg./sec., $t=4.26$ sec., and supporting that $n=2$, we obtain the result $i_d=2.514$ μA. Hence the experimental value agrees nearly with the calculated value within experimental error. Therefore, the reduction of isonicotinic acid seems to correspond to the two electron reduction.

Next, as the result of the wave analysis, the reduction process of isonicotinic acid is found to be irreversible; and this conclusion is also confirmed from the standpoint of A. C. polarography, in which A.C. voltage of an arbitrary amplitude is superposed on the D.C. voltage of polarograph, and A.C. component of the pulsating current resulting electrolysis shows a peak at the half-wave potential of polarographic wave in the case of reversible system, while such a peak does not appear in the case of irreversible system[13,14].

The kinetic current due to the recombination of the dissociated anion with proton was for the first time studied theoretically by R. Brdička and K. Wiesner[9]. Later, J. Koutecký and R. Brdička[10] cleared it up mathematically.

In the dissociation equilibrium of isonicotinic acid

$$HA \underset{k_1}{\overset{k_2}{\rightleftarrows}} H^+ + A^- \quad (2)$$

where HA, A^-, and H^+ denote the undissociated molecule, dissociated anion, and hydrogen ion, respectively, dissociation constant, K, is given by

$$K = k_2/k_1 = [H^+][A^-]/[HA] \quad (3)$$

where k_1 and k_2 are the recombination and dissociation velocity constant, respectively. In the reduction of acid, the undissociated molecule is generally reduced at the more positive potential than the dissociated anion. The reduction wave in the case of isonicotinic acid is considered to be due to the reduction of undissociated molecules and the anion reduction wave seems to be overlapped with the wave of indifferent cation or hydrogen ion in the electrolytic solution. The difference between the dissociation curve (curve (3) in Fig. 2) and the apparent polarographic dissociation curve (curve (2) in Fig. 2) is clearly caused by the kinetic current due to the recombination of dissociated anion with hydrogen ion.

According to J. Koutecký and R. Brdička[10], the change of the concentration of both molecule and anion with time is represented by the algebraic sum of diffusion and recombination terms; that is

$$\frac{\partial a}{\partial t} = D\frac{\partial^2 a}{\partial x^2} + \rho(b - \sigma a) \quad (4)$$

$$\frac{\partial b}{\partial t} = D\frac{\partial^2 b}{\partial x^2} - \rho(b - \sigma a) \quad (5)$$

where a and b the concentration of undissociated molecule and dissociated anion, respectively, and

$$\rho = k_1[H^+], \quad \sigma = K/[H^+]$$

The proper initial and boundary conditions are as follows;

$$a = a_e, \quad b = b_e \quad \text{for} \quad t = 0, \quad x > 0$$
$$a = 0, \quad \partial b/\partial x = 0 \quad \text{for} \quad t > 0, \quad x = 0$$

where a_e and b_e are the equilibrium concentration of a and b, respectively. Eq. 4 can be integrated by means of Laplace transformation, and then the solution is given by

$$\frac{\sqrt{\pi D}}{\alpha}\left(\frac{\partial a}{\partial x}\right)_{x=0} = \frac{1}{(\sigma^2-1)}\left[t^{-1/2}(\sigma e^{-\rho(1+\sigma)t} - 1) + 2\frac{\rho^{1/2}\sigma^2}{(\sigma^2-1)^{1/2}} e^{\frac{\rho t}{\sigma-1}}\left\{\int_0^{\sigma\sqrt{\frac{\rho t}{\sigma-1}}} e^{-x^2}dx - \int_0^{\sqrt{\frac{\rho t}{\sigma-1}}} e^{-x^2}dx\right\}\right] \quad (6)$$

where α denotes the analytical concentration of acid. When $\sigma=0$, i.e., dissociation does not take place at all, Eq. 6 is simplyfied to

$$\left(\frac{\partial a}{\partial x}\right)_{x=0} = \frac{a_e}{\sqrt{\pi D t}} \quad (7)$$

When $\rho \gg 1$ and $\sigma \gg 1$, Eq. 6 is reduced to

$$\left(\frac{\partial a}{\partial x}\right)_{x=0} = \alpha\sqrt{\frac{\rho}{D\sigma}} e^{\frac{\rho t}{\sigma}}\left[1 - \Phi\left(\sqrt{\frac{\rho t}{D}}\right)\right] \quad (8)$$

where

$$\Phi(y) = \frac{2}{\sqrt{\pi}}\int_0^y e^{-y^2}dy$$

and when $\rho \gg 1$, $\sigma \gg 1$, and $\rho/\sigma \gg 1$, Eq. 6 is simplyfied to

$$\left(\frac{\partial a}{\partial x}\right)_{x=0} = \alpha\sqrt{\frac{\rho}{D\sigma}} \quad (9)$$

Therefore, from Eq. 9 and the surface area

12) M. J. Astle and W. V. Mc Connell, *J. Am. Chem. Soc.*, **65**, 35 (1943).
13) B. Breyer, F. Gutmann and S. Hacobian, *Aust. J. Sci. Res.*, **A3**, 558 (1950).
14) I. Tachi, F. Kambara and M. Senda, not published yet.

of mercury drop $q=0.85\,m^{2/3}t^{2/3}$, the average kinetic current, $\bar{i}$, is shown by

$$\bar{i}=\frac{3}{5}\cdot 0.85m^{2/3}t_1^{2/3},nF\alpha\sqrt{\frac{D\rho}{\sigma}} \qquad (10)$$

Since $3/5\times 0.85m^{2/3}t_1^{2/3}$, in Eq. 10 represents the average surface area of the dropping mercury electrode and the product mt_1 is independent of the height of mercury reservoir, when the same capillary is used under the same conditions, the kinetic current shows a constant value independently of the change of the mercury reservoir height. From Eq. 8, the average kinetic current is given by

$$\bar{i}=\frac{0.85m^{2/3}nF\alpha}{t_1}\int_0^{t_1}\sqrt{\frac{D\rho}{\sigma}}e^{\frac{\rho t}{\sigma}}\left[1-\Phi\left(\sqrt{\frac{\rho t}{\sigma}}\right)\right]t^{2/3}dt \qquad (11)$$

when $k_1\to\infty$, the limiting current has no character of the kinetic current, but corresponds to the diffusion current. Denoting it by $\bar{i}_\infty$, from Eqs. 7 and 11 it is seen that

$$\frac{\bar{i}}{\bar{i}_\infty}=\frac{6}{7\sqrt{\pi}y^{7/6}}\int_0^{y_1}F(y)dy=f(y_1) \qquad (12)$$

where

$$F(y)=y^{2/3}e^{y}[1-\Phi(\sqrt{y})]$$
$$y=\rho t/\sigma,\quad y_1=\rho t_1/\sigma \qquad (13)$$

When the kinetic current corresponds to a half of the diffusion current, it can be shown that

$$f(y_1)=0.5$$

and then

$$y_1=0.420(*)$$

When $K\gg[H^+]$, it follows from Eq. 13 that

$$y_1=\frac{k_1[H^+]}{K}t_1$$

$$\log k_1=2\left(p\mathrm{H}+\frac{1}{2}\log y_1\right)-(pK+\log t_1) \qquad (14)$$

The pH value where $f(y_1)=0.5$ in curve (2) (Fig. 2) is 8.8, and $t=4.26$ sec. and

$$K=1.09\times 10^{-5}.$$

Substituting these values into Eq. 14, the recombination velocity constant is equal to

$$k_1=1.22\times 10^{12}\ \text{sec.}^{-1}\ (\text{m./l.})^{-1}$$

Further, it is found that the dissociation velocity constant is

$$k_2=k_1K=1.33\times 10^{7}\ \text{sec.}^{-1}$$

According to J. Koutecký and R. Brdička[10], the thickness of the reaction layer where recombination takes place, μ, is given by

$$\mu=\sqrt{\frac{D}{k_1K}} \qquad (15)$$

Inserting the above mentioned values viz., $D=8.86\times 10^{-6}$, $k_1=1.22\times 10^{12}$ and $K=1.09\times 10^{-5}$ into this equation, it is found that

$$\mu=8.16\times 10^{-7}\ \text{cm.}$$

This value seems to be right in comparison with the other values obtained experimentally concerning some organic acids[17,18].

Summary

(1) Isonicotinic acid shows a single polarographic reduction wave. It is found from the standpoint of the wave analysis as well as of A.C. polarography that the electrode process is irreversible.

(2) The wave height at pH 5.0 is proportional to the concentration of isonicotinic acid in the concentration range from 10^{-4} to 10^{-3} mol per liter.

(3) Since the single reduction wave is considered to be due to the reduction of undissociated molecules, the i-pH curve shows an apparent polarographic dissociation curve.

(4) The kinetic current due to the recombination of dissociated anions with proton is investigated, and the recombination velocity constant and the thickness of reaction layer are determined according to J. Koutecký and R. Brdička's equations.

The authors would like to thank Prof. Dr. T. Takahashi for gifts of isonicotinic acid used in this work. We are also indebted to M. Suzuki, F. Kambara, M. Senda, and S. Koide for their suggestions.

Department of Agricultural Chemistry,
Faculty of Agriculture,
Kyoto University

*) According to J. Koutecký and R. Brdička[10], y_1 is equal to 0.400; but J. Koryta[15] points out the error as to this value. M. Senda[16] newly obtains the plot of y_1 vs. f(y_1) from the numerical calculation, and the above value is obtained from this plot.

15) J. Koryta, *Proc. I.Inter. Polaro. Congr. in Prague*, **1** 798 (1951),
16) M. Senda; not published yet.
17) R. Brdička, *Proc. I. Inter. Polaro. Congr. in Prague*, **3** 286 (1952).
18) I. M. Kolthoff and A. Liberti, *J. Am. Chem. Soc.*, **70**, 1885 (1948).

The Electrostatic Effect of the Solvents on the Frequency Shifts and the Intensity Changes of the Infrared Absorption Spectra

By Eizi HIROTA

(Received April 20, 1954)

Recently a theory was presented by the author[1] on the frequency shifts of the infrared absorption bands in the liquid state in terms of the intermolecular potential by Onsager's theory of dielectrics. The treatment given there, however, was essentially classical, so that it may be desirable to reconsider it in quantum mechanics.

For simplicity let us take a heteronuclear diatomic molecule with one degree of freedom of vibration which may be expressed approximately by a harmonic oscillation. As was stated in the preceding paper[1] the molecules in the liquid are stabilized by the interaction with the surrounding molecules and the energy to be added is given by[2]

$$\Delta H = -\frac{\epsilon-1}{2\epsilon+1}\frac{C}{a^3}[\mu+e'Q]^2 \quad \text{.....(1)}$$

It is easily shown that the first order perturbation energy due to the operator, Eq. (1), gives rise to

$$\int \psi_0 \Delta H \psi_0 d\tau = -\frac{\epsilon-1}{2\epsilon+1}\frac{C}{a^3}\left[\mu^2+\frac{e^2h}{8\pi^2 m\nu}\right] \quad \text{.....(1a)}$$

for the ground state and

$$\int \psi_1 \Delta H \psi_1 d\tau = -\frac{\epsilon-1}{2\epsilon+1}\frac{C}{a^3}\left[\mu^2+\frac{3e^2h}{8\pi^2 m\nu}\right] \quad \text{.....(1b)}$$

for the first excited state, respectively. There ψ_0 and ψ_1 denote the wave functions of the ground and the first excited states of the harmonic oscillator. Then the energy absorbed in the transition, $0\rightarrow 1$, is given by

$$h\nu' = h\nu - \left[\int \psi_0 \Delta H \psi_0 d\tau - \int \psi_1 \Delta H \psi_1 d\tau\right]$$
$$= h\nu\left[1-\frac{\epsilon-1}{2\epsilon+1}\frac{C}{a^3}\frac{e^2}{4\pi^2 m\nu^2}\right] \quad \text{...(2)}$$

Thus the decrease in frequency observed at the transfer from the gas to the liquid state becomes

$$\frac{\Delta\nu}{\nu} = \frac{\nu-\nu'}{\nu} = \frac{\epsilon-1}{2\epsilon+1}\frac{C}{a^3}\frac{e^2}{4\pi^2 m\nu^2}, \quad (2')$$

where

$$C = \frac{(n^2+2)(2\epsilon+1)}{3(2\epsilon+n^2)} \quad \text{.....(3)}$$

This is exactly the same expression as that obtained by the classical consideration in the preceding paper.

The intensity of this absorption band depends upon the squared value of the (0, 1) element of the electric moment, while the latter in the liquid state is increased by the factor C referred to that in *vacuo*;

$$m = C[\mu+e'Q] \quad \text{.....(4)}$$

Therefore the absorption intensity in the liquid state, I_l, is obtained from that in the gaseous state, I_g, by the relation

$$I_l = C^2 I_g \quad \text{.....(5)}$$

To test the above conclusions the recent measurement by Barrow[3] is quoted here. The absorption of the stretching frequency of C=O group of various compounds were measured in the solutions of chloroform and carbon tetrachloride as well as in the vapor. Here are selected the following four examples: acetone, methyl and ethyl acetate, and methyl carbonate. In order to compute the frequency shifts by Eq. (2'), it is necessary to know the values of a's, the effective radii of the molecules. They are usually estimated from the density of the liquid, but in this paper they are treated as adjustable parameters so as to give the best fit with the observed ones in $CHCl_3$ and CCl_4 solutions. In Table I the calculated $\Delta\tilde{\nu}$'s are given to be compared with the observed values. In this table are listed the values a's assumed, together with the frequencies in *vacuo* $\tilde{\nu}$'s (in the unit of cm^{-1}), and the intensities in *vacuo* A's quoted from the paper by Barrow. It is noted that, since $A = N\pi\left(\frac{\partial\mu}{\partial Q}\right)^2/3c^2\ 1000$ given in the unit of mole^{-1} litre cm^{-1} is used, Eq. (2') becomes

1) E. Hirota, This Bulletin, **23**, 397 (1953).

2) Eq. (4*b*) in reference I, in which the energy necessary to polarize the molecule, $\alpha R^2 2$, was omitted. (Cf. C. J. F. Böttcher, "Theory of Electric Polarization", Elsevier Publishing Co., Amsterdam, 1952, pp. 138—139.) This correction being included, the factor C^2 in Eq. (4*b*) in reference 1 should be replaced by C, but it does not essentially alter the conclusion obtained there. C^2 in Eqs. (6*b*), (7*b*). (8*b*) and (8*b'*), should also be corrected to C. About notations used in this paper one should consult with referrence 1.

3) G. M. Barrow, *J. Chem. Phys.*, **21**, 2008 (1953).

TABLE I
FREQUENCY SHIFT

Compound	a (A)	$\tilde{\nu}$(cm^{-1})	A*)	$CHCl_3$ soln. $(\epsilon-1)C/(2\epsilon+1)=0.444$ calc.	obs.	CCl_4 soln. $=0.253$ calc.	obs.
Acetone	1.48	1747	$1.2\ 10^4$	(38.0)	38	21.6	—
Methyl acetate	1.68	1776	1.9	40.3	38	23.0	25
Ethyl acetate	1.73	1772	2.1	41.7	38	23.2	27
Methyl carbonate	2.20	1781	2.9	27.2	25	15.5	18

*) $A=N\pi\left(\frac{\partial\mu}{\partial Q}\right)^2/3c^2$ 1000, given in the unit of mole^{-1} litre cm^{-1}.

$$\Delta\tilde{\nu}=\frac{\epsilon-1}{2\epsilon+1}\cdot C\frac{3}{4\pi a^3}\frac{10^3}{N\pi^2}\frac{A}{\tilde{\nu}} \quad ...(2'')$$

The values of dielectric constants are taken to be 5.0 for $CHCl_3$ and 2.23 for CCl_4, while $n^2=2$ is assumed through out. It follows that $(\epsilon-1)C/(2\epsilon+1)=0.444$ for $CHCl_3$ and 0.253 for CCl_4 solutions. For the last three compounds in Table I. the calculated values of $\Delta\tilde{\nu}$'s for $CHCl_3$ solutions are larger than the experimental values, whereas the contrary is the case for CCl_4 solutions.

The values assumed above for a's are found to be far smaller than the molecular radius $a_0=(3M/4\pi Nd)^{1/3}$, which is the radius of the spheres just filling the entire liquid. The bond moments of C=O and C−O are considered to be greater than those of C−C and C−H, so that the interactions of the bonds C=O and C−O with other molecules may play the main role in this case. The radius of a sphere encircling just this group of oxygen and carbon atoms is taken to be the rough estimate for a. The atomic radii and the bond angles of acetate and carbonate groups are taken from Pauling's book[4], where the two end oxygen atoms in acetate groups are assumed to have radii $0.605=(0.66+0.55)/2$ and the three in carbonate group to have radii $0.623=(2\times0.66+0.55)/3$. The values obtained thus are 1.28A for acetone, 1.75A for two acetates and 2.25A for carbonate. It may be interesting to note that a's used for the calculation of $\Delta\tilde{\nu}$ 1.48A, 1,68A, 1.73A and 2.20A run roughly parallel to these rough estimates.

Another comparison is carried out for the intensity change. As evident from Eq. (5), the intensity ratio I_l/I_g is given by C^2, which depends on ϵ and n, but is free from the value of a. Inserting the values of dielectric constants for $CHCl_3$ and CCl_4 as quoted above and using the intensities in *vacuo* I_g measured by Barrow, one can obtain I_l, the intensities in solutions, which are listed in Table II. It will be seen that the agreement with the observed I_l is very satisfactory.

TABLE II
INTENSITY CHANGE (1)

Compound	A_g*)	A_l*) $C^2=1.49$ $CHCl_3$ soln. calc.	obs.	$C^2=1.265$ CCl_4 soln. calc.	obs.
Acetone	$1.2\ 10^4$	$1.79\ 10^4$	$1.9\ 10^4$	$1.52\ 10^4$	...
Methyl acetate	1.9	2.83	2.8	2.40	$2.2\ 10^4$
Ethyl acetate	2.1	3.13	3.2	2.66	2.6
Methyl carbonate	2.9	4.33	4.2	2.67	3.8

*) See the footnote of Table I.

Further it is also possible to compare the intensities in different solutions; the ratio of the intensities in two solutions is given by

$$I_{li}/I_{lj}=C_i^2/C_j^2 \quad .....(6)$$

where C_i and C_j denote respectively the constants for both solutions. Thus the intensity ratio is a definite constant, determined by the solvents, and common to any absorption bands of any melecules. In Table III. a comparison is made of the intensity ratios $\rho=A\ (CHCl_3)/A(CCl_4)$ of C=O bands of various compounds in chloroform and carbon tetrachloride. It will be clearly seen that the intensity ratios are obtained in the deviations less than 10% from the calculated ratio $\rho_{calc.}=C^2(CHCl_3)/C^2(CCl_4)=1.18$, except in the cases of propionaldehyde (14.7%) and ethyl benzoate (10.1%). According to Barrow, the accuracy of the intensity measurement is about 2% in solutions and about 5% in the gaseous phase. The discrepancies between the

4) L. Pauling, "The Nature of the Chemical Bond" Cornell Univ. Press, 1940, pp. 164, 203, 208 and 209.

TABLE III
INTENSITY CHANGE (2)

Compound	$A_{obs.}$*) $CHCl_3$ soln.	CCl_4 soln.	$\rho_{obs.}=A_{(CHCl_3)}/A_{(CCl_4)}$	$\frac{\rho_{obs.}-\rho_{calc.}}{\rho_{calc.}}$ Deviation in ρ (%)
Diethyl ketone	$1.9\ 10^4$	$1.55\ 10^4$	1.2_2	3.7
Propionaldehyde	2.1	1.55	1.3_5	14.7
Benzaldehyde	2.6	2.1	1.2_4	5.1
Benzophenone	2.4	2.2	1.0_9	−7.4
Acetophenone	2.7	2.1	1.2_8	9.0
Ethyl propionate	3.2	2.8	1.1_4	−3.1
Methyl crotonate	3.4	3.1	1.1_0	−6.9
Ethyl benzoate	3.6	3.4	1.0_5	−10.1
Ethyl carbonate	4.7	4.1	1.1_4	−2.9
Acetyl chloride	3.1	2.5	1.2_3	5.3
Phenyl acetate	3.1	2.9	1.0_7	−9.2
Acetanilide	3.6	3.1	1.1_6	−1.4

$\rho_{calc.}=C^2(CHCl_3)/C^2(CCl_4)=1.49/1.265=1.18$

*) See the footnote of Table I.

calculated and the observed values are of this order of magnitude.

The author wishes to express his gratitude to Professor Yonezo Morino for his kind advice.

Department of Chemistry,
Faculty of Science,
Tokyo University,
Tokyo

A Study of the Effect of Fuchsin Red on the Metabolism of Yeasts

By Krishna BAHADUR

(Received April 7, 1954)

Introduction

In recent years a good deal of work has been done upon the influence of substances which, although not essential as nutrients, still affect the physiological properties of yeast cells[1]. In this paper I have studied the growth and metabolic activity of yeasts in cultures which have the property of absorbing visible light. I selected such a water-soluble dye, which in small doses, does not harm the yeast to a great extent but gives the culture a distinct color. Fuchsin red was chosen as one of such dyes for the study.

These cultures have deep red color. They naturally absorb all the radiations of the visible light except the red light. This absorption of light is followed by simultaneous change in the cells of the cultures. *Chaetomium*[2] and *Serratia* have been found to be mutated by high doses of wave length above 350mμ. The latter bacterium indicates 6 per cent color sector changes by 10^7 erg/cm^2. without noticeable killing. When cells are vitally stained by photodynamic dyes, e. g., erythrosine, the sensitivity to visible light becomes high 3—6).

The influence of dyeing time, concentration, *p*H, and temperature on photodynamic effects can be interpreted in terms of permeability and absorption of the dye. In *Penicillium*[6] and *E. coli* 15 h [7,8] photodynamic and ultraviolet induced mutation processes are similar regarding close curve and correlation to killing. Phage resistance[9] and Sd 4 mutations[10] are also induced by photodynamic action.

1) W. A. Krehl, and S. J. Llao, *Ann. Rev. Microbiol.*, **5**, 121 38 (1951).
2) A. L. Mc Aulay, J. M. Ford, and D. L. Dobie, *Heredity*, **3**, 109 (1949).
3) R. W. Kaplan, *Naturwissenschaften*. **35**, 127 (1948).
4) R. W. Kaplan, *Nature*, **163**, 573 (1949).
5) R. W. Kaplan, *Arch. Microbiol.*, **15**, 152 (1949).
6) R. W. Kaplan, *Planta*, **33**, (1949).
7) R. W. Kaplan, *Naturwissenschaften*, **31**, 547 (1950).
8) R. W. Kaplan, *Microbiol, Genet. Bull.*, **4**, 12, (1951).
9) R. W. Kaplan, *Naturwissenschaften*, **37**, 308, (1950).
10) M. Demerec, G. Bertani, and J. Flint, *Am. Naturalist*, **85**, 119 (1951).

When fuchsin red is present in yeast cultures it stains the cells and effects a change in the physiological properties of yeasts. To study this change varying amounts of fuchsin red were taken in yeast cultures containing sucrose as source of carbon and ammonium sulfate as source of nitrogen. The metabolic substances formed during the yeast growth were estimated to investigate the effect of the dye in the cultures. These studies were done with *Saccharomyces carlsbergensis* and Dhar Yeast[11]

Experimental

Five cultures, each containing 0.2 g. of calcium carbonate, 0.2 g. of magnesium carbonate, 0.2 g. of sodium chloride, 0.2 g. of potassium sulfate, 0.25 g. of disodium hydrogen phosphate and 2.5 g. of ammonium sulfate were prepared. Above substances were digested in dilute hydrochloric acid. The amount of fuchsin red, as mentioned against each culture in the table of *Saccharomyces carlsbergensis*, was added in them. This was done by making a standard solution of fuchsin red and then taking out a certain volume of this solution containing the requisite amount of fuchsin and introducing it in the culture solution. Total volume of each culture was made to 400 cc. with distilled water and *p*H adjusted to 4.5. These cultures were kept in 750 cc. flatbottom pyrex flasks and 20 g. of sucrose were added in each of them. The flasks were cotton plugged and sterilised by heating in an autoclave for 20 minutes at 10 lbs. pressure. Cultures were cooled and seeded with activated sample of *Saccharomyces carlsbergensis*.

Four cultures, each containing the requisite minerals in the above mentioned amounts, were prepared and the amount of fuchsin red mentioned against each culture in the table of Dhar Yeast was added in each of them by the procedure mentioned above. These cultures were kept in 500 cc. flatbottom pyrex flasks and the total volume of each culture was made 200 cc. To each of these cultures 20 g. of sucrose were added as the source of carbon. These cultures were sterilised as mentioned above and after cooling they were seeded with a trace of an activated sample of Dhar Yeast.

Observation

Following tables show the result of the effect of fuchsin red on the growth of yeast, alcohol formation, acid production and sugar consumption in 5 per cent (w/v) sucrose solution using *Saccharomyces carlsbergensis* variety of yeast under non-aerated conditions. The *p*H of the cultures was 4.5 in the beginning and the temperature variations during the period of fermentation was between 29.4 to 32.4°C.

These cultures were analysed after 18 days. The figures mentioned in the following tables are for 100 cc. of the cultures.

TABLE I

Serial Number	Fuchsin dye added in the culture (mg.)	Reducing sugar left in the culture after fermentation (g.)	Total sugar left in the culture (g.)	Sugar consumed during fermentation (g.)	Percentage of sugar consumed calc. on the basis of sugar originally present.
1	0.25	2.13	2.25	2.75	55.00
2	0.50	1.85	1.99	3.01	60.20
3	1.00	1.58	1.66	3.34	66.80
4	2.00	1.31	1.33	3.67	73.40
5	4.00	0.00	0.00	5.00	100.00

TABLE II

Serial no. according to Table I.	Total acid formed during fermentation (g. equiv.)	Percentage of acid formation calc. on the basis of sugar consumed	Ethyl alcohol formed during fermentation (g.)	Percentage of alcohol formation calc. on the basis of sugar consumed	Dry yeast grown in the culture (g.)	Percentage of yeast yield calc. on the basis of sugar consumed
1	0.0238	0.86	0.64	23.27	0.4284	15.57
2	0.0524	1.74	0.71	23.65	0.4148	13.76
3	0.0619	1.82	0.96	28.74	0.3938	11.79
4	0.0762	2.07	1.39	37.87	0.3888	10.59
5	0.2142	4.28	2.01	40.20	0.3288	6.57

11) N. R. Dhar, and Krishna Bahadur., *The Proceedings of the National Acad. of Sci.*, Vol. 19, Part II, 55–9 (1950).

Following tables indicate the results of the effect of fuchsin red on Dhar Yeast cultures containing 10 percent (w/v) of sucrose as source of carbon and ammonium sulphate as nitrogen source, under non-aerated conditions. These cultures were analysed after 10 days and the temperature variation during the period of fermentation was between 26.4° to 29.8°C. The *p*H of the cultures in the beginning was 4.5. The results mentioned below are for 100 cc. of the cultures.

TABLE III

Serial No.	Fuchsin added in the culture (mg.)	Total sugar left in the culture after fermentation (g.)	Reducing sugar left in the culture (g.)	Nonreducing sugar left in the culture (g.)	Sugar consumed during fermentation (g.)	Percentage of sugar consumed calc. on the basis of sugar originally present
1	0.125	8.36	6.86	1.50	1.64	16.4
2	0.250	7.76	6.86	0.90	2.24	22.4
3	0.500	6.86	6.85	0.01	3.14	31.4
4	1.000	7.66	7.18	0.48	2.82	28.2

TABLE IV

Serial No. according to Table III	Total acid formed during fermentation (g. equiv.)	Percentage of acid formation calc. on the basis of sugar consumed during fermentation	Ethyl alcohol formed (g.)	Percentage of alcohol formation calc. on the basis of sugar consumed	Dry yeast grown during fermentation (g.)	Percentage of yeast yield calc. on the basis of sugar consumed
1	0.4324	26.21	0.69	44.07	0.7356	44.85
2	0.4232	18.75	0.58	25.89	0.7440	33.21
3	0.4232	13.37	0.53	16.87	0.7694	24.50
4	0.4232	15.24	0.44	15.67	0.7862	24.36

Inference

Dhar Yeast shows a marked decrease in alcohol forming property up to the concentration of 5×10^{-4} per cent of fuchsin red in the culture after which this decrease becomes constant. *Saccharomyces carlsbergensis* indicates a rapid increase in alcohol forming property up to the concentration of 2×10^{-3} per cent of fuchsin in the culture after which this rise becomes gradual and slow.

The acid producing property of Dhar Yeast rapidly decreases up to the concentration of 5×10^{-4} per cent of fuchsin in the culture after which there is an increase in the acid production; where as *Saccharomyces carlsbergensis* shows a gradual increase in the acid forming property from the very beginning. This increase is gradual up to the concentration of 2×10^{-3} per cent of fuchsin in the culture after which the production of acid increases very rapidly.

The sugar consuming property of Dhar Yeast increases gradually up to the concentration of 5×10^{-4} per cent of fuchsin in the culture after which this shows an upward trend. In the case of *Saccharomyces carlsbergensis* the sugar consuming property gradually decreases with the increase of fuchsin concentration in the culture.

The yield of dry yeast decreases in both cases. Dhar Yeast indicates a more sudden fall but *Sacchoromyces carlsbergensis* shows a very gradual decrease in the yeast yield.

Thus we see that there is a correlation between the radiation induced and spontaneous change in the physiological properties of the microorganism. The different effects of the same influencing factor on different organisms is in accordance with the observation made in the case of *E. coli* whose one strain, particularly streptomycin dependent strain frequently changes spontaneously and after ultra violet radiation, whereas another strain was stable in both respects[12].

Summary

When fuchsin dye is added in the yeast cultures it causes a change in the physiological properties of the yeasts which is characterstic of the variety of yeast used. For

12) M. Demerce, B. Wallace, E. M. Witkin, and G. Bertani, *Carnegie Inst. Wash. Yearbook*, **48**. 154 (1949).

many properties this change becomes more gradual as the concentration of dye increases in the culture. Although there is a vast difference in the nature of change of alcohol forming property of the yeasts studied above, changes of the other properties show a similar trend in both the yeasts under examination, when higher concentrations of fuchsin red is present in the cultures.

The presence of fuchsin in the culture is poisonous to the yeasts. This is indicated by the fact that it hinders their growth. This hindrance is directly proportional to the amount of dye in the culture.

I am much thankful to Prof. N. R. Dhar for his valuable advice in this work.

Chemistry Department
Allahabad University
Allahabad, India

Stoichiometric Investigations of the Liquid State. I. The Relation between the Sound Velocity and the Chemical Structure. (1). The Physical Meaning of the Molar Sound Velocity of the Unassociated Liquid

By Kiyoshi TYUZYO[1)]

(Received April 17, 1954)

Introduction

Thermodynamic quantities such as adiabatic compressibility ($\beta_{ad}=1/\rho u^2$, where ρ is density, u is ultrasonic velocity in the liquid) and ratio of specific heat ($\gamma=\beta_{iso}/\beta_{ad}$ where β_{iso} is isothermal compressibility of liquid) can easily be evaluated from the ultrasonic velocity in the liquid. Therefore, the measurement of the ultrasonic velocity in the liquid is important to clarify the intermolecular force in the liquid[2)].

On the other hand, in 1940, Rao found that K, expressed in the following equation, is a characteristic constant of each liquid and is independent of temperature[3)].

$$K=u^{1/3}V \qquad (1)$$

where V is molar volume of the liquid.

Moreover, in 1941, Rao found that K in Eq. 1 can be given as the sum of increments of the constitutive elements[4)]. That is, K, as well as parachor and molar refraction, is independent of temperature and has the additive property.

K is now designated as molar or molecular sound velocity. It is now possible from this investigation to treat quantitatively the relation between sound velocity and the chemical structure of liquid. Thereafter, investigations of this field were remarkably developed and were dealt with very strictly by Lagemann[5)], Weissler[6)], Schaafs[7)], etc. But the theoretical investigation of molar sound velocity has scarcely ever been performed[7a)].

The present author can satisfactorily interpret the physical meaning of molar sound velocity (K), its temperature-invariance, and its additive property on the basis of the simple theory of liquid state, which will be reported in the following series of papers.

The Physical Meaning of Molar Sound Velocity, K

According to Kincaid and Eyring[8)], the sound velocity in a liquid (u) is expressed by the following equation,

$$u=u_{gas}\left(\frac{v}{v_f}\right)^{1/3}=\left(\frac{v}{v_f}\right)^{1/3}\left(\frac{RT\gamma}{M}\right)^{1/2} \qquad (2)$$

where u_{gas} is sound velocity in a gas, v is molecular volume, and v_f is free volume of a liquid.

v_f is approximately given by the following equation[8)],

$$v_f=\left(\frac{CRT\,V^{1/3}}{N^{1/3}E_{vap}}\right)^3, \qquad (3)$$

where E_{vap} is the energy of vaporization and

1) Present Address: Research Laboratory, Dai-Nippon Celluloid Co. Ltd., Sakai City, Osaka.

2) L. Bergmann, "Der Ultraschall" (1949).

3) M. R. Rao, *Indian J. Phys.*, **14**, 109 (1940).

4) M. R. Rao, *J. Chem. Phys.*, **9**, 682 (1941).

5) R. T. Lagemann and W. S. Dunbar, *J. Phys. Chem.*, **49**, 428 (1945), etc.

6) A. Weissler, J. W. Fitzgerald and I. Resnick. *J. Appl. Phys.*, **18**, 434 (1974), etc.

7) W. Schaafs, *Z. phys. Chem.*, **A 194**, 28 (1944), etc.

7a) Recently, some theoretical explanation of the Rao's relation has been given by O. Nomoto and T. Kishimoto on the basis of the Lennard-Jones, Devonshires' model: *J. Phys. Soc. Japan*, **9**, 59, 66, 73 (1954).

8) J. F. Kincaid and H. Eyring, *J. Chem. Phys.*, **6**, 620 (1938).

C is the packing number of liquid. (This is equal to 2 for cubic packing.)

Then, u is expressed by Eq. 4, making use of Eq. 2 and 3.

$$u = \frac{E_{vap}\,\gamma^{1/2}}{C(MRT)^{1/2}} \tag{4}$$

Therefore,

$$u^{1/3}V = \left[\frac{E_{vap}\,\gamma^{1/2}}{C(MRT)^{1/2}}\right]^{1/3} V \tag{5}$$

In comparison of Eq. 5 and Rao's Eq. 1, the molar sound velocity is expressed as follows,

$$K = \left[\frac{E_{vap}\,\gamma^{1/2}}{C(MRT)^{1/2}}\right]^{1/3} V \tag{6}$$

Namely, Rao's characteristic constant, K, as is shown in Eq. 6, contains several factors such as geometrical configuration of the liquid state (C, V), thermodynamic property of the gaseous state (γ), and property of equilibrium state between liquid and gas (E_{vap}). Therefore, it is rather questionable to conclude simply the additivity of K as was done by Rao[3] and Lagemann[9]. The author will discuss this conclusion in the second paper of this series.

Temperature-invariance of K

In Eq. 6, $E_{vap}^{1/6}$, $\gamma^{1/6}$, $C^{1/3}$ and V are dependent on temperature. But, among them, temperature-variance of $\gamma^{1/6}$ is negligible and $C^{1/3}$ can be regarded as temperature-invariable in the range of ordinary temperature (ca. 0° to 100°C). C must be equal to 2 for the cubic packing. For normal unassociated liquids, this value was computed from the vapor pressure data by Eyring and others and is approximately equal to 2. The present author has examined the temperature-variance of C by calculating it from Eq. 5, using the observed value of u, and found that its temperature-variance does not exceed several percent in the range of 50°C for normal liquids. Examples are shown in Table I. Table II shows the comparison of C values obtained from sound velocity and from vapor pressure. The coincidence of the values from two different methods is satisfactory and both methods give $C=2$ on the average, but in general, the value from sound velocity is somewhat smaller than that from vapor pressure.

As no satisfactory theoretical equation for the temperature-variance of E_{vap} and V can be found, so their values at each temperature were obtained from International Critical Table and other tables.

9) R, T. Lagemann, J. S. Evans, and D. R. McMillan, Jr, *J. Amer. Chem. Soc.*, **70**, 2696 (1948).

TABLE I
THE TEMPERATURE-INVARIANCE OF PACKING NUMBER, C

Temperature (°C)	C
Benzene	
10	1.80
20	1.80
30	1.80
40	1.80
50	1.81
60	1.81
Chloroform	
0	1.82
10	1.82
20	1.81
30	1.81
40	1.81
50	1.81
60	1.81

TABLE II
PACKING NUMBER, C, OF NORMAL LIQUIDS

Substance	C from Sound Velocity	C from Vapor Pressure[10]
n-Heptane	——	1.60
n-Octane	1.61	——
Ethyl ether	1.89	1.92
Benzene	1.80	2.12
Acetone	2.09	1.76
Carbon disulfide	1.76	2.05
Ethyl bromide	1.89	——
Ethylene chloride	1.81	——
Chloroform	1.81	2.44
Carbon tetrachloride	1.77	2.08

γ is the value from the Taschenbuch[11], but in the case of the compound of which γ is unknown, its value is approximately obtained from the following method. As the first approximation, γ-values are determined by the number of atoms constructing the molecule, then the relation between known values of γ and numbers of atoms constructing the molecule is drawn in Fig. 1. As is

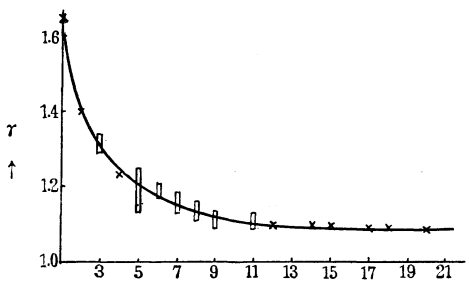


Fig. 1. The relation between the ratio of specific heats (γ) and the number of atoms constituting the molecule in the gaseous state.

10) H. Eyring and J. Hirschfelder, *J. Phys. Chem.*, **41**, 249 (1937).

11) J. D'Ans and E. Lax, "Taschenbuch für Chemiker und Physiker" (1949).

shown in the figure, γ varies in the considerably broad range in the molecules which are made of small numbers of atoms, but the values become fixed dependent only upon the numbers of atoms constructing the molecule when the molecules are made of many numbers of atoms. If the experimental values are connected with a smooth curve as in the figure, γ can be determined from this curve when the number of atoms constructing the molecule is known. (As γ appears in Eq. 6 with 1/6-power, this degree of approximation is quite satisfactory.)

With these treatments, E_{vap}, γ, C and V-values are known, and so K-values can be calculated by Eq. 6 at several temperatures.

Results are shown in Table III for several normal liquids. As is clear from the table, K is almost independent of temperature and this result is consistent with that of Rao and others.

TABLE III
TEMPERATURE-INVARIANCE OF THE CAICULATED K-VALUES FOR NORMAL LIQUIDS

Temperature (°C)	E_{vap} (cal/mol)	ρ(g./cc.)	K_{calc} (c.g.s.)
n-Octane, $M=114.2$, $\gamma=1.05$			
0	7660	0.719	7410
20	7620	0.702	7470
40	7580	0.686	7540
Benzene, $M=78.2$, $\gamma=1.10$			
10	7640	0.890	4370
20	7500	0.879	4360
30	7360	0.868	4360
40	7220	0.858	4370
50	7070	0.847	4370
60	6920	0.836	4370
Ethyl bromide, $M=109.0$, $\gamma=1.19$			
0	6240	1.501	3260
10	6150	1.480	3270
20	6070	1.461	3250
30	6010	1.440	3290
Ethylene chloride, $M=99.0$, $\gamma=1.37$			
0	7870	1.281	3780
10	7780	1.267	3780
20	7670	1.251	3780
30	7550	1.238	3790
40	7430	1.223	3790
50	7300	1.209	3800
Chloroform, $M=119.4$, $\gamma=1.15$			
0	7170	1.525	3620
10	7040	1.506	3620
20	6900	1.487	3610
30	6780	1.467	3620
40	6640	1.449	3620
50	6500	1.429	3620
60	6370	1.409	3630
Carbon tetrachloride, $M=153.9$, $\gamma=1.13$			
0	7740	1.633	4270
10	7460	1.613	4240
20	7210	1.594	4220
30	7080	1.575	4210
40	7000	1.556	4230
50	6930	1.536	4240
Acetone, $M=58.05$, $\gamma=1.1$			
0	7260	0.813	3690
10	7170	0.801	3710
20	7050	0.791	3710
30	6920	0.779	3720
40	6790	0.767	3740
50	6640	0.755	3750
Ether, $M=74.1$, $\gamma=1.08$			
0	6290	0.736	4750
10	6090	0.725	4750
20	5880	0.714	4750
30	5700	0.702	4750
Methyl acetate, $M=74.1$, $\gamma=1.14$			
10	7570	0.946	3950
20	7300	0.932	3930
30	7070	0.918	3930

Comparison of the Calculated and Observed K-values

It was found in the previous paragraph that K calculated from Eq. 6 is independent of temperature and is the characteristic constant of the substance. Next, the K-values calculated from Eq. 6 and observed (Eq. 1) are compared. Results are shown in Table IV[12]. It is clear from the table,

$$K_{calc}/K_{obs}=1$$

(Accuracy is about ±5%.)

TABLE IV
THE CALCULATED AND OBSERVED MOLAR SOUND VELOCITIES, K

Substance	K_{calc}	K_{obs}	K_{calc}/K_{obs}
n-Hexane	6070	6260	0.969
n-Octane	7470	7990	0.936
Benzene	4360	4530	0.962
Carbon disulfide	2810	2940	0.957
Ethyl bromide	3250	3340	0.973
Ethylene chloride	3780	3910	0.967
Chloroform	3610	3730	0.968
Carbon tetrachloride	4220	4390	0.962
Ether	4750	4830	0.983
Acetone	3710	3610	1.027
Methyl acetate	3930	3890	1.010
Ethyl acetate	4770	4810	0.992
Ethyl formate	3260	3730	0.874
Ethyl iodide	3480	3570	0.974
Toluene	6040	6240	0.969
Cyclohexane	5100	5430	0.939

Summary

(1) The physical meaning of Rao's molar sound velocity (K) is given.

(2) It is found that K-values calculated from the theory are independent of temperature in the case of normal liquids.

(3) It is found that the calculated K-values are satisfactorily coincident with the observed ones for normal liquids (aliphatic and aromatic hydrocarbons, ether, acetone, esters, alkyl halides).

12) As the sound velocity, u is ordinarily expressed in the unit of m./sec., so K_{obs} must be converted in the c. g. s. unit. Namely, ordinary K must be multiplied by $(100)^{1/3}=4.62$.

The author expresses his hearty thanks to Prof. Dr. N. Sata of the Osaka University for his valuable encouragement throughout this task. The author also expresses his sincere thanks to Mr. M. Okuyama of the Osaka University for his valuable discussions and Dr. O. Nomoto of the Kobayashi Institute of Physical Research for his kind suggestions, although his opinion is not always consistent with the author's own.

Department of Chemistry, Faculty of Science, Osaka University, Nakanoshima, Osaka

Stoichiometric Investigations of the Liquid State. II. The Relation between the Sound Velocity and the Chemical Structure. (2). The Additivity of the Molar Sound Velocity of Unassociated Liquids

By Kiyoshi TYUZYO[1]

(Received April 17, 1954)

Introduction

According to the first paper of this series[2], Rao's molar sound velocity[3] ($K=u^{1/3}V$) is derived from the simple theory of the liquid state and the calculated molar sound velocity is independent of temperature. Furthermore, the calculated and observed molar sound velocities are coincident with each other with the accuracy of ±5%. The molar sound velocity, K, is expressed by the following equation from the theory,

$$K=\left[\frac{E_{\text{vap}}\,\gamma^{1/2}}{C(MRT)^{1/2}}\right]^{1/3}V \qquad (1)$$

The previous paper may be referred to about the meaning of notations in Eq. 1.

Rao[4] found experimentally that K has the additive property. The additivity of K for normal unassociated liquids will be explained theoretically in this paper.

Calculation of "Atomic-" and Radical Sound Velocity"

If K has the additive property, it is reasonable to assume as follows on the basis of Eq. 1.

$$K=\Sigma K_{\text{a}} \qquad (2)$$

$$K_{\text{a}}=\frac{\gamma^{1/6}}{C^{1/3}(RT)^{1/6}}\left[\frac{\Delta E}{M_{\text{a}}{}^{1/2}}\right]^{1/3}V_{\text{a}} \qquad (3)$$

In Eq. 2 and 3, M_{a}, V_{a} mean the corresponding values for each constitutive atom or radical and ΔE is the energy of vaporization per each element. This value can be approximately substituted by the cohesive energy as shown below. K_{a} may be named as "atomic-" or "radical sound velocity". Lagemann and others[5] have already pointed out that the additivity of K does not completely hold but some constitutive effect is present. As K_{a} contains the packing number and energy factor (C, ΔE), so it is natural that some constitutive effect is present as long as C and ΔE-values are related with the intermolecular interaction. Here, the author does not enter into such a detailed discussion as the influence of intermolecular interaction but calculates only K-values as the first approximation.

Because the packing number and ratio of specific heats seem to be not so remarkably dependent on the species of molecules, and, moreover, because γ enters with the 1/6 power, C enters with the 1/3 power in Eq. 3, γ and C are put equal to 1.4 and 2 respectively. In the ordinary range of liquid (0~100°C), absolute temperature (T) is nearly 300~400° and furthermore, it enters in Eq. 3 with the 1/6 power, and so T is put equal to 300 approximately. Moreover, if ΔE and R are expressed in cal/mol, then Eq. 3 becomes the following.

$$K_{\text{a}}=5.42\times\left[\frac{\Delta E}{M_{\text{a}}{}^{1/2}}\right]^{1/3}V_{\text{a}} \qquad (4)$$

where, of course, $M_{\text{a}}=\sum_{\text{i}}M_{\text{ai}}$. M_{ai} is the atomic weight that constitutes the atoms or radicals and V_{a} is the sum of the constituting atoms (V_{ai}) in the corresponding state.

V_{a} may be put equal to $\sum_{\text{i}}V_{\text{ai}}$ approximately[6]. This approximation is quite satisfactory for the present case. (V_{ai} is the atomic volume in the liquid state.)

ΔE corresponds to the cohesive energy and M.

1) Present address: Research Laboratory, Dai-Nippon Celluloid Co. Ltd., Sakai City, Osaka.
2) K. Tyuzyo, The first paper of this series.
3) M. R, Rao, *Indian J. Phys.*, **14**, 109 (1940).
4) M. R. Rao, *J. Chem. Phys.*, **9**, 682 (1941).
5) R. T. Lagemann, J. S. Evans, and D. R. McMillan, Jr. *J. Amer. Chem. Soc.*, **70**, 2996 (1948).
6) Even the proportionality does not hold between the so-called zero-point atomic volume in the solid state and the atomic volume in the liquid state. Therefore, the atomic volume in the liquid state must be adopted as the Vai-value.

Dunkel has already found the approximate additivity for this quantity[7].

Now, we can calculate atomic or radical sound velocity (K_a) from Eq. 4. The calculated K_a-values from Eq. 4, the observed ones, and the K_{acalc}/K_{aobs} are shown in Table I. It is clear from the table that the calculated K_a-values are approximately equal to the observed ones with the accuracy of about ±10%.

If several assumptions and approximations made for the above calculation are allowed for, this result seems to be quite satisfactory.

TABLE I

CALCULATED AND OBSERVED ATOMIC OR RADICAL SOUND VELOCITY (K_a)

Atom or radical	ΔE[8] (cal/mole)	M_a	V_a[9]	K_{acalc}	K_{aobs}[10]	K_{acalc}/K_{aobs}
$-CH_2-$	990	14.0	22.0	763	905	0.850
$-CH_3$	1780	15.0	27.5	1154	1330	0.868
$-O-$	1630	16.0	7.8	313	345	0.907
$-Cl$	3400	35.5	22.1	993	1055	0.941
$-Br$	4300	79.9	27.8	1179	1137	1.037
$-I$	5040	126.7	37.5	1550	1300	1.191
$>C=O$	4270	28.6	18.8	949	860	1.103
$=CH$	1780	14.0	(22.0)[10a]	(930)	1416	(0.795)

TABLE II

THE CALCULATED AND OBSERVED MOLAR SOUND VELOCITY

Substance	Chemical Formula	$K_{obs}=u^{1/3}V$	$K_{calc}=\Sigma K_{acalc}$	K_{calc}/K_{obs}	Literature
n-Pentane	C_5H_{12}	5390	4610	0.855	(11)
n-Hexane	C_6H_{14}	6260	5380	0.859	〃
n-Heptane	C_7H_{16}	7130	6150	0.863	〃
n-Octane	C_8H_{18}	7990	6910	0.865	〃
n-Nonane	C_9H_{20}	8650	7680	0.888	〃
Ethyl bromide	C_2H_5Br	3335	3100	0.929	(12)
Ethyl iodide	C_2H_5I	3570	3470	0.972	〃
n-Propyl chloride	C_3H_7Cl	4210	3680	0.874	(5)
n-Propyl bromide	C_3H_7Br	4200	3870	0.922	〃
n-Butyl chloride	C_4H_9Cl	5070	4450	0.878	〃
n-Butyl bromide	C_4H_9Br	5020	4640	0.925	〃
n-Butyl iodide	C_4H_9I	5230	5010	0.958	(12)
Methylene chloride	CH_2Cl_2	3040	2760	0.909	(5)
Methylene bromide	CH_2Br_2	3210	3130	0.975	〃
Methylene iodide	CH_2I_2	3690	3870	1.048	(12)
Ethylene chloride	$C_2H_4Cl_2$	3910	3520	0.901	(5)
Ethylene bromide	$C_2H_4Br_2$	4010	3890	0.970	〃
Propylene chloride	$CH_2ClCH_2CH_2Cl$	4760	4290	0.901	〃
Propylene bromide	$CH_2BrCH_2CH_2Br$	4820	4160	0.863	〃
Ethyl ether	$C_2H_5OC_2H_5$	4820	4160	0.863	(2)
Acetone	CH_3COCH_3	3620	3260	0.900	〃
Methyl acetate	CH_3COOCH_3	3890	3570	0.917	(13)
Ethyl acetate	$CH_3COOC_2H_5$	4660	4330	0.929	〃

7) M. Dunkel, *Z. phys. Chem.*, A**138**, 42 (1928).

8) H. Mark and A. V. Tobolsky, "Physical Chemistry of High Polymeric Systems," p. 144 (1950).

9) S. Glsstone, "Textbook of Physical Chemistry," p. 525 (1946).

10) R. T. Lagemann, and W. S. Dunbar, *J. Phys. Chem.*, **49**, 425 (1945).

10a) As the correction for the atomic volume for the double bond is not made, the K_{acalc} of (CH=) is somewhat inaccurate.

11) L. Bergmann, "Der Ultraschall," (1949).

12) R. T. Lagemann, D. R. McMillan, Jr., and W. E. Woolf, *J. Chem. Phys.*, **17**, 369 (1949).

13) R. T. Lagemann. E. G. McLeroy, and O. Milner, *J. Amer. Chem. Soc.*, **73**, 5891 (1951).

Comparison of the Observed Molar Sound Velocities and the Calculated Ones from the Atomic and Radical Sound Velocities.

As an application of the above result, the calculated K from K_{acalc}-values in Table I and the observed ones for unassociated liquids are shown in Table II. The consistency of K_{calc} and K_{obs} is quite satisfactory, and so the above method of calculation is fully reasonable as the first approximation.

Discussion

If the quantities which may be regarded as constant in Eq. 1 are written A, then

$$K=A\left(\frac{E_{vap}}{M^{1/2}}\right)^{1/3}V \qquad (5)$$

From the assumption of Eq.2 and 3, Eq. 5 is

$$K=\Sigma K_a=A\Sigma\left[\left(\frac{\Delta E}{M_a^{1/2}}\right)^{1/3}V_a\right] \qquad (6)$$

On the other hand, from the assumptions,

$$\left.\begin{aligned} M&=\Sigma M_a,\\ E_{vap}&=\Sigma\Delta E,\\ V&=\Sigma V_a. \end{aligned}\right\} \qquad (7)$$

Therefore, from Eq. 5 and 7,

$$K=A\left[\frac{\Sigma(\Delta E)}{(\Sigma M_a)^{1/2}}\right]^{1/3}(\Sigma V_a) \qquad (8)$$

In general, Eq. 6 is not consistent with Eq. 8, and Eq. 8 contains many more cross terms than Eq. 5. Therefore, it is not clear at present whether the discrepancy (about 10%) between the calculated and observed values in Table II is due to the existence of these cross terms or the constitutional effect of ΔE and V coming from the intermolecular interaction. But, considering the fact that the calculated and observed K_a (Table I) has already about 10% difference, the influence of the constitutive effect of ΔE and V seems to be larger than that of the cross terms. (If the influence of cross terms is large, the deviation of the calculated K-value must be larger than that of the calculated K_a-value.) Of course, more detailed investigation is necessary for this point.

Next, as a useful application of Eq. 4, molar cohesion, ΔE, can be reversely calculated if K_a, M_a, V_a are known. ΔE, is derived from the temperature-variance of vapor pressure until now and that method is considerably difficult, but from Eq. 4, its value is very simply calculated.

Summary

(1) The additivity of molar sound velocity has theoretically been derived and the calculated and observed "atomic-" and "radical sound velocity" were shown to coincide with each other with the accuracy of about ±10%.

(2) The molar sound velocity derived from the calculated atomic and radical sound velocity was shown to coincide with the observed value with about 10 % deviation for unassociated liquids. (e. g., paraffins, alkyl halides, ethers, ketones, esters)

(3) The cause of deviation of the calculated and observed values and the application of this theory are briefly discussed.

The author expresses his hearty thanks to Prof. Dr. N. Sata and Mr. M. Okuyama of the Osaka University for their encouragement in this work. The author also expresses his sincere thanks to Dr. O. Nomoto of the Kobayashi Institute of Physical Research for his kind suggestions, although his opinion is not always consistent with the author's own.

Department of Chemistry, Faculty of Science, Osaka University, Nakanoshima, Osaka

Stoichiometric Investigations of the Liquid State. III. The Relation between the Sound Velocity and the Chemical Structure. (3). Molar Sound Velocity and its Additivity for Associated Liquids

By KIYOSHI TYUZYO[1)]

(Received April 17, 1954)

Introduction

The author theoretically calculated the molar sound velocity of unassociated liquid and found its calculated value to be independent of temperature and to be satisfactorily consistent with the observed value[2)]. Then, the author interpreted the additivity of the molar sound velocity and also showed that the calculated atomic or radical sound velocity was satisfactorily consistent with the observed one[3)]. In this paper, results of the same analysis for associated liquids will be reported.

The Temperature Variation of the Molar Sound Velocity of Associated Liquids

According to the first paper, Rao's molar sound velocity, K, is expressed by the following equation.

$$K=\left[\frac{E_{\mathrm{vap}}\gamma^{1/2}}{c(MRT)^{1/2}}\right]^{1/3}V \qquad (1)$$

The previous paper may be referred to about the meaning of notations in Eq. 1.

The temperature variation of K calculated from Eq. 1 is shown in Table I. There are few substances of which all values in Eq. 1 are complete. They are only water, methyl alcohol and ethyl alcohol. As the special case, the liquefied gas, oxygen and nitrogen, are also added in the table.

TABLE I
TEMPERATURE VARIANCE OF MOLAR SOUND VELOCITY OF ASSOCIATED LIQUID AND LIQUEFIED GAS

Temperature (°C)	E_{vap} (cal/mole)	ρ (g/cc)	K_{calc}
Water ($M=18.0$, $\gamma=1.336$)			
0	10170	1.000	1310
10	10050	1.000	1300
20	9920	0.998	1270
30	9800	0.996	1275
40	9700	0.992	1270
50	9570	0.988	1260
60	9460	0.983	1260
70	9340	0.978	1255
80	9210	0.972	1250
Methyl alcohol ($M=32.04$, $\gamma=1.203$)			
0	8540	0.810	2420
10	8450	0.801	2430
20	8350	0.791	2430
30	8220	0.782	2440
40	8080	0.772	2430
50	7950	0.763	2440
Ethyl alcohol ($M=46.07$ $\gamma=1.13$)			
0	9550	0.806	3380
10	9480	0.798	3390
20	9400	0.789	3395
30	9320	0.781	3405
40	9250	0.772	3410
50	9130	0.764	3420
Oxygen ($M=32.00$, $\gamma=1.425$)			
−210	306	1.272	978
−200	270.5	1.224	955
−190	234	1.176	926
−185	217	1.152	909
Nitrogen ($M=28.02$, $\gamma=1.42$)			
−203	192	0.843	1110
−201	184.5	0.834	1110
−199	177	0.824	1100
−197	170	0.815	1090

It is clear from the table that K of water, liquid oxygen and liquid nitrogen are considerably dependent on temperature, but K of alcohols are nearly independent of temperature like unassociated liquids. Weissler accurately measured the sound velocity in a number of alcohols and calculated the molar sound velocity on the bases of the definition, $K=u^{1/3}V$.[4)] Then, he found that K of alcohols are independent of temperature, in contrast with water. This result is quite consistent with the above result of calculation.

In the calculation from Eq. 1, all values are observed ones except $C=2$. But whether $C=2$ or not is questionable. On trial, C was calculated from sound velocity by the following equation[2)].

$$C=\frac{E_{\mathrm{vap}}\gamma^{1/2}}{u(MRT)^{1/2}} \qquad (2)$$

1) Present Address: Research Laboratory, Dai-Nippon Celluloid Co. Ltd., Sakai City, Osaka.
2) K. Tyuzyo, This Bulletin, **27**, 300 (1954).
3) K. Tyuzyo, This Bulletin, **27**, 303 (1954).
4) A. Weissler, *J. Amer. Chem. Soc.*, **70**, 1634 (1948),

The calculated temperature variation of C is shown in Table II. It is clearer than in Table I that C of water, liquid oxygen, and liquid nitrogen are dependent on temperature but those of alcohols are almost constant.

TABLE II

TEMPERATURE VARIANCE OF PACKING NUMBER, C

temperature (°C)	C
water	
0	5.47
10	5.15
20	4.69
30	4.67
40	4.48
50	4.30
60	4.17
70	4.05
80	3.94
liquid oxygen	
−210	1.04
−200	0.93
−190	0.81
−185	0.76
liquid nitrogen	
−203	0.81
−201	0.79
−199	0.76
−197	0.73
methyl alcohol	
0	3.87
10	3.86
20	3.86
30	3.86
40	3.84
50	3.83
ethyl alcohol	
0	3.34
10	3.36
20	3.38
30	3.40
40	3.41
50	3.42

In Table III C-values at 20°C are shown for several associated liquids. The C-values in the third row are the calculated ones from vapor pressure by Eyring and others[5]. The values of C of water, ethylene glycol, and glycerol are much larger than 2, while on the contrary, C those of liquid oxygen and nitrogen, are much smaller than 2. However, in methyl and ethyl alcohol the value is much larger than 2, and the higher the alcohol, the smaller C becomes and its value converges to 2. For fatty acids C is generally 2 except formic and acetic acid. The above facts will be discussed later. Perhaps these are due to the difference in the associated state of the associated liquid.

4) H. Eyring and J. Hirshfelder, *J. Phys. Chem.*, **41**, 249 (1937).

TABLE III

PACKING NUMBER, C, OF ASSOCIATED LIQUIDS (20°C)

Substance	C	C from vapor pressure
water	4.69	—
ethylene glycol	3.17	—
glycerol	2.74	—
oxygen	0.93 (−200°C)	—
nitrogen	0.79 (−201°C)	—
mercury	—	0.21
methyl alcohol	3.86	0.43
ethyl alcohol	3.38	—
n-propyl alcohol	2.57	—
n-butyl alcohol	2.36	—
n-amyl alcohol	2.26	—
n-hexyl alcohol	2.16	—
n-heptyl alcohol	2.10	—
n-octyl alcohol	2.03	—
formic acid	1.46	—
acetic acid	1.51	—
n-propionic acid	1.72	—
n-butylic acid	2.17	—
n-valeric acid	2.04	—
n-caproic acid	1.94	—
n-heptylic acid	1.86	—
n-caprylic acid	1.82	—

The Calculated Values of Molar Sound Velocity

Table IV shows the calculated (C is put equal to 2) and observed molar sound velocity, K. K_{calc} of water, ethylene glycol, glycerol, oxygen, nitrogen, methyl alcohol, ethyl alcohol, formic acid, and acetic acid are considerably different from K_{obs}, but others are consistent with $K_{calc.}$ (about 5% deviation).

TABLE IV

CALCULATED AND OBSERVED VALUES OF MOLAR SOUND VELOCITY, K

Substance	K_{calc}	K_{obs}	K_{calc}/K_{obs}
water	1070	955	1.198
ethylene glycol	3520	3020	1.167
glycerol	4700	4220	1.114
oxygen	955	1234	0.774
nitrogen	1110	1490	0.747
methyl alcohol	2430	1955	1.242
ethyl alcohol	3400	2860	1.188
n-propyl alcohol	3920	3720	1.053
n-butyl alcohol	4620	4625	0.999

n-amyl alcohol	5300	5440	0.973
n-hexyl alcohol	6120	6380	0.958
n-heptyl alcohol	6950	7200	0.965
n-octyl alcohol	7630	8080	0.944
formic acid	1630	1905	0.857
acetic acid	2360	2780	0.850
n-propionic acid	3240	3650	0.888
n-butylic acid	4410	4530	0.974
n-valeric acid	5110	5430	0.942
n-caproic acid	5830	6300	0.927
n-heptylic acid	6550	7210	0.908
n-caprylic acid	7260	8090	0.899

Additivity of Molar Sound Velocity

According to the second paper of this series[3], the molar sound velocity, K, is expressed as the sum of atomic or radical sound velocities, K_a. Namely,

$$K=\sum K_a \tag{3}$$

$$K_a=5.42\times\left[\frac{\Delta E}{M_a^{1.2}}\right]^{1/3}V_a \tag{4}$$

The previous paper may be referred to about the meaning of notations in Eq. 4.

Table V shows the radical sound velocities of hydrogen-bonding radicals calculated from Eq. 4. Generally, the calculated value is larger than the observed, but the deviation is not much larger than that of the normal radicals except amine-radical.

Table VI shows the calculated K using the valve of Table V and the observed one of associated liquids. The consistency is generally satisfactory. Perhaps, the fact that the deviations of $-CH_2-$ and -OH radical compensate each other is the cause of this fact.

TABLE V

RADICAL SOUND VELOCITY OF HYDROGEN-BONDING RADICALS

radical	ΔE(cal/mole)[6]	M_a	V_a[7]	K_{acalc}	K_{aobs}	K_{acalc}/K_{aobs}
—OH	7250	17.0	13.3	869	773	1.124
—COOH	8970	45.0	32.1	1910	1633	1.170
—SH	4250	33.1	28.1	1308	—	—
$—NH_2$	3530	16.0	21.5	1116	842	1.325

TABLE VI

CALCULATED K AS THE SUM OF ATOMIC OR RADICAL SOUND VELOCITY AND OBSERVED ONES FOR ASSOCIATED LIQUIDS

substance	K_{obs}	K_{calc}	K_{calc}/K_{obs}	literature of K_{obs}
water	955	—	—	(8)
ethylene glycol	3020	3272	1.083	〃
glycerol	4220	—	—	〃
methyl alcohol	1955	2023	1.033	(4)
ethyl alcohol	2860	2790	1.011	〃
n-propyl alcohol	3720	3557	0.956	〃
n-butyl alcohol	4625	4324	0.935	〃
n-amyl alcohol	5440	5091	0.937	〃
formic acid	1905	—	—	(8)
acetic acid	2780	3064	1.101	〃
n-propionic acid	3650	3831	1.049	〃
n-butylic acid	4530	4600	1.014	〃
n-valeric acid	5430	5365	0.988	〃

Discussion

Summarizing the results of the previous sections.

(1) The calculated K of alcohols are almost independent of temperature, but that of water is remarkably dependent on temperature. This fact is clearer from the packing number, C. These results are censistent with the experimental results of Weissler. Below, for convenience, the associated liquids such as alcohols and fatty acids series are named as "the associated liquids of the first kind" and water, ethylene glycole, glycerol, etc. are named as" the associated liquids of the second kind."

(2) Packing number is much larger than 2 (normal value) for the associated liquids of the second kind, but is almost 2 for the asoociated liquids of the first kind except

6) H. Mark and A. V. Tobolsky, "Physical Chemistry of High Polymeric Systems," p. 144 (1950).
7) S. Glasstone, "Textbook of Physical Chemistry," p. 525 (1946).
8) L. Bergmann, "Der Ultraschall," p. 263 (1949).

the initial two members of the homologous series.

(3) The consistency of the calculated and observed K is unsatisfactory for the associated liquids of the second kind, but is satisfactory in those of the first kind except the initial two members of the homologous series.

(4) The calculated radical sound velocity is consistent with the observed value with the deviation of about 15% and the calculated molar sound velocity based on the additivity principle is satisfactorily consistent with the observed value in the associated liquids of the first kind. (Data for the associated liquids of the second kind are lacking, but the calculated value of K of ethylene glycol is consistent with the observed one).

Until now, methods of inferring the state of association of associated liquids from sound velocity were those of Lagemann[9] and van Itterbeek[10], but these are both unsatisfactory even qualitatively, as well as quantitatively. The results obtained in this paper are also not so striking, but it seems to be reasonable to divide the associated liquids into the first and the second kind. The author already showed that the associated liquids must be distinguished in the first and second kind by the analysis of the viscous flow[11]. It is a very interesting fact that this is also reasonable in the case of molar sound velocity. According to the author's opinion, it is probable that in the associated liquids of the second kind, there exist no clearly distinguishable associated units and they have a network structure as a whole, and their structures are remarkably deformable and also destroyed with the increase of temperature. In this case it is natural that molar sound velocity shows the several abnormalities as are shown above. On the other hand, in the associated liquids of the first kind, there exist clearly distinguishable associated units, and hydrogen bond connecting this unit is almost strong enough not to be influenced by temperature. Then, except the fact that the unit is large, the molecules of the associated liquids of the first kind are the same as the molecules of the normal liquids. Moreover, E_{vap}, V of Eq. 1 and ΔE, V_a of Eq. 4 contain already the factors of the associated state and so molar sound velocity has no abnormalities. Abnormalities of formic acid and acetic acid probably depend on the special type of association in the liquid state[11,12]. Abnormalities of methyl and ethyl alcohol can not be explained at present.

Lastly, among the methods of determining the state of association of the associated liquids, those methods are quite unsatisfactory which contain the energy of vaporization as an important factor; for example, surface tension, parachor[13] and sound velocity. In the energy of vaporization of the associated liquids, dissociation energy of associated units is contained in addition to the normal cohesive energy. Therefore, it seems to be very difficult to obtain any knowledge about the state of association from the vaporization phenomenon[14]. Those methods which use the properties of the liquids themselves such as viscosity are more effective than those which depend on the quantity of the equilibrium state of liquids and gases such as energy of vaporization for studying the state of association[11,12].

Summary

(1) Associated liquids are analysed with a method similar to that of the previous papers, and the temperature variation of molar sound velocity, comparison with experiment, calculation of the radical sound velocity, additivity, etc. are developed.

(2) It seems to be reasonable to distinguish the associated liquids to the first and second kind. This is consistent with the results of the author's investigation of the viscous flow.

(3) Something about the structure of the associated liquids of the first and second kind, and methods of investigating the state of association are discussed.

The authors expresses his hearty thanks to Prof. Dr. N. Sata and Mr. M. Okuyama of the Osaka University for their encouragement in this work. The author also expresses his sincere thanks to Dr. O. Nomoto of the Kobayashi Institute of Physical Research for his kind suggestions, although his opinion is not always consistent with that of the author.

Department of Chemistry, Faculty of Science Osaka University, Nakanoshima, Osaka

9) R. T. Lagemann, *J. Chem. Phys.*, **12**, 464 (1948).
10) A. van Itterbeek and A. De Bock, *Nature*, **162**, 611 (1948).
11) K. Tyuzyo, *Kolloid-Z.*, **131**, 40 (1953).
12) K. Tyuzyo, The fourth and fifth paper of this series, to be published elsewhere.
13) S. Sugden, "Parachor and Valency", Chap. VIII(1930).
14) K. Tyuzyo, The sixth paper of this series, to be published elsewhere.

LETTER

Die Einwirkung der Wechselspannung auf die Tropfzeit der Quecksilbertropfelektrode

Von Isamu TACHI und Mitsuko OKUDA

(Eingegangen am 27. Feb. 1954)

Die Tropfzeit der in die elektrolytische Lösung getauchten Quecksilbertropfelektrode, whelche sich als eine vollkommen polarisierte Elektrode varhält, verändert sich bekanntlich mit der Variation der Gleichstromspannung, die zwischen der Tropfelektrode und der unpolarisierbaren Gegenelektrode angelegt ist, und zwar beobachtet man eine annähernd parabolische Tropfzeit(τ)-Spannung(E)-Kurve, deren Maximum bei -0.4—0.7 Volt vs. norm. Kalomelelektrode liegt. Die Tropfzeit ist nach der Tateschen Theorie ergeben durch

$$\tau = \frac{2\pi r}{m} \cdot \sigma,$$

worin τ = Tropfzeit in Sek., r = Innerer Radius der Kapillare in cm., m = Ausflussgeschwindigkeit des Quecksilbers in g/Sek., und σ = Oberflächenspannung der Quecksilbertropf in dyn./cm. Hierin ist r/m bei der angegebenen Kapillare und Niveauhöhe konstant. Daher zeigt die τ-E-Kurve die Abhängigkeit der Hg-Lösung-Oberflächenspannung; d. h. es besitzt dieselbe Eigenschaft wie die Elektrokapillarkurve.

Neuerlich haben Frau Fournier[1] und Breyer mit seinem Kollegen[2] die Wechselspannungpolarographie untersucht, worin eine Wechselspannung von geringer Amplitude der gewöhnlichen Gleichstromspannung überlagert wird. Wir haben auch diese neue Art der polarographischen Elektrolyse versucht, und eine neue Erscheinung von der Diskontinuität in τ-E-Kurve gefunden. Also haben wir die Einwirkung der Wechselspannung auf die Tropfzeit versucht. Die verwandte Lösung war 0.1 N KCl, worin das Wasserstoffgas acht Stunden durchgeleitet worden war, und die für zehn Tropfen erforderliche Zeitdauer wurde gemessen. Das Schaltbild ist in Abb. 1 angegeben, und in Abb. 2 ist die Tropfzeit gegen die Spannung aufgetragen. Die Überlagerung der Wechselspannung veranlässt keine beträchtliche Veränderung

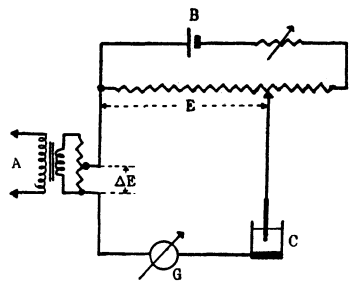


Abb. 1.
Schaltbild
A: Sinusförmige Wechselspannung von 60 Hz.
B: 2~4 Volt. Akkumulator
C: Quecksilbertropfelektrode
G: Galvanometer

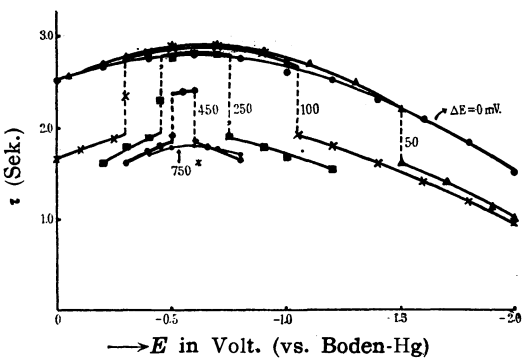


Abb. 2.
τ-E-Kurve
(0.1 norm. KCl bei gewöhnlicher Temperatur)
* Wenn die Amplitude der überlagerten Wechselspannung 755 mV. übersteigt, so wird die Tropfzeit irregulär.

der τ-E-Kurve in der Nähe des dem Elektrokapillarmaximum entsprechenden Potentials. Jedoch, wenn die angelegte Spannung negativer wird und einen gewissen kritischen Potentialwert übersteigt, so ist eine diskontinuierliche Verminderung der Tropfzeit bemerkbar. Infolgedessen stossen wir die Schwierigkeit in der polarographischen Messung der Wellenhöhe auf. Dieselbe Erscheinung ist auch in Bereich der positiveren Gleichstromspannung erkennbar, und der ganze Verlauf der τ-E-Kurve ist in Abb. 2 angegeben. Die beiden kritischen Potentialwerten sind von der Amplitude der überlagerten Wechselspannung abhängig. Abb. 2 zeigt auch den Einfluss der Amplitude (ΔE: Effektivwert) der überlagerten Wechselspan-

1) M. Fournier; *Comp. rend.* **237**, 1673 (1951).
2) B. Breyer und F. Gutman; *Discuss. Faraday Soc.* **1**, 19 (1647).

nung auf die τ-E-Kurve. Daraus ist zu ersehen, dass sich die beiden kritischen Potentialwerten an der kathodischen und anodischen Asten mit wachsender Amplitude etwa symmetrisch zum Elektrokapillarmaximum annähern (siehe Abb. 3); und zwar nach der plötzlichen Veränderung der Tropfzeit, verläuft die τ-E-Kurve zur eigentlichen Elektrokapillarkurve annähernd parallel.

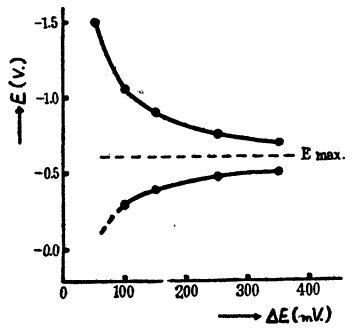


Abb. 3.
Schematische Darstellung des Zusammenhanges zwischen den beiden kritischen Potentialwerten und der überlagerten Wechselspannungsamplitude

Worauf beruht diese Erscheinung, ist theoretisch nicht aufgeklärt; jedoch wäre es zur Untersuchung der Elektrokapillarität bzw. der elektrischen Doppelschicht von Bedeutung.

Landwirtschaftlich-Chemisches Institut,
Fakultät der Landwirtschaft,
Universität Kyoto, Kyoto

A Study of the Growth of Pichia Membranaefaciens Utilising the Energy Obtained by the Oxidation of Different Metallic Hydroxides by Aeration

By S. RANGANAYAKI and Krishna BAHADUR

(Received May 27, 1954)

Introduction

Winogradsky observed long ago that micro-organisms can utilise the energy obtained by the oxidation of mineral substances for their life activity. This statement got confirmation from the findings of Temple and Colmer[1] who could grow *Thiobacillus ferroxidans* by means of energy obtained from the oxidation of ferrous ions.

I have succeeded in growing *Pichia membranaefaciens*[2] in cultures containing only one of such energy sources. In this paper, I am giving the results obtained by growing *this yeast* in cultures containing some metallic hydroxides which by slow aeration liberate energy required for growth. The hydroxides under study were manganese hydroxide, cobalt hydroxide, ferrous hydroxide, stannous hydroxide and cerous hydroxide.

Experimental

Several cultures, each containing 0.30 g. of sodium nitrate, 0.08 g. of potassium hydrogen phosphate, 0.006 g. of calcium carbonate and 0.009 g. of magnesium sulfate, were prepared. These minerals were put into 750 cc. flat bottom pyrex flasks and digested with dilute hydrochloric acid. The total volume of each culture was made to 500 cc. and the *p*H adjusted to 4.5. One gram of the freshly precipitated and dried hydroxide under investigation was added to each culture. The flasks were then cotton-plugged and sterilised by boiling at 15 lbs. pressure for 30 minutes in an autoclave. After cooling, these cultures were seeded with 0.2 cc. of an activated sample of *Pichia membranaefaciens*. This sample contained about 600 cells per cc.

Sterilised air was passed through each culture and the cell-count of the cultures was taken by the method described below. The temperature variation during the period of study was between 29.8°C and 33.0°C.

To take the cell-count of the cultures, first a culture solution was made by the following method. 0.20 g. of calcium carbonate, 0.25 g. of magnesium carbonate, 0.20 g. of sodium chloride, 0.20 g. of potassium sulfate, 0.20 g. of disodium hydrogen phosphate, 10 g. of sucrose and 2.5 g. of ammonium sulfate were weighed out into a flask. These were digested with dilute hydrochloric acid and the total volume of the culture was made up to one litre, adjusting the *p*H to 4.5. Twenty grams of agar-agar were added to it and the solution was sterilised by boiling at 10 lbs. pressure for 30 minutes. On cooling, it solidified. This solution was warmed by keeping it in a water bath. Five cc. of this melted solution were put into a sterilised Petri dish with the help of a sterilised pipette. The solution to be tested was shaken well and 1 cc. of this was added to the agar-agar culture in the Petri dish before it solidified. The dish was closed with the upper lid and kept in an incubator for 24 hours. A small star-like yeast colony developed around each cell. By counting these stars, the number of yeast cells was known. Ten of such Petri dishes were prepared for each culture whose cells were to be counted and the average of these ten countings is shown in the tables.

One culture was kept as control, in which all the other substances were present in the same amount except the source of energy. This control culture was also seeded with the same amount of yeast and aerated similarly. Its cell-count after 2 days and onwards was always zero.

Results

The results obtained by counting the cells in each culture are tabulated below:

No. of days after seeding	Average cell-count					
	Control	Manganese hydroxide	Cobalt hydroxide	Ferrous hydroxide	Stannous hydroxide	Cerous hydroxide
1	0.2	1.8	11.0	1.5	0.5	0.0
3	0.0	3.5	15.0	2.0	1.0	0.0
6	0.0	2.5	19.0	1.0	0.8	0.0
8	0.0	1.5	20.0	0.5	0.1	0.0
14	0.0	0.0	8.0	0.0	0.0	0.0
22	0.0	0.0	2.0	0.0	0.0	0.0
24	0.0	0.0	0.0	0.0	0.0	0.0

1) K. L. Temple and A. R. Colmer, *J. Bact.*, **62** 605-11 (1951).

2) According to the classification scheme of Lodder and Kreger-van Rij.

Discussion

The culture containing cobalt hydroxide as the source of energy material shows good growth of yeast; moreover this growth continues for a fairly long time. The death of yeast in the control culture is due to the fact that it did not contain any source of carbon. Cerous hydroxide is poisonous for the growth of yeast and no yeast cell is seen at any stage. The other hydroxides favour yeast growth in the following order: manganese hydroxide, ferrous hydroxide and stannous hydroxide.

In these cultures, the energy needed for the growth and life activity of the yeast is supplied by the slow oxidation of these hydroxides by aeration. The carbon needed for making the body of the yeast is obtained by the fixation of atmospheric carbon dioxide. Probably the energy needed in this fixation is supplied by the oxidation of the hydroxide.

In these cultures, it is seen that the yeast stops growing after some time and later on, dies out completely as the aeration continues. This is perhaps due to this fact, that the carbon compound synthesised by the fixation of atmospheric carbon dioxide is in a form which can only partially satisfy the carbon need of the organism. It may be that yeast needs carbon food of some other type which cannot be synthesised by this method. Therefore the growth of yeast stops and further aeration in the absence of the essential carbon food proves fatal to the yeast.

Summary

When in *Pichia membranaefaciens* cultures, all other nutrients are present except the carbon source and the hydroxide of some metal is added and the culture aerated, a growth of yeast is observed. Maximum growth is observed in the case of cobalt hydroxide. Cerous hydroxide is poisonous and does not favour any growth.

Chemistry Department, Allahabad University, Allahabad, India

Distribution of Fluorine in Various States in Terrestrial Waters

By Shigeki KOBAYASHI

(Received April 28, 1953)

Introduction

Despite an accumulation of the fluorine studies in terrestrial waters, the distribution of the element in its various states remains untouched, a problem particularly important from the viewpoint of its pathology and hygienics. Filling in the lack of knowledge is the primary motive for the present study.

In effect, the author applied Sanchis' method[1] of fluorine determination in four different ways to thirty-nine samples of various kinds of terrestrial waters in Japan and established the distribution of the element in the three following different states:

(A). The fluorine, which can be determined when Sanchis' method is applied to the supernatant water obtained by keeping the sample still until the suspended matter settles down. This comprises the fluoride ions pre-existent as well as those which can be liberated from certain kinds of complexes such as the ions of silicofluoride or aluminofluoride under the conditions of the application of the method.

(B). Other kinds of dissolved fluorine, which can be converted into silicofluoric acid when the supernatant water is condensed into a smaller volume and treated with concentrated sulfuric or perchloric acid.

(C). The fluorine of the suspended matter, which can be converted into silicofluoric acid when the original sample is evaporated nearly to dryness and treated with concentrated sulfuric or perchloric acid.

Experimental

The sample is cautiously shaken so that the suspended matter is uniformly distributed, and then divided into two fractions.

Fraction 1 is left still until the suspended matter completely settles. The supernatant water is siphoned out into a separate vessel. To a measured portion (50-100 ml.) Sanchis' method is applied directly (a). Another portion is made slightly alkaline with sodium carbonate solution and evaporated nearly to dryness. Then it is distilled with the addition of sufficient amounts of solid silver sulfate and powdered quartz or glass, and some 5 ml. of concentrated sulfuric or perchloric acid. The fluorine in the distillate is determined

1) J. M. Sanchis, *Ind. Eng. Chem.*, Anal. Ed., **6**, 134 (1934).

by Sanchis' method[2,3] (b).

Fraction 2 is shaken again and Sanchis' method is applied to a measured portion of the uniformly distributed suspension (c). Another portion of the same suspension is processed similarly as in (b), and the fluorine content of the distillate is finally determined (d).

By the following equations, the individual amounts of the element in the three different states can be calculated from the data, (a), (b), (c), and (d).

Fluorine in state (A) (a)
" " " (B) (b)—(a)
" " " (C) (d)—(b)

Results

The samples vary one from another in the distribution of the element in its three different states, but can be classified into the four following states, as given in Table I.

TABLE I

DISTRIBUTION OF VARIOUS FORMS OF FLUORINE IN TERRESTRIAL WATERS

Sample	Source	a mg/L	b mg/L	c mg/L	d mg/L
	Waters of Type 1, (a=b=c=d)				
No. 1	Well, Gamagori, Aichi Pref.	0.15	0.15	0.15	0.15
2	Well, Gamagori, Aichi pref.	0.15	0.15	0.15	0.10
3	Well, Oi, Gifu Pref.	0.25	0.35	0.30	0.30
4*	Well, Kasamatsu, Gifu Pref.	0.45	0.50	0.45	0.45
5*	Well, Sendanbayashi, Gifu Pref.	3.8	3.9	3.8	3.8
6	Well, Sendanbayashi, Gifu Pref.	0.10	0.10	0.10	0.10
7	Well, Sendanbayashi, Gifu Pref.	0.10	0.10	0.10	0.10
8	Well, Kamioka, Gifu Pref.	0.10	0.10	0.10	0,10
9	Spring "Kikusuisen", Yōrō, Gifu Pref.	0.25	0.30	0.25	0.30
10	Thermalsprings "Sakakibara-onsen", Sakakibara, Mie Pref.	3.5	3.5	3.5	3.4
11	The botten water of Lake "Kizaki-Ko", Kitaazumi, Nagano Pref.	0.40	0.35	0.40	0.40
12*	River "Wada-gawa", Shimizubara-mura, Nagano Pref.	0.75	0.75	0.75	0.75
13(a)	River "Yumata-gawa" just up its confluence with River "Mizumata-gawa", Nagano Pref.	2.0	2.0	2.0	2.1
14	River "Toyo-kawa" Miya, Aichi, Pref.	0.45	0.40	0.45	0.40
15	River "Sugo-gawa", Okazaki, Aichi Pref.	0.10	0.10	0.10	0.10
	Waters of Type 2, (a=c<b=d)				
No. 16	Well, Gamagori, Aichi Pref.	0.25	0.50	0.25	0.50
17*	Well, Higashikata, Ehime Pref.	0.35	0.60	0.35	0.55
18*	Well, Ōsato, Aichi Pref.	1.7	2.1	1.6	2.1
19	Thermalsprings "Kinryu-onsen" Nagashima, Gifu Pref.	2.0	2.4	1.9	2.4
20	River, Shimecha, Hokkaido.	0.20	0.30	0.15	0.25
21*	River "Takase-gawa", Motoki, Tokiwa-Mura, Nagano Pref.	0.70	1.0	0.75	1.1

2) H. H. Willard and O. B. Winter, *Ind. Eng. Chem.*, Anal. Ed., **5**, 7 (1933).

3) H. Okuno, *J. Faculty Sci., Hokkaido Imp. Univ.*, **3**, (3), 101, (1942).

Waters of Type 3, (a=c<b<d)

Sample	Source	a mg/L	b mg/L	c mg/L	d mg/L
No.22(b)	Well, Sakae-machi, Nagoya City.	0.15	0.40	0.15	1.2
23*	Well, Yokomichi, Ehime Pref.	0.30	0.45	0.30	0.60
24	River "Aki-gawa", Ōi, Gifu Pref.	0.30	0.40	0.25	0.75
25	River "Ibi-gawa", Wakino, Gifu Pref.	0.10	0.30	0.15	0.50

Waters of Type 4, (a=b=c<d)

Sample	Source	a mg/L	b mg/L	c mg/L	d mg/L
No. 26	Well, Ōi, Gifu Pref.	0.35	0.40	0.40	0.90
27	Thermalsprings "Yunoyama-Onsen", Yunoyama, Mie Pref.	12.0	12.5	12.0	20.0
28	The surface water of Lake "Kizaki-ko", Kitasazumi, Nagano Pref.	0.40	0.35	0.40	0.60
29	Swamp "Nakano-sawa", Tokiwa-mura, Nagano Pref.	0.60	0.65	0.60	0.90
30	River "Kago-gawa" just up its confluence with River "Takase-gawa", Nagano Pref.	0.25	0.25	0.25	0.70
31	River "Kashima-gawa", Ōide, Nagano Pref.	0.25	0.25	0.25	0.75
32	River "Titi-gawa" at the foot of Mt. Shiroyama, Nagano Pref.	0.40	0.45	0.45	0.60
33*	River "Takase-gawa", Kutsukake, Tokiwa-mura, Nagano Pref.	0.75	0.80	0.75	1.25
34(c)	River "Takase-gawa" near Kuzu-onsen, Nagano Pref.	2.2	2.2	2.2	3.6
35*	River "Takase-gawa" about 2.5 km. down streem from Kuzu-onsen, Nagano Pref.	0.80	0.80	0.85	1.6
36	River "Mizumata-gawa" just up its confluence with River "Yumata-gawa", Nagano Pref.	2.1	2.0	2.1	2.5
37	River "Kiso-Gawa", Enakyo, Gifu Pref.	0.25	0.25	0.25	0.55
38	River "Togi-Gawa", Togi, Ishikawa Pref.	0.30	0.30	0.25	0.40
39	Water-fall "Yōrō-no-taki". Yōrō, Gifu Pref.	0.30	0.30	0.35	0.50

* Cases of mottled enamel of teeth were found among the people, usually using this water for drinking.
(a), (c) Sample contaminated with thermalsprings water.
(b) Turbid.

Type 1. This type of water dissolves one or more kinds of the ions belonging to (A), but contains no other fluorine compound either dissolved or suspended.

Type 2. This type of water contains the fluorine of (B) in addition to one or more kinds of the ions belonging to (A), but no suspended fluorine compound.

Type 3. This type of water contains one or more kinds of the ions belonging to (A) as well as the fluorine belonging to (B) and (C).

Type 4. This type of water contains one or more kinds of the ions belonging to (A) as well as fluorine (C), but none of (B).

From the result it may be seen that the

statistic exploration of fluorisis cases can be successful only when it is done simultaneously with a differential determination of fluorine in various states in the water, which if ever has seldom been the case in the foregoing studies.

The author expresses his sincere appreciation to Professors K. Sugawara and S. Oana of Nagoya University for their guidance and suggestions. He is also indebted to Dr. T. Koyama and Mr. Y. Morita for their advice and to the members of the Sugiyama Women's College for their help in the present research.

Chemical Laboratory,
Sugiyama Women's College,
Nagoya

Dielectric Behaviour of Hydrated Crystals. II. Potassium Mercury (II) Chloride Monohydrate and Ammonium Mercury (II) Chloride Monohydrate[1]

By Ryôiti KIRIYAMA and Hideko IBAMOTO

(Received October 10, 1953)

Introduction

The water molecule in a salt hydrate crystal, which does not directly coordinate with the metal ion and is situated in an open space in the crystal lattice, will differ to a certain degree from the directly coordinated water molecule in the dielectric behaviour relating to the dipole orientation of the water molecule. In the present paper, potassium mercury (II) chloride monohydrate, $K_2HgCl_4 \cdot H_2O$ and its isomorphous crystal, ammonium mercury (II) chloride monohydrate, $(NH_4)_2HgCl_4 \cdot H_2O$ are dealt with as the typical examples containing the interstitial water of crystallization as confirmed by the X-ray analyses.

Crystal, Specimen and Equipment

A large single crystal of $K_2HgCl_4 \cdot H_2O$ are grown by slow cooling from seed crystal in a slightly supersaturated aqueous solution contained in a glass vessel dipped in a water-thermostat. This solution has been prepared from potassium chloride and mercuric chloride according to the phase diagram. It requires about four or five weeks to obtain a suitable, large, transparent, single crystal.

The crystal of the ammonium salt is obtained in a similar way.

The specimen is made by cutting and grinding, and is inserted directly between silver- or platinum-coated electrodes for the measurement of the capacity and the equivalent resistance of the crystal condenser in a way similar to that described in the previous paper.[2]

Result of Dielectric Measurement

(**a**) **$K_2HgCl_4 \cdot H_2O$.** The permittivities of this rhombic crystal at a room temperature are as follows: $\epsilon_a = 6.7 \pm 0.3$, $\epsilon_b = 6.1 \pm 0.2$, $\epsilon_c = 17.5 \pm 1.0$ (15°C, at 3 Mc and 5 kc). There is a marked anisotropy between the permittivities parallel and perpendicular to the *c*-axis. The temperature dependences of the permittivities and the dielectric losses are shown in Fig. 1, and the temperature coefficients $\frac{1}{\epsilon}\left(\frac{d\epsilon}{dT}\right)$ are as follows:

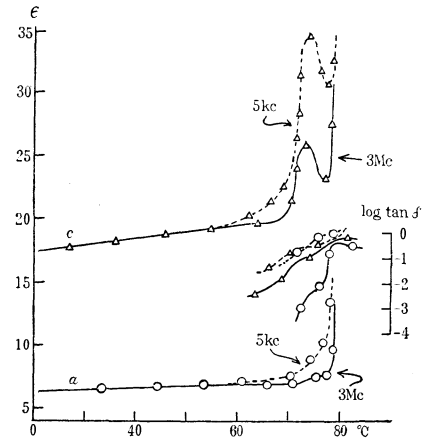


Fig. 1. The temperature dependences of the dielectric behaviour of $K_2HgCl_4 \cdot H_2O$

1) Parts of this investigation were separately read before the annual meetings of the Chemical Society of Japan in April 1949 and 1950, the annual meeting of the Crystallographic Society of Japan in May, 1950 and the Second International Congress of Crystallography at Stockholm in July, 1951.

2) R. Kiriyama and H. Ibamoto, This Bulletin, **27**, 32 (1954).

	−170——−120°	−120——−40°	−40——+70°
a	3×10^{-4}	7×10^{-4}	1×10^{-3}
c	4×10^{-4}	7×10^{-4}	3×10^{-3}

In these measurements, the average rate of heating is 0.2° per minute. The behaviour along the *b*-axis is almost similar to that along *a*. Above 70°C, there is a dispersion between 3 Mc and 5 kc along the *c*-axis, and the permittivity-temperature curve shows a peak at about 110°, while there is no such peak either along the *a*-axis or along the *b*-axis, and the dispersions along these axes are considerably small compared with that along *c*. At about 117°, sudden increases of the permittivities are observed in both *a*-and *c*-directions. When a considerable amount of phosphorus pentoxide powder has been spread at the bottom of the measuring cell, this steep increase at 117° diminishes and a maximum permittivity become measurable, then the ϵ-T curve shows a second peak at certain degrees higher than 117°. Therefore, it may be concluded that the increase at 117° is due to the surface conduction in the adsorbed layer of the dehydrated water molecules on the crystal surface. Similar phenomena were observed in the course of the dielectric measurements of $K_2CuCl_4\cdot 2H_2O$, $(NH_4)_2CuCl_4\cdot 2H_2O$ and $Sr(HCO_2)_2\cdot 2H_2O$ when the dehydration took place suddenly.[2)]

Sometimes we observed a rather rapid increase of ϵ_c at a far lower temperature than that observed in the ordinary case and there arises a terrace on the low temperature side of the peak at 110° in the ϵ_c-T diagram. But this phenomenon is not reproducible and differs somewhat from others. Such a non-reproducible phenomenon may be attributed to some lattice imperfections of the crystal and a qualitative explanation will be given in the next paper of our studies.

For the purpose of making clear the cause of the anomaly at about 110°C, we carried out also the measurement of the time dependence of ϵ_c at constant temperatures, three different points being so chosen out of the temperature region where the anomaly is observed to be of significance from the view point of the results of X-ray experiments. The results are shown in Fig. 2. In the ϵ_c-time diagrams, the curve for 82.5° has two low peaks whereas that for 94° has only one high peak and that for 102.5° has also one high peak which lies nearer to the ordinate axis than that for 94°. After 300–500 hours, these curves seem to tend to an asymptotic value of about 13–15. According to the X-ray experiment mentioned below, the ordinary form transforms gradually into the high temperature form above 82°C. However, the transition velocity from the low temperature form into the high temperature one is so very little above the transition point, that the maximum ϵ_c which corresponds to the peak at about 110°C on the ϵ_c-T curve in Fig. 1 will appear very late as is seen for the appearance of the second peak in the ϵ_c-time curve for 82.5°. And the higher the temperature, the larger the transition velocity, and therefore the corresponding maximum ϵ_c at the higher temperature will appear in the earlier stage of the ϵ_c-time diagram.

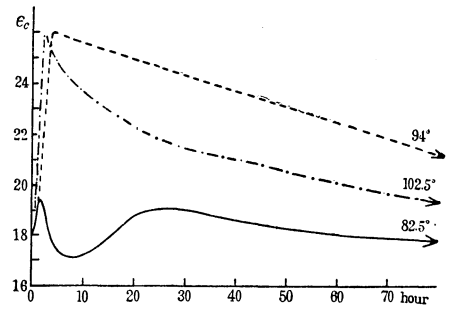


Fig. 2. The time dependences of ϵ_c at constant temperatures for $K_2HgCl_4\cdot H_2O$

(**b**) $(NH_4)_2HgCl_4\cdot H_2O$. The permittivities at 18°C are ϵ_a 7.2, ϵ_b 6.5, ϵ_c 22.3 at 3 Mc. There is also a marked anisotropy observed in the case of the potassium salt mentioned in (**a**). The temperature dependences of the dielectric behaviour are shown in Fig. 3. The sign of the temperature coefficient of the permittivity along each crystallographic axis of the ammonium salt is positive in the neighbourhood of the room temperature, but at lower temperatures the temperature coefficient of ϵ_a becomes negative. It may be

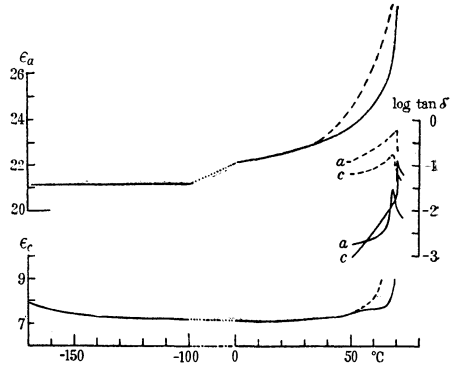


Fig. 3. The dielectric behaviour of $(NH_4)_2HgCl_4\cdot H_2O$. Samples are sandwiched in two mica foils in these cases. Full line-3 Mc, broken line—5 kc.

worth noticing that the negative sign of the temperature coefficient of the permittivity at low temperatures was also found in another ammonium salt, $(NH_4)_2CuCl_4 \cdot 2H_2O$.[2)]

In ϵ-T diagram of this ammonium mercury (II) salt, a peak which is seen in the case of the potassium salt just below the dehydration temperature is not observed. But careful tracing of the ϵ_c-T curve suggests that such a peak may also exist so closely below the dehydration temperature that the peak can not be separated from the steep increase of ϵ_c in the neighbourhood of the dehydration temperature.

Results of X-ray and Thermal Investigations of $K_2HgCl_4 \cdot H_2O$

The change of the crystal structure is investigated by Laue patterns taken with the incident beam parallel to the b-axis at various temperatures (Table I). These results show that the crystal lattice is collapsing gradually above about 82°C. The Debye photographs of the initial and the final stages of 300 hours-heating are taken using Cu $K\alpha$ radiation with Ni-filter at various temperatures (Table II).

From these Laue and Debye photographs, it is concluded that the potassium salt gradually transforms from the low temperature form to the high temperature one above 82°C. The indices of the Debye patterns of this high temperature form are determined wholly in reference to the indices of the ordinary low temperature form, notwithstanding that the relative intensities of the Debye patterns of the high temperature form are essentially different from those of the low temperature one (Table V).

Table I

Structure change of $K_2HgCl_4 \cdot H_2O$ observed from Laue patterns

T(°C)	time(hour)	lattice
25	3	low temperature form
55	3	low (no change)
81	3	low (no change)
107	3	low (Laue spots weaken)
125	3	no spots, fiber patterns of KCl
155	(3)	Debye-rings of KCl only

The second column shows the time of exposure at the temperature given in the first column except the last case. The photograph of the last case was taken also for 3 hours-exposure after 300 hours-heating at 155°.

Table II

Structure change of $K_2HgCl_4 \cdot H_2O$ observed from Debye photographs

T(°C)	initial 10 hours	final 10 hours
25	low	low
60	low	low
75	low	low
80	low	—
82	—	low-high (mixed)
85	low	—
91	—	high (broad)
100	high (broad)	high
120	high (broad)	high (sharp)
128	—	high (sharp)
145	—	high (weak), KCl (strong)

Moreover, the dilatometric experiment using toluene as the dilatometer-liquid shows no discontinuity throughout this transition, whereas the case using mercury shows distinct bending of the dilatometric curve at about 82°. These results suggest that the fine powders of the high temperature form produced by the lattice breaking of the low temperature form are easily wetted by mercury but not by toluene, and there must exist a lattice transformation at about 82° without detectable volume change.

Besides these, the thermal analysis curve obtained by S. Seki and H. Chihara in this laboratory shows that there is no appreciable heat absorption at about the transition point but there are two peaks at 115° and 123°. In this experiment, the average rate of heating is 1.6° per minute and this rate is considerably faster than that in the case of the dielectric measurement. Therefore, the two peaks at 115° and 123° in the thermal analysis curve may be attributed to the latent heat of the delayed lattice transformation and those of the vaporization of the water liberated from the collapsing lattice and of the sublimation of mercuric chloride produced by the decomposition of this double salt respectively.

The microscopic observation of the surface after the partial dehydration at 120° shows numerous small pits distributed randomly on the c-plane and a few semi-cylindrical swellings along the c-axis on the a-plane. Moreover, in the course of the observation of the change of the optical properties with a polarizing microscope for the transparent thin plates, some stripes along the c-axis appear on the surface of the a-plane as the temperature rises and then the crystal collapses gradually, but many nuclei of dehydration are seen at the same time on the c-plane, and as the number of the nuclei increase,

the crystal plate loses its transparency. By the way, these partly dehydrated specimens are considerably hard and tough and they appear in white unglazed ceramic feature.

Discussion

(a) Anisotropy of the Room Temperature Permittivities. For the purpose of discussing the dielectric polarization of this rhombic crystal in the first place, the permittivity along each crystallographic axis is compared with the square of the refractive index for the corresponding axis (Table III).

TABLE III
REFRACTIVE INDICES FOR NaD[3] AND PERMITTIVITIES OF $K_2HgCl_4 \cdot H_2O$

n_a (α) 1.648	n_a^2 2.72	ε_a 6.7
n_b (γ) 1.699	n_b^2 2.89	ε_b 6.1
n_c (β) 1.678	n_c^2 2.82	ε_c 17.5

In this case, the maximum polarization in the optical frequency region is directed along its *b*-axis while that in the radio-frequency region is along its *c*-axis.

The crystal structure of the low temperature form of the potassium salt belongs to space group $Pbam$—V_h^9 and has a unit cell of $a=8.27$, $b=11.63$, $c=8.89$ kX containing four formula units.[4] There is a mirror plane perpendicular to the *c*-axis, therefore the dipoles of a pair of water molecules should be cancelling each other in the direction of the *c*-axis, and this cancellation is confirmed at a room temperature as a fixed four-proton system by the proton nuclear magnetic resonance absorption experiment using single crystals.[5] Consequently, the large polarization along the *c*-axis is mainly due to the atomic polarization of mercury which is surrounded by a less symmetrical chlorine octahedron and may be easily polarizable along the *c*-axis. In fact, the position of the mercury atom is 0.2 Å apart from the center of gravity of the chlorine octahedron (Fig. 4). Such an atomic

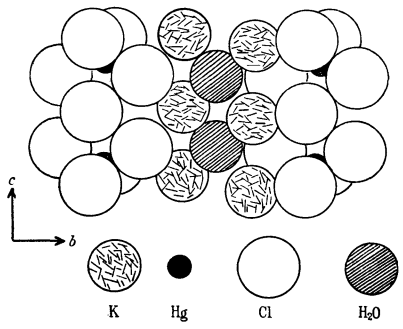


Fig. 4(a). Packing schema of the atomic arrangements in $K_2HgCl_4 \cdot H_2O$

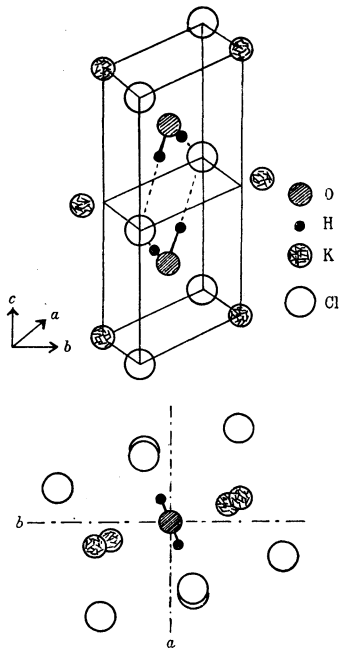


Fig. 4(b). The perspective and projection of the atomic arrangements around the pair of the water molecules in $K_2HgCl_4 \cdot H_2O$

polarization is somewhat analogous to that of the titanium atom in the ferroelectric barium titanate crystal.

In the case of the ammonium mercury (II) chloride monohydrate, the anisotropy of the permittivities, namely the far larger value of ϵ_c compared to those of ϵ_a and ϵ_b, may be attributed to the same cause as in the potassium salt.

(b) The High Temperature Modification of the Potassium Salt. Based on the facts that no detectable volume change is observed at the transition point, and also that the position as well as the indices of the X-ray reflections of the high temperature form coincide completely with those of the ordinary form, it may be concluded that the unit-cell dimensions of the high temperature form must be the same at the transition temperature as those of the low temperature form.

The analysis of the crystal structure of this high temperature form seems to be too difficult to determine precisely from the known data of the Debye photographs only. Fortunately, there are at least two clues for

3) P. Groth, "*Chemische Krystallographie*," Teil **1**, 360 (1906).
4) C. M. MacGillavry, J. H. de Wilde and J. M. Bijvoet, *Z. Krist.*, **100**, 212 (1938).
5) J. Itoh, R. Kusaka, Y. Yamagata, R. Kiriyama and H. Ibamoto, *J. Phys. Soc. Japan*, **8**, 233 (1953).

this crystal structure; one is the above invariableness of the lattice constants at the transition point, and the other the indefinite proportion of the water content in the high temperature form, i.e. the occupation of the possible interstitial positions of the lattice by the water molecules. From these considerations we have tried to determine the atomic arrangement of the high temperature form assuming that the corresponding space group is $Pbnm$—V_h^{16} and all chlorine atoms are in almost hexagonal close packing. The most probable crystal structure for the present among many possible models is gvien after successive trial and error approximations. The atomic coordinates and the relative intensities $I_{obs.}$, the squares of the structure factors $F^2_{cal.}$ of the Debye-patterns are shown in Tables IV and V respectively.

TABLE IV

ATOMIC PARAMETERS OF THE HIGH TEMPERATURE FORM OF $K_2HgCl_4 \cdot H_2O$[6]

$Pbnm$—V_h^{16}, $a=8.3$, $b=11.6$, $c=8.9$ Å, $Z=4$.

		x	y	z
Hg	(4c)	0.40	0.22	0.25
K(I)	(4a)	0.00	0.00	0.00
K(II)	(4b)	0.50	0.00	0.00
Cl(I)	(4c)	0.75	0.06	0.25
Cl(II)	(4c)	0.25	0.44	0.25
Cl(III)	(8d)	0.25	0.19	0.00

The structure principle of the high temperature form is that the mercury atom is surrounded by four chlorine atoms forming a deformed tetrahedron and the potassium atom by slightly deformed chlorine-octahedron. Strictly speaking, such a structure

TABLE V

INTENSITY RELATIONS OF DEBYE-PATTERNS OF $K_2HgCl_4 \cdot H_2O$

			low form		high form	
d (kX)		(hkl)	$I_{obs.}$	$F^2_{cal.}$	$I_{obs.}$	$F^2_{cal.}$
6.75		(110)	vs	0.4	m	0.
5.85		(020)	m	0.2	m	0.1
5.38		(111)	—	0.	s	0.7
4.85		(021)	—	0	m	0.1
4.45		(002)	w	0.1	w	0.1
4.35	$HgCl_2$	(001)	—	—	w-s	—
4.15		(200)	m	0.4	—	0.
3.91		(210)	—	0.	m	0.4
3.72		(112)	vs	1.0	—	0.
3.53		(022)	s	0.7	s	0.4
3.52		(130)				
3.38		(220)	vw	0.1	w	0.2
3.26		(131)	w	0.3	w	0.4
3.13	KCl	(200)	—	—	m-vs	—
3.05		(202)	s	1.0	—	0.
3.00	$HgCl_2$	(200)	—	—	vw-w	—
2.94		(212)	m	0.4	vs	1.0
2.93		(040)				
2.76		(041)	—	0.	m	0.4
2.76		(132)	—	0.1		
2.74		(140)	vw	0.2	—	0.1
2.69		(222)	vs	0.9	vw	0.4
2.69		(310)				
2.64		(301)	—	0.	—	0.4
2.58		(311)	—	0.	vw	0.1
2.52		(123)	—	0.	—	0.4
2.50		(320)	vw	0.2	—	0.
2.43		(042)	w	0.5	—	0.
2.40		(321)	—	0.	w	0.6
2.38		(240)	w	0.4	—	0.
2.25		(330)	vs	1.2	vs	1.0
2.23		(150)				
2.23		(004)				
2.23		(223)				
2.21	KCl	(220)	—	—	vw-w	—
2.18		(322)	—	0.	w	0.5
2.17		(151)	—	0.		
2.11		(114)	m	1.2	vvw	0.
2.10		(242)				
2.02		(303)	s	0.7	w	0.7
2.02		(250)				
2.02		(401)				
2.02		(340)				
1.95		(420)	m	0.9	w	0.4
1.94		(060)				

6) *cf.* Internationale Tabellen zur Bestimmung von Kristalstrukturen, (1938).

without the water molecule is not a high temperature modification of the monohydrate and the remaining water molecules in the lattice are probably in some interstitial positions. From the existence of the reflection of (110) which is a forbidden reflection for the high temperature space group, it will be concluded that in the high temperature form after the phase transition there remain also in several places the tunnel structures parallel to the c-axis, and the water molecules enclosed in these tunnels may have some chances of forming chain-like associations parallel to the c-axis within an adequate temperature range.

(c) The Structure of the Ammonium Mercury (II) Chloride Monohydrate, $(NH_4)_2HgCl_4 \cdot H_2O$. The isomorphism of the ammonium salt and the potassium salt has been confirmed by us structurally by means of X-ray methods. The ammonium salt has a unit cell of the dimensions $a=8.50$, $b=11.97$, $c=9.19$ Å (Cu $K\alpha=1.542$ Å) containing also four formula units. The ammonium salt is so sensitive to moisture that it is difficult to keep the crystal sample without lattice collapsing at just below the dehydration tem-

perature for several hours necessary to obtain the Debye photograph. Therefore, it could not be decided whether or not the hign temperature form of $(NH_4)_2HgCl_4 \cdot H_2O$ exists in a temperature range just below the dehydration point.

(**d**) **The Temperature Dependences of the Permittivities.** Now it is to be discussed what is the cause of the anomalous dispersion which appeared in $K_2HgCl_4 \cdot H_2O$ along the *c*-axis above the transition temperature. The result of the X-ray analysis of the low temperature form shows that there is a characteristic tunnel structure which contains water molecules only. This tunnel is strangulated by the surrounding atoms, consisting of a train of cocoon-shaped spaces with narrow and wide passages alternately. Water of crystallization in such spaces may be looked upon as a zeolitic water, but at room temperatures the fast that the orientations of the water molecules are fixed in the crystal lattice is confirmed. Moreover, there are no marked dispersions in the permittivity-temperature diagrams below the transition point 82° for the practically perfect crystal. Thus it may be concluded that the water molecules in the crystal lattice of the low temperature form are not movable in the whole range of temperatures below the transition point, this water of crystallization being not typically zeolitic.

The phase transition proceeds gradually and the atomic displacements of the chlorines are the smallest and those of the mercuries the largest among the three sorts of atoms, chlorine, potassium and mercury. Besides these, most of water molecules diffuse into the newly constructed lattice and take some suitable interstitial positions, but some of water molecules remain in the remnants of the tunnel structure as described in (**b**). The water molecules confined in these closed capillaries parallel to the *c*-axis will have some chances of chain-like associations of the water dipoles as the lattice loosens moderately when the temperature is maintained in an adequate range. Thus the high ϵ_c appears in consequence of the formation of chain-like clusters of the water dipoles parallel to the *c*-axis and not of the independent simple rotation of the water dipoles. The higher the temperature, the more violent the thermal motion and the more such clusters of water molecules will dissociate. Besides these, the dehydration through the collapsing lattice will become remarkable. The dissociation of the dipole clusters and the diminution of the numbers of the water molecules both cause the dielectric polarization to fall down above 110° as the experiment shows.

Based on this consideration, the changes of ϵ_c at three constant temperatures in the anomalous temperature region may be explained as follows. The first peak on the curve at 82.5°C may be due to the chain-like association of the water molecules enclosed in some original tunnel-structures which have probably some sort of lattice defects of their atomic arrangements. As the lattice transformation proceeds slowly at the constant temperature, these original tunnel-structures will be obstructed gradually and then the chance of the association will be diminished. Therefore, the polarization due to such dipole clusters will fall down, giving a peak of maximum polarization as seen in the figure (Fig. 2). However, in the course of the rearrangement of the atoms, the original tunnel-structures may remain in several places containing water molecules. As this newly constructed lattice is loosened gradually again, these water molecules which have had no chance of dipole association up to this stage owing to the original narrow passages of the tunnel-structure will be able to pass through it and may have some chances of association. Therefore, the dielectric polarization along this direction of the tunnel-structure will rise again. However, these enclosed water molecules may escape rather easily through the loosening lattice and then the polarization will diminish gradually in progress of time. Thus there appears the second peak as seen in the figure. The change at 94° or 102.5° may be explained in a similar way. At such higher temperatures, the transition proceeds rather quickly and the two peaks as seen in the process at 82.5° will fuse in one, and the saddle-shaped fall between two peaks will not be observable in either cases at 94° or 102.5°.

In $(NH_4)_2HgCl_4 \cdot H_2O$, the existence of the high temperature form is not certain as mentioned in (**c**). But the analogous feature of the permittivities below the dehydration temperature may be explained in the same way as in the case of the potassium salt.

The dielectric behaviour and the problem of the zeolitic water of crystallization of potassium tin (II) chloride monohydrate, $K_2SnCl_4 \cdot H_2O$, of which structure is similar to the mercury salts dealt with in the present paper, will be reported in the following paper, Part III.

Department of Chemistry, Faculty of Science, Osaka University, Nakanoshima, Osaka

Dielectric Behaviour of Hydrated Crystals. III. Potassium Tin (II) Chloride Monohydrate and Barium Nitrite Monohydrate[1]

By Ryôiti KIRIYAMA and Hideko IBAMOTO

(Received October 10, 1953)

Introduction

The water of crystallization in potassium mercury (II) chloride monohydrate, $K_2HgCl_4 \cdot H_2O$, which is apparently zeolitic from the view point of the atomic arrangement in its crystal, is fixed tightly in the lattice and shows no orientation polarization of its dipole at a room temperature as reported in the previous paper.[2] The crystal structure of potassium tin (II) chloride monohydrate, $K_2SnCl_4 \cdot H_2O$ closely resembles to that of $K_2HgCl_4 \cdot H_2O$ and in both crystals, a pair of the water molecules which are crystallographically equivalent are enclosed in a cocoon-shaped space facing each other. Brasseur and Rassenfosse who analysed the crystal structure of $K_2SnCl_4 \cdot H_2O$ stated that the water of crystallization is zeolitic based on its continuous dehydration with temperature.[3] It is worth while to decide whether or not the water of crystallization of this crystal is truly zeolitic from the view point of the dielectric behaviour of single crystals as done on other salt hydrates previously reported by the present authors.[2,4]

Although the crystal structure of barium nitrite monohydrate, $Ba(NO_2)_2 \cdot H_2O$ has never been fully analysed, the position of the barium ion has been determined. From the consideration based on the corresponding space group of this crystal structure and the position of the barium ion, it was presumed that the water molecule of this monohydrate is enclosed in a tunnel structure coming from the hexagonal spiral configuration of the lattice and that the water is probably zeolitic.[5] Therefore, it is also interesting to investigate the behaviour of the dielectric properties of this crystal from the standpoint of the dipole orientation and to compare the result with those of the other related crystals.

Crystal, Specimen and Equipment

Transparent, large, single crystals of $K_2SnCl_4 \cdot H_2O$ could not be obtained until now owing to the fact that the effective velocity of crystal growth is exceedingly small. Thus usual crystals exhibit milky white appearance, are more brittle than the transparent ones obtained by us and contain more or less inclusions of the saturated solution between the bundle-shaped fragments parallel to the *c*-axis.

We have succeeded in obtaining these transparent crystals suitable for dielectric measurements (the area perpendicular to the crystallographic axes should be larger than $10 \times 10\,mm^2$) by careful regulation of the temperature of the water-thermostat and the composition of the aqueous solution of this double salt. The composition was maintained usually in excess of the stoichiometric amount of potassium chloride. Besides these, the solution contained a small amount of hydrochloric acid and several grains of metallic tin for the purpose preventing the stannous ion from oxidation. The time required was more than two months.

Frequently, translucent and opalescent crystals were obtained, probably because of a small fluctuation of the temperature of the thermostat or a slight deviation of the composition of the solution. Such crystals have also been investigated for the purpose of comparing the dielectric behaviour of the transparent crystal with that of this translucent one.

Barium nitrite was prepared from double decomposition of barium chloride and sodium nitrite or barium chloride and silver nitrite. The large, transparent, yellow-coloured, single crystal of barium nitrite monohydrate grew up easily from the seed crystal in its aqueous solution. The obtained crystal has the shape of a hexagonal prism with a pyramidal top, but belongs to the class of hexagonal trapezohedron, $62\text{-}D_6$ as the X-ray data show. Colourless crystal could not be obtained and the experiment has been performed using these yellow-coloured crystals.

Good crystals have been selected by a polarizing microscope beforehand, and the specimens for the dielectric measurements are made by cutting and grinding these crystals and pasted by tinfoils with vacuum-grease.

The equipment is the same as those in the previous papers.[2,4]

1) Parts of this investigation were separately read before the annual meeting of the Crystallographic Society of Japan in May, 1950, at that of the Chemical Society of Japan in April, 1951, and at the Second Congress of the International Union of Crystallography at Stockholm in July, 1951.

2) Part II: R. Kiriyama and H. Ibamoto, This Bulletin, **27**, 317 (1954).

3) H. Brasseur and A. de Rassenfosse, *Z. Krist.*, **101**, 389 (1939).

4) Part I: R. Kiriyama and H. Ibamoto, This Bulletin, **27**, 32 (1954).

5) A. Ferrari and L. Cavalca, *Periodico Mineral*, (Rome), **17**, 125 (1948); *Structure Reports* for 1947–1948, Vol. **11**, 355.

Result

(a) **$K_2SnCl_4 \cdot H_2O$**. The permittivities of this rhombic crystal are as follows: $\epsilon_a = 7.3$, $\epsilon_b = 10.1$, $\epsilon_c = 10.0$ (at 15°C; at 5 kc and 3 Mc). There are no dielectric dispersion at a room temperature on the transparent crystals, but a considerable dispersion along the *c*-direction and small dispersion along the *a*-direction are observed with the translucent crystals. Moreover, of the milky-white, opaque crystals the permittivities can not be measured in every direction of the principal axes owing to remarkable conduction.

Thus we have performed further measurements using the transparent crystals throughout the present experiment and the results for somewhat imperfect crystals will be quoted only in comparison with those for the perfect, that is, the transparent ones.

The temperature dependences of the permittivities and the dielectric losses are plotted in Fig. 1. While the values of permittivities

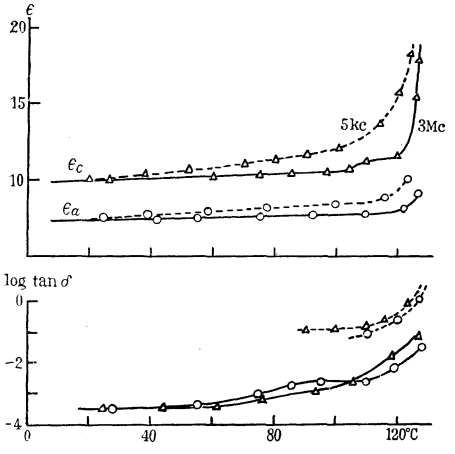


Fig. 1. The temperature dependences of the dielectric behaviour of $K_2SnCl_4 \cdot H_2O$.

are found reproducible in every repeated experiment, the temperature at which considerable dielectric losses appear becomes somewhat lower for every successive experiment. There are distinct dielectric dispersions at higher temperatures, a little along the *a*-axis and considerable along the *c*-axis, between 3 Mc and 5 kc as seen in Fig. 1.

The temperature coefficients of the permittivities $\frac{1}{\epsilon}\left(\frac{d\epsilon}{dT}\right)$ in the temperature range between 20° and 100°C are:

along *a* 6×10^{-4} (3 Mc), 14×10^{-4} (5 kc);
along *c* 6×10^{-4} (3 Mc), 23×10^{-4} (5 kc).

(b) **$Ba(NO_2)_2 \cdot H_2O$**. The room temperature permittivities at 3 Mc and 5 kc are: $\epsilon_a = 8.1$, $\epsilon_c = 7.4$. These values are equal in the limit of experimental error to those at 3 Mc previously reported.[6]

Their temperature coefficients are as follows: along *a* 3×10^{-4}, along *c* 6×10^{-4} in the temperature range between $-170°$ and 80°C.

Up to about 90°C where the dehydration occurs, the permittivities increase monotonously and above 90° the slope of the ϵ-T curve becomes a little steeper than below and at about 100° the values increase rapidly owing to the surface conduction originated by the dehydrated water molecules. The temperature dependence at 3Mc, as an example, is shown in Fig. 2.

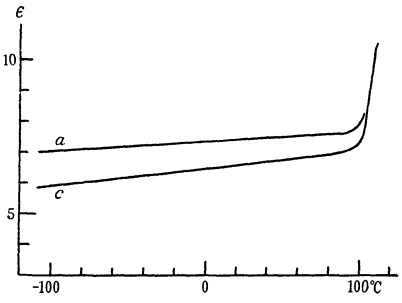


Fig. 2. The temperature dependences of the permittivities of $Ba(NO_2)_2 \cdot H_2O$.

Discussion

(a) **$K_2SnCl_4 \cdot H_2O$**. The anisotropy of the permittivities at room temperature is rather small and the direction of the maximum polarization is in the direction of the *b*-axis and not the *c*-axis. The refractive indices of this crystal were measured by us by means of the minimum deviation method using the prisms obtained by cutting and polishing the transparent, single crystals. The indices and other optical properties are listed in Table I.

TABLE I
OPTICAL CONSTANTS OF $K_2SnCl_4 \cdot H_2O$
Optically negative, axial plane—*b* (010), acute bisectrix—*a*-axis, (*a*-axis—*X*, *b*-axis—*Y*, *c*.axis—*Z*)[7]

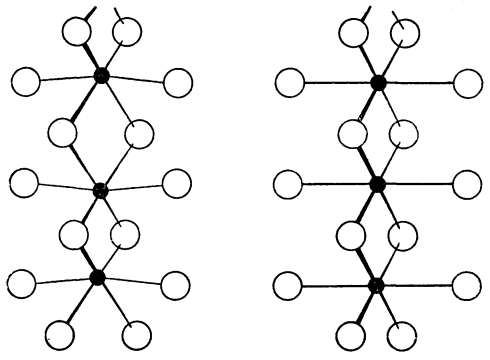
	589mμ	546mμ	436mμ	ε
n_a (α)	1.672	1.685	1.732	7.3
n_b (β)	1.693	1.707	1.752	10.1
n_c (γ)	1.749	1.757	1.798	10.0

It is probable that the direction of the maximum optical polarization coincides with that of the crystallographic *c*-axis because of the dense arrangement of chlorine atoms forming $(SnCl_4)_\infty$ chain along the *c*-axis. However, in spite of its chain-like arrangement of $(HgCl_4)_\infty$ along the *c*-axis, the crystal of $K_2HgCl_4 \cdot H_2O$ does not direct the

maximum optical polarization to that axis.[2] Moreover, it is noticeable that the maximum dielectric polarization of this tin salt occurs in the direction of the b-axis and not in the c-axis whereas in the case of the mercury salt its ϵ_c has much larger value than the others, ϵ_a and ϵ_b.

According to the analyses of the crystal structures, the mercury salt belongs to space group *Pbam*-V_h^9 but the tin salt to *Pbnm*-V_h^{16} in spite of the very similar atomic arrangements.[8,3] However, the results of the proton nuclear magnetic resonance absorption experiments of these crystals suggest that the space group of the tin salt is not *Pbnm* but *Pbam* which is identical with that of the mercury salt.[9] Therefore, it is confirmed that these two salts are not only isomorphous morphologically but also isostructural with each other.

The main difference of the atomic arrangements of these crystal structures is that the tin atom is surrounded by six chlorine atoms in a deformed octahedron; four are near and two in horizontal are distant, taking the c-axis as the vertical direction, while the chlorine octahedron surrounding the mercury atom in the mercury salt is much more deformed than that of the tin salt, namely the almost horizontal two chlorines are near, the other two are remote and the remaining two are more distant (Fig. 3).



$(HgCl_4)_\infty$ $(SnCl_4)_\infty$

Fig. 3. The difference of the atomic arrangements between $(HgCl_4)_\infty$ and $(SnCl_4)_\infty$ chain contained in $K_2HgCl_4 \cdot H_2O$ and $K_2SnCl_4 \cdot H_2O$ respectively.

From these different metal-chlorine distances, it may be concluded that, on the one hand, the two long horizontal Sn-Cl bonds in the $SnCl_6$-octahedron are almost purely ionic and the remaining four are much more covalent than these, and, on the other hand, two short horizontal Hg-Cl bonds in the deformed $HgCl_6$-octahedron are much more covalent than the remaining four Hg-Cl bonds which may be ionic. The electron cloud of a chlorine atom in such a partially ionic, covalent bond as in the oblique Sn-Cl or in the horizontal Hg-Cl may be much more polarizable than that in the purely ionic metal-chlorine binding. Owing to this polarizing effect, the electronic polarization of the tin salt in the vertical direction will become much larger than that expected simply from the dense arrangement of chlorine atoms along the c-axis in the form of $(SnCl_4)_\infty$-chain. On the contrary, the electron cloud of the chlorine atoms in the mercury salt may be more polarizable in the horizontal Hg-Cl direction and less in the oblique ones for light waves. As the result of this polarizing effect, the electronic polarization in the horizontal plane (the maximum refractive index γ is equal to 1.699, which lies along the b-axis) may become slightly superior to that in the direction perpendicular to this plane (along c, $\beta=1.678$) overcoming the polarization effect of the dense arrangement of the chlorine atoms in $(HgCl_4)_\infty$-chain parallel to the c-axis. These are the principal causes of the essential difference of the optical anisotropies between two isostructural crystals.

By the way, it has been recognized generally that the more ionic the bond nature, the larger the atomic polarization or the infrared polarization. From this point of view, it may be assumed that the value of the atomic polarization of the tin atom in the tin salt may be maximum in the direction of the b-axis along which the largest component of the ionic Sn-Cl binding is directed. Owing to this large atomic polarization, the direction of the maximum deformation polarization will tend to the b-axis overcoming the considerably large electronic polarization along c. On the contrary, in the case of the mercury salt, the large atomic polarization of the mercury atom along the c-axis in the deformed chlorine-octahedron will contribute greatly to the deformation polarization as discussed in the previous paper[2] and the electronic polarization perpendicular to this axis will make less contribution to the whole deformation

6) R. Kiriyama, *Kagaku*, **17**, 239 (1947) (in Japanese).
7) P. Groth, *Elemente d. physik. chem. Krystallogyaphie*, 171 (1921).
8) C. M. MacGillavry, J. H. de Wilde and J. M. Bijvoet, *Z. Krist.*, **100**, 212 (1938).
9) J. Itoh, R. Kusaka, Y. Yamagata, R, Kiriyama and H. Ibamoto, *J. Phys. Soc. Japan*, **8**, 293 (1953).

polarization, then the direction of the maximum deformation polarization will agree with the c-axis.

The temperature dependences of the permittivities of this tin salt are plotted in Fig. 1, where ϵ_b is omitted as its curve runs almost precisely on that of ϵ_c especially below 100°C. There are distinct dispersions of the permittivities above the room temperature, but there is no anomalous behaviour such as seen in the mercury salt, and the permittivities and the dielectric losses increase monotonously until the dehydration occurs, and at the dehydration temperature the permittivities increase suddenly as the ordinary hydrated salts.[4]

The result of the thermal analysis shows that there are no peaks up to the dehydration temperature 127°C, and this temperature is fairly coincident with that of the sudden increase of the permittivities 125°C. Moreover, the X-ray oscillation photographs taken at various temperature show that there are no structural changes between a room temperature and 125°C.

Thus we may conclude that the water molecules at the cocoon-shaped interstitial positions can move slightly as the temperature rises above about 105°C. This temperature corresponds to the point of inflection on the ϵ_c-T curves at 3 Mc (Fig. 1). And it is also concluded that from the temperature dependence and the frequency dependence of the permittivities and the dielectric losses the potential barrier against the dipole orientation of the water molecules will be lowered gradually as the temperature rises up to 125°C. And at this temperature the crystal lattice begins to collapse and then the dehydration through the breaking lattice takes place intensely.

In the case of the translucent crystal, the permittivities and the dielectric losses are much larger than those of the perfect, transparent crystal, especially in the c-direction. It may be also concluded that there are some lattice defects and the water molecules have some chances to form chain-like molecular clusters in the c-direction as assumed in the case of the high temperature form of $K_2HgCl_4 \cdot H_2O$.[2] The larger values of the permittivities along the c-axis and the irreproducibillity of them in the translucent crystal of the tin salt may be explained by this model. The remarkable conductivity found in the measurement for the opaque crystal of the tin salt may be attributed to the electrolytic conduction of the saturated solution contained in crystals as the form of liquid inclusion.

(b) $Ba(NO_2)_2 \cdot H_2O$. There are no appreciable dielectric dispersions up to the dehydration temperature in barium nitrite monohydrate. Moreover, the proton magnetic resonance absorption experiment using single crystals carried out by us shows that the water molecules are fixed in the crystal lattice at room temperature and no indications of the protonic movements in the lattice can be detected.[10] Thus, we may conclude from the results of the dielectric measurement that the water of crystallization in such monohydrates as $K_2HgCl_4 \cdot H_2O$, $(NH_4)_2HgCl_4 \cdot H_2O$ and $K_2SnCl_4 \cdot H_2O$ or $Ba(NO_2)_2 \cdot H_2O$ is not movable in the open space of the crystal lattice in spite of the zeolitic feature presumed from the position of the water-oxygen but that it orientates itself into a fixed direction stabilizing the crystalline field by its dipole moment. However, it is noticeable that the imperfect crystals of these substances have often tunnel-like capillaries and the water molecules enclosed in these capillaries will show various kinds of anomalous dielectric behaviour even at room temperature. From these considerations, it will be rather important to reexamine the behaviour of the so-called "zeolitic water" in the hydrated crystals, which might have been misjudged owing to some imperfections of their crystals used for the thermal or dielectric experiments.

In conclusion the authors wish to express their thanks to Prof. I. Nitta for his encouragent and suggestions during this work. Their thanks are also due to Dr. S. Seki and Mr. H. Chihara for their kindness in carrying out the thermal analysis experiment. The expense of this work was partly defrayed by the Scientific Research Grant from the Ministry of Education.

Department of Chemistry, Faculty of Science, Osaka University, Nakanoshima, Osaka

10) J. Itoh, R. Kusaka and R. Kiriyama, *J. Phys. Soc. Japan* (in press).

Studies on the Condensation Polymers of Aromatic Acetoxy Carboxylic Acids

By Hajime HASEGAWA

(Received December 2, 1953)

Introduction

Much work has been done by many investigators on the syntheses of polyesters, especially on the polymers of aliphatic hydroxy carboxylic acid and the copolymers of mono- and di-basic carboxylic acids and glycols. But, as for the syntheses of the polymers of aromatic hydroxy carboxylic acid, no systematic study has been made, although Einhorn[1] made the dimer of salicylic acid by heating with phosphorus oxychloride and Anschütz[2] made the tetramer of it by the same method. This method was used in the present research. In the case of salicylic acid, the formation of the high polymer was not observed. However, in the case of *o*-acetoxy benzoic acid (aspirin), the resin-like substance was obtained. It was considered to be the polymer of salicylic acid, for the violent evolution of acetic acid was observed throughout the reaction with the marked increase of the molecular weight. Starting from this result, the author obtained the high polymers of various kinds of aromatic acetoxy carboxylic acid by heating. The process of the formation of polymers was followed by determining the molecular weight of the resins formed, at several stages of the reaction. From the data obtained, the effect of the position of acetoxy group and carboxyl group on the reactivity of the monomers, was considered. In the case of acetamino carboxylic acids, the formation of the polymer of the high molecular weight by heating was not observed.

Experimental

The monomers used for this research were prepared by the following procedures.

I) *o*-Acetoxy benzoic acid. Aspirin for medical use was purified. M.P. 135°C.

II) *m*-Acetoxy benzoic acid[3]. *m*-Hydroxy benzoic acid[4] was acetylated, using acetic anhydride. M.P. 131°C.

III) *p*-Acetoxy benzoic acid[5] was prepared by the action of acetic anhydride on *p*-hydroxy benzoic acid[6] which was synthesized from salicylic acid. M.P. 182°C.

IV) 3-Acetoxy naphthoic acid-(2)[7] was synthesized from 3-hydroxy naphthoic acid-(2). M.P. 174°C.

V) 2,4-Diacetoxy benzoic acid[8]. β-Resorcylic acid[9] made from resorcinol by Kolbe-Schmitt method was acetylated. M.P. 134°C.

VI) 3,5-Diacetoxy benzoic acid[10] was made by acetylating 3,5-dihydroxy benzoic acid[11] by acetic anhydride. M.P. 155°C.

VII) *o*-Acetamino benzoic acid[5] was made by acetylating *o*-amino benzoic acid. M.P. 180°C.

VIII) *p*-Acetamino benzoic acid[12] was prepared by the action of acetyl chloride on *p*-amino benzoic acid. M.P. 253°C.

IX) 2-Acetoxy-4-acetamino benzoic acid. PAS for medical use, was acetylated by acetic anhydride. The product was recrystallized from hot water which contained a small quantity of alcohol, and was identified with the diacetyl compound of PAS by measuring the acetyl value of the product. Yield-70% of the theoretical amount. M.P. 184°C, with decomposition.

The condensation of the monomers shown above was carried out as follows; 10 g. of monomers were heated in a hard test tube of 1.5 cm. diameter during a definite time at the suitable temperature for each compound, which was listed in Table I. The acetic acid evolved in this reaction was carried off on the outside of a test tube by a slow current of dry carbon dioxide.

o-Acetoxy benzoic acid was chosen as the standard substance for comparison. Hence the process of the reaction of this compound was observed in detail at three different temperatures, 170°C, 240°C and 240°C. This monomer reacted smoothly at these temperatures. Contrary to this compound, *m*-acetoxy benzoic acid, *p*-acetoxy benzoic acid and 3,5-diacetoxy benzoic acid did not react at 200°C. Therefore, the reaction temperature of 240°C was chosen for these compounds. *p*-Acetamino benzoic acid was heated at 300°C, because it reacted smoothly at the higher temperature than its melting point. The polymerization of the other compounds was carried out at two different temperatures (200°C and 240°C), as shown in Table I.

The molecular weight of the resins synthesized in this way was measured by the cryoscopic method using nitrobenzene as the solvent for the

1) A. Einhorn, *Ber.*, **34**, 2352 (1901).
2) R. Ansuchütz, *Ber.*, **25**, 3506 (1892).
3) A. Heintz, *Ann.*, **153**, 340 (1870).
4) H. Offermann, *Ann.*, **280**, 6 (1894).
5) A. Kauffmann, *Ber.*, **42**, 3482 (1909).
6) H. Kolbe, *J. prakt. Chem.*, (2) **11**, 24 (1875).
7) H. Gradenwitz, *Ber.*, **27**, 2624 (1894).
8) M. Bergmann, *Ber.*, **52**, 379 (1919).
9) A. Clibbens, *J. Chem. Soc.*, **107**, 1494 (1915).
10) F. Mauthner, *J. prakt. Chem.*, **136**, 205 (1933).
11) L. Barth, *Ann.*, **159**, 222 (1871).
12) G. Heller, *Ber.*, **43**, 2574 (1910).

TABLE I

Monomer	Reaction temp. (°C)	Color	Solubility in nitrobenzene	Transparency
o-Acetoxy benzoic acid	170	CL→CL	+	TR
	200	CL→LB	+	
	240	P→B	+	
m-Acetoxy benzoic acid	240	B→B	+	TR
p-Acetoxy benzoic acid	240	W	−	OP
3-Acetoxy naphthoic acid-(2)	200	LB→B	+	TR
	240	B→BB	+	
2, 4-Diacetoxy benzoic acid	200	CL→OY	+	TR
	240	OY→R	+	
3, 5-Diacetoxy benzoic acid	240	LB(F)→B(F)	+	TR
o-Acetamino benzoic acid	200	OY	−	TR
	240	R→BB	−	
p-Acetamino benzoic acid	300	LY	−	OP
2-Acetoxy-4-acetamino benzoic acid	200	RB→BB	−	STR

Color; CL=Colorless, LB=Light brown, P=Pink, B=Brown, W=White, BB=Brownish black, OY=Orange yellow, R=Red, LY=Light yellow, RB=Reddish brown, (F)=Fluorescence.
Solubility; +: Soluble, −: Insoluble.
Transparency; TR=Transparent, OP=Opaque, STR=Semitransparent.

polymers of acetoxy compounds, and phenol as the solvent for the polymers of acetamino compounds.

Results and Discussion

i) **The Properties of Polymers.**—With the increase of the molecular weight, the colors of synthetic resins obtained from *o*-acetoxy benzoic acid, *m*-acetoxy benzoic acid, 3-acetoxy naphthoic acid-(2), 2, 4-diacetoxy benzoic acid and 3, 5-diacetoxy benzoic acid change from colorless to brown (Table I), and their hardness increases, and the solubility decreases. Most of them are soluble in nitrobenzene, phenol and pyridine, but are insoluble in alcohol, ether, chloroform and carbon tetrachloride. The resins of the lower molecular weight slightly dissolve in benzene and acetone, but, with the increase of the molecular weight, they become insoluble in these solvents.

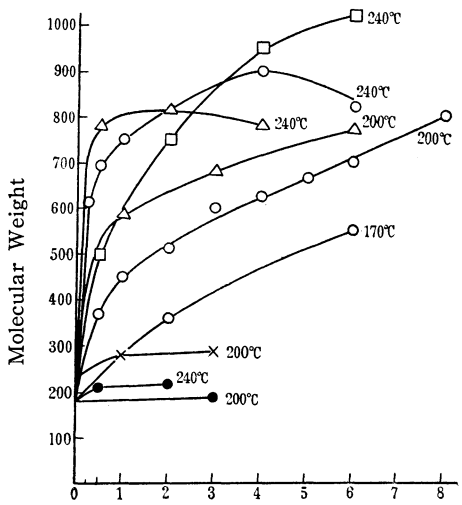
The polymers obtained from *p*-acetoxy benzoic acid and *p*-acetamino benzoic acid were opaque solids and did not dissolve in any solvents. The resins obtained from *o*-acetamino benzoic acid and 2-acetoxy-4-acetamino benzoic acid dissolved in phenol and cresol, but did not dissolve in other solvents.

The polymer (A in Table II) of 2, 4-diacetoxy benzoic acid obtained by heating at 240°C during 4 hrs., and the polymer (B in Table II) of 3, 5-diacetoxy benzoic acid obtained by heating 240°C during 6 hrs. are slightly soluble in nitrobenzene, phenol and pyridine, and the remaining part swells greatly. The degrees of swelling are given in Table II.

TABLE II
DEGREE OF SWELLING (% in volume).

Solvent	Phenol	Nitrobenzene	Pyridine
Polymer (A)	600	430	Soluble
Polymer (B)	280	300	300

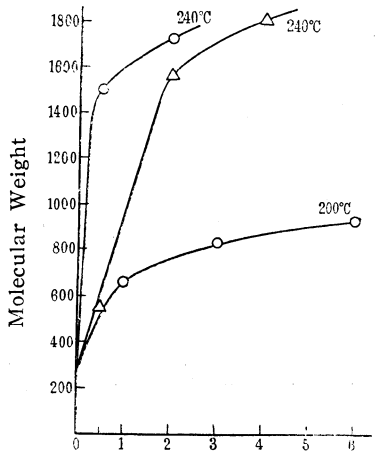
ii) **The Change of Molecular Weight.**—The



○ *o*-Acetoxy benzoic acid
□ *m*-Acetoxy benzoic acid
△ 3-Acetoxy naphthoic acid-(2)
● *o*-Acetamino benzoic acid
× 2-Acetoxy-4-acetamino benzoic acid

Fig. 1

data obtained by measuring the molecular weight in the course of polymerization are shown in Fig. 1 and Fig. 2.



○ 2,4-Diacetoxy benzoic acid
△ 3,5-Diacetoxy benzoic acid
Fig. 2

In these figures, the important points will be the maximum value (p in Table III) of the degree of polymerization (molecular weight of the polymer/molecular weight of its monomer), which can be obtained in the course of reaction, and the reaction velocity (V in Table III) at t (time in hour)=0, which is expressed in the ratio of the change of the degree of polymerization to the change of hour. For example, these values of *o*-acetoxy benzoic acid are calculated as follows:

$$P = 890/180 = 5.0$$

$$V(200°C) = \frac{(370/180) - 1}{1/2} = 2.1$$

As seen from this Table, there is some relation between the chemical structures of monomers and the values of V. Namely, almost the same value of V are observed for *o*-acetoxy benzoic acid and 2,4-diacetoxy benzoic acid. Furthermore, the value of V for *m*-acetoxy benzoic acid is almost the same as the value of V for 3,5-diacetoxy benzoic acid, which is smaller than the value of V for *o*-acetoxy benzoic acid and 2,4-diacetoxy benzoic acid at 240°C. This fact tells us that the monomers, which have the acetoxy group at the ortho-position to the carboxyl group, react faster than the monomers having the acetoxy group at the meta-position to the carboxyl group. But the value of P of *m*-acetoxy compounds is larger than the value of P of the corresponding *o*-acetoxy compounds. Therefore, it seems that *m*-acetoxy benzoic acid and 3,5-diacetoxy benzoic acid are suitable for the preparation of the high polymer of aromatic acetoxy carboxylic acid. As for the value of V of *p*-acetoxy benzoic acid, it cannot be obtained in this research. Therefore, the stability of *p*-acetoxy benzoic acid cannot be discussed in comparison to *o*-acetoxy compounds. However, considering the fact that *p*-acetoxy benzoic acid does not react at 200°C, it seems that *o*-acetoxy compounds react faster than *p*-acetoxy benzoic acid[13]. As for the values of V and P of 3-acetoxy naphthoic acid-(2), they are less than those of *o*-acetoxy benzoic acid. Contrary to the case of acetoxy carboxylic acid, the values of V and P of acetamino compounds are very small. The fact that the color of the product changes rapidly to dark brown may be due to the decomposition of the polymer formed. Therefore, the high polymer will not be obtained from aromatic acetamino carboxylic acid.

TABLE III

Monomer	Reaction temp. (°C)	V	P	Molecular weight
o-Acetoxy benzoic acid	170	0.5	5.0	895
	200	2.1		
	240	9.7		
m-Acetoxy benzoic acid	240	3.6	5.6	1016
3-Acetoxy naphthoic acid-(2)	200	1.6	3.5	811
	240	4.7		
2,4-Diacetoxy benzoic acid	200	1.7	7.2	1720
	240	10.6		
3,5-Diacetoxy benzoic acid	240	3.0	7.7	1820
o-Acetamino benzoic acid	200	0.03	1.2	220
	240	0.4		
2-Acetoxy-4-acetamino benzoic acid	200	0.2	1.2	287

The polymers (A and B in Table II) obtained from 2,4-diacetoxy benzoic acid and 3,5-diacetoxy benzoic acid swell greatly as shown above. These monomers have three functional groups. Therefore, it will be reasonable to assume that their polymers swell, owing to the net work structure formed by the cross linkage, and also their high

13) Y. Tsuzuki, This Bulletin, **5**, 232 (1950).

molecular weight. 2,4-Diacetoxy benzoic acid and 3,5-diacetoxy benzoic acid will be useful to the formation of the net work structure in the polymer.

Summary

We carried out a fundamental research for synthesizing high polymers of aromatic acetoxy carboxylic acid, and observed the influence of the position of the acetoxy group, and found that *m*-acetoxy benzoic acid, 3,5-diacetoxy benzoic acid and 2,4-diacetoxy benzoic acid, are superior as the monomer for the preparation of high polymers of aromatic acetoxy carboxylic acid.

I wish to express my hearty thanks to Prof. K. Yamamoto and Mr. K. Shibata for their kind guidance and valuable suggestions in this study.

Department of Applied Chemistry,
Faculty of Science and Engineering,
Waseda University, Tokyo

The Thermal Polymerization of Acetylene. On the Formation of Cyclooctatetraene

By Zenichiro KURI

(Received January 26, 1954)

Introduction

It has been known for a long time that acetylene is readily but intricately polymerized on heating,[1-4] giving a complex of unsaturated hydrocarbons as well as benzene.[2,10] Nevertheless, in the flow method at the suitable velocity, the propagation stops up to the tetramer and all the products obtained are volatile.[5] On the mechanism of the polymerization Pease, Taylor, and others[5,6,9,10,11] have pointed out from the over-all reaction rate that acetylene reacts in the bimolecular way and so the dimerization of acetylene determines the over-all rate.

On the structure of dimer produced in the primary acts of the photopolymerization of acetylene, Kemula[7] supposed that it would be vinylacetylene. Mignonac[8] got the product consistent with C_4H_4 in the thermal polymerization, but said no word about what it was. Recently Bergman,[12] supposing vinylacetylene to be the dimer, explained the Reppe reaction forming cycloöctatetraene (C.O.T.) under the high pressure.

Some experiments were performed assuming the dimer to be vinylacetylene, and the results were as follows;[13] if one uses a mixture of vinylacetylene and acetylene in the reaction, benzene constituting the main product in the polymerization decreases and also, when making C.O.T. by the catalytic method with high pressure, one can not get any C.O.T. if one uses vinylacetylene as the starting material.

Here, supposing cyclobutadiene (C.B.D.) to be the dimer in the thermal polymerization as well as in the photopolymerization[14] we investigated the thermal polymerization anticipating the formation of C.O.T. by dimerization of C.B.D. and we have obtained C.O.T. as expected.

Experiments

I. Thermal Reactivities and Analysis of C.O.T.

a) Thermal Changes of C.O.T. C.O.T., being a cyclic conjugated double-bonded compound, has unlike benzene little resonance energy and much reactivity.[15,16] It is so labile thermally and photochemically that it causes decomposition, polymerization, and isomerization at high temperatures.[17,18]

1) W. Bone, *J. Chem. Soc.*, **93**, 1197 (1908).
2) N. Zelinsky, *Ber.*, **57**, 264 (1924).
3) H. W. Walker *J. Phys. Chem.*, **31**, 970 (1927).
4) E. Hague, *J. Chem. Soc.*, 378 (1929).
5) R. N. Pease, *J. Am. Chem. Soc.*, **51**, 3470 (1929).
6) P. Schlaepfer and M. Brunner, *Helv. Chim. Acta*, **13**, 1125 (1930).
7) W. Kemula and S. Mrazek, *Z. phys. Chem.*, B**23**, 358 (1933).
8) G. Mignonac and E. Ditz, *C. r.*, **199**, 367 (1934).
9) H. Austin Taylor and A. V. Hook, *J. Phys. Chem.*, **39**, 811 (1935).
10) T. Fujisaki, *J. Inst. Fuel Japan*, **20**, 782 (1941).
11) H. D. Burnham and R. N. Pease, *J. Am. Chem. Soc.*, **64**, 1404 (1942).
12) E. Bergman, "Chemistry of Acetylene Compounds", **91**, (1948).
13) T. Fujisaki, *J. Inst. High Press. Gas Japan*, **15**, 244 (1951).
14) Z. Kuri and S. Shida, This Bulletin, **25**, 116 (1952).
15) I. Tanaka and S. Shida, ibid., **23**, 54 (1950).
16) Y. Mori, I. Tanaka, and S. Shida, ibid., **23**, 168 (1950).
17) I. Tanaka, S. Miyakawa, and S. Shida, ibid., **24**, 119 (1951).
18) I. Tanaka, unpublished.

Thus we adopted the flow method in the thermal polymerization of acetylene and quickly introduced the reaction products to a trap to get C.O.T.

b) Analysis of C.O.T. C.O.T. was analysed by the polarography[19] as in the case of our previous work.[14] Its half wave potential was -1.49 volts vs. S.C.E. At the sensitivity of 2.4×10^{-3} μA/mm. of the galvanometer 1 mm. displacement of the diffusion current corresponded to 2.79×10^{15} molecules of C.O.T. at the experimental conditions.

II. Experimental Details

a) Apparatus and Methods. Acetylene gas was purified by the normal method. The whole arrangement of the experiment is shown in Fig. 1. Purified acetylene is led through A into a liquid air freezing trap B, where the non-condensable gas is removed from the solidified acetylene through a vacuum pump and is fractionated into a reservoir C. From the reservoir, pure acetylene goes through a quartz reaction tube D heated by an electric furnace E, passing a dry ice trap F into the liquid air trap B. Reaction products caught in the trap F are evaporated back into the reaction tube D, after the experiment and are analysed spectrographically in the gas phase.

For the analysis of C.O.T., products in the trap F were directly distilled into a tiny ampoule G using the dry ice bath, and then the ampoule was cut off at the neck. Its contents were dissolved into ethanol-tetramethylammoniumbromide solution, which was submitted to the polarographic analysis.

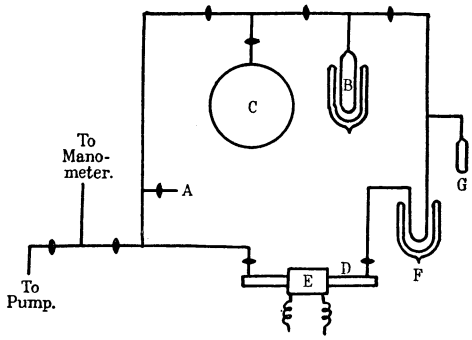
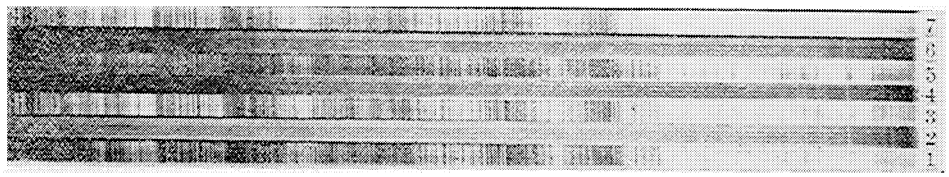


Fig. 1

b) Products of the Reaction. The absorption spectra of the reaction products are shown in Fig. 2. We see the products are benzene in the main and styrene in part. Besides them strong absorption lines characterized by 2808, 2720, 2687Å were always seen in the products of the photopolymerization, but in this case no trace of these lines belonging to the unknown substance appeared. This was a marked difference between the two cases. We suppose that the unknown substance is the intermediate of the polymerization and that it may be polymerized by heating in the thermal polymerization, for those lines disappear rapidly when irradiated with a mercury lamp. The absence of any thermal cracking can be inferred from the fact that there were not found any trace of the spectral lines of toluene and not any carbon or other sediments on the wall after the experiments.



(1), (3), (5) and (7) Iron spectrum (2) Blank (4) Spectrum of the products at 10 mmHg. (6) The same at 5 mmHg.

Fig. 2. Spectra of the products.

c) The Rate of Formation of C.O.T. under the Varied Pressure of Acetylene. If we put the volume passed at the pressure of p mmHg at the experimental temperature, V cc., the pass-time in the furnace, t sec., the height of diffusion current of the polarogram of C.O.T., h mm. (1 mm. corresponds to m mols of C.O.T.), the concentration of acetylene, A mol/cc., we can describe the rate of formation of C.O.T. in terms of the concentration of acetylene as follows.

$$dC/dt=hm/Vt=k_cA^n. \qquad (1)$$

Putting $h/Vt=H$, $\log H$ is seen linear to $n\log A$ and the constant n is determined as far as the reaction satisfies eq. (1). Using the pressure p instead of A, $\log H$ was, in Fig. 3, plotted against $\log p$ at each temperature.

Fig. 3 shows $n=2$ from the slope. It is because of the decomposition of C.O.T. that the line at 575°C lies beneath the one at 570°C. This fact is also seen by the deviation of $\log k_c$ at 575°C. from the straight line vs. $1/T$ as will be written below.

d) The Rate of C.O.T. under the Varied Temperature. At the constant pressure of 250 mmHg, the logarithm of the rate constant k_c of C.O.T. formation was plotted against the reciprocal of the reaction temperature T°K. Fig. 4 shows the result. $\log k_c$ is linear against $1/T$ over the range of 525 and 570°C. The point at 575°C. deviates from the line, which means the decomposition of C.O.T. above at this temperature.

We get the activation energy $E_c=46900$ cal. from the slope of the straight line in Fig. 4. So, the rate of C.O.T. formation is obtained as follows.

19) R. M. Elofson, *Anal. Chem.*, **21**, 917 (1949).

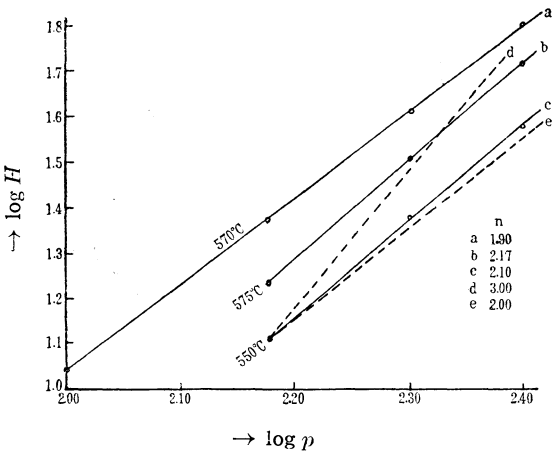


Fig. 3. Rate of formation of C.O.T. vs. acetylene pressure.

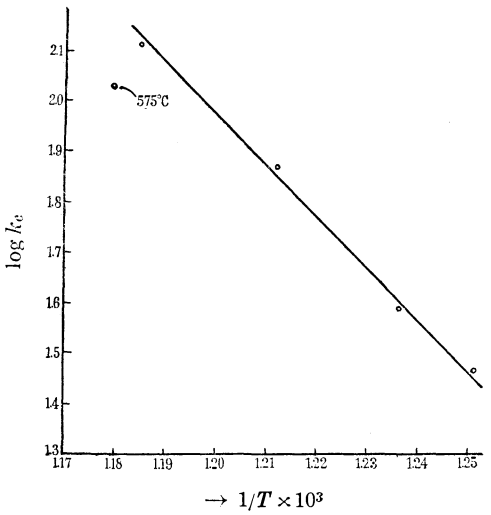


Fig. 4. Rate of formation of C.O.T. vs. reaction temperature.

$$dC/dt = 1.50 \times 10^{11} \exp(-46900/RT)\cdot A^2 \text{ mol. cc.}^{-1} \text{ sec.}^{-1} \quad (2)$$

Discussion of the Experimental Results

As we could determine the rate of formation from acetylene of C.O.T. as stated above, we assumed the following steps of the reaction mechanism.

$$2\ C_2H_2 \xrightarrow{k_1} \begin{matrix}CH{-}CH\\ \|\quad\ \|\\ CH{-}CH\end{matrix} \quad (3)$$

$$\begin{matrix}CH{-}CH\\ \|\quad\ \|\\ CH{-}CH\end{matrix} + C_2H_2 \xrightarrow{k_2} \text{or X} \quad (4)$$

$$2\ \begin{matrix}CH{-}CH\\ \|\quad\ \|\\ CH{-}CH\end{matrix} \xrightarrow{k_3} \quad (5)$$

For simplicity we will abbreviate the concentrations as follows; acetylene A, cyclobutadiene D, benzene B, cycloöctatetraene C, the unknown intermediate X. Under the condition of rapid flowing, we can ignore the steps forming higher polymers than C_8H_8. Then in the stationary state

$$dD/dt = 1/2k_1A^2 - k_2DA - k_3D^2 = 0 \quad (6)$$

$$dB/dt = k_2DA \quad (7)$$

$$dC/dt = 1/2k_3D^2 \quad (8)$$

From eq. (6) we obtain as the stationary dimer concentration

$$D = \frac{-k_2+\sqrt{k_2^2+2k_1k_3}}{2k_3}\cdot A \quad (9)$$

Here the negative root was omitted. We get from eqs. (7), (8) and (9)

$$dB/dt = \alpha\{(1+k_1/\alpha)^{1/2}-1\}A^2 \quad (10)$$

$$dC/dt = 1/2[\alpha\{1-(1+k_1/\alpha)^{1/2}\}+k_1/2]A^2, \quad (11)$$

where $\alpha = k_2^2/2k_3$. The value of k_1/α in eqs. (10) and (11) is of the smaller order than 10^{-3} as far as the values of $(2E_2-E_3)$ are below 25 kcal. In fact the value of k_1/α is much smaller because the one of $(2E_2-E_3)$ is smaller as will be stated below. Thus simplifying eqs. (10) and (11) by the binominal theorem

$$dB/dt = 1/2k_1A^2 \quad (12)$$

$$dC/dt = \frac{k_1^2k_3}{8k_2^2}A^2 \quad (13)$$

We compare eqs. (13) and (2) to find them to be of the same form. The details of the rate constants of eq. (13) may be written as follows,

$$\frac{k_1^2k_3}{8k_2^2} = \frac{(p_1Z_1)^2p_3Z_3}{8(p_2Z_2)^2}\exp -2(E_1-E_2+E_3/2)/RT \quad (14)$$

p_1Z_1 in eq. (14) is given as 4×10^{10} (525~570°C) by Kamenetskii.[20] Z_2 and Z_3 are of the order of 10^{14}. Inserting these values we obtained $p_2^2/p_3 = 10^{-5}$ from the theoretical formula (14) and the experimental one (2). Substituting the various values of p_2 we find the corresponding ones of p_3 as follows.

p_2	10^{-1}	10^{-2}	10^{-3}	10^{-4}	10^{-5}	10^{-6}
p_3	10^{3}	10^{1}	10^{-1}	10^{-3}	10^{-5}	10^{-7}

In general the simpler the reacting molecules, the greater is the steric factor[21] and so $p_2 > p_3$ may be considered. From the values of p_2 and p_3 cited above, p_2 must be $<10^{-5}$, which follows $10^{-5} > p_2 > p_3$. If the dimer would be assumed to have the structure like butadiene biradical, its steric factor p_3 may be approximately of the same order with that

20) D. A. Frank-Kamenetskii, *Acta Phys. Chim. R.S.S.U.*, **18**, 148 (1943).
21) H. Eyring, "The Theory of Rate Process", McGraw-Hill Book Co. (1941) p. 19.

of dimerization of butadiene which is of 10^{-4}.[22] This value of p_3 disagrees with $10^{-5} > p_2 > p_3$.

If C.B.D. is assumed to be the dimer, its steric factor of dimerization p_3 may be greater than that of chain structure 10^{-4}, because the steric factor of the reaction forming a non-linear complex tends to have the greater one than that of the reaction forming a linear complex.[21] Hence, when p_3 of dimerization of C.B.D. is assumed to be 10^{-3}, $p_2=10^{-4}$ is obtained; that is $p_2 < p_3$, which disagrees with the conditions $p_2 > p_3$ mentioned in the case of the chain structure. But that may be explained as follows; the activated state of dimerization of C.B.D. in eq. (5) has a looser structure than that of eq. (4); consequently, $\Delta S^{\ddagger}$ of eq. (5) is greater than that of eq. (4).

Comparing the exponential terms of eqs. (2) and (14) we obtain

$$2(E_1-E_2+E_3/2)=46900 \text{ cal.}$$

As $E_1=29900$ cal according to Kamenetskii[20]

$$E_2-E_3/2=6450 \text{ cal.}$$

Here, E_2 will be of the order of 7~8 Kcal because it is the activation energy for the chain propagation.[11] Consequently E_3 becomes 1~3 Kcal which is so small that this corresponds to the assumption that the reactive dimers react to give C.O.T. as shown in eq. (5).

By calculating the ratio of yields of benzene and C.O.T. from eqs. (12) and (13), we obtain

$$B/C=\frac{4k_2^2}{k_1k_3}$$

$$=\frac{4(p_2Z_2)^2}{(p_1Z_1)(p_3Z_3)}\exp(E_1-2E_2+E_3)/RT \quad (15)$$

That is, the ratio of benzene and C.O.T. is independent of the pressure of acetylene. In fact inserting the values

$$p_2^2/p_3=10^{-5},\ E_2-E_3/2=6450 \text{ cal}$$

etc., into eq. (15) we may compare the evaluated ones and the experimental ones as shown in Table I. The former will not be so accurate, since the experimental values were obtained by assuming the whole weight of the products to be that of benzene which is the main product. Nevertheless they coincide considerably well with each other and especially $(B/C)_{obs.}$ shows independence of pressure.

TABLE I

THE RATIO OF BENZENE AND C.O.T., OBSERVED AND CALCULATED

Temp. °C	Press. mmHg	B/C obs.	B/C calc.
535	250	1.59×10^3	3.72×10^3
550	250	1.28×10^3	3.02×10^3
	200	1.10×10^3	
570	250	4.59×10^2	2.37×10^3
	200	4.10×10^2	
	100	4.22×10^2	

Hence for increasing the yield of C.O.T. it is very efficient to diminish the exponential term of eq. (15) and so the yield as well as the rate of formation of C.O.T. will be increased very greatly if we can decrease, by the use of catalyser, for example, the value E_1, the largest among E_1, E_2, and E_3. On the other hand since the rate of formation of C.O.T. is proportional to the square of acetylene pressure, we may conclude from eqs. (13) and (15) that the use of high pressure and suitable catalyser diminishing E_1 will produce the large yield of C.O.T. This agrees qualitatively with the fact that Reppe[23] obtained C.O.T. in good yield using high pressure and nickel catalyser.

The existence of C.B.D. has not yet been proved, but Kamenetskii[24] considered from the chemical analysis of the polymerization products that the structure of dimer will be C.B.D. or methylenecyclopropene; and again C.B.D. was supposed to be the dimer by Reppe[23], too, who expected but did not succeed in finding C.O.T. in the thermal polymerization products and who said that C.O.T. is too labile thermally to be found in the products.

Concerning the stability of C.B.D., strain energy due to the bent C—C bonds is not so decisive according to Coulson[25], as Penney[26] denied its existence. C.B.D. is probably more stable in a rectangular form having the stretched single bonds than in a square form, after the calculation by Craig[27] and Coulson[28].

It is true that we can not determine these things only by the kinetic consideration we made, and we dare not insist upon our opinion. However from the view-point that the activation evergy E_2 and E_3 are very small, we may state the dimer will not be vinylacetylene but a more reactive and radical-like substance. This might be explained by the butadiene biradical, but we prefer C.B.D.

22) W. E. Vaughan, *J. Am. Chem. Soc.*, **54**, 3863 (1932).
23) W. J. Reppe, "Acetylene Chemistry" (P. B. Report 18852-s) (1949).
24) D. A. Frank-Kamenetskii, *C. R. Acad. Sci. U.S.S.R.*, **37**, 137 (1942).
25) C. A. Coulson and E. M. Moffitt, *Phil. Mag.*, **40**, 1 (1949).
26) W. G. Penney, *Proc. Roy. Soc.*, A**144**, 166: A**146**, 223 (1934).
27) D. P. Craig, *J. Chem. Soc.*, 3175 (1951).
28) C. A. Coulson, Private communication to S. Shida.

at present from the view-point concerning the values of the steric factors p_2 and p_3.

Summary

C.O.T. was found polarographically to exist in the thermal polymerization products of acetylene at the flow method. There did not occur any thermal cracking process below the temperature 570°C. on the experimental conditions. The polymerization of acetylene is fundamentally a bimolecular reaction and the dimer is supposed to be cyclobutadiene from the point of view of the steric factors of the reaction. Benzene is formed by the combination of cyclobutadiene and acetylene. C.O.T. is formed by the dimerization of cyclobutadiene; the rate of C.O.T. formation is of the second order in respect of acetylene. The activation energy and frequency factor of the rate is 46900 cal/mol and 1.50×10^{11} cc. $mol^{-1}.sec^{-1}$., respectively.

The ratio of yield of C.O.T. and benzene is independent of the pressure of acetylene and dependent of the temperature. In order to increase the ratio the activation energy E_1 must be lowered. The high yield of C.O.T. in the Reppe reaction was considered qualitatively.

The author expresses his deepest gratitude to Dr. S. Shida for his encouragement and advice. We are indebted to the budget of the Ministry of Education for our experiments.

Laboratory of Physical Chemistry,
Tokyo Institute of Technology,
Ohokayama, Meguroku, Tokyo

Reactivity of Coke. II. Effects of Heat Treatment of Cokes on Their Specific Surface Areas and Absolute Specific Reaction Rates with Carbon Dioxide at 950°C

By Yoshio KAWANA

(Received February 5, 1954)

Introduction

The reactivity of coke may be considered to depend mainly on its surface properties, crystallographic structure and the catalytic effects of ash in it. These properties are all changed considerably by heat treatment. Accordingly, knowledge on changes of physical and chemical properties of coke by heat treatment is very important for the consideration of the reactivity of coke. Since the conference on the ultra-fine structure of coals and cokes (London, 1943), the physical structure and surface chemical properties of coals and cokes have been actively studied.

The change of adsorption properties of coke or char by heat treatment has been obtained by Maggs[1] and Honda et al.[2] Recently, Boyer and Foucault[3] have obtained the variations of specific surface areas of cokes carbonized from four different coals below 1000°C. Walker et al,[4] and Jolley and Poll[5] discussed the surface area development of carbons during gasification reactions.

In our previous paper,[6] surface areas of cokes were obtained by adsorption of ammonia at 0°C using the simple B.E.T. method, and by these surface area values together with kinetic data, the carbon dioxide-coke reaction was discussed from the standpoint of the absolute reaction rates theory. In this paper, the author obtained the effects of heat treatment of cokes from 1000° to 2000°C on specific surface areas of cokes and absolute specific reaction rates of cokes with carbon dioxide at 950°C.

Experimental

Preparation of Coke Samples.—As original coals, Nakayama lignite, Mitsui Bibai coal, Yatake coal and Hongei anthracite were selected, and after crushing from 20 to 60 mesh (Tyler), their ash contents were reduced by the float-and-sink test in benzene-carbon tetrachloride solution.

1) F. A. P. Maggs, "Proc. Conf. Ultra-fine Structure of Coals and Cokes" B.C.U.R.A., London, 1944, p. 147.
2) H. Honda, Y. Kawana, K. Ouchi and K. Nagata, *J. Chem. Soc. Japan* (Pure chemistry section, in Japanese), **74**, 887 (1953).
3) A. Boyer and G. Foucault, *Compt. rend.*, **257**, 895 (1953).
4) P. L. Walker, R. J. Foresti and C. C. Wright, *Ind. Eng. Chem.*, **45**, 1703 (1953).
5) L. J. Jolley and A. Poll, *J. Inst. Fuel*, **26**, 33 (1953).
6) Y. Kawana, This Bulletin, **26**, 507 (1953).

TABLE I

PROXIMATE AND ULTIMATE ANALYSES OF ORIGINAL COALS

Original coals	Proximate analyses (%) standard basis				Ultimate analyses (%) dry basis					Calorific value (cal./g.)	Fuel ratio	Caking property
	Moisture	Ash	V.M.	F.C.	C	N	H	S	O+errors			
Nakayama lignite	9.95	5.70	44.75	39.60	62.40	1.19	4.96	0.39	24.73	5330	0.884	Non-caking
Mitsui Bibai coal	1.57	8.95	35.27	54.19	77.61	1.79	5.46	0.11	5.95	7650	1.57	Weakly caking*
Yatake coal	0.70	5.82	19.63	73.76	84.15	1.88	4.71	0.59	2.80	8180	3.76	Strongly caking
Hongei anthracite	1.78	1.90	6.79	89.53	91.02	0.98	3.39	0.39	2.29	8250	13.2	Non-caking

* Although Mitsui Bibai coal is usually classified as non-caking, the present sample with the preliminary treatment of reducing ash contents of the coal indicates weakly caking property.

The results of analyses of original coals after this treatment are shown in Table I. These coals were primarily coked at 950°C by an electric furnace, and then both Mitsui Bibai and Yatake cokes were again crushed from 20 to 60 mesh because they solidified in larger blocks, while the other cokes remained as they were. The primary cokes were separately heated in a vacuum carbon resistance furnace at various temperatures from 1000° to 2000°C. The time of heating to desired temperatures and the maximum pressure during heat treatment were respectively about 10—30 minutes and 5—26 mm Hg.

The analytical results and the density of these coke samples are as shown in Table. II.

TABLE II

ANALYTICAL RESULTS(a) AND DENSITIES(b) OF COKES HEATED AT TEMPERATURES FROM 1,000° to 2,000°C

Cokes		Temperature of heat treatment, °C 1000	1200	1400	1600	1800	2000
Nakayama coke	Moisture, %	8.84	8.29	4.14	1.02	—	0.27
	Ash, %	11.18	11.60	12.40	11.00	—	6.36
	Density, g/cc	1.572	1.809	1.571	1.482	—	1.436
Mitsui Bibai coke	Moisture, %	2.42	0.60	0.42	0.20	0.16	0.20
	Ash, %	16.52	17.72	16.97	14.94	13.41	9.56
	Density, g/cc	1.780	1.852	1.894	1.976	2.039	1.917
Yatake coke	Moisture, %	0.72	0.44	0.20	0.20	0.18*	0.24
	Ash, %	8.84	9.46	8.38	6.88	6.70*	4.62
	Density, g/cc	1.809	1.904	2.041	1.959	1.994*	1.927
Hongei coke	Moisture, %	5.52	1.36	0.28	0.14	0.16	—
	Ash, %	4.73	6.16	5.90	6.06	5.78	—
	Density, g/cc	1.808	1.671	1.676	1.674	1.659	1.650

(a) Standard basis (b) The densities of cokes were obtained from the usual liquid displacement method using water at 25°C. The air in the coke sample was eliminated as thoroughly as possible by the rotary pump. (*) This coke was treated at 1780°C.

Apparatus and Procedure.—The apparatus and procedure for determination of the surface area of coke and for reaction rates study of the coke-carbon dioxide system are the same as already stated in the previous paper.[6] The surface area of cokes was determined by the adsorption of ammonia at 0°C following the simple B. E. T. method.[7][8]

After measurement, the sample was heated and the adsorbed ammonia was thoroughly desorbed and then the reaction rates of coke with carbon dioxide at 950°C under constant volume were obtained by measuring the increase of the total pressure of this system against time.

Absolute specific reaction rates, K_a, expressed as the number of molecules reacted per sq. cm per second at 950°C when p_{CO_2}/p_{CO} was equal to unity, were obtained by the kinetic data together with the surface area determination as explained in detail in the first paper.

7) S. Brunauer, P. H. Emmett and E. Teller, *J. Am. Chem. Soc.*, **60**, 309 (1938).
8) S. Brunauer, L. S. Deming, W. E. Deming and E. Teller, ibid., **62**, 1723 (1940).

Results and Discussion

Variations of Specific Surface Areas of Cokes with Heat Treatment.—The B. E. T. plots of adsorption isotherms of ammonia at 0°C for various cokes heated at temperatures from 1000° to 2000° are shown in Fig. 1—Fig. 4. In lower temperatures of heat treatment, good straight lines are obtained, but

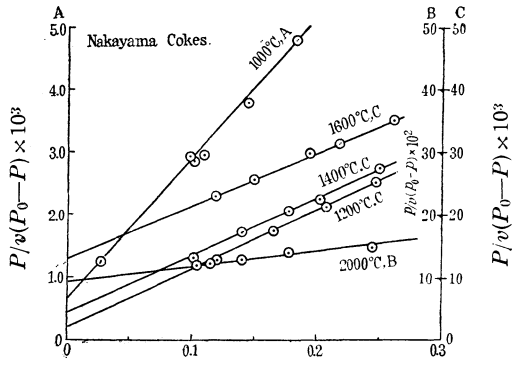


Fig. 1

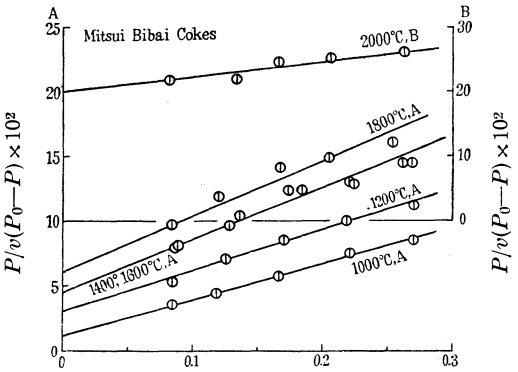


Fig. 2

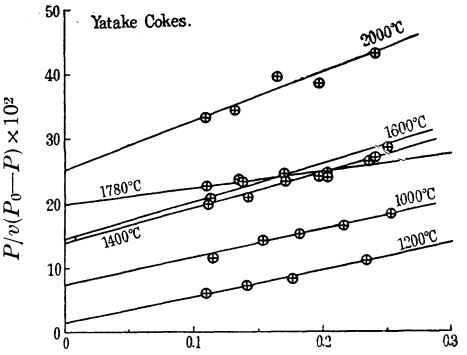


Fig. 3

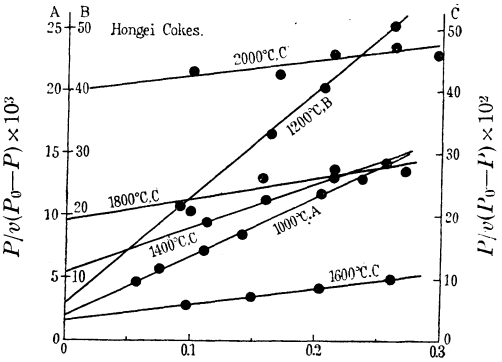


Fig. 4

above 1600°—1800°C, deviations from straight lines become larger and this may be ascribed to smaller adsorption volume. The errors in the surface area values coming from these deviations, however, may not be so large. Various values obtained from Fig. 1—Fig 4 by the usual procedures in the B.E.T. method are summarized in Table III.

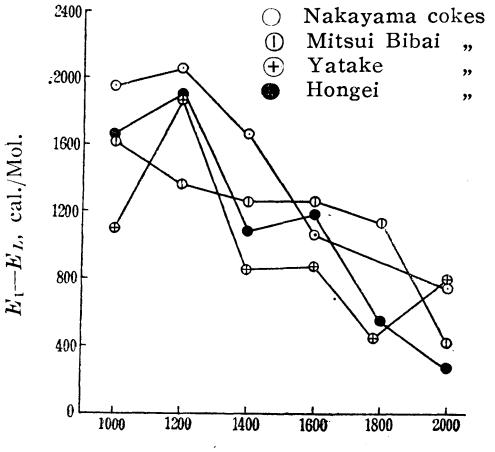
TABLE III. EFFECTS OF HEAT TREATMENT OF COKES ON THEIR SURFACE PROPERTIES AND ABSOLUTE SPECIFIC REACTION RATES OF COKES WITH CARBON DIOXIDE AT 950°C

Cokes	Temp. of heat treatment, °C	Vacuum pretreatment °C, hr (mmHg)	Sample weights	V_m	S	A	C	E_1-E_L	K	K_a molecules
			g	cc	m²	m²/g		cal/Mol		cm⁻² sec⁻¹
Nakayama coke	1000	1000, 19 (10^{-4})	0.3924	43.1	149.4	381	36.3	1950	1.67	8.02×10^9
	1200	1100, 8 (10^{-5})	0.1566	10.5	36.4	232	43.2	2050	3.72	7.64×10^{10}
	1400	1100, 5 (10^{-4})	0.3179	10.5	36.4	115	21.2	1660	1.01	2.45×10^{10}
	1600	1100, 5 (10^{-4})	0.9002	10.9	37.8	42.0	7.09	1060	0.302	5.74×10^9
	2000	1100, 5 (10^{-4})	1.8291	2.80	9.71	5.31	3.89	740	1.75 1.61	1.28×10^{11} 1.17×10^{11}
Mitsui Bibai coke	1000	1000, 4.5 (10^{-3})	3.2387	3.63	12.6	3.89	19.7	1620	0.675	3.81×10^{10}
	1200	1100, 3.5 (10^{-3})	3.6872	2.86	9.92	2.69	12.3	1360	0.865	6.11×10^{10}
	1400	1100, 4 (10^{-3})	5.3936	2.20	7.63	1.41	10.1	1260	0.873	7.84×10^{10}
	1600	1100, 4.5 (10^{-4})	4.4478	2.20	7.63	1.72	10.1	1260	0.969	8.80×10^{10}
	1800	1100, 4.5 (10^{-4})	3.9977	2.03	7.04	1.76	8.02	1130	0.124	1.22×10^{10}
	2000	1100, 4.5 (10^{-4})	3.2879	2.29	7.94	2.41	2.18	420	1.05	9.20×10^{10}

	1000	1000,	5 (10^{-4})	1.1308	1.92	6.66	5.89	7.57	1100	2.73	2.93×10^{11}
	1200	1100,	2 (10^{-3})	2.3473	2.32	8.04	3.43	30.8	1860	1.39	1.23×10^{11}
Yatake	1400	1100,	2 (10^{-3})	2.7940	1.49	5.17	1.85	4.81	850	1.67	2.27×10^{11}
coke	1600	1100,	4 (10^{-4})	3.0608	1.38	4.78	1.56	4.98	870	0.722	1.06×10^{11}
	1780	1100,	4 (10^{-5})	3.1939	2.20	7.63	2.39	2.27	450	0.925	8.45×10^{10}
	2000	1100,	3 (10^{-5})	2.4947	0.96	3.33	1.33	4.25	790	0.310	6.57×10^{10}
	1000	1100,	5 (10^{-3})	2.8936	21.4	74.2	25.6	21.2	1660	2.32	2.17×10^{10}
	1200	1100,	5 (10^{-3})	1.7178	5.66	19.6	11.4	32.1	1890	2.76	1.00×10^{11}
Hongei	1400	1100,	4 (10^{-4})	2.0311	1.24	4.30	2.11	7.37	1080	3.05	5.02×10^{11}
coke	1600	1100,	4 (10^{-4})	6.1565	3.46	12.0	1.95	9.02	1190	2.92	1.60×10^{11}
	1800	1100,	4 (10^{-5})	7.2682	1.90	6.59	0.91	2.75	550	1.35	1.36×10^{11}
	2000	1100,	3 (10^{-5})	7.1644	1.53	5.30	0.74	1.65	270	0.0610	7.66×10^{9}

Before adsorption, coke samples were evacuated at higher temperatures to eliminate the surface oxide and residual volatile matters; "Vacuum pretreatment" in Table III shows the conditions of this preliminary treatment. The quantities of V_m, S, A and C in Table III are respectively monomolecular adsorption volume, total surface area, specific surface area and the B. E. T. constant. The quantity of (E_1-E_L) can be evaluated from C as usual.

The variations of (E_1-E_L) with heat treatment are also indicated in Fig. 5. For all

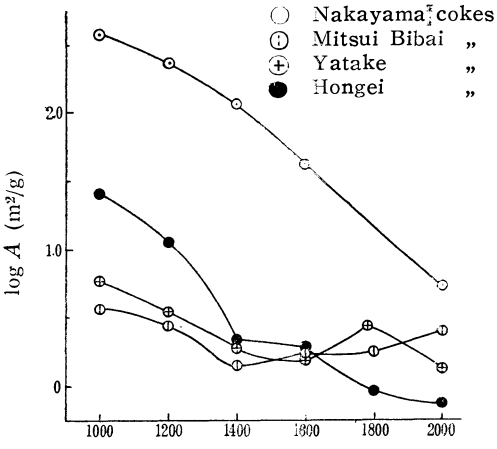


Temperature of heat treatment, °C

Fig. 5. Variations of E_1-E_L with heat treatment.

kinds of cokes, generally speaking, (E_1-E_L) decreases with the increase of heat treatment temperature and the difference due to the rank of original coals can not be clearly seen in Fig. 5. Except for Mitsui Bibai cokes, there seem to be maximum points of (E_1-E_L) at about 1000°–1200°C.

The variations with heat treatment of the specific surface area of cokes are illustrated in Fig. 6. The area of cokes carbonized from non-caking coals such as Nakayama lignite and Hongei anthracite in lower temperature of heat treatment is much larger than that



Temperature of heat treatment, °C

Fig. 6. Effects of heat treatment of cokes on their specific surface areas.

of cokes from other caking coals such as Mitsui Bibai and Yatake coals, but the values of the former cokes decrease rapidly with heat treatment temperature, while those of the latter cokes do not change so much by heat treatment and there may be minimum points at about 1400°–1600°C. The ratios of the area of coke heated at 2000°C to that at 1000°C are respectively about 1.4×10^{-2} for Nakayama, 6.2×10^{-1} for Mitsui Bibai, 2.3×10^{-1} for Yatake and 2.9×10^{-2} for Hongei cokes. It is very interesting to notice that there is a close relationship between the manner of decrease of the area of coke by heat treatment and the caking property of the original coal.

Recently, the views that amorphous carbon consists not only of the so-called "turbostratic structure"[9] but also of a third "three-dimensional covalent cross-linked structure", which plays a great role in the structure of chars and cokes, have been justified by X-ray studies[10] on carbonization products from

9) J. Biscoe and B. E. Warren, *J. Appl. Phys.*, **13**, 364 (1942).

10) J. Gibson, M. Holohan and H. L. Riley, *J. Chem. Soc.*, **1946**, 458.

hexaiodobenzene and hexachlorobenzene and by the wet oxidation rates studies[11] of various kinds of amorphous carbons containing cokes. According to the magnetochemical studies[12] of coals and their related substances, the structure of chars and cokes depends much on both the carbonization temperature and the structure of starting substances; moreover the structure of coke carbonized at about 1100°C may be considered to consist mainly of the three-dimensional covalent cross-linked structure, the change of which to the turbostratic structure or to the graphite one may occur at temperatures higher than 1100°C.

The higher the temperature of heat treatment is, the more the three-dimensional covalent cross-linked structure of cokes is decomposed and the nearer it is to that of graphite; hence, in general, the surface area of cokes decreases with heat treatment temperatures. However, the structure of cokes depends on the kind or rank of original coals as well as the heat treatment temperature, so the specific surface area of cokes heated even at the same temperature may differ a great deal from each other.

It cannot be clearly explained why the specific surface area tends to increase above 1600°C for caking coals, but not for non-caking coals. As the temperature of 1600°C coincides with that of rapid graphitization of cokes,[13] there may be some special relation between the increase of the specific surface area and the graphitization of cokes from caking coals.

Variations with Heat Treatment of Absolute Specific Reaction Rates of Cokes with Carbon Dioxide at 950°C.—The values K and K_a in Table III are respectively rate constants and absolute specific reaction rates, expressed as the number of molecules reacting per sq. cm per second at 950°C when P_{co2}/P_{co} equals unity in the reaction of coke with carbon dioxide, as defined in the first paper. The relations between K_a and the heat treatment temperature are also indicated in Fig. 7. Generally, a regular relation between K_a and the heat treatment temperature is neither seen for all kinds of cokes, nor is there a clear relation between K_a and the rank of original coals for all temperatures of heat treatment. Although the higher the temperature of heat treatment is, the more regular becomes the crystallographic structure of cokes, which approaches to that of graphite, there is not a general tendency of the decrease of K_a with the heat treatment temperature. The irregular changes of K_a by heat treatment may be due to the catalytic effects of the ash which coexists on the surface of coke, and the magnitudes of the changes are comparable with or are larger than those of the specific surface area decrease by heat treatment. According to this result, it may be said that the impurities in coke have stronger effects on the reactivity of coke than the surface area of coke has.

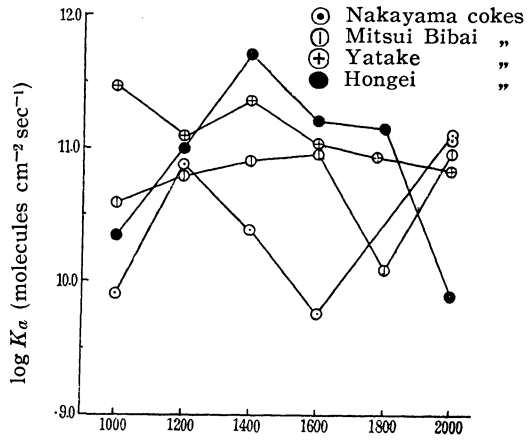


Fig. 7. Effects of heat treatment of cokes on absolute specific reaction rates of cokes with carbon dioxide at 950°C.

On the other hand, in our first paper, it has been concluded that the difference of K_a between pure amorphous carbon and pure graphite at the same temperature will be small, and that for carbons containing some impurities, the catalytic effects of the ash in carbons on the absolute specific reaction rates may be much greater than those of the difference of the crystallographic structure of carbons, that is, the degree of graphitization of carbon, from the absolute reaction rates study of various carbons with carbon dioxide. The same conclusion could again be derived from the above-mentioned results. That is, there are some effects which are much greater than those of the difference of the degree of graphitization of cokes, and these effects have been assumed to be the catalytic effects of the ash in coke.

Summary

The effects of heat treatment of cokes on their specific surface areas and absolute

11) H. E. Blayden and H. L. Riley, *J. Soc. Chem. Ind.*, **54**, 159T (1935); A. F. Balfour, H. E. Blayden, A. H. Carter and H. L. Riley, *J. Soc. Chem. Ind.*, **57**, 1 (1938); H. L. Riley, *J. Chim. Phys.*, **47**, 565 (1950).

12) H. Honda and K. Ouchi, *Reports of the Resources Research Institute* (in Japanese) No. 1 (1952).

13) H. Honda and K. Ouchi, *Sci. Rep.*, Tohoku Univ. Series 1, **37**, 55 (1953).

specific reaction rates of cokes with carbon dioxide at 950°C have been obtained by the same procedure as stated in the first paper.

Generally, the specific surface area of cokes decreases with heat treatment temperature, and the values for cokes from non-caking coals are much greater than those for cokes from caking coals in lower heat treatment temperatures, and there is a close relationship between the manner of decrease of the specific surface area of coke by heat treatment and the caking property of the original coal.

The changes by heat treatment of absolute specific reaction rates of cokes with carbon dioxide at 950°C are very irregular for all the temperatures. There are some effects, which are much greater than those of the difference of the crystallographic structure of cokes, on the absolute specific reaction rates of cokes with carbon dioxide. These effects have been assumed as the catalytic effects of the ash in coke, which may also be larger than those of the surface area of coke on the reactivity of coke.

The author wishes to express his earnest thanks to Mr. A. Baba, Dr. H. Honda and Mr. Y. Yoshida for their kind advice and interest in this study. The author's thanks are also due to Mr. R. Sato for his kind assistance in this experiment.

Shigen-Gijutsu-Shikenjo
Resources Research Institute
Saitama-Kawaguchi
Japan

Surface Chemistry of Synthetic Protein Analogues. IV. On the Monolayers of Electrolytic Synthetic Polypeptides, Poly-L-Glutamic Acid and the Copolypeptide of L-Lysine, L-Leucine and L-Glutamic Acid

By Toshizo ISEMURA and Kozo HAMAGUCHI

(Received March 22, 1954)

Introduction

In the preceding three papers of this series[1-3], we have reported on the properties of the monolayers of some synthetic polypeptides, all of which have non-electrolytic side chains. It was found that the polypeptides having sidechains which are less than four carbon atoms in length, such as poly-DL-norleucine, gave the surface pressure-area curves which closely resembled in shape those of natural proteins. In relation to only the length of side chains, poly-DL-norleucine may be a suitable one as a model of proteins. Strictly speaking, however, this polypeptide may be inadequate because of the lack of electrolytic nature.

The copolypeptide of L-lysine, L-leucine and L-glutamic acid which is described in the present paper should be a more promising protein model for the following three reasons: namely, (1)this copolypeptide has amino groups, carboxyl groups and non-polar hydrocarbon groups in side chains, (2) plausible length of side chain and (3) the configuration of L-type. All of these properties are found in natural proteins in general.

This polypeptide films gave the different surface pressure-area (F—A) and surface viscosity-area (η—A) curves on the substrates of various *p*H values and the results obtained are interpreted in terms of the ionization degree of its amino and carboxyl groups. In addition, further simplified, non-amphoteric, poly-L-glutamic acid monolayers on the substrates of different hydrogen ion concentrations were also examined.

The interest about these electrolytic polypeptides concentrate not only upon the protein model but also upon this polyelectrolytic behaviour of which investigations are recently developed by Kuhn and Katchalsky[4,5] We have investigated the properties of these polypeptides monolayers from the viewpoint of polyelectrolyte in addition to the comparison of these polypeptides with natural proteins.

Experimental

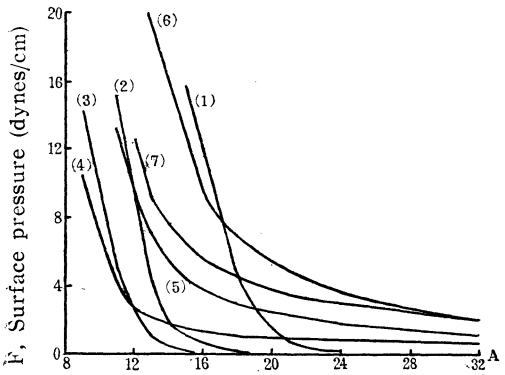
Materials and Methods. The copolypeptide of

1) T. Isemura and K. Hamaguchi, This Bulletin, **25**, 40 (1952).
2) T. Isemura and K. Hamaguchi, ibid., **26**, 425 (1953).
3) T. Isemura and K. Hamaguchi, ibid., **27**, 125 (1954).
4) W. Kuhn, O. Kunzel and A. Katchalsky, *Helv. Chim. Acta*, **31**, 1994 (1948).
5) A. Katchalsky, *J. Polymer Sci.*, **7**, 393 (1951).

L-lysine, L-leucine, and L-glutamic acid and poly-L-glutamic acid were prepared by Dr. H. Tani and Mr. H. Yuki[6] and were used without any further purification. This copolypeptide was spread from its methanol solution and poly-L-glutamic acid from a solution in N/100 sodium hydroxide containing 1 percent isopropyl alcohol. The film of the polyelectrolyte is profoundly affected by the existence of a small amount of salt in the substrate In order to minimize the effect of various salt ions the *p*H of the substrates was adjusted inevitably only with hydrochloric acid or sodium hydroxide without using the buffer. The value of *p*H was measured by using the Beckman glass electrode. The change of the *p*H values before and after experiment, however, did not exceed 0.2 unit at most.

Surface pressure and surface viscosity measurements were carried out by the method of a hanging plate and of damped oscillatory motion of a disc, as reported in the previous papers.[1,3] The area per amino acid residue of the copolypeptide was calculated by assuming that the same ratio of L-lysine, L-leucine and L-glutamic acid as the initial monomer concentration ratio of this polymerization, 1:2:1, was maintained in the copolymer.

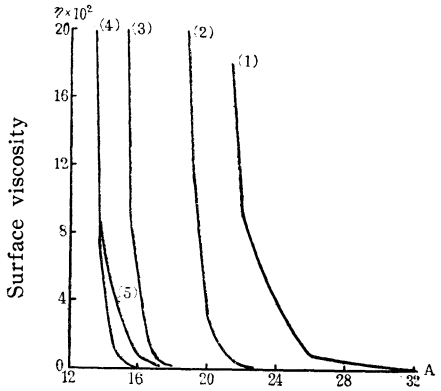
Results. The F—A and η—A curves of the copolypeptide on the substrates of different *p*H values were shown in Figs. 1 and 2. It was found



Area/residue (Å^2)

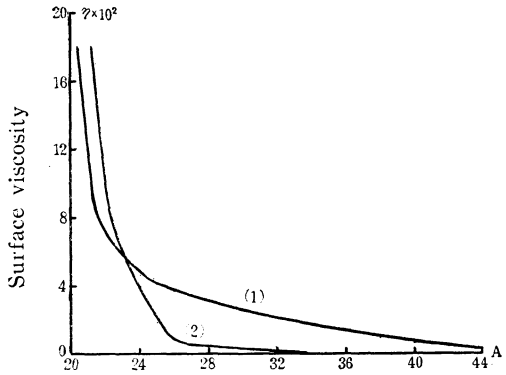
Fig. 1. Surface pressure-area curves for monolayers of the copolypeptide on the substrates of different *p*H values. Curve (1), *p*H 7, (2), *p*H 9.4, (3), *p*H 5.8, (4), *p*H 4.4, (5), *p*H 3.0, (6), *p*H 12.3, and (7) *p*H 1.6. (8°C).

from these figures that the F—A and η—A curves were varied with the substrate *p*H and that the F—A curves on the substrate of which *p*H values lie between 5.8 and 9.4 were of condensed type, but the more acidic or the more alkaline in the outsides of this *p*H range the substrate becomes, the more the F—A curves expand. Furthermore, while in this *p*H range the surface viscosity was very large even at lower pressure region—this is the analogous fact with the case of non-polar polypeptides[3]—it was not sensitive until the surface pressure became considerably high on the either side of this *p*H range. The surface viscosities decrease with the rise of temperature of the substrate at any *p*H value excepting at *p*H 7, where the effect of the temperature was reverse, i.e., the higher the temperature the larger was the viscosity. (Fig 3).



Area/residue (Å^2)

Fig. 2. Surface viscosity-area curves for monolayers of the copolypeptide on the substrate of different *p*H values. Curve (1) *p*H 7, (2) *p*H 8.3, (3) *p*H 9.2, (4) *p*H 5.8 and (5) *p*H 1.6. (7°C)



Area/residue (Å^2)

Fig. 3. Effect of temperature on surface viscosity-area curve for monolayer of the copolypeptide at *p*H 7. Curve (1) 14°C, (2) 7°C.

The F—A and η—A curves of poly-L-glutamic acid were shown in Figs. 4 and 5. Fig. 6 shows the relations of *p*H-area (at constant pressure), and *p*H-surface pressure (at constant area), namely curve (I) shows the plot of the area at 1 dyne/cm. against *p*H (ca. 10°C), curve (II) the same as curve (I) but at the temperature 21°C., curve (III) the surface pressure at 15 Å^2/residue against *p*H, and curve (IV) the area at $\eta=10^{-2}$ surface poises

6) H. Tani, H. Yuki, K. Okawa, S. Sakakibara and C. Oizumi, *Seni Kagaku Kenkyusho Nenpo* (*Mem. Inst. Fiber Research*) **7**, 98 (1953).

against pH. It was noted that the area or surface pressure decreased steeply at about pH 4.6.

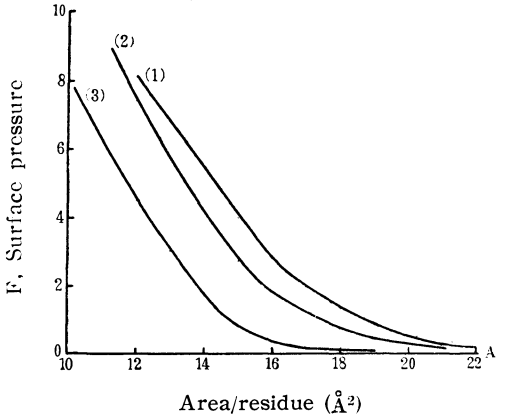


Fig. 4. Surface pressure-area curves for monolayers of poly-L-glutamic acid. Curve (1) pH 1.6~4.6, (2) pH 5.1 and (3) pH 5.6. (10°C).

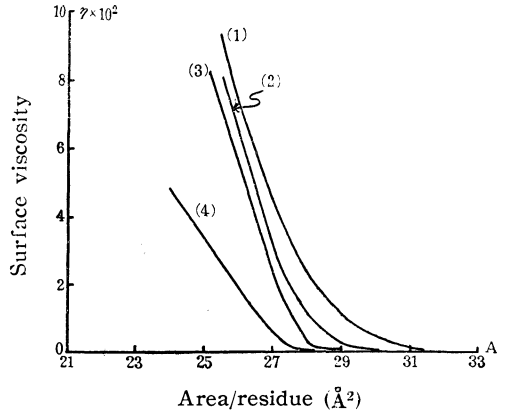


Fig. 5. Surface viscosity-area curves for monolayers of poly-L-glutamic acid. Curve (1) pH 1.6, (2) pH 3.0, (3) pH 4.4 and (4) pH 4.8. (22°C).

Discussion

Compressibility δ was calculated from the F—A curves at various pH by the equation

$$\delta = -\frac{1}{A}\frac{\partial A}{\partial F} \qquad (1)$$

and was plotted against the area. In Fig. 7 the area of the minimum compressibility ($\delta_{min.}$) appearing in the δ—A curves is plotted against the pH of the substrates.

The minima appear at pH 4.4 and 9.6 and the maximum at pH 7 in this curve. The area at $\eta = 2\times10^{-2}$ surface poise was plotted against pH in this figure and this relation is also of W-shape similarly. This relation resembles that found by Gorter, van Ormondt and Dorn,[7] who pointed out that the spreading was maximum at the isoelectric point of the protein. Later, the same relation was also recognized by Bateman and Chambers[8]

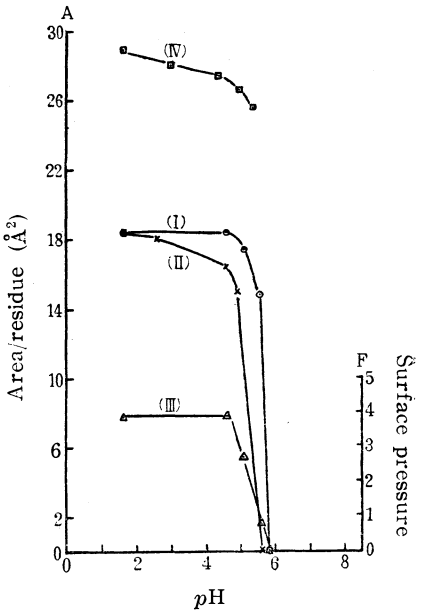


Fig. 6. Monolayers of poly-L-glutamic acid. Curve (I) Area at 1 dyne/cm.—pH curve at 10°C. (II) Area at 1 dyne/cm.—pH curve at 21°C. (III) Surface pressure at 15 Å²/residue—pH curve at 10°C. (IV) Area at $\eta = 10^{-2}$ surface poise—pH curve at 22°C.

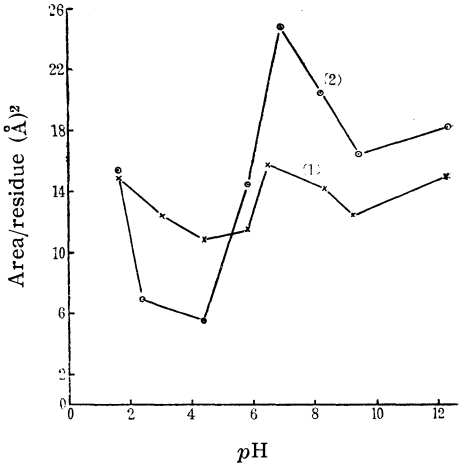


Fig. 7. Monolayers of the copolypeptide. (1) Area at compressibility minimum against pH curve, (2) Area at $\eta = 2\times10^{-2}$ surface poise against pH curve.

7) E. Gorter, J. van Ormondt and F. P. Dorn, *Proc. Kon. Akad.*, Amsterdam, **35**, 838 (1932), cited by McBain, "Colloid Science," (1950).

8) J. B. Bateman and L. A. Chambers, *J. Chem. Phys.*, **7** 244 (1939).

and others. Dervichian,[9] however, suggested that this phenomenon was ascribed to the maximum insolubility of proteins at the isoelectric point. In our case, however, the dependence of the area upon *p*H of the substrate may not be ascribed to the difference of solubility, because the solvent used for spreading is methanol and the area becomes again larger when the *p*H is sufficiently higher or lower.

When the copolypeptide was spread on a large area of the substrate, the polar as well as non-polar side chains and —CO—NH— groups in the main chain would be laid on the surface. With the compression of the film, the non-polar side chains tend to stand up perpendicularly to the surface in air, remaining the main chain on the surface of the substrate. Consequently, the long linear polypeptide would assume more or less extended structure in the spread monolayer.

Now, we shall consider on which *p*H lies the isoelectric point of this copolypeptide. At *p*H 7, some peculiar phenomena were observed, that is, (a), the maximum appeared in the A (at compressibility minimum)-*p*H curve (Fig. 7), (b) the surface viscosity is very high even in larger area and (c) the temperature dependence of the viscosity is opposite to that at the other *p*H values (Fig. 3). Since the number of $-NH_3^+$ ions might be the same as that of $-COO^-$ ions at the isoelectric point, it is probable that the number of salt-linkages between these ions is at its maximum and that the large network structure of the film may be completed. In such a state the resistance against shear becomes very large and the surface viscosity is expected to be high in a larger area. If the salt-linkages between these ions is possible, the degree of hydration and also the hydrophilic tendency of these groups decrease and so it is considered that the F—A curve at the isoelectric point develops from the larger area. With increasing or decreasing the *p*H of substrates from the isoelectric point, either positive or negative charge of the molecules exceeds the other and the number of salt-linkages between NH_3^+ and $-COO^-$ ions decreases. The decrease of the number of salt-linkages results in the lowering of surface viscosity, for the resistance against shear becomes necessarily smaller. All the results and considerations above mentioned lead us to the conclusion that the isoelectric point of this copolypeptide may lie at *p*H 7.

The surface viscosity of the protein monolayer is often discussed in terms of molecular shape in an analogous manner with the viscosity of its bulk solution.[10),11)] In our opinion, the surface viscosity may be entirely different from the bulk viscosity in nature. Therefore, it cannot be considered similarly.

It is well known that the polyampholyte, natural[12,13)] and synthetic,[14,15)] shows a minimum viscosity at its isoelectric point in the bulk solution. This is caused by the coiling of the polyelectrolyte chains by the intramolecular neutralization and no effective free charge in the molecule. On the other hand, the polyampholyte molecule in the monolayer is extended by the surface force. The number of positive and negative ionic groups is maximum in total even though the number of either ionic groups is equal to each other at isoelectric point. As a result, these ionic groups tend to interact intermolecularly forming salt-linkage. This is the reason of maximum surface viscosity and minimum bulk viscosity at isoelectric point.

Surface viscosity depends not only on the interaction between the molecules but also on the degree of molecular packing. There exist two extreme cases of orientation, one of which is that the side chains are directed perpendicular and the other, parallel to the water surface. Between these two extremes the forms or orientations which the polypeptide molecules may prefer on the water surface should be different from the substrate *p*H, depending on the degree of ionization of amino and carboxyl groups. Quantitative analysis of F—A and η—A curves is, therefore, very difficult.

As mentioned above, the F—A curves were of condensed type on the substrates of which *p*H values lie in the range between 5.8 and 9.4, but changed to expanded type if the substrate becomes more alkaline or more acidic than either end of this *p*H range. These facts also relate to the degree of ionization of carboxyl or amino groups; when the number of either positive or negative ions increases, the film expands by the electrical repulsion between the free charges.

The dependence of the degree of ionization (α) of the polyelectrolyte on *p*H may be expressed theoretically by the following equation,[5)]

9) D. Dervichian, *Nature*, **144**, 629 (1939).

10) J. T. Davies, *Biochim. et Biophys. Acta*, **11**, 165 (1953).

11) K. Imahori, This Bulletin, **27**, 146 (1954).

12) E. K. Rideal, "Introduction to Surface Chemistry," p. 431, (1930).

13) H. B. Bull, *Trans. Faraday Soc.*, **36**, 80 (1940).

14) T. Alfrey Jr. and H. Morawetz, *J. Am. Chem. Soc.*, **74**, 436 (1952).

15) T. Alfrey Jr., R. M. Fuoss, H. Morawetz and H. Pinner, ibid., 438.

$$p\mathrm{H}-pK_0=\log\frac{\alpha}{1-\alpha}+\frac{0.4343}{kT}\frac{\partial F(\nu)}{\partial\nu} \quad (2),$$

Where $F(\nu)$ is the free energy of electrostatic field of a molecule having ν ionized groups and K_0 the intrinsic dissociation constant. We cannot find out the relation of pH and α from equation (2), because of the difficult calculation of $F(\nu)$. However, according to Arnold and Overbeek,[16] pK_0 of polymeric acid obtained from extrapolation of titration data to a very low degree of ionization is practically equal to the dissociation constant of a monobasic acid of the corresponding monomeric acid composition. So, the degree of ionization α_L of amino groups and α_G of carboxyl group can be evaluated to a first approximation by assuming the dissociation constant of $-NH_2$ group of lysine (pK_{0L}) and of —COOH group of glutamic acid (pK_{0G}) to be 10.5 and 4.3, respectively, using the following simple equation,

$$p\mathrm{H}-pK_0=\log\frac{\alpha}{1-\alpha} \quad (3).$$

Havinga and M. den Hertog-Polak[17] suggested that the value of pH of the electrolytic surface film may be different from that of the bulk solution. On the other hand, Glazer and Dogan[18] showed that there exists little effect with the surface film of polyampholyte such as proteins. In the present calculation, the pH value of the bulk solution was used as that of the surface phase.

If we assume that the polymerization ratio of lysine and glutamic acid of this copolypeptide is 1 : 1 (this assumption is valid when the isoelectric point lies near pH 7 as mentioned above), equation:

$$|\Delta\alpha|=\alpha_L-\alpha_G \quad (4)$$

may be considered to give a measure of effective free charges. On the other hand, if the inter or intramolecular salt-linkages are possible, the probability of its linkage may be proportional to the product of α_L and α_G. Fig. 8 represents the relation of $|\Delta\alpha|$ and $\alpha_L-\alpha_G$ against pH.

As found from Fig. 8 the pH range in which F—A curves are of condensed type correponds to $\Delta\alpha$ of at most 5%. (In this pH range eqn. (3) may well be applied.) This copolypeptide has, however, the residues of

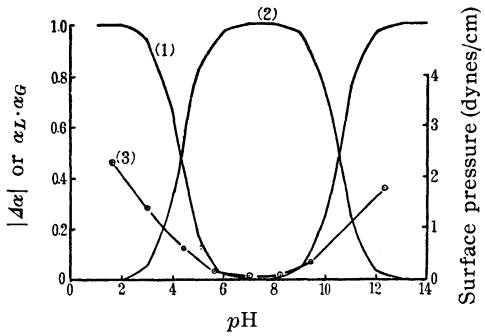


Fig. 8. (1) $|\Delta\alpha|$—pH curve, (2) $\alpha_L\cdot\alpha_G$—pH curve, (3) surface pressure at 30 Å²/residue—pH curve.

lysine, leucine and glutamic acid in the ratio of 1 : 2 : 1 as described above. So, this value of $|\Delta\alpha|$ corresponds to only about 1% ionization of the total number of side chains. It is unfortunate, however, that the pH range which gives the F—A curves of condensed type could not be examined in detail, because of the small amount of the sample. The films which gave the F—A curves of condensed type are characterized by the high viscosity even at low surface pressures (Fig. 9) and this fact corresponds to the cases of nonpolar polypeptides. From these results it is considered that in the pH range which gave the F—A curves of condensed type the molecules forming the film are in such a state that few free charges in molecules exist.

At pH 4.4, $\alpha_L-\alpha_G\fallingdotseq0.5$ (at this pH eqn. (3) cannot be applied but simply qualitatively), namely the number of $-NH_3^+$ ions is greater than that of $-COO^-$ ions by about 50% and the F—A curve is of expanded type. This value of $|\Delta\alpha|$ corresponds to about 10% ionization of the total number of side chains. The film which gives the F—A curves of expanded type is not sensitive for surface viscosity until the film pressure is rather high (Fig. 9). The plots of surface viscosity against surface pressure are shown in Fig. 9. The films which do not bear free charges, for instance, those of non-electrolytic or electrolytic polypeptides which are in the isoelectric state, show the steep curve (I) and increasing the free charges makes the curve flattened for the pressure axis (curve II). Joly[19] measured the surface viscosity against film pressure relations of natural proteins on the aqueous solution of 0.01 N hydrochloric acid. It is found from his results that the more alkaline the isoelectric point is, the more flattened are the η—F curves as shown in curve (II). Consequently,

16) R. Arnold and J. Th. G. Overbeek, *Rec. trav. chim.*, **64**, 190 (1950).
17) E. Havinga and M. den Hertog-Polak, *Rec. trav. chim.*, **71**, 64 (1952).
18) J. Glazer and M. Z. Dogan, *Trans. Faraday Soc.*, **49**, 449 (1953).
19) M. Joly, "Surface Chemistry." *Research* Supplement, Butterworth, p. 157 (1949).

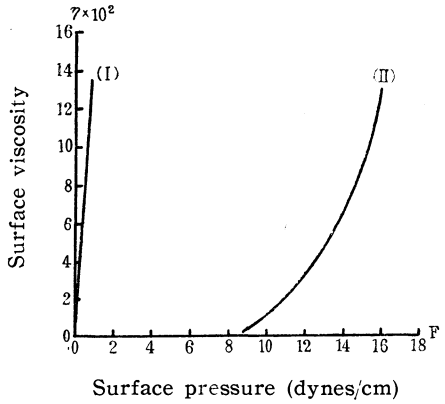


Fig. 9. Surface viscosity-surface pressure curves for monolayer of the copolypeptide. Curve (I) *p*H 7, (II) *p*H 1.6.

the change of the F—A curves to the expanded type must be ascribed to the electrical repulsion of the free charges in polypeptide molecules.

In Fig. 8 surface pressures at constant area are also plotted against the *p*H of the substrate. If the surface pressures exerted at constant area depend markedly on the electrical repulsion between free charges of the molecules, this F—*p*H curve must resemble the $|\Delta\alpha|$ *p*H—curve. This is in fact the case if F—*p*H curve is plotted at a larger area, for instance, 30 Å²/residue; with the lowering of $\Delta\alpha$, F becomes smaller and a minimum point appears at *p*H 7. This fact also supports the theory that the isoelectric point of this copolypeptide lies at *p*H 7. When the surface pressures at smaller area than 25 Å²/residue are plotted against *p*H, there exists discontinuity between *p*H 6 and *p*H 7 and the curve like $|\Delta\alpha|$—*p*H curve could not be obtained, since at such an area region surface pressure depends also on the form or orientation of the molecules.

As is shown in Fig. 7, surface area at constant pressure or at constant viscosity against *p*H curves is of W-shape, and now this curve will be examined in relation to the $|\Delta\alpha|$—*p*H and $\alpha_L \cdot \alpha_G$—*p*H curves. The $\alpha_L \cdot \alpha_G$—*p*H curve shows a maximum at the isoelectric point, *p*H 7, in other words, there exists maximum number of salt-linkages between $-NH_3^+$ and $-COO^-$ ions, the A—*p*H curve shows also a maximum at this *p*H. When the substrate becomes more acidic or alkaline from the isoelectric point, the area becomes smaller, and this region corresponds to the droop of the $\alpha_L \cdot \alpha_G$—*p*H curve. In this region the effect of $\alpha_L \cdot \alpha_G$ is more predominant than that of $|\Delta\alpha|$, i.e., the condensing effect of salt-linkages is more pronounced than the expanding effect of electrical repulsion by free charges. When the substrate becomes still more acidic or alkaline, the area becomes larger again and these regions correspond to the rise of the $|\Delta\alpha|$—*p*H curve, i.e., the effect of electrical repulsion ($|\Delta\alpha|$) is more predominant than that of salt-linkages ($\alpha_L \cdot \alpha_G$). It is of interest that two minima appearing in the curve of W-shape correspond to about pK_0 values of lysine and glutamic acid, respectively.

It is clear from the following reasons that the W-shaped A—*p*H curve is not due to the solubility of this copolypeptide into the underlying water as reported by Dervichian. In the case of poly-L-glutamic acid film, the increase of *p*H shifts the F—A curves to smaller area region and this is clearly due to the increasing solubility of the film substance. A sudden decrease in area and in pressure occurs at *p*H 4.6. The α value at this *p*H calculated from eqn. (3) is approximately equal to 0.6. In the case of the copolypeptide $|\Delta\alpha| \fallingdotseq 0.5$ at *p*H 4.4, based on eqn. (3). In this case, however, there exist the other residues of hydrophobic leucine and non-ionized glutamic acid and if the ratio of lysine, leucine and glutamic acid residues in the molecule is 1:2:1 as described above, this value of $|\Delta\alpha|$ corresponds to about 10% ionization of the total number of the side chains. In such a state, solubility effect cannot be considered in the light of our results of poly-L-glutamic acid.

Next, let us consider about the F—A and η—A curves of poly-L-glutamic acid. The displacement of the F—A curves to a smaller area with the rise of the *p*H of the substrate may be due to the increasing solubility of this polypeptide into the substrate by the ionization of carboxyl groups. It is an interesting fact that both the pressure at constant area and the area at constant pressure or surface viscosity decreased rapidly if the *p*H of the substrate exceeds 4.6. This value of *p*H corresponds to the pK value of glutamic acid.

Berger and Katchalski[20] showed that the reduced viscosity of poly-aspartic acid solution increases rapidly at about *p*H 4.6. Although there have been no experiments on the viscometric behaviour of poly-glutamic acid to be compared with, our present monolayer results may correspond approximately to the bulk data. According to Katchalsky,[5] the rapid increase

20) A. Berger and E. Katchalski, *J. Am. Chem. Soc.*, **73**, 4084 (1951).

of reduced viscosity is due to the elongation of a polypeptide molecule by the electrical repulsion of ionized groups. If the elongation of a polymer molecule into a rod-like filament occurs, the film-forming molecules cannot remain on the surface and dissolve into the underlying water[21]. Our results represent the correspondence between the bulk and monolayer behaviour.

Summary

The surface pressure and surface viscosity of the spread monolayers of the copolypeptide of L-lysine, L-leucine and L-glutamic acid and of poly-L-glutamic acid were measured in relation to substrate *p*H.

The copolypeptide of L-lysine, L-leucine and L-glutamic acid.—The F—A curves in the range of *p*H 5.8 and 9.4 were of condensed type, but at both outsides of this *p*H range they were of expanded type. The area at constant pressure or surface viscosity against *p*H curves were of W-shape and a maximum appeared at *p*H 7. That the isoelectric point of the copolypeptide may lie at *p*H 7 was concluded from the observations of the monolayer properties. The W-shaped curve could be interpreted in terms of the ionization degree of amino and carboxyl groups. At the isoelectric point, *p*H 7, the surface viscosity became maximum. This is in contrast to the bulk viscometric behaviour of polyampholytes.

Poly-L-glutamic acid.—The area at constant pressure or surface viscosity and the pressure at constant area decreases rapidly if the *p*H of the substrate exceeds 4.6. This fact corresponds to the viscometric behaviour of electrolytic polypeptides in solution, i. e., when the elongation of a molecule by the electrical repulsion of ionized groups occurs, the rapid increase in viscosity and in solubility appears in solution and at monolayer, respectively.

The authors wish to express their sincere thanks to Dr. H. Tani and Mr. H. Yuki in the Faculty of Science at Osaka University who gave them the valuable samples of the synthetic polypeptides. A part of the expense for the experiments has been defrayed from a grant given by the Ministry of Education, to which the authors' thanks are also due.

The Institute of Scientific and Industrial Research, Osaka University, Sakai, Osaka

21) T. Isemura, H. Hotta and S. Otsuka,, This Bulletin, **27**, 93 (1954).

Colorimetric Microdetermination of Chromium and Manganese in Aqueous Solutions

By Akiya KOZAWA, Motoharu TANAKA* and Kumazo SASAKI

(Received March 31, 1954)

Introduction

Sometimes it becomes necessary to determine a small amount of chromium and manganese in natural waters and industrial solutions. Heavy metal impurities in the electrolyte (concentrated NaCl solution) have a marked influence on the chlorine-caustic electrolysis by the mercury cell process.[1] In the present study, the method of analysis of chromium and manganese in the electrolyte was established; ferric hydroxide was used as collector and reduction of ferric ion followed by aluminum hydroxide precipitation made it possible to separate chromium from manganese and iron.

Separation of Chromium from Manganese

Chromium and manganese being collected by ferric hydroxide, as will be described later, chromium must be separated from manganese and iron, both of which interfere more or less with the colorimetric determination of chromium.

If an acidic solution containing aluminum and ferrous ions is just neutralized with ammonium hydroxide to bromocresol purple, aluminum hydroxide is precipitated, while a bulk of ferrous iron remains in solution. In this procedure, chromium coprecipitates with aluminum hydroxide and thus manganese

* Department of Chemistry, Faculty of Science, Nagoya University.

1) Gösta Angel and Tage Lundén, *J. Electrochem. Soc.*, 99, 435 (1952).

together with a greater part of iron was separated from chromium.

The following experiment is carried out to check this point.

Various amounts of manganese and chromium are added to 25 ml. dilute sulfuric acid solution (1 : 50) containing 10 mg. of ferric iron and aluminum respectively and then one ml. of 5% hydroxylamine sulphate solution is added. And after boiling to hasten the reduction of any ferric iron to ferrous, the solution is cooled to room temperature and neutralized with ammonium hydroxide (1 : 5) using B. C. P. as indicator.

After filtration, aluminum hydroxide is dissolved with 10 ml. of hot sulfuric acid (1 : 20) and reprecipitated with ammonium hydroxide in the same manner.

Aluminum hydroxide containing chromium on the filter paper is dissolved with 10 ml. of sulfuric acid (1 : 20) and 1 ml. of 85% phosphoric acid,[2] and transferred to a 50 ml. volumetric flask. Chromium coprecipitated with aluminum hydroxide is oxidized to sexivalent state by silver peroxide.[2] After the decomposition of excess of the oxidizing agent by dipping the volumetric flask in boiling water for 2 or 3 minutes, the solution is cooled to room temperature by tap water. Distilled water is added to the mark and 2 ml. of 0.2% of diphenylcarbazide solution (acetone 1 : water 1) are added. The optical density of the solution is then measured by the spectrophotometer at the wave length of 540 mμ.

One ml. of 30% hydrogen peroxide solution and the excess of ammonium hydroxide are added to the jointed filtrates containing iron and manganese.[3] The solution is warmed to about 80°C.

Ferric hydroxide together with all of the manganese is filtered and dissolved with 10 ml. of hot sulfuric acid (1 : 40) containing a small amount of hydrogen peroxide. The solution is boiled to destroy hydrogen peroxide. Then it is transferred into a 25 ml. volumetric flask and manganese is oxidized to permanganate by silver peroxide.[3,4] After the excess of the oxidizing agent is decomposed by the same procedure as before, the volumetric flask is filled with distilled water to the mark and the optical density is measured at the wave length of 535 mμ.

If any chloride is present, the solution becomes turbid; an addition of mercuric sulfate[5] solution, however, is successfully employed to mask the silver chloride formation.

Results are shown in Table I.

TABLE I

SEPARATION OF Cr FROM Mn WHEN PRESENT TOGETHER

No. of experiment	Cr taken μg.	Cr found μg.	Mn taken μg.	Mn found μg.
1	0.0	0.0	44	41
2	4.0	4.0	88	88
3	8.0	8.2	0	0
4	8.0	8.3	22	23
5	8.0	8.2	22	22
6	16.0	16.4	66	68
7	100.	97.0	220	222
8	200.	196.	220	216

As shown in this table, 0—200 μg. of chromium and manganese can be separated and determined.

Coprecipitation of Cr and Mn with Ferric Hydroxide

One litre of water containing 10 mg. of ferric ion and various amounts of chromium and manganese are neutralized with excess of ammonium hydroxide at 30 to 40°C. The precipitate of ferric hydroxide with chromium and manganese is filtered and dissolved with 10 ml. of hot sulfuric acid (1 : 20) and determination of both elements is carried out by the same procedure as in section II. Table II shows the results.

TABLE II

COPRECIPITATION OF Cr AND Mn WITH FERRIC HYDROXIDE

No. of experiment	Cr taken μg.	Cr found μg.	error μg.	Mn taken μg.	Mn found μg.	error μg.
9	4.0	3.9	0.1	22	23	1
10	16.0	15.8	0.2	44	45	1
11	20.0	19.1	0.9	88	85	3
12	100.	97.0	3.0	110	112	2

We can thus determine manganese and chromium with the mean probable error of 2.5% and 2.4% respectively. Results for chromium appear to be slightly low. The use of an empirical curve is therefore recommended for the estimation of chromium.

When this method is applied to nearly saturated sodium chloride solution (purified electrolyte), particular attention should be taken to remove chloride ion by repeated precipitation of ferric and aluminum hydroxide. As shown in Table III, no trace of

2) M. Tanaka, This Bulletin, **23**, 165 (1950). The interference of few mg. of iron can be avoided by phosphoric acid or fluoride.

3) M. Tanaka, *J. Chem. Soc. Japan, Pure Chem, Sect*, **72**, 129 (1950).

4) Y. Murakami, This Bulletin, **22**, 159 (1949); K. Kimura and Y. Murakami, *Mikrochemie*, **36**, 727 (1950).

5) M. Tanaka, *J. Chem. Soc. Japan. Pure Chem. Sect.*, **72** 136 (1950).

manganese or chromium was found in this sample, and the added amounts of these elements were almost quantitatively recovered.

TABLE III

ANALYSIS OF 500 ml. SAMPLE SOLUTION

No. of experiment	Cr added μg.	Cr found μg.	Mn added μg.	Mn found μg.
13	0.0	0.0	0	0
14	8.0	7.8	44	46
15	20.0	19.3	88	87
16	100.	96.0	110	102

Behavioar of Sexivalent Chromium

A sample solution after electrolysis by the mercury cell process contains some free chlorine, so chromium may exist as sexivalent. The brine sample after electrolysis is analysed by the above mentioned procedure; after removal of trivalent chromium and manganese ions by ferric hydroxide, the filtrate is acidified with sulfuric acid and warmed after addition of some sodium sulfite (2–3 g.) for the reduction of chromate to chromic state. Ten mg. of aluminum, collector of chromium, are added to the solution which is subsequently neutralized with excess of ammonium hydroxide. After filtration of aluminum hydroxide, chromium in the hydroxide is determined as is in the case of trivalent chromium. Results are shown in Table IV.

TABLE IV

ANALYSIS OF BRINE CONTAINING FREE CHLORINE

No. of experiment.	Cr III added μg.	Cr III found μg.	Cr IV added μg.	Cr VI found μg.	Mn added μg.	Mn found μg.
17	0.0	0.8	0.0	1.3	0	12
18	8.0	9.0	11.6	11.6	44	56

From these results, it will be clear that small amounts of chromate scarcely ever associate with ferric hydroxide precipitate in our procedure.

Summary

Chromium and manganese less than 100μg. in 500–1000 ml. of solution are separated from a bulk of the solution by ferric hydroxide precipitation and the separation of chromium from manganese and iron can be carried out by the reduction of ferric iron to ferrous followed by the precipitation of aluminum hydroxide. And each element was determined colorimetrically using the silver peroxide as oxydant. No coprecipitation of chromate could be observed in this procedure.

The writers wish to express their hearty thanks to Professor Ken Sugawara for his stimulating interest as well as constant encouragement in the course of this study.

Department of Applied Chemistry,
Faculty of Engineering,
Nagoya University,
Chikusa-ku, Nagoya

Mikroanalyse mit Hilfe von ionenaustauschenden Harzen. II. Über den Nachweis geringer Menge des Chroms mit Wasserstoffperoxyde

Von Masatoshi FUJIMOTO

(Eingegangen am 10. April, 1954)

Einleitung. Wie in der vorhergehenden Mitteilung[1] genau erwähnt, durch mikroanalytische Anwendung der ionenaustauschenden Harze wurde eine neue und verbesserte Tüpfelmethode vorgeschlagen. Bei gegenwärtigem Versuche, hat der Verfasser eine graue bzw. violette Färbung, die bei Anwesenheit von Chromat oder Bichromat mit Wasserstoffperoxyd in die hellgelben anionenaustauschenden Harzkörnchen entsteht, auf den Nachweis geringer Menge des Chroms angewendet und befriedigende Ergebnisse erhalten.

1) I. Mitteilung, Dieses Bulletin, **27**, 48 (1954).

Die in dieser Untersuchung benutzten anionenaustauschenden Harze. Zum Vergleich wurden folgende zwei Arten anionenaustauschender Harze verwendet:

Amberlite IRA-400: Ein aus Styrol und Divinylbenzol dargestelltes starkbasisches Harz von quartärem Ammoniumtypus.

Amberlite IRA-411 (oder XE-98): Ein ebenso starkbasisches Harz wie IRA-400 mit kleinerem Divinylbenzolgehalt.

Beide wurden, vor dem Gebrauch, durch zweimaliges Durchlaufen der 2 N Salzsäure und destilliertes Wassers in die RCl-Form übergeführt. Die Korngrösse ist ungefähr 30 Maschen von Tylerschem Normalsieb.

Versuchsanordnung. Auf einer weissen

Tüpfelplatte versetzt man mit einem Tropfen (0.02 ccm mit Kapillarpipette) der Versuchslösung[2] und einigen Harzkörnchen. Nach drei oder fünf Minuten stehen gelassen, fügt man dazu einen Tropfen verdünnter Schwefelsäure (oder Essigsäure[3]) und verdünnter Lösung des Wasserstoffperoxyds hinzu. Je nach der Mange der Chromat- bzw. Bichromationen in der Probelösung, färben sich die Harzkörnchen grau oder veilchenblau bzw. violettbraun, und diese werden in gleicher Weise als die in der vorhergehenden Mitteilung beobachtet.

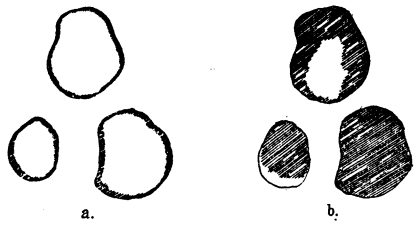


Abb. I. Schematische Darstellung der Färbung der Harzkörnchen
(Cr=2 γ/0.02 ccm als $K_2Cr_2O_7$)
a.=Amberlite IRA-400.
b.=Amberlite IRA-411.

Bestimmung der Bedingungen höchster Empfindlichkeit

1. Massflüssigkeit. Zu diesem Zweck, wurde eine Reihe der Lösungen des Kaliumbichromats (aus heissem Wasser umkristallisiert) dargestellt, deren 1 ccm 10.0 mg, 100-, 10.0-, und 1.00 γ von Chrom enthielten.

Alle folgende Vergleichungen der Bedingungen wurden mit einer Lösung ausgeführt, deren ein Tropfen (0.02 ccm) 2 γ von Chrom enthielt.

2. Einfluss der Harzart. Abb. Ia. und Ib. sind die schematische Darstellung der Färbung an Amberlite IRA-400 bzw. IRA-411. An der IRA-411 wird im Vergleich mit IRA-400 weitgehende Diffusion ins Harzkörnchen der gefärbten Schicht (mit schrägen Linien geschildert) beobachtet, jedoch, waren die Empfindlichkeiten für beide Harze deshalb durchaus dieselbe, weil Verdichtung gefärbter Ionen am Rande der IRA-400 Körnchen diese Differenz vollends kompensierte. Daher wurde bei allen folgenden Versuchen lediglich Amberlite IRA-411 als ein Vertreter angewendet.

3. Einfluss der Konzentration der Schwefelsäure. Azidität des Reaktionsmittels wirkte beträchtlich der Reaktionsempfindlichkeit ein. In Tabelle I wird das Einfluss der Konzentration der Schwefelsäure auf der Färbung dargestellt:

TABELLE I

EINFLUSS DER SCHWEFELSÄUREKONZENTRATION AUF DER FÄRBUNG*

Für 2 γ Cr/0.02 ccm, mit (als $K_2Cr_2O_7$)	0.01 N H_2SO_4	und 10 proz. H_2O_2	nur hell grauisch braun,
	0.1 N H_2SO_4		nur hell grauviolett,
	1 N H_2SO_4		erst deutlich violett,
	10 N H_2SO_4		ebenso deutlich violett.

* Salzsäure trat auch ganz gleichfalls auf.

Von diesem Experiment aus betrachtet, war die Anwendung der ungefähr 1 N Schwefelsäure wünschenswert.

4. Einfluss der Konzentration des Wasserstoffperoxyds. Da scheinlich die konzentrierte Lösung des Wasserstoffperoxyds die Färbung hemmte, wurde eine Reihe der Untersuchungen mit 1 N Schwefelsäure unter verschiedenen Konzentration am Wasserstoffperoxyd folgenderweise ausgeführt. Die Resultate der Experimente stehen in Tabelle II:

TABELLE II

EINFLUSS DER KONZENTRATION DES WASSERSTOFFPEROXYDS

Für 2γ Cr/0.02 ccm, mit 1 N H_2SO_4

		Nach 1,	5,	10,	15, und 25 Min.
und	30 proz. H_2O_2	+ + + +	++++	(+)(+)(+)(+)	(+)(+)(+)(+) — — — —
	10 proz. H_2O_2	+ + + +	++++	+ + + +	+ + + + (+)(+)(+)(+)
	1 proz. H_2O_2	(+)(+)(+)(+)	±++±	± ± ± ±	± ± ± ± ± ± ± ±
	0.1 proz. H_2O_2	— ± ± —	++++	+ + + +	± + + + + + + +

—: nicht erkennbar, ±: unsicher, (+): schwach, +: sicher, ± :etwas stärker, ±: intensiv gefärbt.

2) Nach der Oxydation des Chroms (III) zum Chromate oder Bichromate wird es hergestellt.

3) Die ausgeprägten Einflüsse der Essigsäure auf die scheinbare Deutlichkeit der Färbungen werden an anderer Stelle dieser Mitteilung eingehend erörtert (vgl. s. 350).

In Betracht der Deutlichkeit und der Beständigkeit von der Färbung, sei ein prozentige Lösung des Wasserstoffperoxyds empfehlenswert.

Auf solche Weise, mit Amberlite IRA-411, ein prozentigem Wasserstoffperoxydwasser und 1 N Schwefelsäure wurde folgender Versuch für Erfassungsgrenze durchgeführt.

Bestimmung der Erfassungsgrenze.[4] Die Resultate der Experimente stehen in Tabelle III:

TABELLE III

DIE RESULTATE DER EXPERIMENTE FÜR ERFASSUNGSGRENZE

Zeit nach der Mischung (Min)	Probe	Färbung an zwölf Vertiefungen											
1～ 2	A	−	−	−	−	−	−	−	−	−	−	−	−
	B	±	±	(+)	+	(+)	±	(+)	(+)	(+)	(+)	(+)	(+)
5～ 6	A	−	−	−	±	±	−	±	±	±	−	±	(+)
	B	(+)	(+)	+	+	(+)	(+)	+	+	(+)	(+)	+	+
10～15	A	±	−	±	±	±	±	±	±	±	−	±	±
	B	(+)	+	+	+	(+)	+	+	+	+	+	+	+

A: 0.2 γ Cr (als wässr. Lsg. des $K_2Cr_2O_7$) in 0.02 ccm Probelösung.
B: 0.3 γ Cr (als ,, ,, ,, ,,) in 0.03 ccm Probelösung.
In Bezug auf den Zeichen, −, ±, +, usw., vgl. Tabelle II.

Die Erfassungsgrenze 0.3 γ unter Grenzkonzentration $1:1\times10^5$ für Chrom an dieser Reaktion wurde so festgestellt.

Bestimmung der Erfassungsgrenze für Chrom nach der Oxydation zum Chromate

1. Massflüssigkeit des Chromsalzes wurde aus der in 1 N Schwefelsäure gelösten Lösung des extrareinen Kalichromalauns, deren 1 ccm 0.87±0.003 mg von Chrom enthielt,[5] vorbereitet.

2. Auswahl des Oxydationsmittels. Folgende dreiartige Oxydationsmethoden wurden zu diesem Zweck angewendet, d.h., Oxydation (1) mit wärmer alkalischer Lösung von Wasserstoffperoxyd,[6] (2) mit heissem Bromwasser und (3) mit heisser gesättiger Lösung des Kaliumpermanganats.

Durch Methode (2) war die Oxydation ungeeignet. Methode (1) auch war dann nicht wünschenswert infolge der Niederschlagbildung falls andere Metallionen wie Eisen vorhanden waren, trotz seiner sehr glatten und befriedigenden Oxydationswirkung. Infolgedessen, wurde gegenwärtiger Versuch, mit Hilfe letzter Methode, d.h., durch Kochen der Probelösung mit einem Tropfen gesättiger Lösung des Kaliumpermanganats in einer Mikroeprouvette 1 bzw. 2 Min lang mit einem Mikrobrenner,[7] ausgeführt, dabei überschüssiges Reagens durch Zusatz von Wasserstoffperoxyd glücklicherweise entfärbt wurde.

In gleicher Weise wie die in Tabelle III durchgeführt, war die Erfassungsgrenze für Chromsalze nach der Oxydation zum Chromate 0.3 γ unter Grenzkonzentration $1:6.7\times10^4$.

TABELLE IV

EINFLÜSSE DER BEGLEITSTOFFE

Begleitstoffe	benutzter Verbindungstypus	Menge der Begleitstoffe	Nachweisbare Chrommenge	Grenzverhältnis	Anmerkungen
Fe^{2+} oder Fe^{3+}	$FeSO_4$ oder $FeCl_3$	430 γ	0.25 γ	$1:1.8\times10^3$	——
Ni^{2+}	$NiCl_2$	2.3 mg	0.64 ,,	$1:3.6\times10^3$	——
Co^{2+}	$CoCl_2$	2.7 mg	0.63 ,,	$1:4.4\times10^3$	——
Cu^{2+}	$CuSO_4$	1.4 mg	0.63 ,,	$1:2.2\times10^3$	——
Mn^{2+}	$MnSO_4$	Grosser Überschuss.	0.3 ,,	——	——
UO_2^{2+}	Uranylacetat	910 γ	0.62 ,,	$1:1.5\times10^3$	Neben Blindversuche.
CH_3COOH	Eisessig	Grosser Überschuss.	——	Ziemlich befördert die Färbung.	

4) Hinsichtlich der Bedeutung der Erfassungsgrenze, vgl. Fussnote 1).

5) Die Menge von Chrom wurde folgenderweise bestimmt: Nach der Oxydation mit heisser gesättiger Lösung des Kaliumpermanganats und der (1:1) Schwefelsäure, wurde die Probelösung mit Wasser abgekühlt, filtriert und mit destilliertem Wasser völlig ausgewaschen, wonach die ins Filtrat angesammelte Lösung des Chromats mit bestimmtem Überschusse der 0.1 N Massflüssigkeit des Mohrschen Salzes reduziert wurde, deren Überschuss mit einer Massflüssigkeit des 0.1 N Kaliumpermanganats titriert wurde.

6) Vgl. J. W. Mellor und H. V. Thompson, „A Treatise on Quantitative Inorganic Analysis", 2. Aufl. 1938, s. 533.

7) A. A. Benedetti-Pichler, „Introduction to the Microtechnique of Inorganic Analysis", 1. Aufl. 1942, s. 8.

Einflüsse der Begleitstoffe. Wegen hoher Spezifität der Reaktion konnte man alle Nachweise von Chrom, bei Anwesenheit des grösseren Überschusses von Eisen(II) (III)-, Nickel (II)-, Kobalt(II)-, Kupfer(II)-, Mangan (II)-, Uranyl (II) salze, bzw., Essigsäure, ohne Schwierigkeit durchführen. Die Resultate werden in Tabelle IV kurz gefasst.

Ausgeprägte Beförderung der Färbung mit Essigsäure.[8] Essigsäure befördert so ziemlich die Färbung, dass selbst die mit 1 N Schwefelsäure sich liefernde nur schwach graue Färbung durch ihren Zusatz zur deutlich veilchenblauen Färbung sich verändert. Dabei handelt es sich darum, dass vermutlich eine Art des intensiv gefärbten Chromkomplexsalzes mit Essigsäure sich bildet, jedoch, hier berührt man schlechthin empirischen Ergebnissen. Als Beispiel sei folgende Gegenüberstellung solches Verhältnis klar zu machen:

$$\left.\begin{array}{ll} \text{a)} & RCl \quad +Cr\ 1\gamma^{*} \\ \text{b)} & ROOC\cdot CH_3+Cr\ 1\gamma \\ \text{c)} & ROOC\cdot CH_3+Cr\ 1\gamma \end{array}\right\} \xrightarrow[2\,\text{Min.}]{} +\left\{\begin{array}{l} 1\,\text{N}\ H_2SO_4 \\ 1\,\text{N}\ H_2SO_4 \\ 6\,\text{N}\ CH_3COOH \end{array}\right\} \xrightarrow[1\,\text{Min.}]{} + \text{1proz. } H_2O_2:$$

* als eine Lösung des Kaliumbichromats in der Probelösung vorliegt.

Zum semiquantitativen Vergleich, stellte der Verfasser die scheinbare Intensität der Färbung durch eine Reihe der Zahlen, d. h., −, ±, (+), und +, durch 0, 1, 1.5, bzw. 2, dar. Folgende Abbildung stellt dieses Verhältnis für die an vier Vertiefungen der Tüpfelplatte ausgeführten Reaktionen schematisch dar.

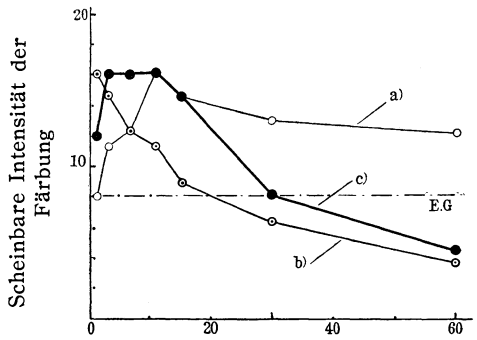


Abb. II. Schematische Darstellung der zeitliche Verwandlung von scheinbarer Intensität der Färbung.

Von dieser Abbildung aus betrachtet, wird es klar, dass, wegen seiner schnellen Entfärbung, Verfahren-b) für empfindlichen Nachweis unbequem ist, und dass c), im Vergleich mit a), dank seiner bis zu 10 Min nach der Mischung entstehenden deutlichsten und zwar beständigsten Färbung, als ein vorzüglichstes Verfahren betrachtet wird, trotzdem nach 10 Min die Färbung etwas schneller als a) verschwindet.

Durch Verwendung der Essigsäure an Stelle der Schwefelsäure wurde der Nachweis geringer Menge des Chromats bemerkenswerterweise deutlich, obgleich diese Erfassungsgrenze mit dem nach Tabelle III erhaltenen Werte identisch war, d. h., 0.3 γ von Chrom unter Grenzkonzentration 1 : 1×10^5.

8) Über diese Wirkung wird der Verfasser später ausführlich diskutieren.

Zusammenfassung

1. Eine empfindliche und sehr spezifische Nachweismethode für Chrom als Chromat mit Wasserstoffperoxyd wird durch einfachste Anwendung von der hellgelben starkbasischen anionenaustauschenden Harze festgestellt. (Vgl. Tabelle II und III).

2. Oxydation des Chroms zum Chromate wird mit heisser gesättiger Lösung des Kaliumpermanganats am günstigsten durchgeführt.

3. Verwendung der Essigsäure an Stelle der Schwefelsäure verbessert bemerkenswerterweise die scheinbare Deutlichkeit des Nachweises, wenn auch die Erfassungsgrenze gar nicht erhöht wird.

Zum Schluss möchte der Verfasser Herrn Prof. Dr. E. Minami für seine freundliche Anregungen über diese Untersuchung seinen herzlichen Dank aussprechen.

Laboratorium der analytischen Chemie,
Chemisches Institut der
wissenschaftlichen Fakultät,
Tokyo Universität, Tokyo

Mechanism of the Formation of Guanidine and its Derivatives by the Fusion of Dicyandiamide with Amine Salt

By Kiichiro SUGINO

(Received April 19, 1954)

This contribution is the abstract of my papers already published in Japanese in the Journal of the Chemical Society of Japan in 1939 and 1944.[1] Some new facts found by the further experiments are added.

I. Mechanism of the Reaction between Dicyandiamide and Ammonium Salt

Dicyandiamide is converted by its reaction with ammonium salt into guanidine salt.

$$C_2H_4N_4+2NH_3\cdot HX=2CH_5N_3\cdot HX$$

This reaction was studied using several ammonium salts in fused state and also in aqueous solution.[2] The difference of the reaction velocity and the yield of guanidine salt due to the difference of ammonium salt was discussed systematically. For each salt, especially the nitrate, the conditions were determined under which the good yield of guanidine salt should be expected. The result was later applied to the commercial preparation of guanidine nitrate by Dr. K. Odo.[3]

The mechanism of this reaction has not yet been clearly explained except that biguanide salt is probably the intermediate product.[4] In order to clarify this mechanism, the following items were studied successively.

a) The condition of the formation of biguanide salt by the fusion of dicyandiamide with ammonium salt.

b) The fusion of biguanide monosalt* with ammonium salt.

c) The thermal decomposition of biguanide monosalt in fused state.

Quantitative determination of the reaction products, the measurement of the heating curve and also the heat of reaction were carried out for each reaction. The main results obtained are summarized as follows.

a) By the fusion of 1 mol. of dicyanidiamide with 2 mol. of ammonium salt, biguanide salt was first formed preceding the guanidine formation. But the former was converted to guanidine salt even at the temperature as low as 120°C according to the reaction (2, 2′) described later. The results are shown in Table I.

TABLE I

Dicyandiamide 4.2 g.
NH_4NO_3 8.0 g.
M. p. of the mixture, 116°C.

Temp. (°C)	Time (hr.)	Biguanide-HNO_3* (g.)	(%)	Guanidine-HNO_3** (g.)	(%)	Insoluble residue of water extraction (g)	Dicyandiamide (unconverted)
120	2	1.79	21.8	—	—	0.01	remains quantitatively
120	3	1.85	22.6	2.25	18.4	0.01	〃 〃
120	4	1.85	22.6	3.26	26.7	0.01	〃 〃

* Determined as nickel-biguanide and reduced to nitrate.

** Determined as picrate and reduced to nitrate.

TABLE II

Biguanide mononitrate 8.2 g.
NH_4NO_3 4.0 g.
M. p. of the mixture, 131°C.

Temp. (°C)	Time (min.)	Guanidine-HNO_3* (g.)	(%)	Insoluble residue of water extraction (g.)	Biguanide
above 180	10	11.7	96	0.02	trace
〃 180	17	10.7	88	0.02	〃

* Determined as picrate and reduced to nitrate.

1) K. Sugino, *J. Chem. Soc. Japan*, **60**, 351, 411 (1939); K. Sugino, M. Yamashita and S. Izumi, **65**, 265, 271 (1944); C.A., **35**. 5097 (1941); 3763 c (1947).

2) K. Sugino, *J. Chem. Soc. Japan*. **60**, 267 (1939).

3) K. Odo, *J. Chem. Soc. Japan* (Industrial Chemistry Section), **52**, 210 (1949).

4) Blair, Braham *J. Am. Chem. Soc.*, **44**, 2342 (1922); Smith, Sabetta, Steibach, *Ind, Eng. Chem.* **23**, 1124 (1931).

* Biguanide dinitrate did not give any guanidine salt by its reaction with ammonium salt. The description of Smith, Sabetta and Steinbach (4) is erroneous.

b) By the fusion of 1 mol. of biguanide monosalt with 1 mol. of ammonium salt, corresponding guanidine salt was obtained in yield as same as that obtained by the reaction between 1 mol. of dicyandiamide and 2 mol. of ammonium salt. The results obtained using nitrate are shown in Table II.*

The phenomenon of the heat evolution due to the guanidine formation was observed in the heating curve of their reactions (Fig. 1).

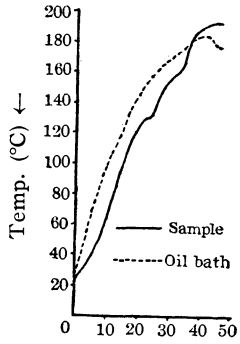


Fig. 1. Biguanide HNO_3 8.2 g. NH_4NO_3. 4.0 g.

But it was not very great compared with the same phenomena found in the heating curve of the reaction between 1 mol. of dicyandiamide and 2 mol. of ammonium salt (Fig. 2). In order to clarify these observations,

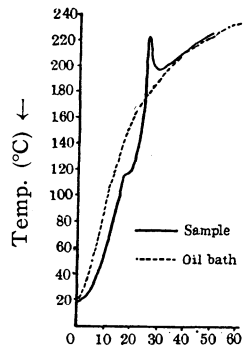


Fig. 2. Dicyandiamide 4.2 g. NH_4NO_3 8.0 g.

the heat of reaction of each reaction must be be determined. For this purpose, the heats of combustion and formation of dicyandiamide and biguanide mononitrate were measured by the usual method (calorimetrical), which were found to be as follows.

Substance	Heat of combustion per g.	Heat of combustion per mol. at constant pressure	Heat of formation per mol. from its elements at constant pressure** (ΔH_f)
Biguanide mononitrate	2274 cal	371.49 Kcal	−90.9 Kcal
Dicyandiamide	3926 cal	329.40 Kcal*	3.76 Kcal

* Later, the heat of combustion of dicyandiamide was measured by Salley and Gray (*J. Am. Chem. Soc.*, **70**, 2650 (1948)), his figure being 331.88 Kcal/mol.

** The heats of formation from the elements, ΔH_f, were calculated using 94.45 and 68.37 Kcal/mol. (18°C) for the heat of formation of gaseous carbon dioxide and of liquid water, respectively.[5] But recently, for these values, 94.05 and 68.32 Kcal/mol. (25°C, 1 atm.) seem to be used commonly.

For the heats of formation of ammonium nitrate and guanidine nitrate, the following data were taken from the literature.

Ammonium nitrate[5] ΔH_f/mol. −87.1 Kcal.,

Guanidine nitrate[6] ΔH_f/mol. −91.8 Kcal.

Then the heats of reaction of following reactions could be calculated which were given as follows.

$$NH_2\cdot C(NH)\cdot NH\cdot CN + NH_4NO_3 = (NH_2\cdot C(NH)\cdot NH\cdot C(NH)\cdot NH_2)HNO_3 + 7.6 \text{ Kcal}$$
$$(NH_2\cdot C(NH)\cdot NH\cdot C(NH)\cdot NH_2)HNO_3 + NH_4NO_3 = 2(NH_2\cdot C(NH)\cdot NH_2)HNO_3 + 5.6 \text{ Kcal}$$
$$NH_2\cdot C(NH)\cdot NH\cdot CN + 2NH_4NO_3 = 2(NH_2\cdot C(NH)\cdot NH_2)HNO_3 + 13.2 \text{ Kcal.}$$

These data seemed to correspond to the heat evolution in two heating curves.

c) The thermal decomposition of biguanide monosalt under fused state was found to give guanidine salt quantitatively as shown in Table III. Melamine was also found in a fair yield in the reaction product.

The most important observation was the existence of regenerated dicyandiamide in the reaction product when biguanide monosalt was cautiously decomposed under fused state at 190–195°C for 2–3 minutes so as to

5) Bichowsky und Rossini, "Thermochemistry of Chemical Substances," (Reinhold Publ. Corp.) 34 (1936).

* The same results were obtained using chloride or sulfate.

6) Calculated by the author from the data of Matignon, *Chem. Centr.*, (1892) II, 199.

TABLE III

Biguanide-mononitrate: 10.00 g. (m.p. 202–3°C).
Conditions: According to Fig. 3.

Guanidine nitrate*		Melamine**		
(g.)	(%)	From solution	From insoluble residue of water extraction (1.67 g.)	(%)
7.31	98.3	0.54	1.05	62
		1.59 g.		
7.20	96.8	—		—

* Determined as picrate and reduced to nitrate.
** The amount of melamine is not quantitative.

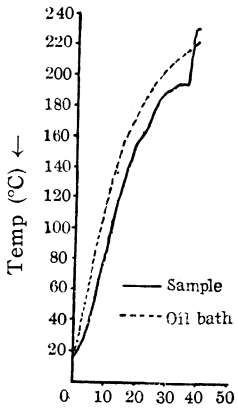


Fig. 3.

prevent spontaneous superheating due to the melamine formation*. For this purpose, about 2.0 g. or less amount of the sample must be used at a time. By extracting the pulverized reaction product by acetone and evaporating the extract to dryness, the crystal of dicyandiamide could be obtained. (From 15,00 g. of the reaction product, about 0.80 g. of dicyandiamide melting at 200°C was isolated. The melting point of the mixture of the sample with pure dicyandiamide was 203–205°C).

Then, the thermal decomposition of biguanide mononitrate may be represented as follows:

$$(NH_2\cdot C(NH)\cdot NH\cdot C(NH)\cdot NH_2)HNO_3 = (NH_2\cdot C(NH)\cdot NH_2)HNO_3 + NH_2\cdot CN$$
$$NH_2\cdot CN = 1/3\, C_3H_6N_6$$
$$(NH_2\cdot C(NH)\cdot NH\cdot C(NH)\cdot NH_2)HNO_3 = (NH_2\cdot C(NH)\cdot NH_2)HNO_3 + \tfrac{1}{2}NH_2C(NH)\cdot NH\cdot CN$$

As the result of these ovservations, the author proposed a mechanism which is summarised as follows.

1) Dicyandiamide is first converted into biguanide monosalt by the addition of 1 mol. of ammonium salt.

$$NH_2\cdot C(NH)\cdot NH\cdot CN + NH_3\cdot HX = (NH_2\cdot C(NH)\cdot NH\cdot C(NH)\cdot NH_2)HX \quad (1)$$

2) Biguanide monosalt is next converted into 1 mol. of guanidine salt and 1 mol. of cyanamide or ½ mol. of dicyandiamide by the thermal decomposition.

$$(NH_2\cdot C(NH)\cdot NH\cdot C(NH)\cdot NH_2)HX = (NH_2\cdot C(NH)\cdot NH_2)HX + NH_2\cdot CN \quad (2)$$
$$(NH_2\cdot C(NH)\cdot NH\cdot C(NH)\cdot NH_2)HX = (NH_2\cdot C(NH)\cdot NH_2)HX + \tfrac{1}{2}NH_2\cdot C(NH)\cdot NH\cdot CN \quad (2')$$

3) The cyanamide or dicyandiamide formed in nascent state, reacts immediately with ammonium salt to give 1 mol. of guanidine salt or 0.5 mol. of biguanide monosalt successively.

$$NH_2\cdot CN + NH_3\cdot HX = (NH_2\cdot C(NH)\cdot NH_2)HX \quad (3)$$
$$\tfrac{1}{2}NH_2\cdot C(NH)\cdot NH\cdot CN + \tfrac{1}{2}NH_3\cdot HX = \tfrac{1}{2}(NH_2\cdot C(NH)\cdot NH\cdot C(NH)\cdot NH_2)HX \quad (3')$$

The biguanide monosalt formed according to the reaction (3′) is again decomposed to guanidine salt and dicyandiamide (2′). The reaction (2) and (3) may take place at higher temperatures (at least above 160°C), whereas the reaction (2′) and (3′) at lower temperatures.

II. Mechanism of the Reaction between Dicyandiamide and Aniline Hydrochloride

The mechanism of the reactian between dicyandiamide and aniline hydrochloride was studied in order to generalise the mechanism of guanidine formation by the reaction between dicyandiamide and ammonium salt.

In this case, it was well known that the phenylbiguanide-HCl (the primary reaction product) was formed quantitatively.[7] Then,

* The heats of reaction of (2), (2′) are endothermic.

7) Lumière and Perrin, *Bull. soc. chim.*, [3] **33**, 205 (1905). Sugino et al, *Japanese Patent* 125272.

TABLE IV

Phenylbiguanide-HCl 15.00 g. (molar ratio 1)

Conditions* (A) 230°C. 2 min.
(B) 230°C. 2 min. after the heat evolution.
(C) 220–230°C. 2 min.

Reaction \ Product	Monophenyl-guanidine***		Guanidine***		Diphenyl-guanidine		Inosoluble residue of Boiling water extraction (melamine derivatives)	Others
	Yield** (g.)	Molar ratio	Yield** (g.)	Moler ratio	Yield** (g.)	Molar ratio	Yield** (g.)	Yield** (g.)
(A) Thermal decomposition of phenylbiguanide-HCl	2.70 2.81	0.29 0.30	1.26 0.96	0.30 0.23	—	—	3.38 3.40	— 2.87
(B) Reaction with ammonium chloride (3.78 g.)	4.68	0.49	1.88	0.45	—	—	1.66	1.57
(C) Reaction with aniline-HCl (9.12 g.)	4.72	0.50	0.67	0.16	5.55	0.37	3.22	2.40

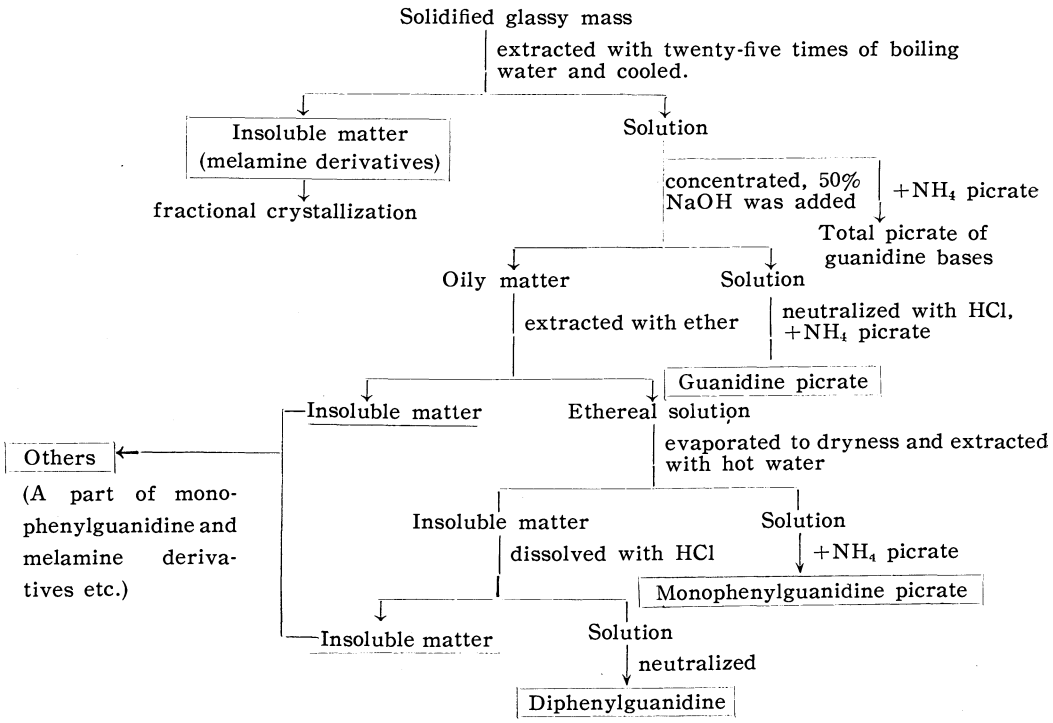
* The mixture melted at (A) 237°C., (B) 230°C. and (C) 185°C. respectively and a small heat evolution occurred spontaneously at about 230°C. By maintaining the mixture at that temperature for 2–3 minutes after the heat evolution, no phenylbiguanide was already present in the fused mass.

** Due to the difficulty of the perfect separation of each product, the yield did not mean the total amount of each product and a part of them may be included in "others". But these data may seem to be useful to compare the amount of each reaction product between three reactions.

*** Determined as picrate and reduced to free base.

TABLE V

SCHEMES OF THE METHOD OF THE SEPARATION OF EACH REACTION PRODUCT



in fused state, the thermal decomposition of phenylbiguanide-HCl and the reaction between phenylbiguanide-HCl and aniline-HCl or ammonium chloride were studied successively.

An example of the quantitative separation of the products of three reactions is shown in Table IV and the method of the separation of each reaction product is also schematically shown in Table V.

It was first observed that the thermal decomposition of phenylbiguanide-HCl in fused state gave not only phenylguanidine-HCl, but also guanidine-HCl. This reaction may be represented as follows by referring the mechanism of the thermal decomposition of biguanide monosalt.

$$(C_6H_5NH\cdot C(NH)\cdot NH\cdot C(NH)\cdot NH_2)HX \longrightarrow \begin{cases} (C_6H_5NH\cdot C(NH)\cdot NH_2)HX + NH_2\cdot CN \\ (NH_2\cdot C(NH)\cdot NH_2)HX + C_6H_5NH\cdot CN \end{cases}$$

If an amine salt should be existed in the reaction mixture, the cyanamides formed would react immediately to give corresponding guanidine salts. So, by the use of ammonium salt, the salt of phenylguanidine and guanidine may be formed.

$$NH_2\cdot CN + NH_3\cdot HX \rightarrow (NH_2\cdot C(NH)\cdot NH_2)HX$$
$$C_6H_5NH\cdot CN + NH_3\cdot HX \rightarrow (C_6H_5NH\cdot C(NH)\cdot NH_2)HX$$

Also by the use of aniline HCl, the formation of the salt of phenylguanidine and diphenylguanidine may be expected.

$$NH_2\cdot CN + C_6H_5NH_2\cdot HX \rightarrow (C_6H_5NH\cdot C(NH)\cdot NH_2)HX$$
$$C_6H_5NH\cdot CN + C_6H_5NH_2\cdot HX \rightarrow (C_6H_5NH\cdot C(NH)\cdot NHC_6H_5)HX$$

The latter two reactions were verified by the experiment. By the fusion of cyanamide (1 mol.) or phenylcyanamide (1 mol.) with aniline HCl (1 mol.), the salt of phenylguanidine or diphenylguanidine was obtained in yield as high as 96% and 92% respectively.

As the result of these successive reactions, a rough estimate of the ratio of the amount of phenylguanidine, guanidine and diphenylguanidine formed by the following reactions may be as follows.

(A) Thermal decomposition of phenylbiguanide-HCl.

(B) The reaction of phenylbiguanide-HCl with ammonium chloride.

(C) The reaction of phenylbiguanide-HCl with aniline HCl.

	Monophenylguanidine	Guanidine	Diphenylguanidine
(A)	1	1	0
(B)	2	2	0
(C)	2	1	1

The results shown in Table IV were in good agreement with this conclusion. But in the reaction (C), the amount of diphenylguanidine seemed to be somewhat larger than that of the other two guanidines. By referring the result of methylbiguanide described later, it is generally noticed that the proportion of different kinds of guanidines formed in these reactions may depend upon the substituent of biguanide as later indicated by Oxley and Short.[8]

If the sufficient amount of amine salt should not exist in the thermal decomposition of phenylbiguanide-HCl, the cyanamides formed might react together and form a mixture of melamine derivatives. Throughout the above three reactions, some amount of melamine derivatives could always be found in the reaction product as shown in Table IV. Melamine derivatives from the reaction (A) and reaction (B) were found to consist mainly of the same compound which was identified as 2.4-dianilino-6-amino-s-triazine (diphenylmelamine). This compound could be synthetized by the mutual reaction of phenylcyanamide and cyanamide.

2.4-dianilino-6-amino-s-triazine.

From the reaction A.

M.p. 201–205°C., m.p. of picrate: 272°C.

Found: C, 64.72, 64.78, H, 5.93, 5.54, N, 30.22

From the reaction B.

M.p. 208–210°C., m.p. of picrate: 272°C.

Found: C, 64.71, 64.76, H, 5.23, 5.58, N, 31.27

From the mutua! reaction of phenylcyanamide and cyanamide.

M.p. 197–202°C., m.p. of picrate: 272°C.

Found: C, 64.75, 64.75, H, 5.50, 5.38, N, 29.69

Calc. for $C_{15}H_{14}N_6$: C, 64.74, H, 5.05, N, 30.21

By summarizing these observations, the author determined the mechanism of the reaction between dicyandiamide and aniline-HCl which are now believed to be as follows.

$$NH_2\cdot C(NH)\cdot NH\cdot CN + C_6H_5NH_2\cdot HX = (C_6H_5NH\cdot C(NH)\cdot NH\cdot C(NH)\cdot NH_2)HX \quad (1)$$

$$(C_6H_5NH\cdot C(NH)\cdot NH\cdot C(NH)\cdot NH_2)HX \longrightarrow \begin{cases} (C_6H_5NH\cdot C(NH)\cdot NH_2)HX + NH_2\cdot CN & (2) \\ (NH_2\cdot C(NH)\cdot NH_2)HX + C_6H_5NH\cdot CN & (2') \end{cases}$$

$$NH_2\cdot CN + C_6H_5NH_2\cdot HX = (C_6H_5NH\cdot C(NH)\cdot NH_2)HX \quad (3)$$
$$(NH_2\cdot CN + NH_3\cdot HX = (NH_2\cdot C(NH)\cdot NH_2)HX)$$

$$C_6H_5NH\cdot CN + C_6H_5NH_2\cdot HX = (C_6H_5NH\cdot C(NH)\cdot NHC_6H_5)HX \quad (3')$$
$$(C_6H_5NH\cdot CN + NH_3\cdot HX = (C_6H_5NH\cdot C(NH)\cdot NH_2)HX)$$

8) Oxley and Short, *J. Chem. Soc.*, **1951**, 1252.

$$2C_6H_5NH\cdot CN + NH_2\cdot CN \rightarrow H_2N-C_3N_3(NHC_6H_5)_2 \quad (4)$$

In the case of phenylbiguanide salt (a unsymmetrical biguanide), two reactions take place in the thermal decomposition. It is converted to (a) phenylguanidine salt and cyanamide and (b) guanidine salt and phenylcyanamide (2), (2'). The cyanamides formed in nascent state react immediately with amine salts and the corresponding salts of guanidines are formed (3), (3'). Some of the cyanamides react together and the phenyl derivatives of melamine (for example: 2.4-dianilino-6-amino-s-triazine (diphenylmelamine)) are obtained as byproducts (4).

III. Mechanism of the Reaction between Dicyandiamide and Methylamine Hydrochloride

The mechanism of the reaction between dicyandiamide and methylamine-HCl was also studied and was found to be almost the same as the case of aniline-HCl. For this purpose, a quantitative study of the following reactions was carried out just the same as in the case of the reaction between dicyandiamide and aniline-HCl.

1. The preparation of pure methylbiguanide-HCl.
2. The thermal decomposition of methylbiguanide-HCl.
3. The reaction between 1 mol. of methylbiguanide-HCl and 1 mol. of ammonium chloride.
4. The reaction between 1 mol. of methylbiguanide-HCl and 1 mol. of methylamine-HCl.
5. The reaction between 1 mol. of dicyandiamide and 2 mol. of methylamine-HCl.

The results obtained are summarized in Table VI.

TABLE VI

Methylbiguanide-HCl: 7.58 g. (molar ratio 1)

Conditions:* Temp. 190°C., Time 2 hrs.

Reaction \ Product	Methylguanidine picrate		Guanidine picrate		Dimethylguanidine picrate	Insoluble residue of water extraction (100 cc.)	Picrate of melamines**
	Yield (g.)	Molar ratio	Yield (g.)	Molar ratio	Yield (g.)	Yield (g.)	Yield (g.)
(A) Thermal decomposition of methylbiguanide-HCl	7.47	0.49	5.46	0.38	—	0.24	0.84
(B) Reaction with ammonium chloride, 2.68 g. (Molar ratio 1:1)	13.09	0.87	12.18	0.85	—	trace	
(C) Reaction with methylamine-HCl, 3.38 g. (Molar ratio 1:1)	15.89	1.05	5.51	0.38	undetermined	nearly zero	
(D) Reaction of dicyandiamide (4.20 g.) with methylamine-HCl, 6.75 g. (Molar ratio 1:2)	17.87	1.18	3.55	0.25	undetermined	trace	

* After two hours and at that temperature, no methylbiguanide was present in the fused mass.

** M.p. 282°C.

The preparation of methylbiguanide-HCl was carried out as follows.

Dicyandiamide (1 mol.) + Methylamine-HCl (1 mol.) —fused at 120-130°C, for 1 hr.→ —dissolved in hot water— < Insoluble matter / Filtrate — $CuCl_2$ (or CuCl) NH_3 soln. was added— < Filtrate / Pink colored precipitate —dissolved in HCl soln. / treated with H_2S→ CuS / Filtrate —evaporated→ Crude Methylbiguanide-2HCl —recrystallization from 80-90% alcohol→ Pure Methylbiguanide-2HCl —dissolved in water and neutralized with equiv. amount of NaOH→ NaCl / Methylbiguanide-HCl —extracted with abs. alcohol→ Pure Methylbiguanide-HCl.

The separation of methylguanidine and guanidine from the reaction mixture could be performed successfully by using the difference of the order of precipitation of those picrates. By adding a saturated solution of ammonium picrate in the reaction mixture, guanidine picrate was first precipitated and when the precipitation of guanidine picrate was almost completed, methylguanidine picrate began to precipitate. So, by carrying out the precipitation cautiously and also recrystallizing, those two picrates could be separated almost completely.

The results seemed to be very similar to that of the reaction of phenylbiguanide-HCl. First, methylbiguanide-HCl also yielded both the salt of methylguanidine and guanidine by the thermal decomposition in fused state just the same as in the case of phenylbiguanide-HCl. Cyanamide and methylcyanamide which were supposed to form at the same time reacted together to give melamine derivatives. By the presence of a suitable amount of an amine salt in the reaction mixture, these cyanamides, if they existed, must be converted to corresponding guanidines. In the case of NH_4Cl, therefore, guanidine and methylguanidine may be obtained and in the case of methylamine-HCl, methylguanidine and sym-dimethylguanidine may also be expected to form. So, similar to the case of phenylbiguanide, a rough estimate of the ratio of the amount of methylguanidine and guanidine formed by the following reactions may be expected as follows:—

(A) The thermal decomposition of methylbiguanide-HCl.
(B) The reaction between methylbiguanide HCl and ammonium chloride.
(C) The reaction between methylbiguanide HCl and methylamine-HCl.

	Methylguanidine	Guanidine
(A)	1	1
(B)	2	2
(C)	2	1

The results shown in Table VI were in good agreement with this assumption. The result of the reaction between 1 mol. of dicyandiamide and 2 mol. of methylamine HCl (D) was found to be almost the same as that of the reaction (C), but the amount of methylguanidine was somewhat larger than in the latter case.

About sym-dimethylguanidine, its confirmation was not carried out in the above experiment. But now, Mr. R. Kitawaki of my laboratory, has again been studying the same reaction in order to confirm this compound in the reaction product. He succeeded in isolating about 9.0 g. of N, N'-dimethylguanidine picrate from the reaction product obtained by the fusion of 21.0 g. of Dicyandiamide with 33.8 g. of methylamine-HCl at 190°C for 1 hr*.

M. p. 159–160°C.

After recrystallization: m. p. 172–4°C.

m. p. of N, N'-dimethylguanidine-HCl derived from the purified picrate: 151–2°C.

m. p. of the mixture of these samples with the same salts of N, N'-dimethylguanidine prepared by the reaction of methylamine with iodocyan or of monomethylcyanamide with methylamine. HCl.*

	Known sample	Mixture
picrate	177°C	175°C
hydrochloride	154°C	153–4°C

As the result of these observations, the mechanism of this reaction could also be formulated as follows.

$$NH_2\cdot C(NH)\cdot NH\cdot CN + CH_3NH_2\cdot HX = (CH_3NH\cdot C(NH)\cdot NH\cdot C(NH)\cdot NH_2)HX \quad (1)$$

$$(CH_3NH\cdot C(NH)\cdot NH\cdot C(NH)\cdot NH_2)HX \rightarrow \begin{cases} (CH_3NH\cdot C(NH)\cdot NH_2)HX + NH_2\cdot CN & (2) \\ (NH_2\cdot C(NH)\cdot NH_2)HX + CH_3NH\cdot CN & (2') \end{cases}$$

$$NH_2CN + CH_3NH_2\cdot HX = (CH_3NH\cdot C(NH)\cdot NH_2)HX \quad (3)$$

$$(NH_2CN + NH_3\cdot HX = (NH_2\cdot C(NH)\cdot NH_2)HX)$$

$$CH_3NH\cdot CN + CH_3NH_2\cdot HX = (CH_3NH\cdot C(NH)\cdot NHCH_3)HX \quad (3')$$

$$(CH_3NH\cdot CN + NH_3\cdot HX = (CH_3NH\cdot C(NH)\cdot NH_2)HX)$$

Mutual reaction of cyanamides $\rightarrow$ Melamine derivatives (4)

In this case, the thermal decomposition of methylbiguanide hydrochloride takes place mainly to the side of methylguanidine formation (2), (This may be the influence of CH_3-group discribed above.) therefore the reaction product consisting of mainly methylguanidine-HCl and the amount of guanidine-HCl seemed to be relatively small. Also, a small amount of N, N'-dimethylguanidine was successifully found in it.

In 1922 Werner[9] also had carried out the reaction between dicyandiamide and methylamine-HCl. He supposed that methylguanidine was only the reaction product according to his supposed mechanism.

$$C_2H_4N_4 \rightleftarrows 2NH_2CN$$

$$2NH_2CN + 2CH_3NH_2\cdot HX = 2(CH_3NH\cdot C(NH)\cdot NH_2)HX$$

$$C_2H_4N_4 + 2CH_3NH_2\cdot HX = 2(CH_3NH\cdot (NH)\cdot NH_2)HX$$

* Unpublished papers of R. Kitawaki,

9) Werner, *J. Chem. Soc.*, **121**, 1790 (1922).

He obtained a picrate which melted at 285°C. and supposed it to be methylguanidine picrate. But the melting point of methylguanidine picrate is about 200°C according to many other researches.[10] This erroneous observation induced the following two erroneous explanations of other investigators. Schenck[11] supposed the picrate obtained by Werner to be ethylenediguanidine picrate and also Kapeller[12] supposed the same picrate to be a mixture of dicyandiamide and picric acid. These observations, of course, were also erroneous. This question continued to be unsolved till 1943, when the author has again studied this reaction.

The author also obtained a picrate melted at 285°C in the reaction product of this reaction. According to the author's mechanism, it was obviously certain that this picrate was a mixture of a large amount of guanidine picrate and a small amount of methylguanidine picrate. It was first formed by adding the picrate solution in the solution of reaction product due to the difference of precipitation velocity of two picrates.

In conclusion, the author wishes to express his thanks to Mr. M. Yamashita for his valuable collaboration in the part III of this research.

Laboratory of Organic Electrochemistry,
Department of Chemical Engineering,
Tokyo Institute of Technology,
Ookayama, Tokyo

10) Phillips, Clarke, *J. Am. Chem. Soc.*, **45**, 1756 (1923).
11) Schenck, *Z. physiol. Chem.*, **155**, 306 (1926).
12) Kapeller, *Ber.*, **59**, 1652 (1926).

Electrolytic Reduction of Dicyandiamide

By Kiichiro SUGINO

(Received April 19, 1954)

This contribution is the abstract of my paper[1] already published in Japanese in the Journal of the Chemical Society of Japan in 1939. Some new and revised explanations are added.

For the structure of dicyandiamide, Bamberger[2] proposed cyanoguanidine formula ($NH_2 \cdot C(NH) \cdot NH \cdot CN$) and with this, he could explain very smoothly the formation of guanidine and methylamine from dicyandiamide by the reduction with Zn and HCl (1893). Bell[3] (1926) however, repeated this experiment and he found that by hydration preceding the reduction (even in cold solution), guanylurea was formed instead and consequently he was led to adopt the original cyclic formula for dicyandiamide. So, it seemed to me that there were many problems regarding the reduction of dicyandiamide. For these reasons, an investigation was made to answer the following two questions.

1. Does dicyandiamide reduce directly ?
2. What kinds of products are given by the reduction ?

As the result of many experiments, it was found that dicyandiamide could be reduced directly only by the electrolytic reduction under special conditions (1% aq. solution of dicyandiamide acidified with H_2SO_4 amounting to 1%).

I. The case in which the electrolysis was stopped so as to let the catholyte remain acidic.

The conditions and the results obtained are shown in Table I.

A new compound (a base) was found to be formed by the following reduction.

$$C_2H_4N_4 + 4H \rightarrow C_2H_8N_4$$

This new compound seemed to be very unstable and could exist only in an acidic medium at room temperature. So, when the electrolysis was stopped so as to let the catholyte still remain acidic and a saturated solution of picric acid was added to the catholyte, the new compound could be precipitated as dipicrate.

Color: Light yellow (plate or needle)

m.p.: It has not the accurate melting point. It began to sinter at 180–200°C and decomposed at 220–230°C.

Found: C, 30.74, 30.62; H, 2.87, 2.70; N, 25.61, 25.62, 25.65.

Calc. for $C_{14}H_{14}N_{10}O_{14}$: C, 30.77, H, 2.56, N, 25.64%.

It was also observed that the dipicrate was easily hydrolysed to give guanidine picrate,

1) K. Sugino, *J. Chem. Soc. Japan*, **60**, 111, (1939); *C.A.*, **34**, 2795 (1940).
2) Bamberger. *Ber.*, **26**, 1584, 1585 (1893).
3) Bell, *Sci. Proc. Roy. Dublin Soc.*, **18**, 207~10 (1926); *C.A.*, **21**, 2444 (1927).

TABLE I

Catholyte			Electrode		Cathodic current density	Time	Temp.	Quantity of electricity consumed*	*p*H of catholyte after electrolysis	Reaction Product			
Dicyandiamide (g.)	H_2O (cc.)	Conc. of H_2SO_4 (%)	Cathode	Anode	(A/dm²)	(hr.)	(°C)	(Ahr.)		(1) Picrate of intermediate product weighed (g.)	(2)** Guanidine picrate obtained by the hydrolysis of catholyte (g.)	(3)** Picrate of intermediate product calculated from (2) (g.)	Yield of intermediate product (Aminomethylene guanidine) (%)
1.00	100	1	Hg	Pt	0.8–1.0	2.3	20–24	1.103	acidic	1.91	—	—	—
1.00	100	1	Hg	Pt	1.0	2.0	26	1.031	acidic	1.72	1.01	1.91	29
1.00	100	1	Pb	Pb	1.0	2.5	23	1.010	acidic	2.80	1.61	3.05	47
1.00	100	1	Pb	Pb	1.0	2.5	23	0.982	acidic	2.77	1.62	3.07	47

* Theoretical value for intermediate product. 1.243.
** (2), (3): Quantitative determination of the new compound. It was carried out as follows:
This compound was converted to guanidine by the hydrolysis according to the reaction (2) in the catholyte and resulting guanidine was weighed as picrate, by which the amount of picrate of original intermediate compound was calculated.

TABLE II

Catholyte			Electrode		Cathodic current density	Time	Temp.	Quantity of electricity consumed	*p*H of catholyte after electrolysis	Reaction Product			
										Guanidine picrate*		Amine-HCl** (mainly ammonium chloride)	
Dicyandiamide (g.)	H_2O (cc.)	Concentration of H_2SO_4 (%)	Cathode	Anode	(A/dm²)	(hr.)	(°C)	(Ahr.)		(g.)	(g.)	(g.)	(%)
1.01	100	1	Hg	Pt	1.0–0.46	—	20–23	2.66	alkali	1.56	46	Undetermined	—
1.00	100	1	Hg	Pt	1.0	7.6	20–23	3.76	alkali	1.31	38	0.40	62
1.01	100	1	Pb	Pb	1.0	6.3	20–23	2.96	alkali	0.89	26	0.88	138

* m.p. 320°C.
Found: N, 29.28.
Calc. for $C_7H_8N_6O_7$: N, 29.16%.
** m.p. above 250°C.
The existence of methylamine was verified by its characteristic odour and also the positive result for chloranil test.

ammonium picrate and formaldehyde almost quantitatively when its aqueous solution was boiled or made alkaline at room temperature.

Guanidine picrate: Yield: 94–120% of the theoretical value* m.p.: 320°C Found: C, 29.50; H, 2.77; N, 29.37 Calc. for $C_7H_8N_6O_7$: C, 29.17; H, 2.80; N, 29.16%.

Ammonium picrate: Long needle, m.p. 280°C (decomp.), Ammonia was evolved quantitatively by heating its aqueous solution with caustic alkali.

Formaldehyde: Yield, 93% of the theoretical value* (determined by the iodometric titration)

The compound itself, in the catholyte, was also found to be hydrolysed to give the same products when the catholyte was treated in the same manner as described above. From these observations, it was concluded that this compound has the constitution of amino-methylene guanidine.

$$NH_2 \cdot C(NH) \cdot NH \cdot CH_2 \cdot NH_2$$

The hydrolysis of the compound (and its dipicrate) may be represented by the following reaction.

$$NH_2 \cdot C(NH) \cdot NH \cdot CH_2 \cdot NH_2 + H_2O = NH_2 \cdot C(NH) \cdot NH_2 + NH_3 + CH_2O \quad \cdots\cdots(2)$$

$$C_2H_8N_4 \cdot 2C_6H_2(NO_2)_3OH + H_2O = CH_5N_3 \cdot C_6H_2(NO_2)_3OH + NH_3 \cdot C_6H_2(NO_2)_3OH + CH_2O \quad \cdots\cdots(2')$$

II. The case in which the electrolysis was continued till the catholyte became alkaline.

When the electrolysis was continued till the catholyte became alkaline, reaction (2) occurred spontaneously and guanidine, ammonia and formaldehyde were obtained as the final products. But a small part of $C_2H_8N_4$ was reduced to guanidine and methylamine.

$$C_2H_8N_4 + 2H = NH_2 \cdot C(NH) \cdot NH_2 + CH_3 \cdot NH_2 \quad \cdots\cdots(3)$$

An example of the results is shown in Table II.

In the high acid concentration of the catholyte, dicyandiamide was first hydrated to guanylurea, which was hardly further reduced in the acidic medium.

From the results of the author, he is induced to think that Bell's conclusion is erroneous and he agrees with Bamberger's one that dicyandiamide is directly reduced. But the author's final reduction products were entirely different from Bamberger's one. And the author's results showed that dicyandiamide should have both guanidine group and N-CN linkage, the latter of which behaves somewhat differently from usual nitrile. By referring the result of Hughe's X-ray analysis later published[4] (1940), the structure of dicyandiamide may be represented as guanylcyanamide rather than cyanoguanidine.

Laboratory of Organic Electrochemistry,
Department of Chemical Engineering,
Tokyo Institute of Technology

* Refer to the reaction (2).

4) Hughes, *J. Am. Chem. Soc.*, **62**, 1258 (1940).

Investigation on the Molecular Structure of Monochloroacetamide by Gas Electron Diffraction and Dipole Moment

By Masao KIMURA, Michiro AOKI, and Yukio KURITA

(Received May 6, 1954)

In the previous investigation, the molecular structures of acetamide and N-methylacetamide were determined by electron diffraction[1]. It was pointed out that the bond length of the peptide bond in gaseous acetamide is longer than that in the crystalline proteins determined by Corey et al.[2] and that the difference is due mainly to the hydrogen bond present in a crystal.

The present investigation deals with the structure of monochloroacetamide. Since the molecule has a carbon-carbon bond as a rotational axis, it is of interest to determine the rotational structure and the bond length of a peptide bond.

1) M. Kimura and M. Aoki, This Bulletin, **26**, 429 (1953).
2) R. B. Corey and J. Donohue, *J. Am. Chem. Soc.*, **72**, 2899 (1950).

Experimental Method and Results

[I] Electron Diffraction. — Since monochloroacetamide is in the crystalline state at room temperature, it was vaporized through a high temperature nozzle[1]. The feature, and the positions of the maxima and the minima were estimated by a visual method and are shown in Fig. 2V and in Table I respectively. Here $q=10\,s/\pi$ and $s=4\pi \sin(\theta/2)/\lambda$. Since the observed q values

TABLE I

OBSERVED q VALUES FOR MONOCHLOROACETAMIDE

Max.	Min.	q	Max.	Min.	q
1		10.6	7		42.7
	2	13.7		8	44.7
2		16.6	8		46.6
	3	19.3		9	49.7
3		21.5	9		52.6
	4	24.4	10		58.5
4		27.3	11		63.2
	5	30.0	12		68.2
5		32.5	13		73.8
	6	34.1	14		79.3
6		37.0	15		83.1
	7	39.7	(16)		91.4
			(17)		96.8

were inaccurate for the minima beyond $q=50$, they were omitted from Table I and were not used for the quantitative comparison with the theoretical values. In Fig. 2V, the features of the 16th and 17th maxima are drawn by a dotted line since they are not very accurate and the first maximum was estimated by use of the theoretical intensity curves to be mentioned later.

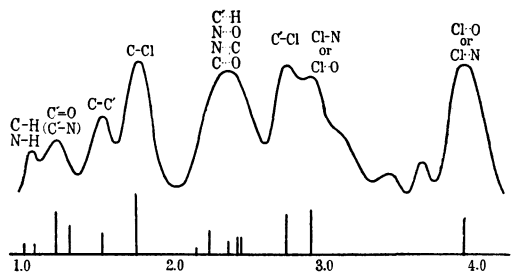


Fig. 1. The radial distribution curve for monochloroacetamide. The vertical bars under the curve show the interatomic distances r_{ij} and $z_i z_j / r_{ij}$ for the structure determined by the present investigation.

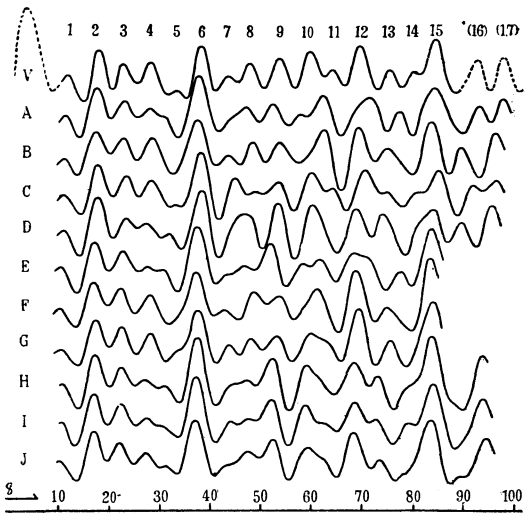
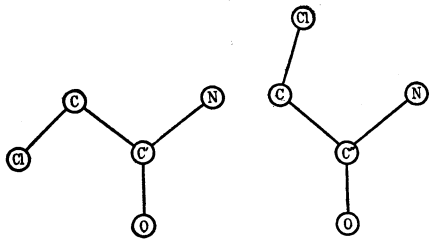


Fig. 2. The visual and theoretical curves for monochloroacetamide.



trans cis

Fig. 3. Monochloroacetamide.

The radial distribution curve,

$$rD(r)=\sum_{q=1}^{\infty} I(q)\exp(-aq^2)\sin(\pi qr/10),$$

calculated by use of the visual curve (Fig. 2V) is shown in Fig. 1, where a was chosen as $\exp(-aq^2_{max})=0.1$. The pair of atoms corresponding to each peak is also indicated in Fig. 1. The peak corresponding to C-Cl bond is very sharp and its bond length was determined to be 1.75 Å. C-C' and C'-Cl interatomic distances could also be determined to be 1.53 Å (the same value as those determined for C-C bond in acetamide, N-methylacetamide[1], glycyl-glycine, etc.[2]) and 2.73 Å respectively, although less accurate than that of a C-Cl bond. The other interatomic distances could not be determined owing to overlapping with the contributions from various interatomic distances (cf. Fig. 3). From the values obtained above, ∠C'CCl can be obtained to be about 113°. The peaks at 2.89 Å and 3.89 Å correspond to Cl···N and Cl···O interatomic distances. From these results alone, we cannot determine the form of the molecule. However, since two peaks are very distinct and are separated from each other by about 1 Å, it is reasonable to consider that the molecule is in the trans or cis configuration, at least approximately.

The theoretical intensity curves were calcutated with the simplified equation,

$$I(q)=\sum_{i\neq j}\sum z_i z_j \exp(-b_{ij}q^2)\sin(\pi r_{ij}q/10)/r_{ij}.$$

Here z_i and z_j are atomic numbers for the ith and jth atoms respectively, and r_{ij} is the interatomic distance between the ith and jth atoms. A factor $\exp(-b_{ij}q^2)$ is related to intramolecular vibrations. The intramolecular vibrations did not affect the features of the theoretical intensity curves, except the rotational vibration about a C-C' bond. Therefore the theoretical curves were mostly calculated for fixed models. When the rotational vibration was taken into account, b_{ij} was taken as 0.0004 for both Cl-O and Cl-N. Some of the intensity curves are reproduced in Fig. 2.

Since there are many parameters involved, we had to be satisfied with an analysis with some assumptions. We used C-Cl=1.75 Å and ∠C'CCl

=113°, which were determined from the radial distribution curve, and also assumed the structure of gaseous acetamide determined by electron diffraction[1] (A form) or the structure of crystalline acetamide suggested by Corey et al. from a probable dimension of polypeptid chain (B form). These assumptions do not contradict with the result obtained from the radial distribution curve and appear to be reasonable since the molecule may be considered to take the structure nearly equal to that of acetamide in the gaseous as well as in the crystalline state (cf. Table II). These assumptions seem to be sufficient at least to estimate the position of C—Cl bond and a probable structure of monochloroacetamide. Thus the only parameter to be adjusted is the rotational angle about a C'—C bond.

TABLE II
THE STRUCTURE OF ACETAMIDE

	A form	B form
Authors	Kimura and Aoki	Corey and Donohue
C=O	1.21	1.23
C−N	1.36	1.32
C−C'	1.53	1.53
State	gas	crystal
method	electron diffraction	X-ray diffraction

In the case of A form, the theoretical intensity curves are shown in Fig. 2 for the models having 180° (the trans configuration, Fig. 2 A), 150° (Fig. 2 B), 30° (Fig. 2 C) and 0° (the cis configuration, Fig. 2D) as rotational angles (cf. Fig. 3). When rotational angles were given values ranging from 60° to 120° the theoretical intensity curves did not agree with the visual one, as expected from the radial distribution curve, and hence are not reproduced in Fig. 2. Curves E, F, G and H are the theoretical curves for the model with B form and the same rotational angle as in curves A, B, C and D respectively. These curves are in agreement to some extent with the visual curve for the maxima in the region $q<37$. But in both A and B form, the theoretical curves (A, B, E and F) for the models having the trans configuration exactly or approximately are not in agreement with the visual one, especially in regard to the 10th and 11th maxima. Moreover in the case of A form the theoretical curve for model C is in fair agreement with the visual one. But the calculated values for the maxima beyond $q=58$ shifted to q values larger than the observed values and the features of the 7th, 8th and 9th maxima were not in agreement with the visual curue. These curves were not in agreement with the visual one, even if we took into account the rotational vibration. In the case of B form, the curves G and H did not agree with the visual one in regard to the 13th and 14th maxima. For the model with the rotational angle of 15° (curve I), however, the theoretical curve was obtained in good agreement with the visual one. When we took into account the rotational vibration for this model, we obtained curve J. In this curve, the features of the 5th maximum, the 7th, 8th and 9th maxima and minima were improved, while the features of the 10th, 11th, 14th and 15th maxima became worse. These results are due entirely to the rather large value of b_{ij}, 0.0004, which was used in the case of taking into account the rotational vibration in N-methylacetamide. Thus the theoretical curve was obtained in good agreement with the visual one by taking into account the rotational vibration with an amplitude smaller than that in N-methylacetamide. The curve is not reproduced in Fig. 2.

Thus the structure of monochloroacetamide was determined as follows: C−Cl=1.75Å, ∠C'CCl =113°, N···Cl=2.89 Å and the twisted angle from the *cis* configuration is about 15°. For the structure of the part corresponding to acetamide the following structure was assumed. : C=O=1.23 Å, C−C=1.53Å, C−N=1.32Å, C−H=1.09Å, N−H= 1.02Å, ∠C'CH=109°28', ∠CC'O=121°, ∠OC'N= 122°, ∠CC'N=117°, ∠C'NH=107°. The interatomic distances r_{ij} and z_{iz_j}/r_{ij} for the structure obtained above are shown in Fig. 1 by means of vertical bars.

[II] Dipole Moment.—The measurement was made in benzene solution at 30°C. The apparatus and the method of measurements have already been reported[3]. The results are shown in Table III.

TABLE III
DIELECTRIC CONSTANT AND DENSITY INCREMENTS OF BENZENE SOLUTIONS AT 30°C
$\epsilon_B=2.2625$, $d_B=0.86629$

$w\times10^5$	$\Delta\epsilon\times10^4$	$\Delta d\times10^5$
30.3	25	—
64.6	60	31
85.5	58	30
88.1	72	—
130.1	76	39

The measurements of dielectric constants of monochloroacetamide could not be made on solutions of concentrations exceeding 0.1 weight percent, because the solubility in benzene is rather small*. Therefore it was difficult to determine the dipole moment of monochloroacetamide very accurately. From the results shown in Table III, the dipole moment of monochloroacetamide can be estimated to be 2.2D∼2.8D. The value thus obtained may be considered to be that in an unassociated state since it was obtained from the measurement on very dilute solutions, although it is known that the molecules of acetamide and its derivatives associate in benzene solutions[4].

The moment of monochloroacetamide was calculated by the use of the valence angles determined by electron diffraction and by assuming the three valence bonds of nitrogen directed in a plane with three valence angles equal to 120°. The bond moments used are:

3) Y. Kurita, T. Nozoe and M. Kubo, This Bulletin, **24**, 10 (1951).

4) W. W. Bates and M. E, Hobbs, *J. Am. Chem. Soc.*, **73**, 2151 (1952); M. E. Hobbs and W. W. Bates, *J. Am. Chem. Soc.*, **74**, 746 (1952).

* The solubility in carbon tetrachloride is smaller than that in benzene.

C—Cl=1.5 D, C—N=0.45 D, C—H=0.4 D, C=O =2.5 D and N—H=1.3 D. The results are 1.4 D, 1.7 D, 2.6 D, 3.5 D and 4.7 D for the configuration with the rotational angles of 0° (the *cis* configuration), 30°, 60°, 90° and 180° respectively. The calculated moment of acetamide is 3.2 D with the assumptions similar to those used for monochloroacetamide. The observed value is 3.44 D[4] in benzene solution. The difference between the calculated and the observed values of acetamide will be due to the values of bond moments used, resonance effect, induction effect and solvent effect. Since monochloroacetamide may be considered to have the same degree of these effects as in acetamide, the calculated value of monochloroacetamide to be compared with the observed one is about 0.2 D larger than those mentioned above. Therefore the configuration of monochloroacetamide may be concluded to take the rotational angle of 60~30° from a comparison of the calculated values with the observed one. Even if the crudeness of the observed and the calculated values is taken into account, the configuration of monochloroacetamide is definitely far from the *trans* configuration*. The discussion on this point will be given later in some detail.

Discussion

According to the results obtained by electron diffraction, C—Cl bond takes the *cis* position to C—N bond. This is due to an electrostatic interaction between C—Cl bond and C=O bond and to a hydrogen bond across Cl···N.

The part corresponding to acetamide does not take the structure of a gaseous acetamide molecule already determined[1], but that similar to a crystalline acetamide with intermolecular hydrogen bonds. This is likely to show a larger contribution of a polar resonance form to the structure of monochloroacetamide than to gaseous acetamide. The effects of an intermolecular hydrogen bond on bond lengths were already pointed out by us in the case of acetamide[1] and hydroquinone[5] by comparing the structure in the crystalline state with that in the gaseous state and by Vaughan and Donohue in carboxylic acids, a peptide and its related compounds from the change of bond lengths owing to the change of the number and the state of hydrogen bonds in crystal[6]. The present investigation shows that an intramolecular hydrogen bond also affects the bond lengths in the molecule.

The result obtained from the measurement of dipole moment is in fairly good agreement with the result obtained by electron diffraction regarding the position of C—Cl bond. As pointed out by Kumler[7], one must take into consideration the state, in which measurements are made, in comparing observed values with calculated ones. So far the effect of a hydrogen bond has not been taken into account by us. But according to the result by electron diffraction, an intramolecular hydrogen bond is present in a gaseous monochloroacetamide molecule. The displacement of charges due to such a hydrogen bond causes mainly the increase of polarity of C=O bond and the shift of a lone pair of an oxygen atom to a hydrogen atom*. As a result, the total moment of monochloroacetamide will increase. Therefore the theoretical moment of monochloroacetamide will possibly be greater than that calculated above. If such is the case, the twisted angle of C—Cl bond from the *cis* configuration becomes smaller and agrees with the result obtained by electron diffraction better than the result mentioned in the experimental part.

Vaughan and Donohue[6] estimated the double bond characters of C=O and C—N bonds to be 70 and 30% respectively in crystalline acetamide, yielding the bond lengths of C=O and C—N equal to 1.23 Å and 1.35 Å respectively**. These values are nearly equal to those obtained in monochloroacetamide. Therefore it is highly probable that an acetamide molecule in crystal has such a structure. Moreover, the contribution of a polar resonance form will probably be smaller in gaseous acetamide than that estimated by Vaughan and Donohue in crystalline acetamide, since the bond lengths are 1.21 Å for C=O and 1.36 Å for C—N in gaseous acetamide.

Summary

1) The structure of monochloroacetamide was determined by gas electron diffraction as follows: C—Cl=1.75 Å, ∠C'CCl=113°, N···Cl=2.89Å, and the twisted angle from the *cis* configuration is about 15°. The structure of the part corresponding to acetamide is nearly equal to that of acetamide with an intermolecular hydrogen bond. This suggests that a monochlorocetamide molecule has an intra molecular hydrogen bond.

* This conclusion is not altered even in the case of the three valence bonds of nitrogen taking a pyramidal form.

5) M. Kimura and S. Shibata, presented at the 4th annual meeting of the Chem. Soc. Japan held on April 7, 1951.

6) P. Vaughan and J. D. Donohue, *Acta Cryst.*, **5**, 530 (1952).

7) W. D. Kumler, *J. Am. Chem. Soc.*, **74**, 261 (1952).

* That the dipole moment of acetamide is 3.90 D in dioxane solution, may be considered to be due to an intermolecular hydrogen bond.

** This values are definitely different from the values obtained by F. Senti and D. Harker. *J. Am. Chem. Soc.*, **62**, 2008 (1940).

2) The dipole moment of monochloroacetamide was estimated to be 2.2 D~2.8 D from the measurement in benzene solution. The observed value was compared with the calculated one. The result agrees with that obtained by electron diffraction in regard to the position of C—Cl bond. The agreement becomes better if the effect of an intramolecular hydrogen bond is taken into account.

We wish to express our thanks to Professors S. Mizushima and Y. Morino of Tokyo University who supplied us with the sample of monochloroacetamide used in this experiment. We wish also to thank Professor M. Kubo of Nagoya University for his helpful advice.

Department of Chemistry, Faculty of Science, Nagoya University, Nagoya

*The Dipole Moments and Molecular Structures of Some Substituted Tropones**

By Yukio KURITA and Masaji KUBO

(Received May 12, 1954)

In our previous paper,[1] we have reported the results of measurements of the dipole moments of tropone and some of its derivatives. The high moment of tropone revealed the importance of contribution to the normal state by the electronic structures of dipolar character and the explanation was made in terms of resonance involving cycloheptatrienium oxide structure.[2] This feature was found to be common to all tropone derivatives including tropolone as well as substituted tropolones, giving rise to the quasi-aromatic properties and other characteristic behaviors of these compounds. The purpose of the present investigation is the elucidation of the effect of various substituents on the electronic state of the tropone ring. We have measured the dipole moments of five tropone derivatives having various substituents at a carbon atom or atoms adjacent to the carbon atom of carbonyl group. All of these substituents are π-electron donors. Some of the substituent groups have an axis of free rotation capable of affecting the value of the resultant moment. The present writers have undertaken to determine the geometrical arrangements of these substituents relative to the tropone ring by means of dipole moment measurements.

Experimental Method and Results

All the measurements were made in benzene solution at room temperature. The dielectric constants were measured with the apparatus described in one[3] of our previous reports. The materials used were synthesized and purified by Nozoe and his collaborators in the laboratory of organic chemistry, Tohoku University. The modified Hedestrand's method[4] was employed throughout. The results are shown in Tables I and II, where the same notations are used as those in the previous reports.

Discussion of Results

The dipole moments of 2-bromotropone, 2,7-dibromotropone and other 2-monosubstituted tropones are summarized in Table III, in which the observed moments are compared with calculated ones. These theoretical moments have been calculated with the following assumptions. (1) The cycloheptatrienone ring has a plane regular heptagon form composed of carbon atoms. Hence the angle between C=O direction and the carbon-substituent bond is equal to 51°26′. (2) The interactions between the tropone ring and the substituent groups have been neglected. In other words, the moment of a substituted tropone has tentatively been assumed to be equal to the vector sum of the moment of tropone, 4.17 D,[1] and the bond moment of the substituent. (3) The bond moments of the substituents in cycloheptatriene are equal to the moments of corresponding substituted benzenes. This assumption may be justifiable since the treatment by molecular orbital

* Read before a symposium on tropolone chemistry held by the Chemical Society of Japan on February 6, 1954.

1) Y. Kurita, S. Seto, T. Nozoe and M. Kubo, This Bulletin, **26**, 272 (1953).

2) W. von E. Doering and F. L. Detert, *J. Am. Chem. Soc.*, **73**, 876 (1951).

3) Y. Kurita, T. Nozoe and M. Kubo, This Bulletin, **24**, 10 (1951).

4) Y. Kurita, T. Nozoe and M. Kubo, This Bulletin, **26**, 242 (1953).

TABLE I

DIELECTRIC CONSTANT AND DENSITY INCREMENTS OF BENZENE SOLUTIONS AT 25°C

	Compounds	m. p.	$w\times10^5$	$\Delta\varepsilon\times10^4$	$\Delta d\times10^5$
I	2-Bromotropone	62°[a]	223	339	98
	at 30°C		483	693	—
			665	946	—
			1341	1919	588
II	2,7-Dibromo-	170[a]—171°	341	422	143
	tropone		558	667	264
			1116	1314	571
			1357	1622	697
III	2-Mercapto-	55°[b]	142	235	49
	tropone		436	675	129
			742	1133	210
			1231	1886	355
IV	2-Aminotropone	104[c]—105.5°	148	194	—
			161	209	57
			185	255	62
			285	366	88
			358	473	107
V	2-Methylmer-	43—44°[b]	221	387	57
	captotropone		536	903	145
			707	1150	199
			714	1160	199

(a) T. Nozoe, S. Seto and S. Matsumura, *Proc. Japan Acad.*, **28,** No, 9, 483 (1952).
(b) T. Nozoe, M. Sato and K. Matsui, *Science Repts. Tohoku Univ.*, I, **37,** 211 (1953).
(c) T. Nozoe, S. Seto, H. Takeda, S. Morosawa and K. Matsumoto, ibid., **36,** 126 (1952).

TABLE II

MOLECULAR POLARIZATIONS AND DIPOLE MOMENTS

	t(°C)	ε_1	d_1(g/cc)	α	β(g/cc)	$P_{2\infty}$(cc)	R_D(cc)	μ(D)
I	30	2.2638	0.86670	14.17	0.438	530.5±3.1	38.7	4.94±0.02
II	25	2.2740	0.87102	11.72	0.546	616.8±5.5	46.5	5.27±0.03
III	25	2.2741	0.87093	15.16	0.280	427.0±0.8	38.7	4.36±0.01
IV	25	2.2729	0.87101	13.00	0.256	326.4±7.3	34.4	3.78±0.05
V	25	2.2772	0.87104	15.66	0.290	483.7±4.1	43.4	4.64±0.02

method,[5,6] the results of ultraviolet absorption spectra,[7] and the studies in organic chemistry[8] have revealed that tropone bears resemblance to benzene in regard to the introduction of substituents in their rings and that the conjugation of the ring with Br, OH, SH, NH_2, etc. in substituted tropones is significant as in the case of substituted benzenes.

In the case of substituents other than bromine, one must take into account free rotation about a single bond between the carbon atom of the ring and oxygen, sulfur or nitrogen atom. In the case of oxygen- or sulfur-containing substituent groups, moments have been calculated for three conceivable configurations, viz., *cis*, *trans* and perpendicular forms. We mean by the *cis* form the configuration in which the hydrogen atom or the methyl carbon atom attached to oxygen or sulfur atom is in the plane of the ring and is near the carbonyl oxygen. The configuration in which the hydrogen atom or the methyl carbon atom is at the greatest distance from the carbonyl oxygen is called the *trans* form. The intermediate position resulting from the rotation of freely rotating atoms or groups about the respective axes of rotation through 90° from either *cis* or *trans* form is termed the perpendicular form. In the case of aminotropone, the configuration in which the two hydrogen atoms in question are equally distant from the carbonyl oxygen and are located at the side of the carbonyl group is designated as the *cis*

5) Y. Kurita and M. Kubo, This Bulletin, **24,** 13 (1951).
6) R. D. Brown, *J. Chem. Soc.*, **1951,** 2670.
7) M. Tsuboi, This Bulletin, **25,** 366 (1952).
8) See papers by T. Nozoe and his collaborators published for the most part in the *Proc. Japan Acad. and Science Repts. Tohoku Univ.* Series I since 1950.

form. The rotation of the hydrogen atoms through 180° and 90° gives *trans* and perpendicular forms respectively in the same manner as before.

For the *cis* and *trans* forms of tropolone, mercaptotropone and their derivatives as well as for the perpendicular form of aminotropone, the lone pair orbitals belonging to the substituent groups overlap with the π-orbital of the ring to the highest extent, favoring the conjugation between the ring and the substituents. On the other hand, the perpendicular forms of tropolone and its analogues as well as the *cis* or *trans* form of aminotropone decrease the conjugation between the ring and the substituent groups. Therefore the moments of the substituents will better be approximated byth ose of alkyl derivatives rather than by those of substituted benzenes. The calculated moments using the former data are given in parentheses in Table III.

TABLE III
DIPOLE MOMENTS OF SUBSTITUTED TROPONES

Substituents	μ_{obs}(D)		μ_{calc}(C)	
Br	4.94		5.3	
Br_2	5.27		6.1	
		cis	Perpendicular	*trans*
OH	3.53[1]	3.1	4.5	5.5
SH	4.36	4.2	4.8	5.4
NH_2	3.78	2.7	3.8	4.7
OCH_3	4.72[1]	3.0	4.1 (4.7)	5.0
SCH_3	4.64	3.6	4.6 (5.0)	5.5
$N(CH_3)_2$	—	2.7 (3.8)	3.6	4.2 (5.0)

In the evaluation of the calculated moments given in Table III, it has been necessary to know the components of the moments of substituents along the direction parallel to the bond between the ring carbon and oxygen, sulfur or nitrogen atom, $\mu_{\parallel}$, and those perpendicular to this direction, $\mu_{\perp}$. These components have been calculated by means of a method similar to that used by Everard and Sutton.[9] These data are given in Table IV. The calculated moments in parentheses in Table III have been obtained using the data given in Table V.

TABLE IV
DIPOLE MOMENTS OF SUBSTITUTED BENZENES

Substituents	μ(D)	$\mu_{\parallel}$(D)	$\mu_{\perp}$(D)
Br	1.57[a]	1.57	0
OH	1.56[a]	0	—1.56
SH	1.19[b]	0.85	—0.83
NH_2	1.52[a]	—1.02	—1.13
OCH_3	1.28[a]	—0.39	—1.22
SCH_3	1.38[b]	0.40	—1.32
$N(CH_3)_2$	1.61[a]	—1.40	—0.79

(a) K. B. Everard, L. Kumar and L. E. Sutton, *J. Chem., Soc.*, **1951**, 2807.
(b) H. Lumbroso and C. Marschalk, *J. chim. phys.*, **49**, 385 (1952).

TABLE V
DIPOLE MOMENTS OF ALKYL DERIVATIVES

Substituents	μ(D)	$\mu_{\parallel}$(D)	$\mu_{\perp}$(D)
OCH_3	1.24	0.62	—1.07
SCH_3	1.57	1.01	—1.20
$N(CH_3)_2$	0.86	0.29	—0.81

The moments calculated for 2-bromotropone and 2,7-dibromotropone are greater than the observed values. Presumably this is due to ortho effect, i. e., to the mutual electrostatic induction of bond moments and to the bond deflection caused by steric repulsion of bulky atoms in ortho position, both decreasing the resultant moments. If the correction is made for the effect of electrostatic induction in the same way as Sutton and his coworkers[10] have done, the moments of these two bromoderivatives are calculated as 5.1 D and 5.6 D respectively in fair agreement with the observed values. Mention should be made here that a similar behavior due to ortho effect has also been recognized in many of the brominated tropolones, phenyltropones and alkyltropolones having a bromine atom or atoms at ortho position to carbonyl carbon.[1,3,4,11]

The observed moments of tropolone and mercaptotropone are nearly equal to the values calculated for the *cis* form, while the moment of aminotropone is close to that of the perpendicular form. In these geometrical configurations, the conjugation between the ring and the substituent groups can attain its maximum possible extent. Moreover a hydrogen bond can be formed between the carbonyl oxygen and the substituent. The hydrogen bond formation will increase the

9) K. B. Everard and L. E. Sutton, *J. Chem. Soc.* **1951**, 2818.

10) J. B. Bentley, K. B. Everard, R. J. B. Marsden and L. E. Sutton, *J. Chem. Soc.*, **1949**, 2957.

11) Y. Kurita, T. Mizuno, T. Mukai and M. Kubo, This Bulletin, **26**, 192 (1953).

trend of electron attraction of carbonyl oxygen, giving rise to the increase of the contribution of cycloheptatrienium oxide structure. This is in conformity with the fact that the observed moment of tropolone is slightly higher than the calculated moment in contradistinction to the case of bromo-derivatives. The magnetic susceptibility measurements by Maruha and Hazato[12] have also indicated that the contribution of the cycloheptatrienium oxide structure is greater in tropolone than in tropone.

The moments of methoxytropone and methylmercaptotropone can adequately be explained either by the perpendicular form or by the mixture of *cis* and *trans* forms. Although the dipole moment data are incapable of settling the problem of the alternative, we think the former viewpoint is nearer the truth on the basis of the following considerations. (1) The fact that the absorption spectra[7] of methoxytropone bear some resemblance to the spectra of tropone rather than to those of tropolone indicates that conjugation taking place between the tropone ring and the methoxy group is weak. (2) The plane configurations are unlikely in view of the steric hindrance acting between the methyl group and carbonyl oxygen or between the methyl group and the hydrogen atom at the position 3 of the tropone ring.

12) J. Maruha and G. Hazato, reported at the annual meeting of the Chemical Society of Japan on April 3, 1953.

Summary

The dipole moments of *ortho*-substituted tropones were measured in benzene solution at room temperature. The values obtained are as follows: 2-bromotropone, 4.94 D; 2,7-dibromotropone, 5.27 D; 2-mercaptotropone, 4.36 D; 2-aminotropone, 3.78 D; 2-methylmercaptotropone, 4.64 D. These values together with those of tropolone and methoxytropone were compared with the calculated moments and the following conclusions were derived. The moments of the bromotropones are lower than those calculated by simple vector addition owing to ortho effect. In tropolone, mercaptotropone and aminotropone, the substituent groups take such configurations that these groups are conjugated with the cycloheptatriene ring in the highest degree and that an intramolecular hydrogen bond is formed between the carbonyl oxygen and the hydrogen atom of each of the substituent groups. In methoxytropone and methyl mercaptotropone, on the other hand, the conjugation is weak and each of the substituent groups lies in a plane nearly perpendicular to the ring.

We wish to express our thanks to Prof. Nozoe and his collaborators in Tohoku University, who kindly provided us with samples used in this experiment. Our thanks are also due to the Ministry of Education in aid of this research.

Chemical Department, Faculty of Science, Nagoya University, Nagoya

Studies on Foams. VIII. Effects of Alcohols on the Foaminess of Soap Solutions

By Masayuki NAKAGAKI and Kōzō SHINODA

(Received May 17, 1954)

In the previous papers in this series[1], the foaminess of aqueous solution has been explained, considering the work required to remove a unit area of adsorption layer. In the present report, this idea is extended qualitatively to three component systems, to elucidate the defoaming and foam-promoting action of alcohols on soap solutions.

As for the foaminess of ternary mixtures, systematic studies have not yet been made, except some solution containing electrolyte, or chemically complex substances, e.g. tannine, saponine, and proteins. Foaminess of aqueous solutions of two simple organic substances was studied by O. Bartsch[2] on nonanoic acid —ethyl alcohol—water, isoamyl alcohol—ethyl alcohol—water, isoamyl alcohol—benzyl alcohol—water, and *m*-cresol—benzyl alcohol—water, and studied by M. Nakagaki[3] on

1) M. Nakagaki, This Bulletin, **23**, 127 (1950); **24**, 269 (1951).

2) O. Bartsch, *Kolloid-Beih.*, **20**, 1 (1924).

3) M. Nakagaki, This Bulletin, **21**, 30 (1948); **22**, 21 (1949).

methyl alcohol—ethyl alcohol—water, and ethyl alcohol—grycerol—water. Few studies, however, on the effects of homologous series of alcohols to soap solution have been reported.

Experimental

Alcohols used were purified by fractional distillation using a glass packed column. A column of 2-ft in height was used for propyl-(b.p. 97.5°C.), and butyl-(b.p. 117°C.) alcohol, 3-ft column for isoamyl-(b.p. 131°C.), hexyl-(b.p. 156°C.), octyl-(b.p. 96°C./16 mmHg.), and decyl-(b.p. 101°C./5mmHg.) alcohol, and 1-ft column for nonyl-(b.p. 96~96.5°C./8 mmHg.), and undecyl-(b.p. 120.5°C./8 mmHg.) alcohol. Heptyl alcohol was Kahlbaum's pure grade material. All these showed definite boiling points.

In fatty acids, caproic-(b.p. 109.5°C./20 mmHg.) and caprylic-(b.p. 120.5°C./9 mmHg.) acids were purified by fractional distillation through a 3-ft column. Capric-(m.p. 31.5°C.), lauric-(m.p.4 4.5°C.), and myristic-(m.p. 54.1°C.) acids were Nihon Yushi's purest grade materials. All these showed definite melting points the same as or somewhat higher than those cited in the literature.

Soap solutions were prepared by the neutralization of above acids with carbonate free potassium hydroxide. Stock solution was about four times as concentrated as the critical micelle concentration (C.M.C.), and 2% excess (to soap) of potassium hydroxide was added to supress hydrolysis of soap.

Foaminess was measured by shaking test in a test tube of 30 cc. in capacity, 15 cm. in height, using 5 cc. of solution. The test tube was immersed in thermostat water. After the temperature became constant, it was taken out and shaken 20 times in 10 sec. Foam height was read after 5 sec (or 30 sec for stable foams) and foam stability was measured as the time required for the foam height to become a half of its original height.

Foaminess of soap solution and alcohol solution

Foaminess of some soap solutions are shown in Figs. 1~3. Fig. 1 shows A_{30}-log C_s relations at 15°C., where A_{30} is the foam height after 30 sec. and C_s is the concentration of soap in mol./l. Fig. 2 shows $t_{1/2}$-log C_s curves at 15°C., where $t_{1/2}$ is the foam stability. Fig. 3 is A_{30}-log C_s relation at 35°C. The foaminess increases with the increase of concentration near to C.M.C. (shown in figures as vertical lines) and then becomes nearly constant or somewhat decreases. At least in dilute solutions near C.M.C., the foam formation of soap solution may be ruled not by micelles but by single ions, since the single ion concentration increases up to C.M.C., and then remains nearly constant. This conclusion coincides with that previously obtained by the studies on the foaminess of dye solutions[4]. Comparing homologous series of soaps, foam height becomes maxi-

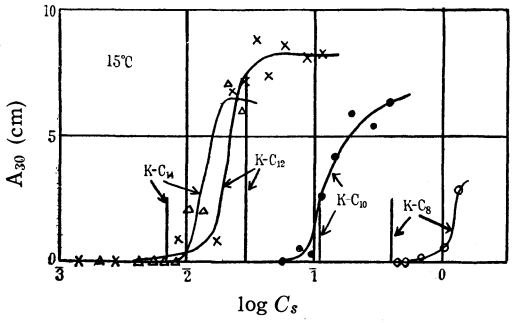


Fig. 1. Foam height of soap solutions at 15°C.

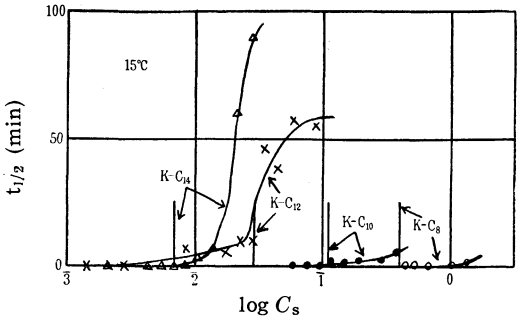


Fig. 2. Foam stability of soap solutions at 15°C.

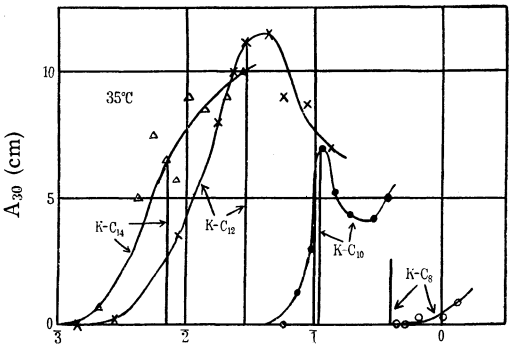


Fig. 3. Foam height of soap solutions at 35°C.

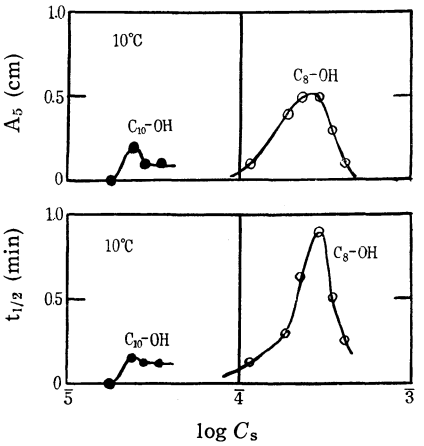


Fig. 4. Foaminess of alcohol solutions at 10°C.

4) M. Nakagaki, This Bulletin, **22**, 200 (1949); **23**, 47, 102 (1950).

mum at about K—C_{12}~K—C_{13} at ordinary temperature.

Foaminess of aqueous solutions of *n*-octyl- and *n*-decyl alcohol are shown in Fig. 4. It is ascertained that the foaminess of alcohol solution is far poorer than that of soap solution. Foam height measured after 5 sec. is smaller than 0.5 cm. for alcohol solutions, while, for soap solutions, it is several cm. even after 30 sec. Foam duration is smaller than 1 min. for alcohols and far more unstable than soap solutions. O. Bartsch[5] reported that the foam formation of homologous series of alcohols showed a maximum at about C_5-OH, and then decreased as alcohols were higher. The results shown here are coincident with Bartsch's, since the higher C_{10}-OH shows smaller foaminess than the lower C_8-OH.

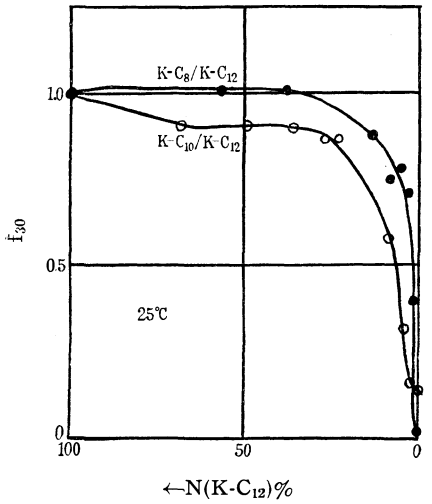


Fig. 5. Foam height of mixed soap solutions at C.M.C. (25°C.).

Foam height of mixed soap solution is measured at C.M.C., since the C.M.C. is considered as a corresponding state of soap solution. As in pure soap solution, C.M.C. can be determined also in mixed soap solution by the change in color of pinacyanol chloride[6]. Fig. 5 shows the relation between f_{30} and the mol. percents of K-C_{12} in two soaps, where f_{30} is defined as the ratio:

$$f_{30}=A_{30}/A^0_{30} \qquad \cdots\cdots(1)$$

A_{30} and A^0_{30} are foam height after 30 sec. for mixed solution and pure K-C_{12} solution at C.M.C., respectively. Foaminess decreases with the increase of the added amount of K-C_{10} or K-C_8. This coincides with the fact that the foaminess of pure soap solution at C.M.C. decreases, as shown in Fig. 1~3, in the sequence of K-C_{12}>K-C_{10}>K-C_8. Higher K-C_{12}, however, dominates the foaminess more influentially than lower K-C_{10} or K-C_8. This is explained by the theory that the nature of foam is dominated by molecules adsorbed at the surface, and the higher soap is adsorbed more strongly than the lower. This also explains the fact that higher K-C_{10} shows its effect at smaller addition than lower K-C_8.

Effects of Alcohols on Soap Solution

Effects of the homologous series of alcohols on the foam height of K-C_{10} and K-C_6 are measured, and f_{30} for K-C_{10} or f_5 (f-values after 5 sec.) for K-C_6 are shown in Fig. 6 as a function of $\log(C_{OH}/C_S)$. C.M.C. of mixed solution[7] is adopted as the concentration to be tested, since the C.M.C. is considered to be a corresponding state for mixed solution of soap and alcohol. C_{OH} and C_S are the concentrations of alcohol and soap in mol./l,

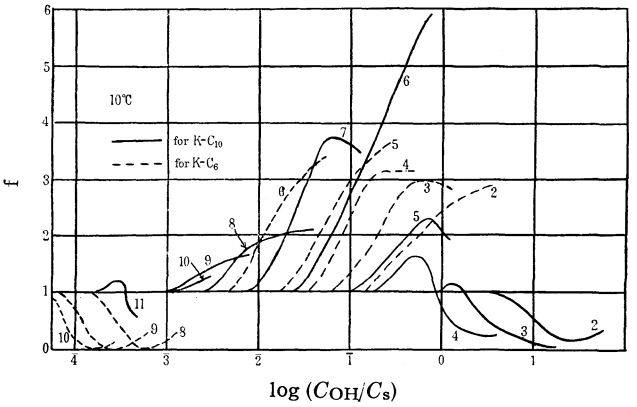


Fig. 6. Foam height ratio of soap-alcohol mixed solution at C.M.C. (10°C.). Numerals show numbers of carbon atoms of alcohol.

5) O. Bartsch, *Kolloid-Z.*, **38**, 177 (1926).
6) K. Shinoda, *J. Phys. Chem.*, **58**, No. 7, (1954).
7) K. Shinoda, *J. Phys. Chem.*, In Press.

respectively. Added amounts of alcohols were smaller than the solubilities of each kind of alcohol in distilled water[8]. In soap solutions, the solubilities of alcohols increase by solubilization, so that the deposition of alcohol drops on the surface cannot be expected.

The effects of alcohols on K-C_{10} are, first, discussed. As for C_2-and C_3-OH, little effects is observed in small addition, but foam height decreases distinctly when the amount of alcohol is increased to $1\sim10^2$ times that of soap. Also for C_4-OH, foam height decreases when the mol. ratio is greater than 1:1, though, at a smaller amount of alcohol, foaminess somewhat increases. The decreases of foaminess of the solution by large addition of lower alcohol (but within the limit of their solubilities) is explained as follows. As stated before[1], the foaminess of a solution is large when the work required to remove a unit area of adsorption layer is large. As the large amount of alcohol is added, the hydrocarbon chain of soap molecule is dissolved easily in bulk solution owing to the oil-dissolving ability of alcohol. The work then, to pull the soap molecule into the solution becomes small, to decrease the foaminess. This effect may be, therefore, named as the defoaming by solvent effect.

For higher alcohols, C_5-$\sim C_{10}$-OH, foam height becomes large with the addition of alcohol, at the ratio of $10^{-3}\sim1$ alcohol to soap. This is compared with the antifoaming action shown as these alcohols are sprinkled upon froth. Such an antifoaming action is explained by S. Ross[9] with a mechanism that a portion of foam membrane is substituted by an oil drop, and this portion becomes thinner to break the foam by the spreading of oil on the surface. In this case, it is necessary for alcohol to exist as an oil drop. When the oil dissolves homogeneously into the bulk after the long lapse of time, the solution becomes again foamable. As shown in Fig. 6, homogeneous dissolution of these alcohols increase foam height. As the number of carbon atoms of these alcohols is somewhat smaller than that of soap, the surface activities of alcohol and soap are about equal, since the hydrophilic property of -OH is weaker than $-COO^-$. Then, a simultaneous adsorption takes place and mixed monolayer is formed, and the surface viscosity may become large, as Matalon and Shulman[10] have shown on the penetration of Na-cetyl sulfate to cetyl alcohol monolayer. The foam promoting action may be attributed to the increase of surface viscosity.

The foam promoting action becomes maximum, as shown in Fig. 6, at C_6-OH and then decreases for higher alcohols. Higher alcohols, C_8-$\sim C_{10}$-OH, having greater surface activity than soap, may expel some of the soap molecules from the surface to decrease the foam height. At last, C_{11}-OH shows a defoaming action in extremely small addition. This alcohol is thought to be much higher in its surface activity than soap, to be adsorbed preferentially to the surface. Then, the greater part of the adsorption layer may be occupied by alcohol molecules, at the addition of $10^{-4}\sim10^{-3}$ to soap. Since the foam height of alcohol is much smaller than soap, the foam height of the mixed solution becomes very small. This effect may be named as defoaming by preferential adsorption.

The defoaming or foam promoting action of alcohol to soap solution is determined by the balance of surface activities between alcohol and soap. The same effects as shown by higher alcohol to higher soap will be shown by lower alcohol to lower soap. Taking the difference of the number of carbon atoms in alcohol and soap as a measure of relative surface activity, alcohols, having 8$\sim$6 carbon atoms less than soap, showed defoaming by solvent effect to K-C_{10}, 5$\sim$0 less showed foam promoting action, and 1 or more larger showed defoaming by preferential adsorption. Then, as for K-C_6 soap, C_2-$\sim$ C_6-OH should show foam promoting action, and alcohols higher than C_7-OH should show defoaming by preferential adsorption. Fig. 6 shows that this estimation is in good agreement with the experiments. C_2-OH and C_3-OH which always showed defoaming effect to K-C_{10} now show foam promoting action to K-C_6, and C_8-, C_9- and C_{10}-OH which always showed foam promoting action now show defoaming action. These three kinds of effects, defoaming by solvent effect, foam promoting action, and defoaming by preferential adsorptions, are entirely different in their phenomenological features, but are closely related in their essential nature.

The defoaming action by preferential adsorption at extremely small addition seems important in its application. The mechanism of defoaming by higher esters, amines, amides, ethers and so on, may be explained by it.

8) K. Kinoshita and K. Shinoda, presented before the 7th Annual Meeting of the Chemical Society of Japan (1954) at Tokyo.

9) S. Ross, *Rensselaer Polytech. Inst. Bull., Eng. Sci. Ser.*, No. 63 (1950).

10) R. Matalon and J. H. Shulman, *Trans. Faraday Soc.*, **43**, 479 (1947).

Summary

Foaminess of soap solution increases with the increasing concentration up to the C.M.C., and then becomes nearly constant. In homologous series, K-C_{12} or K-C_{13} show the greatest foaminess at ordinary temperature. Foaminess of alcohol solution is much smaller than the soap solution. In homologous series of alcohols higher than C_5-OH, the higher foams poorer. For the mixed solution of two soaps, the foaminess becomes smaller when the ratio of lower soap is larger.

The effects of homologous series of alcohols on soap solution are measured and three types are observed: defoaming by solvent effect (by C_2-~C_4-OH for K-C_{10}) is observed at $\log C_{OH}/C_S = 0 \sim 2$; foam promoting action (C_5-~C_{10}-OH for K-C_{10} and C_2-~C_6-OH for K-C_6) at $\log C_{OH}/C_S = 3 \sim 0$: and defoaming by preferential adsorption (C_{11}-OH for K-C_{10} and C_8-~C_{10}-OH for K-C_6) at $\log C_{OH}/C_S = \bar{5} \sim \bar{3}$. These three effects are correlated with each other.

Department of Chemistry, Faculty of Science, Tokyo University, and Department of Physical Chemistry, Faculty of Engineering, Yokohama National University Minamiku, Yokohama

The Catalytic Action of Organic Peroxides on the Polymerization of Ethenoid Compounds. III. The Effects of α-and β-Naphthoyl Peroxide on the Polymerization of Styrene

By Matsuji TAKEBAYASHI, Tadao SHINGAKI and Hisashi MATSUI

(Received May 25, 1954)

The reaction of free radicals in polymerization systems has been widely studied in particular as to the ability of a free radical to initiate and terminate reaction chains.[1] In the previous paper of this series,[2] the authors, studying the polymerization of styrene and of vinyl acetate in the presence of substituted benzoyl peroxides, observed that the activity of a radical derived from a peroxide was related to the distribution of electron density: thus electron repelling substituents increased the activity of a radical, and electron attracting substituents lowered the reactivity, and that the rate of polymerization was in a parallel relation with the rate of decomposition of peroxides, which generated active free radicals.

Recently, it has been found that some amines promote the decomposition of peroxides,[3] and that the peroxide-catalyzed polymerization of styrene is accelerated by adding tertiary amines[4] or polyamines.[5]

The experiments recorded in this paper have been carried out to investigate the effects of α-and β-naphthoyl peroxide on the polymerization of styrene and the influences of some tertiary amines on the effects of naphthoyl peroxides.

First of all, the rate of decomposition of the peroxide (1/6000 mol.) in styrene (1/30 mol.) was measured at 35°C. and 60°C. by the iodometric method. The results obtained are shown in Fig. 1. The date, given in Fig. 1, indicate that α-naphthoyl peroxide decomposes more rapidly than β-peroxide, accompanied by some extent of induced decomposition. Particularly at 60°C., α-peroxide

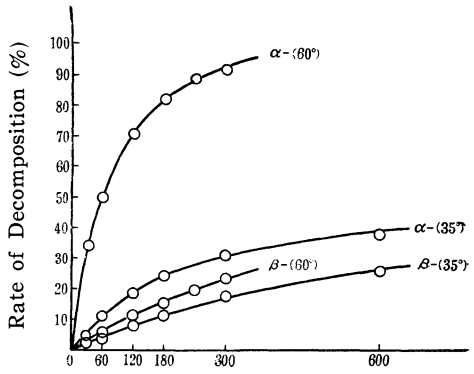


Fig. 1.

1) C. C. Price, "Mechanism of reactions of carbon-carbon double bonds", 70 (1946); W. Cooper, *Nature*, **162**, 897, 927 (1948).

2) M. Takebayashi and T. Shingaki, This Bulletin, **26**, 137 (1953); M. Takebayashi, T. Shingaki and Y. Ito, ibid., **26**, 475 (1953).

3) P. D. Bartlett and K. Nozaki, *J. Am. Chem. Soc.*, **69**, 2299 (1947).

4) L. Horner, *Angew. Chem.*, **61**, 311 (1949); M. Imoto and S. Sai Unpublished: J. Elly, R. N. Haward and W. Simpson, *J. Appl. Chem.*, **1**, 347 (1951).

5) R. Spolsky et al., *Ind. Eng. Chem.*, **42**, 1847 (1950).

decomposed to the extent of 92 per cent, while β-peroxide to that of only 22 per cent during five hours. The decomposition of β-peroxide was observed to be of nearly first order, and the rate was almost equal to that of benzoyl peroxide at 60°C.

In another experiment, the decomposition products of the peroxides in styrene were examined. It was recongnized that the peroxide decomposed to produce mainly naphthoate radical and naphthyl radical, generating carbon dioxide, and that α-naphthoate radical and β-radical did not isomerize each other during the reaction.[6]

If the radicals produced from the peroxides are active ones, the rate of polymerization of styrene will be in a parallel relation with that of decomposition of the peroxides. The above expectation was satisfied in the case of the experiments with 1/30 mol. of styrene and 1/6000~1/3000 mol. of the peroxide at 35°C. and 60°C. in the absence of air. The results are summarized in Table I, and a result obtained for benzoyl peroxide is added to it for the sake of comparison.

TABLE I

Peroxide	Temp. (°C.)	React. time (hr.)	Rate of Polymerization (%)
α-Naphthoyl (1/6000 mol.)	35	10	22
β-Naphthoyl (1/6000 mol.)	35	10	4
α-Naphthoyl (1/6000 mol.)	35	26	34
β-Naphthoyl (1/6000 mol.)	35	26	10
α-Naphthoyl (1/6000 mol.)	60	5	22
β-Naphthoyl (1/6000 mol.)	60	5	16
α-Naphthoyl (1/3000 mol.)	60	5	28
β-Naphthoyl (1/3000 mol.)	60	5	20
β-Naphthoyl (1/3000 mol.)	60	18	89
Benzoyl (1/3000 mol.)	60	18	82
None	60	18	1

In the next place, the influence of tertiary amines (1/6000~1/30000 mol.) on the rate of decomposition of the peroxides (1/6000 mol.) in styrene (1/30 mol.) was examined at 35°C. The data obtained are given in Fig. 2 and 3.

Aromatic amines such as dimethyl aniline and ethyl-benzyl aniline, and urotropine accelerate the decomposition of the peroxides remarkably, while heterocyclic amines such as pyridine and quinoline show practically no influence on the rate of the decomposition in the experimental conditions.

Then the polymerization of styrene with the peroxides and tertiary amines was carried out at 35°C. in the absence of air. The rate of the polymerization and the degree of it ($\bar{P}$) are listed in Table II.

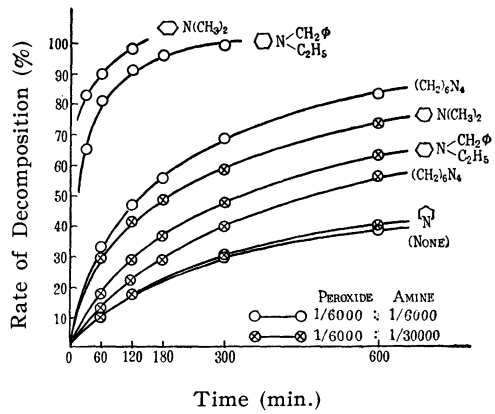


Fig. 2. Rate of decomposition of α-naphthoyl peroxide in the presence of tertiary amines at 35°C.

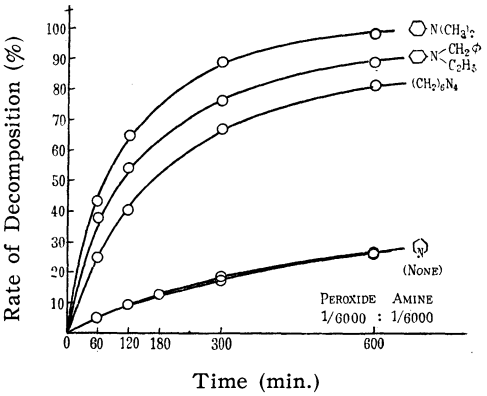


Fig. 3. Rate of decomposition of β-naphthoyl peroxide in the presence of tertiary amines at 35°C.

In the experiments using α-peroxide, the presence of aromatic amines such as dimethyl aniline and ethyl-benzyl aniline, and urotropine show a retarding influence on the rate of polymerization. It has been known that the presence of a little amount of amine accelarates the peroxide-catalyzed polymerization, while a larger amount of amine rather retards.[7] In an experiment, the polymerization was carried out adding a less amount of amines, but a similar result was obtained. It seems that the amines accelarate the decomposition of peroxide so rapidly that the radicals, produced from the peroxide, react to some extent upon each other or combine with other radicals besides reacting as the initiator of reaction chains.

In the experiments using β-peroxide, on

6) Kharasch also has observed this fact in carbon tetrachloride. M. S. Kharash and R. L. Dannley, *J. Org. Chem.*, **10**, 406 (1945).

7) M. Imoto and S. Sai, Unpublished.

TABLE II

In the presence of	React. time (hr.)	Rate of polymerization (%)	$v_i \times 10^9$ mol./l., min.	$\overline{P}$
α-Peroxide (1/6000 mol.) Dimethyl aniline (1/30000 mol.)	10	14.3	18	430
α-Peroxide (1/6000 mol.) Ethyl-benzyl aniline (1/30000 mol.)	10	17.1	24	400
α-Peroxide (1/6000 mol.) Urotropine (1/30000 mol.)	10	17·7	26	380
α-Peroxide (1/6000 mol.)	10	20.3	30	370
α-Peroxide (1/6000 mol.) Pyridine (1/6000 mol.)	26	40.9	20	400
α-Peroxide (1/6000 mol.) Quinoline (1/6000 mol.)	26	40.5	20	400
α-Peroxide (1/6000 mol.)	26	38	19	410
β-Peroxide (1/6000 mol.) Dimethyl aniline (1/6000 mol.)	5	28.9 (60°C.)		
β-Peroxide (1/6000 mol.) Ethyl-benzyl aniline (1/6000 mol.)	5	24.9 (60°C.)		
β-Peroxide (1/6000 mol.) Dimethyl aniline (1/6000 mol.)	10	16.0	17	520
β-Peroxide (1/6000 mol.) Ethyl-benzyl aniline (1/6000 mol.)	10	14.3	14	560
β-Peroxide (1/6000 mol.) Urotropine (1/6000 mol.)	10	3.4	1.3	1400
β-Peroxide (1/6000 mol.)	10	4.0	2.0	1100
β-Peroxide (1/6000 mol.) Pyridine (1/6000 mol.)	26	10.5	2.2	970
β-Peroxide (1/6000 mol.) Quinoline (1/6000 mol.)	26	10.3	2.2	970
β-Peroxide (1/6000 mol.)	26	10.0	2.1	1000

the contrary, dimethyl aniline and ethyl-benzyl aniline influence the peroxide, causing it to accelerate the polymerization. The results indicate that the increase of the rate of polymerization is affected not only by the increase of the amount of active radicals, but also by the activity of β-peroxide-radicals on the initiation of the reaction.

Heterocyclic amines such as pyridine and quinoline manifest practically no influence either on the rate of decomposition of peroxides or on that of the peroxide-catalyzed polymerization of styrene.

The accelerating action of aromatic amines on the decomposition of naphthoyl peroxides seems to be elucidated as follows for the case of dimethyl aniline. The decomposition may be initiated by the addition of dimethyl aniline with its lone-pair of electrons on nitrogen atom to the positively polarized part of the peroxide, giving rise to the formation of an iminium salt.[8] The salt may decompose to produce radicals: RCOO· and R· (R indicates naphthyl radical), ions: $RCOO^+$ and $RCOO^-$, and a radical-cation of dimethyl aniline. Here the radicals, RCOO· and R·, initiate the polymerization, and sometimes react on the peroxide, amine or other radicals. The anion $RCOO^-$ probably forms RCOOH with H^+, and the radical-cation dimerizes giving out H^+, or comes into play for the polymerization.[9]

Heterocyclic amines showed practically no influence on the decomposition of the peroxides in the experimental conditions. However, it has been reported that the decomposition of benzoyl peroxide is accelerated in pyridine.[10] Therefore, the concentration of amine in reaction systems might come in question,

Pyridine, contrary to dimethyl aniline, can hardly be added with its nitrogen atom to naphthoyl peroxide owing to the steric

8) L. Horner and K. Scherf, *Ann.*, **573**, 35 (1951).

9) L. Horner and E. Schwenk, *Ann.*, **566**, 69 (1950).

10) K. Nozaki and P. D. Bartlett, *J. Am. Chem. Soc.*, **78**, 1686 (1946).

strain[11] between them. If the decomposition should be accelerated by pyridine the reaction might be induced by the mutual interaction between pyridine and peroxide radicals.

Experimental

Materials—For the preparation of α-naphthoyl peroxide a modification of the method used by Kharasch and Dannley[6] was found to be useful. α-Naphthoyl chloride was dissolved in 40 cc. of anhydrous toluene; the solution was then added slowly to a vigorously stirred solution of 5 g. of sodium peroxide in 50 cc. of cold water. The temperature was not allowed to rise above 0°C. The stirring at 0° C. was continued for about three hours. Then the α-naphthoyl peroxide separated out as a pale precipitate. The precipitate was collected on a filter, washed with water, and dried. It was then dissolved in chloroform and fractionally precipitated by pouring the solution into methanol on stirring. The procedure was repeated several times. Yield: 55 %. The purity was found to be of 90 per cent by titration. A pure sample decomposed sharply at 98°C. The preparation of β-peroxide was similar to that of α-peroxide, the temperature of the reaction being held at 5~7° C. Yield: 76 %. A sample, the peroxide content of which was 95 %, decomposed sharply at 138° C..

The styrene employed was distilled with steam, dried over a small amount of calcium chloride, and was distilled under reduced pressure just before use. B.p. 63°C./55 mm. The absence of peroxides was ascertained by the test with ferrous ammonium sulfate and ammonium thiocyanate. The aromatic and heterocyclic amines employed were distilled under reduced pressure just before use.

Decomposition of Peroxides—The decomposition of peroxide was carried out in sealed reaction tubes. The tubes were treated with warmed cleaning solution for several hours, left standing in a dilute solution of sodium bisulfate for a short time, then rinsed with distilled water, and dried. The definite amount of the peroxide and amine were mixed with 1/30 mol. of styrene in the reaction tube, the tube was cooled in an ice-salt-bath, then was evacuated and sealed off. The sealed tube was immersed in a thermostat. After the required time the tube was cooled again, and opened. The content of the tube was mixed with 40 cc. of purified acetone in a glass-stoppered flask, and then titrated by the standard solution (1/10N) of sodium thiosulfate according to the direction of Blomquist and Buselli.[12] It was ascertained that no reaction took place between iodine and amine during the titration.

Polymerization of Styrene—The definite amount of the peroxide and amine were mixed with 1/30 mol. of styrene in a reaction tube, evacuated as described above, and then immersed in a thermostat for the reaction time. When the reaction time was over, the tube was cooled in an ice-salt-bath. The reaction products were dissolved in benzene, the polymer produced was precipitated by adding methanol to the solution, and the weight of polystyrene was measured. The molecular weight of the polymer was determined by the viscosity method.

Summary

(1) The rates of polymerization of styrene with α-and β-naphthoyl peroxide have been found to be in a parallel relation with the rates of decomposition of the peroxides at 35° and 60°C.

(2) Aromatic amines such as dimethyl aniline and ethyl-benzyl aniline, and urotropine accelerate the decomposition of the peroxides.

(3) In the experiments using α-peroxide, the presence of the aromatic amines and urotropine show a retarding influence on the rate of the polymerization. In the experiments using β-peroxide, on the contrary, dimethyl aniline and ethyl-benzyl aniline influence the peroxide to accelerate the polymerization.

(4) Heterocyclic amines such as pyridine and quinoline manifest practically no influence either on the rate of decomposition of the peroxides or on that of the peroxide-catalyzed polymerization of styrene.

(5) In respect to the action of amines, a tentative theory has been made.

The authors express their hearty thanks to the Ministry of Education for a Grant in Aid for Scientific Research.

Chemical Laboratory, South College, Osaka University, Osaka

11) H. C. Brown et al., *J. Am. Chem. Soc.*, **64**, 374, 378, 1452 (1945), ibid., **64**. 325 (1942), ibid., **70**, 2878 (1948), ibid., **71**, 445 (1949).

12) A. T. Blomquist and A. J. Buselli, *J. Am. Chem. Soc.*, **73**, 3883 (1951).

Manufacture of Levulose from Jerusalem Artichoke

By Junzo YAMAZAKI

(Received May 25, 1954)

In eight years since 1941, the Japan Levulose Company manufactured 127 tons of pure crystalline levulose (D-fructose) from 6000 tons of tuber of Jerusalem artichoke.

Here will be shown, together with a diagram, the details of the operation performed in 1948, the year of complete mastery of the manufacturing technique.

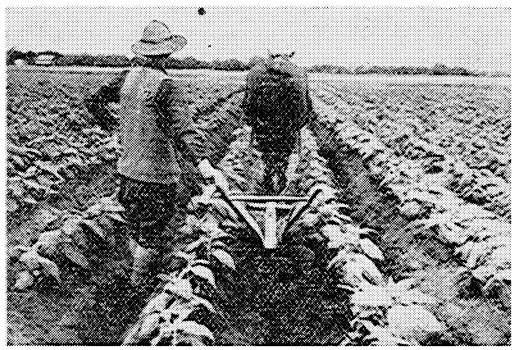


Fig. 1. Cultivation of Jerusalem artichoke in the end of June at Eniwa, Hokkaido.

Cultivation and Drying of Artichoke Tuber

The artichoke used as the raw material for the manufacture of levulose was cultivated mainly in a field (400 acres) of Eniwa, near Sapporo in Hokkaido, using animal power for cultivation and harvesting, as shown in Fig. 1 (photograph). The variety of Jerusalem artichoke used was of a family of white cortex, and the crop was 9 tons per acre. The fresh tuber was washed with water, sliced into cossette, and dried to a water content of 15 percent by the use of a rotary drier. Thus one ton of dried material was obtained from 5 tons of fresh tuber. To this end 800 kg. of coal was required.

TABLE I

ANALYSIS OF JERURALEM ARTICHOKE

(Cultivated in 1947 at Eniwa, Hokkaido)

			After hydrolysis	
	Moisture (%)	Solid matter (%)	Total reducing sugar(%)	Levulose (%)
Fresh tuber*	80.00	20.00	14.80	11.56
Dried tuber**	15.11	84.89	53.35	40.17

* Mean of the analytical values of 11 samples, converted to the basis of moisture content of 80 percent.

** Mean values of 123 tons of the dried cossette.

The dried cossette can well be preserved, is very little damaged by insects, and is suitable for levulose manufacture throughout the year.

The results of analysis of the tubers, both fresh and dried, are shown in Table I.

Manufacture of Levulose

The dried artichoke used for levulose manufacture from 1941 to 1948 amounted to 1142 tons, corresponding to 6000 tons of cultivated fresh artichoke. The average content of levulose in the dried artichoke was 41.3 percent, the maximum content of year average being 44.0, the minimum 38.0 percent. The crystalline levulose manufactured from these material was 127.4 tons in quantity, the average yield being 11.2 percent of the dried artichoke, corresponding to 27.0 percent of the levulose contained in the raw materials.

In order to explain the details of the levulose production we will illustrate the data obtained in 1948. By this year we mastered the technique of manufacture, producing 16.7 tons of crystalline levulose from 123 tons of dried artichoke during the period from January to July.

In Fig. 2 is illustrated each process of manufacture as well as its material balance in the form of a diagram, where the description of water content and thermal data are eliminated. The width of the figure represents the ratio of solid matter, while the content of levulose is shown numerically. All the numerals in Fig. 2 represent those values recalculated from the data totally obtained during this period, so as to correspond to one ton of the material for manufacture.

Diffusion of Dried Cossette

We have used a diffusion apparatus of a type of semi-counter-current diffusion battery which is usually employed for the extraction of beet sugar. This consists of twelve cells, each of 320 l. in capacity, connected with each other in the form of a circle. Each cell is charged with 63 kg. of the material, and hot water is circulated through the cells, so as to extract the contained fructan. Extraction is in general completed when the liquid

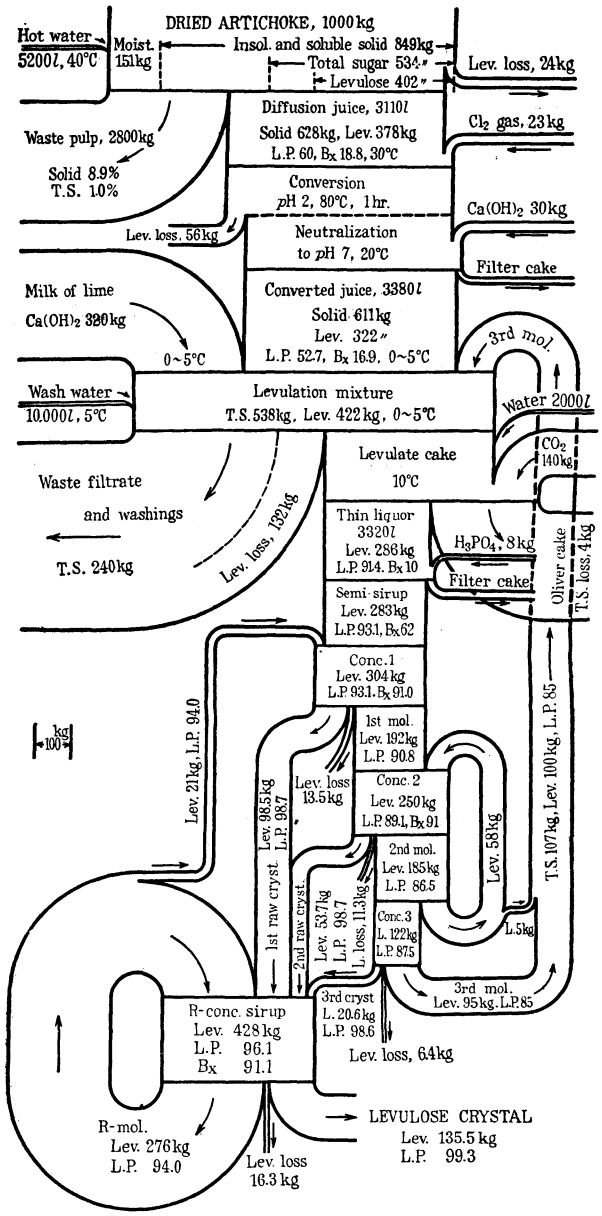


Fig. 2—A process flow diagram of levulose manufacture.

Abbreviations:

T.S.:	Total sugar
L.P.:	Levulose purity
Conc.:	Concentrated sirup
Bx:	Refractometric Brix (% solid)
R:	Refined
Mol.:	Molasses
Lev., L.:	Levulose

passes through ten of the cells, the refractometric solid in the liquid amounting to 18–19 percent. This "diffusion juice" is obtained in a quantity of 200 l. per one charge, is brown in appearance, the total sugar purity (T. S. × 100/solid) being 81, and the levulose purity (Levulose ×100/solid) 60. The yield of levulose of this procedure is 94 percent.

Conversion and Neutralization

A wood tank, 2 m. in height, is filled with this diffusion juice, and chlorine is blown into it at a temperature of 30°C. This is a patented process[1], the characteristic of which is that chlorine destroys any coloring matter, coagulates a part of the impurities, and the hydrochloric acid thereby formed promotes the hydrolysis of polyfructosans. It was once reported[2] that in the oxidation of invert sugar by chlorine, levulose is oxidized at 15°C. to a range of 10 percent, while glucose is destructed by it to the large extent of 80 percent. It is, however, experienced that during the seven months' period the

1) *Japanese Pat.* 92301 (1931).
2) S. Ochi and M. Nakamura, *Repts. Tokyo Imp. Ind. Res. Inst. Lab.*, **24**, No. 5, 46 (1929) (in Japanese).

extent of decomposition or loss in this procedure amount to 14.8 percent for levulose, and to 16.8 percent for other reducing sugars.

It is no doubt possible to prevent the destruction of levulose to a far lesser degree, if hydrochloric acid is used for conversion in place of chlorine, but in this case the filtration of the treated liquor becomes difficult, and, moreover, decolorization as well as clarification can not be carried out with satisfaction. It should be mentioned further that treatment with chlorine has another advantage; this is that in the sugar liquor the growth of moulds is prevented, and thus subsequent operation can easily be performed. The introduction of chlorine is continued until the liquor shows a *p*H between 1.8 and 2.0, and conversion is completed by keeping the liquor at 80°C. for one hour. The liquor is then cooled down to 20°C., and some milk of lime is added to a *p*H 7, when proteinous matters, pectins, etc. are coagulated. On filtering these precipitates a "converted juice" is obtained. The yield of levulose in this process is 85.2 percent.

Precipitation of Levulose ("Levulation Process")

The converted juice is cooled down to 0°–5°C., and milk of lime of the same temperature is added. The necessary quantity of the lime is 1.45 times the quantity equivalent to the total sugar in the hydrolyzate. It is desirable to employ lime of good quality containing more than 67 percent of available CaO, and especially consisting of fine powder. The quality and the quantity of lime has a remarkable effect on the yield of levulose as well as on the amount of carbon dioxide necessary for neutralization. The most important point of this procedure lies in obtaining a compound between levulose and lime ($C_6H_{12}O_6 \cdot CaO \cdot XH_2O$, "lime levulate") in the form of granular precipitate filtrable as easily as possible. Either when the juice is too thick, or when the mixing of the liquors is too rapid, undesirable blocks or fine precipitates are readily formed. To prevent this it is necessary to mix the juice with milk of lime gradually and alternately, and to keep the mixture constantly in a medium of a little excess of lime by stirring well at the temperature between 0° and 5°C. It is, however, unnecessary to add crystal seeds of lime levulate, as already pointed out by Jackson[3]. After thorough mixing for some time, the precipitate is filtered through a filter press, and washed with cold water of 5°C. Washing is continued till the filtrate becomes colorless. The filter cake ("levulate cake") is mixed with cold water, transferred to a carbonator as a thick suspension, and carbon dioxide is introduced until the liquor shows a *p*H 8, keeping the temperature below 10°C. Here levulose is liberated, and by filtering the precipitate of $CaCO_3$ on an Oliver filter, a "thin liquor" of light yellow coloration is obtained. This liquor has a concentration of 10 percent, and a levulose purity (L.P.) 90 to 99 (av. 91.4). In later operations the final (third) molasses, which is removed from raw crystal, is diluted and subjected to levulation process for recovery of levulose, either solely or in admixture with the converted juice.

The process of levulation must be carefully performed, since the loss of levulose in this process is the greatest in the whole procedure, often becoming equal, in quantity, to the final product. The yield of levulose is 65 percent with respect to the artichoke juice, and 80 percent to the molasses. In this illustration the two are mixed and treated, so the yield becomes 68.7 percent on the average.

Evaporation to "Semi-Sirup"

The thin liquor is, while still cold, neutralized with phosphoric or oxalic acid to a *p*H 5.8. After filtration the liquor is concentrated to 62 percent in a vacuum evaporator, and preserved in a tank. The calcium salt in the solution separates out gradually, and finally the value of L.P. increases to 93 on the average.

Crystallization of Raw Crystals

The sirup which has been blended from a few lots of semi-sirups, so as to make the L.P. value to 94, is again thickened by heating in a vacuum evaporator to a "concentrated sirup" having a concentration of 91 percent as regards to solid. This thick sirup is then introduced into a crystallizer, seeded at 52°C. with a fine powder of crystalline levulose, gradually cooled down with constant gentle stirring, so that the seed can grow up sufficiently. Thus the content will be in the state of massecuite, when the temperature is lowered to 30°C. within 24 hours. Then the molasses is removed by means of a centrifuge, where the first raw crystal is obtained. The former (the first molasses), on concentrating, is subjected to repeated (twice) crystallization. In a similar manner the second and the third crop of levulose crystal is obtained, thereby the value of

3) R. F. Jackson, C. G. Silsbee, and M. J. Proffitt, *Sci. Papers Bur. Standards*, No. 519, **20**, 609 (1926).

L. P. is hardly lowered as to the crystal, but is depressed to 85 with the molasses. This molasses with a low L. P., being unfavorable for crystallization, is returned for recovery of levulose to the above mentioned process of levulation.

In practice, the second molasses is concentrated to obtain a third crop of crystal, in so far as the L. P. value is above 87.5. If below, the molasses is blended to a sirup of L. P. 89 by adding the first molasses, and made to yield the second crystal. With the depression of L. P. value the yield of levulose crystal suddenly falls with respect to massecuite, and also the crystallization process becomes tedious, as shown in Table II.

TABLE II
CRYSTALLIZATION OF LEVULOSE

Crystal	No. of Crystallization	Crystals obtained (kg.)	Crystals per one Cryst'n (kg.)	Av. Purity of "Conc."	Yield of Cryst. as to Massecuite (Solid/solid)(%)	Time required for Cryst'n (day)
1st raw	42	12,290	292.6	93.1	29.6	1
2nd raw	35	6,706	191.6	89.1	19.4	2
3rd raw	17	2,574	151.4	87.5	15.1	6
Refined	57	16,810	294.9	96.1	30.7	0.8—1

Crystallization of Refined Crystal

The raw crystal and the sirup (R-mol. of Fig. 2), which is removed from the refined crystal, are made up to a L. P. of 96, decolorized with active carbon, and subjected to crystallization. The crystals, after centrifugation, are washed with a little distilled water, and dried in vacuum at 40°C.

The refined crystals thus obtained are colorless, tilted cubes of a relatively uniform size (from 0.5 to 1 mm.). The L. P. is 99.3 on an average, well in agreement with the Japanese Pharmacopoeia. By recrystallizing from dilute methanol or ethanol we are able to obtain easily a sample of highest purity[4].

In order to obtain further crystals from the mother sirup (L. P. 94) of the refined levulose, some raw crystal is dissolved into it, the excess sirup being returned to the stage of the first raw crystal. Such a somewhat complicated method of preparing refined crystal is, in reality, a most economical process, and favorable for keeping constant the quality of the product.

Steam, Electric Power and Labor

The manufacture of levulose consumed, per one ton of dried artichoke, 6 tons of steam, 1500 KWH of electric power, 345 man hours of labor (in the case of all-night operation) and the chemicals indicated in Fig. 2.

Analytical Procedure

It is of the utmost necessity, for chemical control, to carry out the exact analysis of levulose and the accurate determination of its purity. A number of various analyses were made for each lot of the raw material as well as its intermediates, and finally summed up. The value of refractometric solid was assumed directly as the value of solid in aqueous solutions. The total reducing sugar (T. R. S.) was measured by the titrimetric method of Lane and Eynon[5], after the test liquid was hydrolyzed by hydrochloric acid. The levulose ratio (L. R.) was obtained according to Jackson and Mathews[6] from the titre of T. R. S. and the saccharimetric polarization. It was very fortunate that both of these methods enabled us to perform rapid and accurate determinations. The levulose content (L.) is obtained by means of an equation: $L. = T.R.S. \times L.R.$, and likewise the levulose purity (L. P.) by a relation: $L.P. = L. \times 100/S$. All the analytical procedures required considerable skill and precision; nevertheless, after some experiences, accurate and consistent values were constantly obtained. (Here allow us to mention that Messrs. M. Nakamura†, K. Nishiki, and S. Kidooka of this factory helped us to systematize these analytical methods and carry out practical determinations).

Utilization of Waste Liquor

It is possible to collect nearly 90 percent of the total waste sugar in a concentration of 5 percent from the waste filtrate of the levulate, when combined with the first portion of the filtrate obtained by washing.

This liquor, on neutralizing with carbon

4) Y. Tsuzuki, J. Yamazaki, and K. Kagami, *J. Amer. Chem. Soc.*, **72**, 1071 (1950).

5) J. H. Lane and L. Eynon, *J. Soc. Chem. Ind.*, **42**, 32T (1923), **44**, 150T (1925), A. O. A. C., 5th ed. pp. 498~9 (1940).

6) R. F. Jackson and J. A. Mathews, *Bur. Standards J. Res.*, **8**. 435 (1932).

dioxide or with sulfuric acid, proved to be an active culture media for yeasts.

Experiments culturing Fleischmann's yeast by the so-called "Zulaufsverfahren" with a concentrated liquor, to which was added some ammonium sulfate and phosphate showed that sugar consumption is 92.6 percent and the yield of dry yeast is 49.7 percent with respect to the sugar present in the liquor. The effect was even superior to a control experiment done with malt juice, where sugar consumption was 90.2 percent, yield 49.5 percent[7].

It is, therefore, possible to produce even 1200 lb of fresh yeast by utilizing the waste liquor produced from one ton of dried artichoke.

Cost and Mode of Manufacture

In Japan at present, the mill cost of levulose can not be lowered below $3 per kg., owing to the high price of Jerusalem artichoke. Consequently, raw sugar (sucrose) or beet molasses has been used as the raw materials for levulose manufacture since 1949. It is certain that Jerusalem artichoke has no advantage as raw material, unless the price of fresh artichoke is less than 1/20 of that of sucrose. However, if there is any possibility of utilizing fresh artichoke directly the cost will be equal to that of sucrose, even if the artichoke is, in price, as high as 1/7 of sucrose.

Since the price of this tuber is, in general, lower than this, the cost will be considerably decreased, if such a scheme of production is adopted. If it is possible to produce yeast at the same time, further decrease of the cost by 10 to 20 percent will be expected. One of the best schemes to realize this would be to cultivate Jerusalem artichoke in the vicinity of a beet sugar factory with an attached yeast manufacturing factory, to extract fresh artichoke tuber by using a large diffusion battery during the winter, to preserve the concentrated converted juice till the spring of the next year, and by utilizing the season of cessation of beet sugar production to carry on levulose manufacture. This appears to be a most economical form of levulose production, considering the circumstances that direct extraction of fresh artichoke is at some important points more profitable than the use of dried artichoke.

Japan Levulose Co.,
385 Ichinotsubo, Kawasaki

7) T. Asai, H. Arioka, C. Sakurai, and S. Takahashi, *J. Agr. Chem. Soc. Japan*, **22**, 136~9 (1949) (in Japanese).

Über die Wirkung von Alkynolen als Säurebeizinhibitor

Von Kazumi YAMAMOTO

(Eingegangen am 26. April, 1954)

Einleitung

Zur Entfernung des Rostes von Eisen oder Stahl durch Säurebeize werden verschiedene Substanzen als Beizinhibitor verwendet, die die Auflösung von Eisen oder Stahl an sich schützen. Als solche Substanzen sind Stärke, Mineralöl, organische Basen, Salze des Arsens oder Antimons, Jodide, Phosphate, Benzoate, organische Schwefelverbindungen usw. schon wohl bekannt.

Jüngst hat Reppe[1] in seinem Buche veröffentlicht, dass Propargylalkohol und Butin-2-diol-1.4, welche beide aus Acetylen und Formaldehyd unter erhöhtem Druck hergestellt werden können, vorzügliche Säurebeizinhibitor sind, jedoch eingehende Data sind noch unbekannt.

In vorliegender Abhandlung sollen die Wirkungen der Alkynole erörtert werden.

Arbeitungsmethode

Experiment wurde nach der Einweichungsmethode durchgeführt, unter Verwendung von Probestücken des wohl polierten schweissbaren Stahls in einer Form rechteckiger Platte.

Fünf bis sechs Probestücke wurden in der Inhibitor enthaltenden wässrigen Säurelösung unter Rührung bei einer konstanten Temperatur eingeweicht und einer nach dem andern mit der bestimmten Zeit aufgehoben und nach der Wäsche mit Wasser und Alkohol, in Exsikkator getrocknet und dann gewogen.

Die Ätzung wurde durch den Zerfressungsgrad, der nach folgender Gleichung defeniert wird, ausgedrückt.

1) W. Reppe, "Acetylene Chemistry," Charles A. Meyer Co., N. Y. (1949), S. 96.

$$Z = \frac{\text{Gewichtsverlust des Probestücks (g.)}}{\text{Spezifisches Gewicht Probestücks} \times \text{Oberfläche desselben (cm}^2\text{.)}}$$

Demnach soll der Zerfressungsgrad Z die Dimension von cm. haben und die Tiefe der Ätzung für je eine Einheitsoberfläche des Probestücks bedeuten.

Experiment wurde zuerst in bezug auf die Inhibitorwirkung des Propargylalkohols für Salzsäure bis ins einzelne ausgeführt und danach hinsichtlich der verschiedenen Abkömmlinge.

Experimentelle Resultate

A. Der Effekt der Menge des Propargylalkohols. — Bei der praktischen Rostentfernung wird 8 bis 10 %-ige Salzsäure verwendet. Ich habe jedoch ziemlich konzentrierte Salzsäure, d.h., 20 %-ige, zum Versuch angestellt, um die Wirkung von der Probe auszudehnen. Experimentelle Resultate, die bei 24°C. erhalten wurden, sind in Figur 1 (dicke Linie) und 2 dargestellt.

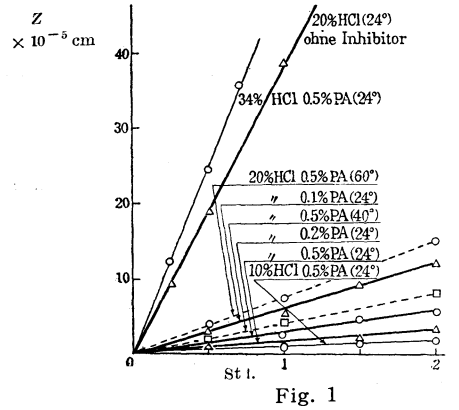


Fig. 1

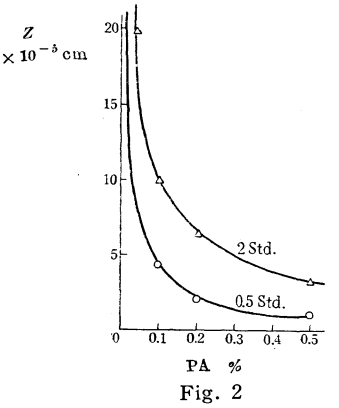


Fig. 2

Bei der Auflösung von Eisen durch Salzsäure ist es schon bekannt, dass sie gegen die Laufzeit in linearem Verhältnis steht. Das ist der Fall auch hier. Von obigen Figuren kann man verstehen, dass die Inhibitorwirkung des Propargylalkohols sehr bemerkenswert its und eine wirksame Grenzkonzentration desselben (0.5%) vorhanden ist.

Auf solche Weise kann der Zerfressungsgrad im Falle der Anwesenheit von Propargylalkohol mit $Z=1.75\times10^{-5}\,t$, wobei t die Laufzeit (Std.) bedeutet, ausgedrückt werden, dementgegen im Falle der Abwesenheit desselben mit $Z=3.75\times10^{-4}t$ (Fig. 1).

B. Einfluss der Temperatur.—Unter der Verwendung von 20%iger Salzsäure, in der Propargylalkohol (0.5%) enthalten ist, wurde der Zerfressungsgrad bei 24°, 40° und 60°C. bestimmt. Die Resultate sind in Figur 1 (punktierte Linie) und 3 dargestellt, von welchen man verstehen kann, dass eine Steigerung der Temperatur die Inhibitorwirkung des Propargylalkohols vermindert.

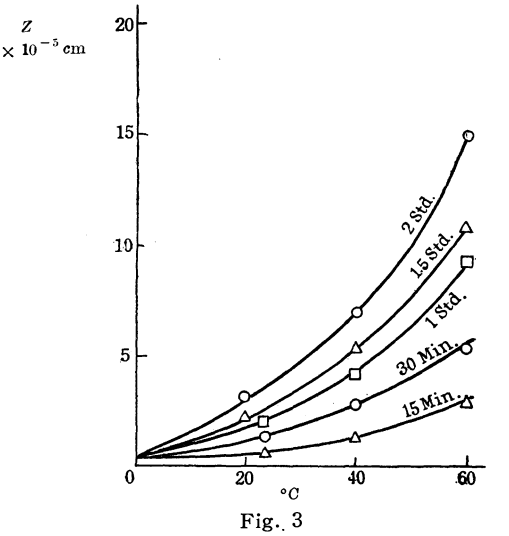


Fig. 3

C. Konzentration der Salzsäure.—Die Auflösung von den Probestücken durch Salzsäure verschiedener Konzentrationen, in der je 0.5 % Propargylalkohol enthalten ist, wurde bei 24° beobachtet.

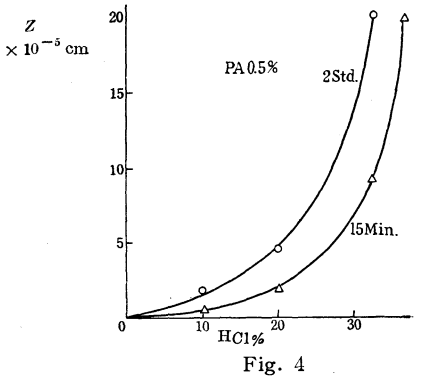


Fig. 4

Die Resultate sind in Figur 1 (dünne Linie) und 4 dargestellt.

Bei der Konzentration von Salzsäure über 25% ist die Inhibitorwirkung eindeutig dahingeschwunden. Es scheint mir, dass dies seinen Ursprung darin habe, dass des Propargylalkohols eigentümliche dreifache Bindung verloren geht, da es wohl bekannt ist, dass Propargylalkohol unter Bildung von Chlorallylalkohol leicht Chlorwasserstoff addiert.[2)]

D. Sparbeizwirkung von anderen Abkömmlingen.—Aus dem Gesagten wurde es klar dass Propargylalkohol bemerkenswerte Sparbeizwirkung hat. Demnach habe ich die Wirkung der unten zusammengefassten verschiedenen Abkömmlinge und der einigen olefinischen und gesättigten Alkohole untersucht, um den Mechanismus der Inhibitorwirkung derselben klar zu erkennen.

Verbindung	Formel	Abbreviation
Propargylalkohol	$HC{\equiv}C\text{-}CH_2OH$	PA
Butin-2-diol-1.4	$HOCH_2C{\equiv}C\text{-}CH_2OH$	BDO
3-Methylbutin-1-ol-3	$(CH_3)^2C(OH)\text{-}C{\equiv}CH$	MB
1,1,4,4-Tetramethylbutin-2-diol-1.4	$(CH_3)_2C(OH)C{\equiv}C\text{-}C(OH)(CH_3)_2$	TMBDO
Hexadiin-2.4-diol-1.6	$HOCH_2C{\equiv}C\text{-}C{\equiv}C\text{-}CH_2OH$	HDDO
Allylalkohol	$H_2C{=}CH\text{-}CH_2OH$	AA
n-Propylalkohol	$CH_3\text{-}CH_2\text{-}CH_2OH$	NPA

Experimente wurden in bezug auf 20%-ige Salzsäure, die je 0.5% von Inhibitor enthielt, bei 24° durchgeführt und deren Resultate sind in Figure 5 illustriert.

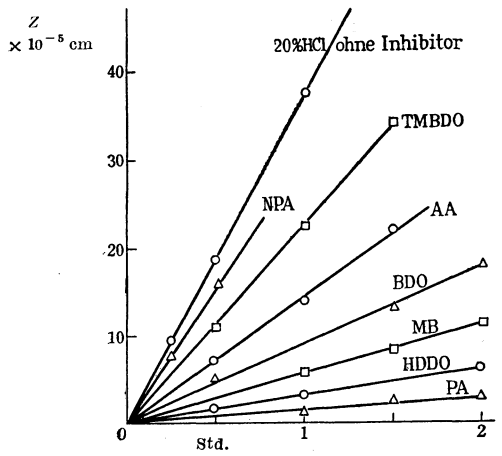


Fig. 5

Wie man von Figur 5 verstehen kann, werden die folgenden Schlüsse gezogen:

1. In bezug auf die gleiches Kohlenstoffatom besitzenden Alkohole nimmt deren Wirkung mit Zunahme von Unsättigungsgrad zu. (PA>AA>NPA)

2. Die Zunahme von Methylgruppe erniedrigt die Wirkung von Acetylenalkohol. Es scheint mir dies auf eine sterische Hinderung zurückzuführen. (PA>MB, BDO>TMBDO)

3. Hexadiindiol ist auch so wirksam wie Propargylalkohol.

E. Das Andere.—Die Sparbeizwirkung von Propargylalkohol für Schwefelsäure anstatt Salzsäure wurde ebenfalls probiert. Diese Resultate sind in Figur 6 gezeigt.

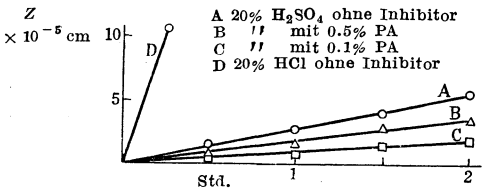


Fig. 6

Nicht nur die Probestücke von Eisen sondern auch die von Zink und Aluminium wurden unter Verwendung von 20%-iger Salzsäure, die 5% von Propargylalkohol enthält ausprobiert. Jedoch Propargylalkohol hat die Inhibitorwirkung für solche Metalle beinah nicht gezeigt.

Betrachtung der Resultate

Der Mechanismus der Sparbeizwirkung bisher bekannter Inhibitoren wird ungefähr in drei Klassen eingeteilt.

1) Inhibitor, der auf der Oberfläche des Eisens unlöslichen, dünnen Film bildet, wie Phosphate, Benzoate. 2) Inhibitor, der an sich positiv geladen ist und der auf der Grenzlinie des Kristalls von Metall, die die Anode der Lokalbatterie bildet, absorbiert wird, wie Stärke, organische Basen, Arsenverbindungen usw. 3) Inhibitor, der die Diffusionsgeschwindigkeit des Metallions auf dem Metall verspätet, wie Mineralöl usw.

Jedoch scheint es mir, dass die Wirkung der Alkynole keiner Gruppe angehört.

Jüngst hat Lüttringhaus[3)] die Sparbeizwirkung der Trithion und der Alkynole durch die chemisch-morphologische -C≡C-CH_2OH-Gruppen-Theorie erklärt.

Nur, mit diesem Experiment möchte ich nicht schliessen und stelle darüber eine Erläuterung auf.

In meiner Arbeit wurde gezeigt, dass auch Methylbutinol, die oben besagte -C=C-CH_2-OH Gruppe nicht hat, die die Sparbeizwirkung bietet, und dass selbst Allylalkohol, wenn es

2) W. Reppe u. a., *DRP* 764595.

3) A. Luttringhaus, H. Goetze, *Angew. Chem.*, **64**, 66 (1952).

auch gering ist, die Wirkung hat. Aber die experimentellen Resultate hinsichtlich der Alkynolabkömmlinge stellen dar, dass die Existenz der Methingruppe (HC≡) nicht gerade bedeutsam ist.

Folglich scheint es mir, dass doppelte oder dreifache Bindung in Molekül auf die Wirkung wesentlich Beziehung habe. Das heisst, die Rolle von OH-Gruppe ist nichts anderes als der Beitrag zur Löslichkeit für wässrige Säurelösung.

Meiner Meinung nach würde π-Bindung ungesättigter Verbindungen auf dem ferromagnetischen Metall wie Eisen durch eine Art induzierter, magnetischer Polarisation aufgebrochen. Und dann würden diese Verbindungen an Oberfläche—Fe—Atome mit Koördinationsbindung unter Bildung von dem Schutzfilme verbunden.

Schlusswort

Gemäss der Suggestion von Reppe wurde Sparbeizwirkung von Propargylalkohol und dessen Abkömmlingen ausgeprobt.

Es wurde beobachtet, dass Acetylenalkohole und Glykole mehr oder wenig Sparbeizwirkung haben und deren Unterschied hauptsächlich auf den sterischen Faktor der Verbindungen zurückzuführen ist.

Diese Wirkung wäre auf Grund der Koördinationsbindung von ungesättigten Verbindungen mit Oberfläche—Fe—Atome zu erklären.

Den Herren Dr. K. Yoshikawa und K. Maki danke ich für ihre fördernde Unterstützung und stetige Leitung zu dieser Arbeit.

Diese Arbeit wurde am 21. Feb. 1953 im Rahmen der Versammlung der japanischen chemischen Gesellschaft-Kyushu-Zweigabteilung in Omuta mündlich veröffentlicht.

Mitsui Chemical Industry Co.
Miike Dyestuff and Chemical Works,
Omuta, Fukuoka

Über die Herstellung von Styrol und Benzol aus Acetylen

Von Kazumi YAMAMOTO und Mitsuo OKU

(Eingegangen am 26. April, 1954)

Einleitung

Reppe[1] hat über die cyclisierende Polymerisation von Acetylen veröffentlicht, die in zwei Gruppen eingeteilt wird, wie folgt:

1) Bildung von Cycloöktateraen unter Tetramerisation von Acetylen

2) Bildung von Benzol unter Trimerisation von Acetylen, und hat gezeigt, dass bei der zweiten Reaktion Styrol als Nebenprodukt erhalten wurde, d.h., 88% Benzol neben 12% Styrol, wovon etwa die Hälfte als polymeres Produkt anfällt.

Cycloöktatetraen, Kohlenwasserstoff von 8-Gliederring, entspricht dem Isomer von Styrol und die Isomerierungswärme zum Styrol ist endothermisch (-36.1 Kcal./Mol.)[2].

Solche leichte Bildung von Styrol oder Benzol zeigt so die Möglichkeit, dass Styrol aus Acetylen, die Reaktionsbedingung gut gewählt, unmittelbar erhalten werden kann. Unsere Arbeit wurde von diesem Standpunkt durchgeführt.

Herstellung von Katalysator

1) Herstellung von Triphenylphosphin: Triphenylphosphin, das der Ausgangsstoff für den Katalysator Bistriphenylphosphin-Nickeldicarbonyl ist, wurde nach Wurtz-Reaktion aus Monochlorbenzol, Phosphortrichlorid und metallischem Natrium hergestellt:

$$3C_6H_5Cl + PCl_3 + 6Na \longrightarrow (C_6H_5)_3P + 6NaCl$$

2) Herstellung von Bistriphenylphosphin-Nickeldicarbonyl: Rose[3] hat Bistriphenylphosphin-Nickeldicarbonyl $(Ph_3P)_2Ni(CO)_2$, wobei Ph den Phenylrest ausdrückt, dadurch hergestellt, ätherische Lösung von Triphenylphosphin bei deren Kochpunkt mit Nickelcarbonyl einwirken zu lassen.

$$2Ph_3P + Ni(CO)_4 \longrightarrow (Ph_3P)_2Ni(CO)_2 + 2CO$$

Smp. 209°

Die Resultate unserer Nachprobe sind in Tabelle I zusammengefasst.

TABELLE I

HERSTELLUNG VON $(Ph_3P)_2Ni(CO)_2$

Ph_3P (g.)	$Ni(CO)_4$ (cc.)	Lösgmittel (cc.)		Reakt.-temp. (°C.)	Ausbeute von Komplex	
					(g.)	(% d. Th.)
13.1	3.2	Äther	30	35	14.6	91.4
13.1	3.2	Benzol	30	55	12.3	77.0
10.0	2.5	Methanol	50	50	9.6	78.7
10.0	3.8	Butanol	50	50	9.5	77.7

4) W. Reppe u. a., *Ann.*, **560**, 104 (1948).

2) W. Johnson, *J. Am. Chem. Soc.*, **72**, 626 (1950).

3) J. D. Rose, *J. Chem. Soc.*, **1950**, 69.

Die Ausbeuten sind zwar ziemlich gut, aber dieses Verfahren an und für sich ist unangenehm, da man sehr giftiges Nickelcarbonyl behandeln muss.

Wir fassten ins Auge, dass Nickelcarbonyl sich leicht durch Einwirkung des unter Druck stehenden Kohlenoxyds auf reduziertes Nickel bildet.

Dann stellten wir auf die Probe, die Komplexverbindung durch Reaktion von Kohlenoxyd mit methanolischer Lösung von Triphenylphosphin, in welcher reduziertes Nickel suspendiert ist, unter erhöhtem Druck und bei erhöhter Temperatur herzustellen.

$$2Ph_3P+Ni+2CO\longrightarrow(Ph_3P)_2Ni(CO)_2$$

Triphenylphosphin wurde so überschüssig verwendet, dass kein freies Nickelcarbonyl blieb. Das Experiment wurde gemäss 4×4-Latin Quadratverfahren in Bezug auf drei Faktoren, Anfangsdruck von Kohlenoxyd, Reaktionstemperatur und Laufzeit durchgeführt. Die Bedingungen waren wie folgt:

Anfangsdruck von CO	11	20	45	60	in at.
Temperatur	50	90	130	170	in °C.
Laufzeit	0:30	1:00	2:00	4:00	in Std.: Min

Andere konstante Bedingungen;

Autoklav	100 ccm. Inhalt
Triphenylphosphin	9 g., Methanol 50 ccm.
Reduziertes Nickel	3 g.

Verarbeitung von Reaktionsprodukt.—Nach Entfernung von nicht umgesetztem Triphenylphosphin mit heissem Methanol extrahiert man den Komplex, der in festem Zustand zurückgeblieben ist, mit Benzol. Der Komplex wird aus der Benzollösung als feiner, schöner Kristall erhalten. Die Resultate sind in Tabelle II zusammengefasst.

TABELLE II

UNMITTELBARE HERSTELLUNG VON KOMPLEX

CO-Atm.	Reaktemp. (°C.)	Laufzeit. (Std. Min.)	Komplex- (g.)	Zurückgewonn. Ph_3P (g.)	Komplex-Ausbeute (%)
11	130	2:00	2.6	5.2	56.1
60	170	0:30	9.2	1.7	100
11	90	4:00	1.0	8.1	91.1
60	130	1:00	8.4	1.0	93.0
11	170	1:00	4.2	4.3	73.2
45	90	1:00	2.6	5.9	69.8
20	90	0:30	1.1	7.5	60.1
60	90	2:00	3.2	5.4	74.2
45	50	2:00	3.4	3.7	52.6
45	170	4:00	11.3	0	100
45	130	0:30	4.2	4.1	70.3
20	130	4:00	4.7	3.9	72.6
11	50	0:30	0.5	7.8	35.6
60	50	4:00	5.5	3.9	88.3
20	50	1:00	0.9	8.1	81.9
20	170	2:00	9.3	0.6	91.2

Erläuterung von Resultaten

1) Betreffs der Ausbeuten wurde ein bedeutender Unterschied in Bezug auf drei Faktoren nicht erkannt. 2) Betreffs der Umsetzung kann man darauf schliessen, dass die Umsetzung des Triphenylphosphins von dem Druck des Kohlenoxyds ziemlich und von der Temperatur bedeutend abhängig ist.

Folglich wurden die besten Bedingungen (60 Atm. CO-Druck, 170°, 30 Min.) bestimmt, worunter der Komplex bei der Feststellungsprobe mit der Umsetzung von 88.5% und der Ausbeute von 100% festgesetzt wurde.

Vorläufige Betrachtung über die Bildung von Styrol

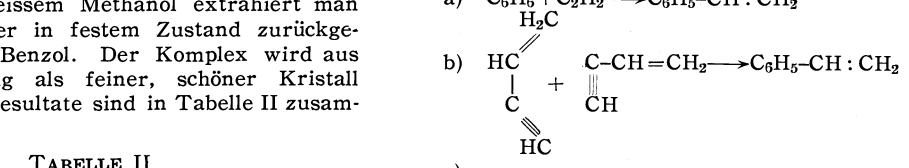
Wie oben gesagt, ist bekannt, dass man bei der cyclisierenden Polymerisation des Acetylens unter Verwendung von Bistriphenylphosphin-Nickeldicarbonyl und einem Lösungsmittel wie Benzol, 88% Benzol und 12% Styrol, wovon etwa die Hälfte als polymeres Produkt sich ausscheidet, erhalten kann.

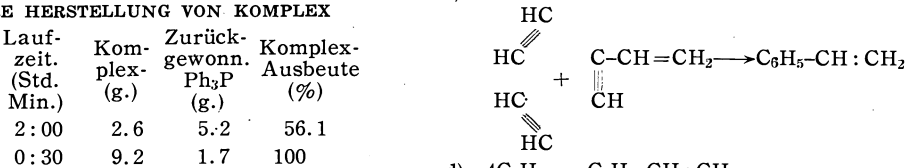
(1) $3CH{\equiv}CH\rightarrow C_6H_6$

(2) $4CH{\equiv}CH\rightarrow C_6H_5CH:CH_2$

Am Anfange unserer Arbeit, die Ausbeute von Styrol zunehmen zu lassen, betrachteten wir zuerst danach, auf welchen Mechanismus die Reaktion (2) verläuft. So nahmen wir folgende vier Reaktionen an:

a) $C_6H_6+C_2H_2\longrightarrow C_6H_5{-}CH:CH_2$

b)


c)


d) $4C_2H_2\longrightarrow C_6H_5{-}CH:CH_2$

Reaktion a), die unter Vinylierung von Benzol verstanden werden kann, muss wahrscheinlich ausserordentlich schwer sein. Reaktion b), die Dimerisation von Monovinylacetylen umfasst, das sich durch Dimerisation von Acetylen bildet, wird aus der Untersuchung von Dykstra[4] vermutet, in der er Styrol aus Monovinylacetylen unter Anwendung von Säure bei 105° mit Ausbeute von 20 bis 50% erhielt. Wir liessen Monovinylacetylen unter Anwendung von besagtem Komplexkatalysator und von Benzol bei 80° während 5 Stunden polymerisieren, aber konnten kein Styrol erhalten, sondern nur gelatineartiges, unlösliches Polymerisat.

4) H. B. Dykstra, *J. Am. Chem. Soc.*, **56**, 1626 (1934).

Demnach berechneten wir die Möglichkeit von Reaktion (c) und (d) thermodynamisch. Wärmetönungen von beiden Reaktionen wurden wie folgt berechnet:

c) $2C_2H_2+C_4H_4 \rightarrow C_6H_5\text{-}CH:CH_2+138.4$ Kcal.

d) $4C_2H_2 \rightarrow C_6H_5\text{-}CH:CH_2+82.6$ Kcal.

Aus diesen Werten wurden Gleichgewichtskonstanten (log Kp) nach Annäherungsgleichung von Nernst ausgerechnet.

TABELLE IV

GLEICHGEWICHTSKONSTANTEN

Temp. °C.	70	80	90	100	110	120
Log Kp (c)	72.74	70.20	67.80	65.52	63.38	61.19
Log Kp (d)	44.90	43.40	41.97	40.61	39.33	38.00

Von diesen wurden Freienergie (konst. Vol.) berechnet.

TABELLE V

FREIEENERGIE

Temp. °C.	70	80	90	100	110	120
$-\Delta Y$ (c) Kcal./Mol.	113.4	111.9	111.1	110.3	109.5	108.2
$-\Delta Y$ (d) Kcal./Mol.	69.8	69.4	69.0	68.4	68.1	67.5

Die Vorzüglichkeit der Reaktion (c) zeigt sich von obigen Werten. Dann haben wir über Mischpolymerisation von Acetylen und Monovinylacetylen gearbeitet.*

Verfahren, worin Monovinylacetylen mit Lösungsmittel in Reaktionsgefäss eingesetzt ist.

Monovinylacetylen wurde unter Anwendung von Nieuwlands Katalysator nach Verfahren von Shimo[5] hergestellt. Die Entfernung von Acetaldehyd, das den Katalysator vergiftet, wurde vorsichtig durchgeführt.

Ein Gemisch von gereinigtem Benzol und Komplexkatalysator Bistriphenylphosphin-Nickeldicarbonyl und Monovinylacetylen wird in Druckgefäss von 300 cc. Inhalt eingesetzt. Man presst nun unter Erwärmen ein Gemisch von 1 Teil Stickstoff und 1 Teil Acetylen auf, bis der Druck 20 at. beträgt. Bei etwa 110° setzt die Reaktion ein. Durch Nachpressen von frischem Acetylen hält man den Druck (ca. 30 Atm.) konstant. Die Temperatur kann im Laufe der Umsetzung auf 60 bis 70° gesenkt werden. Wenn die Absorption von Acetylen langsam wird, so wird das Reaktionsgemisch aus dem Druckgefäss nach Abkühlung herausgenommen, gewogen und mit Wasserdampf abdestilliert. Styrolgehalt in der Oelschicht wird nach KBr-$KBrO_3$-Verfahren bestimmt. Die Ausbeute von Styrol und Benzol wird unter Abziehung der Mengen von Benzol, ausgerechnet, das als Lösungsmittel eingesetzt wurde. Wenn Polyolefin sich nebenbei bildet, soll diese analytische Methode dementsprechenden Fehler begleiten. Aber das Resultat des Feststellungsversuches von Dibromstyrol (Smp. 73°) zeigte, dass Olefin ausschliesslich des Styrols beinahe abwesend war. Das nicht umgesetzte Monovinylacetylen konnte nicht zurückgewonnen werden, da es sich mit dem Abgase bei der Entspannung des Restdrucks im Autoklav verliert.

Die experimentellen Resultate sind in Tabelle VI zusammengefasst.

TABELLE VI

HERSTELLUNG VON STYROL UND BENZOL

Nr.	Bzl. (g.)	Kat. (g.)	MVA (g.)	Temp. (°C.)	Laufzeit (Std.)	Inkremt. (g.)	Benzol (g.)	Benzol (%)	Styrol (g.)	Styrol (%)	S/B
S-1	50	3	5	70–127	15	44.5	19.7	44.2	9.35	21.0	0.48
4	40	3	10	80–110	23	65	35.8	55.0	15.23	23.4	0.43
5	40	3	10	70–110	20	62	34.5	55.7	15.6	25.2	0.45
6	60	3	10	70–100	9	74	25.4	34.3	12.65	17.1	0.5
9	60	3	15	80–120	nicht reagiert						
11	60	3	20	80–120	nicht reagiert						
B-10	50	3	0	70–80	10	100	80.0	80.0	8.0	8.0	0.1

Bemerkungen: S/B ist das Verhältnis der Ausbeuten von Benzol und Styrol. Inkrement bedeutet die Summe von eingesetztem Monovinylacetylen und polymerisiertem Acetylen. Die Ausbeute sowohl von Benzol als von Styrol ist in diesem Inkrement begründet.

1) Mit dem Reaktionsverlaufe (als aufgenommene Acetylenmenge 15 bis 20 l.) wird die Reaktionsgeschwindigkeit langsam. Folglich muss man die Reaktionstemperatur auf 90 bis 120° steigern. Diese Temperatur ist um 20 bis 30° höher als die in dem Falle, in welchem Monovinylacetylen nicht verwendet wird. Es scheint, dass dies seinen Ursprung von höherer Konzentration des Monovinylacetylens hat, die den Verlust von der Aktivität des Katalysators durch Bildung eines schädlichen Nebenproduktes bringt.

5) K. Shimo, Gosei Gomu, S. 168 (1940).

* K. Yamamoto und M. Oku, *J. P.* 198913.

2) Die Ausbeute von Styrol, worin polymeres Styrol nicht umfasst wird, nimmt eindeutig mit Vergleich von der Ausbeute von Nr. B-10 zu.

3) Aus obigen Resultaten wird geschlossen, dass die am Anfange eingesetzten Mengen von Monovinylacetylen ihre Grenzen (bis ca. 20% auf Basis von Benzol) haben und dass auch die Zunahme von der Ausbeute des Styrols also ihre Grenze haben muss.

Verfahren, worin Monovinylacetylen mit Acetylen in Reaktionsgefäss eingepresst wird

Um den oben erwähnten Nachteil zu beseitigen, nahmen wir ein anderes Verfahren auf, worin Monovinylacetylen mit Acetylen in das Reaktionsgefäss nachgepresst wird. Acetylen wird durch druckfesten Verdampfer, worin Monovinylacetylen eingesetzt ist, in

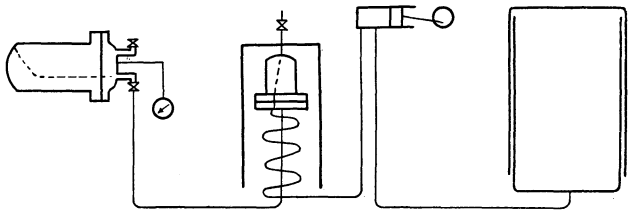


Fig. 1

das Reaktionsgefäss eingepresst. Das Molverhältnis von Acetylen zu damit begleitetem Monovinylacetylen wird durch Regelung der Temperatur von dem Verdampfer willkürlich bestimmt. Die Skizze von dem Reaktionsapparat ist in Figur 1 angegeben.

In Tabelle VII sind Sättigungsdruck von Monovinylacetylen bei verschiedener Temperatur, und in Tabelle VIII Molverhältnisse von dem unter 30 Atm. Druck stehenden, ge sättigten Acetylen-Monovinylacetylen-Gasgemisch angegeben.

TABELLE VII

SÄTTIGUNGSDRUCK VON MVA

MVA-Dampfdruck in Atm.	1	1.82	3.16	5.4	16.98	29.9
Temp. °C.	5	22.4	40	50	110	120

TABELLE VIII

C_2H_2: MVA. BEI 30 ATM. IN MOL.

°C.	C_2H_2	MVA.
22	16	1
60	5	1
80	2	1

Wenn die Reaktion nach folgendem Schema dargestellt wird, so kann man verstehen, dass die Temperatur von dem Verdampfer bei etwa 80° gehalten werden muss.

$$2C_2H_2+C_4H_4\rightarrow C_6H_5\text{-}CH:CH_2$$

Geringe menge Pyrogallol setzten wir in den Verdampfer ein, um die Polymerisation von Monovinylacetylen darin zu hemmen. Experimentelle Resultate nach diesem Verfahren sind in Tabelle IX gegeben.

TABELLE IX

HERSTELLUNG VON STYROL UND BENZOL

Nr.	Bzl. (g.)	Kat. (g).	MVA. (g.)	Verdamp. temp. (°C.)	Reakt.-temp. (°C.)	Laufzeit (Std.)	Inkrement (g.)	Benzol (g.)	Benzol (%)	Styrol (g.)	Styrol (%)	S/B
S13	50	3	4	25	70–90	12	54	35.2	67.7	14.9	28.6	0.42
14	50	3	5	25	70–90	14	76	43.4	57.1	18.6	24.5	0.43
18	50	3	12	60	70–80	11	57.5	25.6	44.5	14.4	25.0	0.56
19	50	3	30	80	70–90	7	50	13.5	27.0	28.5	57.0	2.11

Wie erwartet, nahm die Ausbeute von Styrol desto mehr zu, je grösser Verhältniss MVA/C_2H_2 wird (d.h., je höher die Temperatur von dem Verdampfer wird). Es ist bemerkenswert, dass die Ausbeute von Styrol in Nr. S19 mehr als die von Benzol wurde.

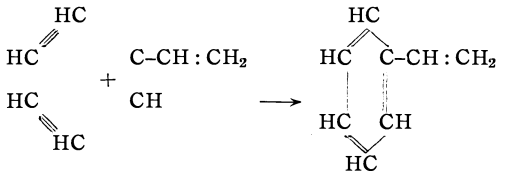
Auf solche Weise haben wir Styrol mit Ausbeute von 57% auf Basis von dem Inkremente erhalten können, das die Summe von aufgenommenem Acetylen und verwendetem Monovinylacetylen bedeutet.

Schlusswort

Bei der cyclisierenden Polymerisation des Acetylens erfolgt die Verwendung von Bistriphenylphosphin - Nickeldicarbonyl - Katalysator die Bildung von Benzol und Styrol und die von Nickelcyanidkatalysator[6] dementgegen die Bildung von Cyclopolyolefin wie Cycloöktatetraen. Diese zwei Katalysatoren müssen in wohl verschiedenen Mechanismen

6) W. Reppe, *Ann.*, **560**, 1 (1948).

einwirken. Der extreme Beweis dafür ist deren Verhalten bei Mischpolymerisation von Acetylen und Monovinylacetylen. In unserem Experiment, in welchem der erstere verwendet wurde, nahm die Bildung von Styrol zu, aber in dem von Hagiwara[7], in welchem der letztere angewandt wurde, dementgegen die Bildung von Cyclopolyolefin hoher Glieder, wie $C_{10}H_{10}$, $C_{12}H_{12}$. Der Mechanismus der Bildung von Benzolring an Komplexkatalysator ist ein Gegenstand späterer Arbeit. Wir haben dargestellt, dass Styrol sich durch Mischpolymerisation von Acetylen und Monovinylacetylen bildet, das durch Dimerisation von Acetylen erhalten wird, d.h.,



Darüber hinaus haben wir einen neuen Weg erschliessen können, bei welchem Styrol in unserem Lande aus leicht zugänglichem Rohstoff wirtschaftlich gut hergestellt werden kann.

7) N. Hagiwara, *J. Chem. Soc. Japan*, **73**, 323 (1952).

Diese Arbeit wird zusammengefasst, wie folgt:

1) Im Verfahren, worin Monovinylacetylen mit Lösungsmittel in dem Reaktionsgefäss eingesetzt ist, betrugen die Ausbeuten von Benzol und Styrol 50 bis 60% und 30 bis 20% beziehungsweise. Die Mengen von dem in Reaktionsgefäss eingesetzten Monovinylacetylen haben ihre Grenzen (bis ca. 20% auf Basis von einem Lösungsmittel).

2) Im Verfahren, worin Monovinylacetylen mit Acetylen in das Reaktionsgefäss eingepresst wird, betrugen die Ausbeuten von Benzol und Styrol 27% beziehungsweise und 57%.

Herr Dr. K. Yoshikawa hat uns immer bei unserer Arbeit geleitet und ermutigt. Ihm und der Mitsui Chemical Industry Co., die uns die Veröffentlichung unserer Arbeit erlaubte, sagen wir unseren herzlichen Dank.

Diese Arbeit wurde am 1. IV, 1954 im Rahmen der 7. Jahresversammlung der japanischen chemischen Gesellschaft in Tokyo mündlich veröffentlicht.

Mitsui Chemical Industry Co., Ltd. Miike Dyestuff and Chemical works, Omuta, Fukuoka

Kupferchromit als Katalysator bei der Propargylalkoholsynthese

Von Kazumi YAMAMOTO, Yōichi HIRUSAWA und Minoru YOSHIMURA

(Eingegangen am 26. April, 1954)

Einleitung

Es ist bekannt, dass Butindiol-1.4 und Propargylalkohol durch die von Reppe[1] gefundene Alkynolsynthese aus Acetylen und Formaldehyd in Anwesenheit von Kupferacetylid als Katalysator unter erhöhtem Druck erhalten werden.

Zur Gewinnung des Propargylalkohols, der wichtiger Ausgangsstoff für organische chemische Industrie ist, handelt es sich darum, auf welche Weise man die Bildung von Butindiol, das sich leichter als Propargylalkohol bildet, hemmen kann.

Murahashi[2] hat mit seinem Mitarbeiter hinsichtlich sowohl des Einflusses des Acetylendruckes als der Reaktionstemperatur und als der Wasserstoffionenkonzentration veröffentlicht. Yamamoto[3] von den Verfassern hat erfunden, dass das als Hydrierungskatalysator wirksame Kupferchromit von Adkins auch für Alkynolsynthese die spezifische Aktivität besitzt.

Wir haben also Reaktionsbedingung unter Anwendung von diesem Katalysator untersucht, Propargylalkohol vorzüglich zu gewinnen. Ferner haben wir die neue Erkenntnis über Selektivität des Chromitkatalysators für einseitige Umsetzung von Acetylen bei Äthinyrierung von Formaldehyd erhalten.

Arbeitungsmethode

Die verwendeten, verschiedenen Kupferchromite wurden gemäss Adkinsscher[4] Methode dargestellt. Das Experiment wurde im allgemeinen wie folgt durchgeführt:

In einem Autoklav von 600 cm^3. Inhalt, der

1) W. Reppe, " Acetylene Chemistry," Charles A. Meyer Co. N. Y. 1949, S. 84.

2) S. Murahashi, B. Ryutani, Mundliche Veröffentlichung bei der 3. Jahresversammlung der japanischen chemischen Gesellschaft, Osaka (1950).

3) K. Yamamoto und K. Sato, *J. P.* 187633.

mit Verdichter durch biegsames Kapillarrohr verbunden ist, erhitzt man Formalin-Kontakt Gemisch bei 120° unter Schüttelung und presst reines Acetylen auf 30 Atm. ein. Durch Nachpressen von Acetylen wird dieser Operationsdruck während des Reaktionsverlaufes, konstant gehalten. In manchen Fällen wurde ein Lösungsmittel wie Methanol oder Aceton verwendet.

Die nach der Filtration von Katalysator befreite Reaktionslösung lässt sich durch Widmersche Kolonne 2 m. lang fraktionieren. Dabei kann Propargylalkohol unter Bildung von Azeotrope mit 56%-igem Wassergehalt bei 97° erhalten werden. Von konzentrierter Mutterlauge wird Butindiol durch Destillation unter vermindertem Druck zurückgewonnen.

Die Ausbeute von Propargylalkohol wurde jodmetrisch bestimmt[5] und die von Butindiol wurde durch Destillation geschätzt.

Experimentelle Resultate und deren Betrachtungen

a) Einfluss der Konzentration von Formaldehydlösung.—Die Resultate der Experimente, in welchen 10 g. von 25 KAF.-Kupferchromit von Adkins als Vertreter, verwendet wurden, sind in Tabelle I zusammengefasst.

TABELLE I

EINFLUSS DER CH_2O-KONZENTRATION

Nr.	Konz. von CH_2O (%)	BDO-Ausbeute (g.)	(%)	PA-Ausbeute (g.)	(%)	Umgesetzt.CH_2O (%)	PA/BDO in Gew.
708	36.9	22.5	57.0	13.5	26.2	38.2	0.61
710	,,	23.0	58.2	13.9	26.8	85.0	0.62
715	17.9	17.4	44.0	17.7	34.4	78.4	1.02
717	11.9	19.2	48.6	19.6	38.1	86.7	1.02
721	,,	19.0	48.2	19.2	37.3	85.5	1.01
723	9.0	15.3	38.7	19.4	37.7	76.3	1.27
727	,,	15.3	38.7	20.1	31.0	78.3	1.33
724	7.4	8.3	31.3	13.7	39.8	71.1	1.65
726	,,	8.5	32.0	13.0	37.9	69.9	1.53
728	6.2	6.5	24.6	14.2	41.3	65.9	2.18
730	,,	6.6	24.8	13.0	37.9	62.7	1.96

BDO = Butindiol-1.4 PA = Propargylalkohol

Auch bei dem Kupferchromit-Katalysator nimmt die Bildung des Propargylalkohols je nach der Verminderung der Konzentration von Formaldehyd zu.

b) Effekt des Lösungsmittels. — Von der unten gezeigten zwei Gleichungen soll vermutet werden, dass die Ausbeute von Propargylalkohol durch Verdünnung von Formaldehyd mit so geeignetem Lösungsmittel, wie das Acetylen gut löst, verbessert werden kann.

$$CH{\equiv}CH + HCHO \longrightarrow CH{\equiv}C{-}CH_2OH$$

$$CH{\equiv}CH + 2HCHO \longrightarrow HOCH_2{-}C{\equiv}C{-}CH_2OH$$

Reppe[1,6] hat Tetrahydrofuran als solches und Kupferacetylid als Katalysator verwendet und Propargylalkohol mit Ausbeute von 59 % erhalten können. Wir haben den Einfluss von Methanol und Aceton, unter Anwendung von 10 g. 25-KAF-Chromit erforscht. Die Resultate sind in Tabelle II gezeigt.

TABELLE II

EFFEKT DES LÖSUNGSMITTELS

Nr.	Lösungsmittel (g.)	37%-CH_2O (g.)	BDO-Ausbeute (g.)	(%)	PA-Ausbeute (g.)	(%)	Umgesez. CH_2O (%)	PA/BDO in Gew.
723	Wasser 225	75	15.3	38.7	19.4	37.7	76.3	1.27
727	Wasser 225	75	15.3	38.7	20.3	39.6	78.3	1.33
666	Aceton 225	75	12.4	31.3	25.0	48.5	79.8	2.02
667	Aceton 225	75	10.8	27.3	25.4	49.2	76.5	2.34
674	Methanol 225	75	3.7	9.4	11.3	21.8	31.2	3.06
675	Methanol 225	75	3.8	9.6	10.8	19.6	30.4	2.38

Wie Tabelle II zeigt, ist Aceton als Lösungsmittel besser denn Methanol. Jedoch eine Sache von grösster Besorgnis ist es, dass Aceton, das auch aktive Carbonyl-Gruppe besitzt, durch das unter Druck stehende Acetylen äthinyliert werden könnte.

4) H. Adkins, *J. Am. Chem. Soc.*, **53**, 1095 (1931); **54**, 1138 (1932).

5) K. Yamamoto, M. Yoshimura, und M. Tanaka, Dieses Bulletin, **24**, 151 (1951).

6) W. Reppe, *J. P.* 148,022.

Es war nicht der Fall. Wie das Fraktionierungsdiagramm (Fig. 1.) zeigt, konnte keine Bildung von Methylbutinol, das bei 82 bis 83° mit Wasser azeotropisch destilliert werden soll, beobachtet werden.

$$CH_3COCH_3+CH{\equiv}CH\longrightarrow (CH_3)_2C(OH)-C{\equiv}CH$$

c) Einfluss der Acetonmenge.—Unter Anwendung besagten Katalysators wurde der Einfluss der Acetonmenge untersucht. Die Resultate sind in Tabelle III gezeigt.

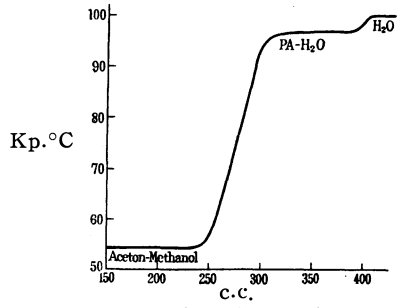


Fig. 1. Fraktionierungskurve von Reaktionsprodukt

TABELLE III

EINFLUSS DER ACETONMENGE

Nr.	36.9% HCHO (g.)	Aceton (g.)	BDO-Ausbeute (g.)	BDO-Ausbeute (%)	PA-Ausbeute (g.)	PA-Ausbeute (%)	Umgesetzt. CH_2O (%)	PA/BDO in Gew.
780	75	—	22.5	57.0	13.5	26.2	83.2	0.6
645	75	75	16.3	41.2	19.9	38.6	79.8	1.22
644	75	112.5	13.6	34.3	19.0	36.9	71.2	2.14
648	75	150	12.6	31.8	20.6	40.0	71.8	1.63
639	75	225	14.6	36.9	22.5	43.7	80.6	1.54
653	50	200	8.5	32.1	18.6	54.0	86.1	2.18
711	50	250	9.0	34.0	19.5	56.6	90.6	2.17

Wie vermutet wurde, ist sowohl die Umsetzung des Formaldehyds als auch die Ausbeute von Propargylalkohol desto höher, je mehr die Acetonmenge steigt. Auf solche Weise haben wir Propargylalkohol mit der Ausbeute von 55 % unter hoher Umsetzung erhalten können.

d) Vergleich der verschiedenen Kupferchromite.—Adkins[4] hat verschiedene Kupferchromite, die kleine Mengen Erdalkalimetall enthalten, entwickelt, wie 25-KAF (Ba), 30-RAC (Ba), 40-KAF (Sr), 39-KAF (Ca). Die zum Vergleich der Aktivität benützte Kontaktmenge war je 10 g.

Auf Tabelle IV ist eindeutig zu sehen dass von diesen Chromiten hinsichtlich der Umsetzung von Formaldehyd und der Ausbeute des Propargylalkohols 25-KAF am wirksamsten ist. Die verwendeten Mengen von 37%-igem Formaldehyd und Aceton waren beziehungsweise 75 g. und 225 g.

TABELLE IV

VERGLEICH DER VERSCHIEDENEN KUPFERCHROMITKATALYSATOREN

Katalysator	BDO-Ausbeute (g.)	BDO-Ausbeute (%)	PA-Ausbeute (g.)	PA-Ausbeute (%)	Umgesetzt CH_2O (%)	PA/BDO in Gew.
25-KAF Cu-Ba-CrO	9.8	24.7	24.1	46.3	71.0	2.46
,,	10.8	27.3	26.1	50.2	77.5	2.60
30-RAC Cu-Ba-CrO	13.3	33.0	24.0	46.1	79.1	1.80
,,	13.7	34.6	24.4	47.3	81.9	1.78
40-KAF Cu-Sr-CrO	14.5	36.7	20.5	39.8	76.5	1.41
,,	14.7	37.2	22.5	43.6	80.8	1.53
39-KAF Cu-Ca-CrO	6.8	17.2	16.7	32.3	49.5	2.45

e) Effekt der Essigsäurenwäsche von 25-KAF.—Im allgemeinen hat üblicher Kupferoxydkatalysator (wesentlich Kupferacetylid) die Neigung zur Butindiolbildung. Dementgegen ist gezeigt worden, dass Kupferchromitkatalysator spezifisches Verhalten bietet. Dies wird durch folgenden Vergleich des Effektes der Essigsäurenwäsche von 25-KAF-Chromit dargestellt. Geröstetes, rohes Chromit wurde in zwei Teile geteilt. Ein Hälfte wurde, so wie sie ist, verwendet, während die andere Hälfte nach der Wäsche mittels 50 %-iger Essigsäure bei 50° unter Rührung während einer Stunde von beigemengtem Kupferoxyd befreit wurde. Katalytische Wirkung dieser beiden Chromite wurde unter Verwendung 75 g. von 37%-igem Formaldehyd mit 225 g. Aceton verglichen (Tabelle V).

TABELLE V

EFFEKT DER ESSIGSÄURENWÄSCHE VON 25-KAF

	BDO-Ausbeute (g.)	(%)	PA-Ausbeute (g.)	(%)	umgesetzt. CH_2O (%)	PA/BDO in Gew.
Rohes Chromit	14.3	36.2	21.4	41.6	77.8	1.50
,,	14.6	36.9	22.5	43.7	80.6	1.54
Gewasch. Chromit	9.8	24.7	24.7	46.3	71.0	2.46
,,	10.8	27.3	27.3	50.2	77.5	2.60

Die gefundenen, analytischen Zusammensetzungen beider Chromite zeigen, dass das Atomverhältnis Cu : Cr unter Berücksichtigung von dem mit Barium sich zu verbindenden Chromatom, nahe an dem Wert von Stroupe[7] 1 : 1 ist.

	Cu %	Ba %	Cr %	Cu:Ba:Cr
Rohes Chromit	31.98	7.71	29.09	10:2.8:10.7
Gewasch. Chromit	22.29	10.06	30.62	10:5.4:16.9

f) Selektvität des Chromitkatalysators.— Die Bildung von Butindiol aus Acetylen und Formaldehyd ist so zu erklären, dass sich zuerst Propargylalkohol aus Acetylen und einem Molekül Formaldehyd auf Katalysator bildet und dann ferner mit einem Molekül Formaldehyd Butindiol ergibt. So soll vermutet werden, dass Chromitkatalysator gegen sekundäre Reaktion, Butindiol aus Propargylalkohol und Formaldehyd, inaktiver als Kupferoxyd (wesentlich Kupferacetylid) sei.

Das experimentelle Resultat, das unter folgenden Bedingungen erhalten wird, ist in Tabelle VI dargestellt.

Ausgangsstoffe; 37% Formaldehyd 30g. (HCHO 11.10 g), Propargylalkohol 9.225g, Katalysator 5 g.

Experiment wurde in Abwesenheit von Luft bei 120° während einer Stund durchgeführt.

Diese Resultate erweisen die Selektivivität des Chromitkatalysators, die auch durch den Effekt der Essigsäurenwäsche von Kupferchromit dargestellt wurde.

7) T. D. Stroupe, *J. Am. Chem. Soc.*, **71**, 569 (1949).

TABELLE VI

BUTINDIOL AUS PROPARGYLALKOHOL

Katalysator	Reaktionsgemisch HCHO (g.)	PA (g.)	BDO (g.)	BDO-Ausbeute % d. Th. an PA
25-KAF	10.38	8.88	0.34	2.40
CuO	9.58	6.89	2.82	19.9
,,	9.45	5.55	3.21	22.7

Schlusswort

Wir haben über die Synthese von Propargylalkohol unter Anwendung von Kupferchromit, das von Adkins als Hydrierungskatalysator entwickelt worden ist, gearbeitet. Und wir haben nicht nur die optimalen Bedingungen darüber finden können, sondern auch die Erkenntnis erhalten, dass die katalytische Wirkung von Kupferchromit von der des Kupferoxyds ziemlich verschieden ist.

Es sei uns gestattet, dem Herrn Dr. K. Yoshikawa, auf dessen Anregung vorliegende Arbeit entstanden ist, an dieser Stelle unseren ergebensten und herzlichsten Dank auszusprechen für die warme und fördernde Leitung an unserer Arbeit.

Diese Arbeit wurde am 20. I, 1951 im Rahmen der japanischen chemischen Gesellschaft Kyushu-Zweigabteilung in Fukuoka mündlich veröffentlicht.

Mitsui Chemical and Industry Co., Miike Dyestuff and Chemical Works, Omuta, Fukuoka

Über die neue synthetische Methode von Carbonäsuren durch Carbonylierung von aromatischen, halogenierten Kohlenwasserstoffen

Von Kazumi YAMAMOTO und Kazutoshi SATO

(Eingegangen am 26. April, 1954)

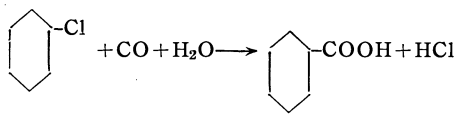
Einleitung

In der Arbeit über die Herstellung von Adipinsäure durch Carbonylierung von Butandiol-1.4 haben wir die Tatsache gefunden, dass Benzoesäure sich durch Einwirkung von Kohlenoxyd auf Monochlorbenzol bildet, welches als Lösungsmittel verwendet wurde.

Auf Grund dieser Erfindung der neuen Reaktion haben wir Carbonylierung von verschiedenen halogenierten, aromatischen

Kohlenwasserstoffen durchgeführt und entsprechende aromatische Carbonsäure erhalten können.

Diese neue Reaktion verläuft wie allgemeine Carbonylierung von Alkohol[1] in Anwesenheit von Wasser und unter Anwendung von carbonylbildungsfähigem Metall oder dessen Halogenid als Katalysator bereits bei 250 bis 300° und 200 bis 300 Atm.

z. B. 

Diese neue Reaktion wird folglich die Verwendbarkeit von aromatischen halogenierten Kohlenwasserstoffen in der organischen synthetischen Chemie vergrössern, d. h., die Herstellung der Benzoesäure aus Chlorbenzol, die der Terephthalsäure aus *p*-Dichlorbenzol, welche als Rohmaterial der synthetischen Faser insbesondere wichtig ist.

Wir wollen etwas über die bisher veröffentlichten, analogen Reaktionen sprechen, bevor wir unsere Arbeit beschreiben.

Hopf[2] hat Essigsäure aus Chlormethan und Kohlenoxyd unter erhöhter Temperatur in Anwesenheit von Aluminiumchlorid erhalten. Frank[3] und Theobold[4] haben auch Essigsäurechlorid oder dessen chloriertes Derivat aus mono- oder polychloriertem Methan unter ähnlichen Bedingungen hergestellt.

$$CCl_4 + CO \rightarrow CCl_3COCl$$
$$HCCl_3 + CO \rightarrow HCCl_2COCl$$
$$H_3CCl + CO \rightarrow H_3CCOCl$$

Groombridge[5] hat auch gefunden, dass oben beschriebene Reaktionen unter katalytischer Einwirkung von Nickel oder dessen Salze glatt verlaufen.

Wir haben am Anfange dieser Arbeit keine Beschreibung über die Reaktion von aromatischem, halogeniertem Kohlenwasserstoff und Kohlenoxyd in einer Literatur finden können.

Unsere Arbeit, wobei ein Autoklav von 18:8 Stahl verwendet wurde, war nicht gerade vollständig, da fortlaufender Versuch wegen der Ätzung der Gefässwand, die auf Einwirkungen von gebildeten Säuren zurück zuführen ist, abgebrochen werden musste.

Beschreibung der Versuche

1. Arbeitungsmethode. Im Autoklav (18:8 Stahl) von 100 cc. Inhalt wird das Gemisch von aromatischem, halogeniertem Kohlenwasserstoff, Wasser und Katalysator eingeschaltet und Kohlenoxyd von 150 bis 200 Atm. nach Verdrängung von Luft eingepresst. Wird das Reaktionsgemisch auf 250 bis 300° gehitzt, so beobachtet man das Auftreten der Umsetzung durch plötzlichen Druckabfall. Die Umsetzung verläuft im allgemeinen in weniger als 30 Minuten.

Als Katalysator gilt in erster Linie Nickel oder dessen Halogenide, insbesondere Nickeljodid. Die Umsetzung verläuft ohne Zugabe von einem Medium, aber im allgemeinen ist die Zugabe von geeignetem Lösungsmittel, wie Glykol, Ester, Benzol usw. erwünscht.

Das Reaktionsgemisch lässt sich aus dem Autoklav herausnehmen und mit Natronlauge behandeln und filtrieren. Gebildete Carbonsäure wird von der auf solche Weise erhaltenen Lösung des Natriumsalzes mit Schwefelsäure niedergeschlagen und umkristallisiert.

2. Experimentelle Resultate. Unsere typenhaften, experimentellen Resultate sind in folgenden Tabellen zusammengefasst.

a) REAKTIONSBEDINGUNGEN

Nr.	Ronstoff (g.)		H_2O (g.)	Katalysator (g.)		Medium (g.)		Reakt.temp. (°C.)	Max. Druck (Atm.)
1	Chlorbenzol	10	10	NiJ_26 Ni	1	Butandiol	15	300	280
2	〃	10	10	NiJ_23 Ni	1	Butylacetat	10	290	261
3	Jodbenzol	10	10	NiJ_23 Ni	1	〃	10	250	250
4	〃	10	10	Ni 3		—	—	300	260
5	*p*-Dichlorbenzol	10	10	NiJ_23 Ni	1	Butylacetat	10	300	240
6	*o*-Chlortoluol	10	10	NiJ_22 Ni	1	〃	10	300	320
7	β-Chlornaphthalin	10	10	NiJ_23 Ni	1	〃	10	280	235
8	*p*-Chlorphenol	10	10	NiJ_23 Ni	1	〃	10	280	240
9	Jodbenzol	10	10	Ni 3		Methanol	10	300	310

b) RESULTATE

Nr.	Druckabfall (Atm.)	Carbonsäureausbeute (g.)		(%)	Nebenprodukt
1	80	Benzoesäure	7.1	65.3	Adipinsäure, Valeriansäure
2	31	〃	10.3	95	Essigsäure, 〃

1) W, Reppe, "Neue Entwicklungen auf dem Gebiet der Chemie des Acetylens und Kohlenoxyds", Springer Verlag (1949) S. 110.
2) H. Hoff, *Ber.*, **64**, 2739 (1931).
3) C. Frank u. a., *Ind. Eng. Chem.*, **41**, 2061 (1949).
4) C. Theobold, *A. P.* 2378048; *C. A.*, **39**, 4084 (1945).
5) W. Groombridge, *E. P.* 621520: *C. A.*, **43**, 6650 (1949).

3	21	〃	6.3	100	〃 〃
4	18	〃	5.5	92	Diphenyl*
5	30	Terephthalsäure	3.5	31	Benzoesäure 4.9 g.*
6	15	*o*-Toulylsäure	6.5	60.5	Essigsäure, Valeriansäure
7	15	*β*-Naphthoesäure	5.5	52.4	Naphthalin 1 g.*
8	Keine Umsetzung				
9	10	Benzoesäuremethyl	1	—	Essigsäure, Methylacetat

* Daneben wurden Essig- und Valeriansäure isoliert.

Betrachtung der Resultate

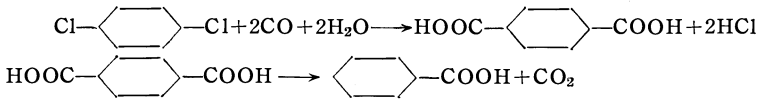
Die Reaktion verlief langsam ohne Zusatz von Reaktionsmedium. Butylacetat liess die Umsetzung als solches glatt verlaufen, wenn gleich es an sich zum Teil durch den Angriff von Kohlenoxyd gemäss der folgenden Gleichung Essig- und Valeriansäure lieferte:

$$CH_3COO\text{-}C_4H_9 + CO + H_2O \rightarrow CH_3COOH + CH_3CH_2CH_2CH_2COOH$$

Der Verlust von Kohlenoxyd betrug im allgemeinen 200 bis 300% an theoretischer Menge, die zur Bildung aromatischer Carbonsäure erforderlich ist. Auch oben erwähnte Nebenreaktion ist natürlich eine der Ursachen, aber eine hauptsächliche Ursache ist die Wassergasreaktion, die durch das Sein von Wasserstoff und Kohlensäure im Abgase bewiesen werden kann.

$$H_2O + CO \rightarrow H_2 + CO_2$$

Wie es in Nr. 5 erkannt wird, bildet sich Benzoesäure, deren Bildung auf die Kohlensäureabspaltung von zuerst gebildeter Terephthalsäure gegründet werden muss.



Man kann Terephthalsäure durch einen anderen, zweckmässigeren Weg herstellen, d.h., durch Oxydation von leicht umkristallisierbarer *p*-Toluylsäure, die nach der neuen Reaktion von *p*-halogeniertem Toluol mit Kohlenoxyd in guter Ausbeute erhalten werden muss. Die Umsetzung von Chlorbenzol verlief bei 290° bis 300°, aber die von Jodabkömmling trat bei 250° unter Anwendung von Nickeljodidkatalysator zusammen mit Nickelpulver als Hilfskatalysator ein. Wenn Alkohol wie Methanol im Reaktionssystem vorhanden ist, so könnte man die Bildung von aromatischem Carbonsäureester vermuten. Unter solcher Annahme wurde das Experiment Nr. 9 durchgeführt. Jedoch Methylbenzoat bildete sich nur in geringem Umfang. Dies soll zeigen, dass die Carbonylierung aromatischen Halogenkohlenwasserstoffes im Vergleich mit der des Methanols bei weitem schwieriger ist. In solchem Falle wurde also die Bildung von Essigsäure und deren Methylester stets beobachtet.

$$CH_3OH + CO \rightarrow CH_3\text{—}COOH \quad \text{und}$$
$$2CH_3OH + CO \rightarrow CH_3COOCH_3 + H_2O.$$

Der Mechanismus der neuen Carbonylierung des aromatischen, halogenierten Kohlenwasserstoffes ist noch nicht aufgeklärt, aber es scheint uns, dass der Abbruch der Bindung zwischen dem Halogen- und Kohlenstoffatom die wichtigste Stufe dieser Umsetzung, von den experimentellen Tatsachen aus gesehen, z.B. die leichtere Umsetzbarkeit von Jodbenzol mit Vergleich von Chlorbenzol oder die beobachtete Bildung von Diphenyl (vgl. Nr. 4), ist.

Die zweite Stufe ist wahrscheinlich die Bildung von Säurechlorid, das sodann durch Verseifung mit Wasser die entsprechende Carbonsäure liefert. Das zur Entwicklung der neuen Reaktion schwierigste Problem ist die Ätzung von Reaktionsgefäss, die ihren Ursprung in erzeugter Salzsäure und Carbonsäure hat und die so heftig war, als dass wir diese Arbeit hätten fortsetzen können.

Wir möchten hier hinzufügen, dass unsere Arbeit unter neuer Gegenmassnahme fortgesetzt wird.

Schlusswort

Wir haben die neue Reaktion zur Synthese von Carbonsäuren aus aromatischen halogenierten Kohlenwasserstoffen in Anwesenheit von Wasser bei erhöhter Temperatur unter erhöhtem Druck von Kohlenoxyd unter Anwendung von Nickelverbindung als Katalysator gefunden.

Diese neue Reaktion gibt die Möglichkeit, dass wichtige Zwischenprodukte für organische chemische Industrie, wie Benzoesäure, Phthalsäure, Terephthalsäure usw., von billigen, leicht zugänglichen Rohstoffen aus mit guter Ausbeute hergestellt werden können.

Für dieses Verfahren zur Herstellung von aromatischen Carbonsäuren haben wir japanisches Patent am 13. Juni 1951 angemeldet.[6]

Zum Schluss sprechen wir dem Herrn Dr.

6) K. Yamamoto und K. Sato, *J. P.* 196859.

K. Yoshikawa für seine Anregung und stetige Leitung zu dieser Arbeit unseren besten Dank aus.

Darüber hinaus zum Teil von Forschungskosten für diese Arbeit wurde die Unterstützung für wissenschaftliche Forschung des Jahrganges 1952 von dem Unterrichtsministrium verwendet. Wir sagen unseren verbindlichsten Dank dafür.

Diese Arbeit wurde am 2. IV. 1953 in der 6. Jahresversammlung der japanischen chemischen Gesellschaft in Kyoto mündlich veröffentlicht.

Mitsui Chemical and Industry Co. Ltd.
Miike Dyestuff and Chemical Works
Omuta, Fukuoka

LETTER

On the Heterogeneity of Calf Thymus Histone

By Nobuo Ui

(Received May 24, 1954)

Since the studies of Kossel and Lilienfeld[1], histones have been a well-known class of proteins, but their chemical and physicochemical properties are not yet clearly understood. Recent workers[2] have discovered a heterogeneity of calf thymus histone, but because of the preparation methods employed in these investigations it is possible that some changes in the protein had been produced during the purification processes.

In the present investigation histone was prepared carefully from acid extracts of calf thymus gland, and examined for its heterogeneity. An attempt was also made to fractionate the preparations.

Method 1. Fresh calf thymus glands were frozen, minced, homogenized in 0.05 M sodium citrate at *p*H 7.0 (or in dilute citric acid) and centrifuged. The sediment was washed with the solvent several times to remove cytoplasmic contaminants and then the histone was extracted from the sediment with 0.1 or 0.2 N sulfuric acid (Extract A). After clarifying "Extract A", the histone was precipitated by addition of two volumes of ethanol at low temperature (sometimes below 0°C.) and reprecipitated several times.

The preparation obtained was free from deoxypentose nucleic acid and its nitrogen content was 18.2%. Tryptophane content was estimated to be less than 0.2%. This preparation was found to be inhomogeneous both in electrophoresis and ultracentrifuge.

Fractional precipitation of the purified histone preparation by ethanol yielded mainly two fractions. Fraction I, precipitated at lower ethanol concentrations, revealed two components in the ultracentrifuge, the sedimentation constants ($s_{20,w}$) of which were 1.9 S and about 7 S respectively in an acetate buffer of *p*H 5.0 and ionic strength 0.2. The heavier component amounted to about one-third of fraction I and its sedimentation constant varied with different preparations. Fraction II, precipitated at higher ethanol concentrations, was ultracentrifugally almost homogeneous ($s_{20,w}=1.0$ S), but electrophoretically not homogeneous.

Fraction II differed from fraction I in the fact that it could not be precipitated by addition of ammonia to its solution, but like fraction I was soluble in H_2SO_4-$HgSO_4$ reagent[3].

Method 2. From the above-mentioned "Extract A" histone could also be salted out by addition of ammonium sulfate. The fraction, which was obtained at 80% saturation of ammonium sulfate, contained two components ($s_{20,w}=2.1$ and 12 S). A second fraction, which precipitated between 80% and 100% saturation of ammonium sulfate, was also inhomogeneous ($s_{20,w}=0.8$, 1.9 and 15 S).

Method 3. According to the method of Mirsky and others[3,4] histone was extracted from thymus nuclei with 0.2 N hydrochloric acid and precipitated by bringing the dialyzd extract to a *p*H value of about 10 by sodium hydroxide. Fractional precipitation, by in-

1) A. Kossel, "The Protamines and Histones," London and New York (1928).

2) L. Ahlström, *Arkiv. Kemi. Mineral. Geol.*, **24**A, No, 31 (1947); E. Stedman and E. Stedman, *Phil. Trans. Roy. Soc. London*, Ser. B. **235**, 565 (1951); J. Grégoire, J. Grégoire, and J. Reynand, *Compt. rend.*, **236**, 1922 (1953).

3) A. E. Mirsky and A. W. Pollister, *J. Gen. Physiol.*, **30**, 117 (1946).

4) M. M. Daly, A. E. Mirsky and H. Ris, *J. Gen. Physiol.*, **34**, 439 (1951).

creasing the *p*H of the solution, yielded at least three different fractions, and a final fraction soluble in alkaline solution was precipitated by adding ethanol at *p*H 10.9. None of these fractions were homogeneous in the ultracentrifuge.

From the above observations it was concluded that calf thymus histone is not a homogeneous protein, but consists of many fractions having different molecular weights and charges.

Studies on the homogeneity of the histone sample which was prepared without using acid are now in progress and will be published soon with the details of the present investigations.

The author wishes to express his sincere thanks to Assistant Professor I. Watanabe for his kind advices and encouragement.

Institute of Science and Technology,
Tokyo University, Komaba-machi
Meguro-ku, Tokyo

Paper Fraction Analyzer

By Nobuo TAMIYA, Yukichi YOSHINO and Tokuro SODA

(Received March 6, 1954)

Since its invention, the fraction collector proved to be widely applicable in various fields of chemistry. The authors tried to construct a very simple apparatus (see Fig. 1) capable of collecting fractions drop by drop on a long moving strip of filter paper[1], and obtained satisfactory results. The drops of the liquid collected on the filter paper were treated by suitable techniques such as are used in paper chromatography.

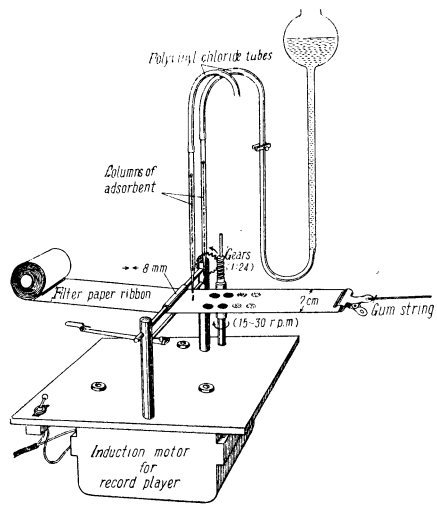


Fig. 1 "Paper fraction collector"

Using a small amount of ion-exchange resin as adsorbent, different metallic ions[2] were collected separately on different parts of the moving paper, as may be seen in Fig. 2. After spraying them with ammonium sulfide solution, the strips of the filter paper were dipped in melted paraffin in order to make the filter paper transparent and in order to stabilize the colors, and the metallic sulfides on the paper were estimated colorimetrically. The coloration is proportional to the concentration of dropped solution, provided that it is not less than 0.030 M/l.

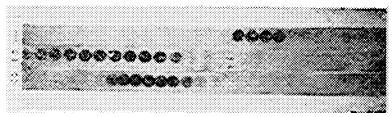


Fig. 2 Strips of filter paper, the colorimetric data of which are shown in Fig. 3. (photographed under ultraviolet light) 1—HgS, 2—CdS, 3—CuS.

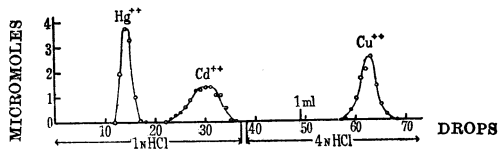


Fig. 3 Separation of Hg^{++}, Cd^{++} and Cu^{++} ions by the paper fraction analyzer. 10 micromoles each of mercuric, cadmium and cupric ions were adsorbed on a column of 0.45 ml. (5.1 cm. in height) of Amberlite IR 120 (180–250 mesh) from sulfates solution (0.033 M/l respectively) in 0.31 N nitric acid. After washing with distilled water, the cations were eluted by hydrochloric acid (1 N and 4 N) at a velocity of 1 drop per minute.

Fig. 4 shows the result of an experiment

1) B. Drake, *Nature*, **160**, 602 (1947).
2) R. Wickbold, *Zeit. anal. Chem.*, **132**, 26 (1951).

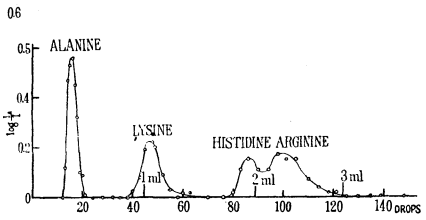


Fig. 4 Separation of amino acids by the paper fraction collector. 1 Micromole each of alanine, lysine, histidine and arginine were chromatographed by a column of Amberlite XE 64 (0.24 ml., 5.0 cm. in height) with a buffer of *p*H 5.95 (mixture of 0.2 M sodium citrate buffer and 0.2 M sodium phosphate buffer at the ratio of 2:1 in volume[4]) at the same rate as in the above experiment.

by this "paper fraction analyzer" in which basic amino acids and alanine were separated by Amberlite XE 64[3,4]. The amino acids on the filter paper were colorimetrically determined after treatment with ninhydrin solution[5] and melted paraffin. Amino acid-ninhydrin coloration thus treated did not change for several months.

The Chemical Institute, Faculty of Science, Tokyo University

3) C.H.W. Hirs, S. Moore, and W.H. Stein, *J. Biol. Chem.*, **200**, 493, (1953).
4) S. Ishii, and T. Ando, "Symposium on Biological Chemistry", October, 1953 (Tokyo).
5) R.R. Redfield, and E.S.G. Barron, *Arch. Biochem. and Biophys.*, **35**, 443 (1952).

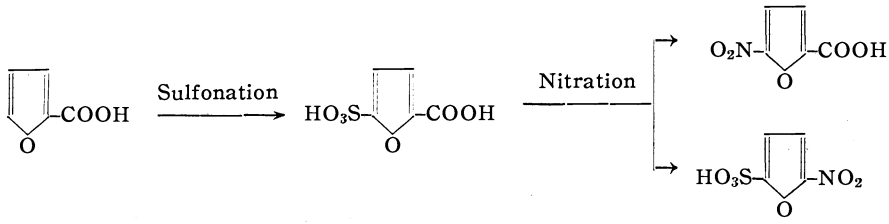
*Studies on Nitration of Furan Derivatives. Part I. On the Nitration of Furan-carboxylic Acid**

By Tadashi SASAKI**

(Received February 6, 1954)

Many types of α-nitrofuran derivatives have been synthesized by Saikachi and the present author to find any chemotherapeutically interesting compound.[1] In every case, the nitration of furan derivatives appears to be the most important. The object of the present studies is to find out the relationship between the structure of furan derivatives and the possibility of their nitration. In this paper the nitration of furan-carboxylic acid is reported.

As to the preparation of nitrofuran-carboxylic acid, there have been several methods,[2] but only a few of them are thought to be applicable for practical use. Hill and his collaborators[3,4] succeeded in carrying out the preparation of nitrofuran-carboxylic acid, in which furan-carboxylic acid was at first sulfonated with fuming sulfuric acid, then nitrated with fuming nitric acid. Their results showed that the product of sulfonation was stable against an acidic reagent and when it was treated with fuming nitric acid, it was converted to nitrofuran-carboxylic acid and nitrofuran-sulfonic acid by nitrosubstitution after decarboxylation or desulfonation as follows:



As, unfortunately, their reports lacked details on the experiments, the present study was carried out. In Part I, the nitration of furan-carboxylic acid was carried out in accordance with the procedure of Hill and White[4] and the relation of the yield of the product to the temperature and the time of reaction was studied. In Part II, the yield of the nitration of sulfofuran-carboxylic acid, obtained by the sulfonation of furan-carboxylic acid, in accordance with the procedure of Hill ane Palmer[3], was investigated. In Part III, the nitration of sulfofuran-carboxylic acid by the mixture of fuming nitric acid and acetic anhydride was studied.

Experimental

I. Nitration of Furan-carboxylic Acid

30 g. of furan-carboxylic acid was sulfonated with 90 g. of fuming sulfonic acid (d=1.951), with stirring below 20°C according to the known method[5]. After allowing it to stand at room temperature for one day, the resulting black viscous mixture was nitrated with 75 g. of fuming nitric acid (d=1.46), by dropping it to the solution at 0°, and then warming it gradually to the definite temperature as shown in Table I, and kept for three hours. The further treatment was the same as the procedure of Hill and White[4]. When the reaction mixture was above 40°, considerable bubbling started and the viscosity of the mixture diminished, the color turning to a light yellow. Above 50° the evolution of nitrogen oxide was observed. As shown in Table I, the lower the temperature of the reaction, the larger the yield of nitrofuran-carboxylic acid. The increasing yield of dinitrofuran with the rising of the temperature of the reaction is probably due to the conversion of nitrofuran-carboxylic acid into dinitrofuran and the conversion is presumably promoted by a catalytic action of the present sulfuric acid. Furthermore, in this reaction the production of nitrofuran-sulfonic acid can hardly be seen. This fact clearly shows that nitrofuran-sulfonic acid is more easily convertible to dinitrofuran than nitrofuran-carboxylic acid is. The effect

* This paper was presented before the Annual Meeting of the Chemical Society of Japan in April, 1949.

** Institute of Scientific Research for Practical Life, Medical Faculty of Kyoto University; Yoshida-konoe-cho, Sakyo-ku, Kyoto, Japan.

1) T. Takahashi, H. Saikachi and T. Sasaki, *J. Pharm. Soc. Japan*, **68**, 42 (1948); **69**, 284 (1949).

2) Four methods are given in Beilstein's Org. Chem., **18**, 287 (Hauptband).

3) H. B. Hill and Palmer, *Am. Chem. J.*, **10**, 380 (1888).

4) H. B. Hill and R. White, Ibid., **27**, 196 (1905).

5) H. Schwanert, *Ann.*, **116**, 269 (1860); H. Hodgson and H. R. Davies, *J. Chem. Soc.*, 806 (1939).

with the time of the reaction at 7° after the addition of fuming nitric acid on the yield is given in Table II. The products in the above experiments were identified by their m.p. which were in good accordance with the description of Hill and White[4].

TABLE I

No.	Reaction Temp.	N.F.C.*	Yield	D.F.*	Yield	N.F.S.*	Yield
1	0 °C	13.5 g.	32%**	1.2 g.	3%	Trace	
2	10	12.0	30	1.5	3.5	—	
3	20	7.0	17	2.0	5	—	
4	30	4.0	10	3.5	8	—	
5	40	4.0	10	3.0	7	—	
6	50	1.0	2.5	4.0	10	—	
7	60	—		3.0	7	—	

* N.F.C.: nitrofuran-carboxylic acid, m.p. 184°.
N.F.S.: nitrofuran-sulfonic acid potassium salt.
D.F.: dinitrofuran, m.p. 101°.

** The maximum yield ever reported.

TABLE II

No.	Reaction Time	N.F.C	Yield	D.F.	Yield	N.F.S.	Yield
8	1 hour*	8.5 g.	20%	0.5 g.	1.2%	Trace	
9	1 day*	11.5	28	1.0	2.5	—	
10	3 days**	10.0	24	1.8	4.0	—	
11	7 days**	9.0	22	2.5	6.0	—	

* After nitric acid was added to a strirred solution at 7°, stirring was continued for one hour at 7°.

** After stirring of the mixture was continued for one hour at 7°, the mixture was left to stand at room temperature of 20° for 1, 3 and 7 days, respectively.

II. Indirect Nitration of Furan-carboxylic Acid*

Nitration was carried on the sulfofuran-carboxylic acid which was obtained from furan-calboxylic acid, after sulfonation similar to that in part I. Sulfofuran-carboxylic acid was obtained in the form of the barium salt by Hill and Palmer[3] and no physical constants of the free acid have been reported. The present author obtained free sulfofuran-carboxylic acid from its salt as follows: the calcium salt which was obtained by the same procedure as the barium salt, was treated with the calculated amount of sulfuric acid and the resulting calcium sulfate was filtered off. After the filtrate was condensed on a boiling water bath till its color changed to black, it was left to stand in a desiccator of conc. sulfuric acid for several days to yield a colorless amorphous solid of sulfofuran-carboxylic acid, which was used for nitration. The yield of the acid was 85% of the theoretical amount, calculated from the starting furan-carboxylic acid.

20 g. of sulfofuran-carboxylic acid was portionwise added to a stirred 60 g. of fuming nitric acid (d=1.46), at several reaction temperatures and the mixture was stirred for a while or left to stand at room temperature as shown in Table III. The following procedure and identification of the products were the same as those described by Hill and Palmer[3]. The results are shown in Table III, which indicates that at lower temperature the yield of nitrofuran-sulfonic acid is comparable to that of nitrofuran-carboxylic acid and the production of dinitrofuran can hardly be seen, but with the rising of the temperature, both yields, of nitrofuran-sulfonic acid and -carboxylic acid, decreased.

III. Nitration of Sulfofuran-carboxylic Acid

11 g. of sulfofuran-carboxylic acid was portionwise added at −5° to the nitrating mixture which was previously prepared by mixing 28 g of fuming nitric acid (d=1.46), with 60 g. of acetic anhydride at −10°. After the addition of sulfofuran-carboxylic acid, stirring was continued for three hours and then the reaction mixture was poured on ice and neutralized with potassium carbonate. Following the procedure of Hill and Palmer[3], there were obtained nitrofuran-carboxylic acid as a main product and dinitrofuran as a by-product and the production of nitrofuran-sulfonic acid could not be seen. The results given in Table IV show that desulfonation takes place more easily to some extent than decarboxylation.

* Indirect nitration means that nitrofuran-carboxylic acid was obtained by the nitration of isolated sulfofuran-carboxylic acid, prepared by sulfonation of furan-carboxylic acid.

TABLE III

No.	Reaction Condition	N.F.C.	Yield	D.F.	N.F.S.	Yield
12	Addition at 10°, stirring at 10° for 5 hrs.	3.5 g.	22%	—	5.0 g.	20%
13	Addition at 10°, stirring at 30° for 5 hrs.	5.0	31	Trace	5.5	22
14	Addition at 10°, stirring at 45° for 5 hrs.	4.0	25	Trace	5.0	20
15	Addition at 10°, standing at 20°* for 3 days	5.0	31	—	4.5	18.5
16	Addition at 23°, stirring at 23° for 6 hrs.	4.0	25	—	4.5	18.5
17	Addition at 23°, standing at 20°* for 3 days	4.0	25	—	5.0	20
18	Addition at 60°, stirring at 60° for 6 hrs	2.0	13	1.0 g. (6%)	1.0	4
19	Addition at −3°, stirring at −3° for 2 hrs	3.5	22	—	4.5	18.5

* Room temperature of 20°.

TABLE IV

No.	Reaction Temp.	N.F.C.	Yield	D.F.	Yield	N.F.S.
20	− 5°C	2.5 g.	16%	0.3 g.	2%	—
21*	− 5	2.8	17	0.5	3	—
22	−10	2.5	16	0.15	1	—

* One drop of conc. sulfuric acid was added to the reaction mixture.

Summary

From the preparative point of view, the nitration of furan-carboxylic acid after sulfonation was studied with the following results:

(1) In order to obtain nitrofuran-carboxylic acid, the nitration of furan-carboxylic acid after sulfonation was carried out without separating the sulfonation product at several temperatures and the yield at 0° was about 32%, the highest ever known.

(2) In order to obtain nitrofuran-sulfonic acid, indirect nitration of sulfofurancarboxylic acid should be carried out at a low temperature, such as below 10°; the yield of which amounts to 20–22%. However, in this case, nitrofuran-carboxylic acid is produced simultaneously as a by-product.

(3) When the nitration of sulfofuran-carboxylic acid was carried out by using acetic anhydride and fuming nitric acid, nitrofurancarboxylic acid and dinitrofuran were obtained, but not nitrofuran-sulfonic acid. This showed that desulfo-nitrosubstitution took place more easily than decarboxy-nitrosubstitution.

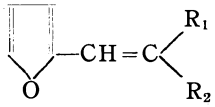
The author wishes to express his gratitude to Professor H. Saikachi of Kyushu University for his kind advice and encouragement in the course of the study.

Institute of Scientific Research for Practical Life, Medical Faculty of Kyoto University, Kyoto

Studies on Nitration of Furan Derivatives. Part II. On the Nitration of Furfurylidene-type Compounds***

By Tadashi SASAKI*

(Received February 6, 1954)

The earliest reported nitro-substituted furan compounds were obtained by the nitration of furan-carboxylic acid[1] or by that of other stable furan compounds such as the products obtained by condensation of furfural with compounds possessing reactive methylene group[2, 3, 4]. In Part I of these studies the former reaction was studied and in the present study the nitration of some furfurylidene compounds belonging to the latter reaction were studied by using two kinds of nitrating reagents, fuming nitric acid (d=1.46) and the mixture of acetic anhydride and fuming nitric acid (d=1.46). Furfurylidene compounds to be nitrated, having a general formula  (where R_1 and R_2 are both electrophilic radicals as shown in the experimental part) were prepared by the condensation of furfural with the corresponding reactive methylene compounds.

Experimental

Nitration was carried out on 13 kinds of furfurylidene compounds described below (shown in Table II) by the following two methods of nitration. In method 1, nitration was carried out at −5∼−10° by using the starting material, acetic anhydride and fuming nitric acid in a ratio of 1:5.6:5.6 in mol. unit. In method 2, the starting material was added portionwise at −5° to a stirred fuming nitric acid which was thrice the amount of the starting material. In both cases, stirring was continued for one hour after the addition. When the nitration product was suspended in the reaction mixture, it was filtered. But when the nitration product was dissolved in the reaction mixture, the reaction mixture was poured on cracked ice, and the resulting oil was treated with the solvent suitable to separate the nitration product in a pure state.

(1) Nitration of Ethyl Furylacrylate.—Ethyl furylacrylate was prepared by Claisen condensation[5].

Method 1: Gilman[4] reported already on this nitration by using the starting material, nitric acid and acetic anhydride in mol. ratio of 1:3.2:5.5, yielding 51%. But the present author's experiment with the same mol. ratio resulted in only 29.5%. Furthermore, the yield of the reaction with 1:5.6:5.6 mol. ratio was 49.5%. The m.p. of the product was in good accordance with that described by Gilman, m.p. 123°[4]. In the second method decomposition occurred and the nitrated product was not obtained.

(2) Nitration of Furfurylideneacetone.—Furfurylideneacetone was prepared by the method of Organic Syntheses[6].

Method 1: When the nitration temperature was −5∼−10°, no crystalline product could be isolated from the red oil which was obtained by pouring the clear red reaction mixture on cracked ice. But when nitration was carried out at −25°, a very small amount of a yellow crystalline product, m.p. 120–135°, was obtained by the addition of a very small amount of alcohol to the red oil which was obtained by pouring the reaction mixture on cracked ice. Its semicarbazone, decomposition point 224°, was identified with that prepared by another method[7].

In the second method decomposition occurred.

(3) Nitration of bis-Furfurylideneacetone.—Bis-furfurylideneacetone was prepared by the method of Organic Syntheses[6].

Method 1: 4.3 g. of bis-furfurylideneacetone, m.p. 52–4°, was dissolved in 10 cc. of acetic anhydride and this solution was nitrated at −5° by the mixture of fuming nitric acid (20g.) and acetic anhydride (30 cc.). In a while, precipitation occurred in the stirred reaction mixture. After stirring was continued for two hours, the reaction mixture was filtered off to give a crude product which was recrystallized twice from acetic acid to a yellow needle crystal, m.p. 198–200° (decomp.) with 5% yield.

Found: N, 8.98, Calcd. for $C_{13}H_8O_7N_2$: N, 9.21%.

In the second method decomposition occurred.

(4) Nitration of Furylacrolein.—Furylacrolein was prepared by König's method[8].

Method 1: When the nitration temperature was −5∼−10°, the nitrated product could not be isolated. The nitration was carried out below −15° and the resulting red solution was poured on cracked ice. The red oil, separated, was dissolved in ethylacetate and the solution was left to stand in an ice box for several days to give a small amount

* Part I, this Bulletin, **27**, 395 (1954).

** A portion of this paper was presented before the Annual Meeting of the Chemical Society of Japan in April, 1949.

1) H. B. Hill and Palmer, *Am. Chem. J.*, **10**, 380 (1888); H. B. Hill and R. White, Ibid., **27**, 196 (1905).

2) B. Priebs, *Ber.*, **18**, 1362 (1885).

3) R. Heuck, Ibid., **28**, 2256 (1895).

4) H. Gilman, *J. Am. Chem. Soc.*, **52**, 2550 (1930).

5) L. Claisen, *Ber.*, **24**, 143 (1891).

6) Org. Syn., Col. Vol. I, 301.

7) This will be reported in Part IV of this study.

8) W. König, *Ber.*, **58**, 2559 (1925).

of a red needle-like crystal, m.p. 112–4°, which was recrystallized from methanol to result in a brilliant red crystal, m.p. 114–5°; the yield was as low as 0.4%. This compound was identical with the specimen prepared by another method which is a more suitable preparation for this compound[9].

In the second method decomposition occurred.

(5) Nitration of Furylacrylic Acid.—Furylacrylic acid was prepared by the method of Organic Syntheses[10].

Method 1: Nitration of furylacrylic acid, F.A.A., was carried out in detail as a standard for nitration of other furfurylidene compounds. Gilman's procedure, slightly modified, was used[4]. The results by changing the ratio of F.A.A. and the nitration mixture are given in Table I, which shows that the maximum yield was obtained when F.A.A., nitric acid and acetic anhydride were in mol. ratio of 1:5.6:5.6. The yield in this mol. ratio was 48.5% at the nitration temperature of −7° and 55% at that of −15°, which seems to indicate that the yield is higher when the nitration temperature is lower. Both yields were higher than that of Gilman whose yield was 40%[4]. In this case, however, the addition of a small amount of conc. sulfuric acid made the yield less and the color of the reaction mixture more reddish. Excess of the nitration mixture decreased the yield and especially the excess of nitric acid resulted in the oxidative destruction occurring during the filtration of the nitration product. On the contrary, the yield became greater when F.A.A. was added directly to the nitrating mixture than when it was added in the form of a solution in acetic anhydride according to the procedure of Gilman[4].

In the second method decomposition occurred.

(6) Nitration of Nitrovinylfuran. Nitrovinylfuran was prepared by Thiele's method[11].

Method 1: The nitration product appeared in the form of a suspension in a red colored nitration mixture. The precipitate was filtered and washed with cold water to give a crude product, m.p. 134–9°, which was identical with that prepared by method 2.

Method 2: Priebs[2] reported on this nitration, in which the yield was not described. A dark red solution, obtained by nitration, was poured on cracked ice and the resulting brown precipitate was filtered and washed with water to give a crude product, m.p. 132–5°, which was identified by mixed melting point with the specimen of Priebs, m.p. 143°, after recrystallization from alcohol.

(7) Nitration of Ethyl Furfuralmalonate.—Ethyl furfuralmalonate was prepared by Knoevenagel's condensation[12].

Method 1: A yellow solution which was obtained by nitration, was poured on cracked ice and the resulting yellow oil gradually solidified. It was filtered to result in a crude product, m.p. 75–83°, which was recrystallized from ethanol and identified with the specimen prepared by method 2.

Method 2: Heuck[3] reported on this nitration qualitatively. The dark blue solution which resulted from the nitration was poured on cracked ice and the resulting oil gradually solidified to give a crude product, m.p. 84–89°, which was identified after recrystallization from ethanol with the specimen prepared by Heuck, m.p. 106–8°[3].

(8) Nitration of Ethyl 3-(2-furyl)-2-Acetylacrylate.—Ethyl 3-(2-furyl)-2-acetylacrylate was prepared by Claisen condensation[13].

Method 1: The reddish blue reaction mixture was poured on cracked ice and the resulting red oil was washed several times with cold water by decantation and mixed with a small amount of ethanol. A crystalline product was separated from the mixture and it was purified by recrystallization from ethanol to give a light yellow, corn-like crystal, m.p. 127–9°.

Found: N, 5.62, Calcd. for $C_{11}H_{11}O_6N$: N, 5.57.

Method 2: The reaction mixture changed to dark red. By the same procedure as method 1, a crude product was obtained. This was recrystallized from ethanol and identified by mixed melting point with the specimen prepared by method 1.

(9) Nitration of Ethyl 3-(2-furyl)-2-Cyanoacrylate. — Ethyl 3-(2-furyl)-2-cyanoacrylate was prepared by Beckert's method[14].

Method 1: The nitrated product appeared in the form of a suspension in the reaction mixture after being dissolved once completely. The precipitate was filtered to give a crude product, decomposition point 145–50°, which was identified with the specimen prepared by method 2.

Method 2: Heuck[3] reported concerning this nitration, but did not describe the yield. The nitrated product was obtained in the form of a suspension in the reaction mixture. By pouring it on cracked ice a crude product, m.p. 130–45°, was obtained which was recrystallized from ethanol to give the same m.p. 153° as described by Heuck[3]. In this case, the addition of one drop of conc. sulfuric acid to the reaction mixture was useful to prevent the mixing of a small amount of the unreacted material.

(10) Nitration of Diacetylvinylfuran.—Diacetylvinylfuran was prepared as follows: 5 g. of freshly distilled furfural, $b.p._{19}$ 62°, and 5 g. of acetylacetone, b.p. 136–137°, were dissolved in 15 cc. of ethanol. To this solution was added 3 cc. of piperidine in pyridine solution (1%) and the resulting mixture was heated in a water bath of 70° for four hours. The solvent was removed under reduced pressure and the residual oil was extracted with ether. The ether layer was washed twice with 15 cc. of water and dried with anhydrous sodium sulfate. After removing ether, the residual dark red oil was distilled under reduced pressure. The greater part distilled at 138–140°/3 mm. Hg., amounting to 6 g., and the yield was 65%.

Found: C, 67.26; H, 5.45, Calcd. for $C_{10}H_{10}O_8$: C, 67.41; H, 5.61%.

Method 1: When the starting material was

9) H. Saikachi et al; *Japan J. Pharm. & Chem.*, **22**, 258 (1950); **23**, 188, 270 (1951).
10) Org. Syn. Col. Vol II, 956.
11) J. Thiele and H. Landers, *Ann.*, **269**, 303 (1909).
12) E. Knoevenagel, *Ber.*, **31**, 2595 (1895).
13) H. Claisen and F. E. Mathews, *Ann.*, **218**, 175 (1883).
14) C. Beckert, *J. prakt. Chem.*, (2), **50**, 17 (1894).

added in the form of a solution in a small amount of acetic anhydride, a clear yellow solution was obtained. After pouring the reaction mixture on cracked ice, the resulting oil was cooled by ice water to give a yellow crystal with a low melting point, 28°.

Found: N, 6.50, Calcd. for $C_{10}H_9O_5N$: N, 6.28%.

Method 2: The nitration product was obtained instantly after the addition of the starting material to stirred fuming nitric acid. After pouring the reaction mixture on cracked ice, the same procedure as that used in the above method 1 was applied for isolating the nitrated product to give a product of m.p. 28°, which was identified with the specimen of method 1.

(11) Nitration of Furfuralmalonitrile.—Furfuralmalonitrile was prepared by Heuck's method[15].

Method 1: A small amount of the nitrated product precipitated from the yellow clear solution. The reaction mixture was poured on cracked ice and the precitate was filtered to give a crude product of m.p. 173° (decomp.), which was identified with the specimen of method 2 after recrystallization from ethanol by a mixed melting point.

Method 2: Heuck[3] reported on this nitration, but did not describe the yield. A clear solution was obtained in the course of the nitration. Following the same procedure as method 1, a crude product of m.p. 173–5° was obtained, which was recrystallized from ethanol to result in raising its melting point to 179°, which was in good accordance with the description of Heuck[3].

(12) Nitration of 2-Cyano-3-(2-furyl) acrylic Acid.—2-Cyano-3-(2-furyl)acrylic acid was prepared by Heuck's method[16].

Method 1: The color of the reaction mixture changed to blue and the nitrated product precipitated gradually. After pouring the reaction mixture on cracked ice, a dark red precipitate was filtered and washed with water to give a crude product of m.p. 241–5° (decomp.), which was recrystallized from ethanol and was identical with the specimen of method 2.

Method 2: The same procedure as method 1 was applied on the dark red reaction mixture. A crude product of m.p. 246–9° (decomp.) was recrystallized from ethanol to give a compound of m.p. 250° (decomp.), the same as that of Heuck[3].

(13) Nitration of Furfuralmalonic Acid.—Furfuralmalonic acid was prepared by Knoevenagel's condensation[17]. Method 1 and 2 were applied to this compound. The evolution of carbon dioxide was observed and the nitrated product could not be isolated. This nitrated product was prepared by another method[10].

The results of the above experiments are summarized in Table II.

TABLE I

NITRATION OF FURYLACRYLIC ACID (F.A.A.)

F.A.A.	Nitration Mixture		Temp. of Nitration	Yield	(decomp. of the Product
	HNO_3	Ac_2O			
mol.	mol.	mol.	°C	%	°C
0.25	0.25	1.40	−7	10.77	228°
„	0.50	1.40	„	23.73	223°
„	0.65	1.40	„	28.02	„
„	1.00	1.40	„	32.32	„
„	1.15	1.40	„	38.88	„
„	1.40	1.40	„	43.09	„
„	1.55	1.40	„	38.88	„
0.25*	0.75	0.75	„	43.60	„
„	1.40	1.40	„	48.50	„
„	1.75	1.75	„	43.00	„
„	1.40	1.40	−15	55.00**	„
„	1.40	1.40	−15	49.00***	„

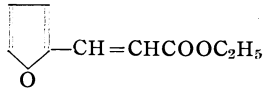
* Furylacrylic acid was added directly into the nitration mixture. In other experiments without asterisk the same acid was added in the form of a solution in acetic anhydride.

** The maximum yield ever known.

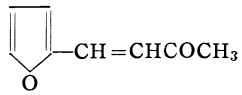
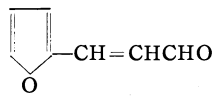
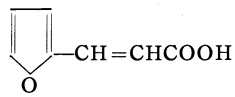
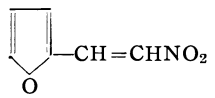
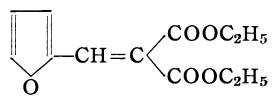
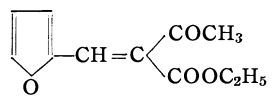
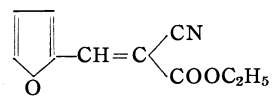
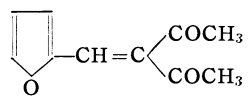
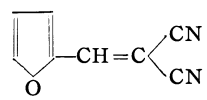
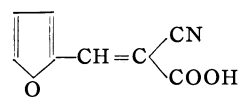
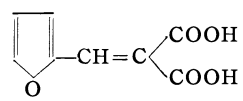
*** One drop of conc. sulfuric acid was added to the reaction mixture.

TABLE II

NITRATION OF FURFURYLIDENE COMPOUNDS

Ex. No.	Compound to be nitrated	Method 1		Method 2	
		Yield %	m.p. of the product °C	Yield %	m.p. of the product °C
(1)		49.5	123°		*

15) R. Heuck, *Ber.*, **28**, 2253 (1895).
16) R. Heuck, Ibid., **27**, 2625 (1894).
17) E. Knoevenagel, *Ber.*, **31**, 2612 (1898).

(2)		0.1	224 (dec.)**	*	
(3)		5.0	200 (dec.)	*	
(4)		0.4	114 (dec.)	*	
(5)		48.5	223 (dec.)	*	
(6)		23.0	134–9	35.8	128–32
(7)		96.5	75–83	92.5	84–89
(8)		10.3	127–9	11.8	128–9
(9)		26.8	145–50 (dec.)	61.0	130–45 (dec.)
(10)		60.0	28	20.0	28
(11)		30.0	173	52.5	173–74
(12)		35.3	241–5 (dec.)	54.9	246–49 (dec.)
(13)		*		*	

* Decomposition occurred and no crystalline product was obtained.

** The m.p. (dec.) is that of its semicarbazone of the produced nitro-furfurylideneacetone.

Summary

The nitration, by using both fuming nitric acid mixed with acetic anhydride and fuming nitric acid alone, was carried out on 13 kinds of furfurylidene compounds,

C_4H_3O–CH=CR_1R_2.

(1) These furfurylidene-type compounds in which R_1 and R_2 are electro-groups are stable against both acidic reagents and can be nitrated without formation of the nitration intermediate.

(2) In the case of a group being –CHO or –$COCH_3$, the nitration temperature must be

kept low enough to avoid decomposition.

The author wishes to acknowledge the help of Professor H. Saikachi for his constructive advice on this work. Gratitude is also extended to Mr. K. Suzuki, Instructor of Kyoto Pharmaceutical College, for assistance given the author in the preparations. Elementary analysis was carried out by Miss H. Iwata and Mr. K. Imaeda, Pharmaceutical Department, Medical Faculty of Kyoto University.

Institute of Scientific Research for Practical Life, Medical Faculty of Kyoto University, Kyoto

On the Distribution and Variation of Nutrient Salts in the Adjacent Water to the Aleutian Islands in the North Pacific

By Rinnosuke FUKAI

(Received February 27, 1954)

Introduction

Oceanographical observations in the salmon fishing ground have been carried out in the region adjacent to the Aleutian Islands on board R. V. "Tenyo-maru", covering over 80 days from May to July in 1952. The author has been engaged in these observations and had an opportunity of analysing a number of water samples on board the vessel. On the basis of the data obtained in the field as well as in the laboratory, the distribution and variation of nutrient salts in the waters of this region have been considered in the present paper.

Although the sea region under consideration has been regarded as one of the most important fishing grounds of the world together with the vicinity of Newfoundland and the North Sea, systematic investigations concerning chemical problems in this region have scarcely been reported except those carried out by Ratomanov (1936)[1] and Barnes and Thompson (1938)[2]. Even in the comprehensive investigation conducted by Barnes and Thompson, the regions mainly concerned were restricted to the eastern side of long. 180° while little information on the Eastern Hemisphere has been available up to now.

Some problems related to the consumption of nutrient salts by marine organisms will also be discussed here.

The Sea Region under Consideration

The region under study is located within the square enclosed by the longitudes of 170°E and 180° and the latitudes of 50°N and 55°N, extending over both sides of the Aleutian Ridge as it is indicated in Fig. 1 with

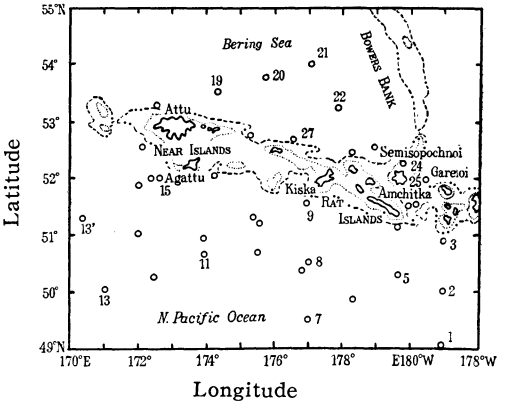


Fig. 1. Oceanographical Stations and Bottom topography near the Western Aleutian Islands. Dotted and broken lines indicate bottom contours of 200 m. and 500 m. depths, respectively.

oceanographical stations and bottom contours. As shown in the figure, the Bering Sea covers an area north of the ridge and the southern area is covered with a portion of the North Pacific. In this region, the Bering Sea forms a very deep basin, while in the east part off the region it becomes much shallower to form the continental shelf of Alaska.

Collection of Samples and Analytical Methods Adopted

Determinations of phosphate-phosphorus, silicate-silicon and dissolved oxygen were made on board ship as soon as possible after collection. Water samples for chlorine and nitrate-nitrogen determinations were brought to the author's laboratory

* Contribution B-No. 137 from the Tokai Regional Fisheries Research Laboratory, Tokyo, Japan.

1) C. E. Ratomanov, "Research of the Sea", Vol. 2, Moscow, 1936 (in Russian with English summary).

2) C. A. Barnes and T. G. Thompson, University of Washington "Publications in Oceanography", Vol. 3, No. 2 (1938).

(Tokyo) and analysed. To the samples for nitrate determination mercuric chloride solution was added in order to avoid the change in concentration due to bacterial growth.

The improved method of Denigès-Atkins[3] was adopted for the determination of phosphate-phosphorus. In this method color development was accomplished by the original procedure, but sea water free from phosphate was used as the media of diluted standards.

Silicate-silicon was estimated by means of Dienert-Wandenbulcke's method in which a buffered potassium chromate solution containing borax was adopted as the color standard. It was standardized against sodium silicate solution both with Beckman's spectrophotometer and by the visual method[4]. Color comparison aboard ship was performed by using improved Hehner tubes with the length of 25 cm.

Stock solutions of standards for phosphate and silicate determinations were prepared in duplicate, one of which served as reference and the other as the working standard, both being checked against each other from time to time. After the completion of the cruise it has been confirmed that the changes in concentration of the reference were negligibly small during the period.

Dissolved oxygen was determined by means of Winkler's iodometric titration[5]; and for chlorine determination the argentometric titration using uranine as the indicator[6] was adopted.

Determination of nitrate-nitrogen was made by colorimetric methods using Harvey's reduced strychnine reagent; and as the artificial color standard the standardized safranine solution was used[7].

Results and Discussion

1. Distribution of Water Temperature and Chlorinity.—As mentioned above, the region under consideration is topographically devided into two areas by the Aleutian Ridge running through the central part of the region. Therefore, it may be convenient to examine the distributions of water temperature, chlorinity and so on separately, by area. Data obtained from several stations within each area in the first decade of June were averaged and considered as representative values for each area.

Fig. 2 shows vertical distributions of water temperature and chlorinity. From the figure it is clear that distributions of water temperature are quite identical in both areas except for slight differences recognized beyond a depth of 200 m. A characteristic feature of

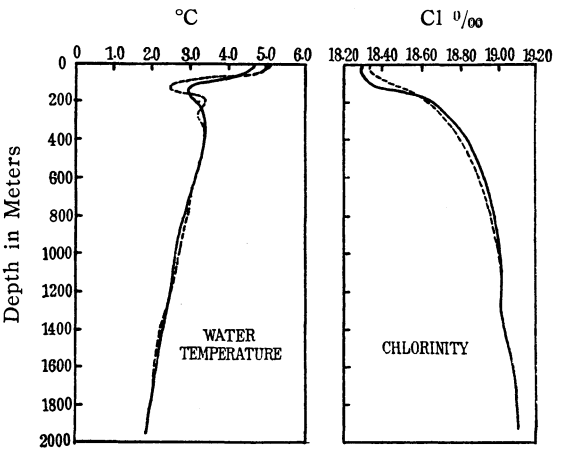


Fig. 2. Vertical distributions of water temperature and chlorinity. Solid lines represent the distributions in the Pacific side of the Aleutian Ridge, and broken lines those in the Bering Sea.

the distribution of water temperature in this region is that the marked temperature minimum and the gentle maximum appear at depths of 100 m. and 400 m., respectively. Below the depth of 400 m. the water temperature falls gradually and the gradients of the fall are much gentler than those in other regions such as tropical waters.

Distributions of chlorinity in these areas also are almost identical and chlorinity increases continuously with depth.

Close agreements in vertical distributions both of water temperature and of chlorinity between these areas suggest that horizontally uniform water masses may exist there. This type of distribution is in striking contrast to those in the Kuroshio or equatorial region.[8]

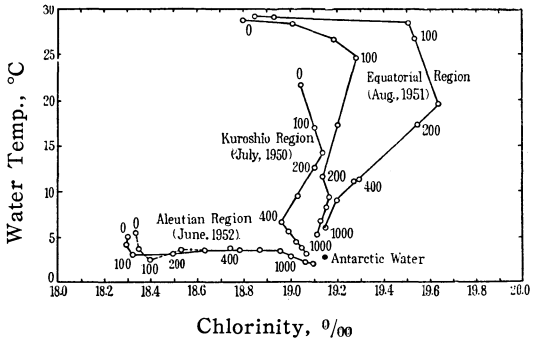


Fig. 3. Temperature-Chlorinity diagram representing water masses in various regions. Numbers in the figure indicate the depths in meters at which temperature and chlorinity for each point were obtained.

3) R. J. Robinson, *J. Mar. Res.*, **7**, 33 (1948).
4) R. Fukai, *J. Oceanogr. Soc., Japan*, in press.
5) W. S. Wooster, "Technical report of the California Cooperative Sardine Program", No. 25, Scripps Inst. of Oceanogr. (1950).
6) Y. Miyake, This Bulletin, **14**, 29 (1939).
7) H. Wattenberg, *Rapp. et Proc.-Verb. des Reunions, Conseil permanent intern. pour l'explosation de la mer*, **103**, 19 (1937).
8) R. Fukai, This Bulletin, **26**, 485 (1953).

In Fig. 3, T–Cl curves which were previously obtained by the author are compared with those from the present data. It should be noticed that although T–Cl curves differ greatly from each other in the upper layers, they tend to converge on a point which represents water temperature and the chlorinity of a water mass having Antarctic origin.

2. Distribution of Dissolved Oxygen.– Vertical distributions of dissolved oxygen in these two areas are shown in Fig. 4 compared

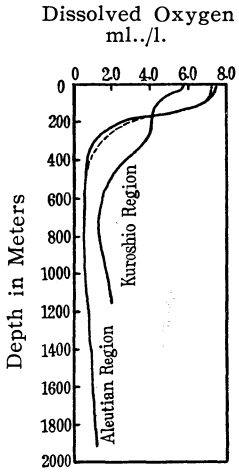


Fig. 4. Vertical distributions of dissolved oxygen. Solid lines: in the Pacific; broken line: in the Bering Sea.

with those in the Kuroshio region. The distributions in the areas are in close agreement with each other as well as those of water temperature and chlorinity. As for characteristic features of the distribution, it may be pointed out that high contents of oxygen are encountered at and near the surface and they suddenly decrease in depths within 100–300m. forming a jumping layer. Oxygen at depths of 400–1000 m. is less than 1 cc. O_2/l., being the minimum value among those oceanic waters of the North Pacific.

As shown in Table I, a remakable fact is

TABLE I
AVERAGE CONTENTS OF DISSOLVED OXYGEN IN THE UPPER LAYERS

Depth m.	O_2 ml./l. obs.	O_2 ml./l. calc.	Saturation percentage
0	7.37	7.23	101.9
10	7.44	7.29	102.1
25	7.46	7.34	101.6
50	7.36	7·37	99.9
75	7.24	7.53	96.1
100*	6.99	7.62	91.7
150	4.94	7.50	65.9

* The layer of minimum water temperature.

that the oxygen contents at the layers of 10 m. and 25 m. are higher than at the surface. This may probably result from photosynthesis by phytoplankton, since this type of distribution without biological support would be destroyed by the strong turbulence prevailing in the region.

The thickness of the euphotic layer may be estimated to be about 50 m. from the fact that the oxygen content at 50 m. layer is just saturated whereas the contents above this layer are supersaturated.

3. Distribution of Phosphate-phosphorus and Nitrate-nitrogen.—Vertical distributions of phosphate and nitrate are given in Fig. 5.

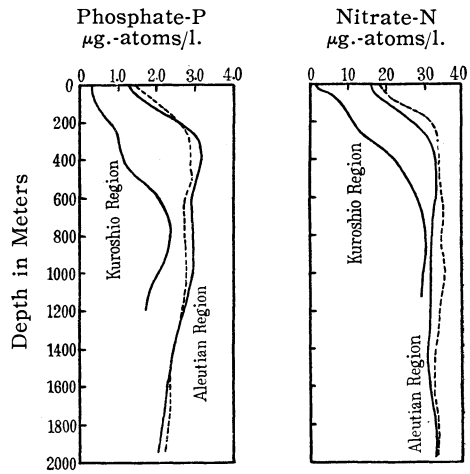


Fig. 5. Vertical distributions of phosphate-phosphorus and nitrate-nitrogen. Solid lines: in the Pacific; broken lines: in the Bering Sea.

The distributions of each of the constituents are almost the same in the two areas. The causes of slight differences recognized between the areas are not clear. Yet it may be remarkable that the phosphate contents at depths within 200–800 m. are lower in the waters of the Bering Sea than in the other area, while the contents of nitrate are higher in the former than in the latter.

Characteristics of the vertical distributions are that the high contents of both constituents are found at and near the surface and that the concentrations increase abruptly in a layer corresponding to the jumping layer of dissolved oxygen. The maximum amount of phosphate appears at a depth within 400–600 m., while the maximum of nitrate is not obvious. Attention is called to the fact that considerable amounts of both constituents (above 1.0 μg.-atoms PO_4-P/l. and 150 μg.-atoms NO_3-N/l.) were present in spite of the fact that abundant crops of phytoplankton existed there. The fact means that the nutrient salts in the upper layers have not been exhausted so that potential ability for organic production could still remain in the layers.

4. Distribution of Silicate-silicon.—Fig. 6 illustrates vertical distribution of silicate in the areas compared with those in the Kuroshio region and in the Northeast Pacific. As

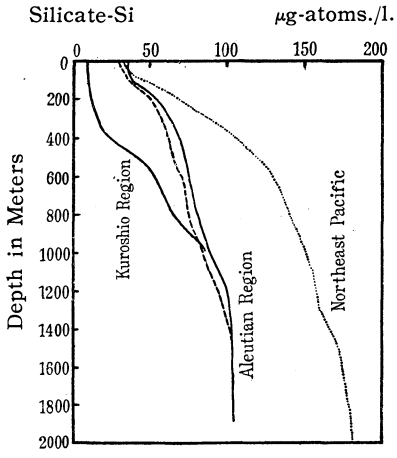


Fig. 6. Vertical distributions of silicate-silicon. Solid lines: in the Pacific; broken line: in the Bering Sea; dotted line: in the Northeast Pacific obtained by Thompson (1938).

in cases of other constituents, considerable amounts of silicate are found at the surface and they further increase in the deeper layers. Referring to some differences in distributions between two areas, the contents are slightly lower on the side of the Bering Sea. It is conspicuous that the distributions differ greatly from those obtained by Thompson.

5. Relationship between Distributions of Nutrient Salts.—As described above, the prevailing features of the nutrient salt distribution are summarized as follows:

(i) Distributions are horizontally uniform except those in limited areas such as the vicinity of islands,

(ii) concentrations are high even in the surface layer,

(iii) and increase further with maximum gradients in depths within 100–300 m.

From the type of distributions, it is expected that parallel correlation may exist between concentrations of these constituents. From Fig. 7 which shows the correlation between phosphate and nitrate, it is concluded that the average atomic ratio of N : P is 12, although points plotted in the figure are somewhat scattered. This value is lower than the normal ratio of 15 proposed by Cooper[9]. As the author has recently pointed out[10], the ratios in the waters below subsurface

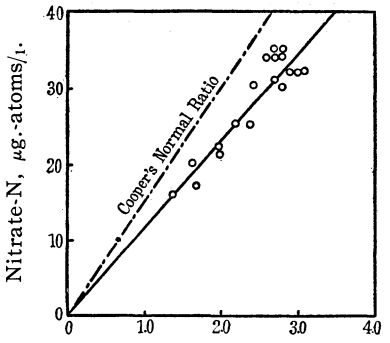


Fig. 7. Relationship between nitrate-nitrogen and phosphate-phosphorus in the adjacent region to the Aleutian Islands.

layers in the Kuroshio region coincide with the normal ratio. So far it has not been conclusive, however, whether the deviation from the normal ratio in the Aleutian region is attributed to local differences or related to the rate of regeneration of these constituents.

In case of the regeneration of these constituents, in general, dissolved oxygen would be consumed. The relationship between phosphate contents and oxygen depletion (the difference between the saturation value and observed value) is shown in Fig. 8. Oxy-

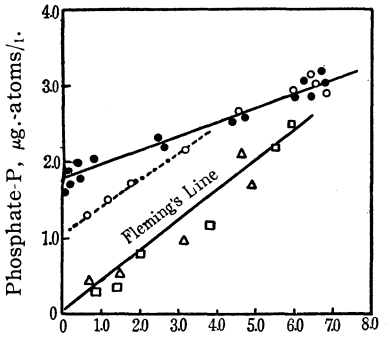


Fig. 8. Relationship between phosphate-phosphorus and oxygen depletion in various regions. Dots designate points for the Aleutian Region in 1st decade of June; circles for those at the end of June. Squares: for the Kuroshio Region; triangles: for the Equatorial Region.

gen depletion may serve as a measure of oxygen consumption.

In the figure, was added a line which was proposed by Fleming[11] on the basis of the proportion between liberated oxygen and as-

9) L. H. N. Cooper, *J. Mar. Biol. Assoc., United Kingdom*, **22**, 177 (1938).

10) R. Fukai, This Bulletin, **25**, 323 (1952).

11) R. H. Fleming, "Proc. the 6th Pacific Science Congress", Vol. 3 (1939).

similated phosphorus, both due to photosynthesis. It can be stated that points plotted for the Kuroshio and Equatorial regions are in close agreement with Fleming's line, while the slope of the line derived from the points for the Aleutian region differs greatly from that of Fleming's line. In addition, the slope had been altered in the course of time and it came to coincide with that of Fleming's line after about a month. This indicates that a constant ratio between phosphate and oxygen depletion has not been maintained during the period and that the decrease in dissolved oxygen has taken place in association with the decrease in phosphate contents in the subsurface layer. Although the mechanism of this decrease in dissolved oxygen may be complicated, it may relate to the decomposition processes in the layer in question. The deficiency of dissolved oxygen in the subsurface layer should be emphasized as a feature in the Aleutian region together with the deviation of N-P ratios from the normal ratio.

6. Quantitative Consideration on the Rate of Organic Production by Phytoplankton.—In the above it has been concluded that the potential ability for organic production still remained in this region at the beginning of June. As the duration of this condition depends upon the rate of organic production, it is desirable to find out the production rate.

Oceanographical observations were repeatedly carried out at sea around 150 nautical miles S. of Attu Island on June 5–6 and 29–30. Table II has been made by averaging a number of data obtained from several stations occupied there. On these materials the following computations have been based.

TABLE II
DATA USED FOR THE ESTIMATION OF THE PRODUCTION RATE

Water layer m.	June 5–6		June 29–30	
	Water temp. °C	PO_4-P μg-at./l.	Water temp. °C	PO_4-P μg.-at./l.
0–25	4.50	1.33	6.08	0.93
25–50	4.29	1.47	5.12	1.19
50–75	4.00	1.60	4.03	1.41

At first, the rise in water temperature may be expressed by

$$\frac{\partial T}{\partial t}=\frac{A_z}{\delta}\cdot\frac{\partial}{\partial z}\left(\frac{\partial T}{\partial z}\right)-V_x\cdot\frac{\partial T}{\partial x}, \qquad (1)$$

where, T is water temperature, A_z, coefficient of eddy diffusivity, δ, specific gravity of sea water, and V_x, current velocity component along x-axis.

In the equation, we may conveniently take x-axis from the west to the east and z-axis from the surface to the bottom. In equation 1, the lateral mixing of water masses was ignored because the horizontal gradients of water temperature were so small; and current velocity components except that along x-axis were of no account.

Let us rewrite equation 1 as

$$A_z=\delta\left(\frac{\partial T}{\partial t}+V_x\cdot\frac{\partial T}{\partial x}\right)\Big/\frac{\partial^2 T}{\partial z^2}. \qquad (2)$$

Since gradients of temperature distribution, current velocity component and specific gravity of sea water are known, we can obtain the value of A_z from the equation 2. The calculated values of A_z are shown in the first column in Table III.

TABLE III
COMPUTED VALUES FOR NET PRODUCTION RATE

Water layer m.	A_z	R PO_4-P μg.-at./l./sec.	Net production rate mg.C/m³./day
0–25	(10)	-5.1×10^{-7}	56
25–50	10	-1.0×10^{-7}	11

On the other hand, the decrease in phosphate contents during the period may be expressed by

$$\frac{\partial C}{\partial t}=R+\frac{A_z}{\delta}\cdot\frac{\partial}{\partial z}\left(\frac{\partial C}{\partial z}\right), \qquad (3)$$

where C is concentration of phosphate R, biological rate of change (rate of net consumption).

In equation 3, the horizontal eddy diffusion and advection were ignored since the horizontal distribution of phosphate was uniform as previously stated. From Eq. 3, we may obtain

$$R=\frac{\partial C}{\partial t}-\frac{A_z}{\delta}\cdot\frac{\partial^2 C}{\partial z^2}. \qquad (4)$$

Then, on the basis of Eq. 4, the value of R can be calculated by introducing into the equation the values of A_z, which have been obtained from Eq. 2, and gradients in phosphate distribution. The values of R thus obtained for each layer are shown in the second column in Table III.

Since photosynthesis by phytoplankton is usually accompanied by the consumption of phosphate, the rate of carbon assimilation can be computed as in the third column of Table III from the values of R, using the proportion given by Fleming.

Few data have been available for comparing these values, except those which were derived from Reiley's data concerning the annual

variations of plankton carbon on Georges Bank[12] (Table IV). The values for the Aleutian region agree well with the value for the spring burst of phytoplankton given by Riley.

TABLE IV

NET PRODUCTION RATES COMPUTED FROM THE DATA OBTAINED BY RILEY ON GEORGES BANK (1947)

Period	Net production rate mg.C/m³./day
Feb.–Mar.	4
Mar.–Apr.	20
Apr.–May	50

Most recently, Nielsen[13] has pointed out on the basis of the results obtained from the determinations using radiocarbon C^{14} that the production rates hitherto estimated were too high, especially in the tropical regions, criticizing the experiments carried out by Riley[14] in the Sargasso Sea. However, Nielsen himself has admitted that Riley's values are reliable so far as the waters on the coastal bank are concerned.

Thus, if we assume that the organic production continues at the rate obtained above, and that the nutrient supply from the substratum is prevented by the development of stratification, the potential ability for organic production is reckoned to last for about 20 days more. Consequently, the production may actually continue till the end of summer without deficiency in nutrient salts.

7. Estimation of the Production Rate based upon the Diurnal Variations of Dissolved Oxygen.—Anchored observations on the diurnal variations of oxygen throughout 24 hours were carried out at Station 24, situated north of Semisopochnoi Island, in the last decade of May. Results obtained are shown in Fig. 9. Values plotted for dissolved oxygen in the figure represent integral mean concentrations from the surface to a depth of 50 m. Although the water was shifted continuously by tidal current during the period, the temperature and chlorinity of water were kept strictly constant. For this reason, it can be assumed that the changes in dissolved oxygen were caused by biological activity in a water mass.

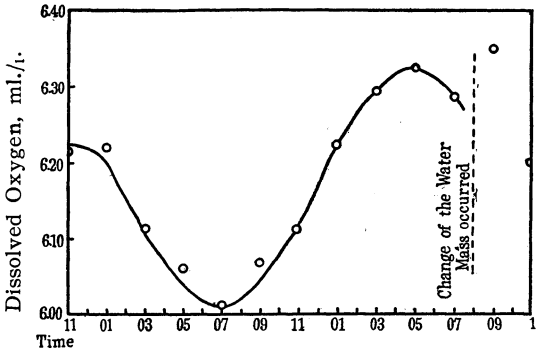


Fig. 9. Diurnal variation of dissolved oxygen at St. 24, off Semisopochnoi Island.

According to the figure, the net increase in the oxygen content amounting to 0.3 ml/l. took place in 10 hours from 7:00 P. M. to 5:00 A. M. (Japanese Standard Time). When this amount of oxygen is converted into the amount of assimilated carbon, we may obtain 165 mg.C/m³.

On the other hand, the author's experiment[15] showed that in case of the carbon assimilation by phytoplankton, 30–50% of assimilated carbon was simultaneously consumed through the respiration processes. Consequently, an estimate of 85 mg.C/m³/day for the net production rate may be obtained by subtracting the quantity for respiration from the net quantity for assimilation during 10 hours.

This value is considered to represent the upper limit for the assimilation rate, since it was estimated for the area in the vicinity of an island, and since carbon was also consumed by zooplankton possessing no assimilating activity. With these views in mind, the values based upon the phosphate consumption seem to be reliable.

Summary

The author was engaged in the oceanographical observations carried out in a region adjacent to the Aleutian Islands in 1952 and obtained a number of data, on which the present discussions are based.

As the results, slight differences in distributions of nitrate-nitrogen, phosphate-phosphorus and silicate-silicon were found between the northern and southern areas separated by the Aleutian Ridge, although distributions are almost the same in the two areas.

Characteristic features in distributions of these nutrient salts are that the high concentrations were found even in the surface layer, increasing further with maximum gradients in depths within 100–300 m.

The ratios of N:P in the region under

12) G. A. Riley, *J. Mar. Res.*, **6**, 104 (1947).
13) E. S. Nielsen, *J. Conseil. perm. intern. pour l'exploration de la mer*, **18**, 117 (1952).
14) G. A. Riley, *J. Mar. Res.*, **2**, 145 (1939).
15) R. Fukai and K. Okubo, not yet published.

study are lower than the normal ratio given by Cooper; and deficiencies in dissolved oxygen were recognized in the subsurface layers. These facts seem to be related to the characteristics of the decomposition processes in the Aleutian region.

On the basis of the rate of phosphate consumption in the upper layers, the net production rate has been computed by introducing some simplifying assumptions; and has obtained the value of 56 mg. C/m^3/day. This value is considered to be reliable, since it coincides with that derived from Riley's data and with that calculated from the data concerning the diurnal variations of dissolved oxygen.

The author is pleased to acknowledge his indebtedness to Prof. Kenjiro Kimura of Tokyo University and Dr. Masao Migita of the Takoi Regional Laboratory for their valuable advice. Acknowledgement is made to Mr. N. Watanabe, who was the leader of the present cruise, for his encouragement and cooperation during the course of the work. The author desires to express appreciation also for the valuable assistance of Miss F. Shiokawa and Miss S. Kojima in the laboratory and all of the members of R. V. "Tenyô-maru," without whose assistance the present work would hardly have been accomplished.

Tokai Regional Fisheries Research Laboratory, Tokyo

Seasonal Variations of Minor Chemical Constituents in the Waters of the Zunan-Kuroshio Region. II. Silicate Contents of Sea Water and Changes in Quality of the Kuroshio*

By Rinnosuke FUKAI

(Received March 20, 1954)

Introduction

In the previous paper[1], the author has studied the problem concerning variations of nitrate and phosphate contents in the waters of the Kuroshio region. The present paper deals with the seasonal variations of silicate contents of water in connection with the changes in quality of the Kuroshio. Although silicate has been regarded as one of the most essential nutrient salts for marine organisms, especially for diatoms, together with phosphate and nitrate, it differs from the other nutrient salts in respect to circulation, the magnitude of the concentration and the physiological significance for organisms.

The author previously made a chemical study on Omura Bay[2] (Nagasaki prefecture, Japan), reporting that, contrary to general expectation, silicate contents of sea water in the estuary of the Kôri river were lower than in the adjacent areas. In this case, however, the physico-chemical state of silicon-compounds colorimetrically determined has not been made clear.

Later, a number of studies were conducted by various authors as to the state of silicon-compounds colorimetrically estimated[3][4], changes in silicate coloration when sea water was diluted with natural fresh water[5] and the state of silicon-ccompounds in hot springs and land waters[6], yielding valuable results.

Although a decisive conclusion has not been reached up to now, it is probable that the most part of silicon-compounds in the oceanic waters may be in a colorimetrically measurable state[7], seasonal variations of which were mainly considered in this paper, not referring to the state of silicon-compounds.

Materials and the Analytical Method

The following discussions are based upon the data obtained for the samples collected from the oceanographical stations illustrated in Fig. 1 of the previous report during the period from January 1950 to Feburuary 1951. The analyses of the samples were carried out as soon as possible after

* Contribution B-No. 144 from the Tokai Regional Fisheries Research Laboratory, Tokyo.

1) R. Fukai, This Bulletin, **25**, 323 (1952).

2) R. Fukai, M. Osako and H. Hamada, *Oceanogr. and Meteorol., Nagasaki Marine Observatory*, **3**, No. 3 (1949) (in Japanese).

3) F. Aoki, *J. Chem. Soc. Japan*, **71**, 634 (1950); **72**, 15 (1951).

4) T. Okura, *J. Chem. Soc. Japan*, **72**, 927 (1951).

5) A. Saeki, *J. Oceanogr. Soc. Japan*, **5**, 41 (1949); **6**, 39 (1950).

6) I. Iwasaki, T. Katsura & T. Tarutani, This Bulletin, **24**, 227 (1951).

7) T. Chow and R. J. Robinson. *Anal. Chem.*, **25**, 646 (1953).

collections either on board ship or on the land, depending on the sea conditions in each observation cruise.

For the analysis was adopted the Dienert-Wandenbulcke's method in which the yellow color of silicomolybdate was developed by addition of ammonium molybdate solution and sulfuric acid. Although further reduction of silicomolybdate by stannous chloride provides the more sensitive method[8], the ordinary method was followed with regard to conditions on board ship. For the color comparison were used the color standard of buffered potassium chromate solution containing borax and improved Hehner tubes with the length of 25 cm., or Beckman's spectrophotometer at a wave length of 380 mμ. Checking experiments were made as to the changes in concentration of silicate which occurred during the standing period of the samples, proving that no change was recognized unless water samples were kept in contact with the glass walls of containers.[9]

Results and Discussions

In order to examine the seasonal variations of silicate in the region under study, it is necessary to distinguish the variations in the surface layers (0–200 m.) from the fluctuations of vertical distributions. The former may be related to prevalence or decline of coastal water masses; and the latter to vertical mixing of water strata due to mechanical disturbance and vartical diffusion.

1. Variations in the Surface Layer.— Variations of silicate contents in the surface layers (0–100 m. and 100–200 m. layers) with those of chlorinity (in 0–100m. layer) at Stations 3 and 6 are shown in Figs. 1 and 2, respectively. The values plotted in the figures are the integral mean values for each water layer.

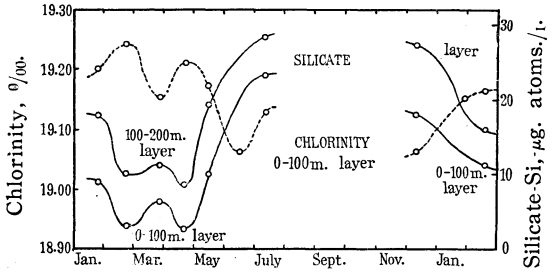


Fig. 1. Seasonal variations of silicate and chlorinity in the surface layers at Station 3. Solid curves: silicate. Broken curves: chlorinity.

From the figure, it is readily noted that chlorinities of the waters in the region decreased in summer, while they increased in winter. It seems to be a remarkable fact that the decrease at Station 6, which is located within the main current of the Kuroshio and is not likely to be affected immediately by land waters, is larger than that at Station 3 located in the mixing region of the Kuroshio with coastal water masses. This may suggest that the decrease in chlorinity of the Kuroshio itself ought to take place before the Kuroshio flows into the region under consideration.

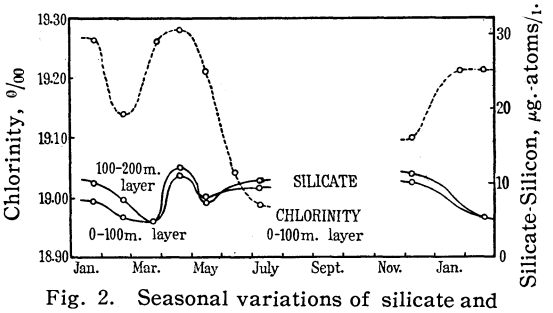


Fig. 2. Seasonal variations of silicate and chlorinity in the surface layers at Station 6. Solid curves: silicate. Brokenc curves: chlorinity.

Silicate contents tend to increase in summer and decrease in winter, being contrary to the variations in chlorinity. This inverse proportionality is remarkable at Station 3. Although the relationship may indicate that silicate contents fluctuate in accordance with the prevalence or decline of coastal water masses, quantitative correlations do not exist.

Now, let us assume that the maximum chlorinity of 19.30‰ represents the normal chlorinity of water in the Zunan-Kuroshio region and that the normal sea water of the region is only mixed up with the fresh water; moreover, let us define the mixing percentage of fresh water, M_f, as follows;

$$M_f = \frac{[\mathrm{Cl}]_n - [\mathrm{Cl}]_s}{[\mathrm{Cl}]_n} \times 100 \qquad (1)$$

where $[\mathrm{Cl}]_n$ is the normal chlorinity, namely 19.30‰ in this case, and $[\mathrm{Cl}]_s$ is the chlorinity in summer.

The values of mixing percentage calculated from the equation 1 did not exceed 2% as shown in Table I. On the basis of the mixing percentage and silicate contents of sea water in summer, silicate contents of assumed fresh water were computed as shown in the last column of Table I. Among these values, the one for July 1950 is three times higher than the mean value for river waters in Japan. This may indicate that the variations of silicate contents in the surface layers are not controlled only by direct invasion of terrestrial water, even at Station 3, located relatively coastward.

8) A. B. Carlson and C. V. Banks, *Anal. Chem.*, **24**, 472 (1952).

9) R. Fukai, *J. Oceanogr. Soc. Japan*, in press.

TABLE I
ESTIMATED SILICATE CONTENTS OF FRESH WATERS

	ΔCl‰	Percentage of fresh water mixed	Si in sea water μg.-at./l.	Estimated Si of fresh water mg.-at./l
Station 3				
May 1950	0.13	0.7	9.7	0.5
July ,,	0.17	0.9	27	2.5
Station 6				
May 1950	0.09	0.5	8.2	1.2
July ,,	0.31	1.6	9.3	0.3

As the other origin of *excess silicate* in sea water, the following may be considered:

(1) the silicate-rich substratum,
(2) the decomposition processes of abundant populations of diatoms in summer,
(3) a water mass having high silicate content and low chlorinity.

Among these cases, the former two can hardly be accepted, since the Kuroshio is a stably stratified and origotrophic water mass of the southern origin. Therefore, the last case should be most probable. It cannot be immediately concluded, however, where the origin of a mixing water mass is.

In the variations of silicate and chlorinity, the conditions are quite different between Stations 3 and 6. This suggests that the causes of the variations are not the same at these stations. Whereas it is probable that the variations in the main current of the Kuroshio are being affected by the water of southern origin such as the adjacent water to Formosa or the water of the East China Sea, the effect of the Oyashio might be taken into consideration as the cause of the variation at Station 3, since the Oyashio from the northern areas of the N. W. Pacific prevails along the coastal region of Japan in summer months.

In order to estimate the silicate content of a water mass of northern or southern origin which is likely to mix with the Kuroshio, the mixing percentage of water masses is computed by using the following equation, defining the normal chlorinity of each water mass from the data previously obtained[10,11];

$$M=\frac{[Cl]_n-[Cl]_s}{[Cl]_n-[Cl]_m}\times 100. \qquad (2)$$

The notations in Eq. 2 are the same as in Eq. 1, except that $[Cl]_m$ designates the postulated chlorinity for the mixing water mass.

From the values in Table II, it may be concluded that the actual circumstances are

TABLE II
ESTIMATED SILICATE CONTENTS OF WATER MASSES MIXED WITH THE KUROSHIO
(July 1950)

Water mass	Cl ‰ of water mixed	Mixing percentage	Estimated Si of water mixed μg.-at./l.	Si found in the Kuroshio μg.-at./l.
Northern				
Station 3	18.35	17.9	130	30
Station 6	18.35	32.6	20	30
Southern				
Station 3	17.50	9.4	250	—
Station 6	17.50	17.2	30	—

not explained so far as only the mixing of different sea waters is concerned. Consequently, the mixing with both fresh and sea water must be taken into consideration.

As described above, the variations of silicate contents in the surface layer are complicated. Nevertheless, it is noteworthy that silicate which appears to originate primarily from land waters is related to the changes in quality of the oceanic water mass such as the Kuroshio.

2. Variations below the Subsurface Layer.—The variations of silicate below the subsurface layer cannot be discussed simply. In general, vertical distributions of silicate contents tend to have parallel correlations with those of phosphate above a depth of 1000 m. In the Kuroshio region, phosphate contents reach the maximum at a depth of about 1000 m., while silicate contents increase continuously.

In Fig. 3 is given the relationship between silicate and phosphate contents above the maximum layer of phosphate, together with the data obtained as to the water samples

10) R, Fukai, This Bulletin, in press (1954).
11) Y. Matsudaira and S. Inoue, *J. of Oceanography, Imperial Marine Observatory, Kobe, Japan*, 705 (1939).

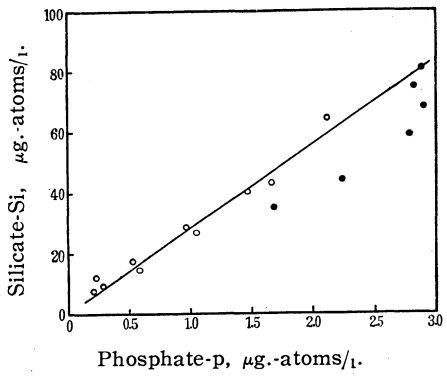


Fig. 3. Relationship between silicate and phosphate. Circles: for the Kuroshio region. Dots: for the Aleutian region.

collected from the Aleutian region. Points in the figure were plotted on the basis of the annual mean values for each of the constituents. A close linear correlation was obtained from these values, although the data for each month were considerably fluctuated. The mean value of Si : P was 28. On the other hand, no linear correlations recognized as to the points for the Aleutian region.

Deviations from the mean ratio of Si : P in the Kuroshio region are especially large in the upper layers. Although relatively close values were obtained as to the waters below subsurface layers, the values tend to fluctuate due to mixing with the waters of deeper layers.

In Fig. 4 are shown the annual mean ver-

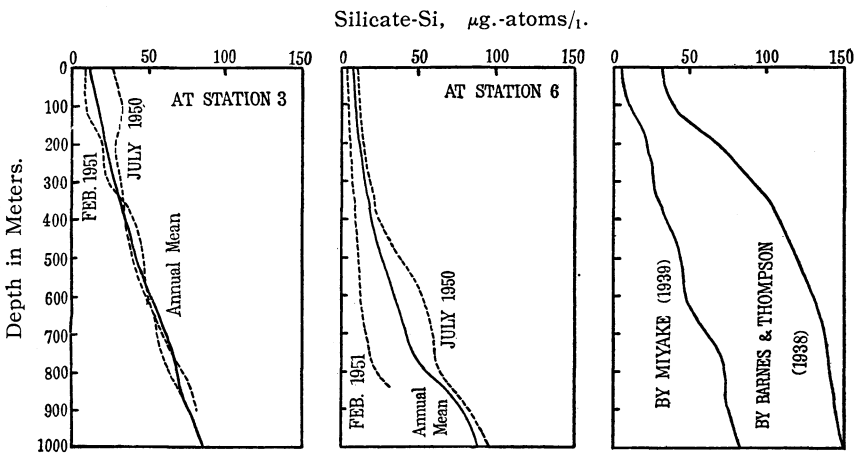


Fig. 4. Vertical distributions of silicate.

tical distributions of silicate and examples of vertical distribution for summer and winter. For a comparison, the vertical distributions obtained by various investigators[12] from the North Pacific were added.

Although the causes for the fluctuation of vertical distributions are not obvious, it should be noted that the whole water column tends to become uniform at Station 6 in winter, suggesting that the mixing with the waters of the substratum due to convection process which may be acting as the controlling factor.

Summary

Seasonal variations of silicate have been considered in the present paper on the basis of the data obtained from the observations carried out from January 1950 to February 1951.

The variations of silicate in the surface layers tend to have an inverse proportionality with those of chlorinity, increasing in summer while decreasing in winter. It is not sufficient to consider that the cause of the variations merely lies in the mixing either with fresh waters from the coast of Japan or with a water mass having low chlorinity and high silicate content. The actual circumstances may probably be caused by the overlapping effect of these two causes.

Although the fluctuation of vertical distributions of silicate below subsurface layer was also complicated, a close linear correlation between annual mean silicate contents and those of phosphate was obtained, to be expressed as the Si : P ratio of 28. However, the vertical distributions fluctuated considerably in the course of time, tending to become uniform in winter.

As the conclusion, it may be estimated that the vertical and lateral mixing of water

12) Y. Miyake, This Bulletin, **14**, 467 (1939); C. A. Barnes & T. G. Thompson, "Univ, of Washington Publ. in Oceanogr.", **3**, No. 2 (1938).

masses is the prevailing factor for the variations of silicate in the region under consideration.

Sincere acknowledgement is made to Prof. Kenjiro Kimura of the Tokyo University for his encouragement and valuable advice during the course of the investigation. The critical reading of the manuscript of Dr. Masao Migita of the Tokai Regional Laboratory is also acknowledged. The author desires to express appreciation for the assistance and untiring zeal of Miss F. Shiokawa throughout the course of the study.

Tokai Regional Fisheries Research Laboratory, Tokyo

Surface Chemistry of High Polymers. V. The Monolayer of Polymethacrylic Acid and its Copolymers with Diethylaminoethyl Vinyl Ether at the Oil/Water Interface

By Hiroshi HOTTA

(Received March 22, 1954)

Previously we studied the monolayer of polymethacrylic acid and its copolymers with diethylaminoethyl vinyl ether at the air/water interface by measuring their surface pressure and potential.[1] Subsequently, we have studied the monolayer of the same samples at the petroleum ether/water interface. The results will be described in the present paper. The effect of the *p*H of substrate on the surface behaviour of polyelectrolyte can be perfectly inferred by comparison between the results at both interfaces. The present investigation provides an useful key to elucidate the nature of the biocolloidal substances.

Experimental

The polymethacrylic acid and its copolymers with diethylaminoethyl vinyl ether (CH_2=CH–O–C_2H_4–N–(C_2H_5)$_2$) (DAV) used in the present study were the same samples as those used in the preceding investigation,[1] and had the composition shown in Table I. Their films were spread from the aqueous solution containing 20% pyridine at the petroleum ether/water interface, using a micrometer syringe according to Alexander and Teorell's method.[2] The *p*H of substrate was adjusted with hydrochloric acid or sodium hydroxide, and measured with "TOYO" *p*H test paper. The occasional test of this value checked by the Beckman glass electrode *p*H meter agreed satisfactorily with each other. The interfacial pressure was measured by ring method,[3] and the interfacial potential by vibrating electrode method using the same apparatus as that described in the previous paper.[4] Detailed descriptions of the spreading technique and of the measurement of interfacial pressure were given in the previous paper.[5] The application of the vibrating electrode method to the measurement of interfacial potential at the oil/water interface has been already tried by Davies.[6, 7] Although the vibrating electrode was immersed in the petroleum ether phase, we took care sufficiently of the amplitude of vibration and the distance of the electrode from the interface not to disturb the film.

TABLE I

THE COMPOSITION OF COPOLYMERS OF METHACRYLIC ACID (MA) WITH DIETHYLAMINOETHYL VINYL ETHER (DAV).

Sample	Mole percentage of DAV in copolymer	Mean molecular weight per vinyl unit
K	31	112
L	20	97
M	0	86

Results

The interfacial pressure (π)-area (A) curves and interfacial potential-area curves at the petroleum ether/aqueous phase at various *p*H interfaces are shown in Figs. 1, 2 and 3, and Figs. 6 and 7, respectively. In these figures, the area was calculated as the mean

1) T. Isemura, H. Hotta and S. Otsuka, This Bulletin, **27**, 93 (1954).
2) A. E. Alexander and T. Teorell, *Trans. Faraday Soc.*, **35**, 727 (1939).
3) A. E. Alexander, "Surface Chemistry" (Supplement of Research) (1949) p. 123.
4) T. Isemura, H. Hotta and T. Miwa, This Bulletin, **26**, 380 (1953).
5) H. Hotta, ibid. **26**, 386 (1953).
6) J. T. Davies, *Nature*, **167**, 193 (1951).
7) J. T. Davies, *Z. Elektrochem.*, **55**, 559 (1951),

area per vinyl unit with the mean molecular weight in Table I. The interfacial moment-area curves, shown by dotted lines in Figs. 6 and 7, were calculated by the usual method as mentioned in the previous paper.[4] Since the measurements of interfacial pressure and potential were carried out separately at room temperature for the reasons of apparatus, the temperature for the two curves was not the same, namely, 17-22°C. for interfacial pressure and 8-11°C. for interfacial potential.

The results for all samples were sufficiently reproducible up to *p*H about 4. On the other hand, the reproduciblity was good for sample K, fairly good for sample L, but somewhat uncertain for sample M in the *p*H range, in which carboxyl groups might be ionized. Therefore, the area in figures is the apparent mean area calculated mathematically in this *p*H range. Uncertainty increases somewhat in the narrower area range. The interfacial potential-area curve for sample M is given only in the case of *p*H 1.6 as a representative in Fig. 7.

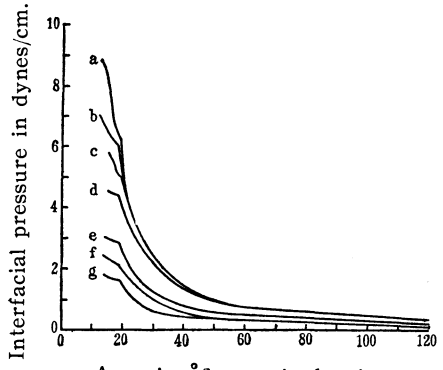


Fig. 1. The interfacial pressure-area curves of sample K at the various *p*H of substrate: curve a, *p*H 1.2; curve b, *p*H 2.8; curve c, *p*H 3.2; curve d, *p*H 3.5; curve e, *p*H 4.0; curve f, *p*H 4.8; and curve g, *p*H 5.7.

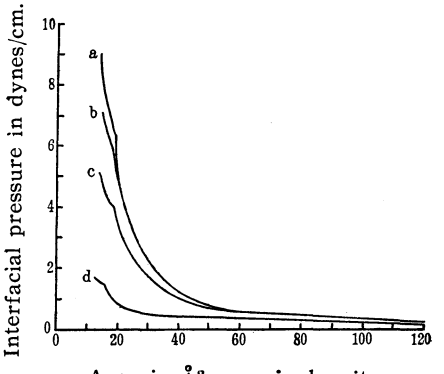


Fig. 2. The interfacial pressure-area curves of sample L at the various *p*H of substrate: curve a, *p*H 1.6; curve b, *p*H 2.6; curve c, *p*H 3.5; and curve d, *p*H 5.8.

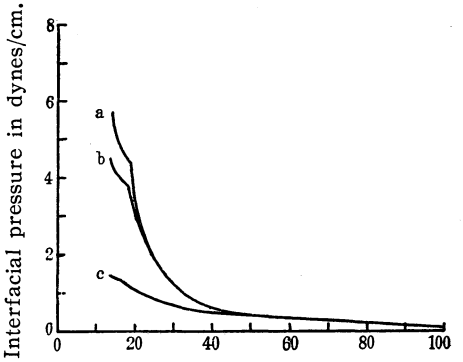


Fig. 3. The interfacial pressure-area curves of sample M at the various *p*H of substrate; curve a, *p*H 1.6; curve b, *p*H 3.0; and curve c, *p*H 3.5.

Discussion

It was concluded from the measurement of surface potential in the preceding paper[1] that, at the air/water interface, the amine groups of the present polyelectrolytes can be ionized by about 20 mol. per cent[8] at the maximum, and that the behaviour of their film can be perfectly understood by Katchalsky's interpretation[9] for the relationship between the state of a molecule and the degree of ionization (or *p*H). In view of the present results, our conclusion was still confirmed.

The film of the present polyelectrolytes is of expanded type as in the case of all other synthetic linear polymers at the oil/water interface[5, 10] as shown in Figs. 1, 2 and 3. The value of $(\pi A)_{A=\infty}$ and the collapse pressure (the interfacial pressure at a kink point) from these figures are plotted against the *p*H of substrate in Figs. 4 and 5, respectively. On comparing these figures with the curve of surface moment against the *p*H of substrate (Fig. 7 in the preceding paper[1]), we noticed that all the curves in these figures are constant up to a certain (and almost same) *p*H, and bend sharply from this *p*H. This tendency might be interpreted as in the case of the air/water interface.[1] That is, up to this critical *p*H the acid groups may be perfectly undissociated and

8) The total ionizable group, namely, the sum of MA and DAV is taken as the unity of the degree of ionization as in the preceding paper.

9) A. Katchalsky, *J. Polymer Sci.*, **7**, 393 (1951).

10) H. Hotta, *Mem. Inst. Sci. & Ind. Research Osaka Univ.*, **11**, 179 (1954).

the amine groups perfectly dissociated; from this *p*H, the total degree of ionization is rapidly affected by the appreciable ionization of the acid group; and at *p*H more than about 6 the film becomes soluble, due to the higher degree of ionization of the acid group. Since the effect of the liberation from lateral cohesion due to the oil phase joins the effect of ionization, the dissociation of the acid group is promoted more and more. Therefore, this effect becomes more considerable at the oil/water interface than at the air/water interface if the *p*H of substrate is the same. It should be more considerable in the case of polyelectrolyte having the higher content of the acid group. The difference of *p*H at a bending point between the three figures can be understood in the light of the effect of the oil phase as mentioned above.

From these reasons, the value of $(\pi A)_{A=\infty}$ for sample M up to a bending point (*p*H 3.5) in Fig. 4 might correspond to that in the undissociated state. Therefore, the length of a statistical kinetic unit in atom unit in the main chain at the oil/water interface, n_{atom}, which is derived from $\left(\frac{kT}{\pi A}\right)_{A=\infty}$, for polymethacrylic acid in the undissociated state is 53 (see Table II). In the range of

TABLE II

THE LENGTH OF STATISTICAL KINETIC UNIT IN ATOM UNIT IN THE MAIN CHAIN (n_{atom})

Sample	n_{atom}
K and L at *p*H 5 (surface isoelectric point)	47
M in undissociated state	53

*p*H more than 3.5 the value of $(\pi A)_{A=\infty}$ increases gradually due to ionization. On the other hand, the values for samples K and L are great at the low *p*H range due to the dissociation of the amine group, but decrease sharply when approaching to *p*H 5, and become 17×10^{-16} erg/vinyl unit for both samples at *p*H 5, which seems to be a surface isoelectric point at the air/water interface.[1] Therefore, the value of n_{atom} for them at this *p*H is 47 (see Table II). The value of $(\pi A)_{A=\infty}$ at the high *p*H range is uncertain, due to the high solubility by the dissociation. The detailed meaning for n_{atom} has been already given in the previous papers.[5,10] On comparing the present values in Table II with the previous ones,[10,11] the value of n_{atom} for the previous non-electrolytic linear polymers (polymethyl methacrylate and amilan) is identical to that for samples K and L, and somewhat smaller than that for polymethacrylic acid. The latter fact may be due to the strong cohesion between undissociated acid groups.[1,11] Of course, all the values are compared in the non-electric state.

The values of $(\pi A)_{A=\infty}$ for samples K and L in Fig. 4 are entirely different at least up to *p*H 3.5, while their collapse pressures in Fig. 5 are completely identical in spite of their

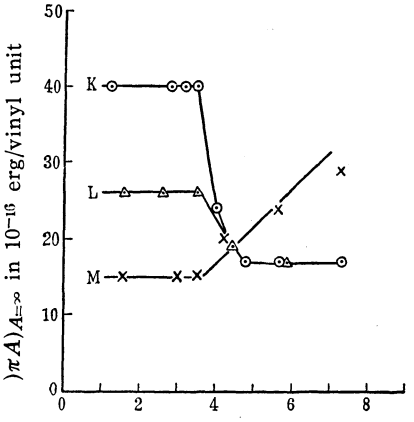


Fig. 4. The $(\pi A)_{A=\infty}$ at the various *p*H of substrate: ⊙, sample K; △, sample L; and ×, sample M.

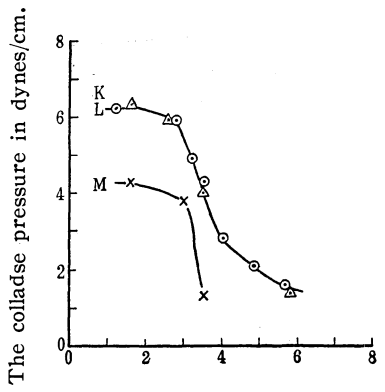


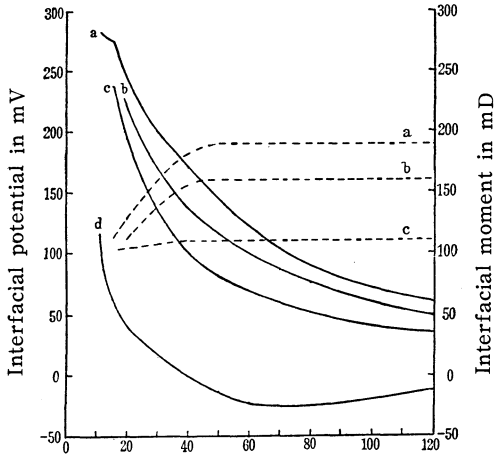
Fig. 5. The collapse pressure at the various *p*H of substrate: ⊙, sample K; △, sample L; and ×, sample M.

different composition as shown in Table I. It is concluded from these facts that the amine groups of these copolymers are perfectly dissociated at the larger area at least up to *p*H 3.5 without the mutual restriction of dissociation due to electrostatic interaction. This may be caused by the liberation from lateral cohesion due to the oil phase. However, the difference between them is no more appeared at the narrow area such as a collapse point similar to at the air/water

11) H. Hotta, This Bulletin, **27**, 80 (1954).

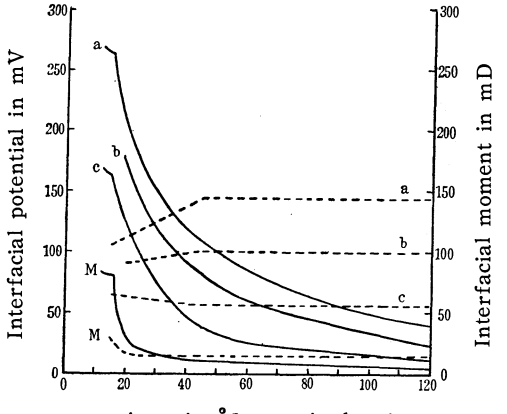
interface, since their dissociation is considerably restricted due to mutual electrostatic interaction, as in the case of condensed film at the air/water interface, and the side chains are immersed into the aqueous phase as discussed in the preceding paper.[1] The present conclusions are also derived from the measurement of interfacial potential as mentioned just below.

The interfacial moments in Figs. 6 and 7 are constant at the area larger than about 50 Å² per vinyl unit, and converge at the narrower area so as to become about 100mD at 10 Å². When the interfacial moment at the constant range is plotted against the *p*H of substrate in Fig. 8, it has the same



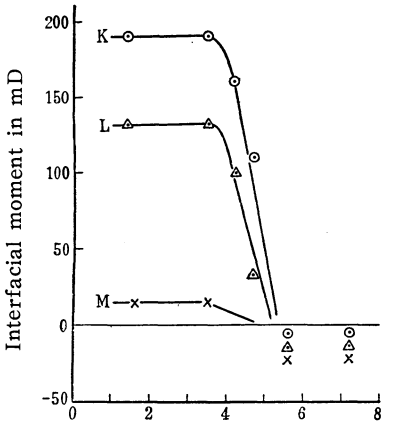
Area in Å² in vinyl unit

Fig. 6. The interfacial potential (or interfacial moment)-area curves of sample K at the various *p*H of substrate. The interfacial moment-area curve is shown by a dotted line. Curve a, *p*H 1.4 and 3.5; curve b, *p*H 4.2; curve c, *p*H 4.7; and curve d, *p*H 5.6.



Area in Å² per vinyl unit

Fig. 7. The interfacial potential (or interfacial moment)-area curves of samples L and M at the various *p*H of substrate. The interfacial moment-area curve is shown by a dotted line. Sample L: curve a, *p*H 1.4 and 3.5; curve b, *p*H 4.2; and curve c, *p*H 4.7. Sample M; curve M, *p*H 1.6.



The *p*H of substrate

Fig. 8. The interfacial moment at the large area plotted against the *p*H of substrate. ⊙, sample K; △, sample L; and ×, sample M.

tendency as in Figs. 4, 5 and Fig. 7 in the preceding paper,[1] which can be interpreted as mentioned above. The points in the negative side of this figure mean only the inversion of sign qualitatively. The interfacial moments for samples K and L up to *p*H 3.5 in Fig. 8 differ considerably from each other, in contrast to their surface moments which are almost identical at the air/water interface. Assuming the perfect dissociation of the amine group and the perfect undissociation of the acid group, the interfacial moment of the dissociated amine group which is evaluated from their interfacial moment at this *p*H range and their composition in Table I, is 600 mD for both samples. In this evaluation the interfacial moment of the undissociated acid group is assumed to be 15mD) from the curve of sample M. This value (600 mD) is completely identical with to that found at the air/water interface.[1] It is analogous to the result reported by Davies[6,7] that the surface potential of $C_{18}H_{37}N(CH_3)^+_3$ on 10^{-2} N-NaCl is identical at the air/water and oil/water interfaces. The interfacial moment extrapolated to 10 Å² (100 mD) is almost identical with that at 10 Å² at the air/water interface.[1] These facts correspond exactly to the results of interfacial pressure measurements mentioned above.

The interfacial moment of polymethacrylic

acid at the larger area in the undissociated state (15 mD) is far smaller than that in the same state at the air/water interface (90 mD)[1] This difference is due to the difference of the type of film at the two interfaces. With the increase of the content of methacrylic acid and the decrease of the total degree of ionization, the bending point of interfacial moment-area curves shifts to a smaller area and approaches to 30 Å^2 found at the air-water interface.

Glazer and Dogan[12] recently investigated the state of ionization of insoluble monolayers by the measurement of maximum surface potential at the air/aqueous phase at various *p*H interface. Although they found that the value of *pK* from their surface technique agrees fairly well with that from the measurement in the bulk solution in the case of protein, but not in the case of the low molecules as stearic acid and octadecylamine, they could not explain the latter disagreement satisfactorily. On the other hand, these facts may be understood in the light of our present investigation. The method of maximum surface potential is applicable to protein, which has a rigid structure even at the larger area as well as at a collapse point.[10] But it is unsuitable to low molecules, which have a loosely packed structure between them at the larger area, for the *pK* from bulk solution corresponds to that at an expanded film. To obtain *pK* by the surface technique for such low molecules, the surface moment in a constant range at the larger area should be investigated. Both methods are consistent only in the case, where the surface moment is constant up to a collapse point such as in the case of polymethyl methacrylate and polymethacrylic acid at the undissociated state at the air/water interface.[11] This is the case of protein.

12) J, Glazer and M. Z. Dogan, *Trans. Faraday Soc.*, **49**. 448 (1953).

Summary

As the result of the comparison of interfacial pressure and potential of polymethacrylic acid and its copolymers with diethylaminoethyl vinyl ether at the various *p*H of substrate between the air/water and oil/water interfaces, it is concluded that their films are of the expanded type without the mutual restriction of dissociation at the larger area at the oil/water interface, and, on the other hand, they are of condensed type with such a restriction even at the larger area at the air/water interface. The difference at the two interfaces disappears at a collapse point, where these films are of condensed type.

In conclusion, the author expresses his hearty thanks to Professor T. Isemura for his kind guidance throughout the present work, and to Mr. S. Otsuka in the Institute who kindly supplied many samples to him.

The Institute of Scientific and Industrial Research,
Osaka University,
Sakai, Osaka

The Effects of Substituents on the Hydrolysis of Substituted Cyanamides in Sulfuric acid Solution

By Teruaki MUKAIYAMA, Shin OHISHI[1] and Hiroshi TAKAMURA[1]

(Received April 21, 1954)

Introduction

Mono- and di-substituted cyanamides are hydrolysed in a sulfuric acid solution to give the corresponding ureas. Several works have already been given on the hydrolysis of cyanamide in aqueous acid solutions. In these earlier communications,[2,3,4], it was shown that the reaction is of the first order with respect to the concentration of cyanamide, and the rate increases steadily with increase in acid concentration. The reaction was also shown as an example of hydrogen-ion catalysis which was accepted by Hammett and Paul as an illustration of specific hydrogen ion catalysis.[5]

1) Laboratory of Organic Chemistry, Tokyo Institute of Technology.

2) H. C. Hetherington and J. M. Braham, *J. Am. Chem. Soc.* **45**, 824 (1923).

3) G. Grube and Motz, *Z. phys. Chem.*, **118**, 145 (1925).

4) G. Grube and G. Schmid, ibid., **119**, 19 (1926).

5) L. P. Hammett and M. A. Paul, *J. Am. Chem. Soc.*, **56**, 830 (1934).

Sullivan and Kilpatrick[6] studied the rate of hydrolysis of cyanamide in solutions of nitric, hydrochloric, hydrobromic and trichloroacetic acids, and they explained the results by assuming a two-stage protolysis, the rate-determining step being the reaction between the hydrated cation of cyanamide, $H^2—N—C=N—H$ (with $H—O^+—H$) and any base present.

Kilpatrick[7] also presented the following paths for the hydrolysis of cyanamide in acid solution,

$$H_2N—C\equiv N \rightleftarrows H—N=C=N—H \quad (1)$$

$$H—N=C=N—H + A \rightleftarrows B^- + H_2N—C^+=N—H \quad (2)$$
(I)

$$H_2N—C^+=N—H + HOH \rightleftarrows H_2N—C(—O^+(H)—H)=N—H \quad (3)$$
(II)

$$H_2N—C(—O^+(H)—H)=N—H + B^- \rightleftarrows A + H_2N—C(—O—H)=N—H \quad (4)$$

$$H_2N—C(—O—H)=N—H \rightleftarrows H_2N—C(=O)—NH_2 \quad (5)$$
(III)

where A is an acid and B is its conjugate base. Step (4) was shown as the rate-determining step.

In the present work, the rate constants of the hydrolysis of mono- and di-substituted cyanamides in 20% sulfuric acid solution were measured. Based on the energies of activation and the entropies of activation obtained, the effect of substituents on the reaction was discussed.

Experimental Part

The hydrolysis of cyanamide to urea is accompanied by a contraction in volume which we made use of to follow the reactions dilatometrically. The experiments were performed in a dilatometer like that described by Broensted, Kilpatrick and Kilpatrick.[8] The dilatometer was a bulb of 10 cc.capacity, from the top of which extended a capillary tube 0.3 mm. in diameter and 15 cm. long. The readings were taken by using a cathetometer.

In order to avoid the formation of air bubbles during the reaction, prior to each run, the solvent was degassed under reduced pressure. The temperature control of the reaction thermostat was accurate to ±0.05° within the temperature range 5~85°C.

As an aqueous sulfuric acid is not suitable for kinetic studies owing to the low solubility of cyanamides, dioxane was used as a diluent. Sulfuric acid concentration was 20% by weight in dioxane-water (3:1) solution. In these experiments the initial cyanamide concentration was 0.1 mol.

Mono-substituted Cyanamides.—Ethyl, *n*-butyl, isopropyl, *t*-butyl, allyl and phenyl cyanamides were used. They were synthesized by adding gradually a solution of an amine (1 mol.) in anhydrous ether to cyanogen bromide[9] (1.5 mol.) in anhydrous ether. The temperature of the reaction mixture was kept below 0°C. (except in the case of phenylcyanamide which was prepared at room temperature). After the reaction was completed, the precipitate (amine hydrobromide) was filtered and then ether and unreacted cyanogen bromide were distilled under reduced pressure. The residual cyanamide was then carefully distilled in vacuo. Methylcyanamide and heptylcyanamide synthesized by the above method could not be distilled.

The attempted distillation resulted in the formation of the corresponding melamines in the claisen distilling flask. They were therefore used without further purification. The boiling points and melting point for the amines and the cyanamides are shown in Table III.

TABLE III

Amine	b.p.(C°.)	reference	Cyanamide	b.p.(C°.)	m.p.(C°.)
ethyl-	16.6		ethyl-	94~95/4 mm.	
n-butyl-	77		*n*-butyl-	117/14 mm.	
n-heptyl-	152	(10)	*n*-heptyl-		
isopropyl-	62	(11)	isopropyl-	108/10 mm.	
t-butyl-	44	(12)	*t*-butyl-	109~110/11 mm.	
allyl-	55	(13)	allyl-	92/3 mm.	
phenyl-			phenyl-		42

6) M. J. Sullivan and M. L. Kilpatrick, *J. Am. Chem. Soc,*. **67**, 1815 (1945).
7) M. L. Kilpatrick, *J. Am. Chem. Soc.*, **69**. 40 (1947).
8) J. N. Broensted, M. Kilpatrick and M. Kilpatrick, *J. Am. Chem. Soc.*, **51**. 428 (1929).
9) Organic Syntheses, **11**, 30.
10) Organic Syntheses, **11**, 58.
11) R. Paul. Bull. soc. chem., (5), **4**, 1121 (1937).
12) Organic Syntheses, **29**, 18.
13) Organic Syntheses, **2**, 732.

Di-substituted Cyanamides.—Di-ethyl, di-*n*-butyl, di-isopropyl, di-allyl and di-benzylcyanamides were used. Diethylcyanamide was synthesized from diethylamine and cyanogen bromide. Di-*n*-butylcyanamide,[14] di-allylcyanamide[14] di-isopropylcyanamide[15] were synthesized from the corresponding bromide or chloride by the action of sodium cyanamide. The boiling points and melting point for these cyanamides are shown in Table IV.

TABLE IV

Cyanamide	b.p.(C°.)	m.p.(C°.)
di-ethyl-	78/16 mm.	
di-n-butyl-	120–121/16 mm.	
di-isopropyl-	93–94/25 mm.	
di-allyl-	107–108/18 mm.	
di-benzyl-		53.5

Dioxane used as the diluent was purified by distillation from sodium metal. The reation products, ureas, were identified by their melting points. Diallylurea, which is not recorded in the literature, melted at 64°C. after recrystallization from petroleum ether (Found: N, 19.6. Calcd. for $C_7H_{12}N_2O$: N, 20.0%)

Results and Disscussion

Under the condition of the experiments, as the concentration of (H^+) and (H_2O) can be considered to be constant during the reaction, the reaction velocity can be expressed as follows:

$$v = k \times \left(\begin{matrix} R \\ R \end{matrix} \!\!>\!\! N - C \equiv N \right) \times K$$

where

$$K = \begin{matrix} R \\ R \end{matrix} \!\!>\!\! N - \underset{\underset{O-SO_3H}{|}}{C} = NH \Big/ \left(\begin{matrix} R \\ R \end{matrix} \!\!>\!\! N - C \equiv N \right)(H_2SO_4)$$

On plotting against time t the logarithm of the contraction in volume, ΔY, which had taken place in a constant period of time beginning at time t, we have obtained a straight line. This indicates a first order reaction rate with respect to cyanamide. The rate constant is given[16] by the gradient of such a plot, as shown in Fig. I. The results are shown in Table I.

The rate data were further analyzed by means of the Arrehenius equation

$$\ln k = \ln A - E/RT,$$

and by the absolute rate equation

$$\ln(k/T) = \ln(R\kappa/Nh) + \Delta S^{\neq}/R - \Delta H^{\neq}/RT$$

The transmission coefficient, κ, was set equal to unity. The calculated kinetic functions are collected in Table II.

14) Organic Syntheses., **1**, 197.
15) W. Traube and A. Engelhardt, *Ber.*, **44**, 3151 (1911).
16) E. A. Guggenheim, *Phil. Mag.*, **2**, 538 (1926).

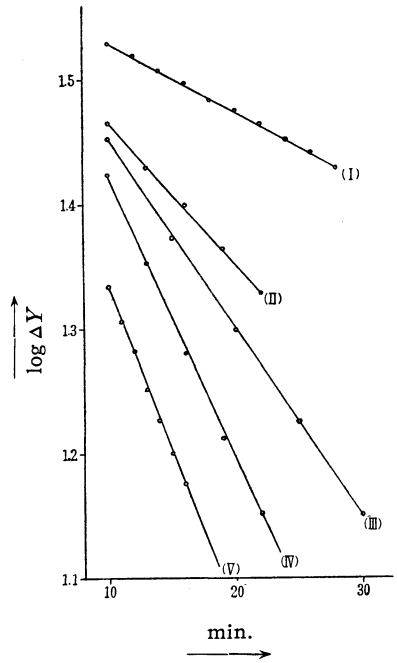


Fig. 1. Hydrolysis of di-ethylcyanamide in 20% sulfuric acid solution: the plot of log ΔY against t.
(I) 26.14° (II) 33.56° (III) 38.50°
(IV) 44.19° (V) 48.15°

TABLE I

THE RATE CONSTANTS OF THE HYDROLYSIS OF SUBSTITUTED CYANAMIDES IN 20% SULFURIC ACID SOLUTION

Cyanamide	t (C°.)	$k \times 10^{-5}$ (sec.$^{-1}$)
methyl-	2.55	5.10
	3.62	6.0
	4.50	6.57
	5.57	7.02
	6.50	7.90
	7.65	8.63
ethyl-	5.55	3.46
	8.25	4.56
	9.21	5.06
	11.25	6.02
	12.15	6.48
	13.10	6.82
n-butyl-	10.0	5.56
	11.13	6.29
	12.15	6.78
	13.20	7.40
	14.18	8.05
	16.78	9.54
n-heptyl-	5.92	5.00
isopropyl	16.52	5.12
	17.32	5.37
	18.06	6.06
	19.08	6.30
	20.10	6.78
	21.20	8.06
	22.50	9.26

t-butyl-	34.10	1.47
	35.07	1.81
	37.47	2.09
	39.0	2.55
	40.83	2.92
allyl-	12.98	6.70
	14.10	7·83
	15.05	8.24
	16.00	9.22
	17.85	11.90
	18.91	14.10
	19.83	14.60
phenyl-	42.75	2.54
cyanamide-	27.07	2.75
diethyl-	26.14	0.394
	33.56	0.613
	38.50	1.06
	41.05	1.25
	44.19	1.72
	48.15	2.06
di-*n*-butyl-	32.45	0.505
	42.55	1.10
	45.92	1.43
	48.60	1.53
	52.10	2.64
	55.20	3.20
di-allyl-	31.10	0.407
	35.16	0.576
	40.03	0.885
	42.88	1.28
	46.80	1.62
	52.50	2.99
di-benzyl-	60.90	0.274
	65.05	0.335
	66.81	0.357
	69.12	0.485
	70.56	0.502
	74.09	0.730
di-isopropyl-	60.90	0.464
	66.04	0.715
	70.74	0.760
	76.22	1.55
	79.81	1.89
	85.04	3.20

TABLE II

THE ACTIVATION ENERGY AND THE ENTROPY OF ACTIVATION FOR THE HYDROLYSIS OF CYANAMIDES IN SULFURIC ACID SOLUTION

Cyanamide	Activation Energy (kcal. mol.$^{-1}$)	Entropy of Activation (cal. mol.$^{-1}$ deg.$^{-1}$)
methyl-	14.8	−26.4
ethyl-	14.4	−29.2
n-butyl-	13.1	−33.6
isopropyl-	17.1	−21.6
t-butyl-	16.6	−28.6
allyl-	19.0	−13.1
di-ethyl-	15.7	−31.4
di-*n*-butyl-	15.9	−30.4
di-allyl-	18.9	−21.6
di-benzyl-	19.5	−21.8
di-isopropyl-	20.2	−23.4

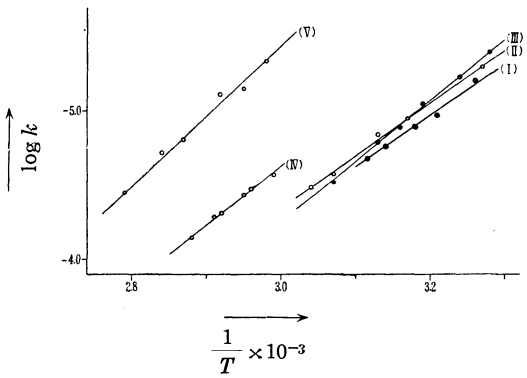


Fig. 2. Hydrolysis of di-substituted cyanamides in 20% sulfuric acid solution: the plot of log k against $1/T$.
(I) di-ethylcyanamide. (II) di-n-butylcyanamide. (III) di-allylcyanamide. (IV) di-benzylcyanamide. (V) di-isoprophylcyanamide.

Cyanamide is hydrolysed to give urea in sulfuric acid solution and the rate of reaction increases as the acid concentration increases. In 10% sulfuric adid solution, the reaction proceeds very slowly.

The effects of substituents on the hydrolysis of the cyanamides in 20% sulfuric acid solution reported in this paper may be summarized as follows:

According to the values of the energies of activation observed for the reaction, the substituents are classified in three groups, (1) normal alkyl groups (13.1–15.9 Kcal.), (2) branched alkyl groups (16.6–20.2 Kcal.) and (3) unsaturated groups (19.0–20.5 Kcal.). The first group contains methyl, ethyl, di-ethyl, *n*-butyl and di-*n*-butylcyanamides, the second isopropyl di-isopropyl and *t*-butyl cyanamides and the third allyl, di-allyl and di-benzyl cyanamides.

As shown in Table I, the rate of reaction for the following eight cyanamides increases in the series:

di-isopropyl- < di-ethyl- < phenyl- < *t*-butyl- < cyanamide < isopropyl- < ethyl- < heptyl-.

The results described above allow the following conclusions to be drawn.

(a) The cyanamide with branched alkyl group requires more energy of activation than the cyanamides with *n*-alkyl group.

(b) The energy required for the hydrolysis of the cyanamides with unsaturated group is nearly equal to those of the cyanamides with branched alkyl group.

(c) In comparing the mono-substituted cyanamide and the di-substituted cyanamide, the latter requires several kilocalories more than the former.

(d) Mono-alkyl cyanamides and mono-isopropyl cyanamide are hydrolysed more easily than the unsubstituted cyanamide.

(e) Phenylcyanamide is hydrolysed more slowly than that which is unsubstituted.

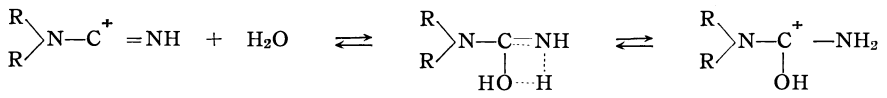
According to the mechanism of hydrolysis of cyanamide in nitric acid solution proposed by Kilpatrick,[7] as mentioned before, the rate-determining step is step (4), which means that (II), the hydrated cation, splits off a molecule of water much more frequently than it yields a proton to an approaching base. In view of experimental results obtained (a)~(e) in this work, however, step (4) is not suitable as the rate-determining step.

On the basis of the electronic effects, supposing that step (4) is the rate-determining step, cyanamides with unsaturated groups would be hydrolysed more readily than the cyanamides with *n*-alkyl groups, because the former cyanamides might be considered to yield a proton to the base more easily than the latter, on account of the negativities of substituents, which make the hydrated cation more acidic. Also, if step (4) limits the reaction, the rates for the hydrolysis of ethylcyanamide, cyanamide and phenylcyanamide should fall into the series,

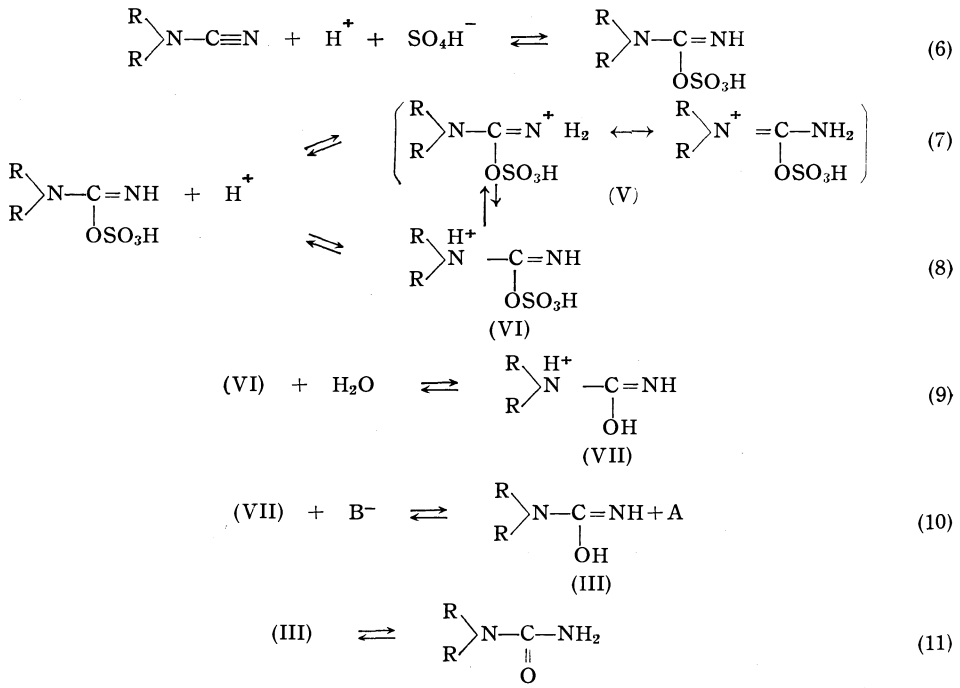
phenylcyanamide > cyanamide > ethylcyanamide.

However, the experiments show the reversed order. The result shows that the cyanamides with electron-releasing groups are hydrolysed more easily than the cyanamide with electron-attracting group, like phenylcyanamide.

These experimental results do not support a mechanism which identifies the rate-determining step with the process of attacking by a water molecule of cyanamide cation.



The results (a)~(e) can be rationalized by considering the following paths for the hydrolysis of cyanamide in 20% sulfuric acid solution.



Under the condition of the experiment, cyanamide-sulfate may be formed in the first place, and by the further protonation, formation of disulfate (VI) and (V) may be expected. The less stable tautomer (VI) is hydrolysed very easily to give an isourea cation, which yields a proton to a base to give urea. On the other hand, the stable tautomer

(V) is more difficult to hydrolyse than (VI) and the isourea is formed via process (8) alone.

It is deemed probable that one nitrogen in a mono-substituted cyanamide has a similiar property to a secondary amine and in a di-subtituted cyanamide to a tertiary amine. As explained by the idea of B-strain introduced by C. H. Brown, the tertiary amines are anomalously weak bases even toward protonic acid. The ability of alkyl amine to add a proton at the nitrogen atom by coordination increases along the series:

$$R_3N < H_3N < RNH_2 < R_2NH.$$

This suggests that a second protonation of cyanamide to form disulfate (VI) is more favorable in cyanamides with *n*-alkyl group and mono-substituted ones than in cyanamides with branched alkyl group and di-subtituted ones, respectively.

As shown in Table V, the basic strength of amines are expressed by their pK_b scale.

TABLE V

ethylamine	ammonia	aniline
3.27	4.75	9.4

The order of the rates for mono-substituted cyanamides (ethylcyanamide, cyanamide and phenylcyanamide) have the same order as to the strength of amines.

Therefore, the second protonation of cyanamide, step (8), can be considered as the rate-determining step.

Summary

The energies and the entropies of activation have been determined for the hydrolysis of mono- and di-substituted cyanamides in 20% sulfuric acid solution.

The effect of substituents are distinctly shown in these kinetic data and the substituents are classified in three groups, (1) normal alkyl group substituted, (2) branched alkyl group substituted and (3) unsaturated group substituted cyanamides. The difference in energy of activation required for the hydrolysis of cyanamides may be explained by assuming the intermediate cyanamide-disulfate, the rate-determining step being the second protonation of cyanamide to give cyanamide-disulfate.

Acknowledgment

The authors wish to express their sincere thanks to Professor T. Hoshino for his many helpful suggestions throughout the course of this work, and to Mr. S. Koyanagi for his help in the early stages of this research.

Department of Physics and Chemistry
Gakushuin Univeasity
Mejiro, Tokyo

Sterols and Other Unsaponifiable Substances in the Lipids of Shell Fishes, Crustacea and Echinoderms. XV. Occurrence of $\Delta^{7:8}$-Cholestenol as a Sterol Component of Star Fish, Asterias amurensis Lütken

By Yoshiyuki TOYAMA and Toru TAKAGI

(Received April 26, 1954)

It was shown in the 5th report[1] of this series that the unsaponifiable substances of the lipid of star fish,* *Asterias amurensis* Lütken, caught around Himagajima Island in Aichi Prefecture contained batyl alcohol as a non-steroid component and hitodesterol** as a sterol component. The present paper describes the results of our studies on the sterol components separated from the star fish of the same species, caught around the southern coast of Hokkaido. The acetate of crude sterol mixture was subjected to fractional crystallization, by which an acetate fraction having a constant melting point of 119—120° and other higher melting fractions were easily separated. The acetate of m.p. 119—120° had a saponification value and an iodine value which agreed closely with the calculated values for cholestenyl acetate. The melting points of the acetate, free sterol and benzoate were found to be close to those reported by previous authors for the corresponding derivatives of $\Delta^{7:8}$-cholestenol (γ-cholestenol). The identity of this star fish sterol with

1) M. Matsumoto, M. Yajima and Y. Toyama, *J. Chem. Soc. Japan*, **64**, 1203 (1943).

* The name of the species *Asterias amurensis* Lütken, was formerly designated as *Asterias rollestoni* Bell.

** Later investigation in our laboratory showed that this sterol has the formula $C_{28}H_{46}O$ or $C_{29}H_{48}O$, having a close resemblance to stellasterol, chondrillasterol and spinasterol, possibly identical with one of them. Cf. The 13th report of this series, Y. Toyama and T. Takagi, This Bulletin, **27**, 39 (1954).

Δ 7 : 8-cholestenol was demonstrated further by conversion of the steryl acetate to Δ 8 : 14-isomer (α-cholestenyl acetate) and Δ 7 : 8, 9-11-cholestadienyl acetate. The higher melting acetate fractions separated from the acetate fraction of m.p. 119—120° yielded, after further recrystallizations a fraction of m.p. 148—153°. Though this fraction was not a single steryl acetate, the easy conversion to its isomer and the saponification and iodine values of the latter appeared to indicate that the fraction of m.p. 148~153° contains predominantly the acetate of Δ 7 : 8-sterol of C_{28} or C_{29} series.

Comparing the above results with those obtained in the previous study, there exists a remarkable difference. While batyl alcohol was easily separated in the previous study, it was not so in the present study. This may be attributable to a far smaller content, if any, of batyl alcohol in the unsaponifiable substances of the present lipid sample. While di-unsaturated hitodesterol was found in the previous study, the sterol mixture of the present lipid sample, as a whole, consisted mainly of mono-unsaturated sterols which contained convincibly Δ 7 : 8-cholestenol. Analogous instances when striking differences exist within an individual lot of aquatic invertebrate of the same species in its unsaponifiable component have already been noted in the case of chiton[2] and corbicula[3]. These facts may possibly be mentioned as a characteristic feature of the unsaponifiable substances of the lipids of some aquatic invertebrates.

Experimental

Some sun-dried star fish, *Asterias amurensis* Lütken, used for these experiments were received from M. Yamada of the Faculty of Fisheries, Hokkaido University. The fish were caught around the southern coast of Hokkaido. The sun-dried material (952 g.) was cut into small pieces. Extraction with ether yielded 84 g. of a dark reddish orange viscous lipid. On treating the lipid with one liter of acetone, an acetone-insoluble oil (73 g.) with the following constants was obtained: d_4^{25} 0.9266, n_D^{25} 1.4733, acid value 71.2, saponification value 162.5, iodine value (Wijs method) 141.5, unsaponifiable matter 15.93%.

Unsaponifiable matter. — The unsaponifiable matter obtained from the acetone-soluble oil by the usual method was a reddish orange solid. The sterol content in the unsaponifiable matter was found to be 52.9% by the digitonide method. The unsaponifiable matter (8.5 g) was recrystallized from 80 cc. of ethanol, yielding a crude sterol (4.2 g.) of m.p. 115–117°. Acetylation of the crude sterol gave a crude steryl acetate of m.p. 115–118° and iodine value* 63.8. Four grams of this acetate was repeatedly recrystallized as shown in Table I.

TABLE I

No. of recrystallization	Solvent	Acetate, crystallized out		Acetate, recovered from mother liquor	
		Yield (g.)	m.p. (°C.)	m.p. (°C.)	Iodine V.
1	Acetone	2.5	125–129	115–116	60.1
2	,,	1.6	127–131	115–116	—
3	,,	0.7	127–137	121–122	66.1
4	Ethanol-ether	0.3	133–145	125–127	66.4
5	Acetone	0.25	140–147	125–132	—
6	,,	0.18	142–147	128–138	—
7	,,	0.12	148–153	135–138	—

Acetate of m.p. 119–120°.—The acetates recovered from the mother liquors of recrystallizations, Nos. 1, 2 and 3, in Table I were united and fractionally crystallized from acetone. After removing a small amount of high melting fraction, a fraction (1.4 g.) of m.p. 119–120° was separated. The melting point was unaltered by further recrystallization from acetone and ethanol-ether, and the fraction recovered from the mother liquors of further recrystallizations showed the same melting point. The fraction of m.p. 119–120° showed $[\alpha]_D^{20} = +5.1°$**, saponification value 131.7 and iodine value 60.5 (calculated for $C_{29}H_{48}O_2$: saponification value 130.8 and iodine value 59.2). Free sterol obtained by saponification of this fraction showed, after recrystallization from ethanol, m.p. 122–123° and $[\alpha]_D^{15} = +4.0$. Benzoate prepared from the free sterol showed, after recrystallization from acetone, m.p. 154–155° and $[\alpha]_D^{15} = +6.8°$.

Δ 8 : 14-Cholestenyl acetate.—The acetate fraction (0.12 g.) of m.p. 119–120° was dissolved in

2) Y. Toyama and T. Tanaka, This Bulletin, **26**, 497 (1953).

3) Y. Toyama and T. Tanaka, This Bulletin, **27** 264 (1954).

* Unless stated otherwise, the iodine values recorded in this paper were determined by the perbenzoic acid method. The pyridine sulfate dibromide method gave an enormously high iodine value of 185.4 for this steryl acetate.

* All rotation were measured with the samples dissolved in chloroform.

15 cc. of glacial acetic acid, and the solution was agitated for 3 hours in an atmosphere of hydrogen in the presence of palladium black. Hydrogen was not absorbed, but isomerization occurred, giving a product of m.p. 76–78° and $[\alpha]_D^{14}=+10.8°$. Free strerol from this product showed m.p. 118–120°.

Δ 7 : 8, 9 : 11-Cholestadienyl acetate.—A solution of 1 g. of the acetate fraction of m.p. 119–120° in 15 cc. of chloroform was mixed with a solution of 2 g. of mercuric acetate in 30 cc. of glacial acetic acid, and the mixture was allowed to stand for 18 hours with frequent stirring.[4] The product, after purification by fractional crystallization from methanol and acetone, showed m.p. 113–115° and $[\alpha]_D^{15}=+32.1°$. It exhibited an ultraviolet absorption curve as shown in Fig. 1

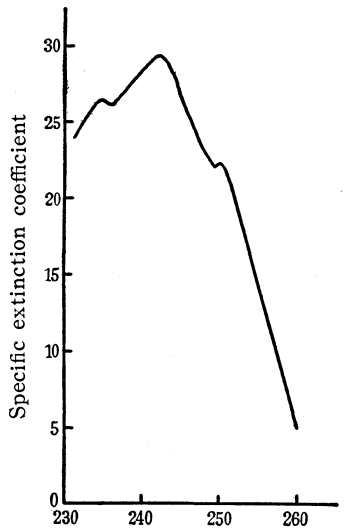


Fig. 1

4) Cf. W. Bergmann and P. G. Stevens, *J. Org. Chem.*, **13**, 10 (1948); W. V. Ruyle et al., *J. Am. Chem. Soc.*, **75**, 2604 (1953).

with the characteristic absorption maxima of 7 : 8, 9 : 11-conjugated sterol; log ε_{235} 4.05, log ε_{243} 4.10 and log ε_{250} 3.98 (Fieser[5] give 4.10, 4.15 and 3.96 for the corresponding values).

Higher melting acetate fraction.—The acetate fraction of m.p. 148–153° in Table I had iodine value 67.5. Free sterol from this fraction had m.p. 146–149° and $[\alpha]_D^{15}=+4.3°$. On treating this acetate fraction in a way similar to that described for the acetate fraction of m.p. 119–120°, it underwent isomerization with little hydrogen absorption. The isomerization product, after recrystallization from methanol, showed m.p. 111–113°, saponification value 125.1 (calculated: $C_{30}H_{50}O_2$ 126.7, $C_{31}H_{52}O_2$ 122.8) and iodine value 60.1 (calculated: $C_{30}H_{50}O_2$ 57.3, $C_{31}H_{52}O_2$ 55.6).

Summary

Sterol mixture of star fish, *Asterias amurensis* Lütken, caught around the southern coast of Hokkaido has been found to consist largely of mono-unsaturated sterols. By fractional crystallization of steryl acetate mixture, an acetate fraction of m.p. 119—120° and a higher melting fraction were separated. The fraction of m.p. 119—120° was identified with the acetate of Δ 7 : 8-cholestenol. The higher melting fraction was not a single steryl acetate, but it appeared to contain predominantly the acetate of Δ 7 : 8-sterol of C_{28} or C_{29} series.

The expence of this study was defrayed in part by a grant from the Hattori Hokokai to whom the authors' thanks are due.

Department of Applied Chemistry,
Faculty of Engineering,
Nagoya University, Nagoya

5) L. F. Fieser, *J. Am. Chem. Soc.*, **73**, 5007 (1951).

Theory of Substitution in Conjugated Molecules[1)]

By Kenichi FUKUI, Teijiro YONEZAWA and Chikayoshi NAGATA

(Received May 17, 1954)

I. Introduction

What we call the *frontier electron theory*, which has been put forward to explain the reactivity of conjugated molecules, was first introduced in discussing the orientation in electrophilic substitutions in non-substituted aromatic hydrocarbons.[2)] Afterwards, this method has been applied not only to electrophilic, but also to radical and nucleophilic substitutions as well as additions in substituted aromatic, heteroaromatic and other conjugated molecules, showing its utility, through a satis-

1) This paper was presented at 7th annual meeting of the Chemical Society of Japan, April 1, 1954.

2) K. Fukui, T. Yonezawa and H. Shingu, *J. Chem. Phys.*, **20**, 722 (1952); K. Fukui, T. Yonezawa and C. Nagata, ibid., **21**, 174 (1953).

factory agreement of theory with experiment, for predicting the reactivity of the π-electron system.[3)]

The frontier electron method is based on the assumption that the reaction should occur at the position of the largest density of the electrons in the frontier orbitals, which are defined according to the type of reaction, namely, the highest occupied orbital in the electrophilic reaction, the lowest vacant orbital in the nucleophilic reaction, and both the above in the radical reaction.

Among the existing theories of the chemical reactivity, the frontier electron method is characterized by the fact that it has not been derived deductively from any physical principle established, but has been found from an intuitive but chemical idea relating to the transition state in the process of substitution. By means of comparing the density distribution of the frontier electrons with the experimental positions of attack in the molecule, it has been recognized, rather as a solid fact than as a theory with a strong physical foundation, that frontier electrons must play some important role in the chemical activation.

In this connection, if a theory of substitution in conjugated molecules could be established in such a form as the frontier electron method which is deduced naturally from the mechanism assumed in the theory, it may be said that this theory would give a physical ground on the frontier electron method, and moreover, the mechanism assumed there would provide us with an important key for obtaining the knowledge of the transition state.

Under these circumstances, the present paper treats a theory of substitution in conjugated molecules, which, therefore, involves not a few assumptions. The validity of them can hardly be demonstrated directly, but can be inferred indirectly on the basis of the availability of the frontier electron method derived from them. This is ture because the agreement of the theory with the experiment proved in the preceding papers[2),3)] is sufficiently satisfactory to convince us that the inference mentioned above is probably reasonable.

II. σ-Part of the Energy of the System

As to the theoretical treatment of a substitution in conjugated molecules, there exists no current theory in which the mechanism of formation and dissociation of σ-bonds is taken into consideration explicitly. Consider a substitution in which the substituent atom X, attached to the r th carbon atom in the substrate π-electron system AX is replaced by a certain atom in a reagent B. The substitution is understood to proceed in such a way that the two σ-electrons shift gradually from AX σ-bond to AB σ-bond. A reaction parameter ρ is introduced, which acts as a measure of proceeding of the reaction and is defined by the following equations:

$$\delta_{AB}=\rho b, \tag{1}$$

$$\delta_{AX}=(1-\rho)a. \tag{2}$$

Here δ_{AB} and δ_{AX} are equal to $\int\chi_A H\chi_B d\tau$ and $\int\chi_A H\chi_X d\tau$, respectively, where χ_A, χ_X are the σ-atomic orbital (real) of the rth atom in A, and of the atom X in AX σ-bond, χ_B is the atomic orbital (real) of B which will form a σ-bond in the reaction, H is the effective Hamiltonian operator for a σ-electron, and a and b are the values of δ_{AX} and δ_{AB} in the isolated molecules AX and AB, respectively. The assumption of (1) and (2) may correspond to the mechanism called "bimolecular" by organic chemists. Then, the initial state is represented by putting ρ equal to zero and the final state by putting ρ equal to unity in the equation.

One electron energy can be obtained by solving the secular equation

$$\Delta\sigma(\varepsilon,\rho)=\begin{vmatrix}\alpha_B-\varepsilon & 0 & \delta_{AB}\\ 0 & \alpha_X-\varepsilon & \delta_{AX}\\ \delta_{AB} & \delta_{AX} & \alpha_A-\varepsilon\end{vmatrix}=0 \tag{3}$$

for any value of ρ, where α_A, α_X and α_B are $\int\chi_A H\chi_A d\tau$, $\int\chi_X H\chi_X d\tau$ and $\int\chi_B H\chi_B d\tau$, respectively.

For simplicity, the changes of α_A, α_B and α_X due to the change of ρ are ignored, because they are expected to have less serious influence upon the essence of the theory than the changes of δ_{AB} and δ_{AX}.# The following results are obtained by some algebraic manipulations of Equation (3):

(1) Among three roots $\varepsilon_1(\rho)$, $\varepsilon_2(\rho)$ and $\varepsilon_3(\rho)$ of Equation (3) ($\varepsilon_1<\varepsilon_2<\varepsilon_3$), $\varepsilon_1(\rho)$ has a maximum value when ρ varies from zero to unity if either one of the following two conditions, i and ii, is satisfied.

i $\alpha_B>\alpha_X$ and $(\alpha_B-\alpha_X)(\alpha_A-\alpha_X)<b^2$, (4)

ii $\alpha_B<\alpha_X$ and $(\alpha_X-\alpha_B)(\alpha_A-\alpha_B)<a^2$. (5)

(2) As long as the condition (4) or (5) is satisfied, $\varepsilon_1(0)$ is equal to the lower σ-level of AX σ-bond in the isolated AX molecule and $\varepsilon_1(1)$ is the lower σ-level of AB σ-bond in the isolated AB molecule. In this case two σ-electrons in AX σ-bond enter into AB σ-bond across a point of the maximum energy along a continuous curve $\varepsilon_1(\rho)$. Thus (4) or (5) may be regarded as the condition which must be satisfied when the substitution

3) K. Fukui, T. Yonezawa, C. Nagata and H. Shingu, *J. Chem. Phys.*, **22**, 1433 (1954); K, Fukui, T. Yonezawa, C. Nagata and H. Shingu, Summary of the Symposium on Atoms and Molecules, *Japan Phys. Soc.*, p. 27 (1953).

But this is a point which may need further investigation. Especially, it should be noted that the assumption of constancy of both α_A etc. and δ_{AB} etc. sometimes leads us to an unreasonable result (compare e.g. the calculation of H_3 molecule by Van Vleck and Sherman (*Rev. Mod. Phys.*, **7**, 167 (1935)), which is, however, not the present case, where the mode of change of δ's is assumed by the equation (1) and (2).

proceeds adiabatically. In the present paper only the case when this condition is satisfied is treated.

(3) The maximum value of $\varepsilon_1(\rho)$, $\varepsilon_1{}^{*}$, is given by

$$\varepsilon_1{}^{*}=\frac{1}{2}[\alpha_A+\alpha_{BX}-\{(\alpha_A-\alpha_{BX})^2+c^2\}^{1/2}], \quad (6)$$

and ρ^{*}, the value of ρ at the maximum point, is also given by

$$\rho^{*}=\frac{1}{2(a^2+b^2)}[[2a^2+(\alpha_B-\alpha_X)[\alpha_A-\alpha_{BX}+\{(\alpha_A-\alpha_{BX})^2+c^2\}^{1/2}]]], \quad (7)$$

where $\alpha_{BX}=(a^2\alpha_B+b^2\alpha_X/(a^2+b^2)$, and $c^2=4a^2b^2/(a^2+b^2)$. Conditions (4) and (5) correspond to the condition that ρ^{*} is in the range from zero to unity.

(4) The higher level $\varepsilon_2(\rho)$, which varies continuously from α_B to α_X when ρ changes from zero to unity, has neither maximum nor minimum at $0<\rho<1$, when the condition (4) or (5) is satisfied.

(5) When the eigenfunctions belonging to the eigenvalues $\varepsilon_i(\rho)$ (i=1, 2, 3) are written as

$$\psi_\sigma{}^{(i)}=c_A{}^{(i)}\chi_A+c_X{}^{(i)}\chi_X+c_B{}^{(i)}\chi_B,$$

the following relations always hold between the coefficients in the wave functions.

$$c_X{}^{(1)}\cdot c_B{}^{(1)}>0$$
$$c_X{}^{(2)}\cdot c_B{}^{(2)}<0$$
$$c_X{}^{(3)}\cdot c_B{}^{(3)}>0$$

All of these characteristics derived mathematically from Equation (3) have an important meaning in constructing the theory of substitution.

The energy $\Delta\varepsilon\sigma$, which is twice as much as the difference between $\varepsilon_1{}^{*}$ given by Equation (6) and $\varepsilon_1(0)$ and hence may be considered as the σ-part of the activation energy in the substitution, is given by

$$\Delta\varepsilon\sigma=\frac{a^2(\alpha_B-\alpha_X)}{a^2+b^2}+\sqrt{(\alpha_A-\alpha_X)^2+4a^2}-\sqrt{\left(\alpha_A-\frac{a^2\alpha_B+b^2\alpha_X}{a^2+b^2}\right)^2+\frac{4a^2b^2}{a^2+b^2}}. \quad (8)$$

The fact that $c_X{}^{(2)}$ and $c_B{}^{(2)}$ have opposite signs is important in connection witn the statement in the next section.

III. Hyper Conjugation in the Transition State

In Section II, it is stated that the coefficients $c_X{}^{(2)}$ and $c_B{}^{(2)}$ in the eigenfunction belonging to $\varepsilon_2(\rho)$ always have opposite signs. Here it is desired to examine generally the quantitative relation between $|c_X{}^{(2)}|^2$ and $|c_B{}^{(2)}|^2$ when ρ is equal to ρ^{*}, but this is too complicated to be carried out analytically. For this reason the case when B is equal to X is at first considered. We could distinguish B from X e.g. by means of labelling them isotopically. In this case eigenfunctions and ρ^{*} are easily written explicitly as

$$\begin{aligned}\psi_\sigma{}^{(1)*}&=2^{-1/2}A^{-1/2}\{(A-\alpha_A+\alpha_B)^{1/2}\chi_A+2^{-1/2}(A+\alpha_A-\alpha_B)^{1/2}(\chi_B+c_X)\}\\ \psi_\sigma{}^{(2)*}&=2^{-1/2}(\chi_B-\chi_X)\\ \psi_\rho{}^{(3)*}&=2^{-1/2}A^{-1/2}\{(A+\alpha_A-\alpha_B)^{1/2}\chi_A-2^{-1/2}(A-\alpha_A+\alpha_B)^{1/2}(\chi_B+\chi_X)\}\\ \rho^{*}&=1/2\end{aligned} \quad (9)$$

where $\psi_\sigma{}^{*}$ corresponds to ψ_σ when ρ is equal to ρ^{*}, and $A=\{(\alpha_A-\alpha_B)^2+2a^2\}^{1/2}$. The orbital $\psi_\sigma{}^{(2)*}$ in Equation (9) is antisymmetric with respect to the plane which is perpendicular to the line connecting B to X across its middle point.

As the reagent B is believed to approach to the rth atom in A from the direction perpendicular to the plane in which all the carbon atoms of AX lie, this plane is considered to cross the line BX at its middle point when ρ is equal to ρ^{*}. Thus the orbital $\psi_\sigma{}^{(2)*}$ is parallel to the π-orbitals in A and is antisymmetric to the above-stated plane. This fact is, therefore, sufficient to make us believe the possibility of a hyperconjugation between the π-orbitals in A and the orbital $\psi_\sigma{}^{(2)*}$.* It is not so unreasonable to consider that the hyperconjugation may take place more or less even when B is not equal to X. It is our opinion similar to Mulliken et al. that this hyperconjugation, taking part in the electronic interaction of the system near the transition state, causes a delocalization of π-electrons from A to the reaction center or vice versa and plays an important role in decreasing the activation energy.

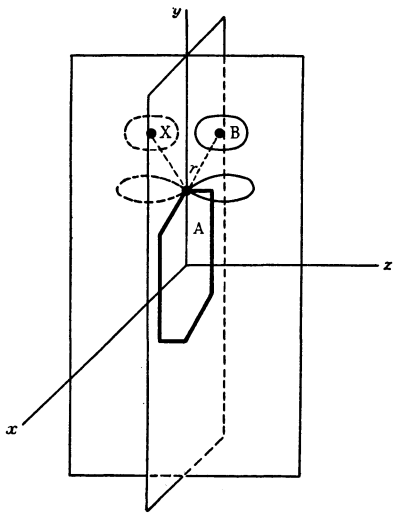


Fig. 1. Schematic diagram of hyperconjugation in the transition state.

IV. π-Part of the Energy of the System

As can be seen in Equation (9) the orbitals $\psi_\sigma{}^{(1)*}$ and $\psi_\sigma{}^{(3)}$ in which coefficient of χ_B is equal to that of χ_X, are free from conjugation with A. In calculating the π-part of the energy, therefore, these orbitals are left out of consideration, even when B is not equal to X, according to the relation mentioned in (5).

The state, in which the total energy of the whole system is maximum, is not always equal to the state $\rho=\rho^{*}$, except when B is equal to X. Thus, in a strict sence, it is not correct to regard the state $\rho=\rho^{*}$ as the transition state. But, in order to avoid complicating the problem and missing more

* This consideration was first introduced by Mulliken et al. (L. W. Pickett, N. Muller, and R. S. Mulliken, *J. Chem. Phys.*, **21**, 1400 (1953).) to explain the stabilization of $C_6H_7^{+}$ ion. Their work modifies the excessively large value of localization energy reported by Wheland (*J. Am. Chem. Soc.* **64**, 900 (1940)).

important conclusions, it might be allowable here to proceed with the discussion taking the state $\rho=\rho^{\ddagger}$ as the transition state. The eigenvalue ε_2 belonging to $\psi_\sigma{}^{(2)}\ddagger\equiv\psi_h$ is denoted by α_h, and the orbital ψ_h is referred to as a *pseudo-π-orbital.*

The empirical classification of substitution reached by organic chemists, i.e. electrophilic, radical and nucleoppilic is naturally introduced into the theory in the following manner. Namely, acoording as the the reagent B is electrophilic, radical or nucleophilic, the orbital ψ_h is considered to be occupied by 0, 1 or 2 electrons, respectively.

Now the π-energy in the transition state can be calculated by means of ordinary LCAO method. The secular equation for the transition state is written as

$$\Delta\pi=\begin{vmatrix} \alpha_h-\varepsilon & \tau & 0 & \\ \tau & \alpha_r-\varepsilon & \beta_{r,r+1} & \\ 0 & \beta_{r,r+1} & \alpha_{r+1}-\varepsilon & \\ \vdots & & \text{(Secular equation for AX)} & \end{vmatrix}=0, \qquad (10)$$

where each α_s and β_{st} is the Coulomb integral of the sth atom and the resonance integral between the sth and the tth atomic orbitals in the isolated AX molecule, and τ is the resonance integral of the quasi-bond between the pseudo-π-orbital and the rth atom in A. The values of these integrals in Equation (10), which concerns the transition state, differ from those in the isolated molecule, but these differences, which are believed to have no any serious influence on the present theory, are here ignored.

In fact, the change in the Coulomb integral α_r caused electrostatically by the approaching reagent in a heterolytic substitution has no longer any essential significance,* so long as a considerable amount of delocalization of electrons, which will be stated below, takes place.

It is rather easy to extend the present theory to the case when a conjugation occurs between AX and B which possesses π-electrons, but this extension is not included in the present paper[4]

Making use of the perturbation theory by regarding τ as small, the π-activation energy for a non-degenerate system** is obtained as

$$\Delta E_\pi=\sum_{j=1}^{N}\frac{(\nu_j-\nu)C_r{}^{(j)2}}{\varepsilon_j-\alpha_h}\tau^2+\nu(\alpha_h-\alpha_B), \qquad (11)$$

where N is the total number of π-orbitals in the isolated AX molecule, ν_j and $C_r{}^{(j)}$ are the number of electrons (0, 1, or 2) and the coefficient of the rth atomic π-orbital in the jth molecular orbital, respectively, the energy of which is ε_j, and ν is 0, 1 or 2 according as the reagent B is electrophilic, radical and nucleophilic, respectively.

The extent of mutual delocalization of electrons between the pseudo-π-orbital and the initial π-electrons system AX, is represented by

$$\Delta q_h=\sum_{j=1}^{N}\frac{(\nu_j-\nu)C_r{}^{(j)2}}{(\varepsilon_j-\alpha_h)^2}\tau^2, \qquad (12)$$

where Δq_h is the difference between the total electron density at BX-part in the transition state and the value ν.

The value of α_h is generally understood to be small for an electrophilic reaction and large for a nucleophilic reaction, but this is not necessarily so in the case when the electron delocalization represented by (12) exists. It can easily be shown that Δq_h is always positive for an electrophilic reaction and is negative for a nucleophilic reaction. The delocalization which occurs in an electrophilic substitution from AX to pseudo-π-orbital makes the value of α_h increase and the delocalization from the pseudo-π-orbital to AX in a nucleophilic substitution makes it decrease, and in both the cases the delocalization will cease after the values of integrals in the whole system become self-consistent. Moreover, in heterolytic reactions, the positive or the negative charge in the activated complex distributes over the whole system and never localizes at the orbital ψ_h. In a homolytic reaction, of course, the value of α_h is very close to that of Coulomb integral of the rth atom in the isolated AX molecule. In these circumstances an assumption is made that α_h is always equal to α_r the value of Coulomb integral of a carbon atom in benzene. This assumption may have room for improvement in case of modification of the theory in such a way that the self-consistency is satisfied, but it seems rather more concise and useful in the present stage to grasp the essential feature of the mechanism of substitution.

Putting α_h equal to α, the first term in the right side in Equation (11) is always negative, and so it is seen that the hyperconjugation in the transition state decreases the activation energy in a substitution.

V. Relation to the Frontier Electron Theory

Since the σ-part of the activation energy, (8), is a constant if the reagent B and the substituent X are fixed, the relative rate of substitution of a definite type in conjugated molecules by a definite reagent can be measured by the amount of the coefficient of τ^2 in Equation (11). This quantity referred to tentatively as *super-delocalizability* and denoted by S_r, that is

$$S_r=\sum_{j=1}^{N}\frac{(\nu_j-\nu)C_r{}^{(j)2}}{\varepsilon_j-\alpha}\beta, \qquad (13)$$

in which the resonance integral of a C-C bond in benzene, β, is multiplied to make it dimensionless. When ε_j is expressed in the form $\alpha+\lambda_t\beta$,

$$S_r=\sum_{j=1}^{N}\frac{(\nu_j-\nu)C_r{}^{(j)2}}{\lambda_j} \qquad (13)'$$

---

* But the change of β_{XR} must be taken into account when the atom X possesses π-electrons or a π-orbital which can conjugate with the π-electrons in A, because a considerable change in the bond AX may occur in the transition state.

4) C. A. Coulson and H. C. Longuet-Higgins, *Proc. Roy. Soc.*, A **195**, 188 (1948); M. J. S. Dewar, *J. Am. Chem. Soc.*, **74**, 3341 (1952); T. Yonezawa, K. Hayashi, C. Nagata and K. Fukui, *Summary of the Symposium on π-electrons*, Jap. Chem. Soc., p. 26 (1952).

** For a degenerate system a similar equation can easily be derived.

\# When AX is an odd molecule an equation of type of (15) should be used instead of (11).

Then S_r is positive for almost all of the usual compounds, and the greater the value, the more reactive is the rth position of the compound.

When AX is an even molecule and its occupied levels are denoted by 1, 2,....., m and the unoccupied levels by m+1, m+2,....., N, S_r is written in three cases as:

(i) For an electrophilic reaction

$$S_r^{(E)} = 2\sum_{j=1}^{m} \frac{C_r^{(j)2}}{\lambda_j},$$

(ii) for a radical reaction

$$S_r^{(R)} = \sum_{j=1}^{m} \frac{C_r^{(j)2}}{\lambda_j} + \sum_{j=m+1}^{N} \frac{C_r^{(j)2}}{(-\lambda_j)},$$

(iii) for a nucleophilic reaction

$$S_r^{(N)} = 2\sum_{j=m+1}^{N} \frac{C_r^{(j)2}}{(-\lambda_j)}. \tag{14}$$

Since, in many compounds especially in large molecules, λ_m and λ_{m+1} are considerably small compared with the other λ's, the magnitude of S_r is determined predominantly by the term whose j is m+1 or m. $S_r^{(E)}$ is large when $2\,C_r^{(m)2}$, i.e. the electron density at the rth atom in the highest occupied orbital, is large, and $S_r^{(N)}$ is large when $2C_r^{(m+12)}$, i.e. the electron density at the rth atom in the lowest vacant orbital, is large. In a radical substitution $S_r^{(R)}$ is large when $C_r^{(m)2}+C_r^{(m+1)2}$ is large, so far as λ_m is approximately equal to $(-\lambda_{m+1})$.

When AX is a neutral odd molecule, in which the mth orbital is partly occupied and its energy is approximately equal to α, the perturbation theory for a degenerate system is available. The π-activation energies are obtained as:

(i) For an electrophilic reaction.

$$\Delta E_\pi = |C_r^{(m)}|\gamma + S_r^{(E)}\frac{\gamma_2}{\beta},$$

$$S_r^{(E)} = 2\sum_{j=1}^{m-1} \frac{C_r^{(j)2}}{\lambda_j} \sim 2\frac{C_r^{(m-1)2}}{\lambda_{m-1}}$$

(ii) For a radical reaction

$$\Delta E_\pi = 2|C_r^{(m)}|\gamma + S_r^{(R)}\frac{\gamma^2}{\beta} + (\alpha-\alpha_B) \sim 2|C_r^{(m)}|\gamma,$$

$$+(\alpha-\alpha_B)$$

$$S_r^{(R)} = \sum_{j=1}^{m-1} \frac{C_r^{(j)2}}{\lambda_j} + \sum_{j=m+1}^{N} \frac{C_r^{(j)2}}{(-\lambda_j)},$$

and in this case the first order perturbation term is dominant,

(iii) For a nucleophilic reaction

$$\Delta E_\pi = |C_r^{(m)}|\gamma + S_r^{(N)}\frac{\gamma^2}{\beta} + 2(\alpha-\alpha_B),$$

$$S_r^{(N)} = 2\sum_{j=m+1}^{N} \frac{C_r^{(m+1)2}}{(-\lambda_j)} \sim 2\frac{C_r^{(m+1)2}}{(-\lambda_{m+1})}, \tag{15}$$

The orbital which determines dominantly the value of S_r in each type of reaction is the same as the *frontier orbitals* which have previously been pointed out by the present authors as playing an important role in the course of reaction. Thus the frontier electron theory is deduced naturally.

If ΔE_π is calculated in the case of naphthalene, as an example, by solving Equation (10) directly without using the perturbation theory, it can be shown that $|\Delta E_\pi|$ of α-position is always larger than that of β-position for any value of γ, and the circumstances are entirely the same concerning 1 and 2 positions in butadiene. The conclusion obtained in the present paper, therefore, never depends on the assumption that the value of γ in (10) is so small that the perturbation method may be used for solving Equation (10).

IV. Summary

A theory concerning the mechanism of substitution in conjugated molecules is stated. The energy of the whole system is divided into σ- and π-parts. When certain relations hold between some integrals of σ-electrons, the σ-part of the energy of the system has a maximum in the process of the reaction, by which the transition state is defined. In the transition state a hyperconjugation may take place between the initial π-electron system and the pseudo-π-orbital in the vicinity of the reaction center. By means of the perturbation method, the π-part of the energy of the system involving the pseudo-π-orbital is obtained. The perturbation energy is always negative and by the magnitude of its absolute value, the reactivity of conjugated molecules can be discussed in a definite type of reaction with a definite reagent. From an approximate expression of this perturbation energy, the frontier electron theory is derived, which has previously been proposed by the present authors, whose coincidence with chemical experiences has already been ascertained. The mechanism stated above, therefore may supply us with a key to grasp a feature of the transition state and at the same time may present us with a physical meaning of the frontier electron theory.

The authors wish to express their heartfelt gratitudes to Professor R.S. Mulliken and to Professor C. A. Coulson for their suggestive discussions on the present problem at the International Conference of Theoretical Physics in Japan, September 1953.

Financial support for this work has been received in part from GAFSR, (1953-59168), Education Ministry, Japanese Government.

Faculty of Engineering,
Kyoto University

Alkylalkoxypolysiloxanes. I. Ethylethoxypolysiloxanes

By Rokuro ŌKAWARA

(Received May 20, 1954)

A series of ethylethoxypolysiloxanes as indicated by formula I and a somewhat similar series[1] were prepared by hydrolyzing the corresponding alkyltriethoxysilane, but the products were not accurately characterized.

$$C_2H_5O\left(\begin{array}{c}C_2H_5\\|\\SiO\\|\\OC_2H_5\end{array}\right)_n C_2H_5 \qquad \text{I}$$

The methylethoxypolysiloxanes[2], having the similar structure as the series I, have also been prepared by the partial hydrolysis of methyltriethoxysilane.

This paper will describe a series of lower members (n=1~4) of ethylethoxypolysiloxanes (series I) which were prepared by a thermal reaction between ethylethoxychlorosilanes and ethyltriethoxysilane at the refluxing temperature.

The thermal reaction between ethyldiethoxychlorosilane and ethyltriethoxysilane was found in the quantitative study of partial ethanolysis of ethyltrichlorosilane to determine the ratio of reaction rate of this competitive consecutive reaction[3]. For the purpose of characterizing these polymerized products, pure ethyldiethoxychlorosilanes and ethyltriethoxysilane were mixed in various mol ratios and refluxed. Changings of the weight, the chlorine content and the boiling point of the mixture were pursued through the reaction. When the chlorine content of the mixture was reduced practically to zero, the mixture was fractionated. A series of linear polymers (series I) was obtained. The first plateau was unreacted ethyltriethoxysilane and subsequent plateaus were the succeeding members of this series. By redistilling these polymers, the presence of a small amount of cyclo-compounds, probably cyclotrimer and cyclotetramer, were found between the succeeding plateaus of linear polymers, but owing to the small amount these cyclo-compounds could not be characterized. Analysis and physical properties of the linear polymers are given in Table II. Properties of the ethyltriethoxysilane are also included for the purpose of comparison.

This thermal reaction was not limited in the case of ethylethoxypolysiloxanes, but the case of ethyl isopropoxy-, ethylmethoxy-, and methylmethoxy-polysiloxanes will soon be reported.

Experimental

Starting Materials.—The ethylethoxychlorosilanes and ethyltriethoxysilane used in this experiment were prepared by the partial ethanolysis of ethyltrichlorosilane[3]. The partial ethanolysis products were fractionated twice through a stedman column of about 20 theoretical plates. Ethylethoxydichlorosilane, ethyldiethoxychlorosilane and ethyltriethoxysilane thus obtained have the following properties.

Ethylethoxydichlorosilane: b.p. 66°C/100 mm Hg, n_D^{20} 1.4100, d_4^{20} 1.0876. Anal. Calcd. for $C_2H_5Si(OC_2H_5)Cl_2$: Cl, 41.0. Found: Cl, 40.4%.

Ethyldiethoxychlorosilane: b.p. 85°C/85 mm Hg, n_D^{20} 1.4007, d_4^{20} 0.9793. Anal. Calcd. for $C_2H_5Si(OC_2H_5)_2Cl$: Cl, 19.4. Found; Cl, 19.1%.

Ethyltriethoxysilane: b.p. 61°C/14 mmHg, n_D^{20} 1.3911, d_4^{20} 0.8963. Anal. Calcd. for $C_2H_5Si(OC_2H_5)_3$: Si, 14.57. Found: Si, 14.50%.

A. Thermal Reaction of Ethyltriethoxysilane and Ethylethoxychlorosilanes: Preparation of the Compounds of the Series I.—Ethylethoxychlorosilane and ethyltriethoxysilane were mixed as shown in Table I. By refluxing, the weight of the mixture and the chlorine content were gradually decreased. After the chlorine content of the mixture practically disappeared, the mixture was further refluxed and tested with Beilstein test to assure that no trace of chlorine compound was found in it. The time needed to produce chlorine free mixture and the highest refluxing temperature attained are cited in Table I.

The products were fractionated through a semimicro stedman column of about 30 theoretical plates under reduced pressure. Unreacted ethyltriethoxysilane was distilled out between 66°–76° C/22–30 mmHg. The disiloxane and trisiloxane fractions were the succeeding plateaus which were obtained at 64°–66° C/0.8 mmHg and 101°–6° C/0.8 mmHg. The amounts in percentage of these plateaus including the intermediate fractions cut on the distillation curve are also shown in Table I.

B. Redistillation of the Polysiloxanes. Isolation and Characterization of Linear Poly-

1) K. Andrianov, *J. Gen. Chem.* (*U.S.S.R.*), **8**, 1255 (1938); **16**, 939 (1946).
2) H. J. Fletcher and M. J. Hunter, *J. Am. Chem. Soc.*, **71**, 2922 (1946).
3) R. Okawara, S. Numa and T. Watase, *J. Chem. Soc. Japan, Ind. Sec.* **57**, 118 (1954) (in Japanese).

TABLE I
RESULTS OF THE THERMAL REACTION

Exp. No.	Starting Material: Compound	(g)	(mol.)	Reaction: Time (hr)	Temp. (°C)	Product: (g)	(%theory)	Polysiloxane Fraction: Monomer (%)	Dimer (%)	Trimer (%)	Residue (%)
1	$C_2H_5Si(OC_2H_5)_2Cl$	11	0.06	45	189	17	90	17	31	22	30
	$C_2H_5Si(OC_2H_5)_3$	11.6	0.06								
2	$C_2H_5Si(OC_2H_5)Cl_2$	8.6	0.05	45	192	20	82	13	10	16	61
	$C_2H_5Si(OC_2H_5)_3$	19.2	0.1								
3	$C_2H_5Si(OC_2H_5)_2Cl$	18.5	0.1	47	212	19.5	91	13	27	27	33
	$C_2H_5Si(OC_2H_5)_3$	9.6	0.05								
4	$C_2H_5Si(OC_2H_5)Cl_2$	9	0.05	62	192	26	88	19	19	29	33
	$C_2H_5Si(OC_2H_5)_3$	24	0.12								

TABLE II
ETHYLETHOXYPOLYSILOXANES

Polymer size	Name	Formula	Boiling Point °C/mm	Density d_4^{20}	Refractive Index n_D^{20}	Molar Refraction Found (Calcd.)*	Molecular Weight Found** (Calcd.)	%Si Found (Calcd.)	%C Found (Calcd.)	%H Found (Calcd.)
Monomer	Triethoxyethylsilane	$C_2H_5O(SiO(OC_2H_5)_2)_1C_2H_5$	61/14	0.8963	1.3911	50.98 (51.08)	—	14.50 (14.57)	—	—
Dimer	Tetraethoxy-1, 3-diethyldisiloxane	— ( )$_2$ —	65/0.8	0.9473	1.4006	79.53 (79.74)	315 (310)	18.12 (18.06)	46.26 (46.49)	9.44 (9.68)
Trimer	Pentaethoxy-1, 3, 5-triethyltrisiloxane	— ( )$_3$ —	101/0.8	0.9750	1.4074	108.4 (108.4)	435 (429)	19.70 (19.64)	44.83 (44.82)	9.39 (9.34)
Tetramer	Hexaethoxy-1, 3, 5, 7-tetraethyltetrasiloxane	— ( )$_4$ —	122/0.8	0.9960	1.4148	137.2 (137.0)	556 (546)	20.63 (20.64)	44.20 (43.92)	8.93 (9.17)

* Calculated from bond refractivities by Warrick, *J. Am. Chem. Soc.*, **68** 2455 (1946)

** Cryoscopic measurements in benzene

mers of Series I.—As the amounts of disiloxane and trisiloxane fraction were small in each experiment, all the polysiloxane fractions except monosilane fraction were gathered (55g.) and again fractionated rigorously through the same column. The distillation curve and the refractive index of the small portions are shown in Fig. I.

The plateaus A, B and C in Fig. I were found to be dimer (tetraethoxy-1, 3-diethyldisiloxane), linear trimer (pentaethoxy-1,3,5-triethyltrisiloxane) and linear tetramer (hexaethoxy-1, 3, 5, 7-tetraethyltetrasiloxane) respectively. Properties of these compounds are given in Table II.

From the knick point of the distillation curve between A and B, and the high refractive index at this portion, the presence of a compound was supposed at this point, but owing to the small amount this compound could not be isolated. Appearance of cyclotrimer (triethoxy-1, 3, 5-triethylcyclotrisiloxane) may be probable at this point, for in the analogous case of ethylisopropoxypolysiloxanes prepared by the same method, the cyclotrimer, which was isolated and characterized, was found

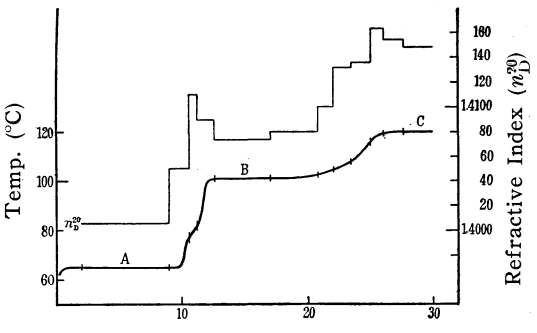


Fig. I. Redistillation curve of ethylethoxypolysiloxanes and the refractive index of the distillates.

A: Dimer
B: Linear trimer
C: Linear tetramer

to be distilled out between the plateaus of dimer and linear trimer. The high refractive index which was found between B and C may also seem to be caused by the presence of cyclo-compound, probably cyclotetramer.

C. Analysis of Silicon.—Silicon was determined by decomposing the sample with concentrated sulfuric acid.

Summary

(1) Ethylethoxypolysiloxanes have been prepared by a thermal reaction of ethylethoxychlorosilanes and ethyltriethoxysilane.

(2) Linear ethylethoxypolysiloxanes containing from 2 to 4 silicon atoms have been prepared and characterized.

(3) Certainly, a small amount of ethylethoxycyclopolysiloxanes were formed by the thermal reaction but they could not be isolated.

Department of Applied Chemistry
Faculty of Engineering
Osaka University
Osaka

On the Synthesis of 8-Hydroxyquinoline

By Akira INOUE, Michio SUGIURA and Yojiro TSUZUKI

(Received May 25, 1954)

Introduction

The object of this investigation is to prepare 8-hydroxyquinoline for the purpose of utilizing quinoline, a constituent of the coal tar bases contained in considerable quantity (ca. 18%). On the synthesis of this substance from quinoline, however, no systematic investigations have been made, in spite of the fact that 8-hydroxyquinoline has been reported to be useful as an organic reagent for the microanalysis of metal irons, as a stabilizer of P.V.A.[1], and a fungicide in the form of its copper salt[2], etc.

The present research was undertaken to find out the best condition of the sulfonation of quinoline, that of the alkali fusion of sulfoquinoline, and that of the preparation of copper 8-hydroxyquinolate in order to obtain 8-hydroxyquinoline as well as its copper salt with good yield.

Sulfonation of Quinoline

The process of sulfonation was adopted as the first stage of the synthesis, because the 8-position of quinoline is, from the view-point of active complex, most active in cationic substitution, is as its highest in electron density (see Fig. 1), and finally because the sulfonic group is expected to enter preferentially into the 8-position considering the previous experimental result.[4]

Purification of Material—Crude quinoline was subjected to fractional distillation with a column of 2 cmϕ×50 cm under reduce pressure. The boiling point of thus purified quinoline was 113–114°C/17 mm. The content was 65% of the crude material. Isoquinoline distilled at 117–118C°/17 mm; the content was 27%.

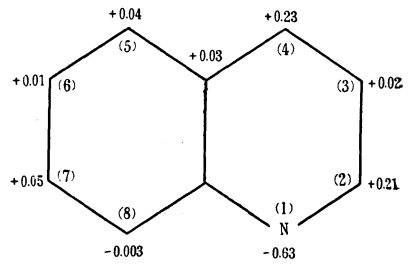


Fig. 1. Electron density of quinoline (C. A. Coulson)

Procedure—50 g. of quinoline was dropped gradually in to 150 g. of 50% oleum (fuming sulfuric acid) contained in a 300 cc. flask, equipped with an air-tight stirrer, a dropping funnel, and a reflux condenser. The temperature was kept below 50°C while adding; then the whole was gradually heated to a given temperature, and kept constant there for some hours, as shown in Table I and II. On pouring the reaction product onto ice, 8-sulfoquinoline separated in the form of white precipitate or crystals (m.p. 312°C), while 5-sulfoquinoline (m.p. 59°C), the main by-product, was dissolved into water.

Results—The influence of the temperature on the yield of 8-sulfoquinoline is shown in Table I. The maximum yield (80.3%) was obtained at 140°C. When the reaction is carried out above this temperature, the product is colored brown, the purification becomes difficult and hence the yield is reduced-

1) F. W. Cox, U.S.P. 2,396,555, March 12 (1946).
2) P. G. Benignus, *Ind. Eng. Chem.* **40**, 1426 (1948).

TABLE I
INFLUENCE OF REACTION TEMPERATURE ON THE YIELD OF 8-SULFOQUINOLINE
(The reaction time: 2 hrs.)

Temp. (°C)	Yield (%)	Temp. (°C)	Yield (%)
100	40.7	130	61.7
110	49.4	135	70.4
120	63.9	140	80.3

The influence of the reaction time on the yield of 8-sulfoxuinoline was investigated at 120° and 140°C. The results are shown in Table II.

TABLE II
INFLUENCE OF REACTION TIME ON THE YIELD OF 8-SULFOQUINOLINE

Time (hr.)	Yield 120°C	Yield 140°C
1	41.7	54.9
2	63.9	80.3
3	53.1	42.4
4	46.9	32.1

G. M. McCasland[3] obtained a lower yield (54%) in the sulfonation of quinoline with 30% oleum at 90°C and 40 hrs. The unfavorable result is probably due to the long heating by which 7- and 5-sulfoquinoline and disulfoquinolines,[4] all soluble in water, are formed. It may be attributed to the formation of these reaction products that the yield decreases, when the reaction is continued further than 2 hrs., as observed in our case (Table II).

Alkali Fusion of 8-Sulfoquinoline

To a quantity of molten (260°C) sodium hydroxide in a graphite crucible is gradually added 20.9 g. (1/10 mol) of 8-sulfoquinoline, and the whole is kept at 300-310°C for 10 to 15 min. Table III shows how the yield of 8-hydroxyquinoline varies with the quantity of sodium hydroxide, which is expressed by a unit of the theoretical quantity, 3 moles of NaOH being theoretically required for one mole of 8-sulfoquinoline.

$$C_9H_6NSO_3H+3NaOH = C_9H_6NSO_3Na+Na_2SO_3+2H_2O.$$

The yield of 8-hydroxyquinoline is expressed by the quantity obtained by distilling with steam for 1.5 hrs.* after alkali fusion.

TABLE III
INFLUENCE OF THE QUANTITY OF SODIUM HYDROXIDE ON THE YIELD OF 8-HYDROXQUINOLINE

NaOH	Yield (%)	NaOH	Yield
1	0	3	38.6
1.5	38.6	3.5	29.0
2	40.7	4	22.1

3) *J. org. Chem.*, **11**, 277 (1946).
4) Claus, Stelzner *J. prakt. Chem.*, [2], **53**, 390 (1896).
* It takes more than one hour, for the black product formed by neutralization with NaOH to turn entirely to a tarry precipitate.

8-Hydroxyquinoline and its Copper Salt

In order to isolate 8-hydroxyquinoline from the product of alkali fusion the following procedure was adopted:

acid decomposition→neutralizaton→steam distillation→8-hydroxyquinoline.

However, complete isolation is not realized by such a simple method, since 8-hydroxyquinoline is slightly soluble in water, and readily soluble both in acid and concentrated alkali, namely, 8-hydroxyquinoline remains in the residue as well as in the filtrate of steam distillation. The following modifications were, therefore, to be made: the product of alkali fusion was decomposed by dilute sulfuric acid, the liquid was carefully neutralized with both concentrated sodium hydroxide and sodium carbonate to a *p*H 7.2, the isoelectric point[5] of 8-hydroxyquinoline, where the solubility in water is the minimum.

These processes were carried out always below 35°C in order to prevent the evaporation of 8-hydroxyquinoline with steam and also to prevent the formation of a cake from the black body formed by the neutralization. The steam distillation is continued for 1.5 hrs. (the quantity of water ca. 1.7 l.), the distillate is cooled, and 8-hydroxyquinoline filtered. The filtrate from 8-hydroxyquinoline, (I), is combined with the filtrate (II), mentioned below. The residue of steam distillation is, after cooling, acidified with dilute sulfuric acid to a *p*H 2.8, so as to precipitate the ferrous 8-hydroxyquinolinate completely, where 8-hydroxyquinoline itself is soluble. The filtrate of ferrous 8-hydroxyquinolinate, (II), is combined with the filtrate (I), and a calculated quantity of crystalline copper sulfate is added, in the state of warm solution, to this combined filtrate, in order to prepare the copper salt of 8-hydroxyquinoline. The crystalline powder of the copper salt, thus formed is filtered at *p*H 2.7–3.2 by treating the mixture with concentrated sodium hydroxide, solution at which *p*H the solubility of the copper salt is least and the precipitate of cupric hydroxide dissolved[6]. The copper salt is washed with warm water, and dried at 100°C in an air-bath. The copper salt is prepared from 8-hydroxyquinoline in the following: an aqueous solution containing a little more than the calculated quantity (0.86 times the weight of 8-hydroxyquinoline) of $CuSO_4 \cdot 5H_2O$ is warmed at 80° to 100° and 8-hydroxyquinoline is gradually added to this warm solution, the precipitate is filtered, while still not, at *p*H 2.7–3.2, and dried at 100°C. The yield of the copper salt is nearly 100%.

In Table IV is shown the yield of 8-hydroxyquinoline including copper salt from 8-sulfoquinoline. Even in respect of the yield the present method is superior to the most

5) I. M. Kolthoff, *Chem. Weekblad*, **24**, 606 (1927).
6) H. Gotô, *Sci. Rept. Tôhoku Imp. Univ.*, 1 ser., **26**, 391 (1937).

recent method (67%) of Skraup synthesis[7] from *o*-aminophenol as well as from *o*-nitrophenol.

TABLE IV

NaOH (theoret. quantity=1)	Yield max. (%)	Yield mean (%)	Experimental condition at the max. yield temp. (°C)	Experimental condition at the max. yield time (min.)
2	61.4	50.3	300–325	5
2.5	77.9	59.3	300–310	10
3	84.1	62.6	300–313	10

8-Hydroxyquinoline obtained from the steam distillate was always pure colorless needles, m.p. 73-74°C. Found: C, 74.64; H, 4.93; N, 9.77. Calc. for C_9H_7NO (145.15): C, 74.48; H, 4.83; N, 9.65%. The copper 8-hydroxyquinolinate obtained from the filtrate was a yellowish green crystalline powder, changed to a brown power on heating and carbonized completely at 245°C. Found: CuO, 21.67; calc. for $C_{18}H_{12}N_2O_2Cu \cdot 1/2\ H_2O$[8] (360.84): 22.05%.

7) W. R. Ashford, *U.S.P*, 2,591,553, July 24 (1951).
8) Y. Nakatsuka. This Bulletin, **11**, 47 (1936).

Summary

1) 8-Sulfoquinoline has been obtained with a yield of 80.3% by sulfonating quinoline with 50% oleum at 140°C for 2 hrs.

2) 8-Hydroxyquinoline has been synthesized by fusing 1 mole of 8-sulfoquinoline with 9 moles of NaOH at 300–315°C for 10 to 15 minutes, decomposing the with dilute sulfuric acid, neutralizing with sodium hydroxide and soda to a *p*H 7.2, and by distilling with steam for 1.5 hrs. The remaining 8-hydroxyquinoline in the residue and in the filtrate was collected in the form of its copper salt. The highest yield of 8-hydroxyquinoline including its copper salt was 84.14%.

3) Copper 8-hydroxyquinolinate has been obtained with a yield of nearly 100% by heating 8-hydroxyquinoline with 0.86 times its weight of crystalline copper sulfate together with a large quantity of water at 80° to 100°C.

The authors are deeply indebted to Mr. K. Arakawa of the Nippon Steel Co., Kawasaki, for his suggestions and help.

Tokyo College of Science
Shinjuku-ku, Tokyo

Rheology of Surface Films. III. A New Type of Surface Rheometer using Electromagnetic Driving Technique[1]

By Kiyoshi INOKUCHI

(Received May 23, 1954)

Introduction

In the course of our effort to establish the standard set of surface rheometry, which involves the rheological measurements of films at liquid surface, the author has previously presented a surface rheometer of wire ring type[2] which enables the film creep to be measured under constant shear stress by using a phototube relay system. This apparatus, although it showed considerable merit in facilitating quantitative analysis of the creep data, was somewhat unsatisfactory in practice, since the construction was comparatively complicated and the operation was not so easy. In addition, it was not readily accessible to the measurements other than the creep test, that is, the stress relaxation test or the dynamic measurement. In order to eliminate these objections and permit wide application to various sorts of measurement, the author again originated a new type of apparatus, using electromagnetic driving technique. The advantage of this equipment lies not only in its ease of operation and simplicity of construction, but also in its accessibility to both static and dynamic measurements. Moreover, the remote control of the instrument, being readily capable using a pair of wires, greatly reduced the experimental care to provide vibration-free operation. The present paper describes the construction of this surface rheometer for static measurement while the description for dynamic measurement will be made in the near future.

Construction of Apparatus

The general view of this apparatus is shown in Fig. 1. Principal construction bears resemblance

1) Presented at the Symposium on High Polymer Chemistry of the Chemical Society of Japan, Oct., 1953, Tokyo.
2) K. Inokuchi, This Bulletin, **27**, 203 (1954).

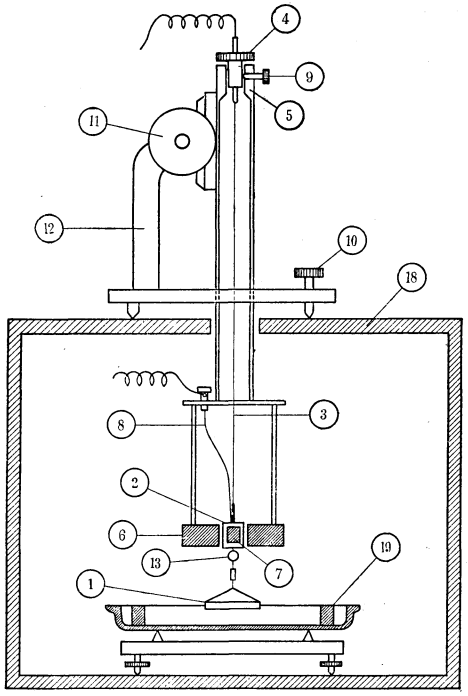


Fig. 1. Elevation view of the instrument.

to the d'Arsonval galvanometer. The actual suspension consists of a ring (1), a moving coil (2), a suspension wire (3), a support rod (4), and a guide (5). The moving coil is just situated between the poles of the permanent magnet (6). The ring is fixed to the moving coil through a small chuck. A light rectangular moving coil is suspended so that its sides lie in the air gaps between the two poles of a permanent magnet and a soft-iron cylinder (7) inside the poles. The suspension wire is an extremely thin strip of copper, which also serves as one of the leads to the coil, the other lead being a loosely hanging thin wire (8) leading upwards from the top of the coil. When the current passes through the coil, a deflecting torque is produced owing to the reaction between the permanent magnetic field and the magnetic field of the coil. Since the pole faces of the permanent magnet are shaped so as to give a radial field and the air gaps between the magnetic poles and iron cylinder are small, the flux density becomes uniform in a radial direction. Hence, the torque causing the coil to rotate turns out to be proportional to the current and constant for all positions of the moving coil as long as its sides are within the pole arcs of the magnet. The magnitude of the torque, therefore, can readily be known by the current of the coil multiplied by a constant.

The level of the coil can be adjusted by raising or lowering the support rod, which is held in place by the screws (9) during run. The centering of the coil is also adjusted by the levelling screws (10) of the stand (12). When the instrument is out of measurement, the support rod is lowered so that the coil becomes mounted on the iron cylinder (7), setting the suspension wire relaxed. The suspension carries a small mirror (13) below the coil upon which a light beam is cast. The beam of light is reflected onto a scale or to a recording photographic paper upon which the deflection is recorded.

The current is supplied from the potentiometer (14), the connection of which is illustrated in Fig. 2. A micro-ammeter (15) is inserted into the cir-

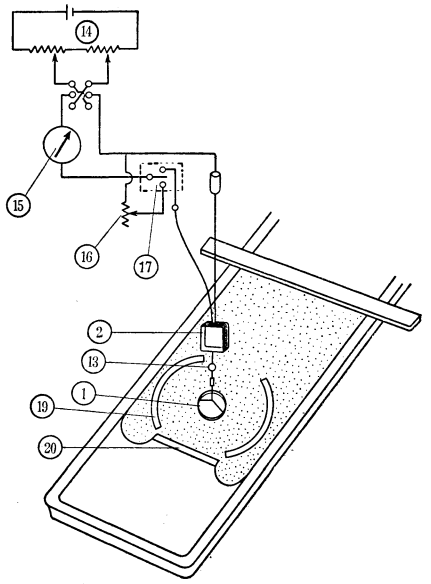


Fig. 2. Schematic illustration of the equipment.

cuit in series with the moving coil (2). In order to avoid the effect due to the eddy current which appears in the coil of the ammeter (15) at the instant of closing the circuit, the coil (2) of the ring provides a resistance (16) parallel with it, the magnitude of which is adjusted to be the same as that of the coil (2). The changeable switch (17) offers the alternative connections of the circuit either to the resistance (16) or to the moving coil (2), the operation of which will briefly be described later.

The ring is a shallow cylinder of platinum, the upper half of which is treated with paraffin, whereas the lower half is left unconditioned. The size of the ring is 3.0 cm. in diameter and 0.3 cm. in height. The moment of inertia of the suspending system was 1.12 g. cm^2. The torsion constant of the suspending wire was 0.016 dyne. cm.

The stand (12) of the instrument was laid on the cabinet (18), only the suspending system being enclosed in it. The instrument was so set that the ring was placed towards one end of the trough, the size of which was $60.0 \times 15.0 \times 10.0$ cm. The ring was provided with a guard (19) of a pair of arc, which was placed in the trough concentric to the ring. The top of the guard was just the same height as the brim of the trough and coated the top face with paraffin for water-repellency.

Determination of Instrumental Constant

The determination of the constant relating the current passed through the moving coil (2) to the deflecting torque applied to it was made as follows. The torsion wire, of which the torsion constant was previously determined, was attached to the moving coil instead of to the ring, and the lower end of the wire was fixed to the ground. The knob (11) was carefully levelled so as to put the wire in proper tension between the coil and the ground. The varying amount of current was let into the coil from the potentiometer, and the respective deflection of the coil was read on the scale by means of a lamp and scale system. As shown in Fig. 3, linear plots were obtained in the current-deflection curve, showing the following equation to be valid

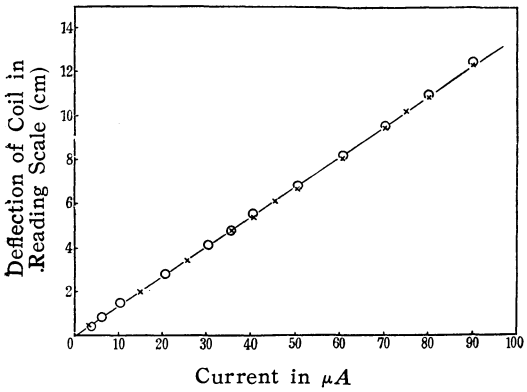


Fig. 3. Current-deflection curve of the moving coil. Circles and crosses represent the plots belonging to different run of measurement.

$$\theta = L \cdot m \qquad (1)$$

where θ is the deflecting angle, m, the current, and L, a constant. Since the deflecting torque,* T, is directly proportional to the deflecting angle θ, the following equation holds

$$T = k \cdot \theta \qquad (2)$$

where k is the torsion constant of the wire attached below the coil. Hence it turns out from the above equations that the torque is proportional to the current as seen in the following equation

$$T = (L \cdot k)m = p \cdot m \qquad (3)$$

where p, being equal to $L \cdot k$, is a constant relating the current to the deflecting torque. In the present apparatus, p was calculated to 0.115 dyne. cm., when m was expressed in microammeter.

Procedure of Operation

The surface of water was cleaned by sweeping with moving barriers. After the ring was lowered so as just to touch the surface of water, the material under test was spread on the surface of the water. By raising carefully the support rod (4) and adjusting the levelling screws (10) for centering the coil, the ring (1) was allowed to be free in suspention. After adequate time was allowed for the equilibrium to be attained, the current was applied to the moving coil (2) of the ring. Prior to the measurement, the current was sent into the circuit turning the switch (17) so that the circuit was closed through the resistance (16), not through the coil (2). In this instant, only the ammeter was actuated by the amount of current which would be applied to the coil in case of measurement. At the time of measurment, the switch (17) was changed to the opposite side so that the current was sent into the coil (2), and the torque was now supplied to the ring without being affected by the eddy current due to the motion of the coil of the ammeter (15).

The deflection of the ring was measured on the scale, or if necessary, recorded on the photographic paper of the rotating drum. Since the deflecting torque of the ring is constant irrespective of the position of the ring if only the current passed through the coil is held constant, the creep curve under constant shear stress can readily be obtained under a constant current throughout the experiment.

If the potentiometer is so adjusted that the deflection of the ring is fixed to a certain value throughout the experiment, and the respective current is measured with time, the stress relaxation curve can readily be obtained.

In calculating the physical constants for the surface viscoelasticity, the film was considered as a mathematical plane. The surface shear modulus of rigidity (G) and surface viscosity coefficient (η) were obtained as follows, respectively, provided that the torque due to the moment of inertia of the rotating system could be ignored,

$$G = \frac{1}{4\pi}\left(\frac{1}{r_1^2} - \frac{1}{r_2^2}\right)\frac{p \cdot m}{\theta} \qquad (4)$$

$$\eta = \frac{1}{4\pi}\left(\frac{1}{r_1^2} - \frac{1}{r_2^2}\right)\frac{p \cdot m}{\dot{\theta}} \qquad (5)$$

where r_1 is the outer radius of the ring, and r_2 the inner radius of the guard coaxial to the ring, respectively.

In the present experimental condition, the stress as well as the strain applied to the film was not uniform throughout the film but varied with the distance from the center of the ring. The stress, S, applied to the outer radius of the ring was given by the following equation, when the moment of inertia of the ring might be ignored.

$$S = \frac{p \cdot m}{2\pi r_1^2} \qquad (6)$$

In our usual experimental condition, in which the film resistance is sufficiently large compared with that of water, the water effect is negligibly small, and the immersion depth of the ring does not matter. However, if the film resistance is so small as to be comparable to that of pure water, the immersion depth would have to be taken into account.

* Since the torsion constant of the suspending wire was suffiiciently small compared with that of the wire attached below the coil, proportional constant between T and θ was simply taken as k, neglecting the deflecting torque due to the suspension wire.

Discussion

Strictly speaking, the deflecting torque, T, should be expressed as follows, taking the torque due to the moment of inertia of the rotating system into consideration

$$T = p \cdot m - I\ddot{\theta} \qquad (7)$$

where I represents the moment of inertia, and $\ddot{\theta}$, the acceleration of the motion of the ring. The author, however, expressed the deflecting torque, T, simply as $p \cdot m$ in equation (4) and (5), neglecting the term $I\ddot{\theta}$. This was because of the fact that, in our usual experiment, $I\ddot{\theta}$ was sufficiently small compared with $p \cdot m$, since very slow creep was mainly subjected to our experiment and the value of I is comparatively small. However, if it were the case, in which $I\ddot{\theta}$ could not be neglected against $p \cdot m$, the correction for the moment of inertia should, of course, be made.

The electromagnetic driving technique very much extended the range of measurement with satisfactory precision. The upper limit of the stress available might be decided by the permissible strength of the current through the wire, in order that over-heating might not occur through the coil. On the other hand, the lower value of the stress might be limited by the extent, to which the stress applied by the current can practically cover the second ary torque due to the torsional drag of the suspension wire, or to the asymmetry of the rotating system, since the present apparatus must satisfy the condition that the deflecting torque is independent of the position of the coil. Using a changeable shunt for the micro-ammeter, the apparatus permitted the measurement over a range of stress from about 3×10^{-3} to about 1×10^{1} dyne per cm. without changing any element of the coil. Such an extremely wide application of the stress is a practical advantage over the previous instrument using a torsion wire, in which a fairly large number of wires must be interchanged in order to apply such a wide range of stress.

The standard deviation of a set of data which appeared in the deflection-current curves was consistently less than 2% and the error inherent to the apparatus was considered to be practically satisfactory. The absolute values of visicosity or elasticity obtained with a different run of experiment using real films however, were found to fluctuate to a considerable extent. This may be due to some uncontrollable experimental conditions which affect the formation of the structure of solid films, and is, of course, not an inherent fault of the apparatus.

Another advantage of this equipment lies in the remote control of operation, which is readily available using a pair of wires. The remote control increases not only the ease of operation, but also serves to provide the vibration-free experimental condition, which is essential for the study of surface films.

In addition to the static measurement, the determination and the analysis of the dynamic modulus is also an important problem of the study. If the alternating current of proper frequency would be introduced into the coil of this apparatus, and the response of the ring would be detected with reference to the input stress, the present apparatus would also be accessible to the dynamic measurement of the film.

Summary

In order to establish the standard set of surface rheometry, which involves the rheological measurement of films at liquid surface, a new type of surface rheometer was devised using electromagnetic driving technique. The advantage of this apparatus lies not only in its ease of operation and simplicity of construction, but also in its accessibility to various sorts of measurement. In addition, the wide range of measurement and remote control of operation provide a practical advantage for the experiment of surface films.

The author wishes to express his hearty thanks to Prof. Taro Tachibana for his helpful advice and encouragement.

Department of Chemistry, Faculty of Science, Ochanomizu University, Tokyo

Spectrochemical Study of Microscopic Crystals. VI.[1] *Light Absorption of Non-planar Quadri-co-ordinated Complexes*

By Shoichiro YAMADA and Ryutaro TSUCHIDA

(Received June 16, 1954)

In the former reports,[1,2] the present authors studied dichroism in the visible and ultra-violet of metallic quadri-co-ordinated complexes possessing planar configuration, and established the common rules on the dichroism. It is known that some metals such as copper (II) and cobalt (II) form non-planar quadri-co-ordinated complexes in addition to planar ones: e.g., $Cu(H_2O)_4^{++}$ in the crystal of $CuSO_4 \cdot 5H_2O$ is square,[3] and $CuCl_4^{--}$ in the crystal of Cs_2CuCl_4 has a distorted-tetrahedral configuration.[4] Complexes with distorted-tetrahedral configuration would probably show more or less remarkable anisotropy of light absorption, whereas complexes with regular-tetrahedral configuration would exhibit very slight or no anisotropy. Measurements of pleochroism may, therefore, be expected to throw some light upon the nature of chemical linkages as well as upon the configuration. For the above purpose Cs_2CuCl_4, Cs_3CoCl_5 and $K_2Co(NCS)_4 \cdot 4H_2O$ have been studied. In the present work absorption spectra of the above compounds in the crystalline state have been quantitatively determined, and the results of the measurements have been discussed in relation to the configuration of the complex ions.

Experimental

Materials. — Cesium cobaltous pentachloride was prepared in blue tabular crystals by spontaneous evaporation at a room temperature of aqueous solution of cobaltous chloride and excess of cesium chloride.[5] The crystals, which belong to the tetragonal system, show straight extinction and very slight dichroism. Measurements of absorption spectra were made on the face (100) with polarized light having its electric vector along the directions of extinction.

Crystals of cesium tetrachloro-cuproate were obtained by evaporating at a room temperature an aqueous solution of cesium chloride and cupric chloride.[4] The orange, tabular crystals thus obtained show a dichroism; they appear orange with electric vector parallel to the b-axis, and yellow with that perpendicular to the above. Optical measurements were performed in the (101) face with reference to the above two directions.

Potassium tetrathiocyanato-cobaltoate tetrahydrate was prepared in blue prismatic crystals by the method of v. Grotthus.[6] The crystals of the orthorhombic system show a definite dichroism in the prism face; they appear blue with the electric vector along the direction of elongation and pale blue with that perpendicular to the above. Dichroism measurement was carried out in the prism face with reference to the above two directions. The absorption spectrum was also determined with its solution in 99% alcohol containing potassium thiocyanate.[7]

Measurements.—Quantitative measurements of absorption spectra of crystals were made at room temperature by Tsuchida-Kobayashi's microscopic method[8] with polarized light in the region covering 7500 to 2400Å. α represents the absorption coefficient of a crystal. Molecular absorption coefficients of a crystal, k, were calculated from the relation, $k=10\alpha M/\rho$, where M and ρ denote formula weight of a complex compound and density of a crystal, respectively.

Absorption spectrum in solution was determined with a Beckman DU quartz-spectrophotometer. ε represents extinction coefficient of the solution.

Results and Discussion

Cesium Tetrachlorocuproate. — According to the result of the crystal structure analysis,[4] the crystal consists of cesium ions and $CuCl_4^{--}$ anions having configuration of flattened tetrahedron. The maximum of the band at the longest wave-length could not be determined, since the band extends into the infra-red beyond the region of the measurement. Comparison of the absorption curve (Fig. 1) with previously reported data of other cupric complex compounds and analogy to cobaltic and chromic complexes indicate that the band with its maximum in

1) Part V of this series, S. Yamada and R. Tsuchida, This Bulletin, **27**, 156 (1954).

2) R. Tsuchida, S. Yamada and H. Yoneda, *J. Chem. Soc. Japan* **69**, 145 (1948); S. Yamada, *J. Am. Chem. Soc.*, **73**, 1182 and 1579 (1951); S. Yamada and R. Tsuchida, This Bulletin, **26**, 72 (1953).

3) C. A. Beevers and H. Lipson, *Proc. Roy. Soc.*, London A**146**, 570 (1934).

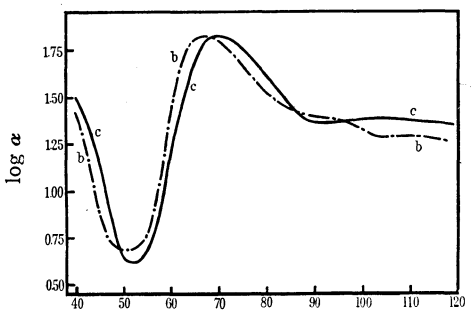
4) L. Helmholz and R. F. Kruh, *J. Am. Chem. Soc.*, **74**, 1176 (1952).

5) H. M. Powell and A. F. Wells, *J. Chem. Soc.*, **1935**, 359.

6) T. v. Grotthus, "Gmelins Handb. d. anorg. Chem.," 8. Aufl., 1932, **58**$_3$, 431.

7) The authors are indebted to the Analytical Laboratory of our department for the measurement of the solution with a Beckman spectrophotometer.

8) R. Tsuchida and M. Kobayashi, "The Colours and the Structures of Metallic Compounds," Osaka, 1944, p. 180.



Frequency, ν, 10^{13}/sec.

Fig. 1. Absorption spectra of Cs_2CuCl_4.

the infra-red region (band A) is considered to be due principally to electronic transitions of co-ordination electrons around the core of the metal atoms, and the band with its maximum at ν=about 70×10^{13}/sec. (band B) may be due largely to the existence of the negative ions in trans-positions.[9]

It is seen from the result of the crystal structure analysis that the b-absorption, absorption with electric vector parallel to the b-axis, is more abundant with the z-component than with the x-component

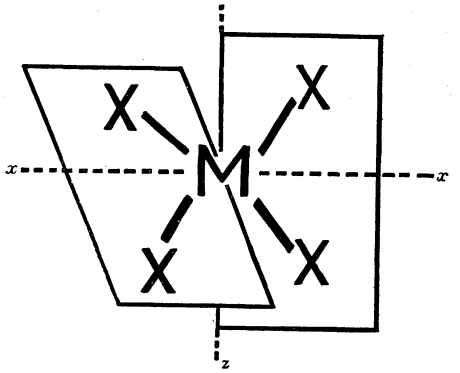


Fig. 2. Flattened-tetrahedral configuration of quadri-co-ordinated complexes.

(Fig. 2.), and that the c-absorption is richer in the x-component. From the configuration of the complex anion, anisotropy is expected for the crystal. The expectation is satisfied by the present measurement, which indicates that for the band B and also possibly for the band A the Z-absorption is bathochromic to the X-absorption. (Table I)

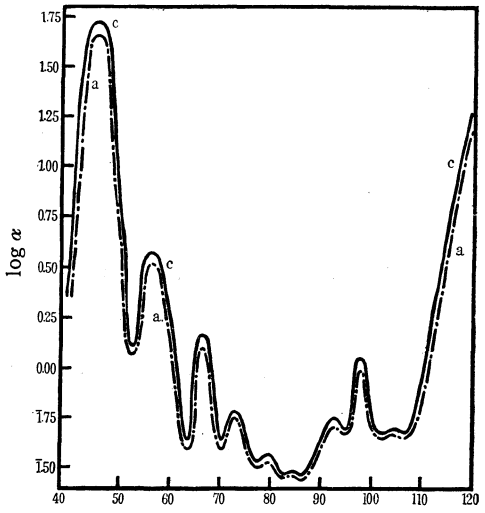
TABLE I

ABSORPTION MAXIMA OF Cs_2CuCl_4 IN THF CRYSTALLINE STATE

	ν,10^{13}/sec.	logα	M
b-abs.	67.0	1.82	9.11×10^4
c-abs.	70.0	1.82	9.11×10^4

The qualitative absorption spectrum of the compound was reported by Helmholz et al.[4] with the solid suspended in the mineral oil, but their results are not in good agreement with ours where a single crystal is used instead of powdered solid in oil.

Tricesium Cobaltous Pentachloride.—According to the X-ray analysis of the crystal,[5] the crystal consists of $CoCl_4^{--}$ cesium and chloride ions, $CoCl_4^{--}$, being regular-tetrahedral. Therefore, very slight or no anisotropy of light absorption can be anticipated for the crystal of the compound. Actually very slight anisotropy of absorption was observed (Fig. 3. and Table II). Slight dichroism may



Frequency, ν, 10^{13}/sec.

Fig. 3. Absorption spectra of Cs_3CoCl_5.

be attributed to the dissymmetrical crystalline field. The above result lends a further support to the regular-tetrahedral configuration of the quadri-co-ordinated complex in this crystal.[5] Recently Katzin et al.[10] reported reflection spectra with powdered solid of dipyridinium and dicesium tetrachloro-

TABLE II

ABSORPTION MAXIMA OF THE CRYSTAL OF Cs_3CoCl_5

ν,10^{13}/sec.	45.0	56.8	66.6	73.2	80.0	84.3	92.8	98.0
logα_α	1.65	0.51	0.10	$\bar{1}$.75	$\bar{1}$.53	$\bar{1}$.43	$\bar{1}$.69	$\bar{1}$.57

9) R. Tsuchida, This Bulletin, **13**, 436 (1938), Such a kind of band was named "third absorption band". See also, F. Basolo, *J. Am. Chem. Soc.*, **70**, 2634 (1948); ibid., **72**, 4393 (1950).

10) L. I. Katzin and E. Gebert, *J. Am. Chem. Soc.*, **75**, 2830 (1953).

11) A. v. Kiss and M. Gerendas, *Z. physik. Chem.*, **A180**, 117 (1938).

cobaltoates, both containing $CoCl_4^{--}$ ions. Their results, however, were only qualitative and limited within the visible region, although the absorption maxima reported by them generally coincide with the results of our present measurement. A. v. Kiss et al.[11] also reported absorption spectra of aqueous solution containing cobaltous chloride and great excess of chloride ions in the visible and ultra-violet. They recorded a number of sharp peaks. Most of the absorption peaks which have been found in the present measurement almost correspond with those reported by them. There were reported, however, other peaks in their work which have not been observed in our measurements.

Inspection of absorption spectra of the crystal leads us to the idea that the absorption bands of the complex anion between $\nu=45$ and 85×10^{13}/sec. may form one series. As reported in our recent communication,[12] wave numbers of the absorption peaks in the above series can be expressed by the following equation,

$$\tilde{\nu}=\nu_0+am-bm(m+1), \qquad (1)$$

where $\tilde{\nu}$ represents the wave-number of a peak, $\tilde{\nu}_0$ the wave-number of the band head, a and b constants, and m positive integer including zero (Table III). The following

TABLE III

A SERIES OF ABSORPTION PEAKS OF Cs_3CoCl_5 IN THE CRYSTALLINE STATE

m in eq.(1)	0	1	2	3	4	5
$(\tilde{\nu})$obs	15.0	18.9	22.2	24.4	26.7	28.0
$(\tilde{\nu})$cal	15.0	18.8	22.0	24.6	26.6	28.1

values have been obtained for a and b: $a=4.37\times10^3$/cm. and $b=2.92\times10^2$/cm. The expression of the form (1) may be derived readily in the approximation, using a familiar expression for an anharmonic oscillator[13] and assuming (a) that the absorption peaks correspond to transitions from the ground electronic state with vibrational quantum number zero to the excited electronic state with m as the vibrational quantum number, and (b) that the vibrational frequency is altered very little in the electronic transitions. Judging from the order of the vibrational frequency and considering that the measurement was made at room temperature, the former assumption may be permissible. The intensity relation of the absorption series may be understood qualitatively on the basis of the above assumed mechanism of the transition.[14] Using the above derived constants and assuming the above mechanism of the transition, the dissociation energy of the complex ion is estimated,[15] in the rough approximation, as 40.2 kcal. per mol. The value thus obtained seems reasonable,[16] favouring the above assumption. The fact that the band peaks can be correlated with electronic-vibrational transitions supports the view that the series of band peaks is due principally to transitions of the coordination electrons of the complex anion.[17,18] A similar fine structure had been reported by Shibata et al.[19] with solution of several metallic compounds at the temperature of liquid air, and an equation had been given to represent wave-numbers of absorption peaks in the fine structure.

Potassium Tetrathiocyanato-cobaltoate Tetrahydrate.—The compound in the crystalline state shows bands at $\nu=50$ and about 100×10^{13}/sec. and one more band in the infra-red; no measurement of the latter band was made in the present work. From comparison of the absorption curves (Fig. 4. and

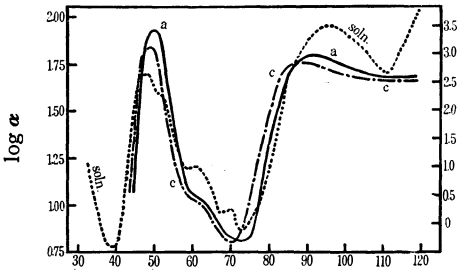


Fig. 4.
Absorption spectra of $K_2Co(NCS)_4\cdot4H_2O$.

TABLE IV

ABSORPTION MAXIMA OF $K_2Co(NCs)_4\cdot4H_2O$

	ν,10^{13}/sec.	logα	M	ν,10^{13}/sec.	logα	M
a-abs.	49.8	1.98	2.18×10^5	91	1.79	1.46×10^5
c-abs.	49.2	1.84	1.58×10^5	88	1.76	1.36×10^5

12) S. Yamada and R. Tsuchida, *J. Chem. Phys.*, **22**, 1273 (1954).
13) See, for example, G. Herzberg, "Spectra of Diatomic Molecules," Van Nostrand Company, New York, 1950, p. 151, etc.
14) For example, Ref. 13), p. 193, etc.
15) See, for example, K. S. Pitzer, "Quantum Chemistry," Prentice-Hall, New York, 1953, p. 255. The equation for diatomic molecules is tentatively assumed in the present estimation.
16) From spectroscopic study, Shibata et al. (Ref. 19) reported 48 kcal. for the dissociation energy of ($CoCl_2$ · acetone).
17) R. Tsuchida, This Bulletin, **13**, 388 (1938).
18) A similar conclusion was formerly drawn by v. Kiss et al, (Ref. 11).
19) Y. Shibata and K. Harai, *J. Chem. Soc. Japan*, **56**, 1 (1935).

Table IV) with that of tricesium cobaltous pentachloride, it is considered that the absorption band at $\nu=50\times10^{13}$/sec. corresponds to the band at $\nu=45\times10^{13}$/sec. in Cs_3CoCl_5, being due mainly to co-ordination electrons, and that the band stretching from $\nu=$about 80×10^{13}/sec. further into the ultra-violet may correspond to "specific band,"[20] which is principally due to the NCS^- ions in co-ordination. The absorption spectrum of cobaltous thiocyanate in aqueous solution containing excess of potassium thiocyanate was reported by Kiss et al.[21] Their data roughly coincide with our result, but differ in detail, probably because their measurements were made with the mixed solution, involving much more complicated factors as compared with ours. It is seen that the crystal of the compound shows the corresponding band peaks in the shorter wave-length than does the solution.

According to the result of the crystal analysis,[22] the crystal consists of potassium ions, $Co(NCS)_4^{--}$ anions and molecules of crystallization water, $Co(NCS)_4^{--}$ ions being determined as tetrahedral. The crystal has been found to exhibit a marked dichroism. That is, as to the band at $\nu=50\times10^{13}$/sec. a-absorption is hyperchromic and hypsochromic to c-absorption, and with the specific band a-absorption is hypsochromic to c-absorption. In consequence, it is readily concluded that the configuration of the anion, $Co(NCS)_4^{--}$, in this crystal deviates considerably from regular-tetrahedron. It is most likely that the complex anion should possess a configuration of distorted-tetrahedron. From analogy to dicesium tetrachlorocuproate, it is supposed that the a-absorption of this crystal corresponds to the X-absorption and that the c-absorption corresponds to the Z-absorption of the $Co(NCS)_4^{--}$ ion.

It is to be noted that there can be found a series of sharp bands with this compound in alcoholic solution as in the crystal of tricesium cobaltous pentachloride. Some of the peaks in the shorter wave-length may be covered under the specific band, since the specific band comes very close to the band series. Though peaks which appear separated from the specific band seem to be rather small in number, wave-numbers at the series of peaks can be represented by the equation of the form (1). The following values have been obtained for a and b; $a=4.8\times10^3$/cm. and $b=4\times10^2$/cm., dissociation energy of the complex being estimated, in the same way as in tricesium cobaltous pentachloride, approximately as 34 kcal.

General Considerations.—It seems of significance that those series of sharp peaks in the above two compounds can be expressed by the equation of a similar form and may reasonably be correlated with electronic-vibrational transitions directly related to the co-ordination linkages in the quadri-co-ordinated complex ions. There have been reported very few metallic complexes which show at room temperature a corresponding electronic absorption band consisting of a series of sharp peaks. One such example, besides the above two compounds, may be found with potassium permanganate in aqueous solution.[23]

The appearance at room temperature of a fine structure in an electronic absorption band of such a kind is probably due to many factors. But the following may be cited as one of the principal factors.[24] Since to a first approximation the only vibrations for which Δv, v being the vibrational quantum number, differs from zero in polyatomic electronic spectra are the totally symmetrical vibrations, the electronic absorption spectra of those complex ions, which have a very small number of totally symmetrical vibrations, will show a simplified vibrational structure. Thus $CoCl_4^{--}$ in the crystal of $CsCoCl_5$ and $M_nO_4^-$ in aqueous solution of potassium permanganate, both being regular-tetrahedral, have only one totally symmetrical vibration and, moreover, contain only simple ions as ligands. Therefore, their electronic absorption might be expected to be more simple than in other complexes of more complicated structure. As for $K_2Co(NCS)_4\cdot4H_2O$, $Co(NCS)_4^{--}$ in this crystal has been presumed, from dichroism measurement, to have flattened tetrahedral configuration. This, however, might be ascribed, at least partly, to the effect of the crystalline field upon the complex ion, and the complex ion in alcoholic solution might be assumed to be nearly regular-tetrahedral. In agreement with the assumption seems to be the fact that the crystal of this compound has been found to be slightly hypsochromic to the solution, and that the splitting of the absorption band is less marked in the crystalline state.

Another point which deserves attention

20) R. Tsuchida, This Bulletin, **13**, 471 (1938).
21) A. v. Kiss and P. Csokan, *Z. physik. Chem.*, A**186**, 239 (1940).
22) G. S. Zhdanov and Z. V. Zvonkova, *Zhur. Fiz. Khim.*, **24**, 1339 (1950); *C. A.*, **45**, 6001e (1951).
23) B. Lange and C. Schusterius, *Z. physik. Chem.*, A**159**, 295 (1932).
24) For example, see G. R. Harrison, R. C. Lord and J. R. Loofbourow, "Practical Spectroscopy," Prentice-Hall, New York, 1948, p. 291.

may be the fact that the above three complex compounds all involve relatively weak linkages. The weakness of the linkage seems to have some relation to the appearance of the electronic band with a fine structure.

It is of significance that there have been found complex-ions with distorted-tetrahedral configurations, intermediate between planar and regular-tetrahedral ones, in contrast to the generally accepted fact that as to magnetic properties there may usually be drawn a sharp line between tetrahedral and planar hybridization. Quadri-co-ordinated cupric and cobaltous complexes are expected to be square when ordinary hybridization of bond orbitals is assumed.[25] In fact this is found not to be the case. One of the reasons for the above fact may be that the linkages between the metal atom and the ligands are too weak to enter into planar hybridization of an ordinary type.[26]

The configuration of complex molecules would naturally be closely related to the hydbridization of bond orbitals in the molecule. The existence of these distorted-tetrahedral complexes, therefore, points to the possibility that the hybridization of bond orbitals, intermediate between tetrahedral and planar ones, may occur with the $CuCl_4^{--}$ and $Co(NCS)_4^-$ ions in these crystals. It is noteworthy that the same central metallic ion has been found to form complexes of different configurations with ligands of varying natures on the one hand, and that with the same ligands different metallic atoms as a centre form complexes of different configurations on the other. Thus it is readily recognized[27] that the natures of both metal atoms and ligands are in close relation to the state of hybridization, the stability of the bonds, and the configurations of the complex ions.

25) R. Tsuchida, *J. Chem. Soc. Japan*, **60**, 245 (1939); R. Tsuchida, M. Kobayashi and H. Kuroya, *Rev. Phys. Chem. Japan*, **13**, 151 (1939); N. V. Sidgwick and H. M. Powell, *Proc. Roy. Soc. London*, A**176**, 153 (1940); L. Pauling, "The Nature of the Chemical Bond", Cornell Univ. Press, Ithaca, New York, 1940.

26) Since the configurations of the above complex ions were determined in the crystalline state, we could not remove another possibility that those complex ions would be non-planar only in the crystalline state where electrostatic forces of surrounding ions on the complex ions might be so strong and the linkages in the complexes so weak that the planar configuration would not be held.

27) N. V. Sidgwick, *J. Chem. Soc.*, **1941**, 433; D. P. Mellor and D. P. Craig, *J. Proc. Roy. Soc. N. S. Wales*, **74**, 474 and 495 (1940); D. P. Mellor, *Chem. Revs.*, **33**, 137 (1943); L. G. Van Uitert and W. C. Fernelius, *J. Am. Chem Soc.*, **76**, 379 (1954).

Summary

Absorption spectra of crystals of dicesium tetrachlorocuproate, tricesium cobaltous pentachloride and potassium tetrathiocyanatocobaltoate tetrahydrate have been quantitatively determined in the visible and ultraviolet region by the microscopic method with polarized light.

In accordance with the flattened-tetrahedral configuration of tetrachlorocuproate anion, the crystal of Cs_2CuCl_4 exhibits anisotropy of light absorption.

It has been found that crystals of Cs_3CoCl_5 are almost isotropic, supporting the regular-tetrahedral configuration of the $CoCl_4^{--}$ ion in this crystal.

It has also been found that $K_2Co(NCS)_4 \cdot 4H_2O$ in the crystalline state shows a marked dichroism. It is concluded from this observation that $Co(NCS)_4^{--}$ ions in this crystal are distorted-tetrahedral, just like the $CuCl_4^{--}$ ions in the crystal of Cs_2CuCl_4.

It has been found that Cs_3CoCl_5 in the crystalline state and $K_2Co(NCS)_4 \cdot 4H_2O$ in alcoholic solution show their second absorption band with a series of sharp peaks, which have been shown to be correlated with electronic-vibrational transitions. This fact is in harmony with the idea on the origins of the absorption bands of metallic co-ordination compounds proposed by one of the authors.

The authors wish to thank the Ministry of Education for a grant.

Department of Chemistry, Faculty of Science, Osaka University, Nakanoshima, Osaka

*Syntheses of Tetracyclohexylsilane and Methylcyclohexylsilanes**

By Motonori KANAZASHI and Michio TAKAKUSA

(Received June 22, 1954)

Preparation of tetracyclohexylsilane[1] and germane[2,3,4] were attempted by several workers with the lithium compound or the Grignard reagent unsuccessfully. Even tricyclohexylalkylsilanes[1,5] could not be obtained due to a large steric hindrance of the cyclohexyl group. The present authors succeeded in making syntheses of these compounds by hydrogenation of methylphenylsilanes and found that the steric hindrance in these molecules was conquerable, though it had a fairly large effect in the case of substitution reaction. In this work, trimethylcyclohexylsilane, dimethyldicyclohexylsilane, methyltricyclohexylsilane, and tetracyclohexylsilane were prepared.

Experimental**

Methylphenylsilanes.—These compounds were prepared from chlorobenzene and corresponding methylchlorosilane by the Wurtz-Fittig reaction in benzene solution.

Trimethylphenylsilane: b.p. 170–171°, n_D^{20} 1.4901, d_4^{20} 0.8687. MR_D: obsd. 50.03, calcd. 50.10.

Dimethyldiphenylsilane: b.p. 101–104° at 2.5 mm Hg., n_D^{20} 1.5593, d_4^{20} 0.9877 MR_D: obsd. 69.45, calcd. 69.92.

Methyltriphenylsilane: m.p. 65–67°.

Tetraphenylsilane: m.p. 229–231°.

Raney Nickel Catalyst.—The catalyst was prepared from Raney nickel alloy, containing 38% of nickel, according to the direction of Adkins' so-called "W-6"[6], except that washing was done in hydrogen atmosphere under 300 mm. in water column instead of 1.5 atm.

Hydrogenation of Methylphenylsilanes.—Hydrogenation was carried out in a stainless-steel shaking type autoclave, 300 cc. in capacity under the condition shown in Table I. Methylcyclohexane was used as a solvent. The catalyst was supplied in two portions as the reaction did not proceed smoothly with an exception of trimethylphenylsilane.

TABLE I

HYDROGENATION OF METHYLPHENYLSILANES

Material	g. (mol.)	Catalyst g. (wt. %)	Solvent g.	Pressure atm.	Temperature °C.	Time hrs.	H_2 (c)	Product	Yield %
		(a)			(b)				
Me_3SiPh	30 (0.2)	4.5(15)	70	110–150	100–140(108)	2	2.98	I	67
Me_2SiPh_2	32.1(0.15)	5 (15)	70	80–100	85–170 (90)	7	5.9	II	62
$MeSiPh_3$	27.4(0.1)	5 (18)	70	60–100	80–170(100)	6	9.0	III	61
$SiPh_4$	51 (0.15)	10 (20)	80	50–100	80–150(100)	7	12.0	IV	63

(a) In the case of trimethylphenylsilane, "W-2" Raney nickel catalyst was used.
(b) The starting temperature of absorption was shown in brackets.
(c) Moles of hydrogen absorbed, to one mole of reactant.

Separation and Purification of Methylcyclohexylsilanes.

Trimethylcyclohexylsilane (I). Out of the hydrogenation mixture[a] a fraction boiling at 67–69° (25 mm.) was collected after removal of the reaction solvent by a fractionating distillation.

Dimethyldicyclohexylsilane (II). A fraction boiling at 94–103° (3–3.5 mm.) was collected.

Methyltricyclohexylsilane (III). A crystalline part was filtered out of the concentrated reaction mixture[a], washed with ethanol-methylcyclohexane mixture and recrystallized from methylcyclohexane[b].

Tetracyclohexylsilane (IV). An aimed product was extracted from the solid phase of the reaction mixture and recrystallized twice with decahydronaphthalene[c], washed with methylcyclohexane and dried in vacuum.

* Presented at the 7th. Annual Meeting of the Chemical Society of Japan held in Tokyo, April, 1954.

1) W. H. Nebergall and O. H. Johnson, *J. Am. Chem. Soc.*, **71**, 4022 (1949).

2) H. Bauer and K. Burschkies, *Ber.*, **65** 956 (1932).

3) O. H. Johnson and W. H. Nebergall, *J. Am. Chem. Soc.*, **70**, 1706 (1948).

4) O. H. Johnson and W. H. Nebergall, ibid., **71**, 1720 (1949).

5) N. W. Cusa and F. S. Kipping, *J. Chem. Soc.*, **1933**, 1040,

** All temperatures reported here were uncorrected.

6) H. Adkins and H. R. Billica, *J. Am. Chem. Soc.*, **70**, 695 (1948).

a) The catalyst was removed by filtration prior to these treatments.

b) This compound was dissolved in hot methylcyclohexane easily, contrasting with the case of IV.

c) This compound was hardly soluble in various solvents:

The solvent recovered from the reaction mixture was fractionated through a 30 cm. distillation column packed with stainless-steel helices, but hardly any benzene or cyclohexane were found in all cases.

Infrared Absorption Spectra.—The spectra were measured using a Perkin-Elmer Model 12-C Spectrometer with a rock salt prism of Government Chemical Industrial Research Institute, Tokyo. Two samples, trimethylphenylsilane and dimethyldiphenylsilane, were run in a potassium bromide cell 0.0125 mm. thick, without using a solvent. The other samples were measured in carbon tetrachloride solution.

$MeSiPh_3$, in about 20% carbon tetrachloride solution, cell thickness 0.1 mm.

I–III, in about 10% 0.1 mm.

IV, in about 3% 0.2 mm. and 1 mm.

Results and Discussion

All these phenylsilanes absorbed the theoretical amount of hydrogen and hydrogenation products were formed. Their physical constants and analytical data are given in Table II.

TABLE II

PHYSICAL CONSTANTS AND ANALYSES OF METHYLCYCLOHEXYLSILANES

Compound	b.p. °C.	b.p. mm.Hg.	n_D^{20}	d_4^{20}	Molar ref. Obsd.	Molar ref. Calcd.(a)	Analyses C Found	Analyses C Calcd.	Analyses H Found	Analyses H Calcd.	
I	67–9	25	1.4477	0.8163	51.24	51.30	(b)		(b)		(c)
II	101–3	3–3.5	1.4850	0.9136	71.50	72.32	74.01	74.91	12.61	12.57	(d)
	m.p.(°C.)										
III	73.0–73.2						78.21	77.99	12.39	12.40	
IV	279–281						79.97	79.91	12.40	12.30	(e)

(a) Calculated from bond refractivities reported by E. L. Warrick, *J. Am. Chem. Soc.*, **68**, 2455 (1946).

(b) Analyses of this compound were unsuccessful due to its explosibility in the combustion tube.

(c) Mass spectra. Parent peaks: mass 156, 157 and 158 (peak height 131, 20.2 and 6.0, respectively).

(d) Mass spectra. Parent peaks: mass 224, 225 and 226 (peak height 52.8, 11.0 and 2.8, respectively).

(e) Analysis. Si %: found 7.71, calcd. 7.79.

Mass-spectrometric data are available for identification of liquid products. The mass of trimethylcyclohexylsilane consisting of the most abundant isotopes of carbon, hydrogen, and silicon, i.e. $C_9{}^{12}H_{20}{}^{1}Si^{28}$, is 156 and this peak was found in the parent group of the spectra of I.[d] Besides, the relative heights of these three peaks (see Table II (c)) accord with those calculated for $C_9H_{20}Si$ based on the known isotopic abundance ratios[7] of involved elements. Other remarkable peaks are: "73, 74, 75" (corresponding to Me_3Si^+), "141, 142, 143" ($Me_2C_6H_{11}Si^+$), and "135, 136, 137" (Me_2PhSi^+). The presence of the last group (135–137), with absence in the intermediate region (p.e. from 152 to 155, or from 137 to 140), reveals contamination of unreacted trimethylphenylsilane, and at the same time shows that no incomplete hydrogenation products were formed (see Table III). The similar results were derived from mass spectra of II, but unreacted dimethyldiphenylsilane was not found.

TABLE III

POSSIBLE PRODUCTS IN HYDROGENATION OF TRIMETHYLPHENYLSILANE AND THEIR MASSES. (Some of fragments of these to be found in mass spectra are also listed)

$Me_3C_6H_{11}Si^+$	156	157	158
$Me_3C_6H_9Si^+$	154	155	156
$Me_3C_6H_7Si^+$	152	153	154
$Me_3C_6H_5Si^+$	150	151	152
$Me_2C_6H_{11}Si^+$	141	142	143
$Me_2C_6H_9Si^+$	139	140	141
$Me_2C_6H_7Si^+$	137	138	139
$Me_2C_6H_5Si^+$	135	136	137
Me_3Si^+	73	74	75

Infrared spectra of the four products and the three materials are given in Fig. 1. The quite identical spectra were obtained for the three methylcyclohexylsilanes. They also accord with spectrum of dicyclohexylsilane reported by West and Rochow[8], except absence of the absorption bands of Si—H[8], in 4.7–4.8 μ and 10.6–10.7 μ, and presence in 7.11 μ and 8.0 μ. Absorption bands in 7.11 μ and 8.0 μ are assigned to methyl group bonded to silicon as reported by Young et. al.[9] The

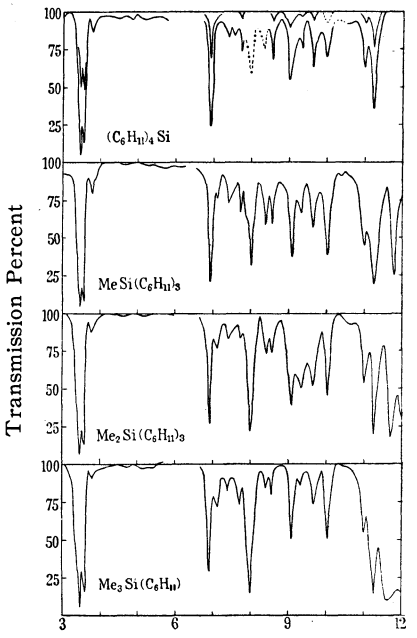
ether, ethanol, carbon tetrachloride, benzene, cyclohexane, and methylcyclohexane. This compelled us to choose a high-boiling solvent for extraction and recrystallization.

d) It is impossible to calculate the ordinary molecular weight from the masses and the relative heights of the parent peaks strictly, unless numbers of included atoms are postulated.

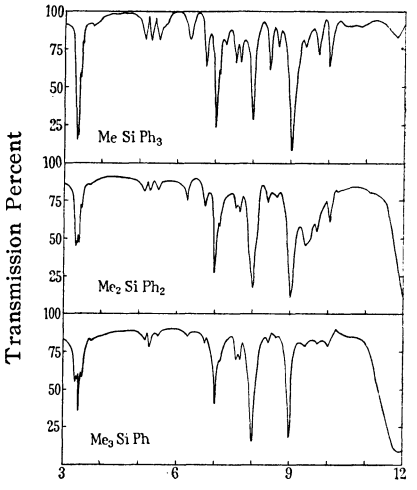
7) G. T. Seaborg and I. Perlman, *Revs. Modern Phys.*, **20**, 585 (1948).

8) R. West and E. G. Rochow, *J. Org. Chem.*, **18**, 303 (1953).

9) C. Young, P. C. Servais, C. C. Currie and M. J. Hunter, *J. Am. Chem. Soc.*, **70**, 3758 (1948).



Wave Length in Microns
Fig. 1 (A).
Infrared spectra of cyclohexylsilanes.



Wave Length in Microns
Fig. 1 (B).
Infrared spectra of methylphenylsilanes.

spectrum of tetracyclohexylsilane is identical with that of dicyclohexylsilane except the absorption bands of Si—H. In these spectra, the absorption assigned to alkene or phenyl group was not found, 3.2–3.4 μ, 7.0 μ and 9.7–9.8 μ. Further discussions, p.e. on the characteristic bands of cyclohexyl bonded to silicon or on the inverted isomerism, could not be made for the lack of data to which to refer.

All these results give a sufficient support to the identification of the prepared substances.

Steric hindrance of cyclohexyl group in organosilicon compounds was first discussed by Kipping and Cusa.[5] Their attempt to introduce one phenyl and three cyclohexyl groups to one silicon atom with Grignard reagent resulted in formation of phenyldicyclohexylcyclohexoxysilane. The reaction involving cyclohexyllithium and silicon tetrachloride[1] was studied by Nebergall and Johnson, and only tricyclohexylchlorosilane was obtained. Concerning it, the following reactions were also reported;

$$(C_6H_{11})_3SiCl + LiAlH_4 \longrightarrow (C_6H_{11})_3SiH$$
$$(C_6H_{11})_3SiH + X_2 \longrightarrow (C_6H_{11})_3SiX$$

where X is Br or I,

$$(C_6H_{11})_3SiCl + KOH \longrightarrow (C_6H_{11})_3SiOH$$
$$(C_6H_{11})_3SiOH + Ac_2O \longrightarrow (C_6H_{11})_3SiOAc$$

but the halogen atom was not substituted for by any alkyl groups. These facts should be attributed to the steric hindrance of the cyclohexyl group. The steric hindrance in organosilicon compounds is small, compared with carbon compounds because of the larger size of silicon and the longer distance in which silicon is bonded to carbon or other atoms.

Steric effects of *tert*-butyl[10], isopropyl[11], cyclohexyl[12], *o*-tolyl[13], and 1-naphthyl[14] have been discussed in previous literatures in silico-organic chemistry. The *t*-butyl has the largest effect of them and the results lead to the natural conclusion that the extent of the group in the surrounding space of silicon atom is a sole factor. From this point of view, cyclohexyl and isopropyl or other secondary alkyl groups have almost equal effects, as far as cyclohexyl is combined with

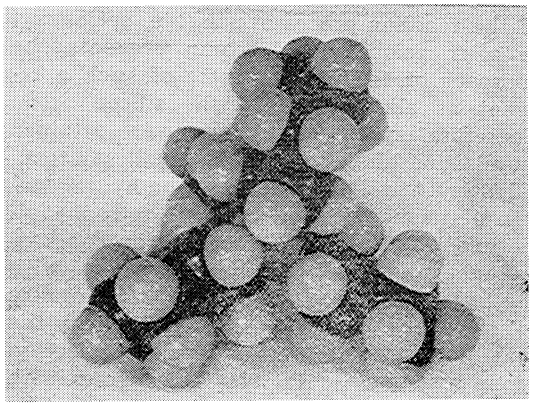


Fig. 2.
Stuart model of tetracyclohexylsilane.

10) L. J. Tyler, L. H. Sommer and F. C. Whitmore, *J. Am. Chem. Soc.*, **69**, 981 (1947); **70**, 2876 (1948); L. H. Sommer and L. J. Tyler, ibid., **76**, 1030 (1954).
11) H. Gilman and R. N. Clark, *J. Am. Chem. Soc.*, **69**, 1499 (1947); C. Eaborn, *J. Chem. Soc.*, **1952**, 2840.
12) Loc. cit.
13) H. Gilman and G. N. R. Smart, *J. Org. Chem.*, **15**, 720 (1950); **16**, 424 (1951).
14) H. Gilman and C. G. Brannen, *J. Am. Chem. Soc.*, 4640 (1951); A. D. Petrov and V. S. Chugunov, *Doklady Akad. Nauk, S. S. S. R.*, **77**, 815 (1951); P. S. Sanin and A. D. Petrov, *Zhur. Obschei Khim.*, **22**, 1124 (1952).

silicon in *e*-bond. And free rotation around C—C bond in it is somewhat prevented because of its ring-form structure.

The stuart model of tetracyclohexylsilane is constructed without much jostling, but the free rotation around the Si—C bond and the inverted isomerism of the cyclohexane ring is prevented entirely as shown in Fig. 2. The inversion is possible with difficulty in models of the other three compounds. The difficulty is diminished with the number of cyclohexyl groups, but these inverted isomers involving *p*-bond seemed to be more unstable than the original isomers involving no *p*-bond. (See Fig. 3.) It is of much theoretical interest to determine whether the inverted

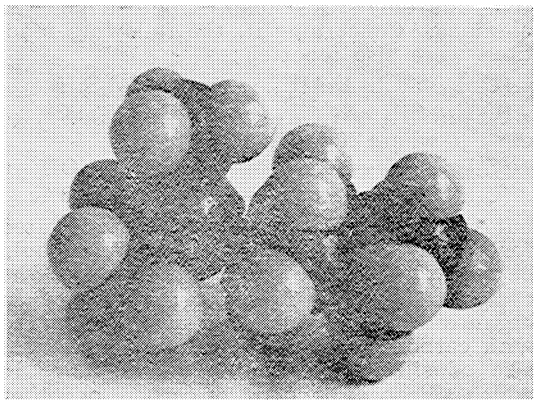


Fig. 3 (1).

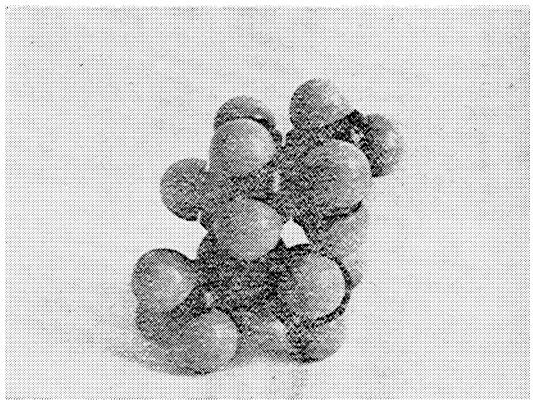


Fig. 3 (2).

Fig. 3. The two forms of stuart models of cyclohexyltrimethylsilane.
Left: Cyclohexyl bonds to silicon in *e*-bond and Si-cyclohexyl rotation is free.
Right: Cyclohexyl bonds to silicon in *p*-bond and the rotation is prevented.

isomer is present or not in the real substance, but this fact is not known from the infrared spectra of these compounds.

Now it is clear that the steric hindrance in them is not essential, or, not a subject of the structures themselves but a subject of the reaction processes; that is, cyclohexyl in a tricyclohexylsilyl group prevents the approach of the active centre of such a reagent as alkyllithium to the silicon atom. Therefore, syntheses of them were attained by addition of hydrogen, the smallest atom.

Ipatiev and Dolgov reported on hydrogenation of triphenylcarbinol[15] and tetraphenylmethane[16]. In both cases, tricyclohexylmethane was produced. Consideration with the Stuart model shows that it is impossible to introduce the fourth cyclohexyl to the central carbon atom in tricyclohexylmethyl group as shown in Fig. 4. This agrees with the results of Ipatiev and Dolgov. The difference in these and our results is explained by differences of atomic sizes and bond lengths. Ipatiev and Dolgov also studied analogous reaction of tetraphenylsilane under high pressure at high temperature without a catalyst[17]. In this experiment, hydrogenation did not take place, and the cleavage of

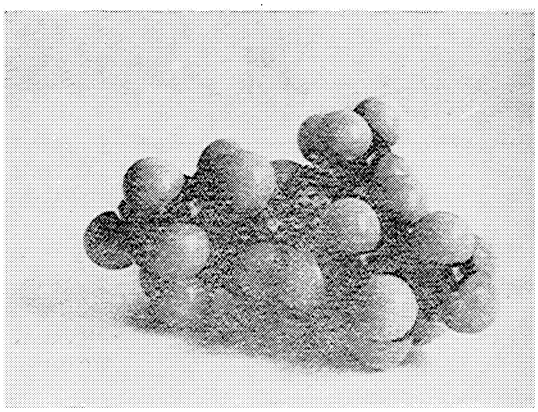


Fig. 4.
Stuart model of tricyclohexylmethyl.

Si—Ph bond with liberation of benzene was observed.

Studies on the steric hindrance of cyclohexyl group in organosilicon compounds are continued and syntheses of hexacyclohexyldisilane, hexacyclohexyldisiloxane and *t*-butyltricyclohexylsilane are under investigation now in this laboratory.

Summary

For new organosilicon compounds containing cyclohexyl group were prepared by hydrogenation of corresponding phenylsilanes. They are: trimethylcyclohexylsilane, dimethyldicyclohexylsilane, methyltricyclohexylsilane, and tetracyclohexylsilane. Physical

15) V. N. Ipatiev and B. N. Dolgov, *Compt. rend.*, **183**, 304 (1926).
16) V. N. Ipatiev and B. N. Dolgov, ibid., **185**, 210 (1627).
17) V. N. Ipatiev and B. N. Dolgov, *Ber.*, **62**, 1220 (1929).

constants and infrared absorption spectra of these compounds were measured and discussions on the steric hindrance were done with Stuart models.

The authors are indebted to Mr. S. Saeki and Mr. T. Yoshimoto for the infrared spectra and Mr. H. Sakai for the mass spectra reported in this paper. They are also grateful to Dr. O. Simamura and Dr. T. Yamada for their helpful advice and encouragement during this work.

Electrotechnical Laboratory, Agency of Industrial Science & Technology
Nagata-cho, Chiyoda-ku, Tokyo

The Nature of the Hydrogen-Bond. I. The Delocalization Energy in the Hydrogen-Bond as Calculated by the Atomic-orbital Method

By Hiroshi TSUBOMURA

(Received June 21, 1954)

Until quite recently it has been assumed that the energy of the hydrogen-bond is mainly electrostatic. Such an assumption seems to be very valid in regard to the experimental evidence that this bond is formed only between molecules which contain polar groups. Also the energies of the electrostatic interaction between hydrogen-bonded molecules calculated by some authors[1,2] agreed fairly well with experimental values of the bond energies and were taken as evidences for the above mentioned assumption.

We face to some difficulties, however, if we try to explain the strengths of hydrogen-bonds of various molecules only from the electrostatic point of view. Let us consider, for example, acetone and ethyl ether. Both act as proton-acceptors in the hydrogen-bond and according to the electrostatic theory we are forced to conclude that the proton-accepting strength of the former is greater than that of the latter since the carbonyl group of the former is much more polar than the C-O group of the latter. But it is known experimentally that the accepting strength of acetone is nearly equal to, or rather less than that of ethyl ether.[3] It is also known that nitriles are moderate proton-acceptors in spite of the strong polarity of their C≡N group.[3]

These phenomena strongly suggest that other sources of the interaction energy exist in the hydrogen-bond. Quite naturally what we can obtain experimentally as the energy of a hydrogen-bond may be, from a theoretical point of view, interpreted as the algebraic sum of the following terms: (1) Electrostatic energy, (2) Dispersion force, (3) Exchange repulsion, (4) Delocalization energy due to the electron-transfer from a proton-acceptor to a proton-donor. Hence, even if the calculated value of the electrostatic energy of a hydrogen-bond agrees with the experimental dissociation energy, we cannot say that the former is the dominant part of the latter. It only shows that the algebraic sum of (2), (3) and (4) is practically zero. Therefore, a complete clarification of the energy of the hydrogen-bond would not be attained until we were able to calculate or estimate these terms precisely.

Unfortunately it is extremely difficult to calculate non-empirically the energy of a hydrogen-bond as the sum of the above mentioned terms. For the energy of a hydrogen-bond is of the order of several kilocalories, that is 0.01 atomic unit, and, to calculate it exactly, we should calculate numerous energy integrals which appear in the course of calculation within the error of, at most, 0.001 atomic unit. Practically, it is almost impossible to carry out such accurate calculations. Nevertheless, it seems important for the discussion of the nature of the hydrogen-bond to calculate, even approximately, each of the above-mentioned terms. The author's aim in this paper is to clarify the nature and to estimate the magnitude of the fourth term, that is, the delocalization energy.

The importance of this term has been quite recently recognized. In 1951, C.A. Coulson[4]

1) N. D. Coggeshall, *J. Chem. Phys.*, **18**, 978 (1950).
2) J. A. Pople, *Proc. Roy. Soc.*, **A205**, 11 (1951).
3) M. Tsuboi, *Kagaku-no-Ryôiki* (*J. Japanese Chem.*), **7**, 611 (1953).
4) C. A. Coulson, "Valence", Oxford Univ. Press (1952), p. 305

described a study of the magnitude of the contribution of various resonance hybrids in the hydrogen-bonded water molecules, and stated that the contribution of the hybrids which is related to the charge delocalization is considerably great. Nukasawa, Tanaka and Nagakura[5] have also emphasized the importance of this term and have proposed that it may conveniently be estimated by use of a second order perturbation theory in terms of molecular orbitals and with some empirical values of the ionization potentials and the excitation energies. Though it seems that their method is very convenient and significant for the qualitative discussion of the problem, it may be also important to carry out an exact non-empirical calculation and to decide whether their qualitative conclusion is correct or not. In this paper the results of the calculations of the hydrogen-bonded water molecules by the atomic orbital method are given.

The Basis of the Calculation

The structure of the two hydrogen-bonded water molecules has been assumed to be that shown in Fig. 1; namely, the two water molecules lie in a

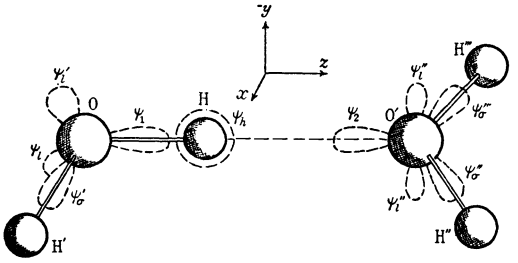


Fig. 1. The assumed structure of the hydrogen-bonded water molecules.

common plane and the hydrogen atom of the proton-donating molecule is situated on the straight line which connects the two oxygen atoms and which, at the same time, coincides with the symmetry axis of the proton-accepting molecule. The individual atoms constituting these molecules have been designated in the way shown in this figure. The O-H and O-O' distances have been taken to be 0.96 Å and 2.70 Å, respectively.

In the present calculation, it is assumed, as is usual, that each of the oxygen atoms has four s, p-hybridized AO's, two of which are directed to the two hydrogen atoms and form electron-pair bonds with the 1s-AO's of the hydrogen atoms, respectively, while each of the remaining two AO's directed toward the opposite side to the O-H bonds, is occupied by two spin-antiparallel electrons and has no influence upon the O-H bonds.

The coefficients of hybridization of $2s$ and $2p$ AO's in these AO's have a strong influence on the electronegativity of oxygen atoms, and therefore on the energy of the hydrogen-bond. The best way is, of course, to make the variation treatment with inclusion of these coefficients. But, since the hydrogen-bond is a week perturbation, one may expect a good result by use of orbitals with constant hybridizations, if the coefficients of the hybridization are properly chosen. The result of the equivalent molecular orbitals obtained by J.A.Pople[6] has shown that the two bonding AO's and the two lone-pair AO's of the oxygen atom in a water molecule can be described by orbitals nearly tetrahedral. Relying upon this result, tetrahedral orbitals have been adopted for the present work. In this case, however, the hydrogen atom of the proton donor finds itself in the middle of the directions of the two lone-pair AO's of the proton acceptor in our assumed configuration of the two water molecules. As the inclusion of the two lone-pair AO's in the calculation complicates the problem, they have been transformed into a $2p_y$ AO and a diagonally hybridized AO (ϕ_2) directed to the H atom. Then, only the latter is to be included in the calculation since the $2p_y$ AO is owing to its anti-symmetric character, unable to interact with the 1s AO of the hydrogen atom. Consequently, the valence AO's of the oxygen atoms we assumed here are as shown in Fig. 1, and their explicit forms are given by the following formulas:[7]

$$\begin{aligned}
\phi_1 &= 1/2(s+\sqrt{3}\,z)\\
\phi_{\sigma'} &= s/2+\sqrt{2}/3x-z/2\sqrt{3}\\
\phi_l &= -s/2+x/\sqrt{6}+z/\sqrt{12}=y/\sqrt{2}\\
\phi_{l'} &= -s/2+x/\sqrt{6}+z/\sqrt{12}-y\sqrt{2}
\end{aligned}$$

where s, x, y, and z denote the $2s$, $2p_x$, $2p_y$, and $2p_z$, AO's of O, and s', x', y', and z', denote those of O', respectively.

$$\begin{aligned}
\phi_2 &= (1/\sqrt{2})(s'-z')\\
\phi_{\sigma''} &= (1/2)(s'+\sqrt{2}x'+z')\\
\phi_{\sigma'''} &= (1/2)(s'-\sqrt{2}x'+z') \qquad (1)\\
\phi_{l''} &= y.
\end{aligned}$$

Since the complete treatment of the problem is extremely tedious, and since the aim of the author is not to carry out a precise calculation for the particular case of water, but to discuss the magnitude and the nature of the delocalization energy for the hydrogen-bond in general, the problem was reduced to the variation treatment of the energy of four electrous over the three atomic orbitals, ϕ_1, ϕ_2 and ϕ_h, in the potential field of the nuclea and of the remaining electrons which are distributed over the inner-shells and lone-pairs of oxygen atoms and other O-H bond..

5) K. Nukasawa, J. Tanaka and S. Nagakura, *J. Phys. Soc. Japan*, **8**, 792 (1953).
6) J. A. Pople, *Proc. Roy. Soc.*, **A202**, 323 (1950).
7) S. Maeda, *Busseiron-Kenkyu*, **70**, 101 (1954). In this paper, S. Maeda reports his results on the SCF LCAO MO calculation of the water molecule. By the transformation of his SCF MO, he obtained as the equivalent AO'S of the oxygen atom approximately tetrahedral ones. It seems that his result also supports the validity of employing the tetrahedral AO's in the present calculation.

orbitals. Such a treatment will give a fairly good result if the assumed distribution of these electrons agrees with the true one for the ground state of the system. According to Pople's result[5], the coefficients of the valence AO's of oxygen and hydrogen in the localized MO of the O-H bond of a water molecule are nearly the same. Hence, it is not so dangerous to replace the potentials of the bonding electrons for the OH′, OH″, and OH‴ bonds (See Fig. 1) by those of the six electrons which occupy, one by one, the valence AO's of the oxygen atoms, $\psi_{\sigma'}$, $\psi_{\sigma''}$, $\psi_{\sigma'''}$, and the 1s AO's of the three hydrogen atoms. Furthermore, the potentials induced by these hydrogen 1s-electrons may be assumed to cansel those of the atomic nuclea of hydrogen, in view of the large distances between these hydrogen atoms and the centres of the orbitals, ϕ_1, ϕ_2 and ϕ_h. Thus, in the present calculation, we assume a core potential arising from the following nuclea charges and electronic clouds.

for O, $+8e$, $(\psi_{1s\sigma})^2$, $(\psi_{\sigma'})^1$, $(\psi_l)^2$, $(\psi_{l'})^2$,
for O′, $+8e$, $(\psi_{1s\sigma'})^2$, $(\psi_{\sigma''})^1$, $(\psi_{\sigma'''})^1$, $(\psi_{2p\pi O'})^2$
for H, $+e$. (2)

The Method of the Calculation

Based on these considerations, five resonance hybrids shown in the following formulas are assumed.

(A) O—H.....O (D) O^- H——O^+
(B) O^- H^+....O (E) O H O^+ (3)
(C) O^+ H^-....O

Eigenfunctions for these can be written as follows:

$$\Psi_A=N_A(\phi_1-\phi_2) \qquad \Psi_D=N_D(\phi_4-\phi_5)$$
$$\Psi_B=N_B\,\phi_3 \qquad \Psi_E=N_E(\phi_7-\phi_8), \quad (4)$$
$$\Psi_C=N_C\,\phi_6$$

in which N_A, N_B, etc., are the normalizing factors and the ϕ's are the four-electron determinantal wave functions:

$$\phi_1=(1\alpha^1\cdot h\beta^2\cdot 2\alpha^3\cdot 2\beta^4) \qquad \phi_5=(1\alpha^1\cdot 1\beta^2\cdot h\beta^3\cdot 2\alpha^4)$$
$$\phi_2=(1\beta^1\cdot h\alpha^2\cdot 2\alpha^3\cdot 2\beta^4) \qquad \phi_6=(h\alpha^1\cdot h\beta^2\cdot 2\alpha^3\cdot 2\beta^4)$$
$$\phi_3=(1\alpha^1\cdot 1\beta^2\cdot 2\alpha^3\cdot 2\beta^4) \qquad \phi_7=(1\alpha^1\cdot h\beta^2\cdot h\alpha^3\cdot 2\beta^4) \quad (5)$$
$$\phi_4=(1\alpha^1\cdot 1\beta^2\cdot h\alpha^3\cdot 2\beta^4) \qquad \phi_8=(1\beta^1\cdot h\beta^2\cdot h\alpha^3\cdot 2\alpha^4),$$

where, for example,

$$(1\alpha^1\cdot h\beta^2\cdot 2\alpha^3\cdot 2\beta^4)=\begin{vmatrix} (1\alpha)^1 & (h\beta)^1 & (2\alpha)^1 & (2\beta)^1 \\ (1\alpha)^2 & (h\beta)^2 & (2\alpha)^2 & (2\beta)^2 \\ (1\alpha)^3 & (h\beta)^3 & (2\alpha)^3 & (2\beta)^3 \\ (1\alpha)^4 & (h\beta)^4 & (2\alpha)^4 & (2\beta)^4 \end{vmatrix},$$

and $1=\phi_1$, $2=\phi_2$, $h=\phi_h$, α, and β are the two spin functions.

By use of these functions, the matrix elements H_{AA}, H_{BB}, etc. were calculated and the lowest root of the secular determinant,

$$|H-S.E|=0$$

was determined. This gives the energy of the O-H...O system in the ground state.

The Hamiltonian is given by the kinetic energy operator plus the three bare-nuclea field potentials and potentials caused by the electrons whose configuration is shown in (2). For ϕ_1 and ϕ_h, however, the core potential of O′ was set equal to

(potential of the neutral oxygen atom)−
$$2\int\phi_2^*(\mu)(e^2/r_{\nu\mu})\phi_2(\mu)d\tau_\mu,$$

and the former was ignored. The values of integrals were taken, if possible, from Kotani, Amemiya and Simose's table[8], and in other cases either directly calculated or estimated by the overlap approximation. Some of the directly culculated integrals were given in the Appendix. Slater-type atomic orbitals were used, and the effective nuclea charge of oxygen for the valence shells were taken to be 4.55. The coulombic integrals between AO's of O and O′ were calculated by the point-charge approximation.

In the calculation of $(\phi_i \mid H \mid \phi_j)$, the terms which arise by twice or more exchanges of electrons were ignored. Also, the exchange integral and overlap integral over ϕ_1 and ϕ_2 were neglected throughout the calculation. All the remaining terms were thoroughly included.

For comparison, the lowest energy of the O-H bond in a free water molecule was also determined. In this case, three resonance hybrids, A′, B′, and C′, similar to the types, A, B and C in (3) may be assumed. The bond eigenfunctions for them are:

$$\Psi_{A'}=N_{A'}(\phi_1'-\phi_2')$$
$$\Psi_{B'}=N_{B'}(\phi_3') \quad (6)$$
$$\Psi_{C'}=N_{C'}(\phi_3')$$

in which the ϕ''s are of the following form, when one uses the same abbreviated formula as used before,

$$\phi_1'=(1\alpha^1\cdot h\beta^2) \qquad \phi_6'=(h\alpha^1\cdot h\beta^2).$$
$$\phi_2'=(1\beta^1\cdot h\alpha^2) \quad (7)$$
$$\phi_3'=(1\alpha^1\cdot 1\beta^2)$$

	A	B	C	D	E
A	−E	0.43−0.70E	0.56−0.70E	0.37−0.26E	0.21−0.32E
B		−(1.28+E)	0.75−0.32E	−(0.17+0.38E)	0.31−0.23E
C			−(0.92+E)	0.36−0.12E	0.34−0.24E
D				−(2.55+E)	−(0.53+0.56E)
E					−(2.25+E)

$=0$ (8)

	A′	B′	C′
A′	−E	0.42−0.69E	0.58−0.69E
B′		−(1.29+E)	0.71−0.31E
C′			−(0.90+E)

$=0$ (9)

8) Kotani, Amemiya and Simose, *Proc. Phys.-Math. Soc. Japan*, **20**, Extra Number 1, **22**, Extra Number.

Results and Discussion

The calculated matrix elements for the O-H . . . O system and for the free molecule are given in (8) and (9), respectively.

As may be seen from these equations, the zero point of the energy was taken at the value of H_{AA} for (8) and at the value of H_{AA}' for (9). Since in absolute value $H_{AA} \neq H_{AA}'$, the zero points of these two equations are not the same. (The calculated values are, $H_{AA}=12.298$, $H_{AA}'=5.429$, in atomic unit.)

TABLE I

	Lowest eigenvalue	C_A^2	C_B^2	C_C^2	C_D^2	C_E^2
(1)	0.3015	0.705	0.088	0.194	0.007	0.008
(2)	0.2756	0.715	0.098	0.187	/	/
(3)	0.2787	0.721	0.088	0.190	/	/

In Table I, (1) shows the result of the solution of the secular equation (8), (2) shows that of the three-dimensional secular equation obtained by dropping the terms, H_{DX}'s and H_{EX}'s, and (3) shows that of the secular equation (9)·C_A^2, C_B^2, etc. are the coefficients for the resonance hybrids, A, B, etc. for the lowest eigenvalue.

From this table, it can be seen that C_C^2 is always larger than C_B^2. This difference occurs mainly for the reason that in the secular determinant, (8) and (9), H_{CC} is larger than H_{BB}, and it means that the structure of O^+H^- contributes more to the ground state of the molecule than the structure of O^-H^+. This is contradictory to the usual chemical concept that the O-H bond is characterized, to a certain extent, by the O^-H^+ structure. Hence, in order to examine the validity of the results here obtained, the dipole moment of the water molecule was calculated. From the supposition of the AO's of the oxygen atom in a valence state, on which the present calculation is based' it is conceivable that the dipole moment of the water molecule consists of two bond dipoles and a lone-pair dipole[9] as shown in Fig. 2. By use of the

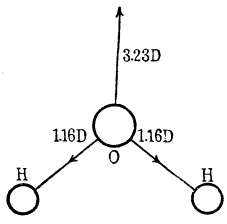


Fig. 2.

coefficients for the lowest-energy-state bond eigenfunction listed in the third row of Table I, the O-H bond moment was calculated to be 1.79D (O^+H^-). The main part of this moment, however, does not arise from the fact that C_C^2 is larger than C_B^2, but it arises from the resonance hybrid indicating homopolar bond (type A). As the calculated lone-pair dipole moment is 3.23 D and directs in the opposite side to the O-H bonds, the total moment amounts to 1.17 D, a value somewhat smaller than the experimental one, 1.84 D. On the contrary, if one assumes, as Pople assumed, that C_B^2 is a little larger than C_C^2, the calculated dipole moment will approach to the experimental value. Therefore, it can be concluded that in the present calculation H_{BB} has been a little underestimated compared to H_{CC}. It seems difficult, however, to avoid errors of this degree in view of the approximation of the method employed in the present work. Further discussions on the validity of the present calculation will be made later in this paper.

The energy of the delocalization due to the D- and E-structures may be given by the difference of the lowest eigen-values listed in the first and second rows of Table I, which amounts to 0.0259 AU., that is, 8.1 kcal./mol. On the other hand, the calculated electrostatic energy of the hydrogen-bond between two water molecules given by Pople[2], is 5.95 kcal./mol. A comparison of these two values allows us to conclude that the delocalization energy is of the same order of magnitude as, or rather larger than, the electrostatic energy.

From a survey of the features of the secular equations, (8) and (9), one can obtain some knowledge on the general character of the delocalization energy. First, we have seen that the inclusion of the D- and E-structures modifies the lowest energy of the system by only 0.0259 AU., a very small value compared to each matrix element. Therefore the problem can be, to some degree of exactness, treated by the second-order perturbation theory for the ground-state of the O-H group with inclusion of the higher energy states, D and E. The ground state of the O-H group may be given by a wave function

$$\Psi_0 = c_A\Psi_A + c_B\Psi_B + c_C\Psi_C \qquad (10)$$

The second-order perturbation energy will then be,

$$(\Delta E)_{0D} = (H_{0D} - S_{0D}\cdot E)^2/(H_{00} - H_{DD}),$$
$$(\Delta E)_{0E} = (H_{0E} - S_{0E}\cdot E)^2/(H_{00} - H_{EE}). \qquad (11)$$

It will be interesting to calculate the perturbation energy by use of (11), and compare the results with the exact value. As a rough approximation H_{00} in (11) may be replaced

9) J. A. Pople, ref. 6. C. A. Coulson, ref. 4.

by H_{AA} since the major part of Ψ_0 consists of Ψ_A. Correspondingly, we get,

$$(\Delta E)_{AD}=(H_{AD}-S_{AD}\cdot E)^2/(H_{AA}-H_{DD}),$$
$$(\Delta E)_{AE}=(H_{AE}-S_{AE}\cdot E)^2/(H_{AA}-H_{EE}), \quad (12)$$

where, for the E, 0.28 may be used. (See (3) of Table I).

The numerical results are:

$$(\Delta E)_{AD}=0.0346\text{AU.}=11\text{ kcal./mol.},$$
$$(\Delta E)_{AE}=0.0066\text{AU.}=2\text{ kcal./mol.},$$

The sum of these two values, 13 kcal./mol., is considerably larger than the true one, 8.1 kcal./mol. This may result from the negative value of $(H_{BD}-S_{BD}\cdot E)$, and $(H_{DE}-S_{DE}\cdot E)$.

From the above equations we can see that the delocalization energy becomes the greater, as the differences between H_{DD} or H_{EE} and other diagonal matrix elements decrease, and it is clear that these differences become the smaller,the larger the electron affinity of O and the smaller the ionization potential of O'*.

We can also see that the energy depends on the resonance integrals, $(H_{DX}-S_{DX}\cdot E)$ and $(H_{EX}-S_{EX}\cdot E)$. (Here X designates the elements A, B and C.) From the survey of the explicit forms of these terms, it can be seen that all of these terms, except $(H_{CE}-S_{CE}\cdot E)$, are approximately proportional to the overlap integral between ψ_2 and ψ_h, denoted hereafter by S_{2h}. Therefore it may be concluded that the delocalization energy increases with increasing S_{2h}. In general, S_{2h} depends on the distance between H and O', the formal charge of O' and the hybridization factor of ψ_2. Concerning the last factor it can be easily shown that S_{2h} has a maximum at a certain hybridization factor α. $(1>\alpha>0)$

Therefore, if one confines his attention within the influence of the overlap integral, he can conclude that the delocalization energy for a proton-acceptor which has an s, p-hybridized lone-pair orbital is, if the hybridization factor is appropriate, larger than the delocalization energy for a proton-acceptor which has pure s- or p-lone-pair orbital. It is interesting to note that, from the electrostatic point of view, a conclusion similar to that mentioned above can also be drawn, concerning the relation between the strength of hydrogen-bonds and the hybridization of the lone-pair of the proton-acceptor[10].

Eqs. (11) also suggest the limit of the accuracy for the obtained value of the delocalization energy. Namely, its accuracy is approximately the same as the accuracy of such terms as $(H_{AA}-H_{DD})$, $(H_{AD}-S_{AD}\cdot E)$, etc. As for the validity of these values, of course, there are many points to be discussed. For example, it is a question whether or not Slater-type AO's give reasonable results for the energy of interaction between atoms which are so separated as in this case. S. Maeda, in private communication, has pointed out that, when we used SCF AO's, the overlap integral, S_{2h}, will become much larger than the value calculated by use of Slater AO's. Also, when we calculate such terms as $(H_{AA}-H_{DD})$, some error will enter into the result on account of the fact that the same screening constant is used for both neutral and ionized states[11]. The correction of this error will increase our value of the delocalization energy.

Influence of the Formal Cahrge at O'

Thus far, it has been assumed that the proton-accepting oxygen atom has no formal charge. This assumption may be valid in many cases where the accepting molecule has only single bonds, because it has been recently accepted that even for a bond, usually thought to be polar, the main part of its polarity arises from the atomic dipole and the bond itself is for many cases nearly homopolar. But when the molecule with which we are concerned is a conjugated double-bond system, such as, for example, phenol or benzoquinone, the oxygen atoms will definitely carry a considerable positive or negative charge. In such cases the formal charge will not only modify the electrostatic interaction energy between proton-donors and proton-acceptors but will also modify the contribution of the delocalization energy by its effect of reducing the ionization potential of the lone-pair of the proton-acceptor and by increasing the overlap integral between the hydrogen 1s AO and the lone-pair AO. The increase of this overlap integral is caused by the change of the screening constant of the oxygen atom due to the formal charge. For instance, the same calculations were made for the case when the oxygen atom, O' has −0.2e formal charge. In this case the matrix elements corresponding to those given in (8) are a little modified and the following results are obtained.

$$H_{AA}-H_{DD}=2.33\text{AU.},$$
$$H_{AD}-S_{AD}\cdot E=0.39\text{AU.}-0.26E.$$

By use of these values and Eq. (12), the second-order perturbation energy arising only from the D-structure is calculated to be 13.5 kcal./mol., showing a 2.7 kcal. increase in comparison with the former result. On the other hand the increase of the electrostatic energy due to the same formal charge is about 1 kcal./mol.

* This has been already pointed out by Nukasawa, Tanaka and Nagakura[5].

10) W. S. Fyfe, *J. Chem. Phys.*, **21**, 2 (1953).

11) W. Moffitt, *Proc. Roy. Soc.*, A**210**, 236 (1951).

Comparison with the Experimental Facts

From the present results of calculation, it has been concluded that the delocalization energy amounts to about 8 kcal./mol. for the hydrogen-bond between water molecules. On the other hand the calculated electrostatic energy for the bond is about 5 kcal./mol. The experimental value of the heat of sublimation for ice is 12.2 kcal./mol., and if one tentatively assumes that about one fourth of this value is attributed to the interaction of non-neighbors, the energy of the hydrogen-bonds may be estimated to be about 9 kcal./mol. Since two hydrogen-bonds exist per one water molecule, the energy of the single hydrogen-bond is estimated to be about 5 kcal./mol. Hence, in order to assume that the theoretical and experimental energy values are consistent, one should consider that a repulsive energy of the order of 8 kcal./mol. is present in the hydrogen-bond. It may be easily understood that this repulsive energy is provided by the difference between exchange repulsion and the dispersion force, since the O-O distance for the hydrogen-bonded molecules must be shortened by the attractive electrostatic and charge-transfer forces, compared to the equilibrium O-O distance which would be attained when only usual dispersion force and exchange repulsion are present.

From the present results, it seems that the disagreement between the order of the experimentally found proton-accepting strengths of some proton-acceptors and the electrostatically predicted ones may be explained by taking into account the delocalization energies. For example, as is described before, the proton-accepting strengths of diethyl ether, acetone and acetonitrile are known to be as follows:

diethyl ether≒acetone>acetonitrile.

In these compounds, it can be concluded that the delocalization energy for the hydrogen-bond grows stronger from right to left in the above formula, and thus compensates or overwhelms the increase of the electrostatic energy from left to right. For, as is concluded previously, the delocalization energy increases as the ionization potential of the lone-pair of the accepting molecule decreases, and the lowest ionization potentials of these molecules, which may be considered to correspond to those of the lone-pairs, are as follows:

diethyl ether[12]>acetone[13]>acetonitrile[12].

The delocalization energies depend, however, not only on the ionization potentials but also on various other terms, for example, the overlap integral between hydrogen and lone-pair AO's which have not yet been clarified for such complex molecules. Hence a precise argument on these points remains to be made in future.

Summary

The delocalization energy for the hydrogen-bonded water molecules has been calculated non-empirically by use of the atomic orbital method, with a simplified model. The delocalization energy thus calculated amounts to about 8 kcal./mol. which is rather greater than the calculated electrostatic energy that has been usually considered to be the most important source of the binding force. The proton-accepting strengths of ether, acetone and acetonitrile have been discussed by use of this result.

Appendix

Some of the integrals calculated by the author are listed below in atomic unit. The notations are the same as those used by J. F. Mulligan (*J. Chem. Phys.*, **19**, 347 (1951)). s, σ, and π are the 2s, 2pσ, and 2pπ AO's of the atom O, and s', σ', and π', are those of the atom O', respectively.

Overlap integrals		Bare nuclea-field-potential energy integrals			Coulomb integrals	
S(s,s')	0.00594	(H : s',s')		0.6066	(s's' : hh)	0.6029
S(s,σ')	0.00867	(H : $\sigma'\sigma'$)		0.6208	($\sigma'\sigma'$: hh	0.6078
S(σ,σ')	0.01260	(H : $\pi'\pi'$)		0.5995	($\pi'\pi'$: hh)	0.6011
S(π,π')	0.00156	(H : s'σ')		0.1166		
		(H : hs')		0.1616		
Exchange integrals		(H : hs')		0.1761		
(Approximate value)		(O' : hh)	=	(s's' : hh)		
(hs' : hs')	0.0359	(O' : hs')		0.2502		
(hσ' : hσ')	0.0483	(O' : hσ')		0.1715		

The author wishes to thank Professor K. Kozima heartily for his valuable advice.

Tokyo Institute of Technology
Ohokayama, Meguro-ku, Tokyo

12) J. D. Morrison and A. J. C. Nicholson, *J. Chem. Phys.*, **20**, 1221 (1952),

13) T. M. Sugden and W. C. Price, *Trans. Farad. Soc.*, **44**, 116 (1948).

The Densities of Polyvinyl Alcohol Film at Moist States

By Hiroshi TADOKORO, Syuzo SEKI and Isamu NITTA

(Received July 9, 1954)

Introduction

Although there exist a considerable number of papers on the sorption of water vapor by high polymers, only a few works have been carried out about the density of high polymers at moist states, and this phenomenon seems to present an important problem for a course of further studies on the mechanism of water sorption. Such density investigations have already been made with wool (A. T. King[1]), native cellulose fibers (E. Filby and O. Maass,[2] A. J. Stamm and M. Seborg[3]) and regenerated cellulose fibers (P. H. Hermans[4]), whereas there, is, as far as the present authors are aware, none yet with synthetic polymers. The synthetic high polymers, whose crystallinity can be changed more or less easily by heat- or mechanical treatments, have an advantage in such density studies, because the density stands in close relation with the crystallinity, which in turn governs the feature of water sorption. The present study was undertaken as a preliminary investigation of such a problem in connection with our previous works[5,6] on the sorption of water vapor by polyvinyl alcohol (PVA), bearing in mind that there might be some analogy between this substance and cellulose.

Experimental

a) Density Measurements.

i) *Sample*: The sample used was purified by the following procedures. The powdered specimen of PVA (average degree of polymerization: 2100) was dissolved in water at about 80°C. The 1% aqueous solution of sodium hydroxide was added to exclude residual acetyl groups on standing overnight. This solution was then neutralized with hydrochloric acid, and dialysed with distilled water for two weeks in order to eliminate inorganic salts, and then PVA was precipitated by adding methanol-acetone mixture. The films used for experiment were cast from about 2.5% aqueous solution of the purified PVA, on a glass plate placed horizontally in an air thermostat at 50° ±5°C. This took about five hours. The films were about 0.05 mm. thick, and were cut in pieces about 1 mm. × 5 mm.

ii) *Apparatus and procedures*: About 500 mg. sample in a weighing bottle was dried at about 60°C. under a high vacuum (10^{-4} mm. Hg atm. or below), until its weight became constant within ±0.2 mg. This procedure required about 10 days. The dry sample in the weighing bottle was placed in a small desiccator, in which the relative humidity was controlled by an aqueous solution of sulfuric acid of a definite concentration This desiccator was thermostated at 25° ± 0.05°C. The sorption equilibrium required about three weeks.

The density measurements were made by the flotation method, by using carbon tetrachloride-benzene mixtures as the flotation media. In this case, a minute amount of water contained in the medium will cause a serious uncertainty on the data. So we have taken special precautions to remove the trace of water, by drying benzene with metallic sodium and carbon tetrachloride with potassium hydroxide. One measurement of density took about 15 minutes. When the specimen was suspended stationarily, another one was then immersed in addition after a short time, and it was found that the latter specimen behaved almost in the same way as the former. Thus, it was confirmed that the adsorbed water in the sample was not appreciably transferred to the flotation medium during the measurement. The density of the flotation medium was determined by use of the bicapillary pyknometer.[8]

All of the density measurements were duplicated with different specimens, and the two corresponding readings coincided with each other within ±0.06% except the sample containing 45.5% water.

The density of the sample in water was measured with the ordinary 10 cc. bottle type pyknometer at 25° ±0.05°C. and found to be 1.312 ±0.003 g./cc.

b) Desorption Measurements.—The sample for these measurements was prepared in the same way as that used for the density measurements, in this case the thickness and size being about 0.02 mm. × 17 mm. × 50 mm.

The apparatus was similar to that described in a previous paper[9] with some modifications to

1) A. T. King, *J. Text. Inst.*, **17**, T53 (1926); **18**, T274 (1927).
2) E. Filby and O. Maass, *Canad. J. Res.*, **7B**, 162 (1932).
3) A. J. Stamm and M. Seborg, *J. Phys. Chem.*, **39**, 133 (1935).
4) P. H. Hermans, "Contribution to the Physics of Cellulose Fibers," Elsevier Publishing Co., Inc., Amsterdam—New York, 1946, p. 73; "Physics and Chemistry of Cellulose Fibers," same publisher, 1949, p, 206.
5) I. Nitta, S. Seki and Y. Yano, *Ann, Report Inst. Fiber Res. (Osaka Univ.)*, **5**, 33 (1950).
6) I. Nitta, S. Seki, Y. Yano and S. Tajima, ibid., **6**, 13 (1952).
7) I. Nitta, S. Seki, H. Chihara, K. Kuriyama and S. Nakajima, ibid., **7**, 24 (1953).
8) M. R, Lipkin, A. D. Davidson, W. T. Harvey and S. S. Kurtz, Jr., *Ind. Eng. Chem, Anal. Ed.*, **16**, 55 (1944).
9) I. Nitta, S. Seki, M. Momotani and K. Satô, *J. Chem. Soc. Japan*, **71**, 378 (1950).

meet the present requirements. The relative humidity was controlled as mentioned above.

About 200 mg. of the sample was suspended from a quartz spring balance (sensitivity: 0.153 mm./mg.) by a glass string. The accuracy of the travelling microscope was ±0.01 mm., and the temperature of desorption was 25° ±0.05°C. The sample was dried under high vacuum (10^{-4} mm. Hg or below) at 60° ±0.05°C. and then the weight of th bone-dry sample was determined.

Fig. 1 shows that the time required to reach

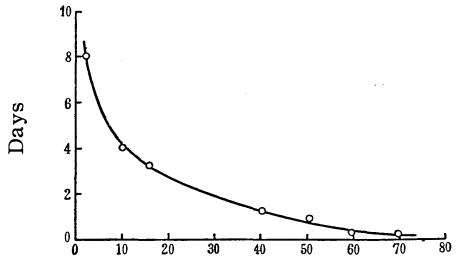
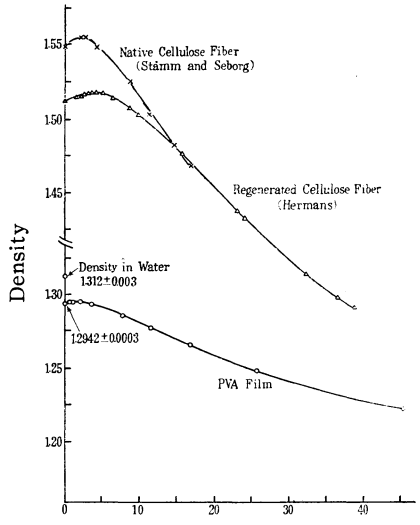


Fig. 1. Relation between time required for desorption equilibrium and final relative humidity.

the desorption equilibrium depends to a remarkable degree upon the relative humidity, indicating that the desorption rate under low relative humidity is very low. The rate-determining process should be the diffusion of water molecules in the polymer film.

Results and Discussion

The densities of the PVA film at moist states are shown in Fig. 2*, and those for



Ffg. 2. Density-water content curves.

native cellulose[3] and regenerated cellulose[4] are also shown for reference. Each density curve showed a conspicuous maximum at about 1.5, 2.5 and 4.5% water content for PVA, native cellulose and regenerated cellulose, respectivery.

The existence of such a maximum has been explained differently by several investigators. Filby and Maass[2] attempted to explain the maximum for native cellulose by assuming a compression of the bound water in the specimen under about 100,000 atm. pressure, whereas Stamm and Seborg[3] estimated this pressure as about 3440 atm. However, this compression hypothesis seems to be superficial and to be only a formal interpretation. On the other hand, Hermans' interpretation[4] is based on the assumption that the apparent volume V_a per 1 g. of polymer in moist state, consists of the following three parts:

$$V_a=(1+a)/d_a=\varphi_w+a+\varepsilon_a,$$

where a is water content in g. per 1 g. bone-dry polymer, d_a, density of the moist polymer whose water content is a g., φ_w, the net volume of the polymer, which should be equal to the specific volume of the polymer measured in water, and ε_a is the volume of the empty space which can be ultimately filled with water molecules but cannot be permeated by the molecules of the flotation medium. As the water content a increases, the empty space ε_a will diminish in proportion and will disappear at last, thereafter the increase in V_a will become equal to the volume of water sorbed and the slope should be 45°. Fig. 3 shows the V_a curves against the water

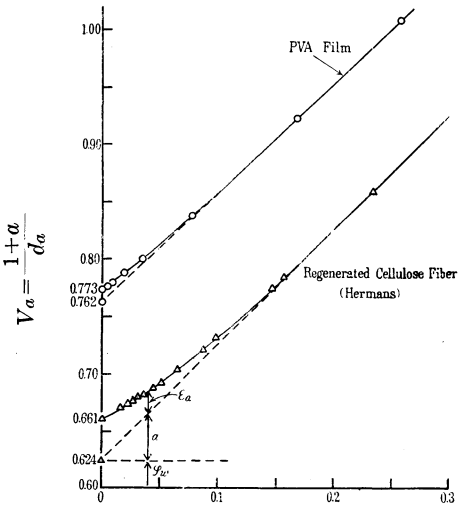


Fig. 3.
Relation between V_a and water content.

* The density of PVA sensibly depends on the temperature and the duration of drying, heat- and mechanical treatments, degree of polymerization, etc. In connection with these, the experiments of the effect of heat treatment on densities are now in progress in this laboratory.

content a for our PVA data together with those for regenerated cellulose by Hermans.[4] In the case of PVA, the slope of the dashed straight line is slightly less than that of regenerated cellulose, whose slope is exactly 45°. This is presumably due to the fact that the interaction of PVA with water is larger than that of cellulose. As to this phenomenon, further study should be made to discover whether the water molecule may infiltrate the crystalline part of PVA or not.

In order to elucidate the nature of the empty space a little more, we calculated the so-called pore size distribution of the PVA film as well as regenerated cellulose fiber from our data of desorption isotherm and of Hermans, by means of Foster's method.[10] The desorption isotherms for PVA and regenerated cellulose[4] are shown in Fig. 4,

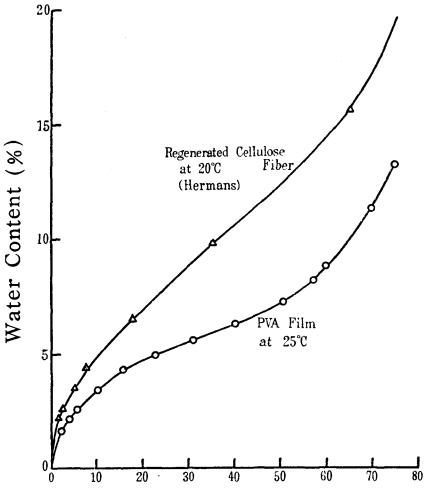


Fig. 4. Desorption isotherms.

and the pore size distribution curves are shown in Fig. 5. $V(\phi)$ in Fig. 5 stands for the

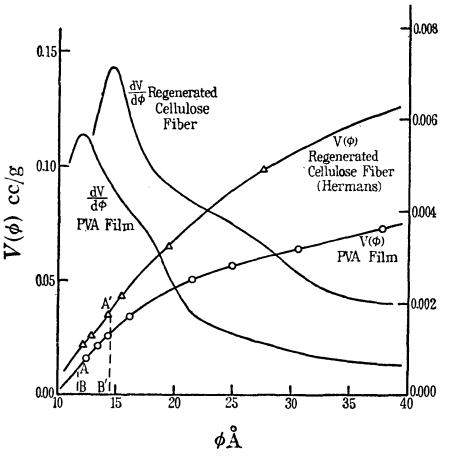


Fig. 5. Pore size distribution curves

integrated volume of pores whose diameter is smaller than ϕ. Although the variation of surface tension with the radius of curvature has been recently discussed theoretically by many authors,[11-15] we did not take this effect into our calculation, as these theories seem to be not yet quite decisive. By differentiating $V(\phi)$ with respect to ϕ the size distribution of the pore was obtained.

The empty volumes $\varepsilon_{a=0}$'s of the present sample and the related substance[3,4] are shown in Table I. In Fig. 5 the pore volumes corresponding to $\varepsilon_{a=0}$'s for PVA and regenerated cellulose are indicated by AB and A'B' respectively. It may be supposed that the pores of the diameter smaller than 11.7 Å. for PVA and 14.5 Å. for regenerated cellulose candot be inhabited by the molecules of the flotation medium, the mixture of carbon tetrachloride and benzene being used as the flotation medium for PVA, and that of carbon

TABLE I

DENSITY DATA AND CRYSTALLINITY

Material	$\varepsilon_{a=0}$ (cc./g.)	Wathr content of max. density (%)	Amorphous part fraction* (%)
PVA film	0.011	1.5	~7** (Nitta Seki, Yano and Tajima[5])
Native cellulose fiber	0.017	2.5	32 (Hailwood and Horrobin[16])
Regenerated cellulose fiber	0.037	4.5	65 (Hailwood and Horrobin[16])

* By sorption method.

** This is the data of the powder specimen which has the same degree of polymerization as the present sample.

10) A. G. Foster, *Discussions Faraday Soc.*, No. 3, 41 (1948).
11) R. C. Tolman, *J. Chem. Phys.*, **17**, 333 (1949).
12) J. G. Kirkwood and F. P. Buff, ibid., **17**, 338 (1949).
13) V. K. LaMer and G. M. Pound. ibid., **17**, 1337 (1949).
14) G. C. Benson and S. Shuttleworth, ibid., **19**, 130 (1951).
15) G. M. Pound and V. K. LaMer, ibid., **19**, 506 (1951).

tetrachloride and nitrobenzene for regenerated cellulose.[7] By use of the covalent and van der waals radii, the diameters of the molecules of the flotation media were estimated as follows:

carbon tetrachloride	~6.6 Å.
benzene	~7.3 Å.
nitrobenzene	~8.5 Å.

In spite of the boldness of the assumptions made above, the maximum diameters given above of the pore unaccessible for the molecules of the flotation media may be said to be in the same order of magnitude with the estimated geometrical sizes of these molecules, though the latter come out somewhat smaller. As the sources of such disagreement, the following factors may be pointed out.

(1) The water and nitrogen* sorption areas of polyvinyl acetal (acetal content 9.6%) measured previously by us were 65.9 m.²/g. and 6.0 m.²/g., respectively.[7] From this it may be reasonably assumed that while water molecules can break into the small space between the PVA molecular chains, nitrogen molecules cannot.[17,18] Accordingly, this fact seems to suggest that the geometrical size of the free molecule is not necessarily a decisive factor, but the mode of interaction between sorbent and sorbate must be also taken into account. Moreover, it may be possible that the pore size will vary as the water content increases.

(2) The filling-in of the pores with flotation medium is, quite probably, a matter out of equilibrium during the measurements of the present case.

(3) The Foster method assumes the Kelvin equation. It is now open to question whether this macroscopic equation can be applied to such a small pore of the molecular dimension.[11–15]

Finally, we may consider the relation among the maximum density of Fig. 2, the quantity $\epsilon_{a=0}$ and the crystallinity determined by the sorption method.[6,16] As shown in Table 1, the water content at which the density shows maximum, and the empty volumes $\epsilon_{a=0}$'s increase in the following order:

PVA < native cellulose < regenerated cellulose

and the % amorphous region measured by the sorption method also increases in the same order.[6,16] This fact may be explained by assuming that mainly the amorphous region of these polymers is accessible to water and has nearly the same fraction of the empty volume.

Summary

(i) The densities of PVA film at moist states were measured at 25°C. with flotation method by using carbon tetrachloride-benzene mixtures. The density against water content curve shows a conspicuous maximum at about 1.5% water content.

(ii) The water desorption expriment was carried out using the same specimen. The pore size distributions of PVA film and regenerated cellulose fibers were calculated by the Foster method from our desorption date and Hermans' data, respectively.

(iii) The results are discussed and compared with those of other investigators obtained with native and regenerated cellulose.

The authors express their sincere thanks to Kurashiki Rayon Co. Ltd. for kindly giving them the PVA samples used for this work, to Dr. K. Hirabayashi and Mr. Y. Sone of the Institute for Chemical Research of Kyoto University, and to Messrs. H. Chihara and K. Suzuki of this laboratory for helpful advice and criticism.

Department of Chemistry, Faculty of Science, Osaka University, Osaka

16) A. J. Hailwood and S. Horrobin, *Trans. Faraday Soc.*, **42**B, 84 (1946).

* These two molecules have nearly the same molecular diameter (N_2: ~4.1 A, H_2O: ~4.0 A.).

17) K. W. Mooney, A. G. Keenan and L. A. Wood, *J. Am. Chem. Soc.*, **74**, 1367, 1371 (1952).

18) T. M. Shaw, *J. Chem. Phys.*, **12**, 391 (1944).

*Electron Diffraction Investigation on Tribromotropolone**

By Masaji KUBO, Masao KIMURA and Katsumi KIMURA

(Received May 28, 1954)

In a series of researches by one of the present writers and his collaborators,[1-7] measurements were made of the dipole moments of tropolone and a number of its derivatives using benzene solutions. The positions of various substituents in these tropolone derivatives were determined from a comparison of the observed moments with the theoretical moment calculated for various conceivable positions of the substituents. In this determination, an assumption was tacitly made that in analogy to ortho and para positions in benzene only carbon atoms 3 (ortho), (para) and 7 (ortho′) are to be considered for the positions of substituents such as halogen atoms or a nitrogroup. One of the present writers and his collaborator[8] calculated π-electron distribution using the molecular orbital treatment and thereby revealed that carbon atoms 3, 5 and 7 have a greater share of π-electrons than carbon atoms 4 (meta) and (meta′). This suggests that electrophilic atoms and radicals preferentially attack hydrogen atoms at ortho, ortho′ and para positions.

Although the conclusions derived from these physico-chemical considerations were found to be in conformity with the results of organic synthesis,[8] it is most desirable that this new type of ring compounds be provided with a more direct experimental proof in favor of the adequacy of the aforementioned assumption. The present investigation was undertaken in order to verify that the three bromine atoms of tribromotropolone are substituted for the hydrogen atoms of tropolone at ortho, ortho′ and para positions. This compound is comparatively complicated for an electron diffraction experiment. Fortunately two of the present writers[10] as well as Heilbronner and Hedberg[11] have already carried out an electron diffraction study on tropolone and elucidated the geometrical configuration of the molecule of this compound. It is anticipated because the atomic number of bromine is high that the positions of bromine atoms in tribromotropolone can be determined by electron diffraction method accurately enough to give a decisive conclusion.

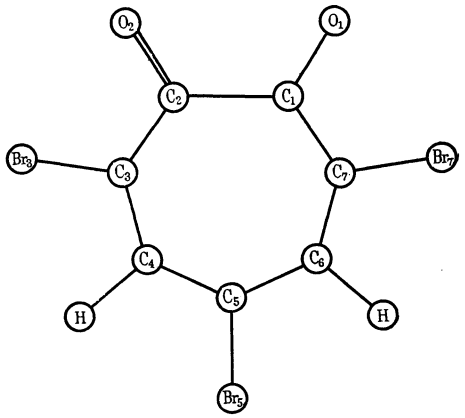


Fig. 1. *o*, *o*′, *p*-Tribromotropolone.

Material and Experimental Method.—A sample of tribromotropolone (m.p. 126°) was synthesized and purified in the laboratory of organic chemistry, Tohoku University. It was evaporated at a temperature 20—30° higher than its melting point and then passed through the high temperature nozzle described in a paper by one of the present writers and his collaborator.[12] The gas molecules ejected into a vacuum chamber interfered with an electron beam having a wavelength of about 0.06 Å. The wavelength was calibrated by means of gold foil. The camera length was 11 cm.

Experimental Results.—The visual intensity curve obtained is shown in Fig. 2. The q-values for the maxima and minima are given in Table I. From the visual intensity curve, a preliminary radial distribution function was calculated. The interatomic distances thus evaluated were used to obtain a preliminary theoretical intensity curve for

* Read before the scientific meeting of the Chemical Society of Japan held on April 4, 1952.

1) M. Kubo, T. Nozoe and Y. Kurita, *Nature*, **167**, 688 (1951).

2) Y. Kurita, T. Nozoe and M. Kubo, This Bulletin, **24**, 10 (1951).

3) Y. Kurita, T. Nozoe and M. Kubo, ibid., **24**, 99 (1951).

4) Y. Kurita, T. Mizuno, T. Mukai and M. Kubo, ibid., **26**, 192 (1953).

5) Y. Kurita, T. Nozoe and M. Kubo, ibid., **26**, 242 (1953).

6) Y. Kurita, S. Seto, T. Nozoe and M. Kubo, ibid., **26**, 273 (1953).

7) Y. Kurita and M. Kubo, ibid., **27**, 364 (1954).

8) Y. Kurita and M. Kubo, ibid., **24**, 13 (1951).

9) See papers by T. Nozoe and his collaborators published for the most part in the *Proc. Japan Acad.* and *Science Repts. Tohoku Univ.* Series I since 1950.

10) M. Kimura and M. Kubo, This Bulletin, **26**, 250 (1953).

11) E. Heilbronner and K. Hedberg, *J. Am. Chem. Soc.*, **73**, 1386 (1951).

12) M. Kimura and M. Aoki, This Bulletin, **26**, 429 (1953).

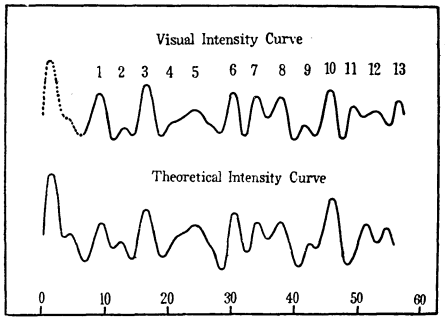


Fig. 2. The visual intensity curve and the theoretical intensity curve of tribromotropolone.

TABLE I

THE q-VALUES FOR THE MAXIMA AND MINIMA OF DIFFRACTION HALOS

Max.	Min.	q obs.	Max.	Min.	q obs.
1		9.42		8	35.64
	2	11.01	8		37.90
2		12.86		9	39.38
	3	14.45	9		41.62
3		16.36		10	43.36
	4	18.63	10		45.30
4		20.58		11	47.13
	5	22.48	11		49.20
5		24.39		12	50.88
	6	27.82	12		53.00
6		30.02		13	54.20
	7	31.61	13		56.30
7		33.73			

the range below $q=8$. As shown in Fig. 2, the visual intensity curve is extended to the region of small q-values by means of this theoretical intensity curve. The final radial distribution curve,

$$rD(r)=\sum_{q=1}^{\max} I_q \exp(-aq^2)\sin\left(\frac{\pi}{10}qr\right), \quad (1)$$

obtained from the visual intensity curve supplemented by the dotted curve is shown in Fig. 3. In this equation, notations have their usual significances. The constant a was chosen to give $\exp(-aq^2)=0.1$ at the maximum q-value. The atomic distance evaluated from this radial distribution curve are given in the third column of Table II. They

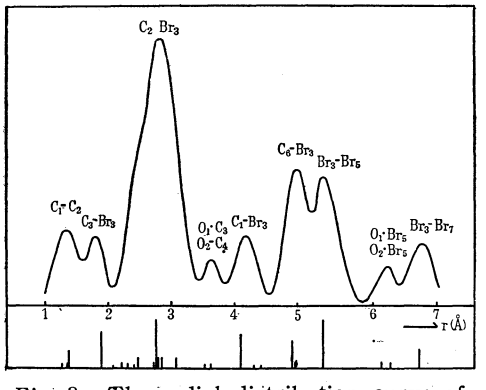


Fig. 3. The radial distribution curve of tribromotropolone.

TABLE II

INTERATOMIC DISTANCES IN TRIBROMOTROPOLONE

Atom pairs	Z_iZ_j/r_{ij}	Distances (exp.)	Distances (theor.)
Br_3–Br_5	38	5.40 A	5.40 A
Br_3–C_2	38	2.80	2.76
Br_3–C_3	28	1.82	1.88
Br_3–C_1	26	4.15	4.10
Br_3–C_6	21	4.96	4.92
Br_3–Br_7	15	6.77	6.74
C_1–C_2	13	1.36	1.36
Br_7–O_1	8	2.80	2.86
Br_3–O_2	8	2.80	2.79
C_1–C_3	8		2.47
C_1–C_4	7		3.08
Br_3–O_1	5	4.96	4.98
Br_7–O_2	5	4.96	4.92
Br_5–O_1	4	6.23	6.28
Br_5–O_2	4		6.14
O_2–C_1	4		2.22
Br_3–H_4	4	2.80	2.74
O_1–C_1	3	1.36	1.36
O_1–C_2	3		2.32
O_2–C_2	3		1.26
O_1–O_2	2		2.42
O_1–C_3	2	3.64	3.64
O_1–C_4	2		4.42
O_2–C_4	2		3.54
O_2–C_5	2		4.30
C_4–H_4	1		1.09
C_3–H_4	1		2.07

are assigned to atom pairs given in the first column. The designation of the atom pairs is evident from Fig. 1. In the second column, the values of Z_iZ_j/r_{ij} are given in arbitrary unit. The atom pairs contributing predominantly to each peak in the radial distribution curve are also given in Fig. 3. It will be seen from Table II and Fig. 3 that the majority of peaks in the radial distribution curve are due to interatomic distance involving a bromine atom or between bromine atoms. Therefore it is possible to determine definitely the location of three bromine atoms relative to each other and also to the tropolone ring. The interatomic distances obtained from the radial distribution curve can adequately be explained if we consider that the three bromine atoms are substituted for hydrogen atoms of tropolone at otho, para and ortho′ positions. If a bromine atom were in meta or meta′ position instead of at para position, the peak at 5.40

Å would be absent and the peak at 3.00 Å should be higher than the peak attributable to C_2–Br_3 distance. If each of three bromine atoms were bonded separately to one of three carbon atoms which, in turn, are bonded together consecutively, even though a peak at 5.40 Å could appear the peak at 3.00 Å would be much higher than it is in actuality and agreement could never be attained with the observed data. Thus it is confirmed that the sample of tribromotroplone under investigation is an *o*, *o*', *p*-derivative.

The radial distribution function of tribromotropolone is not suitable for the determination of the geometrical configuration of a tropolone ring. This is because the only distance obtainable for the determination of ring structure from the radial distribution curve is C–C bond distance equal to 1.36 Å whereas a number of parameters are required for the definite detrmination of the geometrical configuration of the molecule of this compound. In addition the mean amplitudes of various normal modes of vibration will appreciably affect the form of theoretical intensity curves. Considering possible errors inherent in the visual intensity curve, it seems impossible to determine the configuration of the molecule under investigation unless some simplifications be made. Therefore we assumed as follows. (1) The cycloheptatriene ring has a plane regular heptagon form with the length of its edge equal to 1.36 Å, as already mentioned. (2) All three C–Br bonds have the same length and are directed outward from the ring along the lines bisecting the respective ∠CCC angles so that both Br(para)-Br(ortho) and Br(para)-Br(ortho') distances are equal to 5.40 Å, as revealed by the radial distribution curve. (3) The C–H distance is equal to 1.09 Å. (4) The C–O distance is equal to 1.36 Å, while C=O istance is 1.26 Å long, as found in a tropolone molecule.[10]

A theoretical intensity based on these assumptions,

$$I(q)=\sum_{i<j}\sum\frac{Z_iZ_j}{r_{ij}}\sin\left(\frac{\pi}{10}qr_{ij}\right), \qquad (2)$$

in which a constant factor is omitted, has been calculated for a rigid model and is given in Fig. 3. The interatomic distances calculated for this model are given in the last column of Table II. The vertical bars in Fig. 3. are drawn in proportion to Z_iZ_j/r_{ij}. It will be seen that the agreement of the theoretical intensity curve with the visual intensity curve is satisfactory and that the vertical bars in Fig. 3. are in good accord with the heights of peaks in the radial distribution function.

We do not intend to assert that this theoretical intensity curve is the only possible form in agreement with experiment. For instance, the C–C distances in the ring could be a little longer or they might not be exactly equal. Despite these minor reservations, we believe that the problem of the positions of bromine atoms relative to the tropolone ring is undoubtedly settled.

Summary

Tribromotropolone of melting point 126° was investigated in gaseous state by electron diffraction method. The two Br–Br distances equal to 5.40 Å and 6.77 Å respectively were found as distinct isolated peaks in the radial distribution curve. These distances together with the known configuration of tropolone ring already studied gave decisive evidence that in this molecule three bromine atoms are substituted for hydrogen atoms of tropolone at ortho, ortho' and para positions. This conclusion is in good agreement with the prediction of molecular orbital treatment of tropolone and proves the adequacy of the assumption made in the structural determination by dipole moment data, i.e. that electrophilic atoms and groups substiute hydrogen atoms of tropolone at ortho, ortho' and para positions but not those at meta and meta' positions.

We express our deep appreciation to Prof. Nozoe and his collaborators at Tohoku University for providing us with the material used in this experiment and also to the Ministry of Education for supporting this research.

Chemical Department, Faculty of Science, Nagoya University, Nagoya

Dependence of the Molecular Polarization of Carbon Dioxide on Pressure

By Masaji KUBO and Tadashi UCHIDA

(Received June 8, 1954)

One of the present writers[1] has proposed a theoretical formula for the pressure effect on the dielectric constant of gases on the basis of the mutual action of dipoles, namely

$$\left(\frac{\varepsilon-1}{\varepsilon+2}\right)\frac{M}{d}=P=a+\frac{b}{T}+\frac{3ab^2\rho}{8\pi N\beta^3T^2}, \qquad (1)$$

where ρ is the concentration of gas molecules in moles per cc or the reciprocal of molecular volume. The symbol β denotes the radius of the action sphere of molecules. All others have their usual significances. This theoretical equation indicates that the molecular polarizations of nonpolar substances are independent of pressure even when raised to a few hundred atmospheric pressures. The constancy of molecular polarization is in agreement with experiments on hydrogen, nitrogen, methane and air. For polar substances, the equation predicts that the molecular polarization at constant temperature increases linearly with the reciprocal of molecular volume. The results of ammonia conform to this relation. The value of molecular radius which is calculated from the pressure dependence of molecular polarization agrees well with those values obtained from the viscosity of the gas or from the constant b in the van der Waals equation of state. Somewhat exceptional behavior is exhibited by carbon dioxide. Although this gas is nonpolar, the molecular polarization increases slightly but definitely with pressure. It was suggested that this behavior might be due to effects other than dipole-dipole interaction, such as quadrupole interactions, which were neglected in the derivation of the aforementioned theoretical equation. Since then knowledge of the electronic structure of carbon dioxide molecule has been extended to such a degree that it is now possible to give a quantitative interpretation of the pressure dependence of the molecular polarization of this gas. In the present paper the results of a theoretical treatment on this problem will be given.

MacCormack and Schneider[2] used experimental second virial coefficient data for carbon dioxide to investigate the intermolecular potential of this molecule on the basis of a Lennard-Jones model. It was found that the derived force constants varied with temperature, the low temperature data yielding higher values of the collision diameter. They interpreted the results in terms of partial binary association and suggested a T-shaped configuration for the resulting dimer having a separation between the centers of monomeric units, viz. C-C distance, equal to 3.91 Å. A conceivable dimer configuration with the two monomeric molecular axes aligned in parallel was proved to be unstable. The suggested dimer formation could explain adequately the increase of collision diameter at lower temperatures and the dimer configuration led to a Coulomb interaction energy to compare favorably with the heat of dimerization obtained from the temperature dependence of the equilibrium constant of dimerization. The equilibrium constant was obtained from the second virial coefficient observed experimentally at lower temperatures and the coefficient calculated for a monomeric gas on the basis of the Lennard-Jones parameters from the high temperature data. The value of the equilibrium constant K_p of dimerization at 100°C. was found to be equal to 4.51×100^{-4} atm^{-1}.

The T-shaped dimer has no center of symmetry and hence should have a finite overall moment μ, which contributes to orientation polarization. If the degree of association is denoted by w, the molecular polarization P of the gas is given by

$$P=(1-w)P_{mono}=(w/2)P_{dt}. \qquad (2)$$

Inasmuch as the dimer is a loose complex, it is reasonable to suppose that the electronic polarization is unaffected by dimerization. Therefore

$$P=P^\circ+(w/2)(P_{ort}+\Delta P_A), \qquad (3)$$

where P° $(=P_{mono})$ is the molecular polarization of unassociated carbon dioxide, i,e., the limiting value of molecular polarization at approaching zero pressure and P_{ort} is the orientation polarization of dimers,

$$P_{ort}=\frac{4\pi N}{3}\left(\frac{\mu^2}{3kT}\right). \qquad (4)$$

The quantity ΔP_A is the increase of atomic

1) M. Kubo, *Sci. Papers Inst. Phys. Chem. Research* (Tokyo), **27**, 295 (1935); This Bulletin **13**, 167 (1938). Cf. S. Glasstone, *Ann. Repts. Progr. Chem.*, **33**, 130 (1936); P. W. Bridgman, *Revs. Mod. Phys.*, **18**, 70 (1946).

2) K. E. MacCormack and W. G. Schneider, *J. Chem. Phys.*, **19**, 849 (1951).

polarization of dimers over twice the atomic polarization of monomers. Since the force field in monomeric units, viz. CO_2 molecules, will not be altered appreciably by the formation of the loose dimer, the assumption may be made that the vibrational modes of monomeric units remain practically unaffected by dimerization. A carbon dioxide molecule has four $(3\times3-5=4)$ normal vibrations, while the T-shaped dimer molecule has twelve $(3\times6-6=12)$ normal modes. Therefore ΔP_A will be the sum of contributions from four $(12-2\times4=4)$ modes of intermonomer vibrations.

By definition, the equilibrium constant is given as

$$K_p=\frac{p[(CO_2)_2]}{p^2(CO_2)}=\frac{(w/2)}{(1-w)^2p}, \qquad (5)$$

where p denotes the total pressure. Solving this equation for w and expanding the solution in a power series in K_pp, one obtains

$$w=2K_pp(1-4K_pp+\cdots\cdots). \qquad (6)$$

On introducing this in Equation 3, it becomes

$$P=P^\circ+K_pp(1-4K_pp)(P_{ort}+\Delta P_A). \qquad (7)$$

The molecular polarization P can be measured as a function of pressure p and the molecular polarization P° at approaching zero pressure has been obtained accurately ($P^\circ=7.35$ cc.).[3] As has already been mentioned, $K_p=4.51\times10^{-4}$ atm^{-1} at 100°C.[2] Therefore Equation 7 contains only one unknown parameter, $P_{ort}+\Delta P_A$, which can be obtained from experimental data. On the other hand, P_{ort} can be calculated if the dipole moment of a dimer can be estimated and ΔP_A will be obtained if the frequencies, the reduced masses and the effective charges of the four intermonomer vibrations mentioned above are evaluated properly. Subsequently the authors give a comparison of the sum of these two calculated quantitise with the experimental value of $P_{ort}+\Delta P_A$.

The dielectric constant of carbon dioxide at high pressures has been measured by many investigators. Inasmuch as one of the present writers reviewed available data on this problem in his previous reports,[1] references to earlier works need not be comprehensive. The measurements of Keyes and Kirkwood[4] and of Uhlig, Kirkwood and Keyes[5] carried out in the Massachusetts Institute of Technology were revised at the same laboratory by Keyes and Oncley[3] using a new cell. The extensive data by Michels and Michels[6] were critically examined by Keyes and Oncley, who corrected them for the "origin failure" ascribed to a variable displacement of the internal parts of the condenser when subjected to stresses induced by the presence of a high pressure gas. The adjusted data were found to be in good agreement with those obtained by themselves.

In Fig. 1. a plot is made of the molecular

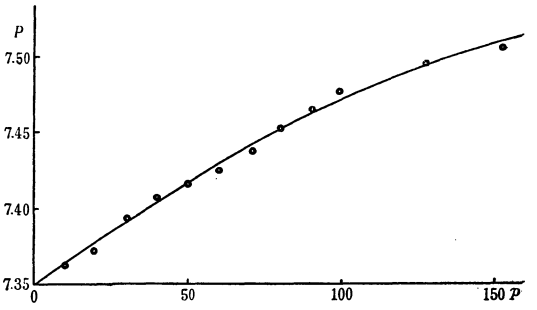


Fig. 1. Dependence of the molecular polarization P(cc.) of carbon dioxide upon pressure p(atm.).

polarization obtained by Keyes and Oncley against pressure rather than against P°/v as is done in the original report, where v denotes the molecular volume.* To convent molecular volume data to pressure, Michels and Michels' p-v-T data[7] were used. The old density data obtained by Amagat and the new by MacCormack and Schneider[8] gave practically identical results. The full line in Fig. 1. depicts the value of P calculated by Equation (7) with $P_{ort}+\Delta P_A=3.30$ cc. Over the entire pressure range studied, the points lie very close to the parabolic line within experimental errors as is expected from Equation (7). If experimental points lie on a parabola, one can give an empirical equation with three constants capable of fitting the curve to experimental points. It should be noted that in Equation (7) there are only two adjustable parameters, viz., P° and $P_{ort}+\Delta P_A$. This indicates that the explanation of the change of polarization with pressure in terms of partial association is adequate.

3) F. G. Keyes and J. L. Oncley, *Chem. Revs.*, **19**, 195 (1936).
4) F. G. Keyes and J. G. Kirkwood, *Phys. Rev.*, **36**, 754, 1570 (1930).
5) H. H. Uhlig, J. G. Kirkwood and F. G. Keyes, *J. Chem. Phys.*, **1**, 155 (1933).
6) A. Michels and C. Michels, *Phil. Trans. Roy. Soc. London*, **231**, 409 (1933).
* Since P° is equal the real volume per mole of molecules regarded as conducting spheres, P°/v is the ratio of the real volume of molecules to the total volume which they occupy.
7) A. Michels and C. Michels, *Proc. Roy. Soc. London*, A**153**, 201 (1935); A. Michels, C. Michles and H. Wouters, ibid., **153**, 214 (1935).
8) K. E. MacCormack and W. G Schneider, *J. Chem. Phys.*, **18**, 1269 (1950).

Estimation of the Dipole Moment of a Dimer

The geometrical configuration of the dimer of carbon dioxide proposed by MacCormack and Schneider[2] is given in Fig. 2. As regards the

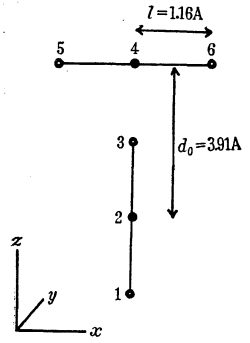


Fig. 2. Geometrical configuration of the dimer of carbon dioxide. Black circles and white circles stand for carbon and oxygen atoms respectively.

charge distribution in a monomeric unit, it may be assumed that each oxygen atom carries $-\kappa e$, while the carbon atom carries $+2\kappa e$. Here e denotes the absolute value of an electronic charge. In a dimer the electric field of each of the three point charges in a monomeric unit polarizes each of the three atoms of the partner monomer. The vector sum of eighteen ($2\times3\times3=18$) induced moments is equal to the over-all moment μ of a dimer. Straightforward calculations yield that the moment is directed antiparallel to the positive z-axis with the following value:

$$\mu=(\alpha_C+2\alpha_O)\kappa e\left[\frac{1}{(d_0-l)^2}+\frac{1}{(d_0+l)^2}-\frac{2d_0}{(d_0^2+l^2)^{3/2}}\right], \quad (8)$$

$$[\ ]=5.59\times10^{14}\ \text{cm}^{-2}.$$

Here α_C and α_O denote the polarizabilities of carbon and oxygen atoms respectively. In this case $\alpha_C+2\alpha_O$ is equal to the polarizability α of a carbon dioxide molecule. This molecule is fairly anisotropic, the polarizability in the direction parallel to the molecular axis $\alpha_\parallel$ ($=4.05\times10^{-24}$cm^3.) being greater than that perpendicular to the axis $\alpha_\perp$ ($=1.95\times10^{-24}$ cm^3).* If the relative position of the two monomeric units in a dimer is taken into account, it is reasonable to assume that α in this case is equal to $(\alpha_\parallel+\alpha_\perp)/2$ rather than $(\alpha_\parallel+2\alpha_\perp)/3$. Hence $\alpha=3.00\times10^{-24}$ cm^3.

Carbon dioxide has been treated from the molecular orbital point of view by Mulliken,[9] Moffitt,[10] Mulligan[11] and Shull.[12] The last author discussed in detail the off-center electron distribution of a carbon atom, which distribution he stated could hardly be interpreted as an ionic character of a C-O bond. Subtracting the terms due to this off-center distribution, he was left with a net equivalent charge distribution in which each of the oxygen atom carries $-0.40e$, i.e., $\kappa=0.40$.

On introducing the values of α and κ in Equation (8), one obtains $\mu=0.322$ D, which corresponds to the orientation polarization at 100°C. given by

$$P_{ort}=\frac{4\pi N}{3}\left(\frac{\mu^2}{3kT}\right)=1.694\ \text{cc}. \quad (9)$$

Contribution of the Four Intermonomer Normal Vibrations to Atomic Polarization

The dimer molecule has a symmetry C_{2v} with symmetry elements of $C_2(z)$, $\sigma_v(xz)$ and $\sigma_v(yz)$. Normal vibrations can be classified into four symmetry types as shown in Table I. Of the four intermonomer normal vibrations mentioned in the foregoing section, one belongs to type A_1, two to type B_2, and one to type B_2. The four normal vibrations in question are shown in Fig. 3.

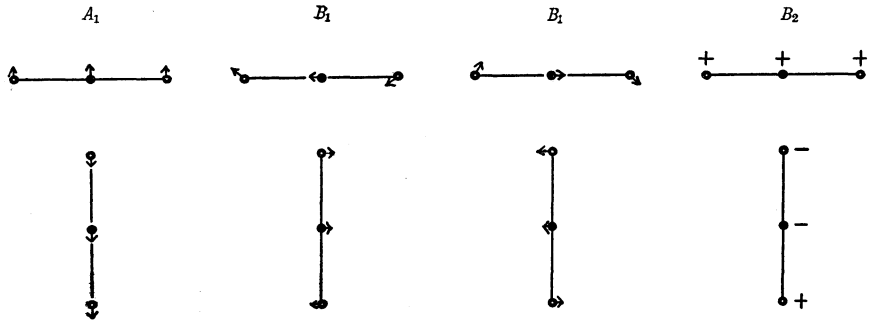


Fig. 3. Intermonomer normal vibrations of the dimer of carbon dioxide.

* Taken from Landolt-Börnstein, Zahlenwerte und Funktionen, 6th ed. 1951, Band I, 3 Teil, p. 511.

9) R. S. Mulliken, *J. Chem. Phys.*, **3**, 720 (1935); *Revs. Mod. Phys.*, **14**, 204 (1942).

10) W. Moffitt, *Proc. Roy. Soc. London*, A**196**, 524 (1949).

11) J. F. Mulligan, *J. Chem. Phys.*, **19**, 347 (1951).

12) H. Shull, *Proc. Natl. Acad. Sci. U. S.*, **38**, 400 (1952).

TABLE I
CLASSIFICATION OF VARIOUS NORMAL VIBRATIONS OF THE DIMER OF CARBON DIOXIDE INTO SYMMETRY TYPES

Symmetry types	Symmetry coordinates	No. of normal vibr.	Translation and rotation	Genuine normal vibr.	Intra-monomer vibr.	Inter-monomer vibr.
A_1	$z_1, z_2, z_3, z_4, x_5+x_6, z_5+z_6$	6	T_z	5	4	1
A_2	y_5-y_6	1	R_z	0	0	0
B_1	$x_1, x_2, x_3, x_4, x_5-x_6, z_5-z_6$	6	T_x, R_y	4	2	2
B_2	$y_1, y_2, y_3, y_4, y_5+y_6$	5	T_y, R_x	3	2	1
Total number		18	6	12	8	4

The contribution of a normal mode of vibration to the atomic polarization is given by[13]

$$Q=\frac{1}{3}\left(\frac{Ne_{eff}^2}{3\pi M_{eff}\nu^2}\right)=\frac{4\pi N e_{eff}^2}{9k_0}, \qquad (10)$$

in which N is Avogadro's number, e_{eff} is the effective charge, ν is the vibrational frequency, M_{eff} is the effective mass associated with the vibration, and k_0 is the force constant. The factor 1/3 was introduced to take into account all the possible orientation in space of a molecule having a linear oscillator. Therefore if the effective charge and the force constant for a particular normal vibration are known, the contribution of the normal vibration to the atomic polarization can be calculated.

Normal Vibration of Type A_1.—Let q denote the increase of C-C distance over its equilibrium value. Apparently q is the normal coordinate of this vibration. The dipole moment which points along the direction of negative y-axis can be calculated in the same manner as in the derivation of Equation (8), even when the vibration is excited. This yields immediately the effective charge given by

$$e_{eff}=\frac{d\mu}{dq}=-2\alpha\kappa e\left[\frac{1}{(d_0-l)^3}+\frac{1}{(d_0+l)^3}-\frac{2d_0^2-l^2}{(d_0^2+l^2)^{5/2}}\right], \qquad (11)$$

$$[\ ]=2.99\times10^{22}\ \mathrm{cm}^{-3}.$$

It should be mentioned here that the polarizabilities of carbon and oxygen atoms enter the equation in the form of $\alpha_C+2\alpha_O$ and no assignment to individual atoms is required.

To obtain the force constant of this vibration, the potential function V was constructed out of the attraction term of Coulomb interactions and the repulsion term of the Lennard-Jones potential assumed to be proportional to the inverse twelfth power of the separation d $(=d_0+q)$, viz.

$$V=\sum\frac{E_iE_j}{r_{ij}}+\frac{\lambda}{d^{12}}, \qquad (12)$$

where E_i denotes a charge in one of the monomeric units, E_j that in the other, r_{ij} the distance between them to be expressed as a function of l, d_0 and q. The values of E's are $+2\kappa e$ for carbon atoms, and $-\kappa e$ for oxygen atoms.

The constant λ was chosen so as to give a minimum of V at $d=d_0$, namely

$$\lambda=2\kappa^2e^2\left[\frac{1}{(d_0-l)^2}-\frac{d_0-l}{[(d_0-l)+l^2]^{3/2}}-\frac{2}{d_0^2}+\frac{2d_0}{(d_0^2+l^2)^{3/2}}+\frac{1}{(d_0^2+l)^2}-\frac{d_0+l}{[(d_0+l)^2+l^2]^{3/2}}\right]\frac{d_0^{13}}{12}, \qquad (13)$$

$$[\ ]=1.60\times10^{4}\ \mathrm{cm}^{-2}.$$

Through cumbersome but straightforward calculations, one obtains the following expression for the force constant:

$$k_0=\frac{d^2V}{dq^2}=2\kappa^2e^2\left[-\frac{2}{(d_0-l)^3}-\frac{1}{[(d_0-l)^2+l^2]^{3/2}}+\frac{3(d_0-l)^2}{[(d_0-l)^2+l^2]^{5/2}}+\frac{4}{d_0^3}+\frac{2}{(d_0^2+1^2)^{3/2}}-\frac{6d_0^2}{(d_0^2+l^2)^{5/2}}-\frac{2}{(d_0+l)^3}-\frac{1}{[(d_0+l)^2+l^2]^{3/2}}+\frac{3(d_0+1)^2}{[(d_0+l)^2+l^2]^{5/2}}\right]+12\times13\frac{\lambda}{d_0^{14}}, \qquad (14)$$

$$[\ ]=-2.51\times10^{22}\ \mathrm{cm}^{-3}.$$

In this equation, the right-hand side of Equation (13) was substituted for λ, leading to:

$$k_0=5.62\kappa^2e^2\times10^{22}\ \mathrm{erg/cm^2}. \qquad (15)$$

Introducing this value as well as that of effective charge in Equation (10), one obtains the following value for the contribution of this normal vibration to atomic polarization:

$$Q(A_1)=0.482\ \mathrm{cc}. \qquad (16)$$

Normal Vibration of Type B_2.—The normal coordinate q of this vibration may be taken as one-half of the difference between y-coordinates of the two carbon atoms. One can determine the displacements of atoms from the plane of a dimer molecule in equilibrium under two conditions, that no translation and no rotation of the dimer molecule as a whole take place, and that the configuration of monomeric units remain unchanged. The result are shown in Table II, where ξ denotes

13) J. H. Van Vleck, "The Theory of Electric and Magnetic Susceptibilities", Oxford Press, 1932, p. 363.

$Md_0/2ml=4.63$, M and m being the masses of a CO_2 molecule and an O-atom respectively.

TABTE II
DISPLACEMENT OF ATOMS FROM THE PLANE OF A DIMER MOLECULE

O-atom, 1	$(\xi-1)q$
C-atom, 2	$-q$
O-atom, 3	$-(\xi+1)q$
Atoms, 4, 5, 6	$+q$

It is obvious from symmetry considerations that the change of moment takes place in a direction parallel to z-axis. Calculations analogous to the foregoing yield the following result:

$$e_{eff}=\frac{d\mu_y}{dq}=-\alpha\kappa e\left[\frac{2+\xi}{(d^0-l)^3}+\frac{2-\xi}{(d_0+l)^3}-\frac{4}{(d_0^2+l^2)^{3/2}}\right], \tag{17}$$

$$[\ ]=2.40\times10^{23}\ \text{cm}^{-3}.$$

Again the assignment of polarizability to individual atoms is not necessary. In this case, however, α should be equal to $\alpha_\perp$ rather than to $(\alpha_\parallel+\alpha_\perp)/2$, because all the y-components of induced moments are perpendicular to the molecular axes of monomeric units. The electrostatic and repulsive interactions being assumed as in Equation (12), the potential function of this normal vibration is calculated as:

$$V=V_0+\kappa^2e^2\left[\frac{(2+\xi)^2}{(d_0-l)^3}-\frac{(2+\xi)^2}{[(d_0-l)^2+l^2]^{3/2}}-\frac{8}{d_0^3}+\frac{8}{(d_0^2+l^2)^{3/2}}+\frac{(2-\xi)^2}{(d_0+l)^3}\right.$$
$$\left.-\frac{(2-\xi)^2}{[(d_0+l)^2+l^2]^{3/2}}\right]q^2-\frac{24\lambda}{d_0^{14}}q^2+\ldots, \tag{18}$$

$$[\ ]=4.35\times10^{23}\ \text{cm}^{-3}.$$

Mentioned should be made here that the third term in this equation due to repulsion is less than 4% of the second term due to electrostatic force and hence the assumed functional form of repulsive potential is rather trivial. The force constant is obviously twice the coefficient of q^2 in the right-hand side of Equation 18. The contribution of this normal vibration to atomic polarization can then be evaluated by the use of Equation (10),

$$Q(B_2)=0.212\ \text{cc.} \tag{19}$$

Normal Vibration of Type B.—There are two normal vibrations belonging to the symmetry type of B_1, both of which are infrared active. Unless some assumptions be made for the force field of the dimer molecule, it is difficult to evaluate the effective charges and the force constants of these normal vibrations. Since the contributions of these vibration are rather minor portions of $P_{ort}+\Delta P_A$ compared with the first term, the writers gave up tedious efforts to evaluate the values of Q and simply assumed that every normal vibration contributes nearly the same amount to atomic polarization. This assumption may be justifiable to some extent because each of the vibrations of symmetry types A_1 and B_2 contributes to ΔP_A an amount of the same order of magnitude as that of the other vibration. The sum of P_{ort} (=1.694 cc.), $Q(A_1)$ (=0.482 cc.), $Q(B_2)$ (=0.212 cc.) and $2Q(B_1)$ (=0.694 cc.), i.e., $P_{ort}+\Delta P_A$ is equal to 3.08 cc. It can be seen that this order of magnitude compares favorably with 3.30 cc. obtained experimentally from the pressure dependence of molecular polarization.

In conclusion, mention should be made of the dielectric constant of ethylene studied by David, Hamann and Pearse.[14] The values of the Clausius-Mosotti function at high pressures were found to exceed the value at the limiting zero pressure. In view of the similarity between the behavior of carbon dioxide and ethylene in this respect, it may be suggested that ethylene also forms a T-shaped dimer molecule which, owing to π-electron transfer, has a finite electric moment.

Summary

The dependence of the molecular polarization of carbon dioxide upon pressure was explained by partial binary association suggested by MacCormack and Schneider on the basis of the second virial coefficient. The theoretical considerations indicate that molecular polarization increases with pressure and that the rate of increase of molecular polarization decrease as the pressure increases. The results of theoretical predictions agree with experiments quantitatively over the entire pressure range if a parameter contained in the theoretical formula is adjusted properly. This parameter can be interpreted as the molecular polarization of dimeric molecules plus the difference between the atomic polarization of dimers and twice the atomic polarization of monomers. The three quantities, the dipole moment of the dimer, the effective charges of four intermonomer normal modes of vibration and the force

14) H. G. David, S. D. Hamann and J. F. Pearse, *J. Chem. Phys.*, **19**, 1491 (1951).

constants of the same, were evaluated theoretically. A numerical value of the aforementioned parameter which is calculated from these three quantities compares favorably with that obtained from the dependence of molecular polarization on pressure.

Chemical Department,
Faculty of Science,
Nagoya University,
Nagoya

A Microphotographic Research on Salt System: $NaNO_2$—KNO_3

By Kaoru SAKAI

(Received May 18, 1954)

Introduction

A considerable amount of microphotographic study on the metallic alloys has been made with the aid of a metallographic microscope, but little has been made on the salt systems. The reason seems to lie in some difficulties of observing directly the state of the etched surface of the salt ingot under the metallographic microscope, because its etched surface is liable to glitter dazzlingly all over the sample. W. M. Magden[1], S. F. Žemczužny[2], E. Shibata & H. Imai[3], A. Kofler[4] have reported microscopical technique of investigating binary salt systems, chiefly for the case of eutectics. But they were not successful in observing the microscopic structures of specimens in the case of solid solution except the silicates and the unhygroscopic salts because of some technical difficulties.

As the $NaNO_2$–KNO_3 system contains the hygroscopic salt ($NaNO_2$), the surfaces of etched specimens become stained during the process of polishing. Besides the specimens of this system are fragile and porous, therefore it is doubtful whether this system belongs to the solid solution type or to the eutectic type. If this system belongs to the former, the dendrite crystals of soild solution can not be observed microscopically by the usual technique, because they are not composed of pure salt like those in the eutectic case. So the author intended to improve the technique and succeeded in taking a clear microphotograph of this system.

Experimental

(1) Thermal Analysis and Electric Conductivity Measurement.—Kagan and Kamuischan[5] made the thermal analysis of the $NaNO_2$-KNO_3 system and found it to be a case of solid solution (It was found somewhat round in the neighbourhood of the temperature minimum 141.1°C, 46 5 Mol.% KNO_3); but it is not so sure unless the microscopical observations are made, because the heat capacities of the specimens are extremely small and the obtained cooling curves are so irregular that it is doubtful whether this system belongs to the solid solution type or to the eutectic type.

The author made a study on phase diagram of this system by means of thermal analysis and electric conductivity measurement by using an electric furnace of sufficiently large heat capacity. The cooling rate was ca. 1°C./45 sec. between 200–300°C., the same as in the research of Kasé[6]. Fig. 1 shows the results obtained. But the author failed to determine the accurate liquidus by these two methods alone because the cooling curves are of very slow slope.

Fig. 1 also shows that the solidus obtained by conductivity method* always lies under that of thermal data. Because in the practice of thermal

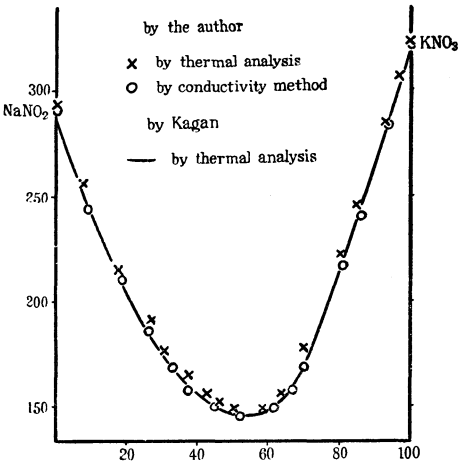


Fig. 1. Phase diagram of $NaNO_2$—KNO_3

1) W. M. Magden, *J. Chem. Soc.*, 458 (1930), 874 (1930).
2) S. F. Žemczužny, *Z. anorg. Chem.*, **153**, 47 (1926).
3) E. Shibata, H. Imai, *J. Sci. Hiroshima Univ.* A**14**, 1 (1949).
4) A. Kofler, *Chem. Ber.*, **85**, 447 (1952).
5) M. Ya. Kagan and N. Kamuischan, *J. Applied Chem.* (U. S. S. R.) 5347 (1932); *Chem. Abstr.*, **27**, 15 (1933).
6) T. Kasé, *J. Applied Phys. Japan*, **7**, 213 (1938).
* The used apparatus is the same as that described in *J. Chem. Soc.* (Japan) Pure Chem. Sec. **75**, 64 (1954).

analysis the thermocouple is set in the centre of the melt, we cannot get rid of the thermal effect occuring from the segregation, but in the case of the electric conductivity there is little error from that source.

(2) Microscopic Method

(*a*) *Method of flattening the surfaces of salt ingots.*—To smooth the surfaces of ingots, it is usually necessary to polish them with the various grades of emery papers and the soft brushes made of flannel. But the ingots of this system are so fragile and porous that their surfaces are liable to be damaged during the process of polishing, and the more they include large amount of KNO_3, the more fragile and porous they become. So the following method is recommended. Mixes of $NaNO_2$ and KNO_3 in various proportions are prepared in a quartz crucible (Fig. 2) which is composed

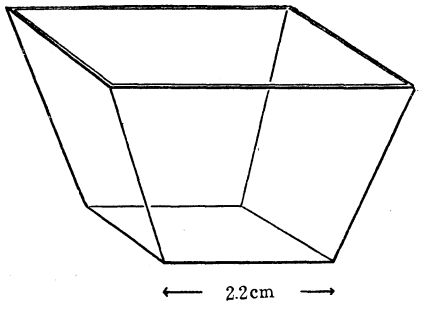


Fig. 2. Quartz crucible.

of five well-polished quartz plates. By the help of this crucible, we are now able to avoid all the troubles in cutting and polishing the surfaces of ingots, because the five surfaces of ingot facing the crucible plates are already as glassy as mirrors.

(*b*) *Method of etching.*—The surfaces of the obtained specimens are etched with etching solution. In this case the author used the saturated KNO_3 solution in 25% alcohol*, because in etching the surfaces of specimens it is recommended to use the saturated solution of the salt of smaller solubility of the two.

(*c*) *Microscopic operation.*—After the above treatment the etched surfaces are pressed on celluloid plates, slightly moistened with amylacetate in which a small amount of celluloid is dissolved. A few minutes later, the celluloid plates are carefully peeled off and examined microscopically.

When the quartz crucible does not react with salt ingot, we have now become able to study phase diagrams of almost all salt systems as easily as those of metallic alloy. Thus, the microphotographic method of studying salt systems can be applied not only to the unhygroscopic specimens but also to the hygroscopic, fragile and porous specimens such as mentioned above.

* E. Shibata used water as the solvent, but it is inadequate because of its high solubility.

Results and Discussions

The dendrite crystals of solid solution are found in the above inserted Photo. 1–5. The shapes of dendrite crystals closely resemble those of Cu-Ni[7,8], Cu-Sn[9] alloys, steel[10] and devitrified glass[11]. The dendrite structure of solid solution occurs in the state of imperfect equilibrium, and when the cooling rate is comparatively rapid, the diffusion of each ion of the mixed salts may be interrupted. So, if the specimens are annealed at the neighborhood of melting points, each ion of salts may diffuse slowly, and the concentration at each part of the melt may become uniform; then the dendrite crystals of soild solution may entirely disappear. See Photo. 6. If the $NaNO_2$—KNO_3 system belongs to a eutectic without any solid solution range, dendrite crystals should not disappear, and moreover, the areas occupied by dendrite crystals in the whole area ought to be varied as the composition changes. But it has been found out by this experiment that the areas of dendrite crystals are always constant on the whole. See Photos. 1–5. This fact also shows that this system belongs to a case of solid solution. And if the cooling rate can be limited within the proper extent to give rise to dendrite crystal, the size of dendrite may become maximum, when the cooling rate is minimum. It is proved by Photos. 1, 3, 4 and 5.

Summary

(1) The phase diagram of the $NaNO_2$–KNO_3 system was constructed by the thermal analysis and the electric conductivity measurements. The solidus on the whole is the same as found by Kagan.

(2) By the microphotographic method it was ascertained that this system belongs to a case of soild solution just as Kagan had inferred and that the nature of dendrite crystals in solid solution of the salts closely resembles those of alloys and devitrified glass.

(2) By the improved technique the microphotographic method of studying salt systems has now become able to apply to almost all salt systems.

7) I. Iitaka, *Bull. Inst. Phys. Chem. Res.* **13**. 1395 (1934).
8) S. H. Carpenter, J. M. Robertson, *Metals*, **1**, 223 (1939).
9) A. Sauveur, *Trans. Amer. Soc. for Steel Treating*, July, I (1923).
10) A. Sauveur, "Metallography and Heat Treatment of Iron and Steel", Chap. 3 (1933).
11) J. Sugie, Study of 'Glass Crystals', 8 (1943).

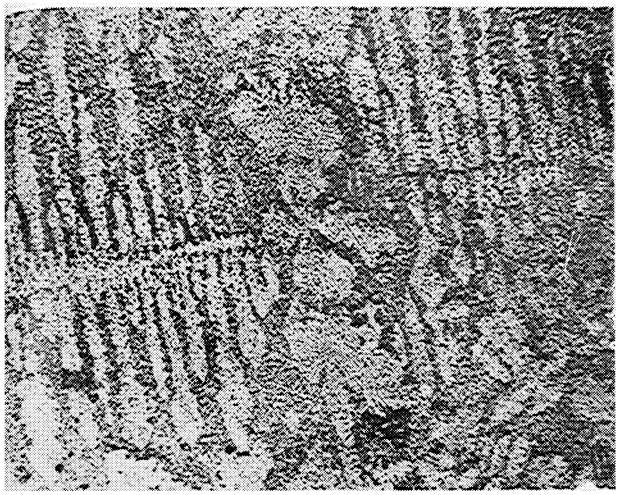


Photo. 1
×80, 24 wt. % KNO_3 (Rapid Cooling)

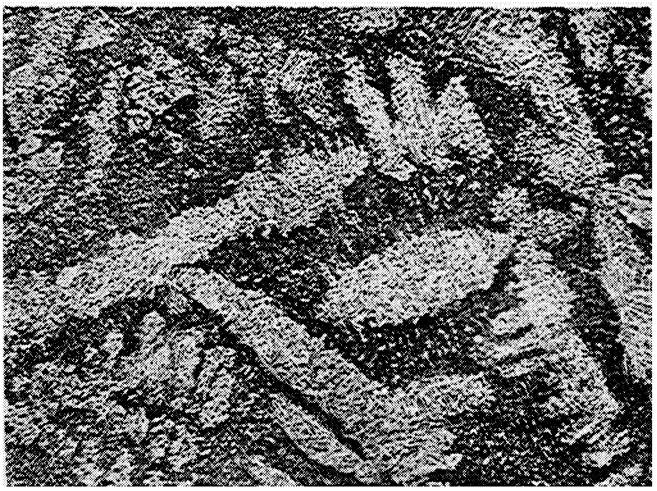


Photo. 2
×80, 34 wt. % KNO_3 (Medium Cooling)

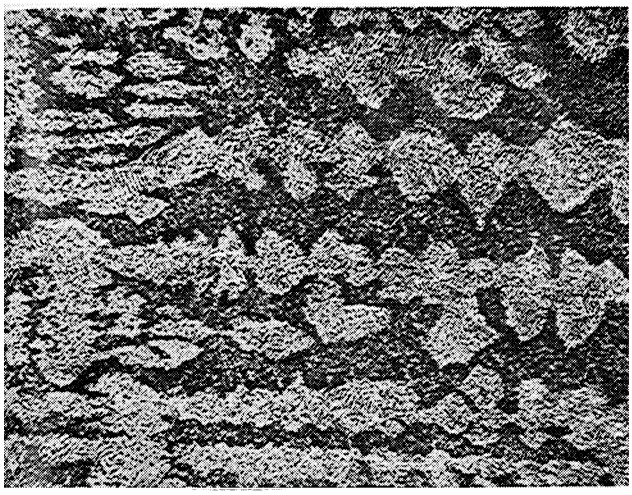


Photo. 3
×75, 51.5 wt. % KNO_3 (Slow Cooling)



Photo. 4
×75, 65 wt. % KNO_3 (Slow Cooling)

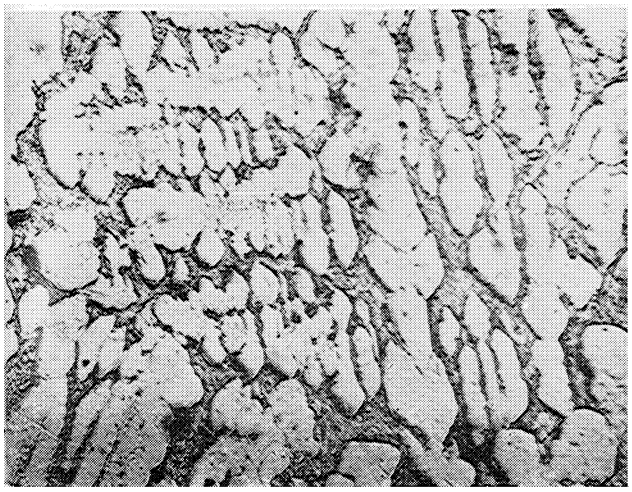


Photo. 5
×75, 82 wt. % KNO_3 (Slow Cooling)

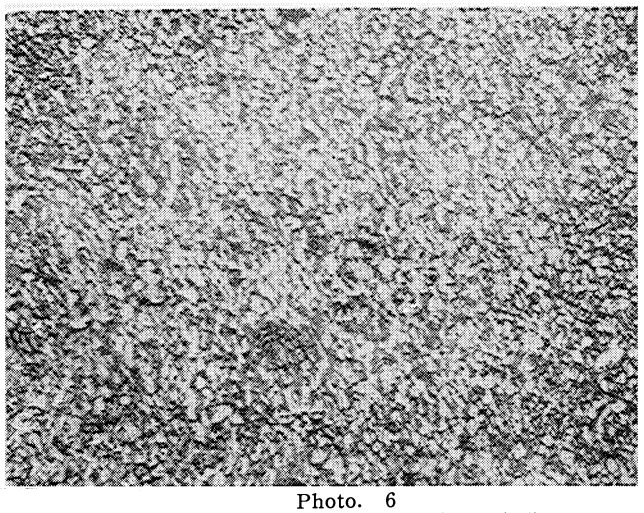


Photo. 6
×80, 82 wt. % KNO_3 (Annealed)

The author wishes to express his sincere thanks to Prof. Eiichi Shibata for his valuable advice and encouragement. This investigation was supported in part by a grant from the Ministry of Education.

Senior High School, Department of Education, Kanazawa University, Kanazawa

Sorption of Gases on Evaporated Nickel Films. I. Sorption of Oxygen

By Zenjirō ODA

(Received June 1, 1954)

Although the sorption of oxygen by evaporated metal films has been studied by various authors[1,2,3,4] there appears some discrepancies in the present view on the sorption mechanism and the structure of evaporated metal films.

The present work was undertaken to understand the behaviour of oxygen adsorbed on the surface more clearly and to examine the applicability of the Cabrera-Mott's theory of oxidation[5] for evaporated metal films.

Experimental

The rate of sorption was measured by a constant-volume method, employing slight modification of the apparatus used by Rideal and Trapnell[3]. A sensitive Pirani gauge and a McLeod gauge were used to measure the pressure ranging from 10^{-6} to 10^{-2} mmHg.

A U-shaped pure nickel filament 0.5 mm. in diameter and 11 cm. long was spot-welded to stem leads and sealed in a vacuum tube. Evacuating the system, the nickel filament was evaporated onto the inner wall of the bulb.

After the bulb was backed for 4 hrs. or longer, the trap was cooled with liquid oxygen and the filament was outgassed at about 1000°C. for half an hr. or longer. Immersing the bulb in melting ice, filament temperature was raised to 1300°C. and maintained at that temperature for a desired period with control of heating current. Since the film thus prepared on the wall of the bulb was unstable, it was kept at 0°C in vacuum for 20 min. before the gas was admitted. Electron diffraction study[6] showed that the films thus prepared consist of fine crystallites with their (110) planes slightly orientating parallel to the base.

The weight of the film was finally determined by weighing the bulb before and after the dissolution of the film.

In measuring the change of electrical resistance of the film in the course of sorption, the test tube described elsewhere[7] was attached to the adsorption apparatus.

Results and Discussions

Although the reaction temperatures were 0°, −78° and −183°C., the sorptions of oxygen were unchanged substantially and found to consist of two stages, i.e., an initial rapid process and a subsequent slow process.

(1) On admitting a known amount of gas to a clean film, a number of increments were consumed at the same very rapid rate and reached an equilibrium pressure of 10^{-6} mmHg. within 5 min.

(2) Subsequent increments were consumed at successively decreasing rate.

A typical example of these uptakes with a film at 0°C. is shown in Fig. 1, where the first fifteen increments are the rapid process, after which the rate of uptake falls with the number of increment.

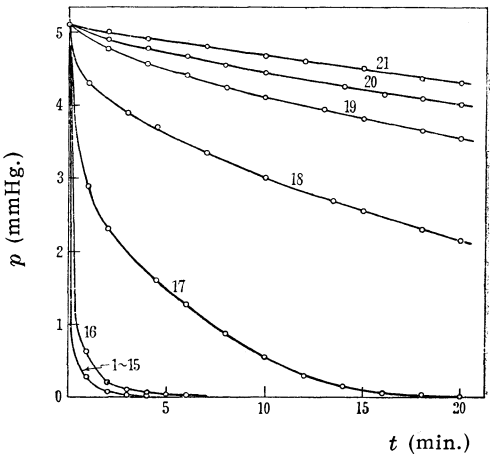


Fig. 1. Sorption of oxygen (T_s=0°C).

1) O. Beeck, A. E. Smith and A. Wheeler, *Proc. Roy. Soc.*, (A) **177**, 64 (1941); O. Beeck, "Advances in Catalysis" II, Academic Press, New York (1950), p. 151.
2) J. A. Allen and J. W. Mitchel, *Disc. Farad. Soc.*, no. 8, 309 (1550).
3) E. K. Rideal and B. M. W. Trapnell, *Proc. Roy. Soc.*, (A)**205**, 409 (1951).
4) W. Scheuble, *Z. f. Phys.*, **135**, 125 (1953).
5) N. Cabrera and N. F. Mott. *Reports on Progress in Physics*. Vol. XII, 163 (1949).
6) K. Ono and Z. Oda, unpublished.
7) Z. Oda, *Ōyōbutsuri* (*J. Appl. Phys., Japan*), **22**, 142 (1953).

TABLE I
RAPID SORPTION OF OXYGEN

Evap. time	Evap. amount[1]	Sorpt. temp.	No. of Ni atom	No. of sorbed O atom	Ni/O atomic ratio
min.	mg.	°C.			
30	7.1	0	7.34×10^{19}	4.44×10^{18}	16.5
30	6.7	0	6.91	4.58	15.1
45	8.4	0	8.67	5.34	16.2
15	2.7	0	2.79	2.36	11.8
30	5.3	−183	5.47	2.96	18.5
		0		4.66	11.7
30	6.3	0	6.51	4.56	14.4
30	6.2	−183	6.92	3.32	20.8
		0		5.08	13.6
30	5.3	0	5.47	2.70	20.3
30	4.2	0	4.34	2.20	19.7
30	8.1	0	8.36	4.72	17.7
30	11.2	−78	11.56	4.46	25.9
		0		5.32	21.7
30	11.0	−78	11.36	4.38	25.9
30	8.8	0	9.09	1.50	60.6[2]
30	5.6	−183	5.78	2.78	20.8
30	6.4	−183	6.61	3.70	17.8

1) The average thickness of film is 141Å/mg. using the bulk density of nickel.
2) run 22, which has been pre-sintered at 240°C. for 30 min.

I. Rapid Process

Sorption amount.—The amount of oxygen sorbed in this stage is given with that of nickel deposited in Table I, where allowance is made for the amount adsorbed by nickel filament. It is noticed that the amount sorbed at −78° and −183°C. were 85 and 60% as much as that at 0°C. respectively. Comparing the mean thickness of film and the corresponding atomic ratio of deposited nickel to sorbed oxygen (Ni/O), it is supposed that the oxygen would penetrate into the film as deep as 40 to 60 Å at this initial stage, if the film had a compact structure without any pores or cracks. However, this does not seem to be the case according to the data of Beeck.[1] The atomic ratio (Ni/O) at 0°C. sorption increases with the deposit, i.e., the oxygen sorbing capacity per unit weight of nickel decreases with increase of the deposit in these experimental regions. In run 22, in which the film was pre-sintered at 240°C. for 30 min. before gas admission, this ratio is about 60 and the sorbed amount is about 1/3 of that of the non-heat-treated films. Electron diffraction study[6] has suggested that the nickel film consists of fine crystallites which grow larger with film thickness and heat-treatment.

From these results, it is reasonable to explain the sorption process of oxygen on the basis of granular structure of film. If this is the case, oxygen will penetrate into the grain boundary at the rapid process and further diffuse in the crystallites with oxidation.

Low-temperature-adsorption of nitrogen.—As has been reported previously, the adsorption of nitrogen at −183°C. on the nickel film shows saturation at a pressure of 2×10^{-2} mmHg or higher. Comparing the number of nitrogen melecules sorbed at this saturation region with that of oxygen rapidly sorbed at −183°C. in Table II, the ratio

TABLE II
SORPTION AMOUNT OF O_2 AND N_2 AT −183°C.

Expt. No.	O_2 sorbed at rapid process moles/10 mg. Ni $\times10^{17}$	N_2 saturation adsorption moles/10 mg. Ni $\times10^{17}$
7	29.05	
9	27.98	
24	24.82	
15		5.20
23		4.06
mean	27.66	4.63

O_2/N_2 is found to be about 6. According to Beeck, one molecule of nitrogen can occupy two surface atoms of nickel. If this relation is applied to the present case, three oxygen molecules will correspond to one surface atom of nickel, so that it is reasonable to expect that even at the temperature of −183°C. oxygen can penetrate into the interior of crystallites to some extent.

Changes of electrical resistance.—It was also expected that the measurement of electrical resistance of film under sorption could furnish considerable insight into the behaviour of sorbed oxygen. After newly prepared film had been stabilized[8] to some extent, a known amount of gas was admitted and changes of gas pressure and film resistance were recorded

8) This stabilization process of evaporated nickel films was discussed in detail in ref. (7).

with time. Data obtained at 0° and −183°C. are shown in Figs. 2 and 3, respectively. It

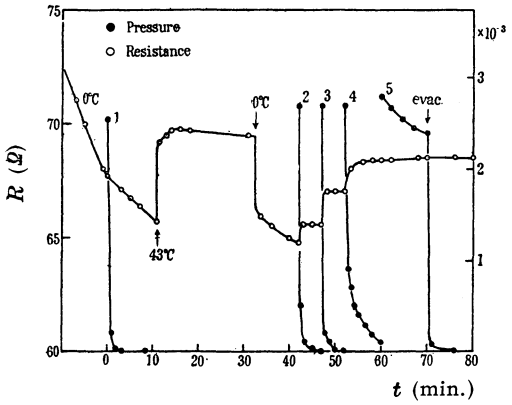


Fig. 2. Changes of electrical resistance with sorption (T_s=0°C)

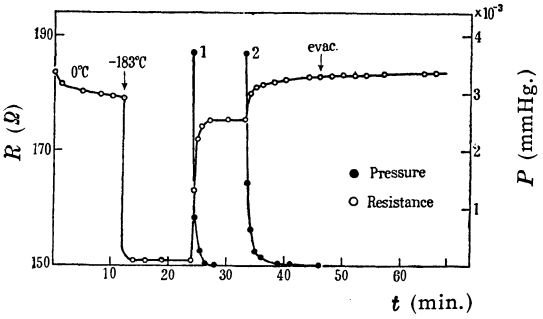


Fig. 3. Changes of electrical resistance with sorption (T_s=−183°C)

should be noticed that similar changes of resistance are observed with sorption at both temperatures.

On the other hand, adsorption of nitrogen and carbon monoxide which is considered to be chemisorbed on the surface gives rise to the increase of resistance within 1% and tend to restore its original value with desorption in the case of the former. Hence, the larger irreversible changes in resistance caused by oxygen uptake appear to account for the fact that oxidation proceeds even at −183°C. in the rapid process.

Estimation of thickness of oxide layer.—It is now possible to estimate the thickness of oxide layer formed in the rapid process at 0°C. from the data shown in Table I and electron diffraction patterns. The values calculated on suitable assumptions[9] are 5 Å and 4.5 A for thicker and thinner films, respectively. These values correspond to approximately 2 layers[10] of nickel atom. However, owing to the variety in size and mutual contact in actual films the effective surface of crystallite is supposed to be reduced and the oxide layer may correspondingly become thicker than ca. 10 Å.

II. Slow Process in Room-Temperature-Sorption

Pressure and temperature dependency of sorption rate.—Reducing the pressure stepwisely on the way of slow sorption, the rate of uptake also falls with pressure. Evaluating the rate of uptake $r_s\left(=-\frac{dp}{dt}\right)$ for each pressure range and plotting log r_s against log p, a straight line is obtained for each run. From the slope of these lines, the rate is well expressed as a function of pressure by the equation

$$-\frac{dp}{dt}=kp^{1/2}, \qquad (1)$$

where k is a constant. Integration of Eq. (1) gives

$$p^{1/2}=\text{const.}-kt/2, \qquad (2)$$

which represents a linear relation between $\sqrt{p}$ and t. In fact, as shown in Fig. 4, the

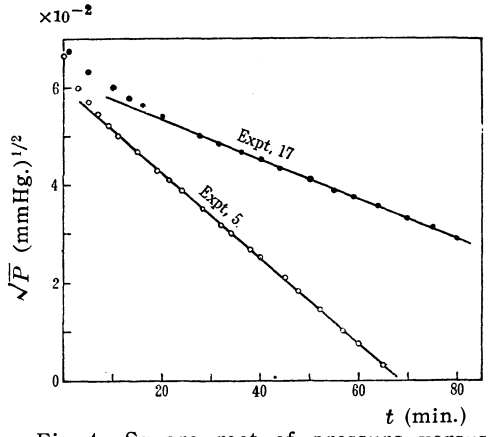


Fig. 4. Square root of pressure versus time (T_s=0°C)

data give a good agreement with Eq. (2) except for those in an early stage. Since the above rate versus pressure relationship inplies the sorption sites to be kept constant in course of one increment, it is naturally anticipated that deviations from linearity are observed at the early stage where the decrease

9) The following assumptions are made: (1) all crystallites composing a film are spheres of uniform size and their surfaces are entirely available for sorption. (2) Oxide layer has a composition of 1:1 atomic ratio and extends from surface to interior concentrically in each crystallite. From Table I O/Ni is given to be 1/20 for thicker films. Hence, atomic ratio of reacted metal to total one is given by

$$\frac{4/3\pi\{r_0^3-(r_0-r_1)^3\}}{4/3\pi r_0^3}=\frac{1}{20}$$

where r_0 and r_1 are the radius of original crystallite and the thickness of reacted layer, respectively. We set r_0=250 Å the magnitude roughly estimated from electron diffraction patterns. For thinner films, one may set O/Ni=1/12 and r_0=150 Å.

10) Estimated from distance between (110) planes (2.48 Å).

of sites is appreciable. Eq. (2) suggests that the dissociation of adsorbed molecules must take place faster than the migration of atoms, and so the dissociation is not a rate-determining step.

To obtain the activation energy E from the measured sorption rate itself, sorption rates were measured with a single film by changing the bulb temperature stepwisely without changing the other surface characters, and k was obtained from a stepwise $\sqrt{p}$ versus t plot. Temperature-dependency of the rate constant k in Eq. (2) is then given by

$$k = k_0 \exp(-E/RT),$$

Hence, by plotting log k against $1/T$ for each experiment, an activation energy of 12.6 ±1 kcal/mol. is obtained as a mean of three experiments.

Recovery of bare metallic surfaces.—The rapid sorption can be observed again by the film which has taken up sufficient gas to show no more rapid uptake, if it is kept in high vacuum at higher temperature than of sorption, but if the film is allowed to be evacuated at 0°C. one finds no such rapid sorption to recover. A few examples are shown in Fig. 5. The cause is considered to

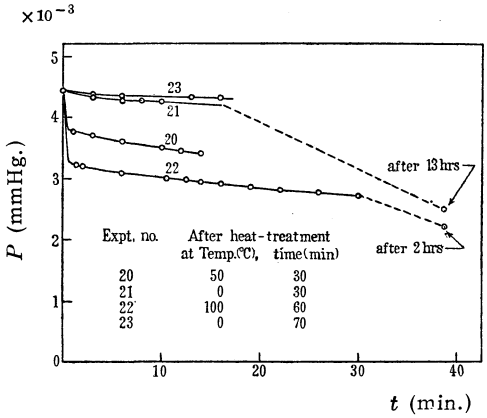


Fig. 5. Effects of heat-treatment on sorption in slow process (T_s=0°C)

be a recovery of bare metallic surfaces due to either the desorption of gas already sorbed or diffusion of metal ions through oxide layers or both. Since there is found no further liberation of gases in the closed system by raising the temperature, this recovery may be attributed to the latter mechanism.

From the above results, the most probable rate-determining step in this slow process is concluded to be the migration of metal ions to the oxygen atoms adsorbed on the oxide surface.

III. Slow Process in Low-Temperature-Sorption

Pressure dependency of sorption rate.—From the sorption rate versus pressure relationship obtained by the same method as described above, the rate of sorption at this temperature is expressed approximately by

$$-\frac{dp}{dt} = k'p, \qquad (3)$$

where k' is a constant. That is, the linear rate law can be applied to the present case.

Desorption and recovery of bare metallic surfaces.—When the temperature is raised to 0°C., rapid sorption occurs again after instantaneous desorption. However, this desorbed amount is far smaller for the case where the system is previously evacuated to 10^{-6} mmHg at −183°C. (1.55×10^{-3} mmHg−l.). than for the case without evacuation (5.55×10^{-3} mmHg−l.). As shown in Fig. 6, if the

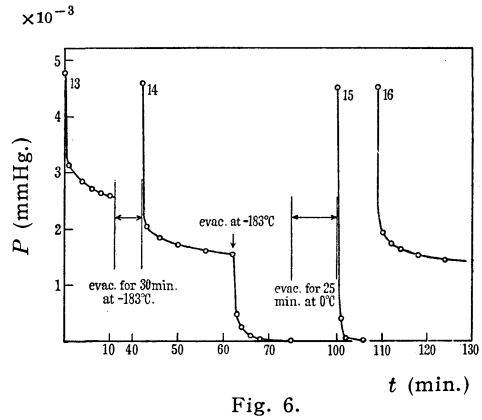


Fig. 6.
Effects of evacuation and temperature raising on sorption rate (T_s=−183°C)

sorption is stopped for half an hr. by evacuating the gas (Curve 13), the supplementary admission of gas (Curve 14) is attended with a more rapid uptake than that of curve 13 which has not been kept in high vacuum. In addition, when the bulb temperature is raised to 0°C. in high vacuum (point c) and allowed to stand for 25 min., subsequent admissions (Curves 15 and 16) at −183°C. are consumed at a rate as rapid as by the initial fresh film. These facts suggest that there occurs such a weak sorption at −183°C. that sorbed gas can be easily liberated even by low temperature evacuation. Therefore, the recovery of bare metallic surfaces observed in this figure is considered to be due to both the desorption and the enhancement of metal ion diffusion through oxide layers by raising the temperature.

Consequently, it is reasonable to consider that in the slow process of low-temperature-sorption, molecular adsorption takes place on the surface of oxide layers which have already

formed at the rapid process, and then these adsorbed molecules slowly dissociate to form oxide layers. The rate-determining step in this process may thus refer to either the adsorption of molecules or the dissociation of adsorbed molecules on the oxide surfaces.

IV. Considerations on the Basis of the Cabrera-Mott's Theory of Oxidation

As noticed above, oxygen can be taken up very rapidly with an almost constant rate in the initial stage of oxidation, but the rate falls abruptly after the oxide layer thickens to ca. 10 Å. Following the Cabrera-Mott's theory, the rate of formation of such a very thin oxide layer is given by

$$dx/dt = A \exp.(X_1/X - W/kT), \qquad (4)$$

where $X_1 = naV/kT$, a is the width of potential barrier between metal and oxide, V is the contact potential difference between metal and adsorbed layer, W is the energy required for a metal ion to migrate from a metal point to a vacant lattice point of oxide, A is a constant related only to the state of metal surface and the size of oxide, and k and T have the usual meanings.

If the oxide layer is very thin, i.e., $X \ll X_1$, the term X_1/X related to the strength of electrical field caused by shift of electron from metal to oxide is comparable to the term W/kT and so the apparent energy of activation becomes smaller. Therefore, in this stage the sorption which gives rise to the formation of vacant cation sites on the oxide surface is very much accelerated. While the rate of sorption is very rapid and appears to be almost independent of temperature, the amount rapidly sorbed is found to decrease as the temperature becomes lower. This is also explained by Eq. (4) as due to the fact that on account of predominance of W/kT to X_1/X with increasing X, the rapid process goes over into a slow one at smaller value of X with lowering the temperature.

In the slow process at room temperatures, the apparent energy of activation E is given by 12.6 kcal/mol. (0.57eV.), which must be represented from Eq. (4) by the following relation,

$$W - naV/X = E. \qquad (5)$$

Although the value of W for nickel has not been known, Cabrera and Mott have given 1.8 and 1.1 eV. for aluminum and copper, respectively. In the present case, also, the value of W is expected to be of the order of 1 eV. Hence, it is found that the field-dependent term naV/X has a large influence on the migration of metal ions even in the slow process.

Summary

While the sorptions of oxygen on the evaporated nickel films are very fast at the early stage and become slow at the later independently of the temperature, oxygen is suppoted to invade the interior even at the early stage of sorption. On the other hand, at the later stage the rate-determining step of low-temperature-sorption is different from that of room-temperature-sorption.

The author wishes to thank Mr. Y. Mizushima for helpful advice and discussion and also expresses his hearty thanks to Mr. T. Ichimiya for his interest and encouragement.

The Electrical Communication Laboratory,
Nippon Telegraph and Telephone
Public Corporation Tokyo

Dichroic Study on Polyvinylalcohol Fibre. IV. *A Theoretical Relation between the Intrinsic Double Refraction and the Dichroism*

By Yasuji KOBAYASHI and Saburo OKAJIMA

(Received July 13, 1954)

The relations between the stretching degree v relative to the isotropic state and the intrinsic double refraction Γ or the dichroism D of a cellulose fibre were already calculated by the authors.[1] Now in this paper the relation between Γ and the dichroic orientation is derived in a more general form.

A. Double Refraction. — The refractive index parallel to the fibre axis z of a refractive indicatrix, whose principal axis points to θ, φ is already calculated as (1), where θ and φ are the latitude and the azimuth.

1) S. Okajima, *J. Soc. Chem. Ind. Japan*, **43**, 351 (1940); S. Okajima and Y. Kobayashi, *J. Soc. Textile and Cellulose Ind. Japan*, **3**, 98 (1947).

$$n_z=\left(\frac{1}{n_\alpha^2}\sin^2\theta+\frac{1}{n_\Gamma^2}\cos^2\theta\right)^{-1/2}. \quad (1)$$

Now developing the right-hand side of (1) into a power series and neglecting the higher terms of $\Gamma_\infty=n_\Gamma-n_\alpha$, n_z is simplified as (2) or (2'),

$$n_z=n_\Gamma-(n_\Gamma-n_\alpha)\sin^2\theta, \quad (2)$$
$$=n_\Gamma\cos^2\theta+n_\alpha\sin^2\theta, \quad (2')$$

while the refractive index parallel to the x-axis of the above refractive indicatrix is given by (3) according to the previous calculation:

$$n_x=n_\alpha+(n_\Gamma-n_\alpha)\sin^2\theta\cos^2\varphi. \quad (3)$$

Now the refractive indices of the fibre $n_\parallel$ and $n_\perp$, parallel and perpendicular to the fibre axis are generally shown by (4) and (5) respectively:

$$n_\parallel=\int_0^{\pi/2}\int_0^{\pi/2}J_\theta n_z\sin\theta\,d\theta\,d\varphi\Big/\int_0^{\pi/2}\int_0^{\pi/2}J_\theta\sin\theta\,d\theta\,d\varphi, \quad (4)$$

$$n_\perp=\int_0^{\pi/2}\int_0^{\pi/2}J_\theta n_x\sin\theta\,d\theta\,d\varphi\Big/\int_0^{\pi/2}\int_0^{\pi/2}J_\theta\sin\theta\,d\theta\,d\varphi, \quad (5)$$

where J_θ is a distribution function of the mers.

Substituting the equations (2) and (3) into the equations (4) and (5) respectively,

$$n_\parallel=n_\Gamma-(n_\Gamma-n_\alpha)\cdot f(J_\theta), \quad (6)$$
$$n_\perp=n_\alpha+1/2\cdot(n_\Gamma-n_\alpha)\cdot f(J_\theta), \quad (7)$$

and $$\Gamma=n_\parallel-n_\perp=(n_\Gamma-n_\alpha)\cdot\{1-3/2\cdot f(J_\theta)\}, \quad (8)$$

where $f(J_\theta)=\int_0^{\pi/2}J_\theta\cdot\sin^3\theta d\theta$,

and $$\Gamma/\Gamma_\infty=f_o=1-3/2\cdot f(J_\theta), \quad (9)$$

as defined by P. H. Hermans[2].

From (6) and (7)

$$(n_\parallel+2n_\perp)/3=(n_\Gamma+2n_\alpha)/3=n_{iso}$$
$$=\text{constant}. \quad (10)$$

The relation (10) was already proved experimentally by the authors[3] in the case of the cellulose fibre.

B. Dichroic Orientation f_D.—When the long axis of a particle of the dye-cellulose complex lies in the direction θ, φ, the coefficients of transparency of the particle, t_z and t_x, for the plane-polarized light vibrating parallel and perpendicular to z are

$$t_z=\beta-(\beta-\alpha)\cos^2\theta, \quad (11)$$
$$t_x=\beta-(\beta-\alpha)\sin^2\theta\cos^2\varphi, \quad (12)$$

where α and β are t_z and t_x at $\theta=0$, respectively, i.e., the principal coefficients of transparency.

The coefficients of light absorption, $K_\parallel$ and $K_\perp$, of a fibre for the plane-polarized light vibrating parallel and perpendicular to the fibre axis are also given by

$$K_\parallel=\frac{\int_0^{\pi/2}\int_0^{\pi/2}J_\theta\cdot k_z\cdot\sin\theta\,d\theta\,d\varphi}{\int_0^{\pi/2}\int_0^{\pi/2}J_\theta\cdot\sin\theta\,d\theta\,d\varphi}, \quad (13)$$

and

$$K_\perp=\frac{\int_0^{\pi/2}\int_0^{\pi/2}J_\theta\cdot k_x\cdot\sin\theta\,d\theta\,d\varphi}{\int_0^{\pi/2}\int_0^{\pi/2}J_\theta\cdot\sin\theta\,d\theta\,d\varphi}, \quad (14)$$

where

$$t_z=10^{-kz},\ t_x=10^{-kx},\ \alpha=10^{-k_\parallel},\ \beta=10^{-k_\perp}, \quad (15)$$

Now developing the right-hand sides of (15) and neglecting the higher terms of every k (k is very small), we obtain

$$\left.\begin{aligned}k_z&=k_\parallel\cos^2\theta+k_\perp\sin^2\theta\\ k_x&=k_\perp+(k_\parallel-k_\perp)\sin^2\theta\cos^2\varphi\end{aligned}\right\}. \quad (16)$$

Then k_z and k_x are of the same forms as these of n_z and n_x respectively and therefore substituting these relations into (13) and (14), $K_\parallel$ and $K_\perp$ can be given in the same forms as $n_\parallel$ and $n_\perp$ respectively, i.e.,

$$K_\parallel=k_\parallel-(k_\parallel-k_\perp)\cdot f(J_\theta), \quad (17)$$
$$K_\perp=k_\perp+1/2\cdot(k_\parallel-k_\perp)\cdot f(J_\theta), \quad (18)$$

and, therefore, the dichronic orientation f_D is

$$f_D=(K_\parallel-K_\perp)/(K_\parallel+2K_\perp)$$
$$=(k_\parallel-k_\perp)/(k_\parallel+2k_\perp)\cdot\{1-3/2\cdot f(J_\theta)\}$$
$$=(k_\parallel-k_\perp)/(k_\parallel+2k_\perp)\cdot f_o \quad (19)$$

and $$1/3\cdot(K_\parallel+2K_\perp)=1/3\cdot(k_\parallel+2k_\perp)$$
$$=\text{constant}. \quad (20)$$

Therefore f_D is directly proportional to f_o. The same relation is already obtained by J. M. Preston,[4] where he assumed that $k_\perp$ is equal to 0 and the proportional constant $(k_\parallel-k_\perp)/(k_\parallel+2k_\perp)$ is equal to 1. Our observation on the ramie fibre, which is dyed with Kongo red, indicates that $k_\perp$ is not 0, although it is very small and difficult to be determined accurately and our old data give the constant 0.89. The latest data on the polyvinylalcohol fibre indicate that the possibility of still larger values of 0.95–1. The details will be described in the following paper.

2) P. H. Hermans "Contribution to the Physics of Cellulose Fibres", 1946.

3) S. Okajima and T. Iwamoto, *J. Soc. Chem. Ind. Japan*, **43**, 355 (1940).

4) J. M. Preston and P. C. Tsien, *J. Soc. Dyers and Col.*, **66**, 361 (1950).

As to the constancy of $k_{\parallel}+2k_{\perp}$, it holds good only when the fibre is dyed very lightly. The old data show some deviations from this relation as shown in Table I, but the latest ones prove this to be true as seen in Table II. In this case a sample of cellulose filament was dyed very lightly with Kongo red and $K_{\parallel}$ and $K_{\perp}$ were measured by using the filtered Hg-line. In order to prove the rule, $K_{\parallel}+2K_{\perp}$ are corrected by dividing by the diameter. The new samples were dyed very lightly but they are sufficient to obtain the exact values of $K_{\parallel}$ and $K_{\perp}$, when Hg-line is used, because this is absorbed so much by the dye as compared with the case where D-line is used.

TABLE I

THE ABSORBTION COEFFICIENT OF A POLYVINYL-ALCOHOL FIBRE DYED WITH KONGO RED

v	Diam., mm.	$K_{\parallel}$	$K_{\perp}$	$\frac{1/3\,(K_{\parallel}+2K_{\perp})}{\text{Diam.}}$
1.00	0.1417	0.170	0.144	1.08
1.43	0.1185	0.174	0.108	1.10
1.69	0.1090	0.182	0.088	1.10
2.07	0.0985	0.196	0.060	1.07
3.08	0.0807	0.214	0.026	1.10
4.11	0.0700	0.224	0.020	1.26
4.99	0.0635	0.228	0.010	1.30

TABLE II

THE ABSORBTION COEFFICIENT OF A CELLULOSE FIBRE DYED VERY LIGHTLY WITH KONGO RED

v	Diam., mm	$K_{\parallel}$	$K_{\perp}$	$\frac{1/3\,(K_{\parallel}+2K_{\perp})}{\text{Diam.}}$
1.00	0.1825	0.468	0.559	2.90
1.05	0.1816	0.485	0.551	2.91
1.14	0.1610	0.497	0.445	2.87
1.27	0.1495	0.525	0.394	2.93
1.38	0.1436	0.536	0.361	2.92
1.54	0.1333	0.559	0.300	2.90
1.66	0.1260	0.598	0.266	2.99
1.81	0.1230	0.567	0.215	2.70
1.90	0.1150	0.578	0.201	2.84
2.11	0.1130	0.578	0.183	2.78
2.21	0.1087	0.582	0.149	2.70
2.28	0.1056	0.594	0.132	2.71
2.40	0.1015	0.615	0.124	2.83
2.55	0.1020	0.611	0.124	2.81
2.56	0.1030	0.611	0.124	2.78
2.69	0.0981	0.671	0.108	3.01

Faculty of Engineering,
Tokyo Metropolitan University,
Tokyo

Some Optical Properties of Cellulose Hydrate

Saburo OKAJIMA, Yasuji KOBAYASHI and Tetsuya KIKUCHI

(Received July 13, 1954)

In the preceding paper[1] a linear relation between the intrinsic double refraction Γ and the dichroic orientation f_D of a fibre was derived as follows:

$$f_D=\frac{K_{\parallel}-K_{\perp}}{K_{\parallel}+2K_{\perp}}=\frac{k_{\parallel}-k_{\perp}}{k_{\parallel}+2k_{\perp}}\cdot\frac{\Gamma}{\Gamma_{\infty}} \qquad (1)$$

As is well known f_O, i.e. Γ/Γ_{∞}, indicates the orientation of the total molecules, while f_D mainly indicates that of the amorphous region. As to the orientations of the crystalline and amorphous regions, the former is higher than the latter according to the general views[2] at present. The above relation (1) was obtained on the tacit assumption of an equal orientation degrees in the crystalline and amorphous regions, but the linear relation is also expected even when the two regions have different orientation degrees, if f_O and f_D are always in proportion. This proportional constant being C, (1) becomes

$$f_D=((k_{\parallel}-k_{\perp})/(k_{\parallel}+2k_{\perp})\cdot C\cdot\Gamma/\Gamma_{\infty},\quad C\leqq 1.$$

In the range of the constancy of C, Γ/f_D is directly proportional to Γ_{∞}. As Γ_{∞} of a certain polymer changes with its crystallinity, Γ/f_D may possibly be a measure of the crystallinity of the polymer.

It is known that the crystallinity of a regenerated cellulose fibre is kept constant during the deformation. Accordingly a linear relation is expected between its f_D and Γ when C is also kept constant and it is actually confirmed experimentally as below. Then Γ_{∞} of the hydrate cellulose may be estimated from the experimental relation (1).

1) Y. Kobayashi and S. Okajima, This Bulletin, **27**, 471 (1954).

2) P. H. Hermans, "Contribution to the Physics of Cellulose Fibre, 1946; J. M. Preston and P. C. Tsien, *J. S. D. C.*, **66**, 361 (1950), etc.

A. Measurements of Γ and f_D of the Fixed Specimens

(1) Preparation of the Anisotropic Filaments.—A sample of the absorbent cotton on the market was purified by extracting with a boiling 1% NaOH solution and dissolved in a cuprammonium solution, from which cellulose was coagulated into an isotropic filament and regenerated as described previously.[3]

This isotropic filament of cellulose hydrate was stretched to various degrees, v, but in Exp. II the decoppering was carried out after being stretched to v which was calculated from the residual dry length relative to the isotropic dry state.

(2) Measurements of Γ and f_D.—The filaments were fixed to the frames as described previously[4] and Γ and f_D were measured with D-line.

An appropriate mixture of tricresylphosphate and dibutylphthalate was used as the mountant. The refractive index was 1.54, which is equal to n_{iso}[5] of the cellulose hydrate.

The dyeing was made with a 1% solution of Kongo red in 50% C_2H_5OH-H_2O and it was carefully controlled so that $K_{\parallel}$ did not go over 0.6 in any case.

Exp. I. A fresh and undried isotropic filament of cellulose was stretched and treated in succession as follows and used for the measurement of f_D.

(a) Dyed with Kongo red.
(b) Stretched to v in water at room temperature.
(c) Air-dried.
(d) Relaxed in water at room temperature.
(e) Air-dried again.

The filament was not allowed to shrink during the treatments (a)-(c) but it was free in (d) and (e). The specimen for Γ was prepared in the same way but a 50% C_2H_5OH-H_2O was used in (a) instead of the dye solution.

In Figs. 1 and 2 Γ and f_D are plotted against v and in Fig. 3 Γ against f_D. According to the

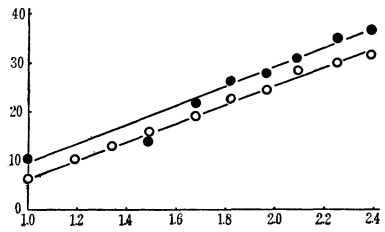


Fig. 1.
○ before Mercerization.
● after Mercerization.

figures Γ and f_D increase almost linearly with v and Γ-f_D is also linear as the theoretical relation (1) requires.

The specimens used for the above measurements

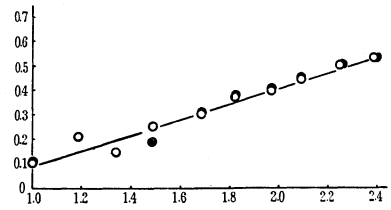


Fig. 2.
○ before Mercerization.
● after Mercerization.

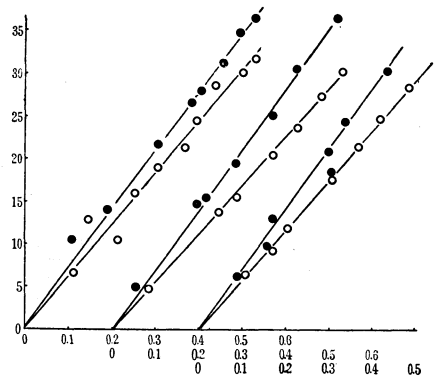


Fig. 3.
○ before Mercerization.
● after Mercerization.

were then washed free from the mountant, mercerized with an 18% NaOH solution at room temperature, regenerated by pouring into a boiling 0.5% acetic acid solution, washed thoroughly and again observed. Of course in these treatments the longitudinal shrinkage was prohibited, otherwise they would shrink and disorientate. As shown in Figs. 1-3, Γ increases after the mercerization, but f_D remains almost unchanged. Both measures are also in a linear relation but the slope grows steeper.

Exp. II. In this experiment an isotropic filament, which was not yet decoppered was stretched in a 5% NaOH solution and then regenerated, washed, and treated as in (c)-(e) of the preceding experiment. The specimens for f_D were dyed after fixing to the frame, while those for Γ were treated, of course, with a 50% C_2H_5OH aq. solution.

In order to observe the effect of the mercerization, separate specimens were mercerized in this case as they were fixed to the frames and then dyed or treated with the 50% C_2H_5OH-H_2O solution. In other words, the mercerization was given to the undyed specimens. Fig. 3 indicates that the result is similar to the above: the linear relation of Γ-f_D holds good and the slope increases after the mercerization also in this case.

Exp. III. The isotropic filament used in the above experiment was decoppered and then stretched as in Exp. I. But the undyed specimens were mercerized as in Exp. II. A similar result is obtained as shown in Fig. 3.

3) S. Okajima and S. Hayama, This Bulletin, **27**, 61 (1954).
4) S. Okajima and Y. Kobayashi, This Bulletin, **25**, 268 (1952); S. Okajima, Y. Kobayashi and R. Yamada, ibid,, **26**, 235 (1953).
5) S. Okajima, *J. Soc. Chem. Ind. Japan*, **49**, 128 (1946); P. H. Hermans, "Contribution to the Physics of Cellulose Fibre", 1946.

B. Measurements of Γ and f_D of the Relaxed Specimens

In the foregoing measurements each specimen was treated in the fixed state to a frame. Now the measurements of Γ and f_D were carried out in the relaxed state. The specimens were cut into the pieces of 3-4 mm lengths after the treatments (a)-(e) mentioned below, and they were inserted into a thin-walled glass capillary in a line and dried at 60°C under the high vacuum (<0.001 mm Hg) as shown in Fig. 4, when one

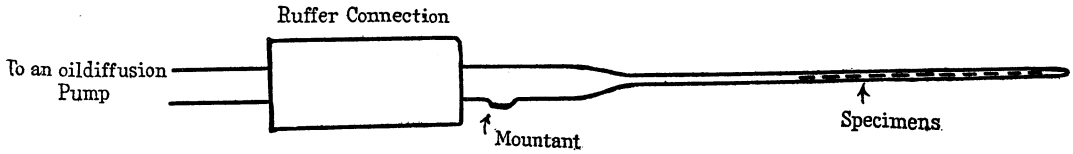


Fig. 4.

drop of the mountant was also placed in the capillary near the open end. After the specimens were dried completely they were mounted. For this purpose the capillary was bent slightly down at the rubber connection, then the mountant streamed down along the inner wall of the capillary and dipped the specimens. The capillary was closed by melting near the open end. $K_{\parallel}$, $K_{\perp}$ and Γ of the specimens in the closed capillary were measured as usual but from the outside of the capillary. Therefore the last drying and the measurements were carried out in the relaxed state in this case as compared with the treatments in A.

The stretching of the isotropic cellulose filament which was prepared as in A was carried out successively in the following order.

(a) Stretched in water at room temperature.
(b) Boiled in water.
(c) In Exp. IV, air-dried at room temperature. In Exps. V and VI, oven-dried at 100°C.
(d) Relaxed in boiling water.
(e) Air-dried again under no tension.

In these treatments (b) and (c) were carried out under tension, while (d) and (e) were carried out in the free state as described in each experiment.

Hg-line filtered through a Mazda's filtere VG1A was used for the following measurement of f_D. Of course the green light is absorbed so much by Kongo red, that the specimens must be dyed very lightly, otherwise $K_{\parallel}$ goes over 0.6. Then the specimens are, on the contrary, so transparent for Na-line, that the same dyed specimens can be used for the measurement of Γ. In Fig. 5 the points ● and ○ are the observed values of the dyed and undyed specimens respectively which show clearly that the effect of the dyeing is negligible. So the same specimens were used for the measurements of Γ and f_D in Exps. V and VI. Of course for this purpose the specimens must be dyed under the conditions which do not cause any disorientation due to swelling and contraction and the condition was accomplished by using the 50% C_2H_5OH aq. solution as the dyeing medium at room temperature.

A small discontinuity can be seen in the early stage of the deformation in Fig. 5, which was already pointed out previously.[6]

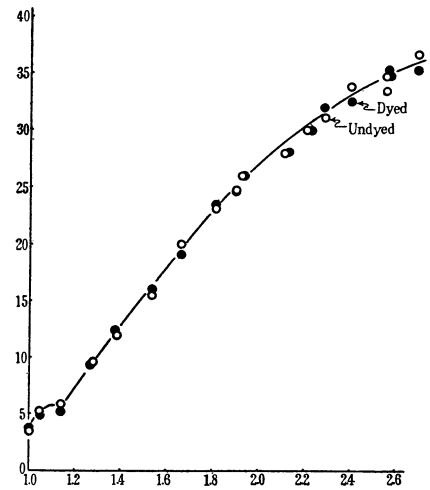


Fig. 5.

Exp. IV. Each specimen was cut into two parts, one of which was dyed with Kongo red as before to measure f_D, while the other half was used for the measurement of Γ after being treated with the alcohol solution. The relation between Γ and f_D is shown in Fig. 6.

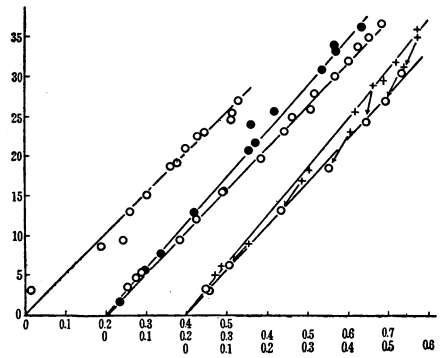


Fig. 6.
○ before Mercerization.
● after Mercerization.

Exp. V. Γ of the unmercerized and mercerized specimens were measured at first and after being dyed, again Γ and f_D were measured. The results

6) S. Okajima and Y. Kobayashi, This Bulletin **24**, 85 (1951).

are similar to the above. The mercerization was carried out under tension to avoid the shrinking of the anisotropic filament.

Exp. VI. A part of the specimens were dyed, air-dried, fixed to the frame, vacuum-dried and $K_{\parallel}$, $K_{\perp}$ and Γ were measured as mentioned in A, except that the same dyed specimens were used for both measurements (VIa). These specimens were cut into pieces after 10 days' vacuum-drying and relaxing in boiling water and again observed in the free state (VIb). As shown in Fig. 6, the slope of the line Γ-f_D becomes less steep by this relaxation, although the linear relation holds goods also in this case.

C. Discussion

All the experimental results prove that a linear relation holds good between Γ and f_D as the theory requires. But the slope θ of the line is not necessarily constant and changes from case to case as shown in the acompanying table. In order to analyze the causes of this fluctuation, the following effects are considered:

(1) The mercerization increases the slop in all cases.

(2) Among Exps. I, II, III and VIa, where the specimens were observed in the fixed state, θ in Exp. II is $56\text{-}57\times10^{-3}$ and slightly smaller than the others. This is because the filament was decoppered under the stretched state. It is interesting to note that this θ increases also to the equal level of 70×10^{-3} after mercerization.

Exp. No.	State of the specimen	$\theta.10^3$ Before merc.	$\theta.10^3$ After merc.
I	Fixed to the frame	60—62	69—70.5
II	„ „	55.5—57	70—71.5
III	„ „	58—59.5	70.5
IV	Relaxed	50	—
V	„	52	58
VIa	Fixed to the frame	60—61	—
VIb	Relaxed	55	—

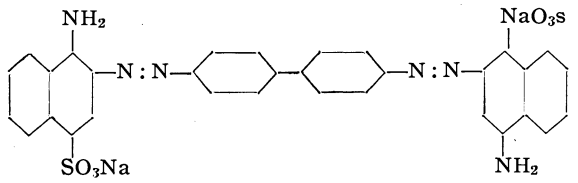
(3) θ in Exps. I, III and VIa are also larger than those in Exps. IV, V and VIb. This seems to be related to the fact that the specimens in the former experiments are dried and observed in the fixed states, while in the latter cases they are in the relaxed states.

Now we consider the meaning of this θ. If the orientation degrees in the crystalline and amorphous regions of a fibre are not different from each other as assumed in the calculation of (1), the linear relation between Γ and f_D means at once the correctness of the formula (1). Then the inclination is equal to

$\Gamma_\infty \div \frac{k_{\parallel}-k_{\perp}}{k_{\parallel}+2k_{\perp}}$ and the fluctuation of this value is nothing but the variation of Γ_∞. Γ_∞ increases generally with the crystallinity, so the value of Γ_∞ indicates quantitatively the relative amount of the crystalline region. So the constancy of Γ_∞ through a series of the varying v is a new support for the specimens of view[7] that the crystallinity is kept constant during the stretching of the cellulose fibre.

As to the absolute value of Γ_∞, the authors[8] obtained 62.4×10^{-3}, while P. H. Hermans[5] 55×10^{-3}, J. M. Preston[9] 54×10^{-3} and A. Frey-Wyssling[10] 49×10^{-3}. These estimations contain some assumptions and the above θ appears to be very valuable for criticising these values of Γ_∞, but the problem is not so simple. The inclination θ is

$\Gamma_\infty \div \frac{C\cdot(k_{\parallel}-k_{\perp})}{k_{\parallel}+2k_{\perp}}$ and knowledge of C or $(k_{\parallel}-k_{\perp})/(k_{\parallel}+2k_{\perp})$ is necessary for this purpose, but it is yet poor. The term $(k_{\parallel}-k_{\perp})/(k_{\parallel}+2k_{\perp})$ is 1 and 0.89 according to Preston's view[11] and the authors' old data respectively, but our latest data show the possibility of a still greater value 0.96. This value was found repeatedly when a polyvinylalcohol fibre of the highest orientation which had been heat-treated after the highest stretching was observed. Considering that the real filament must fall short of the ideally parallel orientation and further that the ordinary polyvinylalcohol sample on the market contains some irregularities in the structure, then $(k_{\parallel}-k_{\perp})/(k_{\parallel}+2k_{\perp})$ of the ideal filament must be still greater than 0.96. But if Kongo red molecule has the structure



7) e. g. H. R. Kruyt, "Colloid Science" II, p. 55, 613 (1949).

8) K. Atsuki and S. Okajima, *J. Soc. Chem. Ind. Japan*, **40**, 360B (1937).

9) J. M. Preston, *Trans. Faraday Soc.*, **29**, 65 (1933).

10) A. Frey-Wyssling, *Helv. Chim. Acta*, **22**, 981 (1939).

11) J. M. Preston and P. C. Tsien, *J. S. D. C.*, **66**, 361 (1950).

and this molecule orientates parallel to a cellulose molecule by means of two NH_2-groups, then $(k_{\parallel}-k_{\perp})/(k_{\parallel}+2k_{\perp})$ may be smaller than 1 because the line connecting the two NH_2-groups is not parallel to the direction of the diazo groups. After all the value can be considered to exist between 1 and 0.96 and it is approximated to 1 in the following discussion.

Now Γ_∞ are 60×10^{-3} and $50\text{–}55\times10^{-3}$ according to the states of the specimens and nearly coincide with the hitherto obtained data by the present authors and the others mentioned above, then C can be considered to be nearly equal to 1 and θ is directly equal to Γ_∞. If C is much smaller than 1, Γ_∞ must also be smaller. This means that the orientation degree of the amorphous region is not especially lower than that of the crystalline region, provided, of course, the dichroism can indicate the orientation of the amorphous region only. But another concept is also possible. Because a simple estimation of $(K_{\parallel}+2K_{\perp})$ from the present degree of dyeing shows that about one molecule of Kongo red is absorbed to 10,000 glucose residues and such small quantities of the dye molecules are not necessarily considered to be absorbed only in the amorphous region but also on the surfaces of the crystallites where the orientations are more or less higher; in other words, the dye molecules seem to be distributed uniformly in the filament. Then C can be equal to 1.

The selective indication of the orientation in the amorphous region may occur only when the more intense dyeing was made and the absorbtion becomes decisively predominant in the amorphous region.

A similar linear relation between Γ and f_D can be seen also in the case of a polyvinylalcohol filament till $f_D=0.89$ or 0.96 as will be described in a separate report. In the case of the cellulose filament the line Γ-f_D is interrupted at $f_D=0.6$ by the breakdown of the sample. Of course it can not be decided at present which of the views is true, but it can be said that f_D is equivalent to f_O.

From these points of view the change of θ can be explained directly by the concept of the change in Γ_∞ and, therefore, the change in crystallinity as below:

(1) The mercerization followed by the hot-regeneration must be considered to increase the relative amount of the crystalline region. This confirms the result of Hermans,[12] who found it by means of the X-ray method. According to him the crystallinity increases by about 10% after the mercerization and our Γ_∞ increases also by the same amount.

(2) The crystallinity of the filament decoppered under tension is slightly lower than that regenerated in the free state. The cause may be that a too excessive strain appears in the filament due to the deswelling at the decoppering process. This strain is released when it is mercerized and the crystallinity increases to the normal level. Therefore the value of Γ_∞ is equal to 70×10^{-3}, irrespective of the slightly lower value of the original Γ_∞ in Exp. II.

(3) As is often mentioned, the relaxed specimens give the smaller value of Γ_∞. The effect of the relaxation may appear principally in the last drying operation. The filament highly dried under tension may cause the crystallization of the metastable portion, among which the smaller or more unstable crystals are destroyed again when the filament is treated in boiling water in the free state. And this recrystallization appears to become more stable if the filament has been dried at a higher temperature and for a longer period because Γ_∞ increases in the order IV to VIb (excepting VIa). They were relaxed similarly in boiling water after air-drying (IV), oven-drying for 1 hr. (V) and oven-drying followed by vacuum-drying for 10 days (VIb) and the larger portion of the crystals appears to survive after the relaxation in the above order.

Therefore the fluctuations observed in the hitherto obtained values of Γ_∞ by the different authors may be related to the small fluctuation of the crystallinity due to the slight difference in the conditions under which the specimens were treated.

(4) The mercerization was carried out before and after the dyeing in Exps. III and I respectively but Γ_∞ increases by the equal amount and arrived at the equal level after the treatment in both cases. Therefore such a crystallization is thought not to be disturbed by the dye molecules. This is very interesting when it is considered that the crystallization of a polyvinylalcohol filament due to heating is fairly disturbed by the dye molecules absorbed as will be reported in a separate paper.

Faculty of Engineering,
Tokyo Metropolitan
University, Tokyo

12) P. H. Hermans and A. Weidinger, *J. Polymer Sci.*, **6**, 533 (1951).

Polymerization by Electric Discharge

By Kiyoteru Otozai, Sanshiro Kume, Shobun Nagai, Tai Yamamoto, and Shouzow Fukushima

(Received June 8, 1954)

In the course of the study on the paper chromatography of poly ethylene oxide[1], we

found that the surface of the liquid polymer was covered by a membrane with the action of the electric discharge by "Tesla coil", the vacuum tester, when polymer was treated in vacuum. In order to ascertain the accelerating effect of the discharge on polymerization, anticipated from this phenomenon, we preliminarily examined the action of the discharge on some polymers and monomers of different type.

(1) **Polyethylene Oxide.** "Carbowax 4,000" was put in a glass ampule, evacuated continually, melted at 60°C., and exposed to the discharge for 10 minutes. With the action of the discharge the surface of the sample was covered with a colorless membrane, which was insoluble and remained fibrous in hot water. The reacted part amounted to about 1%. A colorless, insoluble and fibrous form of the substance indicates presumably that the polymer molecules were awakened to further polymerization in linear structure by the action of the discharge. For a comparison other samples were kept for 10 minutes at 60°C. and 200°C. in a vacuum, but no change was observed and the samples were dissolved completely in hot water.

(2) **Styrene.** Styrene, distilled in a nitrogen stream, was distilled into a glass ampule in vacuum, sealed, placed in water of 11°C., and exposed to the discharge for 30 minutes. As soon as the discharge began a white cloud was produced in the whole space of the gas phase and settled down slowly. The liquid phase became light yellow. The average molecular weight of 15,000 was obtained from the viscosity measurement of a benzene solution of purified colorless polymer, the value of K_m being taken as 1.1. The amount of reaction was about 1%. The light yellow substance, which was produced under the action of the discharge at dry ice temperature for 1 hour, can not be dissolved in benzene.

(3) **Glycine.** The discharge was showered on the crystalline glycine at 13°C., and on the sublimated stream of glycine at 160°C., and on the cold 10% aqueous solution of glycine at 0°C., inan evacuated ampule in all cases. Only in the last case a dust-like colorless substance appeared. In all cases, however, the small amounts of the insoluble colorless substances were obtained, when the samples were dissolved in water. Glycine was detected by paper chromatography of the insoluble product in the first case, after a washing by hot water and hydrolysis by hydrochloric acid. This would suggest that the product was some sort of polymer of glycine.

These effects would be caused by radicals, or ions, or radicalions, produced by the discharge.

We should like to express our sincere thanks to Dr. H. Okuyama, Dr. G. Meshizuka, and Dr. K. Narita for their* guidance about carbowax, styrene, and glycine, respectively.

Department of Chemistry, Faculty of Science, Osaka University, Osaka

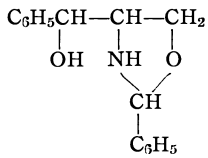
1) S. Kume, T. Yamamoto, K. Otozai, and S. Fukushima, This Bulletin **26**, 93 (1953).

A New Route to DL-*threo*-1-*p*-*Nitrophenyl*-2-*amino*-1, 3-*propanediol*

By Sumio UMEZAWA and Tetsuo SUAMI

(Received June 25, 1954)

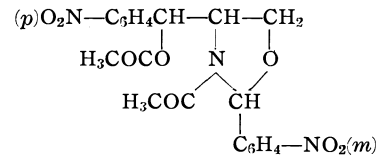
During the course of synthetic investigations of E. Erlenmeyer's *threo* phenylserine[1], we have reduced the latter with a modified Raney nickel catalyst, and obtained a new oxazolidine derivative which appears to be 2-phenyl-4-(α-hydroxybenzyl) oxazolidine (I). Starting from this oxazolidine derivative, we have



(I)

now synthesized DL-chlorampphenicol, an important antibiotic found by scientists of Parke, Davis and Company.

The *threo*-phenylserine ethyl ester was reduced in ethanol at about 50°C. with a modified Raney-nickel which was prepared by the ordinary digestion-procedure at 30°C. for one hour. After working up by evaporation and recrystallization, the above described oxazolidine (41%), m.p. 138–139°C. was obtained. *Anal.* Calcd. for $C_{16}H_{17}O_2N$: C, 75.4; H, 6.67; N, 5.50. Found: C, 75.1; H, 6.58; N, 5.53%. Acetylation of the oxazolidine derivative (I) with acetic anhydride at room temperature



(V)

1) E. Erlenmeyer, *Ber.*, **25**, 3445 (1892).

yielded an N-acetyl derivative (II) (82%), m.p. 145–146°C. *Anal.* Calcd. for $C_{18}H_{19}O_3N$: N, 4.72. Found: N, 4.64%. The failure of II to hydrolyze under Kunz's conditions[2] demonstrated that II is an N-acetyl derivative. Further acetylation of II with acetic anhydride in pyridine gave a viscous product (III), which on nitration with mixed acid (conc. H_2SO_4: conc. HNO_3=1:1) under ice-cooling for 30 minutes, finally at 15°C. for one hour, led to a viscous product (IV) containing a small quantity of crystals. The latter, after recrystallization, appeared to be 2-(*m*-nitrophenyl)-4-(α-hydroxy-*p*-nitrobenzyl)-oxazolidine (V) (12 %), m.p. 192–193°C. *Anal.* Calcd. $C_{20}H_{19}O_8N_3$: N, 9.78. Found: N, 9.44%. V gave *m*-nitrobenzaldehyde on hydrolysis with dilute hydrochloric acid. The main part of IV usually remained viscous and oily. Hydrolysis with dilute hydrochloric acid, followed by neutralization with dilute sodium hydroxide, led to DL-*threo*-1-*p*-nitrophenyl-2-amino-1,3-propanediol, pale yellow crystals (49%), m.p. 143.5–145°C., which did not depress the melting point of an authentic sample obtoined by the synthetic route through *p*-nitroacetophenone[3] and, acylation with methyl dichloroacetate converted the product to DL-chloramphenicol.

It was also shown that the oxazolidine derivative (I) could be directly hydrolysed with dilute hydrochloric acid to DL-*threo*-1-phenyl-2-amino-1,3-propanediol (84%), m.p. 85–86°C., which led to the DL-chloramphenicol by the synthetic route described by Controulis and his coworkers.[4]

Applied Chemistry Department, Faculty of Engineering, Keio University
Koganei, Tokyo, Japan

2) A. Kunz and C. S. Hudson, *J. Am. Chem. Soc.*, **48**, 1982 (1926); M. L. Wolfrom, M. Königsberg, and S. Soltzberg, ibid., **58**, 409 (1936).
3) L. M. Long and H. D. Troutman. ibid., **71**. 2473(1949).
4) J. Controulis, M. C. Rebstock and H. M. Crooks, ibid., **71**, 2463 (1949).

A New Method for Ultra Micro Determination of Ammonia or Organic Nitrogen

By Yoshimi OKADA and Hidesaburo HANAFUSA

(Received July 7, 1954)

The micro-Kjeldahl method is useful for rapid nitrogen analysis of various organic substances of low nitrogen content. However, it would be convenient to determine much smaller amounts of nitrogen in cases where the nitrogen content of the sample is very low or the amount of sample available is limited. For this purpose we replaced titration in this method by colorimetry with ninhydrin[1] and could determine 30 μg. of nitrogen by this modification.

This modified method is the same as the usual micro-Kjeldahl method except that the sample for single determination should contain 20–100 μg. nitrogen and the time of distillation is shortened to 1.5 minutes and 5 cc. of 1/100 N-H_2SO_4 is placed in an adapting flask. After distillation, the solution in the flask (usually 15–20 cc.) is diluted to 25 cc. with a citrate buffer (pH 5.0) and 1 cc. aliquot is taken to determine ammonia colorimetrically[1]. A standard curve was prepared previously with the solution of NH_4Cl (1–10 μg./cc.).

This method is particularly useful for the determination of amide-N of proteins, as the trouble of titration caused by octylalcohol, an anti-foaming reagent, can be eliminated completely. Some results by this method are shown in Table I.

TABLE I
EXAMPLES OF NITROGEN DETERMINATION BY AUTHORS' METHOD

Total-N

Sample	Found %	Calculated %
Acetanilide (354 μg.)	10.39	10.37
,, (425 μg.)	10.43	

Amide-NH_3

Sample	Found %	Reported %
Lysozyme (2.03 mg.)	1.88	1.7–2.0[2]
		1.87[3]
		2.08[4]
Taka-amylase A (2.87 mg.)	1.43	1.47[5]

By further modification of our method, by combining the diffusion method according to Conway[6,7], it would be possible to determine extremely small amounts of nitrogen. Experiments on this possibility are now in progress.

The authors wish to express their thanks to Prof. S. Akabori for his kind advice.

Laboratory of Biochemistry, Faculty of Science, Osaka University

1) S. Moore, W. H. Stein, *J. Biol. Chem.*, **176**, 367 (1948).
2) R. Monier, Y. Gendron, M. Julisz, C. Fromageot, *Biochim. Biophys. Acta*, **8**, 588 (1952).
3) C. Fromageot, M. Privat de Garilhe, ibid., **4**, 509 (1950).
4) J. C. Lewis, N. S. Snell, D.J. Hirshmann, H. Fraenkel-Conrat, *J. Biol. Chem.*, **186**, 23 (1950).
5) S. Akabori, et al., To be published.
6) E. J. Conway, et al., *Biochem. J.*, **36**, 655 (1942).
7) M. Rovery, C. Fabre, P. Desnuelle, *Biochim. Biophys. Acta*, **12**, 547 (1953).

The Structure of the So-called α-Δ⁵-Cholestenone Oxide

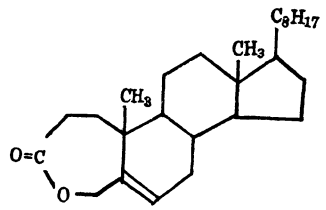
By Susumu MORI and Fumikazu MUKAWA

(Received July 23, 1954)

The structure of the so-called α-Δ⁵-cholestenone oxide has not yet been precisely proved.[1, 2] The study of it has shown that the compound is not an epoxide but a lactone. The reduction of the compound with lithium aluminium hydride in ether gave a diol (m.p. 129°C. Found: C, 80.09; H, 11.94, calcd. for $C_{27}H_{48}O_2$: C, 80.13; H, 11.96%), which was obtained pure in a good yield.

The diol showed a strong absorption peak in 3.0μ (Nujiol mull), indicating the presence of a hydrogen-bonded hydroxyl group, but no longer a peak in the 5.8μ region characteristic of carbonyl function. Oxidation of the diol with chromium trioxide-pyridine complex gave the known 3, 4-seco-Δ⁵-cholestene-3, 4-dioic acid (Diels' acid). Then it was converted into the dimethyl ester, which showed no depression of the melting point on admixture with an authentic specimen.

From a consideration of the results it seems most reasonable to conclude that the so-called α-Δ⁵-cholestenone oxide is an unsaturated lactone as illustrated by formula (I).



(I)

Department of Chemistry, Faculty of Science, Tokyo Metropolitan University, Setagaya, Tokyo

1) L. Ruzicka and W. Bosshard, *Helv. Chim. Acta*, **20**, 244 (1937).
2) Y. Urushibara and M. Chuman, This Bulletin, **22**, 273 (1949).

Procedure for the Preparation of the New Nickel Catalyst

By Yoshiyuki URUSHIBARA and Shigeo NISHIMURA

(Received August 19, 1954)

In a preliminary note[1] one of the authors (Y.U.) reported that metallic nickel and copper precipitated from the aqueous solutions of their soluble salts by means of zinc dust are active catalysts for hydrogenation in the presence of caustic alkali or when digested with aqueous caustic alkali before use. Since then, the activity of the new nickel catalyst has been much improved. The following is the procedure for obtaining the greatest activity that has been so far attained.

Ten grams of zinc dust, as fine as possible, and about 3 cc. of distilled water are put in a round flask of 100 cc. capacity and heated on a boiling waterbath. A stirrer reaching the bottom is installed. Ten cc. of an aqueous solution containing 4.04 g. of nickel chloride, $NiCl_2 \cdot 6H_2O$, is heated to ebullition, and added to the zinc dust by means of a pipet, with vigorous agitation in a few sec. The solids are at once collected on a glass filter by suction, washed with a small quantity of hot distilled water, transferred into 160 cc. of 10 % aqueous caustic soda contained in an Erlenmeyer flask as quickly as possible, and digested at 50–60° for 15–20 minutes with occasional stirring. Then, the supernatant liquid is removed, and the solids are washed with 40 cc. of distilled water of 50–60° two times, and finally with the solvent of hydrogenation, e. g. ethanol. The rinsings are always removed by decantation.

In this way, a catalyst consisting of about 1 g. of nickel and 4.7 g. of zinc, and acting as good as 1 g. of Raney nickel catalyst (e. g. W 7) is obtained and can be used for hydrogenation or reduction of ketones, nitriles, oximes, a double bond conjugated with a carbonyl or a carboxyl group, etc., at the ordinary temperature and pressure.

Free carboxylic acids diminish the activity of the nickel catalyst. Hence, they are neutralized with caustic alkali before introducing the catalyst, or hydrogenated in solution in aqueous alkali. For instance, cinnamic acid is easily reduced to hydrocinnamic acid in solution in aqueous caustic soda.

In case the alkali remaining on the catalyst is undesirable, digestion in a saturated aqueous solution of sodium chloride followed by washing with hot distilled water will remove the majority of the adsorbed alkali. For instance, the reduction of nitrobenzene to aniline is better performed with a so-treated catalyst.

If 80 cc. instead of 160 cc. of 10 % caustic soda is used in digestion, the activity is increased by about 10 %, but the weight of the catalyst amounts to about 10 g. corresponding to the more quantity of matters remaining undissolved.

Department of Chemistry, Faculty of Science, Tokyo University

1) Y. Urushibara, This Bulletin, **25**, 280 (1952).

On the State of Pentosan in Wood Pulps

By Kei MATSUZAKI, Akira HATANO, Tōru ABE and Hiroshi SOBUE

(Received October 9, 1953)

1. Introduction

Many discussions[1,2] have been made on the state of pentosan in wood pulps. However, as our previous report[3] showed, it is difficult to determine a small quantity of pentosan by the phloroglucin or bromate method. Accordingly, the conclusions reached do not seem to be correct. In this research, pentosan determinations by paper chromatography and by the colorimetric method with aniline were applied to the acid-hydrolyzed samples as well as to the alkali-extracted samples, and the state of pentosan in wood pulps was discussed.

2. Experimental Procedures and Results

(1) The Pentosan Contents of Acid-hydrolyzed Pulps.—Five g. each of sulfite rayon pulps from red pine (*Pinus densiflora* S. et Z.) and beech (*Fagus crenata* Blume) were hydrolyzed with 300 cc. of boiling 4N hydrochloric acid for 1, 3, 5 and 7 hours. Since recrystallization of split chains was observed during acid-hydrolysis,[4] the acid-hydrolyzed samples were treated with a boiling 1% sodium hydroxide solution for half an hour to eliminate[5] the recrystallized particles. The pentosan contents of the acid- and acid-alkali-treated samples were determined by paper chromatography.[6] The result is tabulated in Table I. The degrees of polymerization were determined from the viscosities of cupri-ethylene diamine solutions[7] of the samples.

TABLE I

THE PENTOSAN CONTENTS AND DEGREES OF POLYMERIZATION OF ACID-HYDROLYZED AND ACID-ALKALI TREATED PULPS

Time of Acid-Hydrolysis	Treatment	Red Pine			Beech		
		yield %	pentosan* %	D.P.**	yield %	pentosan* %	D.P.**
0	original	···	2.0	720	···	3.0	650
	alkali	88.2	1.25	710	92.6	2.0	620
1	acid	70.5	0.45	111	72.4	0.60	113
	acid-alkali	36.0	0.31	121	41.1	0.50	120
3	acid	47.9	0.30	102	49.2	0.30	102
	acid-alkali	23.9	0.22	87	25.0	0.20	98
5	acid	33.3	0.15	87	35.8	0.10	87
	acid-alkali	11.0	0.10	80	12.7	trace	92
7	acid	23.6	0.13	81			
	acid-alkali	7.1	0.05	80			

* % in the residue, determined by paper chromatography
** Cupri-ethylene diamine solution, $Km = 8.0 \times 10^{-4}$

(2) The Pentosan Contents of Cold Alkali-treated Pulps.—Two g. each of red pine and beech pulps were treated with 50 cc. of 4–17.5% sodium hydroxide solutions for half an hour at 20°C, stirring every five minutes. The samples, pressed on a glass filter to make them free from the residual alkaline solution as far as possible, were treated again with 50 cc. of a sodium hydroxide solution of the same concentration and processed as before, washed successively with water, and 1% acetic acid solution and water, and dried. In another series of experiments, the cold alkali-treated samples whose cellulose micelles are more or less disordered were treated with 200 cc. of 2.5N sulfuric acid at 95–100°C for an hour to remove pentosan thoroughly. The pentosan contents of the samples were determined by the colorimetric method[3] and partly by paper chromatography. The results are tabulated in Table II and Table III.

1) K. H. Meyer, "Hoch polymere Chemie" Vol. 2 (1940) p. 216; H. Maeda, *J. Text. Cell. ind. Japan*, **1**, 669 (1945); H. Sobue, K. Matsuzaki, A. Hatano and Y. Arisawa, ibid., **8**, 79 (1952).

2) A. Meller, *Paper Trade J.*, **124**, No. 9, 104 (1947).

3) T. Abe, K. Matsuzaki, A. Hatano and H. Sobue, This Bulletin, **26**, 255 (1953).

4) H. G. Ingersoll, *J. Applied Phys.*, **17**, 924 (1946); J. A. Howsmon, *Textile Research J.*, **19**, 152 (1949); O. A. Battista, *Ind. Eng. Chem.*, **42**, 502 (1950); A. Meller, *J. Polymer Sci.*, **4**, 619 (1949); P. H. Hermans and A. Weidinger, ibid., **4**, 317 (1949).

5) H. Maeda, *J. Text. Cell. Ind. Japan.*, **1**, 651 (1945).

6) H. Sobue and A. Hatano, *J. Chem. Soc. Japan, Ind. Chem. Sec.*, **54** 460 (1951); **55**, 131 (1952).

7) Tappi Standard T230 Sm-50.

TABLE II
THE PENTOSAN CONTENTS OF COLD ALKALI- AND ALKALI-ACID-TREATED RED PINE PULPS

NaOH, %	Treatment	Yield, %	Pentosan,*%
4	Alk.	97.1	0.93 (0.9)
	Alk.-acid	92.4	0.69
6	Alk.	93.7	0.69 (0.6)
	Alk.-acid	90.4	0.46
8	Alk.	88.9	0.53 (0.5)
	Alk.-acid	85.4	0.35
10	Alk.	85.6	0.42 (0.3)
	Alk.-acid	82.6	0.24
12	Alk.	88.9	0.32
	Alk.-acid	85.4	0.21
14	Alk.	89.0	0.39
	Alk.-acid	86.4	0.19
17.5	Alk.	91.2	0.38
	Alk.-acid	87.5	0.22

* By colorimetric method, except ( ) which was determined by paper chromatography

TABLE III
THE PENTOSAN CONTENTS OF COLD ALKALI- AND ALKALI-ACID-TREATED BEECH PULPS

NaOH, %	Treatment	Yield, %	Pentosan,*%
4	Alk.	95.7	0.73
	Alk.-acid	92.9	0.68
6	Alk.	94.2	0.65
	Alk.-acid	91.4	0.52
8	Alk.	89.8	0.53
	Alk.-acid	86.9	0.38
10	Alk.	88.3	0.48
	Alk.-acid	82.8	0.22

* By colorimetric method

3. Discussion

The foremost interest would be the problem of whether or not the pentosan penetrates into the crystalline region.

From Table I, it is seen that the pentosan contents of the acid-treated pulps and acid-alkali-treated pulps decrease with the time of hydrolysis. The relationship between the yield of residue and the quantity of pentosan removed is shown in Fig. 1. Both the acid- and acid-alkali-treated pulps show a similar tendency, and it is seen that the pentosan content depends mainly on the yields of the residues. If the alkali-treatment helps to remove[5] the particles produced by recrystallization of split molecules in the amorphous region containing most of the pentosan, it would be expected that almost all of the pentosan could be removed. This, however, is not the case as can be seen from Table I and Fig. 1. In Fig. 1, the pentosan contents of the acid-alkali-treated pulps are somewhat higher than those of the acid-treated pulps, when the comparison is made between the samples whose yields of the residues are the same.

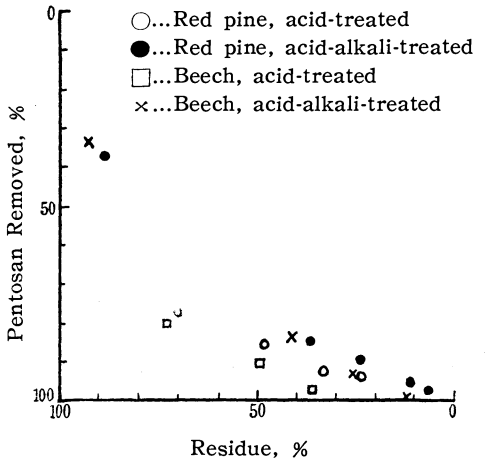


Fig. 1.—Relationship between residue and pentosan removed.

Pentosan removed is expressed as $(1-r)\times 100\%$, where r is the ratio of pentosan content in the treated pulp to that of the original pulps.

It has been asserted that the crystalline region of wood cellulose is 65% by X-ray method[3], and 60–70% by acid hydrolysis followed by dilute alkaline treatment.[5] In Fig. 1, even at 60–70% residue which is thought to consist almost entirely of the crystalline region, 0.5% of pentosan remains in the pulp.

The degrees of polymerization of the acid-alkali-treated pulps were expected to increase for the removal of the recrystallized particles (perhaps of very low D.P.). In Table I, the D.P.'s of the acid-alkali-treated pulps are not apparently different from those of the samples before alkaline treatment. This would be due to the degradation of the high molecular portion.

By using cold caustic solutions of concentrations over 10%, which are believed to be able to penetrate into the crystalline region of cellulose, the pentosan content was reduced to under 0.5%. The after-treatment by the acid of the residues thus treated gave a good effect for pentosan removal. Both pentosan and cellulose molecules in the crystalline region would have been disordered by the conc. alkalies to such an extent that they were readily attacked by the acid solution. Thus wood pulps containing 0.2% of pentosan

8) P. H. Hermans, "Physics and Chemistry of Cellulose Fibers", (1949), p. 517.

were obtained with 82–87% yield, although they are unsuitable for practical use.

These results suggest that the resistant pentosan chains share in building the crystalline region with cellulose chains, although larger portion of pentosan is found in the amorphous region. There remain as yet questions, whether or not the xylose units participate in mixed chain formation.

No great difference was observed between the behavior of pentosan in red pine and beech pulps.

It seems reasonable to deduce the following conclusion from the above discussion.

By intermicellar reactions such as hot alkaline treatment, the pentosan content in the purified pulp would not be reduced to under 0.5%, whereas by intramicellar reactions, such as cold alkaline refinement, the pentosan content could easily be reduced to under 0.5%. This will contribute to the purification processes of wood pulps, since the presence of pentosan is thought to be a cause of poorness in the reactivity of pulps to acetylation and xanthation.[9]

Summary

1. The pulps from the red pine and beech were hydrolyzed with boiling 4N hydrochloric acid solution for 1–7 hours and a part of the hydrolyzed pulps was treated with boiling 1% sodium hydroxide solution for half an hour to eliminate recrystallized particles. The pentosan content decreased as a function of the pulp yield. The degrees of polymerization of these samples were determined.

2. The pulps from the red pine and beech were treated with 4–17.5% sodium hydroxide solution for half an hour at 20° and this procedure was repeated. A part of the samples treated with the alkali was hydrolyzed with 2.5N sulfuric acid solution for one hour at 95–100°. The pentosan contents of these samples were determined.

3. The results show that it is difficult to reduce the pentosan content of wood pulp to under 0.5% by intermicellar reactions such as acid-hydrolysis or dilute hot alkaline refinement, whereas by intramicellar reactions such as cold concentrated alkaline refinement, it is easy to reduce the pentosan content to under 0.5%. The resistant pentosan seemed to be built in the crystalline region of wood cellulose.

4. It has no good effect for pentosan removal to eliminate the recrystallized particles produced by acid hydrolysis with dilute alkali, while acid treatment after cold alkaline refinement gave good result for pentosan removal.

The authors express thanks to Mr. M. Moriya and S. Fukuhara for their aid to the experiment. The expense of the work was defrayed from the Scientific Research Encouragement Grant of the Department of Education.

Department of Applied Chemistry,
Faculty of Engineering,
Tokyo University, Tokyo

9) W. Klauditz, *Holz Roh-u. Werkstoff*, **4**, 314(1941); G. Jayme, *Sevensk Papperstidn.*, **50**, Hägglund Issue 117(1947); R. E. Dörr, *Angew. Chem.*, **53**, 292(1940).

Molecular Structural Studies on Compounds Containing C—O Bond by Electron Diffraction. II. The Molecular Structure of Anhydrous Oxalic Acid[1]

By Shuzo SHIBATA and Masao KIMURA

(Received March 31, 1954)

Introduction

A number of studies[2] have been carried out on the structure of carboxyl group by use of x-ray diffraction, electron diffraction and molecular spectra. However systematic conclusion has not yet been reached for the structure of a carboxyl group. Hence it seems to be desirable to have more abundunt informations regarding the geometrical configuration of the group in order to discuss the character of carboxyl group by theoretical treatments. An oxalic acid molecule contains two carbonyl groups in a conjugated system O=C–C=O. Therefore the structural determination will decide the degree of conjugation between the two carbonyl groups across the central C–C bond.

In the present study we dealt with anhy-

1) Presented at the 5th annual meeting of the Chem. Soc. Japan held on April 4, 1952.

2) Cf. O. Thomas, *J. Chem. Phys.*, **18**, 761 (1950); M. Davies and O. Thomas, "Discussion of the Faraday Soc." 335 (1950).

drous oxalic acid in order to investigate the two subject problems mentioned above, i.e. 1) the stereochemistry of the carboxyl group, 2) the degree of conjugation between the two carbonyl groups. Hendricks,[3] Cox et al.,[4] Robertson,[5,6] Brill et al.[7] and Ahmed et al.[8] have already determined the molecular structures of anhydrous oxalic acid and its dihydrate by x-ray diffraction. Their studies were also undertaken mainly to make clear the two problems mentioned above although the results of their analyses appear to be inconsistent as will be described later. According to their results there exists an intermolecular hydrogen bond in the crystal of dihydrate and the distance O−H···O has a value of about 2.50Å, which is considerably short. This suggests that the structure of a free molecule might be different appreciably from the molecular structure in the crystalline state.

Therefore we attempted to determine the structure of a free anhydrous molecule by gas electron diffraction method and to obtain informations on the properties of carbon-carbon and carbon-oxygen bonds as well as on the effect of a hydrogen bond upon these distances.

Experimental Results

The sample used in the present investigation was anhydrous oxalic acid prepared from oxalic acid dihydrate by heating at temperatures above its melting point and was purified by sublimation. Anhydrous oxalic acid readily sublimes on heating at temperatures above 100°C. The sample was sublimed at about 120°C in a high temperature nozzle.

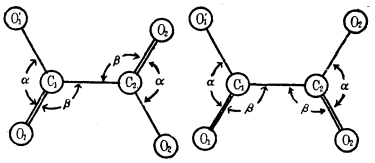
Excellent photographs were taken using an electron wavelength of about 0.06 Å and a camera length of about 11 cm. The characteristic features of the photographs are represented by the visual curve V in Fig. 2, where the dotted portion is drawn by use of the theoretical intensity curves to be mentioned later. That the feature of photograph bears a close resemblance to that of dimethylglyoxal is reasonable on account of the similarity of molecular structure between them. The maxima and minima were measured on the photographs within $q=83$. These observed values are listed in Table I.

TABLE I

OBSERVED AND CALCULATED q VALUES

Max.	Min.	$q_{obs.}$	model L $q_{calc.}$	model L $q_{calc.}/q_{obs.}$	model J $q_{calc.}$	model J $q_{calc.}/q_{obs.}$
	2	14.91				
2		18.07	18.6	1.016	18.5	1.013
	3	21.60				
3		23.87	24.2	1.014	24.2	1.014
	4	26.30	26.0	0.989	26.2	0.995
4		28.94	29.6	1.022	29.6	1.022
	5	32.16	32.4	1.008	32.1	0.998
5		35.56	36.2	1.017	36.1	1.015
	6	40.80	41.6	1.018	41.8	1.025
6		45.40	45.9	1.012	46.0	1.013
	7	48.87	49.4	1.011	49.2	1.006
7		52.43	53.1	1.013	53.0	1.011
	8	56.18	57.0	1.016	56.4	1.005
8		58.93	60.2	1.021	59.9	1.017
	9	62.90	64.0	1.017	63.5	1.009
9		67.25	68.5	1.020	67.9	1.010
	10	71.13	72.4	1.018	72.1	1.013
10		74.34	75.8	1.021	75.4	1.014
	11	77.78	79.6	1.023	79.3	1.021
11		81.12	83.2	1.024	83.0	1.022
average				1.015		1.012
average deviation				0.005		0.006

3) S. B. Hendricks, *Z. Krist.*, **91**, 48 (1953).
4) E. G. Cox, M. W. Dougill and G. A. Jeffrey, *J. Chem. Soc.*, **1952**, 4851.
5) J. M. Robertson and I. Woodward, *J. Chem. Soc.*, **1936**, 1817.
6) J. D. Dunitz and J. M. Robertson, *J. Chem. Soc.*, **1947**, 142.
7) R. Brill, C. Herman and C. L. Peters, *Ann. Physik*, **42**, 357 (1947).
8) F. R. Ahmed and D. W. J. Cruickshank, *Acta Cryst.*, **6**, 385 (1953).



trans form *cis* form

Fig. 1.

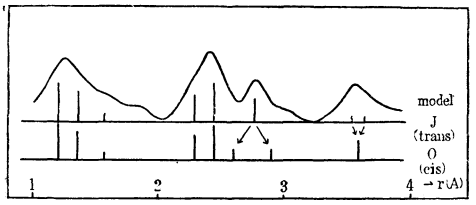


Fig. 2. The radial distribution curve for anhydrous oxalic acid.

The radial distribution curve was calculated by use of the formula

$$rD(r)=\sum_{q=1}^{q=\max.} I(q)\exp(-aq^2)\sin(\pi qr/10)$$

with $\exp(-aq^2_{\max.})=0.1$, and is shown in Fig. 2. The curve has maxima at 1.26, 2.40, 2.75 and 3.55 Å. Each peak may be regarded as made up of the contributions of several interatomic distances. The first peak may be interpreted as representing the bonded $C_1=O_1$ and C_1-O_1' distances, the second peak the non-bonded $C_1\cdots O_2'$, $C_1\cdots O_2$ and $O_1\cdots O_1'$, distances, and the third and the fourth peaks the non-bonded $O_1\cdots O_2'$, $O_1\cdots O_2$ and $O_1'\cdots O_2'$ (see Fig. 1). The last two peaks correspond to the long distances which are related to the rotational configuration about C−C axis. The existence of the third and fourth peaks shows that the four non-bonded O···O distances can be classified definitely into two groups. Accordingly the molecule seems to have, roughly speaking, either the *trans* form or the *cis* form. The sharp feature of the third peak seems to favor the trans form, because if the molecule takes the *cis* form, two equal distances $O_1'\cdots O_2$ and $O_1\cdots O_2'$ in the trans form will turn out to be two different distances $O_1\cdots O_2$ and $O_1'\cdots O_2'$. The possible O−O distances of trans (J) and cis (O) models are shown by bold lines in the radial distribution curve (Fig. 2).

The theoretical intensity curves were calculated with the following simplified equation,

$$I(q)=\sum_{i\neq j}\sum Z_iZ_j\sin(\pi qr_{ij}/10)/r_{ij}$$

Six parameters C=O, C−C, C−O, $\angle\alpha$, $\angle\beta$ and $\angle\gamma$ (a twisted angle) are required for settling molecular forms. The effect of hydrogen atoms is negligibly small on the theoretical intensity curves except the O—H distance which was assumed to be 0.96 Å. If the distance C=O is assumed to be equal to 1.20 Å and the molecule is planar, the parameters involved are as follows C−C/C=O, C−O/C=O, $\angle\alpha$ and $\angle\beta$. Fifty three theoretical intensity curves were calculated for the models with the values ranging from 1.44 to 1.60 Å for C−C, from 1.30 to 1.40 Å for C—O, from 116° to 131° for $\angle\alpha$ and from 112° to 134° for $\angle\beta$. Some of them are reproduced in Fig. 3. in order to illustrate the variation of the relative positions and intensities of maxima and minima with the change of the parameters.

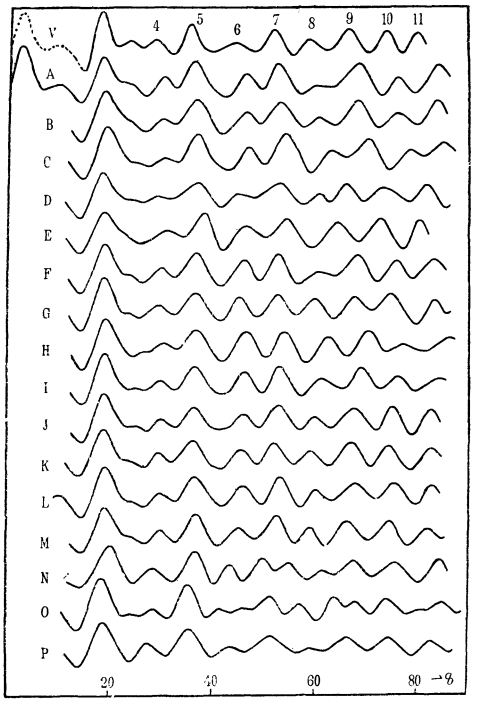


Fig. 3. The visual and theoretical intensity curves.

The models are listed in Table II. The curves A, B, D and E illustrate the effect of $\angle\beta$, the curves F and G that of C−O distance, the curves H, I and J that of C−C distance, and curves B, C, K and L that of $\angle\alpha$. Our analysis could be facilitated by the fact that the calculated intensity curves are not very sensitive to the parameter $\angle\beta$. The curve J in Fig. 3, which is one of the best models, is in good agreement with the observed scattering curve, except that the agreement is not perfect in regard to both the height of the third maximum and the depth of the fifth minimum, which appears stronger on photographs than would be suggested by the calculated intensity curves. This discrepancy may be considered to be due merely to a difficulty in the examination of photographs by visual method. It is found that the models with C−C distance smaller (or larger) than that of the best model can also give the theoretical intensity curves in agreement with the visual curve, if the value of $\angle\alpha$ is decreased (or increased) from that of the best model (e.g. curve L in Fig. 2). These circumstances are shown schematically in Fig. 4. Therefore it is impossible to determine the C−C distance very accurately. Further the theoretical intensity curves were calculated for the models with various twisted angles about C−C axis (Cf. Curves M and N in Fig. 2.). If a twisted angle from the

TABLE II

MODELS FOR ANHYDROUS OXALIC ACID

Model	C=O(Å)	C—O(Å)	C−C(Å)	∠α(degree)	∠β(degree)	∠γ and configuration
A	1.20	1.30	1.48	122	123	planar, *trans*
B	〃	〃	〃	122	120	〃 〃
C	〃	〃	〃	125	〃	〃 〃
D	〃	1.35	1.56	〃	117.5	〃 〃
E	〃	〃	〃	〃	112	〃 〃
F	〃	1.33	1.52	123.5	123	〃 〃
G	〃	1.37	〃	〃	〃	〃 〃
H	〃	1.35	1.48	125	〃	〃 〃
I	〃	〃	1.52	〃	〃	〃 〃
J	〃	〃	1.56	〃	〃	〃 〃
K	〃	〃	1.52	122	〃	〃 〃
L	〃	〃	〃	123.5	〃	〃 〃
M	〃	〃	1.56	125	〃	twisted through 30° from the *trans* form.
N	〃	〃	〃	〃	〃	twisted through 60° from the *trans* form.
O	〃	〃	〃	〃	〃	planar, *cis*
P	〃	〃	〃	〃	〃	free rotation

trans form is less than about thirty degrees, it is possible to obtain theoretical intensity curves in agreement with the visual curve, because the two distances which vary with internal rotation, O_1-O_2' and O_1-O_2 or $O_1'-O_2'$ change in opposite directions so that the effect of the changes is partly compensated each other. However the models with a twisted angle greater than about 30° are unacceptable because the third maximum disappears in the theoretical curves. Therefore electron diffraction data can give no conclusive value of the twisted angle about the C−C axis up to 30°. The free rotational and *cis* models are also discarded because of the disappearance of the third maximum and because of the changes of the 6th and 9th maxima into double maxima respectively. The effect of intramolecular vibrations was taken into account for the interatomic distances except for those related to the internal rotation. The mean amplitudes used in the calculation were estimated using the values for oxalyl chloride.[9] The results are practically the same as those obtained for the fixed models.

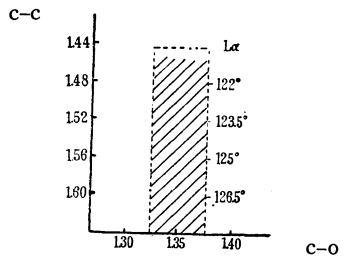


Fig. 4. Parameter chart for oxalic acid. The shaded part shows the region of parameters giving acceptable models when is assumed ∠β=123°.

The effect of the internal rotation can be found in the results obtained from the considerations of the theoretical intensity curves for the models with various twisted angles. But we could not obtain a definite conclusion for the rotational vibration because we must take into account at the same time both the twisted angle in equilibrium and the rotational vibration as well as internal vibrations.

Finally a quantitative comparison with the observed values was made for the maxima and the minima of the best theoretical intensity curves. The results are shown in Table I. For the 2nd and 3rd minima a comparison was not made on account of the inaccuracy of the observed values.

Thus the molecular structure of anhydrous oxalic acid was obtained as follows: C=O 1.22Å ±0.02 Å, C−O 1.37 Å±0.02 Å, C−C 1.54 Å±0.06 Å, ∠O=C−O 125°±3°, ∠O=C−C 122°±5°, and the *trans* form. But the deviation from the *trans* form is permissible within a twisted angle of about thirty degrees.

Although the existence of dimers as in formic acid[10] might be improbable in the gaseous state, the theoretical intensity curves were calculated for the model dimerized in the same type as β form of anhydrous oxalic acid.[3] When O···O distance is equal to about 2.70 Å, the dimerized model gives a theoretical intensity curve in fair agreement with the visual curve. Further investigation on this point, however, has not been carried out.

Discussion of Results

Our analysis gave the following results: First, the length of the central C−C bond is 1.54 Å, a value generally ascribed to a normal single bond, secondly the molecule is

9) Y. Morino, private communication.
10) I. L. Karle and L. O. Brockway, *J. Am. Chem. Soc.*, **66**, 574 (1944).

planar despite the single bond character of the C−C bond. We shall explain the above results and compare the molecular structure of oxalic acid in the gaseous state with that in the crystalline state which has hitherto been reported.

The value of 1.54 Å±0.06 Å was obtained for C−C bond length. This value is equal to C−C bond length in ethane and other saturated hydrocarbons. Therefore C−C bond in an oxalic acid molecule seems to have a small degree of double bond character. Though we cannot say definitely because of the probable errors, the double bond character seems to be less in an oxalic acid molecule than in glyoxal[14] (C−C=1.47 A± 0.02 Å) and in oxalyl chloride.[15] The molecules of these compounds contain carboxyl groups in a conjugated system similar to that of oxalic acid, i.e. O=C−C=O to which the resonating electronic structures such as $O^+-C=C-O^-$ contribute. This suggests that two carbonyl groups in the molecule are not conjugated very much with each other, presumably because the strongly electronegative hydroxyl oxygen atoms prevent an appreciable π electron conjugation across the C−C bond. Therefore the structure of the carboxyl group will be similar to that of a monobasic acid having only one carboxyl group. According to the recent data obtained by Schomaker and O'Gorman,[11] and Karle[13] shown in Table III, the structure of the carboxyl group in anhydrous oxalic acid is in good agreement with that in a formic acid monomer. The dimensions of the carboxyl group obtained have revealed a significant difference of about 0.15 Å, between the two carbon-oxygen bonds, although the difference between them is less than that expected between a pure single and a pure double bond. Accordingly it follows that the resonance form (B2) to be shown later does not contribute very much to the normal state of a carboxyl group in a gaseous oxalic acid molecule.

TABLE III

STRUCTURES OF CARBOXYL GROUP, ESPECIALLY OXALIC ACID

	C=O	C—O	C—C	material	method
Shibata and Kimura	1.22	1.37	1.54	anhydrus oxalic acid	electron diffraction
Hendricks[3]	1.22	1.29	1.57	„ (α form)	x-ray
Cox, Dougill and Jeffrey[4]	1.19	1.29	1.56	„ „	„
Hendricks[3]	1.20	1.30	1.59	„ (β form)	„
Robertson and Woodward[5]	1.24	1.30	1.43	oxalic acid dihydrate	x-ray
Brill, Herman and Peters[7]	1.21	1.28	1.55	„	„
Dunitz and Robertson[6]	1.24	1.25	1.46	„	„
Ahmed and Cruickshank[8]	1.19	1.29	1.53	„	„
Jeffrey and Parry[17]	1.23	1.25	1.56	ammonium oxalate monohydrate	„
Karle and Brockway[10]	1.24	1.42		formic acid monomer	electron diffraction
„ „	1.25	1.36		„ dimer	„
Schomaker and O'Gorman[11]	1.213	1.368		formic acid monomer	„
Karle[13]	1.23	1.36		„	„
Williams[12]	1.225	1.41		„	spectrum
Karle and Brockway[8]	1.24	1.43	1.54	acetic acid monomer	electron diffraction
„ „	1.25	1.36		acetic acid dimer	„
LuValle and Schomaker[14]	1.20		1.47	glyoxal	„
Schomaker[15]	1.20		1.50	oxalyl chloride	„

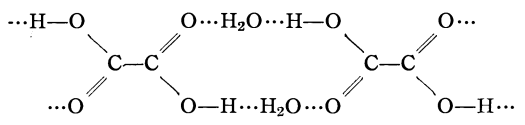
We have come to the conclusion that the molecule takes a planar configuration. To account for this fact some interpretation other than resonance interaction between carboxyl groups is necessary. According to the results obtained from Raman spectra and infrared absorption spectra, oxalyl chloride molecule in the liquid state takes a planar trans configuration rather than the *cis* configuration at room temperature and at higher

11) V. Schomaker and J. M. O'Gorman, *J. Am. Chem. Soc.*, **69**, 2638 (1947).
12) V. Z. Williams, *J. Chem. Phys.*, **15**, 232 (1947).
13) I. L. Karle and J. Karle, *J. Chem. Phys.*, **22**, 43 (1954).
14) J. E. LuValle and V. Schomaker, *J. Am. Chem. Soc.*, **61**, 3520 (1939).
15) The results by V. Schomaker cited in L. E. Sutton and P. W. Allen, *Acta Cryst.*, **3**, 46 (1950).

temperatures.[16] The molecular structure in the gaseous state was also confirmed to be the trans configuration by electron diffraction.[15] Moreover the molecular structure of glyoxal in the gaseous state was found to be the trans configuration, by electron diffraction experiment. The coplanarity of oxalyl chloride and glyoxal may be due to the stabilizing resonance energy associated with some double bond character of carbon-carbon bond. If molecule is planar, a consideration of electrostatic interaction and steric hindrance indicates that these molecules should take the trans rather than the *cis* configuration. On the other hand, since the double bond character which restricts rotation seems to be weak in oxalic acid, a consideration of electrostatic interaction and steric hindrance will indicate the possibility of a nonplanar form. Thus the fact that the molecule have the planar and trans configuration or the form similar to it seems to be due partly to the O—H···O intramolecular hydrogen bond similar to that in salicylic acid. This possibility may be supported by the fact that the distance 2.76 Å between the oxygen atoms (for the best model) is appropriate.

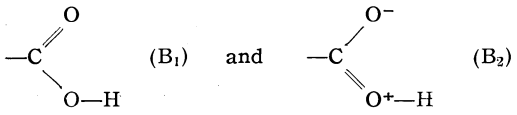
Recently Cox, Dougill and Jeffrey determined the molecular structure of anhydrous oxalic acid (α form)[4] in agreement with a work by Hendricks. Ahmed and Cruickshank carried out a refined analysis using the data obtained by Robertson and his coworkers and by Brill et al. They proposed a new molecular structure of oxalic acid dihydrate. According to these results, as shown in Table III, the C—C bond length is nearly equal to that a normal single bond, 1.54 Å, and two kinds of C—C bonds are equal to 1.29 Å and 1.19 Å respectively, and the molecule is planar.

In general the structure of oxalic acid dihydrate in the crystalline state may be represented by the following schematic formula,[6]

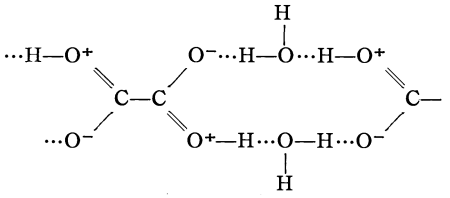


(A)

A carboxyl group may resonate between the two forms,

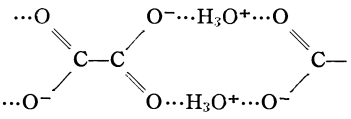


Accordingly the resonance form,



(C)

may contribute to the normal state of oxalic acid dihydrate. If very strong hydrogen bonds are present in a crystal, the contribution of such resonance from (C) will be appreciably large. As an extreme case, a resonance form



(D)

may be considered. If H_3O^+ is separated completely from other part of oxalic acid dihydrate, two C—C bonds in an oxalate ion should be equal to each other as shown by an x-ray analysis of the crystal structure of ammonium oxalate monohydrate.[17]

Taking into account the data of themselves and of Brill et al., Dunitz and Robertson proposed a remarkable feature of results for the structure of oxalic dihydrate, i.e. the C—C bond length 1.46 Å and two C—C bonds, differing in their lengths, 1.24 Å and 1.25 Å. These results are contradictory to that of Ahmed et al. in regard to the C—C double bond character and to the equality of C—C bond length, owing to the contribution of resonance form (D) to a molecule in the crystalline state. If such is actually the case in the crystalline state, the significant discrepancies between their results and ours suggest that the molecular structure is dependent on the molecular environment.

On the otherh and, Ahmed et al. and Cox et al. concluded that the appareciable difference in two C—C bond lengths suggests the absence of H_3O^+ ion in a dihydrate and that the similarity of the molecular structure of anhydrous oxalic acid to that of its dihydrate indicate the interatomic distances unaffected by the environment of the molecule. However more remarkable difference will be found between vapor and solid than between anhydrous oxalic acid (α-form) and dihydrate.

Upon comparison of their data obtained by x-ray with our data obtained by gas electron diffraction, the following facts are found to be noteworthy: the C—C bond has a normal single bond length and two C—O bond lenghts

16) J. S. Ziomek, A. G. Meister, F. F. Cleveland and C. E. Decker, *J. Chem. Phys.*, **21**, 90 (1953).
17) G. A. Jeffrey and G. S. Parry, *J. Chem. Soc.*, **1952**, 4864.

differ from each other. But the hydroxyl C—O bond is very short in crystals than in free molecules by an amount of about 0.07 Å.

The difference between the C—O and C=O bond is less in crystals than in gaseous state. If such is actually the case, this will be due to the difference between the crystalline state and the gaseous state, in other words to the difference in the environment around a molecule. Such changes of interatomic distances owing to intermolecular hydrogen bonds, have already been pointed out, for example, in the cases of acetamide[18] and hydroquinone[19] and also in the difference of the structures between the monomer and the dimer of formic acid. Therefore it seems to be probable that the structure of anhydrous oxalic acid is not exactly the same as that of its dihydrate, because the length of a hydrogen bond of 2.5 Å in a dihydrate crystal is considerably small. However the results of the molecular structure of oxalic acid dihydrate by x-ray method are not conclusive. The result obtained by Ahmed and Cruickshank seems to be more reliable than those by others, since they carried out a refined analysis using the data obtained by Robertson et al. and by Brill et al. But reinvestigation by x-ray diffraction seems to be desirable on the structure of oxalic acid dihydrate.

Summary

The molecular structure of anhydrous oxalic acid was studied by electron diffraction method. The interatomic distances and valency angles were found as follows: C=O 1.22 Å, C—O 1.37 Å, C—C 1.54 Å, ∠O=C—O 125°, and ∠O=C—C 122° with possible errors within 0.02 Å, 0.02 Å, 0.06 Å, 3° and 5° respectively. The molecule takes planar trans configuration. From these data the following conclusions were derived. The central C—C bond seems to have a small degree of double bond character with no appreciable conjugation between two carbonyl groups. The molecule takes the planar trans configuration in spite of the small degree of double bond character in the C—C bond. This fact in connection with the data of other compounds seems to suggest the possibility of the existence of intermolecular hydrogen bonds in a free oxalic acid molecule. Our data of oxalic acid in the gaseous state were compared with the data of oxalic acid in the crystalline state from x-ray diffraction. Significant differences was found between the results on molecular dimensions, especially in hydroxyl C—O bond lengths. From these fact it was inferred that the structure of a molecule (or a carboxyl group) is affected by the molecular environment such as hydrogen bond formation between molecules.

We wish to express our thanks to Prof. M. Kubo of Nagoya University for his helpful advice. Our thanks are also due to Dr. S. Seki and Dr. K. Osaki of Osaka University for their valuable suggestion regarding the x-ray diffraction data.

Department of Chemistry, Faculty of Science, Nagoya University, Nagoya

18) M. Kimura and M. Aoki, This Bulletin, **26**, 429 (1953).
19) M. Kimura and S. Shibata, Presented at the 4th annual meeting of the Chem. Soc. Japan held on April 7, 1951.

Zur Kenntnis über die Hochdrucksynthese von Acrylester. I. Erkenntnisse bei der Acrylestersynthese unter der Anwendung von Nickelhalogenid-Katalysator

Von Kazumi YAMAMOTO

(Eingegangen am 24. April 1954)

Einleitung

Bei der Acrylestersynthese nach dem Reppe-Verfahren er gibt sich zweierlei; das erste ist das stoichiometrische Verfahren (oder die Gewöhnliche-Druck-Synthese), in dem Metallcarbonyl als Kohlenoxydträger verwendet wird, und das andere das katalytische, (oder die Hochdrucksynthese), in dem Kohlenoxyd und Acetylen sich auf Alkohol unter katalytischer Wirkung von Salzen der carbonylbildungsfähigen Metalle, wie Nickel, unter erhöhtem Druck und bei erhöhter Temperatur einwirken lassen.

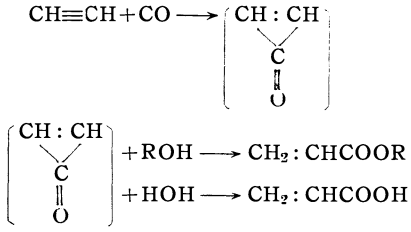
Die Abhandlungen, die fortlaufend veröffentlicht werden sollen, handeln über den Mecha-

nismus der Reaktion, insbesondere über den der Aktivierung des Kohlenoxyds bei dem letzteren.

Die Bildung von Acrylester wird im Sinne der folgenden Gleichung erläutert:

$$CH{\equiv}CH+CO+ROH \longrightarrow CH_2:CHCOOR$$

Reppe[1] hat geschickt die Bildung von Acryl-ester oder Säure aufgeklärt, durch die intermediäre Bildung eines hypothetischen Cyclopropenon-Rings aus Acetylen und Kohlenoxyd, der dann durch Verbindung mit beweglichem Wasserstoffatom, wie Wasser, Alkohol, usw. nach folgendem Schema aufgespalten wird:



Aber man kann den genügenden experimentellen Grund darüber nicht finden, in welcher Weise das Kohlenoxyd an dem Katalysator aktiviert wird, den Cyclopropenonring zu bilden. Darüber nimmt Reppe die Bildung von aktivem, nicht isolierbarem Zwischenprodukt wie $NiBr_2(CO)$, das von Kohlenoxyd und Nickelhalogenid unter der Reaktionsbedingung entsteht, unter Berücksichtigung der Arbeit von Hieber[2] über Kobaltcarbonyljodid $CoJ_2(CO)$ an.

Ausser dem oben erwähnten Metallhalogenid hat Reppe die Komplexverbindungen von demjenigen mit Triphenylphosphin als Katalysator bei der Acrylestersynthese vorgebracht. Was den Mechanismus, wodurch Kohlenoxyd aktiviert wird, anbelangt, ist die zuverlässige Theorie, worüber ich später schreiben werde, bisher nicht veröffentlicht.

Das Allgemeine

Wie vorher erwähnt, werden die Halogenide der carbonylbildenden Metalle als Katalysatoren bei der Hochdrucksynthese von Acrylester aus Acetylen, Kohlenoxyd und Alkohol verwendet. Als solche eignen sich in erster Linie Nickelhalogenide. Die im Experiment benützten Nickelhalogenide wurden nach folgenden Methoden hergestellt.

1. Nickelbromid und Jodid.—Sowohl wasserfreies Nickelbromid als auch Jodid wurde leicht dadurch in einer Form der Lösung erhalten, indem man Brom oder Jod auf Nickelcarbonyl oder auf reduziertes Nickel in Alkohol bei gewöhnlicher Temperatur einwirken lässt.[3,4] Nickelgehalt in der alkoholischen Lösung wurde entweder durch Verdampfung von Alkohol unter erniedrigtem Druck oder durch Titrieranalyse bestimmt. Zu der alkoholischen Lösung des Nickeljodids muss man kleine Mengen reduziertes Nickel beimengen, da es durch Luftsauerstoff unter Jodabspaltung oxydiert wird.[5]

2. Nickelchlorid.—Wasserfreies Nickelchlorid wurde zweckmässig aus Nickelhexaminchlorid hergestellt, das im Vakuum bei etwa 220° über die Stufe Diaminsalz zum Nickelchlorid abgebaut wird.

Acetylen, das von Calciumcarbid erzeugt wurde, wurde durch das übliche Mittel gereinigt, und die Reinheit war mehr als 99% und der Sauerstoffgehalt unter 0.2%.

Kohlenoxyd wurde aus Ameisensäure und Schwefelsäure entwickelt und der darin enthaltene Sauerstoff wurde durch Leitung auf das bei 300° bis 400° erhitzte, reduzierte Kupfer in Kohlensäure umgewandelt, die durch Alkalilauge beseitigt wurde.

Auf solche Weise erhaltenes Acetylen und Kohlenoxyd wurde im Gasometer in gleichem Verhältnis vermischt. Alkohol, wie Äthanol, bzw. Butanol, wird mit Calciumcarbid völlig getrocknet und so verwendet.

Die Aufarbeitung der Acrylestersynthse wurde entweder nach der diskontinuierlichen oder nach der halbkontinuierlichen Methode durchgeführt. Die einzelnen Bedingungen sind je nach den Umständen beschrieben und können folgendermassen zusammengefasst werden:

Diskontinuierliche Methode.—In den Schüttelautoklav, der elektrisch regulierend erhitzt wird, tut man Alkohol und Katalysator hinein und komprimiertes Acetylen-Kohlenoxyd-Gemisch bie zum bestimmten Druck nach dem Verblasen der Luft im Autoklav mit dem Gasgemisch. So beobachtet man hauptsächlich nur die Druckveränderung mit der steigenden Temperatur unter Schüttelung.

Halbkontinuierliche Methode.—Den Autoklav mit dem Verdichter durch biegsames Kapillarrohr verbindend, arbeitet man der Methode (1) gemäss auf. Wenn der Innendruck des Autoklavs bis zu einem Gebiet mit dem Reaktionsverlauf abfällt, so wird frisches Gas-gemisch jederzeit vom Verdichter eingepresst. Die bestimmte Gasmenge, die mittels des Gasometers gemessen wird, wird durch Wiederholung solcher Operation eingepresst. Im allgemeinen verläuft die Reaktion bei 180° unter Gesamtdruck von 30 bis 40 Atm. Die Ausbeute von Acrylester an Alkohol wurde davon ausgerechnet, soweit es nicht anders bestimmt wurde, dass man das ausgewaschene und mit Calciumchlorid getrocknete Öl, das vom Reaktionsprodukt mit Wasserdampf abdestilliert wurde, für Rohacrylester hält.

1) W. Reppe, „Neue Entwicklungen auf dem Gebiet der Chemie des Acetylens und Kohlenoxyds", Springer Verlag, (1949), S. 97.
2) W. Hieber, *Z. anorg. allg. Chem.*, **243**, 145 (1939).
3) K. Yamamoto und K. Sato, *J.P.*, 187, 504.
4) K. Yamamoto und K. Sato, M. Oku, *J.P.*, 195, 106.
5) K. Yamamoto und M. Oku, *J.P.*, 192, 733.

Erkenntnisse bei Äthylacrylat-Synthese

Es dürfte notwendig sein, etwas über die Erkenntnisse bei der Äthylacrylat-Synthese zu beschreiben, z. B. über den Unterschied der katalytischen Fähigkeiten der Nickelhalogenide,*) über die Reaktionsbedigungen, Nebenreaktionen usw.

a) Unterschied der katalytischen Fähigkeiten von Nickelhalogeniden.—Es wurde von Reppe veröffentlicht, dass als Katalysatoren Nickelhalogenide in erster Linie geeignet sind, und dass die wirksamkeit der Halogenide (Nickelfluorid ist unbrauchbar) vom Chlorid zum Jodid stark zunimmt. Bei meiner Nachprobe wurde dies festgestellt, d.h., der Unterschied der katalytischen Fähigkeiten von Nickelhalogeniden ist eindeutig, wie in der Tabelle I gezeigt ist. Das Experiment wurde nach dem halbkontinuierlichen Veafahren durchgeführt.

TABELLE I

Äthanol (g)	NiX_2 (g)		Einleitgsatz. von Gasgem.(%)	Reaktionstemp. (°C)	Laufzeit (Std)	Äthylacrylat (g)	(%)
50	$NiCl_2$	1.5	40	170	20	—	—
50	$NiBr_2$	2.5	100	180	18	45.5	42
50	NiJ_2	3.6	100	165	5	62.5	58

Anmerkung: Autoklavinhalt 600 cm³, Operierender Druck 40 Atm.
Die Kontaktmenge wurde so bestimmt, dass das dem Bromid (5% an Alkohol) entsprechende Nickel erhalten wird, da es mir scheint, dass das katalytische Zentrum das Nickelatom ist. Theoretische Gasgemischmenge ist 48.7 *l.* für 50 g. Alkohol unter normalem Zustand.

b) Reaktionsbedingungen durch Nickeljodidkatalysator.—Wenn man nach dem diskontinuierlichen Verfahren den Reaktionsverlauf beobachtet, so kann man finden, dass die Reaktion in kurzer Zeit über die Latenzperiode (L.P.) hinaus mit dem die Wärmeerzeugung begleitenden Druckabfall verläuft. Die experimentellen Resultate sind unten zusammengefasst. Das Experiment wurde im Autoklav vom 600 cm³ Inhalt, in dem 46 g Äthanol und die bestimmte Menge Nickeljodid (in irgendeinem Falle mit reduziertem Nickel) enthalten sind, dadurch ausgeführt, dass das Gasgemisch (C_2H_2 : CO ist 1 : 1) bis 30 at. eingepresst und unter Schütteln erhitzt wird.

1. Nickeljodidmenge.—In der Tabelle II drückt Atm/Min den verhältnismässig schnellen Druckabfall aus und L.P. die Latenzperiode.

TABELLE II

Nr.	NiJ_2 (g)	Reaktionstemp. (°C)	L. P. (Std)	L. P. (Min)	Laufzeit (Std)	Laufzeit (Min)	Atm/Min
625	2.3	140	6	45	8	—	15/15
627	3.2	140	2	—	2	50	18/6
628	4.6	140	1	15	2	30	31/14

Man kann aus obiger Tabelle ersehen, dass man zur Gewinnung von genügender Reaktionsgeschwindigkeit nur mit Nickeljodid eine ziemlich hohe Konzentration dessen bedarf, und dass die Latenzperiode desto kürzer wird, je höher die Konzentration ist.

2. Reaktionstemperatur. — Unter den gleichen Bedingungen wurde der Einfluss der Temperatur unter Anwendung von Nickeljodid (5% an Äthanol) untersucht.

TABELLE III
EINFLUSS VON TEMPERATUR

Nr.	L. P. (Std)	L. P. (Min)	Reaktions-temp. (°C)	Atm/Min
620	—		120	—
625	6	45	140	15/15
633	2	—	150	20/15
626	1	—	160	30/30

3. Rolle des reduzierten Nickels als Hilfskatalysator.—Es ist bekannt, dass die Hinzufügung von reduziertem Nickel als Hilfskatalysator die Wirkung von Nickeljodid verstärkt. Darauf erforschte ich dessen Effekt unter den bestimmten Bedingungen (Äthanol 46 g. NiJ_2 2.3 g. bei 140°), um den Umfang zu erkennen.

TABELLE IV
NICKEL ALS HILFSKATALYSATOR

Nr.	Nickel (g)	L. P. (Std)	L. P. (Min)	Laufzeit (Std)	Laufzeit (Min)	Atm/Min
625	0	6	45	8	—	15/15
635	0.23	3	—	3	30	28/30
636	0.50	1	15	2	30	20/15

* Jüngst hat Reppe etwas eingehend darüber veröffentlicht: *Ann.*, **582**, 26 (1953).

Es ist hieraus selbstverständlich, dass die Anwesenheit des Nickels im Vergleich mit seiner Abwesenheit entweder die Reaktionstemperatur um ca. 20° erniedrigt oder die Nickeljodidmenge 30 bis 50% ersparen lässt.

In der Tabelle V wurde der Effekt von dem in verschiedenem Verhältnis beigefügten Nickel dargestellt. In solcher Weise ist der Effekt der Beifügung von Nickel als Hilfskatalysator sehr bemerkenswert.

TABELLE V
EFFEKT DER NICKELMENGE

Nr.	NiJ_2 (g)	Nickel (g)	L. P. (Std)	(Min)	Laufzeit (Std)	(Min)	Reaktionstemp. (°C)	Atm/Min
635	2.3	0.2	3	—	3	30	140	20/30
636	2.3	0.5	1	15	2	—	140	15/20
640	0.93	1.0	3	10	2	30	140	17/15
641	0.69	1.2	2	—	3	—	140	35/25
642	0.69	1.2	4	—	5	—	130	25/25
643	0.94	1.0	4	30	5	30	120	25/25

Die Lage der Latenzperioden und Laufzeiten bei den oben beschriebenen Experimenten sind, z.B. in Bezug auf Nr. 627, 628 und 640 aus den Figuren 1, 2 und 3 zu ersehen.

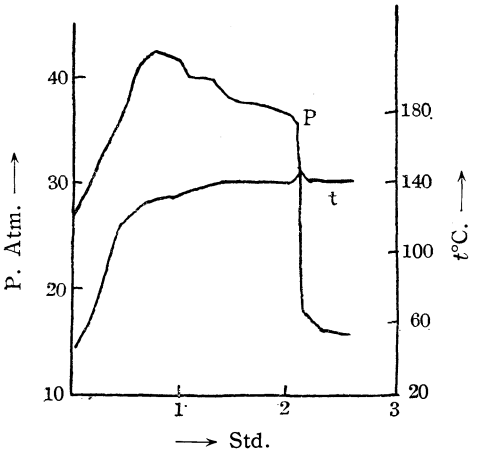


Fig. 1. Nr. 627

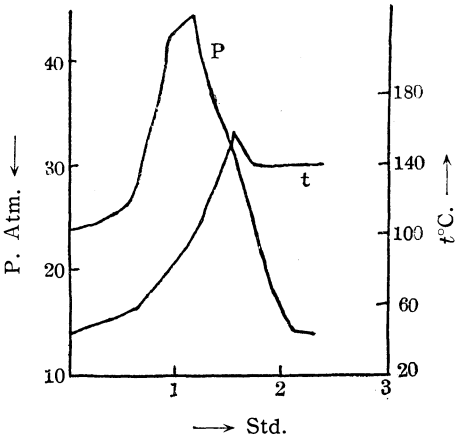


Fig. 2. Nr. 628

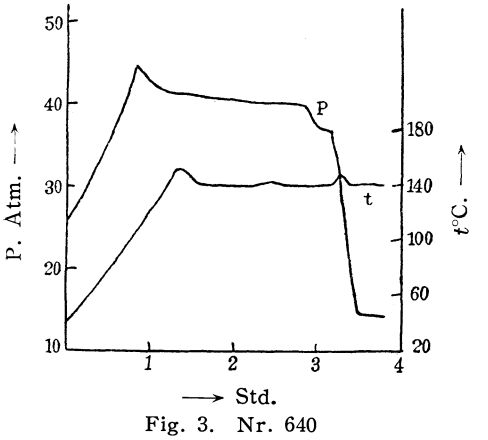


Fig. 3. Nr. 640

c) Über die Nebenreaktionen. — Wenn die eingeleitete Menge von Gasgemisch klein ist, finden die Nebenreaktionen auch in geringem Umfang statt. Mit steigender Gasmenge jedoch werden sie verschieden beobachtet. Abgesehen von der Polymerisation des gebildeten Acrylesters werde ich hier über diese berichten, welche zu dem Reaktionsmechanismus in Beziehung stehen.

1. Nebenprodukte mit niedrigem Siedepunkt. — Man liess das vom Reaktionsprodukt mit Wasserdampf abdestillierte Rohacrylester nach Waschen und Trocknen mit Calciumchlorid abtropfen. 383 g Vorlauf (bis 70°) fraktionierte man als Probe mit Widmer's Kolonne 2 m lang und erhielt die folgenden Resultate.

Die Fraktion 1 enthält eindeutig etwas Acetaldehyd und Äthyläther, welche beide sich von Äthanol herausbildeten. Die Fraktionen 2 und 3, die schwerer als Wasser sind, enthalten noch eine ziemliche Menge Äthyl-

TABELLE VI

FRAKTIONIERUNG VON VORLAUF

Fraktion	Kp. (°C)	Gewicht (g.)	n_D^{20}	Note
1	20— 50	13.3	1.3575	Starker Geruch von CH_3CHO u. $(C_2H_5)_2O$
2	70— 80	29.8	1.4000	Schwerer als Wasser
3	80— 98	103.8	1.3796	Äthylacrylatreich
4	98—100	176.0	1.3990	Reines Äthylacrylat
5	Rest	10.0		

acrylat, das durch Verseifung unter Schütteln mit 2N-Natronlauge bei gewöhnlicher Temperatur grösstenteils beseitigt wird. Von diesen Fraktionen wurde eine Probe als Hauptteil bei der Wiederfraktionierung erhalten, die die physikalischen Eigenschaften, Kp. 73°, n_D^{20}, 1.4980 d_{15}^{20} 1.8158 besass, und deren Jodgehalt 73% analytisch bestimmt wurde. Folglich kann man vermuten, dass der Hauptbestandteil von diesen Fraktionen Äthyliodid (Kp. 72.5°, n_D^{25} 1.5125, d_{15}^{20} 1.9330, Jodgehalt 81.8%) sein dürfte, und dass es sich bei der Acrylesterbildung nebenbei bildet.

Wie es später noch näher beschrieben ist, nimmt die folgende Reaktion eng an dem Mechanismus teil, wodurch das Kohlenoxyd aktiviert wird.

$$NiX_2+4CO \longrightarrow Ni(CO)_4+2X$$

Die Bildungen solcher Nebenprodukte werden demnach unter Annahme der Wirkungen des Jods in naszierendem Zustand völlig aufgeklärt, d.h., wie folgt;

$$\left.\begin{matrix}CH_3CH_2OH\\CH_3CH_2OH\end{matrix}\right\} + 2J \longrightarrow \left[\begin{matrix}CH_3CH_2OJ\\CH_3CH_2J\end{matrix}\right] \longrightarrow \begin{matrix}CH_3CH_2\\CH_3CH_2\end{matrix}\!\!>\!O + J_2 + H_2O$$

$$J_2 + H_2O \longrightarrow HJ + HJO; \quad C_2H_5OH + HJ \longrightarrow C_2H_5J + H_2O$$

$$C_2H_5OH + HJO \longrightarrow CH_3CHO + H_2O + HJ$$

Die Annahme kann ferner dadurch unterstützt werden, dass die Anwesenheit von Jodwasserstoffsäure im Abgase bei der Acrylester-Synthese durch die Behandlung mit Silbernitratlösung bestätigt wird.

2. Hochsiedende Nebenprodukte. — Am Ende der Wasserdampfdestillation vom Reaktionsprodukt wird das als Wasser schwerere Ölprodukt erhalten. Dies siedet bei 78° bis 81° unter vermindertem Druck von 4 mm. Hg. und wird mit der empirischen Formel $C_2H_{3-4}O$ repräsentiert. Behandelt man dies mit konzentriertem wässrigem Ammoniak, so kann man zweierlei kristallinische Substanzen erhalten. Die eine schmilzt bei 242 bis 243° und wird mit der empirischen Formel C_2H_4ON repräsentiert, dementgegen schmilzt die andere bei 262° unter Zersetzung und wird mit der Formel C_2H_3ON benannt. Da die erstere dem Bernsteinsäurediamid ($(CH_2CONH_2)_2$ Smp. 243°) und die letztere dem Fumarsäurediamid ($(CHCONH_2)_2$ Zers. 267°) entspricht, so wird die Anwesenheit von Bernsteinsäure- und Fumarsäurediäthylester in dem ursprünglichen Produkt bestätigt. Ich[6] teilte früher mit meinem Mitarbeiter darüber mit, dass die Bildung von Fumarsäureester ihren Ursprung in der Dehydrierung von Bernsteinsäureester, das sich durch die Anlagerung von Alkohol und Kohlenoxyd an der Doppelbindung von Acrylester bildet, hat. Auch Pino[7] hat jüngst eine derartige Meinung veröffentlicht.

Schlusswort

In vorliegender Abhandlung habe ich vorbereitend die Arbeitsmethode und einiges über die Erkenntnis bei der Acrylestersynthese unter der Anwendung vom Nickelhalogenid-Katalysator mitgeteilt, welche alle bei den folgenden Erörterungen über den Mechanismus der Aktivierung des Kohlenoxyds nötig sein dürften.

Herr Dr. K. Yoshikawa hat mich stets bei meinen Arbeiten leitend unterstützt und ermutigt. Herr K. Sato hat mit mir eifrig mitgearbeitet. Und ich spreche diesen Herren und der Mitsui Chemical Industry Co., die mir diese Veröffentlichung meiner Arbeiten erlaubte, hierdurch meinen herzlichen Dank aus.

Mitsui Chemical Industry Co. Ltd.
Miike Dyestuff and Chemical Works,
Omuta, Fukuoka

6) K. Yamamoto und K. Sato: Vortrag im Kongress der japanischen chemischen Gesellschaft-Kyuschu-Zweigabteilung am 24. 11. 1950.

7) P. Pino, *J. Am. Chem. Soc.*, **74**, 5551 (1952).

Zur Kenntnis über die Hochdrucksynthese von Acrylester. II. Über das Verhalten des unter Druck Stehenden Kohlenoxyds auf das Nickelhalogenid

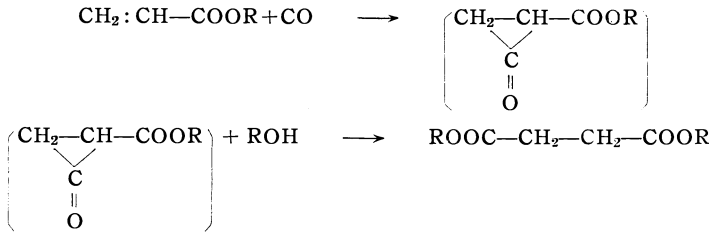
Von Kazumi YAMAMOTO und Kazutoshi SATO

(Eingegangen am 24. April 1954)

Einleitung

Yamamoto[1] hat in Bezug auf die Acrylestersynthese aus Acetylen, Kohlenoxyd und Alkohol unter der katalytischen Wirkung von Nickelhalogenid mitgeteilt, dass die Reaktion über eine Latenzperiode schnell verläuft, und dass die Aktivität von Nickelhalogenide in einer Reihe Jodid, Bromid, Chlorid stark abfällt, und dass sowohl das Alkylhalogenid als auch der Halogenwasserstoff für Nebenprodukte nachgewiesen werden, usw.

Wir möchten hier über die Beziehung zwischen diesen Erscheinungen und dem Reaktionsmechanismus, insbesondere über das Verhalten des Kohlenoxyds, erwähnen. Wie in Mitteilung I erwähnt, wird die Bildung von Acrylester nach der Cyclopropenon-Hypothese von Reppe künstlich aufgeklärt. Auch die von Bernsteinsäureester kann ebenso dieser Hypothese gemäss einbegriffen werden;



Folglich kommt es darauf an, auf welche Weise das Kohlenoxyd aktiviert wird. Reppe hat, wie schon erwähnt, diesen Mechanismus dadurch erklärt, dass mit Kohlenoxyd zunächst das unbekannte, sehr instabile und deshalb sehr reaktionsfähige $NiCOX_2$ entsteht, das unter Abgabe von aktiviertem Kohlenoxyd wieder als rückgebildetes $NiBr_2$ von neuem mit Kohlenoxyd reagiert.

$$NiX_2 + CO \rightleftarrows CO\text{-}NiX_2$$

Aber der experimentelle Beweis darüber wird nicht gezeigt.

Unsere Arbeiten hatten ihren Ursprung an dem grossen Interesse der "Latenzperiode", die in voriger Mitteilung beschrieben wurde. Als wir während der Latenzperiode den Autoklav schnell abkühlten und dessen Inhalt untersuchten, wiesen wir zufällig eine erhebliche Menge Nickelcarbonyl nach. Demnach führte uns das zu einem Zweifel, dass der wirkliche Katalysator nicht das Nickelhalogenid sein könnte, ja vielmehr Nickelcarbonyl ist. Aus diesem Grunde fassten wir damals die erhebliche Wirkung des Nickelhilfskatalysators oder die Erscheinung der Latenzperiode so auf, dass jene als Akzeptor des von Nickelhalogenid freigemachten Halogens wirken, und die Bildung von echtem Katalysator Nickelcarbonyl erleichtern könnte;

$$NiX_2+4CO \longrightarrow Ni(CO)_4+2X$$
$$2X+Ni \longrightarrow NiX_2 \qquad Ni(CO)_4 \longrightarrow Ni+4CO$$

und dass die Latenzperiode die Periode zur Erreicherung einer Konzentration von Nickelcarbonyl sein könnte. Dann haben wir es experimentell feststellen wollen. Diese Arbeiten werden hauptsächlich in vier Klassen eingeteillt, d.h.:

1) Die Bildung von Nickelcarbonyl aus den verschiedenen Nickelverbindungen.
2) Die Bildung von Nickelcarbonyl aus den Nickelhalogeniden in Anwesenheit von dem Zusatzmetell.
3) Der Zusammenhang zwischen der Acrylestersynthese und den oben erwähnten Faktoren.
4) Die Ätzung von dem Reaktionsgefäss.

Reaktion verschiedener Nickelverbindungen mit Kohlenoxyd in Anwessenheit von Alkohol

Nimmt man an, dass Nickelcarbonyl, das mit Acetylen und Alkohol reagiert, durch die Einwirkung von Kohlenoxyd auf das Nickelhalogenid in Alkohol gebildet wird, so

1) K. Yamamoto, Dieses Bulletin, **27**, 491 (1954).

müsste es ein wichtiger Leitfaden zur Lösung vom Mechanismus sein, die Neigung des Nickelcarbonylbildungsbestrebens der Nickelverbindungen zu erkennen.

Das Experiment wurde wie folgt durchgeführt. Man zog 30 cm^3 Äthanol und einige Gramm Nickelverbindung in das Druckgefäss von 130 cm^3 Inhalt (18:8-Stahl) hinzu und erwärmte es nach der Einpressung von Kohlenoxyd (Anfangsdruck 70 Atm). Dieser Kohlenoxyddruck war zwar höher im Vergleich mit dessen Teildruck bei der Acrylestersynthese, aber es dürfte unter Berücksichtigung folgender Sachen zweckmässiger sein:

1) Unterdrückung vom Zerlegen des gebildeten Nickelcarbonyls der erhöhten Temperatur wegen.
2) Vergrösserung vom Reaktionsverlauf.
3) Im Falle der Acrylestersynthese gibt es den Akzeptor von Nickelcarbonyl.

Im Experiment wurde die qualitative Beobachtung gemacht, und die Ausbeute von Nickelcarbonyl vom Unterschied zwischen dem Anfangs-und Enddruck vom Kohlenoxyd berechnet. Man liess den Autoklav langsam erwärmen und hielt die Temperatur, wobei der Druckabfall stattzufinden begann. Als der Druckabfall sehr langsam wurde, steigerte die Temperatur sich wieder. Auf solche Weise beobachtete man den Verlauf der Hauptreaktionstemperatur, der als Kennzeichnung der Reaktionsfähigkeit der Nickelverbindung von Bedeutung wäre. Die Resultate sind in der Tabelle I gezeigt.

TABELLE I

NICKELCARBONYL AUS NICKELVERBINDUNGEN

Nr.	Ni-Verbg. (g)	Reaktionstemp. in°		Laufzeit		$Ni(CO)_4$ (%)	Aufgelös. Fe
		Haupt.	Max.	(Std)	(Min)		
C-12	Ni 6 auf Kiesg.	Raumtemp.	155	4	10	78	+
C-13	Ni 4 auf Kiesg. $(NH_4)_2S$ aq. 0.5	,,	110	1	45	83	+
C-14	NiS 6 $(NH_4)_2S$ aq. 0.5	90–110	170	4	45	24	
C-30	$NiCl_2$6 $(NH_4)_2S$ aq. 0.5	120–150	160	6	—	10	++
C-17	$NiJ_2$10	120–150	180	3	30	100	+++
C-29	Ni-Acetat 8	—	190	2	30	—	
C-31	$NiCl_2$ 5.7	120–150	210	2	30	78	+++

Note: Die letzte Spalte stellt die aufgelöste Eisenmenge qualitativ dar.

Das in den Experimenten Nr. C-12 und C-13 benutzte Nickel ist eben ein und dasselbe, welches als Hilfskatalysator bei der Acrylestersynthese angewandt wurde. Folglich würde vermutlich bei der Acrylestersynthese trotz des niedrigen Teildrucks von Kohlenoxyd eine ziemliche Menge Nickelcarbonyl daraus gebildet werden. Als Eigentümlichkeit der Nickelhalogeniden wie C-17 und C-31 kann man folgendes erörtern:

1) Erhebliche Menge Eisenion ist nachweisbar.
2) Ausser dem Nickelcarbonyl bildet sich die flüchtige Substanz Eisenpentacarbonyl, dessen Nachweis mit der wässrigen Lösung von Sublimat[2] durchgeführt wird.

Da die Quelle von diesem Eisen nichts anderes als die Gefässwand ist, könnte dies als Resultat der folgenden Reaktion aufgeklärt werden;

$$NiX_2 + 4CO + Fe \xrightarrow[\text{Gefässwand}]{} Ni(CO)_4 + FeX_2$$

Eisenhalogenid löst sich in Alkohol und dadurch wird die folgende Ätzung der Gefässwand erleichtert. Die Bildung von Eisenpentacarbonyl dürfte gleich mit der des Nickelcarbonyls sein;

$$FeX_2 + 5CO \longrightarrow Fe(CO)_5 + 2X$$

Dies ergibt die Auflösung von 0.05 bis 0.2% Eisen bei der Acrylestersynthese.

Bildung von Nickelcarbonyl in Anwesenheit von verschiedenen Beimetallen oder verschiedener Verbindung

Von den Resultaten voriger Paragraphen wird vermutet, dass die Bildung von Nickelcarbonyl weitaus leichter wird, wenn das mit dem von Nickelhalogenid freigemachten Halogenatomen leicht zu verbindende Metallpulver hinzugefügt wird. Die unter dieser Annahme durchgeführten Resultate sind in der Tabelle II zusammengefasst.

2) H. Hock u.a., *Ber.*, **61**, 2037 (1928).

TABELLE II

NICKELCARBONYL AUS HALOGENIDEN

Nr.	NiX_2 (g)	Anlage (g)	Reaktionstemp. Haupt.	Reaktionstemp. Max.	Laufzeit (Std)	Laufzeit (Min)	$Ni(CO)_4$ (%)	Gelös. Fe	Note
C-17	NiJ2 10	—	120–150	180	3	30	100	+++	
C-20	,,	Cu 4	Raumtemp.	150	2	30	77		CuJ-Bild.
C-22	,,	Hg_2O 5	,,	180	2	00	39		HgJ_2– ,,
C-31	$NiCl_2$ 5.7	—	120–150	180	2	30	78	+++	
C-23	,,	Cu 4	60–130	142	2	10	43	+	
C-25	,,	A1 2	60–160	178	2	10	34	++	

Note: Jede Anlage kam im Überschuss zur Verwendung. Die Ausbeute von Nickelcarbonyl wurde von dem Druckabfall berechnet.

Wie vermutet erschienen die Effekte der Anlage im Fall des Nickeljodids eindeutig als Erniedrigung der Reaktionstemperatur und Verminderung der Ätzung von der Gefässwand. Bei dem Chlorid war die Lage analog, wenn der auch Grad niedrig gewesen ist. Dies zeigt, dass der Unterschied zwischen dem Jodid und Chlorid in der Bindung Nickel-Halogen sehr wesentlich ist, d.h., bei dem Jodid ist die Bindung mehr nichtionisch als bei dem Chlorid. Der Unterschied ist mit dem der katalytischen Wirkung in der Ordnung analog. Folglich deutet dies auf eine Richtung zur Forschung von neuem Katalysator. Die anfängliche Erwartung war, dass der wesentliche Katalysator bei der Acrylestersynthese nicht das Nickelhalogenid sein könnte, sondern Nickelcarbonyl. Den Fall gesetzt, dass man Nickeljodid mit dem Beimetall wie Cu, Hg, Ag oder Zn verwendet, so könnte unter der Bildung von Nickelcarbonyl die Acrylestersynthese erleichtert werden. Dieses trat nicht ein sondern darüber hinaus wurde die Bildung von Acrylester bei der Verwendung von Nickelcarbonyl vielmehr erschwert. Es bedeutet dies, welche wichtige Rolle die Halogenatome spielen, denn das Beimetall wie Cu nimmt unter der starken Verbindung mit dem Halogenatom dessen Funktion fort.

Beziehung zwischen dem Beimetall und der Ätzung von Gefässwand

Wie schon nach Hieber[3] in Bezug auf die Kobaltverbindung beschrieben, wird die Reaktion von Nickelhalogenid mit Kohlenoxyd in Anwesenheit vom Beimetall im Sinne der Gleichungen dargestellt:

$$NiX_2+4CO \longrightarrow Ni(CO)_4+X_2+Q_1 \quad (1)$$

$$M+X_2 \longrightarrow MX_2+Q_2 \quad (2)$$

wobei das Beimetall M mit der grösseren Wärmetönung Q_2 fester mit den Halogenatomen verbindet, sodass es die Reaktion (1) leicht nach rechts dringen lässt.

Die betreffenden Werte sind hinsichtlich der Jodide und Chloride in den Literaturen wie folgt veröffentlicht:

Jodid	Mg	Zn	Hg	A1	Cu	Fe	Ni
Q_2 in kcal./mol.	84.8	49.8	47.8	44.0	32.2	30.1	23.0
Chlorid	Mg	A1	Zn	Fe	Ni	Cu	Hg
Q_2 in kcal./mol.	151.0	111.3	98.4	82.1	74.5	65.2	61.8

In der obigen Tabelle wechselt die Zusammensetzung der Metalle bei Jodide mit denen von Chloride. Demnach sollten die Zustände der Ätzung von der Gefässwand zwischen der Reaktion von Nickeljodid mit Kohlenoxyd in Anwesenheit von solchen Beimetallen wie Cu oder Hg, entgegengesetzt von denen wie Nickelchlorid unter den gleichen Bedingungen, gehen. Die Folgenden experimentellen Resultate stellen dies dar. In den Tabellen III und IV sind die Bedingungen zur Bildung von Nickelcarbonyl aus Nickelchlorid und Jodid in Anwesenheit von Beimetall gezeigt.

Diese Experimente wurden mehr quantitativ durchgeführt als die in der Tabelle II gezeigten. Die Ausbeuten wurden auf Grund von dem verbrauchten Nickelhalogenid berechnet. Auf solche Weise wurde der Wert von Nr. C-25 in der Tabelle II durch den von C-36 in der Tabelle III korrigiert. Wie aus dem Vergleich der Werte in C-41 und 42 ersehen, ist die Korngrösse von dem Beimetall bemerkenswert. Wenn man das feine Magnesiumpulver wie Korngrösse (c) unter der Berücksichtigung dieser Umstände benutzt, so würde man den grössten Erfolg haben. Dies zeigt, dass sowohl die Ätzung der Gefässwand als auch das Gebiet der Hauptreaktionstemperatur von der Bildungswärme Q_2 beherrscht wird. Ferner ist von dem Resultat in C-49, unter Verwendung

3) W. Hieber, *Z. anorg. allg. Chem.*, **243**, 145 (1939).

TABELLE III

NICKELCARBONYL AUS CHLORID

Nr.	Beimetall (Korngrösse)	Reaktionstemp. (°C)	Laufzeit (Std)	Laufzeit (Min)	Gelöst. Fe (g)	Unreag. $NiCl_2$ als Ni (g)	$Ni(CO)_4$ (%)
C-35	Hg	130–140	2	30	0.35	0.20	87
C-36	Al (c)	16– 70	1	30	0.04	0.00	100*
C-37	Cu (c)	80–120	5	20	0.39	0.47	70
C-41	Mg (a)	70–130	3	20	0.00	0.24	85*
C-38	Zn (c)	65– 80	2	10	0.03	0.33	79
C-42	Zn (b)	75– 85	3	50	0.04	0.26	83

Note: $NiCl_2$ 5.7 g Äthanol 30 cm^3 CO-Anfangsdruck 70 Atm. Beimetallmenge etwas Überschuss. Korngrösse (a) ca. 20 Mesch, (b) ca. 50 Mesch und (c) ca. 100—200 Mesch. * Alkoholatbildung.

TABELLE IV

NICKELCARBONYL AUS JODID

Nr.	Beimetall (Korngrösse)	Reaktionstemp. (°C)	Laufzeit (Std)	Laufzeit (Min)	Gelöst. Fe (g)	Unreag. NiJ_2 als Ni (g)	$Ni(CO)_4$ (%)
C-43	Hg	90–100	2	00	0.03	0.51	73
C-46	Zn (c)	20– 50	3	00	Spur	0.06	96
C-20	Cu (c)	20–100	2	30	Spur	—	90
C-48	Ni (c)	20–100	6	00	0.37	0.11	95
C-49	Ni (b)	90–100	5	30	0.36	0.06	98

Note: NiJ_2 6.9 g Äthanol 30 cm^3.

eines üblichen Nickelpulvers denkbar, dass die Hilfskatalysatorwirkung von Nickel wie anderer Beimetalle, bei der Acrylestersyntese, durch die Wirkung als Akzeptor für freigemachte Halogenatome sein kann.

$$NiJ_2+4CO+Ni^* \longrightarrow Ni(CO)_4+Ni^*J_2$$

Wir sind demnach zum Schluss gelangt, dass das als Hilfskatalysator benutzte Nickel besonders in dem reduzierten, aktiven Zustand nicht zu sein braucht, sondern in der körnigen oder geschnittenen Form auch verwendbar ist.

Lebensdauer von Katalysator und Ätzung von Gefässwand

Wir dachten zuerst die Ätzung der Gefässwand hätte ihren Ursprung in der Bildung von Eisenpentacarbonyl, das sich durch die Einwirkung von Kohlenoxyd unter Druck auf die Gefässwand bildet. Daraufhin wurde Äthanol mit Kohlenoxyd unter 100 Atm Druck bei 150° zwei Stunden lang erhitzt, aber die Bildung von Eisencarbonyl konnte nicht beobachtet werden. Unter Berücksichtigung der Einwirkung von Jod im Molekularzustand wurde die alkoholische Lösung von Jod unter der gleichen Bedingung behandelt, jedoch die Auflösung von Eisen wurde gleichfalls nicht beobachtet, sondern nur die Bildung von Äther. Wir können also nicht umhin anzunehmen, dass die Ätzung ihren Ursprung hauptsächlich in der Einwirkung von Jod in dem naszierenden Zustand hat.

Eisenpentacarbonyl, dessen Anwesenheit durch die Reaktion mit der wässrigen Lösung von Sublimat[2] festgestellt ist, wird sich durch die Reaktion zwischen dem Eisenjodid und dem unter Hochdruck stehenden Kohlenoxyd bilden. Die Auflösung von Eisen bringt nicht nur die Ätzung von Autoklav bei der Acrylestersynthese, sondern gibt auch den Anlass von dem Verlust des Katalysators.

Auch der Zusatz von Nickelpulver kann die Auflösung von Eisen nicht hemmen, wird leicht davon verstanden werden, und wie aus der Tabelle III hervorgeht, ist die Bildungswärme von FeX_2 grösser als die von NiX_2. Wenn man auf Grund der in vorigem Paragraphen beschriebenen Schlussfolgerung, das Reaktionsgefäss mit Nickel bekleidet oder plattiert, so kann man das Hindernis der Ätzung und die Vergrösserung der Reaktionsgeschwindigkeit darauf erwarten. Das Experiment hatte dieses Ergebnis.

In 100 cm^3 Inhalt Autoklav, der dicht vernickelt wurde, setzten wir 24 g Äthanol und 0.12 g Nickeljodid ein und erhitzten dieses Gemisch auf 150 bis 160° unter 30 Atm Druck vom Acetylen-Kohlenoxyd-Gasgemisch. Wir beobachteten dabei den sehr glatten Reaktionsverlauf.

Die starke kondensierende Wirkung des

gebildeten FeJ_2 oder FeJ_3 gibt einen Anlass für die nicht wünschenswerte Polymerisation oder Kondensation von Acetylen oder Acrylester.

Zum Beispiel, wenn die Reaktion in Anwesenheit von Nickelchlorid und Aluminium durchgeführt wird, ist die Bildung von dem harzartigen Produkt wunderbar. Somit wird aufgeklärt, dass die Auskleidung von Autoklav mit Nickel zur Verbesserung der Ausbeute von Acrylester beiträgt[4].

Betrachtungen über die Rolle der Halogenatome in NiX_2

Es wurde bisher beschrieben, dass das Nickelcarbonyl selbst als Katalysator für die Acrylestersynthese nicht genügend ist und dass die Halogenatome dabei eine wichtige Rolle spielen. Dies wurde auch durch das folgende Experiment gezeigt, welches diskontinuierlich im 270 cm^3 Inhalt Autoklav in Anwesenheit von Nickeljodid und Kupfer durchgeführt wurde. Die Resultate sind in der Tabelle V zusammengefasst.

TABELLE V

ACRYLAT-SYNTHESE MIT NiJ_2 UND Cu

Äthanol (g)	NiJ_2 (g)	Cu* (g)	Druck von Gasgemisch	Reaktionstemp. (°C)	Laufzeit (Std)	Laufzeit (Min)	Restdruck Atm
40	2	0	35 at.	160	2	30	0
40	2	1.0	35	150–180	6	40	26.5
40	2	1.0	35	150–180	14	00	25
40	2	0.3	35	160–200	7	00	21

* Die dem Jod in 2 g. NiJ_2 entsprechende Kupfermenge ist 0.4 g.

Mit Anwesenheit von Kupfer wurde die Bildung von Acrylat trotz der Bildung von Nickelcarbonyl beinahe nicht beobachtet.

Die Hinzufügung aber des metalischen Nickels erleichtert die Bildung von Acrylester. Von diesen Tatsachen könnte man erwarten, dass die Erniedrigung der zur Bildung des Cyclopropenons erforderlichen Aktivierungsenergie durch die Bildung irgendeines intermediären Zwischenproduktes erreicht wird, welches sich durch die Umsetzung von Kohlenoxyd und Nickelhalogenid, bevor das Nickelcarbonyl zusammengesetzt wird, bildet und dass das Halogenatom des Nickelhalogenids die wichtige Rolle spielen sollte, mit anderen Worten, dass das Halogenatom vom Nickelhalogenid nicht weggenommen werden müsste. Hierauf möchten wir etwas über die Latenzperiode ausführen. Während der Latenzperiode bei der Acrylestersynthese wurde das Nickelcarbonyl zufällig im Reaktionsgefäss gefunden, und wie schon gezeigt, liess uns diese Beobachtung eine Reihe der Arbeiten ausführen. Jedoch wurde es klar in den Arbeitungsvorgängen, dass die Latenzperiode nicht gerade mit der Bildung des Nickelcarbonyls zusammenhängt, sondern sie hauptsächlich von dem Sauerstoffgehalt im Gasgemisch abhängig ist, d.h., während sie in Abwesenheit von Sauerstoff kaum auftritt, beträgt sie 1 Stunde in Anwesenheit von 0.2% und 1.5 Stunden bei 0.3% bzw. unter den gleichen Bedingungen. Da Nickeljodid durch Sauerstoff unter der Abscheidung von Jod leicht oxydiert wird, so wird die Latenzperiode dargestellt als die beanspruchte Zeit bis zum Verschwinden des abgeschiedenen Jods unter der Umsetzung mit dem Alkohol oder mit der Gefässwand. Auch die Verkürzung der Latenzperiode durch die Hinzufügung von Nickel oder die Steigerung von der Temperatur wird dadurch erläutert. Zur Illustration des Schlusses kann man die folgende Beobachtung anführen. Fügt man absichtlich freies Jod und Eisenpulver ins Reaktionensystem hinzu, so kann man beobachten, dass die Reaktion erst nach der langen Latenzperiode stattfindet.

Selbst eine Nickelverbindung wie Borat, Formiat, Phosphat, Dimethylglyoxymnickel oder Acetoessigsäureester-Nickel als Katalysator für die Acrylestersynthese ist nicht erwünscht. Von den bisher erwähnten Tatsachen zieht man den Schluss, dass die aus Nickel und solchen negativen Atomen oder Atomgruppen zusammengesetzten Verbindungen als Hauptkatalysator gelten, wie sie sich mit dem Nickel nichtionisch verbinden und das Metall leicht angreifen können. Als solche Atome order Atomgruppen kann eine Reihe sogenannter Pseudohalogene von Birkenbach[5] angegeben werden. Deren elektrische Negativität nach folgender Reihe angeordnet sind:

F, CNO, Cl, N_3, Br, CN, SCN, J, SeCN.

Aus dem Resultat der Acrylestersynthese, welches in Anwesenheit von dem nach Grossmans Verfahren[6] hergestellten Nickelthio-

4) K. Yamamoto und K. Sato, *J.P.*, 197, 084.

5) L. Birkenbach, *Ber.*, **58**, 2377 (1925).

6) H. Grossman, *Ber.*, **37**, 565 (1904).

cyanat erfolgte, wurde wie in obiger Reihe vermutet, festgestellt, dass dessen katalytische Fähigkeit, abgesehen von der polymerisierenden Einwirkung, zwischen Nickelbromid und Jodid gestellt wird.[7]

Yatsimirskii[8] hat den Beteiligungsgrad von dem ionischen Charakter in der Bindung zwischen Nickel und Halogenatom wie folgt berechnet:

$NiCl_2$ 53%, $NiBr_2$ 48%, $Ni(SCN)_2$ 45%, NiJ_2 39%

Dies unterstützte auch unsere Meinung.

Zusammenfassung

In der vorliegenden Mitteilung wurde das Verhalten des unter Druck stehenden Kohlenoxyds gegen das Nickelhalogenid in Alkohol in Anwesenheit von den verschiedenen Beimetallen oder anderen Anlagen beschrieben. Zugleich wurde die Rolle des Halogenatoms von Nickel halogenid bei der Acrylestersynthese erörtert, von dem Gesichtspunkt der Ätzung der Gefässwand sowohl, als auch der Lebensdauer des Katalysators aus gesehen.

Darüber hinaus haben wir von diesen experimentellen Resultaten geschlossen, dass die katalytische Fähigkeit der Nickelhalogenide von dem Beteiligungsgrad des ionischen Charakters der Bindung zwischen dem Nickel- und Halogenatom abhängig ist.

Herr Dr. K. Yoshikawa hat uns stets bei unseren Arbeiten leitend unterstützt und ermutigt. Wir sprechen ihm und der Mitsui Chemical Industry Co. Ltd., die uns die Veröffentlichung dieser Arbeiten erlaubte, unseren herzlichen Dank aus.

Diese Arbeiten wurden am 24. 11. 1950 in Kumamoto im Rahmen des Kongresses der japanischen chemischen Gesellschaft — Kyushu — Zweigabteilung mündlich veröffentlicht.

Mitsui Chemical Industry Co. Ltd.
Miike Dyestuff and Chemical Works,
Omuta, Fukuoka

7) K. Yamamoto und K. Sato, *J.P.*, 197, 033.
8) K. B. Yatsimirskii, *Izvest. Akad. Nauk USSR.*, 590 (1948), *C.A.*, **43**, 2329 (1949).

Zur Kenntnis über die Hochdrucksynthese von Acrylester. III. Zur Kenntnis über die Herstellung von Triphenylphosphin-Nickelkomplex-Verbindungen

Von Kazumi YAMAMOTO

(Eingegangen am 24. April 1954)

Einleitung

In den bisherigen Mitteilungen[1] wurde das Verhalten des unter Druck stehenden Kohlenoxyds an Nickelhalogenid Katalysator erörtert. In der vorliegenden Mitteilung sind die Herstellungsverfahren der Triphenylphosphin-Nickelhalogenid-Komplexverbindungen beschrieben, die von Reppe[2] als Katalysator bei der Acrylatsynthese gefunden wurden. Diese Verbindungen, die in der ausgezeichneten Weise allen Anforderungen, z. B. kleine Nebenreaktion, lange Lebensdauer, leichte Zurückgewinnbarkeit wegen deren guter Kristallisierbarkeit, entsprachen, werden im allgemeinen in folgende vier Klassen eingeteilt:

1. $(Ph_3P)_xNi(CO)_{4-x}$
2. $(Ph_3P)_2NiX_2$
3. $(Ph_3P)_2NiX_2RX'$
4. $(Ph_3P)_2NiX_22RX'$

wobei Ph den Phenylrest (C_6H_5)- ausdrückt und x im allgemeinen 1 oder 2, R die Alkyl- oder Arylgruppe, und X und X' dasselbe oder verschiedene Halogenatom ausdrücken.

Über die Aufklärung des Mechanismus der Aktivierung des Kohlenoxyds könnte ich nur die in Copenhaverschem Buch[3] angeführte Annahme von Schweckendiek, der der Mitarbeiter von Reppe ist, und die von McKinley[4] angeben. Wie später ausführlich behandelt, dürfte die erstere einen Widerspruch enthalten und die letztere ginge nur von dem Rahmen des Gedankens nicht aus.

Ich habe darüber einen Erfolg aufgrund der zusammenfassenden Resultate betreffs der Verfahren zur Herstellung, und der chemischen, physikalischen Eigenschaften von Kom-

1) K. Yamamoto, Dieses Bulletin, **27**, 491, 496 (1954).
2) W. Reppe, "Neue Entwicklungen auf dem Gebiet der Chemie des Acetylens und Kohlenoxyds", Springer Verlag (1949) S. 103.
3) Copenhaver und M. Bigelow, "Acetylene and Carbonmonoxide Chemistry", Rheinhold Publ. Co. (1949) S. 259.
4) C. McKinley, *Ind. Eng. Chem.*, **44**, 995 (1952).

komplexverbindungen und betreffs deren Verhalten bei der Acrylestersynthese zu verzeichnen.

Herstellung von Triphenylphosphin.—Triphenylphosphin, das der Grundstoff ist, wurde durch das Verfahren von Michaelis[5] aus Natrium, Chlorbenzol und Phosphortrichlorid hergestellt.

$$3C_6H_5Cl+6Na+PCl_3 \rightarrow 6NaCl+(C_6H_5)_3P$$

Nach Michaelis wird es unter Anwendung von Äther als Lösungsmittel durch Erhitzen bei dessen Kochpunkt 48 Stunden lang mit der Ausbeute von 30% der Theorie auf Grund von Chlorbenzol erhalten. Auch wurde mitgeteilt, dass die Bildung vom harzartigen Produkt erheblich war, wenn Benzol an statt Äthers verwendet wurde. Ich habe es aber dadurch in Benzol mit der Ausbeute von 50 bis 60% erhalten können[5], weil ich die Reaktion bei 60°, 6 Stunden lang in Anwesenheit vom Katalysator wie Äthylacetat, -Malonat, -Acetacetat durchführte.

Herstellung von $(Ph_3P)_xNi(CO)_{4-x}$.—Die Komplexverbindungen dieses Typus sind unmittelbar nicht wichtig für Katalysator bei der Acrylestersynthese und sie nützen zur cyclisierenden Polymerisation des Acetylens[7], aber ich möchte deren Herstellungsveafahren kurz darstellen, da es mit der Herstellung der Komplexverbindungen von $(Ph_3P)_2NiX_2$ und mit dem Mechanismus in Beziehung steht.

Wenn man Triphenylphosphin in Methanol auf Nickelcarbonyl einwirken lässt, so kann man Triphenylphosphin-Nickeltricarbonyl oder Bistriphenylphosphin-Nickeldicarbonyl bei 20° bzw. 50° erhalten:

$$Ph_3P+Ni(CO)_4 \xrightarrow{20°} \underset{\text{Zp. } 123°}{Ph_3PNi(CO)_3}+CO$$

$$2Ph_3P+Ni(CO)_4 \xrightarrow{50°} \underset{\text{Smp. } 206\text{–}9°}{(Ph_3P)_2Ni(CO)_2}+2CO$$

Anstatt des Triphenylphosphins kann man die Komplexverbindung von Triphenylphosphin mit Schwermetallhalogenid verwenden, z. B.;

$$(Ph_3P)_2ZnCl_2+2Ni(CO)_4 \rightarrow 2Ph_3PNi(CO)_3+2CO+ZnCl_2$$

$$(Ph_3P)_2ZnCl_2+Ni(CO)_4 \rightarrow (Ph_3P)_2Ni(CO)_2+2CO+ZnCl_2$$

In diesen Verfahren muss man sehr giftiges Nickelcarbonyl verwenden. Ich habe diese Verbindung dadurch quantitativ herstellen können[8], weil ich Triphenylphosphin und reduziertes Nickelpulver in Methanol bei 150° mit Kohlenoxyd unter Druck von 50 Atm unmittelbar behandelte:

$$2Ph_3P+Ni+2CO \rightarrow (Ph_3P)_2Ni(CO)_2$$

Herstellung von $(Ph_3P)_2NiX_2$.—Reppe hat die folgenden drei Verfahren zur Herstellung der Komplexverbindung von Typus $(Ph_3P)_2NiX_2$ veröffentlicht. Zwei derselben[7] bringen das oben beschriebene Bistriphenylphosphin-Nickeldicarbonyl als Ausgangsstoff zur Verwendung und das andere ist das Verfahren, wodurch die Komplexverbindung aus dessen Bestandteile aufgebaut wird[9].

1. $(Ph_3P)_2Ni(CO)_2+2C_4H_9X+2C_4H_9OH \rightarrow (Ph_3P)_2NiX_2+2C_4H_9COOC_4H_9+H_2$
2. $(Ph_3P)_2Ni(CO)_2+X_2 \rightarrow (Ph_3P)_2NiX_2+2CO$
3. $2Ph_3P+NiX_2 \rightarrow (Ph_3P)_2NiX_2$

Das Verfahren (1) muss im Druckgefäss bei 180° durchgeführt werden, darüber kann die Beimengung von der Komplexverbindung $(Ph_3P)_2NiX_2RX$ nicht vermieden werden. Das Verfahren (2) kann in Benzol bei der gewöhnlichen Temperatur durchgeführt werden. Aber es ist wegen der Bildung von dem harzartigen Nebenprodukt schwierig, den reinen Kristall zu erhalten. Beim Verfahren (3) wird die Komplexverbindung dadurch hergestellt, dass man Nickelhalogenid in das bei 280° geschmolzene Triphenylphosphin unter der Rührung hinzufügt und dann das Reaktionsgemisch schnell abkühlt. Dieses Verfahren ist infolge der thermischen Zersetzung desselben kein gutes, wie in der folgenden Mitteilung erwähnt wird.

Jensen[10] hat darüber mitgeteilt, dass Bistriäthylphosphin-Nickelchlorid aus Triäthylphosphin und Nickelchlorid in Äthanol bei der gewöhnlichen Temperatur hergestellt wurde aber keinen Triphenylphosphinabkömmling ergab. Dementgegen habe ich gefunden, dass diese Komplexverbindung aus dessen Bestandteil durch Erhitzung in Äthanol oder Butanol unter dem Rückfluss beinahe quantitativ erhalten werden kann. Ich habe die bisher nicht veröffentlichte Verbindung nach dieser Methode dargestellt (Tabelle I).

5) A. Michaelis, *Ann.*, **229**, 295 (1885).
6) K. Yamamoto und S. Kunisaki, *J.P.*, 200, 535.
7) W. Reppe und W. J. Schweckeudiek, *Ann.*, **560**, 104 (1948).
8) K. Yamamoto und M. Oku, Dieses Bulletin **27**, 383 (1954).
9) W. Reppe, *F.P.* 961.010, *C.A.*, **46**, 5617 (1952).
10) K. Jensen, *Z. anorg. allg. Chem.*, **229**, 273 (1936).

Tabelle I

Komplexverbindungen $(Ph_3P)_2NiX_2$

Verbindung	Farbe	Smp. in (°C)	P—Gehalt in % Gef.	Ber.
$(Ph_3P)_2NiBr_2$	Intensivgrün	221–22*	8.40	8.36
$(Ph_3P)_2NiCl_2$	Dunkelblau	205–6 **	9.51	9.48
$(Ph_3P)_2NiJ_2$	Violettbraun	225	7.38	7.42

* Nach Reppe[7] 223°, ** Nach Reppe[11] zähe Flüssigkeit.

Diese Verbindungen sind löslich in Aceton, Alkohol und Benzol und nicht in Äther. In der Lösung gibt es Dissoziationsgleichgewicht;

$$(Ph_3P)_2NiX_2 \rightleftarrows 2Ph_3P+NiX_2$$

insbesondere in Methanol ist das Gleichgewicht von links nach rechts bemerkenswert abweichend. Darüber will ich später noch näher beschreiben.

Herstellung von $(Ph_3P)_2NiX_2RX'$.—Reppe[7] hat drei Verfahren zur Herstellung von den Komplexverbindungen dieses Typus, die als Katalysator bei der Acrylestersynthese am wichtigsten sind, veröffentlicht:

1) $(Ph_3P)_2NiX_2+RX' \rightarrow (Ph_3P)_2NiX_2RX'$
2) $(Ph_3P)_2Ni(CO)_2+3RX+2ROH \rightarrow (Ph_3P)_2NiX_2RX+2RCOOR+H_2$
3) $(Ph_3RP)X'+NiX_2+Ph_3P \rightarrow (Ph_3P)_2NiX_2RX'$

In welchem Verfahren es auch sei, verläuft die Umsetzung in Anwesenheit von Alkohol wie Butanol bei 120 bis 200°. Beim Verfahren (1) kann man anstatt des $(Ph_3P)_2NiX_2$ dessen Bestandteile, d.h., Triphenylphosphin und Nickelhalogenid, verwenden[12].

Ich habe ein anderes Verfahren gefunden,[13] in dem das Halogen zusammen mit dem aus Alkylreste bestehenden Alkohol, der dem betreffenden Alkylhalogenid entsprechend ist, anstatt des Alkylhalogenids, verwendet wird. Die Umsetzung verläuft auch in diesem Falle im eingeschlossenen Rohre bei 150 bis 180° und im Endeffekt im Sinne der Gleichung quantitativ.

$$4(Ph_3P)_2NiX_2+6C_nH_{2n+1}OH+2X'_2 \rightarrow 4(Ph_3P)_2NiX_2C_nH_{2+1}X' +C_nH_{2n-1}COOC_nH_{2n+1}+4H_2O$$

Ich soll hier beschreiben, wie diese Umsetzung, die später erwähnt wird, im Zusammenhang mit der katalytischen Wirkung von der Komplexverbindung Typus $(Ph_3P)_2NiX_2$ eine Bedeutung hat.

Ich habe die bisher unveröffentlichten Komplexverbindungen dieses Typus dargestellt und in der Tabelle II zusammengefasst.

Tabelle II

Komplexverbindungen $(Ph_3P)_2NiX_2RX'$

Verbindung	Farbe	Smp. in (°C)	P-Gehalt in % Gef.	Ber.	Bemerk.
$(Ph_3P)_2NiBr_2C_2H_5Br$	Grün	162	7.15	7.28	
$(Ph_3P)_2NiBr_2C_2H_5J$	Violettbraun	160	6.98	6.90	
$(Ph_3P)_2NiBr_2C_4H_9Br$	Blaugrün	178*	6.98	7.04	*Reppe[7] 178°
$(Ph_3P)_2NiBr_2isoC_4H_9Br$	Blaugrün	167	6.90	7.04	
$(Ph_3P)_2NiBr_2C_4H_9Cl$	Hellblau	167–8	7.42	7.45	
$(Ph_3P)_2NiCl_2C_4H_9Br$	Hellblaugrün	167*	7.81	7.84	*Reppe[7] 148–50°
$(Ph_3P)_2NiCl_2C_4H_9Cl$	Blau	176	8.25	8.30	
$(Ph_3P)_2NiBr_2C_4H_9J$	Violettbraun	125	6.71	6.70	
$(Ph_3P)_2NiJ_2C_4H_9J$	Violettbraun	167–8	6.12	6.07	
$(Ph_3P)_2NiBr_2C_6H_5Cl$	Grün	203–5	7.09	7.26	
$(Ph_3P)_2NiBr_2C_6H_5Br$	Aschgrün	210	6.90	6.89	
$(Ph_3P)_2NiBr_2C_7H_7Br$	Gelbgrün	186	6.90	6.97	

Diese Komplexverbindungen sind in Aceton, und Alkohol löslich, dagegen schwer in Benzol und garnicht in Äther. Ich habe die folgende Regelmässigkeit von dem Verhalten dieser Verbindungen gegen Alkohol gefunden, in dem Falle, wenn R Alkyl ist:

1) Gegen gleichen Alkohol ist die Verbindung desto beständiger, je niedriger der Alkylrest in ihr ist.
2) Die eine Verbindung ist desto beständiger gegen Alkohol je höher er ist.

Über das Verhalten gegen Methanol und über die Bedeutung der Beständigkeit soll ich anderweitig noch eingehender sprechen. Darüber bietet die alkoholische Lösung der

11) s. 3) S. 298.
12) K. Yamamoto, H. Izawa und M. Oku, *J.P.* ausgelegt 1952-3625.
13) K. Yamamoto, M. Oku und M. Tanaka, *J.P.* ausgelegt 1952-3173.

Komplexverbindung das sehr charakteristische Verhalten, dass sie bei der Heizung die intensiv eigentümliche Farbe behält, aber beim Erkalten verliert.

Herstellung von $(Ph_3P)_2NiX_22RX'$.—Betreffs des Verfahrens zur Herstellung dieser Verbindungen gibt es keine Beschreibung. Wenn man jedoch darauf das Verfahren, nach der in vorigem Paragraph beschriebenen Methode (1) gemäss unter der Anwendung von überschüssigem Alkylhalogenid durchführt, kann man nichts weiter erhalten, als die Komplexverbindung mit einem Molekül von Alkylhalogenid. Wenn man Bistriphenylphosphin-Nickelhalogenid mit der überschüssigen Menge Alkylhalogenid im eingeschlossenen Rohre bei 150 bis 180° erhitzt, so kann man eine Verbindung, die in Alkylhalogenid unlöslich ist, erhalten. Jedoch bei der Umkristallisation mit Lösungsmittel wie Butanol wandert diejenige zum Monoalkylhalogenidkomplex um. Im Falle, dass R Phenyl ist, kann man die Komplexverbindung dieses Typus als definierter Kristall von dem nach oben beschriebener Methode erhaltenen Reaktionsprodukt durch die Entfernung von überschüssigem Phenylhalogenid unter erniedrigtem Druck gewinnen. Im Falle des Alkylhalogenids ist das Reaktionsprodukt zu zähflüssig, als dass man die Komplexverbindung als Kristall erhalten könnte, selbst durch eine derartige Aufarbeitung.

Falls X' das Halogen mit dem schwereren Atomgewicht als X ist, so darf nicht erlaubt werden, die überschüssige Menge RX' zu verwenden, da man, wegen der Austauschung von Halogen, die erforderliche Komplexverbindung $(Ph_3P)_2NiX_22RX'$ nicht erhalten kann, sondern nur $(Ph_3P)_2NiX'_22RX'$.

In Tabelle III sind diese Komplexverbindungen gezeigt, die von mir hergestellt wurden.

TABELLE III

KOMPLEXVERBINDUNGEN $(Ph_3P)_2NiX_22RX'$

Verbindung	Farbe	Smp. in (°C)	P-Gehalt % Gef.	P-Gehalt % Ber.	Ni-Gehalt % Gef.	Ni-Gehalt % Ber.
$(Ph_3P)_2NiBr_22PhBr$	Hellblaugrün	270	5.64	5.86	5.53	5.56
$(Ph_3P)_2NiCl_22PhCl$	Blau	260	7.65	7.68	6.31	6.68
$(Ph_3P)_2NiJ_22PhJ$	Braun	Unisolierbar				
$(Ph_3P)_2NiBr_22PhCl$	Hellblau	253–5	6.34	6.41	5.92	6.00
$(Ph_3P)_2NiCl_22PhBr$	Hellblau	253–5	6.37	6.41	6.26	6.00

Bemerkenswert ist das, dess die letzten zwei Verbindungeh als gleich angesehen werden könnten. Wie es anderweit beschrieben wird, wurde durch die Erforschung von dem Abbauprodukt bei Methanolyse festgestellt, dass diese Verbindungen mit zwei Arten Halogenatomen nicht nur das Gemisch von je gleicher Menge der einzelnen Homohalogenkomplexverbindungen sind.

Die Komplexverbindung dieses Typus liefert in Alkohol nicht bloss ein Molekül RX leicht, sondern zersetzt sich auch, je nach den Bedingungen, zu Phosphonium- und Nickelhalogenid.

Schwer löslich ist solche in Benzol und Aceton, aber leicht in Nitrobenzol.

Experimentelle Beispiele

1. Triphenylphosphin.—Man tut das Gemisch von 250 g Benzol, 5.7 g Diäthylmalonat und 51.6 g Natriumschnitzen in den Rundkolben vom 1000 cm^3 Inhalt, der mit dem Rückflusskühler, Rührer und Tropfentrichter versehen ist, hinein.

Zu diesem Gemisch fügt man die aus 68 g Chlorbenzol und 32.3 g Phosphortrichlorid bestehende Mischung vom Trichter tropfenweise hinzu, wobei man die Reaktionstemperatur bei 60°C halten muss. Nach 6 Stunden endet die Umsetzung. Wenn man das Reaktionsgemisch nach dem Filtrieren konzentriert, so kann man den Rohkristall des Triphenylphosphins erhalten. Nach der Umkristallisierung aus Methanol erhält man 26.4 g reines Triphenylphosphin (Smp. 79°C).

2. $[(C_6H_5)_3P]_2Ni(CO)_2$.—Man erhitzt das Gemisch von 50 g Triphenylphosphin, 200 g Methanol und 5 g. reduzierten Nickelpulvern in 500 cm^3 Autoklav bei 150°C drei Stunden lang unter 50 Atm Druck von Kohlenoxyd. Da das Reaktionsprodukt in Methanol unlöslich ist, dekantiert man es und zieht mit Benzol aus. Fügt man Methanol zur Benzollösung hinzu, so kann man 43 g $[(C_6H_5)_3P]_2Ni(CO)_2$ erhalten.

3. $[(C_6H_5)_3P]_2NiBr_2$.—Wenn man das Gemisch, bestanden aus 200 g Butanol 24 g Triphenylphosphin und 20 g wasserfreiem Nickelbromid, unter Rückfluss zwei Stunden lang erhitzt, so kann man den feinen, kristallinischen Niederschlag von $[(C_6H_5)_3P]_2NiBr_2$ erhalten.

Die Ausbeute beträgt 35 g nach der Umkristallisierung (aus Butanol).

4. $[(C_6H_5)_3P]_2NiBr_2C_2H_5J$.—Man erhitzt das Gemisch, bestehend aus 10.5 g Triphenylphosphin, 4.4 g wasserfreiem Nickelbromid, 3.1 g Äthyljodid und 15 g Äthanol, im eingeschlossenem Rohr bei 150°C, zewi Stunden lang und kann 15 g $[(C_6H_5)_3P]_2NiBr_2C_2H_5J$ (gef. C 50.3, P 6.98. Ni 6.55%, ber. C 50.8, P 6.90, Ni 6.57%) nach der Umkristallisierung erhalten.

5. $[(C_6H_5)_3P]_2NiBr_2 \cdot 2C_6H_5Br$.—Man erhitzt

das Gemisch, bestehend aus 10 g Triphenylphosphin, 4 g wasserfreim Nickelbromid und 15 g Brombenzol, in eingeschlossenem Rohr bei 250°C, zwei Stunden lang. Beim Erkalten scheidet sich das Reaktionsprodukt als feiner Kristal aus. Wenn man überschüssiges Brombenzol auf dem Wasserbad unter erniedrigtem Druck verdünstet, so kann man ca. 5 g $[(C_6H_5)_3P]_2NiBr_2 \cdot 2C_6H_5Br$ aus den reinen Teilen des Bodenkörpers erhalten.

Falls man den Komplex $[(C_6H_5)_3P]_2NiCl_2 \cdot 2C_6H_5Br$ herstellen will, muss man die stoichiometrischen Mengen Triphenylphosphin, wasserfreies Nickelchlorid und Brombenzol verwenden, dann muss man die betreffenden Kristalle vorsichtig aus den reinen Teilen des Bodenkörpers herausgreifen.

Schlusswort

Die Herstellungsverfahren und einige Eigenschaften von Triphenylphosphin-Nickelkomplexverbindungen, die als Katalysator für die Acrylestersynthese verwendet werden, sind beschrieben worden.

Die Eigenschaften und Struktur betreffender Verbindungen sollen später noch näher gesprochen werden.

Herr Dr. K. Yoshikawa hat mich stets bei meinen Arbeiten leitend unterstützt und ermutigt. Die Herren K. Sato und M. Oku haben mit mir eifrig mitgearbeitet. Ich spreche diesen Herren und der Mitsui Chemical Industry Co., die mir diese Veröffentlichung meiner Arbeiten erlaubte, hierdurch meinen herzlichen Dank aus.

Mitsui Chemical Industry Co. Ltd.,
Miike Dyestuff and Chemical
Works, Omuta, Fukuoka

Zur Kenntnis über die Hochdrucksynthese von Acrylester. IV. Über die Acrylestersynthese unter Anwendung von Triphenylphosphin-Nickelkomplex-katalysator

Von Kazumi YAMAMOTO und Mitsuo OKU

(Eingegangen am 24. April 1954)

Einleitung

In der vorigen Mitteilung[1] wurden die Verfahren zur Herstellung von Triphenylphosphin-Nickelkomplexverbindungen beschrieben.

Es geht über den Rahmen der vorliegenden Abhandlung, die eingehenden Bedingungen über die Acrylestersynthese zu erwähnen. Deshalb sollen nur die Kenntnisse, die die wichtigen Tatsachen über die Forschung vom Mechanismus der Aktivierung des Kohlenoxyds am Komplexkatalysator sind, hier gegeben werden. In der Abhandlung bedeutet Ph den Phenylrest, R den Alkyl- oder Arylrest und X und X' bedeuten das Halogenatom selber oder sich darauf beziehende Arten. Alle Experimente wurden durch das halbkontinuierliche Verfahren[2] durchgeführt.

Wie schon erwähnt, wurde es nach Reppe betont, dass die Triphenylphosphin-Nickelkomplexverbindung als Katalysator für die Acrylestersynthese eine ausgezeichnete Fähigkeit besitzt. Bei unserer Nacharbeitung ist dieses festgestellt worden.

1) K. Yamamoto, Dieses Bulletin, **27**. 501 (1954).
2) K. Yamamoto, Dieses Bulletin, **27**. 491 (1954).

Einfluss, welcher das verschiedene Halogen auf die katalytische Fähigkeit von $(Ph_3P)_2NiX_2$ oder $(Ph_3P)_2NiX_2RX$ ausübt

Es ist schon beschrieben worden, dass die katalytische Fähigkeit von Nickelhalogenid bei der Acrylestersynthese in einer Reihe Cl→Br→J stark zunimmt. Diese Reihe ist ja im Falle des Komplexkatalysators auffallend. Das Experiment wurde nach dem halbkontinuierlichen Verfahren unter der Anwendung vom 600 cm^3 Inhalt Druckgefäss hinsichtlich der Synthese von Butylacrylat, durchgeführt. Die verwendete Menge von Komplexverbindung wurde so bestimmt, dass dejenige menge als Nickelbromid 5% an Butanol erhalten wird, da das Zentrum der katalytischen Wirkung derjenigen katalysatoren das Nickelatom ist.

Unter der Berücksichtigung der Beständigkeit derjenigen katalysatoren für Butanol wurde Butylhalogenid als RX vom $(Ph_3P)_2NiX_2RX$ verwendet. Die Resultate sind aus den Tabellen I, II und beziehungsweise aus der Figur 1 zu ersehen.

TABELLE I

KATALYTISCHE FÄHIGKEIT VON $(Ph_3P)_2NiX_2$

Nr.	BuOH (g)	Katalysator (g)		Einführsatz. von Gasgem. (% d. Th.)	Reakttemp. (°C)	Laufzeit (Std)	(Min)
13	50	$NiBr_2$	2.5	100	180–190	9	00
14	50	$(Ph_3P)_2NiCl_2$	7.5	30	180	3	30
15	50	$(Ph_3P)_2NiBr_2$	8.5	100	180	5	00
16	50	$(Ph_3P)_2NiJ_2$	9.5	100	180	1	10

* Die theoretische Menge vom Gasgemisch für 50 g. Butanol ist 30.0 *l.* unter dem normalen Zustand.

TABELLE II

KATALYTISCHE FÄHIGKEIT VON $(Ph_3P)_2NiX_2RX$

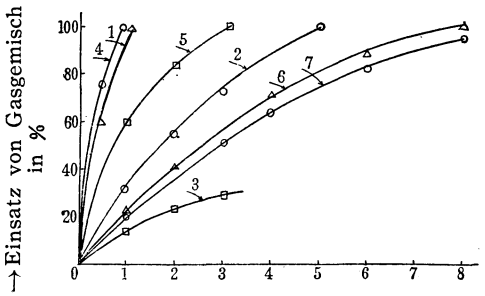
Nr.	BuOH (g)	Katalysator (g)		Reakttemp. (°C)	Laufzeit (Std)	(Min)	Bu-Acrylat (% an BuOH)
35	50	$(Ph_3P)_2NiCl_2BuCl$	8.5	165	8	00	60
36	50	$(Ph_3P)_2NiBr_2BuBr$	10.1	165	3	00	76
37	50	$(Ph_3P)_2NiJ_2BuJ$	11.7	140–50	0	50	50

Note: In allen Fällen war Einführungssatz von Gasgemisch 100% d. Th.

TABELLE III

KATALYTISCHE FÄHIGKEIT VON $(Ph_3P)_2NiX_2BuX'$

Nr.	BuOH (g)	$(Ph_3P)_2NiX_2BuX'$ (g)		Reakttemp (°C)	Laufzeit (Std)	(Min)	Bu-Acrylat (g)	(%)
35	50	„ $NiCl_2BuCl$	8.5	165	8	00	51.5	60
36	50	„ $NiBr_2BuBr$	10.1	165	3	00	65.5	76
51	50	„ $NiCl_2BuBr$	9.1	165	3	40	56.0	65
52	50	„ $NiBr_2BuCl$	9.5	165	4	00	57.0	66
53	50	„ $NiCl_2BuJ$	9.7	140–50	0	55	46.5	54
37	50	„ NiJ_2BuJ	11.7	140–50	0	50	43.0	50



1 $[(C_6H_5)_3P]_2NiJ_2$
2 $[(C_6H_5)_3P]_2NiBr_2$
3 $[(C_6H_5)_3P]_2NiCl_2$
4 $[(C_6H_5)_3P]_2NiJ_2C_4H_9J$
5 $[(C_6H_5)_3P]_2NiBr_2C_4H_9Br$
6 $[(C_6H_5)_3P]_2NiCl_2C_4H_9Cl$
7 $NiBr_2$

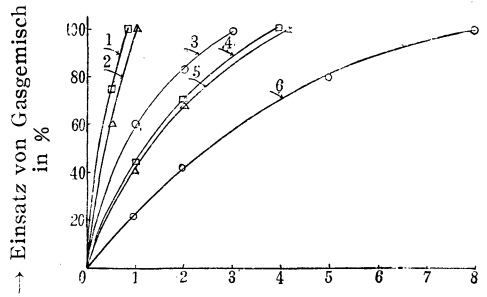
Fig. 1. Katalytische Wirkungen von $[(C_6H_5)_3P]_2NiX_2$ und $[(C_6H_5)_3P]_2NiX_2C_4H_9X$.

Einfluss, welcher das verschiedene Halogen auf die katalytische Fähigkeit von $(Ph_3P)_2NiX_2RX'$ ausübt

Im vorigen Paragraphen wurde der Vergleich der katalytischen Fähigkeit von $(Ph_3P)_2NiX_2RX'$, in dem X mit X' identisch war, gemacht. Im vorliegenden soll derselbe auch im Falle, dass X mit X' nicht identisch ist, gemacht werden.

Die Resultate sind in der Tabelle III gezeigt.

In allen Fällen war der Einführungssatz vom Gasgemisch 100% d. Th. Die Figur 2 illustriert die Reaktionsverläufe.



1 $[(C_6H_5)_3P]_2NiJ_2C_4H_9J$
2 $[(C_6H_5)_3P]_2NiCl_2C_4H_9J$
3 $[(C_6H_5)_3P]_2NiBr_2C_4H_9Br$
4 $[(C_6H_5)_3P]_2NiCl_2C_4H_9Br$
5 $[(C_6H_5)_3P]_2NiBr_2C_4H_9Cl$
6 $[(C_6H_5)_3P]_2NiCl_2C_4H_9Cl$

Fig. 2. Katalytische Wirkungen von $[(C_6H_5)_3P]_2NiX_2C_4H_9X'$

Beobachtet man die Resultate, so werden die katalytischen Fähigkeiten der Komplex.

verbindungen hinsichtlich der Reaktionsgeschwindigkeit in drei Hauptklassen, d. h., Nr. 35 und Nr. 36, 51, 52 und Nr. 53, 37 eingeteilt. Wird das Halogen mit dem schweren Atomgewicht in die Komplexverbindung entweder als Nickel- oder als Alkylhalogenid, d. h., in welcher Form es auch sei, eingeführt, so ist eindeutig zu ersehen, dass deren katalytische Fähigkeit mit der katalytichen Fähigkeit der Verbindung, deren Halogenatome all das Schwere sind, identisch ist.

Diese Tatsache deutet an, dass alle Halogenatome die gleiche Stelle an Nicklatom einnehmen. Darüber hinaus gibt dies die wichtige Suggestion über die chemische Konstitution von diesem Typus Komplexverbindung und über den Mechanismus der Aktivierung des Kohlenoxyds bei der Acrylestersynthese.

Folglich kann man die regelmässige Ordnung über die katalytische Fähigkeit von der Komplexverbindung $(Ph_3P)_2NiX_2RX'$ wie folgt erwarten.

$(Ph_3P)_2NiJ_2RJ \fallingdotseq (Ph_3P)_2NiJ_2RBr \fallingdotseq$
$(Ph_3P)_2NiJ_2RCl \fallingdotseq (Ph_3P)_2NiBr_2RJ \fallingdotseq$
$(Ph_3P)_2NiCl_2RJ > (Ph_3P)_2NiBr_2RBr \fallingdotseq$
$(Ph_3)_2NiBr_2RCl \fallingdotseq (Ph_3P)_2NiCl_2RBr >$
$(Ph_3P)_2NiCl_2RCl.$

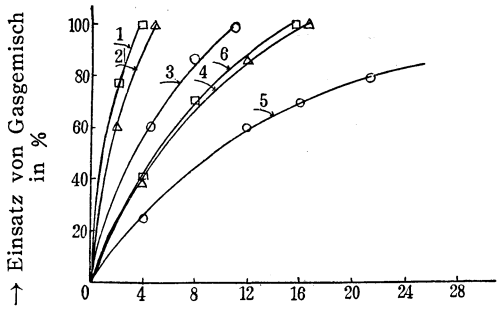
Beschleunigung der Reaktion bei der Äthylacrylatsynthese

Die Synthese von Äthylacrylat aus Acetylen, Kohlenoxyd und Äthanol in Anwesenheit von der Triphenylphosphin-Nickelkomplexverbindung ist im allgemeinen schwerer als die von Butylacrylat.

Dies soll gerade von den schon erwähnten zwei Erfahrungsgesetzen über die Beständigkeit der Komplexverbindung gegen Alkohol induziert werden. Das heisst, bei der Butylacrylatsynthese ist $(Ph_3P)_2NiX_2C_2H_5X$ als Katalysator zwar wirksam, aber bei der Äthylacrylatsynthese ist $(Ph_3P)_2NiX_2C_4H_9X$ nicht mehr zweckmässig. Während die genügende Reaktionsgeschwindigkeit bei derjenigen unter Anwendung von $(Ph_3P)_2NiBr_2C_4H_9Br$ (5% an Butanol) gefunden wird, kann dementgegen bei der anderen die gleiche Geschwindigkeit nicht gefunden werden, es sei denn, dass beinahe die zweifache Menge Katalysator $(Ph_3P)_2NiBr_2C_2H_2Br$ verwendet wird.

Wir haben auf Grund der vorigen Schlussfolgerung geplant, die Reaktionsgeschwindigkeit durch die Anwendung von Äthljodid und Bromid im verschiedenen Verhältnis zusammen mit $(Ph_3P)_2NiBr_2$, dessen Menge dem $(Ph_3P)_2NiBr_2C_2H_5Br$ 5% auf Basis von Äthanol entspricht, zunehmen zu lassen. Das Experiment wurde halbkontinuierlich unter den folgenden Bedingungen durchgeführt; Äthanol 50 g, $(Ph_3P)_2NiBr_2$ 2.2 g, Reaktionstemperatur 180°, Gesamtdruck von Gasgemisch 40 Atm.

Die zur Bildung von $(Ph_3P)_2NiBr_2C_2H_5X$, das den 2.2 g $(Ph_3P)_2NiBr_2$ entspricht, theoretisch erforderlichen Mengen von Äthylbromid und Jodid sind 0.3 und beziehungsweise 0.4 g. Die Figur 3 stellt die Resultate dar.



1 $[(C_6H_5)_3P]_2NiBr_2$+(ÄtBr : ÄtJ = 0 : 1) 5%
2 ,, +(,, = 0.2 : 0.8) 5%
3 ,, +(,, = 0.5 : 0.5) 5%
4 ,, +(,, = 0.8 : 0.2) 5%
5 ,, +(,, = 1 : 0) 5%
6 ,, +(,, = 1 : 0) 10%

Fig. 3. Beschleunigungseffekt von Jodäthyl bei Äthylacrylatsynthese.

Wie man aus der Figur 3 ersehen kann, und man Äthylbromid und Jodid im Verhältnis von 8 : 2 verwendet, kann man die Geschwindigkeit, die mit der bei der Anwendung von 5 g (10%) $(Ph_3P)_2NiBr_2C_2H_5Br$ fast gleich ist, beobachten.

Über die Menge von RX

In den Experimenten im zweiten Paragraphen wurden die definierten Verbindungen $(Ph_3P)_2NiX_2RX'$ verwendet. Aber Reppe[3] hat angedeutet, dass die Anwesenheit von der überschüssigen Menge Alkylhalogenid zur Hemmung vom Auftreten des Katalysatorsabbruchs, insbesondere die Nickelcarbonylbildung, wirksam ist.

Jedoch mit der Zunahme der Menge Alkylhalogenid nimmt die Reaktionsgeschwindigkeit proportional nicht zu. Dies ist in der Figur 4 eindeutig gezeigt, die den Reaktionsverlauf bei der Butylacrylatsynthese unter der Veränderung von dem Molverhältnis von Butylbromid zu $(Ph_3P)_2NiBr_2$ illustriert.

3) W. Reppe, „Neue Entwicklungen auf dem Gebiet der Chemie des Acetylens und Kohlenoxyds", Springer Verlag, (1949) S. 103.

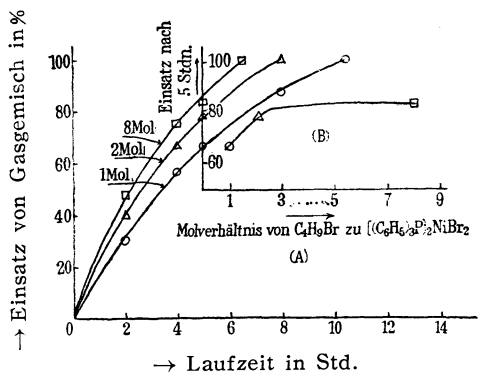


Fig. 4. Einfluss von Butylbromidmenge

Die Figur 4 (A) zeigt die Beziehung zwischen dem Einleitungssatz vom Gasgemisch und der Laufzeit und (B) die zwischen dem Einleitungssatz nach 5 Stunden und dem Molverhältnis von Butylbromid zu Bistriphenylphosphin-Nickelbromid. Aus der Figur 4 (B) scheint es, dass der bedeutende Unterschied zwischen 1 und 2 die Molverhältnisse des Bromids ist. (Arbeitungsmethode und Reaktionsbedingungen folgten denen wie im ersten Paragraphen beschrieben.)

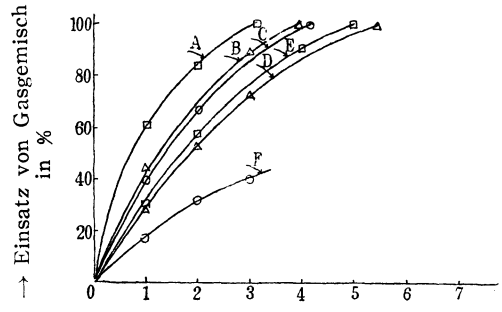
Über die Art und Nummer von Halogenatom

Die Resultate voriges Paragraphen deuten die Möglichkeit des Seins der Komplexverbindung von Typus $(Ph_3P)_2NiX_2 2RX'$, wenn gleich deren Isolierung, falls R Alkylgruppe ist, ausserordentlich schwierig ist. Wir haben den Reaktionsverlauf hinsichtlich der Komplexverbindungen beobachtet, welche eine jede für sich verschiedene Nummer des Halogenatoms gleicher oder verschiedener Art enthalten, um diese Frage durchzuprüfen. Die verwendeten Komplexverbindungen sind folgende:

$(Ph_3P)_2NiBr_2C_4H_9Br$ und dasselbe+C_4H_9Br
$(Ph_3P)_2NiCl_2C_4H_9Br$ und dasselbe+C_4H_9Br
$(Ph_3P)_2Ni(OOCCH_2Cl)_2C_4H_9Br$ und dasselbe+C_4H_9Br

Die Komplexverbindung $(Ph_3P)_2Ni(OOCCH_2Cl)_2C_4H_9Br$, bisher die unbekannte mit Schmelzpunkt 157 bis 158°, wurde aus Triphenylphosphin, Monochloressigsäurenickel und Butylbromid hergestellt, gemäss dem Herstellungsverfahren von dementsprechendem Butylchloridkomplex von Reppe[4].

Die unter gleichen Bedingungen erhaltenen Resultate sind in der Figur 5 illustriert. Die Menge von der als Katalysator verwendeten Komplexverbindung war so gewählt, dass jede Komplexverbindung einen gleichen Nickelgehalt (0.67 g—2.5 g als $NiBr_2$—in 50 g Butanol) enthält.



A $[(C_6H_5)_3P]_2NiBr_2 2C_4H_9Br$
B $[(C_6H_5)_3P]_2NiBr_2C_4H_9Br$
C $[(C_6H_5)_3P]_2NiCl_2 2C_4H_9Br$
D $[(C_6H_5)_3P]_2NiCl_2C_4H_9Br$
E $[(C_6H_5)_3P]_2Ni(OOCH_2Cl_2Cl)_2 2C_4H_9Br$
F $[(C_6H_5)_3P]_2Ni(OOCH_2Cl)_2 2C_4H_9Br$

Fig. 5. Art und Nummer von Halogenatomen in KKomplexverbindungen

Von diesen Resultaten werden die folgenden wichtigen Schlussfolgerungen erzielt:

1) Wenn selbst ein Halogenatom sich in der Komplexverbindung befindet, so hat die betreffende Komplexverbindung die katalytische Wirkung. (Das Chloratom im Monochloressigsäurerest wird dafür gehalten, dass es nicht unmittelbar an der Reaktion teilnimmt.)
2) Betreffs der Verbindungen mit den Halogenatomen der selben Art; je mehr Halogenatome in einer Komplexverbindung enthalten sind, desto grösser wird ihre katalytische Fähigkeit. F<E<B<A.
3) Betreffs der Verbindungen mit den verschiedenen Halogenatomen ist die katalytische Wirkung von der Nummer des schweren Halogenatoms abhängig. D<C.
4) Nicht, dass selbst ein leichtes Halogenatom keine Rolle spielt, sondern es ist von niedrigem Grade. F<D, E<C.
5) Das Sein der Komplexverbindung von Typus $(Ph_3P)_2NiX_2 2RX'$,) worin R Alkyl ist, ist fast gewiss.

Die eingehende Erörterung über die obigen Schlussfolgerungen wollen wir anderweitig beschreiben.

Schlusswort

Die folgenden Resultaten wurden durch die Vergleichung von der katalytischen Fähigkeit der Komplexverbindungen erhalten.

1. In den Komplexverbindungen von Typus $(Ph_3P)_2NiX_2$ und $(Ph_3P)_2NiX_2RX$ nimmt die katalytische Fähigkeit in einer Reihe von Halogen Cl, Br, J stark zu.
2. Von dem Vergleich der katalytischen

4) W. Reppe, *D.B.P.*, 805, 641; *C.*, II, 2251 (1951).

Fähigkeit von $(Ph_3P)_2NiX_2RX'$ (wobei $X \neq X'$) wird erwartet, dass alle Halogenatome die gleiche Stelle an Nickel einnehmen.

3. Die Komplexverbindung $(Ph_3P)_2NiX_2 2RX'$, worin R Alkylrest ist, kann nicht isoliert werden. Das Sein ist aber fast unter den Reaktionsbedingungen gewiss.

4. Betreffs der Nummer und Art des Halogenatoms wurde eine Regelmässigkeit gefunden.

Herr Dr. K. Yoshikawa hat uns immer bei unseren Arbeiten geleitet und ermutigt. Wir sprechen dem Herrn Doktor und der Mitsui Chemical Industry Co., die uns diese Veröffentlichung unserer Arbeiten erlaubte, hierdurch unseren herzlichen Dank aus.

Mitsui Chemical Industry Co. Ltd., Miike Dyestuff and Chemical Works, Omuta, Fukuoka

Zur Kenntnis über die Hochdrucksynthese von Acrylester. V. Zur Kenntnis über die Triphenylphosphin-Nickel-Komplexverbindungen

Von Kazumi YAMAMOTO und Mitsuo OKU

(Eingegangen am 24. April 1954)

Einleitung[1]

Als Literatur betreffs der Eigenschaften des Triphenylphosphin-Nickelhalogenids gibt es nur eine Veröffentlichung von Reppe[2], die aber keine eingehende ist.

Was die Strukturen der bei der Acrylestersynthese wichtigen Komplexverbindungen, wie $(Ph_3P)_2NiX_2RX'$ und $(Ph_3P)_2NiX_22RX'$, worin Ph den Phenylrest, R den Alkyl- oder Arylrest ausdrückt und X und X' selbes oder verschiedenes Halogenatom bedeuten, anbetrifft, gibt es keine. Der von Copenhaver[3] zitierten Meinung von Schweckendiek nach, verbände Alkylhalogenid durch die Nebenvalenz mit Bistriphenylphosphin-Nickelhalogenid $(Ph_3P)_2NiX_2$ und auch seine Annahme über den Mechanismus der Aktivierung des Kohlenoxyds würde sich auf diese Meinung stützen.

Die Struktur oder die chemischen Verhalten von diesen Komplexverbindungen zu untersuchen ist sehr wichtig, um den betreffenden Mechanismus aufzuklären. Wir haben wohl neue Erkenntnisse über die chemischen und physikalischen Eigenschaften derjenigen Komplexverbindungen erworben, die stets Beziehung mit ihrer katalytischen Fähigkeit enthalten.

Thermisches Verhalten der Komplexverbindungen

Wir haben das thermische Verhalten der Komplexverbindungen durch die Thermanowaage beobachtet, um die Kenntnisse über die Konstitution und über den Zusammenhang zwischen der Konstitution und der katalytischen Fähigkeit bei der Acrylestersynthese zu erhalten.

Die Skizze des experimentellen Apparates ist aus der Figur 1 ersehen.

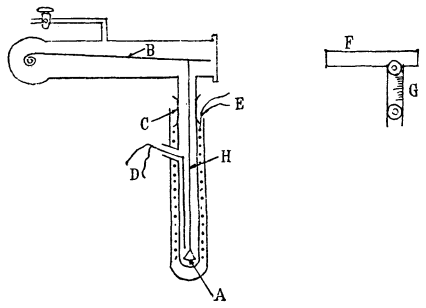
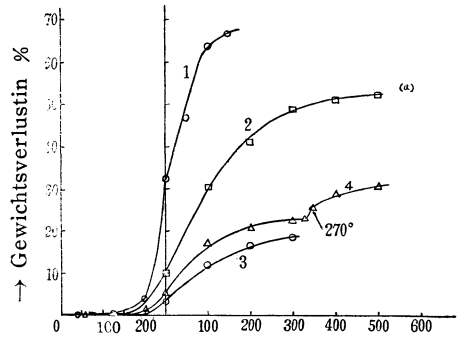


Fig. 1.

Die genau gewogene zirka 70 mg Probe wurde in das quarzige Tellerchen A, das mit dem dünnen Draht H von quarzigem Federhebel B hängt, eingesetzt und mit dem elektrischen Heizapparat E erhitzt. Der mit der Steigerung von der Temperatur zu begleitende Gewichtsverlust der Probe wird dadurch bestimmt, dass man den Aufgang von der Spitze des Hebels durch den mit dem Teleskop F gekuppelten, zuvor korrigierten Kathetometer G beobachtet. Die Geschwindigkeit der Temperatursteigerung, die durch das Thermoelement D gemessen wird, regelt sich in 2°/Min von der Raumtemperatur bis 200° und 1°/Min von 200° bis 250°, wobei die Temperatur konstant gehalten wird. Auf solche Weise wurde die Zersetzungsgeschwindigkeit mit den Gewichtsverlust—Temperatur und Gewichtsverlust-Laufzeit in Kurven dargestellt. Zuerst wurde der thermische

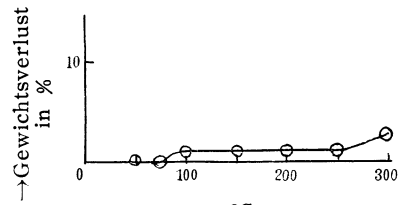
1) Vgl. K. Yamamoto und M. Oku, Dieses Bulletin, **27**, 505 (1954).
2) W. Reppe und R. J. Schweckendiek, *Ann.*, **560**, 104 (1948).
3) J. Copenhaver und M. Bigelow, „Acetylen and Carbonmonoxide Chemistry", Rheinhold Pub. Co. (1949), S. 262.

Abbau von $(Ph_3P)_2NiBr_2$ in der Luft beobachtet. Jedoch der Schmelzpunkt von dem Sublimat, das auf der oberen, inneren Mauer von C in der Figur 1 anklebte, war 153° unter dem Mikroskop. Dieser Schmelzpunkt stimmt gut mit dem des Triphenylphosphinoxyds (Smp. 152–3°[4]) überein. Dies zeigt, dass die Oxydation statt findet. Folglich wurde das nachfolgende Experiment in der Atmosphäre von Stickstoff durchgeführt. Die experimentellen Resultate sind aus den Figuren 2 und 3 zu ersehen.



→°C
→ Laufzeit bei 250° in Min.
1 $[(C_6H_5)_3P]_2NiCl_2$
2 $[(C_6H_5)_3P]_2NiBr_2$
3 $[(C_6H_5)_3P]_2NiJ_2$
4 $[(C_6H_5)_3P]_2NiBr_2C_4H_9Br$

Fig. 2(a). Thermisches Verhalten von Komplexverbindungen.



→ °C.

Fig. 2(b). $[(C_6H_5)_3P]_2NiBr_22C_6H_5Br$.

Aus der Figur 2(b) kann man ersehen, dass $(Ph_3P)_2NiBr_22C_6H_5Br$ ziemlich beständig gegen die Wärme ist. Die anderen Verbindungen zersetzen sich dementgegen schon bei 250°. In jedem Falle wurde das Sublimat, dessen Schmelzpunkt 79° mit dem des Triphenylphosphins völlig übereinstimmte, auf der oberen, inneren Mauer von C und auf dem Draht H in der Figur 1 erhalten. Betreffs einiger Beispiele, bei welchen der Grenzwert des Gewichtsverlustes für konstant gehalten wird, sind die theoretischen Triphenylphosphingehalte sowohl von $(Ph_3P)_2NiX_2$ als auch von $(Ph_3P)_2NiX_2C_4H_9X'$ und die beobachteten Gewichtsverluste, in denen das Gewicht des auf dem Draht H sublimierten Triphenylphosphins für solche nicht beobachtet wird, in der Tabelle I angegeben.

TABELLE I
VERGLEICH VON Ph_3P-GEHALT UND GEWICHTSVERLUST VON KOMPLEXVERBINDUNGEN

Komplex	Gew-verlust. (%) (a)	Theor. Ph_3P-Gehalt (%) (b)	(a)/(b)
$(Ph_3P)_2NiCl_2$	66	80.0	0.88
$(Ph_3P)_2NiBr_2$	56	70.5	0.80
$(Ph_3P)_2NiBr_2C_4H_9Br$	30	59.5	0.50
$(Ph_3P)_2NiCl_2C_4H_9Cl$	33.3	72.0	0.46
$(Ph_3P)_2NiBr_2C_4H_9Cl$	26.4	62.8	0.43

Infolgedessen wird die thermische Zersetzung von der Komplexverbindung Typus $(Ph_3P)_2NiX_2$ wie folgt ausgedrückt werden.

$$(Ph_3P)_2NiX_2 \rightarrow 2Ph_3P+NiX_2$$

Bei dem Typus $(Ph_3P)_2NiX_2RX$ dementgegen wird man sich vorstellen können, dass das von der Zersetzung sublimierte Triphenylphosphin zwar nur ein Molekül ist, ein anderes aber sich in der Bindungsart ganz und gar unterscheidet. Unter der Berücksichtigung des Herstellungsverfahrens (vgl. III. Mitteilung[5]) könnte man diese Zersetzung im Endeffekt im Sinne der Gleichung erläutern.

$$(Ph_3P)_2NiX_2RX \rightarrow (Ph_3RP)X+NiX_2+Ph_3P$$

In der Tat erhitzten wir die Verbindung $(Ph_3P)_2NiBr_2C_4H_9Br$ bei 250°, 6 Stunden lang unter der Anwendung vom Rose -Tiegel in der Atmosphäre des Stickstoffes und erhielten eine kristallinische Substanz aus dem Zersetzungsprodukt durch die Ausziehung mit heissem Wasser und die Umkristallisation. Die Substanz schmilzt bei 235°. Wir stellten wie unten beschrieben fest, dass sie das Triphenylbutylphosphoniumbromid ist.

Darüber hinaus beobachteten wir gegen alles Erwarten, dass die von dem Zersetzungsprodukt von $(Ph_3P)_2NiBr_2C_4H_9Cl$ erhaltene kristallinische Verbindung auch bei 235° schmilzt, und sie wie oben benannt, als Phosphoniumbromid angesehen werden soll.

Wir möchten über solche erstaunliche Umwandlung des Halogenatoms in dem nächsten Paragraphen auch eine andere Erscheinung erörtern.

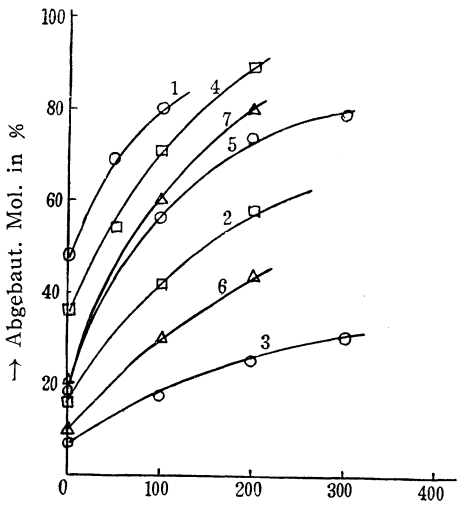
Wenn das Alkylhalogenid sich dagegen mit Bistriphenylphosphin-Nickelhalogenid durch die Nebenvalenz verbände, sollte es zu

4) A. Kosolapoff, *J. Am. Chem. Soc.*, **64**, 2382 (1942).

5) K. Yamamoto, Dieses Bulletin, **27**, 503 (1954).

allererst beim Erhitzen verdünsten, wir aber haben Butylbromid bei der trockenen Destillation von $(Ph_3P)_2NiBr_2C_4H_9Br$ in der Atmosphäre des Stickstoffes nicht fangen können.

Auch die Tatsache, dass das $(Ph_3P)_2NiBr_2$-$2C_6H_5Br$ auch bei 300°C noch keinen bemerkenswerten Gewichtsverlust bietet, dürfte die Nebenvalenz-Theorie von Schweckendiek verneint werden.



1 $[(C_6H_5)_3P]_2NiCl_2$
2 $[(C_6H_5)_3P]_2NiBr_2$
3 $[(C_6H_5)_3P]_2NiJ_2$
4 $[(C_6H_5)_3P]_2NiCl_2C_4H_9Cl$
5 $[(C_6H_5)_3P]_2NiBr_2C_4H_9Br$
6 $[(C_6H_5)_3P]_2NiJ_2C_4H_9J$
7 $[(C_6H_5)_3P]_2NiBr_2C_4H_9Cl$

Fig. 3. Thermische Zersetzung von Komplexverbindungen.

Die Figur 3 illustriert die Zersetzungsneigungen von $(Ph_3P)_2NiX_2$ und $(Ph_3P)_2NiX_2RX'$ mit dem Prozent vom abgebauten Molekül gegen die Laufzeit bei 250°. Davon wird man den Effekt, welcher das Halogen auf die Bindung zwischen dem Nickel und Triphenylphosphinrest ausübt, wissen können. Das heisst, betreffs der Komplexverbindung jedes Typuses, in der Reihenfolge Chlorid→Bromid →Jodid nimmt deren Stabilität zu. Unter Erinnerung der in der vorigen Mitteilung beschriebenen Reihenfolge der katalytischen Fähigkeit von den Komplexverbindungen, könnte man die wichtige Tatsache, dass die katalytische Fähigkeit mit deren Stabilität in der gleichen Ordnung steht begreifen.

Zersetzung von Komplexverbindungen in Methanol

Wir haben vorher zwei Erfahrungsgesetze über die Stabilität der Komplexverbindung $(Ph_3P)_2NiX_2RX'$ gegen Alkohol beschrieben. In Methanol jedoch zersetzt sich die Verbindung, welcher Typus es auch sei. Wir erforschten zuerst das Verhalten von $(Ph_3P)_2NiBr_2$, $(Ph_3P)_2NiBr_2C_4H_9Br$ und $(Ph_3P)_2$-$NiBr_22C_6H_5Br$ als Vertreter jedes Typus qualitativ.

Wird zirca 0.5 g der Probe mit 5 cm^3 Methanol bei Zimmertemperatur behandelt, so löst sich die Komplexverbindung unter Verlöschung der eigentümlichen Farbe und mit spontaner Verdampfung von Methanol kristallisiert das Zersetzungsprodukt aus.

1) Von $(Ph_3P)_2NiBr_2$ kristallisiert Triphenylphosphin (Smp. 79°) beinahe quantitativ aus.

2) Von $(Ph_3P)_2NiBr_2C_4H_9Br$ kristallisiert der wasserlösliche Kristall mit hohem Schmelzpunkt nebst dem Triphenylphosphin aus. Wenn man den ersteren daraus mit heissem Wasser extrahiert und ihn zweimal aus Wasser umkristallisiert, so kann man den farblosen, kubischen Kristall mit Schmelzpunkt 235° erhalten. (*Anal.* gef. P 7.71, C 67.5, H 5.80%)

Fügt man zur wässrigen Lösung von demjenigen die des Silbernitrats hinzu, so schlägt Silberbromid sofort nieder. Also kann man die Substanz für Triphenylbutylphosphoniumbromid erachten, das bisher nicht veröffentlicht wurde. Wir haben es aus Triphenylphosphin und Butylbromid im Butanol bei 180° hergestellt und beobachtet, dass dessen Schmelzpunkt auch bei 235° ist.

$[(C_6H_5)_3(C_4H_9)P]Br$

Gef.	P 7.73	C 65.98	H 5.99	Br 20.1%	
Ber.	7.77	66.20	6.02	20.0	

Dieses Präparat zeigte keine Schmelzpunktdepression bei der Mischprobe mit der aus Produkt sowohl der Methanolyse als der thermischen Zersetzung erhaltenen Probe.

Folglich wurde es festgestellt, dass auch die Zersetzung in Methanol, wie bei der thermischen, verläuft;

$$(Ph_3P)_2NiBr_2C_4H_9Br \rightarrow [Ph_3(C_4H_9)P]Br + NiBr_2 + Ph_3P$$

3) Von $(Ph_3P)_2NiBr_22PhBr$ scheidet Triphenylphosphin nicht mehr aus, sondern wird der wasserlösliche Kristall von Schmelzpunkt 287°, der mit dem des Tetraphenylphosphoniumbromids[6] überein-

6) J. Dodonov, *Ber.*, **61**, 907 (1928).

stimmt, gefunden. Folglich wird die Zersetzung mit der folgenden Gleichung ausgedrückt;

$(Ph_3P)_2NiBr_22PhBr \rightarrow 2(Ph_4P)Br + NiBr_2$

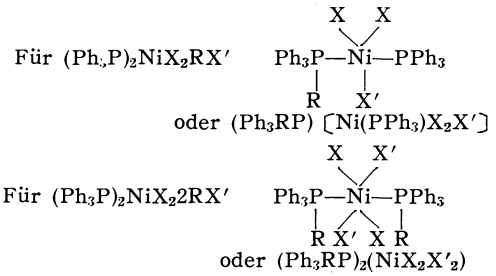
Nachher wurde die Zersetzung von $(Ph_3P)_2NiX_2RX'$ oder $(Ph_3P)_2NiX_22RX'$ untersucht, wobei X beziehungsweise X' verschiedenes Halogenatom bedeutet. In diesen Fällen haben wir eine wichtige Tatsache gefunden, dass als Halogenatom des Phosphoniumhalogenids, wie bei der thermischen Zersetzung, stets das mit schwerem Atomgewicht festgestellt wird. Zum Beispiel wird nur Triphenylbutylphosphoniumbromid (Smp. 235°) bei der Zersetzung sowohl von $(Ph_3P)_2NiBr_2C_4H_9Cl$ wie von $(Ph_3P)_2NiCl_2C_4H_9Br$ gefunden und nicht Triphenylbutylphosphoniumchlorid, das von uns aus Triphenylphosphin und Butylchlorid in Butanol hergestellt wurde, und dessen Schmelzpunkt 227–8° war. Also werden beide Zersetzungen wie folgt gezeigt;

$(Ph_3P)_2NiBr_2C_4H_9Cl \longrightarrow$
$[Ph_3(C_4H_9)P]Br + \frac{1}{2}NiBr_2 + \frac{1}{2}NiCl_2 + Ph_3P$
$(Ph_3P)_2NiCl_2C_4H_9Br \longrightarrow$
$[Ph_3(C_4H_9)P]Br + NiCl_2 + Ph_3P$

Auch bei der Zersetzung von $(Ph_3P)_2NiBr_2$ 2PhCl oder $(Ph_3P)_2NiCl_22PhBr$ wird die gleiche Erscheinung beobachtet, dass die Abbauprodukte jedenfalls Tetraphenylphosphoniumbromid und Nickelchlorid sind. Dies beseitigt die Zweifel, welche zwei derartige Komplexverbindungen, die gleiche Farbe und gleichen Schmelzpunkt[5] haben, jede für sich die Gemische der gleichen Menge von $(Ph_3P)_2NiBr_22PhBr$ und $(Ph_3P)_2NiCl_22PhCl$ sein sollten und bringt dies vielmehr die Möglichkeit hervor, dass beide dieselben Verbindungen sind.

Diese Resultate stellen die in voriger Mitteilung beschriebene Schlussfolgerung „Alle Halogenatome nehmen gleiche Stelle an Nickel ein" dar und zwar verneinen grundsätzlich den Schweckendiekschen Gedanke, dass Alkylhaloganid sich an $(Ph_3P)_2NiX_2$ nur durch Nebenvalenz verbände.

Als solche Strukturen, in denen die Halogenatome die gleiche Stelle an Nickel einnehmen, nehmen wir die folgenden an, abgesehen davon, dass entweder diejenigen die echten Elektrolyte sind oder Nichtelektrolyte;



Unter der Annahme von diesen Strukturen wird man sowohl das thermische Verhalten als auch die Zersetzung von Komplexverbindungen in Methanol sowie die Möglichkeit, dass $(Ph_3P)_2NiBr_22PhCl$ und $(Ph_3P)_2NiCl_22PhBr$ die gleichen Verbindungen seien, gut verstehen können. Über das katalytische Verhalten von $(Ph_3P)_2NiX_2RX'$ möchten wir anderweit noch näher diskutieren.

Leitungsfahigkeit von Komplexverbindungen

Zuerst wurden die Leitungsfähigkeiten von $(Ph_3P)_2NiBr_2C_4H_9Br$ und $(Ph_3P)_2NiBr_22PhBr$ in Aceton, das ein gutes Lösungsmittel für dieselben ist, bestimmt. Wie in der Tabelle II Zeile I und II gezeigt, wurden die Resultate gefunden, dass diese Verbindungen die Elektrolyte sein könnten. Aber auch die Komplexverbindung $(Ph_3P)_2NiBr_2$, die von den Arbeiten von Jensen[7] über Bistriäthylphosphin-Nickelchlorid $[(C_2H_5)_3P]_2NiCl_2$ eindeutig als Nichtelektrolyt angesehen wird, zeigte die Leitungsfähigkeit wie in Zeile III. Dies erläutert, dass auch in Aceton das schon beschriebene Dissoziationsgleichgewicht vorhanden ist.

$(Ph_3P)_2NiBr_2 \rightleftarrows 2Ph_3P + NiBr_2$
$(Ph_3P)_2NiBr_2C_4H_9Br$
$\rightleftarrows (Ph_3C_4H_9P)Br + NiBr_2 + Ph_3P$
$(Ph_3P)_2NiBr_22PhBr \rightleftarrows 2(Ph_4P)Br + NiBr_2$

Folglich gibt es eine Gefährlichkeit, dass die erhaltenen Leitungsfähigkeiten die der Komplexverbindungen für sich nicht bedeutsam sind, sondern die von Nickelbromid und Phosphoniumbromid.

TABELLE II
LEITUNGSFÄHIGKEIT VON KOMPLEXVERBINDUNGEN IN ACETON

Komplex	Temp. (°C)	Verdünnungsgrad (cm³.)	Mol. Leitungsfähigkeit (Ω^{-1})
$(Ph_3P)_2NiBr_2C_4H_9Br$	20	2.5×10^5	72.91
I.		5.0×10^5	84.53
		1.0×10^6	102.3
		2.0×10^6	108.8
$(Ph_3P)_2NiBr_22PhBr$	20	1.9×10^6	210.6
II		3.8×10^6	231.4
		7.6×10^6	235.3
		1.5×10^7	242.9
$(Ph_3P)_2NiBr_2$	20	2.5×10^5	32.9
III.		5.0×10^5	39.08
		1.0×10^6	42.28
		4.0×10^6	45.47
		8.0×10^6	52.13
		1.6×10^7	62.52

9) K. A. Jensen, *Z. anorg. allg. Chem.*, **229**, 273 (1936).

Diese Erscheinung wurde auch in Butanol an $(Ph_3P)_2NiBr_2C_4H_9Br$, wenn der Umfang auch niedrig ist, beobachtet. Die Tabelle III zeigt diese Reultate und die eigentümlichen Leitungsfähigkeiten von Nickel- und Triphenylbutylphosphonium-bromid in den Zeilen I, II, und bzw III. Darüber hinaus stellt die Zeile IV die Leitungsfähigkeit der gleichen Komplexverbindung in Äthanol dar. Die höheren Werte im Äthanol geben das in der Mitteilung III[5] erwähnte zweite Erfahrungsgesetz über die Beständigkeit der Komplexverbindung in Alkohol quantitativer dar.

TABELLE III

LEITUNGSFÄHIGKEIT VON KOMPLEXVERBINDUNGEN IN ALKOHOL

	Komplex	Alkohol	Verdünnungsgrad (cm^3)	Mol. Leitungsfähigkeit (Ω^{-1}) 20°	50°
I.	$(Ph_3P)_2NiBr_2C_4H_9Br$	Butanol	5.0×10^4	6.70	11.05
			2.0×10^5	9.40	16.50
			5.0×10^5	10.36	20.55
			5.0×10^6	20.25	32.85
II.	$NiBr_2$	Butanol	1.9×10^4	1.85	2.39
			7.5×10^4	2.32	2.87
			1.9×10^5	3.25	4.15
			1.9×10^6	7.87	10.54
			1.9×10^7	17.30	23.08
III.	$(Ph_3C_4H_9P)Br$	Butanol	2.38×10^4	5.60	9.85
			9.52×10^4	7.50	13.08
			2.38×10^5	8.90	15.92
			2.38×10^6	13.60	26.40
			2.38×10^7	15.95	28.08
IV.	$(Ph_3P)_2NiBr_2C_4H_9Br$	Äthanol	2.8×10^4	27.6	38.6
			5.6×10^4	33.1	46.3
			2.8×10^5	46.2	65.5
			2.8×10^6	70.3	103.2

Die Tabelle III erläutert, dass die Dissoziation desto grösser wird, je höher die Temperatur ist. Aber unter Anwendung der eingeschlossenen Zelle zeigten die Leitungsfähigkeiten der bei erhöhter Temperatur stehenden Butanollösung von $(Ph_3P)_2NiBr_2C_4H_9Br$ durch den maximalen Wert bei 120° den Abfall (Tabelle IV.)

TABELLE IV

LEITUNGSFÄHIGKEIT DER BUTANOLLÖSUNG VON $(Ph_3P)_2NiBr_2C_4H_9Br$ BEI ERHÖHTER TEMPERATUR

(Verdünnungsgrad 3.1×10^5 cm.^{3} bei 20°)

Temperatur (°C)						
70	100	110	120	130	140	150
Mol. Leitung. (Ω^{-1})						
24.80	30.70	34.10	34.10	30.70	29.22	27.60

Unter Berücksichtigung von der Veränderung seiner Farbe bei der erhöhten Temperatur (vgl. III. Mitteilung) wird dies dadurch aufgeklärt, dass es auf die Verminderung vom Dissoziationsgrad zurückführt. Es ist jedoch eindeutig, dass die oben erhaltenen Data die Erkenntnis, die wir erhalten wollen gerade nicht ergeben. Wenn, demnach, Triphenylphosphin (Smp. 79°), das ein Dissoziationsprodukt ist, verwendet wird, wird man die Leitungsfähigkeit von Komplexverbindungen an und für sich selbst erhalten können, der Verstellung des Gleichgewichts nach links wegen. Das Resultat des von obigem Gesichtspunkt durchgeführten Experiments erläutert, wie in der Tabelle V gezeigt, $(Ph_3P)_2NiBr_2C_4H_9Br$ für sich gewiss ein Nichtelektrolyt zu sein.

TABELLE V

LEITUNGSFÄHIGKEIT VON $(Ph_3P)_2NiBr_2C_4H_9Br$ IN GESCHMOLZENEM TRIPHENYLPHOSPHIN

Verdünnungs-* grad (cm^3.)	Temperatur (°C)	Mol. Leitungsfähigkeit (Ω^{-1})
4.03×10^4	200	**
4.03×10^3	200	**
4.03×10^2	200	**
4.03×10	200	1.43×10^{-4}
4.03×10	180	1.07×10^{-4}
„	160	7.55×10^{-5}
„	140	5.19×10^{-5}
„	120	3.21×10^{-5}
„	100	1.60×10^{-5}
„	80	3.78×10^{-6}

* Diese Werte sind auf der Dichte von Ph_3P d_4^{80} 1.0749[8] gründet, folglich bedeuten sie den Verdünnungsgrad bei 80°.

8) A. Walden, *Z. für phys. Chem.*, **79**, 714 (1912).

** Spezifische Leitungsfähigkeit ist zu gering, als dass sie gemessen werden könnte.

Auch in Bezug auf die Triphenylphosphinlösung von $(Ph_3P)_2NiBr_2$ und $(Ph_3P)_2NiBr_22PhBr$ wurden die Leitungsfähigkeiten bestimmt und die Resultate wurden erhalten, wie aus der Tabelle VI zu ersehen.

TABELLE VI
LEITUNGSFÄHIGKEITEN VON $(Ph_3P)_2NiBr_2$ UND $(Ph_3P)_2NiBr_22PhBr$ IN GESCHMOLZENEM Ph_3P

Komplex	Verdünnungsgrad (cm^3.)*	Temp. (°C)	Mol. Leitungsfähigkeit (Ω^{-1})
$(Ph_3P)_2NiBr_2$	4.06×10^4	200	**
Smp. 219–22°	4.06×10^3	200	**
	4.06×10^2	200	**
	4.06×10	200	4.76×10^{-6}
	„	180	2.75×10^{-6}
	„	160	9.51×10^{-7}
$(Ph_3P)_2NiBr_22PhBr$	3.99×10^4	250	**
Smp. 270°	3.99×10^3	250	**
	3.99×10^2	250	3.74×10^{-4}
	„	220	2.34×10^{-4}
	„	200	1.49×10^{-4}
	3.99×10	250	1.28×10^{-4}
	„	220	8.78×10^{-5}
	„	200	6.78×10^{-5}

*, ** Vgl. Tabelle V.

Struktur der Komplexverbindungen

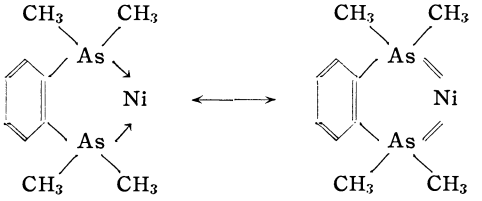
Von den Resultaten der Leitungsfähigkeiten wurde es klar, dass alle drei Typen Komplexverbindungen als Nichtelektrolyte angesehen werden können. Betreffs des $(Ph_3P)_2NiX_2$ kommt es nicht in Betracht, da dessen Konfiguration, welche die das Nickel als Zentralatom enthaltene ebene Konfiguration nach dem Arbeiten von Jensen über den Triäthylphosphinabkömmling analogisch erwartet werden soll, durchaus als Nichtelektrolyt angesehen wird.

Was die anderen zwei Verbindungen betrifft, so steht das nun in Frage. Wir möchten unsere Meinung darüber qualitativ beschreiben, da zur Entscheidung der genauen Konfiguration man die X-Strahlen- oder mindestens magnetische Untersuchungen durchführen muss. Um deren Konfigurationen festzustellen, haben wir die Erkenntnisse über das Absorptionsspektrum oder Dipolmoment suchen wollen, aber die genauen Resultate wegen des Auftretens der Dissoziation in einer Lösung, wie schon beschrieben, nicht erhalten können.

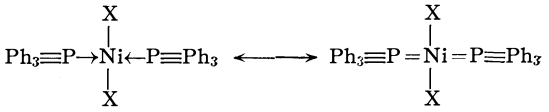
Zum Beispiel, hinsichtlich des $(Ph_3P)_2NiX_2RX'$ kann man bloss von den Resultaten der Leitungsfähigkeit allein keinen Schluss darüber ziehen, denn der Grund ist noch schwach, um die Wesenheit von Ionkomplex $(Ph_3RP)[Ni(PPh_3)X_2X']$, wenn er auch in geschmolzenem Triphenylphosphin elektrolytisch nicht dissoziiert, abzulehnen. Auch bei $(Ph_3P)_2NiX_22RX'$ könnte man eine salzartige Struktur $(Ph_3RP)_2(NiX_2X'_2)$ gar nicht ausser acht lassen.

Aber alles zusammengenommen, ist es hinreichend möglich, dass man die Struktur der 5- bzw. 6-Koordinationskomplexverbindungen annimmt.

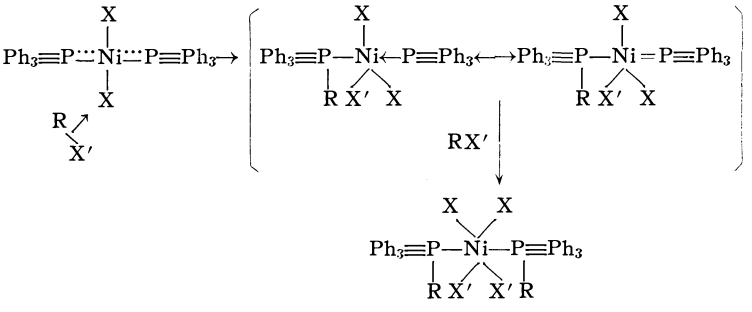
In jüngster Zeit haben Burstall und Nyholm[9] in ihren Arbeiten über [Ni(*o*-Phenylenbisdimethyl-Arsin)$_2$Cl$_2$]Cl veröffentlicht, dass dessen echte Struktur durch Resonanzhybride dargestellt werde, zu welcher die Struktur mit der einfachen Bindung und die mit der Doppelbindung (π-Bindung), die sich unter Anwendung von 3d-Elektronenpaar des Nickelatoms und der vakanten d-Bahn des Arsenatoms bildet, wie folgt beitragen;



Bei $(Ph_3P)_2NiX_2$ möchten wir auch gleiche Erläuterung geben.



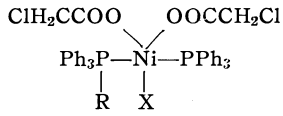
Unter der Annahme des wahrscheinlichen Doppelbindungscharakters der P-Ni Bindung kann man die Anlagerung von RX′ zu der betreffenden Verbindung leicht erklären.



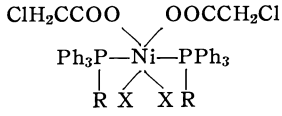
9) A. Burstall und R. Nyholm, *J. Chem. Soc.*, **1952**, 3570.

Auch die sekundäre Anlagerung von RX' kann man ebenfalls dadurch so auffassen und die Resonanzhibride von $(Ph_3P)_2NiX_2RX'$ annehmen, wie oben gezeigt. Die leichte Umwandlung von Dialkylhalogenid zur Monoalkylhalogenidkomplexverbindung könnte man auch durch die verbesserte Beständigkeit von der letzteren aufgrund der Resonanz verstehen.

Ferner hinsichtlich der in der Mitteilung IV[1] beschriebenen Monochloressigsäuresnickel-Komplexverbindungen, wäre es vernünftiger, die 5- bzw. 6-koordinative Verbindung anzunehmen.



und

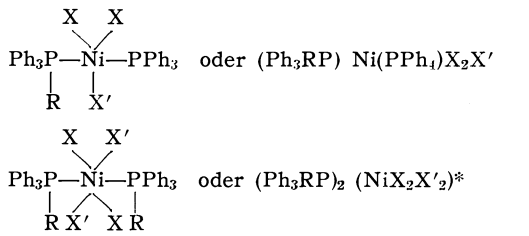


Von den obigen Meinungen und von den Werten der Leitungsfähigkeiten wagen wir die Behauptung, dass solche Komplexverbindungen jede für sich 5- bzw. 6-koordinative Verbindung sind.

Von nun an wollen wir sie bequemlichkeitshalber wie folgt bezeichnen.
(Ph_3RP)-$Ni(PPh_3)X_2X'$ für $(Ph_3P)_2NiX_2RX'$ und
$(Ph_3RP)_2 : NiX_2X'_2$ für $(Ph_3P)_2NiX_22RX'$.

Zusammenfassung

1. Von den Experimenten über das thermische Verhalten sowohl als auch über die Zersetzung der Komplexverbindungen in Methanol wurde gezeigt, dass RX' in $(Ph_3P)_2$ NiX_22RX' oder $(Ph_3P)_2NiX_22RX'$ durch die Nebenvalenz an $(Ph_3P)_2NiX_2$ nicht verbunden ist. Beide Verbindungen sollen vielmehr mit den folgenden Formeln ausgedrückt werden:



Unter der Annahme solcher Strukturen ist aufzuklären, dass alle Halogenatome die gleiche Stelle an Nickel einnehmen, und dass $(Ph_3P)_2NiBr_22PhCl$ und $(Ph_3P)_2NiCl_22PhBr$ eine gleiche Verbindung sind.

2. Es wurde bei der Zersetzung sowohl von $(Ph_3P)_2NiX_2RX'$ als von $(Ph_3P)_2NiX_22RX'$ in Methanol beobachtet, dass das Halogenatom mit schwerem Atomgewicht sich als Phosphoniumhalogenid stets von der Komplexverbindung trennt. Bei der thermischen Zersetzung von $(Ph_3P)_2NiX_2RX'$ ist auch die Lage der Dinge gleich.

3. Durch die Messung der Leitungsfähigkeit der Komplexverbindungen in geschmolzenem Triphenylphosphin erfolgt, dass $(Ph_3P)_2NiX_2$, $(Ph_3P)_2NiX_2RX'$ und $(Ph_3P)_2$ NiX_22RX' all die Nichtelektrolyte sind. Auf Grund dieser Resultate haben wir über ihre Strukturen betrachtet und die Behauptung gewagt, dass die letzten zwei Verbindungen jede für sich 5- bzw. 6- koordinative Verbindung seien.

Die Herren Dr. K. Yoshikawa und K. Ohga haben uns stets bei unseren Arbeiten leitend unterstützt und ermutigt. Wir sagen diesen Herren und der Mitsui Chemical Industry Co., die uns diese Veröffentlichung unserer Arbeiten erlaubte, hierdurch unseren herzlichen Dank.

Mitsui Chemical Industry Co. Ltd.,
Miike Dyestuff and Chemical
Works, Omuta, Fukuoka

* Reppe hat erst in seinen Vorträgen zum Andenken an das 75. Jubiläum der japanischen chemischen Gesellschaft veröffentlicht, dass Komplexverbindung $[(C_6H_5)_3P(C_4H_9)]_2NiBr_4$ bei der Butylacrylatsynthese als Katalysator verwendet wird.

Zur Kenntnis über die Hochdrucksynthese von Acrylester. VI. Mechanismus der Aktivierung des Kohlenoxyds an Triphenylphosphin-Nickelkomplexverbindungen

Von Kazumi YAMAMOTO

(Eingegangen am 24. April 1954)

Einleitung

In der vorigen Mitteilung[1] habe ich vorgeschlagen, die Triphenylphosphin-Nickelkomplexverbindungen von Typus $(Ph_3P)_2NiX_2RX'$ und $(Ph_3P)_2NiX_2RX'$, worin Ph den Phenylrest, R den Alkyl- oder Arylrest ausdrückt und X und X' selbes oder verschiedenes Halogenatom bedeuten, beziehungsweise als (Ph_3RP)-Ni (PPh_3) X_2X' und $(Ph_3RP)_2 : NiX_2X_2'$ zu bezeichnen. In dieser Mitteilung soll der Mechanismus der Aktivierung des Kohlenoxyds an Komplexverbindungen bei der Acrylestersynthese erörtert werden.

Über den betreffenden Mechanismus sind die $Ph_3PNi(CO)_3$-Theorie von McKinley[2] und die Hypothese von Schweckendiek, die in Copenhavers Buch[3] beschrieben ist, bekannt.

Um es kurz zu sagen, ist die Hypothese von McKinley wie folgt: Nickelcarbonyl mit der tetrahedrischen Struktur gibt unter der Umsetzung mit einem Molekül von Triphenylphosphin das wahrscheinlich verzogene Triphenylphosphin-Nickelcarbonyl $Ph_3PNi(CO)_3$, das durch das Nahekommen des Acetylens unter der Abgabe von einem Molekül Kohlenoxyd die Zwischenverbindung $Ph_3PNi(CO)_2(C_2H_2)$ liefert. Das $Ph_3PNi(CO)_3$ wird durch die Einwirkung von Kohlenoxyd auf solche instabile Zwischenverbindung wiedererzeugt, wobei das aktive Cyclopropenon sich bildet. Nach meinem Experiment jedoch hatte das $Ph_3PNi(CO)_3$ die katalytische Wirkung durchaus nicht.

Dementgegen scheine es, dass die Hypothese von Schweckendiek aus den drei verschiedenen Gedanken bestände. Das heisst;

1) $(Ph_3P)_2NiX_2$ gibt mit Kohlenoxyd unter der Abgabe von den Triphenylphosphinresten das sehr aktive $(CO)_2NiX_2$, das wieder mit Triphenylphosphin umsetzt und aktiviertes Kohlenoxyd abgibt.

$$(Ph_3P)_2NiX_2+2CO \rightleftarrows (CO)_2NiX_2+2Ph_3P$$

Dabei spielt Alkylhalogenid die Rolle, die Nebenreaktion vom Katalysator selbst zu hemmen.

2) Bei $(Ph_3P)_2NiX_2RX'$ (er behauptet, dass RX' sich durch die Nebenvalenz mit $(Ph_3P)_2NiX_2$ verbände) wird Alkylhalogenid reversibel durch Kohlenoxyd umgesetzt, wobei das Kohlenoxyd aktiviert wird

3) Der letzte Mechanismus wird nur schematisch dargestellt;

$$2(Ph_3P)_2NiBr_2RBr \xrightarrow{RBr} (Ph_3P)_3(NiBr_2)_2RBr + (Ph_3RP)Br$$

$$(Ph_3P)_3(NiBr_2)_2RBr + CO \rightarrow (Ph_3P)_3(CO)(NiBr_2)_2RBr$$

$$(Ph_3P)_3(CO)(NiBr_2)_2RBr + (Ph_3RP)Br \xrightarrow[C_2H_2]{R'OH}$$

$$CH_2{:}CHCOOR' + 2(Ph_3P)_2NiBr_2RBr$$

Es scheint, dass es seinen Gedanken an der Folgerichtigkeit fehlt. Darüber hinaus wird von mir festgestellt, dass Alkylhalogenid sich nicht nur durch die Nebenvalenz mit $(Ph_3P)_2NiX_2$ verbindet.

Reaktion von Komplexverbindungen mit Kohlenoxyd

Als ein Mittel zur Forschung vom Mechanismus der Aktivierung des Kohlenoxyds am Komplexkatalysator wurden die Verhalten von den typischen Vertretern, wie $(Ph_3P)_2NiBr_2$, $[Ph_3(C_4H_9)P]$-Ni$(PPh_3)Br_3$ und $[Ph_3(C_4H_9)P]$-Ni$(PPh_3)Br_3+C_4H_9Br$ (anstatt des unisolierbaren $[Ph_3(C_4H_9)P]_2 : NiBr_4$), gegen das unter Druck stehende Kohlenoxyd in Anwesenheit von Butanol beobachtet. Ich verhinderte dadurch das Reaktionsgemisch mit der Gefässwand in Berührung zu kommen, indem ich in einem Autoklav 100 cm³ Inhalt ein geöffnetes Glasgefäss von zirca 50 cm³ Inhalt (Figur 1.) einsetzte, in welchem 20 cm³ Butanol und 5 g Komplexverbin-

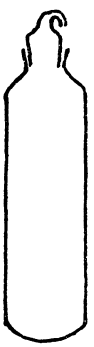


Fig. 1.

1) K. Yamamoto und M. Oku, Dieses Bulletin, **27** 509, (1954).
2) C. McKinley, *Ind. Eng. Chem.*, **44**, 995 (1952).
3) J. Copenhaver und M. Bigelow, „Acetylene and Carbonmonoxide Chemistry", Rheinhold Publ. Co., (1949), S. 261.

dung enthalten waren. Die Reaktionsbedingungen wurden wie folgt bestimmt; Anfangsdruck von Kohlenoxyd 15 Atm Reaktionstemperatur 180°, Laufzeit 1 Stunde.

1) **$(Ph_3P)_2NiBr_2$.** — Unter den Reaktionsbedingungen wurde einiger Druckabfall beobachtet. Nach der Abkühlung wurde die Bildung von Nickelcarbonyl durch die Rauchreaktion mit Bromdampf nachgewiesen. Das Reaktionsgemisch (hellgrün) liegen gelassen, schied sich der weisse Kristall ab, der bei 123° unter der Zersetzung schmilzt, und der als für $Ph_3PNi(CO)_3$ (vgl. Mitteilung III[4]) angesehen werden kann. Nach der Abscheidung vom Kristall die Mutterlauge unter dem Rückfluss gekocht, wurde der andere Kristall vom Schmelzpunkt 206° mit der Bildung des Nickelspiegels erhalten. Dies ist im Sinne folgenden Schemas zu erklären:

$$2Ph_3PNi(CO)_3 \longrightarrow Ni(CO)_4 + (Ph_3P)_2Ni(CO)_2 \text{ Smp. } 209°$$
$$\downarrow$$
$$\rightarrow Ni + 4\ CO$$

Wenn man die Mutterlauge nach der Beseitigung solch unlöslicher Substanzen noch einmal konzentriert, so kann man einen grünen Kristall (ca. 2g) nebst der kleinen Menge Triphenylphosphin (Smp. 79°C) erhalten. Der aus Butanol umkristallisierte schmilzt bei 178° und zeigt keinen Schmelzpunktabfall bei der Mischprobe mit $(Ph_3(C_4H_9)P)$-$Ni(PPh_3)Br_3$···d.h.,$(Ph_3P)_2NiBr_2C_4H_9Br$ ···(Smp 178°).. Das Erstaunliche ist, dass die ursprüngliche Substanz $(Ph_3P)_2NiBr_2$ gar nicht nachgewiesen wurde. Was die Bildung des $[Ph_3(C_4H_9)P]$-$Ni(PPh_3)Br_3$ betrifft, so kann man sich des Herstellungsverfahrens desselben aus $(Ph_3P)_2NiBr_2$ und Brom in Anwesenheit von Butanol erinnern[4]. Das heisst wird der Reaktionsverlauf den folgenden Gleichungen gemäss dargestellt;

$$(Ph_3P)_2NiBr_2 + 2CO \rightarrow (Ph_3P)_2Ni(CO)_2 + 2Br \text{ oder}$$
$$(Ph_3P)_2NiBr_2 + 3CO \rightarrow Ph_3PNi(CO)_3 + Ph_3P + 2Br$$
$$2(Ph_3P)_2NiBr_2 + 4C_4H_9OH + 2Br \rightarrow 2(Ph_3(C_4H_9)P)\text{-}Ni(PPh_3)Br_3 + C_3H_7COOC_4H_9 + 2H_2O$$

Auch bei der Acrylestersynthese unter der Anwendung vom gleichen Glasgefäss wurden die Bildungen von $(Ph_3P)Ni(CO)_3$ und $[Ph_3(C_4H_9)P]$-$Ni(PPh_3)Br_3$ festgestellt. Davon folglich wird die so wichtige Tatsache angedeutet, dass die katalytische Wirkung von der Komplexverbindung $(Ph_3P)_2NiX_2$ wirklich die von (Ph_3RP)-$Ni(PPh_3)X_3$ sei.

2) **$[Ph_3(C_4H_9)P]$-Ni$(PPh_3)Br_3$·····$[(Ph_3P)_2$-$NiBr_2C_4H_9Br]$.** — Unter den ganz gleichen Bedingungen reagiert diese Komplexverbindung mit Kohlenoxyd fast nicht. Sie wurde meistens ohne Veränderung zurückgewonnen.

3) **$[Ph_3(C_4H_9)P]_2$: $NiBr_4$···$[(Ph_3P)_2NiBr_2$-$2C_4H_9Br]$.** — Wie bisher wiederholt gesagt, wurde $[Ph_3(C_4H_9)P]$-$Ni(PPh_3)Br_3$ zusammen mit einem Molekül Butylbromid zur Probe angewandt, da die Komplexverbindung dieses Typus unisolierbar ist. In diesem Falle, wird nach der Reaktion Nickelcarbonyl im Abgase nachgewiesen und die erheblichen Mengen des wasserlöslichen Kristalls mit Smp. 235° und des Nickelbromids wurden vom Reaktionsgemisch aus erhalten. Der Kristall wird für Triphenylbutylphosphoniumbromid (Smp. 235°[1]) identifiziert. Es ist zwar schwierig, den Wiederspruch zwischen solchem Verhalten und der katalytischen Wirkung[5] dieses Typus aufzuklären. Jedoch kann man das Sein der Komplexverbindung dieses Typus und das Auftreten der folgenden Reaktion erwarten:

$$[Ph_3(C_4H_9)P]_2 : NiBr_4 + 4CO \rightarrow 2[Ph_3(C_4H_9)P]Br + \underbrace{Ni(CO)_4 + Br_2}$$
$$\downarrow \quad \uparrow$$
$$NiBr_2 + 4CO$$

Der Mechanismus der Aktivierung des Kohlenoxyds

1) **Mechanismus an $(Ph_3P)_2NiBr_2$.** — Wie in der Einleitung beschrieben, wird nach Schweckendiek der Mechanismus an $(Ph_3P)_2$-NiX_2 gemäss der Gleichung dargestellt:

$$(Ph_3P)_2NiX_2 + 2CO \rightleftarrows 2Ph_3P + (CO)_2NiX_2$$

Es wurde jedoch erklärt, dass die katalytische Wirkung dieser Komplexverbindung, wie in dem vorigen Paragraphen dargestellt, auf die von (Ph_3RP)-$Ni(PPh_3)X_3$ zurückzuführen ist. Die betreffende Gleichung wird wiedergegeben:

$$3(Ph_3P)_2NiX_2 + 3CO + 4ROH \rightarrow 2(Ph_3RP)\text{-}Ni(PPh_3)X_3 + Ph_3PNi(CO)_3 + Ph_3P + 2H_2O + R'COOR$$

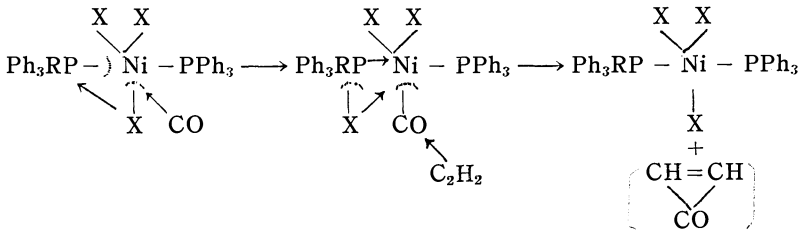
Verläuft demnach diese Umsetzung quantitativ, so soll sich 2/3 Molekül (Ph_3RP)-$Ni(PPh_3)X$ aus einem Molekül $(Ph_3P)_2NiX_2$

4) K. Yamamote, Dieses Bulletin, **27**, 501 (1954).
5) K. Yamamoto und M. Oku, Dieses Bulletin, **27**, 505 (1954)

bilden. Die Wahrheit zu sagen, bleibt die Bildung von demselben wahrscheinlich zwischen 2/3 und 1/3 Molekül, wegen der Nebenreaktion wie Bildung von Nickelcarbonyl. Auf solche Weise begreift es sich, dass die katalytische Fähigkeit der ursprünglichen Komplexverbindung zwischen dem äquivalenten (Ph_3RP)-$Ni(PPh_3)X_3$ und NiX_2 steht.

2) Mechanismus an (Ph_3RP)-$Ni(PPh_3)X_2X'$.—Die wichtige Frage ist also der Mechanismus an der Komplexverbindung (Ph_3RP)-$Ni(PPh_3)X_3$.

Meine von bisher beschriebenen Tatsachen geschlossene Meinung über die betreffende Aufgabe wird schematisch augenscheinlich so dargestellt;



$$(Ph_3RP)\text{-}Ni(PPh_3)X_3 + CO \rightleftarrows (Ph_3RP)X + Ni(PPh_3)(CO)X_2$$

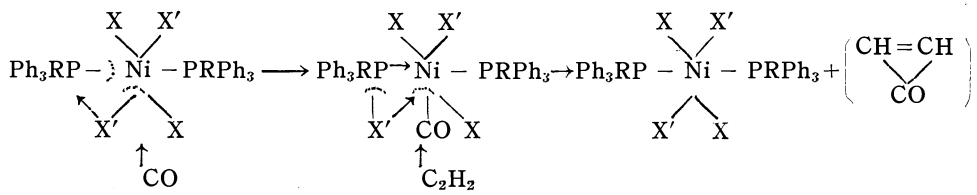
Das heisst, dieser Mechanismus ist so zu erklären, dass zuerst mit Kohlenoxyd das aktive, instabile 4-koordinative $Ni(PPh_3)$-$(CO)X_2$ unter der augenblicklichen Bildung von Phosphoniumhalogenid entsteht, das unter der Abgabe von aktiviertem Kohlenoxyd mit solchem Phosphoniumhalogenid die ursprüngliche Komplexverbindung wiedererzeugt. Der Grad, unter welchem die Bindung zwischen dem Nickel und Halogenatom unter dem Angriffe von Kohlenoxyd abgebrochen wird, ist desto grösser, je nichtionischer die betreffende Bindung ist, d.h., je schwerer das Atomgewicht des betreffenden Halogens ist, desto grösser wird die katalytische Wirkung der Mutterverbindung, wie bei dem anorganischen Nickelhalogenid[5].

Nach dieser Theorie ist das unter der Selektivität von schwerem Halogenatom zur Umsetzung mit Kohlenoxyd so zu erklären, dass die katalytische Wirkung der Komplexverbindung (Ph_3RP)-$Ni(PPh_3)X_2X'$ (wobei $X \neq X'$) beinahe mit der, der mit all demselben, schweren Halogenatom identisch ist.[5]

Auch die Erscheinung, welche bei der Zersetzung von solcher Mischhalogen-Komplexverbindung in Methanol nur Phosphoniumhalogenid mit schwerem Halogenatom stets nachgewiesen wird, trägt sicher gross zur Selektivität von Halogen-Kohlenoxyd-Umsetzung bei. Mit anderen Worten dürfte die Bindungsenergie zwischen dem Phosphoniumrest und Halogenatom sehr bedeutend sein. Auch der in Mitteilung IV[5] beschriebene Schluss über die Art und Nummer vom Halogenatom wird durch diese Theorie aufgeklärt werden. Das heisst, man kann die Zunahme von der katalytischen Fähigkeit mit der zunehmenden Nummer Halogenatom in der Komplexverbindung unter der Vergrösserung der Probabilität des Zusammenstosses vom Halogenatom mit Kohlenoxyd verstehen.

Solche Komplexverbindung, wie sie nur ein Halogenatom besitzt, das mit Nickel unmittelbar gebunden ist, z.B., $(Ph_3P)_2$-$Ni(OOCCH_2Cl)_2RX$ oder (Ph_3RP)-$Ni(PPh_3)$-$(OOCCH_2Cl)_2X$, soll die katalytische Fähigkeit haben[5], da diese Theorie wesentlich auf Grund der reversibelen Umsetzung von Kohlenoxyd mit einem Halogenatom ist.

3) Mechanismus an $(Ph_3RP)_2 : NiX_2X'_2$.—Es ist nun zweifellos, auch im Falle, dass R Alkyl ist, dass die Komplexverbindung $(Ph_3RP)_2 : NiX_2X'_2$ existiert, wenn gleich sie unisolierbar ist. Darüber hinaus drückt sich der Mechanismus der Aktivierung des Kohlenoxyds an dieser Komplexverbindung gemäss dem von (Ph_3RP)-$Ni(PPh_3)X_2X'$ schematisch aus;



$$(Ph_3RP)_2 : NiX_2X'_2 + CO \rightleftarrows (Ph_3RP)X' + (Ph_3RP)\text{-}Ni(CO)X_2X'.$$

Die Erläuterung sowohl vom Schema, als von der Bedeutung von Halogenatom (insbesondere von dem mit schwerem Atomgewicht) ist ebenfalls zu erklären wie in dem vorigen Paragraphen beschrieben. Die Tatsache, dass die katalytische Fähigkeit der Komplexverbindung dieses Typus grösser als die der entsprechenden Verbindung (Ph_3RP)-$Ni(PPh_3)X_2X'$ ist[5], wird man unter der Vergrösserung der Probabilität des Zusammenstosses sowohl von Halogenatom mit dem Phosphoniumrest, der als Halogenakzeptor wirkt, wie von Halogenatom mit Kohlenoxyd mit der zunehmenden Nummer von Halogenatom und Phosphoniumrest verstehen können. Nach meiner Theorie spielt überschüssiges Alkylhalogenid eine wichtige Rolle zur Erhaltung der Komplexverbindung dieses Typus, $(Ph_3RP)_2 : NiX_2X'_2$.

Die in vorigem Paragraphen beschriebene Tatsache, dass das $[Ph_3(C_4H_9)P]$ Br sich durch die Umsetzung von $[Ph_3(C_4H_9)P]_2 : NiBr_4$ mit dem unter Druck stehenden Kohlenoxyd in Abwesenheit von Acetylen als Akzeptor vom aktiven Kohlenoxyd bildete, bestätigt die Gültigkeit der oben erwähnten Theorie.

Um es kurz zu sagen, kann die zur Bildung von Cyclopropenon benötigte Aktivierungsenergie durch die Bildung der intermediären Kohlenoxyd-Komplexverbindung erniedrigt werden.

4) Mechanismus an NiX_2.—Vormals habe ich[6] mit meinem Mitarbeiter über die Acrylestersynthese in Anwesenheit vom Nickelhalogenidkatalysator und über das Verhalten des Kohlenoxyds mitgeteilt.

Ich möchte auf Grund der Erkenntnisse zum Mechanismus der Aktivierung des Kohlenoxyds am Komplexkatalysator wiederum über den betreffenden Mechanismus an NiX_2 Betrachtungen anstellen.

Wie schon mitgeteilt, hätte man von den verschiedenen experimentellen Tatsachen erwarten können, dass die Erniedrigung der zur Bildung des Cyclopropenons erforderlichen Aktivierungsenergie, durch die Bildung irgendeines intermediären Zwischenproduktes, das sich durch die Umsetzung von Kohlenoxyd und Nickelhalogenid, bevor das Nickelcarbonyl zusammengesetzt wird, bildet, erreicht wird.

Folgert man diese Annahme aus dem oben erwähnten Mechanismus am Komplexkatalysator, so dürfte man die Analogie zwischen den beiden Mechanismen finden. Bei der einfachen halogenhaltigen Nickelverbindung existiert nicht eine solche günstige Verbindung wie NiYX, wobei Y den Rest wie $ClCH_2COO$- ausdrückt. Es ist also zwar schwierig, diese Annahme experimentell darzutun, aber der Mechanismus an NiX_2 könnte nach Analogie von demselben am Komplexkatalysator dargestellt werden, wie folgt:

$$NiX_2 + CO \rightleftarrows NiX(CO) + X$$

Dies ist so zu erklären, dass das Nickelhalogenid mit einem Molekül Kohlenoxyd zunächst das unisolierbare, sicher sehr instabile NiX(CO) liefert, das unter Abgabe von aktiviertem Kohlenoxyd mit Halogenatom das Nickelhalogenid wieder erzeugt. Die meisten Halogenatome könnten sich auf solche Weise reversibel verlaufen, aber sie migrieren zum Teil zu unwirksamen Verbindungen. Und dies geht zum Schlusse die wirkliche Konzentration des Nickelhalogenids nieder. Die Hilfskatalysatorwirkung des metallischen Nickels könnte sich daraus erklären, dass das Nickel hauptsächlich die Rolle als Akzeptor dieser migrierenden Halogenatome unter dem Beitrag zur Erhaltung der wirklichen Konzentration des Nickelhalogenids spielt.

Auf solche Weise ist der Mechanismus an der Komplexverbindung mit dem an dem anorganischen Nickelhalogenid-Katalysator im wesentlichen nicht zu unterscheiden. Worauf beruht die Vorzüglichkeit des Komplexkatalysators, wenn das der Fall ist? Meine Antwort für die obige Aufgabe ist wie folgt:

1) Der Zusammenbruch vom Katalysator auf Grund der Migrierung des Halogens ist sehr wenig, da er in eigenem Molekül den mächtigen Akzeptor "Phosphoniumrest" für solches Halogenatom enthalten ist.

2) Die Bindung zwischen Nickel- und Halogenatom nimmt im nichtionischen Charakter durch die Koordination von Triphenylphosphin oder Phosphoniumrest an Nickelatom zu.

Ausserdem soll angegeben werden, d.h., die ausserordentliche Kristallisierbarkeit oder grosse Löslichkeit gegen ein organisches Lösungsmittel auf Grund des zunehmenden organischen Charakters der Nickelverbindung.

Zusammenfassung

Auf Grund der bisher erwähnten Tatsachen habe ich über den Mechanismus der Aktivierung des Kohlenoxyds an Triphenylphosphin-Nickelkomplexverbindungen die folgenden Schlüsse erhalten.

1) Die katalytische Wirkung von $(Ph_3P)_2$-NiX_2 Typus Komplexverbindung ist auf die von (Ph_3RP)-$Ni(PPh_3)X_3$ – $(Ph_3P)_2NiX_2RX$ –

6) K. Yamamoto und K. Sato, Dieses Bulletin, **27**, 496 (1954).

zurückzuführen.

2) Der Mechanismus an (Ph_3RP)-$Ni(PPh_3)$-X_2X' Komplexverbindung ist wie folgt zu formulieren:

$$(Ph_3RP)\text{-}Ni(PPh_3)X_2X' + CO \rightleftarrows (Ph_3RP)X' + Ni(PPh_3)(CO)X_2$$

Das heisst, dieser Mechanismus ist so zu erklären, dass zuerst mit Kohlenoxyd das aktive, instabile 4-koordinative $Ni(PPh_3)(CO)X_2$ unter der augenblicklichen Bildung von Phosphoniumhalogenid entsteht, das unter der Abgabe von aktivem Kohlenoxyd mit solchem Phosphoniumhalogenid die ursprüngliche Komplexverbindung wiedergibt.

3) Der Mechanismus an $(Ph_3RP)_2 : NiX_2X'_2 - (Ph_3P)_2NiX_2 2RX' -$ ist ebenso auch wie folgt zu formulieren;

$$(Ph_3RP)_2 : NiX_2X'_2 + CO \rightleftarrows (Ph_3RP)X' + (Ph_3RP)\text{-}Ni(CO)X_2X'$$

4) Der Mechanismus an Nickelhalogenid ist nach Analogie von dem an Komplexverbindungen zweckmässiger wie folgt, zu illustrieren

$$NiX_2 + CO \rightleftarrows NiX(CO) + X$$

5) Die Vorzüglichkeit der Komplexkatalysatoren wird wie folgt dargestellt:

a) Die Komplexverbindungen sind in eigenem Molekül den mächtigen Akzeptors "Phosphoniumrest" für Halogenatom enthalten.

b) Die Zunahme vom nichtionischen Charakter der Bindung Ni-Halogen auf Grund der Koordination von dem Triphenylphosphin oder Phosphoniumrest an Nickelatom.

Herr Dr. K. Yoshikawa hat mich stets bei meinen Arbeiten leitend unterstützt und ermutigt. Die Herren M. Oku und K. Sato haben mit mir eifrig mitgearbeitet und Beistand durch lebhafte Diskussion über diesen Gegenstand geleistet. Ich sage diesen Herren und der Mitsui Chemical Industry Co., die mir diese Veröffentlichung meiner Arbeiten erlaubte, hierdurch meinen herzlichen Dank.

Mitsui Chemical Industry Co. Ltd. Miike Dyestuff and Chemical Works, Omuta, Fukuoka

Radiochemical Studies on Ultra-Micro Quantities of Organometallic Compounds. II. On the Composition of Polonium Dithizonate

By Tomitaro ISHIMORI

(Received November 11, 1953)

Previously the author[1] has reported on the formation of polonium dithizonate which is extracted into a carbon tetrachloride solution of dithizone (diphenylthiocarbazone) from an aqueous solution under some appropriate chemical circumstances. Further there is a literature[2] which shows that the complex salt can be used in the purification of polonium; however, the present author could not find out any report on the composition of polonium dithizonate.

In the present paper, the composition of polonium dithizonate (formed in a solution acidified with nitric acid) is determined according to the method described in the first paper[3] of this series and the author estimates that two anions of dithizone are bound to one atom of polonium in polonium dithizonate.

(A) Preparation of the Polonium Solution.—The polonium solution used is a solution of radium F which is prepared as follows:

1.5 g. powdered pitchblende are dissolved in nitric acid. The undissolved residue is filtered off after the solution is diluted with water. The filtrate is treated with hydrogen sulfide to precipitate polonium (radium F) with lead and some other elements of the hydrogen sulfide group which may occur in the starting material. The precipitate is dissolved in nitric acid, and the residue containing sulfur is filtered off. The filtrate is diluted until the content of nitric acid becomes about 2.5% (vol.), and then extracted successively with some portions of the chloroform solution of dithizone. The combined chloroform solution is shaken with 10 cc. of (1:1) nitric acid to obtain an aqueous solution of polonium. The aqueous solution is separated, diluted to about 20 cc. with water, and preserved as the stock solution.

1) T. Ishimori and H. Sakaguchi, *J. Chem. Soc. Japan*, **71**, 327 (1950).
2) G. Bouissieres and C. Ferrandini, *Anal. Chim. Acta*, **4**, 610 (1950).
3) T. Ishimori, This Bulletin, **27**, 139 (1954).

The resultant solution contains about 25% (vol.) nitric acid and about 10^{-9} curie radium F (about 10^{-12} g. P_0) per 1 cc. The radioactivity due to the alpha emission of the evaporated residue of the solution is measured by an electroscope (gold leaf type) made by the Scientific Research Institute, Tokyo. The decay of the radioactivity shows that the half-life is about 140 days (Fig. 1). On the other hand, the extremely weak beta-rays are detected by a Geiger-Müller counter. Therefore, this solution seems to contain slight contaminations of radium E and other isotopes.

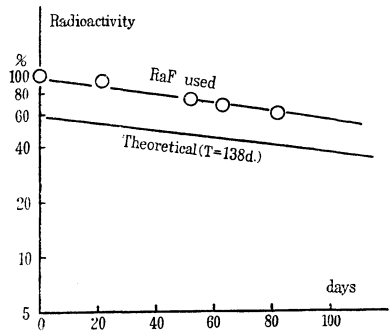


Fig. 1. Decay of RaF

(B) Determination of the Composition of Polonium Dithizonate.—In the first paper[3] of this series, the author gave a method for the determination of the composition of an organo-metallic compound in an ultra-micro amount, basing his conclusions on the following relation:

$$E^{-1}=A+B(HR)^{-n}$$

where, E is extractability, the ratio of the radioactivity due to the total amount of the radioactive metallic cation taken into the system and that extracted into the organic phase, n, the ratio between the number of organic anions and that of the metallic cation, and A and B are constants.

According to the method, the composition of polonium dithizonate is determined by repeating the measurement of extractability for various amounts of dithizone, (HDz), plotting the results in $E^{-1}-(HDz)^{-1,2,3}$ diagrams, and finding out $(HDz)^{-n}$ which is almost linear to E^{-1}. In these experiments, all experimental conditions such as pH and volume of the aqueous phase or volume of the organic phase, must be kept constant. Otherwise the above equation can not be used as the theoretical basis.

(1) Series of Experiments I.—10 cc. of distilled water and 1.0 cc. of the stock solution of polonium are respectively added to six small separating funnels. Though the solutions are not buffered, the pH values are supposed to be fairly constant as they contain about 2.2% (vol.) of nitric acid. Therefore, the necessary condition for a constant pH value[3] is almost satisfied in this case.

5.0 cc. of the dithizone chloroform solutions with various concentrations are prepared by diluting the stock solution of dithizone in chloroform (about 0.4×10^{-3} mol./l.)[4] and added to each separating funnel which contains the diluted aqueous solution of polonium. The funnels are shaken vigorously for a minute.

The separated chloroform layers are evaporated up in glass dishes to measure the radioactivities due to the fractions of radium F which are extracted into the chloroform solution.

The measured intensities[5] are compared with that of the standard specimen which is prepared by evaporating 1 cc. of the stock solution of polonium in a glass dish, and the extractability, E, is calculated.

The results obtained are shown in Table I and Fig. 2(a,b,c).

TABLE I

RESULTS OF (B, 1)

No.	(HDz)	$(HDz)^{-1}$	$(HDz)^{-2}$	$(HDz)^{-3}$	d/m $P_{0\,extd.}$	E^{-1}
1	0.96	1.04	1.09	1.13	11.75	1.31
2	0.42	2.38	5.66	13.5	10.33	1.49
3	0.080	12.5	156	1.95×10^{3}	3.43	4.48
4	0.032	31.2	974	3.04×10^{4}	0.87	17.7
5	0.024	41.7	1740	6.97×10^{4}	0.55	28.0
6	0.000	∞	∞	∞	−0.03	—

E: Extractability; The ratio of radioactivities due to radium F taken (15.39 d/m) and radium F extracted.

(HDz): Amount of dithizone denoted in an arbitrary unit in which $(HDz)=1$ corresponds to about 10^{-6} gram mol. dithizone.

4) The concentration of the chloroform solution of dithizone is determined by titrating known quantities of silver nitrate.

5) The radioactivity is measured by the electroscope mentioned above. The absorption of alpha-particles is checked by adding the stock solution of dirhizone on the specimen of polonium and drying it up. The following table shows that the effect of the absorption is negligible.

ml. dithizone solution (added)	0	1	2
radioactivity measured (d/m)	18.8	19.2	19.4

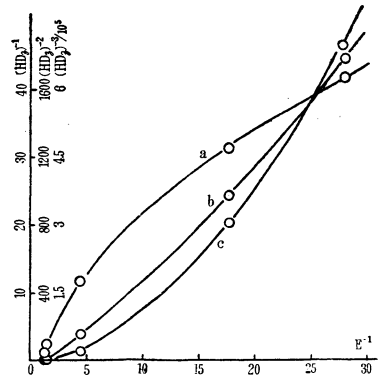


Fig. 2(a, b, c). $(HDz)^{-n}-E^{-1}$ diagram
a: $(HDz)^{-1}-E^{-1}$
b: $(HDz)^{-2}-E^{-1}$
c: $(HDz)^{-3}-E^{-1}$

(2) Series of Experiments II.—Almost the same experiments are repeated, but the procedures are slightly different from that of (1) in the following point: The aqueous solution of polonium is prepared by pipetting 4 cc. of the stock solution of polonium into a 50 cc. volumetric flask, and then adding water to the mark. After mixing thoroughly, 10 cc. of the diluted solution of polonium are taken to each separating funnel respectively. Therefore, the acidity of the aqueous solution is weaker than that of (1).

The results are shown in Table II as well as Fig. 3(a,b,c).

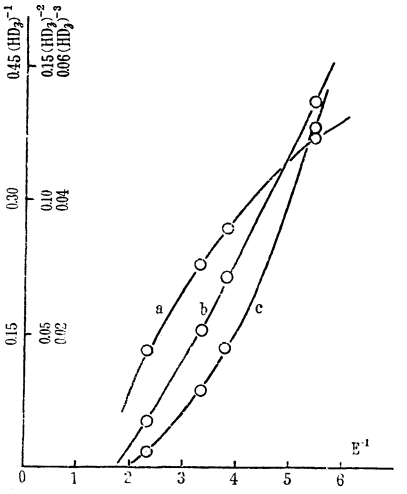


Fig. 3(a, b, c). $(HDz)^{-n}-E^{-1}$ diagram
a: $(HDz)^{-1}-E^{-1}$
b: $(HDz)^{-2}-E^{-1}$
c: $(HDz)^{-3}-E^{-1}$

TABLE II
RESULTS OF (B, 2)

No.	(HDz)	$(HDz)^{-1}$	$(HDz)^{-2}$	$(HDz)^{-3}$	d/m P_0 extd.	E^{-1}
1	7.50	0.133	0.0176	0.0024	6.01	2.33
2	4.38	0.228	0.0519	0.0118	4.20	3.34
3	3.75	0.267	0.0713	0.0181	3.44	3.79
4	2.70	0.371	0.137	0.0509	2.39	5.45

E: Extractability; The ratio of radioactivities due to radium F taken (13.00 d/m) and radium F extracted.
(HDz): Amount of dithizone denoted in an arbitrary unit in which $(HDz)=1$ corresponds to about 10^{-8} gram mol. dithizone.

In these two series of experiments, the acidity of the aqueous solution is different. So the values of extractability given by both series do not coincide for a value of (HDz). However, the results of both series agree in the facts that almost linear relation is found between $(HDz)^{-2}$ and E^{-1} (cf. Fig. 2b and 3b), while the curve of $(HDz)^{-1}-E^{-1}$ is convex (cf. Fig. 2a and 3a) and that of $(HDz)^{-3}-E^{-1}$ is concave. Therefore according to the method described in the first paper of this study,[3] polonium dithizonate is supposed to have two anions of dithizone for one atom of polonium.

So far there is no generally accepted knowledge about the form in which polonium is dissolved in aqueous solutions. However G. v. Hevesy et al.[6] reported bivalent cation Po^{++} in hydrochloric acid solution. On the other hand M. Haissinsky[6] reported that PoO_3^{--} or PoO^{++} is prevailing in dilute nitric acid solution. So we can guess that polonium dithizonate will correspond to the chemical formula $PoDz_2$ or $PoODz_2$.

The author wishes to express has hearty thanks to Prof. Iwaji Iwasaki, Tokyo Institute of Technology, who was kind enough to send him some pitchblende for the preparation of radium F.

Department of Chemistry,
Faculty of Science,
Kyushu University,
Fukuoka

6) Gmelins Handbuch d. Anorganischen Chemie, 8 Auflage, System Nr. 12 (1941). Verlag Chemie, Berlin, S. 103-104.

Polarographic Diffusion Current Observed with Square Wave Voltage. I. Effect Produced by the Sudden Change of Electrode Potential

By Tomihito KAMBARA

(Received February 26, 1954)

In recent years several polarographic electrolyses with rectangular voltage have been reported, providing us many attractive findings. Therefore the present author intends to clear up at first the effects due to the sudden change of electrode potential and then the essential feature of electrolysis with square wave voltage theoretically and further elucidate some experimental results.

Note on the Boundary Condition

In order to discuss the diffusion current observed in the polarographic electrolysis, we must solve the system of differential equations for the diffusions of two materials, i.e. the oxydant (suffix O) and the reductant (suffix R), given by

$$\frac{\partial C_0}{\partial t}=D_0\frac{\partial^2 C_0}{\partial x^2};\quad \frac{\partial C_R}{\partial t}=D_R\frac{\partial^2 C_R}{\partial x^2}. \tag{1}$$

Since before the electrolysis, the initial uniform concentrations $*C_0$ and $*C_R$ govern the system, the initial condition is shown by

$$t=0,\ 0\leqq x\leqq\infty,\ C_0=*C_0,\ C_R=*C_R. \tag{2}$$

The boundary condition, on the other hand, depends on the experimental condition. In the case that the electrolysis is carried out under the application of a constant voltage, it is imagined that each of the concentrations of oxidant and reductant at the electrode surface takes a constant value immediately after the beginning of electrolysis. Such a conception has been given by Cottrel[1] and Ilkovic.[2] We have treated this problem while taking the rates of forward and reverse reactions of the electrode process into consideration[3]; the analogous treatments are also given by Meiman,[4] Smutek[5] and Delahay.[6] In this article, however, let us suppose that the ratio of the concentrations of both forms at the electrode surface is given by the Nernst formula, i.e. the velocities of the electrode processes in two directions are so great that an equilibrium state is always attained thereat. Therefore it is seen that

$$x=0,\ t>0,\ C_R=K_1\cdot C_0, \tag{3}$$

where the equilibrium constant K_1 depends on the electrode potential E_1 and is given by

$$K_1=\exp\frac{-nF(E_1-E_0)}{RT}. \tag{4}$$

In this equation the symbols n, F, R, T and E_0 are used in their usual significances. On the other hand, as for the flows of the diffusing oxidant and reductant, it is obvious that the material flow must be continuous everywhere, provided that there is no accumulation or disappearance at the electrode surface. Accordingly it is found that

$$x=0,\ t>0,\ D_0\frac{\partial C_0}{\partial x}=-D_R\frac{\partial C_R}{\partial x} \tag{5}$$

This condition can be rigorously obtained, as shown by Sevcik,[7] when the amount of oxydant disappearing in unit time is considered to be equal to the amount of reductant produced newly by the electrode reaction in unit time.

As is well known, the general integrals of Eqs. (1) are given by

$$C_0=a_0+b_0\cdot\operatorname{erf}\frac{x}{2\sqrt{D_0t}};$$

$$C_R=a_R+b_R\cdot\operatorname{erf}\frac{x}{2\sqrt{D_Rt}}. \tag{6}$$

From the above cited conditions, it is seen that among four integral constants, a_0, b_0, a_R and b_R, the following relationships hold.

$$\left.\begin{aligned} &a_0+b_0=*C_0;\quad a_R+b_R=*C_R;\\ &a_R=K_1a_0;\quad \sigma b_0=-b_R;\end{aligned}\right\}, \tag{7}$$

where

$$\sigma=\sqrt{D_0/D_R}.$$

Whence

$$\left.\begin{aligned} &a_0=\frac{\sigma *C_0+*C_R}{\sigma+K_1}={}^{\circ}_{1}C_0;\quad a_R=K_1\cdot a_0={}^{\circ}_{1}C_R;\\ &b_0=*C_0-{}^{\circ}_{1}C_0;\quad b_R=*C_R-{}^{\circ}_{1}C_R;\end{aligned}\right\} \tag{9}$$

where ${}^{\circ}_{1}C_0$ and ${}^{\circ}_{1}C_R$ are the respective interfacial concentrations corresponding to the constant potential E_1. Therefore, it follows that

$$\left.\begin{aligned} &C_0={}^{\circ}_{1}C_0+(*C_0-{}^{\circ}_{1}C_0)\cdot\operatorname{erf}\frac{x}{2\sqrt{D_0t}};\\ &C_R={}^{\circ}_{1}C_R+(*C_R-{}^{\circ}_{1}C_R)\cdot\operatorname{erf}\frac{x}{2\sqrt{D_Rt}}\end{aligned}\right\}. \tag{10}$$

Accordingly it is seen that in the integration of linear diffusion equation, upon supposing that the continuity of fluxes and an equilibrium state between the concentrations of two forms hold at the electrode surface, we have the result that

1) F. G. Cottrel, *Z. phys. Chem.*, **42**, 385 (1903).
2) D. Ilkovic, *Collection Czech. Chem. Communs.*, **6**, 498 (1934); *J. chim. physique*, **35**, 129 (1938).
3) T. Kambara and I. Tachi, This Bulletin, **25**, 135 (1952); T. Kambara, ibid., 281.
4) N. Meiman, *J. Phys. Chem. USSR*, **22**, 1454 (1948).
5) M. Smutek, *Chem. Listy*, **45**, 241 (1951); *Collection Czech. Chem. Communs.*, **18**, 171 (1953).
6) P. Delahay, *J. Am. Chem. Soc.*, **75**, 1430 (1953).
7) A. Sevcik, *Collection Czech. Chem. Communs.*, **13**, 349 (1948).

both interfacial concentrations have constant values.

This conclusion is identical with that given by Ilkovic,[2] by whose theory it is supposed that the boundary condition is given by

$$x=0,\ t>0,\ C_0={}^{i}_{i}C_0,\ C_R={}^{i}_{i}C_R. \tag{11}$$

It must be mentioned here, however, that there is no rational reason for the constancies of ${}^{c}_{i}C_0$ and ${}^{c}_{i}C_R$, as pointed out by MacGillavry.[8] It is seen, for example, that even if ${}^{c}_{i}C_0$ and ${}^{c}_{i}C_R$ are both certain functions of time t, it is possible that the ratio ${}^{c}_{i}C_0/{}^{c}_{i}C_R$ might be independent of time. And it is obvious that merely from the condition of an equilibrium state at the surface, the conclusion that the concentrations ${}^{c}_{i}C_0$ and ${}^{c}_{i}C_R$ are constant, respectively, can not result, while their ratio is readily seen to be constant. Nevertheless it is clear that by employing Eq. (5) the identity of the conclusions derived from the above two theories is confirmed. Further it must be remembered that although the same conclusion is attained by employing the two different boundary conditions, such an accordance can not be derived when the solution does not stretch to infinity in one dimension, or the electrode shows not a flat surface but a spherical one.

Discontinuous Change of the Electrode Potential

Now, let us consider the case when the potential of the observation electrode is discontinuously and abruptly changed as shown in Fig. 1; i.e. from $t=0$ the electrolysis begins under the application of potential E_1 and at $t=T$ the potential jumps from E_1 to E_2 discontinuously.

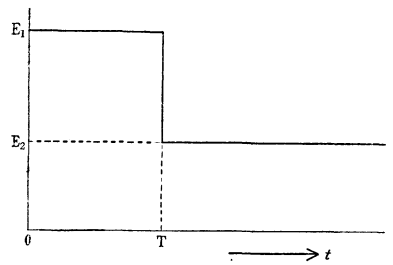


Fig. 1.

(1) Solution by Means of Laplace Transformation.—Let τ be the time elapsed after the potential was abruptly changed from E_1 to E_2; then it is clear that

$$\tau=t-T. \tag{12}$$

Hence our problem comes to integrate the equations:

$$\frac{\partial C_0}{\partial \tau}=D_0\frac{\partial^2 C_0}{\partial x^2};\quad \frac{\partial C_R}{\partial \tau}=D_R\frac{\partial^2 C_R}{\partial x^2} \tag{13}$$

with the initial condition shown by

$$\left.\begin{aligned}&\tau=0,\ x>0,\\ &C_0=a_0+b_0\cdot\operatorname{erf}\frac{x}{2\sqrt{D_0T}}=C_0^{\pm}(x),\\ &C_R=a_R+b_R\cdot\operatorname{erf}\frac{x}{2\sqrt{D_RT}}=C_R^{\pm}(x).\end{aligned}\right\} \tag{14}$$

This condition is required by the above discussions. The boundary condition is, on the other hand, demonstrated by

$$x=0,\ \tau>0,\ D_0\frac{\partial C_0}{\partial x}=-D_R\frac{\partial C_R}{\partial x},\ C_R=K_2\cdot C_0, \tag{15}$$

where

$$K_2=\exp\frac{-nF(E_2-E_0)}{RT}. \tag{16}$$

This condition results from the principle of continuity of fluxes and the assumption of a state of equilibrium between the concentrations of the two forms at the interface.

By means of the Laplace transformation defined by

$$\mathfrak{L}C(x,\tau)=p\int_0^\infty e^{-p\tau}\cdot C\cdot d\tau=u(x,p),$$

we can finally obtain the formulae for u_0 and u_R; i.e. they can be written in the form

$$\left.\begin{aligned}u=&A\cdot e^{mx}+B\cdot e^{-mx}\\ &+b\cdot\operatorname{erf}\frac{x}{2\sqrt{DT}}+2a\cdot\sinh\frac{mx}{2}\\ &-\frac{b}{2}\cdot e^{mx+pT}\left\{\operatorname{erf}\left(\frac{x}{2\sqrt{DT}}+\sqrt{pT}\right)-\operatorname{erf}\sqrt{pT}\right\}\\ &-\frac{b}{2}\cdot e^{-mx+pT}\left\{\operatorname{erf}\left(\frac{x}{2\sqrt{DT}}-\sqrt{pT}\right)+\operatorname{erf}\sqrt{pT}\right\},\end{aligned}\right\} \tag{17}$$

where the subscripts O and R are omitted and the m's are shown by

$$m_0=\sqrt{p/D_0};\ m_R=\sqrt{p/D_R}. \tag{18}$$

Next the four integral constants A_0, B_0, A_R and B_R, can be determined by Eqs. (15) and (16). Then it can be readily seen that the transformations of the interfacial concentrations are given by

$$\left.\begin{aligned}{}^{\circ}u_0&=A_0+B_0=\frac{\sigma^*C_0+{}^*C_R}{K_2+\sigma}=\mathfrak{L}^{\circ}_2C_0;\\ {}^{\circ}u_R&=A_R+B_R=K_2(A_0+B_0)=\mathfrak{L}^{\circ}_2C_R.\end{aligned}\right\} \tag{19}$$

There is no doubt that these equations imply that the interfacial concentrations are independent of time τ and that they are equal to the equilibrium interfacial concentrations which are to be observed when the constant potential E_2 is applied throughout from $t=0$ continuously [Cf. Eq. (9)].

Next we will evaluate the current intensity. From Eq. (17) it follows that

$$\left(\frac{\partial u_0}{\partial x}\right)_{x=0}=\sqrt{\frac{p}{D_0}}(A_0-B_0)=\frac{\sqrt{p}}{(K_2+\sigma)\sqrt{D_0}}\cdot\{(K_2a_0-a_R)+(K_2b_0-b_R)\cdot e^{pT}\cdot\operatorname{erfc}\sqrt{pT}\}. \tag{20}$$

8) D. MacGillavry, *Rec. trav. chim. Pays-Bas*, **57**, 33 (1938).

9) Cf. Table of transformations given in R. V. Churchill: "Modern Operational Mathematics in Engineering." (1944).

Further it is found that

$$\frac{K_2a_0-a_R}{K_2+\sigma}={}^{\circ}_{1}C_0-{}^{\circ}_{2}C_0;\quad \frac{K_2b_0-b_R}{K_2+\sigma}=b_0=*C_0-{}^{\circ}_{1}C_0. \tag{21}$$

Now, for the execution of inverse transformation, the following theorems are useful.

$$\mathfrak{L}^{-1}\sqrt{p}=\frac{1}{\sqrt{\pi\tau}};$$

$$\mathfrak{L}^{-1}\sqrt{p}\cdot e^{pT}\cdot\operatorname{erfc}\sqrt{pT}=\frac{1}{\sqrt{\pi(T+\tau)}}. \tag{22}$$

Hence it is manifest that

$$\left(\frac{\partial C_0}{\partial x}\right)_{x=0}=\frac{*C_0-{}^{\circ}_{1}C_0}{\sqrt{\pi D_0(T+\tau)}}+\frac{{}^{\circ}_{1}C_0-{}^{\circ}_{2}C_0}{\sqrt{\pi D_0\tau}}. \tag{23}$$

(2) Solution by Means of the Principle of Superposition.—It is obvious from the above deduction that when the voltage as shown in Fig. 1 is applied, it can be assumed that the interfacial concentrations in a state of equilibrium take constant values according to the electrode potential, provided that the rate of the electrode process is rapid enough. Accordingly our problem is now to solve the Eq. (1) with the initial condition given by Eq. (2) and with the boundary condition given by

$$x=0,\quad \begin{cases} T>t>0, & C_0={}^{\circ}_{1}C_0; \\ t>T, & C_0={}^{\circ}_{2}C_0. \end{cases} \tag{24}$$

Further it is clear that the applied voltage shown in Fig. 1 is equivalent to the superposition of the two constant voltages, as given by

$$\begin{aligned} E&=E_I+E_{II} && (t>0); \\ E_I&=E_1 && (t>0); \\ E_{II}&=\begin{cases} E_2-E_1 & (t>T); \\ 0 & (T>t>0). \end{cases} \end{aligned} \tag{25}$$

This relation is illustrated in Fig. 2(a) and (b). It may be supposed analogously that as for the interfacial concentration the superposition of two concentrations as shown in Fig. 3(a) and (b) is also effective. Then we can divide the function $C_0(x, t)$ into two parts; namely

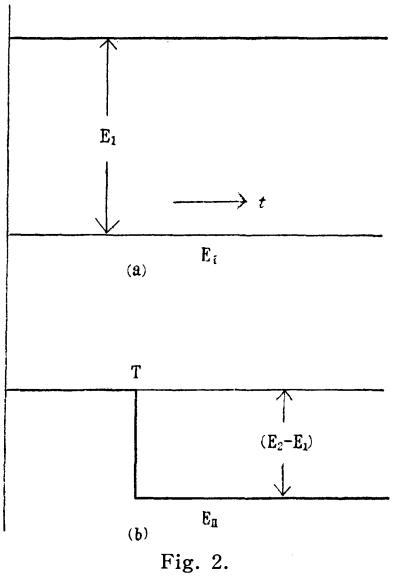


Fig. 2.

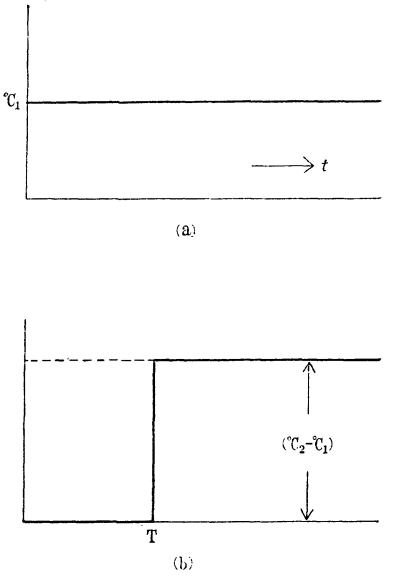


Fig. 3.

$$C_0=C_0(\mathrm{I})+C_0(\mathrm{II}), \tag{26}$$

and we have to integrate the following two equations.

$$\frac{\partial C_0(\mathrm{I})}{\partial t}=D_0\frac{\partial^2 C_0(\mathrm{I})}{\partial x^2};\quad \frac{\partial C_0(\mathrm{II})}{\partial t}=D_0\frac{\partial^2 C_0(\mathrm{II})}{\partial x^2}. \tag{27}$$

The conditions for $C_0(\mathrm{I})$ are shown by

$$\begin{cases} t=0, & 0\leq x\leq\infty, & C_0(\mathrm{I})=*C_0; \\ t>0, & x=0, & C_0(\mathrm{I})={}^{\circ}_{1}C_0, \end{cases} \tag{28}$$

and as for the function $C_0(\mathrm{II})$, the following conditions are valid.

$$\begin{cases} t\leq T, & 0\leq x\leq\infty, & C_0(\mathrm{II})=0; \\ t>T, & x=0, & C_0(\mathrm{II})={}^{\circ}_{2}C_0-{}^{\circ}_{1}C_0. \end{cases} \tag{29}$$

The solutions thereof are clearly given by

$$\left.\begin{aligned} C_0(\mathrm{I})&=*C_0-(*C_0-{}^{\circ}_{1}C_0)\cdot\operatorname{erfc}\frac{x}{2\sqrt{D_0t}}; \\ C_0(\mathrm{II})&=\begin{cases} 0: & (T\geq t) \\ ({}^{\circ}_{2}C_0-{}^{\circ}_{1}C_0)\cdot\operatorname{erfc}\dfrac{x}{2\sqrt{D_0(t-T)}}, & (t>T) \end{cases} \end{aligned}\right\} \tag{30}$$

and there is no doubt that by the sum of these two functions the desired solution is shown as given by Eq. (26). Thus the concentration gradient at the electrode surface is shown by

$$\left(\frac{\partial C_0}{\partial x}\right)_{x=0}=\frac{*C_0-{}^{\circ}_{1}C_0}{\sqrt{\pi D_0t}}+\frac{{}^{\circ}_{1}C_0-{}^{\circ}_{2}C_0}{\sqrt{\pi D_0(t-T)}}, \tag{31}$$

where the second term in the right hand side of the equation should disappear for $t<T$. Eq. (31) is clearly identical with the conclusion of the preceding discussion shown by Eq. (23), since the relationship $\tau=t-T$ holds.

Indeed the solution given by Eqs. (26) and (30)

is obtained only with the assumption that the interfacial concentration has a constant value according to the electrode potential. However, the fact that the solution satisfies the two conditions, i.e. the concentrations of both forms are in an equilibrium state at the electrode surface and also that the fluxes of both forms are continuous at the surface, can be easily verified. Further no discussion may be needed about the facts that for the reductant also a similar relation holds.

Discussion of the Result

In Fig. 4 is shown an example of the variation of concentration distribution near the electrode surface with time. The

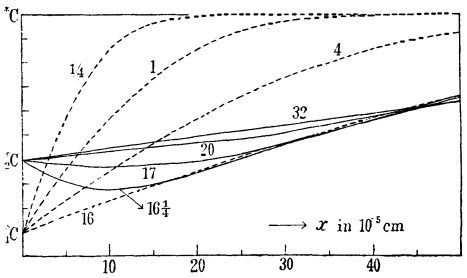


Fig. 4. Theoretical curves representing the variation of concentration distribution of depolarizer with time, drawn with the values: $^{\circ}_{1}C = \frac{1}{10}{}^{*}C$; $^{\circ}_{2}C = \frac{4}{10}{}^{*}C$; $D = 10^{-6}\,\mathrm{cm^2.\,sec^{-1}}$. Figures show the times elapsed after the electrolysis in the unit of 1/100 sec., and the potential is converted from E_1 to E_2 at $T = 16/100$ sec.

legitimacy of the above discussion can be rationally comprehensible from the consideration of special cases. Namely, when the discontinuous jump of the electrode potential at $t=T$ is zero, it follows that

$$E_1 = E_2\,;\ {}^{\circ}_{1}C_0 = {}^{\circ}_{2}C_0\,;\ \left(\frac{\partial C_0}{\partial x}\right)_{x=0} = \frac{{}^{*}C_0 - {}^{\circ}_{1}C_0}{\sqrt{\pi D_0 t}}. \quad (32)$$

This conclusion is, of course, quite in harmony with the Cottrel-Ilkovic theory for the current at a stationary plane electrode. Further, when the condition given by $t \gg T$ is satisfied, viz. when a considerable long time has elapsed after the change of voltage from E_1 to E_2, the hysterisis of the diffusion layer produced by the electrolysis with the application of voltage E_1 during the time interval from $t=0$ to $t=T$ should be ignored, compared with the long history of electrolysis performed after that. This can be well demonstrated by the following equation.

$$\left(\frac{\partial C_0}{\partial x}\right)_{x=0} \approx \frac{{}^{*}C_0 - {}^{\circ}_{2}C_0}{\sqrt{\pi D_0 (t-T)}} \approx \frac{{}^{*}C_0 - {}^{\circ}_{2}C_0}{\sqrt{\pi D_0 t}}. \quad (33)$$

According to the above theoretical treatment, however, it is required that the current intensities at $t=0$ and $t=T$ become infinite. This is clearly irrational; but in order to surmount this difficulty, it is necessary to take the rates of the electrode processes into consideration. As reported in the above quoted papers[3,6]; the mathematical treatment thereof, however, seems to be much more complicated.

Summary

Change of the structure of diffusion layer with time and the course of diffusion current at a stationary and reversible electrode due to the sudden change of the applied voltage are discussed mathematically.

The author wishes to express his sincere thanks to Professor I. Tachi for his kind encouragement.

Department of Agricultural Chemistry, Faculty of Agriculture, Kyoto University, Kyoto

Polarographic Diffusion Current Observed with Square Wave Voltage. II. Basic Theory for a Reversible Electrode

By Tomihito KAMBARA

(Received February 26, 1954)

In the preceding paper[1] the diffusion current, observed when the voltage applied to a reversible electrode is suddenly changed, is discussed theoretically. The theory is so easily to be extended that the electrolysis with a square wave voltage as shown in Fig. 1(a) can be elucidated as follows.

Our problem is now to solve the differential equation:

$$\partial C/\partial t = D \cdot \partial^2 C/\partial x^2 \qquad (1)$$

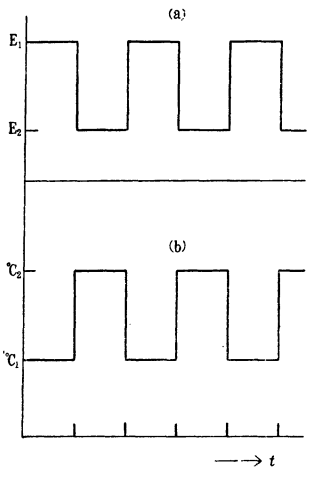


Fig. 1. Changes of electrode potential and interfacial concentration of depolarizer.

with the proper conditions which hold when the square wave voltage $E(t)$ of the period $2T$ shown by

$$\left.\begin{aligned} E(t) &= \begin{cases} E_1 & (0<t<T) \\ E_2 & (T<t<2T) \end{cases} \\ E(t) &= E(t+2T) \end{aligned}\right\} \qquad (2)$$

is applied. Since the concentration of depolarizer shows everywhere the constant value $^*C$ before the electrolysis, the initial condition is given by

$$t=0,\ 0\leq x\leq \infty,\ C = {}^*C. \qquad (3)$$

Next as for the interfacial concentration, it is shown in the previous paper that the conception that the concentrations of the oxidized and reduced forms are at a state of equilibrium at the electrode surface leads to a simplified supposition that each interfacial concentration shows a constant value according to the applied potential. Thus it is seen that the boundary condition is given by $x=0,\ t>0$,

$$C = \begin{cases} {}^\circ_1C & (E=E_1;\ 2nT<t<(2n+1)T) \\ {}^\circ_2C & (E=E_2;\ (2n+1)T<t<(2n+2)T) \end{cases} \qquad (4)$$

where n is an integer. This relationship is illustrated in Fig. 1(b).

(1) Solution by Means of the Principle of Superposition.—Let the function $C(x,\ t)$ be an algebraic sum of the functions $C(\mathrm{I})$, $C(\mathrm{II})$,……, etc.; namely

$$C = C(\mathrm{I}) + C(\mathrm{II}) + C(\mathrm{III}) + C(\mathrm{IV}) + \cdots\cdots, \qquad (5)$$

and it is supposed that each function is governed by Fick's law of diffusion. As shown in Part I of this study, the following relations hold for the function $C(\mathrm{I})$.

$$\left.\begin{aligned} &t=0,\ 0\leq x\leq\infty,\quad C(\mathrm{I}) = {}^*C; \\ &t>0,\ x=0,\qquad C(\mathrm{I}) = {}^\circ_1C; \\ &C(\mathrm{I}) = {}^\circ_1C + ({}^*C - {}^\circ_1C)\cdot \mathrm{erf}\frac{x}{2\sqrt{Dt}} \end{aligned}\right\} \qquad (6)$$

Further, as for the function $C(\mathrm{II})$, the following relations hold.

$$\left.\begin{aligned} &t-T\leq 0,\ 0\leq x\leq\infty,\ C(\mathrm{II}) = 0; \\ &t-T>0,\ x=0,\ C(\mathrm{II}) = {}^\circ_2C - {}^\circ_1C; \\ &C(\mathrm{II}) = ({}^\circ_2C - {}^\circ_1C)\cdot \mathrm{erfc}\frac{x}{2\sqrt{D(t-T)}} \end{aligned}\right\} \qquad (7)$$

When such a calculation is carried out repeatedly, next it is found that $C(\mathrm{III})$ is shown by

$$\left.\begin{aligned} &t-2T\leq 0,\ 0\leq x\leq\infty,\ C(\mathrm{III}) = 0; \\ &t-2T>0,\ x=0,\ C(\mathrm{III}) = {}^\circ_1C - {}^\circ_2C; \\ &C(\mathrm{III}) = ({}^\circ_1C - {}^\circ_2C)\cdot \mathrm{erfc}\frac{x}{2\sqrt{D(t-2T)}} \end{aligned}\right\} \qquad (8)$$

Upon generalizing this procedure, it is found that the concentration of depolarizer $C(x,\ t)$ is demonstrated by

$$C = {}^\circ_1C + ({}^*C - {}^\circ_1C)\cdot \mathrm{erf}\frac{x}{2\sqrt{Dt}} + \sum_{n=1}^{n} (-1)^n ({}^\circ_1C - {}^\circ_2C)\cdot \mathrm{erfc}\frac{x}{2\sqrt{D(t-nT)}}, \qquad (9)$$

which holds at the time interval given by

$$nT<t<(n+1)T$$

That this expression can satisfy the conditions shown by the Eqs. (1), (3) and (4), is

1) T. Kambara, This Bulletin, **27**, 523 (1954).

to be easily verified; and it is comprehensible that the interfacial concentrations are at a state of equilibrium and that the fluxes of oxidant and reductant are continuous at the electrode surface, when the above developed theoretical treatment is applied both to oxidant and reductant.

(2) Solution by Means of the Laplace-Transformation.—Next the above deduced conclusion will be derived by the aid of the Laplace-transformation. Upon applying the Laplace-transformation defined by

$$\mathfrak{L}C(x,\ t)=p\int_0^\infty e^{-pt}\cdot C(x,\ t)\cdot dt=u(x,\ p),$$

the differential equation (1) with the initial condition shown by Eq. (3) is converted into

$$p(u-{}^*C)=D\cdot\partial^2u/\partial x^2. \tag{10}$$

The general solution of this equation is given by

$$u={}^*C+A\cdot\exp\sqrt{\frac{p}{D}}x+B\cdot\exp\left(-\sqrt{\frac{p}{D}}x\right).$$

Since the relationship $u={}^*C$ must always hold for $x=\infty$, the integral constant A is clearly zero. Next the remaining constant B must be determined. Eq. (4), showing the boundary condition, can be written in the form:

$$x=0,\ t>0,\ C=\frac{1}{2}({}^{\circ}_{1}C+{}^{\circ}_{2}C)$$

$$+\frac{1}{2}({}^{\circ}_{1}C-{}^{\circ}_{2}C)\cdot M(T,\ t), \tag{11}$$

where the function $M(T,\ t)$ is the "square wave" or "meander" function shown in Fig. 2 and is defined as follows.

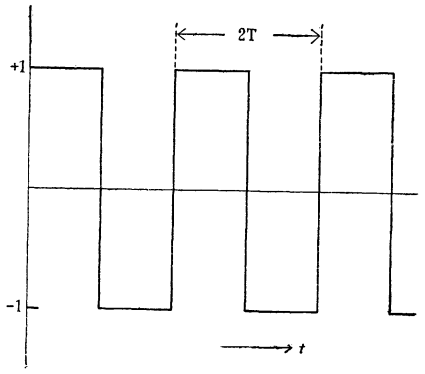


Fig. 2. Schematic representation of square wave function shown by Eq. (12).

$$M(T,\ t)=\begin{cases}+1 & (0<t<T);\\ -1 & (T<t<2T);\end{cases} \tag{12}$$
$$M(T,\ t+2T)=M(T,\ t).$$

Furthermore it can be shown that the function $M(T,\ t)$ has the following transformation.

$$\mathfrak{L}M(T,\ t)=\tanh\frac{pT}{2} \tag{13}$$

If the interfacial concentration is represented by

$$C(0,\ t)={}^{\circ}C=\mathfrak{L}^{-1}\ {}^{\circ}u,$$

it is found that

$${}^{\circ}u=B+{}^*C={}^{\circ}_{2}C+\frac{1}{2}({}^{\circ}_{1}C-{}^{\circ}_{2}C)\cdot\left(1+\tanh\frac{pT}{2}\right)$$
$$={}^{\circ}_{2}C+({}^{\circ}_{1}C-{}^{\circ}_{2}C)\cdot\{1+\exp\ (-pT)\}^{-1};$$

thus the constant B is determined, and it follows that

$$u(x,\ p)={}^*C+({}^{\circ}_{2}C-{}^*C)\cdot\exp\left(-\sqrt{\frac{p}{D}}x\right)$$
$$+({}^{\circ}_{1}C-{}^{\circ}_{2}C)\cdot\exp\left(-\sqrt{\frac{p}{D}}x\right)\cdot\{1+\exp(-pT)\}^{-1} \tag{14}$$

Upon utilizing the expansion:

$$\frac{1}{1+\exp(-pT)}=1-\exp(-pT)$$
$$+\exp(-2pT)-\ \cdots\cdots,$$

Eq. (14) can be transformed into

$$u(x,\ p)={}^*C+({}^{\circ}_{2}C-{}^*C)\cdot\exp\left(-\sqrt{\frac{p}{D}}x\right)$$
$$+({}^{\circ}_{1}C-{}^{\circ}_{2}C)\sum_{n=0}^{n}(-1)^n\cdot\exp\left(\sqrt{\frac{p}{D}}x\right)\cdot\exp(-npT). \tag{14a}$$

In order to execute the inverse transformation, we can legitimately employ the following theorems; i. e.

$$\left.\begin{aligned}&\mathfrak{L}^{-1}\exp\left(-\sqrt{\frac{p}{D}}x\right)=\operatorname{erfc}\frac{x}{2\sqrt{Dt}};\\ &\text{and if we have}\\ &\quad\mathfrak{L}^{-1}f(p)=A(t),\\ &\text{then it is found that}\\ &\quad\mathfrak{L}^{-1}[e^{-kp}\cdot f(p)]=A(t-k).\end{aligned}\right\} \tag{15}$$

It must be noticed here that $A(t-k)=0$ for $t<k$ and that $A(t-k)$ implies the "translated function". There is no doubt that by means of the Eqs. (15) the expression for $u(x,\ p)$ shown by Eq. (14a) can be inversely transformed into Eq. (9).

Thus the basic expression for the concentration distribution in the case that a square wave voltage is applied upon a reversible electrode is theoretically obtained by means of the two mathematically different methods. It follows immediately from the above conclusion that the concentration gradient at the electrode surface is manifested by

$$\left(\frac{\partial C}{\partial x}\right)_{x=0}=\frac{{}^*C-{}^{\circ}_{1}C}{\sqrt{\pi Dt}}$$
$$+\sum_{n=1}^{n}(-1)^{n+1}\frac{{}^{\circ}_{1}C-{}^{\circ}_{2}C}{\sqrt{\pi D(t-nT)}} \tag{16}$$

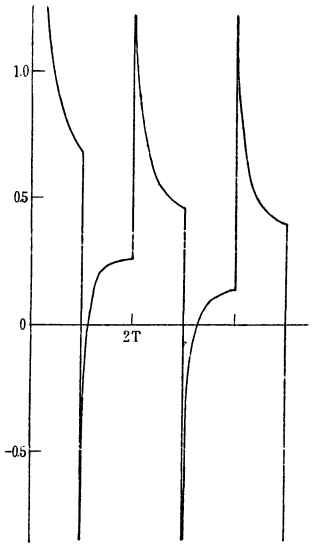


Fig. 3. Schematic representation of the course of instantaneous currents intensity due to the application of a square wave voltage. Curve shows the equation by

$$I=\frac{\alpha}{\sqrt{t}}+\sum_{n=1}^{n}(-1)^n\frac{\beta}{\sqrt{t-nT}},$$

The numerical values employed are as follows:

$$\alpha=3;\quad \beta=1;\quad T=20.$$

The instantaneous current intensity is readily obtainable from this equation, and in Fig. 3 is illustrated an example of the function given by Eq. (16). In our laboratory Dr. Suzuki[2] has investigated the electrolysis with square wave voltage by the aid of a rotating switch and the electro-magnetic oscillograph, and the recordings thereof are, in the case of reversible electrode reactions, quite in harmony with the present theoretical consideration. The validity of the above developed mathematical treatment will be amply and convincingly shown in the following article, in which many experimental facts will be rationally elucidated.

Summary

By means of the principle of superposition and of the Laplace transformation, the differential equation of diffusion is integrated, and the result thus obtained gives the fundamental theoretical expression for the electrolysis with a square wave voltage.

The author wishes to express his sincere thanks to Prof. I. Tachi for his kind guidance. The author's thanks are also due to Dr. M. Suzuki, who helped the author with many oscillographic data.

Department of Agricultural Chemistry, Faculty of Agriculture, Kyoto University, Kyoto

2) M. Suzuki, *J. Electrochem. Soc. Japan*, **22**, 63, 112, 162, 221 (1954); *Memoirs College Agr., Kyoto Univ.*, No. 67 (1954).

Polarographic Diffusion Current Observed with Square Wave Voltage. III. Applications of the Theory

By Tomihito KAMBARA

(Received February 26, 1954)

In Part I of this study,[1] the change of diffusion current produced by the discontinuous change of the electrode potential is discussed, and further in Part II the theory for the electrolysis with a square wave voltage is developed.[1] The conclusion thereof is, employing the same symbols as in the previous studies, that the concentration gradient of the depolarizer at the electrode surface is demonstrated by

$$\left(\frac{\partial C}{\partial x}\right)_{x=0}=\frac{{}^{*}C-{}^{\circ}_{1}C}{\sqrt{\pi Dt}}+\sum_{n=1}^{n}(-1)^{n+1}\frac{{}^{\circ}_{1}C-{}^{\circ}_{2}C}{\sqrt{\pi D(t-nT)}} \tag{1}$$

The instantaneous current intensity i, on the other hand, is shown by

$$i=nFqD(\partial C/\partial x)_{x=0}. \tag{2}$$

Now, writing

$$\alpha={}^{*}C-{}^{\circ}_{1}C\,;\quad \beta={}^{\circ}_{2}C-{}^{\circ}_{1}C\,; \tag{3}$$

$$k=nFq\sqrt{D/\pi}\,; \tag{4}$$

it is seen that

$$I=\frac{i}{k}=\frac{\alpha}{\sqrt{t}}+\sum_{n=1}^{n}(-1)^{n}\frac{\alpha}{\sqrt{t-nT}}\,. \tag{5}$$

Further, for the sake of convenience in the following discussions, some quantities will be introduced as follows. Let i_1 be the diffusion current observed when the electrolysis is

1) T. Kambara, This Bulletin, **27**, 523, 527 (1554).

continuously executed with the constant voltage E_1; then it is seen that

$$i_1=\frac{nFq\sqrt{D}}{\sqrt{\pi t}}\,({}^{*}C-{}^{\circ}_{1}C)=\frac{k\alpha}{\sqrt{t}}, \tag{6}$$

where ${}^{\circ}_{1}C$ is the equilibrium interfacial concentration of depolarizer corresponding to the voltage E_1. Therefore the mean value of the current intensity in the time interval from $t=0$ to $t=t_1$ is shown by

$$\bar{i}_1=\frac{1}{t_1}\int_0^{t_1} i_1\cdot dt=\frac{2k\alpha}{\sqrt{t_1}}. \tag{7}$$

An analogous discussion holds also for the electrolysis with the steady voltage E_2, where it is found that

$$i_2=\frac{k(\alpha-\beta)}{\sqrt{t}}\,; \tag{8}$$

$$\bar{i}_2=\frac{1}{t_1}\int_0^{t_1} i_2\cdot dt=\frac{2k(\alpha-\beta)}{\sqrt{t_1}}. \tag{9}$$

These can be readily seen, since ${}_2{}^{\circ}C$ implies the equilibrium interfacial concentration corresponding to the constant voltage E_2. Thus from these equations it follows that

$$\beta=\frac{\sqrt{t_1}}{2k}(\bar{i}_1-\bar{i}_2)=\frac{\sqrt{t}}{k}(i_1-i_2). \tag{10}$$

Next, some conclusions derived from the theory will be compared with several experimental findings in the section below.

Experiment of Madame Fournier

In the recording of polarographic current-voltage curve, Fournier[2] has experimented while a suitable alternating voltage is superposed onto the constant voltage, which increases negatively as is usual in polarography. The result of her experiment is well understood when the superposed sine-wave voltage is regarded to be equivalent to a square wave voltage of suitable amplitude and frequency. Now, we will compute the mean current which flows during the time interval shown by

$$t_1=2mT,\quad (m\text{: an integer}) \tag{11}$$

where T represents, as in the previous papers, the half-period, and in the case of the dropping mercury electrode t_1 corresponds to the drop time. Eq. (5) can be written as

$$I=\frac{\alpha}{\sqrt{t}}+\beta\left(\frac{-1}{\sqrt{t-T}}+\frac{1}{\sqrt{t-2T}}+\frac{-1}{\sqrt{t-3T}}+\cdots\cdots+\frac{1}{\sqrt{t-(2m-2)T}}+\frac{-1}{\sqrt{t-(2m-1)T}}\right)$$

Thus the integrated value of I is given by

$$\int_0^{t_1} I\cdot dt=\int_0^{t_1}\frac{\alpha}{\sqrt{t}}dt+\beta\left(\int_T^{t_1}\frac{-dt}{\sqrt{t-T}}+\int_{2T}^{t_1}\frac{dt}{\sqrt{t-2T}}+\cdots\cdots+\int_{(2m-2)T}^{t_1}\frac{dt}{\sqrt{t-(2m-2)T}}+\int_{(2m-1)T}^{t_1}\frac{-dt}{\sqrt{t-(2m-1)T}}\right),$$

where the lower limits of the integrals take the values: 0, T, $2T$, ……, etc., because each term containing $(t-nT)^{-1/2}$ in the summation in Eq. (5) must vanish away for $t<nt$ owing to the property of the translated function. Upon executing the integrations, it is found that

$$\int_0^{t_1} I\cdot dt=2\alpha\sqrt{2mT}-2\beta\sqrt{T}\,(\sqrt{2m-1}+\sqrt{2m-3}+\cdots\cdots+\sqrt{3}+\sqrt{1})+2\beta\sqrt{T}\,(\sqrt{2m-2}+\sqrt{2m-4}+\cdots\cdots+\sqrt{4}+\sqrt{2}).$$

For the large value of m, the approximate values of the series appearing in this equation can be estimated by performing integration instead of the summation as follows.

$$\sum_{m=1}^{m}\sqrt{2m-1}\simeq\int_1^m\sqrt{2}\left(m-\frac{1}{2}\right)^{1/2}\cdot dm=\frac{2\sqrt{2}}{3}\left\{\left(m-\frac{1}{2}\right)^{3/2}-\left(\frac{1}{2}\right)^{3/2}\right\};$$

$$\sum_{m=2}^{m}\sqrt{2m-2}\simeq\int_2^m\sqrt{2}\,(m-1)^{1/2}\cdot dm=\frac{2\sqrt{2}}{3}\left\{(m-1)^{3/2}-1\right\}.$$

Hence we obtain

$$\int_0^{2mT} I\cdot dt\simeq 2\alpha\sqrt{2mT}-2\beta\sqrt{T}\cdot\frac{2\sqrt{2}}{3}\left\{\left(m-\frac{1}{2}\right)^{3/2}-(m-1)^{3/2}+1-\left(\frac{1}{2}\right)^{3/2}\right\}.$$

Therefore, upon regarding m to be very large and applying the familiar binomial theorem, the mean value of Fournier current is shown by

$$\bar{i}_F=\frac{k}{2mT}\int_0^{2mT} I\cdot dt=\frac{2k\alpha}{\sqrt{2mT}}-\frac{4k\beta}{3}\cdot\frac{\sqrt{2T}}{2mT}\left(\frac{3\sqrt{m}}{4}+\frac{\sqrt{8}-1}{\sqrt{8}}\right). \tag{12}$$

Inserting Eqs. (7), (10) and (11) into (12) gives

$$\bar{i}_F=\bar{i}_1-\frac{2}{3}(\bar{i}_1-\bar{i}_2)\left\{\frac{3}{4}+\frac{\sqrt{8}-1}{\sqrt{8m}}\right\},$$

which, again owing to the large value of m, can be simplified into

$$\bar{i}_F=\frac{1}{2}(\bar{i}_1+\bar{i}_2). \tag{13}$$

On the other hand, the equation for the polarographic wave due to the reversible electrode reaction is, upon employing the usual notations, demonstrated by

$$\left.\begin{aligned}\bar{i}&=\frac{\bar{i}_d}{2}(1+\tanh\xi)\,;\\ \xi&=\frac{1}{2}\cdot\frac{nF}{RT}(-E+E_{1/2}).\end{aligned}\right\} \tag{14}$$

In the Fournier's investigation, it can be written that

$$E_1=E-\Delta E\,;\quad E_2=E+\Delta E\,;\quad (\Delta E>0) \tag{15}$$

i. e.

2) M. Fournier, *Compt. rend.*, **232**, 1673 (1951).

$$\left.\begin{aligned}&\xi_1=\xi-\Delta\xi\ ;\quad \xi_2=\xi+\Delta\xi\ ;\\ &\Delta\xi=\frac{1}{2}\cdot\frac{nF}{RT}\cdot\Delta E.\end{aligned}\right\} \tag{16}$$

Accordingly the Fournier's current-voltage curve is manifested by

$$\bar{i}_F=\frac{\bar{i}_d}{4}\{2+\tanh(\xi-\Delta\xi)+\tanh(\xi+\Delta\xi)\}. \tag{17}$$

Then, since we have

$$\tanh\xi=-\tanh(-\xi),$$

it is found that the curve:

$$\bar{i}_F=\frac{\bar{i}_d}{2}=\frac{\bar{i}_d}{4}\{\tanh(\xi-\Delta\xi)+\tanh(\xi+\Delta\xi)\}$$

$$=-\frac{\bar{i}_d}{4}\{\tanh(-\xi-\Delta\xi)+\tanh(-\xi+\Delta\xi)\}$$

has a point of symmetry shown by

$$\bar{i}_F=\bar{i}_{d/2}\ ;\quad \xi=0\ ;\quad E=E_{1/2}\ ; \tag{18}$$

which is, of course, identical with the usual half-wave point.

Further the following relations are also found:

$$\left.\begin{aligned}&\bar{i}_F=\bar{i}_d \quad \text{for} \quad E=-\infty\ ;\ \xi=\infty\ ;\\ &i_F=0 \quad \text{for} \quad E=\infty\ ;\ \xi=-\infty\ ;\end{aligned}\right\} \tag{19}$$

Next the inclination of the Fournier's polarogram at the half-wave potential is given by

$$-\left(\frac{d\bar{i}_F}{dE}\right)_{E=E_{1/2}}=\frac{\bar{i}_d nF}{4RT}\cdot\frac{1}{\cosh^2\Delta\xi}\ ; \tag{20}$$

whereas that of the ordinary polarogram is, as is well known, given by

$$-\left(\frac{d\bar{i}}{dE}\right)_{E=E_{1/2}}=\frac{\bar{i}_d nF}{4RT}. \tag{21}$$

Thus it can be concluded that the inclination is made less steep by the superposition of an alternating voltage. The above derived theoretical conclusions have all been confirmed experimentally by Fournier in the case of reversible electrode reaction, e. g. the cathodic reduction of monovalent metal ion; the general aspect of Fournier current is illustrated in Fig. 1.

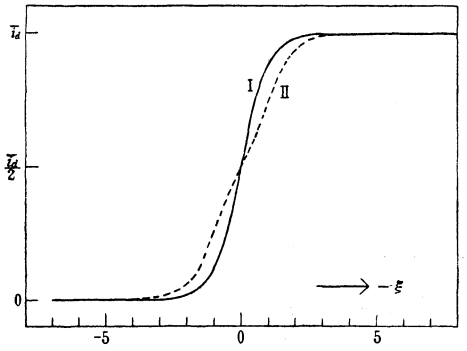


Fig. 1. Curve I shows the ordinary polarogram, and curve II shows the Fournier's polarogram drawn theoretically with the value $\Delta\xi=2$ [Cf. Eqs. (14)-(17)].

Kalousek Apparatus

In the apparatus designed by Kalousek,[3] the electrolysis is performed by applying a square wave voltage; viz. at first the electrolysis is carried out with the potential E_1 for T sec. and then the potential is discontinuously changed to a more positive value E_2; i. e.

$$E_2>E_1, \tag{22}$$

and it may be supposed that the reversibility of the electrode process is to be judged by the intensity of the oxidation current. And thus in this apparatus, it is so designed that only the current flowing during the application of the more positive potential E_2 is recorded by the galvanometer. In order to clear up the observations obtained with this apparatus, at first, we must compute the integrated value of the current, which flows in the half-period shown by

$$E=E_2\ ;\ (2m+1)T<t<(2m+2)T\ (m:\ \text{integer}) \tag{23}$$

It follows from Eq. (5) that

$$\int_{(2m+1)T}^{(2m+2)T} I\cdot dt=\int_{(2m+1)T}^{(2m+2)T}\frac{\alpha}{\sqrt{t}}\cdot dt$$

$$+\sum_{n=1}^{2m+1}\int_{(2m+1)T}^{(2m+2)T}(-1)^n\cdot\frac{\beta}{\sqrt{t-nT}}\cdot dt$$

$$=2\alpha(\sqrt{2m+2}-\sqrt{2m-1})\sqrt{T}$$
$$+2\beta\sqrt{T}(\sqrt{2m}+\sqrt{2m-2}+\cdots\cdots+\sqrt{2})$$
$$-2\beta\sqrt{T}(\sqrt{2m-1}+\sqrt{2m-3}+\cdots\cdots$$
$$+\sqrt{3}+\sqrt{1})$$
$$-2\beta\sqrt{T}(\sqrt{2m+1}+\sqrt{2m-1}+\cdots\cdots$$
$$+\sqrt{3}+\sqrt{1}).$$
$$+2\beta\sqrt{T}(\sqrt{2m}+\sqrt{2m-2}+\cdots\cdots+\sqrt{2})$$

As shown in the preceding section, for the large value of m, it can be written that

$$\sum_{m=1}^{m} m^{1/2}\simeq\int_1^m m^{1/2}\cdot dm=\frac{2}{3}(m^{3/2}-1);$$

$$\sum_{m=1}^{m}(2m-1)^{1/2}\simeq\int_1^m(2m-1)^{1/2}\cdot dm=\frac{1}{3}\{(2m-1)^{3/2}-1\};$$

$$\sum_{m=1}^{m}(2m+1)^{1/2}\simeq\int_1^{m+1}(2m+1)^{1/2}\cdot dm=\frac{1}{3}\{(2m+1)^{3/2}-1\};$$

i. e. the summation is replaced approximately by integration. Thus with the aid of binomial theorem, it is seen that

$$\int_{(2m+1)T}^{(2m+2)T} I\cdot dt=2\alpha\sqrt{T}(\sqrt{2m+2}-\sqrt{2m+1})$$
$$+\frac{4\beta\sqrt{2T}}{3}\left\{2m^{3/2}-2-\left(m-\frac{1}{2}\right)^{3/2}-\left(m+\frac{1}{2}\right)^{3/2}\right.$$
$$\left.+\frac{1}{\sqrt{2}}\right\}\simeq 2\alpha\sqrt{T}(\sqrt{2m+2}-\sqrt{2m+1})$$
$$+\frac{4\beta\sqrt{2T}}{3}\left(\frac{1}{\sqrt{2}}-2\right). \tag{23}$$

Now we must evaluate the integrated value of the total current which flows under the application of potential E_2 during the time interval given by

$$t_1=2(m+1)T. \tag{24}$$

Then it is seen that

3) M. Kalousek, *Collection Czech. Chem. Communs.*, **13**, 105 (1948).

$$\sum_{m=0}^{m}\int_{(2m+1)T}^{(2m+2)T} I\cdot dt=\sum_{m=0}^{m}2\alpha\sqrt{T}\left(\sqrt{2m+2}-\sqrt{2m+1}+(m+1)\frac{4\beta}{3}\sqrt{2T}\left(\frac{1}{\sqrt{2}}-2\right)\right),$$

where it can be shown approximately that

$$\sum_{m=0}^{m}\left(\sqrt{2m+2}-\sqrt{2m+1}\right)\simeq\frac{2\sqrt{2}}{3}\left(\frac{3}{4}m^{1/2}-\frac{\sqrt{8}-1}{\sqrt{8}}\right)\simeq\left(\frac{m}{2}\right)^{1/2},$$

in which the summation is again replaced by integration. Therefore the Kalousek's mean current which flows during the half periods, in which the potential E_2 is applied, is demonstrated by

$$\bar{i}_K=k\sum_{m=0}^{m}\int_{(2m+1)T}^{(2m+2)T} I\cdot dt\Big/t_1=\frac{k\alpha}{\sqrt{t_1}}\left(\frac{m}{m+1}\right)^{1/2}-\frac{4k\beta}{3}\left(2-\frac{1}{\sqrt{2}}\right)\frac{1}{\sqrt{2t_1T}},\qquad(25)$$

where the quantity $\sqrt{m/m+1}$ can be regarded to be nearly unity for the large value of m. Hence, upon inserting Eqs. (7) and (10) into this equation, it is seen that

$$\left.\begin{aligned}\bar{i}_K&=\frac{1}{2}\bar{i}_1=\frac{s}{\sqrt{2T}}(\bar{i}_1-\bar{i}_2);\\ s&=\frac{2}{3}\left(2-\frac{1}{\sqrt{2}}\right)=1.195\end{aligned}\right\}\qquad(26)$$

Eurther the frequency of applied square wave voltage will be introduced according to

$$f=1/2T,\qquad(27)$$

which is equal to the number of revolutions of rotating switch per second. Then it is manifest that

$$\bar{i}_K=\frac{1}{2}\bar{i}_1-s\sqrt{f}(\bar{i}_1-\bar{i}_2),\qquad(28)$$

which is the fundamental equation for the Kalousek current provided that the electrode reaction proceeds reversibly.

The changes of the cathode potential with time due to the employment of Kalousek apparatus Ia, II and III are schematically illustrated in Fig. 2. In the case of apparatus I, it is so designed that the potential E_2 is always kept more positive by a constant value ΔE than the potential E_1; i. e.

$$E_2=E_1+\Delta E.\qquad(29)$$

Accordingly it can be readily found that

$$\bar{i}_1-\bar{i}_2=\Delta\bar{i}=(d\bar{i}/dE)\cdot(-\Delta E),\qquad(30)$$

and further it is clear that the potential E_1 is increased negatively with time, as is usual in polarography. Thus $\bar{i}_1$ is shown by Eq. (14) demonstrating the ordinary polarographic wave. Therefore, it can be readily seen that

$$\bar{i}_K(I\alpha)=\frac{1}{2}\bar{i}-s\sqrt{f}\left(\frac{d\bar{i}}{dE}\right)\cdot(-\Delta E);\qquad(31)$$

viz. the curve observed with the apparatus Ia is the superposition of two currents, namely (1) the current-voltage curve registered with the half decreased sensitivity of a galvanometer, and (2) the derivative curve thereof multiplied by the factor $(-s\sqrt{f})$. It is derived from Eq. (31) that a deep valley due to the oxidation current should be observed near the half-wave potential, which is in complete accordance with Kalousek's findings. Further it is seen that at a sufficiently negative potential, the Kalousek current is just one half the limiting diffusion current (cf. Fig. 3).

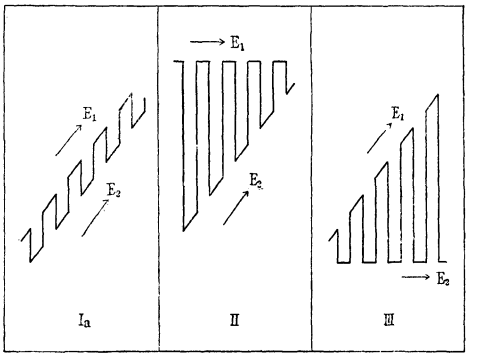


Fig. 2. Changes of the electrode potential with time in the Kalousek's apparatus.

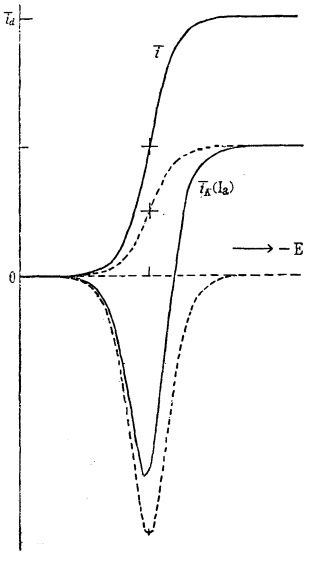


Fig. 3. Kalousek polarogram Ia.

Next in the apparatus II, the potential E_1 is fixed at such a negative value that the limiting current $\bar{i}_d$ is observable, whereas E_2 is increased negatively. Thus from Eq. (28) it follows that

$$\bar{i}_K(\mathrm{II})=\left(\frac{1}{2}-s\sqrt{f}\right)\bar{i}_d+s\sqrt{f}\,\bar{i}.\qquad(32)$$

This conclusion shown in Fig. 4 is quite in harmony with the experiment.

Eurther, in the apparatus III, the potential E_2 is fixed at such a positive value that no appreciable reduction occurs, i. e.

$$\bar{i}_2=0,$$

whereas E_1 is increased negatively. Thus it is seen that

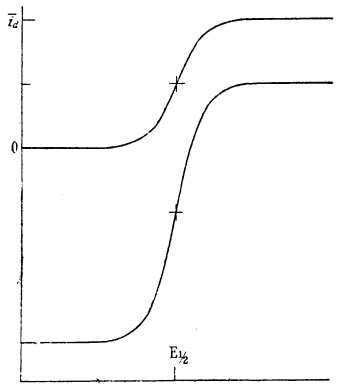


Fig. 4. Kalousek polarogram II.

$$\bar{i}_K(\mathrm{III}) = -\left(s\sqrt{f} - \frac{1}{2}\right)\bar{i}. \tag{33}$$

This equation also agrees well with the Kalousek's observation, and is illustrated in Fig. 5.

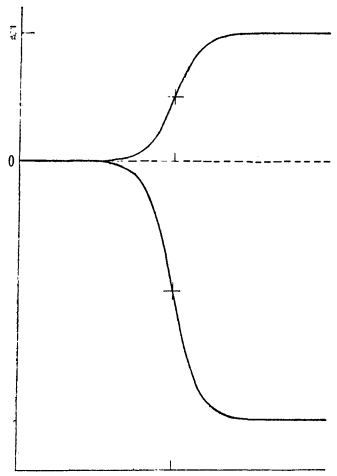


Fig. 5. Kalousek polarogram III.

Ishibashi-Fujinaga Apparatus

In I-F apparatus[4] aiming at the differential polarography and the increased sensitivity, a square wave voltage is applied by means of a rotating switch as in the Kalousek apparatus; furthermore, the rotating current alternator makes the current, flowing under the application of potential E_2, run through the galvanometer in the reverse direction, which is opposite ta the direction of the current flowing while the potential is E_1. This is, as it were, a full-wave rectification of the electrolytic current observed with a square wave voltage. Thus, in order to treat this problem theoretically, it is needed to compute the mean current which flows in the half-period shown by

$$E = E_1;\ 2mT < t < (2m+1)T\ (m;\ \text{integer}) \tag{34}$$

Therefore, at first, we must evaluate the quantity:

$$\sum_{m=0}^{m} \int_{2mT}^{(2m+1)T} I \cdot dt.$$

This calculation is to be executed as is seen in Eqs. (23) and (25); but this is much more simply performable as shown below. When the time interval given by

$$t_1 = (2m+2)T$$

is considerably long, it is already seen that (cf. Eq. (13))

$$\frac{1}{t_1}\int_0^{t_1} i \cdot dt = \bar{i}_F = \frac{1}{2}(\bar{i}_1 + \bar{i}_2).$$

On the other hand, there is no doubt that the following relationship holds.

$$\bar{i}_F = \frac{1}{t_1}\sum_{m=0}^{m}\left\{\int_{2mT}^{(2m+1)T} i \cdot dt + \int_{(2m+1)T}^{(2m+2)T} i \cdot dt\right\}, \tag{35}$$

Thus it follows from the Eqs. (13), (26) and (35) that

$$\frac{1}{t_1}\sum_{m=0}^{m}\int_{2mT}^{(2m+1)T} i \cdot dt = \bar{i}_F - \bar{i}_K$$

$$= \frac{1}{2}\bar{i}_2 + s\sqrt{f}\,(\bar{i}_1 - \bar{i}_2). \tag{36}$$

Hence the mean current observed with I-F apparatus is clearly given by

$$\bar{i}_{IF} = \frac{1}{t_1}\sum_{m=0}^{m}\left\{\int_{2mT}^{(2m+1)T} i \cdot dt - \int_{(2m+1)T}^{(2m+2)T} i \cdot dt\right\}$$

$$= \left(2s\sqrt{f} - \frac{1}{2}\right)(\bar{i}_1 - \bar{i}_2). \tag{37}$$

In the differential apparatus, it is so arranged that

$$\Delta E = E_2 - E_1 = \text{const.}$$

Therefore, from Eq. (30) it follows that

$$\bar{i}_{IF}(\text{diff.}) = \left(2s\sqrt{f} - \frac{1}{2}\right)\cdot\left(\frac{d\bar{i}}{dE}\right)\cdot(-\Delta E). \tag{38}$$

Thus the sensitivity of the derivative curve increases, when the revolution number of a rotating switch is elevated and when a large ΔE is chosen. It is seen that if $f = 16$ c./sec. the height of the peak of the derivative curve is about ten times greater than $\Delta\bar{i}$ corresponding to the given value of ΔE. Next in the I-F apparatus for the increased sensitivity, the potential E_2 is so chosen that no appreciable cathodic current flows; i.e.

$$\bar{i}_2 = 0. \tag{39}$$

On the other hand, $\bar{i}_1$ is the current intensity corresponding to the ordinary polarographic wave and is given by Eq. (14). Hence it follows that

$$\bar{i}_{IF}(\text{incr.}) = \left(2s\sqrt{f} - \frac{1}{2}\right)\cdot\bar{i}; \tag{40}$$

i. e. the observed polarogram exhibits the same effect, that is to be seen with the increased sensitivity of the galvanometer employed; such an effect of increasing the sensitivity, however, depends clearly on the reversibility of the electrode process.

Note—In the above discussions, in which the current intensities under several experimental conditions are well comprehensible from the present theoretical considerations, the reversibility

4) M. Ishibashi and T Fujinaga, This Bulletin, **25**, 63, 238 (1952).

of electrode reaction is always assumed. Accordingly deviations of experimental results from the theoretical conclusion are obviously due to the irreversible character of the process concerned; and hence the degree of such a deviation may be a rational measure of the irreversibility.

The above theory is developed based on the assumption that a stationary plane electrode is employed; thus it may not be quite adequate to apply the theory to the phenomenon obtained with a dropping electrode. But, since the equation for the diffusion current at a plane electrode differs from the Ilkovic equation only by a numerical factor, the present theory seems to be approximately correct. Were it possible to perform the calculation taking the effects due to the curvature and expansion of mercury drop into consideration, although mathematically very hard, it would be a strictly correct.

When in the above treatment the changes of the mercury drop surface given by

$$q=0.85\cdot m^{2/3}\cdot t^{2/3}$$

is employed, then we have the definite integral of the form:

$$\int_{nT}\frac{t^{2/3}\cdot dt}{\sqrt{t-nT}}=\int_{0}\frac{(t'+nT)^{2/3}}{\sqrt{t'}}\cdot dt',$$

which can not be evaluated rationally. But in this integral the effect of the denominator is far greater than that of numerator, so that the error produced by the assumption that the surface area is independent of time may not be very serious.

Summary

The theoretical treatment given in the previous works on the electrolysis with square wave voltage is here applied to the elucidation of experimental results. Thus the experiment by Madame Fournier is satisfactorily explained, and further the findings obtained with Kalousek's and Ishibashi-Fujinaga's apparatus are also rationally clarified.

The author wishes to express his sincere thanks to Professor Tachi for his interest to this study. The author's thanks are also due to Professors J. Heyrovsky, M. Kalousek and J. Koutecky in the Polarographic Institute of the Czechoslovak Academy of Sciences, who helped him with constructive criticism and kind encouragement.

Department of Agricultural Chemistry, Faculty of Agriculture, Kyoto University, Kyoto

On the Reactions Between Some Organic Sulfur Compounds and Silver Ions with Potentiometric Titrations

By Shinichi KIKUCHI, Yoshikata SAKAGUCHI* and Kazumi AKIBA

(Received May 6, 1954)

Introduction

Reactions between organic photographic fog-inhibitors and silver ions were measured by means of silver potentiometric titration in this laboratory. The senior authors, Kikuchi and Sakaguchi reported those on the pyrimidine derivatives[1,2,3] and Kikuchi, Sakaguchi, and Murobushi on the benzimidazoles and rhodanines[4]. The present report intends to clarify the reactions between some organic compounds other than cited before and the silver ion by the same method with an improved device. The substances chosen in this report are as follows:

potassium thiocyanate (I)
thiourea (II)
thiosemicarbazide (III)
benzaldehyde thiosemicarbazone (IV)
piperonal thiosemicarbazone (V)
p-dimetylamino benzaldehyde thiosemicarbazone (VI)
p-acetamide benzaldehyde thiosemicarbazone (VII)
o-nitrobanzaldehyde thiosemicarbazone (VIII)
m-nitrobenzaldehyde thiosemicarbazone (IX)
p-nitrobenzaldehyde thiosemicarbazone (X)
phenyl thiosemicarbazide (XI)
benzaldehyde phenyl thiosemicarbazone (XII)

Some other substance not containing sulfur

* Y. Sakaguchi has been in Fuji Photo. Film Co., since April, 1952.

1) S. Kikuchi and Y. Sakaguchi, *Journ. Sci. Phot. Japan* (in Japanese) **12**, No. 4, 3-7 (1950): abstracted in *Sci. et industr. Phot.*, **23** (2) 307 (1952).

2) Y. Sakaguchi and S. Kikuchi, ibid., **13** No. 4, 126-131 (1951): abstracted in *Sci. et industr. Phot.*, **23** (2) 178 (1952).

3) S. Kikuchi and Y. Sakaguchi, *Sci. et Industr. Phot.*, **23A** 248-260 (1952).

4) S. Kikuchi, Y. Sakaguchi and K. Murobushi, *Bull. Soc. Scient. Photo. Japan* (in English), No. 2, 10-19 (1952).

are also chosen:
hydrazine (XIII)
urea (XIV)
guanidine (XV)
diphenyl guanidine (XVI)

These sulfur compounds are mainly chain compounds and some of these are apparently photographic sensitizers or even fogging agents. The authors wished to know the effect of the substitution of amino group of thiourea in connection of this reaction.

Experimental Part

(a) Pen-recording System of Potential—The silver potential of substances is measured potentiometrically. The voltage difference of a cell which is set up with the calomel and the silver electrode is amplified and read on a pen-writing recorder described in the previous paper[3,5]

(b) Automatic Titrator[7] — The addition of silver nitrate solution to the reagent is done with the automatic titrator designed in this laboratory (Fig. I). A syringe plunger is driven by the system of synchronous motor, gears, belt, and travelling nut. The change of gears enables four steps of the travelling nut's speed (50, 10, 2.5, and 0.625 mm/min.). Besides changes of the connection of belt and pulley make seven stages which are 2, 1.5, 1.25, 1 (standard), 0.75, 0.625, and 0.5. The nut's speed should be changed in 28 steps between 100–0.3125 mm/min. But the combinations of gears and belt make two pairs of the same speed, so 26 steps in total are interchangeable. The size of the syringe may be changeable from 1 to 10 cc also. The present experiment took place under conditions of about 5 cc. syringe and 1.25 mm/min. speed which corresponded to 0.67 cc./5 min.

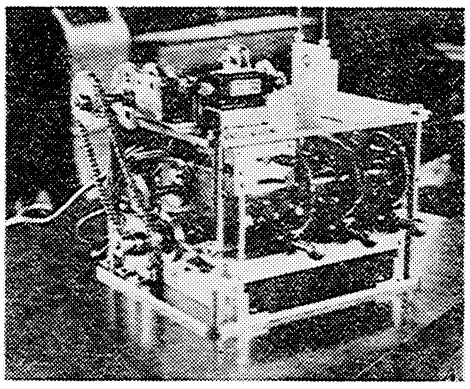


Fig. 1. Automatic titrator

(c) Procedure—0.075 N solution of silver nitrate is added to 50 cc. of 0.001 M/l buffered solution of organic compound in the rate of 0.67 cc./5 min. i.e. 0.00005 M/5 min. under vigorous agitation. In this concentration ratio, five minutes are necessary for an equivalence of Ag. On the other hand, the chart speed of the recorder can be changeable in 5, 10, 20, 60, 120, and 240 mm/min. or mm/hr. Throughout this experiment, the speed 10mm/min. was used, so 50 mm. on the chart corresponds to an equivalent.

If the compound is salted out in buffer solution, it is dissolved in organic solvent as methyl alcohol, then diluted with the buffer solution to the above concentration. A cleaned silver electrode is dipped in the solution and titration is started, and then its potential refered to the saturated calomel electrode is recorded as described above at 50°C.

(d) Buffer Solutions—As buffer solutions, the Walpole's acetate buffers are used for pH 4 and 5, the Sörensen's phosphate buffers for pH 6, 7, and 8, the Sörensen's borate buffers for pH 9, 10, and 11. The formulae for these were given in our previous report[3]. In phosphate buffers, some substances need more silver ions than expected and this showed that the phosphate buffers were inadequate for these substances. So the authors used the citrate buffers for pH 6 and 7, and the modified Sörensen's buffer for pH 8. The formulae of the buffers are given in Table 1.

TABLE I
FORMULAE OF BUFFERS

Sörensen's citrate buffer at 50°C
Solution A
(citric acid 21.008g+I N NaOH 200cc)/1.
Solution B 0.I N NaOH
*p*H 6.0 solution A 52.5 vol% solution B 47.5%
6.8 ,, 61.8 ,, 38.2
Sörensen's glycine buffer at 50°C
Solution A (glycine 7.505g+$NaNO_3$ 8.501g)/1.
Solution B 0.1 N NaOH
*p*H 8.0 solution A 93.5% solution B 6.5%

The sodium chloride of Sörensen's original formula is replaced by a gram equivalent of sodium nitrate to avoid the precipitation of silver chloride. In order to compare the buffering efficiency of the original and modified formulae, the *p*H change at 50°C. is shown in Table 2 when 0.05 N $AgNO_3$ is added to 50 cc. of the buffering solution.

TABLE II
BUFFERING POWER OF TWO BUFFER SOLUTIONS BY ADDITION OF $AgNO_3$

Kind of buffer	0.05N $AgNO_3$cc	0.00	1.00	2.00	3.00	4.00	5.00
glycine	pH	7.97	7.88	7.70	7.50	7.38	7.22
phosphate	pH	7.93	7.90	7.88	7.82	7.80	7.78

The phosphate buffer has a far better buffering power than the glycine buffer.

Results of Experiment

(a) Significance of Silver Potentiometric Titration Curves—As the significance of curves was fully discussed in the previous papers[2,3], the authors intend here to remind the readers of the following.

5) S. Kikuchi and Y. Sakaguchi, *Seisan Ke-kyū* (in Japanese) published by Univ. of To yo. **3** No. 4, 161 (1951).
6) J. J. Lingane, *Anal. Chem.*, **20** No. 4, 285-292 (1948).

i. The silver potential is likely to be less noble when the silver salt of organic compound is hard-soluble and the compound adheres to silver halide as sensitizer, fog-inhibitor or desensitizer.

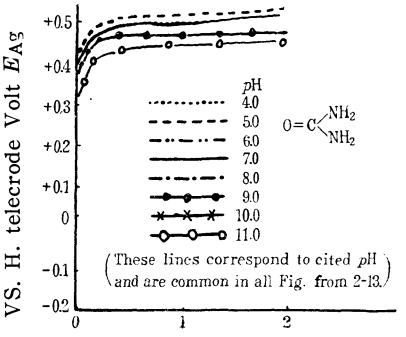
ii. One can discriminate the quality of compounds with their colors of precipitates. Black, brown or grey colors shows the production of silver or silver sulfide which are the reason of sensitization or fogging action. Yellow, yellowish orange, and white colors which are their silver salts are generally the sign for good fog-inhibitors.

iii. The sawteeth form of curve shows the reduction of Ag^+.

iv. The curve of the ineffective substance is same as that of buffer solution.

(b) Potassium Thiocyanate (I) — Potassium thiocyanate gives constant silver thiocyante potentials curves at any pH. The thiocyanate ion is similar to inorganic halogen ions although it contains a sulfur atom.

(c) Urea (XIV), Guanidine (XV) and Diphenyl guanidine (XVI) — From Fig. 2 it may be seen that urea does not react with Ag^+. Guanidine and diphenyl guanidine resemble urea.



Abbreviations

B..... black
Br..... brown
D .....dirty
G.....grey
O..... orange
P..... precipitate
W..... white
Y.....yellow

Fig. 2. Urea.

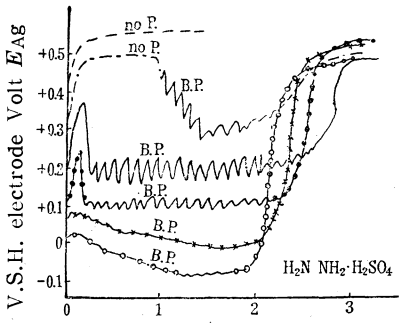


Fig. 3. Hydrazine sulfate.

(d) Hydrazine — The solution of hydrazine sulphate gives, as generally accepted, the curve of reduction of 2 mol. Ag^+ ion in the region more alkaline than pH 6 (Fig. 3).

(e) Thiourea and Thiosemicarbazide—From Fig. 4 the thiourea shows the reduction of 2 mols. of Ag^+ ion in the acid region, while in the neutral and alkaline regions, the curves indicate the decomposition of compound to give black silver sulfide up to 2 mols. equivalent of $AgNO_3$ and the yellow residue with more silver ions. The former is produced by means of =S and the latter by $-NH_2$. The authors suppose that the electronegativity of NH_2 in thiosemicarbazide affects less than thiourea owing to the long distance from the carbon atom attached to =S, so the first gives the silver sulfide more easily than thiourea. (Fig. 4, 5)

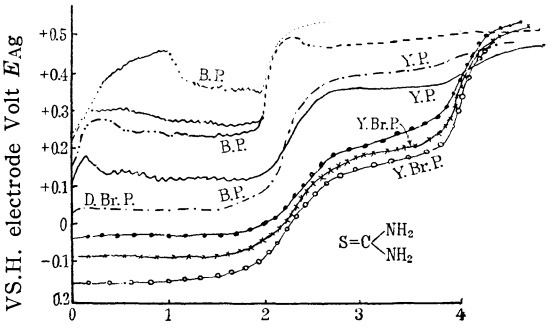


Fig. 4. Thiourea.

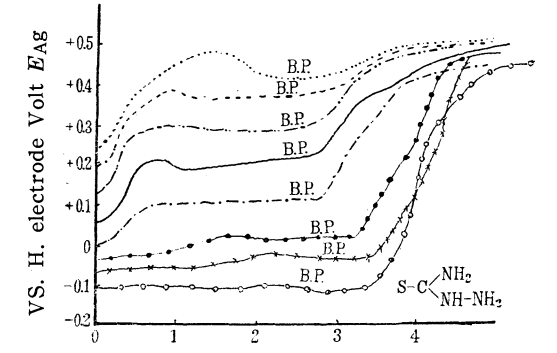


Fig. 5. Thiosemicarbazide.

(f) Benzaldehyde Thiosemicarbazone (IV)— Fig. 6 and 7 are obtained for (IV). In Fig. 6 Sörensen's phosphate buffers were used, the equivalence to Ag^+ becomes larger with pH increase up to 8. The silver equivalent at pH 6, 7, and 8 are 2, 2.5, and 3.5 respectively. Suddenly it turns back to 1 at pH 9. In Fig. 7 where the citrate and the glycine buffers are used, then (IV) gives unit silver equivalent at pH range from 4 to 10, in other word it does not give silver sulfide. In fact, (IV) is the good fog-inhibitor. Perhaps the benzaldehyde group lessons the electronegativity of NH_2 group.

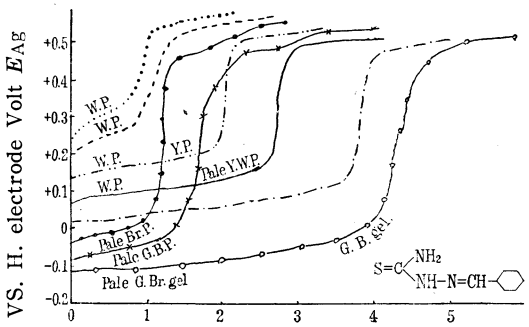


Fig. 6. Benzaldehyde thiosemicarbazone.

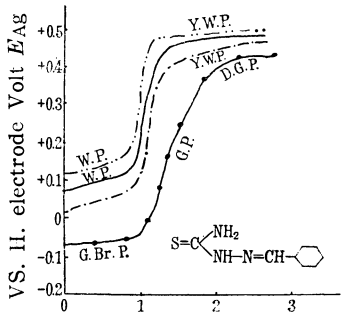


Fig. 7. Case of benzaldehyde thiosemicarbazone with new type of buffer solution.

(g) o-, m-, p- Nitrobenzaldehyde Thiosemicarbazones. (VIII, IX, X)—The curves for three isomers (VIII), (IX), (X) are given respectively in Fig. 8, 9, and 10. At pH 6, 7, and 8 (IX) and (X) they need too much silver ion and at pH 9 the equivalence turns back to unity. New buffers reveal that even at these pH the substances need one Ag^+. The substance (VIII) shows, contrary to (IX) and (X), the unit equivalent even with phosphate buffers. This fact makes us to suppose that silver atom, phosphate ion and some organic substance from the complex form and meta and para forms are more suitable for this complex formation than ortho form.

The colors of precipitates show that these compounds are probably good fog-inhibitors. Indeed the emulsion test with these substances done by Konishiroku Photo Co. reveals that these are good fog-inhibitors though a little desensitizing[7].

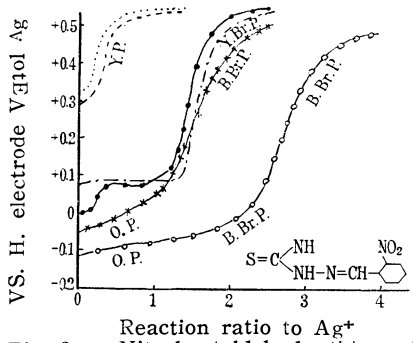


Fig. 8. o-Nitrobentaldehyde thiosemicarbazone.

7) Konishiroku Photo Co., *Report of the Committee of addition agent*, (1952).

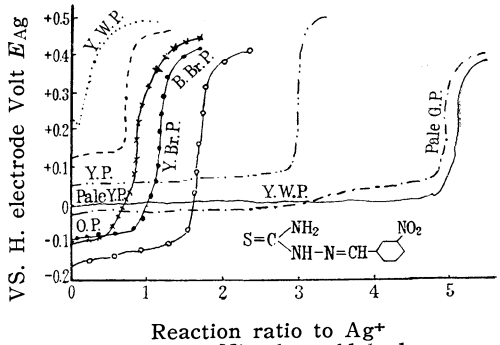


Fig. 9. m-Nitrobenzaldehyde thiosemicarbazone

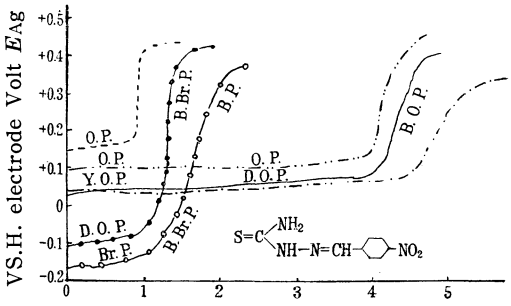


Fig. 10. p-Nitrobenzoldehyde thiosemicarbazone.

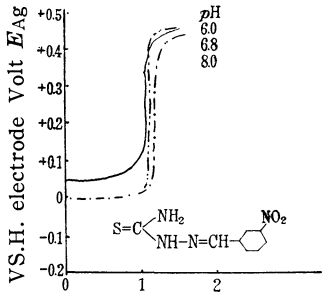


Fig. 11. Case of m-nitrobenzaldehyde thiosemicarbazone with new type of buffer solution.

(h) p-Dimethylamino Benzaldehyde Thiosemicarbazone (VI) and Phenyl Thiosemicarbazide (XI)—The silver potentiometric titration curves are also obtained for (VI) and (XI). The substance (VI) as predicated from its similar structure with (IV) has no tendency to produce Ag_2S, while substance (XI) has this tendency stronger than thiosemicarbazide (III).

(i) Piperonal Thiosemicarbazone (V) and p-Acetamide Benzaldehyde Thiosemicarbazone (VII) and Benzaldehyde Phenyl Thiosemicarbazone (XII)—These compounds have qualities between (IV) and (XI).

(j) The color of the precipitates and the free energy change are shown in Table III when the substances are titrated with Ag^+. To see easily all characters of the tested substances, Table III is dressed in which the symbol $-\Delta F^\circ_{323}$ (standard free energy change at 50°C.) is as previous reports[2,3].

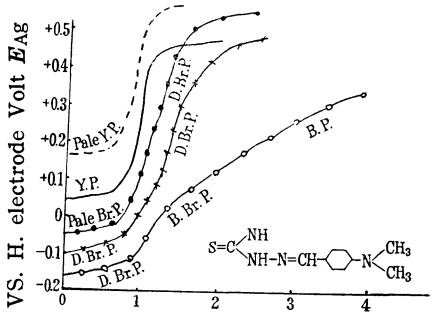


Fig. 12. *p*-Dimethylamino thiosemicarbazone.

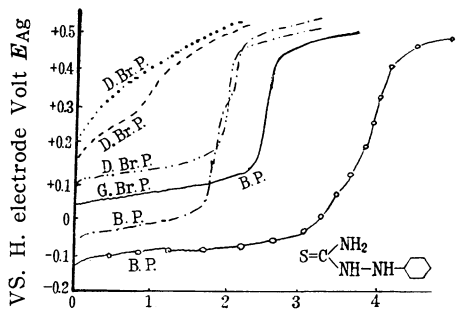


Fig. 13. Phenyl thiosemicarbazide.

TABLE III

PROPERTIES OF SUBSTANCES OBTAINED BY THE REACTION OF ORGANIC SULFUR COMPOUNDS AND THE SILVER ION

Substances	*p*H 5.0		7.0		9.0	
	$-\Delta F^{\circ}_{323}$ kcal/M	Colors of precipitate	$-\Delta F^{\circ}_{323}$	Colors	$-\Delta F^{\circ}_{323}$	Colors
Potassium thiocyanate (I)	15.4	white	15.4	white	15.4	white
urea (XIV)	—	no	—	no	—	no
guanidine (XV)	—	no	—	no	—	no
diphenyl guanidine (XVI)	—	no	—	no	—	no
hydrazine (XIII)	—	no	17–18	silver black ppt.	20	silver black ppt.
thiourea (II)	16	brown, black	19	dirty brown black	22.7	dirty brown, black
thiosemicarbazone (III)	14	brown, black	18	brown, black	22.5	black
benzaldehyde thiosemicarbazone (IV)	17.7	white	20.6	white	22.9	pale greyish brown
piperonal thiosemicarbazone (V)	18.7	white	21.1	white	23.2	pale brown
p-acetamide benzaldehyde thiosemicarbazone (VII)	17.5	white	20	white	22.5	brown black
p-dimethylamino benzaldehyde thiosemicarbazone (VI)	18.9	pale yellow	21.7	yellow	23.5	pale brown
m-nitrobenzaldehyde thiosemicarbazone (VIII)	18.3	yellow	20.8	yellow	23.0	pale brown
phenyl thiosemicarbazide (XI)	18.8	dark brown	20.7	greyish brown	23.5	black
benzaldehyde phenyl thiosemicarbazone (XII)	19	pale yellow	21.5	yellow	22.9	yellow brown

Conclusion

From the silver potentiometric titration of some organic sulfur compounds and their related compounds, the following facts are revealed.

1. In the phosphate buffer, some compounds (IV, V, VIII, X, XII) need too much silver ion because of the complex from of silver and phosphate and these compounds. Then the citrate and glycine buffers were used in order to avoid the complex formation from these compounds.

2. SCN^- radical gives an inorganic silver salt which is not affected with the *p*H change.

3. Hydrazine reduces Ag^+ although it does not give sulfur compound, because of the reducibility of NH_2.

4. Phenyl thiosemicarbazide (XI) gives sulfur most easily, next is thiosemicarbazide (III) and then thiourea (II).

5. We concluded that the sulphur atom is necessary to make good fog-inhibitors, and thiosemicarbazone derivatives which have long chain structure are excellent for the decrease of the electronegativity of NH_2. Thiosemicarbazide derivatives give sulfur compounds and thiocyanate gives silver thiocyanate only.

The authors wish to acknowledge the gift of thiosemicarbazone and thiosemicarbazide derivatives by K. Murobushi (Konishiroku Photo. Ind. Co.) and the suggestions by Y. Koseki (Fuji Photo Film. Co.).

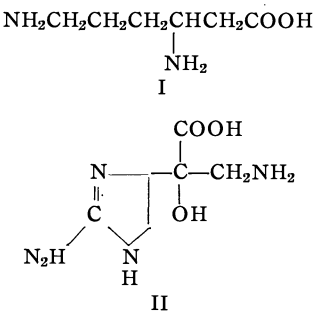
Institute of Industrial Science, Tokyo University, Chiba

*Two Uncommon Amino Acids obtained from Roseothricin**

By Koji NAKANISHI, Toshiko ITO, Mamoru OHASHI, Ichiro MORIMOTO and Yoshimasa HIRATA

(Received May 17, 1954)

Roseothricin is a complex antibiotic comprised from several components and produced by *Streptomyces roseochromogenus*. It was formerly designated H-277 and isolated by Hosoya et al.[1] from the soil of suburban Tokyo during the course of investigations on the production of antibiotics from various molds. Although of rather limited clinical importance due to its somewhat high toxicity, it possesses a high and broad antibacterial spectrum[2]; furthermore, the acid hydrolysis of either roseothricin complex or of the separated components afforded two amino acids, neither of them belonging to the common natural amino acids. Hence chemical investigations have been undertaken on these hydrolysates, and one has been identified as β, ε-diaminocaproic acid (I) (β-lysine)[3]*** or isolysine[4]. The other substance, for which the trivial name of "roseonine" is proposed, has now been shown to be 2-amino-4 (or 5)-(1-carboxy-1-hydroxy-2-amino)-ethyl-2-imidazoline (II), a totally new β-amino acid.****



I

II

The separation of the components of roseothricin complex was accomplished by submitting the substance to paper chromatography, utilizing butanol-ammonia-*p*-toluenesulfonic acid mixture as solvent and *B. subtilis* test plate for location of the active agents.[5] Three substances were obtained, which were designated roseothricin A, B and C, in order of their decreasing flow distance; a fourth component was obtained occasionally. Filter paper cataphoresis (100 v., 4 hrs.) at pH 4.6[5] separated the complex into two fractions, A and B-C. Separation of the complex by means of paper chromatography and filter paper cataphoresis under slightly different conditions have also been reported.[6] Ion exchange chromatography was found to be effective[5] for the separation of A and B-C in fairly large quantities; the complex was absorbed on a column of Amb. IRC-50 (Na-form) column at pH 7, and when eluted with citric acid-HCl buffer at pH 4.6 and gradually lowering the pH by 0.2 units, the following three fractions were obtained: pure A, A-B-C mixture and finally B-C mixture. The separation of B and C has as yet not been accomplished. The toxicity against mice (ID_{50}) weighing 14.4-15.6 g. (intravenous injection) was as follows: A, 155 mg./kg.; B-C, 1 mg./kg.; complex, 14 mg./kg. The respective fractions were active against gram-positive, -negative and acid-fast bacteria, the activity against *Myco. tuberculosis* 607 being of the same order as that of streptomycin; the activity of A was 1/2-1/100 that of B-C and the complex, depending on the species of the strain[1,2,5].

Roseothricin gave a crystalline helianthate (decomp 215–8°, N, 15.51%); reineckate (decomp. 185–190°, N, 22.18%) and picrolonate (decomp. 225–230°, C, 48.23; H, 5.63; N, 20.34%). The ninhydrin, biuret and Fehling reactions were positive, whereas the Pauly, Tollens, maltol, Sakaguchi, Trommer, Nylander, Molisch, Folins, Hopkins-Cole, Millon and Bial reactions were negative[1]. The acid hydrolysis of reseothricin complex and of roseothricin A both afforded two ninhydrin positive products, I and II, which were separated by the solubility differences of the

* Reported at the 6th Annual Meeting, Chem. Soc. Japan, (Kyoto), April, 1953 and at the 7th Annual Meeting, Chem. Soc. Japan, (Tokyo), April, 1954. A communication has appeared in *J. Am. Chem. Soc.* **76**, 2845 (1954).

1) S. Hosoya, M. Soeda, N. Komatsu, S. Imamura, M. Iwasaki, Y. Sonoda and K. Okada, *Jap. J. Exp. Med.*, **20**, 121 (1949): *J. Antibiotics*, **3** (4), 217 (1950).

2) S. Hosoya, M. Soeda, N. Komatsu and S. Imamura, *Jap. J. Exp. Med.*, **20**, 481 (1950); *J. Antibiotics*, **4**, (2), 79 (1951).

3) H. E. Carter, W. R, Hearn, E. M. Lansford, Jr., A. C. Page, Jr., N. P. Salzman, D. Shapiro and W. R. Taylor, *J. Am. Chem. Soc.*, **74**, 304 (1952).

4) E. E. van Tamelen and E. E. Smissman, ibid., 3714.

5) Y. Saburi, *J. Antibiotics*, **6** (8), 402 (1953).

6) S. Hosoya, M. Soeda, N. Komatsu, N. Hara, Y. Sonoda and R. Arai, *Jap. J. Exp. Med.*, **20**, 683 (1950); *J. Antibiotics*, **4** (6), 314 (1951).

picrates. Compound I, $C_5H_{14}N_2O_2$, $[\alpha]_D^{21}$ +19.0° (dihydrochloride in water) was ninhydrin positive, but did not respond normally to the action of the reagent (*vide infra*, Experimental) and therefore it is probably not an α-amino acid. The Van Slyke amino nitrogen determination gave values of one mole of nitrogen after five minutes and another mole after thirty minutes (Table I). The Kuhn-Roth C-CH_3 determination and periodate test were negative. No absorption maximum was seen in the ultraviolet spectrum, and the infrared spectrum of the hydrochloride in nujol also suggested a simple amino acid structure, i.e., 3.6–4.2 μ (broad), 5.81 μ (sharp and strong) 6.25 μ (medium), 6.7 μ (weak). The pK'$_a$ values, 3.20, 9.47 and 10.82 (10°C), indicted that one carboxyl and two amino groups were present, and that probably a β-amino acid grouping was involved, the other amino group occupying the terminal position. The data allowed only two possible structures, viz., β, ε-diaminocaproic acid and α-aminomethyl-δ-amino valeric acid. Two papers by American workers[3,4] on the elucidation of the structure of an amino acid which had been obtained from streptothricin[7], streptolin[7,8] and viomycin[7,9] appeared at this point, and it was found that compound I was identical with the new amino acid, i.e., β, ε-diaminocaproic acid (β-lysine or isolysine).

The infrared spectrum of roseonine (II), $C_6H_{12}O_3N_4$, $[\alpha]_D^{13}$ +51.0° (dihydrochloride in water) (Fig. 1) showed besides bands expected for regular amino acid hydrochlorides, sharp

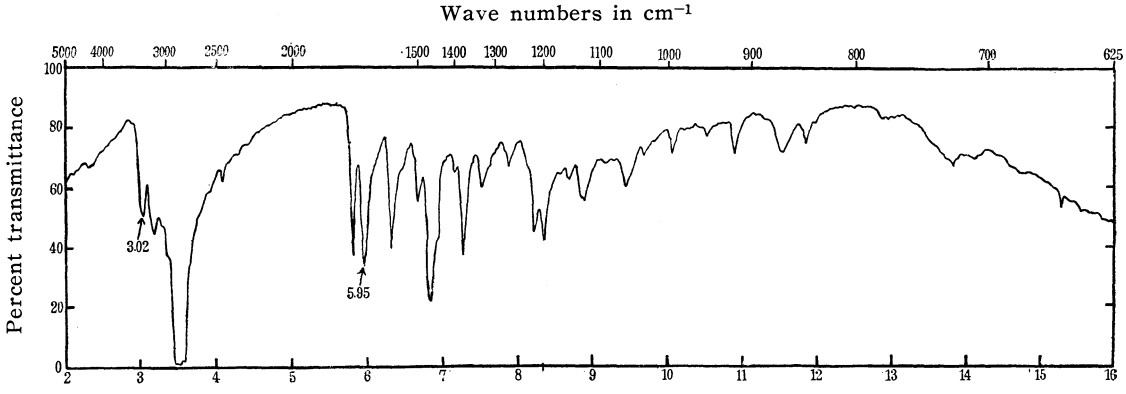


Fig. 1. Roseonine dihydrochloride (Nujol).

absorptions at 3.02 μ and 5.95 μ; the ultraviolet spectrum had an end absorption and a low broad maximum at 262–3 mμ (log ε: 1.22, dihydrochloride in water). Titration of the hydrochloride in aqueous solution gave pK'$_a$ values of 2.4, 9.3 and 11.9 (17°C), the first constant apparently arising from the carboxyl group, and the second and third from nitrogen functions. The 11.9 acidic constant and the 5.95 μ infrared band suggested the possible existence of a guanido group and the low ultraviolet maximum was also comparable with that of guanidine hydrochloride, 265 mμ (log ε: 1.26, in water).

Permanganate oxidation of roseonine at room temperature gave guanidine and a small amount of glycine. When treated with periodate, it consumed one mol. of oxygen in 15 minutes with the formation of one mole each of ammonia and formaldehyde, which meant that one of the two adjacent carbon atoms bearing the hydroxyl and amino groups is at the end of a chain. Coupling this with the formation of glycine and the absence of a strong band in the region 9–10 μ (infrared spectrum) usually associated with primary alcoholic groups, the presence of the grouping $>C(OH)CH_2NH_2$ was clearly indicated. The Van Slyke amino nitrogen determination revealed the existence of two amino groups, one of them being liberated somewhat slowly (*vide infra*, Table I–II). The seresults may be summarized in the following expression III:

$$\left.\begin{array}{l} NH_2—C—N< \\ \quad\quad\| \\ \quad\quad N \\ >C(OH)CH_2NH_2 \\ —COOH \end{array}\right\} C_2H_4 \qquad \text{(No C—CH}_3\text{, N—CH}_3\text{)}$$

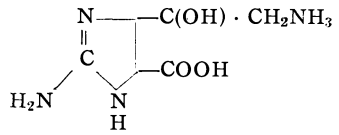
III

7) H. E. Carter, W. R. Hearn and W. R. Taylor, "Abstracts of Papers" 120th Meeting, Am. Chem. Soc., New York, N. Y. September, 1951, p. 3L.

8) E. E. Smissmann, R. W. Sharpe and E. E. van Tamelen, "Abstracts of Papers" 121st Meeting, *Am. Chem. Soc.*, Milwaukee, Wisconsin, April 1952, p. 80.

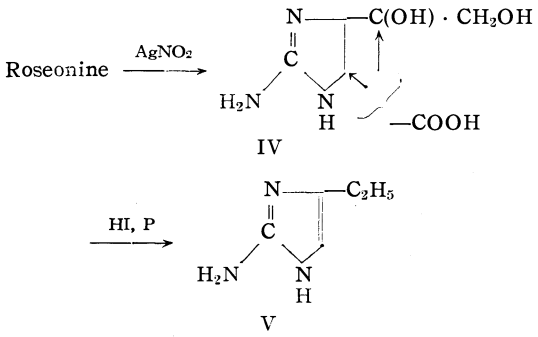
9) T. H. Haskell, S. A. Fusar, R. P. Frohardt and Q. R. Bartz, *J. Am. Chem. Soc.*, **74**, 599 (1952).

It was found at this point that the action of silver nitrite and subsequently hydroiodic acid—red phosphorous brought forth the remarkable conversion of reseonine into an imidazole derivative. Thus silver nitrite reacted normally to convert one amino group into a hydroxyl; the product IV consumed one mole of periodate with the formation of one mole of formaldehyde and it was natural to adopt the view (which received further confirmation, Table I–IV) that the non-guanido amino group had been replaced to give a vic-diol. Heating IV with hydroiodic acid and red phosphorous in a sealed tube gave a substance analyzing as $C_5H_9N_3$ (V); this coupled with *p*-diazobenzenesulfonic acid to give an orange-red color, a reaction which is typical for imidazoles possessing a free imino group and a hydrogen atom (or carboxyl) in positions 2,4 or 5 (Pauly reaction). The bromine decoloration test which is negative for 2-imidazolines but positive for imidazoles containing a free nuclear methine group was also positive. The Kuhn-Roth determination corresponded to one C—CH_3 whereas the N—CH_3 (or N—C_2H_5) determination was negative. Hence V must be 2-amino-4 (or 5)-ethylimidazole. Amongst the conceivable structures for a compound possessing the partial structure III, those represented by II or VI, i.e., 2-



VI

amino-2-imidazoline derivatives, were the only two which could afford V. The possibility of an open chain structure, and hence the formula $C_6H_{14}O_3N_4$ instead of $C_6H_{12}O_3N_4$ was also considered, but all were excluded on grounds of apparent inconsistencies with data hitherto mentioned. The reaction sequences then may be formulated as follows:



IV V

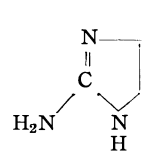
The conversion of IV into V could take place by dehydration of the side chain hydroxyl group, and rearrangement of the double bond to the more stable aromatic system and decarboxylation.

Interesting supporting evidences for the presence of a ring system in roseonine and V were obtained from comparative studies on the Van Slyke amino nitrogen determination (Table I). Comparing 7 with 6 and 8

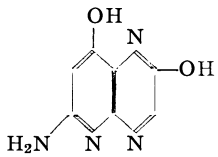
TABLE I

VAN SLYKE AMINO NITROGEN

Compound	Moles of N liberated in 7 min.	Moles of N liberated in 30 min.
1. α,ε-Diaminocaproic acid (I) dipicrate	1.06	2.13
2. Roseonine (II) dihydrochloride	1.02	1.84
3. Roseonine (II) methyl ester dipicrate	1.04	2.00
4. *vic*-Diol (IV) from roseonine	0.09	0.71
5. Compound V monopicrate		0.23
6. 2-Amino-2-imidazoline (VII) monopicrate	0.14	0.86
7. Arginine monopicrate	1.01	1.04
8. 2-Amino-4,6-dihydroxypteridine (VIII)	0	0.29



VII



VIII

respectively, it may be noted that incorporation of the guanido group into either a non-aromatic or aromatic ring exerts a labilizing effect on the guanido amino group. Thus the presence of a 2-imidazoline ring in roseonine was strengthened by the fact that the response of the guanido amino group of roseonine and products (2, 3 and 4) was similar to that of 2-amino-2-imidazoline, namely, about 0.8 mol. in 30 minutes; furthermore, comparison of 5 (0.23 mol.) and 8 (0.29 mol.) also reveal a striking similarity between the two compounds and hence the probable incorporation of the guanido group of V into an aromatic nuclei.

Of the remaining alternative structures II and VI, the latter was excluded on the following grounds: (i) Roseonine is remarkably stable towards dilute and concentrated hydrochloric acid and thus the functional groups are probably not disposed in space so as to permit easy dehydration leading to formation of γ-lactone, -lactam or hydantoin-imide-(2) rings. These relations are satisfied in struc-

ture II: it may also be noted that normal acid dehydration involving the tertiary hydroxyl group would be hindered due to the presence of the carboxyl and an adjacent positive ammonium (NH_3^+) group. (ii) In the periodate treatment, a second mole of the reagent was consumed after 20 hours, a behavior conforming to that of serine, and hence apparently to that of isoserine.

Structure II is also consonant with the fact that the Sakaguchi and biacetyl reactions were negative since it has been reported that N, N'-disubstituted guanidines do not respond to these color tests[10].

Experimental**

I. Hydrolysis of Roseothricin.—A solution of 5 g. of roseothricin (complex or A) in 50 cc. of 20% HCl was heated in a sealed tube for 48 hours at 100°C. and the reaction mixture was evaporated to dryness in vacuo. After addition of 20–30 cc. of water and filtration to remove some tarry product, two spoonfuls of Amberlite IR-4B (OH-form) was added and left overnight when the *p*H was 7–8. The resin was removed and to this there was added 6 g. of picric acid under slight heating upon which a mixture of two picrates and a small amount of resinous product was deposited. The mixture was warmed to bring the picrates into solution, and the resinous material was removed by filtration through cotton. The cooled filtrate containing yellow and orange-yellow picrates was gently rewarmed, when the former dissolved more rapidly. The supernatant was decanted and the separation of the two picrates was effected by repeating the process of dissolution, cooling, warming and separation in the conventional triangular scheme of fractional crystallization. The yellow and orange-yellow picrates corresponded to that of β,ε-diaminocaproic acid and roseonine, respectively. Upon recrystallization from water, each picrate weighed about 2 g. When submitted to paper chromatography using butanol-acetic Acid-water (4:1:5) as solvent, the picrates dissociated and each gave a single spot with ninhydrin, Rf 0.15 (β,ε-diaminocaproic acid) and Rf 0.08 (roseonine).

II. β,ε-Diaminocaproic Acid (I). *Dipicrate*: m.p. 200–1° (water). Found: C, 35.55; H, 3.27; N, 18.19; M.W.[11] 596. Calcd. for $C_{18}H_{20}O_{16}N_8$ (604.40): C, 35.76; H, 3.31; N, 18.54. *Dihydrochloride*: The picrate was dissolved in a small quantity of hot water and the picric acid which precipitated upon acidification with hydrochloric acid was extracted thrice with ether and the solution was concentrated in vacuo. The addition of ethanol gave the hydrochloride which was recrystallized by adding alcohol to the hot aqueous solution, hygroscopic needles, m.p. 146–7° (water and alcohol). Haskell et al. report 153–5° for this derivative.[9] Found: C, 33.60; H, 7.66; N, 12.96; Cl, 31.61. Calcd. for $C_6H_{16}O_2N_2Cl_2$: C, 32.88; H, 7.36; N, 12.79; Cl, 32.36. *N,N-Dibenzoate* (neutral derivative)[3]: The dihydrochloride was benzoylated through the Schotten-Baumann procedure, and the product recrystallized from ethanol, m.p. 159–60°. *p-Hydroxyazobenzene-p'-sulfonate*[3,4] m.p. 243–5° (water). *α-Amino acid test*: (*vide infra*).

III. Roseonine (II). *Dipicrate*: decomp. 237° (water). Found: C, 33.48; H, 3.17; N, 22.09; M. W. 654[11]. Calcd. for $C_{18}H_{18}O_{17}N_{10}$ (646.40): C, 33.45; H, 2.81; N, 22.09. *Dihydrochloride*: From the dipicrate by conventional methods, m.p. 215° (water and alcohol). Found: C, 27.51; H, 5.40; N, 21.55: Cl, 27.97. Calcd. for $C_6H_{14}O_3N_4Cl_2$: C, 27.65; H, 5.41; N, 21.46; Cl, 27.16. *Methyl ester dipicrate*: To a suspension of 20 mg. of the dihydrochloride in 3 cc. of methanol, there was added 0.12 cc. of BF_3 etherate (4 mol. equiv.) and the mixture was refluxed gently for 5 hours. After the addition of 3 cc. of water and picric acid, methanol was removed by boiling and the solution was left at room temperature; the formation of the picrate was slow but the yield was good (35 mg.), m.p. 202° (water). However, there were occasions when the preparation of the ester failed; the cause for this uncertainty was not fully investigated. The ester gave a positive ninhydrin coloration. It was very susceptible to acid hydrolysis. Found: C, 34.66; H, 3.40; N, 21.39. Calcd. for $C_{19}H_{20}O_{17}N_{10}$ (660.43): C, 34.56; H, 3.05; N, 21.22. *α-Amino acid test*—Reaction with ninhydrin: A solution of 33 mg. ninhydrin (2 mol. equiv.) in 5 cc. of water was added to a solution of 26 mg. of the dihydrochloride in 2 cc. of water and heated at 100°. Contrary to the behavior of usual α-amino acids (formation of purple precipitate), no reaction occurred. Hence the mixture was heated in a sealed tube for 3 hours at 150°, upon which ca. 10 mg. of purple brown precipitate was obtained; when 2,4-dinitrophenylhydrazine was added to the colorless solution a small amount of hydrazone, decomp. 110° resulted. However, the same two substances were also produced when ninhydrin alone was treated in a similar manner. A small amount of roseonine picrate was recovered after addition of picric acid to the filtrate of the hydrazone. The behavior of β,ε-diaminocaproic acid was also exactly similar.

Action of periodate: Sodium metaperiodate oxidized II-dihydrochloride at room temperature to give one mole each of formaldehyde (dimedone) and ammonia (titration) after 15 minutes. The consumption of the reagent was 1.01 mol. (15 min.), 1.05 mol. (1 hr.), 2.32 mol. (20 hrs.) for roseonine dihydrochloride, and 1.15 mol. (10 min.), 1.13 mol. (1 hr.), 1.94 mol. (30 hrs.) for serine. Standard techniques were employed for these analyses. Similar results were obtained with periodic acid.

Permanganate oxidation: 100 mg. of II-dihydrochloride and 250 mg. of KOH were dissolved in 5 cc. of water, and 120 mg. of $KMnO_4$ in 5cc. of water

** All melting points were determined on a micro hot stage, and are uncorrected.

10) J. D. Mold, J. M. Ladino and E. J. Schantz, *J. Am. Chem. Soc.*, **75**, 6321 (1953).

11) Obtained from the extinction coefficient by the method of K. G. Cunningham, W. Dawson and F. S. Spring. *J. Chem. Soc.*, 2305 (1951).

was added dropwise with stirring over a period of 2 hours at 30°. After leaving for 2 hours, the mixture was filtered and the brown precipitate washed thoroughly with boiling water. The filtrate and wash solution were combined, and after acidification, taken up to dryness in vacuo. The residue was extracted repeatedly with boiling ether, and the ether extract was left overnight to evaporate when a minute amount of colorless crystals, m.p. 126–31° (with partial sublimation; m.p. depression with malonic acid) was obtained. Though the amount was insufficient to permit further purification, paper chromatography gave only a single spot corresponding to oxalic acid; a simultaneous run showed that neither malonic, succinic nor malic acid was present. The residue from ether extraction was extracted with boiling ethanol, leaving a white inorganic salt. Removal of alcohol gave a hydroscopic crystalline residue. An aqueous solution of picric acid was added; the crystals were first washed with ether and then recrystallized several times from water with addition of active charcoal; 3 mg. of yellow plates, m.p. 315°. No depression observed when mixed with authentic guanidine picrate. Found: C, 29.65; H, 3.13; N, 28.81. Calcd. for $C_7H_8O_7N_6$ (288.18): C, 29.17; H, 2.80; N, 29.17.

The filtrate from the guanidine picrate was acidified and, after extraction of excess reagent with ether, was concentrated in vacuo to give a syrupy mass. This was paper-chromatographed with the following solvents and in each case gave only a single ninhydrin positive spot undistinguishable from glycine. BuOH: AcOH: H_2O 4:1:1 (Rf 0.12). BuOH: AcOH: H_2O=4:1:5 (Rf 0.21). Lutidine: collidine: H_2O=1:1:1 (Rf. 0.15). 40% aq. acetone (Rf 0.45). Phenol: 1% ammonia= 85:15 (Rf 0.38).

Oxidation with $Ba(MnO_4)_2$ also afforded similar results.

vic—Diol (IV): A solution of 130 mg. of II-dihydrochloride was treated with 154 mg. of $AgNO_2$ (2 mol. equiv.) at room temperature for 15 hours, and after filtration of AgCl and concentration in vacuo, a syrupy mass was obtained. White crystals were isolated by the addition of alcohol and filtration; m.p. 190° (water and alcohol), yield 50 mg. Periodate oxidation for 20 minutes produced 0.62 mol. of formaldehyde. Found: C, 37.77; H, 5.62; N, 21.96. Calcd. for $C_6H_{11}O_4N_3$ (189.17): C, 38.09; H, 5.86; N, 22.21. When only one mole of $AgNO_2$ was added the yield of IV was poor, and upon addition of picric acid, unchanged starting material was obtained in good yield. Thus removal of both molecules of hydrochloric acid as AgCl seemed to be necessary for the satisfactory action of $AgNO_2$. Incidentally, $AgNO_2$ is presumably a weaker reagent than HNO_2 as could be seen from the fact that the β-amino group of histamine was converted into a hydroxyl by the latter but not by the former.

Compound V: II-Dihydrochloride (130 mg) was treated with 2 mol. of $AgNO_2$ and the product was worked up to give the syrupy mass as mentioned above. To this there was added 0.48 cc. of HI (b.p. 126°) and 24 mg. of red phosphorus, and the mixture was heated in a sealed tube for 8 hours at 150°. The clear colorless solution was separated from some tarry precipitate and after evaporating to dryness, water was added and the solution was concentrated again; the processes of concentration were carried out under nitrogen. A syrupy residue containing white crystals resulted. The crystals were separated by filtration and analyzed but were not further investigated, m.p. 168°, yield 30 mg. Found: C, 1.24; H, 5.26; N, 9.52; ash, 30.72. The acidic syrup was neutralized with Amberlite IR-4B when addition of picric acid afforded 30 mg. of a yellow picrate, m.p. 182° (water). The syrup as well as the free compound obtained from the picrate gave an orange-red Pauly test. The same picrate was obtained from the reaction product of one mole of $AgNO_2$, but the yield was even lower. Found: C, 39.05; H, 3.72; N, 23.91; M.W. 356[11] Calcd. for monopicrate, $C_{11}H_{12}O_7N_6$(340.25); C, 38.83; H, 3.56; N, 24.70.

Acid treatment: Roseonine is remarkably stable towards acid, and was recovered unchanged after heating 50 mg. of the dihydrochloride with 0.6 cc. HCl in a sealed tube for 8 hours at 150°.

Summary

Roseothricin has been hydrolysed to give two uncommon amino acids, *viz.*, β,ε-diaminocapric acid (I, β-lysine), and 2-amino-4(or 5)-(1-carboxy-1-hydroxy-2-amino)-ethyl-2-imidazoline (II, roseonine) as the sole ninhydrin positive products.

Acknowledgement

The present work was undertaken in collaboration with Prof. S. Hosoya and his associates, Institute for Infectious Diseases, University of Tokyo, to whom the authors are greatly indebted for their continuous support in the problem and generous supply of roseothricin.

Most of the analyses and infrared determinations were carried out by the microanalytical staff at the Institute of Polytechnics, Osaka City University, and the authors wish to make grateful acknowledgements to Mr. S. Senoh and Mr. M. Yamaguchi for their exceedingly generous cooperation.

They also wish to thank Professor F. Egami for his interest and counsel during the course of this study, and the Sanyo Pharmaceutical Co. for preparing a portion of roseothricin.

Department of Chemistry, Faculty of Science, Nagoya University, Nagoya

*** We are very grateful to Professor Carter for information give us on β-lysine.

**** It has been seown by direct comparison that roseonine is identical with streptolidine, a hydrolysis product of streptolin (Communication from Professor E. E. van Jamelen. September 10 (1954).

Heterogeneous Structure of Rayon. IV. Effect of Stretching on the Heterogeneous Structure (1)

By Saburo OKAJIMA and Shigeru HAYAMA

(Received September 16, 1953)

In the previous papers[1] the authors determined the conditions of the peeling-off of rayons by the fibre-heterogeneous acetylation and studied the properties of the skins and cores of some rayons on the market. Now the method has been applied to a series of viscose rayons prepared by a two-bath process in order to study the effect of the stretching of the rayon fiber in the second bath upon its heterogeneous structure.

Experiment

(1) Rayon samples.—The samples used were a series of viscose rayons prepared from an ordinary factory viscose by a two-bath process in the laboratory of the Teikoku Jinken Co. The spinning was carried out as shown diagramatically in Fig. 1, in which the first bath A was composed of 9.70% H_2SO_4 and 0.4% Zn besides some Na_2SO_4, its specific gravity being 1.25. The temperature was kept at 50±1°C and the immersion length was 23 cm.

The second bath B was hot water of 80°C, the immersion length being 35 cm.

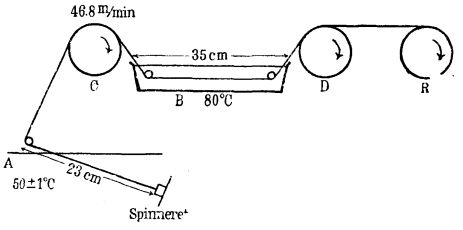


Fig. 1.

The peripheral velocity of the first godet C was fixed to 46.8 m./min. and that of the second one, D, was so controlled as to be able to stretch the yarn in the second bath to various degrees as given in Table I. The yarn collected on a bobbin R was, after being removed from R washed thoroughly, desulfured and bleached as usual. This process was carefully carried out so that the yarn was not stretched during the spinning between D and R. The details of the conditions and some of the properties of the yarns obtained are summarized in Tab. I.

TABLE I

Yarn No	Periph. speed of D, m./min.	Degree of stretch	Denier of the single filament	r	Dry stg., g./den	Dry elong., %
IIa	46.8	1.00	6.37	1.000	1.54±0.06	43.4±1.1
IIb	55.2	1.25	5.09	0.892	2.08±0.08	24.7±0.9
IIc	65.1	1.54	4.15	0.807	2.68±0.12	14.1±0.8
IId	73.0	1.87	3.41	0.753	3.26±0.11	11.1±0.3

The mechanical properties given in the above table were obtained by a test at 20°C and 65% R.H. and the values were estimated stochastically, the confidence coefficient being 95%.

The yarn was extracted with ether for several hours, washed repeatedly with hot water (60°C) and stored after air-drying. This sample was vacuum-dried immediately before use (the weight is W) and the heterogeneous acetylation was carried out for 3~300 hours at 60°C. The composition of the acetylation bath was as follows:

Acetic anhydride	5 g.	} per 0.5 g. sample.
Benzene	15 g.	
Sulfuric acid (1.84)	0.05 g.	

After acetylating the sample to the desired degree it was taken out of the acetylation bath, washed twice with benzol and further with hot water (60°C). It was then vacuum-dried and weighed (W_A). A half of it was peeled-off by pouring into chloroform and keeping over-night at 50°C, washed with water, vacuum-dried and weighed again (W'). From W, W' and W_A, L_2 and L_T are calculated as described in the previous paper.

The other half was used for the determination of the acetic acid content (A%). L_1 is then calculated from A, W and W_A.

The amount of the peeled-off cellulose is therefore $(L_1+L_2)/W$ or directly L_T/W, but the latter is smaller than the former by about 1.5% as was shown in the previous paper and also the present data show the same fact. Then the percentages of the peeled-off shell (P_r) and the layer dissolved during acetylation (P_s), are obtained from the above data as follows:

$$P_r=1-\left(1-\frac{L_T}{W}-0.015\right)^{\frac{1}{2}}=1-\left(1-\frac{L_1+L_2}{W}\right)^{\frac{1}{2}}$$

and

1) S. Okajima, S. Hayama and K. Kobayashi, This Bulletin **25**, 271, 275 (1952).

$$P_s=1-\left(1-\frac{L_1}{W}\right)^{\frac{1}{3}}.$$

Of course P_r and P_s are given on the base of the original radius of the filament.

As to the details of the experimental methods and the notation used refer to the previous papers.

Experimental Results

The results are summarized in Figs. 2–6.

(1) Structural Difference between the Skin and the Core.—In the previous paper it was described that the acetylated shell of the fiber so degradated that it partly dispersed into the acetylation bath and that this rate of dispersion of the skin part was smaller than that of the core. This is true also in the present case (ref. Fig. 2). The

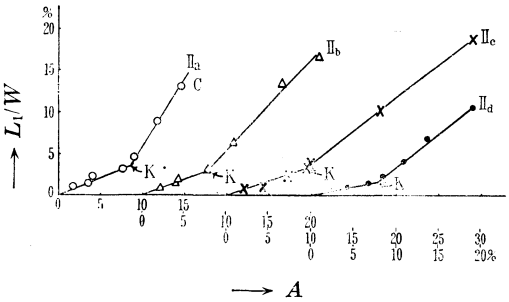


Fig. 2.

relation between the amount of this loss (L_1/W) and the acetic acid content (A) of the acetylated yarn is given by a broken line OKC. The amount of L_1/W corresponding to the inflection point $K-L_K/W$ in Table II—indicates the weight percentage of the outermost skin. These values and the thicknesses estimated from them are given in the second and third lines of the table.

TABLE II

Sample		IIa	IIb	IIc	IId
L_K/W, %		3.3	2.5	2.0	1.7
P_r % calculated from	Fig. 2	1.7	1.5	1.5	0.8
	Fig. 3	1.9	1.4	1.4	0.7

As the slopes of the lines OK and KC decrease in the order from IIa to IId, the rate of acetylation relative to the rate of dispersion of the acetylated portion increases with the growth of the stretching degree both in the skin and in the core. But the absolute rates do not necessarily change similarly.

In Figs. 3 and 4 rP_r and $r(P_r—P_s)$ are plotted against the acetylation time t, where r is the relative mean radius of each filament calculated from the denier, taking the denier of IIa as unity, so that the rate of the dispersion and the apparent rate of acetylation of IIa—IId can be compared directly, irrespective of the difference of their deniers.

As seen from Figs. 3–4, an inflection point appears on each curve, which tells that the

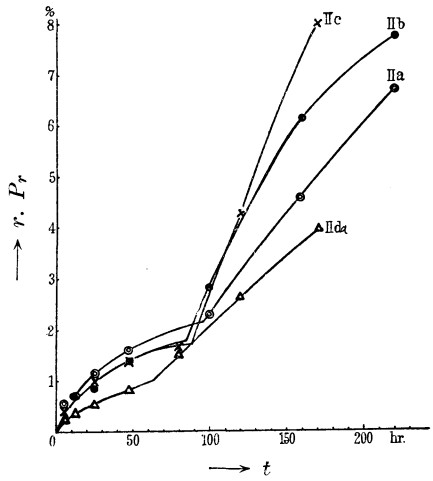


Fig. 3.

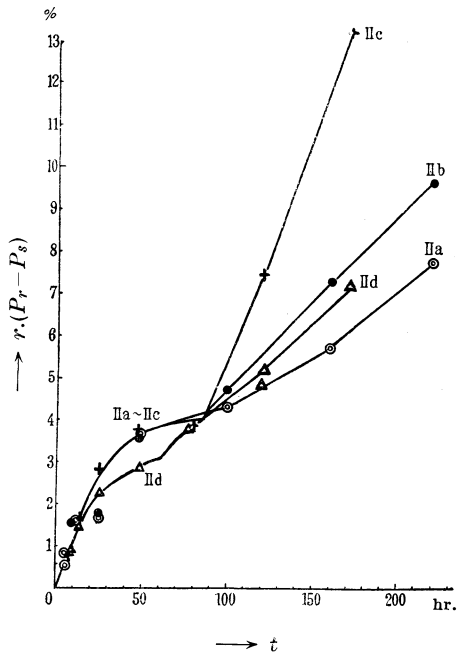


Fig. 4.

outermost skin exists and that the rates of the dispersion and the acetylation increase abruptly when the skin disappears from the filament. This is because the structure of the outermost skin is remarkably dense compared with that of the core or of the transition layer. Then the thickness of the skin layer is estimated also from the curve in Fig. 3 as shown in the fourth line of Table II. A good comformity between the corresponding values in the third and fourth lines

supports this view.

Among IIa—IId the outermost skin becomes thinner in the order from IIa to IId.

As to the effect of the stretching of a rayon fiber on its microstructure, the skin becomes slightly denser while the core becomes looser as the stretching increases, with an exception of IId, the structure of which is extraordinarily denser.

An electronmicrograph taken by Hermans[2] shows that a number of small pores exist within the outermost skin. These pores may be caused by the gasses evolved by the decomposition of viscose. Then we can suppose from the above two figures that the porosity within the outermost skin becomes the larger as the yarn is stretched the higher.

But this generalization can not be applied to the case of the yarn IId, the core of which is thought to have rather greater density and smaller porosity than that of IIb. To this point the authors shall return later.

(2) Orientation Degrees of the Skin and of the Core.—The relation between Γ and P_r is similar to these of the commercial viscose rayons already described in the second report. Three parts of the structure, i.e., the outermost skin, the transition layer and the core are clearly distinguished also here (rf. Fig. 5). The thickness of the outermost

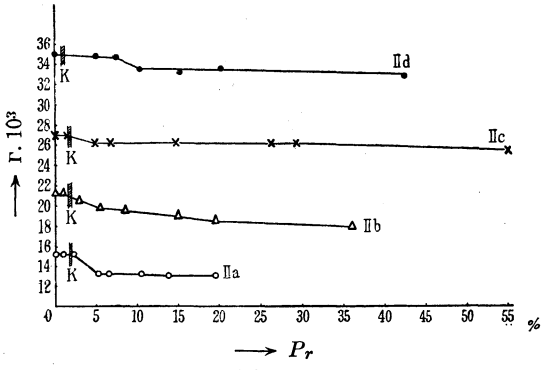


Fig. 5.

skin calculated from the inflection point (Figs. 2—3) coincides well with that found on the corresponding curve as indicated by K with an exception of IId, whose outermost skin is abnormally thick.

As to the orientation degree, both Γ of the skin and of the core grow almost linearly with the stretching degree or the difference between that of the skin and that of the core is kept nearly constant irrespective of the stretching (rf. Fig. 6). So if a fibre of nearly

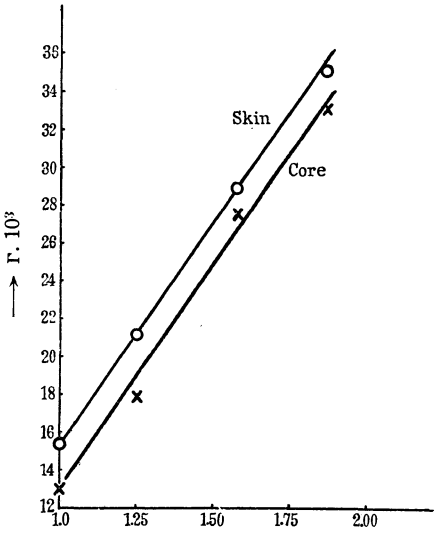


Fig. 6.

isotropic core is prepared by extructing a viscose slowly into a coagulating bath and not drafted[3] or stretched, its skin seems to be of low orientation. That it is truly the case is experimentaly proved. Then the orientation of xanthate molecules due to the high velocity gradient near the spinneret wall is considered to be feasible, if any, or the orientation seems not to be fixed in the hydrate cellulose fibre, even when the high orientation may occur in the viscose.

(3) Abnormality of IId.—As described above some properties of the filaments change systematically in the order from IIa to IId according to the degree of stretching, but IId often deviates from this order.

Many studies have been carried out on the mechanism of the viscose spinning process. They are however fragmentary and the results obtained are not yet conclusive. In order to explain the above results, attempt is made here to consider also this mechanism from author's view point. It is however partly a conjecture for which we hope future experiments will prove.

The first change of a viscose stream extruded from a spinneret orifice into the bath solution is the production of the Zn-xanthate layer on its surface and not the direct regeneration of the Na-xanthate. This layer is assumed to be hydrophobic compared with the ordinary Na-xanthate and cross-linked by Zn. Because of this the cellulose layer

2) P. H. Hermans, *Textile Research J.*, **20**, 105 (1950).

3) "Drafting" and "Stretching" are used as the same thing as "Verzug" and "Verstreckung" of Kauch and Harms; cf. Herbert Brandenberger; Melliand Textilber., **34**, 823 (1953).

regenerated from this Zn-xanthate has also a denser structure. This is the outermost skin considered in this study. It is well known that the addition of $ZnSO_4$ to the spinning bath retards the regeneration to follow. This is considered to be due to the stability of the Zn-xanthate, the retarded penetration of the sulfuric acid (inward) and the enhanced osmotic dehydration of viscose and xanthate (outward), because of the denser structures of the Zn-xanthate and of the hydrate cellulose layers derived from it.

The viscose stream is drafted by the first godet to attenuate the filament so that the orientation occurs during the osmotic dehydration. As the yarn of IIa—IId are drafted equally and the stretching in the second bath is supposed to attenuate the cross section uniformly, the percentage occupied by the outermost skin of each filament must be equal to each other. But the observed thickness of the outermost skin of the yarn is thinner the higher it is stretched. This may be due to the slippage of the yarn on the first godet, the actual drafting not being kept constant as expected.

The drafting brings about the higher orientation of the outermost skin compared with that of the core, because the dehydration of the latter is not sufficiently high to be orientated effectively by this drafting.

Now in the second bath the yarn is stretched to various degrees and at the same time a sudden decomposition occurs because of the high temperature.

The orientation degrees of the outermost skin and of the core are raised further by this stretching and fixed as seen in Fig. 5.

The stretching also accelerates the dehydration of the core by the squeezing action, but at the same time the increase of the density of the outermost skin due to higher stretching retards the penetration of the liquids as shown in Fig. 7. As the result, the actual dehydration goes through a minimum point with stretching.

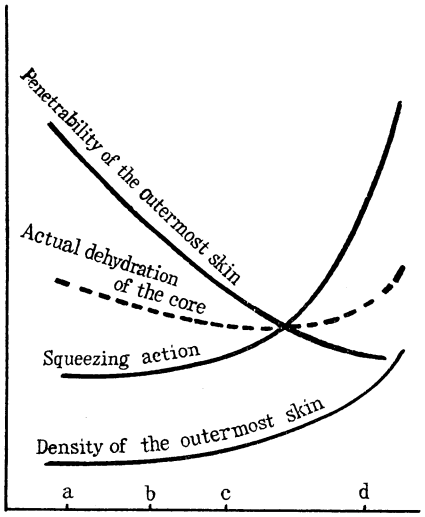
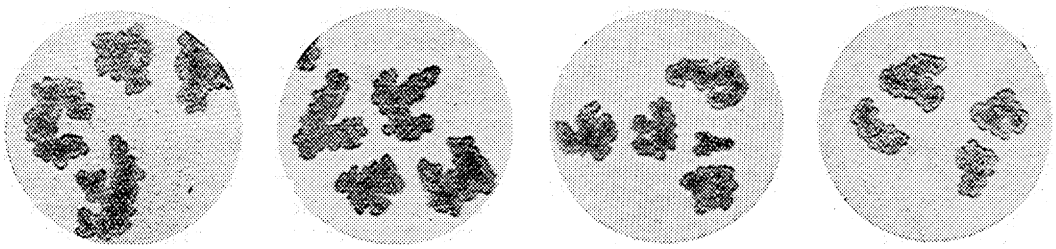


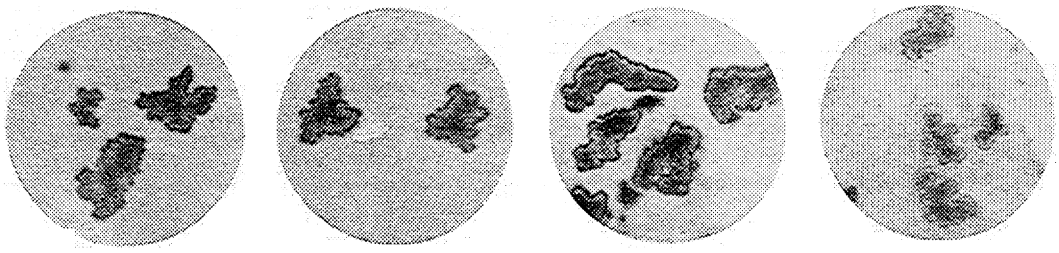
Fig. 7.

Fig. 8.

(a) Dyed with Oxamine pure blue B



(b) Dyed with Oxamine blue 4R



The sudden decomposition of viscose or xanthate evolves gasses and brings about a porous structure. But the more the viscose or xanthate core is dehydrated, the less is the destruction of the structure and the denser is it. So the outermost skin becomes denser in the order from IIa to IId, but the density of the core goes through a minimum (IIc).

In the case of IId the dehydration of the core proceeds and it approaches so near to the state of the outermost skin, that the orientation of that part is fixed effectively similarly to that of the outermost skin and the apparent outermost skin becomes extraordinarily thick. The origin of this outermost skin is thus dual and it can be distinguished only by the acetylation as shown in Fig. 5.

The relation between the outermost skin and the ordinary skin is as follows. The skin layer of an ordinary viscose filament has hitherto been recognized by metachromasis. The thickness of this skin seems to be larger than the authors' outermost skin. According to P.H. Hermans a number of tiny pores exist within an outermost layer (this seems to correspond to the authors' outermost skin), the pores being observed to grow larger toward the centre. Metachromasis is based on the distribution of the pore size so that the skin hitherto observed is thick and its thickness is dependent upon the state of the polydispersity of the dyes used.

Fig. 8 indicates the skins of IIa—IId dyed with Oxamine pure blue B and Oxamine blue 4R. These skins are thicker than our outermost skin and the latter dye seems to give a thicker skin than the former.

The cost of this research has been defrayed by the Grant in Aid for Fundamental Scientific Research from the Ministry of Education, to which the authors' thanks are due. The authors are also grateful to Mr. I. Okamura of the Teikoku Jinken Co. for his kind supply of the samples.

Faculty of Engineering, Tokyo Metropolitan University, Tokyo, and Faculty of Engineering, Yamagata University, Yonezawa

Structural Change in Some Solutions Having Structural Viscosity

By Masayuki NAKAGAKI and Shigeo SAKATA

(Received May 17, 1954)

The amount of liquid flowing out in unit time, Q, from a capillary tube of a in radius and l in length, is proportional to the pressure difference, P, between both ends of the tube. According to Poiseuille, the viscosity of the liquid, η_0, is obtained by:

$$\eta_0 = \alpha P/Q \tag{1}$$

where,

$$\alpha = \frac{\pi a^4}{8l} \tag{2}$$

For some colloidal solutions, however, the viscosity obtained from this equation shows abnormally large value for smaller pressure difference. For such abnormal viscosity, Freundlich and Schalek[1] gave an explanation of "elasticity of flow". Wo. Ostwald[2], on the other hand, named it "structural viscosity", considering that a net-work structure as in jellies has been formed in such solutions. It was assumed that the structure was readily destroyed by pressure, thus exhibiting the usual viscosity for higher pressure.

In the present report, the structural viscosity of vanadium pentoxide (V_2O_5) sol and mercury sulfosalicylate (Hg-SS) sol are measured. Then, the structural changes of these sols by shaking and by the irradiation of ultrasonic wave are observed under the electron microscope, and the structural viscosity is explained by it.

Experimental

V_2O_5 sol was prepared from ammonium vanadate by hydrolysis. 5 g. of ammonium vanadate was put in a mortar and smeared, adding drop by drop 25 cc. of dilute nitric acid (1 volume of $d=1.4$ nitric acid was diluted by 5 volume of water). Then, it was filtered by suction, washed with distilled water repeatedly, till the filtrate showed distinct red color. The precipitate on the

1) H. Freundlich and E. Schalek, *Z. physik. Chem.*, **108**, 153 (1924).
2) Wo. Ostwald, *Z. physik. Chem.*, **111**, 62 (1924).

filter paper was then put in 100 cc. of distilled water and stirred vigorously. The sol was aged about one month.

Hg-SS (mercury sulfosalicylate) was prepared by boiling 4 cc. of sulfosalicylic acid solution (containing 4 g. of solute) with 2 g. of yellow mercury oxide, stirring continuously. After the powders had been completely dissolved by the reaction, the solution was heated to dryness, and the powder obtained was ground. 0.3 g. of powder was dissolved in 200 cc. of water.

The structural viscosity was measured by Ostwald's overflow viscometer, shown in Fig. 1.

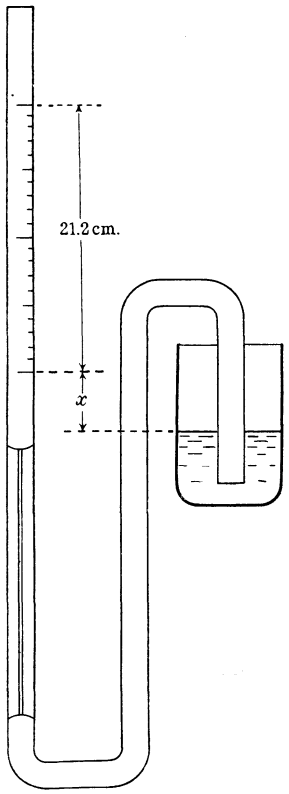


Fig. 1. Overflow viscometer.

A capillary tube of 21.2 cm. in length and 0.67 mm. in inner diameter was connected with a mess-pipette of 2 cc. in capacity. The grade of the pipette from 0.0 to 2.0 corresponded to the height of 21.2 cm. The height indicated by x in Fig. 1 was measured every time. It was usually 3.0—4.5 cm. The time, which 0.4 or 0.2 cc. of liquid required to flow down, was measured by stop watch, to calculate the mean amount of flow, Q. The pressure difference, P, was obtained from the mean difference of liquid levels.

The Electron microscope used was the Hitachi HU-4 type, operated under the direct enlargement of 10,000—5,000 ×. Plates were enlarged, 3—6 times, photographically. If necessary, a shadow was cast by Cr metal.

The ultrasonic apparatus was Shimazu P-200 type, used under the condition of 2 kV., 0.2 A. in input, and output current was also 0.2 A. The frequency was 610 kC.

Structural viscosity

Some of the results obtained for distilled water, V_2O_5 sol (about 0.6%), and Hg-SS sol (about 0.04%) are shown in Fig. 2. P/Q is proportional to the

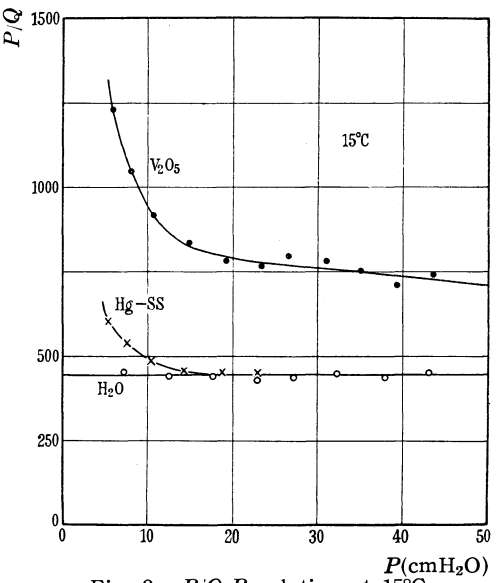


Fig. 2. P/Q-P relation at 15°C.

viscosity, as shown in Eq. (1). Curves for V_2O_5 and Hg-SS, therefore, show structural viscosity, as already known[1,2,3]. As for water, a typical Newtonian liquid, P/Q is constant regardless of pressure P. The mean value of $P/Q=446$ for water gives the α value, using the viscosity of water at 15°C[4], $\eta_0=11.45\times10^{-3}$ dyne. sec./cm.^{2}, $\alpha_{(obs)}=\eta_0/(P/Q)=2.57\times10^{-5}$ (dyne. cm./cmH_2O) (3) where cmH_2O means the pressure expressed by the height of the water column. On the other hand, using the size of capillary tube cited above,

$$\alpha_{(calc)}=\frac{\pi a^4}{8l}g=2.3\times10^{-5}\ \text{(dyne. cm./cm}H_2O\text{)} \quad (4)$$

where the constant of gravity, g, is used to recalculate the pressure to water pressure in *cm.* Values of Eq. 3 and 4 are in good agreement.

The ratio of P/Q for a specimen and for water is equal to the relative viscosity η/η_w. As shown in Fig. 3 and 5, the relative viscosity is linear to $1/Q$:

$$\eta/\eta_w=a+(b/Q) \quad (5)$$

at least in the measured range of pressure. This relation is explained as follows. In the pressure P applied to the liquid, P_0 is used to destroy the net-work structure, and the residue is effective to flow:

$$P_{eff}=P-P_0 \quad (6)$$

P_0 corresponds to the yield value. It is, then, assumed that the flow of broken net-work is Newtonian:

3) Wo. Ostwald and M. Mertens, *Kolloid-Beih.*, **23**, 242 (1927); S. Berkman and H. Zocher, *Kolloid-Z.*, **42** 322 (1927).
4) "International Critical Tables," Vol. 5 (1929), p. 10.

$$Q=\alpha P_{eff}/\eta_N, \tag{7}$$

η_N is the viscosity of this Newtonian flow. The apparent viscosity, η, is

$$\eta=\alpha P/Q=\eta_N+\alpha P_0/Q. \tag{8}$$

Then, the coefficients, a and b, in the empirical equation (5) are

$$\left.\begin{aligned} a&=\eta_N/\eta_w \\ b&=\alpha P_0/\eta_w=P_0/446. \end{aligned}\right\} \tag{9}$$

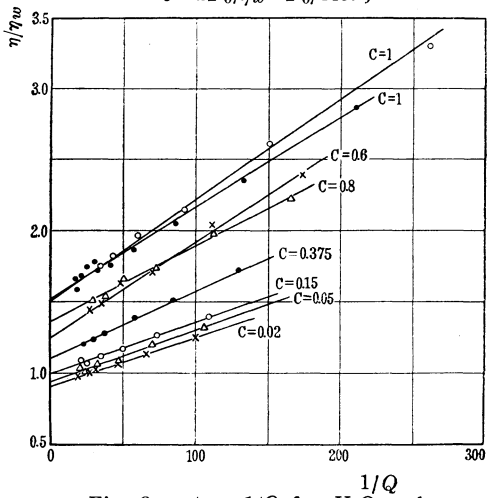


Fig. 3. $\eta/\eta_w-1/Q$ for V_2O_5 sol.

V_2O_5 sol of about 0.6% is diluted to various concentrations, left alone for 2 hrs., and the structural viscosity is measured. The results are shown in Fig. 3. The linear relation of Eq. (5) are verified. The concentration, C, is the relative one, assigning that of original solution (about 0.6%) as 1. Fig. 4 shows (η_N/η_w) and P_0 obtained from the data of Fig. 3, as a function of C. Fig. 4a shows that η_N/η_w increases linearly with the increase of C. Assuming the concentration of the original solution as 0.6%, and the density of V_2O_5 as 3.5[5], the relation.

$$\eta_N/\eta_w=0.91+128\phi \tag{10}$$

is obtained, where ϕ is the volume fraction of dispersed particles. The coefficient 128 is about 51 times larger than Einstein's 2.5. Comparing the fluctuation of plots in Fig. 4a and b, it is concluded that the yield value, P_0, sensitively depends on the structure, or the history of the specimen, while the Newtonian viscosity, or the viscosity after the structure has been broken, depends a little on its history.

As shown in Eq. (10), the relative viscosity becomes smaller than that of the solvent itself at smaller concentration. This is more clearly shown for Hg-SS in Fig. 5. This may be attributed to the slip of liquid on the surface of a capillary tube. The elasticity of flow will usually accompany the slip. Then, the amount of flow, Q, is assumed as the sum of the flow amount by Newtonian flow, Q_η, and the flow amount by slip, Q_s, on the surface of the tube (in this case, liquid is pushed out as a whole). Assuming that the slipping velocity at the tube surface, v_s, is

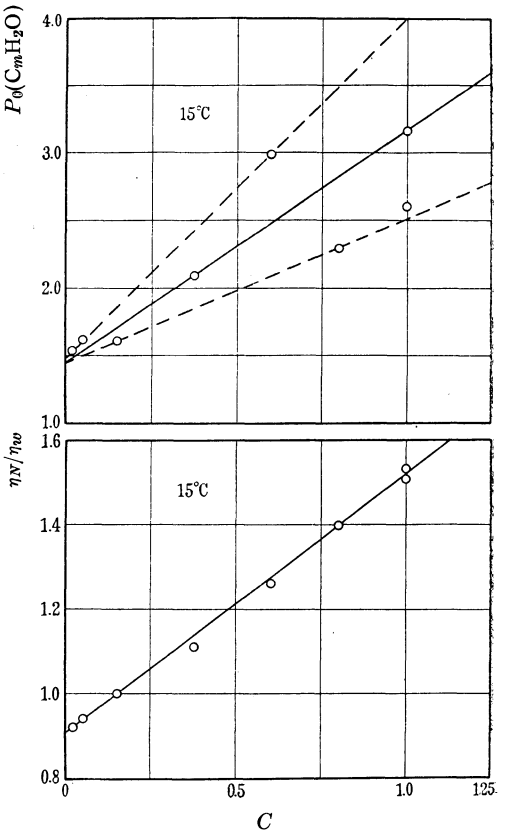


Fig. 4. η_N/η_w and P_0 for V_2O_5 sol.

proportional to the pressure P,

$$v_s=kP \tag{11}$$

Q_s becomes

$$Q_s=\pi a^2kP \tag{12}$$

On the other hand, Q_η is, using Eq. (6) and (7),

$$Q_\eta=\alpha(P-P_0{}^0)/\eta_N^0 \tag{13}$$

Then, the apparent viscosity η is obtained in the same form as Eq. (8)

$$\eta=\alpha P/Q=\eta_N+\alpha P_0/Q \tag{14}$$

But in this case, the apparent Newtonian viscosity η_N and the apparent yield value P_0 are related to their real values, $\eta_N{}^0$ and $P_0{}^0$, by the equation:

$$\left.\begin{aligned} P_0&=P_0{}^0/(1+\beta) \\ \eta_N&=\eta_N^0/(1+\beta) \\ \beta&=\pi a^2k\eta_N{}^0/\alpha \end{aligned}\right\} \tag{15}$$

Owing to this correction factor $(1+\beta)$, the apparent Newtonian viscosity η_N may become smaller than that of water. For example, at the infinite dilution of V_2O_5 sol,

$$\eta_N/\eta_w=\eta_N^0/\{\eta_w(1+\beta)\}=0.91 \tag{16}$$

is obtained from Eq. (10). Then, $\beta\simeq0.10$. If $P_0{}^0\ll P$ at infinite dilution,

$$Q_s/Q_\eta\simeq0.1. \tag{17}$$

For more concentrated sol, the slip may be more important by its greater elasticity, but no method to estimate it is found.

The effect of ultrasonic wave on the structural viscosity of Hg-SS is shown in Fig. 5. The time recorded in this Fig. show that elapsed after the

5) R. Abegg, "Handb anorg. Chem.," Vol. 3, p. 738 (1927).

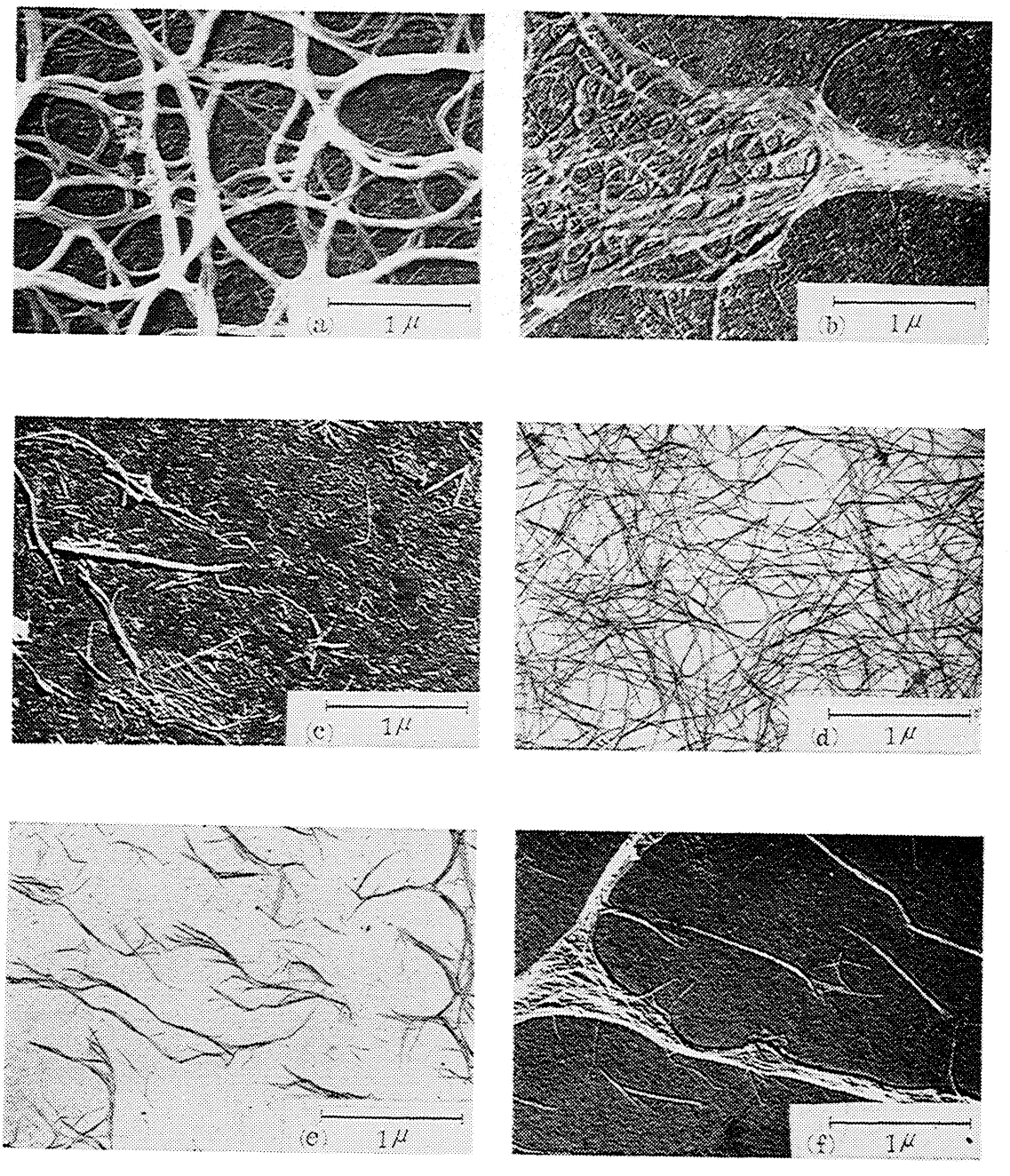


Fig. 6 Electron micrographs for Hg-SS:
(a) No treatment (b) Left alone for 3 min. after shaking
(c) Ultrasonic irradiation
and for V_2O_5:
(d) No treatment (e) Just after shaking (f) Just after shaking

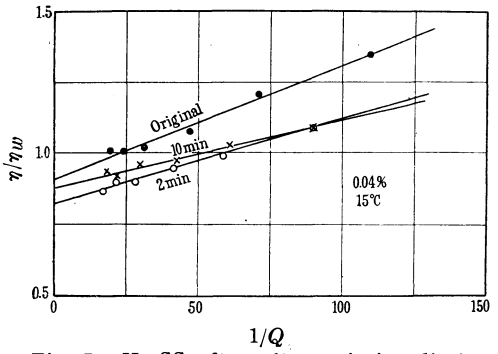


Fig. 5. Hg-SS after ultrasonic irradiation.

end of ultrasonic irradiation. It is shown that the Newtonian viscosity begins to recover after about 10 min., while the yield value does not recover yet. The net-work structure of Hg-SS seems to be destroyed by ultrasonic wave, but broken pieces soon join together to form fibers. Some time is spent, however, before these fibers form rigid knots to complete a net-work. This idea will be supported by electron micrographs shown later. The slip on the wall, however, is so great that a confident conclusion cannot be obtained.

Electron micrograph

Hg-SS has a typical net-work structure as shown in Fig. 6a. The net-work is built of yarns of about 0.1 μ in width, and the latter is a bundle of fibers of about 200 Å in its thickness. After shaking the solution in a test tube for 1 min., the net-work is destroyed and dispersed to single yarn or to single fiber, or on the other hand, they aggregate to a rope of 0.3−1 μ in thickness. Letting the solution stand for about 3 min., (Fig. 6b), the rope again disperses to reproduce a net-work. After 10 min., almost complete net-work structure has been reconstructed. By the irradiation of ultrasonic, (Fig. 6c), the net-work of Hg-SS is torn to pieces of 0.1−1 μ in length. When it is left alone for 3—10 min., broken pieces join together to form fibers, or further coagulaie to yarns and ropes. After 2.5 hrs. they reconstruct a complete net-work structure.

A similar change of structure is observed also for V_2O_5 sol. Original sol (Fig. 6d) has a net-work structure, constructed from fibers of about 100 Å in thickness. By vigorous shaking, the net-work is destroyed and torn to pieces as shown in Fig. 6e, or coagulates to thick ropes of~0.1 μ

The structural changes observed above are favourable to explain their rheological behavior. Destruction of net-work structure may correspond to the lowering of viscosity under higher pressure. The recovery of the net-work structure may explain the recovery of its viscosity and elasticity of flow after keeping the sol standing, and the in thickness as shown in Fig. 6f. After being left alone for 2.5 hrs. or so, they recover a net-work structure again. The recovery of the net-work seems to take more time for V_2O_5 than for Hg-SS. Irradiation of ultrasonic brings nearly the same effects as that by shaking.
dependence of yield value on the history of teh specimen.

Summary

The structural viscosity of V_2O_5 sol is measured by Ostwald's overflow viscometer. A linear relation is found between the relative viscosity (η/η_w) and the reciprocal of flow amount ($1/Q$). Viscosity of Newtonian flow η_N and yield value P_0 are calculated from it. η_N and P_0 is nearly linearly varied with concentration. A decisive conclusion however, cannot be obtained owing to the slip of liquid on the capillary wall.

Hg-SS (Hg-sulfosalicylate) sol also showed a linear relation between η/η_w and $1/Q$. By the irradiation of ultrasonic wave, η_N and P_0 decreases. η_N again increases after about 10 min., but the recovery of P_0 took more time. A clear conclusion cannot be obtained due to the slip.

Electron micrographs showed that Hg-SS has a net-work structure, which is broken by shaking or by the irradiation of ultrasonic wave. When it is kept standing, the net-work is again constructed. V_2O_5 sol showed analogous structural changes.

Department of Chemistry, Faculty of Science, University of Tokyo, and Electron Microscope Laboratory, University of Tokyo

Heterogeneous Structure of Rayon. V. Effect of Stretching on the Heterogeneous Structure (2)

By Saburo OKAJIMA and Shigeru HAYAMA

(Received June 5, 1954)

In the preceding report the effect of the stretching of a rayon fiber in the second bath upon its heterogeneous structure was studied making use of a series of viscose rayons. Now the same experiment was repeated on another series of rayons which were spun by one-bath process but stretched to various degrees.

Experiment

(1) Sample of Rayons.—The spinning was also carried out in the laboratory of Teikoku Jinken Co. by one-bath process using an ordinary factory viscose. A constant volume of viscose was extruded through spinnerets of various orifice sizes and collected with an equal velocity so that the denier of the filament was kept constant. The peripheral velocity of the first godet was so controlled as to equalize it to the extrusion velocity of the viscose so that an equal drafting is given to every filaments. The details of the spinning condition and some of the properties of the yarns obtained are tabulated below.

TABLE I

No.	Diam of orifice, mm.	Stretch	Denier	Dry		Wet	
				Strength, g./den	Elong., %	Strength, g./den	Elong., %
IIIa	0.08	1.06	119.4	1.43	26.2	0.64	35.7
IIIb	0.085	1.20	120.3	1.69	20.5	0.74	29.9
IIIc	0.09	1.35	120.2	2.14	15.9	0.91	20.3
IIId	0.095	1.50	119.7	2.10	12.6	1.06	16.2

Collection velocity: 86.48 m./min.; Number of holes of a spinneret: 25; Bath composition: H_2SO_4 120 g./l, Zn 10 g./l besides Na_2SO_4, sp. gr. 1.25; Bath temperature: 50°C.

In this spinning the spinnerets with uniform holes were prepared with special precautions in order to keep the standard deviation of the denier as small as possible. And the actual standard deviations of the single filaments relative to the mean deniers were 5.8, 6.4, 7.3 and 7.6% in the order from IIIa to IIId.

The other operations were similar to those of the previous experiment, except that one bath-process was adopted in the present spinning.

The acetylation temperature was also controlled but it fluctuates so much that the discussion of the rate of acetylation is abandoned.

Experimental Results

(1) The Structure of the Skin and Core.—The relation between the loss during the acetylation (L_1/W) and the acetic acid content (A) is also similar to that of the previous report (Fig. 1). The weight percentages of the outermost skins IIIa—IIId are 4.6, 4.2, 4.2, and 4.4% respectively, or nearly constant irrespective of the stretching and the mean depth of the outermost skin is estimated to be 2.2% of the total radius. The slope of the line of the skin part, OK, is also nearly constant, but that of the inner structure decreases as the stretching increases. This means that the outermost skin is of nearly equal structure

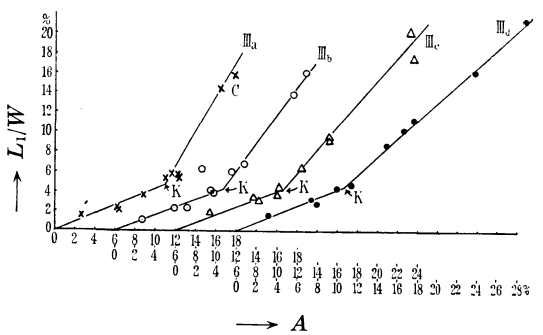


Fig. 1.

in each yarn but the structure within the skin becomes the more difficult to disperse as the filament is stretched the higher.

It is described in the previous paper that the origin of the outer most skin is related to the production of the Zn-xanthate. The constancy of this skin can be explained from this point of view as follows. If the diameter of an orifice is D, then the sectional area of each filament on the first godet will be k_1D^2. Of course the attenuation of a filament occurs due to some complex factors, such as drafting, gelling, dehydration, etc., and the cross section can not be circular. k_1 implies these complex changes of the sectional area and of the form but it is nearly constant and independent on the value of D in the range of the present spinning condition. Now the

thickness d of the Zn-xanthate layer formed is in proportion to the square root of the immersion time t, during which the yarn stays in the bath, so that d is given by

$$d=k_2t=k_3L^{1/2}D,$$

where L is the immersion length and k_2 and k_3 are numerical constants. Therefore d/D is independent on the orifice diameter D.

As the thickness of the outermost skin, which is derived from this Zn-xanthate layer is also proportional to d, and the further shrinkage of the cross section due to the regeneration, stretching and drying occurs uniformly the percentage of the outermost skin, P_r, must always be independent of D as shown above.

(2) **Orientation.**—The radial distribution of the intrinsic double refraction r is given in Fig. 2. The highly stretched filament has larger r.

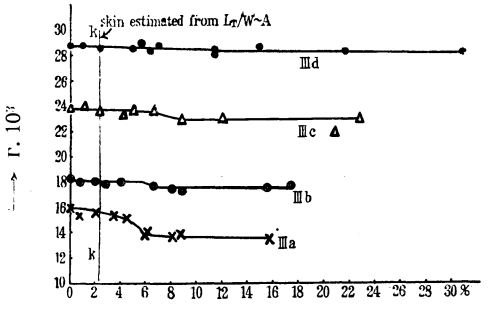


Fig. 2.

On the curves of r—P_r three parts of the structure are seen as already pointed out in the second paper of this study. The outermost skin indicated on these curves grows thicker in the order from IIIa to IIId and the last one appears to be of all skin types. But the skin which appears during the acetylation is a part of it as is indicated by a line k-k, in Fig. 2. So the outermost skin optically indicated as one layer is not simple but is composed of two layers. The inside layer may be caused as follows.

Because the viscose or xanthate close to the Zn-xanthate skin is dehydrated so much by osmotic diffusion and gelates, the flow property of that part is so similar to that of the Zn-xanthate layer, that the orientation of this layer is fixed during the stretching of the filament and the regeneration of cellulose as effectively as in the true outermost skin. The dehydration and syneresis of this layer is further enhanced by the stretching, so the apparent outermost skin thickens with the degree of stretching. For the same reason the destruction of the structure due to the gas evolution within the outermost skin is suppressed in the same order as actually observed in the acetylation.

The cost of this research has been defrayed by the Grant in Aid for Fundamental Scientific Research for the Ministry of Education, to which the authors' thanks are due. The authors are also grateful to Mr. I. Okamura of the Teikoku Jinken Co. for his kind supply of the samples.

Faculty of Engineering, Tokyo Metropolitan University, Tokyo, and Faculty of Engineering, Yamagata University, Yonezawa

Errors in Measuring the Wave-Height of Polarogram. I. Mathematical Discussion

By Yoshikazu YASUMORI

(Received June 16, 1954)

Introduction

In the polarographic quantitative analysis, we may know the amount of material by measuring the wave-height which is obtained after the graphical construction on a polarogram. Therefore it is one of the necessary conditions in the precise polarographic determination, that the polarogram is so taken that the errors of the graphical construction become the least possible.

According to Kolthoff and Lingane[1], any tendency of the limiting current to change with changing applied e.m.f. is greatly magnified by the magnification of a wave and so when the wave is not well-developed, mere magnification of a wave does not necessarily increase the accuracy with which it can be measured. This discussion may hold rather in precision than in accuracy where the so-called errors are related to reliability, precision and accuracy[2]. Therefore a degree of magnification of a wave should be selected in the precise polarographic analysis. In this paper this degree of magnification is discussed mathematically.

Mathematical Calculation of Errors

In order to measure the wave-height of the polarogram *ACB* (Fig. 1), we may use various methods of graphical construction. This discussion holds when the line intersection method[3] treats curves. That is, tangents ξ and η are drawn through the mid-points of straight parts or inflexion-points *A* and *B*, respectively, just before and just after the wave, and a third tangent is drawn through the inflexion-point C of wave. The vertical distance between the two intersection *X* and *Y* thus obtained corresponds to the wave-height *h*.

Now, when the voltage axis represents abscissa and the current axis ordinate, writing coordinates of A, B, C, *X* ane *Y*, as (a_1, b_1), (a_2, b_2), (a_3, b_3), $(x_1, y_1)$and (x_2, y_2), respectively and putting angles at which ξ, η, and ζ intersect the abscissa, φ, ψ and θ, respectively, we have

$$h=f\ (a_1,\ b_1,\ a_2,\ b_2,\ a_3,\ b_3,\ \theta,\ \varphi,\ \psi). \quad (1)$$

But three respective variables in bracket of (a_1, d_1, φ), (a_2, b_2, ψ) or (a_3, b_3, θ) are not independent of one another and the relations between these variables cannot be discussed generally.

On the other hand, the first procedure of construction is to determine (a_1, b_1) etc. and the next is to determine φ etc. And, for instance, on determining (a_1, b_1), b_1 will be

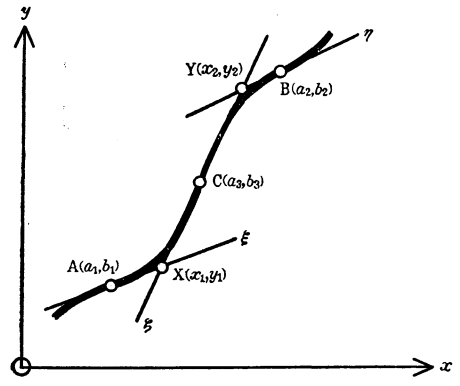


Fig. 1.

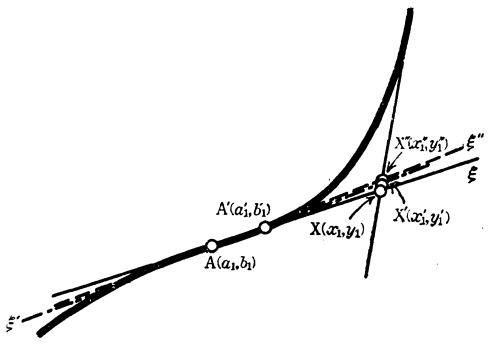


Fig. 2.

1) I. M. Kolthoff and J. J. Lingane, "Polarography," 2nd Ed. p. 328 (1952) Interscience Publishers, New York.

2) K. Ishikawa, *Kagaku-no-Ryoiki*, extra-ed. 10. ("Statistics for Chemists") p. 26 (1953).

3) D. F. Boltz, "Selected Topics in Modern Instrumental Analysis," p. 41 (1952) Prentice-Hall, Inc., New York.

determined after a_1 is fixed. Perhaps the error, which occurs in the determination of b_1, may be negligibly small, if a_1 is fixed. So assuming that b_1 responds strictly to a_1, we have

$$h=f\ (a_1,\ a_2,\ a_3,\ \theta,\ \varphi,\ \psi) \tag{2}$$

Nevertheless another assumption is needed, as two respective variables in a bracket of $(a_1,\ \varphi)$, $(a_2,\ \psi)$ or $(a_3,\ \theta)$ are not independent of each other.

That is, if a point $(a_1',\ b_1')$ is found instead of the actual point $(a_1,\ b_1)$ and a tangent ξ' is erected instead of the actual tangent ξ let us draw through the point $(a_1,\ b_1)$ a line ξ'' in parallel with ξ' (Fig. 2). The difference between the wave-height with ξ' and the one with ξ'' ($|y_1''-y_1'|$) shall be assumed as negligibly small in comparison with the difference between the wave-height with ξ and the one with ξ' ($|y_1'-y_1|$). And the corresponding assumptions of $(a_2,\ \psi)$ and $(a_3,\ \theta)$ shall be considered. With these assumptions the errors in determination of φ, ψ and θ contain those in determination of a_1, a_2 and a_3. Thus writing

$$h=f\ (\theta,\ \varphi,\ \psi) \tag{3}$$

we may calculate the amount of error of h.

Then, by transferring the origin to C in Fig. 1 and displacing the axes parallelly, the following equations can be obtained,

$$\left.\begin{aligned}\frac{b_1^0-y_1^0}{a_1^0-x_1^0}&=\tan\varphi=m\\ \frac{b_2^0-y_2^0}{a_2^0-x_2^0}&=\tan\psi=n\\ \frac{y_1^0}{x_1^0}=\frac{y_2^0}{x_2^0}&=\tan\theta=l\end{aligned}\right\} \tag{4}$$

Where $(a_1^0,\ b_1^0)$, $(a_2^0,\ b_2^0)$, $(0,\ 0)$, $(x_1^0,\ y_1^0)$ and $(x_2^0,\ y_2^0)$ are the coordinates of A, B, C, X and Y, respectively.

Hence we have

$$\left.\begin{aligned}y_1^0&=\frac{(b_1^0-a_1^0m)l}{l-m}\\ y_2^0&=\frac{(b_2^0-a_2^0n)l}{l-n}\end{aligned}\right\} \tag{5}$$

$$h=y_2^0-y_1^0=\frac{(b_2^0-a_2^0n)l}{l-n}-\frac{(b_1^0-a_1^0m)l}{l-m} \tag{6}$$

Now, assuming that the probability density functions of h, θ, φ and ψ are all symmetrical, we have from the familiar formula of error transmission[4]:

$$e_h^2=\left(\frac{\partial h}{\partial\theta}\right)^2e_\theta^2+\left(\frac{\partial h}{\partial\varphi}\right)^2e_\varphi^2+\left(\frac{\partial h}{\partial\psi}\right)^2e_\phi^2 \tag{7}$$

4) S. Miyamoto, "Theory and Calculation of Error," p. 81 (1951) Kosei-sha, Tokyo.

where e_h^2 etc. are the mean squares of errors of h etc., respectively. And from Eq. (6), it follows that

$$\left.\begin{aligned}\frac{\partial h}{\partial\varphi}&=\frac{(a_1^0l-b_1^0)l}{(l-m)^2}(1+m^2)\\ \frac{\partial h}{\partial\psi}&=\frac{-(a_2^0l-b_2^0)l}{(l-n)^2}(1+n^2)\\ \frac{\partial h}{\partial\theta}&=-\left\{\frac{(b_2^0-a_2^0n)n}{(l-n)^2}-\frac{(b_1^0-a_1^0m)m}{(l-m)^2}\right\}(1+l^2)\end{aligned}\right\} \tag{8}$$

Also the relative errors of h are more important than the absolute errors shown in Eq. (7), since the comparative method is usually used in the polarographic quantitative analysis. From Eq. (7) the relative errors are given by,

$$\left(\frac{e_h}{h}\right)^2=\frac{1}{h^2}\left(\frac{\partial h}{\partial\theta}\right)^2e_\theta^2+\frac{1}{h^2}\left(\frac{\partial h}{\partial\varphi}\right)^2e_\varphi^2+\frac{1}{h^2}\left(\frac{\partial h}{\partial\psi}\right)^2e_\phi^2 \tag{9}$$

The Variation of Magnitude of Error with Span Voltage and Sensitivity

When a polarogram is taken with span voltage p times as high and sensitivity q times as high as those with which the original polarogram in Fig. 1 is taken, the new polarogram will be transformed into one of dimensions one pth times in abscissa and q times in ordinate as great as the original. Let us compare the errors of construction on those polarograms as follows.

That is, if the transformation is performed without transferring the point C, the coordinates of A and B will be $(a_1^0/p_1,\ qb_1^0)$ and $(a_2^0/p,\ qb_2^0)$ respectively. Thus

$$\left.\begin{aligned}\tan\varphi_{pq}&=pqm\\ \tan\psi_{pq}&=pqn\\ \tan\theta_{pq}&=pql\end{aligned}\right\} \tag{10}$$

where φ_{pq}, ψ_{pq} and θ_{pq} are angles at which after the transformation tangents ξ, η and ζ intersect abscissa respectively.

Hence from Eq. (8) we have

$$\left.\begin{aligned}\frac{\partial h_{pq}}{\partial\varphi_{pq}}&=\frac{(a_1^0l-b_1^0)l}{(l-m)^2}\cdot\frac{1+p^2q^2m^2}{p}\\ &=\left(\frac{\partial h}{\partial\varphi}\right)\frac{1+p^2q^2m^2}{p(1+m^2)}\\ \frac{\partial h_{pq}}{\partial\psi_{pq}}&=\frac{-(a_2^0l-b_2^0)l}{(l-n)^2}\cdot\frac{1+p^2q^2n^2}{p}\\ &=\left(\frac{\partial h}{\partial\psi}\right)\frac{1+p^2q^2n^2}{p(1+n^2)}\end{aligned}\right\}$$

$$\frac{\partial h_{pq}}{\partial \theta_{pq}} = -\left\{\frac{(b_2^0 - a_2^0 n)n}{(l-n)^2} - \frac{(b_1^0 - a_1^0 m)m}{(l-m)^2}\right\} \frac{1+p^2q^2l^2}{p(1+l^2)} = \left(\frac{\partial h}{\partial \theta}\right)\frac{1+p^2q^2l^2}{p(1+l^2)} \tag{11}$$

And in such a transformation the wave-height varies also. writing the wave-height after the transformation as h_{pq}, it follows that

$$h_{pq} = qh \tag{12}$$

Furthermore, the magnitude of e_θ, e_φ and e_ψ may vary. Now we assume on these variations as follows.

(1) If the curvature on A, B or C of the polarogram in Fig. 1 are greater, or the curve near such a point is linear over a wider range, the amount of e_θ, e_φ or e_ψ will not vary with the transformation.

(2) If the curve near such a point is linear but the linear portion is shorter, the amount of e_θ, e_φ or e_ψ will be inversely proportional to the length of this linear portion.

With the assumption (1), for instance, it is seen that

$$\frac{1}{h_{pq}^2}\left(\frac{\partial h_{pq}}{\partial \theta_{pq}}\right)^2 e_{\theta pq}^2 = \frac{1}{h^2}\left(\frac{\partial h}{\partial \theta}\right)^2 e_\theta^2 \frac{(1+p^2q^2l^2)^2}{p^2q^2(1+l^2)^2} \tag{13}$$

And by partially differentiating Eq. (13) with respect to p or q, we have

$$\frac{\partial}{\partial p}\left\{\frac{1}{h_{pq}^2}\left(\frac{\partial h_{pq}}{\partial \theta_{pq}}\right)^2 e_{\theta pq}^2\right\} = \frac{1}{h^2}\left(\frac{\partial h}{\partial \theta}\right)^2 e_\theta^2 \frac{2(1+p^2q^2l^2)(p^2q^2l^2-1)}{p^3q^2(1+l^2)^2}$$

$$\frac{\partial}{\partial q}\left\{\frac{1}{h_{pq}^2}\left(\frac{\partial h_{pq}}{\partial \theta_{pq}}\right)^2 e_{\theta pq}^2\right\} = \frac{1}{h^2}\left(\frac{\partial h}{\partial \theta}\right)^2 e_\theta^2 \frac{2(1+p^2q^2l^2)(p^2q^2l^2-1)}{p^2q^3(1+l^2)^2}$$

Hence when $pql=1$ ($l \neq 0$), Eq. (13) takes the minimum value. As for

$$\frac{1}{h_{pq}^2}\left(\frac{\partial h_{pq}}{\partial \varphi_{qp}}\right)^2 e_{\varphi pq}^2 \text{ or } \frac{1}{h_{pq}^2}\left(\frac{\partial h_{pq}}{\partial \psi_{pq}}\right)^2 e_{\psi pq}^2$$

it takes the minimum value also, when $pqm=1$ or $pqn=1$, respectively. But if $l=0$, $m=0$ or $n=0$, it takes the smaller value, with the increase of p and q.

Next, with the assumption (2), for instance, it is seen that

$$\frac{1}{h_{pq}^2}\left(\frac{\partial h_{pq}}{\partial \theta_{pq}}\right)^2 e_{\theta pq}^2 = \frac{1}{h^2}\left(\frac{\partial h}{\partial \theta}\right)^2 e_\theta^2 \frac{1+p^2q^2l^2}{q^2(1+l^2)} \tag{14}$$

where

$$e_{\theta pq}^2 = e_\theta^2 \frac{p^2(1+l^2)}{1+p^2q^2l^2} \tag{15}$$

and

$$\frac{\partial}{\partial p}\left\{\frac{1}{h_{pq}^2}\left(\frac{\partial h_{pq}}{\partial \theta_{pq}}\right)^2 e_{\theta pq}^2\right\} = \frac{1}{h^2}\left(\frac{\partial h}{\partial \theta}\right)^2 e_\theta^2 \frac{1+2pq^2m^2}{q^2(1+m^2)} > 0 \tag{16}$$

$$\frac{\partial}{\partial q}\left\{\frac{1}{h_{pq}^2}\left(\frac{\partial h_{pq}}{\partial \theta_{pq}}\right)^2 e_{\theta pq}^2\right\} = \frac{1}{h^2}\left(\frac{\partial h}{\partial \theta}\right)^2 e_\theta^2 \left\{\frac{-2}{q^3(1+m^2)^2}\right\} < 0 \tag{17}$$

Hence, Eq. (14) takes the greater value with increasing p and Eq. (14) takes the smaller value with increasing of q.

As for

$$\frac{1}{h_{pq}^2}\left(\frac{\partial h_{pq}}{\partial \varphi_{pq}}\right)^2 e_{\varphi pq}^2 \text{ or } \frac{1}{h_{pq}^2}\left(\frac{\partial h_{pq}}{\partial \psi_{pq}}\right)^2 e_{\psi pq}^2,$$

the same relationships hold.

Discussion

From the above mathematical calculation, the relative error of h should be minimum when $pql=1$ or $\theta_{pq}=45°$, if the error in construction of the tangent through C in Fig. 1 is more pronounced than other errors and its magnitude varies after the manner shown by the assumption (1). And if the errors in construction of the tangents through B and C are both pronounced and their magnitudes vary after the manner shown by the assumption (1), $1/m > pq > 1/l$, where $l > m$ or $\theta_{pq} > 45° > \varphi_{pq}$, is the necessary condition for the minimum value of the relative error of h.

On the other hand, when in all the errors the assumption (2) holds, the relative error of h becomes smaller, with decreasing p and increasing q.

But we must remember the fact that the manner of variation of error of θ_{pq} etc. can also change with the transformation of the curve.

Department of Agricultural Chemical
Faculty of Agriculture,
Kyoto University, Kyoto

Errors in Measuring the Wave-Height of Polarogram. II. Practical Errors of Graphical Construction

By Yoshikazu YASUMORI

(Received June 16, 1954)

Introduction

In the previous work[1] the errors in measuring the wave-height on a polarogram were mathematically discussed, and it was concluded that the relative errors in graphical construction on a polarogram might vary with the transformation of the polarogram by the changes of span voltage and sensitivity. In this paper the practical variations of errors are investigated for the sake of comparison with the mathematical conclusion.

Experimental

The intersections of tangents were constructed by ten polarographists on the polarograms printed photographically with a same printing ratio (0.45) from variously transformed original polarograms which were recorded of the same samples with various span voltages and sensitivities.

The original polarograms were recorded of the following three samples after oxygen removal with the initial voltage of −0.3V vs. Hg-pool; and the span voltage and sensitivity are shown in Table I.

Sample A: $1\times10^{-4}N$ $Pb(NO_3)_2+2\times10^{-2}N$ $CdCl_2$
Sample B: $1\times10^{-4}N$ $Pb(NO_3)_2+1\times10^{-2}N$ $CdCl_2$
Sample C: $4\times10^{-4}N$ $TlCl+8\times10^{-3}N$ $CdCl_2$
(Each sample contains $1\times10^{-1}N$ KCl as an indifferent salt)

TABLE I
NOTATIONS OF POLAROGRAMS TAKEN WITH VARIOUS SPAN VOLTAGES AND SENSITIVITIES

		Sensitivity microamp./mm.		
		High	Medium	Low
Polarogram	A	0.004	0.010	0.020
	B	0.006	0.015	0.030
	C	0.008	0.015	0.030
Span Voltage	3V	00	01	02
	1V	10	11	12
	0.5V	20	21	22

The polarograph used here was Sargent Model XXI Polarograph, on whose recorder-paper the 1 mm.-scales on current-axis are printed and so

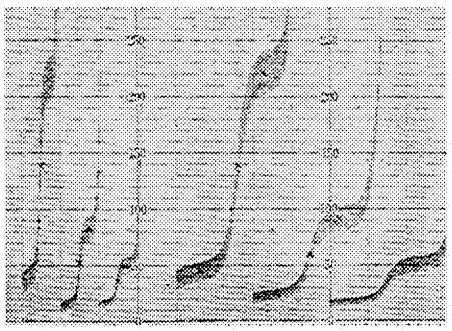


Fig. 3.

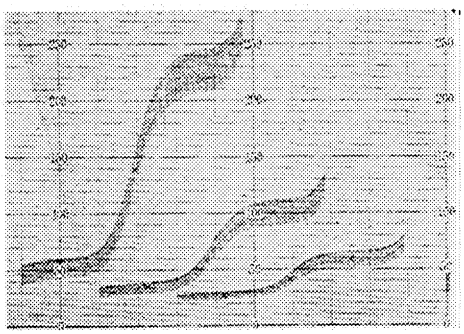


Fig. 4.

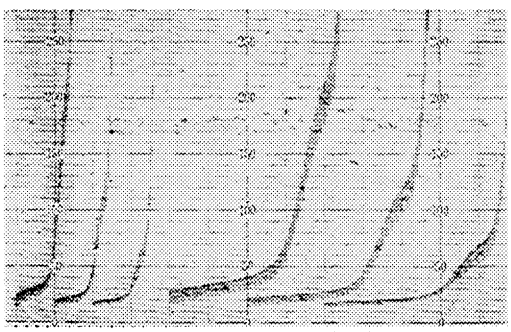


Fig. 5.

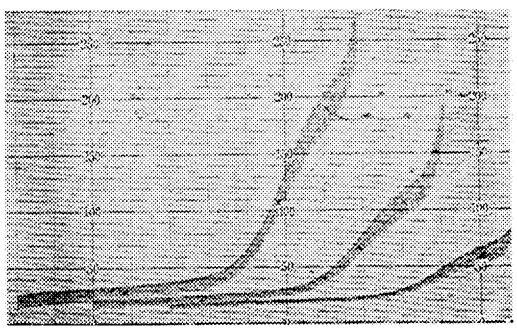


Fig. 6.

1) Y. Yasumori, This Bulletin, **27**, 554 (1954).

the positions of intersections of tangents could be read with these scales.

The tangents in polarogram A (Fig. 3 and 4) and B (Fig. 5 and 6) were drawn through the marked points corresponding to the inflexion-points. In Table II are shown the positions of intersections, in Table III the mean squares of relative deviations of positions of the points from their median to the respective wave-height and in Table 4 the mean squares of relative deviations of thh wave-heights from their median to the respective wave-height.

(The figures in Tables III & IV are values multiplied by 10^4 of the above mentioned.)

TABLE II

THE POSITIONS OF INTERSECTIONS

Sample	Point	Polarogram	Constructer A	B	C	D	E	F	G	H	I	J
A	Y	00	208.1	210.8	208.1	209.0	202.9	205.0	209.3	208.6	209.0	202.3
		01	77.7	79.3	80.0	83.1	79.8	80.3	79.8	81.0	81.1	80.6
		02	48.1	49.7	47.7	50.0	48.2	47.4	48.5	48.8	49.6	49.4
		10	215.0	216.4	214.4	219.8	214.2	210.9	215.0	216.8	215.2	212.5
		11	86.9	90.8	89.2	91.9	89.0	88.7	89.3	89.9	90.2	88.4
		12	48.2	48.7	49.4	50.3	50.3	49.2	48.3	49.8	49.3	49.2
		20	214.0	222.8	214.3	221.2	218.2	218.2	216.1	219.1	219.4	220.2
		21	98.3	97.7	97.1	100.9	100.0	98.3	97.3	98.9	98.5	97.5
		22	57.5	57.9	57.6	58.0	57.6	57.2	57.2	57.9	57.0	57.2
	X	00	44.4	49.9	47.8	46.0	46.3	47.7	47.7	45.7	45.7	49.0
		01	18.8	17.9	19.3	18.6	18.3	18.2	19.7	17.3	18.7	18.4
		02	18.0	19.1	18.5	18.4	18.7	18.5	18.1	17.3	18.0	17.2
		10	51.0	54.8	54.0	51.1	50.2	52.4	51.3	48.6	50.0	52.9
		11	26.8	27.4	27.0	25.7	26.7	26.9	26.2	25.9	26.1	21.8
		12	19.7	18.9	19.1	18.8	17.9	19.3	19.3	18.3	18.5	18.9
		20	55.2	57.2	58.3	53.9	53.4	56.3	56.0	54.2	55.3	55.6
		21	36.2	36.7	36.1	36.0	36.2	37.0	37.6	35.8	35.5	37.0
		22	28.9	28.3	28.3	28.3	28.1	28.4	28.3	28.0	29.9	28.3
B	Y	00	174.1	174.6	175.9	177.0	179.2	175.3	176.0	181.2	178.4	173.5
		01	74.3	74.8	74.0	76.9	75.9	73.8	76.4	77.6	77.7	73.7
		02	37.0	38.7	38.5	39.4	39.4	39.4	37.7	39.8	39.2	37.9
		10	191.2	195.3	192.2	198.8	191.0	191.3	194.1	194.6	194.8	189.3
		11	74.0	75.2	72.4	76.2	74.1	74.0	73.8	74.8	75.3	72.9
		12	35.8	35.9	36.1	37.0	35.1	36.9	35.9	36.8	37.0	35.9
		20	198.4	196.9	195.3	199.2	194.4	192.4	191.7	196.3	193.4	191.8
		21	75.1	76.8	75.7	77.9	76.3	78.3	77.2	78.7	76.8	75.8
		22	37.9	37.2	38.2	38.9	39.9	38.6	38.2	38.8	37.1	38.0
	X	00	46.9	49.2	51.1	47.5	46.6	49.2	50.1	44.3	49.9	50.1
		01	31.1	31.3	31.9	29.3	32.0	29.9	31.5	29.1	29.6	32.2
		02	17.2	18.9	18.7	15.8	15.8	15.9	17.6	15.1	16.2	17.1
		10	86.8	83.2	87.8	82.2	85.3	84.6	83.9	85.1	85.2	84.7
		11	30.1	30.1	31.8	28.3	31.8	30.6	31.0	29.0	30.5	31.0
		12	14.3	15.2	14.7	13.3	14.8	14.2	14.0	14.1	14.2	13.8
		20	85.0	80.1	86.4	82.8	84.8	84.2	83.4	78.3	83.0	88.4
		21	31.2	34.9	33.3	34.9	32.9	33.1	32.2	32.2	34.1	33.4
		22	14.5	17.0	16.0	15.3	15.7	16.0	16.5	15.9	16.0	16.0
C	Y	00	175.0	176.5	158.6	180.7	187.8	166.0	152.2	194.0	167.6	185.5
		01	104.2	99.9	87.2	97.1	99.7	87.0	96.8	100.1	90.0	95.9
		02	59.0	58.8	45.9	60.0	54.9	63.3	62.1	56.2	55.2	55.0
		10	173.8	174.8	155.1	180.9	164.0	166.2	169.5	179.0	184.1	153.4
		11	96.0	97.2	88.8	97.4	96.0	89.9	96.0	97.8	104.0	91.0
		12	55.8	55.8	51.5	55.1	54.0	53.9	53.0	54.5	58.9	56.0
		20	151.4	170.0	164.1	181.8	168.8	172.1	169.5	178.2	178.0	165.1
		21	88.8	100.9	98.6	101.9	94.4	103.0	94.1	96.9	99.8	92.2
		22	53.4	57.0	54.2	56.9	59.1	57.2	57.0	57.7	55.0	55.3
	X	00	33.7	32.5	34.3	31.8	32.4	32.4	33.0	32.4	31.4	32.3
		01	25.7	25.0	25.6	23.4	24.3	24.7	24.4	24.7	24.9	24.8
		02	21.4	20.7	21.9	20.8	20.9	20.7	20.7	21.7	21.1	21.3
		10	40.1	40.1	41.2	40.0	41.9	40.0	40.8	38.8	40.9	40.0
		11	25.2	25.9	26.6	26.3	26.2	26.8	26.4	25.2	26.3	26.4
		12	20.6	21.4	20.5	20.1	21.4	21.7	21.4	20.6	21.7	21.1
		20	36.0	36.4	37.7	34.7	34.5	35.3	39.1	35.1	34.4	35.6
		21	28.2	27.2	26.7	26.5	28.3	27.1	28.2	27.3	27.7	27.1
		22	22.4	21.0	21.9	21.6	20.7	21.0	21.9	21.3	22.1	20.6

TABLE III

THE MEAN SQUARES OF RELATIVE DEVIATIONS OF POSITIONS OF POINTS FROM TMEIR MEDIANS

Span Voltage	Sample	Sensitivity: High Y	High X	Medium Y	Medium X	Low Y	Low X	Sum Y	Sum X
3V	A	3.31	0.98	4.58	2.62	8.01	3.53	15.90	7.13
	B	3.50	2.76	11.56	5.95	24.80	30.47	39.86	39.18
	C	78.3	0.17	62.1	0.74	126.3	1.39	302.7	2.30
1V	A	1.96	1.28	4.41	0.83	5.29	2.69	11.66	4.80
	B	5.95	2.02	6.40	5.06	9.18	5.48	21.53	12.56
	C	54.9	0.40	38.2	0.61	32.1	3.10	125.2	4.11
0.5V	A	2.79	0.85	3.50	1.10	1.35	0.79	7.64	2.74
	B	5.29	6.15	6.60	6.71	12.67	8.29	24.56	21.15
	C	37.7	1.21	38.4	0.77	25.3	3.20	101.4	5.18
Sum	A	8.06	3.11	12.49	4.55	14.65	7.01	35.20	14.67
	B	14.74	10.93	24.56	17.72	46.65	44.24	85.95	72.89
	C	170.9	1.79	138.7	2.12	219.7	7.69	529.4	11.59

TABLE IV

THE MEAN SQUARES OF RELATIVE DEVIATIONS OF WAVE-HEIGHTS FROM THEIR MEDIANS

Span Voltage	Sample	Sensitivity: High	Medium	Low	Sum
3V	A	4.54	6.35	12.53	23.42
	C	82.8	67.1	191.0	340.9
1V	A	4.04	5.43	13.91	23.38
	C	61.9	35.2	29.9	127.0
0.5V	A	4.84	6.55	7.02	18.41
	C	44.9	46.4	36.2	127.5
Sum	A	13.42	18.33	33.46	65.21
	C	189.6	148.7	257.1	595.4

Discussion of the Results

(1) **Polarogram A.** — (*a*) *Intersection Y.* The values of respective sums in Table III become smaller with increasing sensitivity and decreasing span voltage. So this result is coincident with the mathematical result obtained with the assumption (2) in the previous paper. But in the high level of sensitivity and the low level of span voltage, this is not valid. In these levels the errors appear not to vary after such a manner that the assumption (2) alone holds.

(*b*) *Intersection X.* The values of the respective sum in Table III varies after the same manner as in (1, -a). But this is not valid in each level except the low level of sensitivity and the high level of span voltage. In this case, as each value is so small that the error in reading of the intersection may not be ignored, this result cannot be compared with the mathematical result.

(*c*) *Wave-height* (*h*). The values of respective sums in Table IV become smaller with increasing sensitivity, but they are not so affected by the change of span voltage. The cause for this seems to be, that the effect of error e_θ on construction of tangent through a inflexion-point of wave becomes more overwhelming with decreasing span voltage. For the errors of Y and X caused by e_θ are not independent of each other. If the errors of Y and X are independent of each other, the sum of these errors in a certain sensitivity and span voltage in Table III will be equal to the error of wave-height in the corresponding sensitivity and span voltage in Table IV[2], but if these errors are not independent of each other and further errors of Y and X are of the same sign, the sum of these errors will be smaller than the error of wave-height. It is obvious that the effect of error e_θ becomes more pronounced with decreasing span voltage, when the values in Tables III and IV are compared with each other on this standpoint.

(2) **Polarogram B.** — Polarogram B has almost the same wave-form as Polarogram A but its inflexion-points have not been marked on it previously.

(*a*) *Intersection Y.* The values of respective sums in Table III become smaller with increasing sensitivity, but they are not so much affected by the change of span voltage. And each value is greater than the corresponding value in Polarogram A. Perhaps the magnitude of error on construction of tangent may not vary after such a manner as discussed mathematically previously, where the point is not fixed, through which the tangent is to be drawn. The error of construction without the fixing of a point is greater than with the fixing of a point and this tendency becomes more effective when the span voltage and sensitivity are low.

(*b*) *Intersection X* The result is analogous to (2, -a).

(3) **Polarogram C.** — (*a*) *Intersection Y.* The values of respective sums in Table III

2) P. G. Hoel, "Introduction to Mathematical Statistics," (translated into Japanese by G. Taguchi) Kagaku-Shinko-Sha. (Tokyo) (1950) p. 159.

become smaller with decreasing span voltage, but the effect of sensitivity is irregular. And the result in the medium level of span voltage is coincident with the mathematical result with the assumption (1), where the error in construction of a tangent along the curve just after the wave, is more remarkable. Nevertheless, the results in other levels of span voltage are inconsistent with the mathematical result with the assumption (1). In the high level of span voltage, the error in construction of a tangent through the inflexion-point of a wave may become more predominant with decreasing sensitivity.

(*b*) *Intersection X.* Each value in this case is so small that it may be nonsense to discuss this result with the above mathematical result.

(*c*) *Wave-Height h.* When the corresponding values in Table III and IV are compared with each other, it will be found that the error of wave-height is affected mainly by one of intersections (Y), but where the span voltage is low, by both intersections (Y and X), which are not independent of each other.

Summary

When the construction of tangent η on the curve just after the wave in a poralogram is more difficult, but the construction of other tangents are less difficult, it is concluded as follows.

In the case that the construction of η is a little more difficult, a polarogram with high sensitivity is desirable in order to minimize the relative error in measuring the wave-height. And here low span voltage is, to some extent, effective, but a polarogram too enlarged in abscissa is ill-conditioned. Next, in the case of the very difficult construction of η, the relative error of wave-height is minimum, when a polarogram is taken with lowered span voltage, in which the slope of a tangent is tan 45°. Here the error is not always minimum if the polarogram is recorded with lowered sensitivity.

The author wishes to express his hearty thanks to Prof. I. Tachi for his kind encouragement. The authors' thanks are also due to the members of the Polarographic Group in the Faculty of Agriculture, Kyoto University for their kind help in the construction.

Department of Agricultural Chemistry, Faculty of Agriculture, Kyoto University, Kyoto

Studies on Dimethylglyoximo-cobalt(III) Complexes. I. The Preparation and Some Properties of Tris-(dimethylglyoximo)-cobalt(III)

By Akitsugu NAKAHARA

(Received June 21, 1954)

Introduction

Since the work of Tschugaeff[1] a number of dimethylglyoximo-cobalt(III) complexes have been prepared, but the complex-compound having three ions* of dimethylglyoxime about a cobalt atom has never been described. Mann[2] has pointed out that chelating groups fall into two classes: (a) those that can fill all six co-ordination positions, e.g., ethylenediamine, oxalate radical etc.; (b) those which, while capable of filling four positions in the quadri-co-ordinate complex, cannot fill more than four-co-ordination positions when introduced into the sexa-co-ordinate complex. Dimethylglyoxime was cited by Mann as the typical example of the latter case. Thus it has been a definite opinion that the synthesis of tris-(dimethylglyoximo)-cobalt(III) cannot be reached or at least is very difficult[3]. This concept, however, has perfectly been overthrown since the present author has succeeded in preparing this pending compound by a quite simple method. The present paper deals with the method of preparation and properties of this new compound, with some discussions concerning the process of the complex formation.

1) L. Tschugaeff. *Z. anorg. Chem.*, **46**, 144 (1905); *Ber.*, **39**, 2692 (1906); **40**, 3498 (1907); **41**, 2226 (1908).

2) F. G. Mann, *J. Chem. Soc.*, **1933**, 412; H. J. Emeleus and J. S. Anderson, "Modern Aspects of Inorganic Chemistry," 2nd ed., George Routledge and Sons, Ltd. London, (1952), p. 125

3) L. Cambi and C. Corisélli, *Gazz. chim. ital.*, **66**, 91 (1936).

* The following symbols are used: the ion of dimethylglyoxime (DH), $CH_3C(NO)\ C(NOH)CH_3$; the undissociated molecule of dimethylglyoxime (DH_2), $CH_3C(NOH)C(NOH)CH_3$.

Experimental

The Preparation and Identification.—The preparation of tris-(dimethylglyoximo)-cobalt(III) was performed as follows: Six grams of dimethylglyoxime was completely dissolved in 60 ml. of hot water containing 6 g. of potassium hydroxide. After the solution was cooled to 40—50°C, 5 g. of crystalline cobaltous nitrate hexahydrate was added. The mixture was shaken vigorously and thoroughly, and to this 12 ml. of 50% acetic acid was poured. Then the air was bubbled vigorously through the reaction mixture for about three hours. Beautiful orange-yellow acicular crystals gradually were deposited. The mixture was allowed to stand for several hours, and then was filtered by suction. The crude substance was recrystallized from water containing a small amount of acetic acid. Four grams of pure substance was yielded.

In place of potassium hydroxide and cobaltous nitrate in the above described procedure, sodium hydroxide and cobaltous chloride, respectively, can also be used. Therefore, it will be concluded that the resulting products have nothing to do with K^+ and Na^+ or NO^-_3 and Cl^-. In fact, the products did not show any reaction characteristic of those ions. Nevertheless, if the product were not the uncharged complex molecule, the compound would necessarily have H^+ or OH^- as the external ion of the complex radical, and the aqueous solution of the compound would have to show, similarly to the case of $H_3O^+[Co(DH)_2(NO_2)_2]^-$ or $[Co(NH_3)_2(DH)_2]^+ OH^-$, considerably strongly acidic or basic property, respectively.[4] The present compound, however, was found to be neither acidic nor basic. In consequence, it was concluded that the product is an uncharged complex molecule. The results of analyses were as follows: Co, 12.90; C, 32.51; H, 5.98; N, 18.80; H_2O, 9.75 Calcd. for $[Co(DH)_3] \cdot 2.5\ H_2O$: Co, 13.12; C, 32.08; H, 5.83; N, 18.71; H_2O, 10.02%.

Furthermore, as far as the valency of cobalt is concerned, it is reasonably considered to be tervalent since the cobaltous salts in general are very easily oxidized in the presence of glyoximes to cobaltic complexes[5].

Thus it was finally decided that the present substance surely corresponds to the tris-(dimethylglyoximo)-cobalt(III) $[Co(DH)_3] \cdot 2.5\ H_2O$.

Measurements of the Absorption Spectra.—The absorption spectra of the complex and its ligand, dimethylglyoxime, were determined at room temperature with a Beckman Model DU quartz spectrophotometer. The results are shown in Fig. 1. The concentrations used were $1/10^3$—$1/10^5$ and $1/10^2$—$1/10^4$ mol./l., in (a) and (b), respectively. While the measurement of dimethylglyoxime was made in alcoholic solution, that of the complex was made in aqueous solution for the purpose of comparison with the data obtained in bis-(dimethylglyoximo)-derivatives. Molar extinction coefficients ε were calculated from the familiar equation $\varepsilon = \frac{1}{cd} \times \log_{10} (I_0/I)$, where c is the concentration of the compound in mol./l., and d the thickness of the layer in cm.

Description of the Properties.—The clear acicular crystals of tris-(dimethylglyoximo)-cobalt (III) obtained by successful recrystallization are orange-yellow or brownish-yellow. The bright-yellow coloured opaque fibroid crystals which we very often encounter are impure. The pure crystal is quite stable in the atmosphere, and hardly ever decomposes below 200°C. It is somewhat soft to the feel in comparison with ordinary inorganic complexes. This is probably attributable to the feeble intermolecular forces, which are possible in the spherical compound surrounded by many methyl-groups. It is soluble in water, alcohol, chloroform and dioxane, and insoluble in benzene and acetone. In concentrated acetic acid, it decomposes on dissolution.

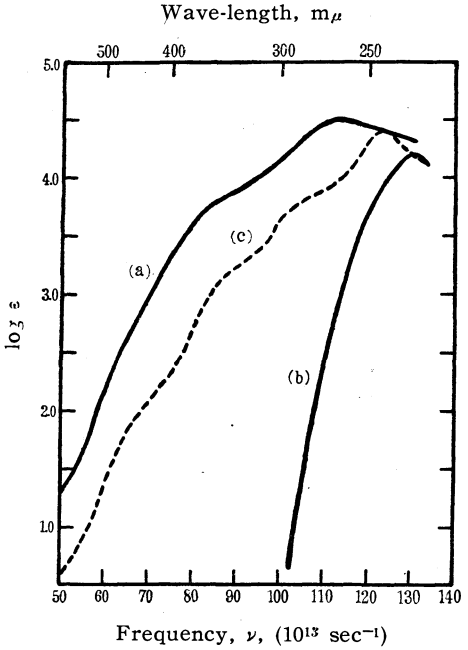


Fig. 1. Absorption spectra of: (a), tris-(dimethylglyoximo)-cobalt(III) in aqueous solution; (b), dimethylglyoxime in alcoholic solution, and (c), bis-(dimethylglyoximo)-diammine-cobaltic chloride in aqueous solution.

Discussion

The Absorption Spectra.—The absorption curve, (a), has only one maximum in the spectral region from 50 to 130×10^{13}/sec., and is quite monotonous. This will probably be due to the large and complicated specific absorption bands[6] of ligands, dimethyl-

4) L. Tschugaeff, *Ber.*, **41**, 2228 (1908); *J. Russ. Ges. chem.*, **41**, 1366 (1909); **41**, 218 (1909); *Z. anorg. Chem.*, **46**, 163 (1905); Gmelins Handbuch d. anorg. Chem., 8. Auflage, **58B**, 276, 324 (1930).

5) L. Cambi and C. Coriselli, *Gazz. chim. ital.*, **66**, 81 (1936); *Chem. Abstr.*, **30**, 8158 (1936).

6) R. Tsuchida, and M. Kobayashi, This Bulletin, **13**, 471 (1938); R. Tsuchida, ibid., **13**, 442 (1938); **13**, 388 (1938).

glyoxime. Although bis-(dimethylglyoximo)-cobalt(III) complexes[7,8] show similar absorption curves on the whole, they differ considerably from the present curve, (a). As is clear from Table I,[8] tris-(dimethylgyloximo)-cobalt(III) has the absorption maximum at 113×10^{13}/sec., while the maxima of bis-(dimethylglyoximo)-complexes are observed in the region from 121.5 to 123×10^{13}/sec. In other words, the former is bathochromic to the latter. Also with respect to the molar extinction coefficients the former is hyperchromic to the latter as shown in Table I.

TABLE I
ABSORPTION MAXIMA FOUND IN THE SHORTER WAVE-LENGTH

Complexes	absorption maxima	
	$\nu_{max.}$	log $\varepsilon_{max.}$
$[Co(NH_3)_2(DH)_2]Cl \cdot 5H_2O$	123.0	4.41
$[Co(NH_3)(DH)_2Cl]$	122.0	4.38
$[Co(DH)_2(NO_2)_2]NH_4 \cdot H_2O$	122.0	4.44
$[Co(NH_3)(DH)_2(NO_2)]$	123.0	4.40
$[Co(H_2O)(DH)_2(NO_2)]$	121.5	4.41
$[Co(DH)_3] \cdot 2.5\ H_2O$	113.2	4.50
Dimethylglyoxime	130.4	4.20

It has long been known that the specific absorption bands are usually shifted bathochromically and hyperchromically with an increasing number of the concerned ligands.[6] If the present absorption band is assumed to be the specific absorption band of dimethylglyoxime, the relation between the absorption maximum of tris-(dimethylglyoximo)-complex and that of bis-(dimethylglyoximo)-derivative agrees with the above mentioned empirical rule. Moreover, judging from the curve in the longer wave-length, dimethylglyoxime seems probably to precede, at least, ethylenediamine in the spectrochemical series.[6] That is to say, dimethylglyoxime is a considerably hypsochromic ligand. The details concerning the absorption spectra of the dimethylglyoximo-cobalt(III) complexes will be reported later.[8]

Stabilities of Dimethylglyoximo-complexes.—According to Nakatsuka and Iinuma,[9] two ions of dimethylglyoxime in the bis-(dimethylglyoximo)-diamine-cobalt(III) complexes generally have a strong tendency to form the planar configuration. Certainly, this opinion is supported by many chemical evidences. For instance, it is necessary to assume such a strong tendency characteristic of dimethylglyoxime, in order to elucidate the reason why any pair of geometric isomers of those complexes has never been obtained, while it is capable of isolating *cis*- and trans-isomers for the bis-ethylenediamine- or bis-oxalato-complexes. The distinguished stability of planar co-ordinated bis-(dimethylglyoximo)-derivative can be recognized also in the fact that any type of complex radical other than the bis-(dimethylglyoximo)-derivative has never been prepared for the last five decades. Although no paper concerning the origin of this characteristic has ever been published, it may be considered that O—H—O hydrogen bonds in the planar configuration as shown in Fig. 2 are necessarily concerned

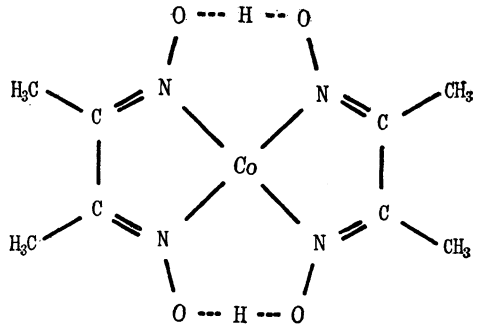


Fig. 2 Planar bis-(dimethylglyoximo)-cobalt(III)-complexes with O—H—O hydrogen bonds.

in the distinguished stability of those complexes.* This is probably because such a kind of hydrogen bond in bis-(dimethylglyoximo)-nickel(II) was demonstrated recently by Godycki and Rundle from the standpoint of X-ray analysis,[10] and directly by means of the measurement of infra-red absorption spectrum.[11] The existence of the above mentioned O—H—O hydrogen bonds in the cobalt(III) complexes will be expected reasonably from the evidence obtained in the nickel complex. If it proves to be the case, we can estimate this energy of hydrogen bond at several kilocalories per mol. from a large number of data.[12] Since there are two hydrogen bonds in one complex radical, the energy of at least 10—15 kilocalories will be expected per mol. On the other hand, so far as the ordinary cobalt(III) complexes are

7) H. Kuroya, *J. Inst. Polytech.*, Osaka City Univ., **1**, No. 2, Ser. C, 11 (1950),
8) To be published later.
9) Y. Nakatsuka and H. Iinuma, This Bulletin, **11**, 48 (1936).
10) L. E. Godycki, R. E. Rundle, R. C. Voter and C. V. Banks, *J. Chem. Phys.*, **19**, 1205 (1951); L. E. Godycki and R. E. Rundle, *Acta Cryst.*, **6**, 487 (1953).
11) R. E. Rundle and M. Parasol, *J. Chem. Phys.*, **20**, 1487 (1952).
12) See, for example, S. Seki, *Chem. and Chem. Ind.* (in Japanese), **6**, 2226—2227 (1953).
* On the contrary, the opinion that the origin of the tendency towards the planar configuration may be attributable to the π-electrons in the conjugated double bond system is out of the question, since tris-(dipyridyl)- or tris-(phenanthroline)-complexes generally are readily synthesized.

concerned, heats of formation are about 30—50 kcal/mol.[13] (Table II). Thus it may be supposed that the present O—H—O hydrogen bonds in the planar configuration contribute to a considerable degree towards the complex

TABLE II
HEAT OF FORMATION OF COBALT(III) COMPLEXES

Complex ions	Heat of formation kcal.
$[Co(NH_3)_6]^{3+}$	51.9
$[Co(NH_3)_5(NO_2)]^{2+}$	53.1
$[Co(NH_3)_5Cl)]^{2+}$	41.7
$[Co(NH_3)_5(H_2O)]^{3+}$	45.0
$[Co(NH_3)_4(NO_2)_2{}^{(1)}_{(6)}]^{+}$	53.1
$[Co(NH_3)_4(NO_2)_2{}^{(1)}_{(2)}]^{+}$	53.9
$[Co(NH_3)_4Cl_2{}^{(1)}_{(6)}]^{+}$	32.0
$[Co(NH_3)_4Cl_2{}^{(1)}_{(2)}]^{+}$	30.2
$[Co(NH_3)_4(NO_2)Cl{}^{(1)}_{(6)}]^{+}$	49.3
$[Co(NH_3)_4(H_2O)(NO_2){}^{(1)}_{(6)}]^{2+}$	45.6
$[Co(NH_3)_4(NO_2)_4]^{-}$	47.0
$[Co(NO_2)_6]^{3-}$	28.1

formation. The origin of the strong tendency towards the planar configuration characteristic of dimethylglyoxime will, therefore, be found in the above described O—H—O hydrogen bonds. It is then quite natural that the synthesis of tris-(dimethylglyoximo)-cobalt(III) should be very difficult in the ordinary conditions, since the planar bis-(dimethylglyoximo)-derivatives are exceedingly stable. The method of preparation of tris-(dimethylglyoximo)-cobalt (III) suggested by the present author, however, is compatible with the above conclusion. Namely, in this condition, the O—H—O hydrogen bonds are interrupted by potassium hydroxide in the process of the complex formation. In such a condition, three ions of dimethylglyoxime will be able to co-ordinate to a cobalt atom, quite similarly to the ethylenediamine or oxalate radical. And it may be supposed that the formation of the original form of the product already is finished before acetic acid is poured. This assumption is supported by the fact that the synthesis of tris-(dimethylglyoximo)-cobalt(III) is unsuccessful if acetic acid is poured on at the beginning. At any rate, the reactions adopted by many investigators differ in the starting form of dimethylglyoxime from the present method; i.e., in the former dimethylglyoxime exists as a molecule and in the latter as a bivalent anion.

13) K. B. Yatsimirski and L. L. Pankova, *J. Gen. Chem. U. S. S. R.*, **18**, 2051 (1948); **19**, 617, 623 (1949); *Chem. Abstr.*, **43**, 2355, 7805, 7806 (1949); **44**, 7701 (1950).

Summary

Tris-(dimethylglyoximo)-cobalt(III) was newly synthesized by making use of dipotassium dimethylglyoximate. The crystals are quite stable in the atmosphere similarly to other so-called luteo-complexes, and orange-yellow in color. It is soluble in organic solvents, e.g., chloroform, alcohol and dioxane, as well as in water, but insoluble in benzene and acetone.

The absorption spectrum of this compound in aqueous solution was measured, and it was concluded that dimethylglyoxime is a considerably hypsochromic ligand.

Some discussions concerning the stabilities of bis-(dimethylglyoximo)-cobalt(III) complexes were given and they reached the following conclusions: (1) the distinguished stability of bis-(dimethylglyoximo)-derivatives is probably due to the O—H—O hydrogen bonds which are expected for the planar configuration of two dimethylglyoximic ions, and (2) the synthesis of tris-(dimethylglyoximo)-cobalt(III) can be successfully achieved only by interrupting the formation of those hydrogen bonds in the course of co-ordination of the ligands.

The author wishes to express his sincere thanks to Prof. R. Tsuchida and Dr. S. Yamada for their guidance and encouragement throughout this work. This study was supported in part by a grant from the Ministry of Education.

Department of Chemistry, Faculty of Science, Osaka University, Nakanoshima, Osaka

A Cytochrome and a Green Pigment of Sulfate-reducing Bacteria

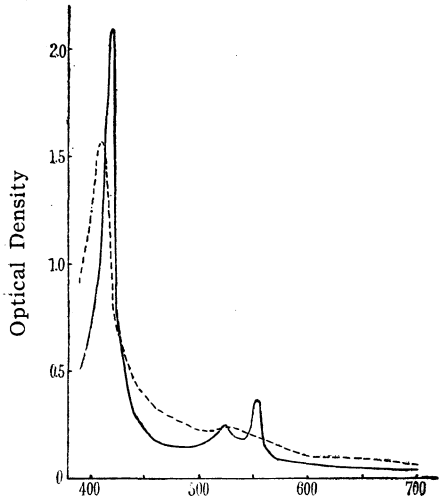
By Makoto Ishimoto, Jiro Koyama and Yutaka Nagai

(Received July 31, 1954)

Some strains of sulfate-reducing bacteria, isolated from paddy fields, were found to contain a cytochrome-like red pigment and a green one in spite of their strictly anaerobic character. In cell suspension, the cytochrome was reduced by molecular hydrogen or by formate, which are the proper metabolites of the bacteria[1], and oxidized by sulfate, sulfite or thiosulfate. So they seem to behave as an intermediary carrier of hydrogen in sulfate reduction in a manner similar to usual cytochromes in aerobic organisms[2]. The presence of the cytochrome and the green pigment was reported recently by Postgate[3] in other strains of sulfate-reducing bacteria, but he did not notice the oxidation of the cytochrome by sulfate.

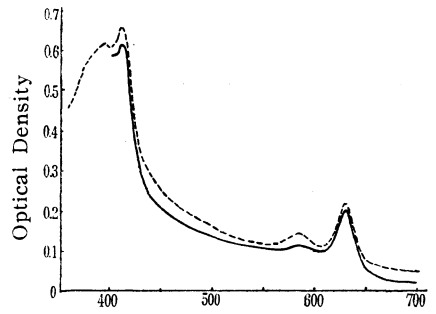
Both pigments could be easily extracted after being made soluble by grinding the cells of the sulfate-reducing bacteria with quartz sand or alumina. A preparation of the green pigment, almost free from the cytochrome, was obtained as precipitate from the saline extract, previously treated with 0.1 M manganese chloride, by addition of its half volume of acetone. The cytochrome, free from the green pigment, was extracted with M/15 disodium phosphate from the residue of the ground cells, which had been treated three times with saline. Their absorption spectra determined by Beckman spectrophotometer, Model DU, are indicated in Fig. 1 and 2.

The cytochrome has absorption maxima at 553 mμ, 524 mμ and 420 mμ in reduced form and at 528 mμ and 410 mμ in oxidized. The absorption bands did not change by the addition of cyanide or carbon monoxide. The



Wave Length (mμ)

Fig. 1. Absorption spectra of the cytochrome of sulfate-reducing bacteria.
Continuous line: reduced form.
Broken line: oxidized form.



Wave Length (mμ)

Fig. 2. Absorption spectra of the green pigment of sulfate-reducing bacteria.
Broken line: before reduction.
Continuous line: after reduction.

reduced form was autoxidizable. This cytochrome resembles fairly well cytochrome-b_4 in respect of the absorption spectra[4], but differs from it in autoxidizability and redox potential. rH_0 of the cytochrome of the sulfate-reducing bacteria falls in between 9.3 and 5.7, when measured by Ball's method[5].

The green pigment had absorption maxima at 630 mμ, 590 mμ and 410 mμ, which were not affected by reduction, but shifted by the addition of pyridine to 590 mμ and 555—545 mμ. This pigment seems to be also a hemoprotein.

1) M. Ishimoto, J. Koyama, T. Omura and Y. Nagai, *J. Biochem.* (Tokyo), **41**, 537 (1954).
2) M. Ishimoto, J. Koyama and Y. Nagai, *J. Japan Biochem. Soc.*, **26**, 304 (1954).
3) J. Postgate, *Biochem. J.*, **56**, xi (1954).
4) F. Egami, M. Itahashi, R. Sato and T. Mori, *J. Biochem.* (*Tokyo*), **40**, 527 (1953).
5) E. G. Ball, *Biochem. Z.*, **295**, 262 (1938).

Department of Chemistry Faculty of Science, Tokyo University

A Semi-empirical Approach to the Self-consistent Molecular Orbitals

By Hideo KON

(Received August 12, 1954)

The semi-empirical ASMO method proposed recently by Pariser and Parr[1] presents a way to calculate the transition energy of a variety of π-electron systems without much labor in conformity with experimental results that is rarely to be found in this kind of calculations. One of the essential points of the method is to alter the values of Coulomb repulsion integrals over atomic orbitals by computing $(pp|pp)$ through the empirical ionization potential and electron affinity values of the atom p and by computing $(pp|qq)$ as the electrostatic interaction between the uniformly charged spheres.

It is of some interest to reflect this reasonable revision of integral values on the form of molecular orbitals. One way might be to resort to the iterative procedure of Roothaan[2], by incorporating Pariser and Parr's semi-empirical scheme into the former. In the present letter, the above mentioned idea is applied to the simple oxygen containing molecules (formaldehyde and glyoxal) as to which no account was given in Pariser and Parr's article.

The best set of coefficients (c_{ip}) in a molecular orbital (ϕ_i) expressed as a linear combination of atomic orbitals (χ_p),

$$\phi_i = \sum_p c_{ip}\chi_p,$$

is obtained by the iterative solution of a set of homogeneous equations derived by Roothaan, with the overlap integrals S_{pq} being replaced by δ_{pq},

$$\sum_q c_{ip}(L_{pq} - \delta_{pq}\epsilon_i) = 0,$$

δ_{pq} being Kronecker's delta. (As to the definitions of L_{pq} and ϵ_i, see ref. 2.) In computing the matrix elements L_{pq}, the simplifications by Pariser and Parr such as; 1) zero differential overlap, 2) neglect of non neighbor resonance integrals are taken in. In addition to this, following assumptions are made: 1) The Coulomb integral α_p can be approximated as the valence state ionization potential (W_{2p}) of the free atom, less the sum only of the Coulomb repulsion integrals $(pp|qq)$. This neglect of Coulomb penetration integrals is found to reduce the labor without having

a significant influence on the numerical results. 2) The resonance integral β_{pq} is proportional for a type of bond (C=C, C=N, or C=O, etc.) to the inverse sixth power of the bond length, the proportionality constants being selected so as to reproduce, as closely as possible, the observed N→V, transition of a particular molecule in the final result by the iterative process. In the case of formaldehyde, −2.95 ev is found suitable for β_{CO} (1.20 Å), and the same value is used for predicting glyoxal N→V_1 transition. The geometricals and numberings for formaldehyde and glyoxal are shown in Fig. 1, together with the computed π-electron densities.

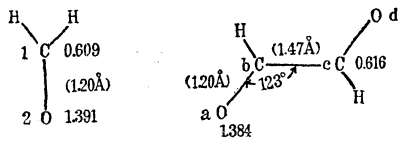


Fig. 1.

The calculated transition energies (E) and self-consistent molecular orbitals are given in the following, where V_1 and T_1 designate the lowest excited singlet and triplet state, respectively.

Formaldehyde,

$E(N\rightarrow V_1)=8.09$ ev, observed, 7.95 ev,[3]

$E(N\rightarrow T_1)=4.75$ ev, — —

$\phi_1=0.5519\ \chi_1+0.8339\ \chi_2$,

$\phi_2=0.8339\ \chi_1-0.5519\ \chi_2$.

Glyoxal,

$E(N\rightarrow V_1)=7.47$ ev, estimated, 7.51 ev*),

$E(N\rightarrow T_1)=5.09$ ev, — —

$\phi_1=0.5541\ (\chi_a+\chi_d)+0.4393\ (\chi_b+\chi_c)$,

$\phi_2=0.6205\ (\chi_a-\chi_d)+0.3390\ (\chi_b-\chi_c)$,

$\phi_3=0.4393\ (\chi_a+\chi_d)-0.5541\ (\chi_b+\chi_c)$,

$\phi_4=0.3390\ (\chi_a-\chi_d)-0.6205\ (\chi_b-\chi_c)$.

*) Estimated roughly from the 57,000 cm^{-1} band of diacetyl, assuming that the two $-CH_3$ groups cause the bathochromic shift of the same magnitude as the difference between the 60,600 cm^{-1} band of acetone and the corresponding band of formaldehyde.

Detailed discussion of these results will be published soon, with the result of calculations for several other molecules which are now in progress.

The author is grateful to Professor H. Tominaga for his kind guidance through the course of this calculation.

1) R. Pariser and R. G. Parr, *J. Chem. Phys.*, **21**, 466, 767 (1953).
2) C. C. J. Roothaan, *Rev. Mod. Phys.*, **23**, 69 (1951); R. G. Parr and R. S. Mulliken, *J. Chem. Phys.*, **18**, 1338 (1950).
3) A. D. Walsh, *Proc. Roy. Soc.* (London), **185A**, 176 (1946).

Department of Chemistry, Faculty of Science, Tôhoku University

The Structure of Trimethylacetic Acid in Condensed Phases as Revealed from Dielectric Studies

By Sei-ichi KONDO and Tsutomu ODA

(Received May 17, 1954)

Introduction

Trimethylacetic acid, $(CH_3)_3CCOOH$, solidifies at 35.2°C, with a very small entropy of fusion, $\Delta S = 2.7$ e.u., as estimated by Pirsch,[1] and gives a cubic crystal. This crystal transforms into another phase of lower symmetry at 7°C with a greater heat of transition. These properties of this compound are very peculiar in contrast to those of the usual lower fatty acids. Formic acid,[2] for instance, has a crystal structure made up of infinite chains of hydrogen-bond between the molecules, and its entropy of fusion is 10.8 e.u.[3]

Timmermans[4] pointed out from these facts that this cubic phase was a kind of plastic crystals, implying that the molecular arrangement in this crystal may have some kind of disorder. This point of view was supported by an X-ray investigation.[5] Our knowledge about the detail of this disordered structure is, however, still quite obscure, and it is the purpose of this paper to add some information to this problem as the result of our dielectric measurements.

Experimentals

1) Purification of the Material.— Trimethylacetic acid was synthesized by the method given in "Organic Syntheses".[6] Special care was taken in drying, so that the sample used was free from moisture as completely as possible. After repeated distillations at low pressure and subsequent recrystallizations, the sample was dried in a desiccator with phosphorus pentoxide for about five days. The material was then sublimed in vacuum of about 10^{-5}mm Hg, and condensed slowly into the measuring cell (shown in Fig.3) in the same vacuum system. The apparatus is shown in Fig.1. The sample thus purified melts sharply at 35.2°C. During the observation there was no noticeable decrease of melting point.

2) Electrical Circuit for the Dielectric Measurement.—Since the amount of the sample obtained was very small, it was necessary to measure small capacities of about 5 pF in the low frequency region. For this purpose we used a revised circuit of the transmitter method shown in Fig.2. With this circuit we were able to observe the capacity from 20 pF to 0.2 pF in the frequency range from 300 cycle to 100 k.c. and the conductance below 10^{-6}

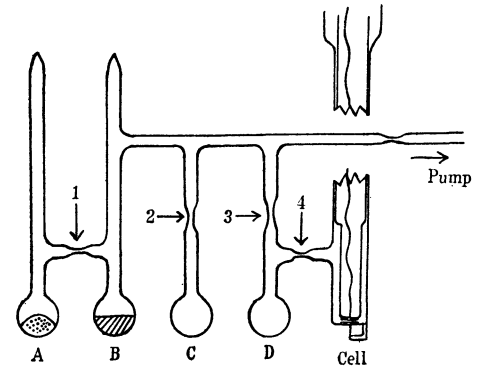


Fig. 1. The process of purification. After distillation and recrystallization, the sample is placed in B with phosphorus pentoxide in A for about five days. Then A is cut off, the system evacuated and half of the sample is sublimed into C, which is cut off. The middle portion of the sample in B is sublimed into D. D and the cell are cut off, and the sample is poured into the Cell. Then D is cut off from the cell.

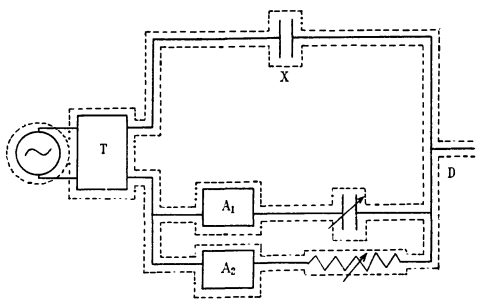


Fig. 2. Electric circuit. T : shielded transmitter. A_1 and A_2 atenuaters. D: detector of zero voltage. X: measuring cell electrode.

1) J. Pirsch, *Ber.*, **70**, 12 (1937).
2) F. Holzberg, B. Post and I. Fankuchen, *Acta Cryst.*, **6**, 127 (1953).
3) Calculated from the values in the "Physico-chemical Constants of Pure Organic Compounds" by J. Timmermans, Elsvier Publishing Co., Inc., (1950), p.379.
4) J. Timmermans, *J. chim. phys.*, **35**, 331 (1938).
5) Y. Namba and T. Oda, This Bulletin **25**, 225 (1952).
6) "Organic Syntheses," Coll. Vol., I., A. H. Blatt, Ed., John Wily and Sons, Inc., New York, N. Y., (1947), p.524.

mho, within the accuracy of ±1% in terms of the absolute value of the dielectric constant. This was examined preliminarily by the measurements on benzene, carbon disulfide, and chloroform. The measurement of the dielectric constant and loss between the frequency range from 100 k.c. to 3 m.c. was carried out by the Q-meter, using the variable precision condenser.

3) Direct Current Conductivity.—The conductivity was measured in the usual way, using the cell shown in Fig.3. The applied voltage was about 10 volts, and a galvanometer of sensitivity 10^{-11} amp./mm. was used. There was no detectable adsorption current.

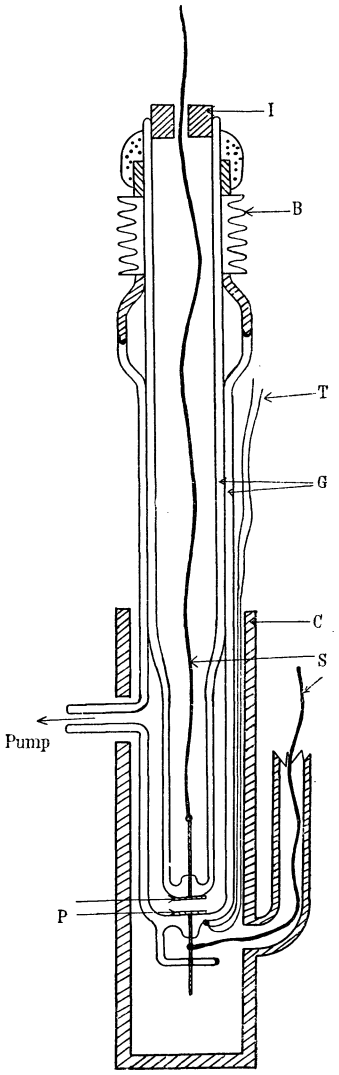


Fig. 3. The measuring cell. G: glass. B: bellows. P: platinum circular parallel electrodes. C: copper block. T: Cu-constantan thermocouple. S: electric leads. I: Polystyrol insulator. C and T are earthed.

4) Electrode Cell.—To facilitate the measurements in vacuum or under dried conditions and to cover a wide temperature range, we used the cell shown in Fig.3, bellows being used in order to keep close contact between the electrodes and the sample during volume change in the solid state. This cell was used for the measurements of both the dielectric constant and the conductivity.

Result

The values of the dielectric constant were obtained in the temperature range from —30°C to +70°C, (shown in Fig. 4). The dielectric constant of tae room temperature phase was found to be have a very small value of 2.62, compared with those of formic and acetic acid.[7] The dielectric loss was of the same order as that of the glass cell, or even smaller and hence this compound falls into the category of insulator. In the frequency range we have studied, there was neither change in the dielectric constant nor loss exceeding the experimental error.

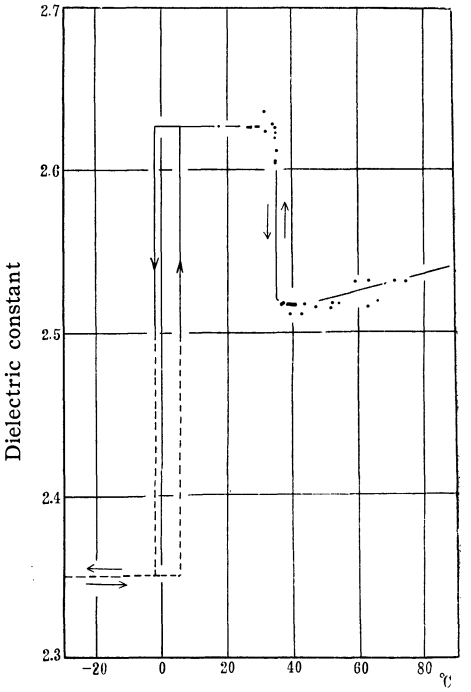


Fig. 4. The dielectric constant vs. temperature curve. The dotted line shows the apparent values of dielectric constant.

On cooling, the dielectric constant increases at the solidifying point. The molecular polarization of both the solid and liquid states near the melting point calculated from the observed values of the dielectric constant and density shows almost the same value, about 38 cc. This will indicate a similarity in the molecular arrangements of the liquid and the cubic modification. This point

of view is also strengthened by the small value of the entropy of fusion. In both states, the value of the dielectric constant is a little higher than the square of the refractive index ($n_D^{20}=1.462$). This difference may be considered as a part of atomic polarization due to the hydrogen-bond, which makes the molecular association possible. The contribution from the orientation polarization is considered to be small.

According to Onsager-Kirkwood's theory,[8] the result given above will indicate that this compound in the two phases, should be composed of nonpolar molecular units, and there seem to be few possibilities of forming chain-like structures.

A reliable value for the dielectric constant of the low temperature phase was not obtained. At the transition point -2°C, the initially transparent crystal with no crack or void becomes suddenly opaque, accompanied by a large volume contraction $\Delta V=10.45$ cc./mol. However, we were able to obtain apparent values of the dielectric constant with powdered crystals at temperatures above and below the transition point. On heating and cooling, the values of the dielectric constant changed almost reversibly. As shown in Fig. 4, the dielectric constant decreases at the transition point and this decrease could be interpreted either by a smaller value of the dielectric constant in the low-temperature modification, or by a kind of preferred orientation of small crystals. The dielectric constant of the cubic phase remained almost constant with varying temperature, while in the liquid state, it has the positive temperature coefficient, contrary to the usual molecular crystals. This might mean a slight increase of the number of the single molecules or the polar association of molecules with increasing temperature. The direct current conductivity (note Fig. 5) showed strikingly small value, being the same magnitude as those of insulators. The hydrogen atoms in the acid radical at lower temperatures, seem not to play a role as the charge carrier and are supposed to be immobile in the stable non-polar molecular units, forming the closed intermolecular hydrogen-bond.

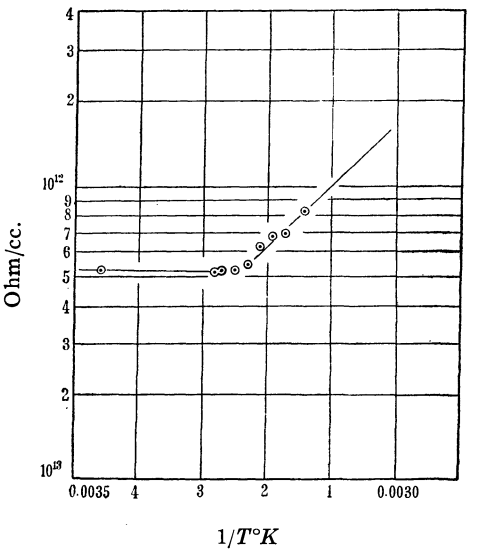


Fig. 5. The direct current conductivity vs. reciprocal temperature curve.

Discussion of the Structure

By the X-ray crystallographic investigation, the crystal shows only three kinds of reflection of face-centered cubic symmetry, $a_0=8.82\pm0.03$Å, containing four molecules in the unit cell. From the symmetry consideration, it was concluded that the structure allows the disordered orientation of molecules.[5]

If we assume the non-polar polymer discussed in the preceeding section to be a dimer, it is possible to obtain a reasonable interpretation of the disordered structure of this crystal. Suppose that the center of mass of each molecule (shown in Fig.6) occupies each lattice point, and this molecule associates with one of the twelve first nearest neighboring molecules by the hydrogen-bond to form a dimer, the four oxygen atoms being coplanar. The shortest intermolecular distance between the oxygen atoms within this dimer comes out to be 2.7 Å, which is a plausible value for the O—H···O hydrogen-bond distance of the fatty acids. We may further assume that this dimer is fairly stable, in view of the fact that the dispersion in dielectric constant is absent. Thus the single molecule may not undergo a dynamical rotation, but the dimer moves as a whole, accompanied by the migration of vacancies which will amount to comparatively large numbers as is seen from the difference of the calculated and observed densities 0.99 and 0.973 at 12.4°C respectively. Such a migration seems to be quite possible, considering the numerical value of the nearest distance of approach between the dimers as is estimated from the van der Waals radii. It is also plausible that the methyl or *t*-butyl radicals, rotate around their C-C bonds and their details would be

7) J. F. Johnson and R. H. Cole, *J. Am. Chem. Soc.*, **73**, 4536 (1951). W. Dannhauser and R. H. Cole, ibid., **74**, 6105 (1952). C. P. Smyth and H. E. Rogers, ibid., **52**, 1824 (1930).

8) See for instance "Theory of Dielectrics" by H. Fröhlich, Oxford Press, (1949), p.104.

clarified through further investigations such as nuclear magnetic resonance absorption. Thus it is concluded that the crystal is made up of dimers orientating randomly, the most stable configuration being such that their axes point to one of the twelve [110] directions, keeping the center of mass of each molecule on the lattice site.

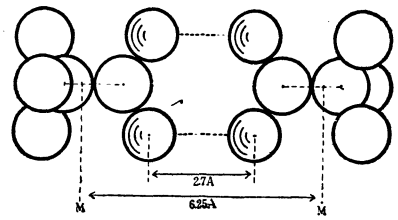


Fig. 6. The schematic model of the dimer of trimethylacetic acid. The steric configulation of *t*-butyl radicals was assumed arbitrarily.

It is interesting to compare the state of association of this compound with that of formic acid. With formic acid, there will be several steps in degrees of association corresponding to the gas, liquid, and solid states.

On the other hand, there seem to be few differences between the liquid and cubic phases of the present material. The bulky *t*-butyl radical seems to be most responsible for such a peculiar structure and properties of trimethylacetic acid.

Summary

The authors have investigated the electric properties of trimethylacetic acid in the liquid and solid states. From the markedly small values of dielectric constant and conductivity, combined with the results of the X-ray investigation, it is proposed that the crystal of the room temperature phase is composed of nonpolar dimer units having disordered orienation.

The authors express their thanks to Professor I. Nitta and Professor T. Watanabe of Osaka University for their continued interest and also for the critical reading of the manuscript by the latter. Thanks are also due to the Ministry of Education for a grant.

Laboratory of Physical Chemistry,
Osaka Liberal Arts
University, Tennoji, Osaka

An Equation of State in Analytical Form (Concluded)

By Tetsuya ISHIKAWA

(Received June 8, 1954)

The substances already exemplified for the verification of the author's equation of state, $(p+a/V^{2-\varepsilon})(V-b)=RT$, $a=3p_cV_c^2$, $b=V_c/3$, were all non-polar or slightly polar which yielded to the condition that at their critical points the pressure independent constants, $\varepsilon's$, converged to a universal constant, 0.077 $\pm$0.008 when V_c is expressed in cc./mol., and for these substances his newly defined association degree, A, which is the ratio of the critical factor to van der Waals' critical factor, 8/3,

$$A=\frac{3}{8}\left(\frac{RT_c}{P_cV_c}\right), \text{ and } \frac{RT_c}{P_cV_c}=\frac{2(1+3V_c^2)}{3} \tag{1}$$

was found to be from the lowest values of 1.22−1.29 for non-polar molecules such as He, A, Kr, N_2, O_2, and CH_4 to the highest values of 1.47−1.49 for slightly polar molecules such as $CH_3CO_2CH_3$, $CH_3CO_2C_2H_5$, and $CH_3CO_2C_3H_7$[1].

For strongly polar substances such as acetone, lower alcohols, acetic acid, and water, $\varepsilon's$ at their critical points always take greater values thus: $(CH_3)_2CO$, $\varepsilon=0.101$; CH_3OH, $\varepsilon=0.139$; C_2H_5OH, $\varepsilon=0.105$; n-C_3H_7OH, $\varepsilon=0.095$; CH_3COOH, $\varepsilon=0.150$; and H_2O, $\varepsilon=0.159$. In these cases, however, A deviates appreciably from the first relation of (1) and takes the form,

$$A=f\cdot\frac{3}{8}\left(\frac{RT_c}{P_cV_c}\right), \tag{2}$$

where f is the deviation factor which may depend upon temperature but can be estimated by putting A from relation (2) into relation (3) in the first report:

$$f=\frac{b}{V-R\beta/\alpha} \tag{3}$$

1) T. Ishikawa, This Bulletin, **26**, 78, 530 (1953); ibid., **27**, 226 (1954); T. Ishikawa, M. Ikeda, ibid., **26**, 516 (1953).

where α and β denote the thermal expansion coefficient and the isothermal compressibility.

Taking f at 20°C into account in the calculation of A, we obtain the values, denoted by the author (20°C) in Table I, in which are also shown the association degrees from other methods by several investigators.

TABLE I
ASSOCIATION DEGREES OF STRONGLY POLAR SUBSTANCES

Liquid	Ramsay[2] (20°C)	Traube[3] (15°C)	Bingham & Spooner[4]	The author (20°C)	The author (crit. pt.)
$(CH_3)_2CO$	—	1.53	1.28—1.31	1.78	1.54
CH_3OH	2.32	1.79	1.89—1.93	1.59	1.71
C_2H_5OH	1.65	1.67	1.90—1.98	1.68	1.53
n-C_3H_7OH	—	1.66	1.78—1.92	1.66	1.50
CH_3COOH	2.13	1.56	1.71—1.95	1.75	1.54
H_2O	1.64	3.06	—	(negative)	1.67

As seen from Table I, the author's values are in fair agreement with other values, his method also may well be applicable to computing the association degree of an abnormal liquid.

The only exceptional case, in which f gives a negative value at 20°C and consequently relation (3) fails, is water. At higher temperatures, however, f changes its sign and this substance behaves like a normal liquid. For example, if we adopt from Kennedy's compressibility data,[5] we can see that e.g., at 200 bars f (α and β being calculated by taking $\Delta t=10$°C and $\Delta p=50$ bars) takes 1.144 at 200°C, 1.106 at 250°C, and 1.011 at 300°C. Judging from these values which approach to 1 as the temperature comes near the critical point, 374.23°C, it is highly probable that even for an abnormal liquid like water, this relation (1) holds good at the critical point (the values of the author [crit. pt.] in Table I are A values thus assumed).

Next, we shall examine the applicability of the new equation to water as an example of the most anomalous case.

Among the critical constants, t_c, p_c, and v_c of water, v_c can not be measured directly and has been obtained by graphical extrapolation from the values of the saturation volume of both liquid and vapour above 340°C.[6] Schroer[7] obtained $v_c=2.56-3.57$ cc./g., but Eck[8] obtained $v_c=2.650-3.630$ cc./g. and decide, as the true critical volume, 3.066 cc./g. which is nearly the value appeared in Henning's "Warmetechnische Richtwerte", p. 17 (VDI-Verlag GMBH, Berlin, 1938), from this the author adopted to evaluate A at the critical point for water in Table I.

Trials of the author's equation by Kennedy's data, using $t_c=374.2$°C, $p_c=217.5$ atm., and either of the above extremities of v_c, turned out to give the best constancy for $(2-\varepsilon)$, but with still unsatisfactory results, in the case of $v_c=2.56$ cc./g, the least value among them, this value being nearly equivalent to $d_c=0.4$ g./cc. which appeared in "International Critical Tables", III, p. 248 (1928).

As we know, from van der Waals' b it is possible to calculate the molecular collision diameter, σ, of a gas from the relation:

$$b=4N\frac{4}{3}\pi\left(\frac{\sigma}{2}\right)^3, \quad \text{where} \quad N\,(\text{Avogadro's number})=6.025\times10^{23}, \tag{4}$$

but in order to let σ nearly coincide with the molecular collision diameter from viscosity, σ_η, b has usually been taken as

$$b=\frac{RT_c}{8p_c}=\frac{3}{8}\left(\frac{RT_c}{p_cV_c}\right)\frac{V_c}{3}=b_{corr}. \quad \text{(already denoted)}, \tag{5}$$

which is a solution (the other solution being $b=V_c/3$) obtained from van der Waals' equation and its two derivatives, $(\partial p/\partial V)_T=0$, and $(\partial^2 p/\partial V^2)_T=0$ at the critical point, notwithstanding that the selection of $b_{corr.}$ from these two is merely conventional so far as van der Waals' equation is concerned.

Now, in Landolt-Börnstein, I, Teil 1, p. 369 (1950), there appears $\sigma_\eta=2.27$ Å, from which b or otherwise $b_{corr.}$ is calculated to be 14.76 cc./mol., whence $v_c=2.457$ cc./g. or otherwise 1.480 cc./g. The former value is very slightly over the saturation volume, 2.450 cc./g, at 374°C (0.23°C below the critical temperature) observed by Eck and therefore may be acceptable, while the latter is too low and must be rejected.

From complete tests of the author's equation by Henning's tables, p. 25 at 0 to 350°C,

2) W. Ramsay, *Z. phys. Chem.*, **15**, 111 (1894).
3) J. Traube, *Ber.*, **28**, 3292 (1895); ibid., **30**, 273 (1897).
4) E.C. Bingham, L.W. Spooner, *Physics*, **4**, 387 (1933).
5) G.C. Kennedy, *Am. J. Sci.*, **248**, 540 (1950).
6) F.G. Keyes, *J. Chem. Phys.*, **17**, 923 (1949).
7) E. Schroer, *Z. phys. Chem.*, **129**, 79 (1927).
8) H. Eck, *Phys. Z.*, **40**, 3 (1939).

the author has learned that this b value gives better constancy for $(2-\varepsilon)$ than $v_c=2.56$ cc./g. i.e., $b=15.39$ cc./mol. above explained, and so the author, adopting also from Kennedy's data, has carried out calculations for $(2-\varepsilon)$ values and their corresponding percentage deviations, 100 $(p_{calc.}-p_{obs.})/p_{obs.}$, for the pressure range 100 to 1000 bars at 200 to 370°C, and 100 to 2500 bars at 380 to 600°C. A half of their results are tabulated in Tables II and III, and the full values of $(2-\varepsilon)$ are diagrammatically shown in Fig. 1, in which the values from Kennedy's data and the values from Henning's tables are denoted by ○ and × respectively.

It follows from Tables II—III and Fig. 1 that the excellent constancies of $(2-\varepsilon)$ and low percentage deviations throughout the temperature studied afford a conclusive proof to the availability of the author's equation for both liquid and vapour states, and that the linearity of $(2-\varepsilon)$ with temperature is strongly confirmed above 250°C as would be expected, the linearity being expressible by $2-\varepsilon=1.771+0.0001683\ (T-T_c)$ where $T_c=647.4$°K.

At the end of this study we shall add another deduction of the new equation from

TABLE II

$(2-\varepsilon)$ VALUES OF WATER AT 200 TO 600°C

p bars	Temperature in °C										
	200	220	240	260	280	300	320	340	350	360	370
100	1.746	1.748	1.749	1.752	1.754	1.757	(1.745)	(1.756)	(1.763)	(1.768)	(1.774)
150	1.746	1.748	1.750	1.752	1.754	1.758	1.760	1.764	(1.744)	(1.749)	(1.756)
200	1.746	1.748	1.750	1.752	1.755	1.758	1.760	1.764	1.766	1.767	(1.745)
250	1.746	1.748	1.750	1.752	1.755	1.757	1.760	1.764	1.765	1.767	1.769
300	1.746	1.748	1.750	1.753	1.755	1.758	1.761	1.764	1.766	1.767	1.768
350	1.746	1.748	1.751	1.753	1.755	1.758	1.761	1.764	1.766	1.767	1.769
400	1.746	1.748	1.750	1.753	1.755	1.758	1.761	1.764	1.766	1.767	1.769
500	1.745	1.748	1.750	1.753	1.755	1.758	1.761	1.764	1.766	1.768	1.770
600	1.745	1.748	1.750	1.752	1.756	1.758	1.761	1.765	1.766	1.768	1.770
700	1.745	1.747	1.750	1.752	1.755	1.759	1.762	1.765	1.767	1.768	1.770
800	1.745	1.747	1.749	1.752	1.755	1.759	1.762	1.765	1.767	1.769	1.771
900	1.743	1.747	1.749	1.752	1.755	1.758	1.762	1.766	1.767	1.769	1.771
1000	1.743	1.745	1.748	1.752	1.756	1.759	1.762	1.766	1.767	1.769	1.771
mean	1.745	1.748	1.750	1.752	1.755	1.758	1.761	1.765	1.766	1.768	1.770

p bars	Temperature in °C										
	390	410	430	450	470	490	510	530	550	570	590
100	(1.787)	(1.784)	(1.788)	(1.795)	(1.799)	(1.804)	(1.808)	(1.810)	(1.813)	(1.814)	(1.818)
150	(1.767)	(1.776)	(1.784)	(1.791)	(1.798)	(1.805)	(1.812)	(1.816)	(1.820)	(1.822)	(1.826)
200	(1.755)	(1.765)	(1.773)	(1.781)	(1.790)	(1.797)	(1.804)	(1.809)	(1.814)	(1.818)	(1.823)
250	(1.754)	(1.759)	(1.767)	(1.775)	(1.783)	(1.791)	(1.799)	(1.806)	(1.813)	(1.818)	(1.824)
300	1.771	(1.762)	(1.765)	(1.771)	(1.779)	(1.786)	(1.794)	(1.802)	(1.809)	(1.814)	(1.820)
350	1.771	(1.771)	(1.768)	(1.770)	(1.776)	(1.783)	(1.791)	(1.799)	(1.807)	(1.813)	(1.819)
400	1.774	(1.773)	(1.773)	(1.772)	(1.776)	(1.781)	(1.787)	(1.794)	(1.802)	(1.809)	(1.815)
450	1.773	1.776	(1.775)	(1.776)	(1.777)	(1.781)	(1.786)	(1.791)	(1.796)	(1.802)	(1.809)
500	1.773	1.775	1.777	1.778	1.779	1.781	1.786	1.791	1.796	1.801	1.807
600	1.773	1.776	1.778	1.781	1.782	1.784	1.787	1.790	1.795	1.801	1.806
700	1.774	1.777	1.780	1.782	1.784	1.787	1.789	1.792	1.796	1.800	1.804
800	1.774	1.777	1.780	1.783	1.786	1.788	1.791	1.794	1.797	1.801	1.805
900	1.774	1.778	1.780	1.783	1.786	1.789	1.792	1.795	1.798	1.802	1.807
1000	1.774	1.778	1.780	1.783	1.786	1.789	1.792	1.795	1.799	1.803	1.807
1200	1.775	1.778	1.781	1.783	1.786	1.789	1.792	1.795	1.800	1.804	1.808
1400	1.775	1.778	1.780	1.783	1.786	1.789	1.792	1.795	1.799	1.804	1.808
1600	1.775	1.779	1.782	1.786	1.788	1.790	1.793	1.796	1.799	1.803	1.807
1800	1.775	1.779	1.783	1.787	1.790	1.794	1.795	1.797	1.799	1.802	1.806
2000	1.774	1.779	1.784	1.788	1.791	1.794	1.797	1.799	1.801	1.804	1.806
2250	1.774	1.779	1.784	1.788	1.792	1.796	1.799	1.801	1.804	1.806	1.808
2500	1.772	1.778	1.783	1.788	1.792	1.796	1.800	1.803	1.806	1.807	1.810
mean	1.774	1.778	1.781	1.784	1.787	1.790	1.793	1.796	1.799	1.803	1.807

TABLE III

PERCENTAGE DEVIATIONS, 100 ($p_{calc.}$—$p_{obs.}$)/p_{obs} FOR WATER AT 200 TO 600°C

p bars	Temperature in °C										
	200	220	240	260	280	300	320	340	350	360	370
100	−21.97	+8.29	+7.53	+4.45	+11.47	+11.86	+4.37	+1.91	+0.65	+0.05	+ 0.00
150	−13.15	+3.45	+3.85	+1.76	+ 5.41	+ 7.67	+5.84	+9.51	+9.41	+6.51	+ 4.15
200	−10.59	+2.30	+1.50	−0.88	+ 3.79	+ 5.03	+5.37	+8.37	+3.40	+4.89	+15.95
250	−11.57	+0.66	+1.21	−1.21	+ 1.75	+ 2.89	+3.22	+6.82	+2.87	+5.39	+ 4.74
300	− 5.82	+0.17	+0.45	−1.44	+ 0.69	+ 1.97	+2.05	+5.54	+2.14	+4.71	+ 5.17
350	− 7.50	+1.14	−0.64	−2.95	− 0.65	+ 0.19	+0.83	+4.63	+1.53	+3.80	+ 4.56
400	− 8.94	−0.17	+0.35	−1.43	− 0.08	+ 0.39	−0.02	+3.47	+1.46	+1.85	− 1.66
500	− 2.57	+1.48	+0.22	−1.60	− 0.47	− 0.38	−0.96	+1.73	+0.70	+0.69	+ 1.08
600	− 1.05	+1.84	+0.77	−1.55	− 0.60	− 0.97	−1.36	+1.23	−0.29	+0.09	− 0.58
700	+ 1.19	+2.20	+1.59	−0.80	− 0.90	− 1.08	−1.73	+0.38	−0.97	−0.58	− 0.48
800	+ 2.77	+3.64	+1.63	−0.47	− 0.52	− 1.09	−1.87	−0.13	−0.72	−1.19	− 1.32
900	+ 3.68	+4.52	+2.55	+1.06	− 0.09	− 1.31	−2.15	−0.48	−1.46	−1.59	− 1.75
1000	+ 5.19	+5.17	+3.35	+1.45	+ 0.57	− 1.00	−1.67	−0.44	−1.51	−1.71	− 1.60
mean	7.38	2.69	1.97	1.62	2.08	2.76	2.43	3.43	1.55	2.54	3.31

p bars	Temperature in °C										
	390	410	430	450	470	490	510	530	550	570	590
100	− 1.31	− 0.83	− 0.78	−1.17	−1.56	−1.29	−1.28	−1.10	−0.70	−0.78	−0.67
150	+ 1.58	+ 0.31	− 0.56	−1.09	−1.47	−1.94	−2.12	−2.12	−1.99	−1.75	−1.25
200	+ 7.76	− 4.16	+ 1.99	+0.68	−0.48	−1.15	−1.67	−1.82	−1.86	−1.71	−1.79
250	+18.70	+ 9.27	+ 5.14	+2.61	+1.08	−0.19	−1.20	−1.69	−2.14	−2.11	−2.18
300	+ 7.90	+15.26	+ 9.04	+5.38	+2.80	+1.19	−0.26	−1.26	−1.82	−1.88	−2.01
350	+ 7.34	+11.40	+13.05	+6.34	+4.94	+2.53	−0.67	−0.65	−1.63	−1.93	−2.12
400	+ 4.18	+ 8.98	+10.56	+8.80	+6.28	+3.66	+2.21	+0.72	−0.68	−1.27	−1.67
450	+ 2.60	+ 3.47	+ 7.99	+8.11	+6.68	+4.70	+3.14	+1.86	+0.77	+0.14	−0.52
500	+ 2.12	+ 4.69	+ 5.84	+6.66	+6.30	+5.36	+3.51	+2.17	+1.17	+0.49	−0.01
600	+ 1.45	+ 3.10	+ 3.67	+4.42	+4.55	+4.59	+3.87	+2.89	+1.73	+0.88	+0.36
700	− 0.23	+ 1.77	+ 1.61	+1.94	+2.58	+2.76	+2.88	+2.49	+1.55	+1.33	+0.99
800	+ 0.45	+ 1.20	+ 1.20	+0.83	+1.13	+1.36	+1.47	+1.47	+1.23	+1.00	+0.64
900	+ 0.22	+ 0.65	+ 1.03	+0.84	+0.93	+0.97	+1.06	+0.92	+0.63	+0.39	+0.17
1000	− 0.64	+ 0.40	+ 0.60	+0.80	+0.87	+0.81	+0.89	+0.68	+0.15	−0.08	−0.12
1200	− 1.13	+ 0.17	+ 0.15	+0.71	+0.84	+0.70	+0.64	+0.37	−0.32	−0.54	−0.56
1400	− 0.82	+ 0.06	+ 0.58	+1.02	+1.07	+0.98	+0.94	+0.51	−0.16	−0.66	−0.67
1600	− 0.62	− 0.58	− 1.10	−1.35	−0.99	−0.20	−0.15	+0.27	+0.08	+0.76	+0.01
1800	− 1.53	− 0.86	− 1.51	−1.98	−2.11	−2.72	−1.07	−0.46	−0.14	+0.32	+0.54
2000	− 0.23	− 0.61	− 1.84	−2.54	−2.92	−2.70	−2.34	−1.70	−1.32	−0.29	+0.40
2250	+ 0.04	− 0.48	− 1.89	−2.61	−3.16	−3.23	−3.21	−2.89	−2.68	−1.48	−0.58
2500	+ 1.27	+ 0.28	− 1.07	−2.48	−2.93	−3.35	−3.44	−2.87	−3.14	−2.04	−1.31
mean	2.96	3.26	3.39	2.93	2.65	2.21	1.67	1.47	1.23	1.04	0.88

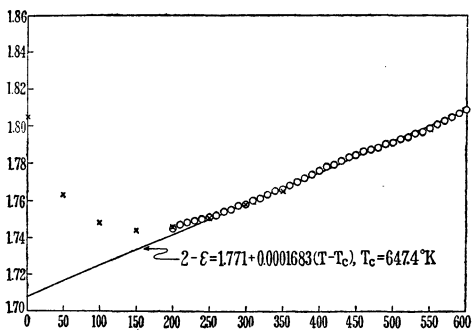


Fig. 1. The temperature dependence of (2−ε) of water.

the standpoint of kinetic theory of gases by taking the idea of molecular association into consideration in the well-known deduction of van der Waals' equation.[9]

In a liquid, single molecules may form themselves into associated molecules[10], each of which is not a fast-combined molecule but is a group composed of no other molecules than singly existing molecules, or more concretely speaking, into cybotactic groups[11], in

9) e.g., S. Glasstone, "Textbook of Physical Chemistry", p. 289 (2nd Edition).

10) T. Ishikawa, This Bulletin, **4**, 5 (1929); T. Ishikawa, T. Baba, ibid., **11**, 64 (1936).

11) G.W. Stewart, *Rev. Mod. Phys.*, **2**, 116 (1930); *Koll. Z.*, **67**, 130 (1934).

each of which the molecules are arranged in a relatively orderly manner, but the groups are not to be regarded as permanent or as having sharp boundaries, for the movement of the molecules must result in a continual shifting of position and exchange of the members of the cybotactic groups with those in the space between.

If the above idea is extended to the gaseous phase, the force exerted on a single molecule about to strike the wall is, as usually regarded, evidently proportional to the density, ρ, but the number of molecules striking the wall at any instant may be proportional to the density slightly less than ρ, because such molecular groups undoubtedly retard their composition of single molecules striking the wall, that is to say $\rho^{1-\varepsilon}$, if the density under consideration is taken as the simplest power form of ρ, where ε is a correction factor dependent on molecular association and therefore probably independent of pressure, so that the cohesive pressure is proportional to $\rho\cdot\rho^{1-\varepsilon}=\rho^{2-\varepsilon}$. Applying volume correction as is usually done, the author's equation readily follows: $(p+a/V^{2-\varepsilon})(V-b)=RT$, in which constant a is the same as that of van der Waals' equation, if ε is small as compared with unity, and constant b is $V_c/3$ which fits a thermodynamic equality $b=V-R\beta/\alpha$ for normal liquids, hence $a=3p_cV_c^2$, $b=V_c/3$, and $RT_c/p_cV_c=2(1+3V_c^{\varepsilon})/3$; this last relation rejects $b=RT_c/8p_c$ (the other solution of b) for the corrected form of van der Waals' equation.

In conclusion, the author expresses his hearty thanks to Nagasaki American Cultural Center who has furnished him with American journals at his request.

Sasebo Commercial Junior College,
Sasebo, Nagasaki

Reactivity of Coke. III. Effects of Some Metallic Additions on the Surface Area of Cokes from Humic Acid and on the Absolute Reaction Rates of the Coke-Carbon Dioxide System

By Yoshio KAWANA

(Received June 8, 1954)

Introduction

It was recognized long ago that certain metallic impurities as well as added salts played an important role in catalyzing the reaction of carbon with carbon dioxide. Particularly, on the catalytic effects of inorganic additions on the reactivity of coke, a number of works have been written and briefly reviewed by M. A. Mayers.[1] The most effective catalysts to coke or pure graphite among them are the metals of the alkali group, usualy applied as the carbonates as well as the oxides and elemental iron or its carbide. Several other materials have been found to have slight or no effect. Though a great number of work have been published, these effects have hardly been treated quantitatively from the standpoint of chemical reaction rates.

In preceding papers[2,3] we have assumed that the catalytic effects of impurities of coke played an important part in the absolute reaction rates of the coke-carbon dioxide system.

In the present study, we have confirmed quantitatively the effects of some metallic additions on the specific surface area of cokes from humic acid and on the absolute reaction rates of the coke-carbon dioxide system. By the comparison between the cokes prepared from humic acid and metal-humates, the catalytic effects of the metallic constituents of the ash in coke have been examined; sodium, calcium, magnesium, iron and aluminium were used as metals which were most commonly found in the coke ash. The reason why humic acid was selected as the parent carbonaceous material was that the inherent mineral matter in coal might be considered to have partly entered into coal as metal-humates in the initial coalification process[4] and that it might be more important in the consideration of the catalytic

1) M. A. Mayers, "Chemistry of Coal Utilization", Editor, H. H. Lowry, John Wiley and Sons, Inc., New York, Vol. **1**, (1945), p.917.
2) Y. Kawana, This Bulletin, **26**, 507 (1953).
3) Y. Kawana, This Bulletin, **27**, 334 (1954).
4) F. Fisher and W. Fuchs, *Brenn. Chem.*, **8**, 291 (1927). E. Biesalski and Berger, *Braunkohle*, **23**, 197 (1924/25).

effects of the ash in coke than the extraneous mineral matter.

Experimental

Preparation of Humic Acid and Metal-humates.—Humic acid was prepared from Takayama lignite. About 200 g. of dried Takayama lignite, bitumen of which had been previously eliminated by benzene-ethanol azeotropic mixture, was treated with ten-times one per cent sodium hydroxide solution for about five hours at the boiling temperature and after settling during about 15 hours, humic acid was precipitated by a little excess of hydrochloric acid from the upper parts of the solution. The precipitates of humic acid were purified by washing several times with distilled water and then by electrodialysis for about twenty days.

Metal-humates were prepared by treating the humic acid with metal chlorides or carbonate solution by the flow method. About 20 g. of humic acid crushed from 20 to 60 mesh was packed into a glass cylinder and 250 cc. of 1N salt solution passed through the humic acid column at a space velocity of about 0.5 and then the metal-humates were washed by distilled water until chlorine ion disappeared. These metal-humates were dried under reduced pressure. Extra-pure sodium carbonate and metal chlorides were used respectively for sodium-humate and the other metal-humates.

TABLE I
DESCRIPTION OF COKES

Cokes	Density g./cc.	Ash, % dry basis	Composition of ash in coke, %					
			$Na_2O+Na_2CO_3$	$CaCO_3$	MgO	Fe_2O_3	Al_2O_3	SiO_2
H-coke	1.630	2.63	—	1.10	0.55	11.46	31.07	51.15
Na- „	1.625	15.51	84.13	—	—	—	—	—
Ca- „	1.842	7.24	—	45.64	—	—	—	—
Mg- „	1.788	5.60	—	—	20.13	—	—	—
Fe- „	1.835	4.08	—	—	—	39.18	—	—
Al- „	1.862	3.40	—	—	—	—	43.20	—

Preparation of Cokes from Humic Acid and Metal-humates.—The experimental conditions for the preparation of cokes from humic acid and metal-humates were as follows. About 20 g. of humic acid or metal-humates packed in a graphite crucible were put into a silica cylinder and evacuated until about 5 mmHg at room temperature and then carbonized at a heating rate of about 5°C per minute until 1000°C under the reduced pressure of 6—8 mmHg and after maintenance at 1000°C for about one hour, the coke sample was cooled down to room temperature. The cokes carbonized from humic acid, sodium-, calcium-, magnesium-, iron-, and aluminium-humate are defined respectively as H-, Na-, Ca-, Mg-, Fe- and Al-coke.

The analytical results and the densities of coke samples are shown in Table I. All cokes, except for Na-coke treated in high vacuum at lower temperature of 500°C, were subjected to vacuum treatment (10^{-1}—10^{-3} mmHg) at 1100°C for half an hour. H-coke is unfortunately not pure and its ash content is 2.63 per cent. The density and ash contents of metal-cokes are remarkably increased as compared with those of H-coke, and the increase of ash contents of metal-cokes is respectively due to metal ions inserted as metal-humates. The chemical analysis of the ash of metal-cokes was made only on the metal ion inserted.

Apparatus and Procedure.—The apparatus and procedure for determination of the surface area of cokes and for absolute reaction rates of the coke-carbon dioxide system at various temperatures were the same as already described in the first paper.[2] The surface area of cokes was determined by the adsorption of ammonia at 0°C using the B.E.T. method. After that, the reaction of this coke and carbon dioxide at the constant temperature ranging from 730°C to 970°C under constant volume was obtained by measuring the increase in the total pressure of this system against time.

The specific reaction rates per unit area of the coke surface Ka expressed as the number of molecules reacted per sq. cm per second when

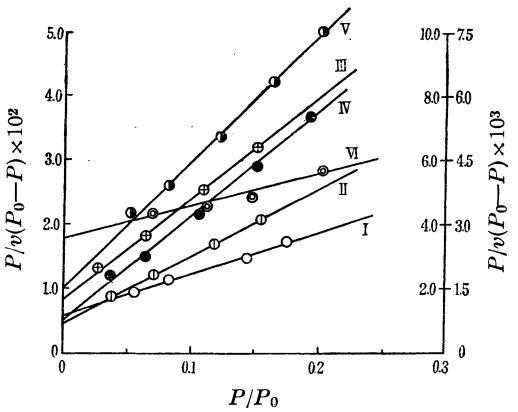


Fig. 1. BET plots of adsorption isotherms of ammonia at 0°C by cokes from humic acid and metal-humates.

	Cokes	Scale
I	H-coke	A
II	Ca-coke	B
III	Mg-coke	„
IV	Fe-coke	C
V	Al-coke	„
VI	Na-coke	A

$P_{co_2}P/_{co}$ was equal to unity, were obtained at various temperatures by the surface area determination together with the reaction rates measurement as already explained in the first paper.

Results and Discussion

Specific Surface Areas of Cokes from Humic Acid and Metal-humates.—The B.E.T. plots of ammonia adsorption at 0°C by cokes from humic acid and metal-humates are shown in Fig. 1 and good straight lines are obtained for a series of relative pressure from about 0.05 to 0.3. According to the usual procedures in the B.E.T. method various values obtained from Fig. 1 are summarized in Table II.

TABLE II

SUMMARY OF SURFACE AREA DATA OF COKES

Cokes	Pre-treatment in vacua °C, hr(mmHg)	Sample weights (g.)	S (m^2)	A (m^2/g.)	A_M/A_H	E_1-E_L (cal./mol.)
H-coke	1100,7 (10^{-4})	0.6306	50.8	80.6	1.00	1295
Na- „	500,2 (10^{-5})	0.3188	53.3	170	2.11	698
Ca- „	1100,1 (5×10^{-3})	0.4262	184.0	433	5.37	1650
Mg- „	1100,1 (10^{-4})	0.2817	100.2	356	4.42	1678
Fe- „	1100,1 (10^{-3})	0.3439	139.4	405	5.02	1900
Al- „	1100,1 (10^{-3})	0.3618	112.0	310	3.84	1660

Before the surface area determination, the coke sample was evacuated at higher temperatures to eliminate the surface oxide and also residual volatile matters; "Pre-treatment in vacua" in Table II shows the conditions of this treatment and the treatment for Na-coke was made at 500°C lest metallic sodium should vaporize by the probable reaction of carbon with sodium oxide.

The specific surface area of metal-coke was about two or five times larger than that of H-coke, and the value of A_M/A_H in Table II is the specific surface area ratio of metal-coke to H-coke. The large specific surface areas of metal-coke compared with H-coke can be expected, as metallic ion exists in highly dispersed state in metal-humate and it is well known that when carbonaceous materials are carbonized with inorganic salts an increase in the surface area is obtained. T.D. Smith[5] had already obtained the similar results with barium mellitate. The values of A_M/A_H must probably depend on not only the valency of the metallic ions, but also their contents in the parent metal-humates.

Absolute Reaction Rates of Cokes from Humic Acid and Metal-humates with Carbon Dioxide.—The reaction rates of the present cokes having the known surface area and carbon dioxide at constant temperature and volume can similarly be expressed by the following equation as already stated in the first paper,

$$dP/dt = KP_{co_2}/P_{co} \qquad (1)$$

where K is a rate constant, P, the total pressure, t, the time, and P_{co_2} and P_{co} denote the partial pressure of carbon dioxide and carbon monoxide respectively.

The specific reaction rates per unit area of the coke surface K_a, expressed as the number of molecules reacted per sq. cm per second at $P_{co_2}/P_{co}=1$, can be calculated by the following equation (Eq. (8) in Ref. (2)) from the rate constant K and the total surface area of the coke S.

$$K_a = a \cdot K \cdot \frac{273}{760} \cdot \frac{1}{60} \cdot \frac{6.02\times10^{23}}{22400} \cdot \frac{1}{S\cdot10^4} \qquad (2)$$

The relations between K_a and $1/T$ for various cokes are shown in Fig. 2 and K_a may be expressed as:

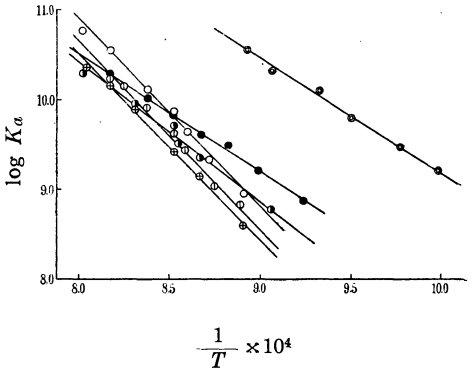


Fig. 2. Relations between log K_a and $1/T$
○ H-Coke, ⊕ Mg-Coke ◑ Al-Coke
① Ca-Coke, ● Fe-Coke ◎ Na-Coke

$$K_a = A \text{ exp. } (-E/RT), \qquad (3)$$

where A is a constant and E, the experimental activation energy. The values of A and E determined by the least squares are summarized in Table III. Although the large difference in A and E among H-, Ca- and

5) T. D. Smith, *J. Chem. Soc.*, **1952**, 923.

TABLE III

THE VALUES OF A AND THE ACTIVATION ENERGIES E

Cokes	$A_{obs.}$ molecules (cm^{-2} sec^{-1})	$A_{calcd.}$ molecules (cm^{-2} sec^{-1})	E (kcal./mol.)
H-coke	4.46×10^{27}	5.57×10^{27} (1173°K)	96.0
Na- „	7.75×10^{21}	4.98×10^{27} (1050°K)	58.3
Ca- „	1.12×10^{27}	5.57×10^{27} (1173°K)	94.0
Mg- „	1.29×10^{27}	„	95.1
Fe- „	1.00×10^{21}	„	60.1
Al- „	8.91×10^{22}	„	71.8

Mg-coke can not be seen, those of Fe-, Al- and Na-coke are much smaller than H-coke.

Provided that the reaction mechanism presented in the first paper may be applicable, the quantity A must be calculated from the following equation applying the absolute reaction rates theory (Eq. (14) in Ref. (2)),

$$A=kT/h\cdot L\cdot f_{co}/f_{co_2}\cdot f_a^{\neq}/f_s \qquad (4)$$

The calculated values of A are also given in Table III, using $L=10^{15}$, $f_a^{\neq}/f_s=1$, $T=1050$°K for Na-coke and $T=1173$°K for the other cokes. The difference between the observed and calculated values for H-, Ca- and Mg-coke is very small, but for Fe-, Al- and Na-coke, it is much greater than expected from the theory. Accordingly, it is concluded that the simple reaction mechanism presented in the first paper may be applicable for H-, Ca- and Mg-coke, but for the other cokes, a more complicated reaction may probably be occurring.

The specific reaction rates per unit area of the coke surface, K_{aM} for metal-cokes and K_{aH} for H-coke at various temperatures, can be calculated from Eq. (3) using the experimental values of A and E, and the ratio, K_{aM}/K_{aH}, is given in Table IV. From these values of K_{aM}/K_{aH}, we can clearly see the effects of metallic impurities on the absolute reaction rates of the coke-carbon dioxide system.

These values for Na-, and Fe-coke at lower temperatures are of the order of 10^1 or 10^2 and under the present experimental conditions it may be considered that metallic sodium for Na-coke and metallic iron or its carbide for Fe-coke would most probably take part in the reaction. These results agree well with those of earlier[1] and recent studies[6] that the most effective catalysts of inorganic additions to coke or pure graphite are the metals of the alkali group and metallic iron or its carbide.

In Ca-, and Mg-coke, calcium and magnesium impurities would exist as the oxides, which intend to inhibit the specific reaction rates per unit surface area to cabron dioxide as seen in Fig. 2 and Table IV. The behavior of Al-coke resembles very much to that of Fe-coke. The ratio of the maximum value of K_a to the minimum at one temperature for various cokes is in the range from 1.74×10^1 at 1000°C to 1.10×10^3 at 700°C evaluated from Table IV. It was already stated that these ratios were about 16 or 20 for various cokes investigated in the first paper and that K_a at 950°C in the second paper[3] changed irregularly with these ratios of 10^1 or 10^2 by the heat treatment of cokes from 1000° to 2000°C, and these experimental facts have been considered as the catalytic effects of the ash in coke. The present results of strong effects of metallic impurities would confirm that these considerations might be most reasonable.

Metallic impurities introduced as metal-humates have strong effects on the specific surface area of cokes from humic acid and on the absolute reaction rates of the coke with carbon dioxide, and the products of A_M/A_H in Table II and K_{aM}/K_{aH} in Table IV represent the effects of metal impurities on the apparent or relative reactivity of the coke. These values of the product are in the range from 1.08 to 1.01×10^3 for all metallic impurities investigated at 700° to 1000°C. That is, all metallic impurities investigated

6) E. A. Gulbransen and K. F. Andrew, *Ind. Eng. Chem.*, **44** 1048 (1952); W. F. K. Wynne-Jones, H. E. Blayden and H. Marsh, *Brenn. Chem.*, **33**, 233 (1952).

TABLE IV

THE RATIOS OF THE SPECIFIC REACTION RATES OF METAL-COKES TO THAT OF H-COKE AT VARIOUS TEMPERATURES

Cokes	K_{aM}/K_{aH}			
	700°C	800°C	900°C	1000°C
H-coke	1	1	1	1
Na- „	4.78×10^2	7.75×10^1	1.74×10^1	4.89
Ca- „	8.7×10^{-1}	7.9×10^{-1}	7.4×10^{-1}	6.9×10^{-1}
Mg- „	4.36×10^{-1}	4.26×10^{-1}	4.07×10^{-1}	3.98×10^{-1}
Fe- „	2.45×10^1	4.36	1.05	3.09×10^{-1}
Al- „	5.36	1.66	6.30×10^{-1}	2.81×10^{-1}

in the present study increase the relative reactivity of the coke.

Summary

The surface area of cokes from humic acid and metal-humates and the absolute reaction rates of these cokes to carbon dioxide at various temperatures have been determined by the same method and procedure as those described in the first paper.

The specific surface area of cokes from metal-humates are about two or five times larger than the coke from humic acid, and this increase is expected from the well-known fact that when carbonaceous materials are carbonized with inorganic salt an increase in the surface area is obtained.

The specific reaction rates per unit surface area K_a of these cokes and carbon dioxide can be expressed by an equation

$$K_a = A \exp. (-E/RT),$$

and the values of A and activation energies E have been determined. The activation energies of cokes from humic acid, Ca- and Mg-humates are about 95 kcal./mol. and a large difference is not seen among them, but those of cokes from Fe-, Al- and Na-humates are about 25–40 kcal./mol. smaller than H-coke. The experimental values of A for cokes from humic acid, Ca- and Mg-humate are in satisfactory agreement with those expected from the application of the absolute reaction rates theory to the reaction mechanism already presented in the first paper, but those of A for cokes from Fe-, Al- and Na-humate are much smaller than expected from the theory. These results may be considered to indicate that the more complicated reaction must be occurring for cokes from Fe-, Al- and Na-humates. Calcium and magnesium impurities have effects of decreasing the specific reaction rates per unit surface area of the coke from humic acid to carbon dioxide and on the other hand, aluminium, especially iron and sodium impurities at lower temperatures have great effects of increasing the specific reaction rates. The effects of these sodium and iron impurities agree well with the earlier results and the present results also confirm that the catalytic effects of impurities in coke play an important role in the absolute reaction rates of the coke-carbon dioxide system, which was assumed in previous papers.

By considering the effects of metallic impurities on both the specific surface area of cokes from humic acid and the specific reaction rates per unit surface area of the coke with carbon dioxide, all metallic impurities investigated increase the relative reactivity of the coke from humic acid and for example, sodium impurities increase the apparent reactivity of the coke about 10^3 times at 700°C.

In conclusion, the author wishes to express his heart-felt gratitude to Mr. A. Baba, Dr. H. Honda and Mr. Y. Yoshida for their valuable suggestions and deep interest in this study. The author's thanks are also due to Mr. R. Sato for his kind assistance, Mr. T. Yamakawa for a gift of humic acid and Mr. Y. Hirose for chemical analysis of the ash in coke.

Resources Research Institute
Saitama-Kawaguchi

On the Thermal Dissociation of Organic Compounds. VI. The Effect of the Substituent and That of the Solvent on the Thermal Dissociation of Ureas

By Teruaki MUKAIYAMA[1], Shōichiro OZAKI and Toshio HOSHINO

(Received June 9, 1954)

Introduction

It is known that, on heating, ureas dissociate thermally into isocyanates and amines.

$$RHN-CO-NHR \rightleftarrows R-N=C=O+H_2N-R$$

The kinetics of the thermal dissociation of urea and some substituted ureas in fatty acid solvents have been studied[2-4] and, in the case of urea in *n*-butyric acid, for example, the mechanism shown by Equations (1)-(4) was suggested.

1) Department of Physics and Chemistry, Gakushuin University, Mejiro, Tokyo.

2) T. Hoshino, T. Mukaiyama and H. Hoshino, *J. Am. Chem. Soc.*, **74**, 3097 (1952).

3) T. Hoshino, T. Mukaiyama and H. Hoshino, This Bulletin, **25**, 392 (1952).

4) T. Mukaiyama and T. Matsunaga, *J. Am. Chem. Soc.*, **75**, 6209 (1953).

$$H_2N-CO-NH_2 \rightleftarrows H-N=C=O+NH_3 \quad (1)$$
$$H-N=C=O+C_3H_7COOH \rightleftarrows C_3H_7CO-O-CONH_2 \quad (2)$$
$$C_3H_7CO-O-CONH_2 \longrightarrow C_3H_7CO-NH_2+CO_2 \quad (3)$$
$$NH_3+C_3H_7COOH \rightleftarrows C_3H_7COONH_4 \quad (4)$$

The dissociation of urea in fatty acid was considered as a general acid catalyzed reaction, which is shown by the following process.

$$H_2NCONH_2+RCOOH \longrightarrow H_3\overset{+}{N}CONH_2+RCOO^- \quad (5)$$
$$H_3\overset{+}{N}CONH_2 \xrightarrow{-H^+} H_2N-C=O \longrightarrow H-N=C=O+NH_3$$

As shown in the previous reports, the rates of dissociation of ureas are deeply dependent on the nature of solvents and the kind of substituents. In the present work, the dissociation of eight substituted ureas in five fatty acids were studied and the relation between the nature of acids and the kind of substituents were discussed.

The reaction can be followed by measuring the rate of evolution of carbon dioxide (Eq. 3), provided it is evolved as soon as formed. Since the reaction temperature was near 155° it is reasonable to believe that this is true, and also that the reverse reaction is negligible under the conditions of the experiments. If reaction (1) is the rate-determining step, then the rate of dissociation is measurable.

On plotting the logarithm of volume of carbon dioxide, ΔY, evolved at regular intervals of time, we have obtained a straight line. This indicates a first order reaction rate. The rate constant is given by the gradient of such a plot,[5] as shown in Fig. 1.

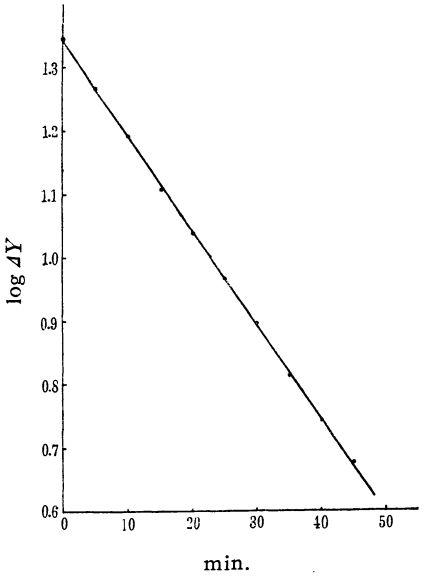


Fig. 1. The plot of t against log ΔY. 1, 1, 3-Triethylurea in n-capric acid at 155.1°C.

Experimental

The apparatus employed was the same as that described in previous reports.[2,3] In this experiment, the reaction vessel was maintained at desired, constant temperature by immersion into the thermostat containing rape-seed oil. In order to prevent the heat loss at this high temperature, the thermostat was surrounded by asbestos and placed in a cabinet thickly filled with glasswool. The temperature control of the reaction thermostat was accurate to ±0.03 within the temperature range 140—160° using a tetraline-mercury regulator.

Preparation of Materials.—*1, 1-Dimethylurea*: the commercial product, m.p. 181°, was used. *1, 3-Diethylurea*: from ethyl isocianate[6] and water, m.p. 110°, recrystallized from petroleum ether. *1, 1, 3-Triethylurea*[7]: from ethyl isocyanate and diethylamine, m.p. 65°, recrystallized from petroleum ether. *1, 3-Diisopropylurea*: from isopropyl isocyanate[8] and water, m.p. 190°, recrystallized from 70% aqueous ethanol. *1, 3-Dihexylurea*: from hexyl isocyanate and water, m.p. 75°, recrystallized from petroleum ether. Found N, 12.79%. Calcd for $C_{13}H_{28}N_2O$: N, 12.28%. *Hexyl isocyanate* was prepared from heptoic acid hydrazide *via* heptoic acidazide by heating in anhydrous benzene, b.p. 71—72°/31 mm. *1, 3-Dibenzylurea*: from benzyl isocyanate[9] and water, m.p. 167°, recrystallized from ethanol. *1, 1-Diethyl-3-isopropylurea*: from isopropyl isocyanate and diethylamine, m.p. 66°, recrystallized from petroleum ether. *1, 3-Di-t-butylurea*: from urea and *t*-butyl alcohol by the method described in Organic Syntheses,[10] m.p. 243° (in sealed tube), recrystallized from 80% aqueous ethanol.

Solvent: n-Butyric and n-caproic acids were distilled after boiling with phosphorous pentoxide and re-distilled employing a fractionating column, b.p. 159–160° and 104–106°/16.5–17mm, respectively. n-Capric acid was twice distilled in vacuo b.p. 121–123°/3.2–3.5 mm. Phenylacetic acid was recrystallized from water and then distilled in vacuo b.p. 117°/4.5 mm. Benzoic acid was used without further purification, m.p. 122°.

The rate constants for the thermal dissociation of ureas were determined under the following conditions: 1, 1, 3-triethylurea (1 mole) in n-capric acid (50 moles), given as an example of a typical run: Fig. 1. Ureas (1 mol.) in a carboxylic acids (50 mol.). The ureas were 1, 1-dimethyl, 1, 3-diethyl, 1, 1, 3-triethyl, 1, 3-diisopropyl, 1, 3-dihexyl, 1, 3-dibenzyl, 1, 1-diethyl-3-isopropyl and 1, 3-di-*t*-butyl. The acids were n-butyric, n-caproic, n-capric, phenylacetic and benzoic.

The results are summarized in Table I. The rates were first order with respect to ureas.

5) E. A. Guggenheim, *Phil. Mag.*, **2**, 538 (1926).
6) T. Curtius and H. Hille, *J. prakt. Chem.*, **64** 401 (1901).
7) Wurtz, Beilstein, IV, 120.
8) O. Hambsch, *J. prakt. Chem.*, **125**, 182 (1930).
9) T. Curtius and E. Boetzlen, *J. prakt. Chem.*, **64**, 316 (1901).
10) "Organic Syntheses," **29**, 18.

TABLE I

THE RATE CONSTANTS OF THE THERMAL DISSOCIATION OF UREAS IN FATTY ACIDS

$k \times 10^2$ (min.$^{-1}$) (at t°C)

ureas \ acids	*n*-butyric acid	*n*-caproic acid	*n*-capric acid	phenylacetic acid	benzoic acid
1, 1-dimethylurea	1.11 (139.5°)	2.97 (155.2°)	1.2 (155.1°)	3.02 (155.0°)	0.545 (155.0°)
1, 3-diethylurea		2.65 (155.2°)	2.66 (155.1°)	2.86 (155.0°)	1.07 (155.0°)
1, 1, 3-triethylurea	4.09 (139.5°)	3.42 (155.0°)	3.39 (155.1°)	10.9 (155.0°)	2.09 (155.0°)
1, 3-diisopropylurea	1.79 (139.6°)	2.61 (155.0°)	3.08 (155.0°)	4.86 (155.0°)	0.967 (154.95°)
1, 3-dihexylurea	1.24 (139.6°)	3.65 (155.0°)	3.26 (155.0°)	2.10 (154.9°)	0.659 (155.0°)
1, 3-dibenzylurea	1.27 (139.6°)	2.68 (155.0°)	2.70 (155.0°)	3.85 (154.9°)	0.418 (155.0°)
1, 1-diethyl-3-isopropylurea	3.15 (139.45°)	6.2 (155.0°)	3.19 (155.0°)	very fast (154.9°)	1.60 (155.1°)
1, 3-di-*t*-butylurea	3.87 (139.4°)	3.93 (155.0°)	6.8 (155.0°)	fast (155.0°)	0.900 (154.95°)

Discussion

According to the results of experiments summarized in Table I, the effects of solvents on the rate of dissociation of ureas are in the following order:

phenylacetic acid, *n*-butyric acid > *n*-caproic acid, *n*-capric acid > benzoic acid.

The *pKa* values for these five acids are shown in Table II.

TABLE II

THE *pKa* VALUES FOR FATTY ACIDS[11]

acid	*pKa*
n-butyric acid	4.82
n-caproic acid	4.85
n-capric acid	4.90
phenylacetic acid	4.31
benzoic acid	4.17

As known from their *pKa* values, if the dissociation of urea proceeds according to a general acid catalyzed reaction (5), the effects of solvents on the rate of dissociation should fall in the order,

Benzoic acid > phenylacetic acid > *n*-butyric acid > *n*-caproic acid > *n*-capric acid.

Benzoic acid, as shown in the above order, should accelerate the rates of dissociation of ureas more than the other four acids. However, the rates of dissociation of ureas in benzoic acid are very slow in comparison with that in other acids and this shows that the previously proposed mechanism (5) is an unsatisfactory one to explain the dissociation reaction.

As to the effects of substituents, it is shown by the present experiment that the rate of dissociation increases in the series,

urea < 1, 1-dimethylurea ≤ 1, 3-dibenzylurea < 1, 3-dihexylurea ≤ 1, 3-diethylurea, 1, 3-diisopropylurea < 1, 3-di-*t*-butylurea ≪ 1, 1, 3-triethylurea, 1, 1-diethyl-3-isopropylurea.

In the process of dissociation of urea, the one nitrogen atom of urea accepts a proton to form an amine and the other nitrogen atom donates a proton to form an isocyanate. Thus, there are two factors which can be considered to dominate the dissociation of ureas.

(a) Ability of one nitrogen atom in urea as a proton-acceptor, namely basicity.

(b) Ability of one nitrogen atom in urea as a proton-donor, namely acidity.

When one compares the relative strength of basities of ureas, those of corresponding amines may be used. A urea nitrogen atom having two substituents is bonded to three carbon atoms and therefore might be expected to behave as a tertiary one. However, by comparing the rate of dissociation of 1, 1, 3-triethylurea with that of 1, 3-diethylurea, the former urea dissociates more easily than the latter. The one nitrogen atom of these two ureas has the same substituent group and therefore the difference in reactivity is due to the difference in the ability of the other nitrogen atom as a protonacceptor. The fact shows that 1, 1, 3-triethylurea has a stronger tendency to accept a proton than 1, 3-diethylurea, namely, the former urea might be more basic. This conclusion does not agree with the consideration that the relative basity of a urea nitrogen atom having two substituents corresponds to that of a tertiary amine. In considering the structure of 1, 1, 3-triethylurea, one of three carbon atoms bonded to a urea nitrogen is that of carbonyl and, be-

11) L. F. Fieser and M. Fieser "Text-book of Organic Chemistry" p. 157 (1952).

cause of the planar configuration of carbonyl group, the B-strain[12] considered to exist in an ordinary tertiary amine is reduced in the urea. Accordingly, it may be reasonable to assume that the relative strength of a urea nitrogen atom having two substituents corresponds to the basity of secondary amine and that of a urea nitrogen having one substituent corresponds to that of primary amine.

The *pKb*[13] values for the corresponding amines are shown in Table III.

TABLE III
THE *pKb* VALUES FOR AMINES[13]

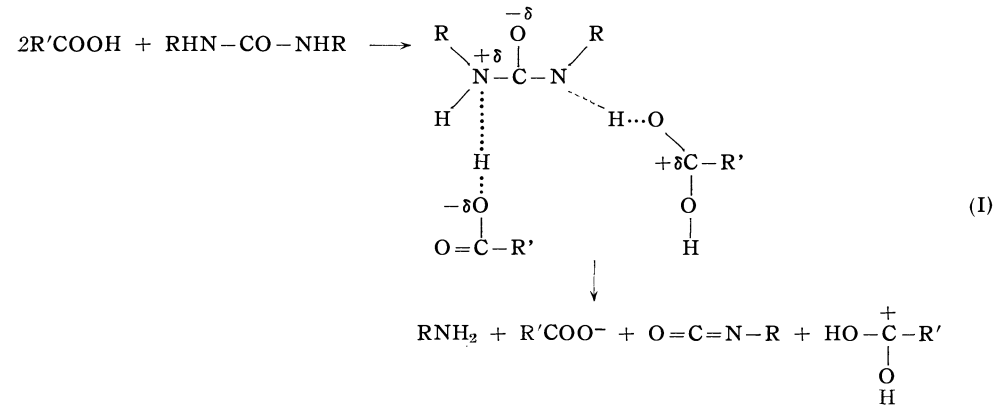
amine	*pKb*
dimethylamine	3.22
trimethylamine	4.13
ethylamine	3.28
diethylamine	2.90
triethylamine	3.36
isopropylamine	3.28
t-butylamine	3.47
benzylamine	4.62
ammonia	4.75

Just as the protonation of urea molecule by the solvent acid is an important factor on the dissociation, the deprotonation of urea molecule by the solvent acid is also an important one. In 1, 3-dibenzylurea, one nitrogen atom is a weak base which facilitates the deproponation and hence the reaction.

The effects of solvents and those of substituents mentioned above are explained by considering the following mechanism.

Under the condition of the experiments, the molar ratio of fatty acid to urea is 50 : 1, therefore the transition state (I) which contains two fatty acid molecules and one urea molecule might be considered as a reasonable one. One acid in the state (I) acts as an acid to donate a proton and the other acts as a base to accept a proton.

Contrary to the expectation that the stronger the acidity of solvent acid the faster the dissociation, the rates of dissociation of ureas in benzoic acid are slower than in the other acids. This slow rate may come from the



The effect of factor (a) on the dissociation reaction is shown in the results that 1, 1-diethyl substituted ureas dissociate faster than other 1-monosubstituted ureas and that urea itself dissociates slower than other substituted ureas. However, the results that the rate of dissociation of 1, 3-dibenzylurea is nearly equal to that of 1, 3-dihexylurea and that 1, 3-di-*t*-butylurea dissociates more readily than 1, 3-diethylurea can not be explained by the factor (a) alone. And factor (b), i.e. the ability of one nitrogen atom in urea as a proton-donor comes into consideration.

fact that the weak basicity of benzoic acid makes the deprotonation of urea in state (I) more difficult. That the rates of dissociation of ureas in *n*-butyric acid are faster than those in *n*-caproic and *n*-capric acids will be explained by considering the difficulty of forming a state (I) in the latter acids because of their spatial requirement. As described in the previous report,[2,4] the rates of dissociation of ureas in acetic, propionic and *n*-butyric acids fall in the following order:

acetic acid>propionic acid>*n*-butyric acid.

This order agrees with the above consideration that the smaller the molecular size the greater the frequency to attack urea molecule.

The effects of substituents controlled by two factors (a) and (b) on the thermal dissociation of ureas can also be explained by considering the state (I), in which two acids

12) In general, secondary amine is a stronger base than a tertiary one. This phenomenon does not agree with the tendency anticipated from the palar effect, and this was explained by the so-called B-strain proposed by H. C. Brown. L. N. Ferguson, "Electron Structures of Organic Molecules" p. 114, (1952).

13) Calculated from the dissociation constants. I. Heilbron et al., "Dictionary of Organic Compounds," Eyre & Spottiswoode Pub. Ltd. London (1946).

act as a proton-acceptor and as a proton-donor to one urea molecule at the same time.

It can be concluded that the thermal dissociation of ureas in fatty acids is more favorable when solvent acids and substituents tend to donate or accept a proton.

Summary

The rate constants of the thermal dissociation of 1,1-dimethyl, 1,3-diethyl, 1,3-diisopropyl, 1,1,3-triethyl, 1,3-dihexyl, 1,3-dibenzyl, 1,1-diethyl-3-isopropyl and 1,3-di-*t*-butyl ureas in *n*-butyric, *n*-caproic, *n*-capric, phenylacetic and benzoic acids were determined. The effects of substituents and those of solvents on the reaction rate were discussed. The transition state of the dissociation containing two fatty acids and one urea molecule was considered and the experimental results were reasonably explained by the proposed mechanism.

The Authors express their hearty thanks to Mr J. Kanai for his help in the early stage of this experiment.

Laboratory of Organic Chemistry,
Tokyo Institute of Technology,
Ookayama, Meguro, Tokyo

Alkylalkoxypolysiloxanes. II. Ethylisopropoxypolysiloxanes

By Rokuro ŌKAWARA and Iwao ISHIMARU

(Received June 15, 1954)

The reaction of secondary alcohol and chlorosilanes has not been so well studied as that of primary alcohol and chlorosilanes. Recently we reported on the preparation of isopropoxypolysiloxanes[1] from isopropanol and corresponding chloropolysiloxanes with good yield. The reaction of isopropanol and diethyldichlorosilane in refluxing benzene was studied by McCusker and Green.[2]

Now we wish to report on the preparation and properties of ethylisopropoxydichlorosilane (I), ethyldiisopropoxychlorosilane (II) and ethylisopropoxypolysiloxanes including ethyltriisopropoxysilane (III). Ethylisopropoxychlorosilanes, i. e. (I) and (II), were prepared by partial isopropanolysis of ethyltrichlorosilane. Data on these materials are given in Table I. In the case of preparing ethylethoxypolysiloxanes[3], in which one ethyl group attaches to each silicon atom, ethylethoxychlorosilane and ethyltriethoxysilane were mixed in various mole ratios and refluxed. In this experiment, the ethylisopropoxypolysiloxanes having the similar structure were prepared by the same method. But in this case the mixture of ethyltrichlorosilane (1 mol.) and isopropanol in a different mole ratio (2.3 to 2.5 mol.) were refluxed. The chlorine content of the refluxing mixture was gradually decreased by a thermal reaction and there was obtained some amount of isopropylchloride in a cold trap. It may be supposed that the thermal reaction occurred at the refluxing temperature between Si-Cl and Si-OC_3H_7 with the result of the formation of siloxane bond and isopropylchloride as follows:

$$\text{Si-OC}_3\text{H}_7+\text{Si-Cl}=\text{Si-O-Si}+\text{C}_3\text{H}_7\text{Cl}. \quad (1)$$

By fractional distillation, the chlorine-free mixture was separated into monomer, dimer and trimer fractions. By a rigorous redistillation of the polymer fractions, a small amount of cyclotrimer was obtained between the plateaus of dimer and linear trimer. Data on these polysiloxanes which belong to the linear-and cyclo-series as indicated by formula (A) and (B) are given in Table III.

$$\text{RO}\left(\begin{array}{l}\text{C}_2\text{H}_5\\|\\\text{SiO}\\|\\\text{OR}\end{array}\right)_n\text{R} \quad \text{R}=\text{CH}(\text{CH}_3)_2\ n=1-3 \quad (A)$$

$$\left(\begin{array}{l}\text{C}_2\text{H}_5\\|\\\text{SiO}\\|\\\text{OR}\end{array}\right)_n \quad \text{R}=\text{CH}(\text{CH}_3)_2\ n=3 \quad (B)$$

To obtain a series of compounds as indicated by formula (C) which have more isopropoxy groups in a molecule than the compounds of formula (A) have, the thermal reaction between (II) and tetraisopropoxysilane (IV) or (II)

1) R. Okawara, T. Tanaka and I. Ishimaru, This Bulletin, **27**, 45 (1954).
2) P. A. McCusker and C. E. Green, *J. Am. Chem. Soc.*, **70**, 2807 (1948).
3) R. Ōkawara, This Bulletin, **27**, 428 (1954).

$$C_2H_5\left[\begin{array}{c}OR\\|\\SiO\\|\\OR\end{array}\right]_n R \qquad (C)$$

$R=CH(CH_3)_2$ $n=2-3$

and hexaisopropoxydisiloxane (V) was carried out.

On fractional distillation of the chlorine-free product, the constant boiling fraction which belongs to the series (C) was obtained. But there is a probability of the compound of the series (C) being contaminated by a small amount of the compound of series (A) or the isopropoxypolysiloxane of the same polymer size which may be formed by side reactions.

Experimental

Starting Materials.—The ethyltrichlorosilane used in this experiment was prepared by the reaction of ethylchloride with copper-silicon and was purified by fractionation through a helices-packed column of about 20 plates. The redistilled fraction having the boiling point 98°–99°C (760mm Hg) was taken as a starting material. Found: Cl, 64.0. Calcd. for $C_2H_5SiCl_3$: Cl, 65.0%.

Isopropanol of Shell Chemicals (b.p. 82.2°C, n_D^{20} 1.3776) was used without further purification. Tetraisopropoxysilane (IV) and hexaisopropoxydisiloxane (V) used for the preparation of the compounds of the series (C) were prepared as already described.[1]

Tetraisopropoxysilane (IV): b.p. 93°–4°C/28 mmHg, n_D^{20}1.3835, d_4^{20}0.8744. Found: Si, 10.59, Calcd. for $(C_3H_7O)_4Si$: Si, 10.62%.

Hexaisopropoxydisiloxane (V): b.p. 82°–3°C/1mmHg, n_D^{20}1.3921, d_4^{20}0.9236. Found: Si, 13.14, Calcd. for $(C_3H_7O)_6Si_2O$: Si, 13.17%.

Exp. No.	Ethyltrichlorosilane (a) (g.)	Isopropanol (b) (g.)	Mole Ratio (b)/(a)	"Refluxing Mixture" (g.)	"Refluxing Mixture" (% theory)	% Cl Found	% Cl Calcd.
1	29.5	27	2.5	41	102	7.9	8.0
2	45.5	40	2.4	61	100	9.8	9.7
3	49	42	2.34	65	100	10.3	10.8

Preparation of Ethylisopropoxychlorosilanes.—*Ethyldiisopropoxychlorosilane (II).* Ethyltrichlorosilane (41g.: 0.25 mol.) was placed in a 500 cc. three-necked flask equipped with an efficient stirrer, a reflux condenser and a dropping funnel. Isopropanol (30g.: 0.5 mol.) was added drop by drop for one hour with vigorous stirring. During the addition the temperature of the mixture was kept at 3° to 5°C. After the addition the mixture was aerated at room temperature (10°C) with dry air to bubble off the hydrogen chloride until the weight of the mixture attained the calculated value. After aerating for 40 minutes the weight of the mixture attained the calculated value (53g.) and the chlorine content of the mixture was 16.6% (calcd. 16.8%). The mixture was fractionated through a semi-micro stedman column of about 20 plates under reduced pressure.

The following fractions were obtained.

The first fraction: 4g., b.p. 70°–76°C/48 mmHg, Found Cl, 18.1%.

The second fraction: 27g., b.p. 76°C/48 mmHg, Found Cl, 16.7%.

The third fraction: 4g., b.p. 76°–78°C/48 mmHg, Found Cl, 13.6%.

The residue: 11g. Found: Cl, 2.1%.

The second fraction (yield: 50% theory) may be considered to be pure (II). (Calcd. for (II): Cl, 16.8%).

Ethylisopropoxydichlorosilane (I). From 41g. (0.25 mol.) of ethyltrichlorosilane and 15g. (0.25 mol.) of isopropanol treated in the same way as above, 44g. of the product (calcd. 47g.) of which the chlorine content is 36% (calcd. 37.9%) was obtained. By fractionating the product through the same semi-micro stedman column under 60 mmHg, 15g. of the fraction boiling at 67°C/60 mmHg was collected. Found Cl, 37.4 Calcd. for (I): Cl, 37.9%. The constants of ethylisopropoxychlorosilanes were determined by the redistilled product and are summarized in Table I.

TABLE I

ETHYLISOPROPOXYCHLOROSILANES

Name	Boiling Point °C/mmHg	Refractive Index n_D^{20}	Density d_4^{20}	Molecular Refraction Found (Calcd.)*	% Cl Found (Calcd.)
Ethylisopropoxydichlorosilane (I)	66–7/59	1.4115	1.0508	44.23 (44.19)	37.4 (37.9)
Ethyldiisopropoxychlorosilane (II)	74–6/48	1.4018	0.9361	54.73 (54.58)	16.7 (16.8)

* Calculated from bond refractivities by E. L. Warrick, *J. Am. Chem. Soc.*, **68**, 2455 (1946).

Preparation of the Ethylisopropoxypolysiloxanes of the Series (A) and (B); (Exp. 1 to 3 in Table II).—The "refluxing mixtures" of Exp. 1 to 3 were prepared by adding isopropanol to ethyltrichlorosilane with vigorous stirring and aerating the products at room temperature until the weight of the products attained the calculated value as described in the preparation of ethylisopropoxychlorosilanes. The amounts of the ethyltrichlorosilane, isopropanol and the product obtained were as follows.

The composition of the product which was used as the "refluxing mixture" was calculated from its chlorine content by assuming that only (II) and (III) were present in it and was given in Table II as "Refluxing Mixture".

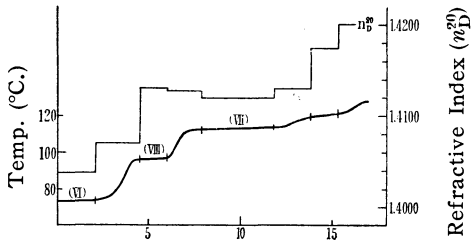


Fig. 1. Redistillation of the polymer fraction of ethylisopropoxypolysiloxanes. (VI): Dimer, (VII): Linear trimer, (VIII): Cyclotrimer

TABLE II

Exp. No.	Refluxing Mixture Compds.* (A) (B)	(g.)	Mole Ratio (A)/(B)	Time (hr.)	Highest Temp. (°C)	Product (g.)	Product (% theory)**	Composition of the product Monomer (%)	Dimer (%)	Trimer (%)	Residue (%)
1	(II)	18.8	1	64	205	29	87.8	60	12	—	28
	(III)	21.2									
2	(II)	35.5	1.5	64	205	43	91.5	47	8	13	32
	(III)	25.5									
3	(II)	41.4	2	112	205	47	96	31	14	7	48
	(III)	23.6									
4	(II)	4.5	0.5	144	210	9.8	86	12	11	—	77
	(IV)	8.6									
5	(II)	10.5	1	64	285	24.9	88.6	0	36	20	44
	(V)	21.4									

* (II): $C_2H_5Si(OC_3H_7)_2Cl$, (III): $C_2H_5Si(OC_3H_7)_3$
(IV): $(C_3H_7O)_4Si$, (V): $(C_3H_7O)_6Si_2O$

** Ratio of the amount of the polysiloxane obtained to the calculated amount of the polysiloxane.

TABLE III

ETHYLISOPROPOXYPOLYSILOXANES

Polymer Size	Name	Boiling Point °C/mmHg	Density d_4^{20}	Refractive Index n_D^{20}	Molecular Refraction Found (Calcd.)*	Molecular Weight Found** (Calcd.)	% Si Found (Calcd.)
	Series (A) and (B)						
Monomer	Triisopropoxyethylsilane (III)	65.4/8	0.8607	1.3938	65.12 (64.97)	241 (234)	11.84 (11.98)
Dimer	Tetraisopropoxy-1,3-diethyldisiloxane (VI)	73/0.8	0.9091	1.4038	98.58 (98.26)	362 (367)	15.64 (15.32)
Linear Trimer	Pentaisopropoxy-1,3,5-triethyltrisiloxane (VII)	112–3/0.8	0.9444	1.4120	131.38 (131.55)	489 (499)	17.14 (16.88)
Cyclotrimer	Triisopropoxy-1,3,5-triethylcyclotrisiloxane (VIII)	96–7/0.8	—	1.4131	—	398 (397)	20.75 (21.23)
	Series (C)						
Dimer	Pentaisopropoxy-ethyldisiloxane (IX)	82–3/0.8	0.9193	1.3962	103.71 (103.65)	404 (397)	13.67 (14.15)
Trimer	Heptaisopropoxy-1-ethyltrisiloxane (X)	114–5/0.8	0.9570	1.4027	141.9 (142.3)	563 (559)	15.21 (15.06)

* Calculated from bond refractivities (Table I footnote)

** Cryoscopic measurements in benzene

The mixture was refluxed until the chlorine could not be detected by Beilstein test. During the course of refluxing a small amount of liquid product was collected in a cold trap. Its boiling point (34.5°C) accorded well with that of isopropylchloride. The time required to produce the chlorine-free mixture and the highest refluxing temperature attained are cited in Table II.

The products were fractionated through a semimicro stedman column of about 30 theoretical plates under reduced pressure. Ethyltriisopropoxysilane (III) was distilled out at 65°C/8 mmHg. The disiloxane and trisiloxane fractions were the succeeding plateaus which were obtained at 73°C/0.8 mmHg and 112°C/0.8 mmHg. The amounts in percentage of these plateaus including the intermediate fractions cut on the distillation curve are also shown in Table II. As the amounts of disiloxane and trisiloxane fractions were small and fairly large amounts of the intermediate fraction was found between them, all the polysiloxane fractions were again fractionated rigorously through the same column. The distillation curve and the refractive index of the small portions are shown in Fig. 1.

Properties of these compounds are given in Table III.

In the preparation of ethylethoxypolysiloxanes[3] carried out by the same method, a smaller amount of cyclotrimer than in this experiment was supposed to be present between the plateaus of dimer and linear trimer, but it could not be isolated.

Preparation of the Ethylisopropoxypolysiloxanes of the Series (C): (Exp. 4 and 5).—In experiments 4 and 5, ethyldiisopropoxychlorosilane (II) and tetraisopropoxysilane (IV) or hexaisopropoxydisiloxane (V) were refluxed until the mixture became chlorine free.

Analysis of Silicon.—Silicon was determined by decomposing the sample with concentrated sulfuric acid.

Summary

(1) Ethylisopropoxychlorosilanes have been prepared and characterized.

(2) By the thermal reaction of partially isopropanolysis product of ethyltrichlorosilane, linear ethylisopropoxypolysiloxanes containing from 1 to 3 silicon atoms and cyclotrisiloxane have been prepared and characterized.

(3) Ethyldiisopropoxychlorosilane and isopropoxypolysiloxanes were refluxed and the two compounds of the series of linear ethylisopropoxypolysiloxanes in which one terminal group is the ethyl one have been synthesized and characterized.

Department of Applied Chemistry,
Faculty of Engineering,
Osaka University,
Osaka

Thermionic Emission from Catalyst for Ammonia Synthesis. I. Electron Microscopic Images of the Catalysts

By Hiroshi UCHIDA and Naoyuki TODO

(Received June 12, 1954)

Introduction

Potash is an important promoter used in iron catalysts for ammonia synthesis and Fischer-Tropsch synthesis. On heating the catalyst, potash or potassium becomes liable to emit electrons or potassium ions from the surface. In this connection, C.H. Kunsman[1] measured thermionic emission from iron catalysts for ammonia synthesis already in 1926 and recently Y. Osumi[2] observed the electronic emission image of the catalyst in the oxidic as well as the reduced state and attained to notably interesting results in comparison with the optical. It can be readily understood that the measurements of the thermoelectronic emission provide detailed knowledge on the state of potash in the catalyst. The authors studied accordingly the thermoionic emission by means of the electronic image observation as well as the quantitative thermionic measurement on the catalysts whose catalytic activity for ammonia synthesis, microscopic structure and surface structure, such as area and average pore size, had already been investigated. Results

1) C. H. Kunsman, *J. Phys. Chem.*, **30**, 535 (1926).
2) Y. Osumi, This Bulletin, **26**, 515 (1953).

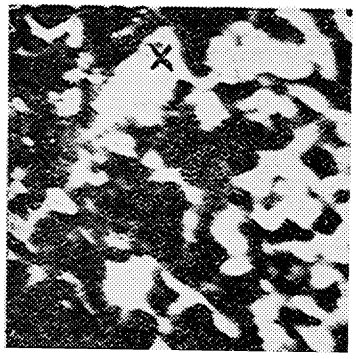


Fig. 1a. Cat. No. 1
Electronic image (830°C)
(Oxide) ×40

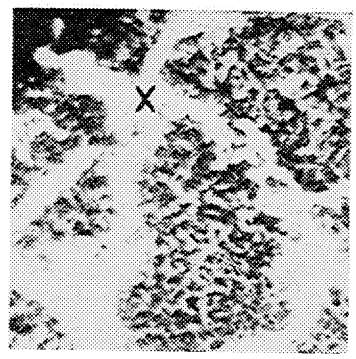


Fig. 1b. Cat. No. 1
Electronic image (450°C)
(Reduced for 5 min.)

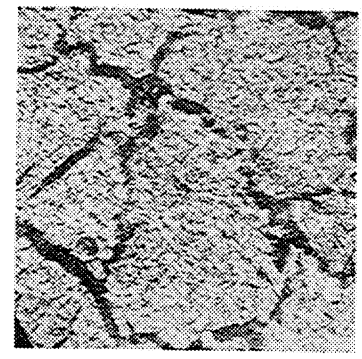


Fig. 1c. Cat. No. 1
Optical image
(After electr. emis.)

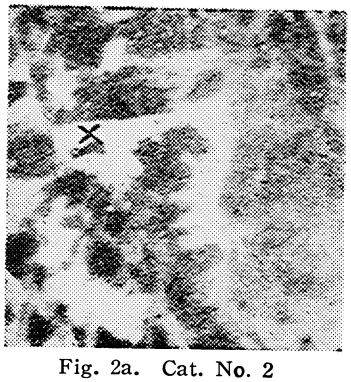


Fig. 2a. Cat. No. 2
Electronic image (870°C)
(Oxide)

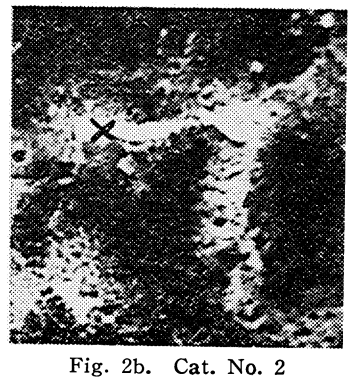


Fig. 2b. Cat. No. 2
Electronic image (680°C)
(Reduced for 20 min.)

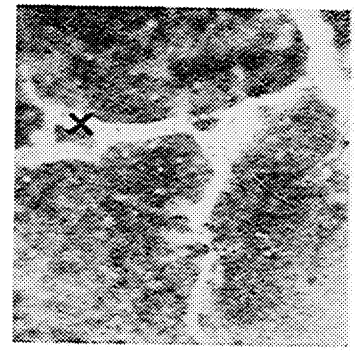


Fig. 2c. Cat. No. 2
Electronic image (760°C)
(After 30 min. observ. of
Fig. 2b)

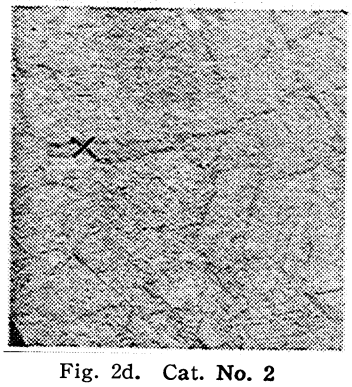


Fig. 2d. Cat. No. 2
Optical image
(After electr. emis.)

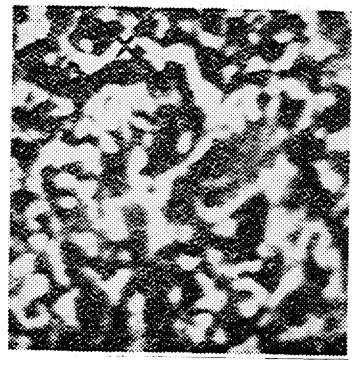


Fig. 3a. Cat. No. 3
Electronic image (800°C)
(Oxide)

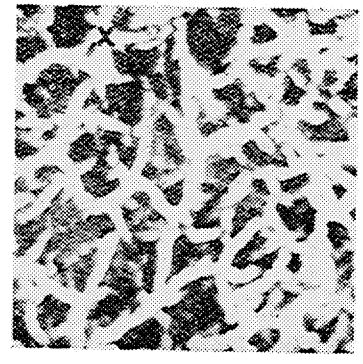


Fig. 3b. Cat. No. 3
Electronic image (780°C)
(Reduced for 5 min.)

obtained on the electronic image observation have lead to a qualitative understanding of potash in the synthetic ammonia catalyst. The results on this thesis will be described in this paper, while the quantitative measurement will be described in the next.

Experimental

Procedures.—The surface electron microscope was of similar type to that used by N. Sasaki[3] and Y. Osumi[2]. Specimens for the electron microscope examination were prepared by polishing with emery paper, finishing with grade 0.5 and finally on cloth to get rid of emery dust from voids. They were of 4 mm. in diam. and 1–1.2 mm. in thickness. The temperature could be raised by heating tungsten filament inserted into the specimen holder and was measured by means of a thermocouple spot-welded as close as possible to the specimen. After the electronic images had been observed on oxidic state, the oxide was reduced at 450°C by passing hydrogen through the microscope at normal pressure. The reduction was stopped at intervals to observe successive alternation of the electronic image. Immediately after the electronic observations, the specimens were removed from the electron microscope to an optical microscope under which they were observed by oblique illumination so that a fair estimate of cracks and hollows on the section was facilitated. The specimens were fused synthetic ammonia catalysts prepared according to a procedure by G. Shima and one of the authors[4] and of the following respective different compositions of the promoters, No. 1: 1% K_2O, No. 2: 5% Al_2O_3, 1% K_2O, No. 3: 4% Al_2O_3, 1% CaO, 1% K_2O, No. 4: 3% Al_2O_3, 2% SiO_2, 1% K_2O, No. 5: 3% Al_2O_3, 2% SiO_2, 1% CaO, 1% MgO, 2.5% K_2O. Their actual potash content was determined by the use of hexyl calcium and found somewhat less than what was expected from the composition of raw material, as shown below respectively, No. 1: 0.86%, No. 2: 0.81%, No. 3: 0.89%, No. 4: 0.71%, No. 5: 1.91%.

Experimental Results

The electronic images are shown from Figs. 1 through 5, in each of which the magnification factor is 40 with an exception of Fig. 4 (×60), together with respective optical micrographs after the electronic observations.*

Catalyst No. 1.—At an earlier stage of 3 minutes, observations showed a bright net work of the emission which gradually decreased in brightness to Fig. 1a which remained almost the same for additional 10 minutes. On reducing the oxide for five minutes, a bright and quite different net work of the emission appeared at such a low temperature as that of 450°C (Fig. 1b). Besides this image, there was not found any homogeneous emission which used to appear on the catalysts containing alumina. On raising the temperature to 750°C, the emission rapidly disappeared. The subsequent optical image is shown in Fig. 1c. In comparison with Figs.1a, b and c, the cracks in the optical image coincide accurately with the net works of Fig.1b, whereas they do not with Fig. 1a.

Catalyst No. 2.—Bright emission patterns were observed together with weaker emission over the whole surface of the oxide (Fig. 2a). On reduction, twenty minutes were required until an abrupt and a very marked change of the image took place as is shown in Fig. 2b. A part of the emissions from the oxide disappeared and new assemblages of fine bright specks appeared. On continuing the reduction for thirty minutes, the specks disappeared and the emission became rather homogeneous over the whole surface across which a few emission bands still shone.** Cracks and a few particular grains surrounded with cracks on the optical image (Fig. 2d) corresponded exactly to the places where the brighter emissions took place on Fig. 2b.

Catalyst No. 3.—As is shown in Fig. 3a, emission images with marked contrast developing appeared on the oxide. A few minutes after the beginning of reduction, the image changed abruptly to a new net work almost independent of the image in the oxide (Fig. 3b). On the continued observations, the emissions decreased in number and brightness till to Fig. 3c which could be closely related to the optical image (Fig. 3d).***

Catalyst No. 4.—The emission was so weak that the image could hardly be observed at the temperatures below 880°C (Fig. 4a). As it had been reported[5], the catalyst, added with silica, contained glassy inclusions on the polished section of the oxide (Fig. 4b). When the emission images were compared with the optical on the oxide, it could readily be detected that the bright emissions occurred from the glassy inclusions. The major part of the emission images remained after the reduction.

Catalyst No. 5.—The emissions became suf-

3) N. Sasaki, R. Ueda. T. Kuroda and H. Okamoto, *J. Soc. Metal, Japan*, **16**, 165 (1950).

4) G. Shima and H. Uchida, *Rep. Chem. Ind. Res. Instit. Tokyo*, **45**, 369 (1950).

* A paper provided with more of photographs will be published in the *Rep. Chem. Ind. Res. Instit., Tokyo.*

** On the electronic images from the oxide, there were observed black specks which began to shine after the oxide was reduced for 20 minutes; specks of this sort were observed only on catalyst No. 2 and the nature has not been accounted for in this paper.

*** When magnesia was used instead of lime, there were not found any emissios on the oxide except for those from the places corresponding to the cracks.

ficient to be observed at 780°C. Among the emission images, some took crystalline appearances (Fig. 5a), corresponding to the crystalline inclusions* which used to appear on the polished sections with increasing amounts of potash, as reported previously[5]. On reduction, the images of crystalline outline remained, whereas those of narrower bands and specks disappeared, and a rather homogeneous emission over the whole surface associated with a number of new narrow bands appeared (Fig. 5b). The emission image obtained after the reduction relates to the optical (Fig. 5c) similar to the findings with catalyst No. 2.

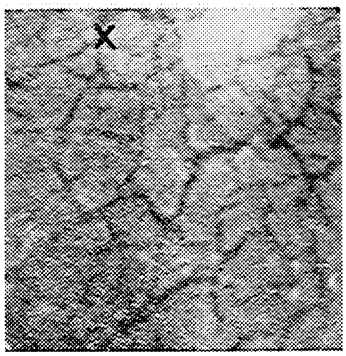


Fig. 3c. Cat. No. 3
Electronic image (850°C)
(After 5 min. observ. of Fig. 3b)

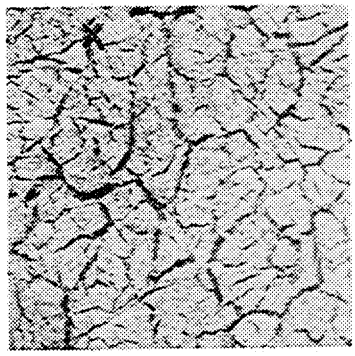


Fig. 3d. Cat. No. 3
Optical image
(After electr. emis.)

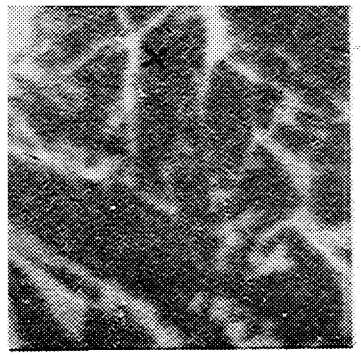


Fig. 4a. Cat. No. 4
Electronic image (900°C)
(Oxide) (×60)

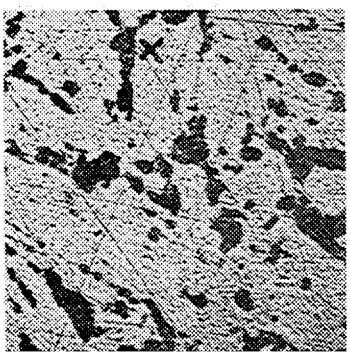


Fig. 4b. Cat. No. 4
Optical image of oxide
by vertical illuminat.
(×60)

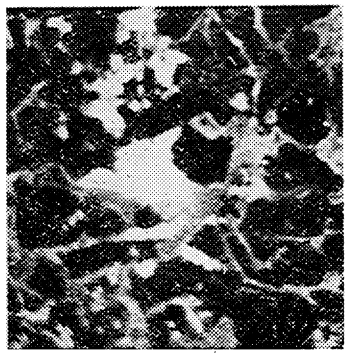


Fig. 5a. Cat. No. 5
Electronic image (850°C)
(Oxide) ×40



Fig. 5b. Cat. No. 5
Electronic image (780°C)
(Reduced for 5 min.)

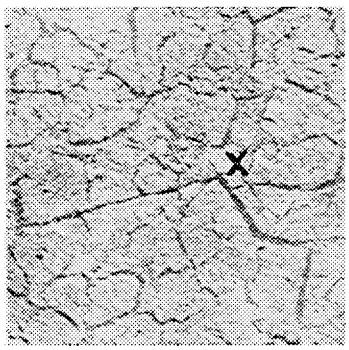


Fig. 5c. Cat. No. 5
Optical image
(After electr. emis.)

Grain Boundary.—On polishing on emery paper and then with red iron oxide on a rotating pad, well marked grain boundaries by ordinary vertical illumination were developed by etching with hydrochloric acid as shown in Fig. 7 at a magnification of X 100. Broader grain boundaries enclose large grains (parent grain) which are divided into a number of fine fragments by unifrom orientation of etch marks on the grains. The catalyst consists of a mosaic like structure of such fine

* On catalyst No. 5, the inclusions could be observed only on the section thoroughly polished with red iron oxide on a rotating pad, in use of which the electronic emission observations were difficult to investigate.

5) H. Uchida, N. Todo and K. Ogawa, *Rep. Chem Ind. Res. Instit., Tokyo*, **46**, 11 (1951).

grains***. Though the specimens polished to such an extent that they were used for the electron emission revealed also patterns shown in Fig. 6, they could be by no means related to the grain boundaries in Fig. 7. It has thus proved that a prediction of grain boundaries from optical patterns on the specimen prepared for the electronic emission is a matter of considerable difficulty. On the other hand, when the section of Fig. 7 was reduced, every crack developed along the etch marks, i. e. the grain boundaries Fig. 9. This could be also confirmed on the other catalysts.

Discussion

It may be estimated with certainty that electrons may easily emit from the place rich in potash or potassium. If additives were always liable to accumulate in the grain boundaries of the oxide, the electronic emission would take place along the boundaries. In this respect, reference is made to a recent article by Y. Osumi[2] who has thought electrons emit mainly from the parts which existed at the grain boundaries as a result of his electronic and optical images comparison. He called this particular part B, distinguishing itself from another part A more abundant in the catalyst. However, in our observations, marked changes of the emission images took place frequently in course of reduction and the places on which the emission was observed in the oxidic state frequently did not correspond to those in the reduced state. Furthermore, the net works of the emission from the reduced, which are quite different from those from oxides, always coincide exactly with the grain boundaries. It, therefore, can not be said reasonably that the emission images from the oxides correspond always to the grain boundaries. Alternation of the emission images in course of the reduction occurred in different manners as described before. Among them, those which were observed on both the oxidic and the reduced were either of relatively wide bands (catalyst No. 2 and 3), or of crystalline outline (catalyst No. 5). Cracks were observed around them on the optical image. They may correspond to interfacial crystallites or grains rather than grain boundaries and the promotors such as potash may segregate in such particular grains. Y. Osumi has already observed that bright emission occurres along the cracks produced by reduction and the fact has been interpreted by himself as being due to migration of active substance such as potash or potassium from beneath to the surface by way of the cracks. The beautiful net work of the emission which coincides with the cracks may therefore give a measure for estimation of the cracks; however, it is not directly related to distribution of potash or potassium in the catalyst. Information concerning the distribution in the oxide may be afforded by another kind of the emission images, which is observed in the oxidic, but is scarcely ever observed at the same places in the reduced. The particular regions where the above kind of the image appears will be searched on the polished and etched section of catalyst No. 3 under an optical microscope. By ordinary vertical illumination (Fig. 7), there are found in the parent grain several shining areas which appear as voids when observed by oblique illumination (Fig. 8). The shining is due to the surface of the grains underlying these having dissolved out with hydrochloric acid. The voids could also be observed more or less marked on the other catalysts; for example, on catalyst No. 2, they were shallow and the areas shining by vertical

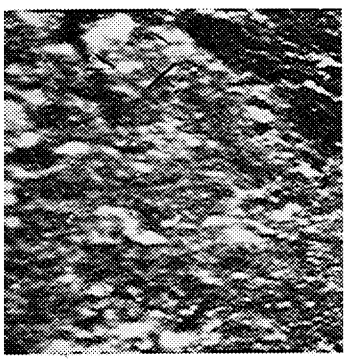


Fig. 6. Cat. No. 3
Oxide by oblique illumination
×100



Fig. 7. Cat. No. 3
Oxide by vertical illumination (Thoroughly polished and etched surface)

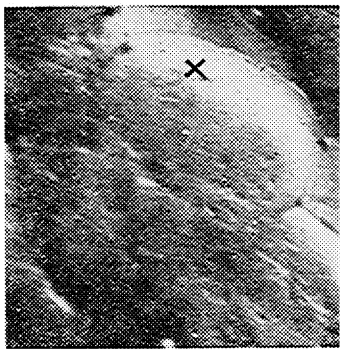


Fig. 8. Cat. No. 3
Fig. 7 by Oblique illumination

illumination were hardly observed. The parent grain may be thus estimated to be divided into those sub-grains which are readily etched with hydrochloric acid and those which are etched with difficulty more or less markedly according to the kind of the catalysts. The voids thus observed on catalyst No. 3 are mostly like the emission images from the oxide in shape and dimension. Since the subgrains readily etched are expected to be rich in potash and to be liable to emit electrons, the bright emission images on the oxide may well be related to the voids, that is to say, to the sub-grains which existed at the voids before they were dissolved out by hydrochloric acid.



Fig. 9. Cat. No. 3
Reduced surface of Fig. 8

On the catalysts No. 2, 3 and 4, the catalytic activities for ammonia synthesis were measured at a pressure of 100 kg./cm², and the surface areas*, the surface concentrations of potash (+lime)**, the average pore radii*** were also measured on the specimens after the use for the activity measurements[6]. The results are shown again in Fig. 10 and Table I together with those on catalyst No. 5 respectively. A catalyst promoted with alumina, potash and magnesia instead of lime has almost the same activity as catalyst No. 2 (Fig. 10). An attempt will be made to account for promoting action of the additives from the view point of the electron emission image. On adding alumina, potash seems to be stabilized in view of the fact that the emissions were retained over the whole surface on prolonged heating with catalyst No. 2, while

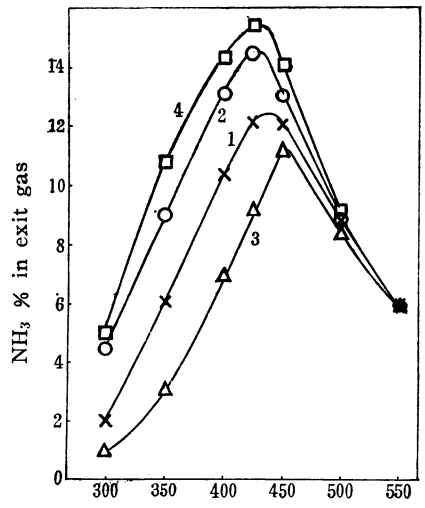


Fig. 10. Ammonia synthesis at 100 kg./cm² and S.V. 5000 in use of 20 cc. Cat. 1; No. 2, 2; No. 3, 3; No. 4, 4; No. 5

they disappeared rapidly with catalyst No. 1. Excellent dispersion of potash is thus observed from the emission image of catalyst No. 2. An addition of lime causes an appreciable increase of the activity as well as the markedly heterogeneous emission which is estimated to be due to the particular subgrains as described above. When magnesia was used instead of lime, there have been found neither the increase of the activity nor the heterogenous emission. The promoting actions of lime for the activity are thus probably ascribed partially to its effect for the formation of the well marked sub-grains in the parent grains, besides that of increasing the surface area (ref. Table I). As for

TABLE I

Catalyst	No. 2	No. 3	No. 4	No. 5
Surface Area, m²/g.	6.11	8.48	7.21	6.0
Surface Concentration of Potash	0.61	0.56	0.20	0.74
Average Pore Radius, Å	400	301	322	460

the addition of lime, A. Nielsen[7] has described that it makes the phase less anisotropic as observed by polarized light and consequently increases the thermostability of the catalyst. On the contrary the surface becomes more heterogeneous on the addition according to our observation and this is consistent with our results[8] that catalyst No. 3 is less thermostable than catalyst No. 2, while the former is superior in the activity to the latter.

** By means of observation under electron microscope on replica of the etched surface, the grains seemed to consist of fine crystallites as small as a few microns in diameter.

* Calculated from isotherms of physical adsorption of CO_2 by means of BET method.

** Represented by ratio of value of chemisorbed CO_2 to that of monomolecular adsorption at 78°C.

*** Average pore radius is calculated by $r=2\times v/S$, where v is pore volume (volume by mercury displacement-volume by water displacement) and S, surface area.

6) H. Uchida and N. Todo, *J. Chem. Soc. Japan* (Industr. Sect.), **56**, 225 (1953).

7) A. Nielsen, "Advances in Catalysis and Related Subjects," Academic Press Inc., New York, **5**, 1 (1953).

8) H. Uchida, *Rep. Chem. Ind. Res. Instit. Tokyo*, **46**, 1 (1951).

On the microscopic examination of catalyst No. 4 containing sillca, glassy grains are present. As potash is liable to segregate in these grains as described, potash is poorer in the major surface free from these grains than it is in catalyst No. 2 and 3, since the total content is almost the same in every three. The part played by the addition of silica may therefore reduce the surface concentration of potash and consequently cause a decrease of the activity. From this view point, a simultaneous addition of potash sufficient to spread in every grain of catalyst with addition of sillica will probably contribute to a recovery of the activity. The estimation is confirmed with the results with catalyst No. 5.

H. Kobayashi et al[9] have found recently that potash can be divided into those soluble in water and those insoluble and that the larger the content of the latter the higher the activity for ammonia synthesis. They have also described a relation between them, according to which a rapid linear increase of the activity is accompanied with the insoluble potash content till to 0.4% potash, beyond which the increase becomes gradually more slow, showing a bend at this content. The value of 0.4% has been considered by them as a limiting content of potash in A part by Y. Osumi. As has been indicated by H. Kobayashi, the activity remains quite low as far as the insoluble content dose not exceed 0.4%. It is therefore necessary to increase the content more and more to obtain any catalyst appropriate for the industrial use. On the basis of our results on the optical as well as the electronic emission images, potash in excess of that possessed by the catalyst distributed homogeneously in the bulk is found locally in the following three kinds of the regions such as, 1 grain boundaries, 2 particular sub-grains in the parent grains, 3 interfacial grain (glassy or crystlline) especially in the particular case where promoters such as silica are used. On reducing the catalysts, they afford a large surface area as shown in Table I respectively. Among the above three, the grain boundaries might contribute to a very small area even if the grains were of the dimension of a few microns. Secondly, the interfacial grains occupy only a small fraction of the total number of the grains and their presence seems not to contribute to an increase of the surface area as well as the activity as it is proved on the latter with catalyst No. 4. In contrast, the particular sub-grains may most contribute to the surface area, as they occupy a wide region of the grains wherein numerous fine pores appear on reduction. It may therefore be probable that the insoluble potash exceeding the limiting value of 0.4% may exist in these sub-grains, so this fact may contribute most to the activity. These sub-grains are liable to appear markedly on addition of lime, and, ndeed the catalyst shows high activity. The authors would finally like to mention that the appearance of the particular sub-grains may be accelerated not only in use of adequate promoters, but may also be favored by maintaining the temperature during the fusion as high as possible so that the segregation of potash in the grain boundaries may be avoided.

9) H. Kobayashi and O. Nishijima, *J. Chem. Soc. Japan* (Industr. Sect.), **57**, 189 (1954).

Summary

The electronic images have been observed on 5 types of the catalysts for ammonia synthesis, which are different in promoter-composition. On heating the oxides from 750 to 900°C, the images of different kinds which were characterized by their respective promoters compositions appeared after a few minutes. On reduction, some of the images remained, while the others disappeared, and during the periods of five to thirty minutes of the reduction, the images turned to the respective characteristic ones again, sometimes being quite different from those of the oxides. On the additional observations, a part of the images weakened or disappeared and rather the homogeneous images over the whole sections became to be observed by raising thetemperature.

Comparing the image with the optical, the net work of the emission after the reduction corresponds to cracks on the section. When the microscopic structure of the section thoroughly polished and etched with hydrochloric acid is adopted for comparison with the above optical image, grain boundaries in the oxide always correspond to the cracks. Therefore, the electronic images on the oxide are not always related to the grain boundaries.

Qualitative explanations on respective promoting effect of alumina, lime and silica are yielded from view point of the electronic image.

It has been proved from the observations of the electronic as well as the optical images that there are the following 3 types of regions which are rich in potash, i.e. the grain boundaries, particular interfacial grains and some of the sub-grains into which the

parent grains are divided. When references are made to the results of the activity for ammonia synthesis, surface area and etc., together with that by H. Kobayashi who has described that the activity is greatly enhanced by the larger amount of potash insoluble in water, the estimation shows that probably potash existing in the sub-grains above may most contribute to the activity for ammonia synthesis.

The authors wish to express their sincere thanks to Professor Nobuji Sasaki and Mr. Ryuzo Ueda of Kyoto University for their valuable advice concerning the electron microscope.

Government Chemical Industrial Research Institute, Tokyo

The Effect of Solvent on Infrared Absorption Bands of Halogenated Hydrocarbon Molecules

By Tsuneo YOSHINO

(Received June 22, 1954)

The intensities of infrared absorption bands have hitherto been measured with two main objects, namely for qualitative and quantitative analyses and for elucidating structural problems, and most of the measurements have been made in solution because the measurements in gaseous state are often difficult. Nevertheless the effects of solvent on infrared absorption bands have scarcely been studied except for the particular case where the hydrogen bond is concerned, and the intensity of the band, especially the area intensity of the band, has often been assumed to be independent of the solvent used. Recently Whiffen[1] has measured an infrared absorption band of chloroform near 760 cm^{-1} and has concluded that the area of the band is approximately independent of solvents although the peak height and the width at half height change considerably with them.

The present work was undertaken to see the effects of solvents on some degenerate and non-degenerate infrared absorption bands of polar and non-polar halogenated hydrocarbon molecules. In particular it seems to be of interest to know whether or not the band area is kept constant for the variety of solvents.

Experimental

Absorption measurements were made for the bands of carbon tetrabromide[2], *cis*-1,4-dibromocyclohexane and *trans*-1,4-dichlorocyclohexane. Following Bartal's method[3] carbon tetrabromide was prepared from acetone and bromine. (m.p. 93°C). The absorption band measured for this compound is the triply degenerate one, the peak frequency of which is about 670 cm^{-1}.

cis-1,4-Dibromocyclohexane[4] was synthesized from chinit and hydrobromic acid by the method used by Rothstein[5] and was separated from *trans*-1,4-dibromocyclohexane by fractional crystalizations using petroleum ether and methanol as solvents, repeatedly one after another. (m.p. 49°C)[6]. The purity was certified by the infrared inspection. The solvent effect was measured for the nine strong bands in the region from 7 to 23μ.

trans-1,4-Dichlorocyclohexane was made from chinit and hydrochloric acid by Rothstein's method[5]. (m.p. 102°C). This compound has two isomeric forms, the abundance ratio of which changes with solvents[7,8]. The solvent effects were, therefore, observed only for the changes of band widths and peak frequencies. The peak frequencies were measured for the bands in the region from 7 to 23μ, but the half intensity widths were measured only for the bands near 475, 565, 760 and 785 cm^{-1}, because the bands of two isomers above 800 cm^{-1} appear in close pairs and the band widths, therefore, cannot be measured accurately.

The spectral data were obtained with Perkin-Elmer Model 112 spectrometer with KBr prism for the region from 14 to 23μ and with NaCl prism for the region from 7 to 14μ. The thicknesses of cells used were 0.102 and 0.103 mm,

1) D.H. Whiffen, *Trans, Faraday Soc.*, **49**, 878 (1953).

2) Since one of the two infrared active bands of carbon tetrachloride lies in the region where KBr is not transparent and the other appears near 780 cm^{-1} as doublet (Fermi resonance), this compound is not suitable to use for the present purpose.

3) A. Bartal, *Chem. Zt.*, **29**, 377 (1905).

4) Detailed report on this compound by Kozima and Yoshino will be soon published in other place.

5) M.B. Rothstein, *Ann. chim.*, **14**, 461 (1930).

6) m.p. in literatures is 48°C or lower. See, for example, 5) or E. L. Bennett and C. Niemann, *J. Am. Chem. Soc.*, **74**, 5076 (1952).

7) K. Kozima and T. Yoshino, *J. Am. Chem. Soc.*, **75**, 166 (1953).

8) T. Yoshino, *J. Chem. Soc. Japan*, **75**, 592 (1954).

which were measured with the interference method. The slit width employed was such that the spectral slit width was nearly equal to, or narrower than half of the half intensity width and kept constant for the variety of solvents. The spectral slit width S was calculated[9] by the following formula, which was obtained by the simple modification of the formula[10] for single pass spectrometer,

$$S=\tilde{\nu}^2\frac{[1-n^2\sin^2(\alpha/2)]^{1/2}}{8\sin(\alpha/2)(dn/d\lambda)}\frac{s}{f}+\frac{\tilde{\nu}}{4l(dn/d\lambda)}$$

where $\tilde{\nu}$ is frequency in cm^{-1}, n is index of refraction at frequency $\tilde{\nu}$, α is prism apex angle, $dn/d\lambda$ is dispersion of prism material, and s, f and l are the slit width, the focal length and the length of prism base in cm. unit respectively.

The absorption curves of solvent and solution were recorded using the same cell, and constancy of recording condition was checked before and after each measurement using the reference cell filled with solvent. Errors due to stray light and non linearity of the amplifier were negligible.

Results and Discussions

The abbreviations used in this paper are as follows:

$\tilde{\nu}_{max}$ = frequency at the peak in cm^{-1}.

ε_{max} = apparent peak intensity in 10^5 cm^{-1} $mol.^{-1}$. The base of logarithm is 10.

ε_{max} (corr.) = peak intensity in 10^5 cm^{-1} $mol.^{-1}$, with Ramsay's slit-width correction[11], assuming Lorentzian curve:

$$a=B/[b^2+(\tilde{\nu}-\tilde{\nu}_0)^2].$$

b' = frequency interval in cm^{-1} between the band center and the half height position on long wave length side.

b'' = the same one on the short wave length side.

$2b=b'+b''$.

$2b$ (corr.) = $2b$ value with slit-width correction.

$\int\varepsilon d\nu$ = band area in 10^{15} cm^2 $sec.^{-1}$ $mol.^{-1}$.

$\log I_0/I$ = absorbance at the peak used to correct ε_{max} and b.

range = integration range in cm^{-1}. Except for the carbon tetrabromide band, the integration range is taken so that the absorption peak lies in its center.

First of all, let us consider the band of carbon tetrabromide. The results are shown in Table I for the various solvents used. The frequencies of the absorption peak in dioxane and in ethyl acetate are higher than those in *n*-heptane and in carbon tetrachloride. These results do not agree with Whiffen's results for chloroform band, which show that the peak frequency becomes highest in *n*-heptane and lowest in dioxane and in general is higher in non-polar solvents and lower in polar solvents.

The apparent half intensity width of the carbon tetrabromide band changes very much with solvents and is smaller in *n*-heptane and in carbon tetrachloride and larger in dioxane and ethyl acetate in accordance with the results of the chloroform band. We see, therefore, that in the carbon tetrabromide band the wider absorption is not accompanied with lower value of peak frequency as was mentioned in reference to the chloroform band.

The large half intensity width is accompanied by the low absorption peak, as is shown in Table I, so that the band areas in various solutions are brought near a definite value, but the differences of the areas are greater than the experimental error. The band area is larger in the solvent which lowers the peak frequency.

TABLE I

Solvent	$\tilde{\nu}_{max}$	ε_{max}	b'	b''	$\int\varepsilon d\nu$	$\log I_0/I$
dioxane	674.8	2.87	14.1	9.3	22.4	0.39
ethyl acetate	672.9	3.05	11.4	13.1	24.1	0.39
n-heptane	672.5	9.15	4.4	3.7	23.8	0.47
carbon tetrachloride	671.8	7.39	5.5	4.8	27.0	0.38

$2S=8.3$

The values of area intensities in Table I were integrated over the frequency ranges from $\tilde{\nu}_{max}-3b'$ to $\tilde{\nu}_{max}+3b''$ cm^{-1}. The band shapes are not symmetric, namely b' is not equal to b''. The solvent changes not only b' and b'' but also the ratio of them. The absorption curve, especially on the high frequency side of the peak, does not fit the Lorentzian curve even if the slit-width correction is made. The absorbance at $\tilde{\nu}_{max}-3b'$ and at $\tilde{\nu}_{max}+3b''$ are about 1/20 and 1/40 of that at the peak respectively and are smaller than those obtained from the Lorentzian

9) The values of n and $dn/d\lambda$ were takec from: C. Schäffer and F. Matossi, "Das Ultraroc Spektrum", Julius Springer, Berlin (for NaCl) and R. E. Stephens, E. K. Plyler, W. S. Rodny and R. J. Spindler, *J. Opt. Soc. Am.*, **43**, 110 (1953) (for KBr).

10) For example, van Z. Williams, *Rev. Sci. Inst.*, **19**, 135 (1948).

11) D. A. Ramsay, *J. Am. Chem. Soc.*, **74**, 72 (1952).

curve (1/10) by use of the peak height and the b' or b'' value with slit-width corrections. Owing to rather rapid decrease of absorption on the wings outwards from the center, the sum of the areas outside of the integration range may by estimated to be about one tenth of the band area and the ratio may not vary with solvents. Therefore the values of band areas in Table I integrated over the finite regions may be used for the comparison of band areas in various solutions in place of the values of infinite integration ranges.

The results of the measurements of the bands of *cis*-1,4-dibromocyclohexane near 505, 640 and 740 cm^{-1} are given in Tables II and III. The shapes of these bands are approximately the Lorentzian form. The Lorentzian curve suitable for the region near the band center does not accurately fit the wings and has a little larger value of absorbance than that observed. The peak frequencies of these bands take lower values in benzene, dioxane and polar solvents and the lower peak frequencies are accompanied with the wider half intensity widths. These effects are in accordance with those observed for chloroform band but the changes of the band widths with solvents are not so large as those in the degenerate bands of carbon tetrabromide and chloroform.

The wings of the absorption band spread over very wide ranges and the area in the wings is not negligible in spite of the small absorbances in the wingths. But as it is hard to obtain the area in the wings with accuracy, the values in Tables II and III were integrated over the definite spectral intervals of about four times of the half intensity widths. The band areas shown in the Table increase with solvents which lower the peak frequency and broaden the band. The area outside of the integration range and its ratio to the integrated area of the broadened band are larger than those of the narrowed band.

TABLE II

Solvnet	$\tilde{\nu}_{max}$ or $\Delta\tilde{\nu}_{max}$	ε_{max}	ε_{max} (corr.)	$2b$	$2b$ (corr.)	$\int \varepsilon d\nu$	$\log I_0/I$
n-heptane	506	0.57	0.63	6.6	5.8	1.43	0.30
cyclohexane	−0.0	0.60	0.67	6.1	5.3	1.39	0.30
carbon tetrachloride	−0.9	0.62	0.67	6.6	5.9	1.48	0.36
benzene	−3.2	0.62	0.67	7.1	6.4	1.61	0.36
chloroform	−3.2	0.56	0.59	8.2	7.6	1.58	0.32
elthyl acetate	−3.6	0.52	0.55	8.1	7.5	1.52	0.34
dioxane	−3.6	0.57	0.59	8.2	7.6	1.71	0.32
n-heptane	645	1.07	1.30	7.3	5.8	2.99	0.28
cyclohexane	−0.0	1.05	1.27	7.3	5.8	2.90	0.30
carbon tetrachloride	−1.1	1.09	1.30	7.5	6.0	3.10	0.31
chloroform	−3.5	1.11	1.25	8.6	7.3	3.18	0.31
cyclohexane	739	0.93	1.19	4.5	3.3	1.61	0.29
benzene	−2.3	0.95*	1.2 *	4.6*	3.4*	1.7 *	0.31*
dioxane	−2.7	1.01	1.24	4.8	3.7	1.88	0.36

$2S$=4.7, 7.0, 4.7, range=23.5, 32.7, 17.7, for the bands near 505, 640, 740 cm^{-1} respectively.
* These values are inaccurate because of the absorption of the solvent.

TABLE III

Solvent	$2S$	ε_{max}	ε_{max} (corr.)	$2b$	$2b$ (corr.)	$\int \varepsilon d\nu$	$\log I_0/I$
dioxane	3.4	0.57	0.59	8.0	7.7	1.71	0.32
	4.7	0.57	0.59	8.2	7.6	1.71	0.32
	6.7	0.56	0.62	8.7	7.6	1.72	0.31
	8.7	0.52	0.61	9.5	7.6	1.70	0.28
n-heptane	3.4	0.59	0.61	6.4	6.0	1.43	0.31
	4.7	0.57	0.63	6.6	5.8	1.43	0.30
	6.7	0.51	0.61	7.2	5.7	1.39	0.27
	8.7	0.47	0.63	7.7	5.4	1.31	0.25

$2S$=23.5
For the absorption curve of dioxane solution, Lorentzian form is a good approximation. Assuming the Lorentzian curve with B/b^2=0.59 and $2b$=7.6, the area intensity with infinite integration range is 2.12 which is 24% larger than the value in the Table.

Then the increment of the band areas above mentioned is not diminished even if integrated over the infinite range. As the areas outsied of the integration ranges in various solutions are different from each other only by a small percent of the integrated area, the increment of band area integrated over infinite range is approximately the same as that shown in Table II and might not exceed 30% for the 505 cm^{-1} band in which the increment is largest.

The transmission measured is the average of the transmissions for the interval of the slit width. Therefore the band area measured, particularly when the integration range is limited, might be smaller than that with infinitely small slit width and this diminution might depend upon the ratio of the band width to the spectral slit width. The area of the band near 505 cm^{-1} was measured with various slit widths for the *n*-heptane (which narrows the band width) and dioxane (which broadens the band width) solutions, but the band areas were found to be independent of slit width as shown in Table III so far as the half intensity width is smaller than twice the spectral slit width. The change in the ratio of the band width to the slit width, therefore, does not make any contribution to the change of the band area with solvents.

The decrease of the band areas in *n*-heptane and cyclohexane is not due to the change of molecules from one form to the other. The reason for this is as follows. As all the bands below 800 cm^{-1} decrease their intensities in the same manner in these solvents, they must belong to one form which is much more populated than the other. Owing to the change of molecules which causes the decrease of the band areas observed, the increase of the band areas of less populated form, if it exists, should be remarkable so far as any of the bands is not covered by the absorption of the more populated form or has appreciable absorbance. But none of the bands which show such a remarkable increase of band area in *n*-heptane or in cyclohexane solution was found in the region from 7 to 23μ. Thus we can see that the change of area intensity without change of molecules takes place for the bands of this compound. Such a change of band area has also been observed for the C=O stretching bands of ketones[12] in chloroform and carbon tetrachloride in accordance with the present results.

In carbon tetrachloride solution the frequency, width and area of the absorption band take intermediate values of those in polar and non-polar solvents.

The shapes of the bands above 800 cm^{-1} are also nearly Loretzian form and the band widths change with solvents as the bands below 800 cm^{-1}. But some of the solvent effects on the higher frequency bands are different from that described before. The peak frequencies of these bands, as shown in Table IV, do not change with solvents and the change of band areas is not

TABLE IV

$\tilde{\nu}_{max}$	$2S$	Range	Solvent	ε_{max}	$2b$	$\int \varepsilon d\nu$
872	3.7	26.3	carbon tetrachloride	1.16	5.3	2.5
			benzene	1.06	5.5	2.4
			chloroform	1.23	5.4	2.7
991	4.2	21.3	cyclohexane	1.68	4.0	2.8
			carbon tetrachloride	1.74	3.9	2.8
			chloroform	1.80	4.1	3.2
			dioxane	1.55	4.5	2.8
1162	5.1	32.5	cyclohexane	0.78	6.4	2.1
			carbon tetrachloride	0.78	6.5	2.1
1206	5.2	30.3	cyclohexane	1.14	7.9	3.5
			carbon tetrachloride	1.12	8.3	3.5
			benzene	1.07	9.7	3.7
1259	5.4	40.6	carbon tetrachloride	1.65	7.1	4.8
			benzene	1.71	7.7	5.3
1341	6.1	22.1	cyclohexane	0.91*	5.9*	2.2*
			carbon tetrachloride	1.09	5.4	2.4
			benzene	0.99	5.5	2.3
			chloroform	1.11	5.7	2.5

* These values are inaccurate because of the absorption of the solvent.

12) G. M. Barrow, *J. Chem Phys.*, **21**, 2008 (1953).

TABLE V

Solvent	$2S$	ν_{max} or $\Delta\nu_{max}$	$2b$	$2b$ (corr.)	$\log I_0/I$
cyclohexane		476	5.2	3.8	0.24
carbon tetrachloride	5.6	−0.8	5.2	3.9	0.41
benzene		−2.0	5.4	4.1	0.35
cyclohexane		566	7.3	6.7	0.48
carbon tetrachloride	4.5	−2.2	7.8	7.3	0.81
benzene		−4.5	8.0	7.5	0.45
cyclohexane		759	3.5	2.9	0.64
benzene	3.3	−3.2	4.1	3.5	0.46
dioxane		−4.2	5.0	4.4	0.43
cyclohexane		786	4.5	3.8	0.40
benzene	3.7	−3.8	5.6	5.1	0.47
dioxane		−4.9	6.0	5.5	0.55

the same for all these six bands nor analogous to that mentioned to the lower frequency bands.

For the bands of *trans*-1,4-dichlorocyclohexane, the solvent effect on the peak frequencies and the widths shown in Table V is the same as that described for the bands of *cis*-1,4-dibromocyclohexane. The peak frequencies of the bands above 800 cm^{-1} which are not given in the Table do not change appreciably with such solvents as cyclohexane, carbon tetrachloride, chloroform and benzene.

So far as the molecules discussed are concerned, the frequency lowering with solvents takes place only for the bands which are related intimately to the stretching and deformation of carbon-halogen bonds. These changes may be due to the perturbation of the solute molecules caused by the action of solvent on the carbon-halogen bonds[13].

We have seen above that the integrated intensity of an absorption band of halogenated hydrocarbon molecules is not kept constant for the variety of solvents and this intensity change is remarkable in low frequency bands. Chako's theory[14] fails to explain this increase of band area, so far as the index of refraction of pure solvent in visible light is used. In this respect it is of interest that the solvent which lowers the peak frequency, broadens the band width and increases the band area is the one which stabilizes the polar form of rotational isomers[15].

In the degenerate bands mentioned above, large changes of band widths and peak heights took place. This remarkable feature might be due to the splitting of degeneracy. The frequency change in the carbon tetrabromide band is different from those in the bands of chloroform and cyclohexane derivatives. This peculiarity of carbon tetrabromide seems to be due to the spherically symmetric form of the molecule and seems to coincide with the action of carbon tetrachloride as non-polar solvents like *n*-heptane and cyclohexane as was seen in the present results.

Acknowledgment

The author would like to express his thanks to Professor K. Kozima for his kind advice and continued interest in this problem.

Tokyo Institute of Technology
Meguro-ku, Tokyo

13) Detailed report on the studies of the solvent-solute interaction using mixed solvents will be published in near future.

14) N. Q. Chako, *J. Chem. Phys.*, **2**, 644 (1934).

15) The elongated form of *trans*-1,4-dichlorocyclohexane corresponds to the polar form in regard to the solvent effect on the abundance ratio. The correspondence was elucidated in 8).

The Spatial Configurations and the Ultraviolet Absorption Spectra of Biphenyl and Some Related Compounds

By Hiroshi SUZUKI

(Received June 29, 1954)

It is well-known that atrop-isomerism occurs when two or more of the ortho hydrogen atoms in biphenyl are replaced by larger atoms or groups. This phenomenon is explained as due to steric hindrance which prevents rotation about the central 1-1′ bond in the biphenyl derivatives. These molecules therefore must have a non-coplanar configuration.

Regarding the spatial configuration of biphenyl itself, on the other hand, there appear to be several conflicting evidences. Thus, the results of X-ray crystal analyses of biphenyl showed the molecule to have a completely planar configuration,[1] while electron diffraction investigations suggested a non-coplanar configuration in which the two benzene rings are perpendicular[2] or at an angle of about 45°[3] to each other. When it is assumed that the molecule of biphenyl is coplanar, the distance between the two nearest ortho hydrogen atoms attached to different benzene rings is about 1.8Å, which is considerably shorter than the usual van der Waals distance 2.0Å; therefore, there should be considerable steric interference between them.

The ultraviolet absorption spectrum of biphenyl is quite different from that of benzene and has an intense characteristic band. This is supposed to be due to the conjugation between the two benzene rings, indicating consequently that the molecule of biphenyl is coplanar or nearly coplanar, since it is generally assumed that such conjugation requires the coplanarity of the two benzene rings. On the other hand, the spectra of the derivatives of biphenyl in which the four ortho positions are substituted, e.g., bimesityl, fail to exhibit the characteristic biphenyl band, and are essentially those of the two corresponding benzene compounds.[4] This is explained by the theory that in these compounds the two benzene rings cannot be coplanar owing to steric interference of the ortho substituents[5] and consequently the conjugation between the benzene rings is destroyed. The occurrence of the conjugation between the two benzene rings in biphenyl is also proved by the fact that the extra-resonance energy has been found to be about 8 kcal./mol.[6] or about 5 kcal./mol.[7] for biphenyl, and further suggested by the fact that in *p*-nitro-*p*′-aminobiphenyl the *p*-nitro group exercises a marked effect upon the basicity of the *p*′-amino group and this effect is diminished by ortho substitution by two methyl groups[8], and also by the fact that the dissociation constants of substituted *p*-biphenylcarboxylic acids are influenced by the substituents, the effect being transmitted through the biphenyl system.[9] Furthermore, on the basis of the assumption of the coplanar configuration, London[10] has computed the energy levels of the biphenyl molecule by the method of antisymmetrized products of molecular orbitals with considerably good agreement between the theoretical electronic transitions and the observed ultraviolet absorption spectrum. These seem to be favourable for the coplanar configuration.

It should, however, be here pointed out that the conjugation requires not necessarily the perfect coplanarity. The conjugation operates by the overlapping of the π-orbitals of the 1,1′ carbon atoms, so it should operate in full at coplanarity. However, partial loss of coplanarity is not necessarily associated with complete loss of conjugation. That is, the

1) (a) J. Dhar, *Indian J. Phys.*, **7**, 43 (1932): *Chem. Abst.*, **26**, 4517. (b) Idem., *Proc. Natl. Inst. Sci. India*, **15**, 11 (1949): *Chem. Abst.*, **43**, 4655.

2) J. L. Karle and L. O. Brockway, *J. Am. Chem. Soc.*, **66**, 1974 (1944).

3) O. Bastiansen, *Acta Chem. Scand.*, **3**, 408 (1949).

4) (a) L. W. Pickett, G. F. Walter and H. France, *J. Am. Chem. Soc.*, **58**, 2296 (1936); (b) M. T. O'Shaughnessy and W. H. Rodebush, ibid., **62**, 2906 (1940).

5) Concerning the effects of ortho substituents on the spectra of biphenyls, see also: (a) M. Pestemer and E. Mayer-Pitch, *Monatsh.*, **70**, 104 (1937); (b) M. Calvin, *J. Org. Chem.*, **4**, 256 (1939); (c) B. Williamson and W. H. Rodebush, *J. Am. Chem. Soc.*, **63**, 3018 (1941); (d) D. W, Sherwood and M. Calvin, ibid., **64**, 1350 (1942); (e) W. H. Rodebush and I. Feldman, ibid., **68**, 896 (1946); (f) R. A. Friedel, M. Orchin, and L. Reggel, ibid., **70**, 199 (1948).

6) (a) L. Pauling and J. Sherman, *J. Chem. Phys.*, **1**, 606 (1933); L. Pauling, "The Nature of the Chemical Bond", (1939), p. 129: (b) M. Szwarc, *Nature*, **161**, 890 (1948).

7) F. Wm. Cagle and H. Eyring, *J. Am. Chem. Soc.*, **73**, 5628 (1951).

8) D. W. Sherwood and M. Calvin, *J. Am. Chem. Soc.*, **64**, 1350 (1942).

9) E. Berliner and E. A. Blommers, *J. Am. Chem, Soc.*, **73**, 2479 (1951).

10) A. London, *J. Chem. Phys.*, **13**, 396 (1945).

perfect coplanarity is not prerequisite to the occurrence of conjugation and consequently to the appearance of the spectrum characteristic of such a conjugated system.

On the basis of such considerations, the apparently conflicting evidences are most satisfactorily interpreted as indicating that biphenyl is non-coplanar in the liquid or gaseous state while in the crystalline state it is maintained in the coplanar configuration presumably by the lattice force which overcomes the steric interference between the ortho hydrogen atoms. Then, the spectrum of biphenyl in the crystalline state should be that of the molecule in the coplanar configuration and the spectrum of biphenyl in the liquid or gaseous state should be that of the molecule in then on-coplanar configuration. Actually, in accordance with expectation, the spectrum of the crystal[11,12] is considerably different from that of the liquid or solution, and the former has the characteristic band at considerably longer wave-lengths than the latter, while the spectrum of the vapor is similar to that of the liquid;[12] so, it may be possible to infer the spatial configurations of biphenyls from their absorption spectra.

Previously,[13] the present author has determined the quantitative relations between the degree of deviation from coplanarity of the molecular configuration and the wave-lengths of the absorption spectrum as well as the extent of conjugation for stilbenes, and showed that the absorption maximum is shifted toward shorter wave-lengths and that the resonance energy is reduced progressively with increasing angle of twist of the phenyl groups out of the plane of the ethylenic linkage. The subject of the present paper is to determine analogous relations for biphenyls and discuss the spatial configurations of biphenyl and some related compounds.

Calculations

The calculations follow a procedure quite similar to the previous one[13] for stilbenes, so only the outline is given. In the present case the exchange integral for the 1-1′ bond is denoted by $\alpha\beta$. The value of the parameter α should vary with the length of the 1-1′ bond and the degree of twist of the benzene rings from the coplanar position around the 1-1′ bond. Since the biphenyl molecule belongs to the symmetry group D_2, the secular equation for the determination of the twelve approximate molecular orbitals as linear combinations of $2p\pi$ atomic orbitals is factorized into the following four equations:

$$\begin{aligned} A_1,\ & x^4+\alpha x^3-5x^2-3\alpha x+4=0,\\ B_2,\ & x^4-\alpha x^3-5x^2+3\alpha x+4=0,\\ B_1,\ & x^2-1=0,\\ B_3,\ & x^2-1=0, \end{aligned}$$

where $x=W/\beta=(Q-E)/\beta$, Q, E, and β having their usual meanings[14]. The numerical values of x obtained by solving these equations for various values of α represent the heights of the energy levels in units of β of the molecule in the spatial configuration prescribed by the corresponding value of α. The levels belonging to A_1 and those to B_2 vary, and those to B_1 and those to B_3 do not vary with α. These are reduced to those of benzene when α is zero. The absorption band characteristic of biphenyls is ascribed to the electronic transition from the highest occupied level to the lowest vacant level. In Table I, the values of the energy difference ΔE between these two levels and values of the extra-resonance energy $R.E.$ for various values of α are recorded. It is seen that the value of ΔE becomes larger and that of $R.E.$ smaller with decreasing value of α.

Since the exchange integral can be taken to be approximately proportional to the overlap integral, the value of α is assumed to vary with the angle of twist and the lengh of the 1-1′ bond R according to the relation

$$\alpha=S(R)\cos\theta/S(1.39\text{Å}),$$

where $S(R)$ is the π-π overlap integral when the bond length is R, and 1.39Å is the bond length between the adjacent carbon atoms in benzene ring. The value of $S(R)$ can be obtained from Mulliken's Table.[15] The value of R is assumed to be determined for any value of θ by the relation

$$\{S(R)-S(1.54\text{Å})\}/\{S(1.48\text{A})-S(1.54\text{Å})\}=S(\theta)/S(0^\circ)=\cos\theta,$$

where $S(\theta)$ is the π-π overlap integral for the angle of twist of θ and $S(0^\circ)$ is that for the angle of twist of 0° at the constant bond length, since the molecule of biphenyl in the crystalline state is coplanar and the length of the 1-1′ bond is 1.48Å according to the X-ray analysis,[1] and since consequently R will vary from 1.48Å, to 1.54Å, the length of the normal C-C single bond, as θ varies from 0° to 90°. Thus, the value of θ being given, the corresponding value of α is easily obtained, and then those of ΔE and $R.E.$ are also obtained according to Table I. When θ is zero and R is 1.48Å, namely, for the coplanar

11) E. Merkel and C. Wiegand, *Z. Naturforsch.*, **36**, 93 (1948).
12) A. R. Deb, *Ind. J. Phys.*, 305 (1953).
13) H. Suzuki, This Bulletin, **25**, 145 (1952).
14) H. Eyring, J. Walter, and G. E. Kimball, "Quantum Chemistry", John Wiley & Sons, Inc., (1944), p. 255.
15) R. S. Mulliken, C. A. Rieke, D. Orloff, and H. Orloff, *J. Chem. Phys.*, **17**, 1248 (1949).

TABLE I

α	1	0.9	0.8	0.7	0.6	0.5	0.4	0.3	0.2	0.1	0
$\Delta E(\beta)$	1.410	1.460	1.512	1.566	1.624	1.682	1.742	1.804	1.868	1.934	2
$R.E.(\beta)$	0.382	0.312	0.248	0.192	0.142	0.098	0.064	0.036	0.016	0.004	0

TABLE II

Compound	Solvent	$\lambda_{max.}$(Å)	$\varepsilon_{max.}$	$\Delta E(\beta)$	α	θ	R(Å)	$R.E.(\beta)$
Biphenyl (crystal)	——	2754[a]	——	1.482	0.858	0°	1.48	0.285
4,5-Methylene-9,10-dihydrophenanthrene	Ethanol	ca. 2720[b]	ca. 18500	1.502	0.819	16.5°	1.482	0.260
9,10-Dihydrophenanthrene	Hexane	2635[c]	18000	1.555	0.720	31.5°	1.489	0.203
2,7-Dihydro-3,4-5,6-dibenzoxepin	Hexane	2500[c]	16500	1.646	0.562	47°	1.499	0.125
2,7-Dihydro-3,4-5,6-dibenzazepinium-1-*spiro*-1'''-piperidinium bromide	Water	2480[c]	15000	1.660	0.538	49°	1.501	0.115
Biphenyl	Heptane	2475	19000	1.664	0.531	50°	1.501	0.112
o-Methylbiphenyl	Heptane	2350	10000	1.759	0.373	63°	1.513	0.056
o,*o*'-Dimethylbiphenyl	Ethanol	(ca. 2270)[d]	6800	1.825	0.267	70.5°	1.520	0.029

a, A.R. Deb, Reference (12). *b*, R.N. Jones, Reference (22).
c, G.H. Beaven et al., Reference (18). *d*, G.H. Beaven et al., Reference (23).

molecule of biphenyl in the crystalline state, α is 0.858 and ΔE is $1.482(\beta)$.

According to Deb,[12] the characteristic band in the spectrum of biphenyl in the liquid state is split up into two broad bands at 36306 cm^{-1} (2754 Å) and 37386 cm^{-1} (2675 Å) in the case of the solid at 30°C, and the band at 36306 cm^{-1} is presumed to be the intrinsic band (ν_0). Consequently, this band corresponds to ΔE of 1.482 β. On the other hand, the "center of gravity of singlets"[16] in the absorption spectrum of benzene, 48000 $cm,^{-1}$ corresponds to ΔE of 2β. Therefore, in order to correlate the position of the absorption maximum with the calculated energy difference ΔE, it is assumed that the former expressed in wave number changes linearly with respect to the change in the latter from 36306 cm^{-1} corresponding to $\Delta E=1.482\beta$ to 48000 cm^{-1} corresponding to $\Delta E=2\beta$. Thus, the position of the absorption maximum of the biphenyl-type compound in which the two benzene rings are twisted to any extent from the coplanar position is easily inferred. Conversely, when the position of the absorption maximum is known experimentally, the degree of deviation from coplanarity, θ, as well as the extent of conjugation, $R.E.$, can be computed.

In Table II, the results of such computations are summarized. It is, for simplification, assumed that the absorption spectrum depends solely on the spatial configuration of the biphenyl skeleton in the compounds, and other effects, for example, the comparatively small bathochromic effect of the alkyl substituent or of the alicyclic bridge, are ignored.

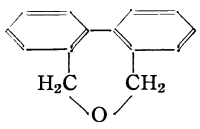
Discussion

As is seen from the Table II, the characteristic absorption maximum is shifted toward shorter wave-lengths and the extra-resonance energy is reduced progressively with an increasing angle of twist.

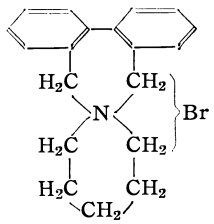
For biphenyl in solution, the angle between the two benzene rings has been computed to be 50°. According to the electron diffraction sector method study by Bastiansen,[3,17] the angle is found to be 45° ±10°, 52° ±10°, 54° ±5°, and 45° for biphenyl, 3, 3'-dichlorobenzidine, 3, 3'-dibromobiphenyl, and 3, 3', 5, 5'-tetrabromobiphenyl respectively. If the actual angle is assumed to be the same for all the non-ortho-substituted biphenyls, it can be given the value 50° ±5° on the average.[17] The agreement between the value obtained here and that found by Bastiansen is surprisingly good, although the former refers to the molecule in solution while the latter to the molecule in the gaseous state. In this connection, the cases of the 2, 2'-bridged biphenyls are of interest. In these compounds the molecule is maintained in the comparatively rigid configuration. According to the models, the angle between the two benzene rings of the biphenyl skeleton in 2, 7-dihydro-3, 4-5, 6-dibenzoxepin (I) and 2, 7-dihydro-3, 4-5, 6-dibenzazepinium-1-*spiro*-1'''-piperidinium bromide (II) in which the 2, 2'-positions of biphenyl are bridged by a 7-membered ring is about 50°, and it is

16) J. R. Platt, *J. Chem. Phys.*, **18**, 1168 (1950).

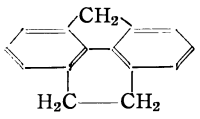
17) O. Bastiansen, *Acta Chem. Scand.*, **4**, 926 (1950).



(I)



(II)



(III)

notable that these compounds show closely similar absorption spectra to that of biphenyl in solution,[18] and that the angle has been computed by the present method to be 47° and 49° respectively. This gives presumably some support to the above estimation of the angle of twist for the isolated molecule of biphenyl. Samoilov and Dyatkina,[19] in contrast to this, have deduced a value of about 30° for this angle in the isolated molecules of biphenyl and of terphenyl by calculations based on the molecular orbital method of the resonance energy and of the interaction between the nearest hydrogen atoms.

According to Beaven et al.,[18] the angle of twist in 9,10-dihydrophenanthrene in which the 2,2′-positions of biphenyl are bridged by a 6-membered ring is estimated to be about 20° from the model, while fluorene in which the 2,2′-positions of biphenyl is bridged by a 5-membered ring is best regarded as a strained planar structure. However, the absorption spectra of these two compounds are similar with the exception that in the latter compound fine structures appear.[20] The X-ray data, according to Jones,[21] favor a non-planar configuration for crystalline fluorene. On the other hand, in 4,5-methylene-9,10-dihydrophenanthrene (III), the conflicting steric requirements of the two bridges would appear to be most favorably compromised in an approximately planar configuration. The above estimations of the angle of twist seem to suggest that it is the case. Thus, this compound has the characteristic absorption band[22] at considerably longer wave-lengths than those of 9,10-dihydrophenanthrene and of fluorene and nearer to that of biphenyl in the crystalline state. This suggests presumably that the molecule of 4,5-methylene-9,10-dihydrophenanthrene is nearer to coplanar and that the molecule of fluorene as well as of 9,10-dihydrophenanthrene deviates from coplanarity to a larger extent as compared with 4,5-methylene-9,10-dihydrophenanthrene. It is doubtful, of course, whether much significance can be attached to the numerical values of the angle of twist shown in Table II especially for these 2,2′-bridged biphenyls, because the straining effects of the 2,2′-bridge linkages in these compounds would be too complicated to be treated by such a simple method. (The above assumption, for example, of the relation between R and θ may be not pertinent to these cases.)

The angle of twist for ortho-methylbiphenyl has been computed to be 63°, which is in best accord with the value 62° deduced from the model in which the length of the 1-1′ bond is 1.51 Å and an ortho hydrogen atom just touches the ortho methyl group.

It is notable that the spectrum of *o,o′*-dimethylbiphenyl is markedly different from that of *o*-methylbiphenyl. If the molecule of *o,o′*-dimethylbiphenyl assumed the trans form in which the ortho hydrogen atoms just contact with the ortho methyl groups, the configuration would be similar to that of *o*-methylbiphenyl, and consequently *o,o′*-dimethylbiphenyl would show a closely similar spectrum to that of *o*-methylbiphenyl. As a matter of fact, the spectrum of *o,o′*-dimethylbiphenyl has no distinct band; however, according to Beaven et al.,[23] it has the inflection at about 2270 Å, which is regarded as a vestigial conjugation band. When this value is taken as a basis for calculation, θ and R are computed to be 70.5° and 1.520 Å. These values are in good agreement with the corresponding values, 70.6° and 1.525 Å, found for 2,2′-dimethylbenzidine dihydrochloride by the X-ray crystal analysis.[24] Considering the fact that the value of the angle between the two benzen rings found for gaseous 2,2′-dichlorobiphenyl by the electron diffraction method,[17] 74°, and that found for crystalline

18) G. H. Beaven, D. M. Hall, M. S. Lesslie, and E. E. Turner, *J. Chem. Soc.*, **1952**, 854.
19) S. Samoilov and M. Dyatkina, *Zhur. Fiz. Khim.*, **22**, 1294 (1948); *Chem. Abst.*, **43**, 2606.
20) R. N. Jones, *J. Am. Chem. Soc.*, **67**, 2127 (1945).
21) Reference (22): Iball, *Z. Krist.*, **94**, 397 (1936): Cook and Iball, *Chemistry and Industry*, **55**, 467 (1936).
22) R. N. Jones, *J. Am. Chem. Soc.*, **63**, 1658 (1941).
23) G. H. Beaven, D. M. Hall, M. S. Lesslie, E. E. Turner, and (in part) G. R. Bird, *J. Chem. Soc.*, **1954**, 131.
24) F. Fowwether and A. Hargreaves, *Acta Cryst.*, **3**, 81 (1950): *Chem. Abst.*, **44**, 7118: A. Hargreaves and W. H. Taylor, *J. Sci. Instruments*, **18**, 133 (1941): *Chem. Abst.*, **35**, 7261.

2,2′-dichlorobenzidine by the X-ray investigation,[25] 72°, are in fact the same within the limits of experimental errors, and that both these compounds have been found to have the structures more similar to the *cis* form than to the *trans* form, it may be not unreasonable to compare the values for 2,2′-dimethylbiphenyl in solution with those for 2,2′-dimethylbenzidine dihydrochloride in the crystalline state, and to infer that the preferred configuration of the former as revealed by its absorption spectrum is similar to the configuration of the latter, which has been found to have the two ortho methyl groups in the *cis*-disposition.[24] At any rate, it seems to be sure that the conjugation between the two benzene rings still occurs, though faintly, in spite of large deviation from the coplanarity of the molecule. In this connection, it is of interest that Theilacker and Ozegowski[26] have found that 2, 2′-dimethyl-4, 4′-bis-(diphenylmethyl)-biphenyl has properties as a true biradical, although their results do not seem to be entirely free from ambiguity. Theilacker[27] mentioned also that the angle of twist was 37°–48° in this compound. In view of the above results, this value is presumably too small.

Lastly, it should be mentioned that the values computed above do not necessarily refer to the rigid configurations of the molecules but to the average or most probable ones. The fairly good agreements of the values computed above with the available data obtained by other methods throughout the cases under discussion may be supposed to prove the validity of such approximate treatments, and further, it is believed that the quantitative relations between the spatial configuration and the absorption spectrum as well as the extent of conjugation for biphenyl-type compounds have been almost satisfactorily determined here.

25) D. L. Smare, *Acta Cryst.*, **1**, 150 (1948); *Chem. Abst.*, **42**, 8045.
26) W. Theilacker and W. Ozegowski, *Ber.*, **73**, 33 (1940).
27) W. Theilacker, *Naturwiss.*, **31**, 505 (1943); *Chem. Abst.*, **38**, 3385.

Experimental

o-Methylbiphenyl was prepared after the Gomberg's procedure[28] by diazotizing *o*-toluidine in concentrated hydrochloric acid and adding the reaction mixture into a stirred mixture of sodium hydroxide solution and benzene. *o*, *o*′-Dimethylbiphenyl was prepared by the action of zinc dust on the diazotized *o*-toluidine in aqueous sulfuric acid solution to which ethanol was added, following the Gattermann's procedure[29] for preparation of biphenyl.

The measurements of the ultraviolet absorption spectra of biphenyl, *o*-methylbiphenyl, and *o*, *o*′-dimethylbiphenyl were carried out with a Beckman Quartz Spectrophotometer Model DU. As the solvent *n*-heptane was used. The concentration of the solutions was $1/3\times10^{-4}$ mole per liter for biphenyl and $1/2\times10^{-4}$ mole per liter for *o*-methylbiphenyl and for *o*, *o*′-dimethylbiphenyl.

Summary

The quantitative relations between the degree of deviation from coplanarity of the molecular configuration and the ultraviolet absorption spectrum as well as the extent of conjugation for the biphenyl-type compounds have been determined by calculations based on the molecular orbital method. On the basis of the results, the spatial configurations of biphenyl, *o*-methylbiphenyl, *o*,*o*′-dimethylbiphenyl, fluorene, 9,10-dihydrophenanthrene, 4,5-methylene-9,10-dihydrophenanthrene, 2,7-dihydro-3,4-5,6-dibenzoxepin, and 2,7-dihydro-3,4-5,6-dibenzazepinium-1-*spiro*-1‴-piperidinium bromide have been discussed.

The author expresses his sincere thanks to Prof. Osamu Simamura, Drs. Saburo Nagakura, Makoto Takahashi, and Fujio Iimura for their kind guidance and encouragement throughout this study. Thanks are also due to the Ministry of Education for a Grant-in Aid for Scientific Research.

The College of General Education,
Tokyo University, Tokyo

28) M. Gomberg and J. C. Pernert, *J. Am. Chem. Soc.*, **48**, 1372 (1926).
29) L. Gattermann, *Ber.*, **23**, 1226 (1890).

Vat Dyes of Acenaphthene Series. VI. Derivatives of Acenaphthene Violet[1]

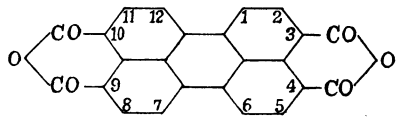
By Toshio MAKI and Harukichi HASHIMOTO

(Received July 1, 1954)

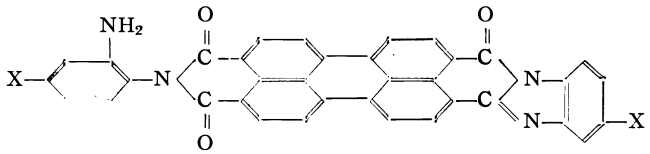
The formation of Acenaphthene Violet (II), a new, deep violet vat dye of maximum fastness, from 3,4,9,10-perylene-tetracarboxylic anhydride (I) and *o*-phenylenediamine was reported in our previous paper[2].

We have now prepared *p,p'*-dichloro derivative of Acenaphthene Violet (III), a brilliant violet vat dye, by condensation of 4-chloro-1,2-phenylenediamine (VII) with (I) at 170°, and also a violet blue dibenzo derivative (V) from (I) and 1,2-naphthylenediamine (VIII) at 150°. As 4-methoxy-1,2-phenylenediamine has been found to be unstable, synthesized by condensing 4-methoxy-2-nitroaniline (IX) and (I) at 200°, and *p,p'*-dimethoxy Acenaphthene Violet (IV) was obtained by its reduction with sodium sulfide via the corresponding diamino-dimethoxyl compound.

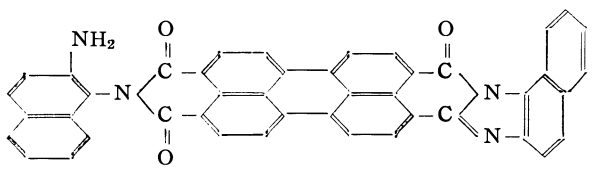
The fastness of the cotton dyeings of these vat dyes are excellent and among them the unsubstituted Acenaphthene Violet has the maximum light fastness, while the violet shade of the dichloro compound is most brilliant.



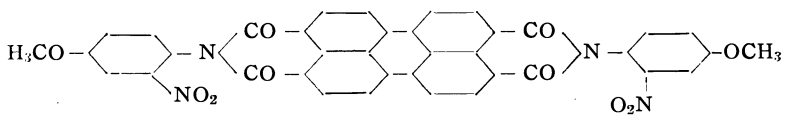
(I)



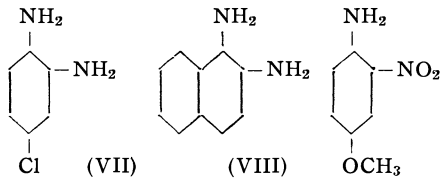
(II) X=H
(III) X=Cl
(IV) X=OCH_3



(V)



(VI)



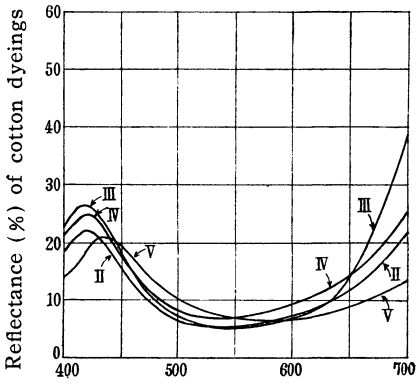
(VII) (VIII) (IX)

	Cotton dyeings		
	Shade	Light fastness	Yield of the theory (%)
Acenaphthene Violet (II)	Violet	8	60.6
Dichloro Derivative (III)	Brilliant violet	7~8	66.3
Dimethoxyl Derivative (IV)	Reddish violet	6~7	49.6
Dibenzo Derivative (V)	Violet blue	7	33.5

1) Read before the 7th Annual Meeting of the Chemical Society of Japan on April 3, 1954.
2) This Bulletin, **25**, 411 (1952).

Constitution		(II)	(III)	(IV)	(V)
Trichromatic coefficient	x	0.2712	0.2632	0.2794	0.2463
	y	0.1963	0.1796	0.2093	0.2074
Brightness Y (%)		6.49	6.55	8.21	7.88
Dominant wavelength (mμ)		564.0c	564.6c	562.8c	461
Color purity (%)		40.8	46.2	37.4	38.1

More accurate comparison of the shades of Acenaphthene Violet and its derivatives were carried out using G.E. recording spectrophotometer with 1% cotton dyeings (IW method) and the obtained reflectance curves (Fig. 1) were analysed according to the I.C.I. system.



Wave length (mμ)

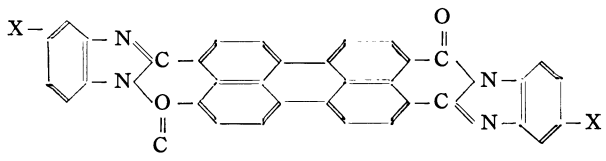
Fig. 1.

These vat dyes of the mono-imidazole type (II–V) are easily soluble in alkaline hydrosulfite and also soluble in 85~90% sulfuric acid. The straight and short conjugation between the two upper (3,10–) carbonyls is considered as the cause of the easy vattability. The associated bis-imidazoles (X–XI), violet blue or blue pigments of highest stability, are the ultimate reaction products and insoluble in alkaline hydrosulfite. Theoretically both *cis*- and *trans*-isomers of the bis-imidazoles may be possible as in the case of 1,4,5,8-naphthalene-tetracarboxylic acid. In the present case, however, the structure of the bis-imidazoles must be *trans*-forms (X–XI) of long and crooked conjugation between the two carbonyls (3,9–) owing to their perfect insolubility against alkaline hydrosulfite. The associated *o,o'*-diamino compounds, the initial condensation products, are insoluble in 85–90% sulfuric acid and have weak dyeing properties of low value.

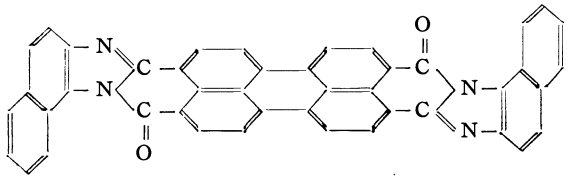
Experimental Part

Dichloro Derivative of Acenaphthene Violet (III).—Perylene-tetracarboxylic anhydride (1, 31 g., 1 mol. ratio) was heated with an excess of 4-chloro-1,2-phenylenediamine[3] (4.8 g., 10 mol. ratio) and 1.0 g. (5 mol. ratio) of glacial acetic acid in an oil bath under reflux at 170° (bath temperature) for 1 hour. The product was heated up with 20 cc. of alcohol, the hot solution was filtered and washed with more alcohol until the filtrate became colorless. The collected precipitate was then treated with 200 cc. of hot aqueous 1% sodium hydroxide. The amount of the unchanged tetracarboxylic acid (alkali soluble) was only a trace. The yield of the crude condensation product was 1.92 g. The crude product was finely powdered, kept with 4 g. of sodium hydroxide, 4 g. of sodium hydrosulfite and 200 cc. of water at 50° for 15 minutes, filtered, and the insoluble part was further treated with 2 g. of sodium hydroxide and 2 g. of sodium hydrosulfite and 100 cc. of water. The part insoluble in the alkaline hydrosulfite, 0.26 g. or 12.9% of the theory, is the blue violet bis-imidazole pigment (X,X=Cl)

3) *p*-Chloroaniline was acetylated with acetic anhydride in benzene to *p*-chloroacetoanilide, m.p. 179.5—180.5° (corr.), in 94.7% yield, converted then into 4-chloro-2-nitroaniline, m.p. 116.4—116.9°, by nitration in conc. sulfuric acid, hydrolysis with 70% sulfuric acid and recrystallisation from water. Yield was 62.9%. The latter was reduced with zinc dust using alcohol and 20% sodium hydroxide and after recrystallisation from water 4-chloro-1,2-phenylenediamine, m.p. 75.0°, was obtained in 50.3% yield. See also Bruyn, *Rec. trav. chim.*, **36**, 127 (1916); Ullmann, Manthner, *Ber.*, **36**, 4027 (1903); *Org. Synth.*, **19**, 70 (1939).



(X)



(XI)

The combined vat filtrate was oxidized by a current of air, the collected precipitate, as a dry powder, dissolved in 42 g. of 99.2% sulfuric acid and 4.3 cc. of water was dropped in under ice cooling to produce 90% sulfuric acid. The insoluble, 0.08 g. or 3.7% of the theory, is the *o,o'*-diamino compound, which dyes cotton in weak, dull violet red of low value from a violet red vat (IW).

The part soluble in 90% sulfuric acid is the main dye, dichloro Acenaphthene Violet (III), the yield was 1.38 g. or 66.3% of the theory. The dichloro compound (III) is a black violet powder, soluble in conc. sulfuric acid and the solution shows blue (thin layer) and violet blue (thick layer) dichroism with weak red fluorescence. Violet precipitate resulted from the conc. sulfuric acid solution by the addition of water. Hydrosulfite vat (IW) is red violet and dyes cotton in brilliant violet of powerful intensity with 1~2% dye, a little more bluish than the chlorine free Acenaphthene Violet (II). The light fastness of the cotton dyeings were found to be 7—8 grade. Found Cl, 10.91; calcd. for $C_{36}H_{16}O_3N_4Cl_2$ (III): Cl, 11.37%.

Dimethoxyl Derivative of Acenaphthene Violet.—A mixture of 1.31 g. (1 mol. ratio) of perylene-tetracarboxylic anhydride and 7.8 g. (14 mol. ratio) of 4-methyoxy-2-nitroaniline (m.p. 124.5—125°, corr.)[4] was heated with 1.0 g. (5 mol. ratio) of glacial acetic acid in an oil bath under reflux at 200° (bath temperature) for 7 hours. The unchanged components were removed with 100 cc. of alcohol and 500 cc. of 1% sodium hydroxide as above. The yield of the dinitro compound (VI) was 1.60 g. or 69.3% of the theory. It is a dark brownish red crystalline powder with a pink streak, soluble in conc. sulfuric acid with violet blue (thin layer) and violet red (thick layer) dichroism without fluorescence. Pink precipitate is formed from the conc. sulfuric acid solution by the addition of water. It dyes cotton in a weak, dull violet red shade of diamino compound from a violet red vat (IW). The vat shows weak orange fluorescence. The powder is a little soluble in boiling nitrobenzene with red-orange color and strong green-yellow fluorescence.

The dinitro compound (1.30 g., 1 mol. ratio) was dissolved in 50 g. of ice cold conc. sulfuric acid and poured into 1,000 cc. of ice cold water. The filtered and neutral washed paste was reduced with 1.1 g. of 55% sodium sulfide (4 mol. ratio) and 15 cc. of water by treating 1 hour at room temperature and 3 hours at 60°. It was then made up to 100 cc. with warm water (60°), the collected precipitate washed neutral and dried at 110° for 5 hours. The yield of the crude product was 1.20 g.

The crude reduction product was treated with 4 g. of sodium hydroxide, 4 g. of sodium hydrosulfite and 200 cc. of water at 50° for 15 minutes. The amount of the hydrosulfite insoluble (dimethoxy bis-imidazole) was only a trace. The soluble part was, after air oxidation, separated with 55.6 parts of 85% sulfuric acid. The part insoluble in 85% sulfuric acid corresponds to the diamino compound (0.24 g. or 20.2% of the theory). It dissolves in conc. sulfuric acid with blue color (without dichroism) and weak red fluorescence, and red violet precipitate is produced from the solution by the addition of water. Hydrosulfite vat (IW) is violet red with weak orange fluorescence and dyes cotton in weak, dull violet red of low value.

The part soluble in 85% sulfuric acid is the main dye, dimethoxy Acenaphthene Violet (IV). It was precipitated by pouring the sulfuric acid filtrate into ice water. The yield was 0.83 g. or 71.6% of the theory (49.6% of the theory from 4-methoxy-2-nitroaniline). It is a dark violet powder with a violet streak. The conc. sulfuric acid solution is blue (without dichroism) with weak red fluorescence, from which a red violet precipitate is formed by water. It is very easily soluble in alkaline hydrosulfite (IW) giving red violet vat with weak orange fluorescence and dyes cotton in a deep reddish violet shade. The grade of the light fastness of its dyeings is 6—7. The substance is a little soluble in boiling nitrobenzene with violet red color and green yellow fluorescence. Found: N, 8.93; calcd. for $C_{38}H_{22}O_5N_4$ (IV): N, 9.12%.

It is interesting that in the case of this methoxyl compound the imidazolization of one of the *o*-amino groups occurs readily at the same time with sodium sulfide reduction even at 60°. When the reduction was carried out at 100° for 3 hours the imidazolization proceeded further, giving 36% of the bis-imidazole pigment (X, X=OCH_3), 16% of the *o,o'*-diamino compound and only 32% of the mono-imidazole dye (IV). The drying temperatures of the products, when they were not higher than 110°, had practically no influence upon the rate of imidazolization.

Dibenzo Derivative of Acenaphthene Violet (V).—Perylene-tetracarboxylic anhydride (1.31 g., 1 mol. ratio) was heated with 5.2 g. (10 mol. ratio) of 1,2-naphthylenediamine (m.p. 95—96°, uncorr.)[5] and 1.0 g. (5 mol. ratio) of glacial acetic acid in an oil bath at 150° (bath temperature) for 1 hour and the unchanged components were removed with alcohol and 1% sodium hydroxide as in the above experiments. The weight of the crude condensation product was 2.10 g. It was then treated twice with 4 g. of sodium hydroxide, 4 g. of hydrosulfite and 200 cc. of water at 50° for 15 minutes and filtered. The amount of the hydrosulfite insoluble was 1.16 g. or 55.3% of the crude product. The part soluble in hydrosulfite was treated, after air oxidation as a dry powder, with 90% sulfuric acid. The amount of the sulfuric

4) *Org. Synth.*, **25**, 78 (1945): 4-Methoxy-2-nitroacetanilide, m.p. 118.7—119.2° (corr.) was obtained in 73.5% yield from *p*-anisidine and then saponified with potassium hydroxide in methanol to 4-methoxy-2-nitroaniline. The yield was 99.3%.

5) Diazotized aniline was coupled with β-naphthylamine in alcoholic solution to 1-benzene-azo-2-naphthylamine, m.p. 102.5—103° in 90.8% yield of the theory. It was then reduced with zinc dust in aqueous acetic acid. The yield of pure 1,2-naphthylenediamine was 53.2%. See Bamberger, Schieffelin, *Ber.*, **22**, 1376 (1889): Yokote et al., *J. Chem. Soc. Japan, Ind. Chem. Section*, **54**, 476 (1951).

acid insoluble was a trace and the soluble part was the main vat dye, dibenzo Acenaphthene Violet (V), which was collected after pouring the sulfuric acid filtrate into ice water. The yield was 0.74 g. or 33.5% of the theory[6]. It is a black violet powder of violet streak, hardly soluble in organic solvents, soluble in conc. sulfuric acid blue without dichroism and fluorescence and a violet precipitate is formed from the solution by the addition of water. The hydrosulfite vat (IW) is red violet, from which cotton is dyed in a violet blue (navy blue) shade of excellent light fastness (grade 7). Found: N, 8.24; calcd. for $C_{44}H_{22}O_3N_4$ (V): N, 8.56%.

The *o,o'*-diamino compounds of the benzene series (N,N'-diphenyldiimide type) were soluble in alkaline hydrosulfite, but the hydrosulfite insoluble of the above 150°-condensation product of 1,2-naphthylenediamine was found to be mainly *o,o'*-diamino compound by the actual estimation of the nitrogen evolution from the corresponding diazo compound. The di(*o*-amino)naphthyl-diimide is soluble in conc. sulfuric acid in blue color without dichroism and fluorescence and is a violet substance in the precipitated state. The hydrosulfite insoluble of 120°-condensation was also the *o,o'*-diamino compound. On the other hand, however, the hydrosulfite insoluble of 170°-condensation was mainly the bis-naphthoimidazole, which had analytically no more free $-NH_2$ groups. The bis-naphthoimidazole (XI) is a blue pigment and its blue conc. sulfuric acid solution shows neither dichroism nor fluorescence.

6) By 170°-condensation the yield of the main vat dye (V) was 17.4% and at 120° 16.5% of the theory.

The authors express their gratitude to The Government Industrial Research Institute, Tokyo for the measurement of reflectance curves using G. E. recording spectrophotometer.

Dyestuffs Research Laboratory,
Department of Applied Chemistry,
Tokyo University, Tokyo

*The Crystal Structure of Diallylsilanediol**

By Nobutami KASAI and Masao KAKUDO

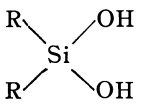
(Received July 17, 1954)

Introduction

The present study is the fourth in a series of organosilanol crystal structure determinations carried out in this laboratory, the previous three compounds examined having been diethylsilanediol[1,2,3], diphenylsilanediol[4], and bis-dimethylhydroxysilyl methane[5].

Diallylsilanediol, $(CH_2=CH\text{-}CH_2)_2Si(OH)_2$, was first prepared by Mr. R. Ōkawara and his coworkers[6].

This compound was selected for study as a typical one of the unsaturated dialkylsilanediols having the formula



.

It is of interest to compare the structure of this crystal, with the cases of the abovementioned compounds especially, in respect to the molecular chain formation through hydrogen bondings or the layer structure.

Experimental

The crystals used in this experiment were recrystallized from their ethyl ether-petroleum ether solution. The crystals are colorless, flat prismatic in habit as shown in Fig. 1; the c-face is a remarkably complete cleavage plane. These properties are quite similar to those of diethylsilanediol. It is well dissolved in oxygen containing organic solvents.

Melting point: 81 ± 0.5°C.

Density: 1.105 (by floatation method at 10°C)

For the structure determination, the oscillation and the rotation photographs were taken around both the b-axis and a-axis using nickel filtered CuK_α radiation.

Some physical constants and the dimensions of

* Read before the 7th annual meeting of the Chemical Society of Japan held in Tokyo, April, 1954.

1) M. Kakudo and T. Watase, *Technol. Repts. Osaka Univ.*, **2**, 50 (1952).

2) M. Kakudo and T. Watase, *J. Chem. Phys.*, **21**, 167 (1953).

3) M. Kakudo, N. Kasai and T. Watase, *J. Chem. Phys.*, **21**, 1894 (1953).

4) T. Watase, M. Kakudo and N. Kasai *Ann. Repts. Textile Research Inst. Osaka Univ.*, **6**, 38 (1952) (in Japanese).

5) M. Kakudo and T. Watase, *Ann. Repts. Textile Research Inst. Osaka Univ.*, **7**, 17 (1953) (in Japanese).

6) R. Okawara, K. Hashitani, and T. Watase, This Bulletin, **26**, 279 (1953).

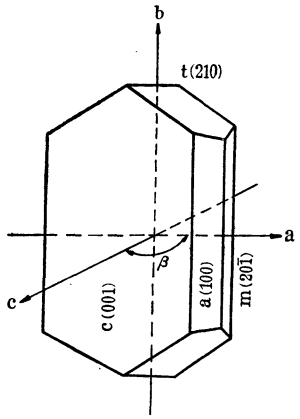


Fig. 1. The crystal form

the unit cell were listed in Table I in comparison with those of diethylsilanediol.

TABLE I

	Diallylsilanediol	Diethylsilanediol
m.p.	81±0.5°C	96±0.5°C
Density	1.105	1.134
System	Monoclinic	Monoclinic
Cleavage	(001)	(001)
Unit cell	a=14.59 kX.	a=14.55 kX.
	b= 4.94 kX.	b= 4.96 kX.
	c=13.37 kX.	c=10.25 kX.
	β=114°30′	β=110°50′
Space group	C^5_{2h}	C^5_{2h}

The physical and chemical properties of these two silanols suggest that they are much like each other not only in their chemical constitution but also in crystal structure.

The unit cell contains four molecules of $(CH_2=CH\text{-}CH_2)_2Si(OH)_2$ (calculated value $z=4.03$).

All the reflexions (hkl) were observed without any speciality, whereas no reflexions (h0l) with h odd or (0k0) with k odd were found. Consequently, the space group corresponds to C^5_{2h}—$P2_1/a$. All the atoms of this molecule are to be in the general positions of C^5_{2h},

$$(x,\ y,\ z)\ (\bar{x},\ \tfrac{1}{2}+y,\ \tfrac{1}{2}-z)\ (x,\ \tfrac{1}{2}-y,\ \tfrac{1}{2}+z)\ (\bar{x},\ y,\ z).$$

The relative intensities of reflexions were estimated by visual method with the standard density scale. The observed structure factors, $|F_{obs.}|$'s, were derived from these values by the usual method.

The Patterson function was first calculated using $F^2_{obs.}$'s. Approximate atomic arrangement was easily assumed from the b-plane projection of Patterson function by comparing with that of diethylsilanediol.

After several trials of structure factor and electron density computations, a good agreement between $F_{obs.}$ and $F_{calc.}$ was obtained for both of F(h0l)'s and F(0kl)'s. The final electron density map is shown in Fig. 2. The atomic parameters

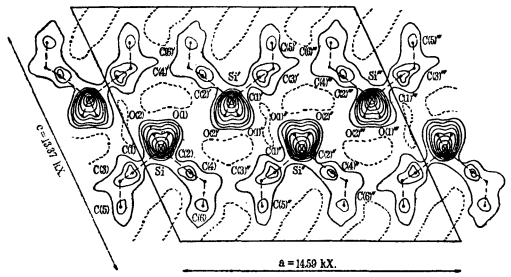


Fig. 2a. The Fourier projection map on the b-plane.

are given in Table II. The observed and calculated F-values are also listed in Table III. The

TABLE II
ATOMIC PARAMETERS

	x	y	z
0(1)	0.084	0.257	0.463
0(2)	0.138	$\overline{0.257}$	0.463
Si	0.082	0.000	0.386
C(1)	$\overline{0.054}$	0.091	0.296
C(2)	0.146	$\overline{0.091}$	0.296
C(3)	$\overline{0.115}$	0.171	0.259
C(4)	0.182	$\overline{0.171}$	0.259
C(5)	$\overline{0.152}$	0.244	0.153
C(6)	0.138	$\overline{0.244}$	0.153

TABLE III
A PART OF CALCULATED AND OBSERVED F-VALUES

(hkl)	$F_{obs.}$	$F_{calc.}$	(hkl)	$F_{obs.}$	$F_{calc.}$	(hkl)	$F_{obs.}$	$F_{calc.}$
001	86	−87	20$\bar{7}$	—	2.2	60$\bar{1}$	28	35
002	36	−27	20$\bar{8}$	11	−1.6	60$\bar{2}$	6	−15
003	30	−18	20$\bar{9}$	—	−11	60$\bar{3}$	30	−34
004	8.0	7.2	400	116	−108	60$\bar{4}$	19	29
005	29	−10	401	36	44	60$\bar{5}$	27	−38
006	25	8.3	402	22	17	60$\bar{6}$	38	40
007	—	11	403	46	−35	60$\bar{7}$	—	−10
008	41	28	404	37	28	60$\bar{8}$	31	−16
009	13	−46	405	20	25	60$\bar{9}$	40	25
0.0.10	25	−11	406	18	−33	800	25	−7.5
200	38	30	40$\bar{1}$	19	24	801	53	32

201	88	−74	$40\bar{2}$	20	−22	802	38	16
202	91	72	$40\bar{3}$	104	108	803	17	13
203	57	−40	$40\bar{4}$	52	−46	$80\bar{1}$	9	7
204	27	24	$40\bar{5}$	17	−22	$80\bar{2}$	9	27
205	18	− 7	$40\bar{6}$	41	38	$80\bar{3}$	51	−71
206	—	2.5	$40\bar{7}$	29	−34	$80\bar{4}$	15	31
207	—	4.5	$40\bar{8}$	15	−21	$80\bar{5}$	10	9
208	19	22	$40\bar{9}$	24	35	$80\bar{6}$	15	−17
$20\bar{1}$	8.3	8.2	600	25	−27	$80\bar{7}$	35	22
$20\bar{2}$	56	−53	601	57	51	$80\bar{8}$	21	−18
$20\bar{3}$	117	80	602	34	−27	$10.0.\bar{1}$	27	−34
$20\bar{4}$	77	53	603	33	− 8	$10.0.\bar{2}$	46	46
$20\bar{5}$	28	33	604	30	20	$10.0.\bar{3}$	—	1.3
$20\bar{6}$	20	−17						

values of $R=\sum||F_o|-|F_c||/\sum|F_o|$ is 0.27 for (h0l) and 0.33 for (0kl) respectively. Calculated structure factors have been corrected for atomic thermal motion by the factor $\exp\{-B(\sin\theta/\lambda)^2\}$ with $B=4.0\times10^{-16}$.

The (F_o-F_c) series map (Fig. 3) indicates,

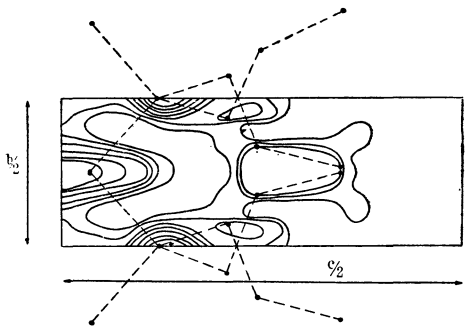


Fig. 2b. The Fourier projection map on the a-plane.

though it may not be said to be accurate, the positions of hydrogen atoms such as are assumed from its molecular structure.

Interatomic distances and bond angles are given in Table IV.

TABLE IV

INTERATOMIC DISTANCES AND BOND ANGLES

(The suffix and number of each atom are the same as in Fig. 2 or Fig. 4.)

Si—0(1)=1.63 Å.,	∠0(1)-Si-0(2)=110°,
Si—C(1)=1.90 Å.,	∠C(1)-Si-C(2)=110°,
C(1)—C(3)=1.54 Å.,	∠Si-C(1)-C(3)=109°,
C(3)—C(5)=1.33 Å.,	∠C(1)-C(3)-C(5)=120°,
C(6)...C(5)″=3.93 Å.,	0(1)′*...0(2)′=2.53 Å.,
C(6)...C(5)‴*=4.16 Å.,	0(1)′*...0(2)=3.75 Å.,
C(6)...C)6)‴*=4.25 Å.,	0(1)′*...0(2)″=3.75 Å.,
C(5)″...C(5)‴*=4.53 Å.,	0(1)′*...0(1)″=3.65 Å.,
C(5)″...C(6)′*=4.16 Å.,	0(1)′*...0(1)″*=3.65 Å.

Discussion

The silicon-tetrahedron was recognized as retaining its ordinary shape and size.

The feature of the whole structure is considerably similar to that of diethylsilanediol as shown in Fig. 4.

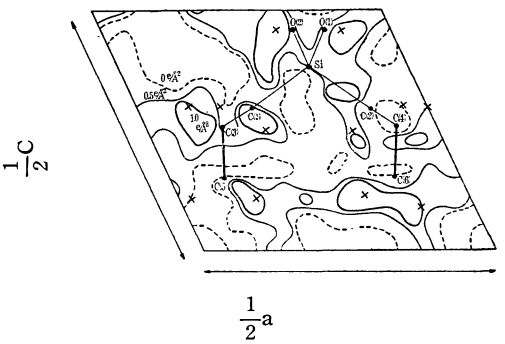
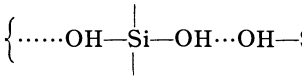


Fig. 3. $(F_o—F_c)$ series map. (The projection on the b-plane)
×: the assumed position of the hydrogen atom.

The OH.....OH distance in molecular chains



parallel to the b-axis is 2.53 Å (2.54 Å in diethylsilanediol). These OH...OH linkages by hydrogen bonds join the molecules to form infinite chains parallel to the b-axis just the same as in the case of diethylsilanediol.

The molecular chains are arranged parallel to each other in a plane (c-plane), and these sheets construct the layer structure, allyl groups of neighbouring molecules contacting back to back as in Fig. 4a. The remarkable

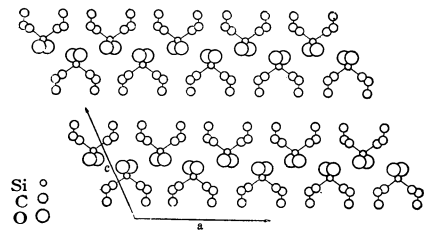


Fig. 4a. The atomic arrangement projected on the b-plane.

cleavage of (001) will be sufficiently understood from such a layer structure.

The feature of approach of OH-groups around an OH-group (Fig. 4b), and interaction

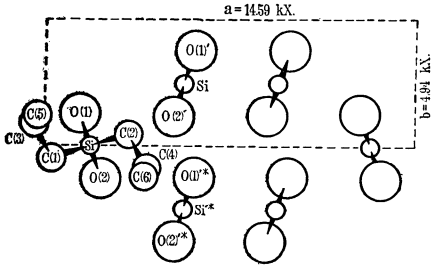


Fig. 4b. The arrangement of hydroxyl groups. (The projection on the plane $Z=\frac{1}{2}$, allyl groups are omitted except two.)

of allyl groups will be explained by the same argument as presented on diethylsilanediol. This structural similarity is to be recognized as an example of isomorphism for the chemical homologues of diorganosilanediols.

The most remarkable result is the fact that the molecular cohesion in the crystal of diorganosilanediol is mainly due to the hydroxyl bond which was formed along the b-axis by strongly polarized OH-groups, and such a way of molecular association characterizes the whole feature of crystal structure of each diorganosilanediol, which we have dealt with.

From the spreading of peaks about carbon atoms in the electron density maps and about hydrogen atoms in the $(F_o—F_c)$ series, it is reasonably supposed that the thermal motion of allyl groups in the crystal may be in a considerable degree. This thermal libration is a noticeable property of the organoradicals directly combined to silicon atom as indicated in many other works. The low interaction of allyl groups, plus the long distance of Si-C bond should bring about a weak barrier to their thermal motion.

It is interesting to note that the peaks for all atoms in the electron-density map of Fig. 2b are elongated in such a manner as to suggest that one of the principal thermal motions is a vibration of the entire molecule along the direction perpendicular to the c-plane. This fact is also in agreement with our consideration that the intermolecular cohesive force of this crystal may be comparatively weak in this direction.

However, the anomaly of (001) reflexions expected to be sensitively influenced by such motion was not observed appreciably, though there were observed a few diffuse Laue spots. The qualitative relation of these diffuse reflexions and the molecular motion will be explained in comparison with diethylsilanediol before long.

Conclusion

The morphology and the crystal structure of diallylsilanediol were presented.

The whole feature of this structure is nearly the same as that of diethylsilanediol previously studied by one of the authors.

Many of the chemical and physical properties of diorganosilanediols can be interpreted in terms of obtained structural principles.

It was verified that the chemical homologues of diorganosilanediols give rise to a structural isomorphism.

The OH...OH distance (2.53 Å) with hydrogen bond is the same as in the case of diethylsilanediol (2.54 Å) within the range of error.

The thermal motion of allyl groups combined to silicon atom is considered as more vigorous than that in the corresponding organic compounds even at room temperature.

The authors wish to express their sincere thanks to Mr. R. Ōkawara who kindly gave them some precious samples.

Department of Applied Chemistry,
Faculty of Engineering,
Osaka University,
Higashinoda, Osaka

*The Alternating Current Polarisation with Respect to Hetero-Pair Electrodes**

By Shigeo NAGAURA and Kazuo SASAKI

(Rceived July 19, 1954)

Introduction

It was long ago when the galvanic polarisation such as the polarisation capacitance and the polarisation resistance, caused by alternating current, came into our knowledge.

As was shown in some reviews made recently by one of the present authors[1] and also by Shaw and Remick[2], many investigators have been concerned with the problem either theoretically or experimentally for the past 70 years or more.

In spite of the fact that the theoretical treatments were carried out in detail from the various standpoints, the experimental investigations did not give us any satisfactory explanation for the nature of the polarisation effect. One of the causes of the present meagre experimental knowledge is the difficulty of the measurement of this sort. Above all it is serious that exact reproducibility can never be attained. In fact, all the investigators have stated that the observed values change, not only from one sample of the liquid to another, or from one set of the electrodes to another, but also change with time for the same set of electrodes and the same sample of liquid.

Here we want to verify a fundamental character of polarisation effect, caused by the application of alternating current, which has been assumed tacitly by prior investigators. In other words, our main subject is to know whether the polarisation characters, measured as to a whole cell, can be attributed to each single electrode or not.

No such attempt has been made so far as we aware.

Robertson[3] attempted to determine the polarisation capacitance for a single platinum electrode immersed in hydrochloric acid solution, along the line indicated by Grahame[4] for dropping mercury electrode.

Though his experiments were carried out also for the polarisation capacitance of the single electrode of solid metal, the effect observed was essentially the direct current polarisation, in which the steady state may be reached, We are going to study the problem in a different way.

Experimental

The measuring devices consist of an ordinary impedance bridge and an audio frequency generator. The latter was made in our laboratory. The frequency was kept at 1440 cycles per second, which was corrected with a standard oscillator. A variable air condenser attached to the balancing arm of the bridge changes in its capacity from 1.11μF. to 0.0001μF.

Since the principal purpose of this experiment was the attribution of the polarisation characters to each component electrode (electrode/soln. interface), several kinds of metals were prepared for electrode materials, each having the same dimension, that is, the disk plate having 2 cm. in its diameter. Metals prepared were Pt, Ni, Cu and Ag. Copper electrode was electropolished before each measurement. Nickel and silver electrodes were prepared by means of electroplating on the copper surface. The solutions investigated were N/100, N/10 and 1N KCl aqueous solution. Alcoholic solutions of KCl in two different concentrations were also investigated. One of these alcoholic solutions was made in the following way: 2 cc. of 1N KCl aqueous solution was dropped into 1 litre of 96% ethyl alcohol and after vigorous shaking the bottle was kept still at 0°C for a day, then the excess precipitation of potassium chloride was separated by careful decantation. A portion of the saturated solution, thus obtained, was diluted by ninefold amount of ethyl alcohol.

Measurements were carried out at 28°C and at 0°C, the former temperature was obtained by means of well regulated thermostat and the latter was kept by means of ice-water mixture.

Figure 1a shows the conductivity cell which is made of Telex glass and has been used for all of the experiments. As is clearly seen, from the figure, both of the two electrodes are allowed to move so as to be able to determine the polarisation resistance in such a way as will be explained in the following article.*

---

* The terms homo-pair electrodes and hetero-pair electrodes are defined as a set of electrodes consisting of the same or different metals, respectively.

1) S. Nagaura, *J. Electrochem. Soc. Japan*, **19**, 249 (1951).
2) M. Shaw and A. Remick, *J. Electrochem. Soc.*, **97**, 324 (1950).
3) W. Robertson, *J. Electrochem. Soc.*, **100**, 195 (1953).
4) D. C. Grahame, *J. Am. Chem. Soc.*, **68**, 301 (1946); *Chem. Revs.*, **41** 441 (1947).

A Short Explanation of the Equivalent Series Circuit

Though most investigators have treated their measured quantities of the polarisation phenomena using the equivalent series circuit, no serious discrepancy has appeared in such treatment.

Warburg first suggested and developed the idea that the diffusion is responsible for the incomplete reversibility of the electrode reactions. By the integration of Fick's law of diffusion with suitable boundary conditions he reached the conclusion that polarisation causes a capacitance in series with the resistance of the electrolyte. His theory has been extended by many authors thereafter, but owing to their different viewpoints, there exist several kinds of equivalent circuits for an electrolytic cell (See Ref. 1). Some of them, however, can not be adopted practically because of the complexity of their circuit elements.

Kohlrausch first found that the inverse electromotive force, Ep, caused by polarisation, is proportional to the amount of electricity passed through the cell, i.e.,

$$Ep=1/C\int Idt. \tag{1}$$

If the current, I,is alternative and expressed as $I=Io\ \sin\omega t$, Eq. 1 then becomes

$$Ep=Io/\omega C\ \sin(\omega t-\pi/2). \tag{2}$$

This means that Ep is equal to the voltage drop which occurs when a.c., $I=Io\ \sin\omega t$, passes through a condenser of capacity C.

Wien suggested that the formula on Ep must have a term with regard to the phase difference, φ, i.e.,

$$Ep=Io/\omega C\ \sin\left\{\omega t-(\pi/2-\varphi)\right\}. \tag{3}$$

This equation means that Ep is equal to the voltage drop which occurs when a.c. is applied to a series circuit consisting of a condenser of capacity $C/\cos\varphi$ and a resistor of resistance $\sin\varphi/\omega C$.

Figure 2a is a schematic expression of the equation 3.

In this work we assume the identical behavior of the two electrodes, thus the equivalent circuit can be expressed as in Fig. 2b.**

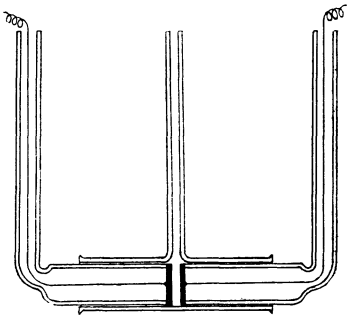


Fig. 1 a. Conductivity cell

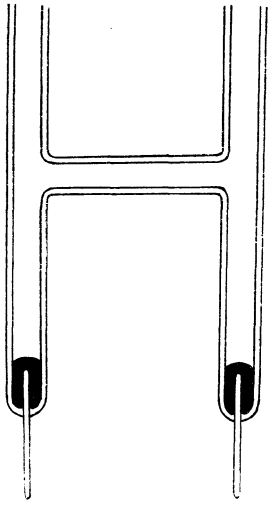


Fig. 1 b. H-Form electrode

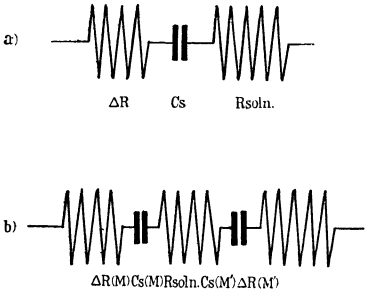


Fig. 2a. Equivalent circuit

Results and Discussion

Reproducibility of the Measurements.—At first, the effect of the immersion time and the reproducibility of the measurements were detected.

Shaw and Remick reported that when the platinum electrodes are combined together electrically and used as the anode for the electrolysis of alkaline cyanide solution before each conductivity measurement, reproducible results were obtained. As far as we repeated their experiment, however, the satisfactory agreement with them was not recognised. Moreover the systematic influence of the electrolysis was not observed. This is shown in Table 1. In Table 1, Rp and Cp are the values of bridge readings and Rs and Cs are of those converted into series circuit, respectively.

From the Table we can not see any regenerative effect of the electrolysis. (Some atten-

TABLE I.*

1)	Anodic treatment; 15 min..			
	Immersion time (min.)	$Rp(\Omega)$	$Cp(\mu F.)$	$Rs(\Omega)$	$Cs(\mu F.)$
	0	711	0.1051	48.7	3.33
	80	628	0.0914	49.4	4.27
	220	619	0.0884	49.6	44.4
2)	Anodic treatment; one hour.				
	0	615	0.0899	49.1	4.45
3)	Anodic treatment; 12 min..				
	0	760	0.1063	49.3	3.03
	10	752	0.1059	49.7	3.11
	50	757	0.1068	49.1	3.04
	105	762	0.1079	48.8	3.03
4)	Anodic treatment; 20 min..				
	0	789	0.1068	49.3	2.71
	20	775	0.1059	49.5	2.71
	50	776	0.1080	49.4	2.58

* The values are arranged in order of the measurements.

It is seen from the table that the values do not depend on the time of anodic treatment but on the immersion time.

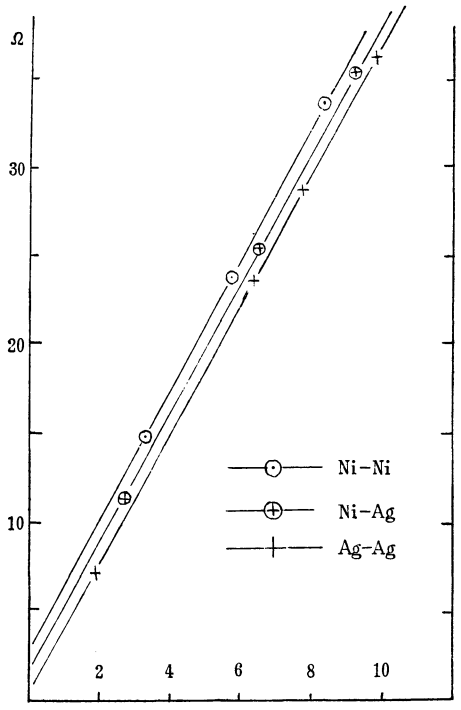


Fig. 3 Determination of polarisation resistance

tion must be given to zero minute values.)

These observations were made by H-form platinum electrodes, which are shown in Fig. 1b, in a wide porcelain bath at room temperature.

Shaw and Remick also stated the effects of immersion as follows:

1) The electrodes were immersed for one hour before taking a reading. Then they were removed from the measuring solution and washed with hot water just before boiling. Finally, the electrodes were returned to the cell and Cs was immediately determined. The result was the same to " one hour value ".

2) The changes of Cs with time, whatever their nature, were essentially independent of any application of the current.

These results were in agreement mostly with our trace experiment.

In consequence, we conclude that the " aging process " of the electrodes makes it impossible to determine the absolute values of the polarisation impedances for all the individual electrode, owing to the incomplete reversibility of the a.c. electrode reactions, and special precautions have to be taken even to obtain relative values which are comparable.

A similar opinion was reported by jaffé and Rider[5] recently. In this connection, Jones and Christian[6] reported that their Cs value with silver electrodes was greater than that for platinum, while Wien had obtained the contrary results. Thus it is also doubtful whether it is possible to determine the order of the Cs values of various metals. From the above arguements, it must be said that absolute order can not be obtained in practice, owing to instability of each metal surface against the action of alternating current and this inability is not because of the experimental mistake.

Thus in the following experiments we took

5) G. Jaffé and A. Rider, *J. Chem. Phys.*, **20**, 1077 (1952).
6) G. Jones and S. Christian, *J. Am. Chem. Soc.*, **57**, 272 (1935).

great care to get reliable data; we need the data only for comparison. In other words, a series of experiments should be completed without delaying.

Additivity of the Polarisation Characters with Respect to a Single Electrode.—Since the arrangement of the balancing arm of the bridge is in parallel, impedances of each element of Fig. 2a is easily calculated by the following relations;

$$Rs=Rt+\Delta R=n(Rp/1+\omega^2Cp^2Rp^2) \quad (4)$$

$$Cs=1/n\cdot Cp(1+1/\omega^2Cp^2Rp^2) \quad (5)$$

where n is the arm ratio of the bridge, and suffixes s and p are taken to mean the series and parallel values, respectively.

As far as we deal with the homo-pair measurements, these series values are easily divided into two parts corresponding to each metal/soln. interface. The values for hetero-pair electrodes may be calculated from the values of homo-pair measurements and also by direct measurements. The results thus obtained for aqueous KCl solutions are tabulated in Table II. Values in Table III are those for KCl saturated ethyl alcohol.

In general, the same kind of experiments were carried out two or three times and the tabulated values are the averages of them.

Although it seems that Cs values for N/100 KCl aq. soln. disprove the simple additivity of the polarisation characters, most of them for N/10 KCl aq. solns. and especially for alcoholic solutions confirm our assumption with relatively high concordance. The Cs values of Cu-Pt system in Table II is something erratic, perhaps due to chemical instability of copper in aqueous solution, while the same system in alcoholic solution gives a good agreement between the observed value and the calculated one. The discrepancies which appear in "N/100 measurements" were

TABLE II

ADDITIVITY OF POLARISATION IMPEDANCES FOR AQUEOUS SOLUTIONS

System	$\Delta R(\Omega)$		$Cs(\mu F.)$	
	Obs.	Calc.	Obs.	Calc.
A) N/10 KCl aq. soln. at 28°C				
Pt-Pt	3.0	—	12.2	—
Ni-Ni	12.6	—	4.5	—
Cu-Cu	3.4	—	21.4	—
Ag-Ag	1.5	—	25.5	—
Ag-Pt	1.5	2.2	11.4	16
Cu-Pt	3.5	3.2	9.3	14
Ni-Pt	6.7	7.8	6.7	6.6
B) N/10 KCl aq.soln. at 0°C				
Ni-Ni	2.6	—	16.1	—
Ag-Ag	0.8	—	37.0	—
Ag-Ni	1.6	1.6	22.3	21.3
C) N/100 KCl aq.soln. at 0°C				
Ni-Ni	40	—	1.4	—
Ag-Ag	5	—	7.6	—
Pt-Pt	uncertain	—	1.6	—
Ag-Ni	10	20	6.8	2.4
Pt-Ni	uncertain	uncertain	4.7	1.5

TABLE III

ADDITIVITY OF POLARISATION IMPEDANCES FOR ALCOHOLIC SOLUTIONS

System	$\Delta R(\Omega)$		$Cs(\mu F.)$	
	Obs.	Calc.	Obs.	Calc.
Ni-Ni	70±30	—	4.8	—
Ag-Ag	130 „	—	12.5	—
Pt-Pt	uncertain	—	9.1	—
Cu-Cu	30±30	—	20.1	—
Ag-Ni	70±„	uncertain	6.5	6.9
Pt-Ni	140 „	„	6.1	6.0
Pt-Cu	50 „	„	12.6	12.5
Pt-Ag	140 „	„	11.1	10.4

not changed by the second runing reexamined one month after the first experiment.

It may be thought that in a dilute solution the solvent molecule as a role to make these discrepancies. In this connection, we made a series of experiments using a dilute alcoholic solution. The result confirmed the additive characters of the effect. This is seen in Table IV.

TABLE IV
ADDITIVITY FOR DILUTE ALCOHOLIC SOLUTIONS

System	Cs (μF.)	
	Obs.	Calc.
Ag-Ag	21.8	—
Ni-Ni	5.0	—
Ag-Ni	8.2	8.1

" N/100 values ", however, are only two sets of electrodes, therefore more detailed investigations with various sets of electrodes are necessary. At the same time the study must be carried out about more dilute solutions.

The polarisation resistance, ΔR,which is often called excess resistance, can be determined by changing the distance of electrodes; since the polarisation resistance is characteristic only of the electrode/solution interface and not affected by inter-electrode distance, if the frequency is kept constant.[1,6] Therefore we can obtain the ΔR value by plotting measured series resistance, Rs, against the electrode separation and read the extrapolated value of Rs at zero distance. Fig. 3a is one of the representative diagram for ΔR determinations. ΔR values for N/100 aqueous potassium chloride solutions and also for alcoholic solutions are very erratic, because our conductivity cell has no elaborate attachment to determine the interelectrode distance and therefore we can read only the order of the magnitude, when the solution is less conductive.

Summary

1) We attempted to prove that the polarisation characters, being measured as to a whole cell, can be attributed to each single electrode. This attempt was verified by most of the experiments.

2) The above success may be one of the experimental justifications to use a simple series circuit as the equivalent circuit of a conductivity cell.

3) Discordant results appearing in " N/100 measurements " are to be studied in more details.

The authors wish to express their great thanks to the effort made by Mr. Koichi Karaki, our former collaborator.

Department of Chemistry,
Institute of Polytechnics,
Osaka City University

Vat Dyes of Pyrazoloanthrone Series. V. Self Condensation of 5-Chloropyrazoloanthrone

By Toshio MAKI and Hideo SEKI

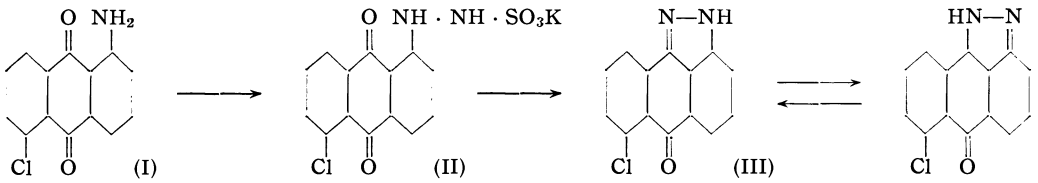
(Received July 24, 1954)

Nuclear chloro derivatives of pyrazoloanthrone have been hitherto prepared from 1,x-dichloroanthraquinone and hydrazine hydrate in pyridine solution.[2] Recently Bradley and Geddes prepared 5-chloropyrazoloanthrone (III) also by this method from 1,5-dichloroanthraquinone,[3] but the obtained product had low and wide range of melting point (275–285°) and only after recrystallization melted at 298°. We have now synthesized 5-chloropyrazoloanthrone (III) from 1-amino-5-chloroanthraquinone (I) via potassium 5-chloroanthraquinonyl-1-hydrazine sulfonate (II) by application of the diazotization, followed by the

1) Read before the 6th Annual Meeting of the Chemical Society of Japan on April 5, 1953.

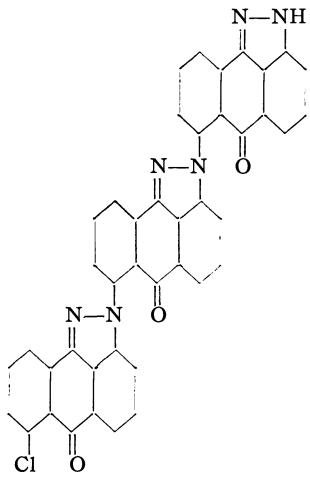
2) Ullmann, *Ber.*, **53**, 826 (1920).

3) *J. Chem. Soc.* **1952**, 1633.

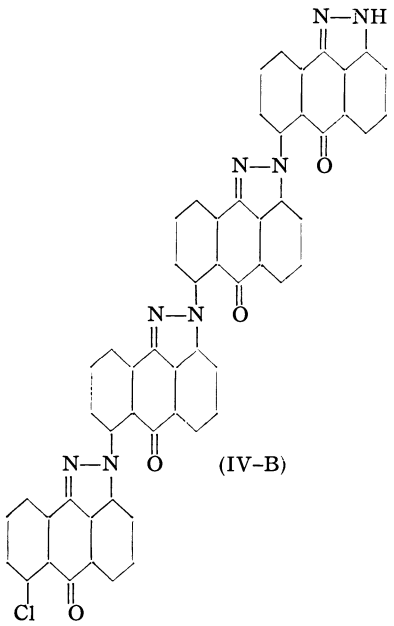


treatment with sulfite and bisulfite and ring closure with conc. sulfuric acid analogous to our synthesis of pyrazoloanthrone from 1-aminoanthraquinone.[4] This method gives 5-chloro-pyrazoloanthrone of high purity in 79% yield of the theory. Even the crude product melted at 301–2° (corr.) and after recrystallization greenish yellow needles of m.p. 305–6° (corr.) were easily obtained.

Among the isomeric chloro derivatives of pyrazoloanthrone the 5-chloro compound is most reactive and we have found that it has an interesting behaviour of polymolecular self condensation, a new type of reaction hitherto never studied in the chemistry of anthraquinone derivatives. When 5-chloro-pyrazoloanthrone alone was heated in boiling nitrobenzene in the presence of sodium carbonate and copper for 25 hours the product was nearly 50%: 50% mixture of 3 molecular and 4 molecular self condensation product (IV-A and IV-B), which was ascertained by its properties



(IV-A)

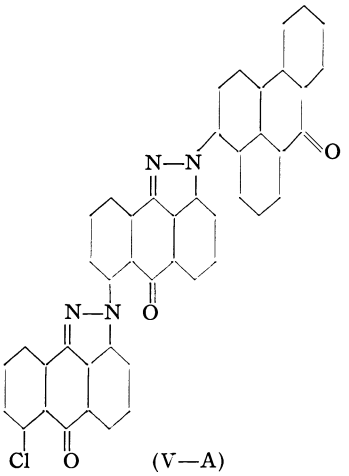


(IV-B)

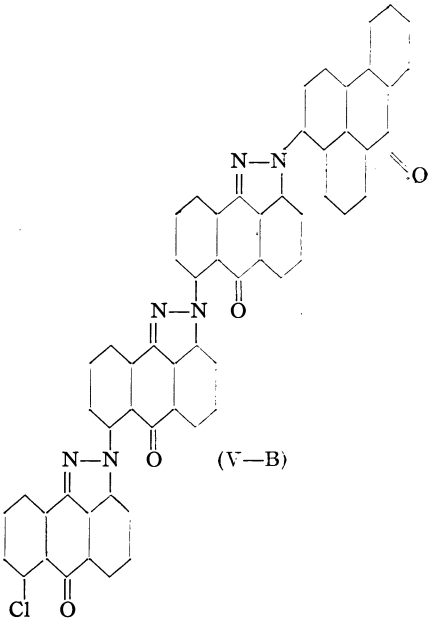
	5-Chloro-pyrazoloanthrone(III)	Self condensation product (IV-A and IV-B)
With aq. NaOH	Orange red solution	No color reaction
m.p.	305—6°	>400°
Cl% found	13.72	4.60
In *o*-dichlorobenzene	Soluble	Insoluble
Appearance	Greenish yellow needles	Yellow brown powder
In conc. H_2SO_4	Orange	Red orange
Precipitate with water	Yellow	Yellow brown

and estimation of the terminal chlorine atoms.

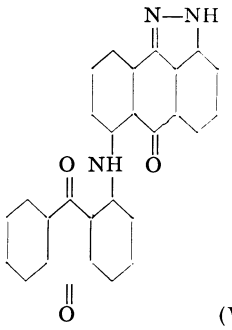
4) T. Maki, T. Akamatsu and M. Maezawa, *J. Chem. Soc. Japan. Ind. Chem. Section*, **54**, 245 (1951).



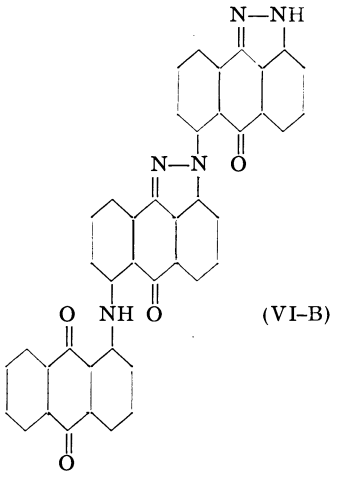
(V—A)



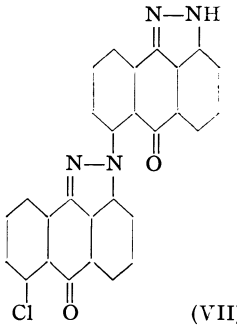
(V—B)



(VI-A)



(VI-B)



(VII)

In the presence of potassium carbonate, even without copper, the self condensation proceeded further and the obtained substance contains 3.80% Cl, which corresponds nearly to the 4 molecular condensation product (IV-B). This polymolecular self condensation occurs also in cases of other syntheses using 2 or more different components. Thus, when 5-chloro-pyrazoloanthrone and 3-bromobenzanthrone were boiled with nitrobenzene in the presence of sodium carbonate and copper for 15 hours the product was found to be a mixture of nearly 45% of (V-A) and 55% of (V-B), 1:2 and 1:3 product respectively, ascertained by the amount of recovered 3-bromobenzanthrone and estimation of Cl% and N% of the substance.

When 5-chloro-pyrazoloanthrone and 1-aminoanthraquinone were similarly boiled with naphthalene for 15 hours the chief product, insoluble in *o*-dichlorobenzene, was a mixture of nearly 34% of (VI-A) and 66% of (VI-B), 1:1 and 2:1 product respectively.

The part soluble in hot *o*-dichlorobezene, in this case, contained bimolecular self-condensation product (VII) and uncombined 1-aminoanthraquinone. The estimation of the amounts of these soluble components was useful for the determination of the proportion of (VI-A) and (VI-B).

Experimental Part

5-Chloro-pyrazoloanthrone (III). — 1-Amino-

5-chloroanthraquinone (I)[5] (12.88g., 1 mol. ratio) was dissolved in 64.4g. of conc. sulfuric acid (97.0%) and sodium nitrite (3.65g., 1.06 mol. ratio), dissolved in 36.5g. of ice cold conc. sulfuric acid, was added at 2° and agitated for 30 minutes at 5°. The diazo solution was poured on 150g. of ice and after the addition of 14.6g. of anhydrous sodium sulfate stirring was continued for 30 minutes keeping the temperature below 10°. The precipitated diazo compound was filtered, agitated with 250g. of ice water and sodium bicarbonately was carefully added until the litmus-neutral point was obtained. The presence of 2 drops of lauryl alcohol is convenient as an antifoaming agent. To the neutralized diazo compound 59.0g. of 16% sodium sulfite (1.5 mol. ratio), freshly prepared from sodium hydroxide and sulfur dioxide, was added, kept 1 hour at 10°, then 1 hour at 30° and to this diazo sulfonate 21.6g. of freshly prepared 36% sodium bisulfite (1.5 mol. ratio), together with 2 cc. of conc. hydrochloric acid and 2 cc. of water, was given, warmed up to 90° and agitated at this temperature for 1 hour. The hot solution was filtered in order to remove a small amount of dark brown insoluble by-product (2.9% of the starting material) and 45g. of potassium chloride was added to the orange red filtrate and allowed to stand over night. The red crystalline precipitate of potassium 5-chloroanthraquinonyl- 1-hydrazine sulfonate (II) was collected and dried in vacuum. The yield was 21.9g. This was then dissolved in 175g. of conc. sulfuric acid (99.6%) and kept at 100° for 3 hours on a boiling water bath. 5-Chloro- pyrazoloanthrone was obtained by pouring the acid solution into water. The yield of the crude product, m.p. 301–2° (corr.), was 10.05g. or 79.0% of the theory. After recrystallization from *o*-dichlorobenzene greenish yellow needles of highest purity, m.p. 305–6° (corr.), were obtained. Its conc. sulfuric acid solution is orange, and a yellow precipitate is formed by the addition of water. Like the unsubstituted pyrazoloanthrone its iminohydrogen is so sensitive to alkali that it dissolves in dilute sodium hydroxide with intense orange red color, which is very useful for its detection even in cases of minute quantities. As shown in our previous report[6] the tautomerism must, of course, exist also in 5-chloro-pyrazoloanthrone. Found: N, 10.74; Cl 13.72; Calcd. for $C_{14}H_7ON_2Cl$ (III): N, 11.01%; Cl 13.92%.

Self Condensation of 5-Chloro-pyrazoloanthrone.—A mixture of 1.268g. (1 mol. ratio) of 5-chloro-pyrazoloanthrone (III), 0.530g. (1 mol. ratio) of anhydrous sodium carbonate and 0.063g. (0.2 atomic ratio) of precipitated metallic copper was kept boiling with 25.4g. of nitrobenzene under reflux and stirring for 25 hours. Nitrobenzene was then removed by steam distillation and the precipitate, after collecting and drying, was dissolved in 30 times to quantity of conc. sulfuric acid and filtered through asbestos in order to remove the insoluble copper. By pouring the conc. sulfuric acid filtrate into water the condensation product was obtained, which was washed neutral and dried at 110°. The yield was 1.10g. or 86.5% of the starting material. It is a yellow brown powder of m.p. higher than 400°, with no color reaction sodium hydroxide and perfectly free from 5-chloro-pyrazoloanthrone. It is insoluble in organic solvents, soluble in conc. sulfuric acid with red orange color, and a yellow brown precipitate is formed from the acid solution by water. Found: Cl, 4.60; calcd. for $C_{42}H_{19}O_3N_6Cl$ (IV-A): Cl, 5.14%; calcd. for $C_{55}H_{25}O_4N_8Cl$ (IV-B): Cl, 3.91%. The substance corresponds neary to 50%: 50% mixture of (IV-A) and (IV-B). Contrary to 2,2'-dipyrazoloanthronyls this substance is insoluble in alkaline hydrosulfite as its constituents have no conjugation between the two carbonyls.

Condensation of 5-Chloro-pyrazoloanthrone with 3-Bromobenzanthrone.[7] — 5-Chloro-pyrazoloanthrone (2.117g., 1 mol. ratio) and anhydrous sodium carbonate (0.974g., 1.1 mol. ratio) were boiled with 31.8g. of nitrobenzene for 1 hour. The heating was interrupted for a short time, 2.834g. (1.1 mol. ratio) of 3-bromobenzanthrone together with 0.106g. (0.2 atomic ratio) of precipitated metallic copper being added, and the whole was further boiled for 15 hours. After distilling off the solvent by steam and removing the insoluble copper with conc. sulfuric acid as in the above experiment, 4.64g. of crude condensation product was obtained. As the crude product is perfectly indifferent to sodium hydroxide and gives no red color it was confirmed that it contains no more 5-chloro-pyrazoloanthrone. It was then boiled with 46.4g. of *o*-dichlorobenzene for 1 hour and filtered, when the purified condensation product, 2.32g. or 50.0% of the crude product, was obtained as the insoluble and 1.94g. (0.75 mol. ratio) of unchanged 3-bromobenzanthrone recovered from the filtrate by steam distillation. So it became known that approximately 0.35–0.4 mol. of 3-bromobenzanthrone had actually condensed with 1 mol. of 5-chloro-pyrazoloanthrone. The purified condensation product is a brown yellow powder of m.p. higher than 400°, insoluble in organic solvents and soluble in conc. sulfuric acid with orange color. Found: N,8.67; Cl, 4.28; calcd. for $C_{45}H_{21}O_3N_4Cl$ (V-A): N, 8.00%; Cl, 5.07%; calcd. for $C_{59}H_{27}O_4N_6Cl$ (V-B): N, 9.15%; Cl, 3.56%. The substance corresponds nearly to a mixture of 45% of (V-A) and 55% of (V-B).

Condensation of 5-Chloro-pyrazoloanthrone with 1-Aminoanthraquinone.[7] —A mixture of 1.015g. (1 mol. ratio) of 5-chloro-pyrazoloanthrone, 0.893g. (1 mol. ratio) of 1-aminoanthraquinone, 0.424g. (1 mol.ratio) of anhydrous sodium carbonate and 0.051g. (0.2 atomic ratio) of precipitated copper was kept boiling with 20g. of naphthalene

5) Obtained by the sodium sulfide reduction of 1-chloro-5-nitroanthraquinone in 91.8% yield and after recrystallization from o-dichlorobenzene melted at 219° (corr.). 1-Chloro-5-nitroanthraquinone was prepared from potassium 5-nitroanthraquinone-1-sulfonate by the chlorate method in 94% yield and a sample of m.p. 316° (corr.) was obtained after recrystallization from *o*-dichlorobenzene. See also T. Maki and Y. Nagai, *J. Chem. Soc. Ind. Japan*, **33**, 464B (1930).

6) T. Maki and T. Akamatsu, *J. Chem. Soc. Japan, Ind. Chem. Section*, **54**, 281, 326 (1951).

7) Compare with *G. P.* 520395, *Frdl.* **17**, 1291

under reflux and stirring for 15 hours. As in the above experiments the crude condensation product was obtained after the steam distillation of naphthalene and after removing the copper by the treatment with conc. sulfuric acid. The yield was 1.61g. The crude product is perfectly free from the starting 5-chloro-pyrazoloanthrone as it shows no red color reaction with sodium hydroxide. A small quantity of chlorine (1.5%Cl) found in the crude substance indicates the presence of about 20% of bimolecular self-condensation product (VII) (calcd. Cl 7.50%), because it can be removed by dissolving in boiling *o*-dichlorobenzene. When the crude product (1.61g.) was boiled with 48.3g. of *o*-dichlorobenzene, hot filtered 0.70g. (44% of the crude product) of chlorine free condensation product was obtained as the insoluble. From the filtrate 0.50g. of unchanged 1-aminoanthraquinone and 0.32g. of the chlorine compound (VII), corresponding to 0.34g. of 5-chloro-pyrazoloanthrone, were recovered. So it was found that about 0.39g. (0.44 mol. ratio) of 1-aminoanthraquinone had actually condensed with 0.67 g. (0.66 mol. ratio) of 5-chloro-pyrazoloanthrone. The purified, chlorine free condensation product is a red brown powder of m.p. higher than 400°, hardly soluble in organic solvents, indifferent against alkali, but soluble in conc. sulfuric acid brown, and brown red precipitate is produced from the acid solution by the addition of water. From these data it is concluded that the substance, insoluble in hot *o*-dichlorobenzene, is a mixture of nearly 34% of 1 : 1 condensation product (VI-A) and 66% of 2 : 1 condensation product (VI-B). Found: N,10.35; calcd. for $C_{28}H_{15}O_3N_3$ (VI-A): N, 9.52%; calcd. for $C_{42}H_{21}O_4N_5$ (VI-B): N, 10.62%.

Dyestuffs Research Laboratory,
Department of Applied
Chemistry, Tokyo University,
Tokyo

Antituberculous Compounds. IV. Thiosemicarbazones and Related Compounds

By Tamio NISHIMURA

(Received August 8, 1954)

α-Bromo-4-nitrocinnamaldehyde thiosemicarbazone has been found to posses *in vitro* action against *Staphylococcus aureus* and *Escherichia coli*.[1] In the present study, semicarbazones and guanylhydrazones of α-bromo-4-nitrocinnamaldehyde (I) and 1-(4-nitrophenyl)-2-bromo-1-buten-3-one were prepared in an attempt to increase the biological effect. Corresponding derivatives of 4-nitrocinnamaldehyde (II) and 4-nitrobenzalacetone were prepared in order to examine the effect of Br-substitution at the α-position of α,β-unsaturated carbonyl compounds. Nitromethane derivatives of I and II were also synthesized.

Furthermore, thiosemicarbazones of 4-nitro, 4-amino, and 4-acetamido-acetophenones were prepared in an attempt to compare their antituberculous activities with those of their vinylogs synthesized previously.[2]

Experimental[3]

α-Bromo-4-nitrocinnamaldehyde.—To a solution of 8.9 g. of 4-nitrocinnamaldehyde[4] in 80 cc. of glacial acetic acid was added 8 g. of bromine. When the red color of the mixture had almost completely disappeared, 6.9 g. of anhydrous potassium carbonate was added. After the evolution of gas had ceased, the mixture was heated in a water bath for ten minutes, giving 11.5 g. of slightly yellow crystals melting at 137–138°. On adding water the filtrate produced a further crop melting at 133–134° which yielded 0.4 g. of the product melting at 136–138° on recrystallization from 10 cc. of ethanol. Both crops were recrystallized from ethanol to give 11 g. (86%) of the desired product melting at 138–139°.[5]

Thiosemicarbazone.—To a suspension of 0.8 g. of α-bromo-4-nitrocinnamaldehyde in 20 cc. of hot ethanol was added 0.3 g. of thiosemicarbazide and the whole stirred in a water bath for ten minutes to give yellow precipitates, yield 1 g. (90%), m.p. 218° (decompn.) Recrystallization from ethanol gave slightly yellow long needles, m.p. about 214° (decompn.). Found: N, 16.88%. Calcd. for $C_{10}H_9N_4O_2SBr$: N, 17.00%.

Semicarbazone.—The crude product obtained by heating a mixture of the aldehyde, semicarbazide, and ethanol was recrystallized three times from ethanol, giving tiny yellow prisms melting at 223° (decompn.) in 32% yield. Found: N, 17.91%. Calcd. for $C_{10}H_9N_4O_3Br$: N, 17.90%).

Guanylhydrazone hydrochloride.—A mixture of 1.3 g. of the aldehyde, 0.7 g. of aminoguanidine bicarbonate[6], and 10 cc. of ethanol was acidified

1) Katsuhiko Tago and Tamio Nishimura, Presented before the Kanto regional meeting of Nippon Saikin Gakkai, June 27, 1953: chemotherapy **2**, 157—161 (1954).
2) Tamio Nishimura, This Bulletin, **26**, 253 (1953).
3) All temperatures are uncorrected.
4) Tamio Nishimura, This Bulletin, **25**, 54 (1952).
5) Reported m.p. 136°; Zincke v. Hagen. *Ber.*, **17**, 1816 (1884). Einhorn and Gehrenbeck, *Ann.*, **253**, 351 (1889).
6) R. L. Shriner and Fred W. Neumann, "Organic Syntheses" Vol. 26, p. 7.

with concentrated hydrochloric acid[7] and heated in a water bath for several minutes. Pale yellow long prisms were obtained from ethanol and conc. hydrochloric acid; m.p. 265° (decompn.), yield 1.4 g. (80%). Found: Cl, 10.35%. Calcd. for $C_{10}H_{11}N_5O_2BrCl$: Cl, 10.17%.

4-Nitrocinnamaldehyde.—This compound was prepared as reported before.[4]

Semicabazone.—A solution of 0.9 g. of the aldehyde, and 0.6 g of acetone semicarbazone in 50 cc. of ethanol was adjusted to pH 3.0 with 10% hydrochloric acid and heated in a water bath for thir'y minutes. Crystals were filtered, washed well with ethanol, suspended in 20 cc. of hot ethanol, filtered hot, and washed again with ethanol to give 1 g. (84%) of the desired product, m.p. 232° (decompn.), yellow plates. Found: N, 23.82%. Calcd. for $C_{10}H_{10}N_4O_3$: N, 23.95%).

Guanylhydrazone hydrochloride.—Tiny yellow prisms (from ethanol and concentrated hydrochloric acid), easily soluble in hot ethanol and hot water and insoluble in hot benzene, yield 64%, m.p. 238° (decompn.). Found: Cl, 13.50%. Calcd. for $C_{10}H_{12}N_5O_2Cl$: Cl, 13.15%.

4-Nitrobenzalacetone.—This compound was synthesized as reported previously.[2]

Semicarbazone.—From 0.96 g. of the ketone and semicarbazide in ethanol was obtained 1.1 g. (89%) of the desired product, m.p. 234° (decompn.), canary yellow crystals. The crude material (0.2 g.) dissolved in 25 cc. of hot pyridine gave tiny needles melting at 235° (decompn.) on adding 40 cc. of water. Found: N, 22.21%. Calcd. for $C_{11}H_{12}N_4O_3$: N, 22.57%.

Guanylhydrazone hydrochloride.—Tiny yellow needles melting at 270° (decompn.) obtained from 0.96 g. of the ketone were recrystallized form 150 cc. of ethanol containing a small amount of concentrated hydrochloric acid, giving 1.2 g. (85%) of the pure hydrochloride melting at 270° (decompn.). Found: Cl, 12.59%. Calcd. for $C_{11}H_{14}N_5O_2Cl$: Cl, 12.50%.

1-(4-Nitrophenly)-2-bromo-1-buten-3-one. — This compound was prepared according to the method reported before.[2]

Semicarbazone.—Long pale yellow prisms (from ethanol) melting at 229° (decompn.) from the ketone and semicarbazide, yield 82%, halogen test positive, Found: N, 17.10%. Calcd. for $C_{11}H_{11}N_4O_3Br$: N, 17.13%.

Guanylhydrazone hydrochloride.—Yellow prisms (from ethanol and concentrated hydrochloric acid), m.p. 249–250° (decompn.), yield 87%. Found: Cl, 9.74%. Calcd. for $C_{11}H_{13}N_5O_2BrCl$: Cl, 9.78%.

ω-Nitro-4-nitrostyrene.—The same procedure as mentioned by David E. Worral[8] in their description of the synthesis of nitrostyrene, was used to prepare this compound.

From 1.5 g. of 4-nitrobenzaldehyde and 0.6 cc. of nitromethane[9] was obtained 0.5 g. (26%) of the desired product melting at 203–204° (decompn.)[10], consisting of yellow prisms (from ethanol).

1-(4-Nitrophenyl)-4-nitro-1,3-butadiene. — The crude material obtained similarly as above from 1.8 g. of 4-nitrocinnamaldehyde and 0.7 g. of nitromethane was recrystallized from ethanol, giving 0.4 g. (18%) of yellow needles, m.p. 200–201° (decompn.). Found: N, 12.69%. Calcd. for $C_{10}H_8N_2O_4$: N, 12.73%.

1-(4-Nitrophenyl)-2-bromo-4-nitro-1,-3butadiene.—α-Bromo-4-nitrocinnamaldehyde (1.3g.) and nitromethane (0.4 cc.) were condensed at 5–12°. On recrystallization from ethanol of the crude product, 0.32 g. (15%) of tiny yellow prisms, m.p. 182–182.5°, were obtained. Found: N, 9.49%. Calcd. for $C_{10}H_7N_2O_4Br$: N, 9.37%.

4-Acetamidoacetophenone.—A suspension of 2.7 g. of 4-aminoacetophenone in 27 cc. of water was treated with 2.7 cc. of acetic anhydride to give 3 g. (85%) of the desired product, consisting of colorless prisms, m.p. 169–170°.[11]

4-Nitroacetophenone.—The procedure described by Sugasawa[12] was used with some modification.

4-Aminoacetophenone (6.75 g.) was dissolved in 65 cc. of water and 8 cc. of nitric acid (sp. gr. 1.42) and diazotized with a solution of 9.6 g. of sodium nitrite in 20 cc. of water. The diazo solution was run slowly into a mixture of water (55 cc.), cuprocupric sulfite (prepared from cupric sulfate (12.5 g.) in water (50 cc.) and sodium hydroxide (4 g.) in water (20 cc.)), and sodium nitrite (13.8 g.). After stirring for two hours at room temperature the reaction mixture was extracted six times with 50 cc. portions of ether, the ether removed, and the residue recrystallized from methanol to give 5.07 g. (63%) of the desired product, m.p. 80–81°. A recrystallized sample showed m.p. 82–82.5°.

4-Aminoacetophenone thiosemicarbazone. — A mixture of 0.68 g. of 4-aminoacetophenone, 0.46 g. of thiosemicarbazide and 25 cc. of water was heated in a water bath for nine houres, but the reaction did not take place. Then the mixture was adjusted to pH 3.2[14] with glacial acetic acid and heated for thirty minutes to give 0.84 g. (81%) of the desired product, slightly yellow plates, m.p. 182–183° (decompn.). Recrystallization from ethanol gave a sample melting at 185° (decompn.). Found: N, 26.55%. Calcd. for $C_9H_{12}N_4S$: N, 26.90%.

4-Acetamidoacetophenone thiosemicarbazone.—A solution of 0.46 g. of thiosemicarbazide in 10 cc. of water was added to a solution of 0.89 g. of 4-acetamidoacetophenone in 10 cc. of ethanol.

7) J. Thiele and R. Bihan. *Ann.*, **302**, 311 (1898).
8) David E. Worrall, "Organic Syntheses" Col. Vol. I. p. 495.
9) F. C. Whitmore and Marion G. Whitmore, Ibid., Col. Vol. I. p. 393.
10) Reported mp. 196—199°. See Johannes Thiele, *Ber.*, 1294 (1899).
11) Klingel (*Ber.*, **18**, 2691 (1885)) and Kunckell (*Ber.* 33, 2641 (1900) reported m.p. 166—167°.
12) S. Sugasawa, N. Sugimoto, J. Iwao and Y. Nakamura, *J. Pharm. Soc. Japan.*, **71**, 225 (1951).
13) H. H. Hodgson, A. P. Mahadevan, and E. R. Ward, "Organic Syntheses" Vol. 28, p. 52.
14) A maximum value of condensation velocity of furfural and semicarbazide was found to be at pH 3.13 by J. B. connant and P. D. Bartlett, *J. Am. Chem. Soc.*, **54**, 2881 (1932).

The whole was adjusted to pH 3.2 with glacial acetic acid, heated in a water bath for one hour, and cooled to yield 1.14 g. (91%) of the desired product, slightly yellow plates, m.p. 223.5° (decompn.) (from ethanol). Found: N, 22.27%. Calcd. for $C_{11}H_{14}N_4OS$: N, 22.39%.

4-Nitroacetophenone thiosemicarbazone. — Similarly was obtained the desired product, yellow needles melting at 240° (decompn.), yield 82%, Found: N, 23.38%. Calcd. for $C_9H_{10}N_4O_2S$: N, 23.38%.

Summary

1) Semicarbazones and guanylhydrazones of 4-nitrocinnamaldehyde, 4-nitrobenzalacetone, α-bromo-4-nitrocinnamaldehyde, and 1-(4-nitrophenyl)-2-bromo-1-buten-3-one, nitromethane derivatives of 4-nitrobenzaldehyde, 4-nitrocinnamaldehyde, and α-bromo-4-nitrocinnamaldehyde, and thiosemicarbazones of 4-amino, 4-acetamido-, and 4-nitroacetophenones were prepared for evaluation of their antibacterial activity.

2) Condensation of the acetophenones with thiosemicarbazide was found to proceed smoothly at pH 3.2 but not at pH 7.

The author wishes to express his appreciation to the Educational Ministry for a Grant in Aid for Miscellaneous Scientific Research under which a portion of this work was carried out.

Chemical Laboratory, The Kitasato Institute, Tokyo

Enzymatic Microdetermination of Nitrate

By Fujio EGAMI, Katsuhira IIDA, Tatsumasa DÔKE and Shigehiko TANIGUCHI

(Received August 23, 1954)

As the color reactions for nitrate so far known are less sensitive and less specific than the Griess-Ilosvay reaction for nitrite, nitrate has often been estimated as nitrite after reduction. However, ordinary reducing agents are not sufficiently specific and it is generally difficult to reduce nitrate quantitatively to nitrite.

We tried, therefore, to reduce nitrate to nitrite quantitatively by a specific enzyme—nitrate reductase,* and to determine nitrate indirectly by the Griess-Ilosvay reaction for nitrite.

Concerning nitrate reductase, R. Sato and one of us (Egami)[1] have shown that a cell-free extract obtained by the ultrasonic destruction of certain strains of *Escherichia coli* contains nitrate reductase, but not nitrite reductase, and nitrate can be reduced to nitrite by the enzyme preparation in the presence of an appropriate hydrogen donor such as formic acid and an intermediary hydrogen carrier such as methylene blue.

Analytical Procedure

Enzyme Preparation.—A strain of *E. coli* (given by Dr. S. Yamagutchi) is cultured at first on the KNO_3(0.1%), peptone (1%), bouillon (1%), agar plate for 15—17 hours at pH 7.4, 37°C. The preparatory culture is inoculated on the peptone bouillon agar plate without nitrate and incubated for 15—17 hours at 37°C. The bacterial cells harvested from 2—3 litre plate culture are washed several times by centrifugation until the supernatant is free from nitrite. The bacterial cells are suspended in 50—60 ml. of distilled water and destroyed by ultrasonic irradiation (490 K.C. for 30—40 min.). Then the bacterial debris are centrifuged off (7000×g. for 30—40 min.) at 0°C. To the cooled supernatant, is added an equal volume of saturated ammonium sulfate solution (adjusted to pH 7.0) under stirring. The formed precipitate containing nitrate reductase and formic dehydrogenase is centrifuged (7000×g. for 30 min.) at 0°C and dissolved in 20—30 ml. of cold water. The enzyme solution is dialysed against running water for 24 hours. Then the enzyme solution is freeze-dried, and 700—800 mg. of the dried preparation is obtained. The dried preparation in evacuated ampoule maintains its activity for at least 3 months in an ice-box.

Solutions required. — a. Enzyme solution: The freeze-dried powder is dissolved in distilled water (2mg./1 ml.).

b. Methylene blue or FAD**(1/200 M), sodium formate (1/5 M), phosphate buffer (1/5 M) (pH

* In this connection, it should be added that R. Williams et al. have used living cells of *E. coil* as reducing catalyst. Their method is for clinical use and less accurate (*J. Lab. Clin. Med. St Louis*, **41**, 157, (1953)).

1) F. Egami and R. Sato, *J. Chem. Soc. Japan*, **68** 39, (1947); **69** 160 (1948); *Proc. Japan Acad.*, **24** 29 (1948).

* Flavin adenine dinucleotide.

* If FAD is used in place of methylene blue, the process of decoloration may be omitted.

7.2) mixed solution.

c. Saturated aqueous solution of uranyl acetate.

d. Griess-Ilosvay reagent:

Solution 1. Sulfanilic acid (10.5 g.), sodium acetate (6.8 g.) and glacial acetic acid (300 ml.) are dissolved in 600 ml. of distilled water. The soluion is boiled for 3 min. and diluted to 1 l.

Solution 2. α-Naphthylamine (5.0 g.) is added to 1 l. of boiling water, then 5 ml. of conc. hydrochloric acid is added to the solution.

Before use, equal volumes of the two solutions are mixed together.

Method of analysis—1. Place 1 ml. of solution a, 0.5 ml. of solution b and 2 ml. of test solution into a Thunberg tube.

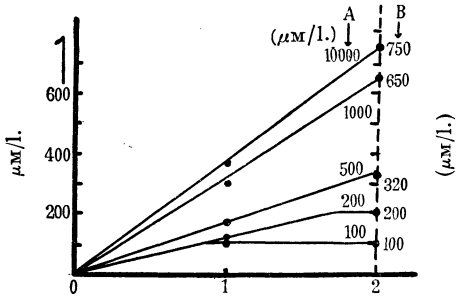
2. Evacuate the tube by aspiration.
3. The tube is allowed to stand at 37°C for 1.5—2.0 hours. Here the reduction takes place.
4. To 2 ml. of solution c in a centrifugal tube, are added 3 ml. of the reaction mixture and a small amount of kaolin powder for decoloration.
5. After centrifugation, to 4 ml. of the clear supernatant is added 1 ml. of Griess-Ilosvay reagent.
6. Then, it is colorimetrically estimated as usual. The authors measured the extinction at 530 mμ with Coleman's spectrophotometer. As blank test solution, the similarly treated solution with 2 ml. of distilled water in place of the test solution should be used.

Remarks.—(1) When nitrite coexists with nitrate, nitrite should be estimated at first as usual, and the value should be subtracted from the total value obtained after reduction.

(2) When the test solution is too concentrated (>100μM/l. nitrate), it must be diluted preliminarily, otherwise the complete reduction can not be attained in 2 hours, as is shown in Fig. 1. So before the accurate analysis, the approximate nitrate concentration must be estimated by measuring the nitrite produced in 2 hours. The test solution is then diluted to an appropriate concentration (10—100μM/l.), and the accurate analysis should be carried out.

Some Examples of Analyses

Some Examples of Analyses with Nitrate and Nitrite Solutions of the Known Concentration.—Some of the experimental results are summarized in Table I, II and III. As shown in Table I and II respectively, nitrate (10—100μM/l.) can be quantitatively estimated by this method and nitrite (50,100μM/l) be quantitatively recovered. Table III shows that the mixture of nitrate and nitrite is quite satisfactorily estimated as the total sum, so nitrate can be determined by subtracting the quantity of nitrite estimated directly as usual.



A: Nitrate concentration in test solution used in enzymatic reduction.

B: Nitrite concentration produced after 2 hours enzymatic reduction.

Fig. 1. Experimental scale for approximate estimation of nitrate concentration.

TABLE I
DETERMINATION OF NITRATE IN STANDARD SOLUTION

Nitrate concn. present (μM/l.)	Nitrite concn. determd. (μM/l.)	Nitrate recovery (%)
10	9.5, 10.5	95, 105
25	25.0, 26.0, 26.5	100, 104, 106
50	48.5, 48.0	97, 96
100	102.0, 99.0, 97.0	102, 99, 97

TABLE II
RECOVERY TESTS OF NITRITE IN NITRATE DETERMINATION

Nitrite concn. present (μM/l.)	Nitrite concn. determd. (μM/l.)	Nitrite recovery (%
50	52.0, 52.0	104, 104
100	98.0	98

TABLE III
DETERMINATION OF NITRATE IN MIXED SOLUTIONS OF NITRATE AND NITRITE

(1) Nitrate concn. present (μM/l.)	(2) Nitrite concn. present (μM/l.)	(3) Nitrite concn. preliminarily determd. (μM/l.)	(4) Nitrate plus nitrite concn. determd. (μM/l.)	(5) Nitrate concn. determd. :(4)—(3) (μM/l.)	(6) Nitrate recovery. (%)
17.0	19.5	19.5	35.0	15.5	91
20.0	6.0	6.0	26.0	20.0	100
20.0	20.0	20.0	38.0	18.0	90
20.0	40.0	40.0	61.0	21.0	105
100.0	40.0	40.0	144.0	104.0	104

Some Examples of Practical Applications.—The method was applied to the estimation of nitrate in human urine, horse serum, spinach leaf extract, sea water and rain water. As a small quantity of nitrate added to these natural test solutions were always quantitatively recovered as shown in Tables IV—VIII, it may be concluded that the method is satisfactory for the estimation of nitrate in these natural samples.

TABLE IV

DETERMINATION OF NITRATE IN HUMAN URINE

Human urine freshly obtained is diluted according to Remarks (2), then used as a sample for accurate analysis. The sample contains no nitrite.

Sample 1. (400 fold diluted)

	Nitrate concn. determd. (μM/l.)	(Mean) (μM/l.)	
Sample alone	15.0		Nitrate concn. in original human urine
	15.0	15.0	$15.0\mu M/l. \times 400 = 6.0 \times 10^{-3} M/l. = 84$ mg. nitrate-N/l.
Sample+ 25μM/l. nitrate.	38.5		Recovery of 25μM/l. nitrate added (μM/l.)
	38.0	38.5	23.5

Recovery (%)

94

Sample 2. (100 fold diluted)

	Nitrate concn. determd. (μM/l.)	(Mean) (μM/l.)	
Sample alone	63.0		Nitrate concn. in original human urine
	61.5		$63.0\mu M/l. \times 100 = 6.3 \times 10^{-3} M/l. = 88$ mg.
	65.0	63.0	nitrate-N/l.
Sample+ 25μM/l. nitrate	87.0		Recovery of 25μM/l. nitrate added (μM/l.)
	86.0	86.5	23.5

Recovery (%)

94

TABLE V

DETERMINATION OF NITRATE IN HORSE SERUM

To the freshly prepared horse serum, is added sodium fluoride (final concn. 1%) as an antiseptic.

This sample contains no nitrite.

	Nitrate concn. determd. (μM/l.)	(Mean) (μM/l.)	
Sample alone	35.0, 34.0		Nitrate concn. in horse serum
	32.0, 33.0		$34\mu M/l. = 0.5$ mg. nitrate-N/l.
	34.0, 35.0	34.0	
Sample+ 25μM/l. nitrate	57.0		Recovery of 25μM/l. nitrate added. (μM/l.)
	57.0	57.0	23.0
Sample+ 50μM/l. nitrate	82.0		Recovery of 50μM/l. nitrate added.
	80.0		(μM/l.)
	80.0	81.0	47.0

Recovery (%)

92

Recovery (%)

94

TABLE VI

DETERMINATION OF NITRATE IN SPINACH LEAF EXTRACT

Minced young spinach leaves are immersed in boiling water, then homogenized and centrifuged (10000×g. for 30 min.). The green supernatant obtained—the dry weight of 1 ml. of this original extract amounts 3.2 mg.—is diluted 200 fold according to Remarks (2), then used as an sample for accurate analysis. This sample contains no nitrite.

	Nitrate concn. determd. (μM/l.)	(Mean) (μM/l.)	
Sample alone	36.0		Nitrate concn. in original spinach leaf extract
	36.0	36.0	36μM/l. ×200=7.2×10^{-3}M/l.=0.1 mg. nitrate-N/ml.
			=0.03 mg. nitrate-N/mg. dry weight
Sample+ 25μM/l. nitrate	60.0		Recovery of 25μM/l. nitrate added (μM/l.) / Recovery (%)
	59.0		
	59.0	59.0	23.0 / 92
Sample+ 50μM/l. nitrate	86.0		Recovery of 50μM/l. nitrate added (μM/l.) / Recovery (%)
	84.0	85.0	49.0 / 98

TABLE VII

DETERMINATION OF NIRATE IN SEA WATER

Prior to the determination of nitrate, the nitrite concn. of the sea water is determined according to Remarks (1). In this case, it is necessary to lower the high salt concn. of the sea water, by which nitrate reductase activity is inhibited. So the ordinary analytical method is slightly modified by adding excess 1 ml. of distilled water at Step. 1 and converting the total volume of reaction mixture to 4.5 ml.

	Nitrite concn. preliminarily determd. (μM/l.)	Nitrate plus nitrite concn. determd. (μM/l.)	Nitrate concn. determd. (μM/l.)	(Mean.) (μM/l.)	
Sample alone	2.0	15.0	13.0		Nitrate concn. in sea water
	2.0	17.0	15.0	14.0	14μM/l.=0.20 mg. nitrate-N/l.
Sample+ 25μM/l. nitrate	2.0	40.5	38.5		Recovery of 25μM/l. nitrate added (μM/l.) / Recovery (%)
	2.0	39.5	37.5	38.0	24.0 / 96

TABLE VIII

DETERMINATION OF NITRATE IN RAIN WATER

Prior to the determination of nitrate, the nitrite concn. of the rain water is determined according to Remarks (1). In this case, the nitrate concn. of the test sample is very dilute. So, the ordinary analytical method is slightly modified by using 3 ml. of the test sample and dissolving the enzyme powder in 3.5 ml. reaction mixture.

	Nitrite concn. preliminarily determd. (μM/l.)	Nitrite plus nitrite concn. determd. (μM/l.)	Nitrate concn. determd. (μM/l.)	(Mean) (μM/l.)	
Sample alone	0.5	6.5	6.0		Nitrate concn. in rain water
	0.5	6.0	5.5	6.0	6.0μM/l.=0.08 mg. nitrate-N/l.
Sample+ 12.5μM/l. nitrate	0.5	18.5	18.0		Recovery of 12.5μM/l. nitrate added. (μM/l.) / Recovery (%)
	0.5	18.5	18.0	18.0	12.0 / 96

Summary

1) On the principle of the colorimetry of nitrite produced by enzymatic reduction, a method of microdetermination of nitrate was established.

2) This method can be applied to 10—100μM/l. nitrate solution. 2 ml. of the solution (1.2—12 μg. NO^-_3 or 0.28—2.8 μg. nitrate-N) is sufficient for an analysis.

3) This method is successfully applied to the estimation of nitrate in human urine, horse serum, spinach leaf extract, sea water and rain water.

Thanks are offered to Mr. M. Tanaka of the Department of Chemistry, Faculty of Science, Nagoya University for his interest and helpful advice.

Department of Chemistry, Faculty of Science, Nagoya University

Diphenylcarbazone as an Internal Indicator in Volumetric Analysis. Part I. Determination of Ferrocyanide by Lead Nitrate

By G. S. DESHMUKH

(Received August 23, 1954)

The standard methods of ferrocyanide determination may be classified broadly as follows: (a) those leading to its quantitative oxidation under certain operative conditions by such oxidants like Ce^{IV}, KIO_3 and $KMnO_4$ [1-3]; (b) those involving the formation of stable complexes of known composition, especially the titration of zinc salt solutions against $K_4Fe(CN)_6$[4] and (c) titrations with $AgNO_3$[5] or $Pb(NO_3)_2$[6] using fluorescein or sodium alizarin sulfonate as adsorption indicators. According to Müller and Gäbler, potentiometric titration of standard lead nitrate against $K_4Fe(CN)_6$ gives reproducible and accurate results.[7]

It is known that in the well known microtest for Hg^{++} by diphenylcarbazone, Pb^{++} interferes due to its reaction with the reagent to develop an intense red or pink color. An aqueous solution of $K_4Fe(CN)_6$ does not, however, produce any characteristic color on the addition of diphenylcarbazone other than the brown or orange color of its alcoholic solution. This, as also the fact that besides Alizarine S no other indicator has been successfully adopted for the titrimetric detemination of ferrocyanide by $Pb(NO_3)_2$, suggested the investigation of this volumetric procedure using diphenylcarbazone as an internal indicator.

Experimental

Standard solutions of lead nitrate were prepared by dissolving accurately weighed quantities of a Merck's guaranteed reagent grade sample in appropriate volume of water; the lead content was checked by the chromate method. Laboratory reagent grade $K_4Fe(CN)_6$ was used for preparing solutions of various concentrations. The quantity of ferrocyanide in an aliquot portion of the solution was determined by standard ceric sulfate with ferroin as the indicator and potentiometrically. To 10 ml. of $K_4Fe(CN)_6$ about 1 ml. of the saturated alcoholic solution of diphenylcarbazone was added and the brown or orange colored solution was titrated slowly with constant stirring against standard lead nitrate. With the formation of lead ferrocyanide, the color faded gradually to pale yellow or brown and the end point was marked with a sharp change to purple. This is easy to detect and does not involve the risk of over-titration. It is, however, possible to rectify the error due to surpassing of the end point by running in a measured quantity of ferrocyanide and continuing the titration as usual. A reverse titration indicating a color change from purple to pale yellow or almost colorless though possible, was found to be less sharp and accurate. The molecular ratio of Pb: $K_4Fe(CN)_6$, calculated from the quantity of $Pb(NO_3)_2$ reacting with ferrocyanide at the equivalent point, showed that the composition of the precipitate corresponds to $Pb_2Fe(CN)_6$ or $2Pb—1K_4Fe(CN)_6$. These results are shown in the Table.

1) H.H. Willard and P. Young, *J. Amer. Chem. Soc.*, **55**, 3260 (1933).
2) R. Lang, *Z. anorg. allgem. Chem.*, **142**, 280 (1925).
3) R.E. Oesper, "Newer Methods of Volumetric Chemical Analysis" Chapman and Hall Ltd. London. (1938) p. 185-87.
4) W.H. Cone and L.C. Cady, *J. Amer. Chem. Soc.*, **49**, 356 (1927). Cf. also I. M. Kolthoff, *Chem. Weekbl.*, **24**, 303 (1927).
5) A.J. Berry and P.J. Durrant, *Analyst*. **55**, 613 (1930).
6) R. Burstein, *Z. anorg. allgem. Chem.*, **164**, 219 (1927).
7) E. Müller and K. Gäbler, *Z. analyt. Chem.*, **62**, 29 (1923).

TABLE I

Expt. No.	Gms. of $Pb(NO_3)_2$ in 250 ml.	Vol. of $Pb(NO_3)_2$=10 ml. $K_4Fe(CN)_6$ ml.	Weight of $K_4Fe(CN)_6$		
			By $Ce(SO_4)_2$ (g.) a	By Diphenylcarbazone (g.)	By Potentiometry (g.)
1	2.2775	16.20	0.0820	0.0820	0.0822
2	2.8060	48.80	0.3044	0.3042	0.3040
3	1.2335	35.5	0.0974	0.0973	0.0973
4	2.8060	24.3	0.1518	0.1516	0.1518
5	3.1416	19.6	0.1358	0.1356	0.1355
6	3.1126	18.6	0.2582	0.2586	0.2584
7	1.2335	14.8	0.04052	0.04054	0.3436
8	4.2162	36.7	0.3436	0.3438	0.3436

It is seen from a comparative study of the data that the above procedure yields accurate and reproducible results. It may also be mentioned that the limitation of using N/30 or even more dilute solutions of $K_4Fe(CN)_6$, inherent in Burstein's method[6] is not necessarily imposed on the present procedure. Since as a precipitant potassium ferrocyanide destroys immediately the pink or red color developed by Pb^{++} with diphenylcarbazone, the general difficulty of the unusual stability of the lead color met with in the case of other internal indicators[8] is not encountered in these titrations.

8) B. S. Evans, *Analyst*, **64**, 2 (1939).

Summary

A simple and direct method of estimating ferrocyanide by standard lead nitrate with diphenylcarbazone as an internal indicator has been described. The results are accurate and compared favorably with those obtained by other classical procedures.

The author wishes to express his sincere thanks to Professor S.S. Joshi for facilities and encouragement during the work and to the National Institute of Sciences of India for award of a research fellowship.

Chemical Laboratories,
Banaras Hindu University,
Banaras, India

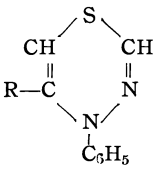
Studies on Organic Sulfur Comqounds. I. Thioformyl Phenylhydrazine

By Tadashi SATO and Masaki OHTA

(Received September 3, 1954)

Thioformylation of amine by dithioformic acid or its potassium salt was first reported by Todd.[1] He suggested that thioformamino derivatives are useful for identification of amines because of their good crystallizability and sharp melting point. He also suggested that thioacylamino derivatives could be used for the synthesis of heterocyclic compounds.

Some kinds of thioformamino- or thioformhydrazino-derivatives have been reported by one of us as intermediates for the synthesis of thiazole- or thiadiazole-derivatives.[2] Concerning our research on the synthesis of 1,3,4-thiadiazine derivatives (I) from, β-thioformyl phenylhydrazine (II), we found it necessary to investigate the properties of thioformyl phenylhydrazine.



(I)

$$\underset{\alpha\ \beta}{C_6H_5NHNHCHS} \rightleftarrows C_6H_5NHN{=}CHSH$$

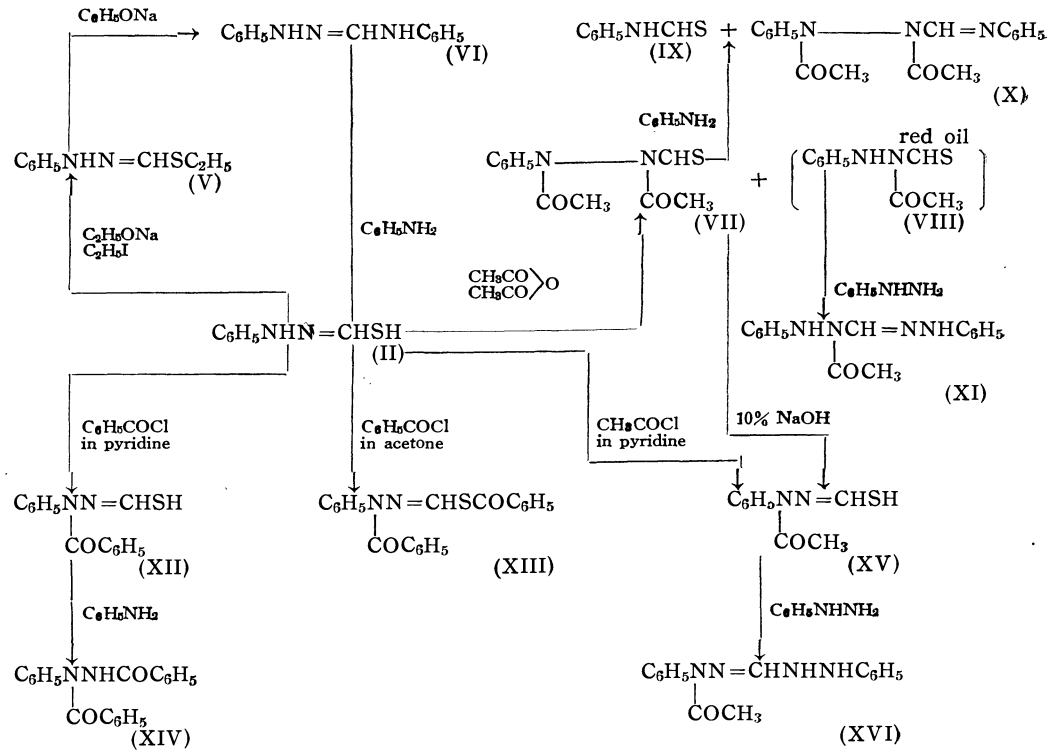
(II)

Baker et al.[3] reported the preparation of thioformyl arylhydrazine derivatives from sodium dithioformate and arylhydrazines.

1) A. R. Todd et al., *J. Chem. Soc.*, **1937**, 361.
2) M. Ohta, *J. Pharm. Soc. Japan*, **71**, 869 (1951); ibid., **73**, 701 (1953).
3) W. Baker et al., *J. Chem. Soc.*, **1950**, 3389.

They obtained (II) as an oil in a crude state and only a small portion of it became crystalline (m.p. 39-41°). They used the crude product in subsequent reactions, and concluded its structure to be (II) by analysis and several reactions. We obtained a compound (m.p. 102°) from phenylhydrazine and potassium dithioformate in a good yield. From various properties described in this report, no doubt remains that the product we obtained has a structure of (II). It is the purpose of this report to determine which hydrogen of two replaceable hydrogens of (II) is replaced, when (II) is submitted to alkylation or acylation.

When (II) was treated with sodium ethoxide and ethyl iodide, ethyl derivative (V) was obtained as an oil. (V) reacted with aniline at room temperature to afford formamidine derivative (VI) liberating ethyl mercaptan.



From this fact it is evident that the ethyl group is attached to the sulfur atom. (V) could be distilled under reduced pressure and was fairly stable compared with the ethyl derivative of thioformyl aniline which is unstable in the presence of moisture.[4]

As for the benzoylation of (II) with one mol. of benzoyl chloride, monobenzoyl derivative (XII) was formed exclusively in pyridine solution. But when the benzoylation of (II) was carried out in acetone solution in the presence of sodium bicarbonate, the principal product was dibenzoyl derivative (XIII), and the formation of monobenzoyl derivative (XII) was small in quantity. When two mols. of benzoyl chloride were reacted with one mol. of (II) in the presence of sodium bicarbonate, dibenzoyl derivative was the sole product. (XIII) did not react with aniline even on warming, which suggests that in dibenzoyl derivative (XIII), unlike in the case of diacetyl derivative (VII), one benzoyl group must be attached to α-nitrogen atom, and the other to sulfur atom.

Monobenzoyl derivative (XII) was soluble in aqueous sodium hydroxide solution, indicating the presence of the mercapto group, so that the benzoyl group should be attached to α-nitrogen. When (XII) was heated with aniline, hydrogen sulfide was liberated and a yellow oil was obtained. From this oil some amounts of colorless crystals (m.p.177°), were obtained. It was identified as α,β-dibenzoyl phenylhydrazine (XIV) from its analytical value, melting point and mixed melting point with an authentic sample. The mechanism by which dibenzoyl phenylhydrazine is formed from monobenzoyl derivative (XII) is unknown.

The reaction of (II) with acetyl chloride

4) O. Wallach and M. Wüster, *Ber.*, **16**, 145 (1883).

gave monoacetyl derivative (XV) in pyridine solution. In the reaction of two mols. of acetyl chloride with one mole of (II) in acetone in the presence of sodium bicarbonate, the formation of diacetyl derivative had been expected on the analogy of benzoylation in the same condition. But the reaction product was a red oil and crystallization or purification were unpossible. This red oil, unlike dibenzoyl derivative (XIII), reacted with aniline to liberate hydrogen sulfide, which is supposed to be due to some by-products.

Monoacetyl derivative (XV) was also soluble in aqueous sodium hydroxide solution, so that the acetyl group should be attached to α-nitrogen and when treated with aniline at room temperature in ethanol, hydrogen sulfide was liberated but the reaction product expected could not be isolated. (XV) reacted with phenylhydrazine to give orange crystals of (XVI), melting at 188°.

When (II) was treated with acetic anhydride at room temperature, diacetyl derivative (VII) was obtained, accompanied by small quantity of red oil (VIII). (VII) was insoluble in 10% sodium hydroxide solution, but on standing, it was hydrolyzed gradually and went into solution. On acidifying with acetic acid, monoacetyl derivative (XV) was obtained. (VII) reacted with aniline liberating hydrogen sulfide and gave thioformyl aniline and (X). This fact leads us to conclude that the two acetyl groups in (VII) must be attached to α-and β-nitrogen atoms of thioformyl phenylhydrazine. The isolation of α,β-diacetyl phenylhydrazine, which should be formed in this reaction, was impossible. The red oil (VIII) obtained as by-product in acetylation of (II) with acetic anhydride, reacted with phenylhydrazine to give colorless crystals, evolving a considerable amount of hydrogen sulfide and heat. This crystal was identified as monoacetyl derivative (XI), probably an isomer of (XVI), from its analytical value. This fact shows that (VIII) must also be monoacetyl derivative and an isomer of (XV). In (XV) as well as in (XVI), it is certain that the acetyl group is attached to α-nitrogen as explained before. Consequently, in (XI) or (VIII) the acetyl group is supposed to be attached to β-nitrogen. This was also confirmed by the insolubility of (VIII) in aqueous sodium hydroxide solution.

The authors are indebted to Mr. A. Kondo for the microanalytical results reported here.

Experimental

N-Phenyl-N'-thioformylhydrazine (II). — A solution of potassium hydrosulfide was prepared by mixing a solution of potassium hydroxide (46 g. in 150 cc. of methanol) saturated with hydrogen sulfide, with a solution of 46 g. of potassium hydroxide in 150 cc. of methanol. The solution was heated to about 50° in a 3 l.-flask equipped with a long Dimroth condenser. Then 30 g. of chloroform was added and constantly shaken. An exothermic reaction occurred which led to violent boiling. After ten minutes the mixture was cooled and filtered. The filtrate was evaporated in vacuo to about 50 cc. The solution of crude potassium dithioformate thus obtained was mixed with a solution of 14 g. of phenylhydrazine in 30 cc. of methanol. The evolution of hydrogen sulfide was recognized at once. The mixture was allowed to stand overnight at room temperature, then diluted with water and acidified with acetic acid. The crystalline precipitates were collected by filtration, washed with water and dissolved in ethanol and filtered from a small amount of insoluble matter. The filtrate was diluted with water to precipitate thioformyl compounds. The crude product was purified by dissolving in dilute sodium hydroxide solution and reprecipitated by acidifying with acetic acid. Colorless leaflets resulted. m.p. 102°. Yield 17 g. (86%). Found: N, 18.21; calculated for $C_7H_8N_2S$: N, 18.41%.

N-Phenyl-N'-ethylmercaptomethylene-hydrazine (V).—To a solution of 5 g. of thioformyl phenylhydrazine in 15 cc. of ethanol were added 15 cc. of sodium ethylate solution (containing 0.8 g. of sodium) and then 5 g. of ethyl iodide at room temperature. After standing overnight at room temperature, most of the alcohol was evaporated under reduced pressure, water was added and extracted with ether. After drying over anhydrous sodium sulfate, ether was evaporated. A small portion of the residual oil was distilled under a pressure of 8 mmHg (bath temperature was 170—180°) and used for analysis. Found: C, 60.47; H, 6.36; calculated for $C_9H_{12}N_2S$: C, 60.00; H, 6.67%.

Benzoylation of (II). (*a*) *in pyridine.*—To a solution of 10 g. of thioformyl phenylhydrazine in 50 cc. of pyridine was added dropwise 9.5 g. of benzoyl chloride in a period of one hour, stirring continuously and cooling with ice-water. After standing overnight at room temperature, water was added, then the oil which soon solidified separated. Recrystallization from ethanol yielded 6 g. of light yellow crystals of N-phenyl-N-benzoyl-N'-mercaptomethylene-hydrazine (XII), melting at 140°. Found: C, 65.75; H, 4.91; N, 10.60; calculated for $C_{14}H_{12}N_2OS$: C, 65.63; H, 4.69; N, 10.93%.

(*b*) *In acetone with two mols. of benzoyl chloride.*—To a solution of 3 g. of thioformyl phenylhydrazine (1 mol.) in 30 cc. of acetone, 4 g. of sodium bicarbonate (2 mols.) were suspended, and 5.5 g. of benzoyl chloride (2 mols.) were added dropwise with constant stirring and cooling. During the addition, the product separated gradually. Stirring was continued for six hours at room temperature and the precipitates were collected by filtration, washed first with aqueous solution of sodium bicarbonate and then with water (yield, 6 g.). When recrystallized from ethanol, fine

needles of N-phenyl-N-benzoyl-N'-benzoylmercaptomethylene-hydrazine (XIII), melting at 137°, were obtained. Found: N, 7.64; calculated for $C_{21}H_{16}N_2O_2S$: N, 7.77%.

(c) *In acetone with one mole of benzoyl chloride.*—To a solution of 3 g. of thioformyl phenylhydrazine (1 mol.) in 30 cc. of acetone were added 2.5 g. of benzoyl chloride (1 mol.) in the presence of 1.7 g. of sodium bicarbonate (1 mol.) in the same manner as described above. After standing overnight the solid was collected and washed with 10% aqueous sodium hydroxide solution. The greater part of the solid was insoluble but when alkali washings were acidified with acetic acid some amounts of solid were obtained, which were identified as monobenzoyl derivative (XII) after the recrystallization from ethanol. The solid which was insoluble in alkali was dibenzoyl derivative (XIII).

Reaction of (XII) with Aniline.—To a solution of 2 g. of (XII) in 40 cc. of ethanol, 0.8 g. of aniline was added and refluxed for four hours. Addition of water to the cooled reaction mixture gave an oil, which was taken up in ether and after drying over anhydrous sodium sulfate, the ether was evaporated. From the residual oil small amounts of crystals were obtained. Recrystallization afforded colorless crystals, melting at 177°. The mixed melting point with authentic sample of N,N'-dibenzoyl phenylhydrazine (XIV) was also 177°. Found: N, 9.28, calculated for $C_{20}H_{16}N_2O_2$: N, 8.86%.

N - Phenyl - N - acetyl-N'-mercaptomethylene-hydrazine (XV).—To a solution of 5 g. of thioformyl phenylhydrazine in 30 cc. of pyridine was added dropwise 2.5 g. of acetyl chloride during a period of one hour, stirring continuously and cooling with ice-water. After standing overnight at room temperature, water was added, then the oil which soon solidified separated. Recrystallization from ethanol yielded 3 g. of light red rhombic crystals (XV), melting at 120–2° to red liquid. Found: N, 14.35; calculated for $C_9H_{10}N_2OS$: N, 14.43%.

N - Phenyl - N - acetyl - N' - phenylhydrazino - methylene-hydrazine (XVI). — To a solution of 1 g. of (XV) in 20 cc. of ethanol 0.6 g. of phenylhydrazine was added at room temperature. The reaction proceeded with liberation of hydrogen sulfide. After an hour water was added and the crystalline precipitates which separated were recrystallized from ethanol. Orange crystals of (XVI), m.p. 188° resulted. Yield, 0.5 g. Found: N, 20,56; calculated for $C_{15}H_{16}N_4O$: N, 20.90%.

N - Phenyl - N,N' - diacetyl-N' - thioformylhy - drazine (VII). — Five grams of thioformyl phenylhydrazine were dissolved in 30 cc. of acetic anhydride, the temperature of the solution being kept under 30° by external cooling with water. After standing overnight at room temperature, water was added to decompose the excess of acetic anhydride. A viscous oil which soon solidified was separated. The solid was collected on the filter, and washed with ether. The crude product weighed 7 g., and melted at 103–4°. Recrystallization from ethanol yielded 6 g. of (VII) as yellow rhombic crystals melting at 107°. Found: N, 11.85; calculated for $C_{11}H_{12}N_2O_2S$: N, 11.86%.

N^{α}-Acetyl-N^{β}, $N^{\beta'}$-diphenyl-formhydrazidine (XI).—From the ether washings in the above reaction, ether was evaporated. The ethanol solution of the residual red oil was treated with phenylhydrazine at room temperature. The reaction proceeded with evolution of hydrogen sulfide and heat. After a little while water was added and the separated solid was recrystallized from dilute ethanol. Colorless needles of (XI), melting at 173° resulted. Found: C, 66.89; H, 6.09; N, 20.41; calculated for $C_{15}H_{16}N_4O$: C, 67.16; H, 5.97; N, 20.90%.

Reaction of (VII) with Aniline.—To a solution of 1 g. of (VII) in a small volume of acetone 0.4 g. of aniline was added and the mixture was kept standing at room temperature for one hour. On addition of water a colorless solid was separated. Recrystallization from dilute ethanol gave 0.3 g. of thioformyl aniline, melting at 140°, which was confirmed by its mixed melting point with authentic sample and analytical value. (Found: N, 10.02, calculated for C_7H_7NS: N, 10.21%.) Addition of water to the mother liquor of the recrystallization gave still greater amounts of solid. This was washed with 10% sodium hydroxide solution to remove thioformyl aniline, and the residue, on recrystallization from dilute ethanol afforded colorless crystals of N,N'-diacetyl-N'-phenyl-hydrazinomethyleneaniline (X), melting at 135°. Found: N, 14.2; calculated for $C_{17}H_{17}N_3O_2$: N, 14.23%.

Hydrolysis of Diacetyl derivative (VII) into Monoacetyl derivative (XV). — One gram of diacetyl derivative (VII) was suspended in 3.5 cc. of 10% sodium hydroxide solution, and stirring was continued until dissolution was completed. Decolorizing with charcoal and acidifying with acetic acid gave an oil which soon solidified. Recrystallization from ethanol yielded colorless rhombic crystals, melting at 120–1°. Mixed melting point with monoacetyl derivative (XV) showed no depression.

Laboratory of Organic Chemistry,
Tokyo Institute of Technology
Ookayama, Tokyo